The Bronze-Age Obsidian Industry at Tell Mozan (Ancient Urkesh), Syria: Redeveloping Electron Microprobe Analysis for 21st-Century Sourcing Research and the Implications for Obsidian Use and Exchange in Northern Mesopotamia after the Neolithic

A DISSERTATION
SUBMITTED TO THE FACULTY OF THE GRADUATE SCHOOL
OF THE UNIVERSITY OF MINNESOTA
BY

Ellery Edward Frahm

IN PARTIAL FULFILLMENT OF THE REQUIREMENTS
FOR THE DEGREE OF
DOCTOR OF PHILOSOPHY

Gilbert B. Tostevin

October 2010

© Ellery Edward Frahm, October 2010

Acknowledgements

Throughout my dissertation, I acknowledge other researchers' contributions. There are, though, individuals and organizations that deserve special recognition here. I thank Professors Giorgio Buccellati and Marilyn Kelly-Buccellati, the Directors of the Urkesh Expedition, for their exuberant support for my research. I also thank Federico Buccellati and Jamal Omar, the Assistant Directors of the Expedition, as well as James Walker, the Unit J3 Supervisor, and the rest of the MZ19 members. The Urkesh Expedition is under the aegis of the International Institute for Mesopotamian Area Studies (www.iimas.org). Export of the obsidian artifacts was graciously approved by the Directorate General of Antiquities and Museums, the Ministry of Culture, Syrian Arab Republic. Over 80% of the geological obsidian specimens in this research were collected by George "Rip" Rapp, Regents Professor Emeritus, University of Minnesota-Duluth, and the late Tuncay Ercan, Directorate of Mineral Research and Exploration in Turkey. Others who kindly provided geological obsidian specimens are cited in Chapter 4. I thank my committee members for their guidance: Professors Gilbert Tostevin, Gilliane Monnier, Peter S. Wells, and Joshua M. Feinberg. The Departments of Anthropology and Geology & Geophysics helped to fund my research. Professors David Kohlstedt and Marc Hirschmann, my supervisors in Geology & Geophysics, allowed and encouraged me to carry out my own research. This work would not have been possible without the loving support (as well as endurance and patience) of my wife, Penny, and my parents, Rose and LeRoy Frahm.

Dedication

For Penny and Liev

"Your love is the true obsidian."

-- Akkadian poem, circa 2nd millennium BCE

Abstract

Obsidian tools continued to be utilized in Northern Mesopotamia well beyond the introduction of metal but have received little archaeological attention. It is widely held that obsidian sourcing can offer little new information during a period in which there is a variety of artifacts and texts available to study. Obsidian, though, is unparalleled in its widespread use and ability to be sourced, so it provides unique information about contact, exchange, and migration. Its sourcing can complement other types of information and be used to test existing hypotheses. Before the recent excavations at Tell Mozan (ancient Urkesh) in northeastern Syria, most of the information about its inhabitants, the Hurrians, was inferred from linguistic or textual evidence. Identifying the sources of their obsidian artifacts can be useful for testing some of the highly debated inferences.

The research at hand involved three primary goals. I sought, first, to demonstrate a sophisticated approach to obsidian studies in the Near East and, second, to redevelop an analytical technique -- electron microprobe analysis -- for sourcing obsidian. Therefore, I assembled and analyzed a reference collection of over 900 geological obsidian specimens from dozens of sources in Turkey as well as Armenia, Georgia, Azerbaijan, and Russia. I sourced a large number of artifacts (n = 97) so that I could explore spatial and temporal patterns on a site level. In addition, this analytical technique, if applied critically, can (i) control for obsidian as a mixture, (ii) measure artifacts non-destructively, and (iii) discern two chemically similar obsidian sources: Nemrut Dağ and Bingöl A. Thus, based on my results, I not only differentiate these obsidians but also pinpoint the collection loci, down to a kilometer, of the Nemrut Dağ obsidians found at Tell Mozan.

My third goal involved identifying the sources of obsidian represented among the Bronze-Age artifacts at Tell Mozan. These results were, in turn, used to explore temporal and spatial patterns of the obsidian sources used at the site, consider broader implications for obsidian use in Bronze-Age Mesopotamia, and examine two issues regarding Urkesh and its Hurrian inhabitants. The overall similarities for two site areas suggest that people living in various parts of Urkesh had similar access to the same obsidian sources. On the other hand, all the sourced obsidian from the temple came from one flow at Nemrut Dağ, and a service courtyard of the palace contains the only Cappadocian obsidian. In fact, the greatest variety of sources is found in units containing palace courtyards.

Regarding the broader implications, there is evidence at Tell Mozan of production of prismatic obsidian blades and bladelets (e.g, flakes with cortex, cores, and early-series blades), suggesting they were not imported from a production center. In addition, there is a prevailing assumption that, if Bingöl B obsidian is found at a site, one can presume that all of the peralkaline obsidian artifacts came from Bingöl A, not Nemrut Dağ. My results reveal that this assumption, based on maximal efficiency, is specious.

The hypothesis of a Hurrian "homeland" as far northeast as Armenia (or beyond) is considered -- but not supported -- in light of my obsidian data. There are no obsidians from northeastern Turkey, Armenia, Azerbaijan, Georgia, or Russia that would point to a link to those regions. The atypical variety of obsidian sources at the site suggests that the city may have had a mountainous hinterland to the north. When compared to the existing data for other Khabur Triangle sites, my results support a possible exchange link between Tell Mozan and Tell Brak, perhaps as part of an early Hurrian kingdom.

Table of Contents

Acknowledgements i
Dedication ii
Abstract iii
Table of Contents v
List of Tables xiv
List of Figures xvi
Introduction 1
Part I: Foundations and Problems 12
Chapter 1: Obsidian: Its Origins, Sourcing, and Issues 12
1.1 - Why All the Interest in Obsidian? 13
1.2 - What is Obsidian, and How is it Formed? 16
1.2.1 - Obsidian as Natural Glass 16
1.2.2 - Obsidian as a Mixture 19
1.2.3 - Formation of Obsidian 29
1.2.4 - Geochemistry of Obsidian 36
1.3 - Fundamentals of Sourcing Studies 39
1.3.1 - Terminology: “Sourcing” versus “Provenancing” 40
1.3.2 - Sourcing, Fingerprints, and Typologies 42
1.3.3 - “Trace-Element Fingerprints” versus Major Elements 44
1.3.4 - The Theory and Postulates of Sourcing 46
1.3.5 - The Goals of Obsidian Sourcing Studies 52
1.4 - Analytical Techniques for Obsidian Sourcing 54
1.5 - Lessons from Ceramics Sourcing 58
1.5.1 - Ceramics as Mixtures and Sourcing Effects 59
1.5.2 - Application to Obsidian Sourcing 64
1.6 - Introduction to EMPA 66
1.7 - Prior Obsidian-Sourcing Studies with EMPA 67
1.7.1 - Merrick and Brown in East Africa 69
1.7.2 - Weisler and Clague in Hawaii 71
1.7.3 - Tykot in the Western Mediterranean 72
1.8 - Research Goals for EMPA and Obsidian Sourcing 74
1.9 - Summary and Concluding Remarks 76
Chapter 2: Obsidian in the Near East: State of Knowledge 79
2.1 - Uses of Obsidian in the Near East 86
2.1.1 - Artifacts from the Epipalaeolithic to the Bronze Age 86
2.1.2 - “Utilitarian/Domestic” versus “Ritual/Symbolic/Elite” 90
2.1.3 - Different Function, Different Exchange? 97

2.2 - The Research of Renfrew, Dixon, and Cann (RDC) 98
2.2.1 - The Archaeological Backdrop 98
2.2.2 - Brief Overview of RDC 104
2.3 - Sourced Obsidian from Mesopotamia and the Northern Levant 109
2.3.1 - The Scope of this Compilation 110
2.3.2 - Sourced Obsidian from the Bronze Age 113
2.3.3 - Sourced Obsidian from the Chalcolithic 116
2.3.4 - Sourced Obsidian from the Neolithic 117
2.3.5 - Summarizing the Results 120
2.3.6 - Putting It in Perspective: Advantages of More Data 121
2.4 - The Stagnation of Near East Obsidian Sourcing 126
2.4.1 - Reasons for the Obsidian Sourcing Stagnation 126
2.4.2 - The Effect of Visual Sourcing Approaches 130
2.5 - Other Issues in Near East Obsidian Sourcing 137
2.5.1 - The Numbers of Obsidian Sources 137
2.5.2 - Are Nemrut Dağ and Bingöl A Indistinguishable? 139
2.6 - Issues with Recent Obsidian Sourcing: Tell Hamoukar 146
2.6.1 - Tell Hamoukar: The Tell and Its Southern Extension 148
2.6.2 - Recent Excavations at Tell Hamoukar 149
2.6.3 - Interpretation of Obsidian in the Southern Extension 150
2.6.4 - An Alternative Interpretation 157
2.6.5 - Sourcing Obsidian from Tell Hamoukar 158
2.7 - Summary and Problems 160
Chapter 3: Tell Mozan, Urkesh, and the Hurrians 163
3.1 - Who were the Hurrians? 165
3.2 - Tell Mozan: The Archaeological Site 169
3.3 - The Geographical Setting and Environment 178
3.4 - The Past Environment and Climate 185
3.5 - Urkesh: The Ancient Hurrian City 189
3.6 - The Features and Layout of Tell Mozan 195
3.6.1 - The Temple(s) 196
3.6.2 - The Terrace and Revetment Wall 199
3.6.3 - The Monumental Staircase 203
3.6.4 - The Plaza 205
3.6.5 - The Royal Palace 205
3.6.6 - The *Âbi* 209
3.6.7 - Road to the Netherworld 211
3.6.8 - The Inner City Wall 212
3.6.9 - Features of the Outer City 212
3.6.10 - Features of Later Habitation Phases 213

3.7 - Outstanding Questions about the Hurrians 215
3.8 - Concluding Remarks 219
Part II: Methods for Sourcing and Their Evaluation 220
Chapter 4: The Geological Reference Collection and Artifacts 220
4.1 - Terminology: “Samples” versus “Specimens” 223
4.2 - Numbers of Geological Specimens 224
4.3 - Homogeneity of Obsidian Sources 225
4.4 - What Constitutes a “Source”? 230
4.5 - Obsidian Fieldwork in Oregon 234
4.6 - Fieldwork Lessons and Specimen Nomenclature 252
4.7 - Assembling the Reference Collection 257
4.7.1 - Turkey Obsidian Specimens 257
4.7.2 - Transcaucasian Obsidian Specimens 266
4.7.2.1 - Azerbaijan 267
4.7.2.2 - Georgia 267
4.7.2.3 - Kabardino-Balkaria Republic 268
4.7.2.4 - Armenia 268
4.7.3 - Excluded Obsidian Sources 269
4.7.3.1 - Unknown Sources in Northeastern Turkey? 275
4.7.3.2 - Northwestern Turkey 276
4.7.3.3 - Aegean Sea 278
4.7.3.4 - Mediterranean Sea 279
4.7.3.5 - Carpathian Sources 280
4.7.3.6 - Afghanistan 280
4.7.3.7 - Iran 281
4.7.3.8 - East Africa and Arabian Peninsula 284
4.8 - Selecting Artifacts for Analysis 285
4.9 - Specimen Preparation - Geological Specimens 286
4.9.1 - Specimen Preparation Requirements for EMPA 286
4.9.2 - Use of Petrographic Thin Sections 287
4.9.3 - Preparing Obsidian Specimen Discs 288
4.9.4 - Grinding and Polishing the Specimen Discs 289
4.9.5 - Documenting the Obsidian Specimen Colors 290
4.9.6 - Conductive Coating for the Discs 290
4.10 - Specimen Preparation - Archaeological Artifacts 292
4.10.1 - Artifact Preparation in Prior EMPA Studies 292
4.10.2 - Artifact Preparation in Prior SEM-EDS Studies 294
4.10.3 - Artifact Preparation in the Present Research 297
4.11 - Summary and Concluding Remarks 300

Chapter 5: Redeveloping EMPA for Obsidian Sourcing 302
5.1 - The Basic Principles of EMPA 305
5.1.1 - Atomic Structure and Electron Shells 307
5.1.2 - The Electron Optical System 309
5.1.3 - Interaction Volume and Spatial Resolution 309
5.1.4 - Electron-Specimen Interactions 311
5.1.5 - Attributes of X-rays 311
5.1.6 - Continuous X-rays 312
5.1.7 - Characteristic X-rays 313
5.1.8 - Secondary Electrons 314
5.1.9 - Backscattered Electrons 314
5.1.10 - Energy- and Wavelength-Dispersive Spectrometers 315
5.1.11 - Electron Microscopy 316
5.1.12 - Quantitative Analysis 316
5.1.13 - Errors in the Archaeological Literature 317
5.1.14 - Additional Information 318
5.2 - Choice of Analytical Conditions 318
5.2.1 - Two Sets of Analytical Conditions 320
5.2.2 - Accelerating Voltage 320
5.2.3 - Beam Current 322
5.2.4 - Beam Diameter 324
5.2.5 - Counting Times 327
5.2.6 - Background Measurements 329
5.2.7 - Number of Analyses 332
5.2.8 - Software Modifications 337
5.2.9 - Choice of Calibration Standards 338
5.2.10 - Data Correction Algorithms 340
5.2.11 - Miscellaneous Procedures 343
5.3 - Challenges to Non-Destructive EMPA for Artifacts 344
5.3.1 - Challenge #1: Non-Flat Artifact Surfaces 346
5.3.2 - Challenge #2: Non-Polished Artifact Surfaces 348
5.3.3 - Challenge #3: Surface Hydration of the Artifacts 352
5.3.4 - Challenge #4: Diagenetic Surface Alteration 357
5.3.5 - Summary of the Challenges to Non-Destructive EMPA 362
5.4 - Concluding Remarks 363
Chapter 6: Evaluating the Analytical Procedures and Source Assignment Methods 365
6.1 - What are the Data? 366
6.1.1 - Elements Selected for Analysis 366
6.1.2 - Data Treatment 372

6.2 - Assessing Precision 376
6.2.1 - Defining Precision 377
6.2.2 - Approaches to Precision in Obsidian Sourcing 378
6.2.3 - Theoretical Precision of EMPA 379
6.2.4 - Assessing Precision in the Present Research 379
6.3 - Accuracy 380
6.3.1 - Defining Accuracy 382
6.3.2 - Approaches to Accuracy in Obsidian Sourcing 382
6.3.3 - Theoretical Accuracy of EMPA 383
6.4 - Assessing Accuracy in the Present Research 384
6.4.1 - Analyzing Standard Materials as Unknowns 385
6.4.2 - Continuing the Accuracy Assessment 389
6.5 - Accuracy Assessment: Analytical "Round Robins" 389
6.5.1 - A "Round Robin" of Basalt Glass Analyses 390
6.5.2 - A "Round Robin" of Obsidian Analyses 393
6.5.3 - Strengths and Weakness of "Round Robins" 397
6.6 - Acquiring NAA and XRF Data for Comparison 400
6.6.1 - NAA by the Max Planck Institute 401
6.6.2 - NAA at the MURR Archaeometry Laboratory 402
6.6.3 - EDXRF at the MURR Archaeometry Laboratory 403
6.6.4 - A "Blind Test" with NAA and XRF at MURR 404
6.6.5 - WDXRF at the University of Wisconsin-Eau Claire 404
6.7 - Discussion of the NAA and XRF Data and EMPA Accuracy 406
6.7.1 - NAA-MPI and EMPA Accuracy 406
6.7.2 - WDXRF-UWEC and EMPA Accuracy 414
6.7.3 - EDXRF-/NAA-MURR and EMPA Accuracy 423
6.8 - (Re)Defining Reliability and Validity 435
6.8.1 - Hughes' Reliability and Validity 441
6.8.2 - Reconsidering Reliability 443
6.8.3 - Reconsidering Validity in Sourcing 445
6.8.4 - What Constitutes Validity in Sourcing? 449
6.9 - Source Discrimination and Artifact Assignment 450
6.9.1 - Graphical-Based Discrimination and Sourcing 451
6.9.2 - Multivariate Discrimination and Sourcing 454
6.9.3 - Issues with the Multivariate Approach 455
6.9.4 - A Compromise Approach and Focus on Geochemistry 457
6.9.5 - Two- and Three-Dimensional Scatterplots 458
6.9.6 - Elements for Source Assignment 466
6.9.7 - Euclidean Distance Measures 469
6.9.8 - A Minimalist Approach to Data Transformation 470

6.9.9 - Using Euclidean Distances to Assign Artifacts to Sources 473
6.10 - Assessing Validity with Georgian Artifacts 480
6.11 - Summary and Concluding Remarks 483
Part III: Results and Implications 485
Chapter 7: The Bronze-Age Obsidian Artifacts of Tell Mozan and Their Sources 485
7.1 - An Instance of "Artificial Obsidian" 486
7.2 - Observations on the Obsidian Industry at Tell Mozan 489
7.2.1 - Quantities of Obsidian and Chert Artifacts 490
7.2.2 - Obsidian Quality at Tell Mozan 491
7.2.3 - Obsidian Tool Types at Tell Mozan 492
7.2.4 - Ground Obsidian and Platform Preparation 494
7.2.5 - Evidence for Production Activities On-Site 494
7.3 - Three Findings from the Analytical Results 504
7.3.1 - Distinguishing Nemrut Dağ and Bingöl A 509
7.3.2 - A Discovery about Meydan Dağ and Tendürek Dağ 512
7.3.3 - Muş, Pasinler, and the Potential for Unknown Sources 514
7.4 - The Urkesh Global Record 516
7.5 - Sourced Obsidian of Site Area A 518
7.5.1 - Sourced Obsidian of Unit A1 518
7.5.1.1 - Feature 16 of Unit A1 518
7.5.1.2 - Feature 29 of Unit A1 519
7.5.1.3 - Feature 67 of Unit A1 519
7.5.1.4 - Feature 606 of Unit A1 520
7.5.2 - Sourced Obsidian of Unit A2 520
7.5.3 - Sourced Obsidian of Unit A6 521
7.5.4 - Sourced Obsidian of Unit A7 522
7.5.4.1 - Feature 56 of Unit A7 523
7.5.4.2 - Feature 63 of Unit A7 524
7.5.4.3 - Feature 69 of Unit A7 524
7.5.4.4 - Feature 121 of Unit A7 525
7.5.4.5 - Feature 148 of Unit A7 526
7.5.4.6 - Feature 261 of Unit A7 527
7.5.4.7 - Feature 465 of Unit A7 527
7.5.4.8 - Feature 480 of Unit A7 528
7.5.5 - Sourced Obsidian of Unit A8 528
7.5.6 - Sourced Obsidian of Unit A9 529
7.5.6.1 - Feature 98 of Unit A9 529
7.5.6.2 - Feature 126 of Unit A9 533
7.5.6.3 - Feature 156 of Unit A9 535
7.5.6.4 - Feature 247 of Unit A9 536

7.5.6.5 - Feature 260 of Unit A9 537
7.5.7 - Sourced Obsidian of Unit A10 538
7.5.8 - Sourced Obsidian of Unit A14 542
7.5.8.1 - Feature 29 of Unit A14 543
7.5.8.3 - Feature 42 of Unit A14 544
7.5.8.3 - Feature 42 of Unit A14 544
7.5.8.4 - Feature 193 of Unit A14 545
7.5.8.5 - Feature 250 of Unit A14 546
7.5.9 - Sourced Obsidian of Unit A15 547
7.5.10 - Sourced Obsidian of Unit A16 548
7.5.10.1 - Feature 26 of Unit A16 549
7.5.10.2 - Feature 83 of Unit A16 549
7.5.10.3 - Feature 208 of Unit A16 550
7.5.11 - Sourced Obsidian of Unit A17 550
7.5.12 - Sourced Obsidian of Unit A18 551
7.6 - Sourced Obsidian of Site Area B 556
7.7 - Sourced Obsidian of Site Area J 557
7.7.1 - Sourced Obsidian of Unit J1 558
7.7.1.1 - Feature 3 of Unit J1 558
7.7.1.2 - Feature 20 of Unit J1 559
7.7.1.3 - Feature 131 of Unit J1 560
7.7.1.4 - Feature 151 of Unit J1 560
7.7.2 - Sourced Obsidian of Unit J2 561
7.7.2.1 - Feature 1 of Unit J2 561
7.7.2.2 - Feature 42 of Unit J2 562
7.7.2.3 - Feature 62 of Unit J2 562
7.7.3 - Sourced Obsidian of Unit J3 563
7.7.3.1 - Feature 100 of Unit J3 563
7.7.3.2 - Feature 101 of Unit J3 565
7.7.3.3 - Feature 105 of Unit J3 565
7.8 - Overview of the Results 566
Chapter 8: Implications for Northern Mesopotamia and the Near East 577
8.1 - Findings from Tell Mozan with Broader Implications 580
8.1.1 - Specialized Blade Production across Mesopotamia? 580
8.1.2 - Gratuze's Assumption about Nemrut Dağ and Bingöl 582
8.1.3 - Peralkalinity and the Nemrut Dağ Sources 585
8.2 - Comparative Data from Prior Obsidian Studies 590
8.2.1 - Sourced Obsidian from the Bronze-Age Khabur Triangle 592
8.2.2 - Sourced Obsidian from Bronze-Age Southern Mesopotamia 597
8.2.3 - Sourced Obsidian from the Bronze-Age Upper Euphrates 599

8.2.4 - Sourced Obsidian from the Bronze-Age Northern Levant 599
8.2.5 - Sourced Obsidian from Bronze-Age Western Iran 600
8.2.6 - Sourced Obsidian from the Chalcolithic Khabur Triangle 603
8.2.7 - Sourced Obsidian from Chalcolithic Northern Mespotamia 604
8.2.8 - Sourced Obsidian from the Chalcolithic Northern Levant 606
8.2.9 - Sourced Obsidian from Chalcolithic Southeastern Turkey 606
8.2.10 - Sourced Obsidian from Chalcolithic Western Iran 608
8.2.11 - A Note about Sourced Obsidian from the Neolithic 609
8.2.12 - Sourced Obsidian from the Neolithic Khabur Triangle 609
8.2.13 - Sourced Obsidian from the Neolithic Middle Euphrates 612
8.2.14 - Sourced Obsidian from the Neolithic Northern Levant 620
8.2.15 - Sourced Obsidian from Elsewhere in Neolithic Syria 625
8.2.16 - Sourced Obsidian from in Neolithic Southern Mesopotamia 626
8.2.17 - Conclusions about the Prior Data 629
8.3 - Starting to Address Copeland's Questions 629
8.3.1 - A Note about Approaches to Exchange 632
8.3.2 - What is the Value of Obsidian? 635
8.3.3 - Possible Transportation via Rivers 636
8.3.4 - The Importance of Location 638
8.3.5 - Obsidian Sources and their Landscapes 643
8.4 - Summary and Concluding Remarks 649
Chapter 9: Implications for Urkesh and the Hurrians 650
9.1 - Urkesh and Ancient Exchange Routes 651
9.2 - Observations on the Obsidian Data 657
9.2.1 - Obsidian Sources at Tell Mozan 657
9.2.2 - Central Anatolian Obsidian at Tell Mozan 660
9.2.3 - Obsidian Sources by Time 663
9.2.4 - Obsidian Sources by Site Area 665
9.2.5 - Obsidian Sources by Site Unit 668
9.3 - Other Evidence of Contact and Exchange at Tell Mozan 674
9.3.1 - Exotic Materials and Items at Tell Mozan 677
9.3.2 - A Lead Figurine at Urkesh from Troy? 680
9.3.3 - The Storehouse of the Royal Palace 681
9.3.4 - Influences of the Early Transcaucasian Complex 682
9.3.5 - "Invisible" Exchange in Northern Mesopotamia 684
9.3.6 - Summary of Contact and Exchange Evidence 687
9.4 - The Existence of a Hurrian "Homeland" to the Northeast 687
9.4.1 - Background of the Debate 688
9.4.2 - Formulating a Hypothesis 691
9.4.3 - Comparison to the Obsidian Data 695

9.5 - The Debate about “The King of Urkesh and Nawar” 696
9.5.1 - “Nawar” as Nagar and Tell Brak: Background 697
9.5.2 - “Nawar” as a Northern Hinterland: Background 699
9.6 - Considering “Nawar” as a Northern Hinterland 701
9.6.1 - Obsidian Distribution in Southeastern Anatolia 702
9.6.2 - Bringing the Obsidian to Urkesh 707
9.6.3 - Comparison to the Data 708
9.6.4 - Interpretation of the Results 710
9.7- Considering “Nawar” as Nagar and Tell Brak 711
9.7.1 - Formulating and Testing the Hypothesis 711
9.7.2 - Comparison to the Obsidian Data 715
9.7.3 - Another Similarity of Urkesh and Nagar 718
9.8 - Implications of the Results Regarding “Nawar” 721
9.8.1 - Could Both Locations Be “Nawar”? 721
9.8.2 - Urkesh and Nagar as Gateways or a Gateway/Central-Place Pair 724
9.9 - The Potential Significance of Nemrut Dağ 729
9.9.1 - Identifying the Collection Loci 729
9.9.2 - Access to Nemrut Dağ and Its Obsidians 733
9.9.3 - Inspiration for the Lower Sacral Area? 738
9.10 - Summary and Concluding Remarks 743
Conclusion 747
Works Cited 757
Appendices 818
Appendix A - Obsidian Sources in the Near East 818
A.1 - Central Anatolian Sources 820
A.2 - Eastern Anatolian Sources 824
A.3 - Northeastern Anatolian Sources 828
A.4 - Transcaucasian Sources 830
Appendix B - Obsidian and Chert Blade-Tools from Tell Mozan by Site Unit 833
Appendix C - Electron Microprobe Analysis Data of Specimens and Artifacts 851
Appendix D - Source Assignments based on Euclidean Distances 913

List of Tables

Page	Table
122	Table 2.1 - Previously Sourced Post-Neolithic Mesopotamian Artifacts
270	Table 4.1 - Obsidian Collection Areas
331	Table 5.1 - Spectrometer Conditions for Major and Trace Elements
341	Table 5.2 - Reference Standards for Major-Element Analyses
342	Table 5.3 - Reference Standards for Trace-Element Analyses
381	Table 6.1 - Precision Based on an Obsidian Reference Specimen
386	Table 6.2 - Analyses of an International Obsidian Reference Specimen
388	Table 6.3 - Trace-Element Analyses of Standard Materials
391	Table 6.4a - G-Probe-2 Selected Results for EMPA
392	Table 6.4b - G-Probe-2 Results for LA-ICP-MS
395	Table 6.5a - Inter-comparison of analytical results for the obsidian source at Sierra de Pachuca, Hidalgo, Mexico from Glascock (1999)
396	Table 6.5b - Inter-comparison of analytical results for the obsidian source at Little Glass Buttes, Oregon from Glascock (1999)
398	Table 6.6 - Inter-laboratory comparison of analytical results for the obsidian source at Sierra de Pachuca, Hidalgo, Mexico
407	Table 6.7 - All NAA-MPI Data for Rapp/Ercan-Collected Specimens from Bassette (1994)
408	Table 6.8 - Example Comparisons of the NAA-MPI Data to the EMPA Data
410	Table 6.9 - Transposed CA01 and CA02 Specimens
410	Table 6.10 - Transposed CA16 and CA17 Specimens
411	Table 6.11 - Example of Bassette's (1994) Specimen Numbering Errors
412	Table 6.12 - Example of Bassette's (1994) Specimen Numbering Errors
413	Table 6.13 - Example of Bassette's (1994) Specimen Numbering Errors
422	Table 6.14 - Comparison of EMPA Data and WDXRF-UWEC Data to Published Values for the Kömürcü Source
424	Table 6.15 - Comparison of WDXRF-UWEC, EDXRF-MURR, and EMPA Data for the Trace Elements

425 Table 6.16a - EMPA Data for Mexican Specimens from MURR Compared to MURR's NAA and EDXRF Data

426 Table 6.16b - EMPA Data for Mexican Specimens from MURR Compared to MURR's NAA and EDXRF Data

428 Table 6.17a: Comparison of EMPA, NAA-MURR, and EDXRF-MURR Data for Armenian Obsidian

429 Table 6.17b: Comparison of EMPA, NAA-MURR, and EDXRF-MURR Data for Armenian Obsidian

430 Table 6.17c: Comparison of EMPA, NAA-MURR, and EDXRF-MURR Data for Armenian Obsidian

475 Table 6.18 - Example of Euclidean Distance Measures and Nearest Neighbors for an Artifact Assigned to Nemrut Dağ (EA25)

476 Table 6.19 - Example of Euclidean Distance Measures and Nearest Neighbors for an Artifact Assigned to Nemrut Dağ (EA22)

477 Table 6.20 - Example of Euclidean Distance Measures and Nearest Neighbors for an Artifact Assigned to Bingöl B

478 Table 6.21 - Example of Euclidean Distance Measures and Nearest Neighbors for an Artifact Assigned to Kömürcü at Göllü Dağ

482 Table 6.22 - Example of Euclidean Distance Measures and Nearest Neighbors for a Georgian Test Artifact

515 Table 7.1 - Comparison of "Meydan Dağ" and "Dogubayezid/Tendurek Dağ" Geological Specimens

568 Table 7.2 - Artifact Source Assignments by Unit

571 Table 7.3 - Artifact Source Assignments by Source

574 Table 7.4 - Artifact Source Assignments by Period

852 Table C.1 - Major-Element Analyses of Geological Specimens

890 Table C.2 - Trace-Element Analyses of Geological Specimens

906 Table C.3 - Major-Element Analyses of Artifacts

910 Table C.4 - Trace-Element Analyses of Artifacts

914 Table D.1 - Source Assignments of Artifacts based on Euclidean Distance to Centroids of Geological Specimens

List of Figures

Page	Figure
2	Figure I.1 - A prismatic obsidian blade from Tell Mozan
4	Figure I.2 - Tell Mozan (ancient Urkesh) against the Tur Abdin mountains
5	Figure I.3 - Location of Tell Mozan in northeastern Syria
20	Figure 1.1 - An example of microscopic minerals and bubbles in obsidian
22	Figure 1.2 - Backscattered-electron images of mineral inclusions in obsidian
26	Figure 1.3 - An example of flow banding, one form of obsidian heterogeneity
27	Figure 1.4 - Examples of macroscopic flow banding in obsidian
28	Figure 1.5 - Flow banding in an obsidian specimen from Glass Buttes, Oregon
31	Figure 1.6 - A cross-section of an obsidian-bearing rhyolitic lava dome
33	Figure 1.7 - An obsidian spine protrudes out of the outer shell of a lava dome
34	Figure 1.8 - The inner obsidian shell is exposed on the dome's forward slope
81	Figure 2.1 - RDC's best-known rendering of their proposed obsidian "supply zones" and "contact zones" during the Neolithic Period
82	Figure 2.2 - RDC's "obsidian interaction zones" during the Neolithic
82	Figure 2.3 - RDC's obsidian distribution patterns during the Neolithic
83	Figure 2.4 - RDC's obsidian sourcing results for the post-Neolithic Period
84	Figure 2.5 - RDC's post-Neolithic obsidian distribution patterns
84	Figure 2.6 - RDC's post-Neolithic obsidian distribution patterns
95	Figure 2.7 - Portrait mask of a bearded man from Egypt, circa 180 CE
115	Figure 2.8 - An obsidian vessel from a Chalcolithic tomb at Tepe Gawra in Iraq
151	Figure 2.9 - Roaf's (1990) obsidian map
153	Figure 2.10 - Reichel's (2007) modifications to Roaf's (1990) obsidian map
170	Figure 3.1 - Satellite image of Tell Mozan
173	Figure 3.2 - Topographic map of the High Mound
174	Figure 3.3 - Topographic map of the Outer City
177	Figure 3.4 - The modern village of Mozan lies near the Royal Palace
179	Figure 3.5 - Khabur Triangle features, sites, and modern cities
181	Figure 3.6 - The Tur Abdin mountains lie about 8 km to the north of Tell Mozan

184 Figure 3.7 - Agriculture and pastoralism are still practiced together
192 Figure 3.8 - One of two lions that served as foundation pegs for the Urkesh temple
198 Figure 3.9 - A partial reconstruction of the temple
198 Figure 3.10 - A square of Unit J3, excavated down to the temple terrace surface
202 Figure 3.11 - The monumental staircase to the temple terrace
202 Figure 3.12 - The revetment wall of the temple terrace
206 Figure 3.13 - Excavations in Area A and the remains of the Royal Palace
235 Figure 4.1 - Nemrut Dağ in Eastern Anatolia from space
236 Figure 4.2 - Nemrut Dağ in Eastern Anatolia from space
239 Figure 4.3 - Nemrut Dağ and its analogue, Newberry Volcano, in central Oregon
240 Figure 4.4 - The caldera of Newberry Volcano as viewed from the caldera rim
242 Figure 4.5 - Göllü Dağ and its analogue, Glass Buttes, in central Oregon
243 Figures 4.6 a and b - The Göllü Dağ-Kömürcü source
244 Figures 4.7 a and b - The Glass Buttes, Oregon source area
247 Figure 4.8 - The “otherworldly” surfaces of a rhyolitic lava dome
258 Figure 4.9 - Field notes by Rapp and Ercan when collecting obsidian at Göllü Dağ
259 Figure 4.10 - Collection areas of Rapp and Ercan at Göllü Dağ and Nenezi Dağ
261 Figure 4.11 - Field notes by Rapp and Ercan when collecting obsidian at Acıgöl
262 Figure 4.12 - Collection areas of Rapp and Ercan at Acıgöl
264 Figure 4.13 - Map of obsidian sources in Central and Eastern Anatolia
291 Figure 4.14 - Geological reference specimens from EA24 prepared for EMPA
306 Figure 5.1 - Schematic of an electron microprobe and its primary systems
310 Figure 5.2 - A backscattered-electron image of obsidian with spot analyses
335 Figure 5.3 - The measured values will approximate a Gaussian distribution
339 Figure 5.4 - For trace elements, the distribution often includes negative values
345 Figure 5.5 - Obsidian can be non-destructively analyzed in an electron microprobe
361 Figure 5.6 - Surface alteration of obsidian artifacts from Anovitz et al. (1999)
415 Figure 6.1a and b - UWEC-WDXRF Data vs EMPA Data for the Major Elements
416 Figure 6.1c and d - UWEC-WDXRF Data vs EMPA Data for the Major Elements
417 Figure 6.1e and f - UWEC-WDXRF Data vs EMPA Data for the Major Elements

418 Figure 6.1g and h - UWEC-WDXRF Data vs EMPA Data for the Major Elements
419 Figure 6.1i and j - UWEC-WDXRF Data vs EMPA Data for the Major Elements
431 Figure 6.2a and b - EDXRF-MURR Data vs EMPA Data
432 Figure 6.2c and d - EDXRF-MURR Data vs EMPA Data
433 Figure 6.2e and f - EDXRF-MURR Data vs EMPA Data
434 Figure 6.3 - BSE image and element maps of a specimen reveal ilmenite
436 Figures 6.4a and b - NAA-MURR Data vs EMPA Data
437 Figures 6.4c and d - NAA-MURR Data vs EMPA Data
438 Figures 6.4e and f - NAA-MURR Data vs EMPA Data
439 Figures 6.4g and h - NAA-MURR Data vs EMPA Data
440 Figures 6.4i and j - NAA-MURR Data vs EMPA Data
459 Figure 6.5 - EMPA data for all obsidian specimens
460 Figure 6.6 - EMPA data for all obsidian specimens
461 Figure 6.7 - EMPA data for all obsidian specimens
462 Figure 6.8 - EMPA data for all obsidian specimens
463 Figure 6.9 - EMPA data for all obsidian specimens
464 Figure 6.10 - EMPA data for all obsidian specimens
465 Figure 6.11 - Nemrut Dağ specimens clearly separated from Bingöl A specimens
488 Figure 7.1 - An unfinished third-millennium Mesopotamian obsidian vessel
488 Figure 7.2 - MgO versus K_2O for ancient glasses from Henderson (2000)
493 Figure 7.3 - Examples of flow bands in artifacts from Area A, the palace complex
493 Figure 7.4 - Examples of artifacts containing mineral inclusions that cause pits
493 Figure 7.5 - Examples of artifacts made of “mottled” obsidian
495 Figure 7.6a - Examples of obsidian blade-tools from Tell Mozan
496 Figure 7.6b - Examples of obsidian blade-tools from Tell Mozan
497 Figure 7.6c - Examples of obsidian blade-tools from Tell Mozan
498 Figure 7.7a - Examples from Tell Mozan of obsidian flake-tools
499 Figure 7.7b - Examples from Tell Mozan of obsidian flake-tools
500 Figure 7.8 - Examples of obsidian trapezes
500 Figure 7.9 - Example of lunates from obsidian blades

500 Figure 7.10 - Examples of notches on blades
500 Figure 7.11 - An obsidian tabular scraper circa about 2200 BCE
501 Figure 7.12 - Examples of a tanged obsidian point and a winged obsidian point
501 Figure 7.13 - Examples of transverse points or end scrapers
501 Figure 7.14 - Examples of likely obsidian borers
501 Figure 7.15 - Examples of obsidian drills or awls
502 Figure 7.16 - Possible fragments of obsidian vessels
502 Figure 7.17 - A prismatic blade with its dorsal surfaces subsequently ground flat
502 Figure 7.18 - A ground and polished obsidian artifact
502 Figure 7.19 - Other obsidian artifacts with evidence of ground surfaces
503 Figure 7.20 - Examples of flakes from Tell Mozan with ground flat platforms
503 Figure 7.21 - A chert nodule from Tell Mozan with a surface ground flat
505 Figure 7.22 - Loose angular and subangular blocks of obsidian
505 Figure 7.23 - Examples from Tell Mozan of decortification flakes
506 Figure 7.24 - Obsidian can fracture into blocks along weak, porous layers
506 Figure 7.25 - Examples from Tell Mozan of flakes with flat, rough surfaces
507 Figure 7.26 - Examples of obsidian blade and flake cores
507 Figure 7.27 - An obsidian blade core
508 Figure 7.28 - Examples from Tell Mozan of probable early-series blades
510 Figure 7.29 - Using trace elements, there appears to be two or three Nemrut Dağ geochemical clusters, one of which overlaps with the Bingöl A cluster
511 Figure 7.30 - Six geochemical clusters are revealed among the Nemrut Dağ specimens, all of which are clearly distinguished from Bingöl A
564 Figure 7.31 - The author excavating Feature 100 of Unit J3, from which one of the obsidian artifacts sourced in this study was recovered
567 Figure 7.32 - Source assignments for the obsidian artifacts from Tell Mozan
587 Figure 8.1 - CNK/A versus NK/A plot of Bingöl A and Nemrut Dağ obsidians
589 Figure 8.2 - CNK/A versus NK/A plot of Bingöl A and Nemrut Dağ obsidians
595 Figure 8.3 - Obsidian from Bronze-Age Sites in the Khabur Triangle
596 Figure 8.4 - Obsidians at Five Bronze-Age Sites in the Khabur Triangle
598 Figure 8.5 - Obsidian from Bronze-Age Sites in Southern Mesopotamia

602 Figure 8.6 - Obsidian from Bronze-Age Sites in the Western Iran
605 Figure 8.7 - Obsidian from Chalcolithic Sites in the Khabur Triangle
607 Figure 8.8 - Obsidian Sources in the Bronze Age and Chacolithic Northern Levant
611 Figure 8.9 - Obsidian at Late-Neolithic Khabur-Triangle Sites - West to East
613 Figure 8.10 - Obsidian at Late-Neolithic Khabur-Triangle Sites - West to East
614 Figure 8.11 - Sources at Neolithic Middle-Euphrates Sites - North to South
616 Figure 8.12 - Sources at Neolithic Middle-Euphrates Sites - By Time
618 Figure 8.13 - Sources at Neolithic Middle-Euphrates Sites - North to South
619 Figure 8.14 - Compiled Sources at Neolithic Middle-Euphrates Sites
621 Figure 8.15 - Sources at Neolithic Upper- and Middle-Euphrates Sites
624 Figure 8.16 - Obsidian Sources in the Neolithic Northern Levant - North to South
627 Figure 8.17 - Obsidian Sources at Various Neolithic Sites in Syria
630 Figure 8.18 - Obsidian Sources at Neolithic Sites in Iraq - North to South
631 Figure 8.19 - Obsidian Sources at Neolithic Sites in Iraq
647 Figure 8.20 - The chaotic surface of a lava dome
652 Figure 9.1 - Urkesh at the crossroads of N-S and E-W transportation routes
654 Figure 9.2 - The Mardin mountain pass viewed from the ruins of the Royal Palace
655 Figure 9.3 - Major transportation routes reconstructed from Roman itineraries
656 Figure 9.4 - Major routes across Northern Mesopotamia in the Classical Period
658 Figure 9.5 - Source assignments for obsidian artifacts from Tell Mozan
661 Figure 9.6 - Number of Sourced Artifacts vs Number of Sources Identified
664 Figure 9.7 - Source Assignments by Time Period
666 Figure 9.8 - Source Assignments by Site Area
667 Figure 9.9 - Obsidian sources in three different site areas superimposed on a map
669 Figure 9.10 - Source Assignments by Site Unit
670 Figure 9.11 - Obsidian sources by unit in Areas J and B
671 Figure 9.12 - Obsidian sources by unit in Area A
672 Figure 9.13 - Obsidian sources by unit in Area A
673 Figure 9.14 - Obsidian sources by unit in Area A
675 Figure 9.15 - Source Assignments by Feature in Unit A9

676 Figure 9.16 - Source Assignments in Unit A9 by Stratigraphy
678 Figure 9.17 - A stone necklace with a large bead of lapis lazuli
678 Figure 9.18 - An example of a bronze dagger from Unit A16
704 Figure 9.19 - Migration routes of nomadic tribes across southeastern Turkey
706 Figure 9.20 - Modern-day pastoralism in the Khabur Triangle of Syria
713 Figure 9.21 - Obsidian Sources at Khabur Triangle Sites during the Bronze Age
714 Figure 9.22 - Obsidian Sources at Bronze Age and Chacolithic Khabur Sites
717 Figure 9.23 - Comparison of Obsidian Sources at Tell Mozan and Tell Hamoukar
719 Figure 9.24 - Comparison of Obsidian Sources at Tell Mozan and Tell Brak
730 Figure 9.25 - Nemrut Dağ, the Taurus Mountains, and the Tur Abdin highlands
731 Figure 9.26 - Obsidian-bearing flows of Nemrut Dağ sampled by Rapp and Ercan
734 Figures 9.27a and b - Atop a lava dome
735 Figures 9.28a and b - High-quality obsidian from the inner shell of a lava dome may be accessible on its forward talus slope
741 Figure 9.29 - The stone-lined necromantic pit, the *âbi*
742 Figure 9.30 - A view of the Nemrut Dağ caldera as seen from the east
833 Figure B.1 - Examples of obsidian blade-tools (blades, segments, etc.) from A1
833 Figure B.2 - Examples of obsidian blade-tools (blades, segments, etc.) from A2
834 Figure B.3 - Examples of obsidian blade-tools (blades, segments, etc.) from A5
834 Figure B.4 - Examples of obsidian blade-tools (blades, segments, etc.) from A6
835 Figure B.5 - Obsidian artifacts recovered together from a single feature
836 Figure B.6 - Examples of obsidian blade-tools (blades, segments, etc.) from A7
837 Figure B.7 - Examples of obsidian blade-tools (blades, segments, etc.) from A8
837 Figure B.8 - Examples of obsidian blade-tools (blades, segments, etc.) from A9
838 Figure B.9 - Examples of obsidian blade-tools (blades, segments, etc.) from A10
839 Figure B.10 - Examples of obsidian blade-tools (blades, segments, etc.) from A11
839 Figure B.11 - Examples of obsidian blade-tools (blades, segments, etc.) from A12
840 Figure B.12 - Examples of obsidian blade-tools (blades, segments, etc.) from A13
840 Figure B.13 - Examples of obsidian blade-tools (blades, segments, etc.) from A14
841 Figure B.14 - Examples of obsidian blade-tools (blades, segments, etc.) from A15

841 Figure B.15 - Examples of obsidian blade-tools (blades, segments, etc.) from A16
842 Figure B.16 - Examples of obsidian blade-tools (blades, segments, etc.) from A17
842 Figure B.17 - Examples of obsidian blade-tools (blades, segments, etc.) from A18
843 Figure B.18 - Examples of obsidian blade-tools (blades, segments, etc.) from B1
843 Figure B.19 - Examples of obsidian blade-tools (blades, segments, etc.) from B2
843 Figure B.20 - Obsidian blades from B3 and B5
844 Figure B.21 - Examples of obsidian blade-tools (blades, segments, etc.) from B4
845 Figure B.22 - Obsidian artifacts recovered together from one feature in Unit B1
845 Figure B.23 - Obsidian artifacts recovered together from one feature in Unit B1
846 Figure B.24 - Examples of obsidian blade-tools (blades, segments, etc.) from J1
846 Figure B.25 - Examples of obsidian blade-tools (blades, segments, etc.) from J3
847 Figure B.26 - Examples of obsidian blade-tools (blades, segments, etc.) from J2
848 Figure B.27 - Examples of chert blades from Unit A7
849 Figure B.28 - Examples of chert blades from Unit A9
849 Figure B.29 - Examples of chert blades from Unit A10
850 Figure B.30 - Examples of chert blades from Unit A14
850 Figure B.31 - Chert blades and a flake from Unit A2

Introduction

Known for its use and distribution during the Neolithic Period, obsidian continued to be used to fashion flaked-stone tools during the Bronze Age in Northern Mesopotamia. Its use was not displaced by copper and its alloys for millennia. In fact, in a few parts of the world, modern use of obsidian scrapers to process animal hides has been documented ethnographically (e.g., Gallagher 1974, 1977; Takase 2004), seven millennia after the rise of metallurgy. Obsidian and metals -- bronze, for example -- have quite different material properties and, thus, performance characteristics. Consequently, obsidian and bronze are best suited to different applications (see Kingery [1996:175-203] for a discussion of what he calls the "materials science paradigm" and its application to archaeology and material culture). Even when employed for similar tasks, there are important differences between obsidian and bronze tools -- for example, the process (including Mauss' body techniques) of butchering an animal will differ using obsidian and bronze blades. From raw-material acquisition to symbolism, these two materials differed. Nevertheless, the significance of obsidian artifacts during the Bronze Age is frequently overlooked.

Similarly, it is thought that obsidian sourcing cannot offer new information during a period in which there is a variety of artifacts, *objets d'art*, and texts to study. Obsidian, however, is an unparalleled in its widespread use and ability to be sourced, so it can offer unique information about contact, exchange, and migration. Its sourcing can complement other sources of information and be used to test hypotheses based on them. For example,

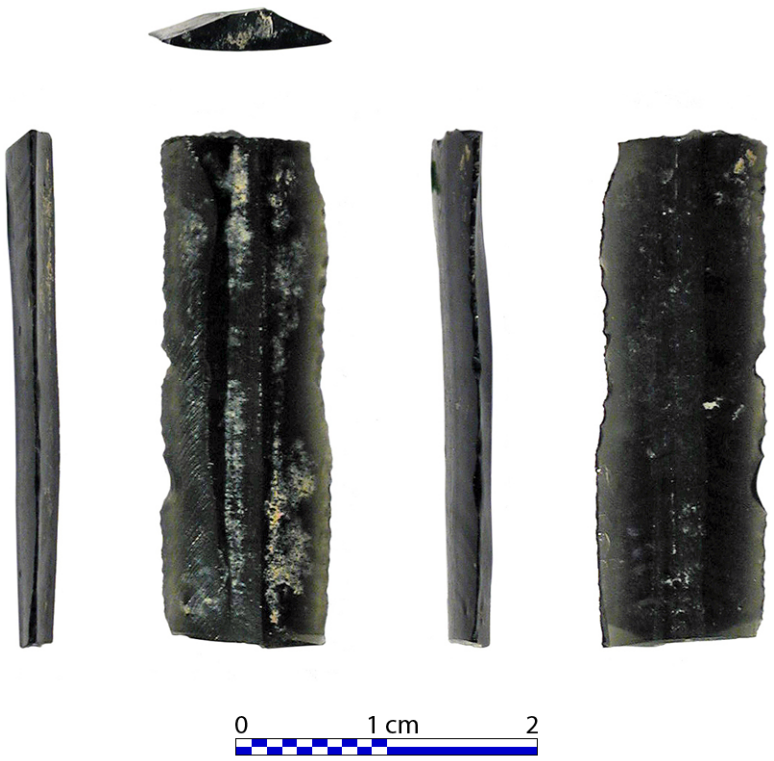


Figure I.1 - A prismatic obsidian blade from Tell Mozan, specifically Unit A12, which includes a monumental sacrificial pit called an *âbi*. This blade may have been used to slaughter juvenile suids and canids in a Hurrian religious ritual known from texts, as discussed in Section 3.6.6. Shown approximately twice its actual size.

before the recent work at Tell Mozan in northeastern Syria, most of the information about the ancient Hurrians was derived from linguistic and textual evidence. Obsidian sourcing can be used to test some of these debated inferences. It is rarely utilized, though, after the Neolithic Period in Near Eastern archaeology. Instead, the Neolithic obsidian distribution patterns, as surmised by Colin Renfrew with colleagues John Dixon and Joseph Cann, are often mistakenly presumed to apply to post-Neolithic contexts.

For the research at hand, I sourced 97 obsidian artifacts from Tell Mozan, the site of ancient Urkesh, the capital of a regional Hurrian city-state during the third and second millennia BCE. To chemically analyze these Hurrian artifacts non-destructively and with high precision, I decided to redevelop electron microprobe analysis (EMPA) for obsidian sourcing. While EMPA is common in the geosciences, it is seldom used for archaeology, including obsidian sourcing. The best known study to use EMPA for obsidian sourcing is that of Merrick and Brown (1984) in East Africa. These two researchers, though, used an instrument so old that it output data onto punch cards. Their results are not demonstrative of what modern EMPA could do for obsidian sourcing today.

My goals were three-fold. First, I sought to demonstrate a sophisticated approach to obsidian sourcing in the Near East, a region where such research has fallen behind that in the New Word. For example, I used, to my knowledge, the largest geological reference collection of Near Eastern obsidians ($n > 900$), and I analyzed a large number of artifacts from Tell Mozan ($n = 98$). I included dozens of obsidian sources in the region, not just a few sources from decades-old research. The chemical similarity of two important sources (i.e., Nemrut Dağ and Bingöl A) is well documented in the literature. Rather than simply ignoring this issue, I selected an analytical technique (i.e., EMPA) that could, if critically used, discern these sources. I also took an approach that treats obsidian as a mixture and considers its major geochemical varieties. Lastly, I appreciate the differences in sources' geology and landscapes, and I consider the probable mechanisms, based on the available archaeological and ethnographic evidence, for obsidian distribution.



Figure I.2 - Tell Mozan (ancient Urkesh, Khabur Triangle, northeastern Syria) against the Tur Abdin mountains, about 8 km to the north, as viewed from the south (photograph by Professor Giorgio Buccellati, Co-Director of the Urkesh Expedition).



Figure I.3 - Location of Tell Mozan in northeastern Syria (original map by GeoAtlas; used here under license to the author).

Second, I sought to develop EMPA for obsidian sourcing, taking advantage of the advancements since earlier studies. As previously mentioned, Merrick and Brown (1984) used an electron microprobe that output its data on punch cards. A contemporary electron microprobe does not have much in common with the instrument they used. Additionally, all of the previous studies involved removing pieces from the artifacts and then polishing them. I, on the other hand, used EMPA non-destructively for the archaeological artifacts, and I chose elements with concentrations that varied over five orders of magnitude. The precision, accuracy, reliability, and validity of my techniques and data were also assessed. When appropriate, I discuss the role of choice in my EMPA and data-analysis techniques. Indeed, doing an analysis involves a series of choices: one starts with an initial analytical scheme in mind, feedback from observations changes the scheme, the new scheme yields feedback, and so on. These actions form an operational sequence and are informed by the theoretical and practical "know how" of a researcher (or *connaissances* and *savoir-faire*, respectively, in the terminology of Pierre Lemonnier). Therefore, it is valid to discuss my analytical choices in the context of anthropological research.

Third, based on Goals #1 and #2, I determined the sources of obsidian used during the Bronze Age at Tell Mozan in northeastern Syria. In addition to considering the spatial and temporal patterns of obsidian sources represented at the site, I used my source data to address two outstanding issues regarding Urkesh and its Hurrian inhabitants. In addition, my findings have broader implications for obsidian use in the Bronze-Age Near East and debunk a few prevalent assumptions in the archaeological literature.

This dissertation is comprised of three parts of three chapters each. Part I is called "Foundations and Problems," and it consists of Chapters 1 through 3. In Chapter 1, I first discuss why obsidian is a central component of archaeological research around the world. I also cover the characteristics, origins, and geochemistry of obsidian. The fundamentals of obsidian sourcing are discussed, as are the most commonly used analytical techniques. Before discussing the use of EMPA to source obsidian, I consider the lessons that should be learned from sourcing studies of ceramics. This chapter concludes with my analytical goals while my archaeological goals are covered in the next chapters.

Chapter 2 largely involves the current state of obsidian sourcing in the Near East, but the roots, especially the work of Colin Renfrew and his colleagues, are also explored. Their work still represents the largest regional-scale obsidian-sourcing study in the Near East, and it rests entirely on a total of 160 artifacts from 53 sites spanning five millennia. Hence, each site is represented, on average, by a mere three artifacts. By comparison, the largest regional-scale study in the New World involved over 9000 obsidian artifacts from more than 130 sites. There is, in comparison to the New World, a severe lack of raw data (i.e., sourced obsidian artifacts) in the Near East, especially from post-Neolithic contexts in Mesopotamia. Thus, a number of issues, most dating back four decades, are still found in the literature. Recent work at another site in northeastern Syria, one widely publicized as an obsidian production center, highlight several of these problems.

Chapter 3 covers the archaeological site of Tell Mozan and its surroundings, what is known about the ancient city of Urkesh, and the site's ancient inhabitants, the Hurrians.

The major archaeological features of this site are discussed because, in Chapter 7, I relate the sourced obsidian artifacts to these features. The landscape of Tell Mozan is important when considering its exchange links to other areas. Lastly, I introduce outstanding issues regarding the Hurrians that I address with my obsidian source data.

Part II is called "Methods for Sourcing and Their Evaluation," and it is comprised of Chapters 4 through 6. Chapter 4 is focused on assembling my reference collection of more than 900 geological obsidian specimens. Unfortunately, most sourcing research in the Near East, including quite recent work, the involves analysis of only a few specimens from just four or five sources, leading to somewhat ambiguous results. I also discuss how I conceptualized my reference collection, including what constitutes an obsidian "source" and how fieldwork may shape such definitions. Debates in obsidian sourcing, such as the appropriate number of specimens and the homogeneity of obsidian flows, are considered as well. I also document how both the geological specimens and artifacts were prepared for analysis. Another issue included here, but usually omitted in other sourcing studies, is my selection criteria for the artifacts analyzed for this research.

Chapter 5 focuses on my goal to redevelop modern EMPA for obsidian sourcing. For the previously mentioned reasons, I do not relegate the information in this chapter to an appendix. I discuss the three principal studies that utilized EMPA to source obsidian: Merrick and Brown in Kenya (1984), Weisler and Clague in Hawaii (1998), and Tykot in the Mediterranean (1995). Besides using data output on punch cards, Merrick and Brown (1984) placed a priority on speed (and titled the article "Rapid Chemical Characterization

of Obsidian Artifacts by Electron Microprobe Analysis"). My first concerns, on the other hand, were accuracy and precision, and my choices reflect those priorities. Tykot had the largest study of the three: he measured 9 to 11 elements, as of 1995, in 433 total analyses on 125 specimens. For comparison, my work here involves about 12,000 major-element analyses and 13,000 trace-element analyses on over 900 geological specimens and over 100 artifacts, each of which was quantitatively analyzed for a total of 20 major and trace elements. The chapter also covers the four main challenges I faced in analyzing obsidian artifacts non-destructively and how I mitigated each of them.

Chapter 6 covers the evaluation of my EMPA data and data-analysis ("statistical") techniques. The four main concepts of assessment -- precision, accuracy, reliability, and validity -- serve as the framework. A review of the literature on assessment theory shows that Hughes (1998) and Nazaroff et al. (2010), the only two earlier obsidian studies to use all four concepts, formulated them somewhat atypically. Thus, I have also endeavored to strengthen their application to obsidian sourcing. I also cover issues of element selection, data treatment, and procedures for ascribing artifacts to sources. I established the validity of my data and procedures using artifacts from Chikiani in Georgia, and all eight artifacts were assigned to that source, suggesting my results are valid.

Part III is "Results and Implications," and it is comprised of Chapters 7 through 9. In Chapter 7, I present the source assignments for the obsidian artifacts from Tell Mozan, and when the information is available, I discuss the stratigraphic contexts of the artifacts. I also document the obsidian artifacts recovered with the ones that I sourced. In addition,

I provide statistics about the prevalence of obsidian and chert flaked-stone artifacts at Tell Mozan, and I offer an initial assessment of the tool types present as well as the likelihood of obsidian-tool production on-site. First, though, I discuss an artifact that I analyzed and concluded is a fragment of "artificial obsidian," as described in texts.

In Chapter 8, I consider the broader implication of my results for obsidian use and distribution in Northern Mesopotamia during the Bronze Age. I also compile the existing obsidian data for Mesopotamian sites; however, I dispense with distribution maps, which are of questionable utility, and instead plot the abundance of obsidian sources represented at each site. The resulting plots show more complex structure than the maps, highlighting the need for much more raw data (i.e., sourced artifacts). By adding textual evidence and ethnographic accounts to the available, but meager, sourcing data, we can start to develop hypotheses of how and why people brought obsidian into Mesopotamia. One implication of my results, though, is that we cannot assume that maximal efficiency was an important factor in source selection. Finally, based on ethnographic and archaeological evidence, I speculate on influences on the use and exchange of Nemrut Dağ obsidians, like culturally based symbolism and "arbitrary" factors like impressive views.

Finally, in Chapter 9, I discuss the implications of my sourcing results for Urkesh and its Hurrian inhabitants. Tell Mozan, situated at the crossroads of east-west and north-south routes, is an ideal location to investigate Bronze-Age obsidian use and distribution in Northern Mesopotamia. In particular, the site lies at the southern outlet of the Mardin Pass into the Tur Abdin foothills, giving us reason to suspect that Urkesh may have been

the equivalent of Burghardt's "gateway city." A large number of sources are represented among the artifacts at Tell Mozan, and this pattern is atypical for contemporaneous cities in the Khabur Triangle. When the source data are examined stratigraphically and by site unit, the palace courtyards seem to have the greatest variety of obsidians. The hypothesis of a Hurrian "homeland" as far northeast as Armenia (or beyond) is considered -- but not supported -- in light of my results. The obsidian data for Tell Mozan and Tell Brak, when compared, suggest a link between to these cities. It may have been that these settlements functioned as "gateway cities" or as a gateway-city/central-place pair. Finally, I consider the potential significance and symbolism of Nemrut Dağ, obsidians from which occur in each site area and for all time periods studied at Tell Mozan.

A final Conclusion section is found after Chapter 9, summarizing my findings and how I achieved the goals set forth here. The appendices follow and include a geological-based discussion of the obsidian sources in Anatolia and the Transcaucasus, photographs of additional obsidian and chert blade-tools from Tell Mozan, and the mean values of my EMPA data for each geological obsidian specimen and artifact.

Part I: Foundations and Problems

Chapter 1:

Obsidian: Its Origins, Sourcing, and Issues

> At the head of the skeletons were two large vases of terra cotta, with covers of the same material. In one of these was a large collection of Indian ornaments, beads, stones, and two carved shells. . . The other vase was filled nearly to the top with arrow-heads, not of flint, but of obsidian; and as there are no volcanoes in Yucatan from which obsidian can be produced, the discovery of these proves intercourse with the volcanic regions of Mexico.
>
> -- John Lloyd Stephens, 1843, *Incidents of Travel in Yucatan*

The above account by American explorer and diplomat John Lloyd Stephens, who was appointed Special Ambassador to Central America by President Martin Van Buren, is among the first published observations of ancient trade evidenced by obsidian discovered far from its geological source. Stephens did not measure any physical properties of these artifacts or conduct chemical analyses. Instead, he observed that obsidian was not native to the vicinity and concluded that the material, either in its raw form or as finished points, must have been transported by people from volcanic areas to this resting place.

In this chapter, I first discuss the reasons why obsidian is a central component of archaeological research around the world. The material properties that make obsidian so desirable for flaked-stone tools is the next topic. I then discuss a common misconception regarding obsidian (i.e., it is completely glass) and consider the implications of the reality

(i.e., it is a mixture of glass and a variety of different mineral inclusions). A few concepts in obsidian geochemistry are introduced, and then I discuss the fundamentals of sourcing studies. I briefly cover the common analytical techniques used for obsidian sourcing, and before discussing the use of electron microprobe analysis to source obsidian, I explain the lessons that have been (or should have been) learned from ceramic sourcing studies. The chapter concludes with my analytical goals for this research, whereas my archaeological goals for the study at hand are discussed in Chapters 2 and 3.

1.1 - Why All the Interest in Obsidian?

Anthropologically obsidian is of interest because it has been used to fashion tools for almost all of human history. Excavations at Olduvai Gorge in Tanzania revealed two obsidian pieces among the *Homo habilis* artifacts in a level dated to between 1.7 and 1.9 million years ago (Leakey 1971:89, 92). Obsidian artifacts have also been discovered at Lower Paleolithic archaeological sites, associated with *Homo ergaster* and *Homo erectus*, within the Awash Valley of Ethiopia. In fact, it comprises nearly a third of one Oldowan lithic assemblage in this valley (Gombore I, level B2) and over half of another (Garba IV, level D) (Piperno et al. 2009:126). The use of obsidian may eventually be shown to date back to hominins' earliest stone tools, circa 2.6 million years ago.

On the other end of the human timeline, obsidian has also been utilized for flaked stone tools in modern times, at least seven millennia after the development of metallurgy. For example, manufacture and use of obsidian scrapers to process animal hides has been

ethnographically documented in Siberia on the Kamchatka Peninsula (Takase 2004) and Ethiopia (Gallagher 1974, 1977; Clark and Kurashina 1981; Brandt and Weedman 1997, 2002; Brandt et al. 1996; Weedman 2005; Weedman Arthur 2008). Obsidian blades have even been used as scalpels in modern surgeries (Buck 1982; Scott and Scott 1982; Sheets 1989; Lynch and Wolfe 1997). In fact, as of this writing, obsidian surgical scalpels may be ordered from Fine Science Tools (although they are not approved for human use). The use of flaked obsidian tools, therefore, spans two million years.

Obsidian has also been used on every continent inhabited by people. In the New World, obsidian use has been studied from northern Alaska and the Aleutian Islands (e.g., Wheeler and Clark 1977, Nicolaysen 2009, Rasic et al. 2009) to Patagonia, the southern region of South America (e.g., Vásquez et al. 2001, Seelenfreund et al. 2002, Stern 2002) and everywhere in between, especially Mesoamerica (e.g., Heizer et al. 1965, Hammond 1972, Sidyrs 1976, Zeitlin 1982) and the American Northwest (e.g., Ambroz et al. 2001, Dillian 2004, Silliman 2005), Southwest (e.g., Shackley 1988, 2005), and Midwest (e.g., Gordus et al. 1968, Griffin et al. 1969, Hatch et al. 1990, Hughes 1992).

Obsidian use was also abundant throughout the Old World: Eastern Europe (e.g., Thorpe et al. 1984, Constantinescu et al. 2002, Rosania et al. 2008); the East African Rift (e.g., Merrick and Brown 1984, 1994; Vogel et al. 2006; Negash et al. 2006) and southern Arabia (e.g., Zarins 1990, Khalidi 2009, Khalidi et al. 2009); Southeast Asia (e.g., Kim et al. 2007; Neri 2007, 2009; Ambrose et al. 2009); the Russian Far East (e.g., Kuzmin et al. 1999, Kuzmin 2006, Phillips and Speakman 2009) and Japan (e.g., Kuzmin and Glascock

2007, Izuho and Sato 2007); Oceania (e.g., Summerhayes et al. 1998, Sand and Sheppard 2000, Torrence 2004, Carter et al. 2009, Torrence et al. 2009); the Mediterranean and the Aegean Seas (e.g., Francaviglia 1984, Tykot 1995, Acquafredda et al. 1999, Bellot-Gurlet et al. 2004); and, of course, Southwest Asia, that is, the Near East.

The study of obsidian is also a core component of much anthropological research because of its multiple uses and contexts. Its use for flaked-stone tools, especially blades and points, occurred around the world (e.g., Mortensen 1973, Lewenstein 1981, Nishiaki 1990, Hirth and Andrews 2002). Obsidian was also used to manufacture carved, ground, and polished artifacts: beads (e.g., Charlton 1993), mirrors like those found at Çatalhöyük (e.g., Vedder 2005), statues (e.g., Wainwright 1927), vessels (e.g., Bevan 2007), cylinder seals (e.g., Gorelick and Gwinnett 1990), and similar objects. Ethnographic research and historical accounts, particularly in the New World, have demonstrated the symbolism and other cultural meanings ascribed to obsidian (Heyden 1988, Saunders 2001, Dillian 2007, Hodgson 2007), showing the value of obsidian beyond its utilitarian applications. Carter (2007) has discussed the "theatricality" of long obsidian blades made for consumption in funerary rituals of the Bronze-Age Cycladic culture of the Aegean area. Jacques Cauvin (1998) and Coqueugniot (1998) consider obsidian symbolism in the Near East. The latter author, in particular, considers texts from ancient Mesopotamia to the Roman Empire and discusses its uses for magic and rituals. Hence, obsidian artifacts may be studied in many contexts, from utilitarian to ritual, from technology to performance.

1.2 - What is Obsidian, and How is it Formed?

Richard E. Hughes, the director of Geochemical Research Laboratory, and Robert L. Smith, a researcher at the U.S. Geological Survey, contend in "Archaeology, Geology, and Geochemistry in Obsidian Provenance Studies" that sourcing "may be compromised by a lack of knowledge about the genesis of obsidians" (1993:79). In his book *Obsidian: Geology and Archaeology in the North American Southwest*, Shackley (2005) asserts that "it is simply not enough to use source provenance data... without a basic understanding of the physical processes that create that material" (7). Therefore, in the following sections, I discuss the properties and formation of obsidian, particularly those characteristics most relevant to this sourcing research. Readers interested in further detail about obsidian and its formation are forwarded to the publications cited above.

1.2.1 - Obsidian as Natural Glass

Obsidian is one type of naturally occurring glass. It is formed under a certain set of conditions by some volcanic eruptions. In particular, obsidian forms when magma cools quickly, before macroscopic minerals can grow in the molten rock. The result is a glassy mass with no overall crystalline structure. Like artificial glass, obsidian is smooth, hard (about 6-7 on the Mohs hardness scale), brittle, and extremely sharp when fractured. In fact, a fresh flake of obsidian has an edge thinner and sharper than a steel surgical scalpel, a mere 3 nanometers thick (Buck 1982:266, Figure 3). Perfect glass, whether artificial or natural, is isotropic, meaning that it is uniform in all directions. Glass is also amorphous,

possessing no ordered, repeating structure of its atoms. When glass is fractured, there are no planes of separation to deviate a crack from its propagation path.

This combination of material properties means that obsidian, when it is struck by a hammerstone or other implement, experiences conchoidal fracture, readily yielding sharp flakes in a manner predictable. Ancient people worldwide realized that these traits make obsidian ideal for fashioning flaked (i.e., knapped) stone tools. Those readers interested in the details about stone-tool features and production are forwarded to Whittaker (1994) and Andrefsky (1998). The same characteristics lend obsidian to grinding and polishing as well, so it was also prized for ground stone objects. Because it was desirable but rare, obsidian was moved and exchanged across hundreds, even thousands, of kilometers in the Americas, Oceania, Africa, the Mediterranean, and the Near East.

Obsidian is an "extrusive" volcanic (or igneous) rock. This means that the magma extrudes, or pushes out onto, or near, the surface of the Earth, and particular types of rock are created at those pressures and temperatures. Extrusive magmas cool quickly, so there is little time for macroscopic crystals to grow before solidification. An intrusive rock, on the other hand, formed from magma that cooled deep within the Earth, and it experienced higher pressures and slower cooling rates, allowing time for large minerals to grow. Take two magmas with a certain composition: the one that extrudes onto the surface and cools very quickly becomes obsidian, whereas the intrusive one remains hot deep underground, cools over millions of years, and becomes large-grained granite.

The term “obsidian” is a classification for rock texture, so actually *in stricto sensu*, there is no compositional component to the definition. The chemistry of obsidian varies, but it tends to form from magmas rich in silica (silicon dioxide). Silica-rich magmas are often termed “silicic,” “felsic,” or “acidic” by geologists. Most frequently, the chemistry of obsidian is described as “rhyolitic,” meaning it is over 69% silica. Rhyolitic lavas can yield rocks with various textures, from porphyritic (comprised of macroscopic minerals) to aphanitic (comprised of microscopic minerals) to glassy (obsidian). The composition of obsidian, as a rhyolitic rock, is usually about 70-77% SiO_2, 10-15% Al_2O_3, 3-5% Na_2O, 1-5% K_2O, and less than 4% total iron oxides (Glascock 1994:115).

Obsidian can have compositions with lower levels of silica (called basaltic, between 45% and 52% silica); however, rhyolitic compositions are much more common precisely because of the high silica content. Magmas rich in silica are more viscous than low-silica magmas. This high viscosity impedes the growth of crystalline minerals, which are more thermodynamically stable, by constricting the motion of atoms in the magma. The silica (SiO_2) molecules bind with the oxygens of neighboring molecules, creating a tetrahedral structure of one silicon atom in the middle of four oxygen atoms. These tetrahedra form a disordered network of silica chains and sheets. There is, therefore, short-range order on the scale of a few atoms but no long-range order like that in crystals.

Silica is called a “glass former” since it facilitates the amorphous structure. Other elements -- like sodium, potassium, and calcium -- bind to this disordered silica network, preventing it from forming crystals. Basaltic magmas have less silica and, therefore, are

less viscous, so microscopic crystals will readily form even when cooled rapidly, making obsidian less likely to form. Readers interested in additional details about the formation of natural glasses are forwarded to Vogel (1971), Bouška (1993), Ohring (1995:160-166), Webb (1997), Zallen (1998), and Mysen and Richet (2005). Furthermore, an overview of obsidian structural research is provided by Zotov (2003).

1.2.2 - Obsidian as a Mixture

I do not intend to suggest, though, that obsidian is a perfect glass and that it is free of any minerals. Unfortunately, one can find statements in geological and archaeological texts that imply obsidian has no minerals whatsoever. For example:

- "Obsidian cools so quickly that crystals have no time to grow and the rock texture is literally as smooth as glass" (Andrefsky 2005:48).
- "Obsidian is a dense volcanic solid often formed in lava flows where the lava cools so quickly that crystals cannot grow" (Goffer 2007:99).
- "The glassy rocks obsidian and pumice contain no crystals because they solidify instantaneously... it cools so quickly that its ions don't have time to become organized into any crystals at all" (Chernicoff and Fox 1997:48).

In fact, even the glassiest obsidian contains a few minerals, but they are microscopic (or even nanoscale [Ma et al. 2007]) and comprise as little as a few tenths of one percent of the total volume. In other varieties of obsidian, the minerals may comprise 5 percent (or more) of the volume. Any abundant, micrometer-scale mineral inclusions are commonly called "microlites" or "crystallites," the former being slightly larger because their mineral species is barely recognizable with visible-light microscopy (though this distinction is not

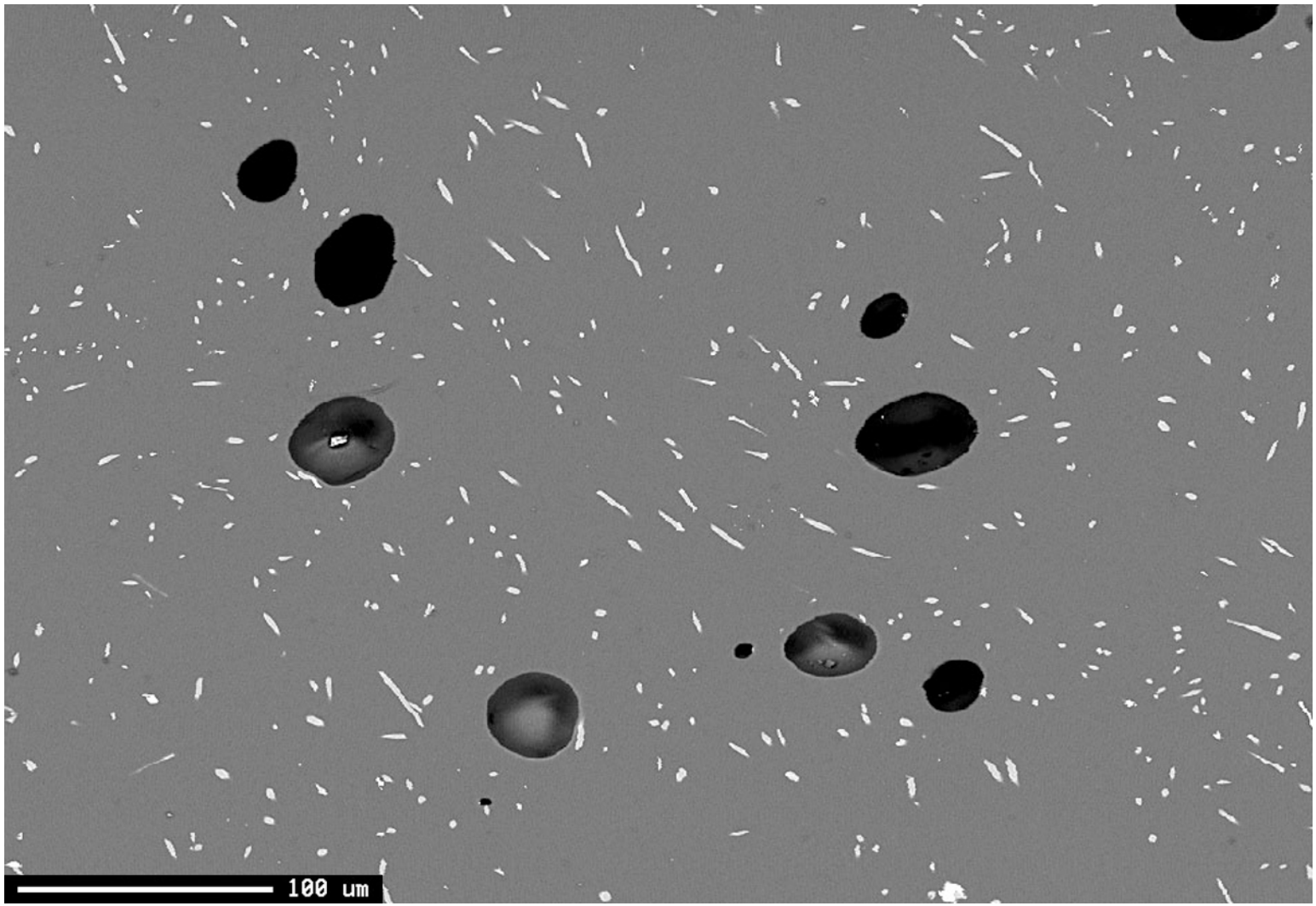


Figure 1.1 - An example of microscopic minerals and bubbles in obsidian (backscattered-electron image by the author).

universal). Any rare, larger inclusions are called "phenocrysts" (or "microphenocrysts"), which simply means the crystal is conspicuously larger than others.

A block of obsidian ordinarily appears black and opaque; however, thinner flakes, especially at the edges, are often transparent with black bands. Pure glass would be clear, like window glass. The black color is a result of microscopic magnetite (one form of iron oxide, Fe_3O_4) grains scattered throughout the glass matrix. The red-brown color in some obsidian varieties is due to hematite (another form of iron oxide, Fe_2O_3, which is basically rust), which forms when magnetite grains oxidize (Iddings 1886:274). Both of these iron oxides range from micrometer- to nanometer-scale (Ma et al. 2007).

Other minerals are also common in obsidian, including silicates such as sanidine, quartz, and plagioclase and oxides such as ilmenite. So-called "snowflake obsidian" has spherical clusters (often several millimeters in size) of needle-shaped cristobalite crystals. Other silicate minerals are also common, including various feldspars, biotites, pyroxenes, and amphiboles. I have also reported zircon, monazite, and other exotic inclusions within certain obsidian varieties (Frahm 2009). Bits of rock, termed xenoliths, from the magma chamber wall may also be included in obsidian. The numerous inclusions in obsidian are also described by various researchers, occasionally in the context of sourcing but usually for geoscience studies (Kayani and McDonnell 1996; Stevenson et al. 1998; Manga 1998; Manga et al. 1998; Castro 1999; Ma et al. 2001, 2007; Castro et al. 2002, 2003; Gimeno 2003; Rózsa et al. 2003a, 2003b, 2006; Acquafredda and Paglionico 2004; Castro and Mercer 2004; Gonnermann and Manga 2005; Kloess et al. 2006).

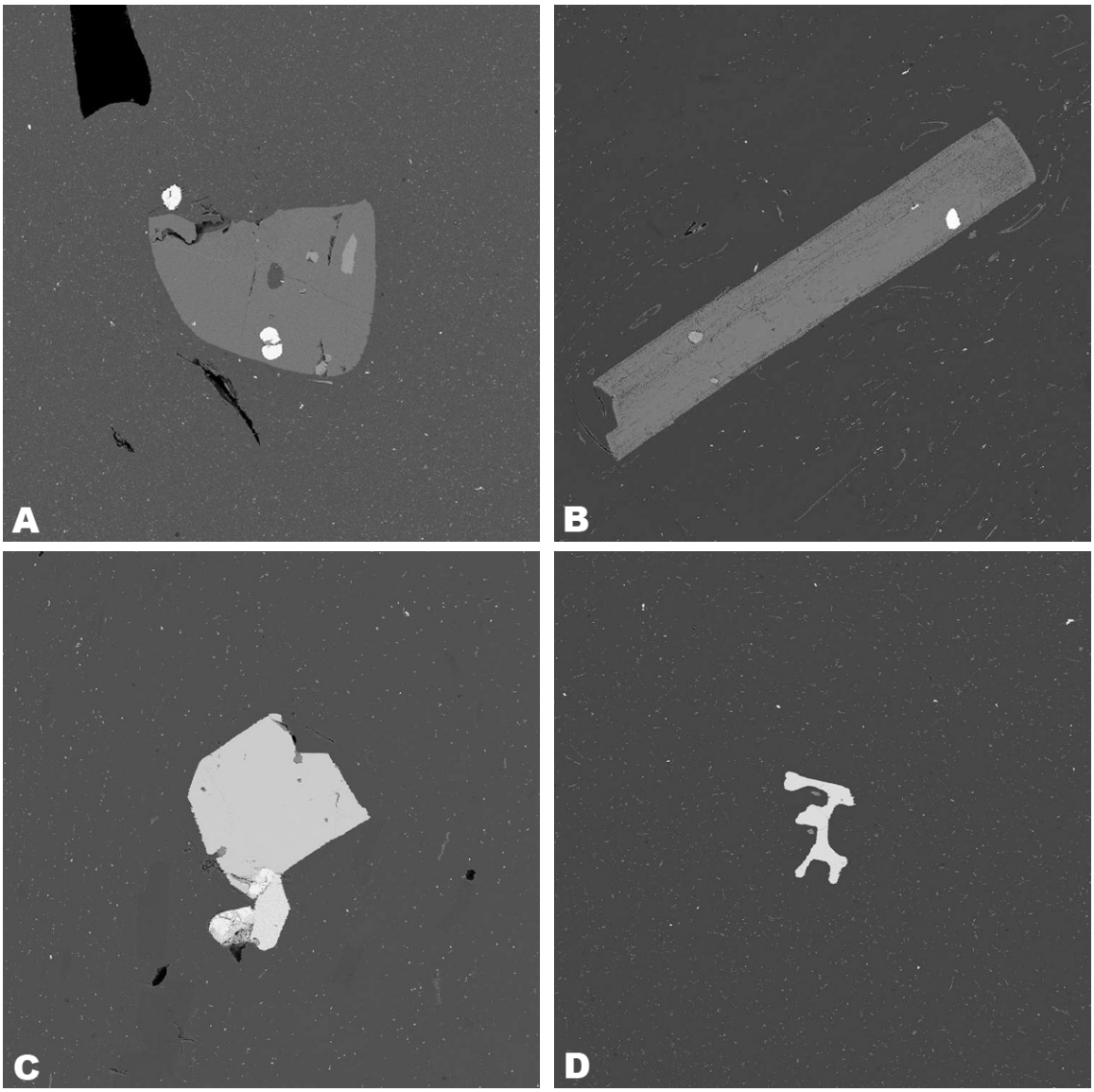


Figure 1.2 - Backscattered-electron images of mineral inclusions in obsidian specimens analyzed in this research. The field of view for all four images is 750 µm (0.75 mm). A) Armenian obsidian with microlites and a pyroxene phenocryst containing amphibole and pyrite grains; B) Armenian obsidian with microlites and a feldspar phenocryst containing monazite; C) Anatolian obsidian with microlites in addition to ilmenite, albite, and zicron phenocrysts; and D) Anatolian obsidian with microlites and an ilmenite phenocryst.

Geoscientists are interested in these inclusions in obsidian for a variety of reasons. First, certain inclusions are useful for dating the obsidian (and its corresponding volcanic eruption). For example, sanidine, a high-temperature form of potassium feldspar, often is found in obsidian and is useful for $^{40}K/^{40}Ar$ and $^{40}Ar/^{39}Ar$ dating, and monazite and zircon are both useful for U/Th/Pb dating. A second application is studying lava flow processes. For example, Stevenson et al. (1998) found that microlites can, under specific conditions, reduce the viscosity of lava. Other researchers (e.g., Manga 1998a, 1998b; Castro 1999) study the orientations of needle-shaped inclusions in obsidian as a means to determine the forces experienced by the molten lava after its eruption. These tiny inclusions align, like proverbial compass needles, with the direction of flow.

A third application is studying the minerals in order to determine how the magma "evolved" -- that is, changed in composition over time -- before it erupted. Crystals form while magma is still in its chamber, and these minerals remove elements from the magma and alter its composition. For example, obsidian is low in Ca because Ca-rich plagioclase [anorthite, $CaAl_2Si_2O_8$] is among the early-forming minerals. Obsidian is similarly low in Mg and Fe because olivine [$(Mg,Fe)_2SiO_4$] is also such a mineral. Based on the minerals still present in the obsidian (i.e., not left behind in the chamber), geologists can determine the pressures and temperatures experienced by the magma as well as its original chemical composition. Analyses of these minerals reveals which elements within the magma were "compatible" with their crystal structures. For example, as mentioned here, olivine is one of the minerals that forms first. Under the conditions in magma chambers, Ni has similar

behavior to Mg and Fe, so it is "compatible" with olivine and readily incorporated into its structure. Other elements are "incompatible" with olivine and stay in the magma. As the conditions change and different minerals form, some elements change from compatible to incompatible and vice versa. Accordingly, studying the partitioning of elements between the glass and the minerals can reveal the magma's history. This topic of incompatible and compatible elements in obsidian is discussed again in Section 1.2.4.

The sizes and abundance of mineral inclusions in obsidian may vary greatly from source to source. In obsidian of sufficient quality for flaked tools (called "weapons-grade obsidian" by Steffen), inclusions are microscopic and scarce, comprising as little as a few tenths of one percent of the total volume. As the sizes and/or abundances of the minerals increase, the suitability of the obsidian for flaked stone tools decreases. The inclusions in the path of a crack, initiated by a knapper, will deflect its propagation in an unpredictable direction. Accordingly, archaeologists have observed the preferential use of high-quality obsidian, even when it is more distant, requiring greater effort to acquire. For example, at Lizard Man Village in Arizona, less than one percent of the points were made of obsidian from the closer but lower-quality source (Kamp 1998:149). In general, obsidians usually are between 95% and 100% glass, but some may be 5% or more crystalline (Cann 1983: 229). Obsidian suitable for flaked tools falls within the former range. For example, the obsidian on Giali in the Aegean Sea contains 5% feldspar crystals, and hence it was only used for stone vessels in Bronze-Age Crete (Renfrew et al. 1965).

The abundance of mineral inclusions in obsidian can also vary within one flow or even an individual specimen. The most dramatic example, shown in Figures 1.3 to 1.5, is called "flow banding" and occurs in many obsidians. The flow bands, which appear to be horizontal light and dark lines, are really planes of highly concentrated microlites (and/or bubbles) in the obsidian. Due to the often dark color of these bands, it is usually assumed that they consist wholly of iron oxides, magnetite in particular; however, silicate minerals can also comprise the bands. For example, Castro et al. (2002, *inter alia*) investigated the pyroxenes in the flow bands of obsidian from two sources in California and one source in Oregon, and they also noted feldspar and oxide inclusions in every specimen (2004). The density of these pyroxenes varied over an order of magnitude within the obsidians (2003). At the Mono-Inyo volcanic chain, Swanson et al. (1989) observed that the "abundance of microlites varies dramatically, even on the thin-section scale. Microlites are concentrated in bands, their alignment defining a flow banding in the obsidian" (167). The flow bands may vary greatly in width. Castro et al. (2002) found that the bands vary between a tenth of a micrometer to a few millimeters (214), and Gonnermann and Manga (2005) state that bands can even be dozens of centimeters in width (135-136).

The concentration of flow bands within a certain obsidian specimen can affect its overall chemical composition. Stevenson et al. (1996) point out that microlites can "vary in concentration within [obsidian] flows" and that "adjacent microlite-rich and -poor flow banding, together with the wide range of microlite compositions, means that composition of the melt can vary significantly within flows" (298). Similarly, Castro et al. (2004) note



Figure 1.3 - An example of flow banding, one form of obsidian heterogeneity (Newberry Volcano; photograph by the author).

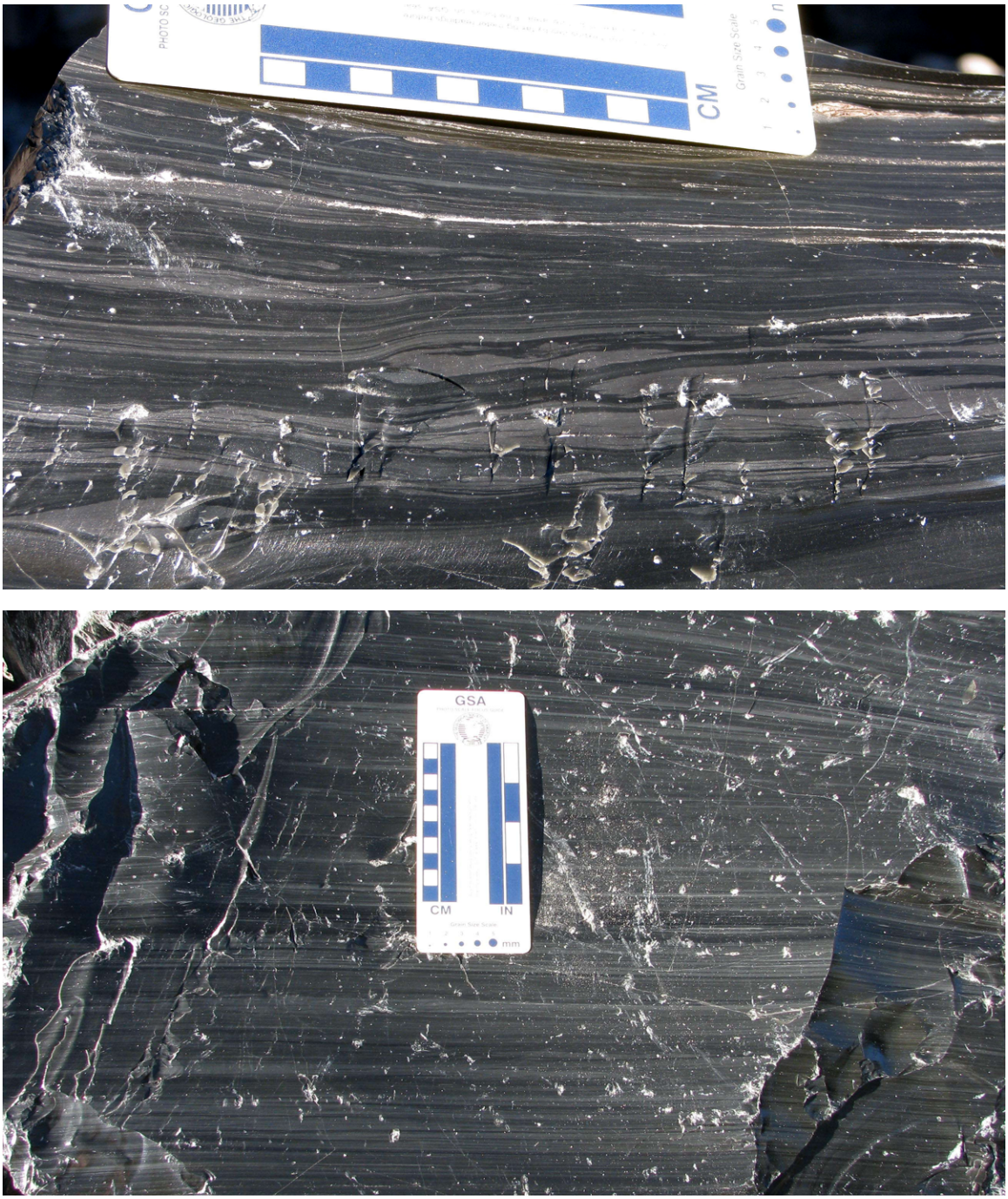


Figure 1.4 - Examples of macroscopic flow banding in obsidian. The bands are planes of abundant mineral inclusions (iron oxides and various silicates) and/or bubbles. These are examples from Newberry Volcano (photographs by the author).

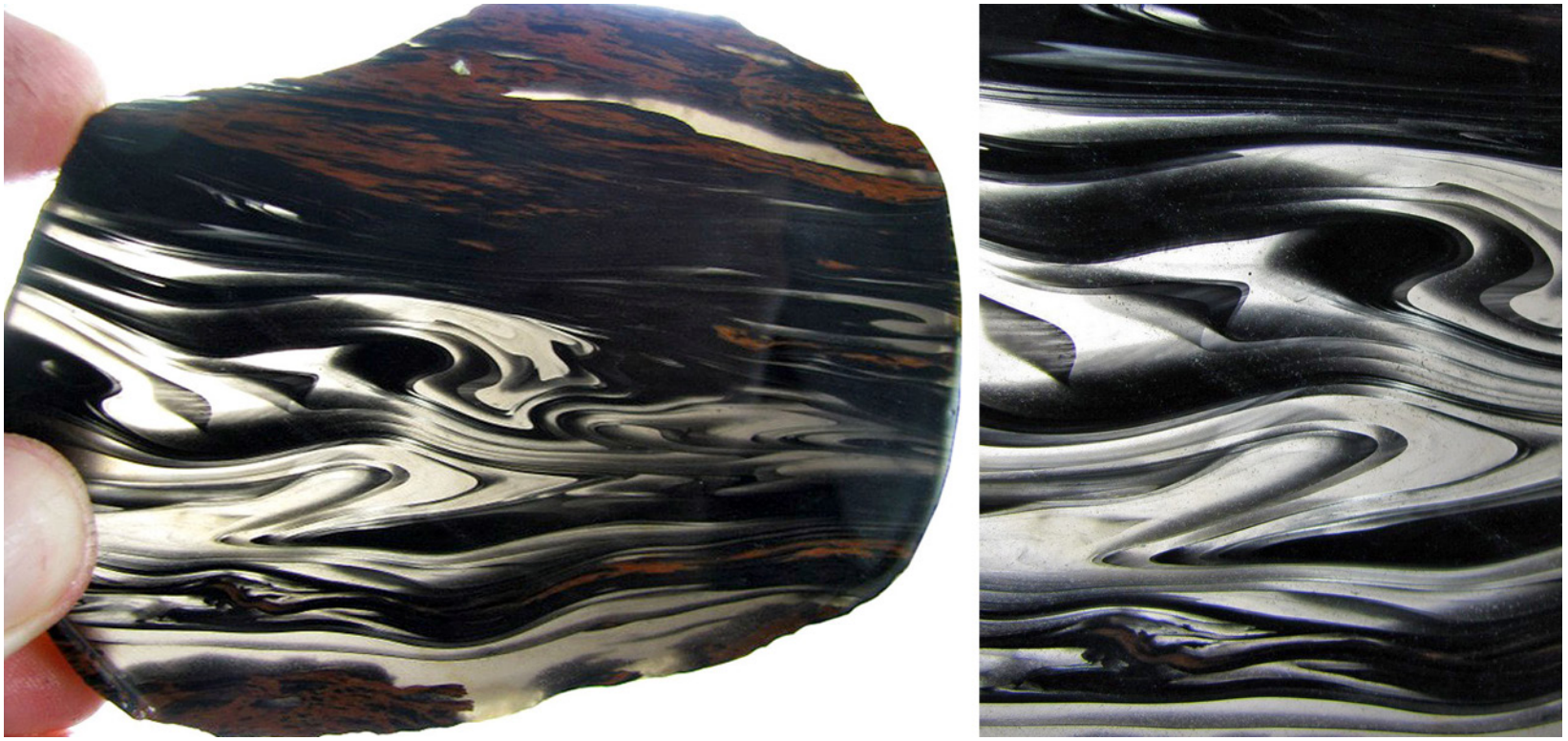


Figure 1.5 - Flow banding in an obsidian specimen from Glass Buttes, Oregon (from the collection of the author).

that, with respect to the mineral inclusions in obsidian, "the relative abundances of these phases vary dramatically within particular samples" and that the flow bands have two kinds of variation: (1) modal (i.e., "adjacent bands have the same mineral assemblage but contain different volume fractions, size distributions, and/or number densities" of the inclusions present) and (2) mineralogical (i.e., "adjacent bands differ by virtue of their constituent mineral assemblages"). For example, they discovered that the bands in Big Glass Mountain obsidian had modal differences: pyroxenes in the bands varied in size, shape, and abundance. At Obsidian Dome, however, the bands exhibited both modal and mineralogical variation: only some bands had plagioclase.

Flow banding, a dramatic example of how inclusions can vary, is a very common feature in obsidian. For the obsidian specimens they studied, both Swanson et al. (1989) and Castro et al. (2002) call flow bands "ubiquitous." Regarding their formation, Castro et al. (2004) state that the bands "arise from degassing, crystallization, and deformation processes" although "relatively little is known about the origin" precisely. Given such influences, however, these "flow bands must contain important information regarding the chemical and physical evolution of obsidian." This means that these bands reflect the formation processes of obsidian, discussed in the next section.

1.2.3 - Formation of Obsidian

As discussed in Section 1.2.1, obsidian will form only under particular conditions: when viscous, silica-rich lava oozes onto or near the surface so that it cools quickly. This

high viscosity of the lava affects how it erupts. Low-silica lava flows easily in "rivers" of molten rock, covers extensive areas, and forms ropy *pāhoehoe* surfaces. High-silica lava, on the other hand, forms structures called "lava domes." Such domes are small, normally only covering less than a dozen square kilometers. Fink (1987) explains that the "blocky, inhospitable surfaces of silicic lava domes, along with their relatively small volumes and restricted global distribution, have until recently relegated them to positions of obscurity in the geological literature" (v). The outer shell of lava domes is comprised of pumice, a porous rock created by the release of water and gasses, once dissolved in the magma but released at surface pressures and temperatures. The porosity decreases with depth until a vesicular glass is reached and, beneath that, a bubble-free obsidian layer (although, when lava containing too much water or gas erupts, tool-quality obsidian might not be present). Beneath this obsidian "inner shell" is a crystalline core, which cooled slowly enough for rock-forming minerals to grow. The temperatures of these lava domes cool to only a few hundred degrees in a matter of days (Ericson et al. 1976:36). The same rhyolitic magma, if it is emplaced at a depth of 5 kilometers, retains about 80% of its initial temperature for over one million years and eventually becomes granite (36).

This inner shell of obsidian can be deeply buried across much of the dome. Tool-quality obsidian can be gathered where the glass layer is exposed either on the talus slope at the dome perimeter or by later faulting. Hughes and Smith (1993:81) explain:

> Most rhyolite lavas cool and crystallize leaving at least a basal obsidian zone. However, unless this base is catastrophically exposed by faulting early in its postdepositional history, by the time it is exposed by erosion only hydrated glass,

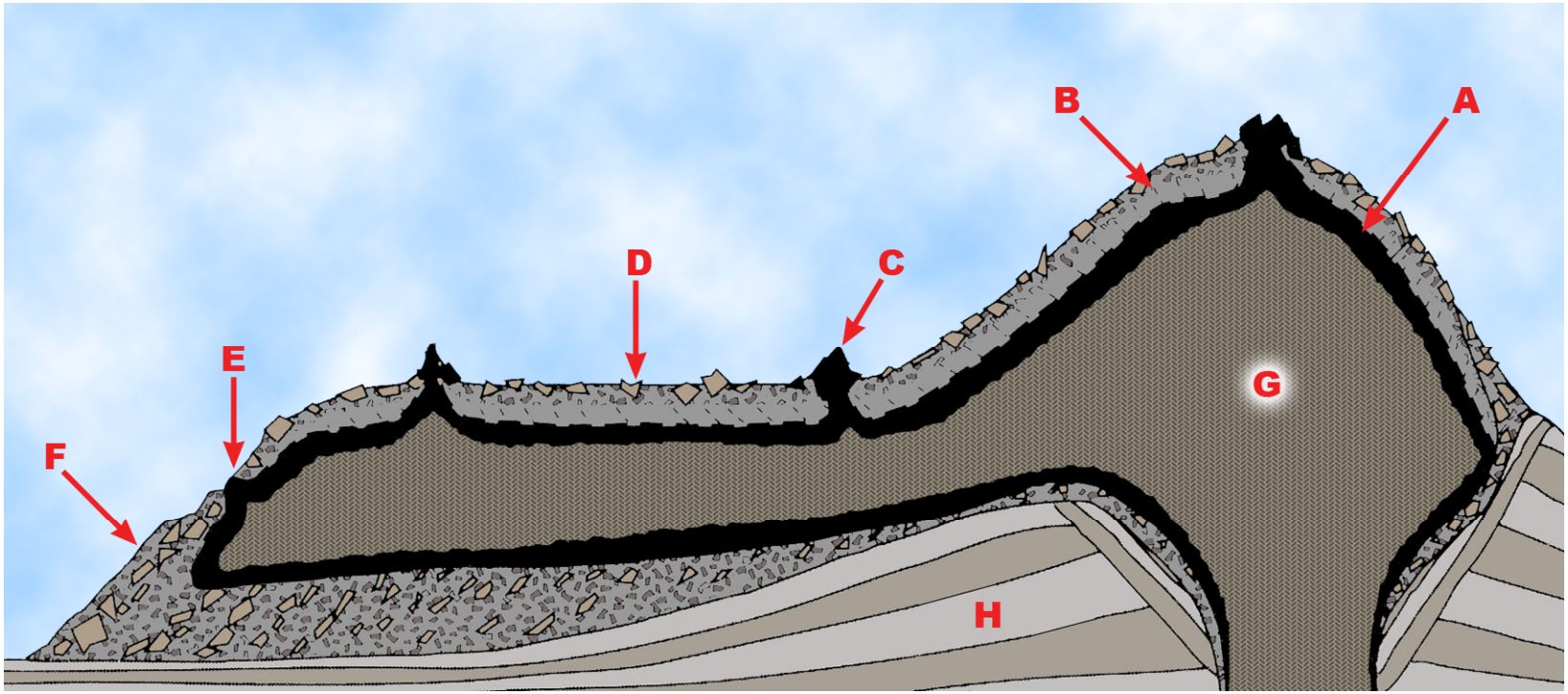


Figure 1.6 - A cross-section of an obsidian-bearing rhyolitic lava dome: A) inner shell of obsidian; B) outer shell of porous glass (i.e., pumice); C) protruding obsidian spine; D) blocky surface of the dome; E) part of the inner obsidian shell exposed along the forward slope; F) talus slope of mostly pumiceous blocks; G) crystalline interior; and H) existing pumice cone onto which the rhyolitic lava dome erupted (based on a figure from Hughes and Smith 1993; redrawn and modified by the author).

> occasionally with obsidian remnants, will remain... By far the majority of such deposits will be completely hydrated before they are exposed.

Spines of obsidian may also protrude through the outer shell of a lava dome. Hughes and Smith (1993:81) suggest that many artifacts were made from this material:

> Thus most obsidian artifacts were probably made from obsidians formed in the upper parts of very young lava flows or domes. Obsidian from the upper part of such bodies is far less uniform than that from the basal zone, and it is more likely to show striking variations in color, texture, and other physical properties, while still retaining its chemical homogeneity.

This variation explains, in part, the limitations of visual obsidian sourcing (e.g., Bettinger et al. 1984, Moholy-Nagy and Nelson 1990, Aoyama 1996, Tenorio et al. 1998, Braswell et al. 2000, Carter and Kilikoglou 2006, Carter et al. 2008). Furthermore, if Hughes and Smith (1993) are correct and most artifacts were fashioned from this material with varied textures (that is, its physical character, including the minerals and their sizes, shapes, and arrangement), it is even more important to treat obsidian as a mixture.

Forces experienced by the obsidian may cause a network of cracks throughout the layer. An obsidian flow with a large surface area and extensive crack network will have a shorter existence than a mass of crack-free obsidian. Water infiltrates the cracks, causing hydration of the obsidian and, consequently, the formation of perlite, which is useless for flaked-stone tools since it no longer fractures conchoidally. Crack-free obsidian, though, might exist for 10 million years or more before the last small nodules (called marekanites or Apache tears in the American Southwest) are obliterated. Abundant phenocrysts in an obsidian may also increase the speed of hydration because, as strain increases in hydrated portions of the obsidian (due to an increase in its volume), the inclusions can facilitate the



Figure 1.7 - An obsidian spine protrudes out of the outer shell of a lava dome (Newberry Volcano; author included for scale).



Figure 1.8 - The inner obsidian shell is exposed on the dome's forward slope (Newberry Volcano; author included for scale).

spread of cracks. Hughes and Smith (1993) explain that "the persistence in the geologic record of any crack-free obsidian mass is largely a function of its volume and shape after initial cooling and its post-cooling cracking history" (81).

Over time the outer pumice shell erodes, and weathered obsidian nodules wash downstream as alluvium. These secondary deposits may be a few kilometers in diameter, but particularly old obsidian can be distributed, in the right landscape, over much broader areas. This long-range transport has been documented in the American Southwest, where some obsidian sources are more than 10 million years old. For example, Shackley (2005) reports that small nodules have been found up to 100 km from Cow Canyon, Arizona and Mule Creek, New Mexico sources (26). Similarly, the Rio Grande River has transported obsidian from Valles Caldera and Mount Taylor in New Mexico to Chihuahua, Mexico, a distance of over 250 kilometers (26). In places where the long-range alluvial transport of obsidian occurs, there are important implications for sourcing.

Both Hughes and Smith (1993) and Shackley (2005) discuss a few other volcanic processes that can create obsidian, but the latter argues that these "uncommon methods… rarely produced artifact-quality obsidian" (26). The mechanisms include: (i) pyroclastic deposits around a volcanic vent might include obsidian blocks ejected with abundant ash and pumice (Hughes and Smith 1993:84-85); (ii) agglutinates produced by rhyolitic lava fountains, but those "that yield artifact-quality obsidian are rare" (85); and (iii) ash sheets that, while still hot from eruption, are compacted and weld together into glassy layers, but Shackley (2005) states that "rarer still is obsidian formed" this way (27).

Discussions regarding obsidian formation are found in Ericson et al. (1976), Cann (1983), Fink and Manley (1987), Hughes and Smith (1993), Bouška (1993), and Shackley (2005) for those readers interested in greater detail.

1.2.4 - Geochemistry of Obsidian

There are three basic geochemical types of obsidian called *alkaline*, *calc-alkaline*, and *peralkaline*. Many obsidian-producing volcanoes occur in volcanic arcs, usually one or two hundred kilometers from and parallel to a subducting plate boundary. Within such volcanic arcs, alkaline or calc-alkaline obsidian is most common. Calc-alkaline obsidian has high concentrations of Ca and alkalis like K and Na. Alkaline obsidian also has high levels of K and Na, but it has been depleted in Ca due to differences in magma generation or evolution. Sometimes alkaline and calc-alkaline obsidians are considered to be only a single geochemical type. On the other hand, peralkaline obsidian is higher in Fe, and it is produced occasionally in volcanic arcs and more commonly at divergent plate boundaries (also called constructive or extensional boundaries). The geochemical types tend to have slightly different hues: alkaline and calc-alkaline obsidian is ordinarily gray or black, and peralkaline obsidian is commonly tinted brown or green.

The concentrations of trace elements, not only major elements, also vary between these geochemical types. Alkaline and calc-alkaline obsidians usually have higher levels of Ba and Sr, and peralkaline obsidian has high Zr and Nb contents, frequently over 1000 ppm. As noted in Section 1.2.2, some elements are *compatible* with the minerals in the

magma, and others are *incompatible* with the minerals and are instead concentrated in the magma. Different minerals form in alkaline, calc-alkaline, and peralkaline obsidians, and the presence of these different "hosts" in the magma leads to these variances in the trace-element concentrations. For example, while Zr is high in the glassy matrix of peralkaline obsidians, it is much lower in alkaline and calc-alkaline obsidian because zircon ($ZrSiO_4$) and other Zr-bearing minerals form and remove it from the glass. While Ba is high in the glass component of alkaline and calc-alkaline obsidian, feldspars in peralkaline obsidians easily accept Ba and, as a result, reduce its concentration in the glass phase. As Rollinson (1993) reports, "there are degrees of compatibility and incompatibility and trace elements will vary in their behaviour in melts of a different composition" (103).

The implication is that elements are not always "compatible" or "incompatible" in magma. Instead, the conditions and composition affect the elements' behaviors, and thus, the ratio of a particular element in the solid phase (i.e., the minerals) and liquid phase (i.e, the magma) will change. There are, though, general trends. For example, Cr, Co, and Ni are easily absorbed into the minerals. Elements such as Ga and Ge are evenly partitioned between the minerals and magma. Incompatible elements remain in the magma for a few reasons. For example, elements like Ba, Sr, and Rb are often classified as "incompatible" elements because their radii are too large to fit into most minerals, and consequently, they tend to remain in the liquid magma. As just mentioned, though, Ba is readily accepted by feldspars in peralkaline obsidian, so it is a compatible element under those circumstances. Other elements are considered incompatible because their charge is frequently too high to

fit into most minerals. This is the case with the +3-charged La and Ce, the +4-charged Ti and Zr, and the +5-charged Ta and Nb. Yet as noted earlier, ilmenite ($FeTiO_3$) is abundant in obsidian, and zircon ($ZrSiO_4$) forms in alkaline and calc-alkaline obsidian. In addition, U, which is normally incompatible, is compatible in zircon. In another example, studying obsidian from Northern Ireland, Brooks et al. (1981) found Le and Ce concentrated in the epidote (a silicate mineral) rather than the glass: La was 5% in the epidote and 60 ppm in the glass, and Ce was 10% in the epidote and 165 ppm in the glass. Clearly elements like Ti, Zr, La and Ce are not always incompatible elements in all obsidians.

The ratio between the concentration of an element in a specific mineral and that in the magma is called the partition coefficient or *D*. For example, for compatible elements, $D >> 1$, such as Ba into feldspars in rhyolitic magmas. Best (2003) explains:

> No single partition coefficient describes the behavior of a particular trace element in all magmas. The composition of the magma and that of the mineral both affect the value of D. Coefficients for the same element in the same mineral generally increase as the magma becomes more silicic; variations of a factor of 10 are common... Decreasing magma temperature (T) also corresponds with increasing coefficients. Cooler, more silicic melts are more tightly structured, causing trace elements to be rejected and forced into coexisting crystals. (39)

Thus, as the magma changes in chemical and mineralogical composition over time and as pressure and temperature change, the partitioning of trace elements between the minerals and magma also change, and new minerals also form. Therefore, one cannot assume that any particular element is always incompatible in obsidian.

Nevertheless, using only "incompatible elements" to source obsidian is frequently mentioned in the literature (e.g., Lees and Roach 1993; Shackley 1998a, 1998b; Ambroz

et al. 2001; Hall and Kimura 2000; Shackley and Dillian 2002; Tykot 2004; Bellelli et al. 2006; Reepmeyer and Clark 2010). For example, Green (1998) maintains that various techniques "have now become more than adequate for source assignment, as long as they measure incompatible elements with a fair degree of certainty" (228). This, it appears, is intended as a way to control for variations in the types and abundances of inclusions (i.e., a way to control for obsidian being a mixture of glass and minerals) when using bulk (or "whole-rock") analytical techniques. As we have established, though, one cannot assume that a specific element is always incompatible. For example, measuring Ba in an alkaline obsidian largely reflects its concentration in the glass, but measuring Ba in an peralkaline obsidian can reflect the abundance of feldspar inclusions.

1.3 - Fundamentals of Sourcing Studies

Archaeologically it is advantageous to determine from where an artifact or its raw material originally came. For hunter-gatherers, determining the sources of raw materials, such as obsidian, can indicate their procurement and utilization patterns and, in turn, their territory size or organization of production. For complex societies, sourcing can indicate exchange systems and allow inferences about the economic and/or political organizations of the people involved. Sourcing, though, involves its own theoretical basis and series of postulates as well as issues of much discussion and debate.

1.3.1 - Terminology: "Sourcing" versus "Provenancing"

The term "provenancing" is often used as a synonym for archaeological sourcing, and two terms -- "provenience" and "provenance" -- are frequently used interchangeably, so this terminology must be discussed. Both "provenience" and "provenance" come from the French *provenir*, "to come from," referring to the origin of something. Rapp and Hill (1998:134) argue for the following distinction between these two terms:

> *Provenience* is a common archaeological term referring to the precise location at which an artifact was recovered (from a survey or excavation). Without provenience data, artifacts have little archaeological value. By *provenance*, however, geoarchaeologists mean something quite different. The provenance of an artifact is the location, site, mine that is the origin of the artifact *material*.

I have followed their definitions elsewhere (e.g., Frahm 2002); however, adherence to the distinction between these terms is far from universal. Various authors, including those of many archaeological dictionaries, equate these two terms and even treat them as alternate spellings (e.g., "The term *provenance,* or *provenience*, as the word is often also spelled," Goffer 2007:42; also see Mignon 1993:88, Kipfer 2000:458, Bahn 2001:369, Wilson and Pollard 2001:507, and Darvill 2008:367 for examples of treating the words as synonyms). Harbottle (1982:16) offers a hypothesis about the usage of two terms:

> Provenience (= provenance). It *ought* to mean *only* where something is found... But among art historians it generally means *presumed origin*... Some archaeometry papers have also used the term to mean *source* or *origin* (Wilson 1978). One suspects that we are seeing here an Old World-New World bias, the art-historical usage being common among Old World archaeologists.

Pollard et al. (2007) also attribute this ambiguity to differences between the United States and Great Britain and between art history and archaeology:

> … relating to *provenance* (or, in the US, *provenience*…). The term here is used to describe the observation of a systematic relationship between the chemical composition of an artifact… and the chemical characteristic of one or more of the raw materials involved in its manufacture. This contracts sharply with the use of the same term in art history, where it is taken to mean the find spot of an object, or more generally its whole curatorial history.

About the distinctions proposed by Rapp and Hill (1998), Pollard et al. (2007:5) write:

> In fact, a recent North American textbook on geoarchaeology has used the term *provenience* for find spot, and *provenance* for the process of discovering the source of raw materials... Although this is an elegant solution to a terminological inexactitude, it has not yet been universally adopted, at least in Europe.

I prefer the definitions of Rapp and Hill (1998); however, because the distinction between the terms is not widely accepted and has caused confusion (e.g., Millet and Catling 1966), I prefer the term "sourcing," rather than "provenancing," and use it here (for an opposing opinion on the appropriateness of the term "sourcing," see Shackley 2008b:196). Other researchers, when quoted, might use the terms "provenance" and "provenancing." When I have included such quotations, the terminology will be consistent with that of Rapp and Hill (1998). Furthermore, when I use the term "provenience," its usage will be consistent with the definition from Rapp and Hill (1998), meaning where the artifact was unearthed. I suspect that, at least in part, the popularity of the term "provenancing" is due to debates over what constitutes a "source" in such studies. In Chapter 4, I consider this issue and provide the "source" terminology that I used in my research.

1.3.2 - Sourcing, Fingerprints, and Typologies

A diagnostic pattern of elements is commonly termed a chemical or compositional "fingerprint." In some ways, a fingerprint is an apt nickname for a characteristic pattern of elements. Fingerprints are, of course, used as a means of identification, and chemical fingerprints are utilized to identify raw-material sources. Siblings frequently have similar ridge patterns, and geological materials with the same "parentage" have similar chemical fingerprints. Fingerprints are classified by pattern types, the size of the patterns, and their location on the fingers. Similarly, chemical fingerprints can be classified by the elements present, their quantities, and their distributions in the material.

Unfortunately, this analogy is not a perfect one. There are hundreds of millions of fingerprints in databases around the world, and no two sets are identical. Our fingerprints are so unique that they are widely considered an infallible means of identification. When a person touches a dime, it is claimed, there are sufficient lines on that coin to establish a positive identification to the exclusion of any other person on Earth. This, though, is not true of chemical "fingerprints" of geological materials. Such patterns of elements are not nearly as characteristic as the ridge patterns on our fingertips.

Another analogy for chemical fingerprints, although just as imperfect, are ceramic typologies. Ceramics are very frequently used to date archaeological sites and strata, and they are also utilized to study a variety of cultural aspects, such as settlement patterns and exchange networks. Ceramic artifacts are sorted into types based on technological (e.g., clay, temper), morphological (e.g., size, shape), and stylistic (e.g., cord marking, painted

patterns) features. Consider, for example, two ceramic types used by the Hurrians at Tell Mozan: Khabur ware and Nuzi ware. There are commonalities: both types, for example, are wheel-made. The former, however, is characterized by painted red-brown horizontal lines with geometric, usually triangular, patterns of the same color whereas the latter has white curled or wavy lines on a brown or black background.

Typologies are artificial constructs, idealized classifications, used to sort ceramics by time and place. Ceramic types are derived from a collection of sherds and vessels, and commonly no one sherd possesses all properties of the type into which it has been sorted. Of the two typologies mentioned above, some traits are distinctive (e.g., red-brown bands versus white curls) while others are shared (e.g., wheel-made). It is the overall pattern of the traits that characterizes a type, not any one. Furthermore, there are variations within a type: patterns on Khabur vessels can be either hatched or cross-hatched, and "there are no two examples of Nuzi Ware with exactly the same white painted design" (Stein 1984:27). There are also very similar types, and sherds will be found that could be sorted into more than one type. The same circumstances occur in chemical fingerprinting.

Therefore, chemical fingerprints are, on one level, similar to other archaeological types. The formation of types depends on categorization of artifact attributes, and trends in archaeological types, in turn, are used to delimit cultural units and patterns. Chemical fingerprints are used to source artifacts based on not form or decoration but composition. Like ceramic types, chemical fingerprints are used to make inferences about the group of people who made and/or used the artifacts. It must be remembered, though, that ceramic

types reflect where the artifacts were manufactured, whereas sourcing studies involve the origin of the raw materials from which they were manufactured.

Typologies intended to answer questions about where artifacts were manufactured have also been formulated based on chemical fingerprints and groups. These are not true "sourcing" studies *per se* -- analytical techniques are used to characterize and chemically group the artifacts, not trace them back to their geological sources. Banterla et al. (1973), for example, utilized neutron activation analysis to classify terra sigillata potsherds "into homogeneous groups when it [was] impossible to place them stylistically or by any other means" (209). Such studies can, in some cases, be useful but are not "sourcing" studies because the geological origin of the raw material is not sought.

1.3.3 - "Trace-Element Fingerprints" versus Major Elements

These fingerprints are almost automatically called "trace-element fingerprints" by most authors. What constitutes a "trace element" is not rigorously defined, though, and a chemical fingerprint can also be demarcated by major and minor elements.

With respect to volcanic glasses, Zotov (2003) defines major elements as greater than 1%, minor elements as 0.1% to 1.0%, and trace elements as below 0.1%. Andrefsky (1998) somewhat similarly defines major elements as greater than 2%, minor elements as 0.1% to 2%, and trace elements as below 0.1%. Discussing obsidian sourcing, Glascock (1994) states that trace elements "are present at concentrations far less than 1%" (115). Best (2003), a petrologist, takes a different stance. He explains that elements above 0.1%

"are said to be major elements, whereas trace elements contain <0.1 wt.% of the element, or more conventionally, <1000 ppm. This limit is rather arbitrary. Some elements are not consistently major or trace elements" (19). He explains that, because ten oxides -- Na_2O, MgO, Al_2O_3, SiO_2, P_2O_5, CaO, K_2O, TiO_2, MnO, and iron oxide -- comprise about 99% of most rocks, these might be considered the "geological" major elements. Shaw (2006) has a very similar stance, explaining that geochemists "define *major elements* as those which give the sample whatever distinctive character is has" while *trace elements* have very low concentrations and do not contribute (1; emphasis in original).

In this research, I adopt definitions of major and trace elements much like those of Best (2003) and Shaw (2006), corresponding to my two rounds of analysis. In the initial round, I analyzed for the ten oxides listed by Best (2003) plus Cr_2O_3, SO_3, F, and Cl, four other elements common in rock-forming minerals. These fourteen elements I consider to be the "geologically major elements," even if some of the concentrations are below 0.1% in obsidian. The six elements measured in the second round of analysis -- Zr, Nb, Ga, Zn, Ba, and Ce -- are considered to be "trace elements," even though the concentrations of Zr and Ba are greater than 0.1% in some of the obsidian specimens.

Merrick and Brown (1984) argued that "trace element analysis is undoubtedly the most elegant and reliable means of characterizing obsidian" (235), but in their study, they showed that CaO, TiO_2, and Fe_2O_3 are sufficient to differentiate Kenyan obsidian sources. In a statement typical of many authors, Herz (2001) states that major elements "generally be used as a tool for sourcing obsidian because of a relatively narrow variation in major

elements" (454). It is true that trace elements can vary over several orders of magnitude; however, because trace elements occur, by definition, at low concentrations, they may be hard to measure accurately and precisely compared to major elements. Most importantly, studies have demonstrated that major elements are, at least in part, also useful in obsidian sourcing (e.g., Anderson et al. 1986 and Glascock et al. 1999 in North America; Fralick et al. 1998 and Santley et al. 2001 in Mesoamerica; Bellot-Gurlet et al. 1999 and Lazzari et al. 2009 in South America; Willams-Thorpe et al. 1984 in Eastern Europe; Tykot and Chia 1997 in Indonesia; Sand and Sheppard 2000 and Reepmeyer and Clark 2010 in the South Pacific; Francaviglia 1984, 1995, Tykot 1995, *inter alia*, Acquafredda 1996, 1999, and Le Bourdonnec et al. 2006, 2010 in the Mediterranean). Hence, I include major elements in this study to reveal their usefulness in the Near East. In fact, I show that major elements are crucial to distinguish important Near Eastern obsidians.

1.3.4 - The Theory and Postulates of Sourcing

Glascock (2002) argues that identification of archaeological materials "that were exchanged between different areas and different societies are the most tangible evidence that an archaeologist can hope for when looking to establish contact between prehistoric peoples" (1). Matching an artifact to the source of its raw material initially seems rather conceptually simple; however, archaeological sourcing studies necessitate a set of tasks and assumptions which are briefly discussed in this section.

The so-called "Provenance Postulate," normally credited to Weigand et al. (1977), explains how successful sourcing depends on measurement of compositional differences, and it has since been reformulated and rephrased by various researchers. One of the most succinct articulations of the Provenance Postulate is that of Neff (2000:107): "Sourcing is possible as long as there exists some qualitative or quantitative chemical or mineralogical difference between natural sources that exceeds the qualitative or quantitative variation within each source." Rapp and Hall (1998) add a needed clause that is missing in Neff's formulation: "there is a demonstrable set of physical, chemical, or mineral characteristics in raw-material source deposits *that is retained in the final artifact*" (134).

Pollard et al. (2007) conceptualize the Provenance Postulate in terms of five basic conditions that must be satisfied: (1) *characterizability*, meaning that an artifact has some sort of compositional fingerprint that is unique to its source, particularly in comparison to all other likely sources; (2) *uniqueness,* meaning that the source is geographically unique, at least sufficiently so for the research question (e.g., obsidian from Valles Caldera, which has been alluvially transported all the way to Chihuahua violates this condition when one sources artifacts found in the Rio Grande river valley); (3) *predictability*, meaning that a chemical fingerprint should be either anthropogenically unaltered or, if altered by human processing, affected in a predictable manner; (4) *measurability*, meaning that techniques used to analyze the artifacts and raw materials need sufficient accuracy and precision for distinguishing the sources; and (5) *stability*, meaning that any diagenetic alteration of the artifacts must be either inconsequential or predictable (15).

Wilson and Pollard (2001) list somewhat different "major assumptions underlying every provenance study" (507-508). These six sourcing assumptions are:

1. Some compositional trait of the raw material is preserved, either unaltered or in a predictable manner, in the artifact, acting as a "fingerprint" of the source.
2. The "fingerprints" of different raw-material sources vary and are relatable to their geographical distribution. Further, the amount of *inter*-source variation must be larger than the amount of *intra*-source variation in the "fingerprints."
3. Analyses can measure "fingerprints" in the artifacts with sufficient accuracy and precision to be able to distinguish the possible raw-material sources.
4. There is no mixing of raw materials, either through processing or recycling, or that the mixing is sufficiently predictable that one can somehow account for it.
5. Any diagenetic alteration of the artifact was inconsequential to the fingerprint or affected the fingerprint in a recognizable and predictable manner.
6. Any patterns of raw-material movement can be interpreted in terms of human behaviors such as exchange systems or territorial mobility.

Wilson and Pollard (2001) point out that it is astonishing "that the provenance hypothesis has been so successful -- if these *ab initio* requirements had been explicitly stated before any such work had been attempted, it might be that no reasonable researcher would have embarked on the quest!" (508). These conditions are usually taken for granted, but Rapp and Hill (1998) contend these assumptions really "can be justified only through empirical work, which requires large data sets of high analytic accuracy" (134).

Rapp and Hill (1998) divide sourcing studies into three main components: (1) the identification and sampling of all possible raw-material sources (that is, both primary and secondary geological deposits); (2) selecting an analytical technique that can measure the compositional fingerprint with sufficient accuracy and precision in both the raw materials and the artifacts; and (3) using a statistical or data analysis technique to assign artifacts to the most likely raw-material sources (135). They also highlight two "inherent problems" in souring studies: (1) adequate representation of all potential sources in the database and (2) establishing that the artifact has not suffered any alteration that negates comparison to the raw materials (135). There are two parts to the second issue: anthropogenic alteration (i.e., processing, mixing, or recycling) and post-depositional alteration. The latter is often easier to overcome because surface alteration can be removed. Hall (1971) proposes that, when a surface or spot technique is used, an artifact should be "rubbed down" to expose a fresh surface that is representative of the interior. Rapp and Hill (1998) contend that only analytical "characterizations unaffected by processing, manufacturing, use, or post-burial diagenesis can be used for provenance determination" (135).

One objection to using "sourcing" (instead of "provenancing") is an assertion that one does not ever conclusively identify the source of an artifact. Instead, one statistically assigns an artifact to the most probable source, but this does not ensure that it came from that source. For example, there is the potential that the artifact may have originated from a source not included in the database. It is also possible for two sources to have chemical

fingerprints so similar that an artifact could potentially be attributed to both, though it can only be assigned to one. Harbottle (1982:15) contends that

> with a very few exceptions, you cannot unequivocally source anything. What you can do is characterize the object… and also characterize the equivalent source materials, if they are available, and look for similarities to generate attributions. A careful job of chemical characterization, plus a little numerical taxonomy and some auxiliary archaeological and/or stylistic information… will produce groupings of artefacts that make archaeological sense. This, rather than absolute proof of origin, will often necessarily be the goal.

Wilson and Pollard (2001) similarly contend that, if "a 'statistical' match is demonstrated, then one can only say it is *possible* that the two may derive from the same source" (510). In fact, they argue that "only mis-matches between source material and test object can be conclusively demonstrated… [Sourcing] proceeds by systematic elimination of possible sources, rather than by positive attribution" (510).

Fortunately, the conditions needed for successful sourcing are mostly satisfied by obsidian. Obsidian has a small number of sources because (1) only some volcanoes have the right conditions for its formation; (2) glass is unstable, so obsidian lasts only 10 or 20 million years at most; and (3) many obsidians contain too many minerals to make flaked-stone tools, further restricting the number of possible sources. This rarity makes it likely that obsidian was traded or otherwise moved long distances, and it is possible to assemble a complete source database. This is not the case for a lithic material like chert. Obsidian, as noted in Section 1.1, has been used around the world and for most of human history, so its study is applicable in a variety of archaeological contexts. Some obsidian sources still have evidence of quarrying and debitage from workshops, so its procurement can also be

studied. The flaked obsidian artifacts themselves can be examined as well for indications of the techniques used to fashion them. Unlike metal or ceramic artifacts, obsidian is not processed, mixed, recycled, or otherwise compositionally altered during the manufacture of tools. Obsidian artifacts hydrate, but the alteration is limited to the outer layer. Lastly, as Glascock et al. (1998) maintain, the "composition of obsidian at any particular source or flow is, with few exceptions, homogeneous and different sources... are compositionally different from each other" (17). Therefore, if one follows the steps outlined by Rapp and Hill (1998) -- sampling of all possible sources, selecting a suitable analytical technique to measure the chemical fingerprints, and choosing a statistical technique to assign artifacts to the most likely sources -- obsidian sourcing should be possible.

This does not mean that obsidian sourcing is without challenges, discussions, and debates. Many outstanding issues, both theoretical and practical, in obsidian sourcing are most recently discussed in *Archaeological Obsidian Studies: Method and Theory*, edited by M. Steven Shackley (1998a). He lists some of the frequent questions:

> How certain can we be that a piece of debitage less than 7 mm in diameter and 1 mm thick is actually from the source assigned by the analyst? How many samples are a minimum number to characterize a source? How variable is obsidian source chemistry in a single source? (3)

When relevant to my research, these issues and others, such as what comprises a "source" of obsidian, are discussed in later in this dissertation. For example, issues about obsidian sources and their sampling are discussed in Chapter 4, and evaluating the effectiveness of my analytical and statistical techniques are discussed in Chapter 6.

1.3.5 - The Goals of Obsidian Sourcing Studies

Recall that the sixth and last assumption of sourcing studies, according to Wilson and Pollard (2001), is that any patterns of obsidian movement can be interpreted in terms of human behavior, like exchange or territorial mobility. Glascock (2002) asserts that the identification of "actual goods in the archaeological record that were exchanged between different areas… are the most tangible evidence that an archaeologist can hope for when looking to establish contact between prehistoric peoples" (1). Sourcing studies can easily establish whether obsidian was moved locally or over long distances. Exchange implies social contact and, therefore, transmission of ideas between groups. With the application of various middle-range theories, some archaeologists hope to make inferences about the economic, political, or social organization of the people involved. Many of these studies have theoretical underpinnings in Lewis Binford's concept of space utility: "Space utility is gained when energy and matter can be put to work over a greater geographical area by transporting them beyond the geographical area from which procured" (1967).

The information from sourcing studies is often used to address questions about the procurement and utilization of obsidian in antiquity. For hunter-gatherers, the movement of obsidian is commonly interpreted as evidence of their foraging radius, territory size, or seasonal mobility (e.g., Mellars 1996:141-168, Andrefsky 1998:219-229; Shackley 2005: 118-133). Mellars (1996) points out that lithic sourcing research, when applied in Middle Palaeolithic contexts, can reveal the cognitive planning processes of Neanderthal groups (141). For complex societies, like those in Mesoamerica, sourcing is used to investigate

economic systems and the exchange mode by which the raw material or finished artifacts changed hands (e.g., Braswell and Glascock 2002). Sourcing has also often been applied to studying issues of ethnicity, migration, and relationships among groups (e.g., Shackley 2005:134-146). The value of this raw material may be explored due to differences in the exchange of everyday and prestige goods (e.g., Ammerman et al. 1990). Mellars (1996) contends that sourcing studies "can provide a direct insight into patterns of movement of human groups over the landscape" (141), so Molyneaux (2002) uses obsidian sourcing to consider issues of landscape, particularly landmarks and cognitive mapping. Gender and social identity have even been investigated using obsidian sourcing (e.g., Shackley 2005: 147-171). The concepts of *supply zone*, *contact zone*, and *monotonic decrement* from the early obsidian sourcing research of Colin Renfrew and his colleagues (Dixon et al. 1968, Renfrew et al. 1968) will be discussed in the next chapter.

The limitations of obsidian sourcing should also be briefly acknowledged here. In a discussion on the application of obsidian sourcing in the American Southwest, Shackley (2002:69) points out some of the information that is inaccessible via sourcing:

> It will not tell us how long that obsidian nodule was carried or exactly how it was procured. The range designated by obsidian geochemical analyses could be the result of procurement a few weeks or a few years before it entered an archaeological context. It is certainly possible that the glass could have been obtained through exchange rather than direct procurement with a distant relative while in the uplands or lowlands.

These, and other, limitations must be kept in mind during any sourcing study.

A thorough discussion on all applications and aims of obsidian sourcing as well as its role in studying exchange systems is well beyond the scope of this dissertation. Entire books have been written on these topics, including Earle and Ericson (1977), Ericson and Earle (1982), Torrence (1986), and Dillian and White (2009). My own goals for obsidian sourcing in the present research are explained at the end of Chapter 3.

1.4 - Analytical Techniques for Obsidian Sourcing

M. Steven Shackley, the director of the Geoarchaeological XRF Laboratory at the University of California-Berkeley and the author of *Obsidian: Geology and Archaeology in the North American Southwest*, wrote: "Just about the most frequently asked question by archaeology students is: 'Which instrument is best to analyze my stone objects?' The answer, unfortunately, is: 'It depends...'" (2005:89). This question, though, is not limited to students. Which techniques are "best" is a topic of much discussion.

It is only a small exaggeration to claim that nearly every analytical technique has, at some point, been utilized to study obsidian. These techniques include (in no particular order; with at least one citation, although not necessarily the first or most important one): atomic absorption spectroscopy [AAS] (Wheeler and Clark 1977, Michels 1982), optical emission spectroscopy [OES] (Cann and Renfrew 1964), back-scattered electron [BSE] imaging (Burton and Krinsley 1987), electron microprobe analysis [EMPA] (Merrick and Brown 1984), electron paramagentic resonance [EPR] (Daraban et al. 2002), fission-track [FT] analysis (Duranni et al. 1971), electron spin resonance [ESR] (Duttine et al. 2003),

Fourier Transform infrared spectrometry [FT-IR] (Conde et al. 2009), inductively coupled plasma atomic emission spectroscopy [ICP-AES] (Stevenson and McCurry 1990), laser-ablation inductively coupled plasma mass spectrometry [LA-ICP-MS] (Gratuze 1999, de B. Pereira et al. 2001), Mössbauer spectroscopy (Longworth and Warren 1979), neutron activation analysis [NAA] (Gordus et al. 1967), nuclear reaction analysis [NRA] (Murillo et al. 1998), particle-induced X-ray emission [PIXE] and gamma-ray emission [PIGME] (Nielson et al. 1976), Raman spectroscopy (Bellot-Gurlet et al. 2004, Carter et al. 2009), Rutherford backscattering spectroscopy [RBS] (Murillo et al. 1998), scanning electron microscopy [SEM] with energy-dispersive X-ray spectrometry [EDS] (Biro and Pozsgai 1984; Acquafredda et al. 1996), secondary ion mass spectrometry [SIMS] (Anovitz et al. 1999), spectroscopic ellipsometry [SE] (Frahm 2009, unpublished), thermoluminescence [TL] (Huntley and Bailey 1978), transmission electron microscopy [TEM] (Swanson et al. 1989, Stevenson et al. 1996), X-ray diffraction [XRD] (Okuno et al. 1996), and X-ray fluorescence [XRF] (Bennet and D'Auria 1974, Nelson et al. 1975).

In a *Nature* article on analytical techniques in archaeological research, Ashworth and Abeles (1966) contend, "There are many different methods of chemical analysis, but the majority of them can be disregarded" (9). The same can basically be said of obsidian sourcing. Some of the above techniques were used to study obsidian for geoscience, not sourcing, research -- this includes TEM and XRD. Other techniques -- for instance, RBS and SE -- were only used in very small-scale "proof-of-concept" tests, some of which did not even analyze a single artifact. A few -- like BSE -- worked in a specialized situation

to resolve two sources but have limited widespread applicability. Others -- such as NRA and RBS -- have not seen widespread use in obsidian sourcing. Still other techniques are so new to obsidian sourcing -- like EPR and ESR -- that they are currently being assessed, often in just one area of the world. Furthermore, some analytical techniques -- SIMS, for example -- would be too expensive for analyzing large numbers of geological specimens and artifacts. The common thread of all these issues is that the techniques have been used to analyze only small numbers of obsidian specimens and artifacts, making it challenging to rigorously evaluate their widespread usefulness to obsidian sourcing.

The list of frequently employed techniques for obsidian sourcing is actually much shorter. Green (1998) contends that four techniques "stand out" from the others: neutron activation analysis (NAA), X-ray fluorescence (XRF), inductively coupled plasma-mass spectrometry (ICP-MS), and proton-induced X-ray emission/gamma-ray emission (PIXE/PIGME) (228). Shackley (1998a) emphasizes the same ones: "nearly every archaeologist who sends his or her samples to an analyst anywhere on the globe will send it to a lab that uses [XRF, NAA, ICP-MS] or PIXE/PIGME, particularly the former two" (3). Glascock et al. (1998) agree and state "XRF and NAA have proven to be highly cost effective and, therefore, are the methods most frequently used to source artifacts" (19). Carter similarly claims that "NAA and XRF represent the mainstay techniques," and he asserts that these analytical techniques were responsible for the growth of obsidian sourcing after the early work of Colin Renfrew and his colleagues, John Dixon and John Cann, who used optical emission spectroscopy (OES) semi-quantitatively (2010, in prep).

In fact, all of the current laboratories in North America that either are dedicated to obsidian sourcing or provide obsidian sourcing as a routine service use NAA and/or XRF for the analyses. NAA of obsidian has been done at the Archaeometry Laboratory of the University of Missouri Research Reactor Center (MURR) for two decades, and XRF has been recently added to their repertoire. Both NAA and XRF of obsidian are conducted at McMaster University in Ontario. XRF is used at two privately-owned obsidian-sourcing laboratories: Northwest Research Obsidian Studies Laboratory in Corvallis, Oregon and Geochemical Research Laboratory in Portola Valley, California. The Geoarchaeological XRF Laboratory at the University of California-Berkeley uses, of course, XRF to source obsidian; however, this facility is scheduled to shut down soon.

Given the prevalence of XRF and NAA in the field of obsidian sourcing and that a component of my dissertation is assessing a different analytical technique for sourcing, I compare my data to that from both XRF and NAA in Chapter 6 as part of the assessment of my technique. I also discuss these techniques in Chapter 6 so that readers have a basic familiarity with them and how they compare to EMPA. Here, though, I briefly cover the specimen requirements, which are usually destructive, and I describe how XRF and NAA are both bulk (or "whole-rock") analytical techniques that provide an overall composition of specimens, even those that are mixtures like ceramics or even obsidian.

In X-ray fluorescence (XRF), a specimen is bombarded by X-rays with a specific energy and wavelength (commonly about 40 keV and 0.03 nm, respectively). As a result, the specimen reemits X-rays with energies and wavelengths characteristic of the elements

present. The X-rays are easily reabsorbed, so only the specimen surface, from a depth of less than 1 mm to over 1 cm, is analyzed. Thus, XRF is classified as a surface analytical technique, and it is also often considered a bulk technique because the area analyzed is on the order of a few square millimeters to square centimeters. The ideal specimen for XRF has a flat, smooth surface, so one either (1) polishes specimens, (2) grinds specimens into fine powders and then fuses them into discs, or (3) analyzes unaltered specimens with the understanding that there will be additional, but perhaps acceptable, error.

In neutron activation analysis (NAA), specimens are exposed to a neutron source, usually inside a nuclear reactor, making some of the elements radioactive. The elements are identified and their concentrations measured using characteristic gamma rays emitted during their radioactive decay. Neutrons easily penetrate most materials, so the core of a specimen is irradiated as much as its surface. In addition, gamma radiation is penetrative enough that photons emitted at the core of a specimen can be detected. These two factors make NAA a bulk analytical technique. NAA is almost always destructive, necessitating a specimen of 50-100 mg or more be removed from an artifact, subjected to the neutrons, and eventually discarded as low- to medium-level radioactive waste.

1.5 - Lessons from Ceramics Sourcing

Julian Henderson, an archaeologist at the University of Nottingham and an expert in ancient glass technology and sourcing, has called obsidian studies "a macrocosm of the development of archaeological science" (2000:305). He explains that obsidian "might be

claimed is one of the better candidates for chemical characterisation" and, therefore, "has produced some exceptional results" (305). On the other hand, Wilson and Pollard (2001) contend that ceramics "account for the vast majority of all [sourcing] studies undertaken" and tend to provide "a greater challenge than lithics in that there is a much greater degree of anthropogenic manipulation of the raw material" and in that they are complex mixtures of materials (511). Therefore, researchers doing ceramic sourcing studies have dealt with challenges not faced, or commonly ignored, in obsidian sourcing studies and have learned from them. The lessons learned by ceramic researchers can also be applicable in obsidian sourcing, and one of these -- dealing with mixtures -- is the topic here.

1.5.1 - Ceramics as Mixtures and Sourcing Effects

The use of NAA in archaeological research was originally suggested by J. Robert Oppenheimer (Sayre and Dodson 1957:35). Oppenheimer is known as "the Father of the Atomic Bomb," but while he pursued physics, he had a wide range of interests, including geology and classics (Carnes 1999). In 1954, Oppenheimer suggested that Edward Sayre and Richard Dodson, chemists he knew from the Manhattan Project but who were then at Brookhaven National Laboratory, use NAA to analyze sherds from Mediterranean vessels and figurines. In 1956, Oppenheimer invited archaeologists and chemists to the Institute for Advanced Study to discuss NAA, and Sayre and Dodson presented their results at this meeting and in an *American Journal of Archaeology* paper in 1957.

The aim of Sayre and Dodson (1957) was to determine whether the ceramic sherd compositions "as revealed by neutron activation would correlate with and be indicative of the regions of origin" (36). They analyzed fifteen sherds from five archaeological sites in the Mediterranean region. The observed radioactivity was dominated by signals from the sodium and manganese contents of the ceramics, and they "found that the ratio of sodium to manganese activities, which are predominant among the [radioisotopes] formed, show such correlation" between origins and chemistry (36). In other words, Sayre and Dodson (1957) focused on Na and Mn simply because those were the two strongest signals in the spectrum they were capable of measuring at the time. The chemists were optimistic (e.g., "The indication of this preliminary investigation is that sherds from certain regions show characteristic impurity patterns," 40), but they suggested caution due to the small number of specimens analyzed and the lack of information about inter- and intra-source variations and how manufacturing processes affect the ceramic composition.

Eight years later, in 1965, Ralph A. Johnson and Fred H. Stross, scientists at Shell Development Company, analyzed Valley of Mexico ceramic sherds using NAA. Johnson and Stross (1965) analyzed the eleven sherds for Na and Mn, citing the analyses of Sayre and Dodson (1957), and Mn concentrations were converted into percentages. An article by archaeologists James A. Bennyhoff and Robert F. Heizer followed and presented their interpretations of the data. They separated the Cuicuilco and Teotihuacán sherds into two groups based on their Mn content: one with 890-720 ppm Mn and the other with 660-430 ppm Mn. Bennyhoff and Heizer concluded that the two groups represented two different

clay sources. They argued that exchange occurred between the sites because three sherds from Cuicuilo had Mn contents similar to those from Teotihuacán. Also as a result, they point out, the two ceramic types represented (and therefore the associated cultural phases) must have been contemporaneous for such exchange to exist.

Ceramic analyst Anna O. Shepard (1966) questioned their interpretations in a later article. She asserted their study "raises fundamental questions about choice of analytical methods and interpretations about choice of analytical methods and interpretation" (870). Foremost of her objections is the choice of Bennyhoff and Heizer to use NAA. NAA can measure the overall (or "bulk") composition of a sherd with high sensitivity, but it cannot determine the distributions of the measured elements within the ceramic. Hence, Shepard asserts that NAA "does not identify the potters' raw materials" (1966:871). Ceramics are mixtures composed of clay, mineral and/or rock inclusions that occur naturally within the clay, and temper particles that have been deliberately added, not to mention pigments and slip and/or glaze layers. Shepard points out that choosing bulk analytical techniques, like NAA, to analyze ceramics "raises problems of interpretation: did the significant elements come from the clay, or from the temper, or from both?" (871).

Shepard's solution was to use EMPA to investigate Mn distributions in the sherds from Cuicuilco and Teotihuacán. She stated that, in this case, use of EMPA "to determine the location of the manganese was a perfect selection of a highly specialized instrument" for a specific problem (1966:871). Analyses with EMPA revealed Mn occurred primarily in the clay, not the temper, in the form of inclusions only one or two microns in diameter,

and the concentration of Mn within these inclusions was as much as 15%. Only a small variation in the abundance of these natural inclusions, perhaps due to layering within one clay bed used over a long time, may yield the observed pattern in overall Mn contents. In fact, a quick calculation reveals that, if these inclusions are 15% Mn and the overall sherd concentration of roughly 500 ppm (average for the Teotihuacán sherds), the abundance of the inclusions in that ceramic is about 0.3% of the volume. At roughly 800 ppm (average for Cuicuilco), the inclusions comprise about 0.5% of the volume. That tiny difference in the inclusion abundance produces the two compositional groups.

In 1997, archaeologist Glenn Summerhayes published "Losing Your Temper: The Effect of Mineral Inclusions on Pottery Analyses." He analyzed pottery from Papua New Guinea using EMPA and PIXE-PIGME (proton-induced X-ray and gamma-ray emission) to investigate their production and distribution. He emphasizes "in particular the problem of compensating for the chemical noise that arises when mineral inclusions are added to a clay in the manufacturing process of pottery" (108). If one does not consider this noise in the data, it can lead archaeologists to create erroneous models of ceramic technology and exchange. He points out that ceramics made from a single clay source will have different overall compositions if there are different quantities of minerals and/or different varieties of minerals. EMPA avoids this problem by separately analyzing clay and inclusions, both naturally occurring and deliberately added. Accordingly, a compositional group "defined using this technique is made up of the ceramic matrix only" (111).

Other ceramic researchers have similar conclusions about the effects of inclusions on chemical analyses of ceramics, especially the addition of "noise" to any compositional groups. For instance, Olin and Sayre (1971) showed, based on analyses of tempered and non-tempered 16th-century British pottery, that adding temper to ceramics could "dilute" the measured concentrations of elements in the clay. Bishop (1980) held that the addition of temper may dilute some elements' concentrations and enrich others and that the degree of this effect would vary from element to element. Studying Guatemalan pottery, Arnold et al. (1978), found that the ash-tempered ceramics differed in composition from the clay alone. Rice (1978), also using materials from the Valley of Guatemala, made mixtures of clay and temper in different proportions and found statistically significant differences in some element concentrations. Testing materials from the same region, Bishop and Neff (1987) showed that temper, when added in different amounts, can produce compositional groups within ceramics made using materials from just one source.

Neff et al. (1988, 1989) rigorously investigated how temper can affect the overall composition of the resulting mixture, focusing, in particular, whether temper can hide the use of multiple clay sources. They identify a number of factors that affect the magnitude of the chemical "noise" due to temper: the compositions of the clay and temper, the initial differences between the clays, and the amount of temper and its heterogeneity. They note that this chemical "overlap increases with increasing temper no matter what combination of components is mixed" (1989:65) and that the "heterogeneous temper more drastically attenuates the separation between clay source-related compositional groups" (1988:170).

Based on the experiments, Neff et al. (1989) conclude that "tempering may create as well as destroy compositional patterning" (68) when temper is added in different amounts or if it has multiple components itself. Ultimately, though, they deduced...

> for the simulated components used in this study, temper characteristics had little effect on the practical separability of clay source-related groups when clays and tempers were mixed in proportions which approximate real-world proportions. This result suggests that compositional investigations need not exclude tempered ceramics from analysis. The confounding effect of temper may not be as serious as is commonly assumed, at least for situations in which untempered clays are quite distinct. (1988:170)

In other words, if the raw clay sources are "quite distinct" initially, the resulting ceramics are, in practice, separable into clay-source groups, regardless of the temper characteristics when added in real-world abundances, despite the additional "noise" in the compositional data. When the different clay sources are not so distinct, though, the effects of temper are more severe and can cause the compositional groups to overlap.

1.5.2 - Application to Obsidian Sourcing

Although not often treated as such, obsidian, like pottery, is a mixture, that is, two or more substances that are not chemically combined with each other. The glassy matrix is one substance, microscopic black magnetite crystals are another, and each other type of mineral inclusion is a different substance as well. Various researchers have addressed the issue of sampling mixtures to obtain a representative composition (e.g., Benedetti-Pichler 1956, Kratochvil and Taylor 1981, Smith and James 1981), and statistical equations have been used in the chemical analysis of archaeological ceramics to determine representative

specimen sizes (e.g., Bromund et al. 1976, Bower et al. 1986). Such equations depend on knowing the abundance and size of each type of inclusion within a specific volume. The abundances, sizes, and compositions of inclusions in obsidian vary from source to source, but, to my knowledge, such sampling questions have not been widely used by researchers utilizing a bulk analytical technique, like neutron activation analysis (NAA), to determine representative specimen sizes for obsidian from the different sources. The only example of which I know is Francaviglia (1984), who explained:

> The size of the single samples has been conditioned either by the natural size or by number and size of macroscopic inclusions within each single piece. It is evident that if in a piece of obsidian there are inclusions of 2-3 mm in size, with an average distance of 10 mm from each other, it would be necessary to collect samples containing at least some 20 inclusions. Otherwise, the sample would no longer be representative. (312)

I would argue this situation is far from "evident" as such observations in the literature are rare. The alternative to making observations about inclusion size and abundances, doing these calculations, and analyzing specimens of only a calculated size is instead to utilize a technique that can measure only the glass and avoid inclusions. Both Shepard (1966) and Summerhayes (1997) chose electron microprobe analysis (EMPA) to separately analyze the components of ceramics, so I selected the same technique to measure only the glass of both geological obsidian specimens and obsidian artifacts.

1.6 - Introduction to EMPA

One of my goals in this research was to determine if electron microprobe analysis (EMPA) is reliable and valid for obsidian sourcing, and this was tested by studying Near Eastern geological sources of obsidian and artifacts from the Bronze-Age archaeological site of Tell Mozan. EMPA is an analytical technique used to measure the composition of a small area on a specimen surface. A beam of accelerated electrons is focused onto the specimen, producing highly magnified images of the surface as well as X-rays indicative of the elements present. Like any tool, EMPA is better suited to address some problems than others: a wrench, which excels at tightening and loosening nuts and bolts, can serve as a crude hammer to drive nails, but is useless for turning screws. My goals, therefore, included evaluating the validity of modern EMPA for obsidian sourcing.

Part of what makes EMPA such a useful analytical tool is that, unlike many other analytical techniques, it permits simultaneous investigation of structure and composition: the electron beam simultaneously creates highly magnified electron images of a specimen surface as well as X-rays indicative of the elements present and their concentrations. The structural information investigable using EMPA should, however, be clarified. Kingery (1996) defines "structure" as how "the component parts of an object or assemblage… are arranged and how their interactions result in particular properties. There are many levels of structure" (176). Such levels include macrostructure, microstructure, crystal structure, and atom-electron structure. In EMPA, the electron images and element maps can reveal information about a specimen's microstructure. Features smaller than 100 nm (10^{-4} mm)

can be seen and those larger than 1 μm (10^{-3} mm) can be analyzed. Information about the crystal structure of a specimen cannot be *directly* collected but may, in some instances, be inferred. Therefore, EMPA permits the investigation of both components -- structure and composition -- of geochemical and materials-science characterization.

1.7 - Prior Obsidian-Sourcing Studies with EMPA

The first suggestion to utilize EMPA for archaeological sourcing of volcanic glass came from ceramics research. Since the 1960s, geologists had utilized EMPA to analyze volcanic glass fragments in ash for tephrachronology, matching the composition of these glassy fragments to a particular eruption. These ash layers, once matched to an eruption, could serve as a time marker. In a paper on the potential of EMPA for sourcing ceramics and investigating their manufacture, Ian Freestone (1982) suggested:

> The application of the microprobe to [ceramic] provenance studies may provide useful supplementary data to standard thin section work… where identifiable rock fragments exist in the fabric but these have a petrography which is not sufficiently definitive to identify their source, microprobe analysis may allow a more precise determination. *A good example of this is volcanic glass inclusions, the chemistry of which may be highly diagnostic of the source region.* (107, emphasis added)

Freestone explains that these volcanic glass fragments are common in Mesoamerican and Mediterranean ash-tempered ceramics. Analyses of the fragments, he claims, may reveal compositions "characteristic of volcanoes from a particular 'petrological province' and in some areas of a particular volcano" (109). He includes an example of such an analysis on

an ash-tempered Anatolian sherd and concludes that EMPA "of volcanic glass inclusions is likely to provide a good indication of provenance" (110).

Despite predictions that EMPA would become useful for obsidian sourcing (e.g., Kempe and Templeman 1983:45-46) and its dominance in tephrachronology, only three sizable studies have used EMPA with the goal of obsidian sourcing: Merrick and Brown in Kenya (1984), Weisler and Clague in Hawaii (1998), and Tykot in the Mediterranean (1995, *inter alia*). A few obsidian studies claimed to use a "microprobe" but really used scanning electron microscopy with energy-dispersive spectrometry (SEM-EDS), not true EMPA-WDS (Keller and Seifried 1990; Biró and Pozsgai 1984; Biró et al. 1986). Tykot (1997) mistakenly cites Merrick and Brown (1984) as one such study; however, they did, in fact, use EMPA-WDS (232). SEM-EDS is sometimes used in obsidian sourcing, often supplemented by other techniques (e.g., Abbès et al. 2003), and some of the studies were quite small and did not analyze even a single artifact (e.g., Acquafredda et al. 1996, 1999; Le Bourdonnec et al. 2006). Consequently, I will overlook these SEM-EDS studies at the moment and concentrate on those that actually used EMPA-WDS. During the course of this dissertation, another team presented their research at Italian conferences on sourcing Mediterranean obsidian via EMPA (Le Bourdonnec et al. 2005b, 2010; Sanna et al. 2010). I exclude this project here for three reasons: (1) the same sources were studied by Tykot (1995, *inter alia*) in greater detail with EMPA; (2) these three conference papers were published after I started my research, and two were published only this year; and (3) the conference papers do not provide sufficient analytical details to evaluate. Additionally,

during the course of this research, I learned of the work of Keiji Wada and his colleagues (Wada et al. 2003, Wada 2009) to study Japanese obsidians, and similarly these papers do not include sufficient details to asses their analytical methods.

1.7.1 - Merrick and Brown in East Africa

After their initial study with XRF and wet chemical methods, Harry Merrick and Francis Brown (1984) used EMPA to analyze obsidian outcrops in central Kenya as well as artifacts from the same area. They held that this analytical technique could be "a very useful tool... whenever differences in the concentrations of major and minor elements are sufficient to distinguish between obsidian sources" (1984:230).

Over 50 obsidian sources in the Kenya Rift Valley and the surrounding highlands were sampled, and wet chemical and XRF analyses of these obsidian specimens revealed their compositions. Merrick and Brown identified 22 chemically differentiable obsidians that correlated with different sources. In particular, they realized that their Fe, Ca, and Ti contents could be used to distinguish them by EMPA. The iron alone separated them into three groups. They point out that, while earlier studies used trace elements as an "elegant and reliable means of" obsidian sourcing, there will be areas like East Africa where major and minor elements can sufficiently distinguish the sources (235).

There were, though, some limitations in their study. The three analyzed elements were present at relatively high concentrations: between 10% and 0.1% (1000 ppm). They note that, in some cases, trace elements and/or additional elements might be necessary for

sourcing. For example, Merrick and Brown note that trace elements might "be necessary in many cases to distinguish between chemically similar sources," and they also point out that "some source assignments could not be satisfactorily made to individual source areas within the Eburu volcanic complex using only the three elements" (235). Future electron microprobes, they speculate, will be able to analyze additional elements concurrently, and "should provide sufficient data to distinguish most sources if they can be characterized on the basis of major and minor elements" (235). In other cases, Merrick and Brown (1984) explain, those "artifacts requiring additional trace element analysis for assignment" could be first analyzed with EMPA and identified for further analyses (235).

Merrick and Brown also put a high priority on speed. The instrument they used -- the University of Utah's ARL-EMX, a microprobe from the 1960s that output the data on punch cards -- could measure only three elements simultaneously, so Merrick and Brown selected just three elements for analysis. In fact, it took them a mere six hours to analyze 260 artifacts -- each artifact was analyzed for an average of 1.4 minutes. For comparison, in the present research, I analyzed each artifact for 20 elements over a total of almost two hours. Merrick and Brown even called their article "Rapid Chemical Characterization of Obsidian Artifacts by Electron Microprobe Analysis, " and their goal was to demonstrate "the utility of the electron microprobe in rapidly and relatively inexpensively establishing the probable source of obsidian artifacts" (1984:235).

Merrick and Brown (1984) note that obsidian almost always contains microscopic mineral inclusions, such as quartz and feldspar, within its matrix (231). Their procedures

apparently included avoidance of these inclusions since they state “microphenocrysts are easily avoided when analysing with the electron microprobe” (231).

1.7.2 - Weisler and Clague in Hawaii

Marshall Weisler and David Clague (1998) utilized EMPA to characterize basaltic obsidian sources and artifacts from Hawaii. The distribution of obsidian, they maintain, indicates the scale, complexity, and duration of interaction among prehistoric societies of the islands of Oceania, citing the obsidian sourcing studies on Aegean and Mediterranean islands. During the 1950s and 1960s in Hawaii, obsidian “was thought of little scientific value and was routinely discarded on the back dirt piles” (113). In fact, the only previous sourcing study of Hawaiian obsidian was done by Weisler (1990).

Weisler and Clague (1998) analyzed artifacts from nine sites and specimens from the West Moloka’i Volcanics geological province, aiming to investigate contact between prehistoric groups on the Hawaiian island of Moloka’i. They explain:

> During late prehistory it is generally believed that each traditional land unit *(ahupua’d)* was economically self-sufficient (Handy and Pukui 1958; Earle 1978) and that exchange of resources was primarily between productively specialized households within *ahupua’a.* Examination of the distribution of fine-grained basalt and volcanic glass resources in relation to political boundaries suggests, however, that some form of interaction or exchange must have occurred. Taking the island of Moloka'i as an example, we analyzed volcanic glass source samples and artifacts from two different settlement regions. (114)

They state that EMPA “is especially well-suited to... these specimens since only the glass itself is analyzed by excluding phenocrysts and other inclusions” (114).

Weisler and Clague analyzed for eleven elements (Na, Mg, Al, Si, P, S, K, Ca, Ti, Mn, and Fe), and they selected two plots -- TiO_2 vs. MgO and TiO_2 vs. CaO -- to highlight the chemical differences among sources (117). These were not trace elements within the specimens: TiO_2 varied between 2% and 5%, MgO varied between 3% and 7%, and CaO varied between 7% and 11%. Weisler and Clague found that the compositions of most artifacts, when plotted, fell into "a tightly defined array that overlaps the array defined by unaltered lava and glass samples from West Moloka'i" (121). Fifty artifacts from the six sites originated from nine outcrops (122). About 70% of the artifacts derived from three sources, and 47% came from the source nearest the sites.

Although they analyzed only the glassy matrix using EMPA, Weisler and Clague also identified the tiny minerals found in the nine obsidian varieties from West Moloka'i. One type of obsidian, for instance, contained abundant olivine crystals while another type contained scarce crystals of plagioclase and clinopyroxene. Because the specimens were prepared as thin sections, it is likely these minerals were identified petrographically under a visible-light microscope. The minerals were useful for differentiating some sources -- a few types of obsidian, Weisler and Clague note, "are distinguished by mineralogy as their glass compositions are similar, and in some cases, overlapping" (121).

1.7.3 - Tykot in the Western Mediterranean

Robert H. Tykot (1995, *inter alia*) also used EMPA to study obsidian artifacts and sources of the western Mediterranean. He wanted to address the spatially and temporally

dynamic economic and social role of obsidian in the western Mediterranean, and because obsidian artifacts have been unearthed at over a thousand sites and comprise as much as 100 percent of lithic assemblages, a sizable number of analyses was necessary (1996:46). Therefore, Tykot was interested in "low-cost, major-element analysis for determining the provenance of hundreds of artifacts" (1998:72), and he chose EMPA. As of 1995, he had measured 9 to 11 elements in 433 total analyses on 125 specimens (114). By 1998, Tykot had nearly 2000 analyses on about 700 specimens. Hence, his study is the largest of the three prior projects discussed here. In comparison, the present research incorporates over 12,000 major-element analyses and 13,000 trace-element analyses on over 900 geological obsidian specimens from southwest Asia and more than 100 artifacts, each of which was quantitatively analyzed for 20 major and trace elements.

Prior studies had shown that archaeologically significant Western Mediterranean obsidian sources could be characterized by major and minor elements (e.g., Francaviglia 1984, 1988). Based on initial experiments with ICP-MS, Tykot corroborated this finding (1996:45; 1997:473-475). Accordingly, Tykot decided to use EMPA "since the precision of the microprobe is superior to laser ablation ICP-MS, only a tiny l - 2 mm sample needs to be removed, sample preparation is minimal, and the per-sample cost is equally low -- a fraction of the price of XRF or NAA" (1998:75). Note that his preparation of artifacts for analysis was destructive, just like the two other projects discussed.

Recall Merrick and Brown (1984) stated that small mineral inclusions in obsidian "are easily avoided when analysing with the electron microprobe" (231), and Weisler and

Clague (1998) also apparently avoided inclusions actively to guarantee that only the glass was analyzed (114). Tykot, though, seems to have taken a different approach. He spread out the electron beam more than prior researchers, and two to four points "were tested, in case a phenocryst contributed to the analysis." (1995:113). The broader beam, he hoped, would "ensure that microlites or other heterogeneous inclusions did not contribute to the analysis" (1997:474). He was confident that he could recognize an analysis that involved an inclusion, and he claims that "it was necessary to purge the results of only a few of the 433 analyses" due to the contributions of minerals (1995:113-114).

Based on his results, Tykot concluded there were chronological and geographical differences in the utilization of Sardinian obsidian sources (1998:70). He claims that the exploitation of multiple Sardinian sources clarifies obsidian procurement and distribution in Neolithic Italy, but these findings raise issues about exchange mechanisms when, as he showed, several island sources were concurrently used (70). He wonders, for example, if there are functional and aesthetic differences among sources (1996:62). More sourcing data are needed, and Tykot asserts that EMPA "allows comprehensive sourcing of entire obsidian assemblages and the effective statistical comparison of spatially and temporally dynamic obsidian source exploitation patterns" (1998:79).

1.8 - Research Goals for EMPA and Obsidian Sourcing

As I discuss in Chapter 5, EMPA has greatly advanced since the original research of Merrick and Brown (1984), who used an instrument built in the 1960s that output data

on punch cards. Merrick and Brown (1984) had a straightforward research goal: to show "the utility of the electron microprobe in rapidly and relatively inexpensively establishing the probable source of obsidian artifacts... by relying heavily on differences in major and minor elements" (235). The subsequent researchers, to varying degrees, shared this same goal, and all three analyzed tiny, polished chips from obsidian artifacts.

Here I mention my goals regarding developing and evaluating modern EMPA for obsidian sourcing. Most importantly, I decided to analyze the artifacts non-destructively, which apparently has not been previously attempted on a sizable artifact set.

- *Glass-only analyses:* As previously established, obsidian is a mixture, so I used EMPA to analyze only the glass component of the geological obsidian specimens and artifacts. I expected that glass-only analyses might "tighten" some of the chemical fingerprints for Near Eastern sources. Comparisons of EMPA data to XRF and NAA data can reveal how measured concentrations are affected by bulk ("whole-rock") versus spot analyses due to inclusions.
- *Non-destructive artifact analyses:* I sought to analyze the obsidian artifacts without removing any chips or polishing away the exteriors to expose fresh material. Instead, I analyzed the artifact exteriors that had been affected by post-depositional processes, namely hydration and diagenetic alteration (or weathering). I hoped that at least a few of the measured elements would be either negligibly or predictably altered, meaning sourcing would be possible.

- *Trace-element analyses:* EMPA has been regarded as an analytical technique suited to major and minor elements but not trace elements. I sought to assess the ability of EMPA to analyze trace elements in obsidian specimens, ranging in concentration from dozens to thousands of parts per million. I accomplish this using analytical conditions optimized for trace elements, modifications to the software, and at least ten analyses per specimen or artifact.
- *Evaluation of accuracy, precision, reliability, and validity:* In Chapter 6, I use the basic framework suggested by Richard Hughes (1998), including *accuracy* and *precision* as well as *reliability* and *validity*, to assess my EMPA and data analysis techniques for sourcing obsidian artifacts.

1.9 - Summary and Concluding Remarks

The study of obsidian is a central component of much archaeological research for three principal reasons: (1) obsidian tools have been used for almost all of human history, from at least two million years ago until modern times; (2) obsidian has also been used on every continent inhabited by people; and (3) obsidian has been used for multiple uses and in a variety of contexts, from scraping hides to providing magical protection. The present research, though, focuses on a particular time, location, and technology: the flaked-stone tools, especially prismatic blades, from Bronze-Age strata of Tell Mozan, ancient Hurrian city of Urkesh, within the Khabur Triangle of northeastern Syria.

Although obsidian is best described as volcanic glass, it is not a perfect glass free of minerals. All obsidians contain mineral inclusions in the glassy matrix. The minerals are often microscopic (or even nanoscale), but their existence can frequently be observed as "ribbons" or bands within obsidian, especially in thin flakes. The varieties, sizes, and abundances of these minerals may vary greatly from source to source, and their presence will affects the overall (i.e., bulk) composition of obsidians, possibly obscuring the subtle differences between chemically similar sources. To control for these differences, earlier studies have focused on trace elements that tend to remain in the glass (i.e., incompatible elements) rather than concentrate within the minerals (i.e., compatible elements). This is, however, a largely false dichotomy. The conditions experienced by the lava as well as its geochemical variety (i.e., peralkaline or calc-alkaline) and the minerals present will affect the partitioning of elements between the glass and inclusions.

It will always be better to treat obsidian like the mixture that it is and, if possible, analyze its components separately. A spot analytical technique, like EMPA, can measure the glass composition independent of the inclusions. The two most analytical techniques most frequently used in obsidian sourcing -- XRF and NAA -- can only measure the glass and minerals together. These two techniques, which are very sensitive for trace elements, are also popular because "sourcing" is often considered synonymous with "trace-element fingerprinting." Major elements, though, may also be useful for sourcing when measured precisely and, as discussed in Chapter 2, are crucial for discerning two chemically similar obsidian sources in Turkey (i.e., Nemrut Dağ and Bingöl A). As shown in Chapters 5 and

6, with the proper choices, EMPA can analyze the major elements in obsidian with higher precision than other techniques commonly used for sourcing.

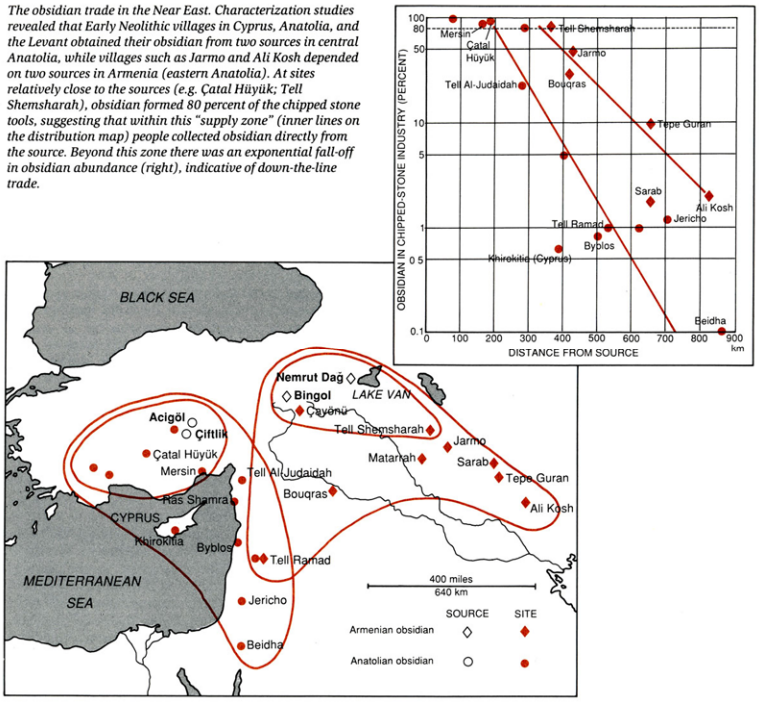
Despite such benefits, EMPA has rarely been used for obsidian sourcing. Its most well-known application is the work of Merrick and Brown (1984) in East Africa. These two researchers, though, used an instrument built in the 1960s that output data on punch cards, and EMPA has greatly advanced since their research. Merrick and Brown (1984) also placed a priority on speed, analyzing 260 artifacts in six hours, rather than precision and complete analyses. Additionally, all three prior studies involved analyzing polished chips removed from artifacts, making their analyses destructive.

As part of my research, to source artifacts from the previously mentioned context (i.e., Bronze-Age Syria), I redeveloped EMPA, taking advantage of recent advancements, for obsidian sourcing in a new century. Key components of this redevelopment included: (1) glass-only analyses to remove the effects of mineral inclusions on bulk compositional data; (2) non-destructive analyses of artifacts, involving no cutting or even polishing; (3) measuring trace elements at concentrations much lower than those measured in the earlier studies using EMPA; and (4) a rigorous evaluation of the accuracy, precision, reliability, and validity of my techniques. The successes of these goals led to new information about obsidian use in the Near East, as I discuss in Chapters 7, 8, and 9.

Part I: Foundations and Problems

Chapter 2:

Obsidian in the Near East: State of Knowledge



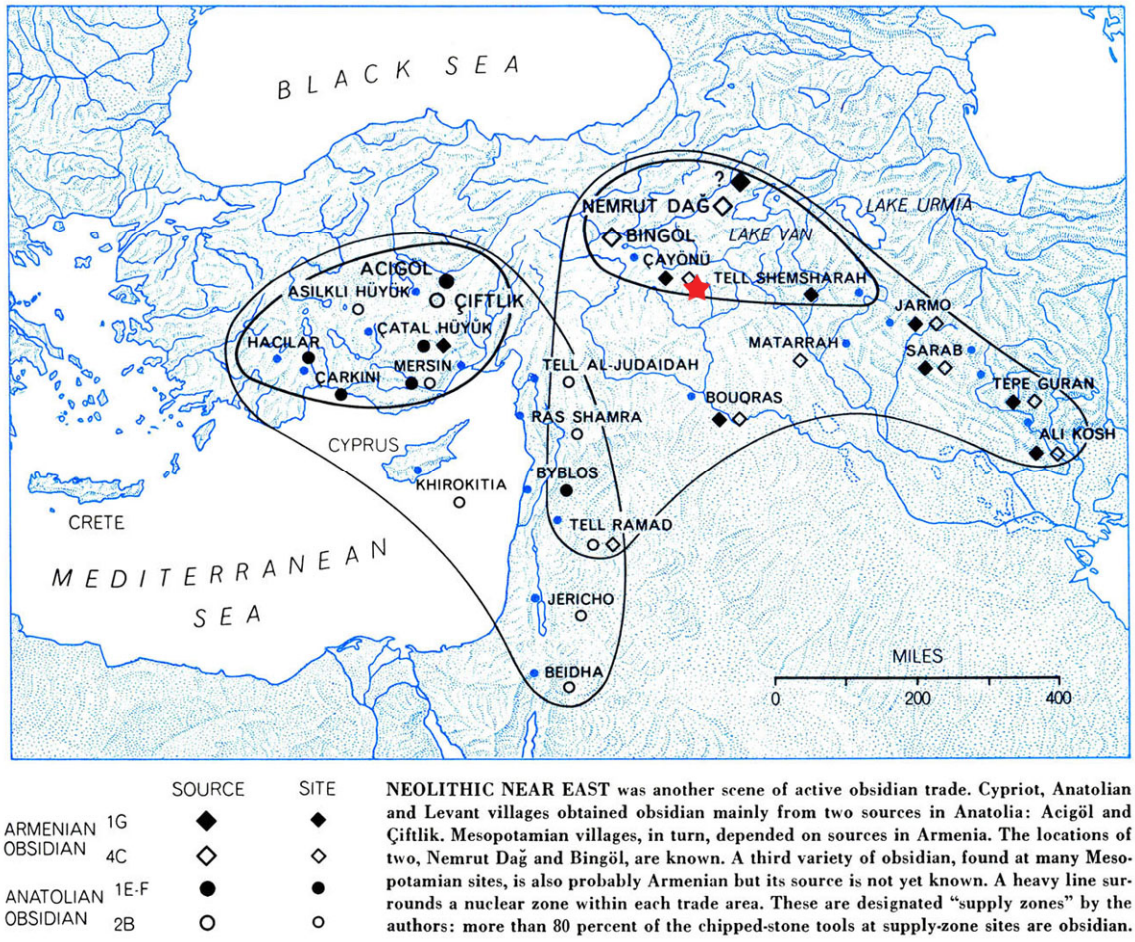
-- Colin Renfrew and Paul Bahn, 2008, *Archaeology: Theories, Methods, and Practice*

I have taken the unusual step to quote figures, rather than text, at the start of this chapter to emphasize their importance in obsidian sourcing in the Near East. This graph and map are, in fact, the most reproduced illustrations in all of obsidian sourcing and are from the research of Colin Renfrew, John Dixon, and Joseph Cann (RDC). The graph in

the upper right shows "fall-off curves" for obsidian abundance in the lithic assemblages at a set of Near Eastern archaeological sites, and it first appeared in Renfrew et al. (1968: 328) and Dixon et al. (1968:87). The map in the lower left corner is a redrawn version of a figure in Dixon et al. 1968 (Figure 2.1) that shows the distribution of obsidian during the Neolithic. Similar maps for Neolithic appear in Renfrew et al. (1966, 1968), Renfrew and Dixon (1976) (Figure 2.2), and Dixon (1976) (Figure 2.3). These figures have been reproduced in other publications, including Colin Renfrew and Paul Bahn's introductory textbook, now in its fifth edition and the source of the figures at the start of this chapter. The post-Neolithic distribution maps appear in Renfrew et al. (1968), Dixon et al. (1968) (2.4), Dixon (1976) (Figure 2.5), and Renfrew and Dixon (1976) (2.6). These later maps are especially important for my research on the Bronze Age.

These figures from RDC, now over four decades old, simultaneously popularized obsidian sourcing and, arguably, stagnated it in the Near East. Their work still represents the largest regional-scale obsidian-sourcing study in the Near East, and it rests entirely on a total of 160 artifacts from 53 archaeological sites spanning five millennia. Each site on that map is represented, on average, by a mere three artifacts. By comparison, the largest regional-scale study in the New World was done as part of a pipeline expansion project in the 1990s: over 9000 obsidian artifacts from over 130 Oregon, California, and Idaho sites were sourced (Skinner 1995), that is, almost 70 artifacts per site.

Four decades after RDC, obsidian sourcing research in Near Eastern archaeology lags behind that in the New World, and in comparison, there is a serious lack of raw data,



NEOLITHIC NEAR EAST was another scene of active obsidian trade. Cypriot, Anatolian and Levant villages obtained obsidian mainly from two sources in Anatolia: Acigöl and Çiftlik. Mesopotamian villages, in turn, depended on sources in Armenia. The locations of two, Nemrut Dağ and Bingöl, are known. A third variety of obsidian, found at many Mesopotamian sites, is also probably Armenian but its source is not yet known. A heavy line surrounds a nuclear zone within each trade area. These are designated "supply zones" by the authors: more than 80 percent of the chipped-stone tools at supply-zone sites are obsidian.

Figure 2.1 - RDC's best-known rendering of their proposed obsidian "supply zones" and "contact zones" during the Neolithic Period. Figure from Dixon et al. (1968). A red star has been added to mark the location of Tell Mozan (ancient Urkesh) in Syria.

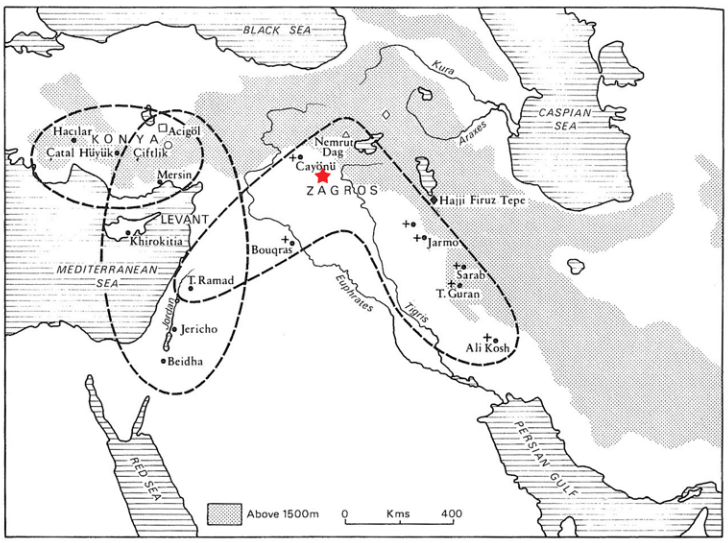


Figure 2. Obsidian interaction zones *c.* 7,500-5,500 B.C. In the Levant zone the obsidian is predominantly of group 2b (from Çiftlik); in the Konya zone, of group 1e-f (from the Acigöl region); in the Zagros zone, of group 4c (from the Nemrut Dağ area) and of group 1g. Find-spots of group 1g obsidian are indicated by a cross. The single known find-spot of group 3 obsidian of this period is indicated by a lozenge.

Figure 2.2 - RDC's "obsidian interaction zones" during the Neolithic, circa 7500 to 5500 BCE. Figure from Renfrew and Dixon (1976). A star marks the location of Tell Mozan.

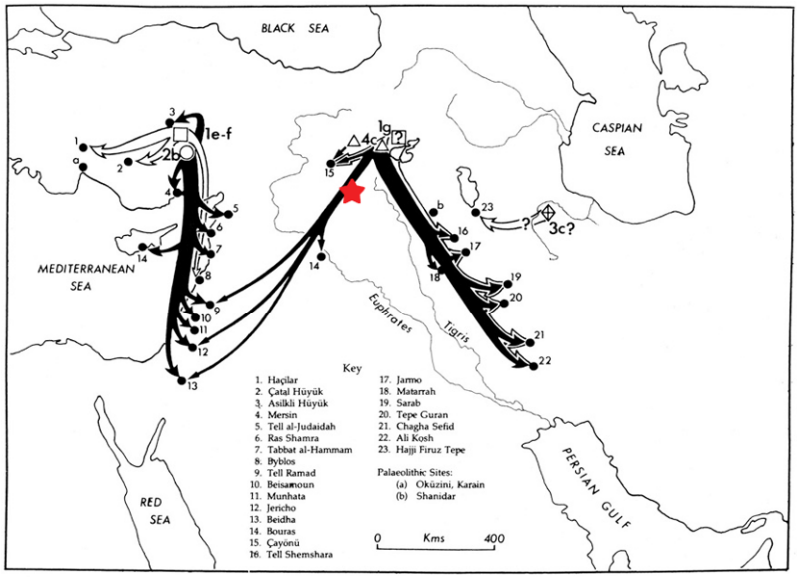


Figure 15.13. Sources and dispersal of Near Eastern obsidian, 7000 B.C.–ca. 5200 B.C. The arrows link sources to sites but are not intended to imply a specific route or mechanism of trade. Data are from references 3, 4, 8, 50, 51, and 71.

Figure 2.3 - RDC's obsidian distribution patterns during the Neolithic, circa 7000 to 5200 BCE. Figure from Dixon (1976). A red star marks the location of Tell Mozan.

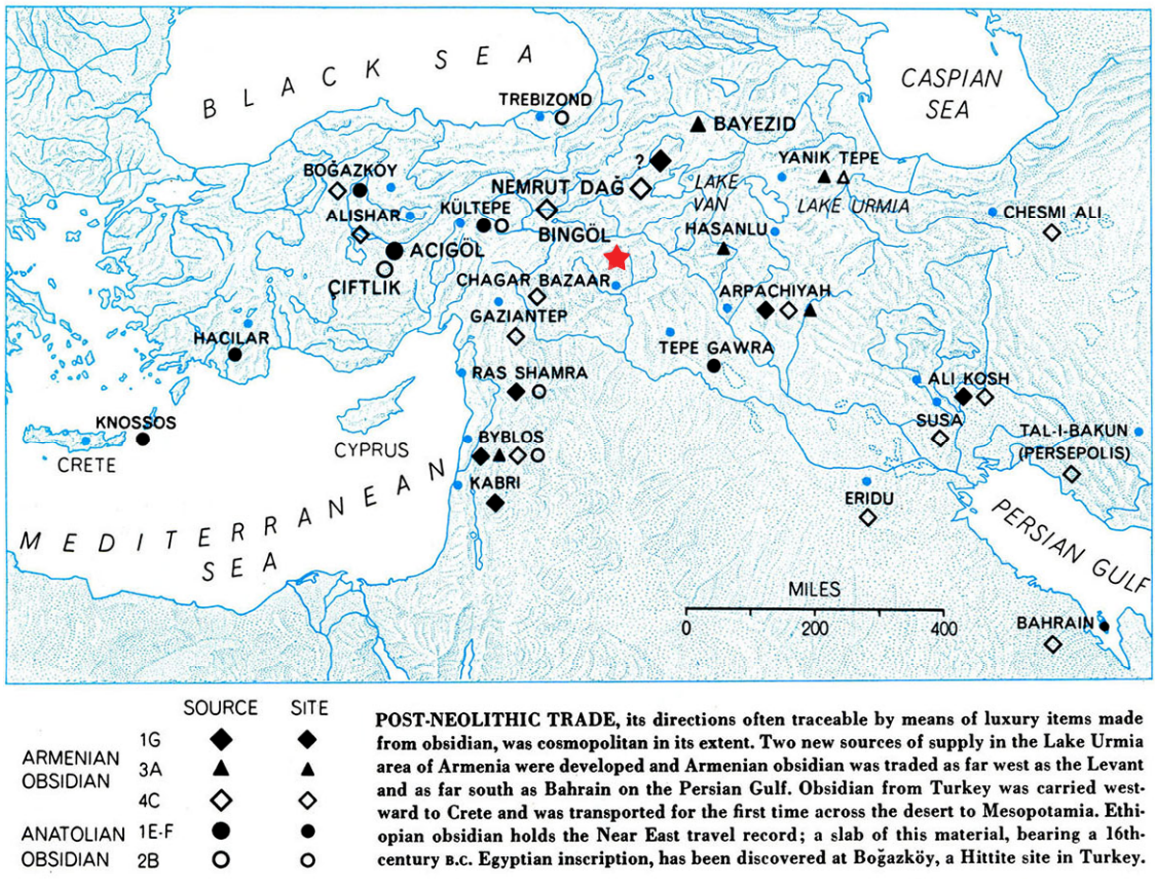


Figure 2.4 - RDC's obsidian sourcing results for the post-Neolithic Period. Figure from Dixon et al. (1968). A red star has been added to indicate the location of Tell Mozan.

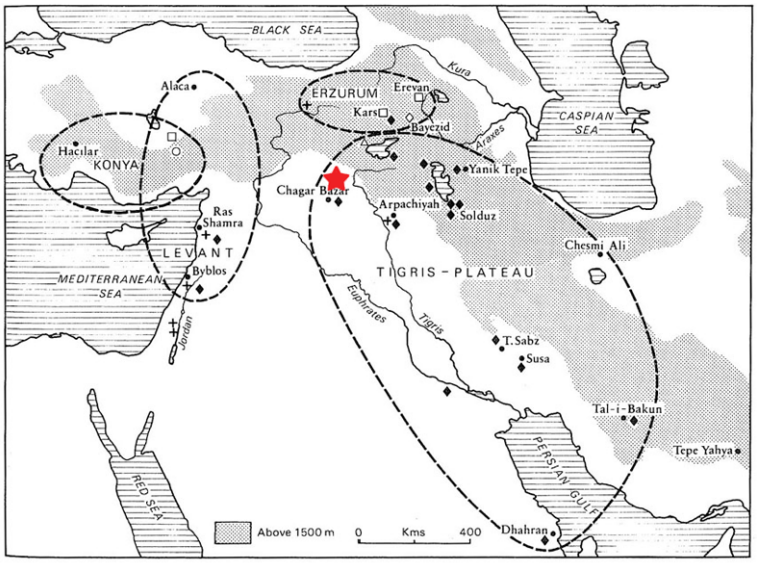


Figure 3. Obsidian interaction zones *c.* 5,000-3,000 B.C. In the Erzurum zone the obsidian is predominantly of group le-f (from sources in the VAA area); in the Tigris-Plateau zone, of group 4c and group 3. Find-spots of group lg obsidian are shown by crosses; of group 3 obsidian, by lozenges.

Figure 2.5 - RDC's post-Neolithic obsidian distribution patterns, circa 5000 to 3000 BCE.

Figure from Renfrew and Dixon (1976). The red star marks the location of Tell Mozan.

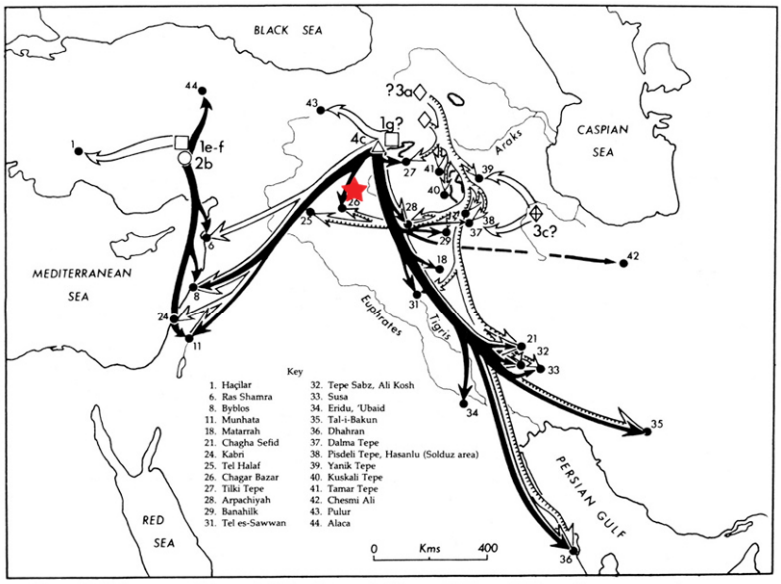


Figure 15.14. Sources and dispersal of Near Eastern obsidian, ca. 5,200 B.C.–2000 B.C. (data sources and comments as for Fig. 15.13).

Figure 2.6 - RDC's post-Neolithic obsidian distribution patterns, circa 5200 to 2000 BCE.

Figure from Dixon (1976). The red star marks the location of Tell Mozan.

that is, sourced artifacts, particularly from post-Neolithic contexts in Mesopotamia. For example, in a paper titled "Obsidian Trade in the Near East in Neolithic and Bronze-Age Times" (Gratuze et al. 1995), the entire Bronze Age is represented by only nine artifacts from Ras Shamra (ancient Ugarit; circa 1300 BCE) on the Mediterranean coast of Syria. By my estimates, prior to my research, only 41 obsidian artifacts have been sourced from all of Bronze-Age Syria. My research increases this sum by 230%, and my analyses were non-destructive, which will be necessary to continue this work.

In this chapter, I start by discussing the uses of obsidian in the ancient Near East, and I argue that a dichotomy often found in the literature, between flaked-stone/utilitarian and ground-stone/ritual-elite, is specious. Regarding RDC's initial research, I discuss the archaeological *zeitgeist* that led to their endeavor to source obsidian in the Mediterranean, Aegean, and Near East. I briefly consider the models (e.g., monotonic decrement, down-the-line exchange, the gravity model) developed to describe their obsidian data as well as some criticisms of these models. The main problem, though, was that their raw data (i.e., sourced artifacts) were insufficient. As I reveal, a lack of data remains today, particularly after the Neolithic, in Mesopotamia. In fact, for reasons that I discuss, obsidian sourcing had diminished in the Near East since the mid-1980s whereas it has flourished in the New World. Consequently, a number of issues, most dating back to RDC, are still found in the literature. Recent work at another site in northeastern Syria, one widely publicized as an obsidian production center, highlight several of these problems.

2.1 - Uses of Obsidian in the Near East

Numerous obsidian-sourcing studies, both in the Near East and elsewhere, report the probable geological origins of the obsidian used to make artifacts without discussing how obsidian artifacts were likely used. Here I attempt such a discussion. Obsidian has been utilized in Southwestern Asia since at least 30,000 BCE: flakes, likely from eastern Turkey, have been found at Shanidar Cave in Iraq, a site inhabited by Neanderthals. My research, though, is focused primarily on the Bronze Age (circa 3500 to 1300 BCE). The following discussion has largely been informed by Akkermans and Schwartz's book *The Archaeology of Syria* (2003), Steven Rosen's *Lithics after the Stone Age* (1997), and the references cited within and supplemented by Mortensen (1973) at Neolithic Choga Mami in Iraq; Nishiaki (1993, 2000, 2003) on Neolithic and Chacolithic Syria, particularly Tell Kosak Shamali; and Copeland (1989, 1996) and Verhoeven (1999) at Neolithic Tell Sabi Abyd in Syria. I largely restrict the discussion only to uses of obsidian, but chert tools, in general, have been subjected to more functional analyses. I shall also focus on Northern Mesopotamia rather than Greater Anatolia or the Southern Levant.

2.1.1 - Artifacts from the Epipalaeolithic to the Bronze Age

During the Epipalaeolithic, obsidian first occurs at archaeological sites as flakes, often unworked. Blades and bladelets eventually become part of the flaked-stone toolkit, as do small geometric microliths, typically made from bladelets and having a number of shapes, such as triangles, trapezes (i.e., trapezoids), and lunates (i.e., half-moon shapes).

It is widely believed that the microliths are the remnants of composite tools. They could have been used as projectile points or barbs by inserting them into a grooved wood shaft and hafting them using bitumen. If set end-to-end in a bone or wooden handle, they may have been useful as knives, perhaps for reaping plants. Microwear research suggests that microliths were indeed mounted in such composite tools and that bladelets, bearing wear-marks of cutting wild grasses, were employed as sickles.

The Epipalaeolithic lithic industries continued during the Pre-Pottery Neolithic A (PPNA): the blades, bladelets, and geometric microliths, especially lunates, dominate the assemblages. During the tenth millennium BCE, a new type of projectile point emerges: the so-called El Khiam point, named for the site (and contemporary town) in Lebanon, is fashioned out of a blade and has a triangular point and side notches. These points clearly were mounted on spears and used for hunting. Microliths decreased in popularity during the ninth millennium BCE, and blade production seemingly became more standardized as their sizes and shapes are more uniform. These blades were, in turn, modified to produce other types of tools, like the aforementioned El Khiam projectile point or scrapers, borers, and burins (a blade with a chisel-like corner, probably for carving bone or wood). Blades were occasionally denticulated (i.e., finely notched), and based on bitumen traces and the microwear evidence, they were mounted in crescent-shaped wood, bone, or antler handles and used as sickles and knives for cutting grassses and reeds. In the Pre-Pottery Neolithic B (PPNB), there were several types of notched and tanged projectile points, including the

leaf-shaped Byblos point, and scrapers. Parallel-sided bladelets, commonly unretouched, predominate most obsidian assemblages during this period.

Uses of obsidian seems to vary quite a bit during the Late (Pottery) Neolithic. On one hand, there is a use of simple flakes, largely or totally unmodified, as expedient tools and probably for a variety of purposes that require no particular tool shape. On the other hand, specialized tools -- sickle blades, points, scrapers, burins, and borers -- were still in use. Blades, sometimes denticulated, were apparently broken into short segments for use as sickles, probably for reaping plants or perhaps for shearing animals. At Yarim Tepe in Iraq, obsidian scrapers and blades from eighth-millennium levels bear use-wear evidence of their application in butchering and maybe hideworking (Merpert and Munchaev 1993). At about this period, the large projectile points, like the Byblos and Amuq points, become less common and are supplanted by smaller points and transverse arrowheads. Verhoeven (1999) has examined chert tools from sixth-millennium levels of Tell Sabi Abyad in Syria and discusses evidence for plant- and wood-processing, butchering, hideworking, boring, and carving (Table 6). In the sixth- and fifth-millennia, blades and unmodified flake tools dominate the lithic assemblages at most sites. In the Khabur Triangle of northern Syria, it appears that chert nodules were frequently just smashed into pieces using a hammerstone, and the random fragments were employed as expedient tools. At the same time, polished obsidian vessels, beads, and jewelry first appear in Mesopotamia.

During the fourth millennium BCE, projectile points are already rare, and formal borers and similar tools decrease in popularity. One significant development is a type of

prismatic blade known as the Canaanean blade, first identified in the Southern Levant but can be found throughout Mesopotamia and the Levant. These long and wide blades have parallel sides and two parallel ridges down their entire dorsal surfaces, and the result is a trapezoidal cross-section. The "Canaanean" label tends to describe only chert blades with this form, not similar obsidian blades. Some have proposed that sites like Tell Brak were production centers for such blades and that these products were distributed over a certain region. These artifacts are commonly identified as sickle blades. Some (Anderson 1998, Anderson and Chabot 2001, Anderson et al. 2007), though, have proposed that the blades and their segments were instead used as "teeth" on an agricultural implement known as a threshing sledge. Much like a raft of logs or planks lashed together, a threshing sledge is used to cut straw and separate grain, and the bottom is covered with blades or fragments, chert or obsidian, as many as 2000 pieces (Anderson 1998:154). A second important tool is the tabular scraper, fashioned from large retouched flakes.

During the third millennium BCE, microborers, notches, and bladelets occur with less frequency and usually with specialized purposes, like working mother-of-pearl in the palace at Tell Hariri (ancient Mari) in eastern Syria. Chert and obsidian were still used to make projectile points despite the appearance of metal spearheads. Blades, including the prismatic types, continued to be utilized, at least in part, as harvesting tools. During the second millennium, sickle blades were more often the Large Geometric type, which some authors have also suggested were produced at specialized sites.

Blades, which were used as sickles, were the most common lithic tools and lasted from the Epipalaeolithic to the Bronze Age. It is hardly surprising that obsidian, with its especially sharp edges, was chosen for cutting and scraping tools. Sickles were probably used for harvesting grasses and cereals, both wild and domesticated, but they also might have been used for cutting reeds, woodworking, or even tilling soil. When mounted in a row, the blades could have been used for any cutting application. The possibly misnamed "borers" might have been used for engraving and similar tasks. "Scrapers" might also be misnamed because, in addition to scraping, suggested applications include butchering and shearing. Notched blades could have various purposes, perhaps scraping wood and bone. Simple flake tools, retouched or not, might have been used in any application that needed a sharp cutting or scraping edge. The uses of obsidian vessels, for example, are even less evident. Intact obsidian vessels have been recovered in Mesopotamia only from a fourth-millennium-BCE tomb at Tepe Gawra and the three-millennium-BCE tomb of a queen or priestess in the Royal Cemetery of Ur (Coqueugniot 1998).

2.1.2 - "Utilitarian/Domestic" versus "Ritual/Symbolic/Elite"

Flaked-stone tools are commonly named for their suspected functions (e.g., sickle blades, borers, scrapers, projectile points), and ground obsidian artifacts (beads, mirrors, rings, and vessels) are often recovered from mortary and/or elite contexts. Consequently, some researchers have labelled flaked-stone tools as "utilitarian" and "domestic" artifacts while suggesting that ground-stone artifacts are likely affiliated with "ritual and elite" use

or have "symbolic value." Although it is tempting to make such associations, these two categories reflect the techniques used to manufacture the artifacts and should not directly be used as proxies for "utilitarian" versus "ritual" applications.

An examination, though, of Near Eastern textual sources reveals why ground and polished artifacts are often associated with ritual uses. The Chicago Assyrian Dictionary Project (hereafter abbreviated CAD) has assembled a comprehensive dictionary of terms from Akkadian-language texts, circa the third and second millennia BCE, recovered from Near Eastern archaeological sites. The Akkadian word *surru* has been translated obsidian or chert. Based on contextual evidence, *surru* refers to a stone that (1) can be flaked and have a sharp edge; (2) can also be ground into beads; (3) can be considered a valuable or precious stone; and (4) has a characteristic appearance: shiny, transparent, black or green, sometimes with lines (i.e., flow bands) (1962:257-259). Association of this term with the dull, opaque, grey and tan chert in this region seems questionable.

Assuming that *surru* refers to obsidian, the Akkadian texts from Mesopotamia and the Levant indicate a variety of "ritual and elite" uses for ground obsidian objects. There are, for example, references to necklaces made using beads of obsidian, gold, lapis lazuli, and other stones. One necklace is described as having "five lapis lazuli beads, fifteen of obsidian, fifteen small (beads of) *pappardillu*-stone" (257). Some of the necklaces, made of obsidian beads and other stones, had apotropaic purposes -- that is, they were intended to ward off evil and diseases (258). Such beads were sometimes also put on the forehead or toted around in a leather bag as magic charms (258). One tablet instructs: "You string

hulālu and black obsidian [beads] and place [them] on [the magic figurine]" (258). Other texts explain that an obsidian-like stone is used "to dispel the wrath" of a certain god and that "you crush black obsidian into [bitumen]" as an elixir (258).

Jacques Cauvin (1998) argues that obsidian beads were more than only decorative and had magical-religious significance ("signification magico-religieuse," 81). Beads of obsidian, gold, lapis lazuli, carnelian, and other stones, he suggests, had purposes beyond aesthetics -- each material would have had a specific meaning, perhaps symbolizing such concepts as power, authority, wealth, piety, and sanctity. Coqueugniot (1998) agrees that obsidian had important roles in magical rituals ("un rôle important dans la magie et… les rituels d'ensorcellement," 352) in Mesopotamia. Like Cauvin (1998), he believes that the stone beads in necklaces were chosen and arranged chiefly for symbolic reasons. He also notes that obsidian beads may have been sewn to clothes for protection or luck. There is, for example of an obsidian amulet (circa the early first millennium BCE), now housed in the Metropolitan Museum of Art, that is inscribed with a spell to protect from Lamashtu, a goddess who tormented pregnant women and kidnapped their babies. Coqueugniot also discusses the symbolism of obsidian in the Levant, Anatolia, Egypt, and the Aegean area. Especially noteworthy are the "two-finger" obsidian amulets from pharaohic Egypt (circa first millennium BCE), depicting the index and middle fingers and placed on a mummy's embalming incision, perhaps to hold closed and protect the wound.

Highly polished obsidian mirrors have been discovered in Anatolia (Çatal Hüyük, circa seventh millennium BCE) and the Levant (Tel Kabri, circa fourth millennium BCE)

and described by classical authors (Decourt 1998). Cauvin (1998) contends that polished obsidian mirrors were most likely used for divination and were equivalent to crystal balls rather than cosmetic mirrors. Coqueugniot claims, like Cauvin, that magic abilities were attributed to obsidian mirrors, such as revealing hidden worlds during divination rituals ("la vision des choses cachées avec l'usage de l'obsidienne dans des rites de divination," 358). Mirrors have long been associated with magic and witchcraft, particularly as a tool for scrying, that is, seeking spiritual visions or divination in a reflective surface, including a crystal ball or a vessel of water (e.g., Moyer 2008a, 2008b).

Akkadian texts also suggest, though, that the "utilitarian" obsidian blades also had symbolic and ritual uses. One tablet describes bloodletting using an obsidian blade: "You make an incision in his temple with an obsidian blade and draw blood" (CAD 1962:259). Another tablet mentions self-mutilation as an act of mourning: "Instead of saying, as you have, 'Let us go and talk with our brothers (the Assyrians),' let us (rather) tear our heavy garments (and) take the [obsidian] knife (to slash ourselves as a sign of mourning)" (259). In the Levant, a text instructs that balsam trees in the Eid Gedi oasis should not be cut by iron or bronze tools but instead by blades made of bone and stone such as obsidian (Faure 1987:87-88). Coqueugniot (1998) interprets this passage to mean that metal blades were considered unclean and/or unnatural compared to obsidian and other rocks and, therefore, unsuited to specific tasks. According to Egyptian texts, obsidian blades were used to cut umbilical cords, to circumcise, and to eviscerate corpses during mummification (Aufrère 1991:563-567), that is, for cuts at the beginning and end of life.

Jacques Cauvin (1998) contends that, because chert was available in the Near East and because it can perform similarly for flaked-stone tools, the use of obsidian was more about flashiness than functionality. Thus, he maintains, that the presence of obsidian is a cultural, not technological, phenomenon ("un phénomène de nature culturelle," 379) and that people transported obsidian far because it was exotic. He argues that, for sites in the Southern Levant and Southern Mesopotamia, obsidian tools are sufficiently rare that they could not have been a key part of their utilitarian technological systems. Projectile points of obsidian, Cauvin claims, seem to be works of art and likely were considered too fragile and valuable to risk loosing or breaking during hunting or warfare.

Various authors (e.g., Cauvin 1998, Coqueugniot 1998) have connected obsidian symbolically to eyes and vision, linking obsidian mirrors to inlays used to depict eyes in anthropomorphic sculptures throughout the Near East. The polished obsidian inlays and beads utilized for pupils on Egyptian masks and sarcophagi (Figure 2.7) are often cited examples. In Neolithic Mesopotamia and Anatolia, though, eyes were represented using obsidian blade segments and flakes. At Yanik Tepe in Iran, small obsidian flakes serve as the transparent eyes for the representation of a face on a bowl sherd, near its rim (Burney 1962:138, Plate 43, Figure 12). Obsidian fragments also represent eyes in the relief of a human head at Bouqras in Syria (Akkermans et al. 1983:346; 1978-1979:156, Figure 11). At Hacilar in Turkey, anthropomorphic vases and figurines have small obsidian chips for eyes (Mellaart 1970:139, Plate 172, Figs. 1, 2, and 5). Also in Turkey, a life-sized (about



Figure 2.7 - This portrait mask of a bearded man (right) from Egypt, circa 180 CE, is terracotta with inlaid obsidian eyes. (Photograph by the author; taken in the Egypt and Ancient Near East Gallery of the Minneapolis Institute of Art).

2 m tall) limestone statue found at Göbekli Tepe (officially called the "Balıklıgöl Statue" but locally dubbed "The Snowman") has blade segments for eyes.

Carter (2007) discusses the "theatricality" of long, "flamboyant" obsidian blades made for consumption during funerary rituals of the Bronze-Age Cycladic culture of the Aegean region. Complete, unused, and particularly fine obsidian blades have been found in Early Bronze Age Cycladic burials. The earliest grave assemblages include individual blades much like those utilized in other segments of society. Over time, entire blade "sets" were included in burials, and their lengths markedly increased, necessitating new knapping techniques that were not used in other contexts and producing what Carter calls a "necrolithic" technology. He suggests that, given the techniques necessary to make the blades, their production might have been a "theatrical" performance.

Across the world, in the Americas, symbolic and "ritual" uses of obsidian knives, blades, and lances have been documented archaeologically, ethnographically, and through historical accounts in various regions, particularly Mesoamerica (e.g., Aztec bloodletting, human and animal sacrifice, spiritual dances, ceremonial weapons; Griffen 1969, Michels 1971, Taube 1991, Bayman 1995, Saunders 2001, Carballo 2005), the American Midwest (e.g., found in Hopewell mortuary areas, possibly for processing and disposal of the dead; Anderson et al. 1986, Hatch et al. 1990), and California (e.g., bifacial knives and sacks of obsidian fragments used in dances; Dillian 2002, Hodgson 2007).

2.1.3 - Different Function, Different Exchange?

Though we cannot simply equate flaked-stone obsidian artifacts with "utilitarian" and "domestic" or ground-stone artifacts with "ritual and elite" use or "symbolic value," the two technologies are, for the most part, distinct (I show several exceptions from Tell Mozan in Chapter 7). Despite being made from the same material, different techniques must be used to produce prismatic blades over 15 cm long versus a stone bowl with sides only a few millimeters thick. Furthermore, their functions are distinct, so their roles in exchange systems might be as well. This was observed by M. James Blackman (1984) regarding the obsidian artifacts excavated at Tal-e Malyan in western Iran:

> Two general categories of objects may be defined based on function: utilitarian items -- tools (mostly blades), cores, and debris; and luxury items -- ground and polished bowls, bead/rings, and cylinders. The presence of spent cores and core trimming debris indicates that the blades were struck from the cores at the site rather than arriving as finished products... The luxury items, ground and polished objects, may well have arrived at Tal-e Malyan as finished products. Although a ground stone industry was present at the site, only relatively soft stone materials such as talc, chlorite, marble, and limestone appear to have been worked... It is likely that the luxury items and the raw material for the utilitarian items were being exchanged in terms of function rather than material type. As such, these two categories of object may have been included in different aspects of the exchange system. (22)

This is my major criticism of the work of RDC -- their post-Neolithic distribution pattern in Dixon et al. (1968) includes one of the obsidian vessels from a burial at Tepe Gawra in Iraq. They sourced the vessel to Central Anatolia, making it the farthest west occurrence of obsidian from these sources. This was the only obsidian vessel, though, in their work, and the same level at Tepe Gawra includes dozens of obsidian blades and a few cores. It

is unclear why the blades and cores were ignored in favor of this vessel. This brings us to our discussion of RDC and the influence of their initial research.

2.2 - The Research of Renfrew, Dixon, and Cann (RDC)

My intention is not to review all the research of Renfrew and his colleagues with respect to ancient obsidian trade (Aspinall et al. 1972; Cann and Renfrew 1964; Renfrew et al. 1965, 1966, 1968; Dixon et al. 1968; Cann et al. 1968, 1969; Renfrew 1969, 1970; Durrani et al. 1971; Dixon 1976; Hallam et al. 1976; Renfrew and Dixon 1976; Shelford et al. 1982). A complete review of their work would require an entire chapter, and I have already mentioned my major criticisms: (1) their distribution maps are based on very few geological specimens and, on average, two or three artifacts from about fifty sites, and (2) they have confounded their results by including ground-stone obsidian (i.e., a vessel from Tepe Gawra) with the flaked-stone artifacts because these two technologies likely played different roles in Near Eastern exchange systems. Others have offered various criticisms of RDC's results and models over the years (e.g., Wright 1969; Wright and Gordus 1969; Hodder and Orton 1976), some of which I will mention. I start, though, with an overview of topics of archaeological interest leading up to their research.

2.2.1 - The Archaeological Backdrop

Many archaeologists cite the research of RDC in the Mediterranean and Near East during the 1960s as the start of obsidian sourcing. Their collaboration is surely the most

well-known obsidian sourcing work; however, the quotation from John Lloyd Stephens in Chapter 1 reveals that the idea of using obsidian as evidence of exchange or mobility was not new. Indeed, the work of RDC built on that of a variety of researchers. For example, in the Mississippi Valley, Squier and Davis (1847) noted the discovery of obsidian points in burial mounds, and they proposed that comparing these artifacts to geological obsidian occurrences "might serve to throw some degree of light upon the origin and connections of the race of the mounds" (212). The initial research of RDC was, in part, an attempt to confirm or refute a widespread belief that obsidian from the Aegean island of Melos was the source of most obsidian artifacts unearthed in the Mediterranean and Near East. This belief was strongly influenced by Kroeber's cultural diffusion hypothesis (Kroeber 1940). It was thought that, just as ideas or cultural elements such as religions and languages may diffuse outward from one source area into surrounding regions, so too can technologies or materials like obsidian spread from a core to other areas and cultures.

Some early investigations of obsidian in the Mediterranean and Near East seemed to support Melian origins for many widespread artifacts. For example, in 1909, Thomas Eric Peet, known principally for his research as an Egyptologist, claimed that circulation of obsidian across the Italian mainland and Mediterranean islands "is a question of great interest and importance" (150). The obsidian flakes and cores found at an archaeological site in southern Italy, Peet argued, appeared, "judging from its transparency and lustre, to be from Melos and not Italian" (150). Cornaggio-Castiglioni and colleagues (1962, 1963) even used the same analytical technique as RDC (i.e., optical emission spectroscopy), and

they concluded, based on their manganese and phosphorous measurements, that obsidians at Italian archaeological sites primarily originated from Melos.

There were, of course, advocates for localized obsidian use as well. In the 1880s, Jean-Jacques de Morgan, a French archaeologist and mining geologist, surveyed obsidian outcrops in Armenia and eastern Turkey. He asserted, based on his visual inspection, that obsidian artifacts unearthed in Mesopotamia and Iran came from these, or nearby, sources and arrived there via exchange (de Morgan 1927). In 1904, in a report on excavations on the Aegean island of Melos, archaeologist R.C. Bosanquet expressed disappointment that it was not possible to discern obsidian from Melos and other sources. Bosanquet realizes that "it is only in the Eastern Mediterranean that we may safely treat obsidian as evidence of trade-relations with Melos" (229). Provisionally, he hypothesizes that Lipari, Sardinia, and Pantelleria islands were the sources of obsidian exploited in the Mediterranean and "the Caucasus and Russian Armenia for any found in the Black Sea and in eastern Asia Minor" (229). In 1927, Near Eastern archaeologist Gerald Wainwright studied obsidians used by the Egyptians. Obsidian does not occur locally, so he writes:

> … the presence of obsidian objects in a non-volcanic country is proof of trade with some centre of volcanic activity. Unhappily the scientific identification of any given piece of obsidian with specimens from any one deposit is beset with difficulties, so that it is at present impossible to say categorically that the given piece did, or did not, come from a certain locality. (77)

He discusses current thought about obsidian exchange across the Near East and asserts a preoccupation with "Melian obsidian trade has so engrossed archaeologists' attention as to blind them generally to other possibilities" (77). Wainwright contends:

> … when obsidian is found to be in such common use as it is in Armenia and Mesopotamia it is hardly possible to refer so vast a trade to an island so small and so remote as Melos until all possibilities of a nearer provenance have been exhausted. As a matter of fact there is a great obsidian field close at hand in Armenia itself upon which the Near East may have drawn without the necessity of going all the way to the farther side of the Aegean. (78)

Thus, popular opinion, chemical evidence (Cornaggio-Castiglioni et al. 1962, 1963), and at least one visual investigation (Peet 1909) proposed that Melian obsidian -- and, with it, Aegean culture -- had diffused throughout the Mediterranean and Near East. On the other hand, some argued that various local sources were more likely used, and two visual-based studies (de Morgan 1927, Garstang 1953) supported this hypothesis.

There were other influences on their work as well. For example, Grahame Clark, one of Renfrew's professors at Cambridge, published *Prehistoric Europe: The Economic Basis* in 1952. In this book, he argued that archaeologists can examine cultural elements of ancient societies, such as their social organization or perhaps even more abstract ideas, by studying the sources of the societies' raw materials and their movement. In particular, he focused on stone axes in Neolithic Europe, and this continued to be a topic of interest to Clark into at least the 1960s (e.g., Clark 1965). Clark, and likely Renfrew, would also have been familiar with other early archaeological sourcing studies, as covered by Pollard and Heron (1996:3-6), including Thomas' petrographic examinations that allowed him to identify the sources of the Stonehenge bluestones (Thomas 1923). In addition, interest in the transportation and storage of raw materials was gaining momentum as Lewis Binford formulated the concept of space utility (1965): "Space utility is gained when energy and

matter can be put to work over a greater geographical area by transporting them beyond the geographical area from which procured" (Binford 1967).

It was within this archaeological *zeitgeist* that Colin Renfrew approached Joseph Cann about characterizing and potentially sourcing Melian and other obsidians:

> There was an important obsidian source on the Cycladic island of Melos. When I began to think about the Cyclades, I saw that this presented a fascinating problem and that it ought to be possible to do something with it technically. An old school friend of mine, Joe Cann… was a fellow of St. John's College at that time and a research worker in the Department of Mineralogy and Petrology. It seemed very natural to discuss the problem with him, and we looked together at things like refractive index and specific gravity, which turned out to be no use at all, and it was he who suggested the optical emission spectroscopy approach. Then we did it very much together. We selected the material systematically and sat there grinding up the samples with pestles and mortars. A senior technician in their department ran the samples through the spectroscope, and Joe read off the data from the resulting photographic plates. What would emerge then would be a table of figures, and we had great fun together working out how we might best interpret those figures… (Renfrew in Bradley 1993:74)

In case it is still not clear from the above paragraph, the research of RDC was not initially conceptualized as an anti-diffusionist model, as is sometimes claimed:

> … the obsidian work arose out of the specific wish to characterize the Aegean material. Then when the result came through, it did prove to be anti-diffusionist in the sense that there was no Aegean obsidian in the West Mediterranean and no so-called liparite in the Aegean through the Bronze Age and into the Neolithic… so it did undermine the idea of very long-distance links in the Neolithic period. But that came as the result of the study; it was not an *a priori* belief. (74)

Thus, their obsidian sourcing research started as a way to investigate the Cycladic culture of the Early Bronze Age. These Aegean islands were settled in the fifth millennium BCE, and the Cycladic culture, a mixture of Anatolian and Greek influences, reached its height

during the third millennium before its assimilation into Minoan culture during the second millennium. Their later publications (Renfrew et al. 1965; Renfrew 1972, 1975) used the obsidian sourcing results to investigate development of the Minoan state and Mycenaean Greece and their roles in Bronze-Age Aegean exchange systems.

Although first developed for studying the Bronze-Age Aegean, obsidian sourcing has scarcely been applied to Bronze-Age Mesopotamia. Instead, the Neolithic revolution in the Near East, especially the origin of urbanism and agriculture, was an emerging topic of interest at this time. It was hoped that the distribution of obsidian across the Near East may reflect the spread of agriculture in the Fertile Crescent. In particular, archaeologists, especially researchers at the University of Chicago Oriental Institute, sought the Neolithic villages where agriculture arose and the mechanisms by which this invention spread from village to village, which were considered, at this time, to have been fairly isolated. The spread of obsidian throughout the Near East, even during the Neolithic, showed that these settlements were not isolated and hinted that, as obsidian moved, so too could have ideas, such as agriculture. Large Neolithic villages, such as Çatal Höyük, soon were interpreted to be obsidian trading centers, as proposed by Mellaart. Obsidian sourcing was also seen as a way to explore Gordon Childe's theories about nomads versus sedentary farmers. He had already proposed that the long-distance spread of exotic materials like obsidian could be explained by nomadism and the mobility of pre-agriculturalists.

Therefore, I suspect that the excitement about obsidian sourcing in the Near East and Aegean (which has been likened to a "gold-rush" by Özdoğan 1994:423) was due to

existing topics of great archaeological interest in those regions. In the Aegean, it was the development of the Minoan state and Mycenaean Greece and their roles within exchange systems, notably the circulation of Melian obsidian, during the Bronze Age. In the Near East, it was the rise of agriculture and the mobility of human groups during the transition from pastoral nomadism to sedentary agricultural villages. The interconnectedness of the Neolithic villages could also be explored using obsidian sourcing. It seems that, as these topics were "answered," there was less interest from Near Eastern archaeologists in the tool used to do so (i.e., obsidian sourcing). Thus, particularly for post-Neolithic contexts, obsidian sourcing has seen relatively little recent use in the Near East.

2.2.2 - Brief Overview of RDC

In 1962, RDC started their research as described in the prior section. They settled on optical emission spectroscopy (OES), which required 60 mg of powdered material, as their analytical technique. The analyzed artifacts outnumbered the geological specimens, and in fact, the obsidian distributions in Renfrew et al. (1966) are based on: (1) chemical analyses of 33 geological obsidian specimens from all of Anatolia and 132 artifacts from 42 Near Eastern archaeological sites, (2) obsidian abundance in the lithic assemblage of fourteen sites, and (3) the proportion of green obsidian among the obsidian artifacts of a dozen sites. Another 28 artifacts from even sites were added in Renfrew et al. (1968). In other words, their model is largely built on a total of 160 artifacts from 53 sites, and each site is, on average, represented by just three obsidian artifacts. Their analytical data were

supplemented by the color reports from twelve sites -- their assumption was that all green obsidian "derives from the... source at Nemrut Dağ" (1966:58).

RDC argued that, based on the obsidian source and abundance data, the observed distribution patterns could reveal exchange mechanisms and, perhaps, whether nomadic bands or settled agriculturalists were involved. This endeavor introduced the concepts of "supply zone" and "contact zone" as well as the use of fall-off curves (which actually are straight on their logarithmic plot) and the so-called "Law of Monotonic Decrement," that is, the quantity of obsidian decreases at a particular rate as a function of distance from its geographical source. RDC propose that, within a supply zone (where at least 80% of the lithic assemblage is obsidian), the artisans themselves, without intermediaries or traders, would have collected raw obsidian from the source. Beyond the supply zone, within the contact zone, obsidian was acquired via contact with other groups. Therefore, according to RDC, obsidian served as an indicator of "contact" between different Neolithic groups, and one may, in turn, define the range of the groups and their contacts. Çatal Höyük was a major influence on the size of the "supply zones" -- the abundance of obsidian there, at various times, ranged from 89% to 97%, and this site is roughly 250 km from Göllü Dağ and Acigöl. This data point had a large effect on the observed fall-off rate, so the supply zone radius, at least for Central Anatolia, is about 300 km.

Their obsidian distribution patterns covered three basic geographical regions: the Levant, Cappadocia (especially the Konya Plain, where Çatal Höyük is), and the foothills of the Zagros Mountains (eastern Mesopotamia, east of the Tigris River). RDC proposed

that, based on the different "fall-off rates" for the two main obsidian source areas and the distribution patterns, Central Anatolian obsidians may have been circulated by sedentary villagers (agriculturalists) whereas Eastern Anatolian obsidians may have been spread by migration of nomadic groups (pastoralists). In particular, RDC offered a model of "down the line" exchange, in which obsidian moved between groups by a series of exchanges, to account for exponential decline in its abundance with distance. One implication of such exchange is that there need not be traders or formal organization.

Later, additional components were added to the RDC model, specifically obsidian interaction zones and the gravity model. An "obsidian interaction zone" is an area within which all the sites have at least 30% of obsidian from a particular source, and a particular site can belong to more than one interaction zone. These overlaps mostly occur at sites in the Levant, like Tell Ramad in the Damascus Basin. The zones were intended to describe the spatial distribution of obsidian, not the mechanisms of exchange. The gravity model added an "attractiveness" to certain obsidian sources that would have been related to, for example, raw-material quality. If obsidians from various sources were available at a site, their relative abundances in the lithic assemblage would reflect the inhabitants' perceived "attractiveness" of those obsidians. In other words, it was suggested that more attractive obsidians should "outcompete" the less attractive obsidians.

When it was discovered that, especially in the fifth millennium BCE and later, the fall-off rate was always non-monotonic, the model was further revised. First, geographic features were added as a component, so distances were revised to include natural barriers

such as mountains and deserts. Second, redistribution from a central place was suggested as another explanation. Obsidian could have moved monotonically among central places, from which it could have been redistributed to neighboring settlements. Development of central place theory in archaeology was closely related to obsidian. This explanation was desirable because the origin of urbanism was another topic of great interest, and sites like Çatal Höyük and Jericho were being called the "first cities." Another suggestion was that obsidian followed the exchange of other materials, which had different starting points and ending points and which perhaps preceded the circulation of obsidian.

Wright (1969) offered some early criticisms of RDC's techniques. He suggested that the mass of artifacts, not just their counts, would be more insightful regarding to the amount of obsidian present at a site. He also proposed that RDC should not have simply lumped together all of the obsidian abundance data, regardless of time period, onto only one graph to show the fall-off. Their fall-off model, Wright argued, was not an accurate description for obsidian distribution from the Eastern Anatolian sources:

> The generalizations mentioned above which Renfrew derived from his graph seem to hold strictly only for the Central Anatolian supply zone and not for the Van sources... I have... added data not available to Renfrew (e.g., Çayönü). In contrast to Renfrew, I have not considered an entire site as one datum point, but have plotted the individual levels or phases: for example, Jarmo I and Jarmo II are plotted separately. (Wright 1969:51)

In addition to the issue of timing, Wright argues that the type of site -- permanent farming village versus seasonal nomadic settlement -- must also be considered. He suggests other factors as well: the availability of chert locally, the uses of obsidian at a site, and whether obsidian arrived at a site as raw material or finished artifacts. The existence of additional

obsidian sources in Central Anatolia -- besides Acigöl and Çiftlik (i.e., Göllü Dağ) -- was also proposed by Wright as a result of recent field surveys. In his study, he supplemented his obsidian data with information about the circulation of other materials, such as copper and turquoise, from Anatolia into Mesopotamia and the Levant.

Other criticisms primarily involved their fall-off curves, supply and contact zones, and obsidian interaction zones. In Hallam et al. (1976), an obsidian interaction zone was defined as the area within which at least 30% of the artifacts originated from a particular obsidian source. Henderson (2001) points out that, "by increasing the percentage for the definition of an interaction zone from 30% to 50%, we could produce a rather different, more contracted pattern leading to a different archaeological interpretation" (310). Their "down-the-line" interpretation was questioned by Hodder and Orton (1976), who showed that simple random-walk patterns, generated with computer simulations, could reproduce the curves reported by RDC. Thus, it seemed that quite different processes could lead to the observed fall-off curves. This determination was made while Schiffer was developing the concept of site formation processes, so it was accepted that a map of obsidian artifacts might not accurately reflect the true nature of exchange systems. Thus, Crawford (1978), among others, left out the mathematical component of modeling obsidian circulation, and he focused on ethnographic approaches to consider exchange.

Another issue, for me, is that most of the RDC artifacts date to the Neolithic. Not a single Bronze-Age artifact from Syria was sourced by them. Three blades from Eridu in southeastern Iraq, near Ur, were analyzed (Renfrew et al. 1966). Though these blades

likely date to the fourth or third millennia BCE, they came from unstratified contexts, and a sourced obsidian bowl from Tepe Gawra (Renfrew et al. 1966, 1968; Dixon et al. 1968) probably dates to the Chalcolithic rather than the Bronze Age. In western Iran, Renfrew et al. (1966) analyzed one Bronze-Age artifact from Susa and another from Tepe Hasanlu (near Lake Urmia). In other words, at most, only six Bronze-Age artifacts from four sites were sourced by RDC. Clearly the soundness of using their post-Neolithic maps, such as that in Dixon et al. (1968) (Figure 2.4), for the Bronze Age should be doubted. Yet their post-Neolithic maps -- and even their Neolithic maps -- have often been used to postulate where obsidian found at Chalcolithic and Bronze-Age sites originated. Such speculations are made because: (1) there are many other materials (including texts) to study during the Bronze Age, so little attention is given to lithics compared to the Neolithic Period and (2) obsidian sourcing decreased in the Near East after the early 1980s.

2.3 - Sourced Obsidian from Mesopotamia and the Northern Levant

I have mentioned a decline in obsidian sourcing in the Near East and lack of data, particularly from post-Neolithic periods. It is, though, difficult to believe that, in one of the regions where obsidian sourcing was first developed, relatively few artifacts actually have been sourced over the last forty years. This deficit has been documented elsewhere (e.g., Özdoğan 1994), but the best way to prove that such a lack exists is to inventory the numbers of sourced artifacts in Mesopotamia and the Northern Levant and then compare those numbers to New World obsidian studies. There is, to my knowledge, no such other

compilation for the region. The closest is a set of review articles from 1998 (Chataigner et al. 1998, Chataigner 1998, Cauvin and Chataigner 1998), but these are incomplete and outdated. Thus, hopefully this list will be useful for other archaeologists.

2.3.1 - The Scope of this Compilation

In the following sections, I outline the scale of prior obsidian sourcing research in the region traditionally considered Northern and Southern Mesopotamia and the Northern Levant. Thus the geographical area for the discussion includes all of Syria, Lebanon, and Iraq as well as southeastern Turkey (south of the Taurus Range) and western Iran (west of Lake Urmia and the Zagros Range). The Southern Levant, the Arabian Peninsula, eastern Iran (the Zagros Range and to the east), and most of Anatolia (in the Taurus Range and to the northwest) are beyond the scope of consideration here. It is a bit of shorthand when I state that a certain researcher "sourced" some number of artifacts. I do not mean to imply that all of those artifacts are necessarily *correctly* sourced (i.e., some may be attributed to an incorrect origin) -- instead, I mean the researcher went through the process of sourcing (as discussed in Section 1.3) and, to the best of their knowledge and abilities at the time, assigned each artifact to its likely "source" (the definitions of which vary, as discussed in Chapter 4) based on its composition or other property (e.g., age). In Chapter 4, I discuss which of these studies used deficient geological reference collections, and in Chapter 8, I evaluate the findings of these studies most relevant to my research.

I have excluded from this tally, though, a few questionable studies. For example, Hammo (1984) used crude (by today's standards) magnetic measurements in his effort to source a few obsidian artifacts from three sites in Iraq, including Tell Shemshara and Tell al-Uhaymir (ancient Kish). The only obsidian artifact from Tell al-Uhaymir was assigned to the Eastern Anatolian sources using his measurements. All artifacts from the other two sites were supposedly from an "Abyssinian, Arabian, or other unnamed source." I am not opposed to the idea of obsidian from East African Rift sources in Mesopotamia so long as a mechanism can be proposed (e.g., part of a small toilette table, made from East African obsidian and carved with the inscription of a 17th-century-BCE pharaoh, was discovered at the ancient Hittite capital of Boğazköy and was quite likely "a gift sent by the Pharaoh to the Hittite king" [Dixon et al. 1968:88]). However, Renfrew et al. (1966) sourced five obsidian blades and one flake from Tell Shemshara to sources in the Lake Van area (about 200 km away), not the East African Rift sources (more than 2000 km away), so Hammo's (1984) method was likely faulty (and is generally considered so).

As is the case in all of archaeology, there is the problem of "grey literature," such as unpublished site and laboratory reports, posters presented at conferences two or three decades ago (before the advent of digital posters that can be preserved and disseminated online), and other inaccessible documents and data. Occasionally conference posters and presentations can be connected to later publications that impart the findings and data (e.g, the artifacts sourced and discussed in Yeğingil 1990 were eventually published in Bigazzi et al. 1996, and Al Isa et al. 1990 was later published as Gratuze et al. 1993). Other times

the conference presentation is only partially published (e.g., the sourced Uruk artifacts of Schneider 1992 were previously published in Schneider 1990, but his data and results for two unspecified Syrian sites apparently went unpublished). In one instance, I was able to find a bit of second- and third-hand information on a conference poster -- the results from a site presented by Schneider (1994), Tell Mashnaqa, was mentioned in a brief site report by Thuesen in an article by Weiss (1994) and as a personal communication (Chataigner 1998), but there are no details (e.g., number of artifacts sourced) or data. The results and data from other conference presentations, though, (e.g., Capannesi et al. 1990) appear lost entirely, and the findings are not even included in the abstracts.

One must be careful to avoid "double counting" artifacts when compiling artifacts as I have done here. For example, Francaviglia (1994) sourced a set of obsidian artifacts from four Neolithic sites in northern Iraq (Yarim Tepe, Tell Magzalia, Tell Sotto, and Kül Tepe), and the exact same artifacts are covered by Bader et al. (1994), Chataigner (1994), and Gratuze (1994). Abbès et al. (2003) present newly analyzed artifacts from Jerf el Ahmar in Syria, but they also discuss previously sourced artifacts from the nearby sites of Cheikh Hassan (Abbès et al. 2001) and Mureybet (Bellot-Gurlet 1998). Artifacts sourced in Gratuze et al. (1993) were reanalyzed in Gratuze (1999), and many of Wright's (1969) artifacts came from RDC. There are other examples as well. The result is an impression that more artifacts have been sourced than have been in reality.

2.3.2 - Sourced Obsidian from the Bronze Age

The number of sourced obsidian artifacts from Bronze-Age sites (circa 3500 BCE to 1200 BCE) in Syria is low, only a few dozen. None are found in the work of RDC, nor have I been able to identify any sourced artifacts prior to the 1990s. Gratuze et al. (1993) sourced nine artifacts (of unknown types) from Late Bronze Age levels (circa 1300 BCE) at Ras Shamra (ancient Ugarit), a port city on the Mediterranean coast of Syria (three of them were reanalyzed by Gratuze 1999). Hall and Shackley (1994) sourced 21 retouched obsidian blades -- all surface finds but estimated to be circa the second millennium BCE based on the ceramics -- from two sites in northeastern Syria: Tell Hamoukar (ten blades) and the smaller Hirbet Tueris (eleven blades). Pernicka et al. (1997) sourced one artifact (of unknown type) from another site in northeastern Syria -- Tell Mulla Matar -- dated to the Early Bronze Age (third millennium BCE). Finally, Chabot et al. (2001) sourced ten artifacts -- all blade fragments -- from Bronze-Age (third millennium BCE) strata of two sites -- Tell ʻAtij (six fragments) and Tell Gudeda (four fragments) -- both also located in northeastern Syria. These 41 artifacts from six archaeological sites are, to the best of my knowledge, the entirety of sourced Bronze-Age Syrian obsidian.

Including Iraq does not considerably increase the number of sourced Bronze-Age artifacts. Gratuze et al. (1993) sourced just one Middle-Bronze-Age artifact (of unknown type) from Tell as-Senkereh (ancient Larsa) in southeastern Iraq, roughly 25 km southeast of Uruk. Renfrew et al. (1966) sourced three artifacts (all blades) from Tell Abu Shahrain (ancient Eridu) also in southeastern Iraq, just 12 km southwest of Ur. These blades came

from unstratified contexts, but this settlement reached its height during the late fourth and third millennia BCE. Schneider (1990) sourced eleven artifacts (including blades, flakes, and a core) from the Riemchengebäude (3400-3100 BCE) and surface finds (likely about 3200-2900 BCE) at Uruk. The research of RDC (Renfrew et al. 1966, 1968; Dixon et al. 1968) includes a carved obsidian bowl (Figure 2.8) from a burial tomb at Tepe Gawra in northern Iraq, about 15 km from modern Mosul. At the time, it was thought that the tomb (and the bowl) dated to about 3200 BCE in the Early Bronze Age (Wright 1969), but later research suggests that its stratum (Level X) dates to about 3800 BCE, placing it instead in the Chalcolithic (Rothman 2002:3). Consequently, there are roughly 16 sourced Bronze-Age obsidian artifacts from four sites in Iraq, possibly fewer.

In Lebanon, Gratuze (1999) sourced sizable chunk (over 15 kg) of obsidian from Tell Arqa, a site inhabited from the Neolithic to the Middle Ages, and attributes the chunk to the Bronze Age. At the same site, though, Thalmann (2006) sourced a similar obsidian chunk, perhaps the same one, as well as associated blades and debitage, and he attributed them to the sixth- or fifth-millennium Neolithic Period. In southeastern Turkey, Otte and Besnus (1992) sourced a singular EBA artifact from Hassek Höyük on the Euphrates. In western Iran, Renfrew et al. (1966) sourced one EBA artifact from Susa (near the modern town of Shush) and one from Tepe Hasanlu (near Lake Urmia). Mahdavi and Bovington (1972) sourced seven EBA artifacts from Tepe Hasanlu, and Blackman (1984) sourced 44 Bronze-Age artifacts from Tal-i Malyan (ancient Anshan). Accordingly, we have roughly 53 additional Bronze-Age artifacts from five archaeological sites.

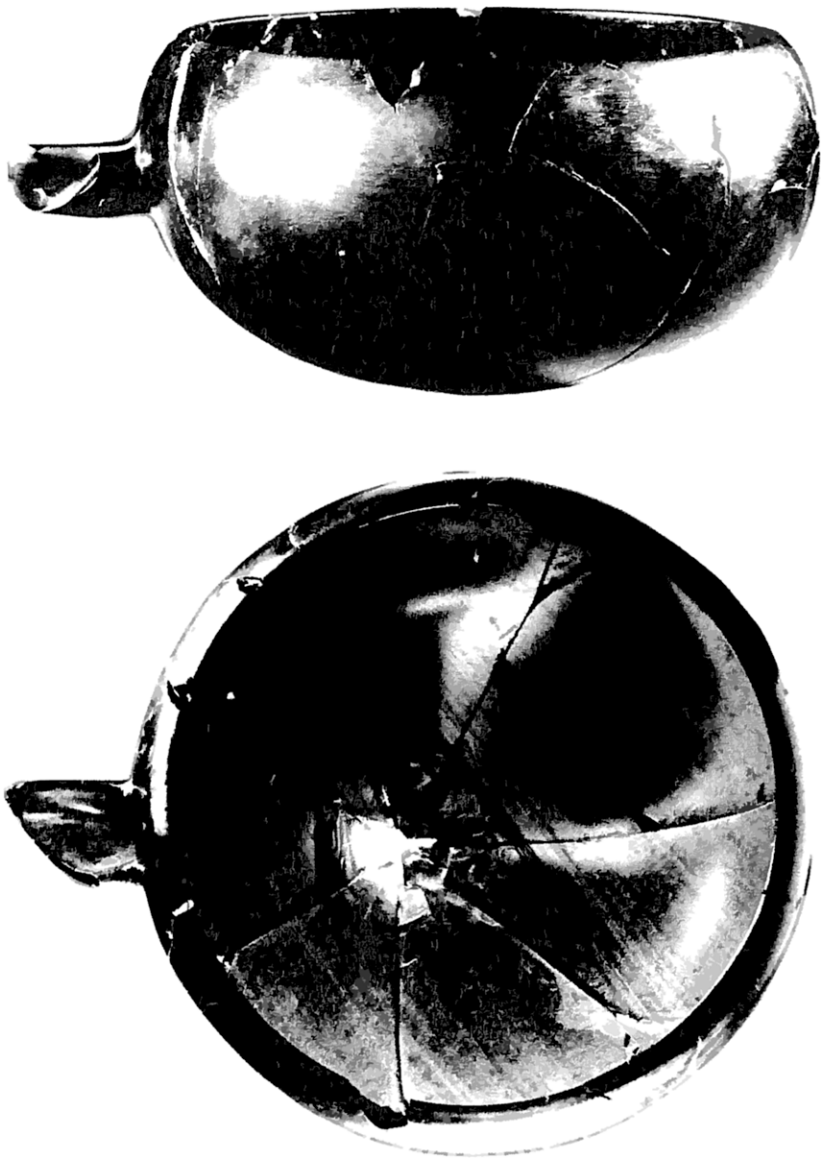


Figure 2.8 - An obsidian vessel, about 20 cm in diameter, from a Chalcolithic tomb in Level X, circa 3800 BCE, at Tepe Gawra in northern Iraq, near Mosul. (Images based on photographs in Renfrew et al. 1966 from the University of Pennsylvania Museum).

2.3.3 - Sourced Obsidian from the Chalcolithic

The number of sourced Chalcolithic (about 4500 to 3500 BCE) obsidian artifacts from Syria has only recently improved. Cann and Renfrew (1964) sourced two obsidian artifacts from Chagar Bazar but only one from a Chalcolithic context. Chagar Bazar, one of the Syrian sites excavated by British archaeologist Max Mallowan and his wife Agatha Christie, lies in the so-called Khabur Triangle (another name for the Upper Khabur River basin) in northeastern Syria. Wright (1969) and his colleagues also sourced two artifacts from Chagar Bazar, but I suspect that these were the same two artifacts sourced by Cann and Renfrew (1964). For almost four decades, this was the only sourced obsidian artifact from the Syrian Chalcolithic. In 2003, using fission-track dating, Oddone and colleagues sourced 21 artifacts from the Chacolithic levels (circa 4000-3500 BCE) of Tell Afis in far northwestern Syria, about 45 km southwest of modern Aleppo. In 2009, Khalidi and her colleagues sourced 8 artifacts from Tell Brak (ancient Nagar) as well as 32 artifacts from Tell Hamoukar -- the artifacts came from Late Chalcolithic levels, and both sites lie in the Khabur Triangle. These 62 artifacts from four archaeological sites are, to my knowledge, the entirety of sourced Chalcolithic Syrian obsidian artifacts.

Outside of Syria, the numbers of sourced Chacolithic artifacts are also rather low. In Lebanon, Renfrew et al. (1966) sourced one Chacolithic artifact from Byblos, a city on the Mediterranean coast. In southeastern Turkey, Pernicka (1992) sourced 17 Chacolithic artifacts from Hassek Höyük, and it seems these same artifacts were also sourced by Otte and Besnus (1992) in the same volume. To my knowledge, the only sourced Chacolithic

obsidian artifact from Iraq is the previously noted carved bowl from Tepe Gawra -- it was initially dated to the EBA (Wright 1969), but later archaeologists instead dated its stratum to the Chalcolithic (Rothman 2002). In western Iran, Renfrew et al. (1966) sourced three obsidian artifacts from Tal-i-Bakun (just south of Persepolis) and three from Pisdeli Tepe (near Tepe Hasanlu). Mahdavi and Bovington (1972) sourced three Chacolithic artifacts from Susa, two artifacts from Tepe Jaffarabad (near Susa), and five from Marvdasht (near Persepolis). Niknami et al. (2010) quite recently sourced 60 artifacts from 22 Chacolithic sites in northwestern Iran, but its appears that only three artifacts came from sites west of Lake Urmia. Therefore, apart from Syria, there are approximately 38 Chacolithic sourced obsidian artifacts from Mesopotamia and the Northern Levant.

2.3.4 - Sourced Obsidian from the Neolithic

Much greater attention has been paid to sourcing Neolithic obsidian artifacts from Syrian sites. Cann and Renfrew (1964) sourced one artifact (a flake) from a Halaf-Period stratum (circa about 6000 to 5200 BCE) at Chagar Bazar. Renfrew et al. (1966) sourced two blades (one blade from Ubaid Period, circa roughly 5200 to 4000 BCE, and the other from the Pre-Pottery Neolithic, or PPN) from Ras Shamra (ancient Ugarit), and they also sourced two obsidian blades (circa the PPN) from Tell Ramad in southwestern Syria near Damascus. Renfrew et al. (1968) sourced six artifacts, all blades, (circa 6000 BCE) from the eastern Syrian site of Bouqras. Therefore, RDC's obsidian distributions for Neolithic Syria are based on eleven artifacts from four archaeological sites.

Later researchers have also concentrated on the Neolithic Period of Syria. Epstein (1977) sourced 64 artifacts from Tell Aswad (circa 8000-6500 BCE) within the Damascus basin. McDaniels et al. (1980) also sourced 54 artifacts from Tell Aswad in addition to a hundred artifacts from Abu Hureyra (in the Middle Euphrates area) and 24 artifacts from Ghoraife (near Tell Aswad). Pernicka et al. (1997) sourced 38 artifacts from five Middle-Euphrates sites: Halula (six PPNB artifacts, ten pre-Halaf artifacts, three Halaf artifacts), Dja'de (one pre-Halaf artifact, five PPNB artifacts), Jerf el Ahmar (one PPNA artifact), Cheikh Hassan (two PPNB artifacts), and Mureybet (five PPNA and five PPNB artifacts). Copeland (1989) reports that six artifacts from Tell Sabi Abyad were sourced by Boerma. Francaviglia and Palmieri (1998) sourced 50 artifacts, apparently circa the Late Neolithic, from four sites within the Khabur Triangle of northeastern Syria: Tell Barri (22 artifacts), Tell Hamoukar (16 artifacts), Tell Halaf (seven artifacts), and Tell Brak (five artifacts). Gratuze et al. (1993) sourced 71 obsidian artifacts from seven sites: Cheikh Hasan (three PPNA artifacts) and Mureybet (ten PPNA-PPNB artifacts) from the Middle Euphrates region; Tell Assouad (five PPNB artifacts) in northern Syria; Kashkashok (eight Halafian artifacts) in the Khabur Triangle; and Qdeir (25 PPNB artifacts), El Kowm (seven PPNA and PPNB aritfacts), and Umm el Tlel (eight PPNB artifacts) near the oasis of Palmyra in the desert. Abbès et al. (2001) sourced 19 artifacts from Cheikh Hassan, and Abbès et al. (2003) reports the sources of 40 artifacts from Mureybet and 44 from Jerf el Ahmar in the Middle Euphrates region. Le Bourdonnec et al. (2005a) analyzed 26 artifacts from four unspecified Middle Euphrates archaeological sites (but given his coauthors, likely Cheikh

Hassan, Jerf el Ahmar, Mureybet, and one other site). Maeda (2003) sourced a number of artifacts from three sites in the El-Rouj Basin in far northwestern Syria: four blades from Tell Abd el-Aziz, 44 artifacts from Tell Aray, and 367 from Tell el-Kerkh. Therefore, in the four decades since the original research of RDC, roughly 946 Neolithic artifacts from 22 archaeological sites throughout Syria have been sourced, and almost 40% of them are from a single 5 × 5 m square at one site in far northwestern Syria.

In northern Iraq, Cann and Renfrew (1964) sourced five Neolithic artifacts (Halaf and Ubaid phases) from Tell Arpachiyah near modern Mosul. Also in the north, Renfrew et al. (1966) sourced five obsidian blades and one flake from Tell Shemshara (circa Early Neolithic), seven blades and two flakes from Jarmo (circa 7000-6000 BCE), and a flake and a blade from Tell Matarrah (circa 5800-5300 BCE). Thus, the work of RDC included 22 artifacts from four sites. Epstein (1977) sourced 79 artifacts from Choga Mami (circa 5500-4200 BCE), and in southern Iraq, Gratuze et al. (1993) sourced five artifacts (Ubaid phase) from Tell el-'Oueili (near Larsa). Francaviglia (1994) sourced numerous artifacts from northern sites in Iraq: 62 artifacts from Yarim Tepe, 19 artifacts from Tell Magzalia, 17 artifacts from Tell Sotto, and four artifacts from Kül Tepe (the same ones are discussed in Chataigner 1994 and Bader et al. 1994). Therefore, about 208 artifacts from ten sites have been sourced from Neolithic Iraq in the last forty years.

Renfrew et al. (1966) sourced six artifacts from Byblos in Lebanon and two from Tilki Tepe in southeastern Turkey. At Çayönü, also in southeastern Turkey, Renfrew et al. (1968) sourced five artifacts, and Bigazzi et al. (1996) sourced 50 artifacts also from this

site (some of the same artifacts were sourced earlier in Yegingil et al. 1990). In the same vicinity, Cauvin et al. (1986) sourced 21 artifacts from Cafer Höyük, and Le Bourdonnec (2008) sourced a hundred artifacts from Göbekli Tepe. Bressy et al. (2005) sourced nine artifacts (Ubaid and Halaf phases, circa 5700 to 4300 BCE) from Tell Kurdu in the Amuq Valley, near ancient Antioch and modern Antakya. In western Iran, Renfrew et al. (1966) sourced four artifacts from Sarab, eight from Tepe Guran, seven from Ali Kosh, and three from Hajji Firuz Tepe, and Renfrew and Dixon (1976) sourced one blade from Tepe Sabz in the southwest. Pullar et al. (1986) sourced twelve artifacts from Tepe Abdul Hosein. Thus, roughly 228 Neolithic artifacts from twelve sites in Lebanon, southeastern Turkey, and western Iran have been sourced in the last four decades.

2.3.5 - Summarizing the Results

I believe that this tally is fairly accurate -- Chataigner et al. (1998) estimated that, among "the artefacts from the Near East analysed in the past 30 years, there are... about... a total of 750" (533). According to my inventory, there are about 1600 sourced obsidian artifacts from all of Mesopotamia and the Northern Levant from the Pre-Pottery Neolithic through the Late Bronze Age. From the Bronze Age (circa 3500 to 1300 BCE), there are only about 110 sourced artifacts from 15 archaeological sties -- only 41 of these artifacts come from six Syrian sites. Even if I have overlooked a study here or there, the point is still that only a few artifacts from the Near East have been sourced compared to the New World. Obsidian sourcing data is particularly thin for Bronze-Age Mesopotamia, and the

four main reviews of Near East obsidian research end at the Calcholithic: Wright (1969) and Chataigner (1998) both end at 3500 BCE; Cauvin and Chataigner (1998) end at 3700 BCE; and Chataigner et al. (1998) end at 4000 BCE. Furthermore, in one article that claims to examine obsidian use in the Neolithic and Bronze Age (Gratuze et al. 1995), the entire Bronze Age is represented by nine artifacts from Ras Shamra (circa 1300 BCE) on Syria's Mediterranean coast. Clearly, there are little data for Bronze-Age Mesopotamia, even on the level of sourcing at individual archaeological sites.

2.3.6 - Putting It in Perspective: Advantages of More Data

The number of sourced obsidian artifacts from New World sites exceeds that from Near Eastern sites by one or two orders of magnitude. In the 1960s and 1970s already, at Berkeley, Robert Jack and Thomas Jackson analyzed over 1500 obsidian artifacts, mostly from California (Shackley 2008a). Forty years later, about 100,000 New World obsidian artifacts have been sourced. I mentioned in Chapter 1 three XRF laboratories: Shackley's Geoarchaeological XRF Laboratory at Berkeley, Skinner's Northwest Research Obsidian Studies Lab, and Hughes' Geochemical Research Laboratory. These three labs, over the years, have sourced over 72,000 obsidian artifacts from the United States (Skinner, 2010, personal communication). The University of Missouri Research Reactor Center (MURR) has, under the supervision of Michael Glascock, also sourced 24,000 New World artifacts (Boulanger, 2010, personal communication). Of these, about 9200 of these artifacts were from Mexico, 6300 from the United States, 2400 from Guatemala, 1900 from Argentina,

Table 2.1 - Previously Sourced Post-Neolithic Mesopotamian Artifacts

Country	*Period*	*Site*	*Authors*	*Number*
Syria	Bronze Age	Ras Shamra	Gratuze et al. (1993)	9
Syria	Bronze Age	Tell Hamoukar	Hall and Shackley (1994)	10
Syria	Bronze Age	Hirbet Tueris	Hall and Shackley (1994)	11
Syria	Bronze Age	Tell Mulla Matar	Pernicka et al. (1997)	1
Syria	Bronze Age	Tell ‘Atij	Chabot et al. (2001)	6
Syria	Bronze Age	Tell Gudeda	Chabot et al. (2001)	4
			Sum	***41***
Iraq	Bronze Age	Tell as-Senkereh	Gratuze et al. (1993)	1
Iraq	Bronze Age	Tell Abu Shahrain	Renfrew et al. (1966)	3
Iraq	Bronze Age	Uruk	Schneider (1990)	11
			Sum	***15***
Lebanon	Bronze Age?	Tell Arqa	Gratuze (1999)	1
Turkey	Bronze Age	Hassek Höyük	Otte and Besnus (1992)	1
Iran	Bronze Age	Susa	Renfrew et al. (1966)	1
Iran	Bronze Age	Tepe Hasanlu	Renfrew et al. (1966)	1
Iran	Bronze Age	Tepe Hasanlu	Mahdavi and Bovington (1972)	7
Iran	Bronze Age	Tal-i Malyan	Blackman (1984)	44
			Sum	***53***
Syria	Chalcolithic	Chagar Bazar	Cann and Renfrew (1964)	1
Syria	Chalcolithic	Tell Afis	Oddone et al. (1993)	21
Syria	Chalcolithic	Tell Brak	Khalidi et al. (2009)	8
Syria	Chalcolithic	Tell Hamoukar	Khalidi et al. (2009)	32
			Sum	***62***
Iraq	Chalcolithic?	Tepe Gawra	Renfrew et al. (1966, 1968)	1
Lebanon	Chalcolithic	Byblos	Renfrew et al. (1966)	1
Turkey	Chalcolithic	Hassek Höyük	Pernicka (1992)	17
Iran	Chalcolithic	Tal-i-Bakun	Renfrew et al. (1966)	3
Iran	Chalcolithic	Pisdeli Tepe	Renfrew et al. (1966)	3
Iran	Chalcolithic	Susa	Mahdavi and Bovington (1972)	3
Iran	Chalcolithic	Tepe Jaffarabad	Mahdavi and Bovington (1972)	2
Iran	Chalcolithic	Marvdasht	Mahdavi and Bovington (1972)	5
Iran	Chalcolithic	near Lake Urmia	Niknami et al. (2010)	3
			Sum	***19***

and 1600 from Belize. In comparison, MURR has sourced zero artifacts from Syria, Iraq, or Lebanon and only 59 from Turkey. Note that MURR alone has sourced 1600 obsidian artifacts from Belize, a country the size of Massachusetts, and this is the same number of sourced artifacts from all of Mesopotamia and the Northern Levant.

The abundance of data in the New World, thanks to the fact that obsidian sourcing is considered a routine element of excavation in many regions, has allowed researchers to recently develop and test sophisticated models of obsidian procurement, distribution, and use. The nuances of these studies are beyond the scope of this discussion, so I shall only list various examples from the past fifteen years here. In North America, particularly the Pacific Northwest, California, and the Southwest, these studies include: Bayman (1995), Shackely et al. (1996), Hess (1997), Peterson et al. (1997), Bayman and Shackley (1999), Roth (2000), Clark (2001), Dillian (2002), Shackley (2005:118-133, 147-171), Silliman (2005), Bohn (2007), Eerkens et al. (2008), Taliaferro et al. (2009), and Park (2010). In Mesoamerica, these studies include: Darling (1998), Aoyama et al. (1999), Santley et al. (2001), Saunders (2001), Norris (2002), Barrett (2003), Moholy-Nagy (2003), Carballo (2005), Benitez (2006), and Hirth (2006). In South America, the studies include: Burger et al. (2000), Yacobaccio et al. (2004), Lazzari (2005, 2006), Tripcevich (2007), Ogburn et al. (2008), Lazzari et al. (2009), and Tripcevich (2009).

Basically the only archaeological site in Southwest Asia where obsidian sourcing approaches this level of sophistication is Çatal Höyük. This is due, in large part, to there being sufficient data (i.e., sourced artifacts) from the site. In the last decade, at least 660

artifacts have been analyzed: 100 artifacts in Carter et al. (2006) using ICP-AES/-MS at Grenoble; 35 in Carter et al. (2005, 2006) at Aberystwyth; 42 in Carter and Shackley (2007) using EDXRF at Berkeley; 72 artifacts in Poupeau et al. (in press) using PIXE at Bordeaux; 51 in Poupeau et al. (in press) using SEM-EDS at Bordeaux; 24 in Poupeau et al. (in press) using EDXRF at Berkeley; 48 in Carter et al. (2008, in prep) using EDXRF at Berkeley; 42 in Carter et al. (2008, in prep) using PIXE at Paris; 45 in Carter et al. (in prep) using ICP-AES at Stanford; and at least 100 artifacts in Carter (2009, in prep) using PXRF at Çatal Höyük. This amount of data has revealed details of obsidian procurement and circulation patterns in this Neolithic village (e.g., Carter et al. 2006, 2008; Carter and Shackley 2007). If these researchers at Çatal Höyük had stopped when one or two dozen artifacts had been sourced and it was clear that the obsidian mainly came from Göllü Dağ and Nenezi Dağ, the nuanced intra-site spatial and temporal patterns would not have been noticed. Furthermore, the recently reported obsidian blades from Eastern Anatolia, which are entirely unexpected based on the distribution patterns of RDC and comprise just 0.1% of the obsidian assemblage, would have been missed -- this is an important discovery that moves Neolithic circulation of Eastern Anatolian obsidian much farther west (Carter et al. 2008). There are advantages to sourcing more than a few artifacts.

If Çatal Höyük informs us about a Neolithic village on the Konya Plain of Central Anatolia, what about Mesopotamia and the Northern Levant? At the start of the chapter, I mentioned a pipeline expansion project in the American Northwest in which, on average, about 70 obsidian artifacts per archaeological site were sourced. In Mesopotamia and the

Northern Levant, how many sites meet this standard? Prior to my research, just *three* did: (1) Epstein (1977) sourced 79 artifacts from Choga Mami in southeastern Iraq, east of the Tigris; (2) McDaniels et al. (1980) sourced 100 artifacts from Abu Hureyra in the Middle Euphrates region of Syria; and (3) Maeda (2003) recently sourced 367 artifacts from one 5 × 5 m excavation square at Tell el-Kerkh in far northwestern Syria, near Latakia on the Mediterranean coast. All three are Neolithic sites, meaning that there were no thoroughly sourced sites from the Chalcolithic or later. My analyses of 97 obsidian artifacts from the Bronze-Age strata of Tell Mozan in the Khabur Triangle of northeastern Syria adds much needed spatial and temporal diversity to the Mesopotamian data.

Rare studies like Epstein (1977) also reveal an unanticipated diversity of obsidian sources used by the inhabitants of a particular site. RDC indicate that obsidian from only one or two sources, perhaps three at most, was utilized at Neolithic sites in Mesopotamia and the Levant (Renfrew et al. 1966, 1968; Dixon et al. 1968). Epstein (1977), however, identified eight different geochemical clusters in the obsidian analytical data from Choga Mami. One might expect such a result to have a profound effect on obsidian research in the Near East, but there was a problem. The clusters were found in artifacts alone, and no geological obsidian specimens seem to have been analyzed. Therefore, these groups are given labels -- B1, B2, B3, B4, G1, G2, G3, and T2 -- based on their color (B for black, G for green, and T for transitional) and clustering on plots. Epstein and other University of Bradford researchers made some associations between clusters and sources: for example, G1 was deemed to be a Nemrut Dağ source, and B1 was a Göllü Dağ source. Some other

clusters, however, remained of unclear origin (e.g., B2) while Bradford researchers added even more clusters (e.g., B5). McDaniels et al. (1980) also suffered from this problem as this work, too, was done at the University of Bradford. Being unable to link the artifacts to their geological sources hurt these two otherwise notable studies, and the advantages of sourcing greater numbers of artifacts per site went unappreciated.

2.4 - The Stagnation of Near East Obsidian Sourcing

Now that a relative lack of obsidian sourcing data from the Near East, particularly for the Bronze Age, and the advantages of sourcing greater numbers of artifacts per site have been established, the reasons and effects should be considered. First, I discuss three previously suggested reasons for this decline. Then I suggest another factor, popularized by RDC as well, for a lack of analytical sourcing: visual-based approaches.

2.4.1 - Reasons for the Obsidian Sourcing Stagnation

A few explanations have been proposed for why obsidian sourcing has seen little subsequent use in the Near East, especially in Mesopotamia. Tristan Carter, the obsidian expert at Çatal Höyük, has suggested that criticisms of RDC's research, particularly that the observed obsidian distribution patterns are not necessarily explained by their models, essentially had a chilling effect and affected "a broad retreat from using sourcing data to address such large-scale questions" (Carter, 2010, in prep). Subsequently, Carter argues, obsidian sourcing in the Near East has been restricted to either single sites or very small-

scale region studies. Indeed, most recent studies focus on one site or perhaps two or three sites in one river valley (e.g., Otte and Besnus 1992; Abbès et al. 2001, 2003; Chabot et al. 2001; Oddone et al. 2003; Bressy et al. 2005; Khalidi et al. 2009). Did such criticisms themselves cause a chilling effect on future work, or did archaeologists conclude that the large-scale regional economics was much too complex to investigate with their approach? Whatever the actual cause, only one recent meta-analysis by Chataigner (1998) has come close to such wide-reaching obsidian research in the Near East.

Mehmet Özdoğan, an archaeologist who specializes in Neolithic Turkey, proposes another explanation: the work of RDC is a very good, albeit flawed, initial study and laid the framework, but it was presented with, and was perceived to have, such authority that the findings seemed conclusive. Özdoğan explains that the work of RDC...

> could have had a stimulating impact for a more thorough and systematic survey of obsidian sources, and a lot could have been achieved during the last 25 years. However, regardless of the incipient nature of the evidence and the minimal number of specimens obtained from sources, their paper sounded conclusive for source identifications and almost dismissed the possibility of other sources of obsidian being present in Anatolia. (1994:425)

Indeed, as will be discussed in Section 2.5.1, the initial four to six obsidian sources that RDC recognized are still portrayed in recent articles as *the* Anatolian sources, despite the presence of dozens of obsidian sources in Turkey and the Transcaucasus. Özdoğan holds that too much authority was given to their geochemical clusters:

> However, when initial results were presented as final, inevitably those who were not well accustomed with the particularities of research in Anatolia accepted the published facts as conclusive and intensified their research on elaborating the exact paths of the trade networks... Accordingly, in the course of these two

> decades, hundreds of obsidian artifacts were analyzed... in the hope of matching their finds to one of the 'obsidian cluster groupings of Renfrew,' and hence very little had been done for eventual documentation of the sources... We felt agitated at seeing how genuinely surprised some of our colleagues were, on hearing that there was yet no thorough documentation of obsidian sources in Turkey. It is contemptuous even to think how much has been published and debated on trade or exchange systems based on obsidian cluster groups from Anatolia. (1994:427)

Therefore, Özdoğan suggests that the results of RDC seemed so definitive that, instead of spurring further development of obsidian sourcing procedures (e.g., seeking new sources, analyzing greater numbers of geological specimens and artifacts per site), time was spent developing models with insufficient data (i.e., sourced artifacts).

Olwen Williams-Thorpe (1995), in an article on the status of obsidian sourcing in the Mediterranean and Near East, showed that the number of published studies increased steadily from the mid-1960s until the mid-1980s. After about 1985, the number of papers decreased precipitously, reaching mid-1960s levels by the mid-1990s. He considered the possible reasons for a drop in obsidian studies in this region:

> The decrease of papers in recent years is probably a reflection of several factors: first, the basic distributions are now established and it becomes rather less exciting to simply 'fill in the gaps.' Second, archaeological science has become increasingly focused on environmental and biochemical studies in recent years; in such a climate, lithic studies may gain less attention. And third, it is probably simply a reflection of fashion: obsidian research was a bandwagon on which many workers (including the present author) jumped with enthusiasm, but it has now lost its initial momentum. (235, 237)

There are two basic hypotheses provided here: (1) obsidian sourcing in the Near East has fallen out of favor as a popular topic in archaeological science and has been replaced by environmental archaeology; and (2) obsidian sourcing in this region is, for the most part, "complete," and future work need only follow a prescribed formula. He continues:

> The increase and now fall-off of archaeological obsidian research papers conforms to a well-established pattern of scientific research, reflecting the initial recognition of a problem, the increasing input to problem solving, followed by the decline in scientific attention as approaches (and interest?) are exhausted (pers. comm. anonymous referee; Crane 1972). (237)

Again the explanation is that the "problem" of obsidian sourcing has been "solved" to the point where it requires little further attention. Williams-Thorpe recognizes that this is not actually the case and that critical momentum seems to have been lost:

> Developing a provenancing basis for obsidian (and other artefacts) produces an initial data base of results which remains valuable. However, a further aim of the development is that provenancing should become a routine part of post-excavation work. Without this, much of the point is lost... Obsidian studies in the area under review have become rather static. (237, 240)

Thus Williams-Thorpe has identified a likely explanation: obsidian sourcing here is often considered so complete that more data (i.e., sourced artifacts) are rarely collected. This is essentially the same explanation as that offered by Özdoğan.

Recall that I also made a suggestion in Section 2.2.1. The excitement regarding obsidian sourcing in the Near East and Aegean likely was due to existing topics of great interest in those two regions. In the Near East, it was the rise and spread of agriculture as well as the mobility of human groups and their interconnectedness during their transition from pastoral nomadism to sedentary villages. As these topics became "answered," there was less interest from Near Eastern archaeologists in the tool used to do so (i.e., obsidian sourcing). This explanation is related to those suggested by Williams-Thorpe (1995) and Özdoğan (1995): the line of investigation was considered "complete."

Regardless of what combination of these explanations is true, there are two more factors to consider. First, there is a cost for the chemical analyses for obsidian sourcing, and there are many other costs to excavation and investigating the unearthed materials, so chemically sourcing the obsidian artifacts may, out of necessity, not be one of the highest priorities. Second, the chemical analyses have traditionally been destructive. Recall that RDC powdered at least 60 mg of each artifact. The partial destruction of artifacts is, to a certain extent, much less tolerated in Near Eastern archaeology. As a result, visual-based approaches are commonly considered a low-cost, non-destructive technique to "source" large numbers of obsidian artifacts on-site. The major question, though, is the efficacy of visual-based sourcing of Anatolian and Transcaucasian obsidians.

2.4.2 - The Effect of Visual Sourcing Approaches

The color differences between calc-alkaline/alkaline and peralkaline obsidians is a reason that obsidian sourcing has been relatively infrequent in the Near East, especially in Mesopotamia and the Levant. Recall from Section 1.2.4 that the geochemical varieties of obsidian tend to have different hues: calc-alkaline/alkaline obsidian is commonly gray or black whereas peralkaline obsidian is often tinted brown or green. RDC noted this trend and used it to supplement their chemical data. First in the Mediterranean, color was used to discern peralkaline Pantelleria obsidian from calc-alkaline Lipari obsidian at Neolithic archaeological sites on Malta (Cann and Renfrew 1964). Similarly, Renfrew et al. (1966) found green-tinted obsidian with peralkaline compositions in the Near East:

> … a green colour in transmitted light proves to be a frequent (although not a necessary) property of peralkaline obsidians, which are of rare occurrence… In the Near Eastern region the only source of peralkaline obsidian is Nemrut Dağ on Lake Van, so that a similar separation is warranted… The obsidian from Nemrut Dağ, like other peralkaline obsidians, is typically green in colour when seen in transmitted light, although this is not always the case… and it seems likely that nearly all of the Near Eastern obsidian which shows this green colour derives from Lake Van. (Renfrew et al. 1966:31, 39)

These observations were substantiated, at least in part, by Herb Wright of the University of Minnesota-Twin Cities, who visited Nemrut Dağ. Wright observed an obsidian layer, two or three meters thick, along the northern caldera wall, and he reported that "much of the obsidian is full of feldspar phenocrysts, but some clear black and some opaque olive green types (in places interlaminated) were also found" (Wright quoted in Renfrew et al. 1966:39). Accordingly, Renfrew et al. (1966) concluded that "obsidian which is green in color in transmitted light… probably derives from the group 4c source at Nemrut Dağ on Lake Van" (58), so green-tinted obsidian artifacts were attributed to Nemrut Dağ, and this information was used in their reconstructions and fall-off curves.

To supplement their chemical data, RDC asked investigators at numerous sites to report, by stratum or period, the numbers of flaked-stone artifacts, obsidian artifacts, and "green" obsidian artifacts. For example, Frank Hole provided the data for Jarmo in Iraq, Sarab in Iran, Deh Luran in Iran, and Basal Tabbat al-Hammam in far northwestern Syria while Henri de Contenson supplied data for Bouqras in northern Syria and Tell Ramad in southwestern Syria. Joan Crowfoot Payne provided these data for Jericho as well as Tell al-Judaidah in Turkey, and Jacque Cauvin supplied the data for Byblos in Lebanon. The

numbers for Tell Shemshara in Iraq, Tepe Guran in Iran, and Çatal Höyük in Turkey were supplied by Peder Mortensen of the University of Copenhagen.

Later Mortensen described the chert and obsidian tools from the Samarran culture (circa the sixth millennium BCE) at Choga Mami in Iraq (1973). No analytical obsidian sourcing was conducted at that time, but Mortensen assembled the same data that he had for Tell Shemshara, Tepe Guran, and Çatal Höyük for RDC. He writes:

> In transmitted light 80% of the 240 pieces of obsidian from Choga Mami showed a clear or smoky greyish colour, indicating a Cappadocian origin. 48 specimens (i.e., 20% of the material) had a distinct greenish tinge which might suggest that these pieces came from one of the two Near Eastern sources of peralkaline obsidian, Bingöl or Nemrut Dağ in Eastern Anatolia near Lake Van (cf. Renfrew, Dixon and Cann 1966, 31 ff., and 1968, 319 ff.). The two types of obsidian seem to be equally distributed through the sequence. (39)

The assumption that green-tinted obsidian originated from Nemrut Dağ or the peralkaline Bingöl (i.e., Bingöl A) sources is reasonable as long as one realizes that (1) not all of the Nemrut Dağ obsidians are green-tinted (as Herb Wright noted and as I have observed for specimens from one of the post-caldera flows); (2) the peralkaline Bingöl (i.e., Bingöl A) obsidians can be brownish, not just greenish; and (3) the calc-alkaline Bingöl (i.e., Bingöl B) obsidians occur near the peralkaline ones and are gray or black.

Mortensen's equating of gray obsidians with Cappadocian (i.e., Central Anatolian) sources, on the other hand, is completely unfounded. In fact, there are numerous sources of calc-alkaline/alkaline obsidians within Eastern Anatolia -- such as Meydan Dağ (a.k.a. Ziyaret), Süphan Dağ, Tendürek (a.k.a. Doğubayezid), the Kars sources, and sources near Pasinler, Erzurum, and Erzincan -- and the Transcaucasus. Subsequent chemical analyses

of 79 Choga Mami obsidian artifacts by Epstein (1977) revealed that most of the gray or black ones seemingly came from the calc-alkaline Bingöl sources and either Meydan Dağ or Tendürek, all located in Eastern Anatolia. Only a single artifact originated from Göllü Dağ in Central Anatolia (and a few artifacts had uncertain origins).

Visual-based obsidian sourcing has been used recently with some success at Çatal Höyük in south-central Turkey; however, this is a special case. Of the obsidian artifacts at Çatal Höyük sourced using modern techniques, around 99.9% of them came from only two sources in Central Anatolia: East Göllü Dağ and Nenezi Dağ, about 200 km from the site (Carter and Shackley 2007, Carter et al. 2008a). The remaining 0.1% of the obsidian artifacts -- five blades -- are greenish and have the peralkaline composition of Bingöl A or Nemrut Dağ, about 650 and 825 km away, respectively (Carter et al. 2008a). For visual-based souring, therefore, the choice is a binary one between two nearby sources, and the rare third possibility is distinctive. Working at Çatal Höyük with Tristan Carter, Nurcan Kayacan and Marina Milić have developed a twenty-type classification scheme, based on color and texture (i.e., mineral size and abundance, the presence of banding, etc.), for the obsidian artifacts unearthed at the site. Their classifications for Nenezi Dağ include: grey matte with inclusions (spherulites); intensively black, sprinkled; grey, matte with rough surface; grey with sprinkled surface; and grey, matte, sprinkled, rough surface (Carter et al. 2008b:222). The Göllü Dağ obsidians have classifications such as: transparent with sprinkled grey inside; transparent with tiny white stripes; and dark blue sprinkled (222). Their classification of "opaque black shiny" corresponds to both Nenezi Dağ and Göllü

Dağ obsidians (222). This scheme has been substantiated, at least in part, using chemical analyses. Besides a continuing need for chemical corroboration of the types, the greatest weakness of visual-based sourcing is inter-observer variability, but otherwise, the trained observers have demonstrated good reproducibility of their scheme.

It should also be noted that, in this scheme developed by Çatal Höyük researchers, some of the Nenezi Dağ visual classifications include "green" in the description: smooth, slimy greenish-grey; greenish-grey almost matte (smoky); greenish-grey with dark stripes inside or on the surface; ashy greenish-grey; and opaque green. The peralkaline obsidian from either Bingöl or Nemrut Dağ, on the other hand, is described as "green oily" (Carter et al. 2008b:222). The appearance of "greenish-grey" and "opaque green" would seem to undermine the usual assumption that green-tinted obsidian comes from either Bingöl A or Nemrut Dağ in Eastern Anatolia. The distinction between (1) "slimy greenish-grey" and "opaque green" obsidians from Nenezi Dağ and (2) "green oily" obsidian from Bingöl or Nemrut Dağ is not overt. Even at a site at which there is a 99.9% chance that an artifact originated from one of only two sources and at which there has been extensive chemical obsidian sourcing, visual-based sourcing is not without difficulties.

Nevertheless, visual-based sourcing, or at least visual classifications, are still used in the Near East. A recent example is the research of Güner Coşkunsu at Mezraa Teleilat, a site on the Euphrates in southeastern Turkey (Coşkunsu 2007). While studying the Late Pre-Pottery Neolithic (PPN) to Pottery Neolithic (PN) transition at the site, she examined

a sample of the flaked obsidian and chert tools, and she developed a classification scheme for obsidian based on color, texture, and transparency. She explains:

> A sourcing analysis has not yet been undertaken. The following types have been defined: 1- colorless (very translucent); 2- opaque very shiny black; 3- opaque black; 4- translucent green; 5- semi-translucent green; 6- opaque green; 7- cloudy gray; 8- translucent brown; 9-semi-translucent brown; 10- opaque very shiny brown. According to macroscopic characteristics, East Anatolia's Van and Bingöl sources were in greatest demand by Mezraa Teleilat inhabitants, although Central Anatolian obsidians were also occasionally used. A peralkaline obsidian that is characterized by a green tinge under transmitted light is related to East Anatolia's peralkaline Bingöl A or Nemrud obsidian sources... The colorless transparent obsidian was probably obtained from Cappadocia; although East Anatolian sources also include colorless obsidian... Black and brown obsidian might have been brought from Bingöl... although brown and black obsidian are also available from Cappadocian sources. (37-38)

There are, of course, several problems here. First, there have been no chemical analyses to corroborate her scheme based on colors and textures or even to determine the numbers of obsidian sources or geochemical groups represented at the site. Mezraa Teleilat is in a location where its inhabitants could have obsidian from just two or three sources, such as Bingöl or Nemrut Dağ as well as one of the Central Anatolian sources like Göllü Dağ, or from numerous sources, maybe five or six throughout the region. Second, green obsidian is presumed to have originated from Bingöl or Nemrut Dağ; however, some of the Nenezi Dağ obsidians have been described as "greenish-grey" and "opaque green" by researchers at Çatal Höyük. Third, not all Bingöl and Nemrut Dağ obsidians have greenish tints, and fourth, as recognized by Coşkunsu, black, brown, and transparent obsidians occur in both Central and Eastern Anatolia. Accordingly, there is no way to know if her types represent anything other than appearance, and her conclusions must be considered carefully:

> Most of the obsidian was imported from East Anatolia's obsidian sources, while Central Anatolian obsidian was rarely present. The Neolithic inhabitants sought two specific types of obsidian from eastern sources -- not black, gray, or brown, but green obsidian, particularly the translucent and semi-translucent types. Since Phase IV, these two types were most widely used obsidians and in demand at Mezraa Teleilat. A slight shift in quantity and importance from the translucent green to the semi-translucent green obsidian occurred after Phase IV. (41)

Without knowing the actual sources of the obsidian utilized at Mezraa Teleilat (i.e., Is the green obsidian actually from Bingöl and/or Nemrut Dağ, or does it include green obsidian from Nenezi Dağ?), it cannot be decisively argued that most obsidian was imported from Eastern Anatolia, much less that the inhabitants preferentially sought greenish obsidian or that it was more "in demand" than black, grey, or brown obsidians. Nor is there reason to believe that "translucent" and "semi-translucent" greenish obsidians came from different sources (or arrived at the site via different mechanisms). Unfortunately, Coşkunsu notes that her approach is more the norm than the exception: "It should be noted, however, that no serious counting or chemical laboratory analysis has been done to differentiate eastern from Cappadocian obsidian in many prehistoric sites" (2007:41).

Therefore, a belief in the efficacy of visual-based sourcing is a reason for minimal analytical obsidian sourcing in the Near East. Black and grey hues are frequently equated with calc-alkaline/alkaline obsidians which, in turn, are usually (mistakenly) equated with Central Anatolian sources. Brown and especially green hues are equated with peralkaline obsidians which, in turn, are equated with either Bingöl and Nemrut Dağ, in particular, or Eastern Anatolian sources, in general. These assumptions are additionally problematic if no analytical work has corroborated the visual-based types or if the calc-alkaline/alkaline sources in Eastern Anatolia are ignored, as discussed in Section 2.6.3.

2.5 - Other Issues in Near East Obsidian Sourcing

There are two other important subjects in Near East obsidian sourcing that should be discussed, particularly because they are often ignored, even in recently sourcing work: (1) the number of obsidian sources in Anatolia and the Transcaucasus, although much of this discussion is relegated to Appendix A, and (2) the difficulty, but not impossibility, of distinguishing the Bingöl A and Nemrut Dağ peralkaline sources.

2.5.1 - The Numbers of Obsidian Sources

The obsidian distribution maps in Dixon et al. (1968) (Figures 2.1 and 2.4 here) show four to six obsidian "sources" in the Near East. Acigöl and Çiftlik (typically called Göllü Dağ today) in Central Anatolia (called "Anatolia" by RDC) are marked with closed and open circles, respectively. In Eastern Anatolia (called "Armenia" by RDC), Nemrut Dağ and Bingöl are represented by open diamonds, and a closed diamond with a question mark and no name (other than its chemical group: "1G") is positioned north of Lake Van: this was subsequently identified as a second variety (i.e., calcalkaine) of Bingöl obsidian. A closed triangle marks the position of the town of Bayezid (or Doğubeyazıt) northeast of Lake Van (based on the label for a British Museum obsidian specimen). A few volcanoes have been suggested over the decades as the actual source of this specimen: Süphan Dağ, Meydan Dağ, Tendürek Dağ, and Mount Ararat (or Ağrı Dağ).

Four decades later, some studies still compare artifacts only to these few obsidian sources. For example, Le Bourdonnec et al. (2005a) compared artifacts to four "relevant

sources" of obsidian in the Near East: East Göllü Dağ (one of the three Göllü Dağ/Çiftlik sources), Nenezi Dağ (a volcano about halfway between Acigöl and Göllü Dağ), and the Bingöl sources, which have two varieties (peralkaline and calcalkaline) known as Bingöl A and B, respectively. Bingöl A and Nemrut Dağ obsidians are geochemically similar, so Le Bourdonnec et al. do not even bother to analyze any specimens from Nemrut Dağ. In other words, they consider *fewer* sources than RDC -- no source of obsidian north of Lake Van is included in their study. Bressy et al. (2005) analyzed obsidian from four sources -- two Göllü Dağ sources (Komürcü and Kayırlı) as well as Bingöl A and B -- and relied on previously published values for the obsidian sources at Nemrut Dağ, Ziyaret (a name for Meydan Dağ), and Pasinler (a basin in the Erzurum-Kars Plateau).

Dozens of obsidian "sources" (I discuss this term later in Chapter 4) are present in Turkey and the Transcaucasus (Georgia, Russia, Armenia, and Azerbaijan). Using even the most conservative definition of obsidian "sources," there are about two dozen sources in Turkey alone. The number of named obsidian sources and "sub-sources" in Turkey is at least three dozen. If one counts the individual obsidian flows and outcrops, there are at least 90 locations in Turkey where people could have collected obsidian (Rapp, personal communication). Regardless of how one defines an obsidian "source," there are many more than the four, five, or even six obsidian sources considered in RDC and most of the recent studies. Armenia has dozens more sources. In Appendix A, I discuss the principal obsidian sources that exist in Turkey and the Transcaucasus.

It has been argued (e.g., Wilson and Pollard 2001:510) that sourcing really shows mismatches between artifacts and possible sources rather than actually proving a specific source for the artifacts. In other words, in this view of sourcing, improbable raw-material sources are ruled out until one or more most likely sources remain. There will always be a possibility that some other source, either undiscovered or just not included in the study, has a chemical "fingerprint" very similar to that of the suspected source. This possibility increases as fewer obsidian sources in a particular region are included in a sourcing study. Therefore, all of the obsidian sources in a region must be included in sourcing studies to be conclusive (Rapp and Hill 1998:137; Shackley 2002:59-60).

2.5.2 - Are Nemrut Dağ and Bingöl A Indistinguishable?

It is often stated in the literature how difficult it is to differentiate the peralkaline obsidians from the Bingöl A and Nemrut Dağ sources. This challenge is apparently due to some magmatic relationship between these two volcanic systems, potentially involving magma mixing, and the cause remains uncertain. In one recent sourcing study, Khalidi et al. (2009), using EDXRF and ICP-MS, state that it is "not yet possible to fully distinguish between these two sources solely using elemental analysis" (884). Using ICP-MS/-AES, Fréderic Abbès and his colleagues make a similar statement:

> Actuellement, sur la base des analyses chimiques réalisées, il est difficile d'attribuer sans equivoque certaines obsidiennes peralcalines de la région à l'une ou l'autre des sources de Bingöl ou du Nemrut Dağ. [Currently, on the basis of chemical analyses carried out, it is difficult to source unequivocally certain peralkaline obsidians from the region to one or the other sources of Bingöl or Nemrut Dağ.] (2001:13)

Thus the chemical data from this collaboration has a combined "fingerprint" for Bingöl A and Nemrut Dağ (Abbès et al. 2001, 2003; Bellot-Gurlet and Poupeau 2006). Carter et al. (2008) mention artifacts "made of obsidian from the mountains of Bingöl and/or Nemrut Dağ" (900) and explain that the "geochemical similarity of these volcanoes' peralkaline raw materials means that we unfortunately cannot tell which specific source(s) supplied the raw materials" using EDXRF and PIXE (902). Using NAA, Bernard Gratuze and his colleagues report a rather similar result: "At this time, we are still not able to distinguish between the Nemrut Dağ and the Bingöl 'A' sources" (Gratuze et al. 1993:16, Gratuze et al. 1995:502-503). Based on their PIXE analyses, Le Bourdonnec et al. (2005a) consider the Nemrut Dağ obsidians to be part of a "Bingöl A" geochemical group: "obsidians with a Bingöl A composition can be collected both around Bingöl and also associated with the Nemrut Dağ volcano" (596). Similarly, Rosen et al. (2005:780) explain:

> Unfortunately, despite a large chronological gap in their age of formation, some of the Nemrut Dağ outcrops (of Quaternary age) are very similar in chemical composition to Bingöl (late Miocene) making it difficult to confidently assign artifacts to one source rather than the other.

A solution to the problem is actually implied in this sentence: using a chronometric, not a chemical, technique to distinguish them. In fact, Bigazzi et al. (1996, 1997) used fission-track dating to show that two Bingöl A specimens are 3.2 to 4.0 million years old and one specimen from Nemrut Dağ is 24,000 years old. The use of fission-track dating, though, or another technique ($^{40}K/^{40}Ar$ and $^{40}Ar/^{39}Ar$ dating) has not caught on for discerning these obsidians sources due, at least in part, to high cost and low accessibility. Therefore, many

Near Eastern obsidian sourcing studies still suffer from an inability to differentiate Bingöl A and Nemrut Dağ (e.g., Pernicka 1992, Bader et al. 1994).

One common "solution" to failing to chemically distinguish Bingöl A and Nemrut Dağ obsidians is simply to ignore one source or the other. For example, some researchers discuss Nemrut Dağ as a source and never mention the Bingöl sources (e.g., Mahdavi and Bovington 1972, Schneider 1990, Niknami et al. 2010). Others consider Nemrut Dağ and Bingöl B but do not discuss Bingöl A or explain why artifacts are ascribed to Nemrut Dağ rather than Bingöl A (e.g., Pernicka et al. 1997). Still others (e.g., Gratuze 1999) consider Bingöl A and B but do not even mention Nemrut Dağ. In this last instance, one must turn to earlier publications to locate the reasoning: "if, at one archaeological site, we find the artifacts have the two compositions of the Bingöl area, we may suppose that the artifacts come from Bingöl" (Gratuze et al. 1993:16, 1995:503). Simply ignoring either Bingöl A and Nemrut Dağ violates a fundamental assumption of sourcing: all potential sources of material have been included in the study. Chataigner (1998) contends that distinguishing Bingöl A and Nemrut Dağ obsidians is important because their distribution were probably different in antiquity, so this issue should not be ignored.

The problem of discerning Bingöl A and Nemrut Dağ obsidians dates back to the original work of RDC. Cann and Renfrew (1964) analyzed three "Lake Van" geological specimens from the British Museum: two from "south rim of the crater, Nemrut Dağ" and one from "within crater, Nemrut Dağ" (129). Six artifacts (two from Arpachiyah in Iraq, two from Eridu in Iraq, one from Chagar Bazar in Syria, and one from Gerzeh in Egypt),

based on their analyses, had similar compositions (133). Together these three specimens and six artifacts define their "Group 4c" from the "Lake Van" vicinity (117). Later, they added two more Nemrut Dağ specimens also from the British Museum -- a third from the "south rim of the crater" and one from the "southwest rim of the crater" -- and 35 artifacts to Group 4c (Renfrew et al. 1966:67, 72). Soon they added one geological specimen from "east of Bingöl" (apparently from a Bingöl A source, Çavuşlar or Orta Düz) and six more artifacts to the "Group 4c" definition (Renfrew et al. 1968:322, 324).

There are two issues with RDC's Group 4c definition that were repeated by other researchers and that made distinction between Bingöl A and Nemrut Dağ obsidians even more challenging. The first is too few geological reference specimens to account for the small chemical variations within obsidian sources. RDC relied heavily on archaeological artifacts for their group definitions, and they had just five Nemrut Dağ specimens and one Bingöl A specimen. Forty years later, Carter et al. (2008) compared Çatal Höyük artifacts to three Nemrut Dağ specimens and a single Bingöl A specimen (902). Bellot-Gurlet and Poupeau (2006) relied on only eight Bingöl A and Nemrut Dağ specimens (3), and Bressy et al. (2005) used five Nemrut Dağ and two Bingöl A specimens (1564). Clearly, for such geologically complex sources, these are too few specimens. For this study, I analyzed 40 specimens from the Bingöl sources (with at least eight more specimens to be analyzed in the next phase of this research) and one hundred specimens from Nemrut Dağ. I discuss the origins of my geological reference collection in Chapter 4.

The second problem, closely linked to having too few reference specimens, is best described as "lumping" -- that is, assuming that all obsidian specimens from, for instance, Nemrut Dağ belong to a single geochemical group. In turn, one may draw an oval around the "lumped" data points on scatterplots or use it to predefine groups for multivariate data analysis. "Lumping" is dubious, however, for geologically complex sources, as I discuss in Chapter 4. There are at least two Bingöl A sources, and Altınlı (1964) identified about twenty lava flows at Nemrut Dağ, suggesting that numerous obsidian deposits were likely present and compositionally distinct. As a result, I discuss in Chapter 6 how I decided not to identify *a priori* groups in my specimens, so I did not use discriminant function or cluster analysis. Instead, I treated each specimen individually in my data analysis, so that the individual flows are not lumped or averaged and can be discerned.

At the University of Michigan, Gary Wright and his colleagues started to identify subgroups within RDC's Group 4c using NAA (instead of optical emission spectroscopy) and fieldwork. Wright (1969) explains: "The field inspection of Nemrut Dağ by Watson and me in November, 1968, confirmed Altınlı's observations that more than one obsidian flow is represented at Nemrut Dağ" (10). After collecting specimens and analyzing them using NAA, they showed that the specimens "from two of the flows may be differentiated on the basis of Mn, Sc, Fe, and Zr" (10). The Fe, Mn, and Zr concentrations were higher in the flow dubbed Nemrut Dağ-B while Sc was higher in Nemrut Dağ-A. Based on this result, Wright concluded that most of the "4c" artifacts analyzed by RDC originated from Nemrut Dağ-B. He also reported "a flow located about 50 km east of Bingöl" (15), likely

the Orta Düz source (which has a "Bingöl A" composition). Analyses revealed that four specimens from this source fit within RDC's Group 4c, that they could be discerned from Nemrut Dağ-A and -B obsidians, and that only one artifact, unearthed from the Neolithic site of Çayönü in southeastern Turkey, matched this Bingöl source.

Others also distinguished groups in obsidian from Nemrut Dağ. Blackman (1984) found at least two, possibly three or four, different Nemrut Dağ compositional groups, but he did not analyze any Bingöl specimens. He used a different nomenclature than Wright: Nemrut I, II, III, and IV. Yellin and colleagues also reported two groups in Nemrut Dağ obsidians, which they called NMRD1 and NMRD2. Additional nomenclatures followed for Bingöl A and Nemrut Dağ geochemical groups (e.g., G1, G2, and G3 at the University of Bradford; A1 and A2 at C.N.R. Rome). Some studies reinforced the groups of Wright and those of Blackman (while simply giving them different names), and others suggested revisions (e.g., Blackman's Nemrut I and II should actually represent only one group and are possibly part of the same flow). Many of these studies were not actually informed by field experience -- few, if any, of these researchers had obsidian specimens collected from the field with geological knowledge of the region. These different laboratories also used various elements to distinguish the sources (e.g., Mn, Zr, Y, and Rb at Rome; Fe and Sc at Bradford; Rb and Sr at Freiberg; Ba and Zr at Heidelberg). These schemes to distinguish Nemrut Dağ and Bingöl A are summarized by Chataigner (1994).

In a meta-analysis of earlier obsidian studies, including his own, Poidevin (1998) noted three ways to distinguish Bingöl A and Nemrut Dağ sources. First, he reported the

Ba content is higher in the Nemrut Dağ obsidians compared to Bingöl A. Second, a plot of Al_2O_3 versus Fe_2O_3 reveals three clusters: (1) obsidian from the caldera interior, that he terms "Nemrut Lake" (and others term "post-caldera") and is high in Fe while low in Al; (2) obsidian from the southern exterior slope, that he terms "Nemrut South" (and others term "pre-caldera") and is low in Fe while high in Al; and (3) obsidian from Bingöl that has intermediate amounts of Fe and Al. His third approach is, in a way, the most obvious: the degree of "peralkalinity" of these obsidians. This is typically shown on what is called a CNK/A vs. NK/A plot -- that is, $(CaO + Na_2O + K_2O) / Al_2O_3$ vs. $(Na_2O + K_2O) / Al_2O_3$. The plot shows that the "Nemrut Lake" obsidians are more peralkaline than the "Nemrut South" obsidians and that the Bingöl A obsidians fall between them. This graph was also used to claim that Blackman's Nemrut III is actually equivalent to Nemrut Lake and that Blackman's Nemrut I, II, and IV are all equivalent to Nemrut South. Others (e.g., Bressy et al. 2005) have used such a plot and added a third Nemrut Dağ cluster, called "Nemrut Caldera," which falls close to the Bingöl A cluster. In Chapter 8, I reveal, however, that these claimed equivalences are not nearly so straightforward.

If there are multiple schemes to differentiate Bingöl A and Nemrut Dağ obsidians, why do so many studies (e.g., Gratuze et al. 1993, 1995; Abbès et al. 2001, 2003; Bellot-Gurlet and Poupeau 2006; Khalidi et al. 2009) claim that it is difficult, if not impossible, to do so? The problem apparently has three factors: (1) the necessary elements -- Ca, Na, K, and Al -- not being measured, (2) the elements being measured with poor precision by a particular analytical technique, and (3) poor inter-laboratory reproducibility when using

data from one technique or laboratory with data from another. For example, Rosen et al. (2005) assert that, to attribute artifacts to either Bingöl A and Nemrut Dağ, "such specific attributions could be confirmed through analysis of both artifacts and geological samples using the same instrument" (780). Chataigner (1998) showed the potential problem with using data from multiple laboratories: she compiled the Fe_2O_3 and A_2O_3 data from various laboratories -- Rome, Grenoble, Orleans, Strasbourg, Freiburg, and Berlin -- and put them on a single scatterplot. Due to poor reproducibility among these laboratories, the clusters for Bingöl A and Nemrut Dağ are diffuse and overlap. Consequently, she asserts that, to distinguish these sources, one must either use the data from a single laboratory or ensure that data from laboratories are consistent. Poidevin (1998) similarly claims that his inter-laboratory comparison of Bingöl A and Nemrut Dağ data reveals a problem:

> This clearly shows a major analytical problem and a lack of calibration between laboratories and compared to international standards... the bulk of the dispersion is directly attributable to analytical problems. (141, "Ceci témoigne à l'évidence d'un problème analytique majeur et d'une absence de calibrage entre laboratoires et par rapport à des étalons internationaux... l'essentiel de la dispersion est directement imputable à des problèmes analytiques.")

Their findings reinforced calls for obsidian analyses to include internationally recognized reference standards and estimates of accuracy and precision. In Chapter 6, I discuss these issues and the actions I took to ensure accurate and precise data.

2.6 - Issues with Recent Obsidian Sourcing: Tell Hamoukar

Özdoğan (1994) holds that relying too much on the work of RDC has "sometimes lured archaeologists into over-simplistic and, in most cases, baseless remarks" (423), and

I have warned against using RDC's obsidian distribution maps after the Neolithic simply because their data for the Chalcolithic and Bronze Age are especially sparse. While their "down-the-line" exchange model was widely criticized, the prevalence (and, accordingly, perceived authority) of the RDC distribution maps (particularly Figures 2.1 to 2.3) seem to influence the amount of obsidian sourcing done at Near Eastern sites. The existence of a perception that Near Eastern obsidian sourcing is "complete" is supported by Özdoğan (1994) and Williams-Thorpe (1995), as discussed in Section 2.4.1.

I have also discussed a variety of other issues in obsidian sourcing. For example, among the criticisms of RDC, Wright (1969) suggested that the mass of artifacts, not just their raw counts, would be insightful regarding the amount of obsidian present at a site. I mentioned that, as RDC were refining obsidian sourcing, a subject of interest was the rise and interconnectedness of Neolithic villages. In fact, at the time, large Neolithic sites like Çatal Höyük and Jericho were often interpreted as obsidian trading centers, and Mellaart claimed that Çatal Höyük arose and grew by controlling the distribution of obsidian from nearby Hasan Dağ, a hypothesis that was later refuted. I also pointed out that all obsidian sources in a region must be included in sourcing studies. The subtleties of distinguishing the Nemrut Dağ and Bingöl A obsidian sources were also discussed.

Recent work at post-Neolithic Tell Hamoukar in northeastern Syria is an example of relying on RDC's distribution maps while ignoring their obsidian quantity predictions as well as later developments in obsidian sourcing and its criticisms.

2.6.1 - Tell Hamoukar: The Tell and Its Southern Extension

Like numerous archaeological sites in this region, Tell Hamoukar is comprised of a High Mound (i.e., the "tell" itself, Arabic for "hill") about 13 hectares in area (32 acres, 0.13 square kilometers; Gibson 2000) and a Lower Town (or Outer City) as large as 100 hectares (245 acres or a full square kilometer; Gibson 2000). This settlement dates back to at least 4000 BCE. The area of the High Mound was settled about 3500 BCE, and the lower town reached its maximum extent around 2200 BCE. To the south is an area called the Southern Extension, initially noted during an archaeological survey of the Hamoukar vicinity. Ceramic sherds recovered from surface collection and soundings indicated that an area of about 280 hectares (700 acres, 2.8 square kilometers; Reichel 2006a) had been inhabited but not as densely as the High Mound or Lower Town. The sherds were dated to about 4500 to 4000 BCE. In the survey report, Jason Ur (2002:18) offered two likely explanations for the Southern Extension based on its sherd distribution:

> Two interpretations of the southern extension of Tell Hamoukar can be offered at present. Settlement may have been seasonal, with the inhabitants returning annually to different areas within the site through time. Another possibility is that the settlement was permanent but dispersed in small clusters of houses. The distribution of sherd density appears to support either of these interpretations.

Consequently, there are two main possibilities. First, the Southern Extension could be an area of seasonal encampments for itinerant agricultural workers who labored in the fields around Tell Hamoukar, harvesting crops and then either moving on to other settlements or returning to the outlying villages. Second, this area could instead be a pastoral habitation with space between the houses for livestock such as goats. This, too, could be a seasonal

settlement if the Southern Extension inhabitants practiced transhumance, that is, seasonal movement of people and their livestock between high pastures in the hot summer and low pastures in the cool winter. Herders at Hamoukar would have taken their animals into the southeastern Taurus Range to the north during the hot summer. Some combination of the two practices -- mixed farming involving both rainfall-dependent agriculture and animal husbandry -- is another possible interpretation for use of this area. It must also be pointed out that the Southern Extension dates to 4500 to 4000 BCE and that the earliest published dates from the High Mound are about 4000 to 3800 BCE. Therefore, apparently, there is no evidence that these two areas were simultaneously inhabited.

2.6.2 - Recent Excavations at Tell Hamoukar

In 2005, the expedition excavated three trenches in the Southern Extension. Their findings included a pot-sherd pavement framed by postholes, suggesting a tent, as well as remains of a room containing storage jars, suggesting a less transient settlement (Reichel 2006a:75). Obsidian tools and debitage indicated that these blades and points were made there. A year later, six new, large (10 × 10 m) trenches were excavated, and in addition to more Chalcolithic architecture and ceramics, they found what was characterized as "vast amounts of obsidian fragments" (Reichel 2007:65). Khalidi et al. (2009) state that about 3000 "obsidian products" (i.e., projectile points, blades, flakes, debitage) were recovered, of which over 80% are "blade fragments" (882, 889). They also report that the Southern Extension's lithic assemblage is more than 95% obsidian (889).

Also in 2005, the Hamoukar expedition unearthed widely publicized evidence that the settlement was attacked and suffered extensive destruction at around 3500 BCE. The evidence included a collapsed wall, two burned administrative buildings and an industrial area also burned, twelve graves, and over a thousand egg-shaped clay balls, interpreted to be sling bullets, found in rooms with collapsed walls and roofs. Most of these balls were found on the southern end of the site, so it was put forth that Hamoukar had been attacked by an army from the south (Reichel 2006b:9-10, Wilford 2007).

2.6.3 - Interpretation of Obsidian in the Southern Extension

The 2006-2007 Annual Report for the Tell Hamoukar expedition, published by the Oriental Institute of the University of Chicago, was written by the excavation co-director, Clemens Reichel, then at the University of Chicago and now at the University of Toronto. This annual report features an uncredited figure from Michael Roaf's *The Cultural Atlas of Mesopotamia and the Ancient Near East* (1990:34). Roaf was a director of the British School of Archaeology in Iraq, and he presently is Professor of Near Eastern Archaeology at the University of Munich. His obsidian distribution map -- see Figure 2.9 here -- is a somewhat updated version of the original RDC obsidian maps.

On his obsidian distribution map, Roaf replaced the symbols from the RDC maps with color-coded circles, and he made a few updates, especially for the Eastern Anatolian sources. For example, he separates the Bingöl and Nemrut Dağ sources, but it is unclear if his "Bingöl" source corresponds to the perakaline Bingöl A, the calc-alkaline Bingöl B,

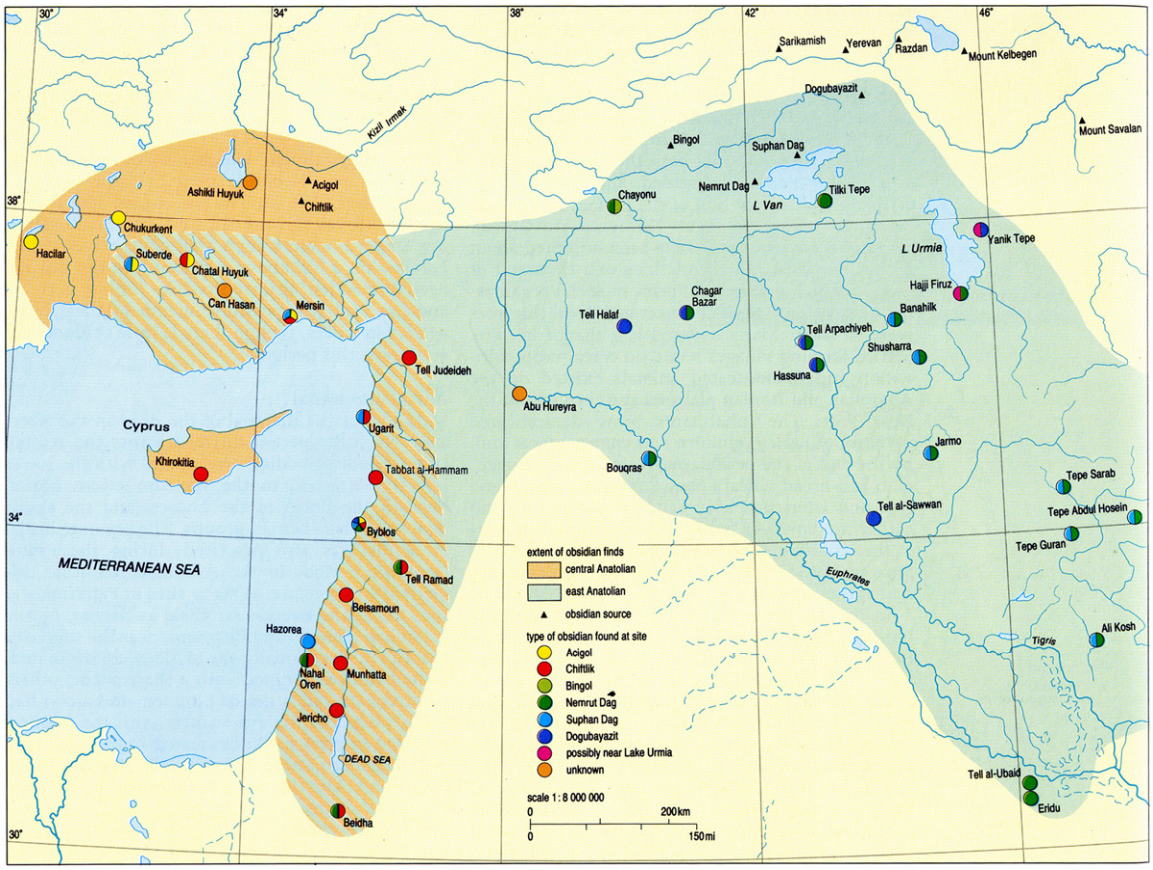


Figure 2.9 - Roaf's (1990) obsidian map is an updated, although somewhat problematic, version of RDC's obsidian maps. For example, he separates the Bingöl and Nemrut Dağ sources, but it is not clear if his "Bingöl" source corresponds to the perakaline Bingöl A, the calc-alkaline Bingöl B, or both. He misidentifies Meydan Dağ obsidians as Süphan Dağ obsidians, and Doğubeyazid is likely Tendürek Dağ. In addition, the circles do not show sources proportions, so the half-blue/half-green circles, for instance, are misleading.

or both. In Roaf's color scheme, dark green represents obsidian from Nemrut Dağ while, for example, light blue is Süphan Dağ (in my opinion, more likely Meydan Dağ) and dark blue represents Doğubeyazid (in my opinion, Tendürek Dağ). Many Mesopotamian sites, therefore, have half blue/half dark-green circles, showing mixed origins of their obsidian, regardless of the proportions (i.e., if 75% of the obsidian at a site came from Nemrut Dağ, the circle will still be half, not three-quarters, dark-green). Only Tell al-'Ubaid and Eridu in far Southern Mesopotamia have full dark-green circles.

Dr. Reichel (or another expedition member) modified Roaf's original figure -- see Figure 2.10 here (Figure 14 in Reichel 2007). A dashed circle was added around the Lake Van region, encompassing the lake as well as Nemrut Dağ, Bingöl, and Süphan Dağ, and this circle is labelled as "obsidian sources close to Hamoukar." An arrow, heavy dot, and label were also appended to the map to single out and highlight Nemrut Dağ. Hamoukar has also been added to the map and is represented by a heavy dot. Nemrut Dağ and Tell Hamoukar have been connected by a straight, dashed line, running almost directly north-south parallel to the 42° E longitude. The straight line must be intended to suggest some sort of a direct connection between Nemrut Dağ and Tell Hamoukar. This line apparently is not intended to indicate a literal route because, of the 200 km between them, about 150 km is quite mountainous terrain. This distance through southeastern Taurus range would be cut in half using a route to the southwest from Nemrut Dağ.

In another supplement to Roaf's map, a dashed, arcing line connects Hamoukar to Tell al-'Ubaid and Eridu in far Southern Mesopotamia, 750 km away. This line bypasses

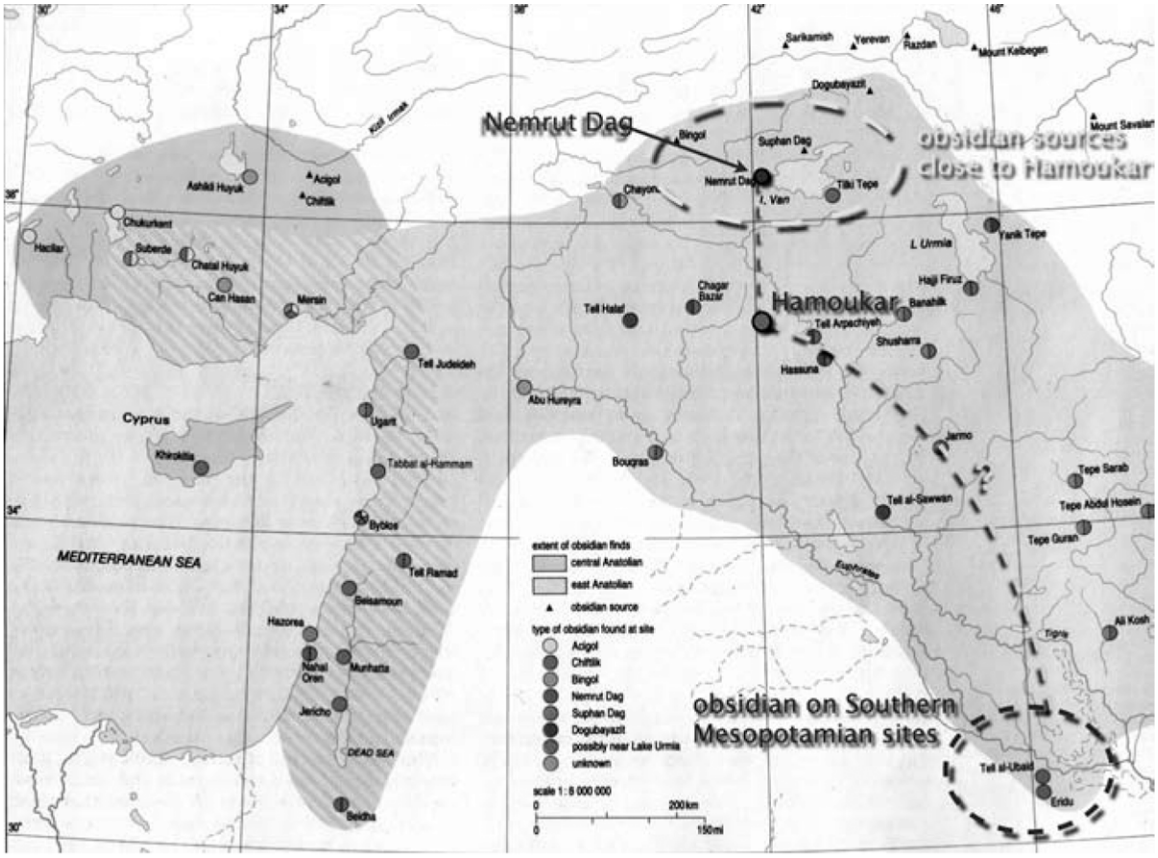


Figure 14. Map showing location of Hamoukar in relation to obsidian sources an possible trade connections with Southern Mesopotamia

Figure 2.10 - Reichel's (2007) modifications to Roaf's (1990) obsidian map. Note the addition of Tell Hamoukar, which has been connected via dashed lines to Nemrut Dağ in the north and to Tell al-'Ubaid and Eridu in the south.

other sites like Jarmo and Tell al-Sawwan, and it follows neither the Euphrates nor Tigris. Clearly the line is also not meant to indicate an actual route. In fact, the arc implies a less direct connection than the straight line between Nemrut Dağ and Hamoukar. The caption suggests that the line indicates "possible trade connections with Southern Mesopotamia." It is unclear if Tell al-'Ubaid and Eridu are highlighted because they are the southernmost archaeological sites on this map or because they are the only two sites with all dark-green circles, indicating that only Nemrut Dağ obsidians were used there.

In the text of the report, Reichel (2007) contends that their "evidence suggests that Uruk culture attacked and destroyed Hamoukar" and that the reasons might involve "vast amounts of obsidian fragments" unearthed in the Southern Extension (65). Based on the abundance of debitage, especially blade fragments, he labels the entire area an "obsidian-producing facility" (65). The implication (intended or not) of such a label is that all 280 hectares (700 acres, 2.8 square kilometers) of the Southern Extension is an industrial area dedicated to producing finished obsidian tools. Reichel writes:

> The discovery of a 280 hectares obsidian-producing facility at Hamoukar dating to the fifth millennium B.C. gives reason to pause and ponder… The only logical way to explain the size of our Southern Extension is as a shifting settlement. Even though it is abundantly clear that a production facility of this magnitude extended far beyond the needs of Hamoukar itself, its main purpose had to be export. This raises two important questions -- what were the sources of the obsidian, and where were the markets for the tools made from it? (2007:65)

I certainly agree that there is "reason to pause and ponder." For example, as Gary Wright (1969) pointed out, with respect to the research of RDC, we should consider not only the proportion of obsidian in the lithic assemblage but also its mass.

The average mass of the blade fragments at Tell Hamoukar has not been published yet; however, in my experience, such obsidian fragments are often only 1 gram or less. If we are a bit generous and allot 2 grams, on average, for each of the 2500 blade fragments, their total mass would be 5 kilograms (11 pounds). This means that just a single obsidian block or nodule with a diameter of 16 cm (6.3 inches) could, in theory, have yielded all of the recovered obsidian fragments. As I discuss in Chapter 4, John Whittaker, a lithics specialist, visited the Kömürcü obsidian source at Göllü Dağ in Central Anatolia, and he found nodules there with diameters of 15, 20, and even 25 cm (Whittaker, 2007, personal communication). The largest of these nodules would be about 20 kg. Also, as mentioned in Section 2.3.2, an obsidian chunk with a mass over 15 kg (33 pounds) was discovered at Tell Arqa in Lebanon, about 430 km (270 miles) from the Central Anatolian sources. The proposal, therefore, that the Southern Extension is an "obsidian-producing facility" seems unlikely. Furthermore, because a study of the fragments has not been published yet, it is unclear if these fragments represent blade production debris (e.g., errors and broken core-reduction blades) or broken blades at the end of their use-lives.

Reichel (2007) continues the report by speculating about the origin of the obsidian artifacts recovered from the Southern Extension of Tell Hamoukar. He writes:

> The next source of obsidian from Hamoukar is about 70 miles to the north at the Nemrud Dagh volcano to the west of Lake Van… Scientific analyses have matched the chemical fingerprint of Nemrud Dagh obsidian in blades from Ur and Eridu from the sixth and fifth millennia B.C. Even if a chemical analysis of the Hamoukar obsidian is still lacking, the fact that Hamoukar is in direct line between the Nemrud Dagh and Southern Mesopotamia seems to be more than a coincidence. A large-scale obsidian-producing facility at Hamoukar could also answer another important question raised in connection with Hamoukar's early

> urban adventure -- why did people move into the confines of a city in an area that by its geographic and climatic conditions allows rain-fed agriculture, hence favoring a village and subsistence-based lifestyle? (65-66)

First, it must be noted that the straight-line distance between Nemrut Dağ and Hamoukar is 120 miles (200 km), not 70 miles. Second, it is unclear why Reichel highlights Nemrut Dağ obsidian at three far Southern Mesopotamian sites -- Ur, Eridu, and, on the map, Tell al-'Ubaid -- and ignores neighboring sites with previously sourced obsidian, like Chagar Bazar, Kashkashok, Tell Arpachiyah, Tell Shemshara, Jarmo, and others. Third, it is easy to draw a straight line between Nemrut Dağ and two archaeological sites, and it would be entirely coincidental. Fourth, it overlooks two prior sourcing studies: Hall and Shackley (1994) sourced ten blades from the surface of Tell Hamoukar and concluded that nine of the blades came from Nemrut Dağ while one blade came from an unknown source, and Francaviglia and Palmieri (1998) sourced sixteen artifacts from Tell Hamoukar and found that all of them originated from Nemrut Dağ and/or Bingöl. Fifth, based on the obsidian distribution maps of RDC, which do not distinguish between Nemrut Dağ or Bingöl, it is equally probable that obsidian from Tell Hamoukar came from either source -- one or the other cannot be assumed based on their work alone. Reichel (2007) continues:

> A large-scale export of obsidian tools to the south would have required a significant surplus production and resulted in an accumulation of wealth that had to be protected by a wall -- such as the Late Chalcolithic city wall of Hamoukar discovered in 1999. Such a powerful position in the obsidian trade could also have contributed to Hamoukar's ultimate doom -- before the widespread use of copper in the later fourth millennium B.C., lithics not only were used for household tools but also for weaponry. If Hamoukar attempted to monopolize access to the Nemrud Dagh obsidian sources and the manufacture of tools from it, then it may have been seen as a threat to vital interests of the Uruk state and hence had to be eliminated. (66)

There is no suggestion of a mechanism by which the inhabitants of Tell Hamoukar could have tried to control access to an obsidian source about 200 km (120 miles) away. More importantly, though, there is little reason to suspect that Tell Hamoukar has an abundance of obsidian artifacts that would suggest it controlled access, or nearly so, to the sources at Nemrut Dağ or Bingöl. This hypothesis seems to stem from the fact that over 95% of the lithic assemblage is obsidian. Tell Hamoukar is located within RDC's "supply zone" for the Eastern Anatlian obsidians, and for sites within this zone, RDC claimed that obsidian comprises at least 80% of the flaked-stone tool assemblage. Consider, for example, Tell Shemshara in northern Iraq, approximately 360 km (200 miles) southeast of Nemrut Dağ. As reported in Renfrew et al. (1966), about 88% of the lithic assemblage is obsidian circa 5000 BCE and about 90% was obsidian circa 5100 BCE. Other strata at Tell Shemshara were over 90% obsidian. Another example is Çatal Höyük, which, like Tell Hamoukar, is about 200 km (120 miles) from its primary obsidian sources. The lithic assemblage there is about 96% obsidian circa 5600 BCE and 97% obsidian circa 5700 BCE. Therefore, the proportion of obsidian artifacts at Tell Hamoukar is not unprecedented. Reichel seems to have ignored this part of RDC's research while, at the same time, using their distribution maps to make predictions about the obsidian sources exploited.

2.6.4 - An Alternative Interpretation

Until more data from Hamoukar are published, I propose the following alternative hypothesis. Recall from Section 2.1.1 the applications of obsidian blades, and also recall

that the Southern Extension dates to 4500 to 4000 BCE while the easiest published dates from the High Mound are about 4000 to 3800 BCE, meaning the two areas may not have been inhabited simultaneously. The Southern Extension, as proposed by Jason Ur (2002), had been inhabited sparsely and, at least in part, seasonally. It could represent a time of mixed farming involving both rainfall-dependent agriculture and animal husbandry. The herders may have practiced transhumance and moved livestock between high pastures in the hot summer and low pastures in the cool winter. In particular, they would have taken their animals into the Taurus Range during the hot summer. While there each year, either via direct access or exchange, a few chunks of obsidian from Nemrut Dağ were obtained and brought back to Tell Hamoukar to provide sickle blades, butchering knives, and hide scrapers for the subsequent year. Inevitably, the tools broke, left scattered fragments, and were discarded after use. When the settlement became more urban and agricultural, such forays to the north became less common for inhabitants of the High Mound, so obsidian tools also were less common. There is no need to invoke expansive "obsidian-producing facilities" and "monopolized access to obsidian sources."

2.6.5 - Sourcing Obsidian from Tell Hamoukar

Khalidi et al. (2009) endeavored to source 32 obsidian artifacts from Hamoukar's Southern Extension with two analytical techniques: XRF and LA-ICP-MS (laser-ablation inductively coupled plasma mass spectrometry). The geological specimens analyzed for comparison originated from only three Eastern Anatolian sources -- Bingöl A (Çavuslar,

two specimens), Bingöl B (Çatak, one specimen), and Meydan Dağ (one specimen) -- and from two of the three sources at Göllü Dağ in Central Anatolia (Kalatepe and Birtlikeler, unknown number of specimens) (882). Of the artifacts, Khalidi and colleagues assign 27 obsidian fragments to Bingöl A, two fragments to Bingöl B, one to Meydan Dağ, and two to an unidentified source (884). Khalidi et al. (2009) analyzed geological specimens from just five obsidian sources: Kalatepe (a non-standard name for Komürcü) and Birtlikeler (a non-standard name for East Kayırlı) at Göllü Dağ, Bingöl A and B (Çavuslar and Çatak, respectively), and Meydan Dağ. Consequently, it is not surprising that their data revealed an "unknown source," which they labelled "source X" (881).

Furthermore, Khalidi et al. (2009) explain that their analyses could not distinguish between the obsidians from Bingöl A and Nemrut Dağ (883, 884). Peralkaline fragments are attributed to Bingöl A because, due to the presence of obsidian from Bingöl B at Tell Hamoukar, they contend, "it is highly probable" that these fragments "thus correspond to the Bingöl A source and not to Nemrut Dağ" (883). This interpretation is originally from Gratuze et al. (1993), who argued "if, at one archaeological site, we find the artifacts have *the two compositions* of the Bingöl area, we may suppose that the artifacts come from Bingöl," (16; emphasis added). Thus, Khalidi et al. (2009) conclude that their access to "obsidian sources such as Bingöl appears to have been direct" (886) and that the presence of so many blade fragments "reaffirms the likelihood of its population having been direct actors in obsidian exchange with the Bingöl source area" (889). This article does not cite Hall and Shackley (1994), who sourced artifacts from Tell Hamoukar. Francaviglia and

Palmieri (1998) are referenced but not in the context of having sourced obsidian artifacts from Hamoukar previously; instead, they are only cited as an example of researchers who could not differentiate obsidians from Bingöl A and Nemrut Dağ.

For the hypothesis put forth by Reichel (2007), it is crucial to know if the obsidian at Tell Hamoukar came either via exchange or direct access (1) primarily from the closest obsidian source, Nemrut Dağ approximately 200 km (120 miles) away, (2) primarily from the Bingöl sources, over 260 km (160 miles) away, or (3) from some combination of both Nemrut Dağ and Bingöl, about 130 km (80 miles) apart. Khalidi et al. (2009) report that most obsidian artifacts at Tell Hamoukar are green, indicating that their compositions are peralkaline and that their sources are Nemrut Dağ and/or Bingöl A. Unfortunately, these researchers chose analytical techniques that could not distinguish those sources. Khalidi et al. (2009) concede that it is possible that "some of the samples related to the Bingöl A obsidian source are in fact from Nemrut Dağ" (884). Indeed, perhaps half or even all of them are. Furthermore, they maintain: "It is not yet possible to fully distinguish between these two sources solely using elemental analysis" (884). This statement, as discussed in Section 2.5.2, is not entirely true, and the issue could be resolved.

2.7 - Summary and Problems

This chapter is intended to reveal the current status of obsidian sourcing in Near Eastern archaeology and how the research of RDC, now four decades old, simultaneously popularized obsidian sourcing and, to an extent, also stagnated it in the Near East. Each

site on the RDC obsidian distribution maps is represented, on average, by three artifacts, and the data for post-Neolithic contexts is particularly rare. Nevertheless, their maps are still used to assume what obsidian sources were used at specific sites, even contexts from the Chalcolithic and Bronze Age. As a result, four decades later, there are only about 110 sourced obsidian artifacts from all of Bronze-Age Mesopotamia and the Northern Levant, and 41 of those are from Syria. Even when the Neolithic and Chalcolithic are included in the tally, there are only 1600 sourced obsidian artifacts from the region. In comparison, a regional-scale study in the New World was done as part of a pipeline expansion project in the 1990s: over 9000 obsidian artifacts from over 130 Oregon, California, and Idaho sites were sourced (Skinner 1995), that is, roughly 70 artifacts per site. Very few studies in the Near East -- just three or four -- have sourced this many obsidian artifacts at one site. All in all, about 100,000 obsidian artifacts have been sourced in the New World, mostly from the Pacific Northwest, the Southwest, and Mesoamerica. Clearly there is a serious lack of primary data (i.e., sourced artifacts) for Mesopotamia. As a result, Near Eastern obsidian studies have, both practically and theoretically, fallen behind.

It is not enough simply to "do more obsidian sourcing" in the Near East: there is a wide variety of issues to consider, from considering the role of artifact type or technology in its exchange (i.e., the likely different exchange modes of flaked obsidian blades versus polished obsidian bowls) to including all known obsidian sources in the region and using appropriate techniques capable of distinguishing chemically similar sources, like Nemrut Dağ and Bingöl A. Archaeologists should be familiar with the data and theories of RDC

(as well as those of their critics) so that the past errors are not repeated, and their findings should be considered provisional, not definitive -- the recent discovery of obsidian blades from Nemrut Dağ or Bingöl A at Çatal Hüyük exemplifies this.

More obsidian data from the Near East is clearly needed, especially large numbers of sourced artifacts from major post-Neolithic sites. Developing non-destructive analyses is critical so that more obsidian artifacts will be available for sourcing.

Part I: Foundations and Problems

Chapter 3:

Tell Mozan, Urkesh, and the Hurrians

> Three Tells compete for the honour of our attention: Tell Hamdun which is geographically in an interesting sector; our first selection, Tell Chagar Bazar; and a third, Tell Mozan -- this is much the largest of the three… Soundings must be made at all three mounds. We make a start with Tell Mozan… Three trial trenches are selected at different levels of the Tell. There is a murmur of "Inshallah!" and the picks go in.
>
> -- Agatha Christie, 1946, *Come, Tell Me How You Live*

Tell Mozan is the site where I decided to conduct this study of nearly one hundred obsidian artifacts from a Near-East Bronze-Age city. In 1934, this site was surveyed by archaeologist Max Mallowan and his wife, Agatha Christie. After brief excavations, he instead chose Chagar Bazar (about 22 km south) for detailed study. Tell Mozan remained unstudied for half a century, until Giorgio Buccellati and Marilyn Kelly-Buccellati began excavations in 1984. Buccellati and Kelly-Buccellati suspected that Tell Mozan might be the Hurrian capital city of Urkesh, which they established in 1995. In 2006, I joined their

expedition for its nineteenth season to participate in the excavations and study the flaked-stone artifacts, concentrating on those manufactured from obsidian. Almost a hundred of these artifacts were approved for export to conduct laboratory analyses.

In this chapter, I briefly explain what is known about the ancient Hurrians, which is especially scant before the Late Bronze Age. I then describe the archaeological site of Tell Mozan as well as the geographical setting and surrounding landscape. The ancient and current climates and environments are likewise covered. I discuss the identification of Tell Mozan as the ancient Hurrian capital of Urkesh, which was known from myths preserved by the Hittites. Major archaeological features at the site are briefly described, some of which offer the only physical evidence of Hurrian practices or aesthetics. Lastly, I introduce a few of the issues about the Hurrians that could be addressed with additional information about their resource-procurement areas.

An overview of the Near Eastern world from the Chalcolithic until the Iron Age, or even just Northern Mesopotamia during the Bronze Age, is well beyond the scope of the chapter. Instead, those readers interested in placing Tell Mozan and the Hurrians in a wider context are directed to books written about the region and period. In particular, I recommend *A Companion to the Ancient Near East* by Daniel Snell (2005), *A History of the Ancient Near East ca. 3000-323 BC* by Marc Van De Mieroop (2007), *The Ancient Near East c. 3000-330 BC,* by Amélie Kuhrt (1995), and *The Archaeology of Syria* by Peter M. M. G. Akkermans and Glenn Schwartz (2003).

3.1 - Who were the Hurrians?

Our knowledge about the Hurrians is so fragmentary that many authors use words like "mysterious" and "enigmatic" to introduce them. It is hard to explain the issue more succinctly than Gernot Wilhelm in the preface for his 132-page book *The Hurrians*:

> The Hurrians were one of the most important ancient Eastern civilizations, and yet we have far less information, linguistic as well as historical and cultural, about them than we do about the Sumerians, the Babylonians, the Assyrians, the Hittites, or the Canaanites. However, the very contradiction between the obvious importance of the Hurrian role in the ancient Eastern world and the fragmentary evidence about it has given rise to a variety of assessments and even to rank speculation. (1989:v)

Indeed little is known about the Hurrians compared to contemporaries like the Sumerians and Akkadians. Entire books on the Near Eastern world leave out the Hurrians or merely mention them (or one of their kingdoms) in passing on a handful of pages.

The ancient Hurrians lived in Northern Mesopotamia and seem to have occupied a transitional zone between Anatolia (contemporary Turkey) and Lower Mesopotamia. The earliest evidence of the Hurrians dates to at least the mid-third millennium BCE, although most books still mistakenly claim the Hurrians did not appear in this area until the second millennium BCE. The Hurrians are often portrayed as immigrants or invaders from some homeland, frequently cited as southeastern Turkey or the Transcaucasus region. Hurrian city-states and kingdoms arose in the region, the largest of which was the Mitanni Empire circa 1500 to 1350 BCE. The Hurrians "disappeared" (e.g., became invisible historically) in about 1300 BCE, when the Assyrians assumed control in northern Syria.

From the start, I wish to emphasize that "Hurrian" is still, at present, a language-based identification for a group and carries the flaws of any such designation. The term "Hurrians" should essentially be considered as shorthand for the phrase "speakers of the Hurrian language" or, when contemplating ancient name lists, "individuals with Hurrian-lanaguage names." Similarly we should, at least for now, understand "the Hurrian city of Urkesh" to mean more properly "the Hurrian-dominated city of Urkesh." Such issues are covered by van Dassow (2008:68-69) and Buccellati (2005:4-6).

The problem is that, until recently, information about the Hurrians was basically limited to textual sources (name lists, seal impressions, and texts from Hittite archives and from vassal city-states on the periphery of a second-millennium Hurrian kingdom) and subsequent linguistic analyses. Most information about the Hurrians comes from a series of mid-second-millennium texts. Assyriologist Gonzalo Rubio (2008) writes that, "before the Urkesh discoveries... our knowledge of the Hurrians in the third millennium B.C. was limited mostly to personal names" in a few texts (8).

The Hurrian language, with the Urartian language, constitutes the extinct Hurro-Urartian linguistic family. These languages are neither Semitic nor Indo-European. The relationship of the Hurrian and Urartian languages was initially assumed to be lineal, and by extension, the ninth-century-BCE Urartians were thought to be the direct descendants of the earlier Hurrians. The assumption proved unfounded, and Hurrian and Urartian are most likely descended from a common predecessor. The early literature, though, contains information about the Urartians improperly applied to the Hurrians.

Some Hurrian myths and rituals were preserved in archives, unearthed in 1906, of the Hittite capital of Hattuša (the modern town of Boğazkale, formerly called Boğazköy). There are only about forty Hurrian texts, mostly religious and literary, from Hattuša. The Hittite archives also included Akkadian documents that refer to a "land of Hurri" and the "people of Hurri" (Wilhelm 1989:2). A few official Hittite texts also mention Hurrians, usually in the context of second-millennium military campaigns.

The textual evidence also includes name lists and names on seal impressions from sites throughout Northern Mesopotamia. In most cases, the presence of Hurrians at some site is inferred on the basis of Hurrian-language names discovered in lists. Of course, not every individual having a Hurrian name must have spoken Hurrian and followed Hurrian cultural practices, or vice versa. As mentioned previously, van Dassow (2008:68-69) and Buccellati (2005:4-6) cover such issues. von Dassow likens the endeavor to "recreating a city on the basis of pages torn at random from the city's phone book!" (xviii).

More information comes from "Hurrian" texts from Nuzi (modern Yorghan Tepe in Iraq) and Alalakh (modern Tell Atchana in Turkey), discovered during excavations in the first half of the twentieth century. These texts, though, describe the Mitanni Empire, an expansive Hurrian-dominated territory circa 1500 to 1350 BCE. These cities were on opposite sides of the Mitanni Empire: Alalakh in the west, near the Mediterranean coast, and Nuzi in the east, over 700 kilometers away. The two cities were only "Hurrianized" during the Mitanni expansion. This situation is not unlike attempting to learn about the Roman state by studying local documents from two border cities on opposite ends of the

empire. The local culture and practices were retained, at least in part, by the people, and locals still oversaw the government there. Accordingly, the texts at Nuzi and Alalah are sometimes contradictory (Wilhelm 1982:61), and these texts are written in the Akkadian language, not Hurrian. Readers interested in the process of "Hurrianization" at Alalakh are directed to a recent volume by Eva von Dassow (2008).

Numerous archaeologists have sought alternatives to relying on the name lists and texts as a means to trace the movement of the Hurrians. Ceramic types, of course, have attracted the most attention in such endeavors. Archaeologists first tried to link Khabur ware with the Hurrians (Akkermans and Schwartz 2003:308); however, Kramer (1977) concluded that the region in which Khabur ware is found was too culturally complex to associate it with just one group. Other ceramic types have been similarly explored for a link to the Hurrians -- Khirbet Kerak, Bichrome, and Nuzi wares -- but all were rejected for reasons of geographical or temporal distribution (Stein 1997:126-127).

In her book *The Ancient Near East: c. 3000-330 BC*, Amélie Kuhrt lists some of the many outstanding questions about the Hurrians, and she writes: "If we want to try to answer any of these questions it is essential to examine the sources for the Hurrians, which are exclusively linguistic: there are no artefacts or buildings that can with any certainty be defined as 'Hurrian' in type" (1995:284). Fortunately, this is no longer the case. In the same year that Kuhrt's book was published, Buccellati and Kelly-Buccellati finally proved that Tell Mozan is the Hurrian city of Urkesh.

Tell Mozan is among a very few conclusively Hurrian settlements. Many second-millennium tells in the Syrian Jezireh are often assumed to be Hurrian sites with little, if any, archaeological evidence (Buccellati and Kelly-Buccellati 2002b:127). For instance, two second-millennium cities of the Hurrian Mitanni empire, Waššukanni and Taite, are suspected to be Tell el Fakhariya and Tell Hamidiya, respectively; however, excavations have yet to prove these identifications. Other sites, like the previously mentioned Nuzi and Alalakh, only became "Hurrianized" during the expansion of the Mitanni Empire in the middle of the second millennium, and, consequently, the "resulting ethnic picture is complex, if not hopelessly confused" (Speiser 1953:319).

If one wishes to study the material culture of the Hurrians, especially before the mid-second millennium BCE, Tell Mozan is the place to work and study.

3.2 - Tell Mozan: The Archaeological Site

Tell Mozan lies in the northeast corner of Syria (latitude 37º 03' 27" N, longitude 40º 59' 50" E) at about 450 meters above sea level. The site is 7 kilometers southeast of the Syrian city of Amuda and 20 kilometers west of Al Qamishli. The Turkey border is 6 kilometers to the north, and the Iraq border is 70 kilometers southeast. The Euphrates River is to the west and south of Tell Mozan, and the Tigris River is to the east and north of Mozan. This places the site in the middle of the Syrian Jezireh (Arabic for "island," referring to the land between the Tigris and Euphrates).



Figure 3.1 - Satellite image of Tell Mozan (used in compliance with Google Maps' terms of use; imagery ©2010 DigitalGlobe and GeoEye; map data ©2010 Basarsoft).

The earliest evidence of occupation is a set of Halaf ceramic sherds, recovered in a deep sounding right above virgin soil. This intricately decorated ceramic type, named for the nearby archaeological site of Tell Halaf, dates to the end of the so-called Halaf Period, circa 5200 BCE (Akkermans and Le Mière 1992:1). A floor was revealed in the stratum directly above the Halaf sherds, and three Ninevite V cups sat on this surface. This type, named for Nineveh in Iraq, has diagnostic painted and incised patterns and dates to about 3000 BCE (Wilkinson 2000:225). This layer also included charcoal carbon dated to 2920 ± 170 BCE (Buccellati 2000:12). Halaf sherds were also noticed in the fields around the mound (Buccellati and Kelly-Buccellati 1995b:389).

This discontinuity -- ceramics from the end of the sixth millennium and the start of the third millennium -- remained until 2006, when fourth-millennium Late Chalcolithic ceramics were unearthed in multiple squares (Buccellati 2007:1, 3). Therefore, it seems the site was occupied continuously beginning in the mid-fourth millennium, if not earlier (Buccellati 2008b:1). The site was eventually abandoned between 1350 and 1300 BCE, when the Assyrians assumed control throughout northern Syria, and it was not resettled in antiquity (Buccellati and Kelly-Buccellati 2006:6, 2007c:141). This absence of later occupation periods has aided the preservation of the site.

As its name indicates, this site is a tell (Arabic for "hill"), that is, an accumulation of cultural material, mostly architectural mudbrick, built up by occupation over millennia and subsequently eroded into a mound. There is no naturally occurring hill at the site. A sounding, excavated in the process of digging a well for the fieldhouse, revealed cultural

materials (including ceramics) down to the level of the encompassing agricultural fields (Buccellati and Kelly-Buccellati 1997b:60, 2006:8). Geoarchaeologist Arlene Rosen's book *Cities of Clay: The Geoarchaeology of Tells* (1986) discusses the anthropogenic and natural formation processes of tells. As is common practice, Tell Mozan is named for the nearest village. In this case, Mozan, a small farming village comprised of perhaps one to two dozen households, sits at the northwest base of the mound.

The archaeological site is comprised of two major components: the conspicuous earthen mound, dubbed the High Mound by the expedition directors, and the much lower and less apparent surrounding area, designated the Outer City.

As noted by Agatha Christie in the quotation at the start of this chapter, Mozan is one of the largest tells in the vicinity. The High Mound is about 20 hectares (roughly 50 acres or 0.2 square kilometers) (Buccellati and Kelly-Buccellati 2007c:141). The peak of the High Mound rises an imposing 28 meters above the surrounding farmland (Buccellati and Kelly-Buccellati 2004:6), dominating the flat landscape for several kilometers all around. Its perimeter is roughly egg-shaped with its maximum dimension, approximately 600 meters, oriented north-south (Figure 3.2). Despite its name, the High Mound is not a single, congruous hill. Instead, it consists of seven lobes or sub-hills, some of which are separated by gullies (Kelly-Buccellati 1988:43). There is a flatter, central depression that is several meters below the highest points and has noticeably fewer sherds exposed on the surface (43). Such irregular topography is common among tells in the region and reflects spatial and temporal habitation patterns and subsequent erosion.

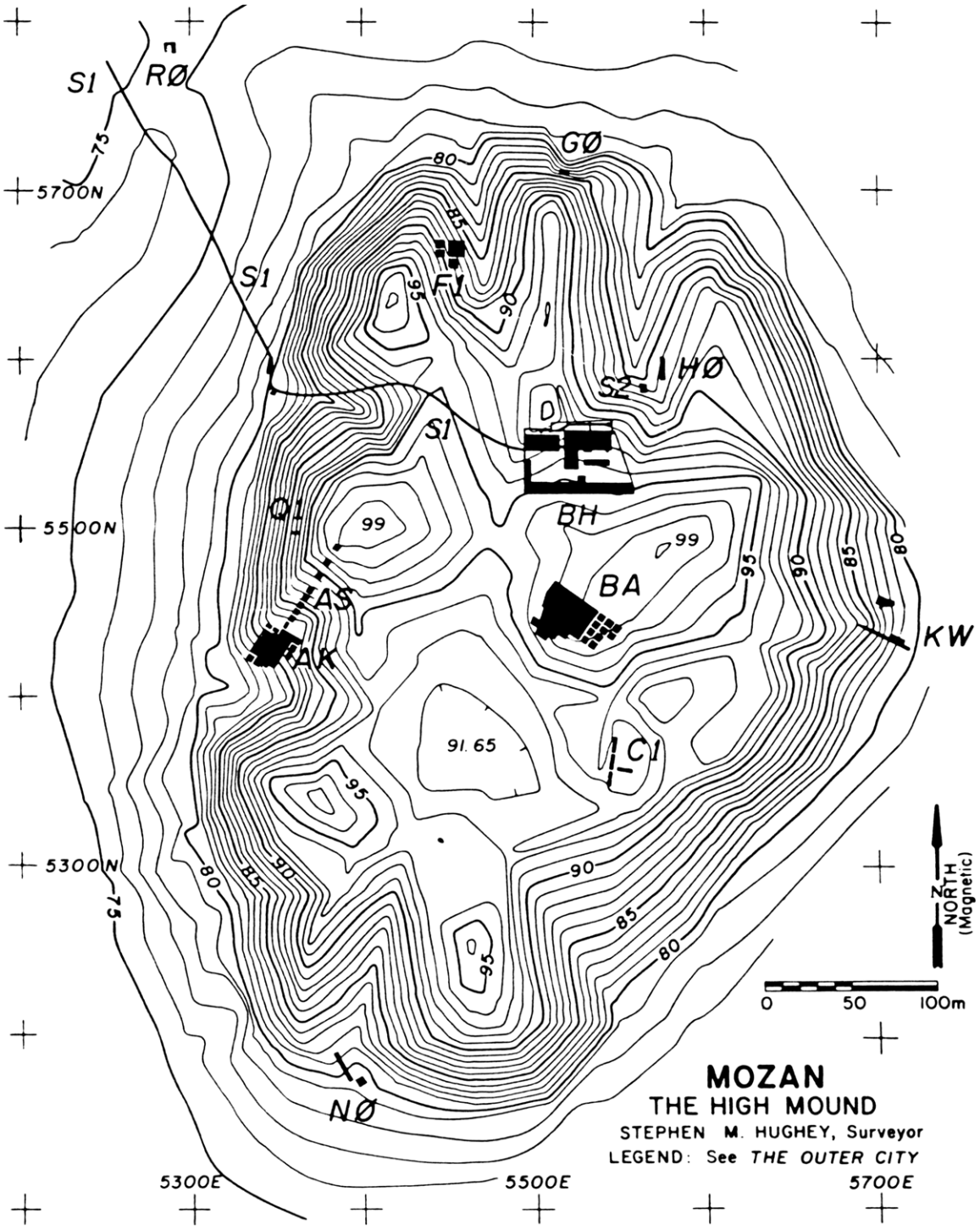


Figure 3.2 - Topographic map of the High Mound (Urkesh expedition image).

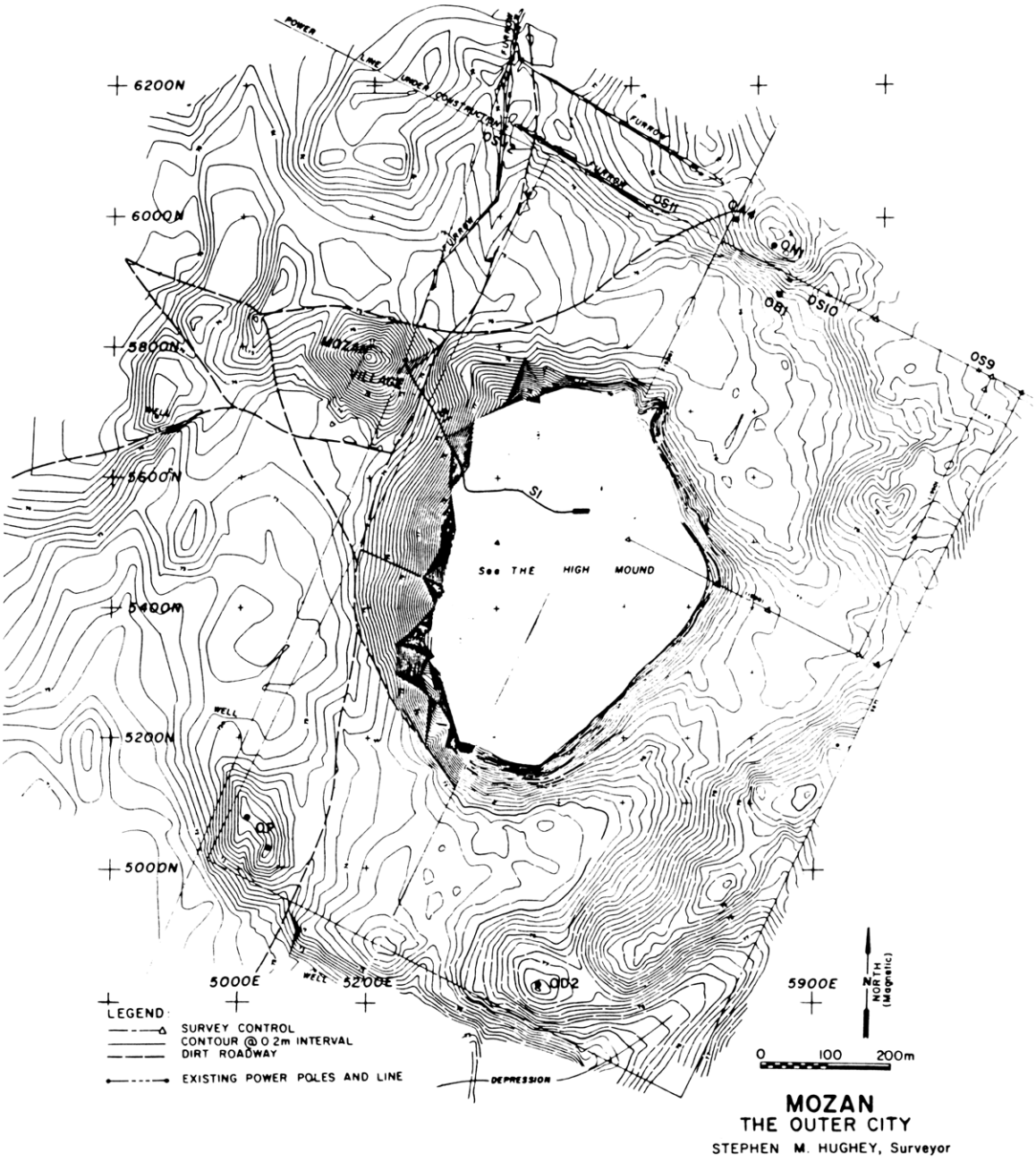


Figure 3.3 - Topographic map of the Outer City (Urkesh expedition image).

In contrast, the Outer City can easily go unnoticed by a visitor. Extending about 300 to 400 meters from the base of the mound is a slight rise that appears to encircle the High Mound (Thompson-Miragliuolo 1988:50). Low rises can be observed from the tell, usually when the sun is low, to the north and the south, but no such rises are apparent to either the east or the west. The rises are usually interpreted to be the remnants of an outer city wall, some portions of which have been destroyed due to plowing for at least several decades (Kelly-Buccellati 1988:43, Buccellati 2000:18). Thompson-Miragliuolo (1988) suggested that these rises could instead be interpreted as satellite settlements (50), much like those noted at nearby sites like Tell Brak (Ur et al. 2007).

Surface collections, archaeological soundings, and a series of holes for electrical lines revealed abundant cultural material within the perimeter but little outside, strongly suggesting that these rises represent a discrete boundary of cultural activity (Thompson-Miragliuolo 1998; Buccellati 2000:18). Moreover, geophysical surveys (Buccellati and Kelly-Buccellati 2004:7) have revealed a continuous, circular feature interpreted to be the stone foundations of a wall around the city. Numerous carved, limestone slabs have been unearthed in the surrounding fields by plowing and probably represent remnants of this outer wall foundation (Thompson-Miragliuolo 1998:55). It should be also noted that geomorphological studies have shown the ancient landscape in this area, exposed during the Chalcolithic period (circa 4000 BCE), is now buried as much as three meters beneath the current agricultural plains (Deckers and Riehl 2004).

The Outer City is clearer in satellite photographs than in person. Halos of lighter colored soil surround the High Mound in Google Earth (which, as of this writing, uses GeoEye and DigitalGlobe images; see Figure 3.1). This demarcation is more apparent in declassified Corona spy satellite imagery from the 1960s. In particular, image D025-055 1105-1 FWD, taken on 5 November 1968, shows Tell Mozan. The contemporary village of Mozan is contained entirely within the Outer City area. The village sits on a low rise, as seen on a topographic map of the site (Figure 3.3). The precise history of this rise is unclear, but a pit in Mozan village revealed fourth- to second-millennium-BCE sherds to a depth of nearly three meters (Deckers 2007:26). The abundance of ceramics from the third millennium BCE indicates this was the major occupation period of the village area (26). The reason why contemporary farmers would resettle this rise is simple: the locals attest that, as recently as two or three decades ago, winter floods usually swamped some fields in the vicinity (26). During especially severe years, even the village itself flooded (26). Placing the modern village on this small rise, within the outer-wall remnants of the ancient Outer City, must have been a strategy to avoid flooding.

Together the High Mound and the Outer City cover an area of about 130 to 150 hectares (about 320 to 370 acres or 1.3 to 1.5 square kilometers) (Buccellati and Kelly-Buccellati 2007c:141). It extends nearly one and a half kilometers on its north-south axis and about one kilometer on its east-west axis (Buccellati and Kelly-Buccellati 1988:25). Buccellati and Kelly-Buccellati (2001a) observe that its size "may not seem very big to a modern city dweller, but it was bigger than Ebla, one of the great centers of ancient Syro-



Figure 3.4 - The modern village of Mozan lies near the Royal Palace and within the Outer City (photograph by the author).

Mesopotamia" (24). With the Outer City, Tell Mozan is one of the largest archaeological sites of Syria inhabited during the third millennium BCE (1988:1, 2004:6). More about the layout and features of the site will be discussed in Section 3.6.

3.3 - The Geographical Setting and Environment

Tell Mozan sits at the north-middle of the so-called Khabur Triangle, essentially another name for the Upper Khabur River drainage basin. This area contains numerous important ancient sites, including (from west to east) Tell Halaf, Tell el-Fakhariyah, Tell Beydar, Chagar Bazar, Tell Brak, Tell Barri, Tell Leilan, and Tell Hamoukar. The entire area, especially the vicinity of Tell Mozan, is a transitional region between the Anatolian highlands to the north and the Mesopotamian plains to the south.

The Khabur River (also spelled as Habur) is a 320-km-long principal tributary of the Euphrates. The Khabur originates in mountain springs of southeastern Turkey, flows southward, and crosses into Syria at Ra's al-'Ayn. It then flows southeast to Al Ḥasakah, where it merges with the Jaghjagh River, and meanders south to join with the Euphrates at Deir ez-Zor. The Khabur Triangle consists of the area north of the confluence at Al Ḥasakah, and it is roughly defined by Ra's al-'Ayn on the west, Al Ḥasakah on the south, and, for lack of a better landmark, the town of Al Malikiyah on the east.

The region consists of a dendritic drainage system that, while roughly triangular, looks more like a tree leaf. This drainage basin includes dozens of named (e.g., Jarrah, Avedji, Khanzir, Kuneizir, Darah, Radd) and unnamed wadis. The term "wadi" (Arabic

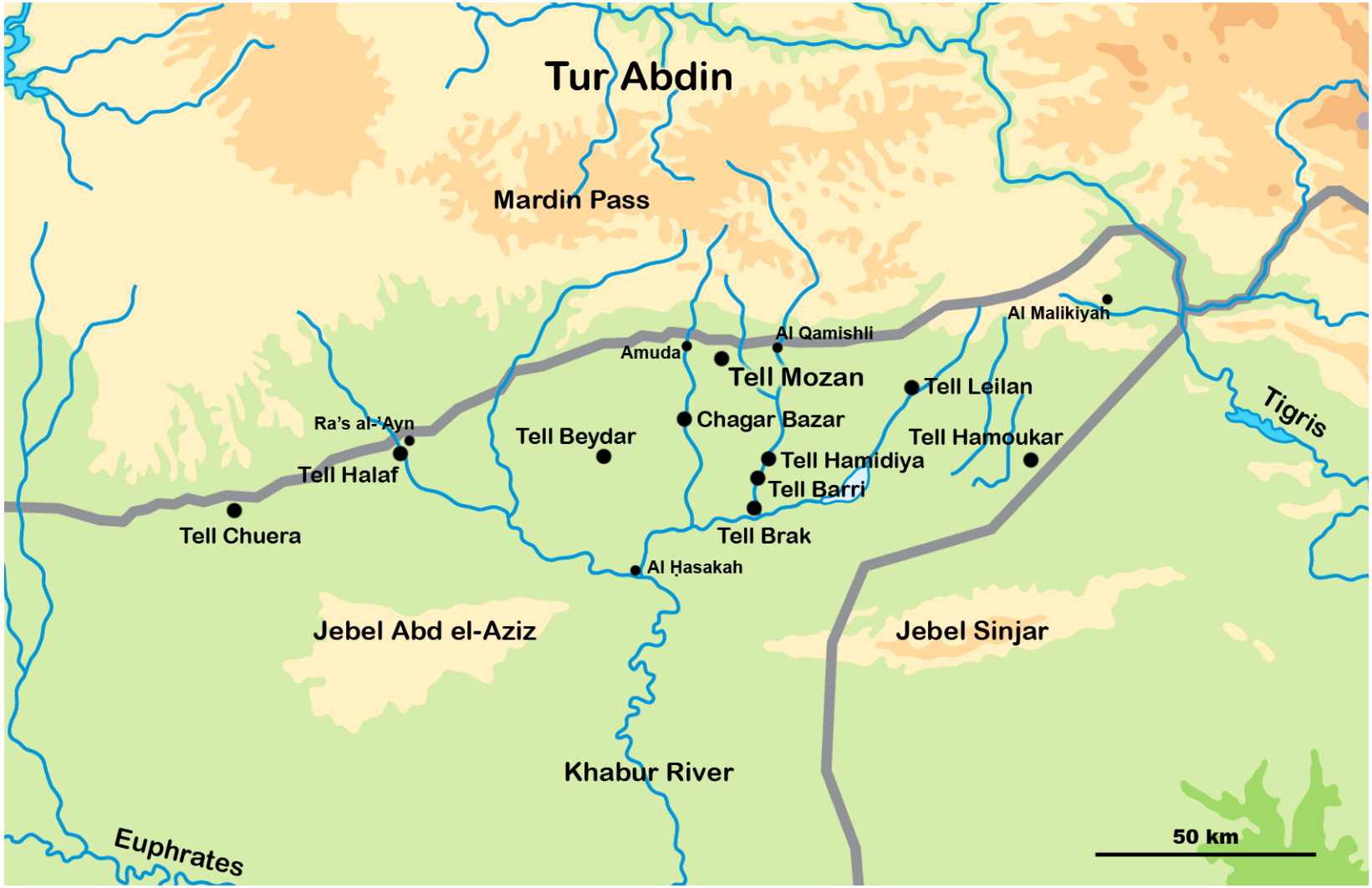


Figure 3.5 - Khabur Triangle features, sites, and modern cities (original map by GeoAtlas; used under license to the author).

for "valley") usually refers to an ephemeral streambed, sometimes dry but intermittently filled either seasonally or when it rains. The term, though, is also sometimes applied to streams and rivers (e.g., the Nahr Jaghjagh) that would naturally flow year round but run dry during arid summers as a result of damming and irrigation.

The Khabur Triangle has such a shape due to the regional geography. The wadis and rivers originate in the front range of the Taurus Mountains, known as the Tur Abdin (Syriac for "the mountain of the servants [of God]"). These wadis and rivers converge at Al Ḥasakah due to two mountain ranges: Jebel Abd el Aziz on the west and Jebel Sinjar (across the border in northwest Iraq) on the east (Figure 3.5). The Cornell Syria Project classified both Abd el Aziz and Sinjar as part of the same tectonic area and as geological features known as half-grabens (Brew et al. 2001:604). The two small mountain ranges each formed along a fault, or a fracture in the Earth's crust. On one side of the fault, the tectonic plate pushed upward, and it slipped downward on the opposite side. In this case, each short fault is oriented east-west, so the mountains have the same orientation. Jebel Abd el Aziz is about 100-kilometers long and 920-meters tall, and on the other side of the Khabur River, Sinjar is approximately 150-kilometers long and 1460-meters tall (Brew et al. 1999:291). The rise of these two mountains blocked the southward flow of wadis and rivers and diverted their flows into the Khabur River at Al Ḥasakah (Kolars and Mitchell 1991). Brew et al. (1999) discuss the relevant tectonics in detail.

The three major mountain ranges that shaped the Khabur Triangle are all visible from the top of Tell Mozan. Looking north, the Tur Abdin range fills one's view. On a



Figure 3.6 - The Tur Abdin mountains lie about 8 km to the north of Tell Mozan, which appears in the foreground. The Outer City of Urkesh extends to about the electrical tower in the middle of the photograph. (Photograph by the author).

clear day, the peaks of Jebel Sinjar are visible on the southeast horizon, and Abd el Aziz is visible on the horizon in the southwest. Another geological feature is also evident on the southwestern horizon just to the left of Abd el Aziz: a cinder-cone volcano known as Sharat Kovakab about 60 kilometers away. I suspect, and hope to establish with future research, that Sharat Kovakab is the source of the vesiculated basalt used at Tell Mozan to manufacture ground-stone tools, such as millstones. This volcano, though, is not the type that erupts magma with the proper conditions to create obsidian.

The rest of the view from Tell Mozan, with the exception of a handful of smaller tells, is filled by semi-arid steppe as far as the eye can see. In *Geobotanical Foundations of the Middle East* (1973), Michael Zohary classifies the modern flora as Mesopotamian steppe vegetation. Low shrubs are scattered across the rolling plateau, and the only trees occur in irrigated orchards, near a well or oasis, or at the base of the tell, where trees can use rainwater that runs off the mound. A garden and a cotton field are irrigated with rain run-off in the same way. The surrounding fields contain winter wheat, planted in fall and harvested in summer. The wheat grows in soils that consist of clay, silt, and loam (a mix of clay, silt, and sand) and are often fine-grained and calcareous (chalky).

Much of this sediment is recent, and it originates from the calcareous Tur Abdin range to the north in Turkey and was deposited by alluvial (water-driven) and colluvial (gravity-driven) processes. The fine silty layer that covers everything after a sandstorm testifies to aeolian (wind-driven) sedimentary processes throughout this region as well. Wilkinson et al. (2001) and French (2003) describe the geomorphology and soils at Tell

Brak, located about 45 km south of Tell Mozan, while McCorriston (1992) and Deckers and Riehl (2007) discuss the wider Upper Khabur Basin. Much of the agriculture in this area is quite recent. Hole (2009) points out that, a mere seven decades ago, most of the land in northeastern Syria was utilized by nomadic groups, like various Bedouin tribes, for sheep and camel grazing before irrigated farming proliferated (4). Shepherding still exists in the region (Figure 3.7b), but this lifeway is a dying one.

The climate in the region of Tell Mozan is semiarid, marginally suited to rain-fed agriculture, and characterized by dry, hot summers and wet, mild winters. In the nearby city of Al Qamishli, January has a mean high temperature of 11º C (51º F), a mean low of 2º C (36º F), and a mean precipitation of 78.2 mm (3.08 inches). July has a mean high of 41º C (105º F), a mean low temperature of 23º C (74º F), and a mean precipitation of 0.3 mm (0.01 inches). The annual precipitation at Tell Mozan is 425 mm, most of which falls between autumn and spring, occasionally as snow in winter. Rainfall abates to 250 mm at Al Ḥasakah (about 65 km south of Mozan) and eventually to less than 150 mm at the desert's edge (McCorriston and Weisberg 2002:486; Hole 2009:6).

Within the Khabur Triangle, only two major archaeological sites do not currently have an immediately adjacent watercourse. One site is Tell Mozan, and the other is Tell Hamoukar (Gibson et al. 2002:45-46, Figure 2). Today, Wadi Darah (sometimes spelled Dar'a) is a few kilometers south of Mozan and is presently the nearest seasonally active wadi (Buccellati and Kelly-Buccellati 1997b:60). This, though, was not always the case. The same Corona satellite imagery which exposes the Outer City also reveals, during the



Figure 3.7 - Agriculture (a) and pastoralism (b) are still practiced together in this part of northeastern Syria. Winter wheat is the primary crop there. (Photographs by the author).

1960s, a tributary of Wadi Khanzir flowed just west of the High Mound and near Mozan village (Deckers and Riehl 2007:343, Figure 1). Additionally, these declassified images suggest that a relict wadi possibly coursed through the tell (Deckers and Riehl 2007:343, Figure 7). In addition to these wadi remnants mentioned by Deckers and Riehl (2007), Google Earth images indicate a second relic wadi approximately 2 kilometers east of the High Mound and a third about 1.5 kilometers west. Such watercourse changes are likely due, at least in part, to a series of dams and canals that were built throughout Turkey and Syria in recent decades and have changed the flow of seasonal streams.

3.4 - The Past Environment and Climate

Paleoecological studies have shown how the environment of Tell Mozan differed during its height and how the site's inhabitants enjoyed a desirable niche. Fragments of charcoal indicate the presence of an oak park woodland in the Khabur Triangle (Hillman 2000; Deckers and Riehl 2004:343; Deckers 2006). The piedmont steppe was probably more like a savanna, having light tree coverage (Buccellati and Kelly-Buccellati 2007c: 146). Deckers and Riehl (2004) propose the current woodlands in the Taurus mountains approximate the flora surrounding Tell Mozan during the Bronze Age (343).

In addition to regional studies of plant remains, notably McCorriston (1992) and McCorriston and Weisberg (2002), both covering the Upper Khabur Basin, two studies have investigated the natural and cultivated plants specifically at Tell Mozan. Calvin (1988) examined carbonized grains collected from two spots. One set of grain samples

contained 93% domestic bread wheat (*Triticum aestivum* L.), 3% wild barley (*Hordeum spontaneum*), and 2% wild einkom (*Triticum boeoticum* Boiss. em. Thiem.) (83-84). In the second sample, the species proportions were almost identical (85). Calvin concluded that the two "small samples indicate nothing unusual, but in fact, reflect a much expected dependence on domestic bread wheat by the population" (86).

In her studies of the vegetation at Tell Mozan, Riehl (2000) reports some species indicate moderate to moist site conditions (236). She collected charred wood and seeds from Middle Bronze Age levels of the High Mound (Riehl 2006). The wood fragments originated from a variety of trees, including (roughly in order of decreasing abundance) poplar or willow, olive, ash, elm, plane, pistachio, juniper, and cedar (Deckers and Riehl 2004). The seeds of three cereal species were also identified: two-row barley (*Hordeum distichum*), emmer wheat (*Triticum dicoccum*), and bread wheat (*Triticum aestivum* or *durum*) (343). Her identifications differ from Calvin (1988) at the species level but are otherwise similar. Deckers and Riehl (2004) claim that, in particular, the bread wheat indicates favorable growing environs due to its greater water demands (343). Legumes were recognized as well among the seed remains: bitter vetch (*Vicia ervilia*), grass pea (*Lathyrus sativus/cicera*), lentil (*Lens culinaris*), chick pea (*Cicer arietinum*), and bean (*Vicia faba*) (Riehl 2000; Deckers and Riehl 2004:343). Scattered grape (*Vitis vinifera*) and fig (*Ficus carica*) seeds were also found (343), and Riehl (2006) postulates that the seeds represent collection from wild trees in the vicinity. Visitors to the site today will see fig trees growing in the courtyard of the expedition fieldhouse.

Stable carbon isotope analysis has also been conducted on the archaeobotanical remains at Tell Mozan (Riehl et al. 2008). The ratio of ^{12}C to ^{13}C in plants is dependent, in part, on climate. In particular, because the lighter (^{12}C) and heavier (^{13}C) isotopes are absorbed differently depending on how efficiently plants use water (e.g., Farquhar et al. 1989; Ehleringer 1989, 1993), the ratio has been used as a proxy for water conditions in the past, such as annual rainfall (Miller et al. 2001), humidity (Edwards et al. 2000), and moisture of the soil (Chen et al. 2005; Wang et al. 2005). Riehl and colleagues used the carbon isotopic ratios to investigate growing conditions throughout the Khabur Triangle during the Bronze Age (Riehl et al. 2008). The $\Delta^{13}C$ values from botanical remains at Tell Mozan indicate that the site had "good natural water availability" during the Early Bronze Age and that it was among those sites with a low evaporation rate, "resulting in well-balanced moisture conditions" during that time (1020). Later, in the Middle Bronze Age, the values suggest decreased water availability (1018).

Relict wadis, as discussed earlier, indicate more abundant water in the antiquity, and Deckers and Riehl (2007) discuss the fluvial history of extant wadis in the Khabur basin. At a transect excavated near Tell Ḥamīdī, roughly 23 kilometers due south of Al Qamishli, sediment sizes indicate that the Jaghjagh had a stronger, steadier flow during the mid-fourth to mid-third millennium BCE (345). Water was sufficiently abundant, according to the botanical evidence, that the Jaghjagh sustained a riverine gallery forest with willows and swamps populated with sedges. After the mid-third millennium, a rise in the deposition of fine-grained, silty sediments suggest that either the wadi had shifted

or its flow diminished (346). Drier conditions have been reported for the end of the third millennium BCE (Courty 1994; Bar-Matthews et al. 1998:211). Consequently, Deckers and Riehl (2007) conjecture that the Wadi Jaghjagh slowed as a result of either these drier conditions or a reduction in trees, and therefore an increase in erosion, due to intensifying land use in this area for agriculture (346). Information about similar fluvial evidence near Tell Mozan is reported by Deckers (2007:25-27).

Faunal remains also indicate wetter conditions in northeastern Syria. The bones recovered at archaeological sites include various animals not currently found in the area, including Indian elephants (*Elephas maximus*) along the Lower Khabur River Valley and the Euphrates (Becker 2005) and lions (*Felis leo*) at Tell Mozan and other archaeological sites (Uerpmann, personal communication). Perhaps the best faunal evidence of plentiful water is the Eurasian beaver (*Castor fiber*). Beavers are not currently found in Syria, but their bones and teeth have been noted at archaeological sites throughout the Jezireh: Tell Abu Hureyra and Tell Hadidi (Legge and Rowley-Conwy 1986), Tell es-Sweyhat (Weber 1997), Tell Mulla Matar (Vila 1998), Tell Sheik Hassan and Jerf al Ahmar (Gourichon and Helmer 2004), and Tell Sheikh Hamad and Tell Bder along the Lower Khabur River Valley (Becker 2005). In addition, a stone carving of a beaver was found at Tell Halaf (Brentjes 1964:184), and an Akkadian text complained that beaver dams would impede shipping on the Euphrates at times (Landsberger 1934:86).

3.5 - Urkesh: The Ancient Hurrian City

As noted in the introduction to this chapter, Giorgio Buccellati and Marilyn Kelly-Buccellati began excavating Tell Mozan in 1984 with the hypothesis that it was the site of the Hurrian city of Urkesh (alternately spelled as Urkish or Urkeš). Buccellati and Kelly-Buccellati often refer to Urkesh as a Hurrian "capital" (e.g., 1997a; 2002b), but their use of this term is not meant to imply that Urkesh was a seat of power for an empire like that of the Akkadians or Assyrians. Instead, Urkesh was an urban center that appears to have administered an extensive hinterland, including mountainous territory to the north. This territorial control will be discussed later in Chapter 9. Despite its importance, Urkesh did not appear to develop beyond a city-state (Buccellati 2003). Instead, farming villages in the vicinity probably had Hurrian inhabitants who were, through linguistic and cultural traditions, linked to Urkesh (Buccellati and Kelly-Buccellati 2001a:26).

At this point, it should be noted that the terms "Urkesh" and "Tell Mozan" are not interchangeable. Tell Mozan was inhabited by the mid-fourth millennium BCE, possibly much earlier, and abandoned by 1300 BCE. During some fraction of this period, the city was called Urkesh, the capital of the Hurrians. We do not know what it was called when first settled or when it was eventually deserted. Urkesh, therefore, should be considered one of the settlements whose remains form Tell Mozan. Buccellati and Kelly-Buccellati (2007) advise that there is "every reason to believe that this city is indeed Urkesh from" the mid-fourth millennium (150). The city was definitely named Urkesh circa the late-third millennium, roughly 2200 BCE, and it was likely Urkesh for centuries before and

after, encompassing most of the Bronze Age. It is also possible, though, the settlements at Tell Mozan, over the millennia, went by a variety of names.

Furthermore, although the contemporary village of Mozan does not sit atop the High Mound, this tell is still a cultural space, not quite a ghost town. For instance, the area that I helped excavate in 2006 (Unit J3 within the central depression) had been the village's soccer field. Shepherds bring their flocks across the tell. It is not unusual for local youths and teens to hang out on the tell some evening. A small orchard sits at the northwestern base of the tell, taking advantage of the rain runoff, and a cotton field sits on the southeastern corner for the same reason. Two small cemeteries, circa the 1940s, sit atop the tell: one on a southwestern hilltop (for one of the small villages to the south) and another on a northeastern high point (for Umr'rabie'e to the east). A third cemetery, in collaboration with the Mozan villagers, was relocated onto lower ground. Lastly, the fieldhouse, inhabited by archaeologists from Syria, Italy, and several other countries for a few months every year, sits on the northern side of the tell.

Before the identification of the site, the city of Urkesh was known as "the ancient religious and political center of Hurrian civilization... from historical, mythological, and ritual texts" (Buccellati and Kelly-Buccellati 2003:224). Myths designate Urkesh as the abode of the god Kumarbi, father of the Hurrian deities (Buccellati and Kelly-Buccellati (2002b:127). One myth called the "Song of Silver," preserved in Hittite archives, relates the tale of a young god, Silver, who lives in a mountainous hinterland. When he asks his mother about his father, she tells Silver that his father is Kumarbi, the "father" of Urkesh,

where he resides and rules. The young god then travels to Urkesh in search of his father, but Kumarbi is not there. Instead, the ancestral god is off roaming through the highlands. The full tale is reported in Hoffner (1990:46-7). Buccellati and Kelly-Buccellati (2001a) suggest the myth may well be symbolic of the Hurrian landscape at the height of Urkesh, signaling a kinship between people living in the urban center and those in the mountains (26). This link between the city of Urkesh and its resource-rich, mountainous hinterland will be discussed further in later sections, particularly in Chapter 9.

Such texts, discovered in Hittite archives, remained the only evidence of Urkesh until two arsenical-copper lion sculptures appeared in a *souq* in Amuda in 1948. One of these lions is now displayed in the Louvre, and the other is in the Metropolitan Museum of Art (Figure 3.8). The stone tablets held by the lions were scribed in Hurrian, starting with the phrase "Tiš-atal, king [*endan*] of Urkesh, built the temple of Nergal." Hence, these lions are foundation pegs, the Mesopotamian equivalent of building cornerstones. Foundation pegs were often deposited at the foundation of a monumental structure, such as a palace or temple, and attribute its construction to the king at the time. In addition to commemorating the responsible king, foundation pegs are also thought to have provided spiritual protection, a task seemingly well suited to a pair of lions.

For four decades, Near Eastern historians and archaeologists presumed these lion sculptures came from a tell in the vicinity of Amuda, but which one, in a region peppered with tells, was unknown. Placing Urkesh in the vicinity of Amuda was consistent with an Old Babylonian travel itinerary, which placed the city "in the western half of the Khabur



Figure 3.8 - One of the two lions that served as foundation pegs for the Urkesh temple. This lion is displayed in the Metropolitan Museum of Art (photograph by the author).

Triangle" (Goetze 1953:62-63). A common thought (e.g., Drower 1973:417, Kuhrt 1995: 285) was that the lions came from a tell in Amuda (called Tell Amuda in the literature but Tell Shermola locally) (Buccellati and Kelly-Buccellati 1988:89).

Visits to Tell Amuda/Shermola by Buccellati and Kelly-Buccellati (1988) and a subsequent inspection by Bunnens and Roobaert (1988) revealed no evidence of a major third-millennium settlement. Buccellati and Kelly-Buccellati then turned their attention to Tell Mozan, which we have established is one of the largest in the area. Their earliest excavations in 1984 on a summit of the tell quickly revealed the foundations of a temple, dating to about 2500 BCE, very near the mound surface (2001a:19).

Excavations in 1995 uncovered hundreds of *bullae*, that is, clay lumps that were molded around a cord, which was, in turn, wrapped about a shipping container. The wet clay was imprinted with a seal, usually denoting the destination or owner, and one could not tamper with a shipment without damaging the *bulla*. Some of these seal impressions discovered at Tell Mozan had legible Hurrian inscriptions. The name "Urkesh" appeared on some, and others revealed the name of a previously unknown Hurrian king: "Tupkish, *endan* [king] of Urkesh" (Buccellati and Kelly-Buccellati 2001a:18). Just as important is where these *bullae* were found: in an accumulation, which built up over time, in a service wing of the royal palace. This deposition pattern suggests that shipping containers were opened in the room and their contents either stored or distributed while the broken *bullae* fell to the floor and remained there (22). These *bullae* and their resting place established

that Tell Mozan was indeed Urkesh. I will further discuss this room in the service area of the royal palace, and its contents, later in Sections 3.6.4.

The *bullae*, and the palace around them, date to about 2200 BCE (Buccellati and Kelly-Buccellati 2007a:1). The previously mentioned temple, which sits atop 25 meters of cultural material, dates to approximately 2400 BCE. I stated in Section 3.1 that other materials at Tell Mozan date to 3000 BCE and earlier, back to the mid-fourth millennium, maybe farther. Even the latest of these dates moves back the presence of the Hurrians in Syro-Mesopotamia by centuries. Before the 1990s, most textual evidence of the Hurrians dated to the second-millennium BCE, so it was widely taken for granted that they arrived in Syro-Mesopotamia then. Buccellati and Kelly-Buccellati (2001a:23) write:

> Besides identifying Tell Mozan as Hurrian Urkesh, our excavations demonstrate that Hurrian civilization developed in northern Mesopotamia much earlier than formerly believed. For example, a distinguished encyclopedia of Near Eastern archaeology, published just four years ago, observes that the evidence indicates "a Hurrian presence in northern Syria and Anatolia as early as 2000 B.C.E." That is the common view: that the first Hurrian kingdoms, including Urkesh, came into existence at the very end of the third millennium B.C. as a result of the collapse of the Akkadian Empire in southern Mesopotamia.

A notion that Urkesh arose as a city-state after the fall of the Akkadian empire cannot be reconciled with the archaeological evidence, including the existence of the royal palace, built by a Hurrian *endan* (or king), during the height of the Akkadian period. The glyptic evidence, in fact, indicates that a daughter of Naram-Sin of Akkad, who ruled during the peak of the empire, resided at Urkesh, likely as a queen (Buccellati and Kelly-Buccellati 2001c:63). Furthermore, the oldest examples of the Hurrian language have already been

mentioned here: the inscriptions on the two copper lion sculptures and their stone tablets as well as the *bullae* from the palace (Buccellati 1999:244).

I have already mentioned here a few of the major archaeological features of Tell Mozan: the High Mound, the Outer City and the foundations of its outer wall, the royal palace, and a temple. In the next section, I shall describe these and other features of the archaeological site in more detail. After that, I will discuss outstanding questions about the Hurrians that may be addressed using obsidian sourcing.

3.6 - The Features and Layout of Tell Mozan

The overall layout of Tell Mozan is known as a *Kranzhügel* (German for "wreath mound"). The term was coined by Max von Oppenheim, German diplomat and amateur archaeologist who excavated Tell Halaf prior to World War I, during his surveys of Syria (Akkermans and Schwartz 2004:256). Crawford (1991) describes this settlement type as an "upper town, or citadel, [that] sits in the middle of a further ring of land enclosed by a fortification wall" (123). This type of settlement appears to have arisen during the mid-third millennium in the Khabur Triangle, primarily to the south and west of Tell Mozan (122,128). Besides Tell Mozan, other prominent *Kranzhügel* sites are Tell Chuera, Tell Beydar, and Tell es-Sweyhat. Of these, only Tell Chuera can be argued to be a Hurrian settlement with any confidence (Buccellati and Kelly-Buccellati 2001a:26).

There is variation among *Kranzhügel* sites. For instance, Crawford (1991) points out that the land between the "citadel" and outer wall sometimes contains structures but,

in some examples, is nearly vacant, leading to a hypothesis that it was a stockade area for urban pastoralists (123). This seems quite a substantial distinction. It is just as important that these features might not actually be contemporaneous. Indeed, that appears to be the case at Tell Mozan: the outer city wall was not constructed until the inner city wall was razed, and a terrace might have predated both features. The usefulness of the *Kranzhügel* designation is therefore questionable. Instead, I will describe here the important features of Urkesh, including their dates and relationships to the other features.

Much of the information covered here was initially published in articles available online in the Urkesh Electronic Library, part of the expedition website: www.urkesh.org. This information is supplemented by discussions with the expedition directors as well as my own observations from fieldwork at the site in 2006.

3.6.1 - The Temple(s)

As mentioned earlier, the first excavations on the High Mound quickly revealed the foundations of a temple, sitting atop over 25 meters of cultural material. The temple remnants were dated, based on the ceramic types and seal impressions, to approximately 2500 BCE (Buccellati and Kelly-Buccellati 2001a:19-20). Later the temple was linked stratigraphically to a layer carbon-dated to about 2350 BCE (2004:16). These remains sat right below the current surface of the tell. Its height over the surrounding agricultural plains would have been about 30 meters, rivaling the ziggurat at Ur.

The excavations uncovered a foundation of limestone boulders, roughly carved, on which mudbricks were laid (1997b:61). Based on its foundation, this temple was an open room about 9 by 16.5 meters (61). It was entered via a stone ramp about 8-meters long (61). Plan views were published in Buccellati and Kelly-Buccellati (1997b), and a CG reconstruction is found in Buccellati and Kelly-Buccellati (2007b).

As noted earlier, texts preserved in Hittite archives state that Kumarbi, father of the other deities in the Hurrian pantheon, rules from Urkesh. The previously discussed stone tablets, held by the lion sculptures, state that "Tiš-atal, king of Urkesh, built the temple of Nergal," not Kumarbi. Because the temple remnants are close to the modern surface, it is certainly possible these lion sculptures were discovered in the 1940s while digging graves for the Umr'rabie'e cemetery (about 50 meters from the temple) or even during surface collection. It is also likely that the prominent temple at Urkesh would be dedicated to Kumarbi, the god closely linked to the city in Hurrian myths. How can we reconcile these? Astour (1968) maintains that "Kumarbi" is actually a title rather than a personal name and that this deity's real Hurrian name (as of the article's publication) was unknown. Buccellati suggests that "Nergal" is really a logogram for a Hurrian name and that "Nergal" and "Kumarbi" may well be one in the same (2005b:10). For these reasons, Buccellati and Kelly-Buccellati propose that the temple of Urkesh was likely dedicated to the Hurrian ancestral god Kumarbi (2006:6, 25; 2007b:72).

Both earlier and later versions of the temple likely sat in this location. Buccellati and Kelly-Buccellati (2006) maintain that, while the "current" form of the temple dates to



Figure 3.9 - A partial reconstruction of the temple (photograph by the author).



Figure 3.10 - My square of Unit J3, excavated down to the temple terrace surface paved with *baqaya*. The circular pit is a second-millennium *tannur* (photograph by the author).

about 2400 BCE, a series of temples most likely sat there, being periodically rebuilt over millennia (6, 16). The terrace on which the temple(s) sat is the next topic.

3.6.2 - The Terrace and Revetment Wall

The temple remains lie on a massive platform or terrace, sitting not far below the modern tell surface and outlined by a stone wall (Buccellati and Kelly-Buccellati 2001a: 25). The use of stone for the wall, as well as apparent curation in the past, has protected the terrace from erosion over three millennia. Sitting atop this terrace, the temple would have been about 30 meters over the agricultural plains in antiquity. The temple dates to about 2400 BCE, so the terrace on which it sits must predate that period. The terrace, in its "current" form, could date as early as 2700 BCE (2001a:25).

Geophysical surveying, a combination of magnetometry and ground-penetrating radar (GPR), revealed an oval-shaped feature (2004:16). The resulting maps exhibited an unbroken line in the shape of an oval, about 40 by 60 meters, suggesting the presence of a continuous feature like a wall (2006:4; 2007a:1; 2007c:148). Excavations between the temple and the central depression of the tell revealed a stone wall, about 3 meters tall, which the expedition directors have termed the "revetment wall" for reasons that we will discuss shortly. The idea that this terrace was an oval, based on the geophysical surveys, persisted until the 2006 field season. During that season and subsequent ones, excavated squares revealed three bends in the revetment wall, one fairly sharp, evidencing that this terrace is instead an asymmetrical polygon in shape (2007a:2-3).

The wall, as noted already, is about 3 meters tall and about a meter wide, roughly the thickness of two boulders used in its construction (2006:12). Its irregularly shaped limestone boulders are held in place using only mud mortar (12). These stones have not been carved to fit together tightly. Instead, the rocks have just been roughly hewn. The wall also has no substantial foundation; instead, it is merely set into the ground about 30 centimeters (Buccellati 2009b:24). Given its composition and dimensions, the wall could not have mechanically functioned *sensu stricto* as a retaining wall for the terrace. It must have instead been a revetment wall to halt erosion and likely also for aesthetic purposes (Buccellati and Kelly-Buccellati 2006:12). Consequently, because this wall is too weak to be a retaining wall, Buccellati (2009b) proposes that it was "designed to serve almost as an ornamental crown around a preexisting [fourth-millennium] slope" (24). Buccellati and Kelly-Buccellati (2006) furthermore suggest that the revetment wall may well have served as "a barrier that arrests the view of the onlooker and marks the threshold between the two worlds, the sacred [above] and the profane [below]" (26).

Buccellati (2009b) reports that, during the 2008 season, a subtle triangular pattern built into the wall was observed. The "zig zag" pattern is expressed by differences in the sizes of boulders. He notes that this pattern, similar to early pictograms for "mountain," could have been intended to reinforce links to the alpine north:

> I would therefore suggest that the triangular pattern has a subtle ideological nuance, namely, that it recalls the mountains which are ever present in the background landscape of the city..., and of which the Temple Terrace itself is like an echo. The pattern is well known as a motif in cylinder seals of the same time period, including one from Urkesh... that we have interpreted as representing the god Kumarbi "walking in the mountains," as the myths say. (24)

Connections, both physical and ideological, of the Hurrians to the mountains to the north will be a recurring theme later, particularly in Chapter 9.

The terrace surface, or *glacis*, was paved, at least in part, with *baqaya* (Arabic for "remainder"), which is the Mozan villagers' term for a variety of local clay, very hard and reddish, after it is separated from the gravel components (Buccellati and Kelly-Buccellati 2007a:5). The locals are familiar with this clay product because it is still used in the area as a durable material for building subfloors (5). One possible function of the *baqaya* was to facilitate even rainwater runoff and to prevent erosion of the terrace (2005a:4). Across the *glacis*, the *baqaya* pavement varies from 30- to 50-cm thick (2006:9). It is joined to an interior coating of the revetment wall and is level with the top (9). Two or more rings of sizable stones circled the *glacis* concentrically (2006a:5; 2006:11), and there are also indications that the terrace was paved using mudbricks (2007b).

Excavations down to the exterior base of the wall revealed a ceramic assemblage indicative of about 2400 BCE, about the same date as that of the temple (2005b:3). The elevation of the terrace at this time indicates that the temple sits "above layers that were considerably earlier in date or... on a massive artificial fill" or some combination of both (2006:8). In 2005, Late Chalcolithic sherds were found beneath the *glacis* surface and interpreted as an anomalous occurrence, part of fill brought in from elsewhere, possibly the Outer City, to build up the terrace height (2006:3; 2007a:3). Then, beginning in the 2006 season, more exposures revealed fourth-millennium deposits so consistently that an earlier phase of the terrace, dating to that time, seems most likely (2007a:3). The size of

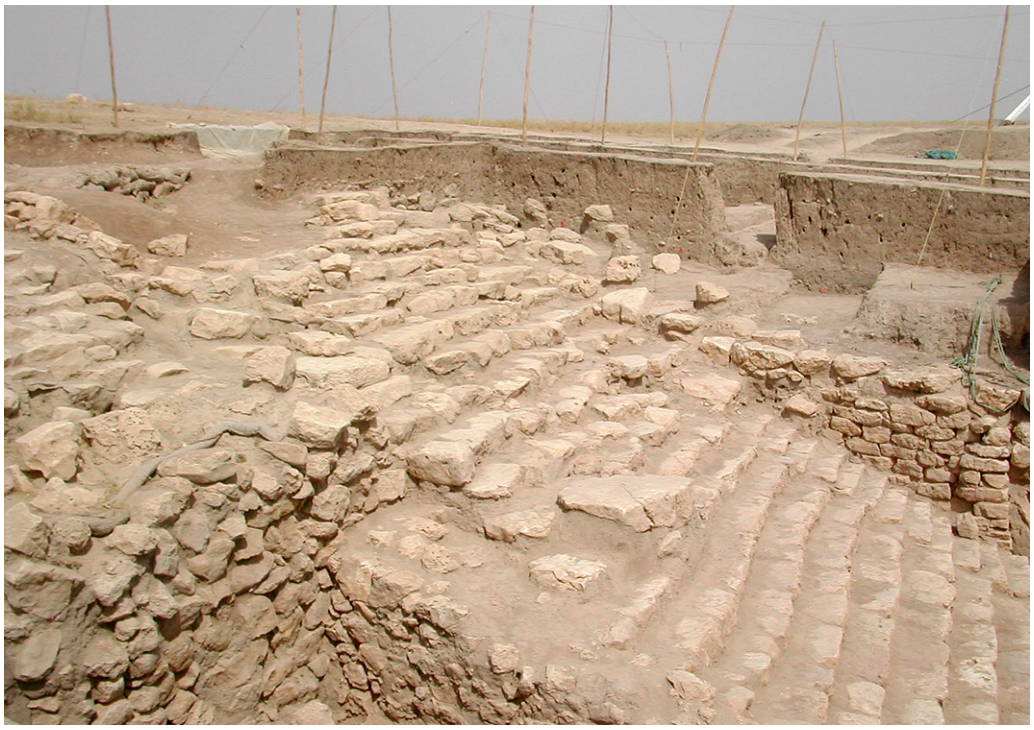


Figure 3.11 - The monumental staircase to the temple terrace (photograph by the author).



Figure 3.12 - The revetment wall (left) of the temple terrace (photograph by the author).

this antecedent was probably about that of the later terrace (2007c:148). Buccellati and Kelly-Buccellati (2006) infer the existence of an earlier temple terrace, which served as an "inner core" and around which fill, including Late Chalcolithic sherds, was packed to level off the later phase with the top of its new revetment wall (5).

Excavation in conjunction with ground-penetrating radar and magnetometry have shown that, by the mid-third millennium, buildings sat on the northern and eastern parts of the terrace while the western and southern portions were free of structures (2007b:23). Buccellati and Kelly-Buccellati (2004) offer that the buildings may have been related to the temple (16). Stratigraphic evidence, uncovered by additional excavations, reveal that the revetment wall is so well preserved because it was maintained from its construction to roughly a thousand years later (2004:17). After about 1500 BCE, natural sedimentation processes started to cover the wall, completely obscuring and protecting it by the time the site was deserted circa 1350 BCE (2006:6). This finding suggests that, even though the city was smaller during the second millennium (a trend throughout the region during this time), Tell Mozan retained its function as a religious center (2004:17).

3.6.3 - The Monumental Staircase

The terrace was accessed via a monumental stone staircase on the southern edge of the revetment wall (Figure 3.11). At the bottom of the staircase is the plaza, the topic of the subsequent section. The 24 massive steps are adjoined on the west by a trapezoidal

"apron" consisting of stone steps roughly twice as tall and wide as those of the staircase, somewhat resembling an ancient amphitheater (Buccellati 2009b:24).

The monumental staircase was assumed to be symmetrical, with only half of it initially exposed during the 2005 season. During subsequent seasons, though, this has proved incorrect. Instead, Buccellati and Kelly-Buccellati (2007a) propose, based on the findings about the asymmetric shapes of the terrace and its staircase, that symmetry "was clearly *not* part of the stylistic preferences of the Hurrians" (3).

Three phases of the staircase's construction have been identified, resulting in an important conclusion (2005b:5). The lower portion of the exposed staircase was built contemporaneously with the terrace wall and the plaza, roughly 2400 BCE (5). This is the middle phase. Beneath the surface of the plaza are older stone steps with a distinct appearance, so they must date to a prior phase (6). This evidence of an older staircase, lying beneath the later one, is thought likely to correspond to the earlier version of the temple terrace, dating to the fourth millennium (2007c:149). The upper portion of the exposed staircase dates to a later period, roughly 1500 BCE, meaning a staircase to the terrace was used by the inhabitants for more than a thousand years (2005b:6). Such an apparent continuity of the religious features, from potentially the fourth through second millennia, suggest a cultural continuity as well (2007c:149).

3.6.4 - The Plaza

The bottom of the third-millennium phase of the monumental staircase connects to a plaza, which is thought to stretch west all the way to the palace. Between the base of the revetment wall and the plaza, which sits roughly 2 meters lower, is an escarpment, a sloped surface that joins these two features (2006:5).

As noted previously, the central depression on the High Mound had a marked lack of sherds while second-millennium remains are abundant elsewhere (2006:3). An initial geophysical survey indicated that the nearly sherdless area in front of the terrace wall had no discernible structures or features (4). Excavations corroborated that the accumulated sediment against the revetment wall and on the open plaza was devoid of any structures, not even pits or *tannurs* (2005b:4). Buccellati and Kelly-Buccellati (2005b) interpret this to mean that the plaza remained open and in use until the mid-second millennium (4). It seems that sedimentation started covering the plaza during the Khabur period, circa 1800 BCE, when new structures constructed on the southern portion of the terrace blocked the flow of rainwater from clearing the plaza of sediment (2006:5).

3.6.5 - The Royal Palace

The plaza area appears to connect the monumental staircase to the royal palace on the western edge of the High Mound. The entire palace, based on its known dimensions, is projected to cover more than 3500 square meters (2003:225). It was constructed circa 2250 BCE, which corresponds to the Akkadian period (2001b:76). The palace consists of



Figure 3.13 - Excavations in Area A and the remains of the Royal Palace built by Tupkish. The palace walls are covered with green and tan canvas over steel frames to protect them. A white canvas dome is covering the *âbi*. (Photograph by the author).

two major areas: the service wing and the formal wing, where the royal family lived and presided over the government (2004:10). The service wing has been excavated entirely, covering a thousand square meters (2003:224). Designated as area AK, the service wing is 5 meters above virgin soil (1995a:4), and the floor of the formal wing (AF) is 2 meters above the service wing (2002a:13). Whereas the formal wing became deeply covered by later structures, the service wing remained near the tell surface.

As mentioned in Section 3.2, Tell Mozan was eventually confirmed as Urkesh by a collection of *bullae* found in the service wing of this palace. Based on over a thousand seal impressions on these *bullae*, corresponding to roughly 80 different seals, the room in which they were found was used during the middle to late Akkadian period, circa 2250 to 2150 BCE (2002b:128,132). The *bullae*, as noted earlier, were originally molded around a cord, which was wrapped around a shipping container. The abundance and depositional pattern of the *bullae* suggests that shipping containers were opened in this area and their contents either stored or distributed (2001a:22). This particular portion of the palace has been termed the "storehouse" in the Urkesh literature, but Buccellati and Kelly-Buccellati (1997a) explain that this palace area was "not a long-term warehousing depot, but rather the provisioning center for the immediate needs of the court" (91). It probably contained supplies for use by the royal family as well as goods from city workshops, the hinterland, and nearby and distant settlements for redistribution (2002b:128).

In addition to the storerooms (termed Sector B), the service wing is comprised of three additional sectors: a kitchen (D), workspaces (C), and an area too eroded to deduce

its uses (A) (2004:10). The ceramics, both sherds and entire vessels, as well as other artifacts in the various palace rooms have suggested their likely functions. Room D1 is interpreted as a kitchen because it contained a *tannur* and a set of andirons for a hearth (Buccellati 2000:21). A thick-walled room perhaps offered cool storage for perishables (Buccellati and Kelly-Buccellati 1995a:28). There was also an open workspace (Sector F), termed the service-area courtyard, which connects to the kitchen and the storerooms. Walker (2003) proposes that cobbled paths in this area functioned to protect the surface from pack animals carrying supplies into and out of the palace (55).

The floor surfaces of these two wings exhibit the status difference between them. The floors of the service wing were covered by a thin plaster coat while the floors of the formal wing had high-quality plaster pavements (Buccellati and Kelly-Buccellati 2002a: 13). The courtyard in the formal wing has a flagstone surface (13), but the workspace in the service wing has only earthen and pebble-paved floors (Walker 2003:54).

Stratigraphic evidence suggests that the service wing of the palace remained in use, although in a different capacity, after the formal wing was demolished (Buccellati and Kelly-Buccellati 2002a:13). The excavations within the formal wing "have shown evidence of localized destruction, followed by an immediate re-occupation, though of a type clearly not in keeping with its earlier palace functions" (2001b:60). For instance, a *tannur* was put in the courtyard, likely part of a domestic habitation (60).

This palace is sometimes called the "Tupkish palace" because it was constructed during the reign of Tupkish and his queen Uqnitum (2004:15). Two subsequent *endans*

(the Hurrian term for king) also lived there: Tar'am-Agade's husband and Ishar-napshum (15). It remains unknown when the first royal palace was constructed at Tell Mozan or if it lay in the same location (2005a:42). Buccellati and Kelly-Buccellati (2001b) mention the possibility that, after the formal wing of the Tupkish-era palace was destroyed, a new palace was constructed nearby, perhaps slightly to the south (60).

3.6.6 - The Âbi

Buccellati and Kelly-Buccellati (2004) propose that the palace, built by Tupkish circa 2300 BCE, was intended to function as a connection between two existing religious structures: the temple, as discussed in Section 3.6.1, and the *âbi*, described here (9). The plaza, discussed in Section 3.6.4, linked these royal and sacral structures.

Located just south of the palace, the *âbi* is a large, circular, stone-lined pit, about 5 meters in diameter. It has been excavated down 8 meters (2007c:149), and the bottom has not been reached. The hypothesis that the feature was a well was considered, but the deposition pattern is inconsistent with such a use (2004:13). A well would be expected to have irregular accumulations of material dumped inside it. Instead, the accumulations were "very regular, as if within a house" (13). In addition, the faunal evidence indicated some use other than that of a well. Bones of juvenile suids and canids (i.e., piglets and puppies) were unearthed in those highly regular deposits, a combination does not match the faunal remains found elsewhere throughout the site (13).

The mix of piglets and puppies, though, is found in texts from the Hittite archives that describe a Hurrian ritual for evoking spirits of the underworld (13). The name "*âbi*" originates from these texts (13). The texts describe a practice in which one either digs a shallow pit or inscribes a circle in the soil using a pin or dagger, and piglets and puppies are slaughtered within that pit or circle (13-14). This massive stone-lined *âbi* appears to be a monumental construction for containing a long sequence of shallow pits and circles for this ritual (14). This pit, then, was probably where a Hurrian religious figure would consult or appeal to the spirits of the underworld (2004:9).

In addition to the suid and canid skeletons, which were the most abundant, there were lesser amounts of sheep, goat, and donkey remains (Collins 2004:55). Bones from an adult dog were also found (55). An adult canine discovered in another area of the tell (J4) was identified by Drs. Hans-Peter and Margarethe Uerpmann as a Saluki or similar dog (2007:28). This is not surprising because Parker et al. (2004) analyzed the DNA of modern dogs and concluded that Salukis were among the first breeds to branch off from wolves in the Middle East. Examination of the skeletal remains revealed butcher marks on the bones, except for those of the canids (Collins 2004:55). The Hittite texts suggest that the necks of the suids and canids would have been ritually slit.

Only a few artifacts were recovered in the âbi, including a small anthropomorphic vessel and a jar spout with a suid head shape (Buccellati and Kelly-Buccellati 2004:14). Also recovered in the pit were some bronze pins and silver rings (Collins 2004:55). The

accumulations also included ash, pebbles, and seeds (54). A few of the ceramic vessels were recovered whole (Buccellati and Kelly-Buccellati 2004:14).

The lowest excavated level of the âbi dates to circa 2400 BCE, contemporaneous with the third-millennium temple terrace (2006:6). Not much later, roughly at the time of the palace construction, circa 2300 BCE, the âbi was covered using a corbel arch, and a square antechamber was added on the western side, toward the setting sun (2007c:142). The currently exposed level of the âbi is about 6 meters above virgin soil. It is certainly possible that additional excavations would reveal that this structure dates back as far as the fourth millennium (142). Perhaps the original stone-circle base dates back so far that it rests on virgin soil, even with the ancient agricultural plain.

The *âbi* is one of the features of Tell Mozan that is distinctly Hurrian and differs from anything in Lower Mesopotamia (2007c:147). This is the only known example of such a structure, offering a contrast to the religious practices of Hurrian contemporaries such as the Sumerians and the Akkadians (Buccellati 2005a:20).

3.6.7 - Road to the Netherworld

Against the palace wall is a platform with an apparently associated stone drain (Buccellati and Kelly-Buccellati 2004:14). Buccellati and Kelly-Buccellati (2004) have proposed that this drain is another Hurrian ritual structure described in Hittite texts: the road to the Netherworld (14). They state that, if true, the drain "is the counter-part of the

âbi: through the latter, the spirits of the Netherworld come to the surface" and "through the former, humans send liquids down into the earth" (14).

3.6.8 - The Inner City Wall

In Section 3.2, I discussed the Outer City and the remnants of a perimetral wall, most likely for defense. The entire High Mound, though, was also once encircled by a wall. The inner city wall is the principal reason for the steep slopes of the High Mound today (2004:8). This wall was 5 to 6 meters tall and about 8 meters thick, and it dates to about 2700 to 2600 BCE (2001a:20). A *glacis* seems to have extended out 15 meters, beyond which the presence of a moat has been inferred (1995b:387). With such a form, this inner city wall apparently served a defensive purpose.

The city wall no longer served a defensive function by the time that the Tupkish palace was constructed. During the mid-third millennium, the moat was backfilled, and the wall remnants were razed (Buccellati 2000:13, 24). The material cast into the moat was apparently from a burned building and contained sealings and ceramics dating from 2600 to 2400 BCE (Buccellati and Kelly-Buccellati 1988:65-82; 1997a:79). It has been hypothesized that this was about when the Outer City wall was constructed as a means to defend the wider settlement, so the inner wall was rendered ineffective.

3.6.9 - Features of the Outer City

The Outer City was briefly discussed earlier in Section 3.2, so only a few of the previously unmentioned features will be covered here. Additionally, the Outer City has

been hard to study systematically, so there is less to discuss. As mentioned already, the ancient landscape is buried beneath several meters of recent sediment (which covers the evidence of past habitation), and wadis likely flowed through portions of the Outer City at various times during the past (which could have erased it).

Excavations in the Outer City, near the north edge of the High Mound, revealed an administrative building, based on the cultural materials uncovered, contemporaneous with the mid-third-millennium terrace (2001a:24). The existence of such a structure in the Outer City indicates that, during this period, official government buildings were not confined to the High Mound (24). Other work exposed houses as well as burials dating typologically to the early third millennium (2004:8; Buccellati 2000:12). Parts of the Outer City might have been left vacant (Buccellati and Kelly-Buccellati 2004:8), but it is possible that evidence of settlement was destroyed in those areas.

The Outer City appears to have reached its greatest extent during the mid-third millennium (8). A dearth of second-millennium material indicates that, by this period, habitation at the site retracted back onto the High Mound (8).

3.6.10 - Features of Later Habitation Phases

As mentioned in Section 3.6.5, the formal wing of the palace was abandoned by the start of the second millennium (Buccellati and Kelly-Buccellati 2004:15). Houses were initially built only to the north of the palace, but after its abandonment, dwellings expanded into the area (15). Consequently, these strata above the royal palace contained

late-third-millennium and second-millennium residential buildings (Buccellati 2000:24). In fact, the hill to the north of the palace appears comprised largely of houses constructed after it was deserted (Buccellati and Kelly-Buccellati 2004:15).

Besides four residential complexes, sixteen burials, dating to about the end of the third millennium or the start of the second, were excavated in the strata above the palace (Buccellati 2000:29). These burials contained a variety of bronze artifacts, including a dagger and straight pins for clothing, and a tube-shaped gold bead (Buccellati and Kelly-Buccellati 2005a:40). Small structures, somewhat house-like, contained the burials, and there appears to have been an open area between the burials and other nearby structures, creating "a small quarter of the dead" in that area (2004:15).

Occupation during the second millennium BCE seems to have been limited to the highest parts of the tell (1995b:389), and the Mittani-period (circa 1500 BCE) settlement is the final major phase here (2004:16). Buccellati and Kelly-Buccellati (2005a) think that Mittani-era houses may also have existed atop the Tupkish palace but that they were destroyed by erosion and construction of a road to the top of the tell (30).

Late-phase habitation also encroached on the temple terrace vicinity. In Unit J2, the stratigraphic layers atop the terrace, deposited during periods of scattered occupation, contained three *tannurs* (2006:12). In Unit J3, I helped to uncover another *tannur*, which extended deep enough to cut into the *baqaya*. These bread ovens, most likely features of domestic habitation, are interpreted as belonging to a concluding period of scattered occupation, when Tell Mozan was no longer a Hurrian religious center (12).

3.7 - Outstanding Questions about the Hurrians

The preceding sections set out that, by the start of the third millennium, Urkesh was already a religious and political urban center, making it the earliest known Hurrian settlement in Syro-Mesopotamia (Buccellati 2005b:18). This leads us to a discussion of two outstanding questions regarding Hurrians that could be addressed by archaeological evidence from Tell Mozan, in particular, their sources of obsidian and other evidence -- either physical, textural, or glyptic -- for exchange at this site. I should stress there are a great many unanswered questions about the Hurrians, many more than could possibly be addressed by any single line of archaeological investigation. Therefore, I will not discuss here those outstanding questions -- such as a debate about the validity of "Hurrians" as an ethnic category -- that the present work cannot meaningfully address.

1. A debate about the existence of a Hurrian "homeland" to the northeast, maybe as far as northeastern Turkey, Armenia, or Georgia (or even beyond).

Ephraim Speiser (1953), who was awarded a Guggenheim Fellowship in 1926 to explore Northern Mesopotamia for Hurrian ruins, argued that "the original home of the Hurrians cannot have been far from the Lake Van district" in southeastern Turkey (325). His suggestion has been persistent, and many researchers cite Lake Van as a Hurrian core. For example, Wilhelm (1989) suggests that the mountainous area south of Lake Van can be presumed "to have been the oldest homeland of the Hurrians" (41). Akkermans and Schwartz (2003) claim the Hurrians likely "originated in the eastern Taurus [in southeast Turkey] or western Zagros highlands [in Iran]" (285). Some researchers have suggested

even more a far-flung Hurrian homeland in Armenia, Georgia, or beyond. For example, Steinkeller (1998) believes it quite likely "their homeland was located somewhere in the Trans-Caucasian region, quite possibly in Armenia" (96).

Others disagree with hypotheses about a Hurrian homeland in this area. Benedict (1960) contends that the "belief that the area around Lake Van was an integral part of the Hurrian cultural and political area in the second millennium B.C. rests upon evidence of the most dubious sort" (102). He states that such ideas are based on debunked arguments regarding direct cultural links between the Hurrians and the ninth-century-BCE Urartians, whose territory was centered about Lake Van (i.e., the specious assumption that Urartians were the direct, lineal descendants of the Hurrians) (101-102).

Nevertheless, linguistic, and therefore cultural, associations between the Hurrians and the later Urartians have been carried even farther. Russian linguists I. M. Diakonoff and Sergei Starostin have argued that the Hurro-Urartian family has certain similarities to Northeastern Caucasian languages, while others argue that Armenian has loanwords from the Hurro-Urartian languages. Already tenuous, these claims are sometimes advanced as evidence that the Hurrians originated in the Transcaucasus region, perhaps as far north as Georgia. Such proposals have met serious doubt and debate. This is not to state that they are necessarily wrong, just without convincing evidence.

The Hurrians are often regarded as immigrants or invaders who arrived at the time that Hurrian names become visible in textual and glyptic evidence. von Dassow (2008) asserts that, although Hittite texts do not refer to Hurrians until the middle of the second

millennium BCE, "there is little reason (and no evidence) for postulating that speakers of Hurrian entered the Near East from elsewhere rather than being indigenous to the area where they are first attested" (71). Similarly, Amélie Kuhrt (1995) holds it likely that "the Hurrians were a cultural-linguistic group *always* located among the foothills and mountains fringing the northern Mesopotamian and Syrian plains" (288, emphasis in original). She points out that the Hurrians, "as far as we can tell, were from prehistoric times connected with this region -- we do not need to visualise them as a group migrating from somewhere further north or east" (289). Therefore, we have an alternative proposal that the Hurrians were indigenous to the Syro-Mesopotamian area.

Given the abundance of obsidian in eastern Turkey and the whole Transcaucasus region, seeking obsidian from sources in these areas may yield evidence of exchange and contact, perhaps even direct, with these highlands. With careful consideration, obsidian from, for example, sources in Armenia or Georgia would help establish a historical link to that region. Taking into account other evidence of exchange and contact at Tell Mozan may strengthen such hypotheses or may instead be of little utility.

2. The debate regarding "The king of Urkesh and Nawar" and either an Urkesh northern hinterland or an alliance or kingdom with Nagar (Tell Brak).

Related to this debate about a possible northern Hurrian "homeland" are issues of the mountainous Urkesh hinterland and a potential alliance with another city.

A large copper tablet, first described by Thureau-Dangin in the early twentieth century, bears the inscription of a Hurrian ruler, Atal-šen, identifying him as "king of

Urkesh and Nawar" (Buccellati and Kelly-Buccellati 2001a:26). Thureau-Dangin first equated "Nawar" with the country of "Namar" in the Zagros Mountains in modern Iran, implying a wide-ranging empire. Later, in the 1980s, a clay tablet from the fourteenth-century-BCE strata at Tell Brak proved that Nawar instead existed in or near the Khabur Triangle (Wilhelm 2002:175). Tell Brak has been identified as the ancient city of Nagar, so various scholars (e.g., Oates 1987, Oates and Oates 1993) have proposed that "Nawar" and "Nagar" were one and the same based on the similar names.

Buccellati and Kelly-Buccellati hold that "Nawar" and "Nagar" are not the same. Instead, they argue that Nawar refers to an area, not another city, which encompassed the mountainous region to the north of Urkesh. Their arguments are set forth in Buccellati (1988:33) and Buccellati and Kelly-Buccellati (1997a:93), and I discuss their arguments in Chapter 9. In their hypothesis, Nawar is a region equivalent to what they term the "Hurrian urban ledge," a territory or hinterland along the foothills of the Taurus range and extending north some distance into the mountains. This region appears to have been the center of Hurrian urbanism, based on the very few cities in the Khabur Triangle with any evidence of being Hurrian-controlled (e.g., Tell Chuera).

This identification of a mountainous hinterland for Urkesh also relates to some of the evidence I have already mentioned of a Hurrian ideological link to the highlands. For example, in Section 3.2, I noted the Hurrian "Song of Silver" myth, in which Silver lives in the highlands, visits Urkesh in search of Kumarbi, and learns that the ancestral god is roaming the mountains. In another Hurrian myth, the half-brother of Silver is Ullikummi,

a monstrous stone (or perhaps lava) deity -- the mountains are the only source of stone in this region. Additionally, in Section 3.6.2, I mentioned the recently discovered triangular pattern in the temple terrace wall. Observable from the lower plaza, this pattern is similar to early pictograms for "mountain," and Buccellati (2009b) suggests that it was probably intended to reinforce links to mountainous lands to the north.

With the exception of potential Iranian sources, the geological sources of obsidian in the Near East all lie north of Tell Mozan. A few of the obsidian sources are almost due north, others are far west in Cappadocia, and many more lie to the northeast, toward Lake Van and as far as Armenia and Georgia. The hinterland of Urkesh, basically the resource use area or catchment area of its ancient inhabitants, may be investigated by establishing which obsidian sources were exploited by them. Incorporating other evidence of contact or exchange may also clarify the Hurrians' landscape interactions.

3.8 - Concluding Remarks

Both of the issues raised in Section 3.7 will be further discussed in Chapter 9, as I discuss the sources of obsidian at Tell Mozan and consider the implications for Urkesh and the Hurrians. The geographical setting of Tell Mozan and its surrounding landscape will be important when considering the settlement's exchange links to other regions. The contemporary climate and environment will be raised again when I discuss issues related to post-depositional conditions and alteration. I also relate the distribution of obsidian to the main archaeological features unearthed at Tell Mozan, so knowing the general layout and proposed uses of the structures will be meaningful in later chapters.

Part II: Methods for Sourcing and Their Evaluation

Chapter 4:

The Geological Reference Collection and Artifacts

> Since the early 1960s considerable research has been devoted to locating Anatolian obsidian sources and determining chemical fingerprints for them... However, as of 1996, this database may be misleading for two reasons: not all potential source deposits have been sampled, and many deposits were not sampled systematically -- with full knowledge and coverage of the geology of the site.
>
> -- George "Rip" Rapp and Christopher Hill, 1998, *Geoarchaeology*

> The characterization of obsidian is quite a complex question, and to be reliable, it demands an extraordinary degree of care in sample collection and analysis.
>
> -- Garman Harbottle, 1982, *Contexts for Prehistoric Exchange*

> Almost all work on Anatolian obsidian is, however, still based on the random and hasty collection of source material, either from a few reputed sources or from those that are easily accessible.
>
> -- Mehmet Özdoğan, 1994, *Obsidian in Anatolia: An Archaeological Perspective on the Status of the Research*

Michael Glascock of the Archaeometry Laboratory at the University of Missouri Research Reactor Center (MURR) and his colleagues list the principal factors that lead to flawed sourcing (1998:20). The first two problems that they cite are "failure to locate all possible sources" and the "collection and analysis of too few specimens from each" (20). A third problem is that earlier studies also assumed there was a single obsidian source per

volcano or lava dome complex. Researchers referred to *the* Açigöl source and *the* Çiftlik source in Central Anatolia, but Rapp and Hill (1998) point out the reality:

> Rapp and his colleagues have defined eight separate signatures, not simply one for Açigol and one for Çiftlik. In the eastern part of the Açigöl caldera three separate flow signatures can be defined. In the western part of the caldera there is only one distinct signature -- from the youngest of the obsidians in central Anatolia. In the Çiftlik area three separate sources can be distinguished. The eighth source is from the obsidians at Nenezi Dağ, about halfway between Açigöl and Çiftlik. (138)

These problems are evidenced by the numbers of geological specimens analyzed in some obsidian sourcing studies. Renfrew et al. (1966) and Wright and Gordus (1969) analyzed 33 geological specimens (including, for example, five specimens from Nemrut Dağ) from all of Anatolia. Mahdavi and Bovington (1972) analyzed only five geological specimens, one from each of five Anatolian source regions. In the research of Gale (1981), Anatolia is represented by only six geological specimens. The situation slightly improved with the work of Blackman (1984), who analyzed 13 geological specimens from Central Anatolia and 32 specimens from Eastern Anatolia and the Transcaucasus.

These problems might be expected in the early studies; however, even in the years since Rapp and Hill (1998) pointed out insufficient surveying and source sampling in the Near East, the numbers of geological obsidian specimens analyzed have not dramatically increased. Consider the following reference collections in studies from the last ten years: 33 geological specimens from 18 areas in Armenia (Badalian et al. 2001); 19 specimens from five source areas in Anatolia (Abbès et al. 2003); 48 specimens from nine areas in the Transcaucasus (Chataigner et al. 2003); 18 obsidian specimens from only four areas

in Anatolia (Bressy et al. 2005); 19 specimens from Central Anatolia (Bellot-Gurlet and Poupeau 2006); four specimens from four areas in Anatolia (Le Bourdonnec et al. 2005a); and one specimen from each of three sources in Iran (Niknami et al. 2010). Such issues are quite evident in Khalidi et al. (2009). Artifacts were compared to only about a dozen geological specimens from only four Anatolian sources (Bingöl A/Nemrut Dağ, Bingöl B, Meydan Dağ, and Göllü Dağ), so it is not surprising that their chemical data revealed an "unknown source," which they have labelled "source X" (881).

There are at least three exceptions to the low numbers of geological specimens in Near East obsidian sourcing studies. First, in 1973, Sebastian Payne, then a researcher at the British Institute of Archaeology at Ankara and now chief scientist at English Heritage, conducted a very thorough survey and collection of Central Anatolian obsidian. In 1975, he explained in a letter that he collected about 400 specimens with their locations marked precisely on maps (a few examples were reproduced in Todd 1980). He also stated these obsidian specimens were sent for analysis to Hugh McKerrell at the National Museum of Antiquities of Scotland. McKerrell was fired shortly thereafter, and the museum returned specimens to their owners. Payne's specimens apparently sat unanalyzed until the 1990s when Yellin (1995) chose 188 of them for NAA. A second exception is Gratuze (1999), who analyzed 127 specimens from 17 Anatolian and Aegean sources.

My research is a third exception. For this dissertation, I analyzed more than 900 geological specimens, including 453 from Eastern Anatolia (including, for example, 100 specimens from 11 areas of Nemrut Dağ), 281 from Central Anatolia, 151 from Armenia,

and smaller numbers from Georgia, Azerbaijan, and Russia. In addition, I have hundreds more specimens awaiting analysis in the next phases of my research.

This chapter covers a variety of topics: how I assembled this geological reference collection from various sources; how I conceptualized this collection, including the issue of what constitutes an obsidian "source" and how it was informed by fieldwork; debates in obsidian sourcing, including an appropriate number of specimens and the homogeneity of obsidian flows; and how geological specimens and artifacts were prepared for analysis for this study. Another issue included here, but usually omitted in sourcing studies, is my selection criteria for the Tell Mozan artifacts analyzed in this research.

4.1 - Terminology: "Samples" versus "Specimens"

I refer to an individual piece of geological obsidian for analysis as a "specimen," not a "sample" like most researchers. I avoid the word "sample" in this context because, in statistics, it refers to a representative subset of some population. In one sense, the term "sample" would be very apt: pieces of obsidian are collected from a large occurrence in a way that, ideally, would be representative of the whole, and extrapolations are made from their examination to the entire occurrence. A statistical sample, however, always consists of multiple values or observations. It never consists of just one value or observation. On the other hand, a "sample" of obsidian would, as most researchers use the word, refer to a single piece. Following the statistical definition, a "sample" of obsidian from a particular source would include all of the pieces collected there intended to represent the whole. To

avoid the statistical term and its implications, I instead use the word "specimen" since the obsidian pieces are "a portion of material for use in testing or study." "Sampling" refers, therefore, to the larger process of collecting specimens and samples done in a systematic and representative way. This meaning of "sampling" is consistent with uses of this term by the contributors in *Sampling in Archaeology* (Mueller 1975).

Many researchers also refer to artifacts as "samples" when chemical analyses are involved. The term "sample" used in this context implies either a representative subset of artifacts chosen from the entire corpus or a representative piece removed from an artifact. Mostly, however, authors simply use "sample" as a synonym for "artifact." Carter (2009) has argued that calling an archaeological artifact a "sample" reduces it to merely material for chemical analyses, not a human-made object that embodies other information as well, such as the morphological traits that indicate how a stone tool was made. Hence, I follow his practice of calling an artifact such, not a sample or specimen.

4.2 - Numbers of Geological Specimens

If most studies mentioned at the beginning of the chapter have too few geological specimens, it raises the question of how many specimens are sufficient to characterize an obsidian source. The cited studies clearly have too few specimens to have been collected systematically, though there is no clear answer or consensus about what is adequate. As discuss later in Section 4.7.1, Rapp collected at least ten specimens from each area that he considered an individual flow or deposit in Turkey. Hughes (1994) similarly collected

ten specimens from each source within the Casa Diablo complex of California. Shackley echos a need for systematic collection: "It is no longer enough to chemically characterize a source of obsidian by grabbing five samples from a road cut" (1998a:6). He also argues that, for each obsidian source, a sufficient number of specimens "to analyze may only be discernible experimentally. Five is certainly not enough. Ten might be" (2002:60). The key issue is the compositional homogeneity of obsidian flows and deposits and, therefore, the number of specimens needed to analytically characterize them.

4.3 - Homogeneity of Obsidian Sources

The homogeneity of obsidian sources, especially in comparison to the differences between sources, has been a topic of considerable interest. Some of the earliest work on source uniformity was done by Richard Laidley and David McKay at the NASA Manned Spacecraft Center (Laidley 1968, Laidley and McKay 1971). The two analyzed obsidian specimens from five flows, including Big Obsidian Flow (BOF), at Newberry Caldera in Oregon (discussed later in Section 4.5). For example, BOF was sampled at intervals of 30 meters across a 1500-meter transect (Laidley and McKay 1971:336). Their specimens were analyzed using X-ray fluorescence (XRF) and other techniques for eleven elements: Na, Mg, Al, Si, Ca, Ti, Mn, Fe, Zn, Rb, U, and Th. Only two elements, Mg and Rb, had a statistically significant variance across the transect (338). They concluded:

> The BOF is remarkably homogeneous in major element composition and slightly less homogeneous in trace element composition. Within the flow, there is no chemical variation that can be related to sample locality. Consequently, a sample taken from any point in the flow would be representative of the entire flow. (341)

Their analyses also demonstrated that BOF and the other four sources in the caldera were compositionally similar, due to the same host rock and magma chamber for the flows, but still distinguishable -- almost every element showed significant variation.

Also notable is that Laidley and McKay (1971) observed correlation among some elements in the BOF specimens: Ca, Fe, Ti, and Mn varied directly as did Si and K (340). As a possible explanation for these relationships among elements, they suggest that either the elements might be segregated within the glass itself or that

> … the observed microlites and phenocrysts of such minerals as feldspar, pyroxene, or ilmenite are responsible for the observed correlations. The relationships also indicate that very minor though detectable variations in the content of these phases are present in these samples. The samples collected averaged about 10 cm on a side, and perhaps a larger specimen would minimize differences in the amounts of these phases (339).

Their suggestion, therefore, is that variations in the abundances of tiny mineral inclusions might be the cause of, or at least one contributing factor to, element correlations. This, in turn, could lead to heterogeneity within a source or a "diffuse" elemental fingerprint for a source. In theory, their suggestion -- the use of larger specimens -- could help to mitigate the effect of centimeter-scale variations in mineral abundances; however, their specimens, about 10 centimeters in diameter, are already much larger than those in most studies. The practical implications are also worrisome: an obsidian block about 10 centimeters on each side is over 2 kilograms (4.5 pounds), so collecting and transporting numerous specimens of such size (or even greater!) poses considerable challenges. Instead, one could analyze

the glass alone, avoiding the minerals and ensuring that their differing abundances are not contributing to the analyses. This is a key point in the present research.

Returning to the subject of obsidian source homogeneity, other studies have found that obsidian sources can vary in uniformity. For example, Gordus et al. (1968) analyzed over a thousand obsidian specimens from sixty flows in North America. They found that trace elements (like Mn, Sc, La, Rb, Sm, Ba, and Zr) could vary as much as 40% relative within a particular flow; however, the variation among sources could be a factor of ten or more (over 1000% relative). Similarly, Stross et al. (1971) analyzed Californian obsidian specimens using X-ray fluorescence, and the element concentrations had relative standard deviations between 5% and 15% (213). They concluded that "the variability between all the sources is such that in one or the other plot it almost always considerably exceeds the variability within a given source and that from the measuring error" (213). Bowman et al. (1972) observe that some obsidian sources are highly homogenous, varying less than 1% relative. For the Mediterranean sources, Acquafredda et al. (1999) noted the "monotony of the glass composition in the same lava flow" (317).

Only a very few researchers have noted that specific obsidian sources are actually heterogeneous to some degree. For example, Harry R. Bowman and his colleagues Frank Asaro and Isadore Perlman (Bowman et al. 1972, 1973a, 1973b) noted that obsidian from Borax Lake in California exhibited a continuous range of compositions. This continuum, they maintain, suggests the mixing of two magmas with distinct compositions in different proportions (1973a). The effect for sourcing studies, however, is not detrimental. In fact,

they state, the pattern is so unique "that the judgement of provenience is just as definitive as it would be if the flow were extremely homogeneous" (1973b:123). This, though, is a clear example of heterogeneity within one obsidian source.

Two studies, also of Californian obsidian, by Richard E. Hughes are often cited as providing examples of heterogeneous obsidian sources. Hughes (1988) showed the Coso Volcanic Field had geochemically different obsidian outcrops and, therefore, could not be considered a single obsidian source, as had been previously assumed. This volcanic field covers 160 square kilometers and consists of 38 rhyolitic lava domes and flows, of which most have obsidian exposures (Wood and Kienle 1990:239-240). These domes and flows formed in a series of eruptive events, not just a single one (239). Based on his specimens and XRF analyses, Hughes revealed that at least four different obsidian compositions (of sufficient quality for stone tools) occurred in the volcanic field (1988:259). Hughes gave these "subsources" names: Joshua Ridge, Sugarloaf Mountain, West Sugarloaf, and West Cactus Peak. Furthermore, he showed that the obsidian artifacts from two archaeological sites only originated from the latter three (261). Later work (e.g., Eerkens and Rosenthal 2004, Ericson and Glasock 2004) reinforced Hughes' "subsources" at Coso, including his terminology. Draucker et al. (2002) analyzed specimens collected from four outcrops of the Sugarloaf Mountain obsidian in an effort to differentiate among them, but they found that this "subsource" could not be further subdivided chemically. A similar study of West Sugarloaf obsidian produced a similar result (Draucker 2007).

In the Casa Diablo area of California, Hughes (1994) reports a second instance of what he calls "intra-source chemical variability" (263). The area covers about 150 square kilometers in the Sierra Nevadas and includes over 20 obsidian exposures (264). Hughes cites many researchers, including himself, who assumed there was a single, homogeneous Casa Diablo source. His analyses, though, revealed three obsidian "varieties" in the area, and he gives each of them location-based names: Sawmill Ridge, Lookout Mountain, and Prospect Ridge (264, 266). Hughes does not label them "subsources" (as he did at Coso); however, he continues to mention a single Casa Diablo source (e.g., "geochemical types... of obsidian *within* the Casa Diablo source," 268, emphasis in original).

Though commonly cited as such, Hughes' observations are not actually examples of obsidian flow heterogeneity or intrasource variability. Instead, these volcanic regions were assumed to have either a single source of obsidian or multiple obsidian sources with identical geochemistries. The differences identified by Hughes exist because the obsidian varieties were produced by different eruptive events, not because there is heterogeneity in a single lava flow or dome. Similar assumptions -- that a large volcanic area has only one obsidian source -- have been made around the world, and subsequent research recognized multiple "subsources" (e.g., at Glass Buttes, Oregon [Ambroz 1997, Ambroz et al. 2001], San Martin Jilotepeque, Guatemala [Braswell and Glascock 1998], the Jemez Mountains, New Mexico [Glascock et al. 1999]). As noted at the start of this chapter, the same trend occurred in Anatolian obsidian studies. At issue, really, are varied definitions of the term "source" in the literature, as discussed in the next section.

4.4 - What Constitutes a "Source"?

In his chapter "Tracing to Source" in *Science and the Past,* Hughes (1991) draws an analogy between the chemical analyses of artifacts for sourcing and the classification of objects based on visual characteristics. He notes that a particular "object's appearance is the first way we recognise where it comes from: a Volkswagen 'Beetle' is an instantly recognisable shape even if the VW badge has fallen off the car; likewise we recognise a Rolls Royce" (99). The analogy is not carried through, though, to an underlying issue in sourcing research: what is the definition of a "source"?

In the above example, the "sources" of Volkswagen and Rolls Royce automobiles are complex. Should the source of a "Bug" be considered the Volkswagen Corporation, or would a particular factory be the source? On the other hand, Volkswagen is a German company, so one might call Germany its source. Bugs, though, were also manufactured in Ireland, South Africa, Brazil, Australia, and Mexico. To clutter the issue further, Rolls Royce Motors was sold to Volkswagen in 1998. Depending on the definition of "source," a 1963 Volkswagen Bug and a 2010 Rolls Royce sedan may have identical sources. This analogy stresses the importance of a clear "source" definition, and there will be different definitions for different archaeological materials (i.e., the definition for the "source" for a multi-component material like pottery differs from that for obsidian or chert). The core problem, as described by archaeologist Roger Green, is "characterizing the size of the dot which pinpoints [an artifact's] supposed origin" (1998:227).

In his review chapter on the status of obsidian studies, Green (1998) observed "a fair degree of variation in the terminology employed by authors when describing different levels of 'source' discrimination" (226-227). He reported that geoscientists, for the most part, had three levels of distinction: (1) the broadest being *source systems* or *source areas*, (2) the highest-resolution being *source localities,* and (3) "*source subsystems* and *locality complexes* lying somewhere in between" (227). Archaeologists, he found, tend to use an assortment of terms: source regions and subregions, source and subsources, systems and subsystems, loci and localities, etc. Just within the same volume, he noted:

> Summerhayes et al. are very explicit about what they mean by geographic regions with a number of sources, and source localities as specific sampling loci where naturally occurring obsidian specimens were collected. All source localities within a geographic region are for them a regional group, within which similarities in chemical composition make it possible to distinguish subgroups or "chemical groups." Other authors, such as Glascock et al. also speak of geographic regions, but they also talk of subregions, source areas and complex source areas, and chemical or compositional subgroups for these, while Shackley speaks of four distinct chemical groups for a named source region. (227)

Here Green alludes to two major differences in how a "source" is defined: the geographic definition (i.e., location in space where the obsidian flow or secondary deposit occurs and where humans collected the material) and the geochemical definition (i.e., a mathematical cluster in the compositional data, often called a "chemical group"). These definitions do not necessarily yield identical sources. Harbottle (1982) warns: "One must never assume that the physical and mathematical source have to coincide" (31).

Wilson and Pollard (2001) describe a typical mathematical definition for a source, stating that chemically similar specimens "can be agglomerated into chemically coherent

'groups' which will 'characterize' a single 'source'" and, in turn, that "'sources' can then be distinguished as discrete clouds of points in multivariate space" (509). Hughes (1998) similarly claims that obsidian "sources are defined, geochemically speaking, on the basis of chemical composition -- not spatial distribution" (104). He notes that such a definition has led to the term "chemical group" (or variations like "chemical type"), which have no geographical implications, being often used to describe sources.

Neff (1998) provides an example of a geographic definition, explaining that "the theoretical concept of interest here is 'source,' defined as a location or set of locations in geographic space" (116). A source, in his terminology, can be defined by coordinates on a map. Similarly, Harbottle (1982) considers "the *source* as the ultimate starting point -- the clay bed, obsidian flow, mine of flint or copper or marble quarry, which is the natural deposit of a material" (16). Rapp and Hill (1998:134) give a virtually identical definition for a source. For them, a source is where people collected the raw material and started its distribution. Ericson et al. (1976) consider an obsidian source to correspond to "a single volcanic event" (218). Other researchers have implicitly defined a source geographically. For example, some use the term "geological source" (Braswell and Glascock 2002:35) or refer to obsidian sources having particular geographic locations (e.g., "the primary source in the Valles Caldera in the Jemez Mountains," in Shackley 2002:56). Still others refer to sources being a particular distance from an archaeological site or state that sources should be described using geographic coordinates (e.g., Shackley 2008b:198).

Clearly geographical definitions of "source" prevail in the literature, and the term "chemical group" (or similar ones like "chemical type") is commonly used to refer to the mathematical concept of "source" described above. I shall follow these trends here. My use of the term "source" refers to a geographical location, and I use "geochemical group" to refer to the mathematical concept described by Wilson and Pollard (2001:509). These definitions are appropriate, I maintain, because, in "sourcing" studies, archaeologists are concerned with placing obsidian in geographical space, not just multidimensional vector space. Therefore, a "source" of obsidian can be represented on a map with a dot, but this leaves us with the issue of, as Green described it, "the size of the dot which pinpoints [an artifact's] supposed origin" (1998:227) and a plethora of terms.

As Green (1998) noted, varied nomenclatures are found in the literature: sources and subsources; sources areas and sources; source systems and subsystems; regions and subregions; localities and locality complexes; and source localities and sampling loci. It is often unclear how these terms relate to one another, and different researchers often will apply different terms to the same obsidian-bearing region. For example, Glass Buttes in central Oregon, which has obsidian exposures with at least seven different compositions, has been described in a variety of ways: as a sole obsidian "source" (Dillian et al. 2006), as one "source area" (Skinner 2010), as a "source complex" (Skinner et al. 1999), and as a "complex" comprised of multiple "subsources" (Ambroz et al. 2001). Note that the two intermediate, and most similar, terms here -- "source area" and "source complex" -- come from a researcher who did extensive fieldwork at Glass Buttes. The two extremes, on the

other hand, are from researchers who analyzed specimens at the University of California-Berkeley (Dillian et al. 2006) and the University of Missouri (Ambroz et al. 2001). Field experience, it seems, may affect one's interpretation of a "source."

4.5 - Obsidian Fieldwork in Oregon

As I discuss later, I did not collect the specimens analyzed for this work. Instead, specimens for this study were gathered by geologists and archaeologists who work or live in the region. If, though, fieldwork affects how one defines an obsidian "source" (and the related terms), I wanted to have field experience in a place at least volcanically similar to Anatolia and the Transcaucasus, so that I could benefit from observing first-hand how the obsidian occurs at different "sources." Furthermore, I wanted to have the experiences of finding and gathering obsidian from different volcanoes so that I could better understand the experiences of people doing the same in antiquity. Given the importance of obsidian from Nemrut Dağ and Göllü Dağ, I sought similar locations.

Nemrut Dağ is an active stratovolcano (the last reported volcanic activity was 400 years ago), and it has relatively young obsidian deposits. For example, one specimen was fission-track dated to 24,000 ± 14,000 years old (Bigazzi et al. 1994:24), and another was dated to 34,000 ± 6000 years old (Bigazzi et al. 1997). Nemrut Dağ experienced a major caldera collapse, creating a circular basin or crater approximately 7 km (4 miles) by 8 km (5 miles) in diameter. The western half of the caldera is filled with a lake, and the eastern half is covered by subsequent lava domes and rhyolitic flows, both bearing obsidian. The

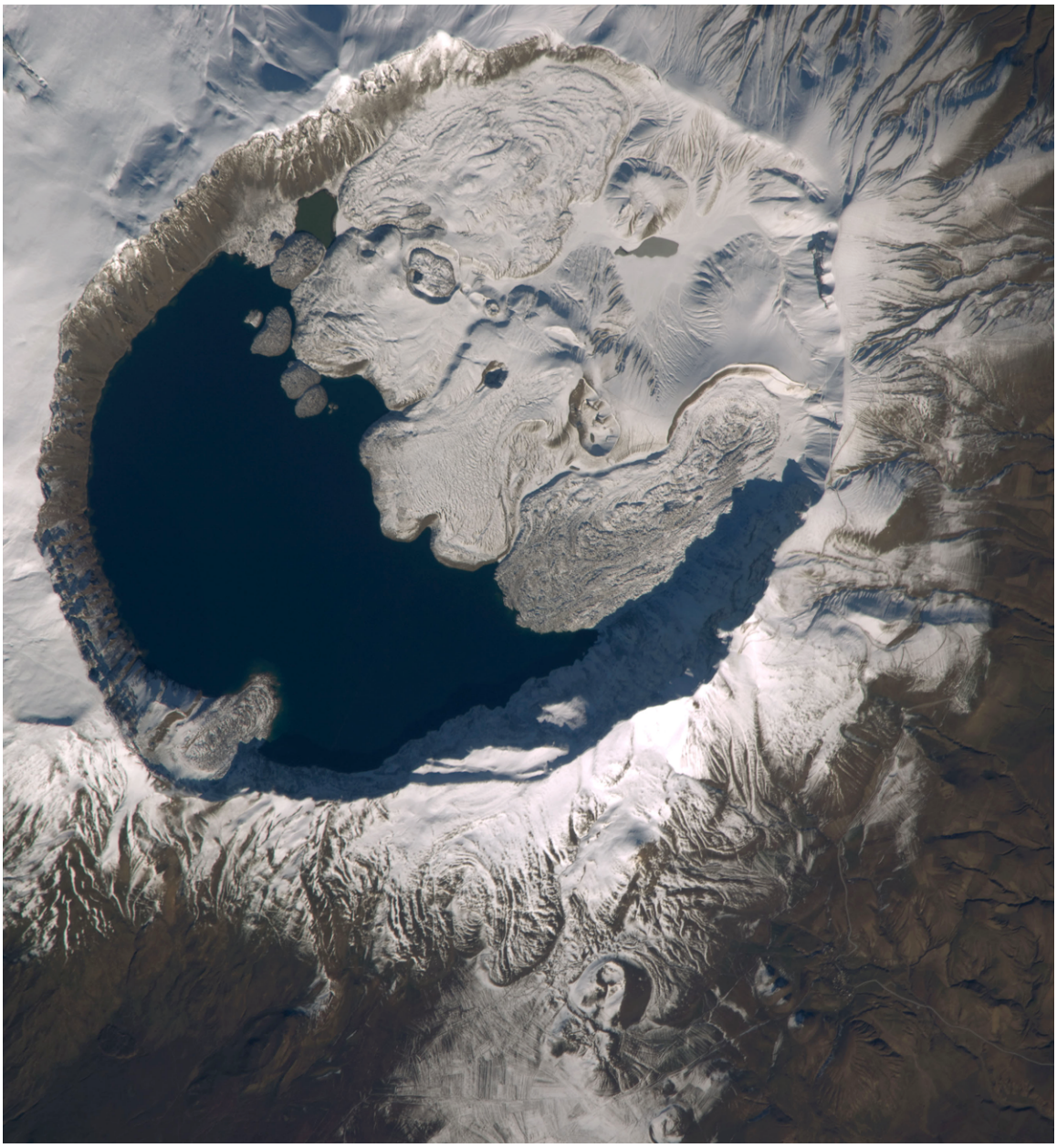


Figure 4.1 - Nemrut Dağ in Eastern Anatolia from space; north is the upper left corner (composite of Photographs ISS018-E-10205 and -10206, taken on 3 December 2008 by the International Space Station crew; available online at the NASA/JSC Gateway to Astronaut Photography of Earth website thanks to the ISS Crew Earth Observations Experiment and the Image Science and Analysis Laboratory, Johnson Space Center).



Figure 4.2 - Nemrut Dağ in Eastern Anatolia from space; north is the top of the image. (Photograph ISS015-E-08780, taken on 15 May 2007 by the International Space Station crew; available online at the NASA/JSC Gateway to Astronaut Photography of Earth).

impressive caldera is clearly the reason that Nemrut Dağ has been called "one of the most spectacular volcanoes of eastern Anatolia" (Yılmaz et al. 1998:175).

Göllü Dağ is a stratovolcano as well, but its obsidian is older. The obsidian flows were dated to 1.0 to 1.5 million years ago (Bigazzi et al. 1998, Yegingil et al. 1998). It is a lava dome complex, more than 10 km in diameter, and there are multiple geochemically distinct obsidian deposits on its flanks. Göllü Dağ is also highly eroded and dissected by channels due to small streams, exposing the subsurface obsidian. John Whittaker, one of my Anthropology professors at Grinnell College and a lithics expert, visited the Kömürcü village area of Göllü Dağ, and he described the area as follows:

> If you continued on through the village to the north and a bit east, the road went up a drainage, and there was the obsidian. Going north, the obsidian was all in rhyolite slopes to the right, with the mass of the volcano to the left. Drainages coming off the volcano had nothing but bits in them, but the whole slope to the right was ridges of rhyolite and veins of obsidian, sometimes just little droplets and pebbles, sometimes veins that were breaking up into masses with some pieces 15-20-25 cm. The slopes were littered with black stuff, mostly small nodules, but many flakes and some blades. (personal communication, 2007)

His photographs of this area illustrate how it is "littered with" small obsidian nodules and flakes as a result of erosion and human exploitation for ten millennia.

John E. Dixon, a coauthor with Colin Renfrew on a number of obsidian sourcing papers (Renfrew et al. 1965, 1966, 1968; Dixon et al. 1968; Renfrew and Dixon 1977) and a geologist interested in the magmatism and structural evolution of the Mediterranean and Aegean regions, discussed Near Eastern obsidian in his chapter in "Advances in Obsidian Glass Studies" (1976). He points out that the tectonics and volcanism of Eastern Anatolia

and the Transcaucasus region is roughly analogous to the Cascade Range of the American Northwest, stretching from southern British Columbia into northern California (305-306). In particular, Dixon lists Newberry Caldera and Crater Lake, both of which are located in Oregon and are examples of calderas similar to that of Nemrut Dağ. Therefore, I decided to do fieldwork in Oregon, in part, to discover how obsidian "sources," defined either by geography or geochemistry, are manifested on the landscape.

Newberry Caldera, part of Newberry National Volcanic Monument, served as my analogue for Nemrut Dağ. While Nemrut Dağ is a stratovolcano, Newberry Volcano is a shield volcano; however, both have erupted lava ranging in composition from basaltic to rhyolitic. Both are considered potentially active. Newberry Caldera was possibly formed as long as 500,000 years ago, and the Nemrut Dağ caldera is thought to be approximately 270,000 years old (Ulusoy et al. 2008). These two calderas are very similar in size. Both are about 7 km (4 miles) by 8 km (5 miles) in diameter and roughly 400 m (1300 ft) deep. Nemrut Dağ has a large lake (and a few small ones) that covers the western third or so of its caldera, and Newberry Caldera has two large lakes (Paulina and Eastern Lakes) in the northern half. Each caldera floor has subsequent lava domes and rhyolitic flows that bear obsidian. Obsidian at Nemrut Dağ has been dated to 24,000 ± 14,000 and 34,000 ± 6000 years old, meaning it is among the youngest in the Near East. At Newberry Caldera, the obsidian is even younger. I explored the three flows that were 7300 (Interlake Obsidian Flow), 3500 (East Lake Obsidian Flows), and 1300 (Big Obsidian Flow) years old. The

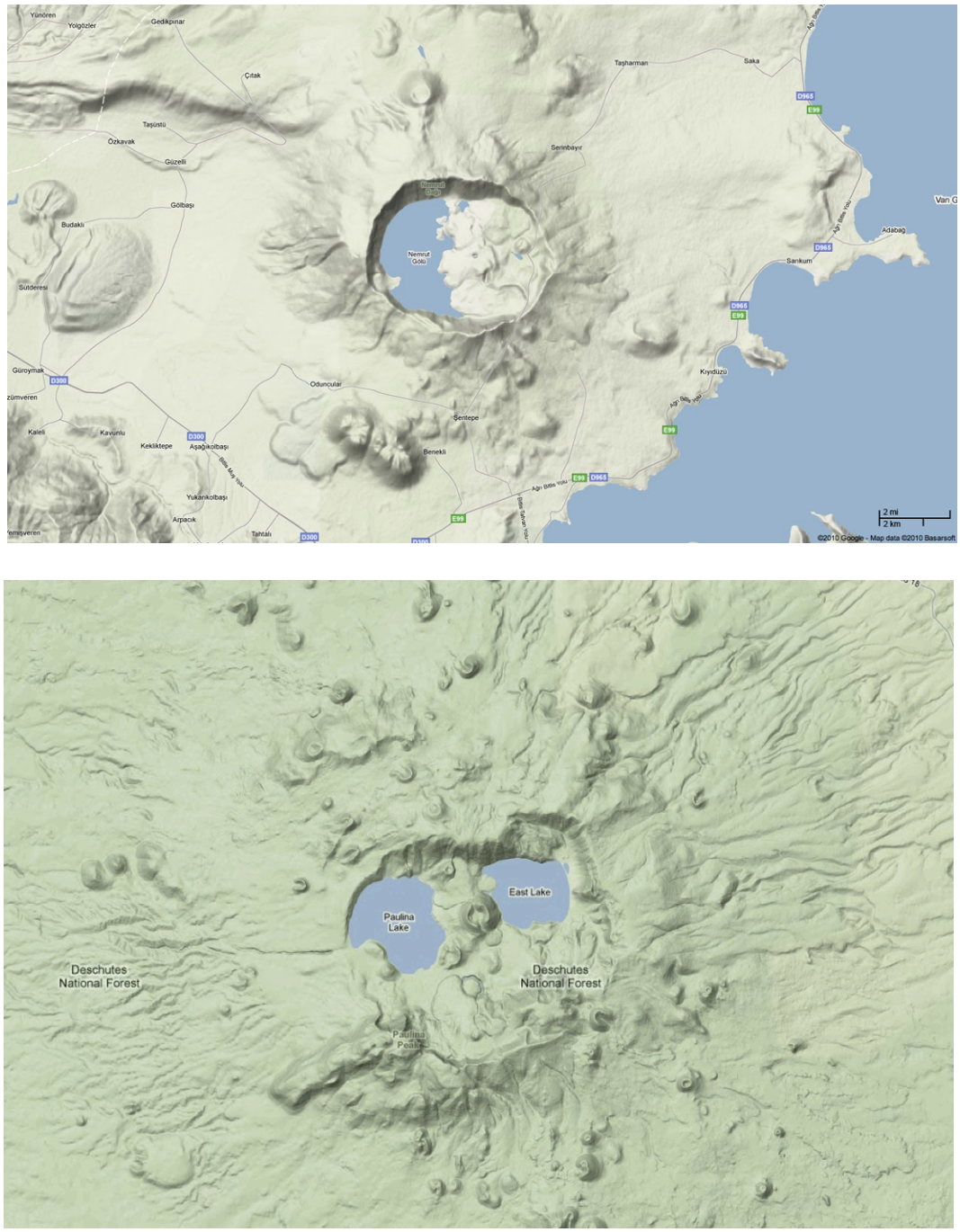


Figure 4.3 - Nemrut Dağ (top) in Eastern Anatolia and its analogue, Newberry Volcano (bottom), in central Oregon. Both are volcanic calderas of about the same size. (Used in compliance with Google Maps' terms of use; ©2010 Google; map data ©2010 Basarsoft).



Figure 4.4 - The caldera of Newberry Volcano as viewed from the caldera rim. Both caldera lakes are pictured: Paulina Lake on the left and East Lake on the right. The rise between the two lakes is a cinder cone. Between the two lakes and behind the cinder cone is Interlake Obsidian Flow. Big Obsidian Flow fills lower right portion of the photograph. Beyond Big Obsidian Flow, close to East Lake, is East Lake Obsidian Flow. Smaller lava domes are hidden by the trees. (Photograph by the author.)

geology of Newberry Caldera is described in detail by MacLeod et al. (1981). Given all their similarities, Newberry Caldera well represented Nemrut Dağ.

Glass Buttes in central Oregon served as my analogue for Göllü Dağ. As noted in the previous section, the area has obsidian exposures with seven to nine compositions and has been described by various researchers as a "source" (Dillian et al. 2006), as a "source area" (Skinner 2010), as a "source complex" (Skinner et al. 1999), and as a "complex" of "subsources" (Ambroz et al. 2001). Göllü Dağ also has multiple compositionally distinct obsidian deposits. Glass Buttes and Göllü Dağ are both lava dome complexes of roughly the same size. Göllü Dağ is about a dozen kilometers across, and Glass Buttes covers an area of about 10 km by 20 km. The obsidian at Göllü Dağ is among the oldest known in Central Anatolia, dated to 1.0 to 1.5 million years ago (Bigazzi et al. 1998, Yegingil et al. 1998). Glass Buttes obsidian is even older, between 4 and 6.5 million years old (Walker et al. 1974, Godfrey-Smith et al. 1993). Both of the volcanic complexes are also highly eroded and dissected by channels from small streams and springs. Ma et al. (2007) notes that the "surface obsidian flows have long since been eroded away" at Glass Buttes (552), and Russell (1905) described this complex as the "remnants of ancient... volcanoes, now deeply dissected by erosion" (49). Much like at Göllü Dağ, Waters (1927) observed that obsidian, which occurs as sizable chunks "in the dry stream channels and as loose blocks in the pumiceous sand of the Glass Buttes region, is rarely found in place" (451). These similarities make Glass Buttes and Göllü Dağ reasonable parallels.

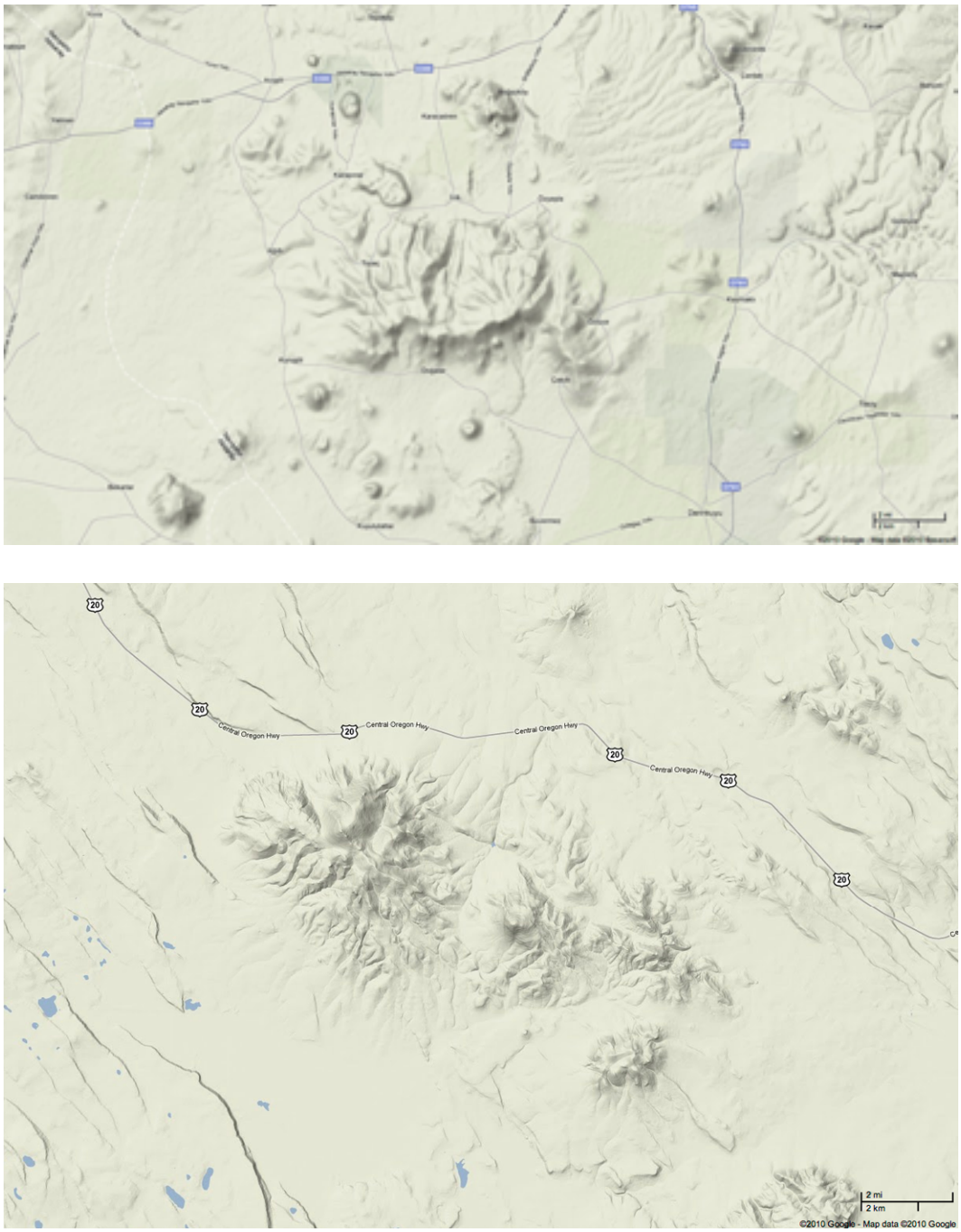
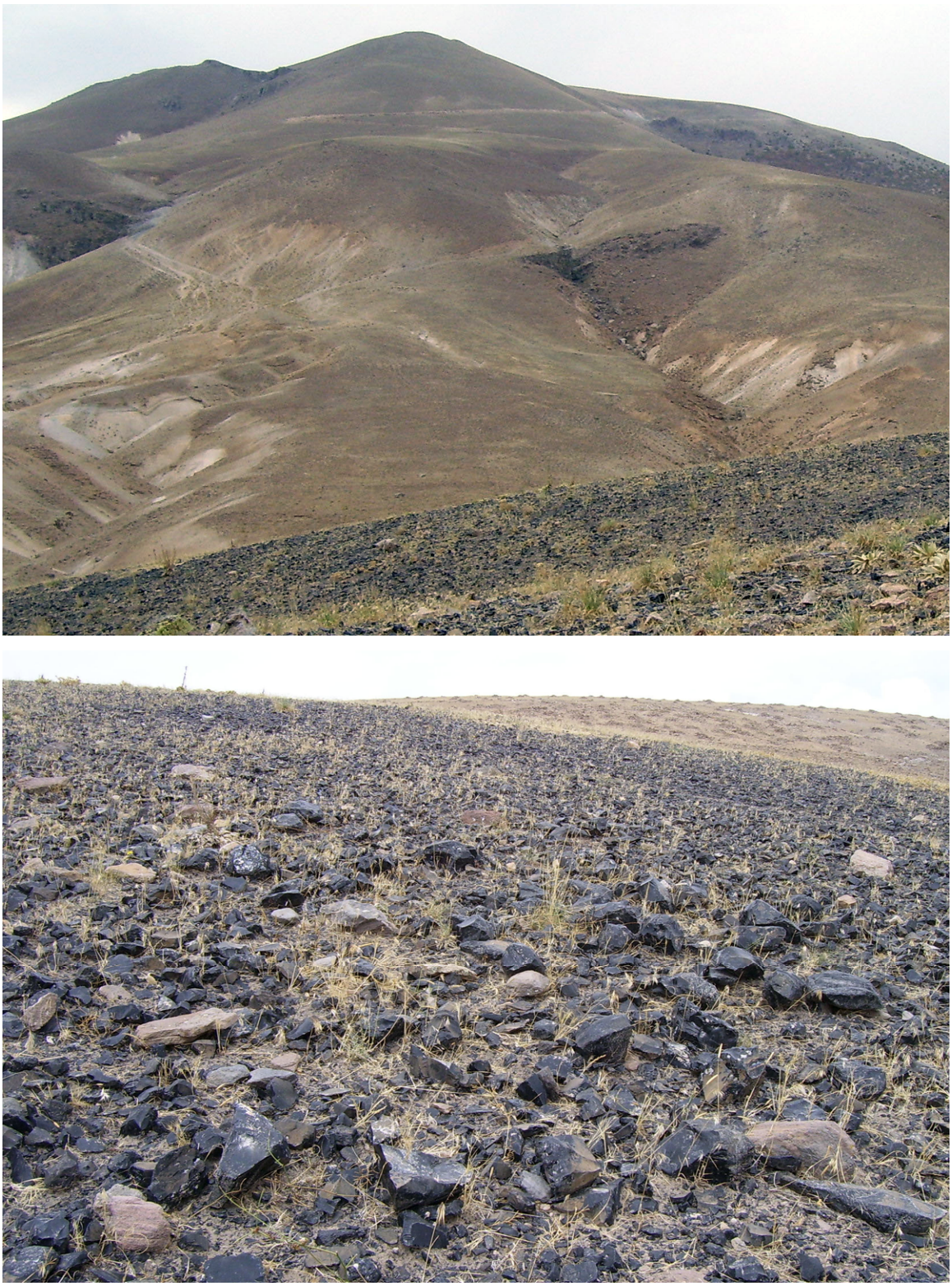


Figure 4.5 - Göllü Dağ (top) in Central Anatolia and its analogue, Glass Buttes (bottom), in central Oregon. Both are eroded volcanic complexes of about the same size. (Used in compliance with Google Maps' terms of use; ©2010 Google; map data ©2010 Basarsoft).



Figures 4.6 a and b - The Göllü Dağ-Komürcü source (photographs by John Whittaker).



Figures 4.7 a and b - The Glass Buttes, Oregon source area (photographs by the author).

The experiences of seeking obsidian at Newberry Caldera and at Glass Buttes are quite different. At Newberry Caldera, one enters ordinarily through a channel, cut by the only stream to drain one of the two lakes, where the caldera wall has been eroded to only a few meters tall. From this vantage point, one is surrounded the caldera walls, hundreds of meters tall, which contain massive obsidian flows hidden by evergreens. If one hikes a trail along the caldera rim, one is looking down into a deep depression several kilometers across, and three massive, gray, rocky lava flows are apparent as discrete features among the trees and rises of reddish-yellowish ash. From the top of one obsidian flow, the other two are often visible. For example, when standing on the East Lake Obsidian Flows and looking west, one sees Big Obsidian Flow (BOF) on the left and Interlake Obsidian Flow on the right. From either the caldera rim or atop a flow, the flows appear to be similar but separate features and readily could be considered different "sources." One does not need to resort to geochemical analyses to regard them as distinct.

Walking up to the edge of one of the Newberry flows, one has the impression of encountering a wall in the middle of the forest. BOF, for example, is 20 meters (65 feet) tall, 1800 meters (6000 feet) across, and covers 2.8 square kilometers (700 acres). Large obsidian chunks, over a meter in diameter, can be found at the bottom of the slope. If one ascends the slope of sharp pumice blocks, about two-thirds of the way up, one may gather obsidian from a layer exposed in some spots along the periphery. Atop the flow, spires of obsidian protrude from the pumice chunks. Some of these spires have collapsed, creating a pile of obsidian pieces useful for tool production. Obsidian is abundant, and it occurs in

angular blocks of almost any size. Also these shiny, black rocks are quite easy to identify, simply scattered across the flow among the dull, gray pumice.

The top of BOF presents a different experience. Its upper surface is composed of a series of ridges, and when standing between these ridges, the gray, rocky, nearly lifeless surface is all one can see other than sky. It is little exaggeration to say that the surface of BOF seems otherworldly -- atop BOF in 1964, Apollo 7 astronaut R. Walter Cunningham tested a spacesuit for use on the Moon, and over the next two years, dozens of astronauts trained for lunar missions on BOF and nearby lava fields. One cannot move from one of these quasi-lunar landscapes to another without walking at least 2 kilometers through the forest. Furthermore, erosion has not yet transported obsidian too far from its parent flow, much less out of the caldera and down the sides of the volcano. Thus, one essentially can only find obsidian at one of the three lava flows in caldera, and these imposing flows can even surround one with bizarre, even transcendental, scenery.

In comparison, visiting Glass Buttes and finding obsidian there is quite a different experience. The two low, eroded mountains of Glass Buttes -- known as Glass Butte and Little Glass Butte -- are typical of the area known as the High Desert or High Lava Plains in central and southeastern Oregon. This region has had many names over the years: the Great Sandy Desert and Rolling Sage Plain were popular terms in the nineteenth century, and the locals today call it the Oregon Outback. Low shrubs, particularly sagebrush, and occasional juniper trees grow on this semi-arid plateau. The mountains in this area were created by volcanism between 2 and 15 million years ago. As noted earlier, Glass Buttes



Figure 4.8 - The “otherworldly” surfaces of a rhyolitic lava dome, specifically Big Obsidian Flow at Newberry Volcano in central Oregon (photographs by the author).

obsidian formed between around 4 and 6.5 million years ago. Since then, weathering and erosion have worn down these ancient mountains. There are no conspicuous lava domes, massive obsidian outcrops, or steep slopes of sharp pumice blocks. As noted by Ma et al. (2007), "surface obsidian flows have long since been eroded away" (552). The only hard basalt outcrops from eruptions during the same period. The remaining low mountains, at first glance, seem completely unremarkable on the landscape.

Eventually, though, one notices that small black pebbles, just a few millimeters in diameter, scattered over the ground are obsidian. At some spots, larger obsidian cobbles, from 5 to 30 or 40 cm in diameter, can be found emerging from the clay soil, which is the eroded remnants of igneous rocks. Just as Waters (1927) described, obsidian is found not in outcrops but as rounded chunks "in the dry stream channels" or in the soil (451). One also finds, in areas where the larger cobbles occur near the surface, many obsidian flakes. Recall how Whittaker described the scene at Göllü Dağ: drainage channels had small bits of obsidian, one area had obsidian pieces ranging from pebbles to chunks between 15 and 25 centimeters, and the slopes near Kömürcü "were littered with black stuff, mostly small nodules, but many flakes and some blades." The scene is similar at Glass Buttes not only because both lava dome complexes are old but also because they have been exploited for obsidian for millennia. The flakes at Glass Buttes, though, are not the products of ancient obsidian workspaces. Instead, they are the waste of modern rock collectors and knapping hobbyists. Thus, one must either dig or search for cobbles recently eroded out of the soil, especially in stream channels, to find any sizable obsidian pieces.

Ambroz et al. (2001) created a map of the spatial distributions of seven chemical groups of obsidian at Glass Buttes. Even with this map and a GPS unit in hand, a visitor to Glass Buttes would be hard pressed to identify the spatial boundaries of these different chemical groups. On the western slope of the larger Glass Butte, obsidian collected from the rises are one group (Group B) while that from the channels between them are another (Group G), and almost immediately to the northeast and southeast is Group A (Ambroz et al. 2001:743). Other than the occasional barbed-wire fence, there are no clear boundaries or demarcations. One can wander within the Group A area or from Group A to Group B with no change of the landscape to indicate that there was ever a series of distinct domes from individual eruptions, very different from the situation at Newberry. Fieldwork and chemical analyses are still being done to identify the geographical boundaries of the nine known chemical obsidian groups at Glass Buttes (Skinner 2010).

Recent fieldwork and analyses have even suggested that multiple chemical groups of obsidian may be collected from one location at Glass Buttes. At a natural basin where water collects, a few kilometers from the mountains, Skinner (2010) discovered obsidian nodules from five chemical groups. Note that this required XRF analyses conducted in a laboratory to establish, not just visual inspection. Equally as important, he observed that, around this water source, abundant obsidian flakes were scattered across the ground, so it "was clearly a prehistoric place of interest" (Skinner 2010). There are two interpretations for this result. First, erosion could have carried obsidian from five different eruptions to a single water basin at the foot of Glass Butte a few kilometers away. This is possible since

Shackley (1992, 1995) showed an example of ancient obsidian, over 20 million years old, that had been transported 100 km by water. This suggests that people may have collected obsidian from one location, though the cobbles originated from five flows and correspond to five different chemical groups, that also served as a water source. The other possibility is that people collected obsidian nodules from the mountain, gathered at the water source, and discarded unwanted nodules (from each of five distinct chemical groups) in the basin while working there. Other secondary deposits, either natural or artificial and with mixed chemical obsidian groups, almost certainly exist near Glass Buttes.

The research of Ambroz et al. (2001) offers a possible clue to ancient conceptions of obsidian "sources" at Glass Buttes. Their chemical analyses of obsidian artifacts from an archaeological site, called the Robins Springs site, on the western slope of Glass Butte mountain revealed the use of obsidian from five chemical groups and none from the other two known groups. Although not pointed out in the article, there is an interesting trend in their data. The five chemical groups identified at this site all, according to the map, occur on the larger Glass Butte mountain, and the only two unrepresented groups are the two of the smaller Little Glass Butte mountain to the southeast. One artifact was traced to Yreka Butte, over 5 kilometers west of Glass Butte, farther than Little Glass Butte. The fact that all Glass Butte chemical groups are represented at the Robins Spring, in numbers roughly corresponding to distance from this site, while no Little Glass Butte obsidian groups were found, might hint that the larger mountain was considered a viable or acceptable obsidian "source" while the smaller mountain was not. Factors such as material quality or nodule

size may have been important influences, but based on my fieldwork and experience with flaking the obsidian, I did not observe any major differences in quality or size between all the Glass Butte groups and the two Little Glass Butte groups.

In summary, at Newberry Caldera and likely also Nemrut Dağ, the individual lava flows are identifiable as such, so one can readily recognize them as discrete "sources" of obsidian. Laidley and McKay (1971) showed that BOF and the other flows in the caldera were compositionally similar, due to the same host rock and magma chamber, though still distinguishable by their chemistries. For Newberry Caldera and perhaps Nemrut Dağ, the geographical obsidian "sources," as perceived by an observer on the ground, are identical to the geochemical "sources." At Glass Buttes, and perhaps Göllü Dağ, the distributions of chemical "sources" for each mountain are indistinguishable on the ground. A "source" would likely be perceived as a local geographical feature (like the water basin), an entire mountain (as indicated by Ambroz et al. 2001), or simply a dense cluster of nodules. The perceived geographical "sources" are not the same as the geochemical "sources" at Glass Buttes. The perceived geographical "sources" might, in comparison to the distribution of the geochemical "sources," be higher resolution (e.g., a natural basin or a nodule cluster) or lower resolution (e.g., one mountain or another). Their actual geographical "sources" are known only from chemical analyses of rigorously collected specimens with precisely defined locations, not from observations on the ground. To assess how geographical and chemical "sources" coincide, geological and archaeological surveys as well as the critical chemical analyses of collected specimens and artifacts are needed.

4.6 - Fieldwork Lessons and Specimen Nomenclature

A key component of this research is assessing the abilities of EMPA to distinguish chemical "source" groups using geological reference specimens, and I was confident that, at least in theory, this was likely. Based on the literature and my experience at Newberry Caldera and Glass Buttes, though, I decided that linking the geochemical "source" groups to their geographical "sources" required critical consideration.

One consideration was that, as discussed later in Section 4.7, I did not personally find the geological obsidian specimens in the field. Instead, the specimens were collected over three decades by a number of individuals. Rapp et al. (2000) identify this one cause of variability in their native-copper sourcing database, and that is likely also the case here and in the vast majority of sourcing studies. In the work of RDC, for example, of the five total specimens from Açigöl, considered one source at that time, Giorgio Pasquaré of the University of Milan collected two, and Herb Wright of the University of Minnesota-Twin Cities collected three (Renfrew et al. 1966:62). These obsidian specimens were probably given to RDC with their origins labelled as "Açigöl," and they lumped all five together to describe chemically the "Açigöl source" (or "Group 1e" of their system). Today, though, we know of five different flows and chemical groups at Açigöl (Rapp and Hill 1998:138), a fact obscured by low specimen numbers and lumping their data.

For every specimen collected, especially before the common use of GPS, there is imprecision in its location description, some more so than others. For example, as noted above, "Açigöl" is an inexact description for the specimen location or chemical "source"

group due to the presence of multiple obsidian-bearing flows there. It might, though, be adequate as a geographical "source" for archaeological studies on a sufficient scale, when it might not matter that the obsidian came from one of three eastern flows or from only a few kilometers to the west. Gordus et al. (1971) argues in favor of giving specimens with imprecise locations a broad geographical name, like "Yellowstone" (226). This would be acceptable if all such specimens were not lumped into one "Yellowstone source" because over a dozen distinct flows and chemical groups occur there. Thus we have an argument against uncritical "lumping" of geological specimens to "sources."

I received many geological specimens with labeled origins that would be tempting to call "sources" because they matched source names found in the obsidian literature, like Nemrut Dağ, Açigöl, and Nenezi Dağ. A few specimens had much less specific locations, like "Lake Van" or "Armenia." Some specimens had good descriptions of their locations in relation to volcanic features, like those from Nemrut Dağ (e.g, "NE interior of caldera" and "SE outside slope of caldera"). Others listed locations that, after experience at Glass Buttes, seem potentially problematic (e.g., "river bed, 600 m W Catkoy" and "ephemeral river, W Catkoy") due to secondary deposition and possible mixing.

Obsidian collected by Rapp and Ercan came in multi-specimen bags, each with a two-letter and two-number code, such as EA12 or CA09. The letters stood for the region: EA for Eastern Anatolia and CA for Central Anatolia. The numbers corresponded not to a particular volcano but were simply given to each location where obsidian specimens were collected. For example, the full description for the specimens labeled CA09 was: "CA09,

Açigöl, Korudağ, interior of caldera." I was hesitant to consider such a description these specimens' "source" (or a related term such as "source area") before I had determined their compositions and without having personally collected them. I decided to retain this numbering scheme and to integrate additional specimens into it.

I considered a variety of terms and concepts for these units -- EA12, CA09, etc. -- as, on one level, these would be a unit of analysis in my research. The term "locality" is commonly used in geology to define a small geographical area where a particular mineral or rock is found (e.g., olivine from San Carlos, Arizona; hornblende from Kakanui, New Zealand). The term, though, has already been applied by various researchers (e.g., Baugh and Nelson 1987, Shackley 1988, Wada et al. 2003, Izuho and Sato 2007, Godfrey-Smith et al. 1993, Park 2010) inconsistently to describe various scales of obsidian sources, from "subsources" to "source areas." "Deposit" was also considered, but Rapp (2002) defines this as "a coherent occurrence of rocks." This term, though, does not necessarily describe a site of secondary deposition, like the basin at Glass Buttes or locations in the Southwest where obsidian has been transported over 100 km. The term "outcrop" has similar issues. "Mine" and "quarry" implies that the location was a site of ancient human activity, which certainly was not necessarily the case for all of these specimens.

I decided that these units -- EA12, CA09, etc. -- would be considered "collection areas." This term reflects their nature: a space, of any scale, that the specimens' original collector considered to be a single area where obsidian occurs. It is not necessarily equal to either a geographical or chemical-mathematical "source" of obsidian. The "collection

area" size can vary from collector to collector. For one person, a "collection area" might be one or two meters in diameter, and for another person, it might be an entire volcano or lava dome complex. When I was sent bags of obsidian specimens with individual labels, each bag was considered a "collection area." Therefore, what constitutes one "collection area" is determined by each collector, not me. They are emic, not etic, descriptions. Still, each specimen was treated separately, as discussed in Chapter 6.

When I refer to the "source" of obsidian artifacts, I refer to the relevant collection area or areas as well as the volcano and, if available, geographical locations known in the literature (e.g., Kömürcü village at Göllü Dağ). I avoid the alphanumeric scheme of RDC because it is imprecise, convoluted, and only specifies chemical group -- consider:

> The position remains, then, that there are two major source regions for western Asia: Cappadocia (central Turkey), with the group 2b source at Çiftlik and the group 1e sources at Acigöl; and VAA, with sources of groups 1f, 1g, 3 and 4c. It is known that there are several flows in the Acigöl region... they will probably fall within the broad group 1e-f. (Renfrew and Dixon 1976:139)

This passage is followed by arguments for revisions to their Group 3 and its subdivisions 3a, 3b, 3c, 3d, including the need for additional subdivisions: 3a' , 3a'', and 3c' (139). It is more meaningful and intuitive, in my opinion, to state that obsidian came from Acigöl or Nemrut Dağ rather than Group 1e-f or Group 4c, respectively.

There are challenges to using geographical "sources," such as variations in names found in the archaeological and geological literature. For example, Todd (1980) explains that Güneydağ, an area on the northwestern side of Acigöl, is called Güneydağ Tepe, Göl Dağ, or Güneş Dağ by some researchers (30). Another example is that Sebastian Payne,

who collected obsidian specimens while at Mineral Research and Exploration Institute of Turkey (MTA), labelled an obsidian occurrence on the southwestern side of Göllü Dağ as "Sırça Deresi," which, according to the local inhabitants, was the name of a small nearby valley; however, others label this area "Bozköy" on their maps (34).

There are also instances where I have decided to use the volcano name to describe a geographical source rather than the most commonly used name. For example, RDC and others refer to two primary source areas in Central Anatolia: Acigöl and Çiftlik. Acigöl is the name of a caldera and its associated lava domes, but Çiftlik is the name of a town, not the volcano or lava dome complex. I instead use its official name from the Smithsonian's Global Volcanism Program: Göllü Dağ. "Ziyaret" is a Turkish word for "meeting place" or "pilgrimage place" and has been applied to at least two volcanoes in the Lake Van area (Bressy et al. 2005:1563). Therefore, I prefer to use the official volcano name -- Meydan Dağ -- rather than a local nickname applied to multiple places. In another example, RDC labeled one of their chemical groups (Group 3) as "Bayezid" because they suspected that its geographical source was somewhere near the town of Bayezıd, more commonly called Doğubeyazıd. This town, however, is surrounded by mountains and volcanoes, including Mount Ararat immediately to the northeast. Instead, in this vicinity, obsidian more likely originated from Tendürek Dağ, about 15 to 20 km southwest of the town. This, therefore, seems the better name to describe the geographical source.

4.7 - Assembling the Reference Collection

As established, one of the common criticisms of early, and even modern, sourcing studies is poor geological specimen collection schemes. Most studies, though, provide no or little information about how their specimens were collected, so their collection scheme or the resulting database cannot be assessed. In this section, I discuss how the geological specimens in this study were gathered and assembled into one collection.

4.7.1 - Turkey Obsidian Specimens

Most of the geological specimens from Turkey (646 out of 771) were given to me by George "Rip" Rapp, Regents Professor of Geoarchaeology *Emeritus* of the University of Minnesota-Duluth. Rapp earned a doctorate in geochemistry from Pennsylvania State, and he was a geoscience professor at the University of Minnesota-Twin Cities before he joined the University of Minnesota-Duluth. Based on his archaeological and geological experience, he realized that specimen collection for Anatolian obsidian sourcing studies could be done more systematically, as evidenced by the quote at the start of this chapter. To remedy these problems, during 1991 and 1992, Rapp and the late Dr. Tuncay Ercan of the General Directorate of Mineral Research and Exploration collected over 900 obsidian specimens (about 10 specimens from over 80 flows and deposits).

Rapp retained some of the specimens from each collection area at the University of Minnesota-Duluth. The rest were sent for analysis to Prof. Ernst Pernicka, then at the Max Planck Institute in Heidelberg. A small number of the specimens -- only 15 -- were

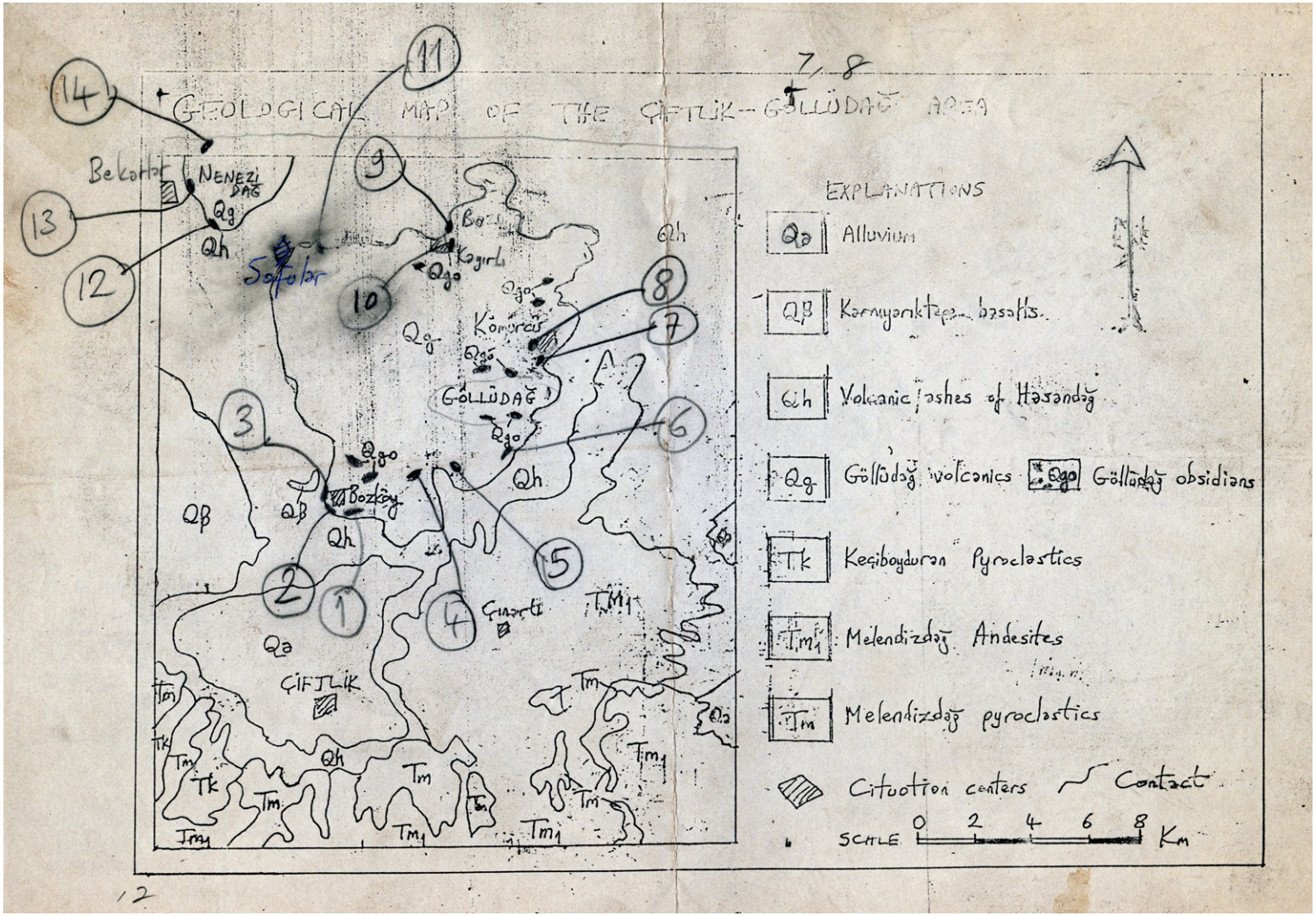


Figure 4.9 - Sample of the field notes by Rapp and Ercan when collecting specimens at Göllü Dağ (collection of the author).

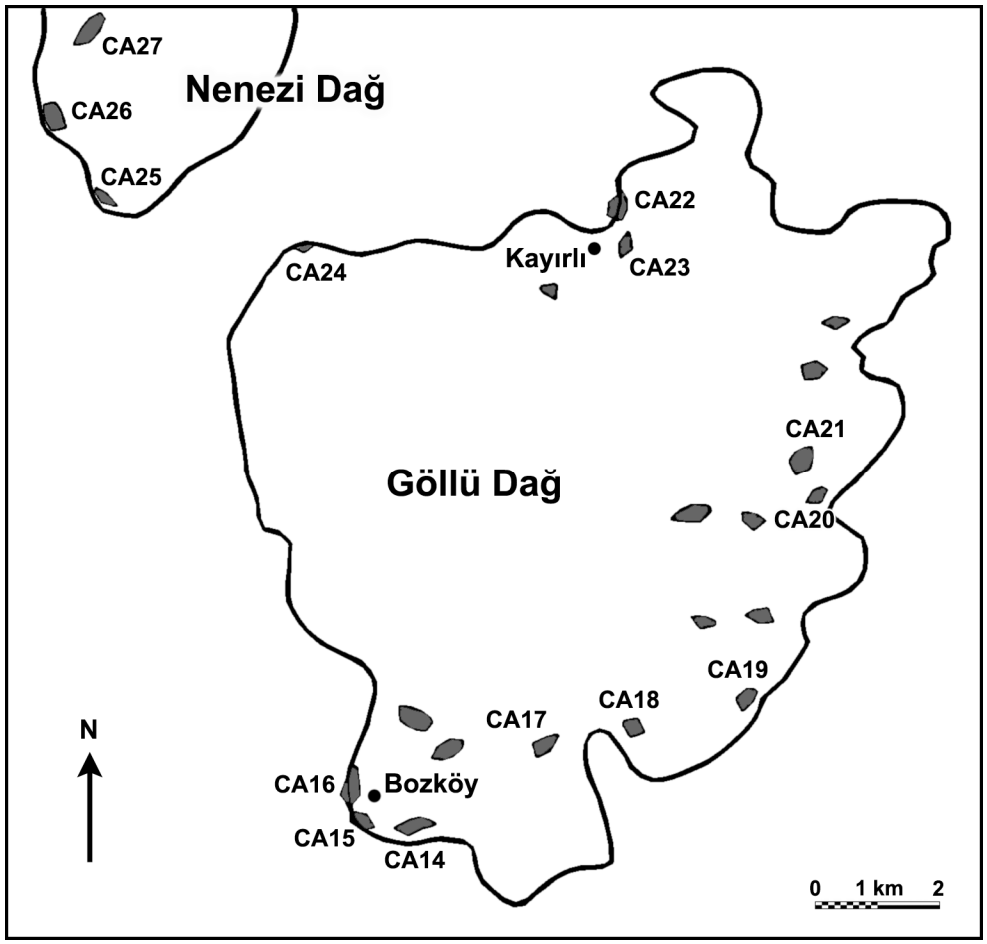


Figure 4.10 - The obsidian collection areas of Rapp and Ercan at Göllü Dağ and Nenezi Dağ; the gray spots represent obsidian outcrops (redrawn by the author; based on the field notes and maps of Rapp and Ercan and Figure 6.2 in Rapp and Hill 1998).

analyzed with NAA for a Master's thesis (*Geochemische Untersuchungen an Obsidianen Zentralanatoliens, Türkei* or *Geochemical Studies of Central Anatolian Obsidian, Turkey*; Bassette 1994) supervised by Pernicka. The NAA data were included in this thesis, and I compare them to my data in Chapter 6. Results using Rapp and Ercan's specimens were included in a conference talk on obsidian sourcing at two archaeological sites on the Biga peninsula in northwestern Turkey (Pernicka et al. 1996). Neither their data nor specimen numbers are included in the published version. One other project also made use of the specimens collected by Rapp and Ercan. A doctoral student of Pernicka, Kirstin Kasper, seemingly used some of the specimens in her dissertation study of Eastern Anatolian and Transcaucasian obsidian exchange during the Neolithic. Her data and dissertation are not publicly available, so no comparisons can be made to my data.

In a discussion with Professor Rapp in 2004, I learned that the obsidian study that he originally envisioned in 1991 did not occur, and with his support, I decided to take on this research. In 2002, an exploratory study that I conducted with EMPA and a variety of obsidian specimens from the American West showed promise, and I decided, based on a review of the literature, that modern EMPA should be reassessed for obsidian sourcing. That year, I received the specimens that Rapp had kept in Duluth, and I sent a request to Pernicka, who had since relocated to the University of Tübingen, to return the remaining specimens from Rapp and Ercan's collection. After a year, I received the specimens that had not been consumed by the NAA studies -- the process of NAA involves irradiation by neutrons, so any specimens analyzed with this technique must be discarded as radioactive

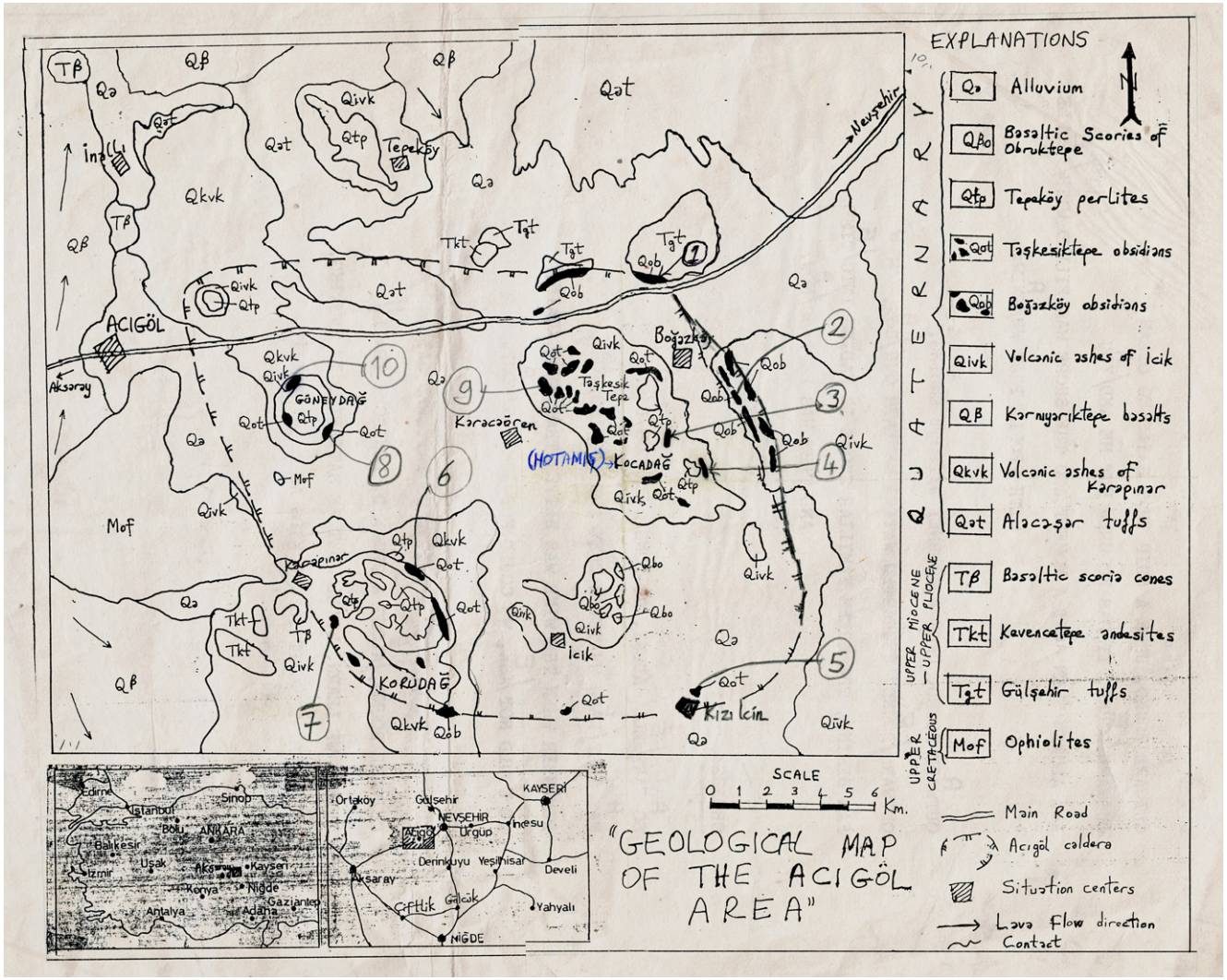


Figure 4.11 - Sample of the field notes by Rapp and Ercan when collecting specimens at Acıgöl (collection of the author).

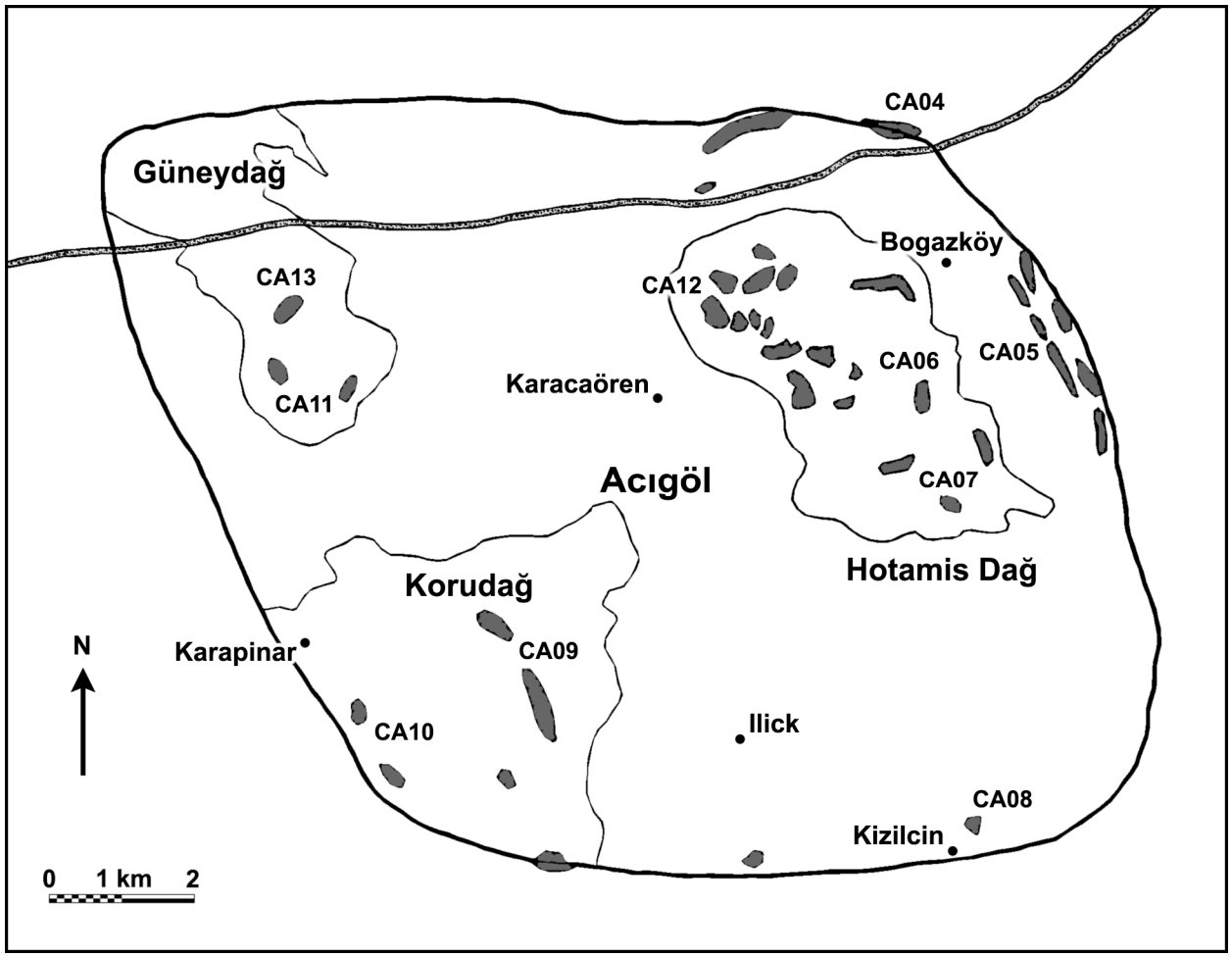


Figure 4.12 - The obsidian collection areas of Rapp and Ercan at Acıgöl; the gray spots are obsidian outcrops; the dotted line is a road (redrawn by the author; based on the field notes and maps of Rapp and Ercan and Figure 6.2 in Rapp and Hill 1998).

waste. In the end, I had over 640 specimens from the original 900 collected by Rapp and Ercan. They had gathered at least ten specimens from each of about 80 different obsidian flows and deposits ("collection areas") in Central and Eastern Anatolia, so I was left with, on average, five to eight obsidian specimens per collection area.

Comparisons to sources described in the literature (as of 2005) revealed the Rapp and Ercan collection was largely complete. There were only two main exceptions. First, prior studies had showed the importance of the Bingöl obsidian sources. Ercan and Rapp collected at least ten obsidian specimens from each of four Bingöl areas, but the majority of specimens from two collection areas must have been analyzed by NAA and discarded. There was only one specimen left, from Rapp's set in Duluth, from collection area EA47 and three specimens from EA49, two from Rapp. The other EA47 and EA49 specimens must have been subjected to NAA at the Max Planck Institute. Given the archaeological importance of the Bingöl locality and that there are two distinct chemical groups at these sources, it is not surprising these specimens received extra scrutiny. Therefore, I needed to supplement the Bingöl material with additional specimens.

Second, an obsidian locality described by Giulio Bigazzi and colleagues (Bigazzi et al. 1996:552, Figure 1; Bigazzi et al. 1997:66, Figure 10) was not represented in those specimens collected by Rapp and Ercan. Near the city of Muş, roughly halfway between the Bingöl and Nemrut Dağ source areas, are obsidian sources. They are also described by Yılmaz et al. (1987) and Ercan et al. (1995). Take note that the paper from Ercan and colleagues post-dates his fieldwork with Rapp in 1992. Mentions of the Muş locality are

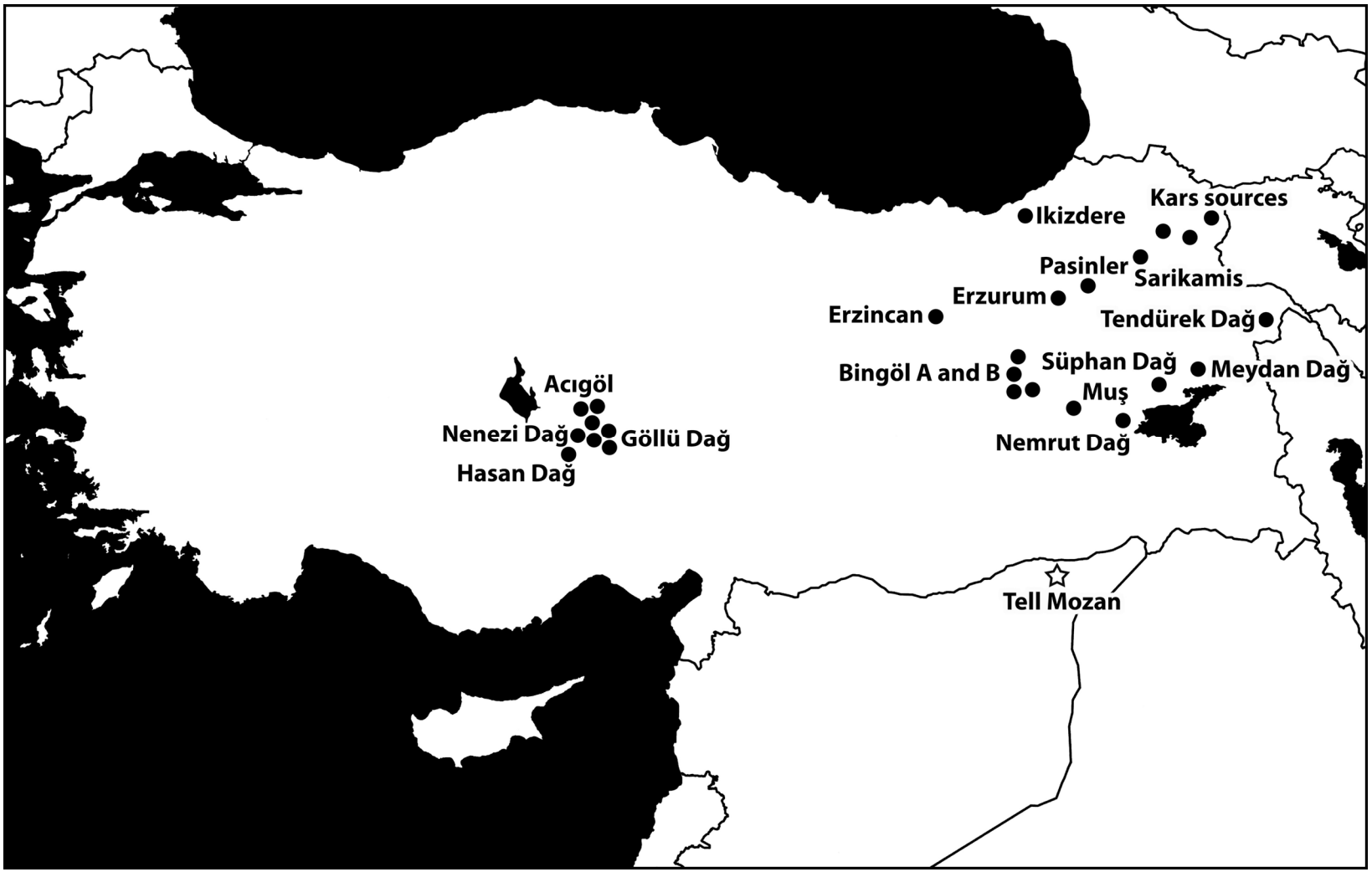


Figure 4.13 - The obsidian sources in Central (left) and Eastern (right) Anatolia in relation to Tell Mozan (map by the author).

missing from most earlier publications. Its discovery, at least by modern geologists, was apparently quite recent. Ercan must only have learned of its existence after 1992. In fact, Ercan collected these specimens for Bigazzi and his colleagues, who utilized fission-track dating as a means to determine the ages of obsidian in Turkey.

Therefore, for this research, I required obsidian specimens from the Muş locality as well as supplementary specimens from the Bingöl locality. I contacted Giulio Bigazzi at the Institute of Geochronology and Isotope Geochemistry in Pisa, Italy and one of his colleagues, Zehra Yeğingil in the Physics Department at Çukurova University in Adana, Turkey. Drs. Bigazzi and Yeğingil kindly provided me with specimens from the Bingöl and Muş localities and the corresponding collection area numbers used on the geological maps in Bigazzi et al. (1997). In particular, they sent me specimens from four of the six collection areas from the Muş locality and specimens from all five of their Bingöl areas. Because their research involved fission-track dating of the obsidian, their articles do not include any chemical data for inter-laboratory comparisons. More specimens from these areas were sent by Bernard Gratuze of the Institut de Recherche sur les Archéomatériaux but not received in time to include in this phase of the research.

Additional specimens from Turkey were sent to me from John Whittaker, who, as noted in Section 4.5, is a lithics expert and archaeology professor at Grinnell College. I was interested in specimens collected by archaeologists, not only geologists, because they might have different selection criteria for gathering obsidian and different conceptions of "collection areas" for geological specimens. Whittaker, who was participating in a study

abroad program in Istanbul, surveyed two of the primary obsidian source areas in Central Anatolia: Açigöl and the Kömürcü village area of Göllü Dağ. In addition to the Kömürcü and Açigöl specimens, he sent me obsidian from the Lake Van area.

A few specimens of Anatolian obsidian came from two additional sources. First, I obtained sizable specimens from Erzurum and Nemrut Dağ from Hasan Diker, a rock and mineral dealer from Turkey, who personally collected them. Second, I found a company, Stonex Madencilik Ltd. in Turkey, that owns an obsidian quarry near Meydan Dağ. The company generously provided me with large specimens and a report from their geologist, including maps and photographs of the obsidian outcrops.

In summary, over 90% of the specimens from Turkey were originally collected by George "Rip" Rapp and/or Tuncay Ercan of the General Directorate of Mineral Research and Exploration, making for a fairly coherent collection. The other 10% were contributed by an archaeologist, a rock collector, and a mining company. The result approximates, at least, what Rapp envisioned: a geological collection with obsidian sources systematically sampled "with full knowledge and coverage of the geology" of the region (Rapp and Hill 1998:137-138). His call, though, to include "all potential source deposits" spurred me to add hundreds of obsidian specimens from outside Turkey to my collection.

4.7.2 - Transcaucasian Obsidian Specimens

Compared to Anatolia or the Aegean and Mediterranean areas, the Transcaucasus region has much less attention for obsidian sourcing research until quite recently. One of

the key reasons is that, as former Soviet republics, these nations were largely inaccessible to Western researchers until 1991. The few systematic studies in this region have showed that obsidian from Transcaucasian sources principally remained in the region and was not exchanged over great distances, like that from Central and Eastern Anatolia, probably for geographical reasons (e.g., Blackman et al. 1998; Barge and Chataigner 2003; Chataigner et al. 2003). Nevertheless, the Transcaucasian obsidian sources were of particular interest in this research due to the hypothesized connections of the Hurrians to the Transcaucasus, as discussed in Section 3.7 and Buccellati and Kelly-Buccellati (2007c).

4.7.2.1 - Azerbaijan

Azerbaijan has only one main obsidian source: the Kel'bedzhar volcano, which is also known in the literature as Kechel Dağ and Merkasar. I received obsidian specimens from this area from two individuals: M. James Blackman at the Archaeology Division of the Smithsonian Institution (via Michael Glascock at the Archaeometry Laboratory at the University of Missouri Research Reactor Center; MURR) and Khikmet I. Makhmudov of the Azerbaijan National Academy of Sciences and Baku State University.

4.7.2.2 - Georgia

Georgia also has a single major obsidian source: Chikiani volcano (also known in the literature as the Paravani Lake source). I received specimens from this volcano from a few people: M. James Blackman at the Smithsonian (via Michael Glascock at MURR);

Irina Demetradze of the Ilia Chavchavadze State University in Tbilisi, Georgia; Sergey Karapetyan (via Khachatur Meliksetian), both of the Armenian Institute of Geological Sciences; Ruben Badalyan of the Armenian Institute of Archaeology and Ethnography; and Nino Sadradze and Givi Maisuradze of the Institute of Geology in Tbilisi, Georgia. Obsidian artifacts also sent by Irina Demetradze and Nino Sadradze played a key role in evaluating my sourcing procedures, as discussed in Chapter 6.

4.7.2.3 - Kabardino-Balkaria Republic

Another obsidian source occurs across the northern Georgian border into Russia, in particular, the Kabardino-Balkaria Republic. It is known as the Baksan River source, and the obsidian apparently derives from the Mount Elbrus volcano, where the Baksan River originates. My specimens of this area were also collected by M. James Blackman of the Smithsonian and sent to me by Michael Glascock at MURR.

4.7.2.4 - Armenia

Armenia poses a greater challenge for assembling a complete geological reference collection than Azerbaijan, Georgia, or the Kabardino-Balkaria Republic. This is the case because Armenia has over 20 obsidian-bearing volcanoes, the majority of which have not been adequately sampled for systematic sourcing research, and because, in comparison to Anatolia and the Aegean, sourcing Armenian obsidian is a recent line of study undertaken by only a few researchers (e.g., Keller at al. 1996; Blackman et al. 1998; Poidevin 1998;

Oddoone et al. 2000; Badalian et al. 2001; Chataigner et al. 2003; Barge and Chataigner 2003; Cherry et al. 2007; Pinhasi et al. 2008).

Rapp and his colleagues once noted that, in their native copper sourcing research, they collected geological specimens from the field but also relied on "geologists, private collections, mining companies, museums, other universities, and commercial suppliers" to provide additional specimens (Rapp et al. 2000:35). I had to use these sources as well to assemble a reasonable, though imperfect, Armenian obsidian collection. For example, I obtained a number of specimens collected by researchers at the Smithsonian Institution: one set collected by M. James Blackman and another set collected by Ivan P. Savov (as a postdoc) and the late James F. Luhr. In addition, I received specimens from the Robert L. Smith obsidian collection, now curated at the Smithsonian. I was sent specimens as well from Armenian researchers: Ruben Badalian, Institute of Archaeology and Ethnography; Albert Harutyunyan, Geology and Exploration Technology, State Engineering University of Armenia; and Khachatur Meliksetian and Sergey Karapetyan at the Armenian Institute of Geological Sciences. Obsidian, given its extent, is also a popular material from which to make souvenirs and gifts in Armenia, so I also obtained several initial specimens from the Hrazdan volcanic cluster from commercial suppliers.

4.7.3 - Excluded Obsidian Sources

As has been mentioned several times now, sourcing research requires all potential sources of material to be located and sampled. At some point, though, one must choose a

Table 4.1 - Obsidian Collection Areas

Eastern Anatolia (EA) collection areas

Area	*Name*	*Location Notes*
EA01	Sarikamis	ca. 10 km N Mescitli village; Ciplak Dag
EA02	Sarikamis	ca. 6 km N Mescitli village; Ciplak Dag
EA03	Sarikamis	ca. 1 km NE Mescitli village; near Sarikamis-Karakurt road
EA04	Sarikamis	ca. 5 km SE Hamamli village; Aladag
EA05	Sarikamis	ca. 3 km NNW Sehitemin village; Aladag
EA06	Sarikamis	between Mescitli and Sehitemin, river bed
EA07	Meydan Dag	also known as Ziyaret
EA08	Meydan Dag	also known as Ziyaret
EA09	Meydan Dag	also known as Ziyaret; actually Tendurek Dag?
EA10	Meydan Dag	also known as Ziyaret
EA11	Meydan Dag	also known as Ziyaret
EA12	Suphan Dag	Rutudag, N Suphan Dag
EA13	Suphan Dag	SE slope Suphan Dag
EA14	Suphan Dag	0.5 km SW Dizginkale village
EA15	Suphan Dag	1 km S Dizginkale village
EA16	Suphan Dag	ca. 7 km SE Suphan Dag; Ahuruk Dag
EA17	Suphan Dag	Kucukkale Tepe, ca. 5 km S Suphan Dag
EA18	Suphan Dag	Nernek Dag, W side
EA19	Suphan Dag	Nernek Dag
EA20	Nemrut Dag	N crater rim (Sivri Tepe)
EA21	Nemrut Dag	N shore of Nemrut Golu (Cavus Tepe)
EA22	Nemrut Dag	NE interior of caldera; near Tatuan town
EA23	Nemrut Dag	SE outside slope of caldera (Yarbasi Tepe)
EA24	Nemrut Dag	E shore of Nemrut Golu
EA25	Nemrut Dag	SE corner of Nemrut Golu
EA26	Nemrut Dag	E outside slope of caldera
EA27	Nemrut Dag	NW EA22, near SE shore of Ilig Golu
EA28	Nemrut Dag	SW outside slope of caldera
EA29	Nemrut Dag	SE interior of caldera
EA30	Tendurek Dag	ca. 15 km W Dogubayezid
EA31	Tendurek Dag	ca. 15 km W Dogubayezid
EA32	Tendurek Dag	ca. 15 km W Dogubayezid
EA33	Pasinler	Hasanbabu Dag (NW Tizgi village)
EA34	Pasinler	Hasanbabu Dag (NW Tizgi village)
EA35	Pasinler	Hasanbabu Dag (NW Tizgi village)
EA36	Kars-Digor	10 km S of Digor, 40 km SE Kars, NE flank of Yaglica Mt
EA37	Kars-Digor	11 km S of Digor, 40 km SE Kars, NE flank of Yaglica Mt
EA38	Kars-Akbaba Dag	ca. 15 km S Kars
EA39	Kars-Arpacay	NW Akuzum village, ca. 55 km E Kars
EA40	Kars-Arpacay	SW Akuzum village, ca. 55 km E Kars
EA41	Erzurum	ca. 20 km SW Erzurum town, near Tambura village
EA42	Erzurum	ca. 20 km SW Erzurum town, near Tambura village
EA43	Erzincan	Agili Tepe, ca. 30 km E Erzincan
EA44	Erzincan	Agili Tepe, ca. 30 km E Erzincan
EA45	Erzincan	Degirimen Tepe, ca. 20 krn E Erzincan (Kertah Koy)
EA46	Erzincan	Degirimen Tepe, ca. 20 km E Erzincan (Kertah Koy)
EA47	Bingol	NE Cavuslar Koyu
EA48	Bingol	NE Cavuslar Koyu
EA49	Bingol	NE Cavuslar Koyu

Table 4.1 - Obsidian Collection Areas (Continued)

EA50	Bingol	NE Cavuslar Koyu
EA51	Ikizdere	Haros Dag, SE Rize
EA52	Bingol	Arcuk; 35 km N of Bingol town, near Arcuk village
EA53	Bingol	Alatepe; 38 km NE of Bingol town, near Alatepe
EA54	Bingol	Catak; 5 km N of the above sample, near Catak village
EA55	Bingol	Cavuslar; 33 km NE of Bingol town, near Cavuslar village
EA56	Bingol	Cavuslar; 200 m E of the above sample
EA57	Mus	20 km NE of Mus town, near Mercimekkale; near Anzar village
EA58	Mus	21 km NE of Mus town, near Mercimekkale; near Anzar village
EA59	Mus	24 km NE of Mus town, near Mercimekkale; near Anzar village
EA60	Mus	25 km NE of Mus town, near Mercimekkale; near Anzar village
EA61	Mus	Ziyaret Tepe
EA62	Mus	20 km NE of Mus town, near Mercimekkale; near Anzar village
EA63	Erzurum	"near Erzurum"
EA64	Nemrut Dag	"Mount Nemrut, Turkey"
EA65	Lake Van	"Lake Van area, East Turkey"
EA66	Lake Van	"Lake Van area, East Turkey"
EA67	Lake Van	"Lake Van area, East Turkey"
EA68	Meydan Dag	Stonex Ltd mines; near Erciş town
EA69	Meydan Dag	Stonex Ltd mines; near Erciş town

Central Anatolia (CA) collection areas

Area	*Name*	*Location Notes*
CA01	Catkoy	river bed, 600 m W Catkoy
CA02	Catkoy	river bed, 800 m W Catkoy
CA03	Catkoy	ephemeral river, W Catkoy, small obsidian in tuffs
CA04	Acigol	WTHD; white tuff north of Hotamis Dag
CA05	Acigol	southeast of Bogazkoy, Asmanbasi Tepe
CA06	Acigol	Hotamis Dag, SE rim of obsidian dome
CA07	Acigol	Kirkiz Tepe, SE of Hotamis Dag
CA08	Acigol	Kizilcin village; Hotamis Dag
CA09	Acigol	Korudag, interior of caldera
CA10	Acigol	W slope of Korudag, separate flow (?)
CA11	Acigol	Guneydag, W caldera ("Acigol crater")
CA12	Acigol	Hotamis Dag, W rim (Taskesik Tepe)
CA13	Acigol	Guneydag, N side
CA14	Bozkoy	S Bozkoy ("Golludag-Bozkoy")
CA15	Bozkoy	S Bozkoy, 500 m towards Bozkoy from CA14
CA16	Bozkoy	Bozkoy, stream gravels
CA17	Golludag	S little Golludag
CA18	Golludag	1 km E CA17, from quarry
CA19	Golludag	S large Golludag
CA20	Golludag	Komurcu village ("Golludag-Komurcu")
CA21	Golludag	2 km NW CA20, from river bed draining Golludag
CA22	Kayirli	Kayirli villlage, NW Golludag ("NW Golludag")
CA23	Kayirli	Kayirli villlage, 1.2 km S CA22, river-bed
CA24	Sofular	Sofular village, near crater lake (hot springs)
CA25	Nenezi Dag	S side Nenezi Dag
CA26	Nenezi Dag	W side Nenezi Dag, near Bekarlar village

Table 4.1 - Obsidian Collection Areas (Continued)

CA27	Nenezi Dag	NW side Nenezi Dag
CA28	Hasan Dag	Hasandag, SE Taspinar village
CA29	Hasan Dag	Hasandag, SE Taspinar village, 1 km S CA28
CA30	Hasan Dag	Hasandag, SW Kecikalesi village
CA31	Hasan Dag	Hasandag, S Kecikalesi village
CA32	Komurcu	Kocatepe/Kumurcu source area of Gollu Dag
CA33	Acigol	colluvium in the road cut along the highway

Azerbaijan (AZ) collection areas

Area	*Name*	*Location Notes*
AZ01	Kel'bedzhar	M. James Blackman collection, sample #AZO-073
AZ02	Kel'bedzhar	also known in the literature as Kechel Dağ and Merkasar
AZ03	Kel'bedzhar	also known in the literature as Kechel Dağ and Merkasar
AZ04	Kel'bedzhar	also known in the literature as Kechel Dağ and Merkasar

Kabardino-Balkaria (KB) collection areas

Area	*Name*	*Location Notes*
KB01	Baksan River	M. James Blackman collection, sample #CBO-008
KB02	Baksan River	M. James Blackman collection, sample #CBO-009

Georgia (GE) collection areas

Area	*Name*	*Location Notes*
GE01	Chikiani/Paravani	M. James Blackman collection, sample #GEO-002
GE02	Chikiani/Paravani	Paravani Lake Area, Javakheti Region, South Georgia
GE03	Chikiani/Paravani	Paravani Lake Area, Javakheti Region, South Georgia
GE04	Chikiani/Paravani	Paravani Lake Area, Javakheti Region, South Georgia
GE05	Chikiani/Paravani	Paravani Lake Area, Javakheti Region, South Georgia
GE06	Chikiani/Paravani	Paravani Lake Area, Javakheti Region, South Georgia
GE07	Chikiani/Paravani	Chikiani, South Georgia, near the border with Armenia
GE08	Chikiani/Paravani	Chikiani volcano (Georgia); Javakheti ridge (2 samples)
GE09	Chikiani/Paravani	Chikiani (dark black); Javekhety highland near Lake Paravani
GE10	Chikiani/Paravani	Chikiani (black); Javekhety highland near Lake Paravani
GE11	Chikiani/Paravani	Chikiani (limpid black); Javekhety highland near Lake Paravani
GE12	Chikiani/Paravani	Chikiani (brown); Javekhety highland near Lake Paravani
GE13	Chikiani/Paravani	Chikiani (gray); Javekhety highland near Lake Paravani

Armenia (AR) collection areas

Area	*Name*	*Location Notes*
AR01	Hrazdan Cluster	obsidian from commercial source, Hrazdan region
AR02	Hrazdan Cluster	obsidian from commercial source, Hrazdan region

Table 4.1 - Obsidian Collection Areas (Continued)

AR03	Hrazdan Cluster	obsidian from commercial source, Hrazdan region
AR04	Hrazdan Cluster	obsidian from commercial source, Hrazdan region
AR05	Hrazdan Cluster	obsidian from commercial source, Hrazdan region
AR06	Gutansar	originally misidentified at Sevakar; actually Gutansar
AR07	Hatis	M. James Blackman collection, sample #ARO-008
AR08	Hatis	M. James Blackman collection, sample #ARO-009
AR09	Mets Arteni	M. James Blackman collection, sample #ARO-011
AR10	Mets Arteni	M. James Blackman collection, sample #ARO-012
AR11	Gutansar-Gutansar	M. James Blackman collection, sample #ARO-061
AR12	Gutansar-Gutansar	M. James Blackman collection, sample #ARO-062
AR13	Ankavan	M. James Blackman collection, sample #ARO-084
AR14	Ankavan	M. James Blackman collection, sample #ARO-087
AR15	Gutansar-Gyumush	M. James Blackman collection, sample #ARO-094
AR16	Sizevit Yeni-el	M. James Blackman collection, sample #ARO-164
AR17	Sizevit Yeni-el	M. James Blackman collection, sample #ARO-165
AR18	Artik/Arteny	Sample #1: City-Artik, Village-Arteny
AR19	Artik/Arteny	Sample #2: City-Artik, Village-Arteny
AR20	Artik/Arteny	Sample #3: City-Artik, Village-Arteny
AR21	Chazencavan/Abovian	Sample #4: City-Chazencavan, City-Abovian
AR22	Varik/Dar-Alages	Sample #5: City-Vaik; additional note for "Dar-Alages"
AR23	Spitaksar	4-20-04; NMNH: Field #4-20-04
AR24	Dry Fountain	Erevan Dry Fountain; 6-26-04; NMNH: Field #6-26-04
AR25	Spitaksar	8-29B-04; NMNH: Field #8-29-04
AR26	Geghasar	8-30A-04; NMNH: Field #8-30A-04
AR27	Hatis	9-31A-04; NMNH: Field #9-31A-04
AR28	Hatis	9-31D-04; no corresponding SI-NMNH sample
AR29	Unknown	"136 - old red obsidian (exact eruption center unknown)"
AR30	Gutansar	9-32B-04; NMNH: Field #9-32B-04
AR31	Brusok	11-35A-04; NMNH: Field #11-35A-04
AR32	Pokr Arteni	11-36A-04; NMNH: Field #11-36A-04
AR33	Pokr Sevkar	3-12A-08 (red), "red obsidian"
AR34	Pokr Sevkar	3-12A-08 [black], "rhyolite obsidian"
AR35	Pokr Sevkar	3-12C-08, "rhyolite obsidian"
AR36	Metz Satanakar	4-15A-08
AR37	Metz Sevkar	4-18A-08
AR38	Bazenk	5-20A-08; "rhyolite obsidian"
AR39	Brusok	no specimen number
AR40	Erevan	Robert L. Smith collection #211; NMNH #52092; VG 00458
AR41	Pokr Arteni	#4673: Poqr Arteni
AR42	Pokr Arteni	#KM-786: Poqr Arteni; LAT 40.3451, LON 43.7822
AR43	Pokr Arteni	#KM-587: Poqr Arteni; LAT 40.3462, LON 43.7806
AR44	Gutansar	#1389: Gutansar
AR45	Gutansar	#KM-47: Gutansar; LAT 40.3671, LON 44.6875
AR46	Gutansar	#1676: Jraber extrusive (Gutansar)
AR47	Gutansar	#KM-451: Jraber extrusive; LAT 40.3619, LON 44.6385
AR48	Hatis	#756d: Atis
AR49	Fontan	#3370: Fontan
AR50	Alapars	#4561: Alapars
AR51	Geghasar	#1419: Geghasar
AR52	Geghasar	#1422: Geghasar
AR53	Geghasar	#KM-135: Geghasar; LAT 40.1813, LON 44.9881
AR54	Geghasar	#KM-35: Geghasar; mistakenly listed as "Mets Sevkar"

Table 4.1 - Obsidian Collection Areas (Continued)

AR55	Spitaksar	#1419: Spitaksar
AR56	Metz Satanakar	#237: Mets Satanakar
AR57	Metz Sevkar	#3223: Mets Sevakar
AR58	Bazenk	#3177: Basenk
AR59	Damlik	#KM-1890: Damlik, LAT 40.5966, LON 44.4835
AR60	Damlik	#1780: Damlik
AR61	Khorapor	#4571: Khorapor
AR62	Sizevit Yeni-el	#4498: Sizavet
AR63	Aghvorik	#KM-273: Aghvorik; LAT 41.085, LON 43.7098
AR64	Arqayasar	#1740: Arqayasar
AR65	Sevkar/Sevakar	obsidian piece "found near Sevkar village (black rock)"
AR66	Aghvorik	Aghvorik; Javakheti ridge
AR67	Mets Arteni	Mets Arteni; Arteni volcano; Aragats massif
AR68	Pokr Arteni	Pokr Arteni; Arteni volcano; Aragats massif
AR69	Damlik	Damlik volcano; Tsaghkuniats ridge
AR70	Ttvakar	Ttvakar volcano; Tsaghkuniats ridge
AR71	Kamakar	Kamakar volcano; Tsaghkuniats ridge
AR72	Hatis	Akunk I deposit; Hatis volcano; Gegham ridge
AR73	Hatis	Akunk II deposit; Hatis volcano; Gegham ridge
AR74	Hatis	Zar deposit; Hatis volcano; Gegham ridge
AR75	Hatis	Kaputan deposit; Hatis volcano; Gegham ridge
AR76	Gutansar	Jraber deposit; Gutansar volcano; Gegham ridge
AR77	Gutansar	Fontan deposit; Gutansar volcano; Gegham ridge
AR78	Gutansar	Karenis deposit; Gutansar volcano; Gegham ridge
AR79	Geghasar	Geghasar volcano; Gegham ridge
AR80	Metz Satanakar	Mets Satanakar volcano; Syunik ridge
AR81	Metz Sevkar	Mets Sevkar volcano; Syunik ridge
AR82	Bazenk	Bazenk volcano; Syunik ridge

boundary, based on the literature if possible, outside of which geological sources need not be included. This decision is basically a matter of practicality: any extraneous specimens cost time and money. For my research, it was clear that obsidian sources in, for example, the Russian Far East, Japan, and Iceland could be safely left out. In this section, I discuss those obsidian sources that I decided to exclude (i.e., Aegean, Mediterranean, Carpathian, East African, and Arabian sources) and those regions for which I could not obtain reliable specimens (i.e., Iran, Afghanistan, and northwest Turkey and its Aegean coast).

4.7.3.1 - Unknown Sources in Northeastern Turkey?

Brennan (1996) asserted that "there are many more obsidian sources in Turkey yet to be located… in the Bayburt Plain and Erzurum areas" (27). He further maintains that, based on the regional geology, "it is likely that numerous primary sources of obsidian are present in the Erzurum area" (29). Brennan even repeats that "it is apparent that there are numerous sources of obsidian present especially in the Erzurum area, none of which have yet been adequately analyzed" (30). His evidence supports, though, the presence of only two sources. Analyses of obsidian artifacts from five archaeological sites in the Bayburt Plain revealed six chemical groups that did not correspond to Hotamis Dağ, Göllü Dağ, or Hasan Dağ in Central Anatolia or Nemrut Dağ or Suphan Dağ in Eastern Anatolia. It seems that they are missing several known obsidian sources, including Meydan Dağ and Tendürek (Doğubeyazıd) in Eastern Anatolia. More importantly, my collection includes specimens, gathered by Rapp and Ercan in 1991 and 1992, from six "collection areas" in

this region: two west of Erzurum and four east of Erzincan. Hence, it is quite likely that I have specimens from these six "unknown" sources. Unfortunately, Brennan includes his data only as graphs of Rb versus Th and La/Sc versus Cs/Sc, so I cannot compare his data to that from my specimens. Nevertheless, Brennan (1996) may still be correct: there may be obsidian sources not yet discovered in northeastern Turkey.

4.7.3.2 - Northwestern Turkey

Obsidian sources were not discovered in northwestern Turkey until the late 1980s (Ercan et al. 1989, Keller and Seifried 1990:61, Bigazzi et al. 1993). The region in which they occur is known as the Galatian massif, that is, a group of mountains formed by faults and folds in the crust. Two newly located obsidian sources were termed Sakaelı-Orta and Yağlar by Keller and colleagues (Keller and Seifried 1990:61), and they postulate a third source in the region, nicknamed "Galatia-X," based on a scatter of obsidian debitage that matched no other known sources (62). The obsidian deposits at Sakaelı-Orta and Yağlar are smaller than, for example, Acıgöl and Göllü Dağ in Central Anatolia, and they are the oldest in Turkey, dating to between 16 and 25 million years ago (Ercan et al. 1990, 1994; Bigazzi et al. 1993). These deposits have been described as "perlite and obsidian pebbles (diameter up to 10 cm)" (Bigazzi et al. 1993:591) and as "nodules in tuffs," that is, rocks consisting of fused volcanic ash (Ercan et al. 1994:506).

Clearly the small "pebbles" or "nodules" (called "marekanite" or, in the American Southwest, "Apache tears") at Sakaelı-Orta and Yağlar are of limited utility compared to

the larger obsidian blocks at other sources. In fact, obsidian artifacts are rare at sites in this part of Anatolia (Pernicka 1996:515), and the obsidian from Sakaelı-Orta and Yağlar "seems to have been diffused by man only in western Anatolia, in the Troad," and only a few Neolithic sites (Cauvin and Chataigner 1994:531). Chataigner et al. (1998) state that obsidian artifacts from these sources "were recovered from some villages close to the Sea of Marmara (Fikirtepe, Pendik, Ilıpınar)… These are, up to now, the only evidence of the use of obsidian from the massif of Galatia by prehistoric populations" (523). Only a very few researchers have included Sakaelı-Orta and Yağlar in their sourcing studies (Oddone et al. 1997, Gratuze 1999). Because, though, these two obsidian sources do not appear to have been involved in long-distance exchange and because reliable specimens are hard to locate, I excluded obsidian from the Galatia massif from this study.

There are a few obsidian sources, although not of tool-quality material, located in western Anatolia. Two small occurrences, known as Kütahya (in the Kalabak valley near Eskişehir) and Foça (near the Aegean coast north of Izmir), were not discovered until the 1990s. Ercan et al. (1994) reported that "obsidians observed in Kütahya and Foça are not suitable for use as tools and therefore have no archaeological value" (506). Chataigner et al. (1998) similarly maintain that any "prehistoric exploitation of these obsidians appears unlikely" (523). I, therefore, left out these sources from this study.

Ercan et al. (1994) describe the source at Foça as "thin obsidian beds intercalated with perlites... found in Neogene deposits" (506). The Rapp-Ercan collection included a few specimens of perlite (that is, hydrated volcanic glass) from Foça. Perlite commonly

starts as obsidian, and over time, it is infiltrated and saturated by groundwater. Based on analyses of their water contents, these Foça perlite specimens were shown to be volcanic glass that experienced subsequent hydration rather than obsidian with a high initial water content (Conde, Ihinger, and Frahm 2009a, 2009b). Zielinski et al. (1977) studied perlite and obsidian at four Rocky Mountain sources. They noted marked chemical differences, beyond simple hydration, between obsidian and perlite. The conclusion was "significant errors can be made in estimating the original composition of rhyolitic obsidian simply by relying on abundances of elements in associated perlite" (1977:426). Therefore, perlite is of little use in obsidian sourcing, and it is not useful for flaked stone tools, so these Foça specimens were not included in my analytical database.

4.7.3.3 - Aegean Sea

The Aegean obsidian sources -- namely, Sta Nychia, Adhamas, and Dhemenegaki on the island of Melos; Soros on Antiparos; and the island of Giali -- have been a subject of archaeological interest for over a hundred years. In 1904, Robert Bosanquet wrote the chapter "The Obsidian Trade" in the report *Excavations at Phylakopi in Melos*. Renfrew and his colleagues quickly applied their sourcing technique to the Aegean (Renfrew et al. 1965, Dixon et al. 1968) and showed that Aegean obsidian was not moved far from these island sources. Since then, numerous researchers have characterized or sourced obsidian from this region (e.g., Durrani et al. 1971, Filippakis et al. 1981, Schmidbauer et al. 1986, Torrence 1986, Duttine et al. 2003, Arias et al. 2006, Georgiadis 2008). The research has

corroborated that Aegean obsidian did not travel far from its origins. For example, to the west, Aspinall et al. (1972) identified no Aegean obsidian beyond Greece, and to the east, Bigazzi et al. (1993) found just Anatolian, no Aegean, obsidian at four sites near Istanbul. I decided that, for this research phase, I could exclude Aegean obsidian.

4.7.3.4 - Mediterranean Sea

Like the obsidian sources in the Aegean Sea, the Mediterranean sources have long been a subject of interest, and they were among the early applications of RDC's sourcing techniques (Cann and Renfrew 1964; Dixon et al. 1968, Hallam et al. 1976). Their early work showed that, much like the Aegean sources, Mediterranean obsidian remained in the vicinity of its sources: Malta, Pantelleria, Lipari, Palmarola, and Sardinia. Mediterranean obsidian is still popular for archaeological studies and as a sort of experimental "testbed" for analytical techniques, so numerous researchers have characterized or sourced obsidian from the region (e.g., Ammerman et al. 1978; Ammerman 1979; Longworth and Warren 1979; Gale 1981; Francaviglia 1984, 1988; Randle et al. 1993; Tykot 1995; Kayani and McDonnell 1996; Acquafredda et al. 1996, 1999; Scorzelli et al. 2001; Vargo et al. 2001; Duttine et al. 2003; Stewart et al. 2003; Acquafredda and Paglionico 2004; Bellot-Gurlet et al. 2004; Bigazzi et al. 2005; Le Bourdonnec et al. 2005b; Lugliè et al. 2007; Bressy et al. 2008; De Francesco et al. 2008). Studies that actually sourced artifacts at a number of sites corroborated that Mediterranean obsidian was not transported east of the Ionian Sea. Consequently, I also decided to exclude the Mediterranean sources.

4.7.3.5 - Carpathian Sources

Obsidian also occurs in eastern Europe, namely Hungary and Slovakia, and these occurrences are commonly known as the "Carpathian" sources. Various researchers have characterized these sources and attributed obsidian artifacts to them (e.g., Nandris 1975; Williams-Thorpe et al. 1984; Biró et al. 1986; Bigazzi et al. 1990; Kilikoglou et al. 1997; Yanev et al. 1997; Constantinescu et al. 2002). Kilikoglou et al. (1996) found Carpathian obsidian in Macedonia, but Bigazzi et al. (1993) identified only Anatolian, no Carpathian, obsidian at four archaeological sites near Istanbul. Aspinall et al. (1972) observed that, at that point, no Carpathian obsidian artifacts had been found in the Aegean. Decades later, Carpathian obsidian was discovered on sites on the Aegean islands and the western coast of Turkey but no farther to the east (Georgiadis 2008). Because Carpathian obsidian has not been found beyond the Aegean coast, I excluded these sources.

4.7.3.6 - Afghanistan

Given the presence of lapis lazuli, almost certainly from the Badakhshan province of Afghanistan, at Tell Mozan and across Mesopotamia, I sought to include obsidian from that area. There is reportedly one source of volcanic glass in Afghanistan: the Zardqadah volcano in the Dasht-i-Nawyr basin, reported by Pierre Bordet (1972): "The obsidian of Zardqadah is a local anomaly… there are many fragments on the north side of Zardqadah" (297). I have not yet found anyone with specimens from Zardqadah or chemical data for such specimens. Based on Bordet's account, though, it is not clear if the "fragments" are

of useful size or quality for flaked stone tools. In fact, accounts of obsidian artifacts from sites in Afghanistan are also sparse. Davis and Dupree (1977) located two Epi-Paleolithic sites, both within the Dasht-i-Nawyr volcanic basin, where "virtually all of the tools were manufactured from obsidian, a material which has not been found in any archaeological context before in Afghanistan" (139). They suspected Zardqadah as a likely source (144), but they did not have any geological specimens for comparison. I tried to track down and gain access to these artifacts for analysis but was unsuccessful.

4.7.3.7 - Iran

I also worked to obtain obsidian specimens from Iran, given established exchange patterns between Mesopotamia and Iran by the third-millennium BCE (Kohl 1978, Potts 1993, Matthews and Fazeli 2004) and the fact that the volcanic features in eastern Turkey and Armenia extend into Iran (Dostal and Zerbi 1978, Innocenti et al. 1982). Information about Iranian obsidian sources, however, is sparse, incomplete, and even contradictory at times. Some accounts of Iranian obsidian are little more than hearsay. For example, in a paper on Iranian geomaterials, Beale (1973) gives a third-hand account:

> Local villagers at Yahya claim that obsidian exists in the volcanic mountain areas of Baluchistan, to the east of Yahya. Obsidian has been found by the French geologist Girod in the mountains 55 kilometres east of Bam (Fig. 1) (as communicated to Professor Movius, Harvard University, autumn 1971) (136).

In addition, in the few very studies of Iranian obsidian localities, the compositional data are scant. Niknami et al. (2010) analyzed just one specimen for each of three volcanoes,

and Khademi et al. (2007) analyzed an unknown number of specimens from Sahand and Sabalan volcanoes and published their data for none (nor any information about where or when the specimens were collected). A discovery, which I discuss here shortly, based on my analyses of specimens sent from Iran, further complicates the picture.

Many claims for local origins of obsidian at Iranian archaeological sites seem to be based on appearance (e.g., Burney 1962) or the lithic technology (e.g., Rafifar 1991). Various sourcing studies, though, have proved that much of the obsidian at Iranian sites originated from Turkey and Armenia (e.g., Mahdavi and Bovington 1972; Renfrew 1977; Blackman 1984, 1994; Pullar et al. 1986; Badalyan et al. 2004; Glascock 2009). It must be noted that many of these studies (1) do not include any geological obsidian from Iran and (2) have at least a few artifacts without matching geochemical groups. For example, in Blackman (1984), of the eight geochemical groups identified among the artifacts, only half correspond to known obsidian sources. For the remaining groups, Blackman (1984) suggested additional surveys in eastern Turkey and Armenia. The missing sources might be Iranian, but these studies also often have sources missing in both Turkey and Armenia and suffer from too few source specimens. For instance, Mahdavi and Bovington (1972) compared artifacts to only two sources in Eastern Anatolia and three in Central Anatolia represented, apparently, by only one specimen each (151).

To import geological obsidian specimens from Iran, I acquired a license from the Office of Foreign Assets Control, a division of the U.S. Department of the Treasury. Dr. Ahmad Jahangiri, a geologist at the University of Tabriz, did not find any obsidian in the

department's collection from Mounts Sahand and Sabalan. Those specimens he did find reportedly came from three areas of the Urumieh-Dokhtar-Magmatic Arc: three from the Gareh-Chman region (roughly 100 km southeast of Tabriz), one from the Maku volcanic complex (near the border of Iran and Turkey), and one from Shahr-e-Babak (in southeast Iran, possibly one of the occurrences mentioned by Beale 1973).

Unfortunately, based on my analyses, I found that the specimens supposedly from the Gareh-Chman area were a mix of artificial glass and obsidian that actually came from Gutansar in Armenia. From what I was told, these specimens came from a departmental rock collection, not freshly gathered material, so the professor who sent them to me only had the specimen card information to follow. Such problems with geological collections, assembled over several decades, are not uncommon. For instance, here at the University of Minnesota, one obsidian specimen in the collection of the Department of Geology and Geophysics is labeled: "Gunnison, Colo. or National City, Calif." Not only are there two possibilities, but the obsidian source closest to National City is about 150 km to the east. Unfortunately, other obsidian researchers have noted very similar problems with obsidian specimens from museum collections in Iran (Glascock 2009).

For these reasons, I have removed all of the specimens sent from the University of Tabriz collection. Until obsidian specimens can be obtained either directly from the field in Iran or from field geologists who personally collected specimens, Iran and its possible obsidian sources will not be represented in my collection (and others).

4.7.3.8 - East Africa and Arabian Peninsula

Obsidian also occurs in the southern Red Sea and East African Rift areas: Yemen and Saudi Arabia on the Arabian side and Eritrea, Ethiopia, Kenya, and Tanzania on the African side. The evidence of obsidian from this region in Mesopotamia and Anatolia is sparse. In fact, to my knowledge, the sole example comes from the work of RDC. Dixon et al. (1968) state that part of "a little toilette table of obsidian made in Egypt and bearing a hieroglyphic inscription of Pharaoh Chian, of the 16th century B.C., has been found at Boğazköy, the capital of the ancient Hittite kingdom in Turkey" and suggest that it likely was "a gift sent by the Pharaoh to the Hittite king" (88). All of the other evidence seems speculative, circumstantial, or unconfirmed, essentially rumors.

Obsidian sources of Red Sea and East African Rift have been studied by various geologists and archaeologists (e.g., Francaviglia 1985, 1990; Zarins 1990; Khalidi et al. 2009 on the Arabian side and Muir et al. 1976; Merrick and Brown 1984, 1994; Poupeau et al. 2004; Raynal et al. 2005; Vogel et al. 2006; Negash and Shackley 2006; Negash et al. 2006, 2007; Brown et al. 2009; Morgan et al. 2009; Piperno et al. 2009 on the African side). Most of these researchers in East Africa, though, focus on Paleolithic sites. Work, like that of Bavay et al. (2000), on sourcing ancient Egyptian obsidian is rare, meaning it is difficult to evaluate the likelihood of such obsidian in Mesopotamia.

Given the extreme rarity of reliable reports of southern Red Sea and East African Rift obsidian in Mesopotamia and Anatolia, I decided that it was sensible to exclude these sources from this phase of my research. I have, though, already gathered specimens from

various obsidian sources in Yemen, Eritrea, Ethiopia, Kenya, and Tanzania in anticipation of adding this region in a future phase of this obsidian sourcing work.

4.8 - Selecting Artifacts for Analysis

At Tell Mozan, I conducted a survey of all the lithics, including obsidian artifacts, excavated at the site since 1984 and stored at the field house. Artifacts that are especially rare or ascetically pleasing are sent to the regional archaeological museum at Deir ez-Zor, so these objects were not included. I did this survey, in part, to develop selection criteria for the obsidian artifacts that I would request to export for analysis. The lithics collection includes over 800 obsidian pieces, including tools like blades, flakes, debitage, and a few cores. When my selection criteria were applied to the entire corpus, 97 obsidian pieces fit the criteria and were approved for export by the Syrian Directorate General of Antiquities and Museums. My criteria for these artifacts were included in the 2006 expedition report by Buccellati and Kelly-Buccellati (2007a) and are repeated here:

> Selected samples cannot:
> - be recognizable as a tool (includes projectile points, blades, bladelets, borers, scrapers, knives, celts, notches, deticulates, trapezes, burins, and choppers).
> - have a cross section that is typical of the above tools, especially blades.
> - be a core or pieces that refit to form a core (possible cores were examined for features such as striking platforms and negatives of bulbs of percussion).
> - be ground- or polished-stone (for example, no beads or drilled objects).
> - have any apparent retouch (includes both the ventral and dorsal sides).
>
> Selected samples must:
> - be either debris from tool making or some other unrecognizable fragment.
> - be less than 2 cm in diameter, fitting the definition for chip debris (debris larger than 2 cm is classified as a chunk, and it is commonly assumed that most tool types require flakes larger than 2 cm in diameter).

These definitions of "chip debris" and "chunk debris" are based on Rosen (1997:30), who also excluded small broken blades from these waste classes. By number, then, about 15% of the entire Tell Mozan obsidian corpus was exported and analyzed for this research. By weight,the fraction is much lower, only a few percent. I hope that, based on these results, larger artifacts, especially blades, will also be approved for export.

4.9 - Specimen Preparation - Geological Specimens

For the present research, over 900 specimens of obsidian from geological sources were prepared for EMPA. About two-thirds of the specimens were mounted individually and, as a result, could have their magnetic properties measured for ongoing research into magnetism-based obsidian sourcing (Feinberg et al. 2009, Johnson et al. 2009, Feinberg et al., in preparation). The remaining third of the specimens were sufficiently small that they were prepared together in mounts of two to six specimens. The specimens were all mounted and polished using a set of standard techniques.

4.9.1 - Specimen Preparation Requirements for EMPA

The ideal specimen for EMPA has a polished flat surface. Rough surfaces lead to errors in the data correction schemes (Goldstein et al. 1981:338, 449). This is due to the fact that EMPA is a surface analytical technique (Beaman and Isasi 1972:51). The beam electrons penetrate just a few micrometers (μm) into a specimen, so surface roughness or irregularities on this scale will affect the electrons and the X-rays they yield. A "mirror"

finish is often considered ideal. Calculations by Lifshin and Gauvin (2001) showed that a surface with grooves only 0.5-µm deep can lead to errors (171).

4.9.2 - Use of Petrographic Thin Sections

The majority of rock and mineral specimens analyzed by geologists using EMPA are prepared as petrographic thin sections. Specimens prepared this way are sliced thinly, adhered to a glass slide, and polished to a thickness of 30 micrometers (0.03 millimeters). Using a petrographic microscope, thin sections are observed under transmitted, polarized light to identify the minerals based on their optical properties. Archaeologists interested in the mineral content of artifacts, especially ceramics, will frequently use polarized-light petrography in their studies (e.g., Kempe and Templeman 1983).

I decided against preparing my specimens as thin sections for three main reasons. First, and most importantly, I did not intend to observe the specimens with a petrographic microscope. In fact, most mineral inclusions in obsidian are too small for polarized-light petrography. Second, most specimen material is exhausted during the preparation of thin sections -- if a 3-millimeter-thick rock slice is prepared as a thin section, 99 percent of the material is polished away. The specimens could not be easily replaced, and consequently, conservation of the material was important. Lastly, preparing thin sections is either time-consuming or expensive. The cost to have specimens prepared as thin sections, including the additional polishing required for EMPA, is $30-40 per slide. Preparing more than 900 specimens as thin sections would have been time- or cost-prohibitive.

4.9.3 - Preparing Obsidian Specimen Discs

I instead mounted the obsidian specimens in clear acrylic discs, 1-inch (25-mm) in diameter and 1/8-inch (3-mm) thick. These discs were ideally sized for the specimen holders of the electron microprobe. Acrylic has a molecular formula of $(C_5O_2H_8)_n$, which means that it contains no elements of interest in the present research. Therefore, it is not a potential source of contamination. I drilled holes in the discs, using a milling machine in the Geology and Geophysics Machine Shop. About two-thirds of the specimens were mounted individually in discs with a single large hole. The rest were smaller specimens mounted in discs with multiple holes, usually two or four. The mean exposed area of the specimens is over 100 square millimeters (1 square centimeter).

Large obsidian specimens were reduced in size two ways. For some specimens, I took advantage of obsidian's properties and used percussion flaking techniques to remove pieces for mounting. My "hammerstones" were porcelain and agate pestles. Porcelain is comprised of clay minerals (phyllosilicates that contain some combination of Na, Mg, Al, Si, K, Ca, and Fe oxides), and agate is comprised almost entirely of chalcedony, a micro- and crypto-crystalline variety of silica (SiO_2). Although these materials contain elements of interest in the obsidian, contamination was not an issue because any specimen surface struck by a pestle was either polished away later or not analyzed.

Some of the large obsidian specimens were cut using a Buehler IsoMet low-speed precision sectioning saw. Gravity pulls the specimens down on a rotating wafering blade, and a precision holder allowed serial sections to be cut from some specimens. The blades

from Allied High Tech Products had metal-bonded diamonds on their cutting edges. Like the pestles, elements of interest for the obsidian were also present in the blades (Al, Si, P, Mn, and Fe); however, contamination was not an issue because the specimen surfaces cut by the blades were either polished down or not exposed for analysis.

The specimens were mounted in the drilled holes in the acrylic discs using a two-part epoxy. I chose EpoxySet from Allied High Tech Products as the embedding medium because it sets hard and clear, has a low viscosity and excellent adhesion, and is vacuum-compatible (meaning it is stable in high-vacuum environments, such as the interior of the electron microprobe). The ingredients of EpoxySet are mostly comprised of chains of H, O, and C, so contamination was not an issue. To remove bubbles in the fresh epoxy, discs were placed in a Buehler "Cast N' Vac" vacuum impregnation system.

4.9.4 - Grinding and Polishing the Specimen Discs

I polished all the specimen discs using a LECO semi-automatic grinding/polishing machine and a custom holder for preparing eight discs at once. The grinder/polisher head applied 15-20 PSI of pressure, and the polishing wheel spun at 500 RPM. The discs were polished for two to three minutes at each of eight stages. I ground the specimens using a set of three silicon carbide abrasive paper discs on the polishing wheel: 240 grit (54 μm), 400 grit (24 μm), and 600 grit (16 μm). The silicon carbide (SiC) particles were adhered to the paper with resin, and water was used to remove debris -- only with soft and ductile materials like lead do these particles pose a contamination risk.

After grinding the specimen discs flat, I polished them using a set of five abrasive polishing suspensions. These suspensions were polycrystalline diamonds -- 15 µm, 9 µm, 6 µm, 3 µm, and 1 µm in diameter -- in propylene glycol lubricant mixed with water, and they were sprayed on fabric polishing pads. From 15 to 6 microns, these pads were made of woven nap-free nylon, and from 3 to 1 microns, they were either low-napped synthetic velvet, woven wool, or woven silk for a "mirror" finish. The pads were rinsed with water between each polishing step to remove debris and any remaining diamonds, and a glycol- and water-based lubricant was also used to aid debris removal.

4.9.5 - Documenting the Obsidian Specimen Colors

Before conductive carbon coats were applied to the specimen discs, giving them a silver-tinted appearance, I scanned them at 300 dpi with a flatbed photograph scanner (an Epson Perfection 3170). Each disc was scanned with a 24-block RGB-CMYK color card for calibration and consistency. I acquired the images in the interest of documenting their colors and textures, given the importance of visual-based obsidian sourcing (Bettinger et al. 1984, Moholy-Nagy and Nelson 1990, Tykot 1995, Aoyama 1996, Tenorio et al. 1998, Braswell et al. 2000; Carter and Kilikoglou 2006; Carter et al. 2008).

4.9.6 - Conductive Coating for the Discs

All specimens for EMPA must have electrically conductive surfaces, but obsidian, acrylic, and epoxy are excellent insulators. The surfaces of the specimen discs, therefore,

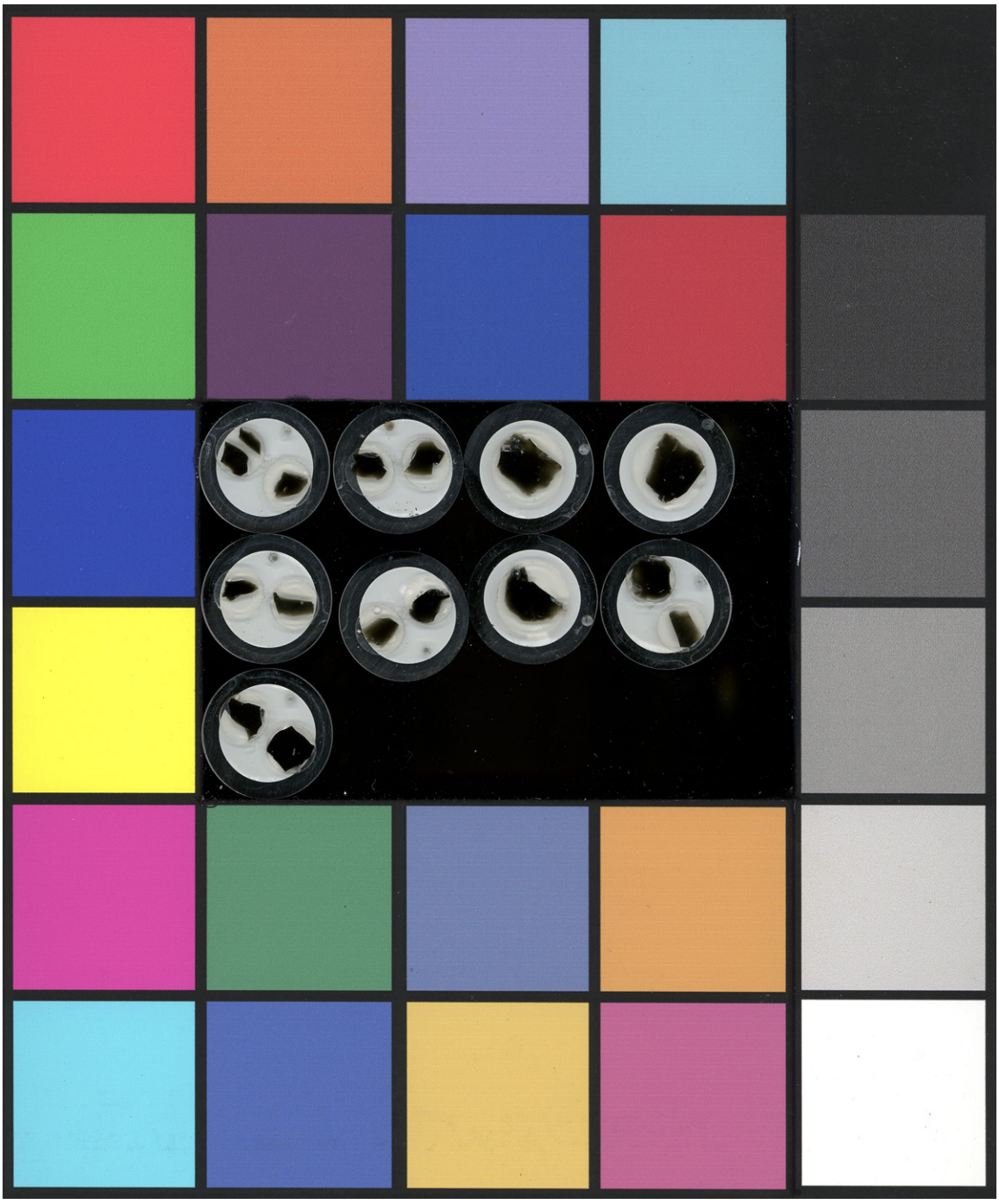


Figure 4.14 - Sixteen geological reference specimens from collection area EA24 of Nemrut Dağ prepared for EMPA: mounted in epoxy and acrylic discs and polished; scanned with a photographic color card to document the colors of the obsidians.

had to made conductive. Specimens for observation with high-vacuum scanning electron microscopy (SEM) are coated using various metals, including gold and palladium. While such metals adhere well to surfaces for high-magnification electron imaging, they impede quantitative analyses with EMPA. Instead, my specimens were coated with a thin layer of carbon, only 15 to 20 nanometers thick, which minimally impedes the beam electrons and X-rays. Carbon coats were applied to each of the specimen discs with the JEOL JEE-420 Vacuum Evaporator in the Electron Microprobe Laboratory.

4.10 - Specimen Preparation - Archaeological Artifacts

The preparation, or lack therefore, of the archaeological artifacts is part of what is novel in this research. I set out to establish, in part, if EMPA could be employed in a way non-destructive to artifacts. If EMPA could indeed be used non-destructively, it would be a great advantage of this technique when applied to obsidian sourcing. Much information about lithic artifacts is embodied in their shapes, so the ability to analyze artifacts without altering (i.e., cutting or chipping) them would be extremely desirable.

4.10.1 - Artifact Preparation in Prior EMPA Studies

Let us first consider how the artifacts were prepared in earlier obsidian sourcing studies that utilized EMPA. These three projects -- those of Merrick and Brown (1984), Tykot (1995, *inter alia*), and Weisler and Clague (1998) -- are also discussed in Chapters 1 and 5, where I discuss their analytical approaches and procedures.

Archaeologist Harry Merrick and geologist Francis Brown, who first used EMPA for obsidian sourcing, described their preparation technique as follows:

> Our method of sample preparation was to cement small fragments of obsidian artifacts into wells drilled in a fixed pattern into epoxy resin disks (3.1 cm diam. x 10 mm thick). The obsidian fragments were mounted so that the upper part of each fragment protruded above the surface. The disks were then ground flat and polished by standard techniques... We also noted that the fine fraction of obsidian debitage which passed through a 4 mm mesh screen, but which was recovered in 1 mm mesh was ideally suited for mounting directly into disks (1984:231).

Their specimen preparations, therefore, involved mounting either obsidian microdebitage or small pieces removed from larger artifacts. Merrick and Brown (1984) state that such grinding and polishing is necessary because Paleolithic artifacts from tropical East Africa should have "heavily altered chemically" surfaces, so the "removal of the altered surficial layer is required" to expose fresh material for EMPA (230). How these small pieces were removed from artifacts is unclear. The diameters of the pieces were apparently just a few millimeters, causing "only minor damage to an artifact" (230).

Tykot (1995) claims that "only a tiny 1 - 2 mm sample needs to be removed" from archaeological artifacts (111). He elaborates on his preparation techniques:

> Cylinders one inch in diameter were made using Epotek two-part epoxy, and allowed to harden for 48 hours. Up to 18 holes 2 mm in diameter and 3 mm in depth were drilled in the flat surface of the hardened disk, fresh epoxy was poured in the holes, and the disk was evacuated to remove air bubbles. Obsidian samples, cut earlier with a fast-speed diamond saw if necessary, were inserted in the holes (filled with still-wet epoxy), and covered with an additional later of wet epoxy. The entire disk was allowed to harden for 48 hours before a series of successively finer grit grinding papers were used to produce a flat surface in which all samples were visible. 10- and then 1-micron diamond paste were used to fine polish the surface. (112)

Tykot does report how pieces were removed from the artifacts: “samples were removed... either by flaking or using a high-speed diamond saw” (126). The artifacts that he studied were Neolithic-era (circa 6000-3000 BCE) and made of obsidian from the Mediterranean islands of Sardinia, Palmarola, Lipari, Pantelleria, and Melos.

Weisler and Clague (1998) had their obsidian specimens -- both geological source specimens and archaeological artifacts, or at least small pieces of them -- prepared as thin sections (116). Most of their specimens were 1 millimeter or greater in diameter, but they claim that specimens as small as 30 to 50 micrometers can be analyzed, although handled and prepared with difficulty. Weisler and Clague prepared the specimens as thin sections because they included basic petrographic observations, the kind made via polarized-light microscopy rather than EMPA (121). They analyzed artifacts less than one millenium old (circa 1100 to 1400 CE) from the Hawaiian island of Moloka’i.

In summary, all obsidian sourcing studies with EMPA-WDS involved destructive specimen preparation techniques for the archaeological artifacts as well as the geological reference specimens. None of the prior studies even mention attempting non-destructive analyses of the artifacts as, perhaps, an experiment or initial test.

4.10.2 - Artifact Preparation in Prior SEM-EDS Studies

It is also worth considering how obsidian artifacts have been prepared for analysis with the related technique of scanning electron microscopy (SEM) and energy-dispersive spectrometry (EDS). Compared to EMPA-WDS, SEM-EDS has two primary advantages

that make it more conducive to analyzing entire artifacts non-destructively. First, an EDS spectrometer is less severely affected by an irregular specimen surface, and second, most SEMs have stages capable of titling and rotating the specimen toward the detectors. Few researchers, though, have taken advantage of these capabilities.

T. K. Biró and colleagues (1984, 1986) analyzed Central European ("Carpathian") and Mediterranean obsidians and artifacts from Hungarian archaeological sites. For their specimen preparation, they removed a "small fragment of the obsidian" artifacts to mount in epoxy, cut flat, and then polish (1986:265). They state that a non-destructive approach was tested: "we tried to use chipped fresh and hydrated surfaces of archaeological pieces, with and without carbon coating" (271). Their data, presented as element ratios for seven artifacts, are hard to evaluate, particularly because there is no indication which data came from polished flat, freshly chipped, or hydrated surfaces. Their conclusions are only that "reliability... was weakened in the case of the naturally hydrated surfaces by the effect of the chemical alterations in the near-surface layers of the obsidian" (271) and that a beam-normal and "polished surface gives better and more reliable results" (265). The degree of alteration and how accuracy and/or precision are affected is unclear.

Burton (1986, 1989, 1993) and Burton and Krinsely (1987) used SEM-EDS with backscattered-electron images (BSE) to characterize obsidian sources and artifacts in the American Southwest. Burton describes the preparation of artifacts:

> The sample must have a highly polished surface, but because obsidians are generally very homogeneous (as was empirically determined during the initial BSE studies), only a small facet, approximately 0.1 cm^2, is needed. This facet is

> made by lightly grinding a surface on the artifact with 600 grit silicon carbide and then polishing the surface with 1-micron diamond powder. (1989:665)

Burton based his characterizations on the rare mineral inclusions within the obsidian, so a polished flat surface was needed to remove any topographic contrast.

Acquafredda et al. (1996, 1999) employed SEM-EDS to analyze obsidian from six Mediterranean sources, and they sought to demonstrate that their technique might be used for non-destructive sourcing of artifacts. The only requisite specimen preparation was the application of a thin, conductive carbon layer, which may be removed later. Acquafredda and colleagues analyzed both thin sections and freshly fractured obsidian, and they found the two surface types "give quite comparable data" (1999:319). It must be noted, though, that Acquafredda and colleagues did not analyze any archaeological artifacts, nor did they address the issue of diagenetic changes to surface chemistry.

Similarly, Le Bourdonnec et al. (2006) utilized SEM-EDS to examine specimens of geological obsidian from four Mediterranean islands. They describe their preparation techniques: "Slices of about 1 cm^2 were cut from each sample and included in an araldite resin. About six to eleven samples were mounted together" (1153). Like Acquafredda et al. (1996, 1999), Le Bourdonnec et al. (2006) did not analyze any archaeological artifacts or address surface alteration of artifacts. They do, though, make a prediction with regard to the future of minimally destructive analyses: "one may expect that in a near future the [use] of SEM–EDS for 'small' archaeological pieces" (1156).

Abbès et al. (2003) used SEM-EDS and PIXE (proton-induced X-ray emission) to analyze three geological specimens and twenty artifacts from the Neolithic archaeological

site of Jerf el Ahmar in the Middle Euphrates Valley of Syria. Abbès and colleagues state that "most... analyses were made in destructive mode, from polished sections. Only four samples were treated non-destructively" (163). These four "samples" were, one assumes, artifacts, but it is unclear why these four were selected for non-destructive analyses, not others. Were the four artifacts complete and considered too important to sample? Were they debitage sufficiently small to fit on the SEM specimen holder? Were they selected at random? Abbès et al. also offer no direct information on how the results for these four artifacts differed from the ones analyzed destructively. The only hint that non-destructive analyses were somehow inadequate comes from their conclusion: "elemental analysis by ICP, PIXE or SEM-EDX *in destructive mode of analysis* are equally efficient" (emphasis added; 165). What of the non-destructive artifact analyses?

To summarize, only a few researchers (Biró et al. 1984, 1986; Abbès et al. 2003) have conducted experiments with non-destructive SEM-EDS analyses of archaeological obsidian artifacts. Their findings from these tests, however, went largely unreported and are difficult to assess. Their non-destructive results were deemed less "reliable," but it is unclear how the evaluation was made. A few other researchers (Acquafredda et al. 1996, 1999; Le Bourdonnec et al. 2006) used SEM-EDS to analyze the unprepared surfaces of geological obsidian specimens but not any archaeological artifacts.

4.10.3 - Artifact Preparation in the Present Research

This research differs from prior studies, in part, in that the analyzed artifacts were not ground, polished, cut, or chipped. I did not destructively prepare the artifacts for two

reasons. First, I always envisioned that a key component of this work was investigating a non-destructive approach to obsidian sourcing using EMPA. Thus, despite the challenges discussed in Chapter 5, I did not want to abandon that component. Second, my export agreement with the Syrian Directorate General of Antiquities and Museums specified that I would only do non-destructive tests on the approved artifacts and that I would return the artifacts intact. If I wished to investigate using EMPA as a destructive technique, another agreement would be necessary. As it was, almost 18 months passed between when I first filed a request and when I had all the artifacts in this research.

The artifacts were cleaned using isopropyl alcohol (IPA) and KimWipes cleaning tissues, primarily to remove fingerprints and other residues from handling. IPA dissolves non-polar molecules such as oils and fats, and it quickly evaporates. Because EMPA is a surface analytical technique and the instrument operates under a high vacuum (below 10^{-4} Torr), a clean surface is necessary. KimWipes are comprised of wood pulp, so any future residue studies must keep this potential source of contamination in mind. Cleaning with IPA and KimWipes removed loose material from the artifacts, but they were not scrubbed to remove any adhered sediments or residues. I analyzed the material affixed to a few of these artifacts: it was mostly calcite from the sediments at Tell Mozan.

Just like the geological specimen discs, the obsidian artifacts required a thin layer of carbon to be electrically conductive. Such a carbon coat, roughly 15 to 20 nanometers thick, was applied to the artifacts with the same JEOL JEE-420 Vacuum Evaporator. The carbon layer can easily be removed from an artifact with acetone or IPA.

Artifacts were placed whole in the electron microprobe using one of two holders, both made by JEOL, for irregularly shaped specimens. The maximum specimen size for the largest of the two holders is 10 cm x 10 cm x 2 cm. None of the artifacts analyzed in the present research approached this size, according to my artifact selection criteria listed in Section 4.8. No obsidian blades or blade segments discovered so far at Tell Mozan exceed these dimensions; only the largest core fragments do. Nevertheless, the specimen holders and instrument airlock impose a size limit on large artifacts, which would have to be either cut or chipped to remove a suitably small piece for EMPA.

Because the artifacts were not ground, polished, cut, or chipped, I consider these analyses to have been non-destructive. I cannot argue, though, that there is no alteration whatsoever. Carbon coats can be easily removed, but museum conservators would likely consider their application and removal to be an alteration. Arguably, the only permanent alteration is at the exact spot where the electron beam strikes, as noted in Chapter 5. At each analysis spot, there is heat-induced "beam damage" in a circle about 30-µm (0.03-mm) in diameter and just one to two micrometers deep -- the spots can only be seen under a microscope. For comparison, the pits produced by LA-ICP-MS are commonly an order of magnitude greater in diameter and depth than EMPA spots.

These "beam damage" spots are areas with slight chemical alteration due to heat, namely the emission of volatiles (especially water). Under the analytical conditions that I used, the maximum temperature increase where the beam strikes (not the entire artifact) was on the order of 10º C for the major-element analytical round and 100º C for the trace-

element round. An increase of 10º C is trivial, but with an increase on the order of 100º C for 10 minutes, water in the hydration rind may be expelled. Some studies, though, have found that the hydration layers on artifacts in a forest fire remain largely unaffected after experiencing temperatures of 200º C for hours (Schroder 2002:8).

4.11 - Summary and Concluding Remarks

Sourcing studies require adequate sampling all of potential raw-material sources, otherwise the attributions of artifacts to sources may be compromised. During the initial work of RDC, only 33 geological obsidian specimens from all of Anatolia were analyzed for comparison to the artifacts. Such a low number of reference obsidian specimens was excusable four decades ago; however, even after calls to improve reference collections of the Near Eastern obsidians, this number has not markedly increased. In some cases, even fewer specimens were analyzed: 19 specimens from five source areas (Abbès et al. 2003), 18 specimens from four areas (Bressy et al. 2005), and four specimens from four areas in Anatolia (Le Bourdonnec et al. 2005a), to name a few. On the other hand, my collection is, to my knowledge, the largest obsidian reference collection from all of Anatolia and the Transcaucasus area. I analyzed over 900 specimens, including 453 from Eastern Anatolia (including a hundred specimens from Nemrut Dağ), 281 from Central Anatolia, 151 from Armenia, and smaller numbers from Georgia, Azerbaijan, and Russia. I discussed how I assembled my reference collection and prepared all the specimens for EMPA, and I also documented how I selected and prepared the artifacts for analysis.

The process of assembling both the geological and archaeological collections also raised a series of important issues. One issue, for example, is the tendency of researchers to call geological specimens and artifacts "samples," despite, I contend, such a term being inappropriate for both. A second issue is that entire volcanic complexes -- whether Göllü Dağ in central Turkey, the Coso Volcanic Field in California, or Glass Buttes in Oregon -- are frequently considered one "source" of obsidian with "intrasource" chemical variation, but this reflects neither the geological nor geographical reality that there are multiple lava flows in these vast complexes. This raises the issue of different uses of the term "source" in obsidian studies. Most definitions fit into two categories: (1) the mathematically based geochemical cluster or "clouds of points in multivariate space" (Wilson and Pollard 2001: 509) and (2) a geographical location that could be marked on a map. Both definitions are valid, but both are also missing two important elements: (1) how the source is manifested (i.e., the physical landscape) and (2) how individuals perceive the source (i.e., the mental landscape). Young obsidian-bearing flows in a caldera (e.g., Nemrut Dağ, and Newberry Volcano) are manifested, and hence perceived, differently than older, highly eroded flows in extensive volcanic fields (e.g., Göllü Dağ and Glass Buttes).

An important methodological development -- perhaps the most important one -- is that I analyzed the artifacts non-destructively. Unlike previous sourcing studies that used EMPA, the artifacts for this study were not polished, cut, or chipped. There are only tiny spots, about 0.03 mm in diameter and 0.001 mm deep, within which water was driven out of the obsidian, but that is the only permanent alteration of the artifacts.

Part II: Methods for Sourcing and Their Evaluation

Chapter 5:

Redeveloping EMPA for Obsidian Sourcing

> This review should be most useful to the novice embarking upon what at first glance might appear to be a torturous journey into the depths of quantitative electron beam microanalysis. Hopefully, all will emerge enlightened and emboldened with the courage to perform such analyses with confidence.
>
> -- D.R. Beaman and J.A. Isasi, 1972, *Electron Beam Microanalysis*

> …. one has to be wary of merely reveling in the details of the archaeometric techniques at the expense of considering the anthropological significance of the case studies themselves.
>
> -- Tristan Carter, in prep, "Obsidian Provenance Studies"

Throughout this dissertation, I strive to balance the two considerations expressed by the above quotes: How much should I discuss the nitty-gritty details of EMPA and its application to obsidian sourcing versus the archaeological interpretations of the obsidian sources used by the Hurrians, the inhabitants of Tell Mozan? This chapter is the one most heavily skewed toward the former, and I ask the indulgence of the reader to include these discussions here instead of an appendix. Consumers of any analytical data should not see the technique as a proverbial "black box." To assess such data, to recognize the strengths

and limitations, one must grasp the foundations of the analytical technique. This, in turn, requires some understanding, at least conceptual, of the physics involved.

In *The Quantum Dice* (1993), Russian physicist Leonid Ponomarev puts physics in an anthropological context. Ponomarev contends that "physics is a vast country with a rich and deep culture" (13). I would argue that consumers of EMPA data should learn at least some of the fundamental physics involved, otherwise, as Ponomarev puts it, one "will know as much about it as tourists know about an unfamiliar country whose culture is foreign to them and whose language they do not understand" (13). If unaware of these fundamentals, one "will only retain some highlights -- for instance, bright neon signs and posters" (13). Therefore, as Ponomarev recommends, we "must first get acquainted with the customs and culture of the country" in order to appreciate why I elected to re-develop and re-evaluate EMPA for obsidian sourcing and to assess the analytical procedures, both extant and novel, that I used in the research presented here (13).

Despite predictions that EMPA would become useful for obsidian sourcing (e.g., Kempe and Templeman 1983:45-46), as discussed in Section 1.7, only three substantial studies have used this analytical technique with the goal of sourcing: Merrick and Brown in eastern Africa (1984), Weisler and Clague in Hawaii (1998), and Tykot in the western Mediterranean (1995, *inter alia*; Tykot and Ammerman 1997).

The prior studies involved different instruments, procedures, and approaches, and they were, of course, products of their times. For example, Merrick and Brown used the University of Utah's ARL-EMX, a microprobe from the 1960s that output data on punch

cards (1984:232). Weisler and Clague (1998) and Tykot (1995) also utilized instruments now considered obsolete: an ARL-SEMQ and a Cameca MBX, respectively, both built in the 1970s. Consequently, the studies do not represent the capabilities of modern electron microprobes. The studies had additional limitations too. Merrick and Brown (1984) put a priority on speed (and titled their article "Rapid Chemical Characterization of Obsidian Artifacts by Electron Microprobe Analysis"), so they just measured three elements (as the old ARL-EMX instrument had only three spectrometers) and analyzed 260 artifacts in six hours. My top priority, though, was accuracy and precision, so it took roughly 200 hours to analyze over 100 artifacts. For their study, Weisler and Clague (1998) measured more elements (11) but do not provide enough details to evaluate the work. Tykot (1995, *inter alia*) had the largest study of the three. He measured 9 to 11 elements, as of 1995, in 433 total analyses on 125 specimens (114). For comparison, my research here involved over 12,000 major-element analyses and 13,000 trace-element analyses on over 900 geological obsidian specimens from southwest Asia and more than 100 artifacts, each of which was quantitatively analyzed for a total of 20 major and trace elements. All of these previous studies were also, as discussed in Section 4.10, destructive to the artifacts. In the present research, I analyzed all of the artifacts non-destructively.

This chapter covers the analytical procedures that I developed for this research. I compare my procedures to those in the earlier sourcing studies as well as those described in the EMPA literature. Geochronologists often use EMPA to analyze tiny volcanic glass shards and chemically match them to a specific volcanic eruption. Therefore, this type of

research, called tephrachronology, is quite similar to obsidian sourcing, so I also compare my procedures to those used in such studies (see Steen-McIntyre 1985 for an overview of tephrachronology). The chapter also covers four major challenges for analyzing obsidian artifacts non-destructively and how I mitigated each of them. I start this chapter, though, with a brief overview of electron microprobe analysis.

5.1 - The Basic Principles of EMPA

Electron microprobe analysis (EMPA), also called electron probe microanalysis, is an analytical technique used to determine the composition of small areas on specimens. EMPA is closely related to scanning electron microscopy (SEM) and X-ray fluorescence (XRF), and it combines them to offer both electron imaging of a specimen and an ability to measure elements' concentrations using characteristic X-rays.

As in SEM, the specimen is bombarded by a beam of high-energy electrons. This beam is focused onto a specimen surface by a set of apertures and electromagnetic lenses. These accelerated electrons generate characteristic X-rays from a small volume (often on the scale of just a few cubic micrometers) of the specimen. Modern SEMs are commonly outfitted with energy-dispersive spectrometers (EDS) to measure such X-rays, but EMPA utilizes a series of wavelength-dispersive spectrometers (WDS), which have better X-ray resolutions and minimum detection limits, to determine the elemental composition of the specimen. All elements -- except H, He, and Li -- can be detected because every element emits a particular and known series of X-rays. EMPA has a high spatial resolution with a

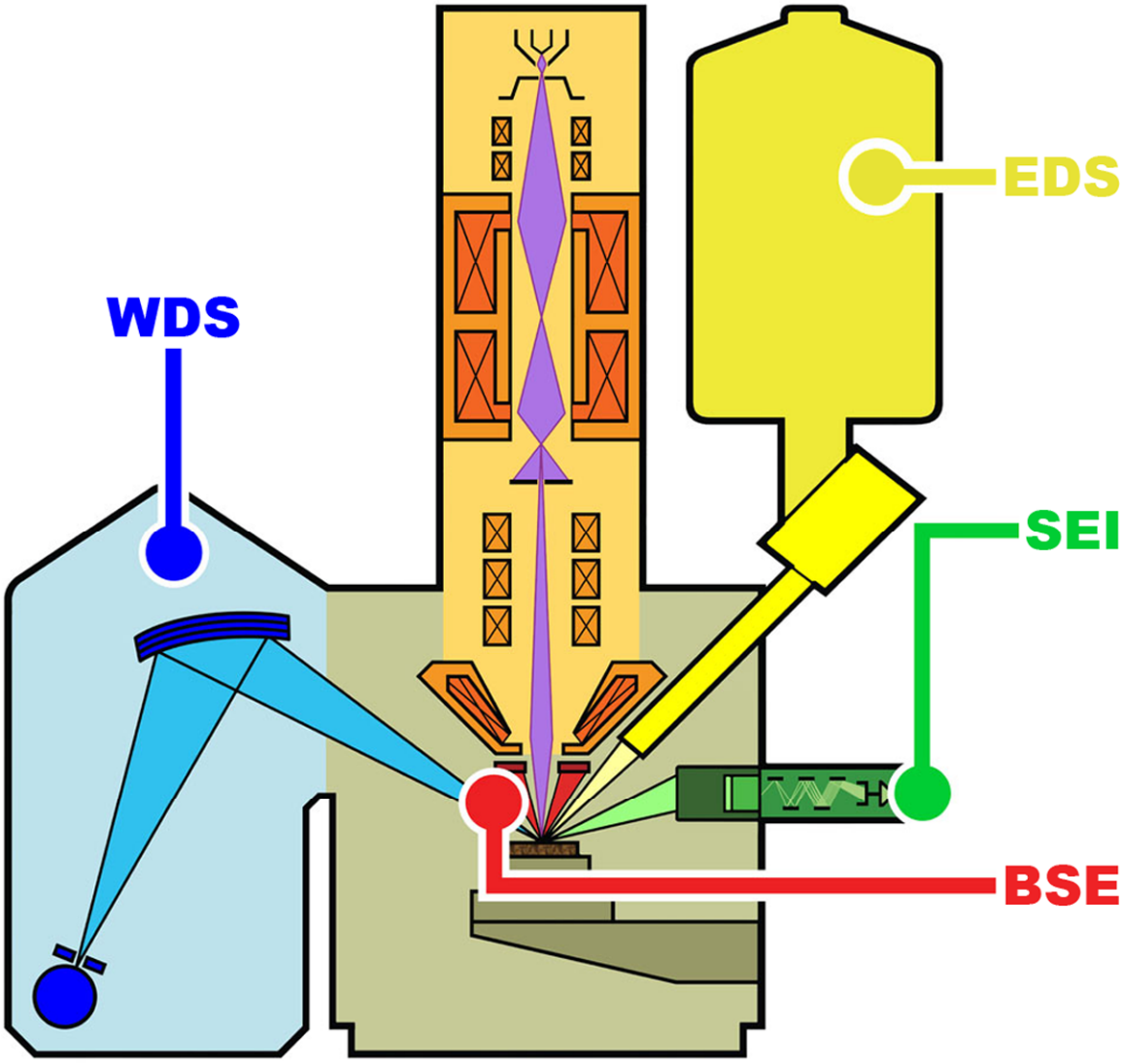


Figure 5.1 - Schematic of an electron microprobe and its primary systems. WDS (blue): wavelength-dispersive spectrometer. EDS (yellow): energy-dispersive spectrometer. SEI (green): detector for secondary-electron (topographic) imaging. BSE (red): detector for backscattered-electron (compositional) imaging. The electron optical column is orange, and the electron beam itself is purple. The specimen chamber and stage are tan, and the specimen is brown. (Illustration by the author; based on several illustrations from JEOL).

relatively high sensitivity, and the individual analyses are reasonably short, requiring only a few minutes in most cases. In addition, an electron microprobe can function as a SEM and obtain highly magnified electron images of a specimen.

5.1.1 - Atomic Structure and Electron Shells

In 1913, Niels Bohr proposed that electrons cannot assume any orbit in an atom. He stated that electrons are restricted to particular orbits, and any other orbits are simply not allowed. Such special orbits are quantized, meaning that the electrons in these orbits have particular quantities of energy. They are ordinarily called energy levels or electron shells. In reality, the shells are volumes of space, not actually circular orbits. The inner shell holds electrons with the lowest energy, and outer shells have higher energies. Bohr hypothesized that electrons may instantly "jump" from one electron shell to another. He stated that energy must be added to an electron for it to jump to a higher shell and energy must be released by an electron for it to jump to a lower shell. These transitions involve absorption and emission, respectively, of electromagnetic radiation. These "packets" of radiation are known as photons. The energies of these photons depend on the difference between the two shells involved in the electron transition.

The transitions of electrons and the resulting photons must obey the conservation of energy. An electron does not emit a photon when it merely remains in a specific shell. In this case, there is no change in its energy and, therefore, no photon. When an electron jumps to a lower shell, something must happen to the surplus energy. The electron emits

this extra energy in the form of a photon. For an electron to jump up to a higher shell, it requires additional energy, and this energy must come from some source. This necessary energy comes from the absorption of a photon. In any transition between two shells, the energy of the electron changes, and a photon constitutes the difference.

Starting with the innermost one, the electron shells are termed the K-, L-, M-, and N-shells. The K-shell is the lowest-energy electron shell, and electrons in this innermost electron shell are most tightly bound in an atom. The "energy spacing" of these electron shells is different for each element. The electron shells for one copper atom are identical to those for any other copper atom, but the shells of copper differ from those of all other elements. Additionally, when an electron jumps from, for example, the L-shell to the K-shell in a specific element, it always emits a photon with the same energy. Each time an electron undergoes the same downward transition, it emits the same photon. The energy of the photon is equal to the difference between the two shells. Because the wavelength of a photon is inversely proportional to its energy, a transition between the same electron shells always yields a photon with the same wavelength.

Because the "energy spacing" of the electron shells is different for every element, the transitions that electrons can undergo are different for every element. Every element has a unique set of allowed electron transitions. The unique transitions produce photons with characteristic energies and wavelengths. When the transitions involve inner electron shells, the emitted photon falls in the X-ray portion of the electromagnetic spectrum. The X-rays have both energies and wavelengths specific to the element from which they were

emitted. This is the basis of EMPA. Emitted characteristic X-rays are identified by their wavelengths to ascertain the composition of a specimen. The high-energy electron beam that bombards the specimen enables such electron transitions.

5.1.2 - The Electron Optical System

The electron microprobe contains an electron optical column, which produces the beam of high-energy electrons and controls its diameter when focused on a specimen. At the top of the column is an "electron gun." Electrons are negatively charged particles, so they are accelerated by applying a voltage, usually 15,000 or 20,000 volts. This is called the accelerating voltage, and it can be optimized for the specimen at hand. As the beam is accelerated toward the specimen, a set of electromagnetic lenses focuses the electrons like a glass lens focuses visible light. Coils at the bottom of the column raster the beam across a specimen surface to produce an image, just as a SEM does.

5.1.3 - Interaction Volume and Spatial Resolution

EMPA is a spot analytical technique, meaning that the electron beam is focused onto one spot and compositional information is collected from only a small volume, not the entire specimen. The beam electrons interact with a microscopic volume, just a few cubic micrometers. The tiny interaction volume of EMPA permits a researcher to obtain highly localized compositional data and to examine specimens so small that they cannot be studied using other analytical techniques. It also allows one to measure the chemical

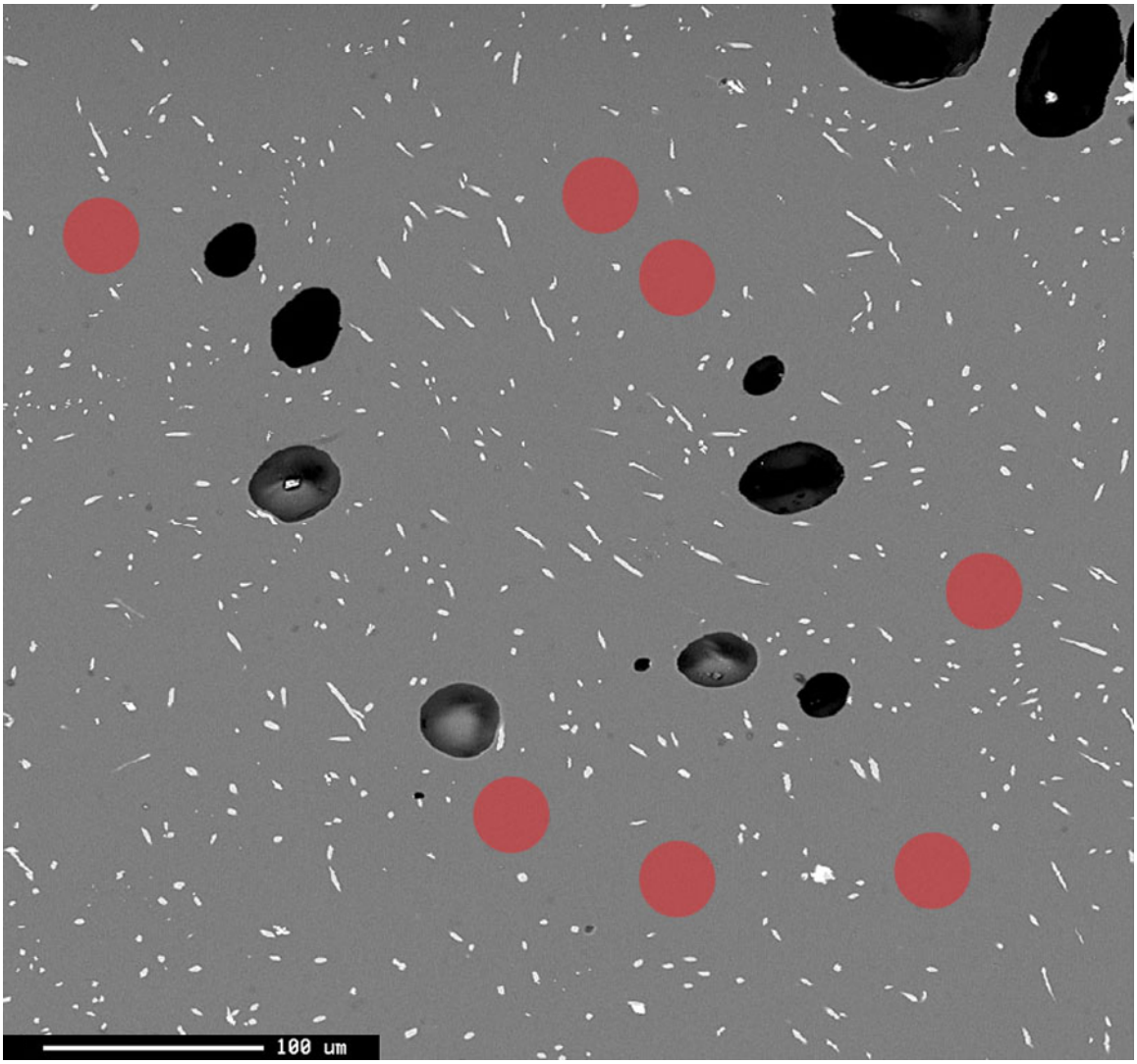


Figure 5.2 - A backscattered-electron image of obsidian showing microscopic bubbles and a variety of microlite inclusions in the glass matrix. The superimposed red circles show spots where one can use a 30-micron (0.03-mm) electron beam to analyze the glass component without interference from the inclusions. (BSE image by the author).

variation across a specimen surface. Therefore, EMPA is well suited to study specimens of mixed components, like different minerals, that one wants to analyze separately and *in situ,* leaving their contextual relationships unaltered and observable.

5.1.4 - Electron-Specimen Interactions

The energy of the electrons is chiefly lost in the form of heat generation within a specimen. Consequently, significant amounts of heat are ordinarily produced within the specimen, and this can cause damage within the electron interaction volume. The change in temperature is small for materials with high thermal conductivities, such as metals. In poor conductors, the temperature can rise as much as 200º Celsius at the point of impact. Damage to a heat-susceptible specimen may be minimized by increasing the diameter of the electron beam and/or decreasing its intensity.

5.1.5 - Attributes of X-rays

X-rays fall in an energetic part of the electromagnetic (EM) spectrum and, like all EM radiation, have the characteristics of both particles and waves. As a result, they have both an energy and a wavelength. The wavelengths of X-rays are between approximately 0.01 and 10 nanometers. These are shorter wavelengths (and, therefore, higher energies) than visible and ultraviolet light. Like all forms of EM waves, they travel at the speed of light, move only in straight lines, and are electrically neutral.

Two different processes within the specimen generate X-rays, and both processes result from bombardment by the electron beam. The first process is known as continuous X-rays, and it produces a distribution of X-rays across all wavelengths. A second process is characteristic X-ray emission, which involves the electron shell jumps discussed above and generates X-rays at wavelengths specific to each element.

5.1.6 - Continuous X-rays

Continuous X-rays (also called background X-rays) are produced from a process called *bremsstrahlung*. This term is German for "braking radiation," a fairly appropriate description of the process. The beam electrons are accelerated and then hit the specimen with a lot of energy. These electrons are decelerated by interactions with atoms within a specimen and lose energy, in part, via the release of X-rays. The degree of the "braking" determines the energy of X-rays emitted. A beam electron can lose a small amount of its initial energy, all of it, or any amount in between. After this process happens millions of times in a specimen, the result is a continuous spectrum of X-rays.

Unlike characteristic X-ray emission, this *bremsstrahlung* spectrum is similar for every element. The continuous X-rays provide no useful information about a specimen's chemistry, and they limit the minimum amount of an element that can be detected. These "background" X-rays can obscure the characteristic X-rays, particularly in trace-element analysis. During EMPA, *bremsstrahlung* measurements are taken near the characteristic X-ray "peaks" to subtract the contributions of continuous X-rays.

5.1.7 - Characteristic X-rays

Characteristic X-rays are produced by a different phenomenon, called inner-shell ionization, than continuous X-rays. These X-rays have wavelengths and energies specific to the elements from which they are emitted, and they are produced as a result of electron transitions between the inner electron shells. When exposed to a beam of electrons, each element in a specimen generates a set of characteristic X-rays, and due to the uniqueness of these X-rays for each element, they can be detected using spectrometers as a means to determine the specimen's elemental composition. During EMPA, an analyst searches for characteristic X-ray peaks, emerging out of the *bremsstrahlung* spectrum, at wavelengths that correspond to elements present within the specimen.

Characteristic X-rays are created when orbital electrons in an atom "fall" from an outer electron shell to an inner one. Because the inner electron shells are normally filled, an electron in one of those shells must be removed to create a vacancy. When a specimen is bombarded, a beam electron may knock an orbital electron in an atom from its electron shell. This process is known as inner-shell ionization. Just about instantly, an outer-shell electron jumps down to fill this vacancy in the inner shell. Electrons in outer shells have higher energies than electrons in inner shells. Consequently, an electron that falls into the vacated position must lose some of its energy. Its excess energy is emitted in the form of a characteristic X-ray, corresponding to the energy difference between the outer and inner shells involved in the jump. These X-rays are unique to the element from which they are emitted because the shell "spacing" differs for every element.

5.1.8 - Secondary Electrons

Secondary electrons are a result of the same process of inner-shell ionization that creates characteristic X-rays. A secondary electron is the electron freed from its shell by one of the high-energy beam electrons that strike a specimen. These electrons have very low energy, so those emitted within a nanometer of the specimen surface can escape and be detected. As a result, secondary electrons are quite sensitive to specimen topography. Accordingly, secondary electrons are used for imaging by both electron microprobes and scanning electron microscopes (SEMs). Many people have seen examples of secondary-electron (SE) images: electron microscopists will normally use ants or spiders, table salt, or pollen as examples of SEM images to show the public.

5.1.9 - Backscattered Electrons

Backscattered electrons (BSEs) are energetic beam electrons that have essentially "ricocheted" out of the specimen. These electrons are deflected back toward the surface by atomic interactions in the specimen and can subsequently be collected by detectors to form an image. BSEs have much higher energies than SEs, so they are less affected by a specimen's topography. Instead, BSEs are strongly affected by the mean atomic number of the elements in the interaction volume. For elements with high atomic numbers, more beam electrons are deflected back out of a specimen as BSEs compared to elements with low atomic numbers. The dependence on atomic number is used to create images, called backscattered-electron images, that show compositional information.

5.1.10 - Energy- and Wavelength-Dispersive Spectrometers

As previously mentioned, X-rays have characteristics of both particles and waves and, for that reason, can be described in terms of their energies or wavelengths. The two types of spectrometers integrated into electron microprobes detect both characteristic and continuous X-rays based on their energies and wavelengths. The energy-dispersive (ED) spectrometer sorts X-rays electronically with respect to their energies, and modern SEMs are also ordinarily outfitted with an ED spectrometer. Electron microprobes also possess several wavelength-dispersive (WD) spectrometers, often four or five. ED spectrometers are faster, but WD spectrometers take more accurate measurements.

The heart of an ED spectrometer is a solid-state detector that creates an electrical pulse proportional to the energy of a detected X-ray. The pulses are electronically sorted, and the entire spectrum is recorded simultaneously. The resulting spectrum is displayed as a histogram with X-ray energy on the horizontal axis and the intensity (the number of X-ray counts at a certain energy) on the vertical axis. ED spectrometers collect an X-ray spectrum swiftly. The ED spectra, though, suffer from overlapping X-ray peaks, and the background X-ray levels are higher, meaning ED spectrometers are usually not sensitive enough to reveal the tiny signals produced by trace elements.

WD spectrometers use a phenomenon called Bragg diffraction to separate X-rays by their wavelengths. When light passes through a prism, it separates into the constituent colors, each with its own wavelength. The same phenomenon occurs with X-rays in WD spectrometers. The incoming X-rays are dispersed with respect to their wavelengths by a

crystal. A WD spectrometer is "tuned" to a single wavelength at a time, and as a result, it has a better X-ray resolution than an ED spectrometer, meaning fewer X-rays overlap and the elements present can be more readily identified and quantified.

5.1.11 - Electron Microscopy

In an electron microprobe or SEM, an image is produced by scanning the electron beam over a specimen in a television-like raster, and the output from an electron detector is displayed on a screen. As I described earlier, there are two different types of electron signals from a specimen: secondary electrons (SEs) and backscattered electrons (BSEs). Both SEs and BSEs can be collected by detectors and used to produce highly magnified images of a specimen. SE images reveal topographic features of the surface while BSE images show variations in the mean atomic number across a specimen.

BSE images have bright areas where the mean atomic number is higher and dark areas where it is lower. Variations in a BSE image, though, show relative differences in mean atomic number; the elements present cannot be identified without measuring their characteristic X-ray emissions. BSE images are useful to determine the relationships of different constituents of a specimen, like the minerals within a rock. These images may also be used to choose points for characteristic X-ray analysis.

5.1.12 - Quantitative Analysis

Quantitative elemental analysis in EMPA, like almost all analytical techniques, is basically a comparative method. It entails the measurement of characteristic X-rays from

a specimen and a set of reference standards under the same analytical conditions, like the accelerating voltage and beam current (that is, the number of electrons in a beam). Using this approach, one can quantitatively determine the elemental composition of a specimen with high accuracy and precision. Quantitative analyses have three primary steps. First, one measures the characteristic X-ray count rate on standards, the composition of which is well-known already. Second, one measures the X-ray count rate on the specimen, and software calculates the ratio of these two rates. Third, the software calculates correction factors for various physical effects within a specimen and then applies the corrections to the raw data, resulting in the elements' concentrations in the specimen.

5.1.13 - Errors in the Archaeological Literature

Unfortunately, a number of misleading, oversimplified, and inaccurate statements regarding EMPA can be found in the archaeological literature. For example, Kempe and Templeman (1983) state that the "beam can be trained on areas as small as 10 μm square" (45), but analysis areas approaching 1 μm^2 are possible. Herz and Garrison (1998) state "electrons from a filament are accelerated by about 30 KeV toward the specimen" (222). Not only are the units incorrect (kV is the proper unit to describe a voltage), but also the value is not really correct. For most geological materials, an accelerating voltage above 25 kV is actually undesirable (Reed 1993:155), and ordinarily instruments in geoscience laboratories operate at 15 or 20 kV. Herz and Garrison (1998) also claim that "the lower limit of percentage composition detected is only about 0.1%" (223), which is 1000 ppm.

The EMPA detection limits, however, approach 100 ppm, even 30 ppm, under favorable conditions. When explaining the difference between EMPA-WDS and SEM-EDS, Herz (2001) claims that "WD has higher detection limits... than ED" (452) when the reverse is true: WDS has lower, better detection limits than EDS. He also states that XRF involves "a powdered sample, as does SEM and the probe" (2001:452). Such misstatements must be cleared up if EMPA and other techniques are to be used effectively.

5.1.14 - Additional Information

Readers interested in further information about EMPA are directed to two books: *Electron Microprobe Analysis and Scanning Electron Microscopy in Geology*, Second Edition (2005) by Stephen J.B. Reed and the voluminous *Scanning Electron Microscopy and X-ray Microanalysis*, Third Edition (2003) by Joseph Goldstein, Dale Newberry, and colleagues. References written in the 1990s and earlier are largely out-of-date in terms of the technical details about the instruments and data processing.

5.2 - Choice of Analytical Conditions

Many individuals unfamiliar with analytical techniques often expect that modern instruments (like the electron microprobe) function more or less like a microwave oven: put the specimen inside, enter one or two settings, and press a button. Some new users, it seems, expect to find a big, red "Analyze" button on the front of the microprobe. This "microwave paradigm," as I call it, has been reinforced by a recent advertising campaign

by a major instrument manufacturer: the advertisements feature a person in a suit, unseen except for their arm, pressing a single button labeled "Direct to Answers." Instead, doing an analysis involves a series of choices, especially at the outset. One starts with an initial analytical scheme in mind, feedback from observations changes the scheme, the modified scheme yields new feedback, and so on. These actions form an operational sequence and are informed by the theoretical and practical "know how" of an analyst (or *connaissances* and *savoir-faire*, respectively, in the terminology of Pierre Lemonnier).

The role and importance of informed choices is also recognized in the literature on EMPA. In their book, Goldstein et al. (1981) emphasize "those instrument parameters which the microscopist can and must manipulate to obtain optimum information from the specimen" (v). Likewise, Long (1995) points out: "Precision is affected by a number of factors: the stability of the primary beam and of the spectrometer and detector are clearly important. . . but [so is] the expertise of the operator in choosing and setting the optimum operating conditions" (15). Reed (1996) states the "range of options as regards operating conditions, type of analysis, etc. requires the user to make a lot of choices" (272), and he refers to "suitable" and "appropriate" analytical choices throughout his book (40, 54, 96). Similarly, Reed (2005) holds: "It is difficult even for an experienced operator to arrive at optimal choices for all the relevant parameters" for a quantitative analysis (137). Lifshin and Gauvin (2001) even provide what they call a process map (essentially an operational sequence) of steps during which an analyst makes choices.

5.2.1 - Two Sets of Analytical Conditions

As I discuss later in Chapter 6, I decided to analyze both the geological specimens and obsidian artifacts for fourteen of the elements important in mineral formation (what I somewhat misleadingly term "major elements": Si, Ti, Al, Cr, Fe, Mn, Mg, Ca, Na, K, P, F, S, and Cl) and six geochemically interesting "trace" elements (Zr, Nb, Ga, Zn, Ba, and Ce). Reed (2005) points out that, because "ideal conditions for trace and major elements differ, it is desirable to employ a separate procedure for each, with different accelerating voltages and beam currents" (139). I sought to measure elements in obsidian that vary in concentration over five orders of magnitude. Obsidian is usually about 75% SiO_2 (that is, about 35% Si), and I wanted to measure elements at concentrations of 30 ppm (0.0030%) and below. Therefore, I decided to analyze these two sets of elements in separate rounds with somewhat different conditions, which I discuss next.

5.2.2 - Accelerating Voltage

Choosing an accelerating voltage -- that is, the voltage applied to beam electrons to give them sufficient energy to produce characteristic X-rays in a specimen -- is one of the first decisions that an analyst must make. The accelerating voltage of the instrument at the University of Minnesota-Twin Cities can vary between 0.2 and 40 kV. In practice, though, these extremes are never used for analyses. Too low an accelerating voltage will not give the beam electrons sufficient energy to generate X-rays. Too high a voltage may yield undesirable effects, such as a greater reliance on correction algorithms, extra energy

(and, therefore, heat) in the specimen, and worse spatial resolution. Reed (1993) suggests "a lower limit of 10 kV is advisable" and "it is undesirable to use too high an accelerating voltage for quantitative analysis (i.e. above 25 kV)" (155). Most electron microprobes in geoscience departments, including the instrument at the University of Minnesota, operate at 15 kV to balance these phenomena in geological specimens.

Though "a higher than normal accelerating voltage enhances peak intensities and peak-to-background ratios" (Reed 2005:139) and, therefore, may have slightly improved the detection limits of trace elements, a "normal" accelerating voltage of 15 kV was used in the present research. I chose to do this both "technical" and, for lack of a better word, "cultural" reasons. On the technical side, I did not want to increase the heat added to the obsidian specimens. On the "cultural" side, changing the voltage requires adjustments to the electron optical system that novice users are typically incapable of making. Given the number of sessions required for my research, I selected, even for the trace-element round, the 15-kV voltage most often used by researchers in the lab.

The three prior obsidian sourcing programs that used EMPA (Merrick and Brown 1984; Weisler and Clague 1998; Tykot 1995, *inter alia*) also had accelerating voltages of 15 kV. In a study into the mechanism of so-called "rainbow" Mexican obsidian, Ma et al. (2001) also used 15 kV with EMPA. A voltage of 15 kV is also the norm in EMPA-based tephrachronology research (e.g., Smith and Westgate 1969; Smith et al. 1977; Kyle and Jezek 1978; Nielsen and Sigurdsson 1981; Mehringer et al. 1984; Vreeken et al. 1992; Hanson et al. 1996; Eastwood et al. 1999; Eden et al. 2001; Shane et al. 2003; Foit et al.

2004; Aksu et al. 2008; Allan et al. 2008; and Payne et al. 2008). Higher voltages seem limited to a single EMPA laboratory: Hang et al. 2006 and other researchers used 20 kV at the University of Edinburgh. Lower voltages (13 kV in Tryon et al. 2009) are even more rare. Among obsidian studies using SEM-EDS, higher voltages are the norm: Le Bourdonnec et al. (2006, 2010) and Lugliè et al. (2008) utilized 20 kV, whereas Biró and Pozsgai (1984) used a voltage of 25 kV for unspecified reasons.

5.2.3 - Beam Current

Deciding on the beam current -- the number of electrons in the beam -- is another choice that the analyst must make. Reed (2005) explains that using a "high beam current gives high X-ray intensities, but contrary factors should also be taken into account. For instance, samples prone to damage under electron bombardment may require the use of a low beam current" (136). Obsidian is one such material susceptible to damage under the energetic beam, namely the migration of Na and K. Beam damage, though, is effectively mitigated by a larger beam diameter, as discussed in the next section.

The electron microprobe at the University of Minnesota-Twin Cities is capable of currents from 1 picoAmp (pA; 10^{-12} Amps) to over 1 microAmp (μA; 10^{-6} Amps). SEMs usually run in the range of tens to hundreds of pA (10^{-11} to 10^{-10} Amps) for high-resolution imaging. EMPA involves higher currents, though, because the number of X-rays emitted is directly proportional to the beam current. The greater the beam current, the faster that sufficient X-rays are counted for a precise analysis. Reed (2005) states that "a current in

the range 10-100 nA is usual, except for trace elements requiring a higher current" (136). For most geological research and materials, beam currents of 20-30 nA are very common. Besides the aforementioned Na and K migration, there is another problem with analyzing obsidian at a high beam current for trace-element analyses.

If the beam current is greatly increased to acquire sufficient counts from the trace elements in a specimen, the X-ray generation rate for major elements can yield excessive counts for these elements and overwhelm the X-ray detector, causing an erroneous result. Rates over 50,000 counts per second cause such problems (Reed 2005:112). Obsidian is usually about 75% silica (SiO_2) by weight, which corresponds to about 35% silicon. My initial tests of analytical conditions revealed that, above a beam current of roughly 80 nA, the count rate for Si became too high for the X-ray detector to process. Accordingly, this was one of the reasons that I analyzed the specimens and artifacts in two separate rounds: major elements (actually the common mineral-forming elements) in one round, and trace elements in another round with a much higher current. This also allowed Na and K to be analyzed with a current less likely to cause marked migration.

Unlike the accelerating voltage, beam currents used in prior studies vary. Merrick and Brown (1984) used 50 nA, whereas Weisler and Clague (1998) utilized 10 nA. Tykot (1995, *inter alia*) does not provide the beam current that he used to source Mediterranean obsidian. Ma et al. (2001) studied Mexican "rainbow" obsidian using a current of 15 nA. Using SEM-EDS, Biró and Pozsgai (1984) had a 20-nA current. Zhang et al. (1997) used EMPA in a study of volcanic glasses and analyzed them with a current of 3 nA. Looking

through the tephrachronology literature, the beam currents used to analyze volcanic glass fragments vary from 100 nA (Smith and Westgate 1969; Smith et al. 1977) down to only 4 nA (Adams et al. 2006). After a series of initial experiments, I selected 50 nA for the major-element round and 600 nA for the trace-element round. It should be emphasized that I was able to use such high currents only because I (1) separated the major and trace elements and (2) defocussed the beam, as discussed next.

5.2.4 - Beam Diameter

The diameter of the electron beam on a specimen surface can be varied from fully focused (less than 1μm) to 300 μm. The ability to analyze an area on a micrometer scale is, in fact, one of the key advantages of EMPA. On the other hand, Reed (2005) explains:

> An essential characteristic of EMPA is its spatial resolution (normally approximately 1 μm), but sometimes it is appropriate to use a deliberately broadened beam (e.g. to determine the average composition of a devitrified melt). The beam can be enlarged for this purpose by defocussing the final lens, or alternatively the beam may be scanned in a raster. (144)

Similarly, Toya and Kato (1983) point out that a broad beam is used "for average analysis of the specimen and analysis of specimens vulnerable" to damage under an electron beam (28). Caution is needed, when taking this approach, due to the requirement of WDS for a precise geometry between the specimen, beam focal point, and spectrometers. Too broad an electron beam will increase the error. Reed (2005) asserts that its diameter "should be limited to less than 100 μm to minimise spectrometer defocussing, which affects different elements to a varying degree" (144). Some researchers instead prefer to scan or raster the

beam across a small area on a specimen, but Spray and Rae (1995) warn that rastering the beam also produces analytical error due to geometrical effects (330).

As mentioned in the prior section, increasing the diameter of the electron beam is the most efficient way to minimize Na and K migration (Reed 2005:141). In an artificial soda-lime glass (like windowpanes or jars) and with a focussed electron beam, half of the Na has migrated out from under the beam after only a few seconds (Toya and Kato 1983: 86). After about 15 seconds, half of the K has moved out from under the beam (86). For interested readers, Spray and Rae (1995) offer a detailed discussion of possible Na and K migration mechanisms (326-329). Reducing the current density in the specimen, done by spreading out the beam, reduces the Na and K migration effect. Various researchers have investigated how large an electron beam must be spread to minimize migration in glasses and other susceptible specimens. Toya and Kato (1983) state that, with a beam current of 50 nA, an analyst must spread out the beam diameter to at least 30 μm to avoid Na and K migration in natural and artificial glasses (86). In tests with basaltic glass, Spray and Rae (1995) showed that, using a low current of just 2.5 nA, a 20-μm beam diameter yields Na values near "the quoted international standard value" (326).

Looking at the tephrachronology literature, a wide range of beam diameters have been used, frequently limited by the size of the tiny volcanic glass fragments in the study. On one end of the scale, Payne et al. (2008) used a beam diameter of just 1 μm (and, as a result of the beam-induced damage that surely resulted, have data with totals often below 95%). Other researchers, like Mehringer et al. (1984), Eastwood et al. (1999), and Tryon

et al. (2009), have used a slightly larger diameter: 5μm. Most studies seem to have used a 10-μm beam (e.g., Federman and Carey 1980; Froggatt 1983; Shane et al. 2002; Adams et al. 2006; Hang et al. 2006; Aksu et al. 2008). Broad electron beams, like 20 μm (Allan et al. 2008) or 30 μm (Hanson et al. 1996), are somewhat rare.

Hunt and Hill (2001) suspected that EMPA analyses on volcanic glass fragments, conducted for tephrachronology, suffered from Na and K migration (and, as an effect, the apparent enrichment of other elements). The accelerating voltage, electron beam current, and beam diameter all determine the power density at the analysis spot and, therefore, the degree of Na and K migration. Hunt and Hill (2001), consequently, conducted a series of tests on Lipari obsidian, varying the beam diameter for a constant voltage and current. A beam diameter of at least 10 μm, they concluded, yielded "accurate" data (107). For their analytical conditions and a 10-μm beam, the power density at the analysis spot was about 2.3 W/mm^2. This, then, was a target for my major-element round.

Merrick and Brown (1984) selected a beam diameter of 20 μm, meaning that their beam covered an area of about 314 μm^2 on the specimen surface. With a beam current of 50 nA, the power density in that area was 2.4 W/mm^2. Note that this is virtually identical to the maximum established by Hunt and Hill (2001), suggesting Na and K migration was not a severe problem for their quantitative analyses. Weisler and Clague (1998) utilized a 5-μm beam, which covered an area of about 20 μm^2. With a beam current of 10 nA, their power density was triple that of Merrick and Brown: 7.5 W/mm^2. Tykot (1995, *inter alia*)

used a broad beam with a 40-μm diameter, covering 1250 μm^2. Because his beam current was not given, the power density for his analyses cannot be calculated.

I based my choice of beam current and diameter on not only the tests of Hunt and Hill (2001) but also my own tests. On a set of 104 obsidian specimens (one from almost all of the Anatolian collection areas), I conducted analyses with beam diameters of 10 μm (78 μm^2 analytical area), 30 μm (706 μm^2), and 50 μm (1960 μm^2). I discovered that the 10-μm beam caused marked Na and K migration in the obsidian specimens (and possibly other beam damage). The broader electron beams -- 30 and 50 μm -- produced equivalent results, but it was more difficult to avoid mineral inclusions with a 50-μm beam. Thus, I selected a 30-μm beam diameter for the major- and trace-element analytical rounds. With a 15-kV accelerating voltage, 50-nA beam current, and 30-μm beam diameter, the power density for the major elements is 1.1 W/mm^2, less than half that of Hunt and Hill (2001). The Na and K measurements should be accurate. For the trace-element round, a 600-nA beam current yielded a power density of 12 W/mm^2, just 60% greater than that of Weisler and Clague (1998) during their analyses of Hawaiian obsidians.

5.2.5 - Counting Times

The amount of time taken to count the characteristic X-rays from an element, and to measure the background X-ray level at that wavelength, is another choice that must be made by an analyst. The more X-rays counted for an element, the better the precision of the measurement. Reed (2005) states that, for the major elements within a specimen and

typical beam currents, a counting time of 10 seconds is often sufficient for a precision of ±1% relative (77). This 10 seconds spent counting on the characteristic X-ray "peak" for a particular element would normally be accompanied by 5 seconds spent measuring each of two background (or continuum) X-ray levels. Increasing the X-rays counted, by using a higher beam current and/or longer counting times, will decrease the minimum limits of detection (Reed 1996:86). Goldstein et al. (1992) explain that, in analyses of germanium in meteorites, the minimum detection limit was calculated to be 20 ppm, but this required a current of 200 nA and counting times of about 30 minutes (501).

For trace-element analyses, the precision of the background X-ray measurements are equally as important as that of the characteristic X-ray peak measurement. Therefore, as Scott et al. (1995) state, "the optimum peak and background counting times are equal" for trace elements (104; the relevant equations are on pp. 139-140). I further discuss the importance of background measurements in the subsequent section.

Merrick and Brown (1984) explain: "Counting time ranged from 10 to 12 sec per analysis" (232); however, it is unknown how this time was divided between the peak and background measurements or even if the background levels were measured at all. Tykot utilized "counting times of 10-80 seconds per element" (1995:113), but again, there is no indication of how the time was divided between the peak and background measurements or which elements or specimens had longer counting times and why. The counting times used by Weisler and Clague (1998) are not reported in their paper.

Tephrachronology researchers usually report a total counting time of 10 (Smith et al. 1977; Kyle and Jezek 1978; Froggatt 1983; Hang et al. 2006), 20 (Hanson et al. 1996; Eastwood et al. 1999), or 30 seconds (Federman and Carey 1980; Nielsen and Sigurdsson 1981) per element. Only a few are more specific. Mehringer et al. (1984) counted for 10 seconds on the X-ray peak and 10 seconds on for background measurements. Tryon et al. (2009) counted for 20 seconds on the peak and 10 seconds on each background. Foit et al. (2004) had four sets of peak/background times: 10 seconds / 5 seconds for Na, Mg, Al, and Si; 30/5 for Cl and K; 22/7 for Ca and Ti; and 52/20 for Fe.

For this research, I chose to use different counting times for the major- and trace-element rounds. For the major-element round, the counting time was 25 seconds on the characteristic X-ray peak and 25 seconds on both background measurements (75 seconds total). This was true for all elements except Na, which was counted for 10 seconds on the peak and then 10 seconds on each background because its migration was minimal during that 30 seconds under the electron beam. For the trace-element round, I used 50 seconds on the peak and 50 seconds on both background measurements (150 seconds total). Both sets of counting times follow the recommendation of Scott et al. (1995) that, for elements at trace levels, peak and background counting times should be equal.

5.2.6 - Background Measurements

As mentioned in the prior section, measurement of the background X-ray level is important in quantitative analyses, especially those of trace elements. Reed (2005) states

that the detection limit for a particular element "is the concentration which corresponds to a peak that can just be distinguished from statistical background fluctuations" (139). The erroneous measurement of background X-rays can affect even major and minor elements; the effects of such errors are simply more pronounced for trace elements (Goldstein et al. 1981:436). If, for example, a background measurement is overlapped by the X-ray peak from a different element, the difference between the peak and background intensities can be low, sometimes negative (Reed 2005:114). An error for the background measurement can also occur if it is taken on either side of a "step" (termed an "absorption edge") in the background X-ray continuum (114). In addition, the background is curved and has other non-linearities of which an analyst must be aware (139). Goldstein et al. (1992) explains the process of background measurement in greater detail (376).

> In the present research, I followed the recommendation of Goldstein et al. (1981):
>
> > The background intensity using a WDS is obtained after a careful wavelength scan is made of the major peak to establish precisely the intensity of the continuum on either side of the peak. Spectrometer scans must be made to establish that these background wavelengths are free of interference from other peaks in all samples to be analyzed. (436)

To inform the placement of X-ray background measurements and search for interferences or discontinuities in the spectrum, I conducted a set of long, qualitative wavelength scans, some even taking a full day, on obsidian specimens. My spectrometer settings, including background positions for each element, are listed in Table 5.1.

Table 5.1 - Spectrometer Conditions for Major and Trace Elements

Element	Na	Cl	Si	Ti	Fe	Mg	S	Al	Ca	Mn	Si
X-ray	K-alpha	K-alpha	K-alpha	K-alpha	K-alpha	K-alpha	K-alpha	K-alpha	K-alpha	K-alpha	K-alpha
Spectrometer	1	2	3	4	5	1	2	3	4	5	1
Crystal	TAP	PETJ	TAP	PETJ	LIFH	TAP	PETJ	TAP	PETJ	LIFH	TAP
Measure Order	1	1	1	1	1	2	2	2	2	2	3
Peak Position	129.36	151.24	77.25	86.77	134.06	107.35	171.95	90.52	106.29	145.55	77.27
Background +	5.50	5.00	5.00	4.00	5.00	5.50	5.00	5.50	6.00	4.00	5.00
Background -	4.50	4.00	6.00	3.50	5.00	6.00	5.50	5.00	4.00	4.00	6.00
Peak Time (sec)	10	25	25	25	25	25	25	25	25	25	25
Back Time (sec)	10	25	25	25	25	25	25	25	25	25	25
PHA Gain	32	16	64	64	64	32	16	64	64	64	32
High V. (volts)	1688	1664	1724	1774	1696	1688	1664	1724	1774	1696	1688
Base L. (volts)	0.70	0.50	0.70	0.50	0.50	0.70	0.50	0.70	0.50	0.50	0.70

Element	P	F	K	Cr		Zr	Nb	Ga	Ce	Ba	Zn
X-ray	K-alpha	K-alpha	K-alpha	K-alpha		L-alpha	L-alpha	L-alpha	L-alpha	L-alpha	K-alpha
Spectrometer	2	3	4	5		1	2	3	4	5	4
Crystal	PETJ	TAP	PETJ	LIFH		PETJ	PETJ	TAP	LIF	LIFH	LIF
Measure Order	3	3	3	3		1	1	1	1	1	2
Peak Position	196.97	200.63	118.50	158.62		194.21	183.28	122.71	176.67	192.36	98.41
Background +	4.00	5.00	5.50	4.00		5.25	4.50	5.00	5.50	4.00	3.50
Background -	5.00	5.00	5.00	4.00		4.00	5.25	4.00	5.50	4.00	3.50
Peak Time (sec)	25	25	25	25		50	50	50	50	50	50
Back Time (sec)	25	25	25	25		50	50	50	50	50	50
PHA Gain	16	128	64	64		16	16	64	64	64	64
High V. (volts)	1664	1744	1774	1696		1676	1664	1724	1700	1696	1700
Base L. (volts)	0.50	0.70	0.50	0.50		0.70	0.50	0.70	0.50	0.50	0.50

5.2.7 - Number of Analyses

Many researchers using spot analytical techniques (i.e., EMPA, SEM-EDS, PIXE, and LA-ICP-MS) acquire more than one analysis per specimen. Analyzing three spots is seemingly most common (e.g., Bíró et al. 1986; Constantinescu et al. 2002; Bellot-Gurlet et al. 2005, 2008; Le Bourdonnec et al. 2005a; Ambrose et al. 2009; Reepmeyer and Clark 2010). The goal of taking three measurements is typically stated as attempting to average out any chemical heterogeneity, especially the contribution of any mineral inclusions that fall within the analysis spot. For example, using EMPA, Tykot (1995) states that "at least three points per sample were tested, in case a phenocryst contributed" to the composition measured (113). Similarly, using PIXE, Bellot-Gurlet et al. (1999) write that, "to account for possible local heterogeneities (e.g., due to crystalline inclusions), the composition of each sample was measured at three points" (856). Lugliè et al. (2007), also using PIXE, state that "to take possible elemental variations of composition on a millimetre scale into account, three to four such 'spot' measurements per sample were taken" (431). The only other explicitly stated goal of taking multiple spot analyses per obsidian specimen, to my knowledge, is checking instrument stability (Draucker 2007:9).

Just a handful of researchers using spot techniques have acquired greater numbers of analyses per specimen for obsidian sourcing. Using LA-ICP-MS to source Californian obsidian artifacts, Eerkins et al. (2008) collected five analyses per specimen. Abbès et al. (2003) acquired SEM-EDS data from five spots and PIXE data from three to six spots on Near Eastern obsidian. With SEM-EDS, Le Bourdonnec et al. (2006, 2010) analyzed 10

to 17 spots per specimen. Like the researchers listed earlier, the reason for acquiring that number of analyses per specimen was "to check for sample homogeneity and detect local variations due to the presence of phenocrysts" (2010:95).

For the present research, I analyzed each of the geological specimens and artifacts at least 20 times between both the major- and trace-element rounds -- the average was 27 analyses. In the major-element round, the specimens and artifacts were analyzed usually 10 or 20 times but sometimes 30 or 40 times. During the trace-element round, they were ordinarily analyzed 10 or 20 times but, on occasion, as many as 50 times. As previously explained, I analyzed the glass matrix and strived to entirely avoid the mineral inclusions using backscattered-electron images and reflected-light microscopy. Consequently, I did not collect so many analyses because I was concerned about inclusions affecting the data. Instead, I analyzed the obsidian at least 10 times for each element in order to improve the precision due to the character of X-ray emission and detection.

The emission and detection of X-rays -- whether one uses PIXE, EMPA-WDS, or SEM-EDS -- is a random and statistical process. This randomness occurs for any process involving the emission and detection of radiation. Long (1995) explains:

> Even with perfect stability of specimen and analytical instrumentation, it is necessary to take into account the quantum nature of the secondary signal, which will consist of X-ray photons, light photons, ions, electrons, etc. In every case, repeated measurements of intensity will show variations about some mean value due to the random nature of the emission process, no matter how constant the behaviour of the apparatus. (15-16)

Hence, for any analytical technique, even with a perfectly homogeneous specimen as well as a perfectly stable instrument, two successive measurements will differ by some amount due to the random nature of radioactive emission and detection. In the case of SEM-EDS and EMPA-WDS, Goldstein et al. (1981) explain the number of characteristic X-rays that are generated in a specimen and that escape to be counted by the detectors "is completely random in time but has a fixed mean value" (430). If one plots a number of X-ray counts from a series of successive measurements for a fixed time, the resulting histogram would show a Gaussian distribution (Goldstein et al. 1981:431). For example, a set of analyses on pure silicon metal would yield a histogram centered at 100% and, with an accuracy of ±1%, having a few analyses near 99% and others near 101%.

Therefore, I acquired at least 10 analyses for each element on each specimen and artifact so that my data approximated a Gaussian distribution. While a sample size of 30 or more would have been ideal (if analysis time had not been a consideration), at least 10 observations per element for each specimen was considered the minimum for the Central Limit Theorem to apply. As a result, after collecting a series of X-ray measurements and converting that data to concentrations, the mean of the resulting Gaussian distribution "is considered to be the most probable value of" the actual value (Goldstein et al. 1981:431). Accordingly, my goals for acquiring at least 10 analyses per specimen or artifact included increasing the precision of the concentration data, especially for trace elements, based on the statistical nature of X-ray emission and detection. Two modifications to the software, as discussed in the next section, aided this statistical treatment.

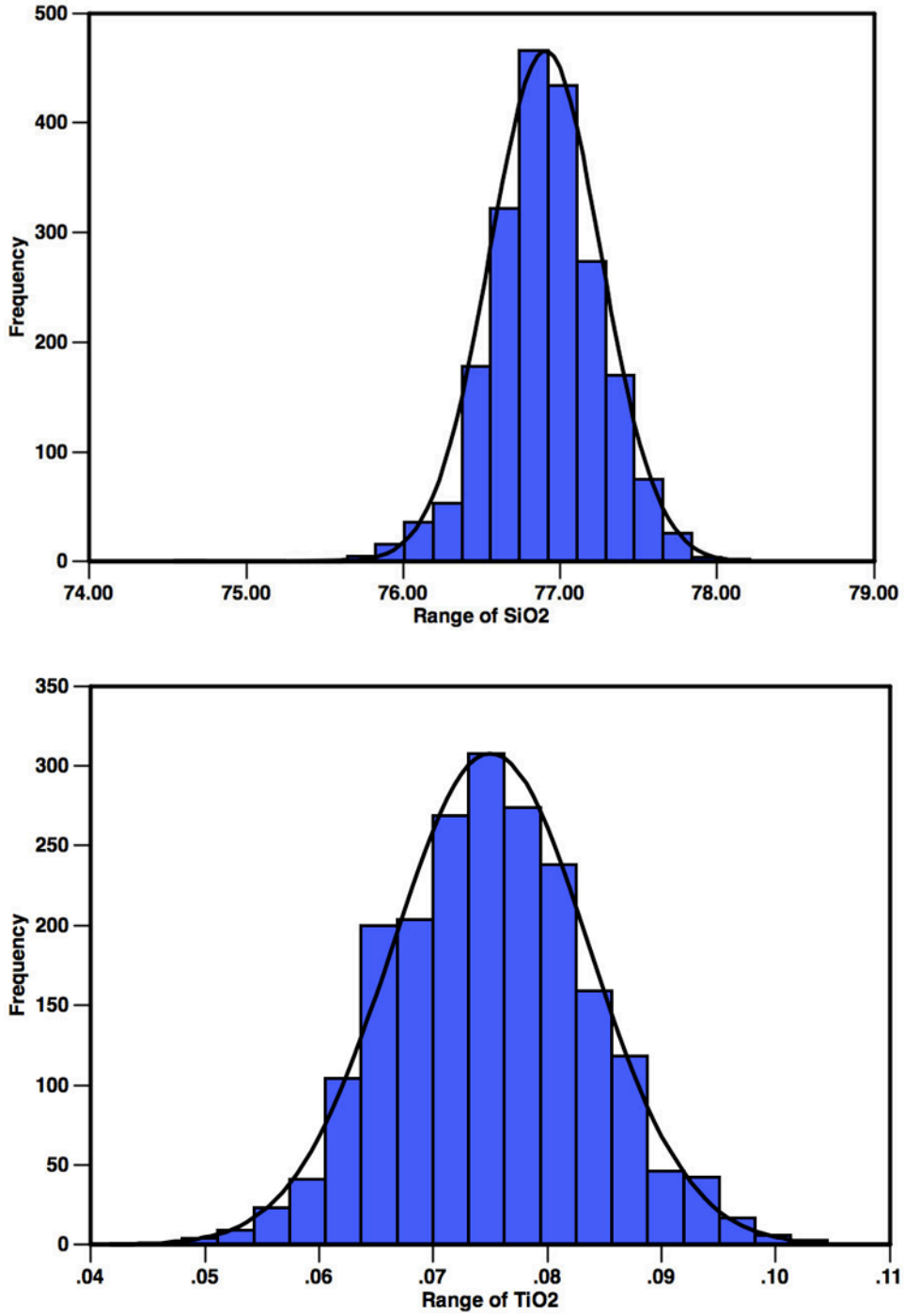


Figure 5.3 - Because the emission and detection of radiation (e.g., X-rays, gamma rays) involve some degree of randomness, the measured values will approximate a Gaussian distribution, and the means are the most accurate values (the author's data and plots).

Collecting a series of 10 or more analyses also improved the detection limits. As discussed earlier, Goldstein et al. (1992) reported that, in analyses of germanium in iron-nickel meteorites, the detection limit was 20 ppm, but this necessitated counting times of 30 minutes (501). With such long counting times for a single measurement, the stability of the instrument as well as the specimen under electron bombardment become an issue: is there instrument "drift" or beam-induced damage to the specimen that occurs over the course of half an hour? For specimens like iron-nickel meteorites, even with high beam currents, beam damage is not much of a problem. Such damage, on the other hand, is an important issue for insulators like obsidian and other glasses.

Recall that, for the trace elements, I set the software to count for 150 seconds total (counting for 50 seconds on the characteristic X-ray peak and then 50 seconds on each of two background X-ray level measurements). There is, in terms of the numbers of X-rays counted, little difference between 10 analyses of 2.5 minutes each and a single 25-minute analysis. In both cases, X-rays are counted for a total of 25 minutes, and mathematically, it does not matter if these X-ray counts are summed into just one measurement or divided among 10 measurements, summed, and averaged. One benefit of taking multiple, shorter measurements is that the instrument and a specimen are required to be stable for only 2.5 minutes at a time, not 25 minutes. A well-maintained and optimized electron microprobe can be stable for this length of time; however, the stability of glass for so long, especially when measuring trace elements, is questionable. Therefore, it seemed a better strategy to measure the obsidian specimens in a series of shorter analyses.

5.2.8 - Software Modifications

Two modifications to the JEOL proprietary software, made with support from the JEOL software specialists, increased the precision of the Gaussian distributions and, thus, the mean concentration values, especially for the trace-element data.

The first modification to the EMPA software was made with significant assistance from David Videchak, the National Service Support Specialist for electron microprobes at JEOL USA. Consider that 1 ppm equals 0.0001%, but the JEOL proprietary software, by default, reports concentration data to three decimal places, not four. For routine analyses, three decimal places are beyond adequate -- in general, spectrometric methods are precise to no more than three significant figures. The detection limits of EMPA is normally listed in the low double-digit-ppm range: 30 ppm (Birks 1963:2), 20 ppm (Goldstein 1967), and even 15 ppm (Scott et al. 1995:105). Recently, researchers have claimed that, using their advanced procedures, EMPA can measure single-digit-ppm concentrations with favorable analytical conditions and specimens (e.g., Donovan et al. 2007).

I wanted the software to output the compositional data to four decimal places to increase the precision of the average values for such low concentrations. After contacting David Videchak at JEOL USA, he instructed me how to make the changes to the software to achieve this. Thus, the electron microprobe at the University of Minnesota-Twin Cities is one of only a few that outputs data to four, not three, decimal places.

The second modification was initially tested and implemented at the University of Minnesota, and it was developed by Peter McSwiggen, an electron microprobe trainer for

JEOL USA, and Masayuki Otsuki, an electron microprobe specialist at JEOL Japan. This modification permitted negative concentrations to be reported, not automatically changed to zero. Admittedly, the ability for the microprobe software to report a negative value for an element concentration is not immediately apparent as an advantage.

As discussed in the previous section, X-ray emission and detection is a statistical process, and repeated measurements will, when plotted on a histogram, form a Gaussian distribution. For trace elements, which have concentrations very near zero, one "tail" of the Gaussian curve can fall into the negative range. This occurs because the X-ray peaks from trace elements are tiny and often hardly distinguishable from the background X-ray level. On occasion, at random, the background level measurements will be slightly high, and the peak measurement will be low. As a result, the background level subtracted from the peak intensity will be negative. By default, the JEOL software automatically changes all such results to zero values. This markedly alters the shape of the histogram so it is no longer a Gaussian function, and the mean will be too high without the negative data. An ability to include the negative values allows the proper Gaussian distribution to be plotted and, therefore, the correct mean to be determined. As a result, this software modification considerably improved the precision of my trace-element analyses.

5.2.9 - Choice of Calibration Standards

As explained in Section 5.1.12, quantitative EMPA, like nearly all techniques, is a comparative method. Characteristic X-rays are measured from the specimen and a series

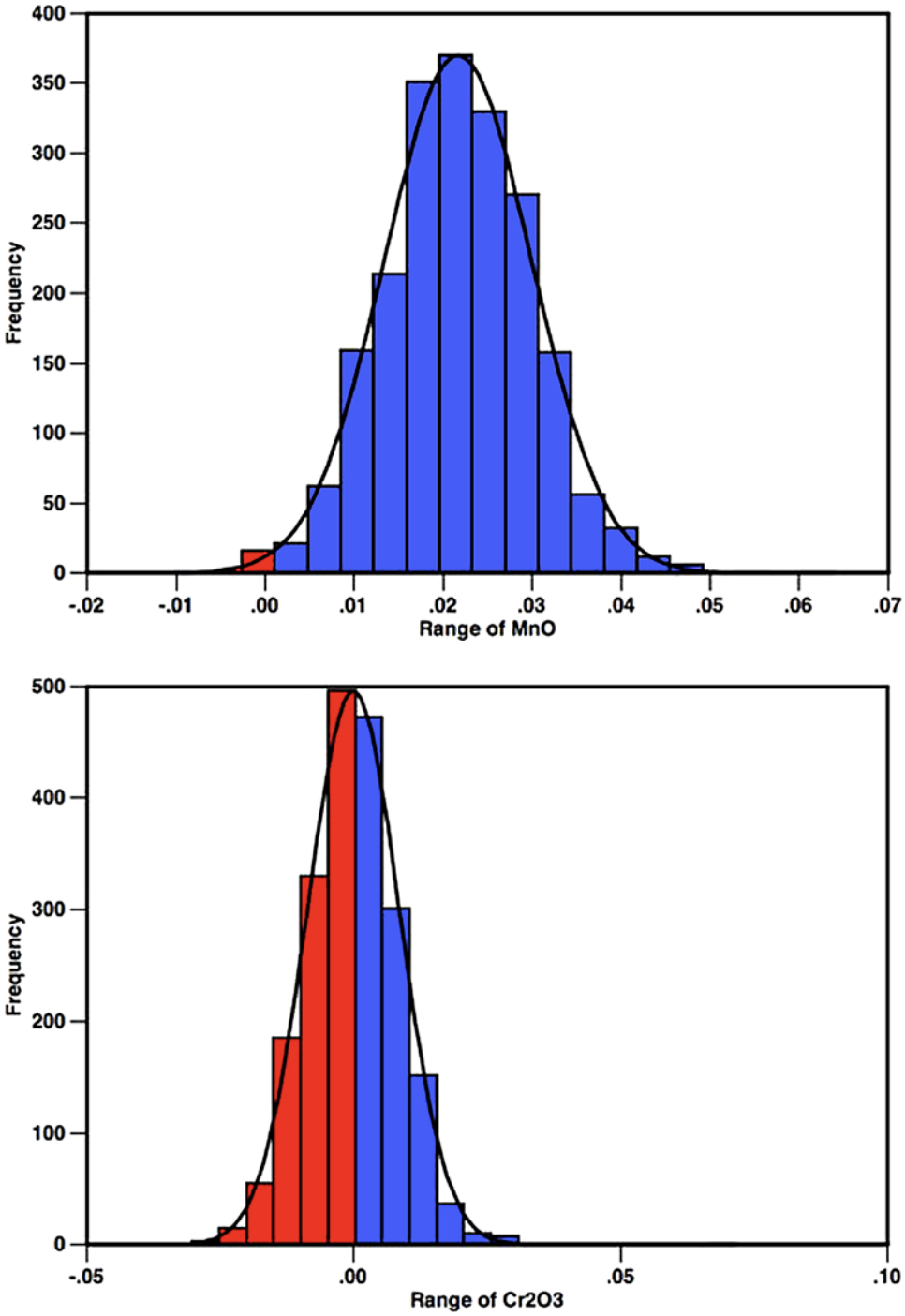


Figure 5.4 - For trace elements, the Gaussian distribution often includes negative values (red), so it is important that the instrument software be modified to report those negative values: Cr_2O_3 = 0.003% with negatives as zeros, Cr_2O_3 = 0.000% with negative values.

of reference standards using the same analytical conditions. With suitable standards, one can quantitatively determine the elemental composition of a specimen with high accuracy and precision. Choice of calibration standards may be complex and is discussed in detail by Reed (1993:159-160, 1996:142-143). In fact, a recent article in *Microscopy Today* on this topic was entitled "Standard Choice for the Electron Microprobe: Making the Right Compromise" (Kratcher 2001), referring to the competing considerations.

Merrick and Brown (1984) measured only four elements in their obsidian artifacts -- calcium, titanium, and iron -- and seem to have utilized geological "source obsidians... for standardizations" (231). Weisler and Clague (1998) only briefly mention "natural and synthetic standards" (116), and Tykot (1995) simply reports that the data were "calibrated against international standards" (113). Tephrachronology papers typically make similarly obscure statements regarding their choice of standards (e.g., "Calibration was made using mineral and synthetic standards" [Froggatt 1983:190] and "… calibrated using a sequence of minerals and metals of known composition" [Payne et al. 2008:44]). Just a few studies report the calibration standards selected for all elements (Mehringer et al. 1984; Foit et al. 2004; Allan et al. 2008; Tryon et al. 2009). My calibration standards for both the major- and trace-element analytical rounds are listed in Tables 5.2 and 5.3.

5.2.10 - Data Correction Algorithms

Raw X-ray measurements must be adjusted for various physical effects within the specimens and the standards to be converted into accurate element concentrations. These

Table 5.2 - Reference Standards for Major-Element Analyses

Na:	albite (plagioclase); locality: Amelia County, Virginia source: Harvard Collection #131705 (Carl Francis) publication: McGuire et al. 1992, *American Mineralogist* 77:1087-1091
Mg, Ca, Ti, Fe:	hornblende (amphibole); locality: Kakanui, New Zealand source: Smithsonian Institution, USNM #143965 (Eugene Jarosewich) publication: Jarosewich et al. 1980, *Geostandards Newsletter* 4(1):43-47
Si, Al:	1: rhyolite glass; locality: Yellowstone National Park, Wyoming source: Smithsonian Institution, USNM #72854/VG-568 (E. Jarosewich) 2: basalt glass; locality: Makaopuhi Lava Lake, Hawaii source: Smithsonian Institution, USNM #113498/VG-A99 (E. Jarosewich) 3: basalt glass; locality: Indian Ocean source: Smithsonian Institution, USNM #113716 (Eugene Jarosewich) 4: tektite glass; synthetic material source: Smithsonian Institution, USNM #2213 (Eugene Jarosewich) publication: Jarosewich et al. 1980, *Geostandards Newsletter* 4(1):43-47
K:	microcline (feldspar); locality: Asbestos, Quebec, Canada source: University of Chicago #258 (E.J. Olsen via Ian Steele) publication: Smith and Ribbe 1966, *Journal of Geology* 74(2):197-216
Cr:	chromite (spinel); locality: Tiebaghi Mine, New Caledonia source: Smithsonian Institution, USNM #117075 (Eugene Jarosewich) publication: Jarosewich et al. 1980, *Geostandards Newsletter* 4(1):43-47
Mn:	manganoan hortonolite (olivine); locality: Franklin, New Jersey source: University of Chicago #27 (Clifford Frondel via Ian Steele) publication: Frondel 1965, *The American Mineralogist* 50:780-782
F, P:	apatite (phosphate); locality: Durango, Mexico source: Smithsonian Institution, USNM #104021 (Eugene Jarosewich) publication: Jarosewich et al. 1980, *Geostandards Newsletter* 4(1):43-47
Cl:	meionite (scapolite); locality: Brazil source: Smithsonian Institution, USNM #R6600-1 (Eugene Jarosewich) publication: Jarosewich et al. 1980, *Geostandards Newsletter* 4(1):43-47
S:	pyrite (sulfide); locality: unknown source: Micro Analysis Consultants (MAC), St. Ives, Cambridgeshire

Table 5.3 - Reference Standards for Trace-Element Analyses

Zn:	gahnite (spinel); locality: Brazil source: Smithsonian Institution, USNM #145883 (Eugene Jarosewich) publication: Jarosewich et al. 1980, *Geostandards Newsletter* 4(1):43-47
Ga:	gallium arsenide; synthetic material source: Micro Analysis Consultants (MAC), St. Ives, Cambridgeshire
Zr:	zircon (silicate); locality: unknown source: Smithsonian Institution, USNM #117288-3 (Eugene Jarosewich) publication: Smithsonian Department of Mineral Sciences standards website
Nb:	niobium; synthetic material source: Micro Analysis Consultants (MAC), St. Ives, Cambridgeshire
Ba:	synthetic ancient glass source: The Corning Museum of Glass, specimen C (Robert H. Brill) publication: Brill 1971, *Proc. of the IXth International Congress on Glass*
Ce:	artificial rare-earth element glass source: University of Oregon, specimen REE3 (Drake and Weill) publication: Drake and Weill 1972, *Chemical Geology* 10:179-181

effects include differences in electron backscattering and interaction volume size because of atomic number (Z) differences, absorption of characteristic X-rays (A), and generation, or fluorescence (F), of extra characteristic X-rays. These are known collectively as ZAF corrections, and they are particularly important for major elements (and less important for trace elements). In this research, I used the ZAF correction scheme written into the JEOL operating software. Merrick and Brown (1984) describe their approach:

> Data were punched directly onto cards and reduced using a simple linear regression. More sophisticated techniques of data reduction are available, but were not employed as the increase in precision and accuracy is marginal for these materials, and the computing expense is considerably increased. (232)

Modern software applies corrections almost instantaneously, so obviously their concerns about computing costs are outdated and their approach obsolete. Both Tykot (1995) and Weisler and Clague (1998) used the Bence-Albee correction scheme, a set of empirically derived coefficients mainly used by geologists before computers were sufficiently fast to calculate corrections directly. It is important to report which correction scheme was used because work has shown that, for certain specimens and conditions, differences may arise among correction methods (Lifshin and Gauvin 2001:175-176).

5.2.11 - Miscellaneous Procedures

I used four other procedures to improve accuracy and precision of the quantitative analyses. First, spectrometers may "drift" a bit over time, and this can particularly affect elements with narrow X-ray peaks (i.e., the wavelength range of emitted X-rays is small),

like Al and Si. Accordingly, every five or ten analyses I set the spectrometers to "repeak" for Na, Si, Al, and K -- in other words, the spectrometers rescanned the X-ray spectrum in the vicinities of those elements in order to find their new peak centers. Second, I used the autofocus system to assure that the specimen had the proper placement with respect to the spectrometers. Third, I analyzed for Na and K first to minimize the effects any migration would have on the results. Lastly, I did not directly measured for O in the major-element round. Instead, as is typical for geological analyses (Goldstein et al. 1992:470), O atoms were assigned to the other elements by valency (i.e., as a ratio).

5.3 - Challenges to Non-Destructive EMPA for Artifacts

There are four principal challenges to using EMPA for non-destructive analysis of obsidian artifacts. The first two challenges involve the specimen requirements of EMPA: an ideal specimen has a surface that is (1) flat and perpendicular to the electron beam and (2) highly polished. The characteristics of obsidian work in favor to mitigating these two challenges. In particular, the second challenge would pose a much greater problem if the material of interest was instead chert, quartzite, or most other rocks. The third and fourth challenges involve post-depositional processes that affect the artifacts' surfaces. Data on the effects of these processes on the analytical results is sparse, even contradictory. Thus it is difficult to predict to what degree the results will be affected.

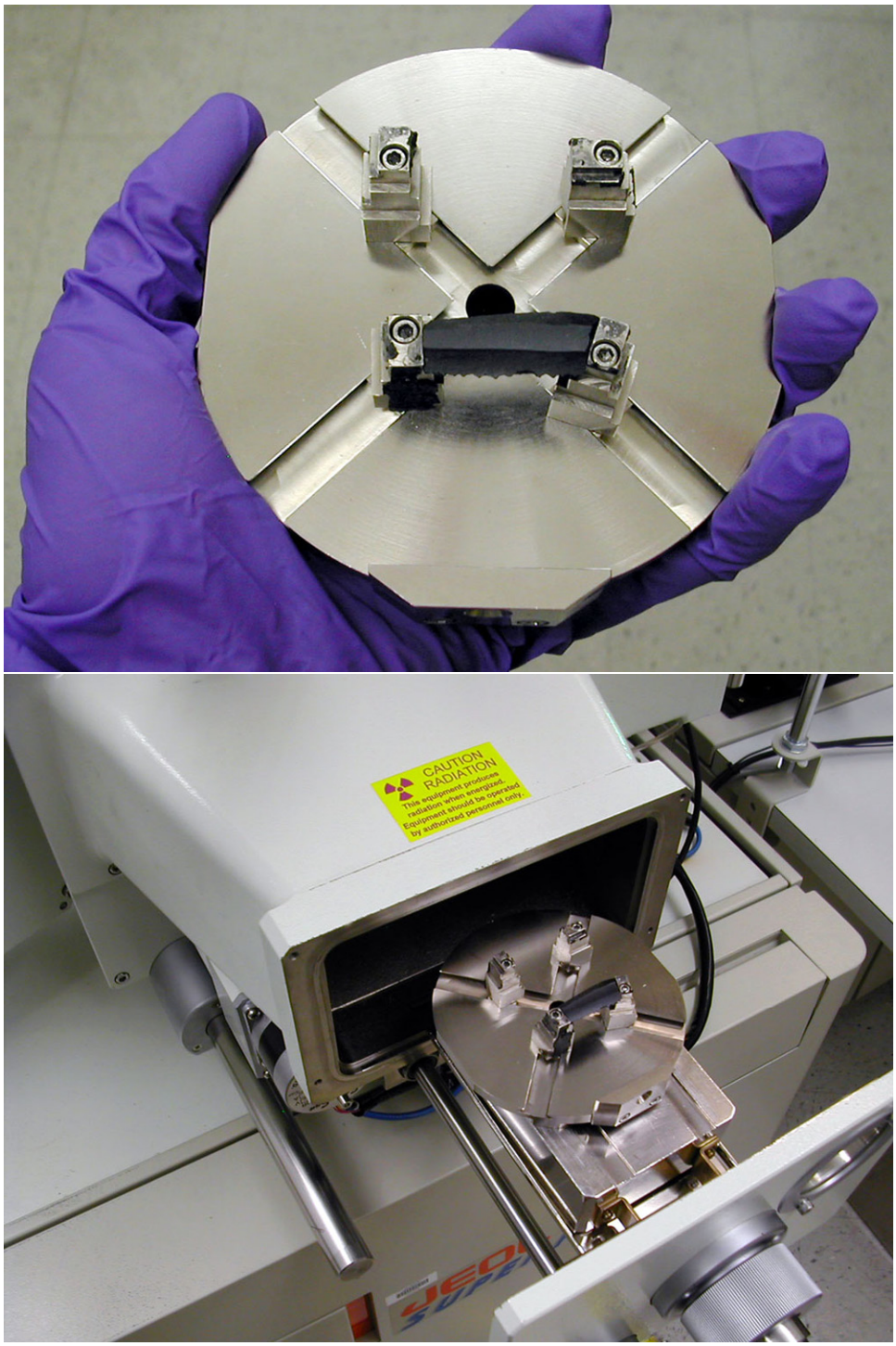


Figure 5.5 - A carbon-coated obsidian blade can be analyzed in the electron microprobe without having to remove a piece or leaving it radioactive (photographs by the author).

5.3.1 - Challenge #1: Non-Flat Artifact Surfaces

The first challenge to using EMPA to source obsidian non-destructively is that the artifacts do not have perfectly flat surfaces. Conchoidal fracture, the process which by a brittle and homogeneous material like obsidian breaks and which humans have exploited for over a million years to fashion stone tools, produces only curved surfaces. Prismatic blades, for example, are ordinarily convex on the ventral surface, and the dorsal side has concave surfaces (unless a blade's surfaces have been ground flat; see Chapter 7 for one example of such a blade from Tell Mozan). Projectile points, though, may be covered with dozens or even hundreds of small, concave flake scars.

Trying to analyze a curved surface is similar to trying to analyze a tilted surface. Goldstein et al. (1981) point out that the "chief difficulty in handling tilted specimens is that the [data] correction model is predicated on normal beam incidence. The effect of a titled specimen... has not been extensively investigated" (336). An assumption built into the data-correction algorithms is that the electron beam is perpendicular to the specimen surface. This condition is required for two reasons. First, the penetration depth of beam electrons into a specimen is only accurately determined with normal incidence. Without knowing the penetration depth accurately, various effects within the specimen, especially the reabsorption of the emitted X-rays, will be miscalculated, leading to error. Second, a flat specimen also means that the geometry between the beam and the five spectrometers, known as the take-off angle, is known and constant. A tilted specimen, on the other hand, has a different take-off angle for each spectrometer (and thus different elements), causing

further miscalculations of X-ray absorption. Accordingly, it is usually recommended that specimens be tilted no more than a degree or two from perpendicular to the electron beam and parallel to the plane of the specimen stage (Reed 2005:146).

There are always specimens -- whether artifacts or forensic evidence -- that cannot be altered for EMPA. For these reasons, Goldstein et al. (1981:338) claim:

> There exists a broad class of irregularly shaped specimens which do not meet the geometrical requirement of the ideal specimen... The x-ray intensities measured from such irregularly shaped specimens differ from those of the flat standards both because of compositional differences and because of 'geometrical effects.'

Reed (2005) states EMPA "is normally carried out on flat well-polished specimens using a focussed electron beam at normal incidence... [In] the cases of analysis under non-ideal conditions… steps can be taken to minimise the loss of accuracy" (143). In this case, the challenge was to determine how to analyze curved flake scars on artifacts when the ideal specimen for EMPA is flat and lying in a plane parallel to the stage.

With the artifacts, I took the approach that, while the majority of a curved surface approximates a specimen tilted to varying degrees, there are locally flat areas, parallel to the plane of the specimen stage and perpendicular to the electron beam. For a convex surface, its apex can be essentially flat as well as perpendicular to the beam on a scale of several micrometers. The same is true of the trough of a concave surface. Their tangents are normal to the beam and parallel to the specimen stage. The radii of the flake scars are on the order of millimeters or centimeters, so on a micrometer-scale (three or four orders of magnitude smaller), some spots in the scars are effectively flat.

I located these flat, stage-parallel, beam-perpendicular areas in flake scars using a reflected-light microscope attached to the microprobe. The microscope is usually used to position a specimen at the proper height for analysis (i.e., positioned for the proper Bragg angle between the specimen and the X-ray spectrometer), which is also the focal point of the microscope. A focussed image, seen through the microscope on an LCD monitor, and sharp crosshairs indicate that the specimen is sitting at the correct height. If the specimen is tilted to either side, the horizontal line of the crosshairs diverges, and if the specimen is tilted forward or backward, the vertical line diverges. Thus, I surveyed the flake scars for areas in the correct plane by seeking locations where the microscope image as well as the vertical and horizontal lines of the crosshairs appeared sharp.

In summary, I was able to minimize the error from analyzing non-flat surfaces by identifying areas within the artifacts' flake scars that were effectively flat, stage-parallel, and beam-perpendicular. This error should be relatively small.

5.3.2 - Challenge #2: Non-Polished Artifact Surfaces

The second challenge to using EMPA to source obsidian non-destructively is that the artifacts did not have polished surfaces. Goldstein et al. (1992) argue that a specimen for EMPA must have a "highly polished surface... There exist physical effects such as the specimen's surface roughness... which can also influence the interactions of electrons and the propagation of x-rays. Such effects strongly modify the x-ray spectra obtained from... rough objects such as fracture surfaces." (415). Reed (2005) also asserts that "absorption

and other corrections are affected by roughness (irregularities of much less than 1 μm can have a significant effect)" (146). Calculations by Lifshin and Gauvin (2001) showed that grooves only 0.5-μm deep can produce errors for some elements (171). Initially, it seems that trying to analyze an unpolished artifact would be too error-prone.

Consider, though, that obsidian's fracture surfaces are extremely smooth. A rock like granite has a rough fracture surface because its crystalline structure causes a crack to deviate, causing breaks along crystal boundaries and cleavage planes. Even chert, with a fine-grained micro- to cryptocrystalline structure, has a fracture surface that, at least on a microscopic scale, is rough. Glasses, on the other hand, are amorphous and conchoidally fracture as a crack propagates, yielding very smooth fracture surfaces. Therefore, under a reflected-light microscope, the fracture surfaces of flint and other cherts appear rough and dark, whereas obsidian looks bright and smooth. Hurcombe (1992) explains, though, that "although the surface of the obsidian is much brighter and smoother than that of flint, it is by no means a flat, featureless plane" (25). This is due to the fact that, as we established, obsidian is not a perfect glass, and it contains tiny mineral inclusions.

The microscopic minerals within obsidian cause deviations in the path of a crack, but the effect is not so severe as to compromise its propagation. Cotterell and Kamminga (1987) explain that inclusions "cause the path of a crack to deviate from the ideal... After a small disturbance caused by a local inhomogeneity in the material a crack either returns to propagate stably along its original path, or continues to deviate," meaning that the path is unstable and the crack goes awry (679). The former case is what appears commonly to

occur near inclusions within obsidian: there are only local aberrations around the mineral inclusions, leaving the remainder of the fracture surface quite smooth.

This proposal -- the extremely smooth fracture surface of obsidian is interrupted only by small perturbations due to microscopic mineral inclusions -- is supported by the microscope-based observations made by Linda Hurcombe (1992):

> The flaked surfaces of the two rocks are very different. Flint surfaces appear rough under the microscope... In contrast obsidian fracture surfaces are very smooth indeed, and therefore appear to be bright microscopically. However, an obsidian surface does have distinct features... There are surface irregularities of varying size... which are crystals within the amorphous silica matrix... As a crack which detaches the obsidian flake propagates, occasionally these irregularities cause a small stress fissure after them... The irregularities have another feature around them -- microscopic ripple marks. (24)

Patel et al. (1998) studied obsidian from Kenya and the Mediterranean island of Sardinia and made observations similar to those of Hurcombe (1992):

> The surface pits were studied by cleaving a Sardinian and a Kenyan sample in the laboratory and examining the freshly exposed surfaces under an optical microscope using the transmission and reflective modes. In transmission mode, inclusions were seen inside both obsidian samples and found to vary in number density across the surface, roughly in proportion to the number density of the surface pits observed in the reflective mode at the same region. (1052)

The researchers also examined specimens of Lipari obsidian, and they found

> inclusions only along dark bands that could be seen by the naked eye... On the surface, it was found that pits had only formed along the dark bands. Some samples appeared clear with no visible bands and on examination, no inclusions were seen and no pits had formed on the cleaved surface. These observations suggest that the pits only form in regions where inclusions exist. The mechanism

> of pit formation is not clearly understood, but may be due to some sort of stress build-up around the inclusions during fracture. (1052)

These findings by Hurcombe (1992) and Patel et al. (1998) establish that irregularities in the fracture surface of obsidian are due to the effect of inclusions.

The fact that inclusions within obsidian create surface aberrations in an otherwise smooth surface was an advantage in the present research. As noted by Hurcombe (1992), smooth obsidian appears bright in reflected-light microscopy, and irregularities caused by inclusions are readily apparent under the microscope. As discussed in the prior section, I used the reflected-light microscope affixed to the electron microprobe in order to find the areas in flake scars in the proper plane for analysis. I was also able to use the microscope to select very bright, and thus very smooth, areas on the artifacts for analysis and to avoid mineral inclusions by watching for the surface aberrations they cause.

A fresh fracture surface of obsidian is, in general, smoother than all but the finest polishes. I was able to use this fact to analyze obsidian artifacts, over four millennia old, without polishing them. This approach would be much less successful with flint artifacts because the fracture surfaces of cherts, despite being micro- or crypto-crystalline, are too rough on a micrometer scale. Using a reflected-light microscope, inclusions were readily avoided, as were use-wear and, if possible, some types of altered surfaces. For example, obsidian surfaces hydrate with time, and this process can lead to spalling of the hydrated layer, causing an uneven surface. This is only a secondary reason that obsidian hydration is a challenge to non-destructive artifact analysis using EMPA.

5.3.3 - Challenge #3: Surface Hydration of the Artifacts

Hydration is one of the two obsidian surface effects that lead to complications for non-destructively analyzing artifacts. Obsidian hydration is actually a primarily physical process, not a chemical one. A fresh obsidian surface contains microscopic cracks. Over time, water absorbs into the surface via these fissures. As this happens, not only does the density of this hydrated layer increase but also the mechanical strain it experiences. This denser, strained layer is evident under a polarized-light microscope due to a greater index of refraction. This forms the basis of obsidian hydration dating (OHD), much too large a topic to explore in depth here. Recent overviews of OHD include Green (1998:231-233), Stevenson et al. (1998), Beck and Jones (2000), and Ambrose (2001).

The breakthrough that lead to OHD came in 1955, when USGS geologists Robert L. Smith and Clarence S. Ross showed that the perlite was hydrated obsidian and that the ensuant change in density and strain was observable under a microscope (Ross and Smith 1955). Five years later, Smith and fellow USGS geologist Irving Friedman first formally described OHD (Friedman and Smith 1960), and their publication was accompanied by a paper, demonstrating New World archaeological applications, from Cliff Evans and Betty Meggers (1960). They held that obsidian hydration was a fairly straightforward diffusion phenomenon affected principally by soil temperature, observing that the rates varied over two orders of magnitude between arctic and tropical environments.

Complications, though, in OHD emerged. Friedman et al. (1966) held that it was possible to adopt a regional hydration rate if one limited the size of that region to a fairly

"uniform" environment (326). Ten years later, Friedman and Long (1976) noted that soil temperatures "vary with soil diffusivity, albedo, snow cover, climate," and more and that a rise of 1º C increases the hydration rate by 10% (34). Leach and Hamel (1984) pointed out that "the humidity of the environment in which a piece of obsidian comes to rest does influence hydration too" (399). Tests have shown this rate is also affected by liquid water versus water vapor (Abrajano et al. 1986, Bates et al. 1988), by burial depth (Jones et al. 1997; Ridings 1991, 1996), and by vegetation cover and localized variations in the soil properties (Jones et al. 1995, 1997). Consequently, Jones et al. (1997:514) argue that the rate should be determined at the site, not the regional, level. Others have suggested that, because hydration is so environmentally sensitive, obsidian artifacts should be utilized to investigate paleoclimates, not for dating (Anovitz et al. 2006).

The composition of the obsidian also affects its hydration rate, so the rate must be determined for each obsidian source. Still, though, no fewer than fifteen hydration rates, either empirically or experimentally derived, have been published for the Coso Volcanic Field source in southern California (Beck and Jones 2000:137). One primary variable is the initial water content of the obsidian. Mazer et al. (1992) and Stevenson et al. (1998) demonstrated that intrinsic water content of obsidian was the major variable affecting its hydration rate. The magma composition, its cooling rate, and low-temperature hydration affect the abundances of two hydrous species (OH hydroxyl groups and molecular H_2O), and it is the OH content that controls the hydration rate. Colleagues at the University of

Wisconsin-Eau Claire and I have been researching my obsidian collection using FT-IR to further explore this variable (Conde et al. 2008; 2009 a, b, c).

Even fundamental issues, such as the proper hydration rate equation, are still not completely answered (Anovitz et al. 2009). Consequently, Anovitz et al. (2006) contend that "while this approach is conceptually simple, the technique has, generally, not proven successful" (517). Furthermore, obsidian researchers have written articles with titles like "Where in the World Does Obsidian Hydration Dating Work?" (Ridings 1996) and "The Failure of Obsidian Hydration Dating" (Anovitz et al. 1999). Due to these challenges to successful OHD and the abundance of other datable materials (particularly ceramics that are stylistically diagnostic), most Near East archaeologists seem little interested in OHD, and few reliable hydration rates are available for the region.

With all of the complicating factors for OHD, it was difficult to predict the depth of the hydrated layer on Bronze-Age artifacts from Tell Mozan. The layer might be a few tenths of a micron in young artifacts in arid environments to a maximum of about 50 μm in old artifacts in humid climates (Herz and Garrison 1998:78,81; Patel et al. 1998:1047). As mentioned earlier, the hydration rate varies for obsidian from different sources, but the sources exploited for artifacts at Tell Mozan were not known prior to the present research. Furthermore, Jones et al. (1997:514) assert the hydration rate should be established at the site level. Given the features of the tell and the factors that affect OHD, it is possible that there are even intra-site hydration rate variations at Tell Mozan.

The obsidian artifacts I analyzed came from two different parts of Tell Mozan: the royal palace (Area A), the temple atop the summit (B), and the monumental staircase and terrace area (J). Area A lies on the western edge of the High Mound, where the rain runs down the slope into the surrounding fields. On the other hand, Area J is the middle of the tell and depressed a few meters, so it floods during the spring. Sedimentation and erosion rates also vary in these parts of the tell, meaning the burial depths of the artifacts, and the soil temperatures they experienced, differed over time. It seems quite likely that artifacts deposited in Areas A, B, and J experienced different hydration rates.

Without making a series of assumptions, it was not possible to calculate the depth of the hydration rind on the Tell Mozan obsidian artifacts. Based on hydration data from other Bronze-Age Near East archaeological sites, the rinds could be on the order of 5-μm thick (Friedman et al. 1960:513-518; Rosen et al. 2005:779). Thinner rinds, on the order of just tenths of micrometers, are also possible. Friedman et al. (1969) reported "the lack of any hydration on many of the artifacts examined from Jarmo, Iraq" (67). Jarmo lies in the foothills of the Zagros Mountains in northern Iraq, and it was a Neolithic agricultural settlement inhabited between about 7000 and 5000 BCE. A lack of observable hydration rinds on artifacts from a site similar to, but older than, Tell Mozan means that the artifacts in the present research could have nearly nonexistent rinds.

The depth of the obsidian hydration rind is important because, of course, EMPA is a surface analytical technique. The penetration of the energetic beam electrons as well as the generation and emission of characteristic X-rays are limited to the upper surface, only

a few micrometers in depth. I used a Monte Carlo simulation software package (Electron Flight Simulator) to calculate the depths in a silica-rich specimen like obsidian. Based on these simulations, I learned that, under the analytical conditions that I used, characteristic X-rays were emitted from the topmost 2.0 to 2.5 μm of obsidian. If the hydrated layer is only tenths of a micrometer deep, most X-rays will be emitted from the unaltered interior. If, on the other hand, the hydrated layer is greater than 3-μm deep, all of the characteristic X-rays will be emitted from the hydrated layer of the artifacts.

What is the effect of hydration on EMPA analysis of the obsidian? If hydration in obsidian is simply the absorption of water, I would expect the resulting chemical analyses to be "diluted" by the amount of absorbed water. In fact, obsidian hydration is essentially that simple a phenomenon. As discussed in Section 2.2, silica (SiO_2) molecules bind with the oxygens of neighboring molecules, creating a tetrahedral structure of one silicon atom in the middle of four oxygen atoms. These tetrahedra, in turn, form a disordered network of silica chains and sheets. The absorption of water molecules disrupts this network. The water breaks Si–O–Si bonds and, in turn, forms Si–O–H H–O–Si pairs (Ernsberger 1977, Bartholomew et al. 1980, Yanagisawa et al. 1997). In one sense, then, this hydrated layer is simply obsidian "diluted" with water; however, as will be discussed in the next section, the disrupted silica network may release other elements in the glass.

The degree of this "dilution" depends on the concentration of the water within the obsidian. Unfortunately, various studies have found different values for the concentration of water when the hydration layer is saturated. For example, Friedman et al. (1969) state

that the layer "consists of a glass containing about 3.5% water by weight" (67) Similarly, Ericson (1975) found maximum water contents between 2 and 2.5 weight % (156). Jezek and Noble (1978) likewise claim that hydrated obsidian, based on their analyses, contains "about 3 weight percent H_2O" (266). To the contrary, Anovitz et al. (1999) report "water concentration in obsidian apparently peaks near 10 weight %" based on their analyses of obsidian specimens from Mexico and the American West (741). Similarly, Riciputi et al. (2002) found water at concentrations of 8 to 10% in artifacts from a site in Mexico. It is hard to know, therefore, if analyzing the hydrated layer would add 2 or 3% relative error to EMPA data, or if that error would actually be 10% or more.

To summarize, hydration layers on the Tell Mozan artifacts were expected to have an effect on the analyses, but the extent was unknown. Not only were the hydration layer thicknesses unknown, but so too was the water content of these layers. A layer just a few micrometers thick and containing just 3% water would have minimal effect on the EMPA data. On the other hand, a layer that is 5-µm thick and contains 10% water would have a marked effect on the data. At the start of this study, it was not possible to know which of these conditions would apply to the artifacts from Tell Mozan.

5.3.4 - Challenge #4: Diagenetic Surface Alteration

Hydration is accompanied by chemical alteration of the obsidian surface, what is generally termed weathering. These two phenomenon are related but distinct. Friedman et al. (1969) explain that the hydration layer "should not be confused with the patina that

develops on many materials as a result of alteration or chemical weathering" (62). They note, though, the link between the hydration layer and surface alteration:

> Diffusion of alkalis and other ions is very rapid in the high water content layer. Consequently, alteration and solution are speeded up in this layer as compared to the non-hydrated obsidian. Conceivably the chemical environment present in certain soils will speed up this chemical attack. Obsidian in areas of hydrothermal activity would seem especially prone to this vicissitude. Artifacts from sites near hot spring localities in Central California show a high degree of this form of alteration... However, except for a few sites, we have found little evidence for pronounced alteration of the hydrated layer by physical or chemical agents. (67)

Alkalis are those elements that comprise Group 1 (the first column) on the periodic table: lithium (Li), sodium (Na), potassium (K), rubidium (Rb), cesium (Cs), and francium (Fr). Other researchers have also found alteration of alkalis on the surface of obsidian artifacts. For example, using nuclear reaction analysis (NRA), Coote and Nistor (1982) studied the depletion of sodium on the exterior of archaeological obsidian.

Unfortunately, information about the depths and degrees of such surface alteration on archaeological obsidian is scarce. Most knowledge about the alteration of obsidian is inferred from the weathering of artificial glass (e.g., Doremus 1975, 1979; Pantona 1976; Adams 1984; Schreiner et al. 1984; Ford and Cox 1988; Schreiner et al. 1988), lab-based hydration experiments on natural and artificial glasses (e.g., Schreiner 1989, Tremaine and Frederickson 1988, Anovitz et al. 2009), high-temperature experiments on silica-rich melts (e.g., Doremus 2000 and references therein), and studies of vitreous geological materials like perlite and glassy fragments in volcanic ash (e.g., White 1984). Only a few

researchers have directly studied the surface alteration of obsidian artifacts by measuring the concentrations of elements versus depth from their exteriors.

Tsong et al. (1978) employed a form of optical emission spectroscopy to measure the abundances of hydrogen (H), lithium (Li), sodium (Na), magnesium (Mg), aluminum (Al), silicon (Si), potassium (K), and calcium (Ca) as a function of surface depth in a set of Guatemalan artifacts. These element concentrations were compared to a fresh surface on one of the artifacts. The analyses showed a correspondence between the depths of the hydration layer and the chemically altered surface. The hydration depth was measured to be 2.0 μm, and it was a "depth around 2 μm where the signals of H, Na, K, and Li... reach an equilibrium level" (340). At the obsidian surface, Na was depleted by about 30%, and K by about 20%. Though the effect was less pronounced than for the alkalis, Ca and Mg were also depleted near the surface and leveled off at 2 μm. On the other hand, Si and Al exhibited "very little variation of concentration with depth" (341).

Patel et al. (1998) analyzed the surfaces of Sardinian obsidian artifacts with SIMS (secondary-ion mass spectrometry), primarily interested in the concentrations of nitrogen and carbon on their exteriors. They discovered that Na and K were depleted to a depth of about 0.1 to 0.15 μm, reached their maximum enrichment at 0.2 to 0.25 μm, and returned to their bulk concentrations at about 0.4 to 0.45 μm. The depths, unfortunately, cannot be compared to the thickness of the hydration layer because Patel et al. (1998) did not report it. Like Tsong et al. (1978), Sanjay Patel and his colleagues found that Si and Al "show a near constant distribution" (1049). Ultimately, they concluded that the distributions of N

and C could not be used for dating because their presence is a "result of what is probably a complex biologically-driven process during diagenesis" (1054).

Anovitz et al. (1999) also used SIMS to analyze the surfaces of obsidian artifacts from Mexico and the American West. As mentioned earlier, Tsong et al. (1978) reported a correspondence of alkali depletion and the hydration layer. This was not supported by the findings of Anovitz et al. (1999). In fact, they noted that "in most cases water uptake is not balanced by alkali loss... the depths at which alkali concentrations become constant are significantly less than that of water" (742). Their concentration versus depth data for nine artifacts are summarized in their Figure 3, reproduced here as Figure 5.6. In one of the artifacts (A; Otumba, Mexico obsidian source), the hydration front was measured at a depth of 3.1 μm optically, but Na, K, and Ca reach their unaltered, bulk concentrations at roughly 0.3 μm. In another artifact (D; Zaragosa, Mexico obsidian source), the hydration front had a depth of 2.2 μm, but Na, K, and Ca reach the bulk concentrations at about 0.4 or 0.5 μm. The conflict between their findings and those of Tsong et al. (1978) cannot, at present, be fully resolved, but Anovitz et al. (1999) assert that SIMS provides data "more detailed than those obtainable" by the technique of Tsong et al. (1978).

Many researchers who have analyzed obsidian with surface analytical techniques, including SEM-EDS and PIXE, express at least some concern about surface alteration or the effect of weathering and/or hydration (e.g., Ambrose et al. 1981, Ambrose 1998, Kim et al. 2007). Despite these concerns, details about how the surface of obsidian is actually altered post-depositionally are rare. Judging from recent data, measured using SIMS, the

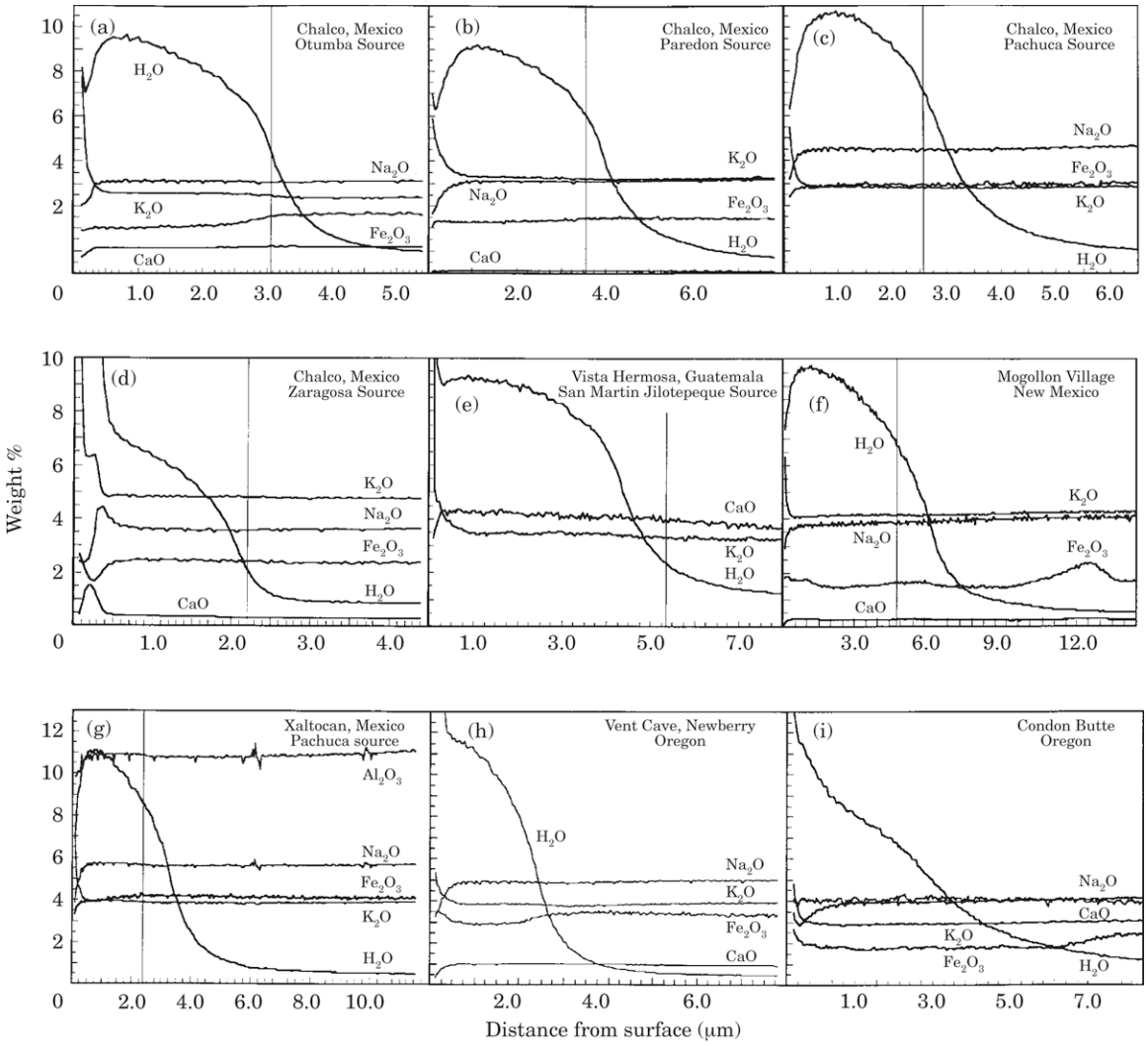


Figure 5.6 - This figure from Anovitz et al. (1999:742) shows how the concentrations of H_2O, Na_2O, K_2O, Fe_2O_3, and CaO vary with depth (in micrometers) from the surfaces of nine North American obsidian artifacts. These profiles were measured using secondary-ion mass spectrometry (SIMS). These are the only available recent data for the depth and degree of chemical alteration and the correlations (if any) to the hydrated layer. In many of these obsidians, the chemically altered layer is just a few tenths of a micrometer deep, much more shallow than the hydrated layer, suggesting these are two separate processes.

chemical alteration can be much more shallow than the hydration layer, even a full order of magnitude thinner. As noted earlier, my simulations showed that, under the analytical conditions that I used, characteristic X-rays were emitted from the topmost 2.0 to 2.5 μm of the obsidian artifacts. If their surface alteration is limited to only the upper few tenths of micrometers, their effect on my analyses should be only moderate. In addition, not all elements will be affected equally. Some, in fact, may remain largely unaffected, so using those immobile elements for source discrimination will be preferable.

5.3.5 - Summary of the Challenges to Non-Destructive EMPA

Of the four challenges to using EMPA non-destructively for artifacts, the first two involve specimen requirements: an ideal specimen for EMPA has a surface that is (1) flat and perpendicular to the beam and (2) highly polished. I minimized the former challenge by identifying areas on the artifacts' surfaces that were effectively flat, stage-parallel, and beam-perpendicular. Regarding the latter, a fracture surface of obsidian is smoother than all but the finest polishes, and both inclusions and irregular surfaces can be avoided. The error should be relatively small from these two challenges. This would not be true if, for example, I tried to analyze chert projectile points, nor would my procedures work as well for a ground-stone obsidian artifact, like a bowl or cylinder seal.

The third and fourth challenges involve post-depositional processes that affect the artifacts' surfaces: hydration and surface chemical alteration. Unfortunately, detailed data on the effects of the processes are sparse, even contradictory. For example, reports about

the concentration of water within a hydration rind vary from 2 or 3% to over 10%. All of the factors that affect obsidian hydration -- temperature, relative humidity, soil properties and more -- made it difficult to calculate the depth of the hydrated layer on artifacts from Tell Mozan. The depth of any surface alteration, such as depletion or enrichment of K or Na, was also difficult to predict, though the latest data suggested a thickness of just a few tenths of a micrometer. Alteration data for other elements are rare.

Ultimately I could do nothing to address the last two challenges directly because I was committed to non-destructive analyses. Two factors work in favor of the Tell Mozan artifacts having thin hydration and surface alteration layers: (1) these artifacts date to the Bronze Age and (2) were buried in, at least what is currently, an arid climate. In contrast, both the hydration and surface alteration layers on, for example, the artifacts noted at the start of Section 2.1 -- several obsidian pieces in *Homo habilis* levels of Olduvai Gorge in tropical Tanzania -- should be much thicker. Similarly, Mesoamerican artifacts should be expected to have thicker hydration rims and, thus, surface alteration layers: the hydration rate in tropical climates can be ten times faster than in dry ones.

5.4 - Concluding Remarks

My research extends the limits of how EMPA has been used in obsidian sourcing and shows the modern capabilities of this technique. As explained in Chapter 1, the key components of my redevelopment of EMPA for obsidian sourcing include: (1) glass-only analyses to remove the effects of inclusions; (2) non-destructive analyses of artifacts; and

(3) measuring trace elements at concentrations much lower than those measured in earlier studies. I discussed in this chapter how I accomplished these goals.

The next step is to show not only that the EMPA analyses are accurate and precise but also that EMPA (when combined with my statistical approach) is a valid and reliable technique for obsidian sourcing, especially when artifacts are analyzed non-destructively, which was done, to my knowledge, for the first time in this research.

Part II: Methods for Sourcing and Their Evaluation

Chapter 6:

Evaluating the Analytical Procedures and Source Assignment Methods

> Some... have made what I consider the mistake of focussing on precision versus the archaeological accuracy we seek in source provenance studies...
>
> -- M. Steven Shackley, 2005, *Obsidian: Geology and Archaeology in the North American Southwest*

> Further consideration of geological, geochemical, and archaeological factors involves the concepts of *reliability* and *validity*, reliability involving mainly issues of measurement and instrumentation, and validity combining measurement issues with noninstrumental purpose.
>
> -- Richard E. Hughes, 1998, *On Reliability, Validity, and Scale in Obsidian Sourcing Research*

In the above quotations, both Shackley and Hughes assert that we should really be concerned with *something* beyond pure analytical precision and accuracy. Shackley calls this "archaeological accuracy" whereas Hughes contends that the concepts of "reliability" and "validity" provide a better framework. While the concepts of precision and accuracy arose in engineering and the natural sciences, reliability and validity originated mainly in education and the social sciences, especially psychology. These concepts, therefore, were originally applied to the evaluation of tests and surveys in education and psychology, so it is not evident how they can be applied to analytical techniques that yield large amounts of

quantitative geochemical data. Further, reliability and validity are less rigorously defined than precision and accuracy, which themselves vary a bit in meaning. Nevertheless, these four concepts -- precision, accuracy, reliability, and validity -- will serve as my framework to assess my EMPA and data-analysis procedures for non-destructively sourcing obsidian artifacts. Since Hughes (1998) called for all four concepts to be included in evaluation of obsidian-sourcing techniques, use of this framework has been almost nonexistent. Aside from a few one-off uses of the word "reliability" in papers without defining or discussing it (Bavay et al. 2000:8, Constantinescu et al. 2002:375), only Nazaroff et al. (2010) have previously utilized Hughes' framework in their evaluation of PXRF for obsidian sourcing in Mesoamerica. Here I not only use his framework but also consider its foundations and attempt to strengthen its application in obsidian sourcing.

6.1 - What are the Data?

Before discussing Hughes' framework for assessing sourcing techniques, what is being evaluated must first be defined. In this case, at least for precision and accuracy, the EMPA results are the subject of evaluation. More specifically, it involves the quantitative elemental measurements and any subsequent data processing applied to them.

6.1.1 - Elements Selected for Analysis

Selecting the elements to be measured is one of the first steps of EMPA. Each of the elements to be analyzed must be chosen beforehand, and a series of choices is needed

for each element, including which spectrometer to use, for how long to count the X-rays, where in the spectrum to measure the background X-ray levels, and what standard to use for calibration of that element. Accordingly, one must balance the need for a "complete" analysis for a particular research question with time spent measuring elements of little or no importance to the work at hand. Although EMPA is technically capable of quantifying over 80 elements, this is never done for practical reasons. Even studies with quantitative analyses of 20 elements, like my research, are unusual. Therefore, one must be selective, on both theoretical and practical grounds, of elements for analysis.

Naturally, a closely related issue is the suite of elements chosen for discrimination of obsidian sources. Harbottle (1982), a researcher at Brookhaven National Laboratory, wrote: "One often hears in discussions at symposia the query of 'which elements are best to analyze, to discriminate sources of some archaeological material from one another, and which elements need not concern us?'" (18). The reality, though, is that a diagnostic set of elements used in a given region to differentiate chemical groups might not be adequate for differentiation in another region. The variation between specific elements of different chemical groups will vary between and within regions. Thus, one must discover -- either empirically or using prior studies -- a set of elements useful for discriminating the sources in the region of interest (Glascock et al. 1998; Shackley 1998a, 1998b).

There are two basic lines of thought about element selection for sourcing obsidian artifacts. The first can be summarized as "more is better." For example, Harbottle (1982) maintains that "multielement methods are needed, and the more elements the better" (18).

Harbottle argues this because he considers sourcing to be a form of taxonomy. Therefore, he applies taxonomic theory and practices to his approach to sourcing studies. He claims, for example, that taxonomic classifications based on numerous traits are superior to those based on a few traits. With this reasoning, he asserts: "You get the best classifications out of the most information, and therefore the best analytical technique a priori is the one that yields reliable data on the largest number of elements" (39). In summary, his advice is to "analyze for everything that you can, at whatever level of precision you can conveniently reach, and let the computer decide which combinations of elements can effect the desired group discriminations. Make no a priori assumptions" (18).

Today it is not unusual to find studies in which obsidian specimens were analyzed for 27 (e.g., Braswell and Glascock 1998 and Aoyama et al. 1999 in Mesoamerica; Abbès et al. 2003 and Bressy et al. 2005 in Near East), 28 (e.g., Bavay et al. 2000 in East Africa; Burger et al. 2000 in Mesoamerica; Glascock et al. 2007 in North America; Eerkens et al. 2008 in California), and even up to 36 elements (e.g., Carter et al. 2006 in the Near East; Bellot-Gurlet et al. 2008 in Mesoamerica). These numbers of elements are the maximum for which a particular technique (e.g., NAA in Glascock et al. 2007) or pair of techniques (e.g., ICP-MS and ICP-AES in Carter et al. 2006) are capable of analyzing.

The second line of thought regarding element selection involves critical selection (and exclusion) for instrumental, geochemical, and practical reasons. Hughes (1984), for example, points out that "it is commonly believed that the inclusion of larger numbers of variables in discriminant analysis results in a 'better' classification, [but] in fact this is not

necessarily the case" (3). He claims that including "poorly measured, weak, or redundant variables... can actually increase the number of misclassifications" (3). This includes any elements either measured with poor precision or that tend to vary within an obsidian flow (7). Hughes also provides Fe as an example of an element "much more variable" within an individual flow than Ba, Zr, and Rb, so it "probably would not be [a] good [candidate] for inclusion" with the distinguishing elements (7). This comment reflects, of course, the analysis of obsidian with a bulk analytical technique (XRF) so that the abundance of iron oxide inclusions highly affects the measured Fe concentrations. My analyses of the glass, not the inclusions, means that Fe may, in fact, become a useful element for distinguishing obsidian sources when a spot analytical technique like EMPA is used.

The second approach to element selection utilizes empirical observations of the geochemical trends in obsidian. For instance, Rapp and Hill (1998) note that Mn, Ba, Sc, Rb, La, and Zr can "vary by as much as three orders of magnitude among obsidian flows, while varying by less than 50 percent within a single flow" (137). Other researchers have also reported elements that are especially variable among obsidian sources. For example, Gordus et al. (1971) note the usefulness of Na, Sc, Ba, and Zr in distinguishing Near East obsidians (23). Also in the Near East, Carter and Shackley (2007) measured ten elements that had been useful in prior studies: Ti, Mn, Fe, Zn, Ga, Rb, Sr, Y, Zr, and Nb. Kim et al. (2007) analyzed only four elements in Southeast Asian obsidians (Fe, Rb, Sr, and Zr), and De Francesco et al. (2008) analyzed five (Nb, Y, Zr, Rb and Sr) in the Mediterranean. Of course, a key example is Merrick and Brown (1984) who utilized EMPA to measure only

three elements (Ca, Ti, and Fe) in East African obsidians. Such empirical criteria can also be used to exclude elements (e.g., Craig et al. 2007: "Ni, Cu, and Ga... are rarely useful in discriminating glass sources and are not generally reported," 2015).

Correlation among elements has affected their selection in some research. Wilson (1978) asserts that, for ceramic sourcing at least, elements with correlated concentrations provide less information than uncorrelated elements. He states that, when two "elements are perfectly correlated, there is no point in measuring more than one element" (223). In fact, Perlman and Asaro (1969) explain that, for this very reason, they do not measure all rare earth elements (REEs) in ceramics. Harbottle (1970) found a correlation between Ni and Cr in Mycenaean Greek sherds, and he later argued that "redundant variables" should be left out of archaeological sourcing studies (1984:3). Wilson (1978) concluded that "it is of dubious value to measure elements that are correlated with many others or which are highly correlated with a particular element" (223). Other researchers disagree. Glascock et al. (1998) explain that element concentrations within any geological material are never truly independent, and consequently, "the practice of not considering correlated elements results in a loss of potentially useful information" (24). In some obsidian sourcing work, excluding those elements correlated with Fe (from magnetite) has been considered a way to reduce the effect of different inclusion abundances. Even if this was effective, it is not necessary in this research because I am only analyzing the glass.

Instrumental limitations can also affect element selection. In an extreme example (Frahm 2007), a handheld XRF instrument (a Thermo Fisher Scientific NITON analyzer)

had 21 factory-preset elements (Mo, Zr, Sr, Rb, Pb, Se, As, Hg, Zn, Cu, Ni, Co, Fe, Mn, Cr, V, Ti, Sc, Ca, K, P) for its "bulk analysis" setting. Some elements either cannot be analyzed by a certain analytical technique or are not analyzed well (e.g., Nb, P, Pb, S, and Si by NAA). In other cases, it is the concentrations of elements in obsidian or inferences between particular elements in obsidian that pose problems. For example, elements at the single-digit-ppm level and lower cannot be measured with EMPA. Various elements have X-ray peaks that overlap in EDXRF and SEM-EDS (e.g., Sr with Si, Ti with Ba, Mo with S and Pb, Cr with Mn, Mn with Fe) but not in WDXRF and EMPA-WDS. Other times, a few elements may be much easier to measure than others. Recall from Section 1.5.1 that Na and Mn were initially two of the easiest elements to quantify with NAA, so these two elements were often used in early ceramic sourcing studies (e.g., Sayre and Dodson 1957, Johnson and Stross 1965). For the same reason, Na/Mn ratios have been used in obsidian studies with NAA (e.g., Mahdavi and Bovington 1972, Hatch et al. 1990).

As I explained in Chapter 5, I conducted two rounds of analyses. For the "major" element round, I measured fourteen elements: Si, Ti, Al, Cr, Fe, Mn, Mg, Ca, Na, K, P, F, S, and Cl. These are the elements that comprise major rock-forming minerals in igneous rocks. To choose elements for the "trace" element round, I conducted a test with Ba, Zr, Zn, Nb, Pb, La, Ce, Th, Ga, and As measured in 104 obsidian specimens, each one from a different collection area. Based on the test results, I selected six of these ten elements for analysis in all of the specimens and artifacts: Zr, Nb, Ga, Zn, Ba, and Ce. These elements had, based on my initial tests, sufficient concentrations and precision to include. Further,

Zr, Nb, Zn, and Ba had proved useful in many prior obsidian sourcing studies in the Near East and elsewhere. I analyzed for Ce to include one of the rare earth elements (REEs), a popular series of elements for obsidian sourcing. Ga was included because it was used in earlier studies of Anatolian obsidian (e.g., Carter and Shackley 2007).

Two elements that have been particularly useful for obsidian sourcing around the world -- Sr and Rb -- had to be excluded from this study. The X-ray peaks for Sr and Rb do not directly overlap with that for Si; however, their energies and wavelengths are very similar. In a silicate mineral with both Si and Sr or Rb as major elements, these elements likely could be measured with acceptable accuracy. In obsidian, however, which is about 75% SiO_2, the "tails" of the primary Si peak and its tiny satellite peaks will interfere with measuring the small X-ray peaks due to trace amounts of Sr and Rb. I tried to find a way to measure the Si, Sr, and Rb X-ray peaks and use overlap correction factors, empirically determined, to calculate adjusted concentrations. Finding suitable standards to derive and test the correction factors was problematic, and a third round of analysis would have been necessary. Sr and Rb were thus excluded for technical reasons.

6.1.2 - Data Treatment

Shackley (2005) has called for obsidian characterization studies to report the data "in a manner that is easy to interpret" and in a format that is compatible with later studies (101). For elemental data, this means reporting the data as quantitative concentrations of elements or their oxides. This has not always been the case, and various researchers have

reported their data only as raw, instrument-specific X-ray counts or ratios (e.g., Ambrose et al. 1981; Brown 1983; Biró et al. 1984, 1986; De Francesco et al. 2008; Godfrey-Smith and Haywood 1984; James et al. 1996; Kunselman 1994). Without making the necessary corrections to convert X-ray counts into element concentrations, their data are only semi-quantitative, and no one could replicate their results or generate comparable data without using the same instrument under identical conditions. Hughes (1998) likens the situation to sending off specimens to a laboratory for radiocarbon dating and receiving their results in units of decay counts rather than radiocarbon or calendar years.

Even today many researchers report and interpret their data only as element ratios, and Shackley (2005) explains that such an approach has pitfalls. For example, one source might have unique concentrations of Nb and Zr, for example, but its Nb/Zr ratio might be the same as another source. Also, without knowing the Zr concentration used to calculate these element ratios, the actual concentrations cannot be determined by us. Some studies even calculated the element ratios with a mix of corrected concentrations and uncorrected raw counts, meaning that the data must be considered semi-quantitative and incomparable to other data. Still, the use of such ratios is common, especially in the Mediterranean and Near East (e.g., Gratuze et al. 1995 in the Near East normalized to Na; Brennan 1996 in the Near East normalized to Sc; Briois et al. 1997 in Near East normalized to Na and Zr; Gratuze 1999, Abbès et al. 2001, and Khalidi et al. 2009 all in the Near East normalized to Zr; and Le Bourdonnec 2008 in the Near East normalized to Ga).

Sometimes normalizing to either an element or 100% is required by the analytical technique. For example, Carter et al. (2006) had to normalize their LA-ICP-MS data for Anatolian obsidians to SiO_2 at an assumed concentration (69.895%), and they considered their concentration data to be "approximate" as a result (903). In another instance, Craig et al. (2007), using a portable XRF analyzer with Peruvian obsidians, explain that "values for each analysis were constrained to 100%" by the proprietary software (2016). In their PIXE analyses of North American obsidians, Bellot-Gurlet et al. (2005) point out that the major elements "were calculated with their sum as oxides normalized to 100%" (584), yet the reason, whether it was a constraint of PIXE or not, is not clear.

Others have chosen to normalize their data to a total of 100% or some other value. The most notable example is Tykot (1995, *inter alia)*, who normalizes his EMPA data to a total of either 99.00% (Tykot 1995, 1997, 2002, *inter alia*; Rosen et al. 2005) or 100.00% (Tykot 1996; Tykot and Chia 1997). When he analyzed an Egyptian artifact, "the results were normalized to 100% and [then] averaged" (Tykot 1996:177); however, in Indonesia, the data were "averaged and [then] normalized to 100%" (Tykot and Chia 1997:177). In his dissertation research on Mediterranean obsidian, Tykot (1995) states that, with "each sample, the three (or more) analyses were each normalized to total 99.00% (allowing 1% for water and trace elements) and averaged" (475). This reasoning is elaborated in Rosen et al. (2005): "The resulting data were then normalized to 99% to eliminate the effects of variable water content" (780). The unnormalized values for the six artifacts analyzed are

included in the paper, and with the exception of a sum of 99.16%, the original totals for the rest of the analyses fall between 97.90% and 98.60% (780).

Such normalization is ordinarily considered unacceptable in EMPA. Goldstein et al. (1992) point out that "the analytical total should fall within 99-101% if the specimen corresponds to the ideal bulk case and the analysis is conducted with careful attention to instrument operating conditions" (471-472). Reed (2005:125) similarly claims:

> . . . the oxide sum should be close to 100% (between 99% and 101% is acceptable for most purposes). A low total can be caused by beam-current drift, poor spectrometer calibration, etc., but may occur for other reasons, such as the presence of water or an element not included in the analysis. Normalisation to 100% is undesirable because it disguises these effects.

Goldstein et al. (1992) states that, because all elements "are independently measured" in EMPA, a "*nonnormalized* analytical total conveys significant information" (emphasis in original, 471). If a total is less than 98%, the possibilities include an error with the beam current or spectrometer, a missing element, and specimen preparation or geometry issues (472). Whatever the cause, they assert that it is "better to report the 'raw' analysis since subsequent processing may mask the magnitude of the correction and instill a false sense of confidence" in the quality of the analyses (1981:347).

Rosen et al. (2005) explain that normalization to 99% is intended "to eliminate the effects of *variable* water content" (emphasis added, 780); however, the prior publications (Tykot 1995, *inter alia*) suggest that these data were normalized to 99.00%, not 100.00%, to leave a percent for water and trace elements (although the water content of obsidian is commonly less than 0.3%). The normalization instead seems to have more to do with the

data quality. Looking at the original data in an appendix of Tykot (1995), one notices that about 1 in 12 of his analyses have totals below 97%. Of these, nearly half are below 90% (including one below 81%). Most of his analyses fall in the range of 97% to 98.5% or so, but a few high totals (e.g., 101.04%, 101.40%) are also present. It is impossible to tell if one or two elements are responsible for the low totals or if there is a source of systematic error (e.g., unstable electron beam or counting electronics) to blame.

For the present research, I report the data as fully quantitative analyses with each element independently calibrated to standards. The data for the major elements are given as weight percent oxides, and the trace elements are reported in parts per million. I have not processed my data beyond (1) applying the ZAF correction algorithms to convert the raw X-ray counts into element concentrations (as discussed earlier in Section 5.2.10) and (2) averaging the analyses on each specimen (as discussed in Section 5.2.7) because the mean "is considered to be the most probable value of" the actual concentration (Goldstein et al. 1981:431). For the major elements, the oxygen was not measured directly. Instead, it was assigned by stoichiometry (e.g., for every two Al atoms, three O atoms were added to the analysis). All of the data at each stage, from over three-quarters of a million X-ray measurements to the mean element concentrations for each obsidian geological specimen and artifact, are digitally archived and could be reprocessed.

6.2 - Assessing Precision

Sufficient precision is essential because all sourcing research involves measuring geological specimens and artifacts and seeking tight clusters within the data -- elemental,

isotopic, magnetic, etc. -- to differentiate sources and identify these characteristic signals in artifacts (Harbottle 1982:14, 27; Wilson and Pollard 2001:509). I start, therefore, with accessing the precision of EMPA for obsidian analyses using my procedures discussed in Chapter 5, and a discussion of accuracy will follow in Section 6.3.

6.2.1 - Defining Precision

The *precision* of a set of measurements is sometimes known as the reproducibility or repeatability, and its definition is rather well refined in the sciences. In *Introduction to Error Analysis*, John R. Taylor (1996) defines precision as the degree to which a series of measurements with the same conditions give identical results. Most scientific definitions of precision are fundamentally consistent with Taylor's formulation.

The National Institute of Standards and Technology (NIST) separates the concept of precision into two parts: repeatability and reproducibility. *Repeatability* is "agreement between the results of successive measurements... carried out under *the same conditions*," whereas reproducibility is "closeness of agreement… under *changed conditions*" (Taylor and Kuyatt 1994; emphasis added). Repeatability requires: the same procedure, observer, instrument, conditions, and location in a short time period. If any of those criteria change or a longer period of time passes, *reproducibility* is involved.

Given the large number of specimens needed for sourcing research, many sessions over months or years are often required, meaning that the conditions will inevitably vary, even if everything else remains the same. Therefore, repeatability and reproducibility are

hard to sparse in sourcing research, so the broader concept of precision suits our purpose here. Repeatability and reproducibility, as defined by NIST, will be important in Section 6.8.2, though, when we examine the concept of reliability.

6.2.2 - Approaches to Precision in Obsidian Sourcing

It is generally accepted in sourcing research that precision is determined by taking repeated measurements on a certain specimen over time, not as a calibration standard, but as an unknown. For example, in their study of Egyptian obsidian artifacts using ICP-MS, Bavay et al. (2000) assessed their precision with 5 to 12 repeated analyses on 17 obsidian specimens (8). Based on measurements of their standards over a few years, Bellot-Gurlet et al. (2005) estimated the precision of PIXE in the CNRS-Bordeaux facility to be about 5 to 10% (587). For their PIXE analyses of Romanian obsidian artifacts, Constantinescu et al. (2002) checked their precision using a series of replicate measurements on a particular artifact (374). Craig et al. (2007) used XRF to characterize Peruvian obsidians, and they analyzed three obsidian specimens from known sources "at the beginning and end of the [analytical sessions] to assure stability of the system and monitor instrument drift as well as to determine the precision" (2016). To source Californian obsidians with LA-ICP-MS, Eerkens et al. (2008) analyzed a certain obsidian specimen daily, and the results "showed excellent precision from day to day" (672). Gratuze (1999) used LA-ICP-MS to analyze Anatolian and Aegean obsidian, and the precision for each element was determined from 20 analyses on a particular specimen over a period of one week (874).

6.2.3 - Theoretical Precision of EMPA

The precision of EMPA depends on counting statistics (i.e., the numbers of X-ray counts from the standards and specimens) and instrument stability (i.e., reproducibility of the WD spectrometer mechanisms, stability of beam position on the specimen). For low X-ray counts, counting statistics prevail in determining precision. For high X-ray counts, the reproducibility of the instrument prevails. Beaman and Isasi (1972:50) point out that, theoretically at least, "precision well below 1 percent is possible (0.1 percent at 100 s and 0.5 percent at 10 s)… [but] the production of small errors (0.5 to 1 percent) has become a real source" of imprecision. Fortunately, like accuracy, EMPA precision has improved as instrument stability and electronics have improved. The minimum obtainable precision is 0.5% relative for elements at concentrations above 10 wt % in a specimen. For elements at concentrations between 1 and 10 wt % in a specimen, a precision of 1 to 3% relative is attainable (1972:56). Below concentrations of 1%, the precision worsens as X-ray counts decrease (56). As the X-ray peak counts approach the X-ray background counts for trace elements, precision worsens. For trace elements, the only way to increase precision is to increase the measured X-ray counts by (i) increasing the counting time, (ii) increasing the number of X-rays generated, or (iii) increasing both. For major elements, precision may be improved by ensuring stability and calibrations over time.

6.2.4 - Assessing Precision in the Present Research

I analyzed a specimen of obsidian from Yellowstone National Park (Smithsonian Standard VG-568, USNM Specimen #72854) multiple times with each batch. As a result,

the specimen was analyzed more than 600 times over a period of 16 months between July 2008 and November 2009. During this period, the analyst, the procedures, the instrument and its location, and the basic conditions remained constant. Over 16 months, however, a few conditions are bound to change somewhat: the electron gun filaments break and must be replaced every month or two; the electron optical system is disassembled, cleaned, and realigned every six months; the detector gas measure and mixture varies slightly; etc. All of these factors affected the precision. The data can be found in Table 6.1, including the relative standard deviation (standard deviation / mean × 100%) as a measure of precision. The precision for major elements (> 10 wt %) was better than 1% relative. For the minor elements (0.1 - 10 wt %), the precision was better than 5% relative, except for iron (which was still better than 10% relative). For the trace elements (< 0.1 wt %), the precision was at least 10% relative and worsened as the concentrations decreased. These results suggest that precision becomes poor below the 100-ppm level. Therefore, I concluded that EMPA indeed has enough precision for major and minor elements as well as some trace elements (particularly those above 100 ppm) for obsidian sourcing.

6.3 - Accuracy

Any particular obsidian sourcing study does not actually need accurate analyses if its data are precise and internally consistent. Accuracy is essential, though, if one wishes to use the data from one study with data from another study. In comparison to precision, accuracy is harder to define and, for a particular study, to determine. Therefore, accuracy is the second concept from Hughes' (1998) framework that I consider.

Table 6.1 - Precision Based on an Obsidian Reference Specimen

	n > 600 ‡		*% RSD* †			
			major	minor	trace	
	mean	*std dev*	> 10 wt%	10 - 0.1 wt%	0.1 % - 100 ppm	< 100 ppm
SiO_2	76.905	0.353	0.46			
Al_2O_3	12.031	0.103	0.86			
K_2O	5.008	0.075		1.5		
Na_2O	3.679	0.151		4.1		
FeO(T)	1.122	0.110		9.8		
CaO	0.433	0.016		3.7		
Cl	0.098	0.011			11	
TiO_2	0.075	0.009			12	
MgO	0.030	0.005			17	
MnO	0.022	0.008			36	
P_2O_5	0.004	0.008				> 100
F	0.002	0.004				> 100
SO_3	0.001	0.008				> 100
Cr_2O_3	0.000	0.009				> 100
Total	99.385	0.373				

Specimen: Rhyolitic Obsidian, Yellowstone National Park, Wyoming
Smithsonian Standard #VG-568, USNM Specimen #72854

Notes: † %RSD: Percent relative standard deviation = standard dev/mean × 100%
‡ Data acquired over 16 months between July 2008 and November 2009.

6.3.1 - Defining Accuracy

The *accuracy* of a specific measurement, as defined by NIST, is "closeness of the agreement between the result of a measurement" and the actual (or accepted) value of the quantity being measured (Taylor and Kuyatt 1994). Accuracy is commonly expressed as the percent relative error of a measurement (i.e., the difference between the measured and actual values divided by the actual value given as a percentage). In the second edition of their book *Statistics in Spectroscopy*, Howard Mark and Jerry Workman, both researchers familiar with spectrometry, state that assessing accuracy is challenging "because the usual statement of 'accuracy' compares the result obtained with 'truth'" (2003:214). They note that "'truth' is usually unknown, making this comparison difficult" (214). Thus, to assess the accuracy of my EMPA measurements on obsidian, I had to find ways to determine, or at least estimate, "true" element concentrations in my specimens.

6.3.2 - Approaches to Accuracy in Obsidian Sourcing

The consensus seems to be that accuracy should be checked against specimens of known compositions analyzed as an unknown; however, these specimens often vary from study to study. Acquafredda et al. (1999), using SEM-EDS in the Mediterranean, claimed to use "many reference materials (standards from Micro-Analysis Consultants Ltd.)" as a means to check accuracy (319). Glascock et al. (1999) explain that, at their NAA facility, NIST SRM #1633a (coal fly ash) is analyzed with each batch (865). With their ICP-AES of Mexican obsidian specimens, Fralick et al. (1998) also measured USGS standard SY-2

(syenite) with each run (1026). Eerkens et al. (2008) analyzed Californian obsidians with LA-ICP-MS, and "USGS andesite standard (AGV-2) was analyzed each day and showed good agreement" with published values (672). Gratuze (1999), who used LA-ICP-MS as well, analyzed NIST SRM #612 (trace elements in glass) for accuracy.

Some researchers have, though, analyzed obsidian standards to evaluate accuracy. At the Berkeley Geoarchaeological XRF Laboratory, USGS standard RGM-1 (obsidian) is analyzed with each run (e.g., Bayman and Shackley 1999, Negash and Shackley 2006, Craig et al. 2007). For NAA of Aegean obsidians, Arias et al. (2006) utilized NIST SRM #278 (obsidian) to check the accuracy. Bellot-Gurlet et al. (2005) explain that "accuracy [was] checked using international rock standards," including NIST SRM #278 (obsidian) and USGS standards RGM-1 (obsidian), BHVO-1 (basalt), and BIR-1 (basalt) (587). For XRF of North American obsidians, Anderson et al. (1986) checked their accuracy against a series of nine USGS standards, including RGM-1 (obsidian).

6.3.3 - Theoretical Accuracy of EMPA

The accuracy of EMPA depends on factors such as the suitability of the standards and choice of analytical conditions. For quantitative analyses, accuracy better than ±1% relative is attainable for major elements (Reed 2005:1). Goldstein et al. (1981) states that the accuracy is commonly about 1 to 2% relative (9), while Beaman and Isasi (1972) state that the accuracy should be 1 to 3% relative (6). Note that the older references cite worse accuracy. Accuracy has improved as microprobe stability and electronics have improved.

With a stable instrument and when one has investigated and minimized any experimental errors, an accuracy of 1 to 2% relative is attainable for elements heavier than Na ($Z > 10$) and with concentrations above 10 wt % in the specimen. For light elements (i.e., $Z \leq 10$), an accuracy of about 5 to 10% relative should be expected (Goldstein et al. 1981:9). For elements at concentrations between 1 and 10 wt % in a specimen, an accuracy of 1 to 5% relative is attainable for many specimens. Below a concentration of 1 wt %, the accuracy worsens as concentrations decrease, largely due to counting statistics.

6.4 - Assessing Accuracy in the Present Research

To establish the accuracy of the EMPA data using my procedures, as discussed in Chapter 5, I sought various ways to compare my results to other data sets, some of which could be considered "true" values for the elemental concentrations whereas others simply offered another data set for comparison. Hughes (1998) reports the two main approaches:

> Generally speaking, reliability in obsidian sourcing research can be measured by the extent to which (1) the measurements obtained correspond, within specified limits of analytical uncertainty, to values recommended for international rock standards and (2) the values subsequently obtained agree with values determined using the same, or different, instrumentation at another laboratory. (108)

I started my assessment of accuracy with the former approach, briefly outlined in Section 6.3.2, most frequently used in obsidian sourcing: analyzing a well-characterized material, particularly a glass or rock standard from an internationally recognized body like NIST or the USGS, as an unknown (rather than used as a calibration standard). In later sections, I discuss my endeavors to assess accuracy using the latter approach.

6.4.1 - Analyzing Standard Materials as Unknowns

To assess the major elements, I analyzed an obsidian specimen from Yellowstone National Park (Smithsonian Standard VG-568, USNM Specimen #72854) multiple times for each round. The results of these analyses are found in Table 6.2. This table includes three sets of published compositions for VG-568: (1) Jarosewich et al. (1980), working at the Smithsonian Institution three decades ago and published in *Geostandards Newsletter*; (2) Streck and Wacaster (2006), working at Oregon State University's EMPA facility and published in the *Journal of Volcanology and Geothermal Research*; and (3) Rowe et al. (2008), working at and published by the USGS. I also calculate the percent relative error with respect to the mean values from these published analyses.

Despite being acquired over thirty years ago, the compositional data in Jarosewich et al. (1980) are considered the "official" values by the Smithsonian Institution. Some of these values, however, seem suspect when compared to my own analyses as well as those of Streck and Wacaster (2006) and Rowe et al. (2008). For example, TiO_2 is reported at a concentration of 0.12 wt% in Jarosewich et al. (1980). Streck and Wacaster (2006) report 0.08 ± 0.03 wt% TiO_2, Rowe et al. (2008) report 0.08 ± 0.01 wt% TiO_2, and I measured a TiO_2 concentration of 0.075 ± 0.009 wt% (which would round to 0.08 ± 0.01 wt%) in this standard. The MnO concentration reported in Jarosewich et al. (1980) -- 0.30 wt% -- also is suspect. Streck and Wacaster (2006) report 0.02 ± 0.02 wt% MnO, Rowe et al. (2008) report 0.02 ± 0.02 wt% MnO, and I measured a MnO concentration of 0.022 ± 0.008 wt% (which would round to 0.02 ± 0.01 wt%). On the other hand, the NaO_2 values in Rowe et

Table 6.2 - Analyses of an International Obsidian Reference Specimen

Specimen: Rhyolitic Obsidian, Yellowstone National Park, Wyoming; Smithsonian Standard #VG-568, USNM Specimen #72854

	Frahm		**Jarosewic et al. 1980‡**	**Streck and Wacaster 2006†**		**Rowe et al. 2008****		**Published values including Jarosewic et al. 1980**		**Published values excluding Jarosewic et al. 1980**	
	n > 600 *		n = ?	n = 9		n = 17					
	mean	*std dev*	*mean*	*mean*	*std dev*	*mean*	*std dev*	*mean*	*rel error %*	*mean*	*rel error %*
SiO_2	76.905	0.353	76.71	76.96	0.53	76.55	0.67	76.74	*0.2%*	76.76	*0.2%*
TiO_2	0.075	0.009	0.12	0.08	0.03	0.08	0.01	0.09	*20%*	0.08	*6.3%*
Al_2O_3	12.031	0.103	12.06	12.17	0.12	12.44	0.19	12.22	*1.6%*	12.31	*2.2%*
Cr_2O_3	0.000	0.009	-	-	-	-	-	-	-	-	-
FeO(T)	1.122	0.110	1.23	1.08	0.05	1.11	0.07	1.14	*1.6%*	1.10	*2.5%*
MnO	0.022	0.008	0.30	0.02	0.02	0.02	0.02	0.11	*81%*	0.02	*10%*
MgO	0.030	0.005	< 0.10	0.03	0.02	0.03	0.02	0.03	*0.0%*	0.03	*0.0%*
CaO	0.433	0.016	0.50	0.45	0.03	0.39	0.02	0.45	*3.1%*	0.42	*3.1%*
Na_2O	3.679	0.151	3.75	3.52	0.11	3.51	0.24	3.59	*2.4%*	3.52	*4.7%*
K_2O	5.008	0.075	4.89	4.93	0.2	4.91	0.13	4.91	*2.0%*	4.92	*1.8%*
P_2O_5	0.004	0.008	< 0.01	0.00	0.01	0.01	0.01	0.01	*20%*	0.01	*20%*
F	0.002	0.004	-	-	-	-	-	-	-	-	-
SO_3	0.001	0.008	-	0.002	0.002	0.00	0.00	0.00	*0.0%*	0.00	*0.0%*
Cl	0.098	0.011	-	0.101	0.005	0.12	0.01	0.11	*11%*	0.11	*11%*
Total	99.385	0.373	99.44	99.31	0.64	99.18	0.92	99.31	*0.1%*	99.25	*0.1%*

* Data acquired over 16 months between July 2008 and November 2009.

‡ Jarosewich, Nelen, and Norberg, 1980, "Reference samples for electron microprobe analysis," *Geostandards Newsletter*, volume 4, pp. 43-47; these concentration values, acquired over thirty years ago, are considered the "official" values from the Smithsonian Institution.

† Streck and Wacaster, 2006, *Journal of Volcanology and Geothermal Research*, vol. 157, pp 236-253.

** Rowe, Thornber, Gooding, and Pallister, 2008, U.S. Geological Survey Open File Report 2008-1131; acquired during six sessions over six weeks.

al. (2008) and Streck and Wacaster (2006) might be low due to alkali migration under the electron beam, and the Al_2O_3 value seems high in Rowe et al. (2008).

I calculated the percent relative error with respect to the mean published values, both including and excluding Jarosewich et al. (1980). As noted in Section 6.3.3, one can expect an accuracy of 1 to 2% relative for elements above 10 wt % in the specimen. The SiO_2 (36 wt% Si) had a relative error of 0.2%, much better than anticipated. For elements between 1 and 10 wt % in a specimen, an accuracy of 1 to 5% relative was expected. The Al_2O_3 (6.5 wt% Al) had a relative error of about 2%, K_2O also had an error of 2%, FeO(T) had an error of 1.5 to 2.5%, and Na_2O had an error of 2.4 to 4.7%. Below a concentration of 1 wt %, accuracy worsens. When the data in Jarosewich et al. (1980) are excluded, the error, even for the trace elements, does not surpass 20% relative. Therefore, based on the analyses of VG-568, I considered the major-element data accurate.

To assess the trace elements, I analyzed two artificial glass standards: NIST SRM #610 (trace elements in glass; containing Zr, Nb, Ga, Zn, Ba, and Ce at roughly 450 ppm) and Corning 951RX glass (USNM #117085; containing different amounts of Zr, Zn, and Ba). My analyses of the glass standards are found in Table 6.3. Eight sets of published values are available for SRM #610, and these data are included in the table. I calculated relative errors based on the averages of these published values, and the error ranges from 3% relative (Zn) to 31% relative (Ba), with the rest about midway (13% for Ce, 16% for Zr, 17% for Nb, and 18% for Ga). For 951RX, the error was even lower: less than 1% for

Table 6.3 - Trace-Element Analyses of Standard Materials

NIST SRM #610: Trace Elements in Glass

	Zr	Nb	Ga	Zn	Ba	Ce
	0.0555	0.0519	0.0330	0.0487	0.0466	0.0588
	0.0536	0.0474	0.0359	0.0486	0.0585	0.0524
	0.0485	0.0548	0.0366	0.0513	0.0612	0.0433
	0.0548	0.0545	0.0342	0.0464	0.0537	0.0514
	0.0511	0.0550	0.0342	0.0507	0.0573	0.0459
	0.0529	0.0460	0.0375	0.0431	0.0599	0.0442
	0.0467	0.0554	0.0369	0.0455	0.0566	0.0597
	0.0482	0.0529	0.0352	0.0437	0.0569	0.0474
	0.0531	0.0512	0.0364	0.0451	0.0530	0.0521
	0.0508	0.0531	0.0375	0.0449	0.0575	0.0480
Mean - EMPA	0.0515	0.0522	0.0357	0.0468	0.0561	0.0503
St Dev	0.0030	0.0032	0.0015	0.0029	0.0042	0.0057
Dulski 2001	0.0456	-	-	-	0.0452	0.0456
Gao et al. 2002	0.0439	0.0420	0.0437	0.0455	0.0425	0.0448
Hollocher & Ruiz 1995	0.0444	-	0.0433	0.0428	0.0420	0.0431
Nebel et al. 2009	0.0447	-	-	-	-	-
Pearce et al. 1997	0.0440	0.0420	0.0438	0.0456	0.0424	0.0448
Reed 1992 (NIST)	-	-	-	0.0433	-	-
Rocholl et al. 1997	0.0423	0.0497	0.0425	0.0505	0.0412	0.0444
Rocholl et al. 2000	0.0457	-	-	-	0.0431	0.0447
Mean - Published	0.0444	0.0446	0.0433	0.0455	0.0427	0.0446
Relative Error vs EMPA	16%	17%	18%	3%	31%	13%

Corning 95IRX Glass: USNM #117085

	Zr	Nb	Ga	Zn	Ba	Ce
	0.5190	0.0001	-0.0010	0.6395	0.0168	0.0005
	0.5232	0.0042	0.0006	0.6495	0.0161	0.0065
	0.5285	0.0016	0.0016	0.6386	0.0132	0.0016
	0.5239	0.0000	0.0007	0.6406	0.0104	0.0025
	0.5232	0.0061	-0.0002	0.6431	0.0196	-0.0053
	0.5374	0.0023	-0.0003	0.6414	0.0083	-0.0035
	0.5234	0.0031	0.0030	0.6634	0.0167	-0.0030
	0.5272	0.0005	0.0017	0.6502	0.0186	-0.0070
	0.5214	0.0000	0.0013	0.6483	0.0207	0.0039
	0.5194	0.0049	0.0004	0.6319	0.0119	-0.0061
Mean - EMPA	0.5247	0.0023	0.0008	0.6447	0.0152	-0.0010
St Dev	0.0054	0.0022	0.0012	0.0087	0.0041	0.0046
Corning/CalTech	0.5800	-	-	0.6300	-	-
Carpenter et al. 2002	0.5840	-	-	0.6321	0.0152	-
Mean - Published	0.5820	-	-	0.6311	0.0152	-
Relative Error vs EMPA	10%	-	-	2%	0%	-

Ba at about 150 ppm, 2% for Zn, and 10% for Zr. Therefore, based on the analyses of the Corning 951RX glass, I considered the trace-element data accurate.

6.4.2 - Continuing the Accuracy Assessment

In a recent paper, Hancock and Carter (2010) point out that, "although analytical chemistry is not a democratic process, the agreement of specific elemental concentration data between (among) independent analytical techniques adds credibility to the relative accuracy of their numbers" (245). Therefore, I sought ways to compare my EMPA data to data from other analytical techniques, particularly techniques commonly used to source obsidian. In *Statistics in Spectroscopy*, Mark and Workman point out that accuracy often is evaluated using "round robins" and other interlaboratory comparisons (214). I utilized both of these approaches and first discuss analytical "round robins."

6.5 - Accuracy Assessment: Analytical "Round Robins"

In an analytical "round robin," pieces of a specimen (or specimens) are sent out to a number of laboratories to analyze, and the results are compiled and shared. It is usually assumed that, with a large number of participating laboratories using different techniques, the resulting average values represent a good approximation of "true" values. Individual laboratories can, in turn, use these values to assess their own procedures. I participated in an international round robin, involving basalt glass, during its course, and I also was able to test my procedures against Mexican obsidian specimens analyzed during a round robin in 1996. Both are discussed in the following two sections.

6.5.1 - A "Round Robin" of Basalt Glass Analyses

During the early stages of my present research, I participated in a proficiency test, called G-Probe-2, for analytical laboratories using microbeam techniques, such as EMPA, SEM-EDS, and LA-ICP-MS. This was an international "round robin" largely intended to assist the laboratories in assessing their data accuracy and to evaluate the current status of interlaboratory agreement. Sixty-four microanalytical laboratories (most of them EMPA) and seven facilities with bulk analytical techniques (ICP-MS, NAA, XRF) participated in this program. The University of Minnesota's Electron Microprobe Laboratory was one of the participants, and I was the analyst for the test. Analysts were instructed to use typical analytical conditions and strategies rather than to devote extraordinary time and attention beyond that used in routine analyses. I conducted these analyses well before deciding on the conditions and procedures that I used for my obsidian analyses. The specimen was a basalt glass (NKT-1G) prepared by the U.S. Geological Survey as a powdered and fused form of NKT-1 (peralkaline basalt that occurs near Knippa, Texas).

Table 6.4a shows the results from about half of the EMPA labs, and Tables 6.4b and 6.4c show the results from all of the LA-ICP-MS labs and all of the SEM-EDS labs, respectively. These data were originally published in Potts et al. (2005). The three tables include the mean values calculated from all of the submitted data. For our purposes here, I consider these mean values to be the "true" elemental concentration values. Table 6.4a also includes my measured values and the percent relative error for the elements based on the test-wide mean values. My data, compared to the "true" values, show good accuracy,

Table 6.4a - G-Probe-2 Selected Results for EMPA

	G-Probe-2	Frahm - UMN		Lab 1B	Lab 2B	Lab 3B	Lab 4B	Lab 5B	Lab 6B	Lab 7B	Lab 9B	Lab 10B	Lab 11B
	mean	*mean*	*rel error*	*EMPA*	*EMPA*	*EMPA*	*EMPA*	*EMPA*	*EMPA*	*EMPA*	*EMPA*	*EMPA*	*EMPA*
SiO_2	38.68	38.60	0.2%	38.36	38.29	38.87	38.55	38.71	39.50	37.23	38.50	38.51	39.46
TiO_2	3.95	3.96	0.3%	3.98	3.96	4.01	3.95	3.91	4.01	3.88	3.92	3.91	4.01
Al_2O_3	10.20	10.35	1.4%	10.18	10.16	10.07	10.42	10.08	10.07	10.16	10.48	10.48	10.75
FeO(T)	12.10	12.36	2.1%	12.14	12.13	12.32	12.32	12.12	12.15	13.03	12.36	12.45	12.06
MnO	0.21	0.19	10.5%	0.20	0.19	0.22	0.21	0.20	0.22	-	0.20	0.21	0.21
MgO	14.33	14.79	3.1%	14.38	14.12	14.33	14.13	14.28	14.38	13.99	14.88	14.85	14.66
CaO	13.21	13.43	1.6%	13.23	13.13	13.31	13.21	13.12	13.21	13.04	13.45	13.63	13.46
Na_2O	3.48	3.33	4.5%	3.48	3.37	3.48	3.50	3.59	3.43	3.32	3.33	3.46	3.55
K_2O	1.28	1.38	7.2%	1.19	1.26	1.29	1.26	1.33	1.27	1.27	1.24	1.24	1.34
P_2O_5	0.97	0.95	2.1%	0.48	0.92	0.94	0.97	1.06	0.97	-	-	-	1.04

	Lab 15B	Lab 18B	Lab 19B	Lab 22B	Lab 25B	Lab 26B	Lab 28B	Lab 31B	Lab 32B	Lab 33B	***All EMPA***		
	EMPA	*EMPA*	*EMPA*	*EMPA*	*EMPA*	*EMPA*	*EMPA*	*EMPA*	*EMPA*	*EMPA*	*mean*	*std dev*	*rel error*
SiO_2	38.18	38.42	38.81	39.46	40.12	38.33	38.94	38.77	38.44	37.94	38.67	0.63	0.0%
TiO_2	4.07	3.89	4.08	4.04	4.05	3.99	3.89	4.10	3.97	3.74	3.97	0.09	0.4%
Al_2O_3	10.29	10.38	10.15	10.15	10.83	9.29	10.10	10.32	10.04	10.88	10.26	0.34	0.6%
FeO(T)	12.12	12.21	12.09	12.31	12.16	12.12	11.95	12.54	12.28	11.58	12.22	0.28	1.0%
MnO	0.21	0.20	0.20	0.23	0.21	0.22	0.21	0.22	0.20	0.21	0.21	0.01	0.6%
MgO	14.43	14.56	14.51	14.42	14.28	14.50	14.32	15.08	14.20	14.03	14.42	0.29	0.6%
CaO	13.38	13.19	12.95	12.99	13.12	13.30	13.13	13.27	13.14	12.98	13.21	0.17	0.0%
Na_2O	3.44	3.56	3.53	3.60	3.29	3.52	3.48	3.76	3.43	3.78	3.50	0.13	0.4%
K_2O	1.26	1.32	1.31	1.32	1.32	1.31	1.29	1.27	1.17	1.22	1.27	0.05	0.5%
P_2O_5	1.06	0.97	0.98	0.91	1.01	0.98	0.96	0.97	0.99	1.01	0.95	0.13	1.7%

Table 6.4b - G-Probe-2 Results for LA-ICP-MS

	G-Probe-2	16B	17B	24B	36B	44B	49B	54B	*All LA-ICP-MS*		
	mean	*LA-ICP-MS*	*LA-ICP-MS*	*LA-ICP-MS*	*LA-ICP-MS*	*LA-ICP-MS*	*LA-ICP-MS*	*LA-ICP-MS*	*mean*	*std dev*	*rel error*
SiO_2	38.68	-	38	35.95	47.3	40.67	-	49.27	42.24	5.81	9%
TiO_2	3.95	-	3.85	4.17	-	3.94	-	3.43	3.85	0.31	3%
Al_2O_3	10.20	-	8.75	10.8	-	11.06	9.13	12.89	10.53	1.66	3%
FeO(T)	12.10	-	13	12.8	-	14.04	-	7.18	11.76	3.10	3%
MnO	0.21	0.16	0.27	0.22	-	0.22	-	0.16	0.20	0.05	2%
MgO	14.33	-	14	13.8	-	14.3	-	9.77	12.97	2.14	10%
CaO	13.21	-	14.5	-	7.63	13.99	13.20	-	12.33	3.18	7%
Na_2O	3.48	-	4.1	2.73	-	3.91	-	1.50	3.06	1.20	12%
K_2O	1.28	-	1.85	1.07	-	1.65	-	0.58	1.29	0.58	1%
P_2O_5	0.97	-	0.62	0.70	-	1.02	-	-	0.78	0.21	20%

Table 6.4c - G-Probe-2 Results for SEM-EDS

	G-Probe-2	23B	32B	47B	52B	57B	*All SEM-EDS*		
	mean	*SEM-EDS*	*SEM-EDS*	*SEM-EDS*	*SEM-EDS*	*SEM-EDS*	*mean*	*std dev*	*rel error*
SiO_2	38.68	38.47	38.44	39.19	38.55	35.25	37.98	1.56	2%
TiO_2	3.95	4.08	3.97	4.05	3.85	9.05	5.00	2.27	27%
Al_2O_3	10.20	9.75	10.04	10.15	10.09	7.3	9.47	1.22	7%
FeO(T)	12.10	12.04	12.28	11.77	12.17	17.36	13.12	2.38	8%
MnO	0.21	0.23	0.20	0.20	0.20	0.5	0.27	0.13	27%
MgO	14.33	14.31	14.20	15.10	14.35	11.47	13.89	1.40	3%
CaO	13.21	13.6	13.14	12.75	13.24	12.38	13.02	0.47	1%
Na_2O	3.48	3.72	3.43	3.31	3.42	2.54	3.28	0.44	6%
K_2O	1.28	1.25	1.17	1.27	1.25	0.50	1.09	0.33	15%
P_2O_5	0.97	1.02	0.99	0.96	0.98	1.43	1.08	0.20	11%

with relative errors of a few percent, or less, for the major and minor elements. The only trace element -- MnO at about 0.2 wt% -- had an error of 10% relative.

The tables also reveal that, at least for these elements, EMPA has better precision and accuracy than LA-ICP-MS and SEM-EDS. For the twenty EMPA laboratories listed, the maximum and minimum values for SiO_2 are 37.23% and 40.12% with an average and standard deviation of 38.67 ± 0.63%. For the only seven LA-ICP-MS laboratories listed, the maximum and minimum values for SiO_2 are 35.95% and 49.27% with an average and standard deviation of 42.24 ± 5.81%. For the five SEM-EDS facilities, the maximum and minimum values for SiO_2 are 35.25% and 39.19% with an average and standard deviation of 37.98 ± 1.56%. Similar patterns are seen for the other elements.

The G-Probe-2 test illustrates that EMPA has generally good accuracy, using even "routine" procedures, for vitreous geological specimens. It also demonstrates the amount of variation that might be encountered among laboratories using different procedures and analytical strategies. While insightful, this test has two principal shortcomings regarding the research at hand: (i) it did not involve laboratories that specialize in obsidian sourcing and that have established, hopefully well tested, procedures, and (ii) it did not involve my procedures, as described in Chapter 5, for obsidian characterization.

6.5.2 - A "Round Robin" of Obsidian Analyses

In 1996, Michael D. Glascock, the director of the Archaeometry Laboratory at the University of Missouri Research Reactor Center (MURR), organized an analytical "round

robin" in order to reveal the consistency (or a lack thereof) in obsidian characterization at laboratories involved in sourcing research. A call to participate in this "round robin" was announced in the *Bulletin of the International Association for Obsidian Studies* (Glascock 1996). Of the nine laboratories that responded, eight submitted data for a report compiled by Glascock (1999). The eight laboratories supplied ten datasets involving five analytical techniques: NAA, LA-ICP-MS, ICP-AES/MS, PIXE/PIGME, and XRF. Specimens from two well-known obsidian sources -- Sierra de Pachuca, Hidalgo, Mexico and Little Glass Buttes, Oregon -- were sent to each laboratory. Each of the participating laboratories also wrote up a summary of their analytical procedures for the report. Glascock (1999) shared the data "as is" and made "no evaluation or comments about the accuracy or precision of any particular laboratory or any of the analytical methods" (13).

Tables 6.5a and 6.5b give the results, as published in Glasock (1999), but edited to include only the elements I measured using EMPA. Some of the variations are notable. Consider the values reported for Mg in Sierra de Pachuca obsidian: 2100 ppm (Orleans), 844 ppm (Rome), 344 ppm (Rio), 326 ppm (Grenoble), and 286 ppm (Orleans) -- nearly a full order of magnitude separates the highest and lowest values. Also consider the values given for Ca in Sierra de Pachuca obsidian, ranging from 2362 ppm (Orleans) on the high end to 640 ppm (Rio, respectively) on the low end. For Little Glass Buttes obsidian, Mg follows the same basic pattern with the highest (3640 ppm) and lowest (501 ppm) values both from Orleans; however, Ca varies but much less dramatically.

Table 6.5a - Inter-comparison of analytical results for the obsidian source at Sierra de Pachuca, Hidalgo, Mexico from Glascock (1999)

	A	B	C	D	E	F	G	D	I	J
	MURR	Orleans	Orleans	Rio	Grenoble	Grenoble	ANSTO	Rome	Ashe Analytics	NW Research
	INAA	FNAA	LA-ICP-MS	ICP-AES/MS	ICP-AES/MS	PIXE	PIXE/PIGME	XRF	XRF	XRF
Element	n = 5	n = 2	n = 3	n = 1	n = 3	n = 7	n = 3	n = 1	n = 1	n = 1
F (ppm)							2850 ± 190			
Mg (ppm)		2100 ± 600	286 ± 6	344	326 ± 1			844		
Na (%)	3.80 ± 0.09	4.45 ± 0.40	3.76 ± 0.17	3.91	3.92 ± 0.07	3.83 ± 0.08	4.53 ± 0.27	3.74		
Al (%)		6.19 ± 0.04	6.51 ± 0.22	6.52	5.52 ± 0.21	6.06 ± 0.04	6.57 ± 0.35	5.78		
Si (%)		34.3 ± 0.3	35.2 ± 0.1			35.7 ± 0.05	36.2 ± 2.0	35.3		
P (ppm)			196 ± 1		26 ± 1					
Cl (ppm)	1460 ± 150					1647 ± 116				
K (%)	3.78 ± 0.24	4.23 ± 0.06	3.46 ± 0.03	3.69	3.11 ± 0.07	3.39 ± 0.03	3.83 ± 0.17	3.47		
Ca (ppm)		1160 ± 240	2362 ± 105	640	750 ± 11	769 ± 5	894 ± 31	786		
Ti (ppm)		1300 ± 60	1190 ± 7	1050	1049 ± 22	1028 ± 29	1118 ± 65	1258		1141 ± 96
Mn (ppm)	1149 ± 20	990 ± 140	1048 ± 4	837	1231 ± 50	1006 ± 24	1265 ± 85	1161	1095 ± 70	1124 ± 48
Fe (%)	1.58 ± 0.02	1.72 ± 0.10	1.66 ± 0.01	1.66	1.62 ± 0.06	1.56 ± 0.02	1.81 ± 0.12	1.89	1.64 ± 0.11	1.72 ± 0.08
Zn (ppm)	191 ± 12	240 ± 2	219 ± 2	206		221 ± 4	292 ± 19		224 ± 14	224 ± 6
Ga (ppm)				30.5		29 ± 1				
Zr (ppm)	888 ± 40	1020 ± 5	1058 ± 143	796	1005 ± 12	1008 ± 13	1097 ± 92	1055	991 ± 35	965 ± 9
Nb (ppm)		91 ± 1	116 ± 9	63. 8	91.2 ± 0.9	97 ± 13		91	91.2 ± 3.8	99 ± 2
Ba (ppm)	30 ± 12	21 ± 6	9.3 ± 0.6	12.6	16.6 ± 3.8				20 ± 9	14 ± 14
Ce (ppm)	92.0 ± 1.6	93 ± 2	91 ± 3	90	92.7 ± 0.6				133 ± 13	

Table 6.5b - Inter-comparison of analytical results for the obsidian source at Little Glass Buttes, Oregon from Glascock (1999)

	A	B	C	D	E	F	G	H	I	J
	MURR	Orleans	Orleans	Rio	Grenoble	Grenoble	ANSTO	Rome	Ashe Analytics	NW Research
	INAA	FNAA	LA-ICP-MS	ICP-AES/MS	ICP-AES/MS	PIXE	PIXE/PIGME	XRF	XRF	XRF
Element	n = 5	n = 2	n = 3	n = 1	n = 3	n = 7	n = 3	n = 1	n = 1	n = 1
F (ppm)							357 ± 8			
Mg (pprn)		3640 ± 1690	501 ± 15	656	603 ± 16			1266		
Na (%)	2.84 ± 0.06	3.34 ± 0.08	2.97 ± 0.07	2.92	2.83 ± 0.06	2.85 ± 0.07	3.35 ± 0.14	2.86		
Al (%)		7.03 ± 0.20	7.09 ± 0.11	7.74	7.08 ± 0.19	6.98 ± 0.03	7.45 ± 0.34	6.67		
Si (%)		34.9 ± 0.1	35.6 ± 0.1			36.0 ± 0.05	38.6 ± 0.8	35.9		
P (ppm)			244 ± 3	45.3	74 ± 5			87		
Cl (ppm)	113 ± 29									
K (%)	3.52 ± 0.16	3.90 ± 0.05	3.43 ± 0.05	3.6	3.15 ± 0.06	3.24 ± 0.03	3.57 ± 0.02	3.44		
Ca (ppm)		5900 ± 30	6813 ± 69	5432	6219 ± 246	5565 ± 97	6230 ± 50	5933		
Ti (ppm)		690 ± 25	595 ± 5	600	527 ± 34	786 ± 36	691 ± 16	659		570 ± 97
Mn (ppm)	327 ± 6	297 ± 30	269 ± 5	303	333 ± 10	291 ± 11	357 ± 9	387	298 ± 13	349 ± 47
Fe (%)	0.62 ± 0.01	0.65 ± 0.03	0.684 ± 0.028	0.61	0.650 ± 0.036	0.607 ± 0.011	0.702 ± 0.023	0.79	0.573 ± 0.015	0.66 ± 0.08
Zn (ppm)	31 ± 7	90 ± 3	26.5 ± 0.5	29.3		27 ± 2	36 ± 1		24.2 ± 2.6	41 ± 7
Ga (ppm)				15.9		15 ± 2				
Zr (ppm)	118 ± 7	99 ± 10	83 ± 7	106	106 ± 2	105 ± 8	107 ± 3	105	96.3 ± 2.6	109 ± 8
Nb (ppm)		12 ± 1	9.1 ± 0.1	7.88	7.92 ± 0.10			8	7.1 ± 1.2	8 ± 2
Ba (ppm)	1270 ± 20	1550 ± 130	1080 ± 2	843	1237 ± 14				1270 ± 13	1338 ± 14
Ce (ppm)	48.4 ± 1.0	46 ± 2	43 ± 1	48.5	49.7 ± 0.6				50 ± 7	

In early 2009, Glascock sent me obsidian specimens from Sierra de Pachuca and a new XRF dataset, recently acquired by MURR researchers, for the source. I analyzed the Sierra de Pachuca specimens using the same procedures that I used for my Anatolian and Transcaucasus obsidian specimens. This was done entirely without consulting the data in Glascock (1999) or the recent XRF data so that it was basically a blind test. I reformatted the data from Glascock (1999) for Table 6.6 and added my own EMPA data and the new XRF data. Then I calculated mean values based on the elemental concentrations reported by the eight laboratories, and I gauged the relative error of my measurements with respect to those mean values. My EMPA data, compared to the means and standard deviations of the compiled values, show favorable agreement. The relative error for my MgO and CaO data initially seem high; however, recall the extreme variability in the reported values for those two elements, making any comparisons problematic. A few other comparisons also are ambiguous. For example, F was only measured by one laboratory, and P_2O_5 had two differing means (450 ppm versus 60 ppm) from two facilities. Various elements, though, have an error of 5% relative or less: SiO_2, TiO_2, Al_2O_3, FeO, MnO, K_2O, and Zr. Even the two trace elements with concentrations in the low three-digit-ppm range (Nb at about 100 ppm and Zn at about 300 ppm) have only about 30% relative error.

6.5.3 - Strengths and Weakness of "Round Robins"

One strength of analyzing a specimen (or two) in analytical "round robins" is that one expects the accuracy of the cumulative result from all participating laboratories to be

Table 6.6 - Inter-laboratory comparison of analytical results for the obsidian source at Sierra de Pachuca, Hidalgo, Mexico

	Frahm EMPA			Overall Results				MURR INAA		MURR XRF		Orleans FNAA		Orleans LA-ICP-MS	
	mean	std dev	rel error	mean	std dev	max	min	mean	std dev	mean	std dev	mean	std dev	mean	std dev
SiO_2	75.7	0.4	0.1%	75.6	1.5	77.4	73.4					73.4	0.6	75.3	0.2
TiO_2	0.189	0.010	1%	0.19	0.02	0.22	0.16			0.158	0.024	0.217	0.010	0.198	0.001
Al_2O_3	11.30	0.07	3%	11.65	0.77	12.42	10.43					11.70	0.08	12.30	0.42
FeO (T)	2.17	0.03	1%	2.16	0.13	2.43	2.01	2.03	0.03	2.04	0.15	2.21	0.13	2.13	0.01
MnO	0.140	0.011	2%	0.14	0.02	0.16	0.10	0.148	0.003	0.103	0.008	0.128	0.018	0.135	0.001
MgO	0.052	0.005	60%	0.13	0.13	0.35	0.05					0.348	0.099	0.047	0.001
CaO	0.105	0.019	29%	0.15	0.08	0.33	0.09					0.162	0.034	0.330	0.015
Na_2O	5.02	0.30	7%	5.38	0.42	6.11	5.04	5.12	0.12			6.00	0.54	5.07	0.23
K_2O	4.63	0.09	5%	4.39	0.39	5.10	3.75	4.55	0.29	4.60	0.20	5.10	0.07	4.17	0.04
P_2O_5	0.003	0.009	-	0.03	0.03	0.04	0.01							0.045	0.000
F	0.002	0.004	-	0.29	0.02	0.29	0.29								
Cl	0.186	0.010	20%	0.16	0.01	0.16	0.15	0.146	0.015						
Zr (ppm)	953	40	3%	985	84	1097	796	888	40	957	62	1020	5	1058	143
Nb (ppm)	124	29	31%	95	10	116	84			84	8	91	1	116	9
Ga (ppm)	46	16	-	28	4	31	23			23	2				
Zn (ppm)	291	31	29%	225	29	292	191	191	12	207	19	240	2	219	2
Ba (ppm)	37	35	-	18	7	30	9	30	12			21	6	9	1
Ce (ppm)	77	42	-	99	17	133	90	92	2			93	2	91	3

Table 6.6 - Inter-laboratory comparison of analytical results for the obsidian source at Sierra de Pachuca, Hidalgo, Mexico (continued)

	Rio	Grenoble		Grenoble		ANSTO		Rome	Ashe Analytics	NW Research
	ICP-AES/MS	ICP-AES/MS		PIXE		PIXE/PIGME		XRF	XRF	XRF
	n = 1	mean	std dev	mean	std dev	mean	std dev	n = 1	n = 1	n = 1
SiO_2				76.4	0.1	77.4	4.3	75.5		
TiO_2	0.175	0.175	0.004	0.171	0.005	0.186	0.011	0.210		0.190
Al_2O_3	12.32	10.43	0.40	11.45	0.08	12.42	0.66	10.92		
FeO (T)	2.13	2.08	0.08	2.01	0.03	2.33	0.15	2.43	2.11	2.21
MnO	0.108	0.159	0.006	0.130	0.003	0.163	0.011	0.150	0.141	0.145
MgO	0.057	0.054	0.000					0.140		
CaO	0.090	0.105	0.002	0.108	0.001	0.125	0.004	0.110		
Na_2O	5.27	5.28	0.09	5.16	0.11	6.11	0.36	5.04		
K_2O	4.45	3.75	0.08	4.08	0.04	4.62	0.20	4.18		
P_2O_5		0.006	0.000							
F						0.285	0.019			
Cl				0.165	0.012					
Zr (ppm)	796	1005	12	1008	13	1097	92	1055	991	965
Nb (ppm)	63. 8	91	1	97	13			91	91	99
Ga (ppm)	31			29	1					
Zn (ppm)	206			221	4	292	19		224	224
Ba (ppm)	13	17	4						20	14
Ce (ppm)	90	93	1						133	

better than the result from any one particular laboratory, meaning the result is, as close as is typically possible, the "true" concentration values for the specimen. Round robins also allow us to assess the accuracy and precision of different analytical techniques as a whole and compare them to other techniques. The weakness of round robins is that usually only one specimen, rarely two, is sent out and analyzed, so when inaccuracies are observed, it is difficult to generalize because any systematic error at a particular laboratory cannot be discovered in just one or two specimens. To identify systematic error, it is helpful to have comparative data for a series of specimens. As discussed in Section 1.4, XRF and NAA are the predominant analytical techniques in obsidian sourcing. Consequently, I sought to compare my EMPA data to data from these two technique for a large number of obsidians specimens so that I could have additional measures of my accuracy.

6.6 - Acquiring NAA and XRF Data for Comparison

Glascock (1998) explains "XRF and NAA have proven to be highly cost effective and, therefore, are the methods most frequently used to source artifacts" (19). Therefore, I decided that data sets from XRF and NAA would be best for assessing the accuracy of EMPA. Four comparative data sets, with specimens from obsidian collection areas in my own collection, comes from three sources: (1) the Max Planck Institute (using a reactor at the University of Mainz), (2) the Archaeometry Laboratory at the University of Missouri Research Reactor Center, and (3) the Materials Science Center, University of Wisconsin-Eau Claire. These four data sets and their usefulness for assessing accuracy are discussed

in the following sections. In addition, I was sent specimens of Mexican obsidian as a sort of "blind test" of my EMPA procedures for obsidian characterization.

Readers interested in information about XRF in general are directed to two recent books: Jenkins (1999) and Beckhoff et al. (2006). Those interested in current overviews of archaeological XRF applications are forwarded to Ferretti (2000), Moens et al. (2000), Pollard et al. (2007:101-109), and Pollard and Heron (2008:33-45). Readers interested in NAA are referred to Kruger (1971), De Soete et al. (1972), Keisch (1972), Friedlander et al. (1981), Ehmann and Vance (1991), and Alfassi (1990). Those interested in overviews of archaeological applications of NAA are directed to Neff (2000), IAEA (2003), Pollard et al. (2007:123-136), and Pollard and Heron (2008:50-56).

6.6.1 - NAA by the Max Planck Institute (NAA-MPI)

As I mentioned in Section 4.7.1, only 15 of the specimens collected by Rapp and Ercan were analyzed using NAA for a Master's thesis (Bassette 1994) at the Max Planck Institute in Heidelberg. Staff from the institute assisted Bassette with these analyses. The analyses were done at the TRIGA (Training, Research, Isotope, General Atomics) Reactor of the Institute of Nuclear Chemistry in either 1993 or 1994. I have not been able to find any other examples of obsidian analyses done at this facility. For the rest of this chapter, I will refer to this particular data set as the *NAA-MPI data*.

Bassette ground the obsidian specimens into fine powders, of which 200 mg each was analyzed using NAA and compared to two standards materials. These two standards

were USGS standard SDO (shale) and "TONY," an in-house clay standard. No obsidian standards or reference specimens were analyzed. Twenty-five elements were measured: Na, K, Sc, Cr, Fe, Co, Zn, As, Rb, Zr, Sb, Ba, Cs, La, Ce, Nd, Sm, Eu, Tb, Yb, Lu, Hf, Ta, Th, and U. Eight of these elements (Na, K, Cr, Fe, Zn, Zr, Ba, and Ce) were analyzed by EMPA in specimens from the same collection areas: CA03, CA04, CA07, CA08, CA10, CA11, CA12, CA14, CA15, CA20, CA21, CA22, and CA23. A little more information about the analytical procedure is available in Bassette (1994).

6.6.2 - NAA at the MURR Archaeometry Laboratory (NAA-MURR)

I sent 94 specimens from Armenia, Azerbaijan, Georgia, and Central and Eastern Anatolia to the Archaeometry Laboratory at the University of Missouri Research Reactor Center (MURR), led by Dr. Michael D. Glascock, for NAA. Glascock and his colleagues have considerable experience analyzing obsidian, particularly from the New World. They have analyzed 6000 geological specimens from 400 New World sources and about 25,000 obsidian artifacts. MURR is the best place to obtain NAA data for obsidian. I asked that they use their normal procedures for obsidian analyses. For the remainder of this chapter, I will refer to this particular data set as the *NAA-MURR data*.

Using two separate irradiation events, MURR can readily measure 28 elements in obsidian: Ba, La, Lu, Nd, Sm, U, Yb, Ce, Co, Cs, Eu, Fe, Hf, Rb, Sb, Sc, Sr, Ta, Tb, Th, Zn, Zr, Al, Cl, Dy, K, Mn, and Na. Of these, ten elements were duplicated in my EMPA analyses: Ba, Ce, Fe, Zn, Zr, Al, Cl, K, Mn, and Na. The obsidian specimens are usually

crushed into small fragments for NAA. About 100 mg of obsidian is needed for the short irradiation and about 150 to 200 mg for the longer irradiation, although MURR has been refining procedures to reduce this amount. The standard materials were National Institute of Standards and Technology (NIST) standard reference materials (SRMs) #688 (basalt), #1633a (fly ash), and #278 (obsidian). More information about MURR's procedures may be found in Ericson and Glascock (2004), in Glascock et al. (2007).

6.6.3 - EDXRF at the MURR Archaeometry Laboratory (EDXRF-MURR)

I sent also 133 specimens to the MURR Archaeometry Laboratory for EDXRF to compare to my EMPA results. There are two types of XRF: energy-dispersive (EDXRF) and wavelength-dispersive (WDXRF). Energy-dispersive (ED) spectrometers sort X-rays with respect to their energies. EDXRF systems acquire entire X-ray spectra quickly, but they suffer from overlapping X-ray peaks due to the poor resolution of ED spectrometers (130-180 eV) with respect to the "natural width" of X-ray peaks (2-10 eV). Glascock and his MURR colleagues have used EDXRF to analyze obsidian since 2001. For the rest of this chapter, I refer to this data set as the *EDXRF-MURR data*.

They used an ElvaX EDXRF system to measure eleven elements: K, Ti, Mn, Fe, Zn, Ga, Rb, Sr, Y, Zr, and Nb. Of these, eight of them were duplicated in my EMPA data: K, Ti, Mn, Fe, Zn, Ga, Zr, and Nb. The energy resolution is 180 eV, and the beam size on the specimen surface was roughly 3 × 4 mm. Each specimen was analyzed for 5 minutes. ElvaX proprietary software was used for spectra deconvolution and calculating elemental

concentrations. The obsidian specimens were of sufficient size to analyze whole, not as a powder (at least 8 mm across and 3 mm thick). Their standards were obsidian specimens, analyzed by multiple techniques, from North and South America in the MURR collection. For additional information regarding MURR's EDXRF procedures, readers are forwarded to Glascock et al. (2007) and Glascock et al. (2008).

6.6.4 - A "Blind Test" with NAA and XRF at MURR

At the same time I sent Near Eastern specimens to MURR, Michael Glascock sent me 36 specimens from 12 obsidian sources in Mexico. This series of obsidian specimens served as a sort of "blind test" because I was not familiar with the geology and chemistry of Mexican obsidian. Only after I had completed my EMPA analyses of these specimens did Glascock send me the corresponding NAA and EDXRF data.

6.6.5 - WDXRF at the University of Wisconsin-Eau Claire (WDXRF-UWEC)

In addition to the EDXRF-MURR data, I sought to compare my EMPA data with WDXRF data as well. WDXRF, unlike EDXRF, uses Bragg diffraction to sort the X-rays by their wavelengths. WD spectrometers are mechanically "tuned" to one wavelength at a time, and as a result, they have much better resolutions than ED spectrometers (about 5 eV versus 130-180 eV), meaning that fewer X-ray peaks overlap and that elements can be better identified and quantified. These analyses were conducted at the Materials Science Center at the University of Wisconsin-Eau Claire by my collaborators Giselle Conde and

Professor Phillip Ihinger as well as the laboratory manager, Jill Ferguson. The Materials Science Center houses a Bruker/Siemens SRS3000 WDXRF system. For the rest of this chapter, I will refer to this data set as the *WDXRF-UWEC data*.

I brought them 78 geological specimens: one from each of 78 different collection areas. There was sufficient material for major-element analyses of all specimens (800 mg of powdered obsidian) and for trace-element analyses of eight specimens (4 grams). The powders were prepared as fused disks or pressed pellets, which were ground flat and then polished. The major-element analyses included ten elements -- Na, Mg, Al, Si, P, K, Ca, Ti, Mn, Fe -- that were also analyzed using EMPA. The trace-element analyses included nineteen elements: Ba, Ce, Co, Cr, Cu, Hf, La, Nb, Nd, Ni, Pb, Rb, Sc, Sr, Th, V, Y, Zn, and Zr. Of the trace elements, I analyzed five of them -- Ba, Ce, Nb, Zn, and Zr -- using EMPA. Obsidian characterization was new to this laboratory.

For the calibration of the X-ray intensities, a set of Siemens XRF standards were used in addition to standards from the US Geological Survey (USGS), including AGV-2 (andesite), ALB-1 (albite), BHVO-1 and BHVO-2 (basalt), GSP-2 (granodiorite), MRG-1 (gabbro), QLO-1 (quartz latite), RGM-1 (obsidian; Glass Mountain in California), SY-3 and SY-4 (both syenite), and W-2 (diabase). Unlike the EDXRF-MURR data, for which the standards consisted of a series of obsidian specimens, these data were calibrated to a series of minerals and only one specimen of obsidian from California.

6.7 - Discussion of the NAA and XRF Data and EMPA Accuracy

In the previous sections, I explain how I obtained XRF and NAA data sets to help assess the accuracy of my EMPA data. In the following sections, I discuss these data sets and their usefulness (or, in some cases, lack thereof) for evaluating accuracy. These data sets are all independent, so agreement between them suggests good accuracy; however, if the data sets exhibit systematic differences, one (or both) has poor accuracy. Three of the four data sets -- NAA-MPI, NAA-MURR, and EDXRF-MURR -- exhibit good agreement with my EMPA data. The "blind test" with Mexican obsidians from MURR also suggests accurate EMPA data. One of the four data sets -- WDXRF-UWEC -- exhibited systematic differences with my EMPA data for the major elements, and a comparison to the literature values for a particular source -- the Kömürcü source of Göllü Dağ -- strongly suggest that my EMPA data are more accurate than the WDXRF-UWEC data.

6.7.1 - NAA-MPI and EMPA Accuracy

Table 6.7 shows the complete NAA-MPI data (from Bassette 1994:89-96) for the Rapp-Ercan collection. When my EMPA data from several of the collection areas -- for example, CA22 and CA23 -- are put beside the NAA-MPI data for the same ones, the two data sets show excellent agreement (Table 6.8). Note that there was one analysis of one specimen for each collection area in the NAA-MPI data, whereas there were ten analyses of nine specimens for each collection area in my EMPA data. Thus, sometimes the NAA-MPI data matches one or two of the specimens analyzed with EMPA rather than the mean

Table 6.7 - All NAA-MPI Data for Rapp/Ercan-Collected Specimens from Bassette (1994)

		CA03	CA04a	CA04b	CA07	CA08	CA10	CA11	CA12	CA14	CA15	CA20	CA21	CA22	CA23
Na	wt%	3.07	3.17	3.13	3.45	3.41	3.20	3.36	3.04	2.98	3.00	3.03	3.00	3.18	3.18
K	wt%	3.83	3.97	3.67	3.62	3.60	3.81	4.03	4.08	4.17	3.79	3.88	3.91	3.73	3.88
Fe	wt%	0.77	0.80	0.74	1.24	1.22	0.61	0.62	0.76	0.59	0.54	0.59	0.63	0.77	0.75
Sc	ppm	1.120	1.225	1.143	1.445	1.437	2.198	2.236	1.142	1.959	1.930	1.932	1.509	1.300	1.247
Cr	ppm	2.98	3.00	2.81	3.10	3.28	3.54	3.73	2.83	2.75	2.90	2.75	4.04	3.30	3.30
Co	ppm	0.46	0.39	0.41	0.78	0.79	0.40	0.19	0.43	0.23	0.18	0.21	0.24	0.96	0.48
Zn	ppm	39	24	38	56	51	35	38	41	15	22	17	30	26	24
As	ppm	6.6	6.9	6.9	6.5	6.6	11.7	13	6.8	8.9	8.4	7.7	6.6	7.1	7.1
Rb	ppm	172	164	169	153	154	231	265	174	197	182	189	132	161	150
Zr	ppm	99	101	108	194	188	87	83	114	60	75	80	79	120	121
Sb	ppm	0.66	0.60	0.69	0.64	0.62	1.16	1.29	0.67	0.90	0.93	0.83	0.65	0.99	0.74
Cs	ppm	8.71	8.48	8.88	7.70	7.65	13.70	15.40	8.72	9.25	8.80	7.47	5.56	7.63	7.32
Ba	ppm	326	306	323	457	457	6	5	317	89	85	199	736	554	521
Hf	ppm	3.88	3.67	3.93	5.21	5.19	4.01	4.22	3.92	3.11	3.03	3.36	2.89	3.88	3.51
Ta	ppm	2.57	2.46	2.66	2.37	2.36	3.92	4.44	2.60	2.78	2.70	2.79	1.82	2.03	1.84
Th	ppm	29.2	29.1	28.4	26.7	26.4	37.8	38.1	29.2	22.7	21.7	22.6	25.2	28.9	28.4
U	ppm	8.60	8.09	8.50	7.90	7.80	12.60	13.60	8.68	8.74	9.02	8.94	6.12	7.38	7.50
La	ppm	27.5	29.2	28.4	34.8	34.0	15.5	14.8	27.9	23.6	22.6	23.2	31.7	39.7	39.0
Ce	ppm	50.9	62.5	52.5	62.3	61.9	36.2	35.4	51.8	43.2	43.6	48.6	52.6	69.0	68.7
Nd	ppm	17.7	17.0	18.2	21.4	22.3	16.4	16.5	19.1	17.0	15.8	16.9	17.6	19.3	18.8
Sm	ppm	3.78	4.04	3.83	4.41	4.41	4.93	5.35	3.84	3.96	3.73	3.79	3.06	4.02	4.79
Eu	ppm	0.35	0.32	0.35	0.61	0.59	0.08	0.08	0.37	0.14	0.14	0.19	0.36	0.53	0.49
Tb	ppm	0.52	0.51	0.50	0.60	0.60	0.78	0.86	0.52	0.54	0.52	0.54	0.37	0.47	0.43
Yb	ppm	2.44	2.50	2.75	2.60	2.52	3.35	3.76	2.37	2.32	2.39	2.39	1.68	2.13	1.94
Lu	ppm	0.428	0.366	0.438	0.454	0.450	0.586	0.645	0.428	0.315	0.358	0.319	0.267	0.319	0.294

Table 6.8 - Example Comparisons of the NAA-MPI Data to the EMPA Data

NAA-MPI	Frahm										
CA22	**CA22-P1**	**CA22-P2**	**CA22-P3**	**CA22-R1**	**CA22-R2-A**	**CA22-R2-B**	**CA22-R2-C**	**CA22-R2-D**	**CA22-R2-E**	**CA22**	
n = 1	*n ≥ 10*	*n ≥ 10*	*n ≥ 10*	*n ≥ 10*	*n ≥ 10*	*n ≥ 10*	*n ≥ 10*	*n ≥ 10*	*n ≥ 10*	***mean***	***std dev***
4.29	4.03	4.13	4.15	4.21	4.22	4.31	4.24	4.12	4.28	**4.19**	**0.09**
4.49	4.62	4.58	4.53	4.38	4.60	4.36	4.56	4.67	4.38	**4.52**	**0.12**
0.99	1.04	1.02	1.02	0.97	0.98	1.00	0.99	0.98	1.02	**1.00**	**0.02**
5	-	-	11	15	-	3	-	-	-	**-**	**-**
26	28	24	17	45	72	68	80	12	32	**42**	**25**
120	131	138	141	134	132	140	117	135	143	**135**	**8**
554	590	590	602	600	596	584	611	601	576	**595**	**11**
69	81	111	48	107	75	112	107	69	61	**86**	**24**

NAA-MPI	Frahm										
CA23	**CA23-P1**	**CA23-P2-A**	**CA23-P2-B**	**CA23-P2-C**	**CA23-P2-D**	**CA23-P3-A**	**CA23-P3-B**	**CA23-P4-A**	**CA23-P4-B**	**CA23**	
n = 1	*n ≥ 10*	*n ≥ 10*	*n ≥ 10*	*n ≥ 10*	*n ≥ 10*	*n ≥ 10*	*n ≥ 10*	*n ≥ 10*	*n ≥ 10*	***mean***	***std dev***
4.29	4.12	4.04	4.16	4.15	4.11	3.99	3.91	4.11	4.28	**4.10**	**0.11**
4.68	4.74	4.57	4.61	4.62	4.61	4.51	4.39	4.63	4.54	**4.58**	**0.10**
0.96	0.80	0.86	0.84	0.89	0.85	0.83	0.82	0.86	0.90	**0.85**	**0.03**
5	-	40	-	-	-	22	-	14	-	**-**	**-**
24	31	48	36	44	41	67	27	45	21	**40**	**13**
121	124	132	144	136	129	136	80	117	134	**126**	**19**
521	581	605	598	580	601	601	490	603	600	**584**	**37**
69	88	84	73	95	31	108	42	78	60	**73**	**25**

for all for the specimens. Unfortunately, such data comparisons quickly revealed an issue with the NAA-MPI data: specimen-handling problems in Germany.

Throughout my research, I tracked which specimens had been retained by Rapp in Duluth for over a decade and which had been studied by Pernicka and his two students in Germany, as discussed in Section 4.7.1. The specimen numbers included a "R" or "P" to denote this. As Table 6.9 demonstrates, I had noticed, during the course of my analyses, that CA01-R1 matched CA02-P1 while CA01-P1 matched CA02-R1-A and CA02-R1-B. I initially attributed this mismatch to obsidian mixing in the field, as discussed in Section 4.5, that happened to coincide with the "R" and "P" subsets. Collection area CA01 was described by Rapp and Ercan as "river bed, 600 m W Çatköy" while CA02 was described as "river bed, 800 m W Çatköy.," so alluvial transport seemed likely. I noticed this same problem, however, for CA16 and CA17 -- as shown in Table 6.10, the CA16-P specimens match the CA17-R specimens and vice versa. This, too, could potentially be attributed to transport and mixing in the field. CA16 was described as "Bozköy, stream gravels" while CA17 was described as "S little Göllüdag" -- these are adjacent regions of Göllü Dağ, and one is explicitly a stream bed. It seemed, though, quite a remarkable coincidence that the mixing, if actually to blame, occurred only along "R" and "P" lines.

Comparison to NAA-MPI data revealed another issue. Table 6.11 shows that the NAA-MPI data for CA04 matches my data for CA05, not CA04, including both the "R" and "P" specimens. Similarly, the NAA-MPI data for CA14 matches my data for CA15, not CA14, again for both the "R" and "P" specimens. Somewhat differently, Table 6.13

Table 6.9 - Transposed CA01 and CA02 Specimens

		CA01-P1	CA01-R1	CA02-P1	CA02-R1-A	CA02-R1-B
SiO_2	*wt%*	75.92	75.36	74.95	76.12	76.16
TiO_2	*wt%*	0.026	0.073	0.090	0.029	0.030
Al_2O3	*wt%*	12.54	12.94	13.15	12.57	12.60
Cr_2O_3	*wt%*	-	0.001	-	-	-
FeO(T)	*wt%*	0.754	0.912	1.107	0.772	0.762
MnO	*wt%*	0.073	0.051	0.057	0.070	0.074
MgO	*wt%*	0.012	0.067	0.099	0.012	0.012
CaO	*wt%*	0.379	0.764	0.788	0.409	0.409
Na_2O	*wt%*	4.230	4.100	4.328	4.129	4.028
K_2O	*wt%*	4.310	4.873	4.651	4.359	4.303
P_2O_5	*wt%*	0.002	0.008	0.015	-	0.008
F	*wt%*	0.004	0.001	0.003	0.003	0.001
SO_3	*wt%*	-	0.001	-	0.002	-
Cl	*wt%*	0.073	0.124	0.125	0.080	0.081
Zr	*ppm*	80	121	143	75	82
Nb	*ppm*	65	71	55	76	99
Ga	*ppm*	47	50	64	49	50
Zn	*ppm*	88	92	37	81	73
Ba	*ppm*	36	343	435	53	37
Ce	*ppm*	-	72	119	-	-

Table 6.10 - Transposed CA16 and CA17 Specimens

		CA16-P1	CA16-R1	CA16-R2	CA17-P1	CA17-P2	CA17-R1-A	CA17-R1-B
SiO_2	*wt%*	76.67	76.45	75.97	76.77	76.73	76.97	77.03
TiO_2	*wt%*	0.056	0.050	0.049	0.057	0.053	0.057	0.056
Al_2O3	*wt%*	12.57	12.54	12.39	12.53	12.47	12.53	12.59
Cr_2O_3	*wt%*	-	-	-	-	-	-	0.002
FeO(T)	*wt%*	0.649	0.642	0.652	0.662	0.442	0.676	0.678
MnO	*wt%*	0.061	0.064	0.063	0.062	0.064	0.064	0.058
MgO	*wt%*	0.030	0.033	0.029	0.036	0.028	0.035	0.036
CaO	*wt%*	0.433	0.443	0.418	0.455	0.423	0.454	0.456
Na_2O	*wt%*	3.229	3.090	3.130	3.875	3.097	3.886	3.939
K_2O	*wt%*	5.929	6.000	5.962	4.598	5.882	4.635	4.708
P_2O_5	*wt%*	0.001	0.001	0.004	0.006	0.006	0.011	0.003
F	*wt%*	0.005	0.003	0.001	0.002	0.002	0.002	-
SO_3	*wt%*	0.002	-	0.002	-	-	-	0.003
Cl	*wt%*	0.099	0.097	0.096	0.094	0.088	0.098	0.101
Zr	*ppm*	94	77	88	78	79	82	73
Nb	*ppm*	86	105	94	81	111	91	72
Ga	*ppm*	56	47	61	46	58	50	44
Zn	*ppm*	49	68	45	17	34	34	29
Ba	*ppm*	94	92	95	166	92	167	164
Ce	*ppm*	80	85	37	80	86	91	80

Table 6.11 - Example of Bassette's (1994) Specimen Numbering Errors

		Bassette/NAA-MPI CA04 *specimens = 2* *analyses = 2*		Frahm - EMPA CA04 *specimens = 11* *analyses = 120*		Frahm - EMPA CA05 *specimens = 21* *analyses = 210*	
		mean	st dev	mean	st dev	mean	st dev
Na_2O	*wt%*	4.25	0.04	3.33	0.09	4.16	0.10
K_2O	*wt%*	4.60	0.26	5.99	0.06	4.58	0.05
FeO	*wt%*	0.99	0.05	0.58	0.08	1.07	0.07
Cr_2O_3	*ppm*	4	-	-	-	-	-
Zn	*ppm*	31	10	87	13	59	13
Zr	*ppm*	105	5	129	10	159	12
Ba	*ppm*	315	12	393	9	452	10
Ce	*ppm*	58	7	65	19	81	25

Table 6.12 - Example of Bassette's (1994) Specimen Numbering Errors

		Bassette	Frahm						Frahm					
		CA14	**CA14-P1**	**CA14-P2**	**CA14-R1-A**	**CA14-R1-B**	**CA14**		**CA15-P1**	**CA15-R1-A**	**CA15-R1-B**	**CA15-R2**	**CA15**	
		n = 1	*n ≥ 10*	*n ≥ 10*	*n ≥ 10*	*n ≥ 10*	***mean***	***std dev***	*n ≥ 10*	*n ≥ 10*	*n ≥ 10*	*n ≥ 10*	***mean***	***std dev***
Na_2O	*wt%*	**4.02**	4.13	4.10	3.98	3.97	**4.04**	**0.08**	4.01	3.92	4.00	3.99	**3.98**	**0.04**
K_2O	*wt%*	**5.02**	4.53	4.54	4.50	4.52	**4.52**	**0.02**	4.66	4.72	4.73	4.69	**4.70**	**0.03**
FeO	*wt%*	**0.76**	0.70	0.69	0.73	0.72	**0.71**	**0.02**	0.59	0.43	0.42	0.44	**0.47**	**0.08**
Cr_2O_3	*ppm*	**4**	1	3	-	-	-	-	-	-	-	-	-	-
Zn	*ppm*	**15**	43	47	47	36	**43**	**5**	27	42	35	14	**29**	**12**
Zr	*ppm*	**60**	82	78	86	80	**82**	**3**	80	72	71	82	**76**	**6**
Ba	*ppm*	**89**	461	488	451	433	**458**	**23**	88	67	89	67	**78**	**12**
Ce	*ppm*	**43**	108	122	105	90	**106**	**13**	41	68	70	82	**65**	**17**

Table 6.13 - Example of Bassette's (1994) Specimen Numbering Errors

		Bassette	Frahm				Frahm					
		CA08	**CA08-P1**	**CA08-P2**	**CA08-P**		**CA08-R1-A**	**CA08-R1-B**	**CA08-R1-C**	**CA08-R1-D**	**CA08-R**	
		n = 1	*n ≥ 10*	*n ≥ 10*	***mean***	***std dev***	*n ≥ 10*	*n ≥ 10*	*n ≥ 10*	*n ≥ 10*	***mean***	***std dev***
Na_2O	*wt%*	**4.60**	4.053	4.217	**4.13**	**0.12**	4.296	4.321	4.401	4.463	**4.37**	**0.08**
K_2O	*wt%*	**4.34**	4.379	4.219	**4.30**	**0.11**	4.471	4.451	4.434	4.423	**4.44**	**0.02**
FeO	*wt%*	**1.57**	0.797	0.736	**0.77**	**0.04**	1.157	1.227	1.166	1.252	**1.20**	**0.05**
Cr_2O_3	*ppm*	**5**	-	30	**-**	**-**	-	25	-	-	**-**	**-**
Zn	*ppm*	**51**	48	42	**45**	**5**	56	55	62	52	**56**	**4**
Zr	*ppm*	**188**	73	79	**76**	**5**	204	196	187	186	**193**	**8**
Ba	*ppm*	**457**	-	10	**-**	**-**	473	471	486	469	**475**	**8**
Ce	*ppm*	**62**	54	70	**62**	**11**	98	111	115	87	**103**	**13**

shows that the NAA-MPI data for CA08 matches my data for the CA08-R specimens but not the CA08-P specimens. The situation is just like the mismatches of CA01/CA02 and CA16/CA17 except NAA data is available for comparison. Mixing in the field was again possibile, but another perfect division between the "R" and "P" specimens is unlikely. It appears, given the NAA-MPI data, that several of the "P" specimens were mixed up after they were analyzed by NAA. Mixing in a laboratory, not the field, seems to be to blame. One wonders if this issue was noticed by the German researchers and that is why Bassette reports data for only 13 of the 31 collection areas available to him.

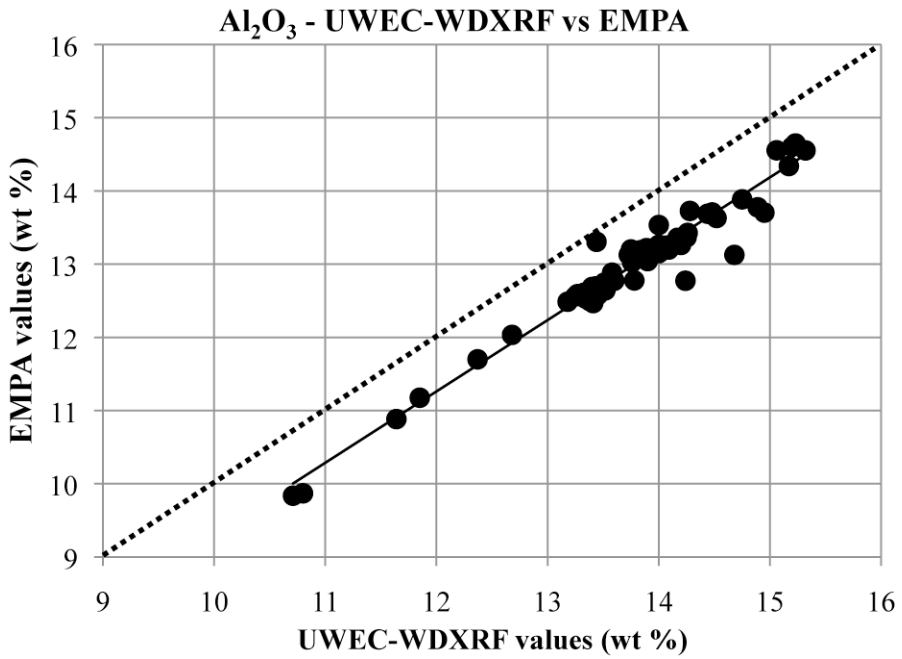
For the specimens that I can directly compare and be confident that there were no mix-ups, these data sets show excellent agreement. Because NAA and EMPA operate on entirely different physical principles (i.e., gamma-emission during radioactive decay after a nucleus captures an extra neutron versus characteristic X-ray emission after inner-shell ionization due to high-energy electron bombardment), these two analytical techniques are independent, so agreement of their data suggests good accuracy for both.

6.7.2 - WDXRF-UWEC and EMPA Accuracy

Figures 6.1a to 6.1j reveal how the WDXRF-UWEC and EMPA data compare. A few elements, like like Si and Mn (Figure 6.1i and j), show reasonably good agreement, but the other major elements show significant differences, especially Al, Na, and Mg. Fe shows marked variances between the data sets (Figure 6.1g), which I expected due to the differences between spot analyses of the glass (EMPA) and bulk analyses of the glass and

Figure 6.1a and b - UWEC-WDXRF Data vs EMPA Data for the Major Elements

a)



b)

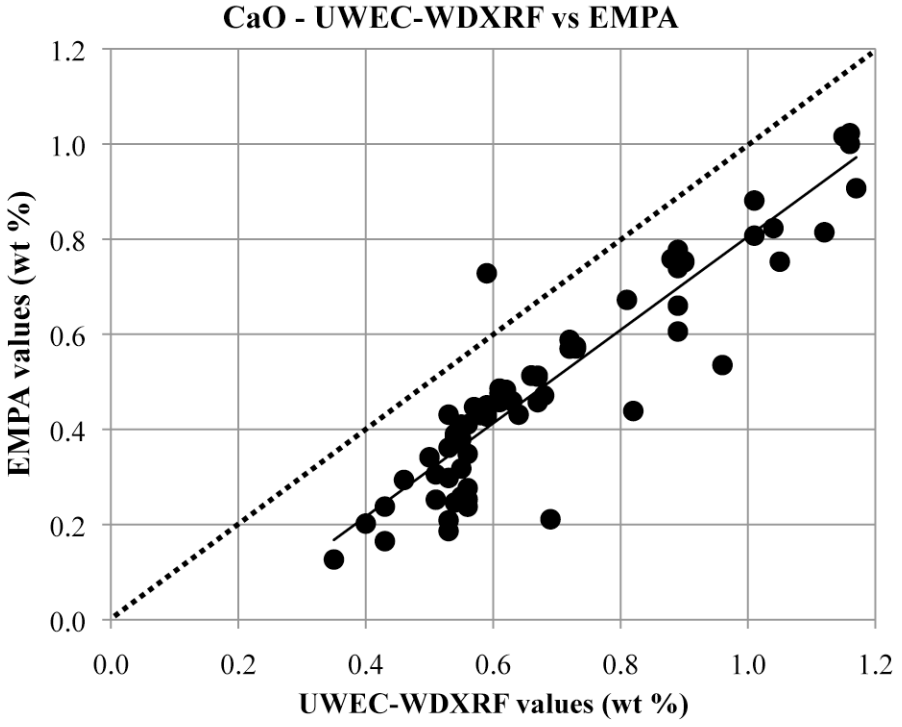
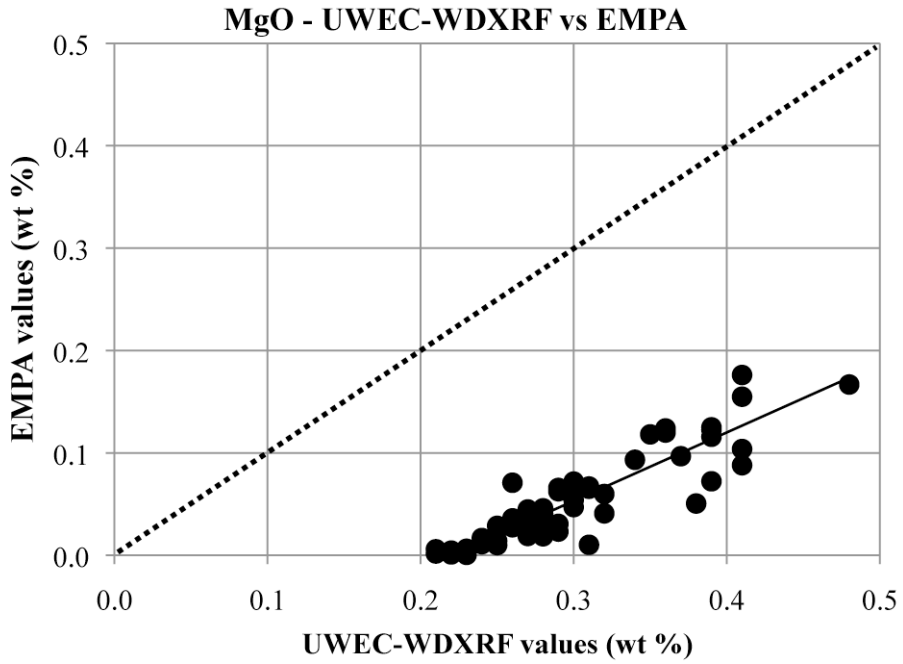


Figure 6.1c and d - UWEC-WDXRF Data vs EMPA Data for the Major Elements

c)



d)

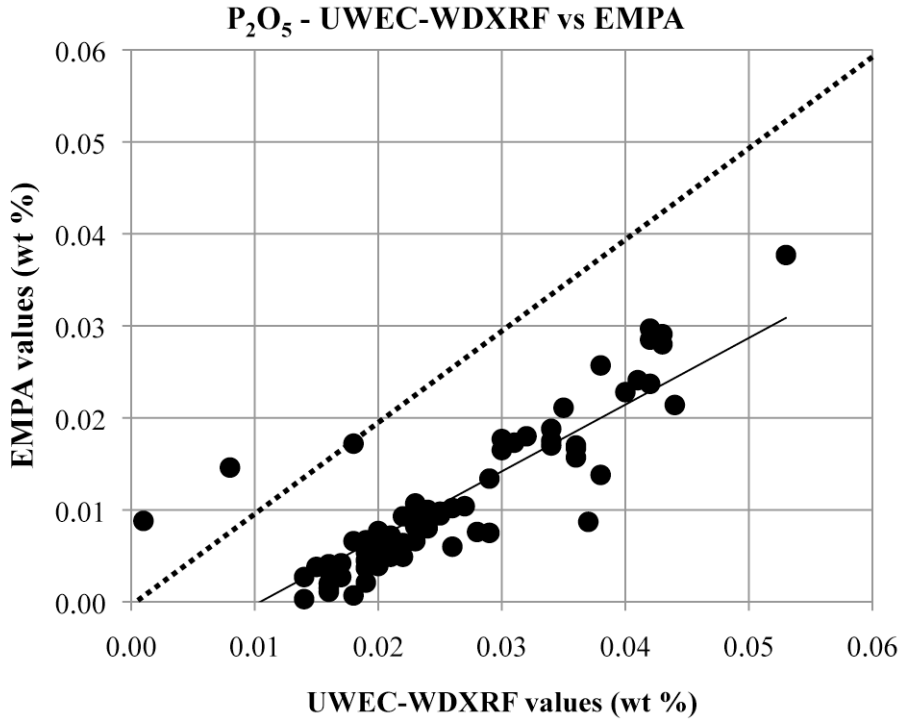
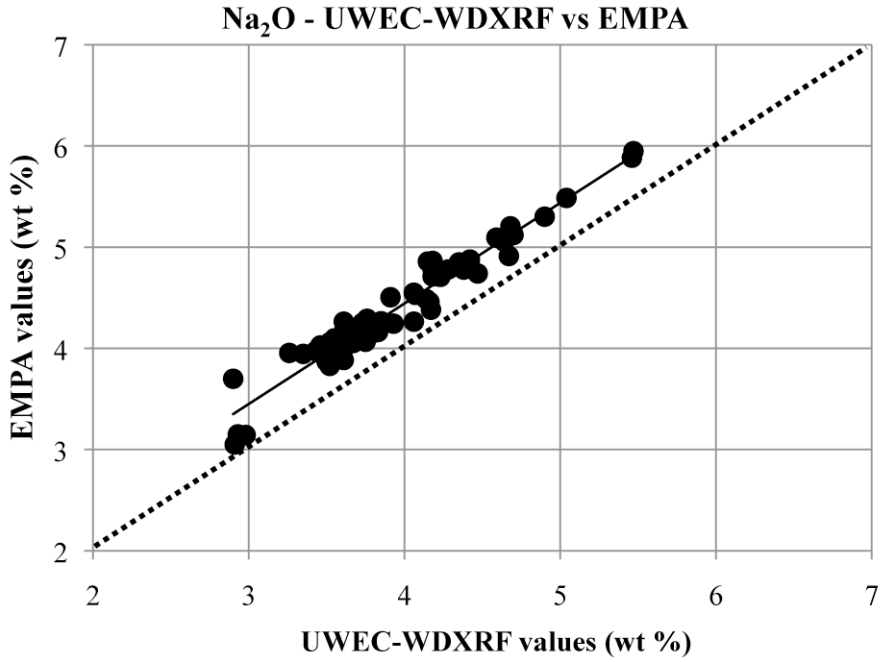


Figure 6.1e and f - UWEC-WDXRF Data vs EMPA Data for the Major Elements

e)



f)

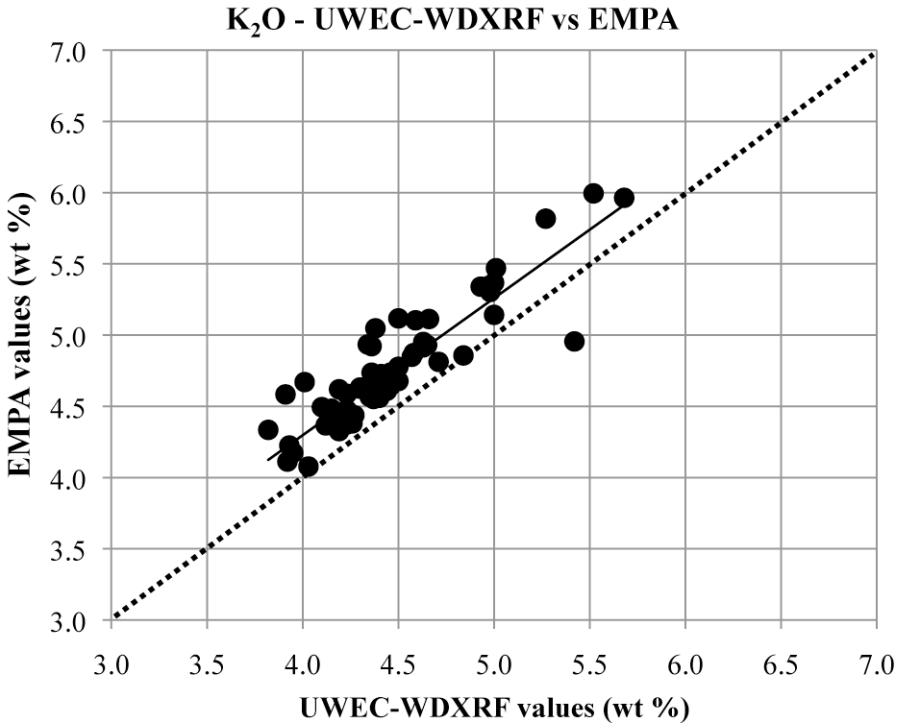
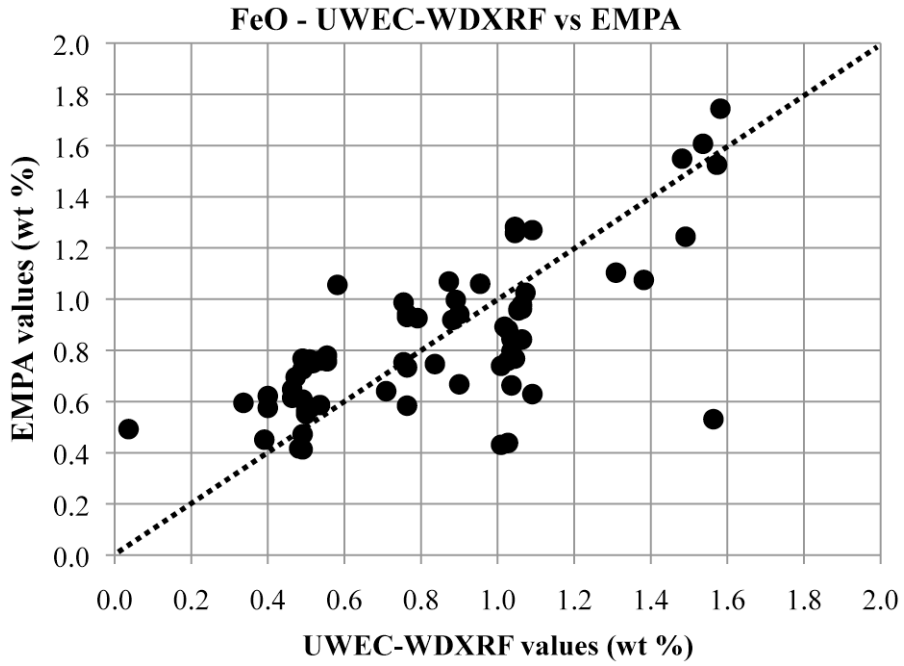


Figure 6.1g and h - UWEC-WDXRF Data vs EMPA Data for the Major Elements

g)



h)

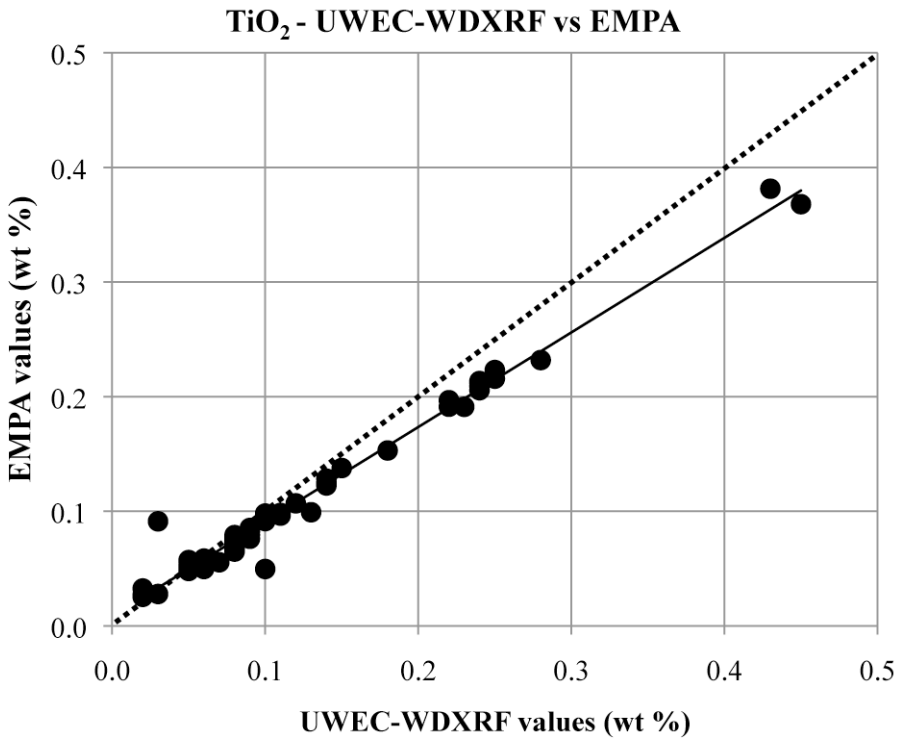
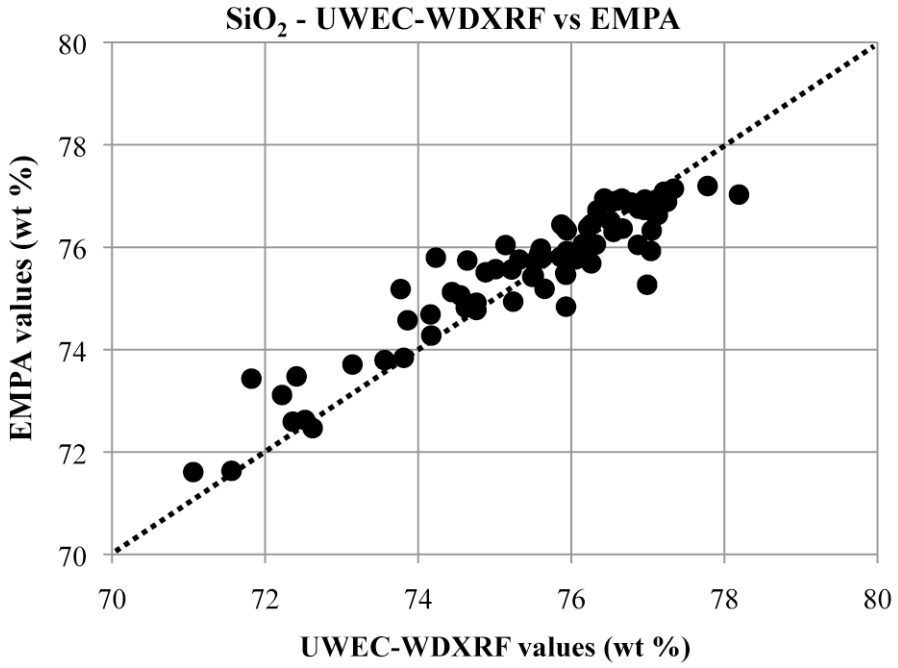
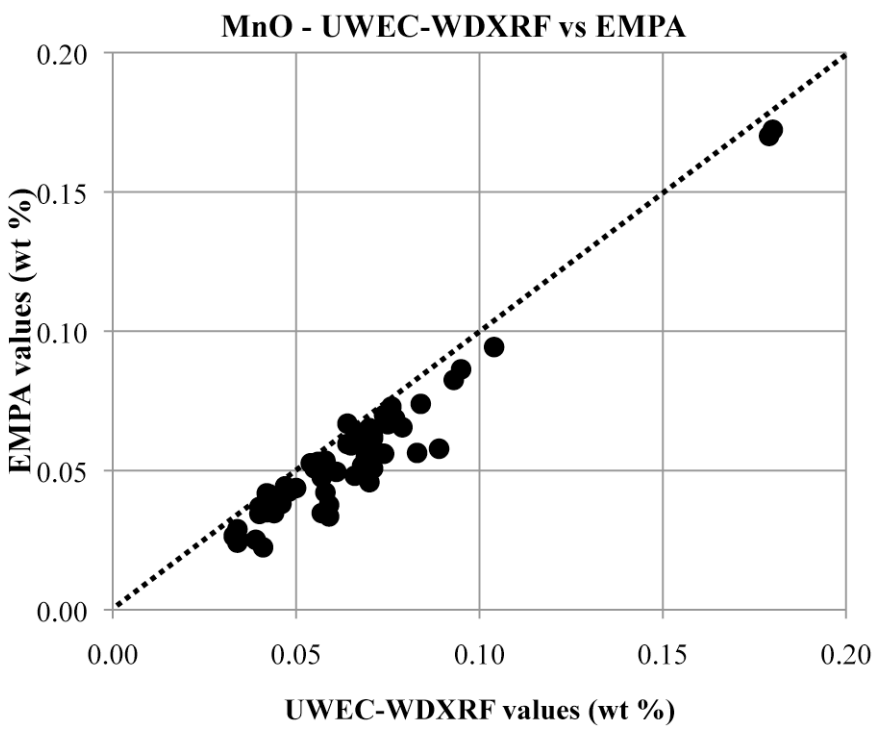


Figure 6.1i and j - UWEC-WDXRF Data vs EMPA Data for the Major Elements

i)



j)



inclusions together (XRF). Ti exhibits another issue (Figure 6.1h): the WDXRF-UWEC Ti values increasingly diverge from the EMPA values as its concentration rises, and I also attribute this to the presence of inclusions, namely ilmenite ($FeTiO_3$).

The other major elements show notable systematic deviations that indicate errors in the calibration of the WDXRF-UWEC and/or EMPA data. Mg and P (Figure 6.1c and d) have the largest deviations, with WDXRF-UWEC data for MgO almost a full order of magnitude higher than the EMPA data. In addition, Al_2O_3 and CaO values are high in the WDXRF-UWEC data (Figure 6.1a and b), whereas Na_2O and K_2O values are low in the WDXRF-UWEC data (6.1e and f). For these four elements, the linear-regression lines are nearly parallel to the dotted 1:1 ratio lines, indicating that there were systematic errors in the calibrations (i.e., using X-ray intensities from standards to calculate concentrations in unknowns). The question is which data set had the calibration errors.

Recall from Section 5.2.3 that Na_2O and K_2O both tend to migrate out from under an intense electron beam. Therefore, I expected that the Na_2O and/or K_2O concentrations might be low in the EMPA data, despite my endeavors to minimize the migration effects, and that XRF analyses may yield more accurate concentrations. I noted, though, that the Na_2O and K_2O values were actually lower, not higher, in the WDXRF-UWEC data, which was completely unexpected and suggested an error in that data set.

I decided that a comparison to the literature values for a particular obsidian source may reveal whether the EMPA and/or WDXRF-UWEC data had calibration errors. I was initially reluctant to use literature values because, as discussed in Chapter 4, (1) different

researchers have used a variety of names for the same sources (e.g., the Güneydağ source on the northwestern side of Acigöl is also called Güneydağ Tepe, Göl Dağ, Güneş Dağ, or even just Acigöl) and (2) I could not be certain that what Rapp and Ercan recognize as an individual particular collection area would coincide with what other researchers consider a collection area. My solution was to pick an especially well-studied and discrete source, and the Kömürcü source of Göllü Dağ best fit these two requirements.

Table 6.14 shows my EMPA data and the WDXRF-UWEC data for the CA20 and CA32 collection areas, both at Kömürcü. This table also includes the Kömürcü data from six different studies: Keller and Seifried (1990), Olanca (1994), Yellin (1995), Martinetto (1996), Cauvin in Poidevin (1998), and Gratuze in Poidevin (1998) as well as the overall mean values for all six publications. Note that the mean published Al_2O_3 value is 12.57% and that my values are 12.57 ± 0.06% and 12.56 ± 0.05%. The WDXRF-UWEC values, though, are 13.33% and 13.44%. The literature values evidently support the EMPA data. Similarly, the Na_2O literature values (4.04% mean) support my values (4.05 ± 0.10% and 3.98 ± 0.04%) rather than the WDXRF-UWEC values (3.52% and 3.53%). The same is true for both MgO and CaO. Consequently, it seems that the EMPA calibrations, at least for these elements, are superior to the WDXRF-UWEC calibrations and that, based on the Kömürcü literature values, the EMPA data have superior accuracy.

Recall that the WDXRF-UWEC calibration standards included only one obsidian standard (USGS RGM-1) among a series of other rocks. This might be appropriate for a "generic" geological calibration but insufficient for obsidian. As I mentioned earlier, the

Table 6.14 - Comparison of EMPA Data and WDXRF-UWEC Data to Published Values for the Kömürcü Source

	Keller and Seifried (1990)		Olanca (1994)	Yellin (1995)	Martinetto (1996)	Cauvin in Poidevin (1998)		Gratuze in Poidevin (1998)		Literature Values Combined	Frahm - CA20		Frahm - CA32		WDXRF-UWEC	
	Mean	*St Dev*		*Mean*		*Mean*	*St Dev*	*Mean*	*St Dev*	*Mean*	*Mean*	*St Dev*	*Mean*	*St Dev*	CA20	CA32
SiO_2	76.89	0.06	76.37			75.89	0.46			*76.38*	76.95	0.15	76.63	0.22	76.66	77.13
TiO_2	0.07	0.01	0.06			0.07	0.00	0.05	0.01	*0.06*	0.06	0.00	0.06	0.01	0.06	0.05
Al_2O_3	12.85	0.02	12.36		12.47	12.60	0.08			*12.57*	12.57	0.06	12.56	0.05	13.33	13.44
FeO(T)	0.86	0.01	0.87	0.87	0.95	0.98	0.01	0.73	0.19	*0.88*	0.70	0.02	0.61	0.03	0.47	0.49
MnO	0.06	0.01	0.07		0.07	0.06	0.01			*0.07*	0.06	0.00	0.06	0.01	0.06	0.066
MgO	0.05	0.04	0.06		0.20	0.01	0.01			*0.08*	0.04	0.00	0.03	0.01	0.26	0.27
CaO	0.48	0.01	0.49		0.40	0.51	0.01			*0.47*	0.45	0.00	0.45	0.01	0.59	0.59
Na_2O	4.18	0.04	4.05	4.16	3.82	3.99	0.17			*4.04*	4.05	0.10	3.98	0.04	3.52	3.53
K_2O	4.48	0.05	4.36		4.53	4.56	0.14			*4.48*	4.61	0.03	4.64	0.04	4.44	4.46
P_2O_5	0.01	0.01				0.01	0.01			*0.01*	0.01	0.00	0.01	0.01	0.02	0.019
Zr	77	1	79		70	85	4	71	10	*76*	80	3	43	8	-	106
Nb	20	1	22		25	28	3	21	3	*23*	86	4	63	9	-	28
Zn			22					17	4	*20*	26	12	61	13	-	39
Ba	166	12	143	160	155	131	25	161	30	*153*	178	7	150	47	-	112
Ce			43	46	42			39	16	*43*	61	15	45	17	-	43

EDXRF-MURR data used a set of obsidian specimens as standards. Richard E. Hughes and M. Steven Shackley, two obsidian researchers who use XRF, have also used multiple obsidian standards. Shackley's XRF calibration scheme for obsidian specimens involves 16 standards, including three obsidians (RGM-1 from the USGS and JR-1 and JR-2 from the Geological Survey of Japan) (Negash and Shackley 2006; Craig et al. 2007). Hughes (1988) tested his calibration scheme with three obsidian standards (RGM-1 in addition to NBS-278 from the National Bureau of Standards [today NIST SRM #278] and JR-1 from the Geological Survey of Japan) as well as three granite standards. I gave UWEC a series of obsidian powders with known compositions to use as standards, including NIST SRM #278 and 15 different obsidian specimens analyzed by wet chemistry in the University of Minnesota's Rock Analysis Laboratory (from well-known geologists Norman Bowen and Chester Longwell). These obsidian specimens have not been analyzed, but their analyses would reveal further information about the calibration errors.

Eight obsidian specimens were also analyzed for trace elements at UWEC. Table 6.15 shows the WDXRF-UWEC data with the EDXRF-MURR and EMPA data for trace-element analyses of these specimens. The EMPA data shows reasonably good agreement, except for Nb (which appears too high in the EMPA data), with the WDXRF-UWEC and EDXRF-MURR data, which is discussed in the subsequent section.

6.7.3 - EDXRF-/NAA-MURR and EMPA Accuracy

Table 6.16 shows the EDXRF-MURR and NAA-MURR data in comparison to the EMPA data for eight Mexican obsidian sources, based on a series of specimens sent to me

Table 6.15 - Comparison of WDXRF-UWEC, EDXRF-MURR, and EMPA Data for the Trace Elements

		Zr	Nb	Zn	Ba	Ce
	EMPA - Frahm	159 ± 12	78 ± 9	59 ± 13	452 ± 10	81 ± 25
CA05	WDXRF-UWEC	188	24	68	383	58
	EDXRF-MURR	153	17	40		
	EMPA - Frahm	43 ± 8	63 ± 9	61 ± 13	150 ± 47	45 ± 17
CA32	WDXRF-UWEC	106	28	39	112	43
	EDXRF-MURR	83	20	24		
	EMPA - Frahm	47 ± 8	75 ± 9	76 ± 16	23 ± 9	46 ± 16
CA33	WDXRF-UWEC	112	41	55	n.d.	32
	EDXRF-MURR	102	26	26		
	EMPA - Frahm	117 ± 7	74 ± 7	59 ± 14	601 ± 14	97 ± 24
EA04	WDXRF-UWEC	140	16	69	565	54
	EDXRF-MURR	112	16	29		
	EMPA - Frahm	287 ± 7	93 ± 7	103 ± 16	83 ± 20	60 ± 20
EA09	WDXRF-UWEC	318	39	104	48	74
	EDXRF-MURR	268	27	67		
	EMPA - Frahm	289 ± 9	92 ± 9	89 ± 11	69 ± 10	89 ± 33
EA30	WDXRF-UWEC	327	38	127	44	75
	EDXRF-MURR	283	29	63		
	EMPA - Frahm	108 ± 8	80 ± 3	55 ± 17	509 ± 24	64 ± 24
EA63	WDXRF-UWEC	122	17	49	467	45
	EDXRF-MURR	84	12	29		
	EMPA - Frahm	1413 ± 23	138 ± 9	292 ± 8	27 ± 6	258 ± 6
EA64	WDXRF-UWEC	1093	64	234	10	254
	EDXRF-MURR	1108	73	235		

Table 6.16a - EMPA Data for Mexican Specimens from MURR Compared to MURR's NAA and EDXRF Data

	Guadalupe Victoria, Puebla						Malpais, Hidalgo					
	EMPA-Frahm		NAA-MURR		EDXRF-MURR		EMPA-Frahm		NAA-MURR		EDXRF-MURR	
	mean	*std dev*	*mean*	*std dev*	*mean*	*std dev*	*mean*	*std dev*	*mean*	*std dev*	*mean*	*std dev*
SiO_2	77.025	0.283					75.940	0.319				
TiO_2	0.099	0.008			0.107	0.015	0.126	0.010			0.131	0.013
Al_2O_3	13.091	0.109					13.409	0.099				
Cr_2O_3	0.000	0.008					0.001	0.008				
FeO (T)	0.466	0.111	0.548	0.008	0.59	0.03	0.862	0.113	0.946	0.014	0.93	0.03
MnO	0.063	0.009	0.067	0.002	0.046	0.005	0.044	0.010	0.054	0.001	0.033	0.007
MgO	0.086	0.008					0.112	0.033				
CaO	0.475	0.030					0.871	0.031				
Na_2O	4.306	0.188	4.41	0.12			4.040	0.171	4.17	0.12		
K_2O	4.093	0.115	4.08	0.20	4.11	0.07	4.125	0.060	4.02	0.23	4.13	0.11
P_2O_5	0.027	0.009					0.033	0.010				
F	0.002	0.003					0.002	0.004				
SO_3	0.000	0.009					0.001	0.009				
Cl	0.077	0.011	0.062	0.011			0.058	0.008	0.051	0.007		
Zr	63	24	54	9	73	5	120	29	96	4	104	8
Nb	65	20			13	3	71	20			14	3
Ga	51	14			12	1	44	18			14	1
Zn	23	54	27	1	28	3	49	40	37	1	35	5
Ba	984	36	931	36			879	34	783	11		
Ce	30	52	27	1			39	56	50	1		

	Otumba, State of Mexico						Tepalzingo, Hidalgo					
	EMPA-Frahm		NAA-MURR		EDXRF-MURR		EMPA-Frahm		NAA-MURR		EDXRF-MURR	
	mean	*std dev*	*mean*	*std dev*	*mean*	*std dev*	*mean*	*std dev*	*mean*	*std dev*	*mean*	*std dev*
SiO_2	75.056	0.423					73.461	0.666				
TiO_2	0.151	0.011			0.177	0.008	0.157	0.018			0.265	0.015
Al_2O_3	13.613	0.119					13.532	0.272				
Cr_2O_3	-0.001	0.008					-0.002	0.008				
FeO (T)	0.977	0.236	1.112	0.019	1.08	0.04	2.276	0.178	2.353	0.026	2.17	0.17
MnO	0.042	0.011	0.049	0.001	0.043	0.011	0.057	0.009	0.063	0.002	0.043	0.008
MgO	0.153	0.072					0.018	0.006				
CaO	1.040	0.058					0.856	0.099				
Na_2O	4.038	0.121	4.00	0.12			4.718	0.308	4.77	0.13		
K_2O	4.221	0.118	4.11	0.25	4.27	0.17	4.474	0.127	4.18	0.24	4.36	0.23
P_2O_5	0.036	0.009					0.007	0.008				
F	0.003	0.004					0.003	0.004				
SO_3	0.000	0.009					-0.001	0.008				
Cl	0.061	0.007	0.056	0.005			0.117	0.010	0.098	0.008		
Zr	137	29	138	7	143	11	472	31	486	14	448	35
Nb	70	23			15	4	97	24			41	5
Ga	48	22			16	1	45	30			23	1
Zn	35	42	40	1	40	5	186	34	146	1	125	8
Ba	865	33	761	15			962	91	892	13		
Ce	35	71	52	1			133	75	138	2		

Table 6.16b - EMPA Data for Mexican Specimens from MURR Compared to MURR's NAA and EDXRF Data

	Paredon, Pueblo						El Paraiso, Queretaro					
	EMPA-Frahm		NAA-MURR		EDXRF-MURR		EMPA-Frahm		NAA-MURR		EDXRF-MURR	
	mean	*std dev*	*mean*	*std dev*	*mean*	*std dev*	*mean*	*std dev*	*mean*	*std dev*	*mean*	*std dev*
SiO_2	76.536	0.401					76.124	0.410				
TiO_2	0.134	0.008			0.131	0.016	0.130	0.008			0.101	0.014
Al_2O_3	12.192	0.096					10.974	0.080				
Cr_2O_3	0.000	0.008					0.000	0.007				
FeO (T)	1.095	0.080	1.089	0.144	1.12	0.03	2.664	0.088	2.508	0.039	2.52	0.18
MnO	0.043	0.010	0.046	0.001	0.025	0.006	0.026	0.009	0.030	0.001	0.045	0.002
MgO	0.051	0.018					-0.001	0.003				
CaO	0.341	0.051					0.155	0.053				
Na_2O	3.849	0.192	3.90	0.09			4.810	0.257	4.87	0.12		
K_2O	5.101	0.059	4.93	0.25	4.75	0.10	4.524	0.039	4.42	0.25	4.40	0.24
P_2O_5	0.005	0.008					0.001	0.007				
F	0.002	0.004					0.002	0.004				
SO_3	-0.002	0.008					-0.001	0.007				
Cl	0.142	0.013	0.119	0.009			0.193	0.009	0.154	0.013		
Zr	216	19	193	8	213	17	1231	35	1110	48	1247	92
Nb	102	22			41	4	98	22			69	6
Ga	61	21			16	1	59	23			28	1
Zn	113	41	55	1	53	4	312	36	234	14	244	20
Ba	98	41	59	9			20	38	37	16		
Ce	75	86	110	2			96	55	142	4		

	Pico de Orizaba, Veracruz						Sierra de Pachuca, Hidalgo					
	EMPA-Frahm		NAA-MURR		EDXRF-MURR		EMPA-Frahm		NAA-MURR		EDXRF-MURR	
	mean	*std dev*	*mean*	*std dev*	*mean*	*std dev*	*mean*	*std dev*	*mean*	*std dev*	*mean*	*std dev*
SiO_2	76.898	0.487					75.696	0.362				
TiO_2	0.079	0.009			0.091	0.015	0.189	0.010			0.158	0.024
Al_2O_3	13.020	0.099					11.302	0.073				
Cr_2O_3	-0.001	0.007					-0.001	0.008				
FeO (T)	0.389	0.357	0.457	0.015	0.54	0.03	2.174	0.032	2.032	0.026	2.04	0.15
MnO	0.066	0.008	0.072	0.002	0.043	0.005	0.140	0.011	0.148	0.003	0.103	0.008
MgO	0.071	0.010					0.052	0.005				
CaO	0.340	0.026					0.105	0.019				
Na_2O	4.217	0.151	4.29	0.09			5.019	0.296	5.12	0.12		
K_2O	4.418	0.091	4.19	0.25	4.29	0.08	4.628	0.092	4.55	0.29	4.60	0.20
P_2O_5	0.028	0.009					0.003	0.009				
F	0.002	0.004					0.002	0.004				
SO_3	0.000	0.008					0.010	0.014				
Cl	0.049	0.007	0.049	0.007			0.186	0.010	0.146	0.015		
Zr	48	29	32	7	58	6	953	40	888	40	957	62
Nb	52	31			14	3	124	29			84	8
Ga	41	18			12	1	46	16			23	2
Zn	72	27	25	3	24	3	291	31	191	12	207	19
Ba	797	39	724	42			37	35	31	12		
Ce	6	46	14	2			77	42	92	2		

by Glascock, and Table 6.17 shows the same three data sets for twelve obsidian collection areas in Armenia, based on specimens that I sent to MURR. Both tables show very good agreement for most elements. The Al contents were measured by NAA for the Armenian obsidian specimens but not the Mexican ones. Measurement of Al in obsidian with NAA is complicated by the abundance of Si, which produces the same radioisotope, ^{28}Al, under neutron bombardment, leading to poor precision. Two trace elements -- Nb and Ga -- are higher in my EMPA data than in the EDXRF-MURR data set, and recall that Nb was also higher in my data than in the WDXRF-UWEC data. Table 6.3 showed good agreement for Nb and Ga with the glass reference standards, but in the double-digit-ppm range, their accuracy might be reduced due to interferences or other effects.

Figures 6.2a through 6.2f show the correspondence between the EDXRF-MURR and EMPA data. The dotted line on each graph represents a 1:1 ratio, and the data points would fall on this line if these data sets were identical. Notice that the elements with the greatest deviations from this line are TiO_2, FeO, and MnO -- these elements have greater concentrations for some specimens in the EDXRF-MURR data. I expected that the high concentrations of Ti, Fe, and Mn were due to inclusions measured in the EDXRF-MURR bulk analyses but not the EMPA spot analyses of the glass. To confirm this hypothesis, I identified those specimens with high Ti contents in the EDXRF-MURR data, and I found ilmenite ($FeTiO_3$) inclusions, some rather large, in the specimens that I examined (Figure 6.3). The FeO concentrations are almost always greater in the EDXRF-MURR data due to the abundance of iron-oxide inclusions -- magnetite (Fe_3O_4), hematite (Fe_2O_3), limonite

Table 6.17a: Comparison of EMPA, NAA-MURR, and EDXRF-MURR Data for Armenian Obsidian

	AR06 Specimens: Gutansar, Armenia						AR47 Specimens: Gutansar, Armenia					
	EMPA-Frahm		NAA-MURR		EDXRF-MURR		EMPA-Frahm		NAA-MURR		EDXRF-MURR	
	mean	*st dev*	*mean*	*st dev*	*mean*	*st dev*	*mean*	*st dev*	*mean*	*st dev*	*mean*	*st dev*
SiO_2	74.59	0.11					73.94	0.16				
TiO_2	0.175	0.002			0.300	0.013	0.174	0.002			0.309	0.015
Al_2O_3*	13.99	0.04	13.28	0.31			13.91	0.05	13.90	0.47		
Cr_2O_3	0.000	0.002					0.002	0.002				
FeO (T)	1.09	0.01	1.04	0.01	0.967	0.011	1.05	0.02	1.03	0.01	0.996	0.029
MnO	0.077	0.002	0.083	0.001	0.064	0.007	0.075	0.005	0.082	0.001	0.067	0.005
MgO	0.214	0.003					0.199	0.011				
CaO	0.984	0.013					0.976	0.010				
Na_2O	4.37	0.04	4.48	0.09			4.43	0.04	4.39	0.05		
K_2O	4.23	0.03	4.27	0.06	4.16	0.12	4.20	0.03	3.88	0.16	4.19	0.08
P_2O_5	0.034	0.003					0.032	0.001				
F	0.003	0.001					0.005	0.001				
SO_3	0.004	0.003					0.005	0.002				
Cl	0.039	0.002	0.028	0.001			0.040	0.002	0.027	0.001		
Zr	148	6	134	5	174	3	147	6	139	11	182	6
Nb	70	6			29	2	73	18			32	1
Ga	40	4			16	1	33	12			17	1
Zn	82	14	41	1	48	6	58	14	43	1	51	2
Ba	489	9	421	5			486	9	410	19		
Ce	83	14	55	1			97	11	55	1		

	AR41 Specimens: Pokr Arteni, Armenia						AR42 Specimens: Pokr Arteni, Armenia					
	EMPA-Frahm		NAA-MURR		EDXRF-MURR		EMPA-Frahm		NAA-MURR		EDXRF-MURR	
	mean	*st dev*	*mean*	*st dev*	*mean*	*st dev*	*mean*	*st dev*	*mean*	*st dev*	*mean*	*st dev*
SiO_2	76.46	0.02					76.32	0.07				
TiO_2	0.076	0.001			0.126	0.003	0.082	0.004			0.088	0.005
Al_2O_3*	13.13	0.05	13.60	0.11			12.87	0.01	13.94	0.24		
Cr_2O_3	-0.002	0.001					0.000	0.002				
FeO (T)	0.47	0.00	0.50	0.00	0.616	0.012	0.47	0.01	0.51	0.00	0.621	0.033
MnO	0.076	0.002	0.081	0.001	0.055	0.005	0.071	0.002	0.076	0.002	0.052	0.001
MgO	0.049	0.000					0.054	0.001				
CaO	0.514	0.002					0.515	0.009				
Na_2O	4.22	0.05	4.12	0.02			4.18	0.03	4.10	0.00		
K_2O	4.61	0.03	4.58	0.05	4.52	0.07	4.66	0.01	4.32	0.01	4.48	0.27
P_2O_5	0.010	0.001					0.007	0.001				
F	0.003	0.002					0.001	0.001				
SO_3	0.002	0.001					0.004	0.002				
Cl	0.041	0.000	0.027	0.004			0.039	0.002	0.023	0.000		
Zr	50	8	59	13	87	4	64	2	53	5	89	1
Nb	89	19			30	1	65	1			29	1
Ga	42	11			13	1	40	16			14	1
Zn	99	1	41	1	33	1	88	7	38	1	34	2
Ba	163	11	109	7			283	3	192	12		
Ce	66	13	34	1			55	3	34	1		

* The measurement of aluminum in obsidian by NAA is complicated by the abundance of silicon, which produces the same radioisotope, ^{28}Al, under neutron bombardment.

Table 6.17b: Comparison of EMPA, NAA-MURR, and EDXRF-MURR Data for Armenian Obsidian

	AR37 Specimens: Metz Sevkar, Armenia						AR66 Specimens: Aghvorik, Armenia					
	EMPA-Frahm		NAA-MURR		EDXRF-MURR		EMPA-Frahm		NAA-MURR		EDXRF-MURR	
	mean	*st dev*	*mean*	*st dev*	*mean*	*st dev*	*mean*	*st dev*	*mean*	*st dev*	*mean*	*st dev*
SiO_2	76.92	0.13					72.95	0.14				
TiO_2	0.081	0.002			0.067	0.001	0.315	0.002			0.299	0.022
Al_2O_3*	12.54	0.10	13.64	0.34			14.52	0.02	15.50	0.85		
Cr_2O_3	0.000	0.002					0.002	0.002				
FeO (T)	0.47	0.02	0.49	0.00	0.634	0.050	1.41	0.30	1.55	0.01	1.322	0.034
MnO	0.053	0.002	0.055	0.000	0.036	0.003	0.059	0.006	0.064	0.001	0.062	0.003
MgO	0.039	0.002					0.339	0.024				
CaO	0.494	0.007					1.363	0.046				
Na_2O	3.97	0.04	4.09	0.18			4.40	0.01	4.29	0.05		
K_2O	4.81	0.10	4.48	0.18	4.64	0.17	4.43	0.08	4.24	0.25	4.08	0.13
P_2O_5	0.001	0.002					0.065	0.002				
F	0.002	0.001					0.004	0.000				
SO_3	0.003	0.002					0.004	0.001				
Cl	0.045	0.004	0.027	0.005			0.041	0.005	0.025	0.006		
Zr	51	7	35	7	82	3	218	2	223	15	232	7
Nb	69	6			26	1	36	14			14	1
Ga	43	4			14	1	38	1			17	1
Zn	80	21	28	1	26	5	63	16	48	2	52	1
Ba	28	9	-	-			984	10	903	12		
Ce	65	19	42	2			135	21	79	1		

	AR67 Specimens: Metz Arteni, Armenia						AR69 Specimens: Damlik, Armenia					
	EMPA-Frahm		NAA-MURR		EDXRF-MURR		EMPA-Frahm		NAA-MURR		EDXRF-MURR	
	mean	*st dev*	*mean*	*st dev*	*mean*	*st dev*	*mean*	*st dev*	*mean*	*st dev*	*mean*	*st dev*
SiO_2	76.40	0.02					75.67	0.13				
TiO_2	0.059	0.003			0.069	0.001	0.103	0.002			0.192	0.010
Al_2O_3*	13.23	0.06	13.64	0.47			13.61	0.05	14.20	0.26		
Cr_2O_3	0.001	0.003					0.000	0.001				
FeO (T)	0.36	0.02	0.44	0.01	0.563	0.014	0.48	0.11	0.73	0.01	0.740	0.054
MnO	0.092	0.003	0.097	0.001	0.066	0.004	0.051	0.001	0.056	0.000	0.042	0.002
MgO	0.035	0.006					0.101	0.006				
CaO	0.487	0.010					0.874	0.017				
Na_2O	4.11	0.04	4.12	0.05			4.10	0.03	4.13	0.02		
K_2O	4.80	0.10	4.46	0.25	4.51	0.01	4.53	0.05	4.43	0.24	4.26	0.27
P_2O_5	0.006	0.002					0.014	0.003				
F	0.001	0.002					0.003	0.002				
SO_3	0.005	0.001					0.003	0.000				
Cl	0.042	0.002	0.026	0.004			0.054	0.004	0.031	0.006		
Zr	29	14	41	15	87	9	47	9	79	4	99	5
Nb	87	5			38	2	61	7			15	1
Ga	43	2			14	1	44	4			15	2
Zn	67	20	46	1	33	2	30	16	33	1	34	4
Ba	75	5	28	7			756	3	652	22		
Ce	52	16	26	1			107	9	56	1		

* The measurement of aluminum in obsidian by NAA is complicated by the abundance of silicon, which produces the same radioisotope, ^{28}Al, under neutron bombardment.

Table 6.17c: Comparison of EMPA, NAA-MURR, and EDXRF-MURR Data for Armenian Obsidian

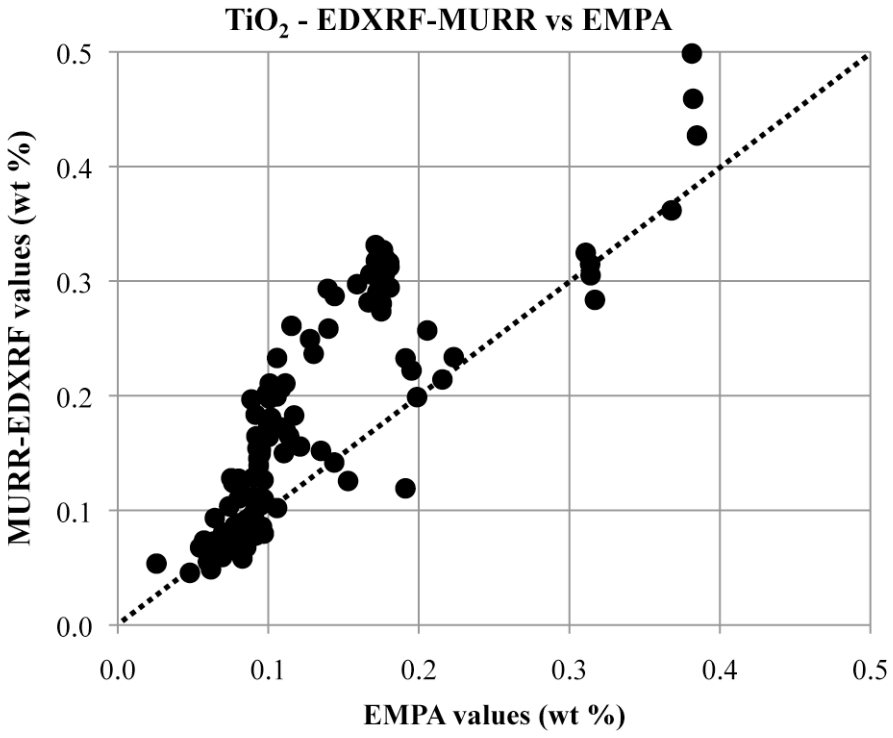
	AR70 Specimens: Ttvakar, Armenia						AR72 Specimens: Hatis, Armenia					
	EMPA-Frahm		NAA-MURR		EDXRF-MURR		EMPA-Frahm		NAA-MURR		EDXRF-MURR	
	mean	*st dev*	*mean*	*st dev*	*mean*	*st dev*	*mean*	*st dev*	*mean*	*st dev*	*mean*	*st dev*
SiO_2	75.58	0.02					74.66	0.19				
TiO_2	0.109	0.004			0.222	0.016	0.125	0.035			0.248	0.050
Al_2O_3*	13.73	0.01	14.01	0.09			13.93	0.14	14.54	0.54		
Cr_2O_3	-0.003	0.002					0.002	0.002				
FeO (T)	0.51	0.00	0.81	0.01	0.773	0.036	0.65	0.10	0.91	0.15	0.902	0.130
MnO	0.050	0.000	0.059	0.000	0.054	0.023	0.057	0.005	0.065	0.001	0.055	0.006
MgO	0.116	0.001					0.186	0.054				
CaO	0.745	0.010					1.016	0.179				
Na_2O	4.30	0.04	4.38	0.01			4.26	0.09	4.31	0.06		
K_2O	4.50	0.04	4.72	0.03	4.13	0.03	4.43	0.13	4.22	0.04	4.14	0.15
P_2O_5	0.014	0.005					0.027	0.012				
F	0.003	0.001					0.003	0.002				
SO_3	0.002	0.000					0.004	0.001				
Cl	0.048	0.023	0.026	0.006			0.043	0.013	0.030	0.001		
Zr	82	3	78	3	102	20	94	34	75	6	129	42
Nb	55	15			16	5	61	27			22	6
Ga	41	1			14	1	40	4			15	2
Zn	35	6	29	2	34	2	47	8	36	1	38	8
Ba	830	3	727	35			594	61	548	11		
Ce	116	21	60	1			112	56	47	1		

	AR79 Specimens: Seghasar, Armenia						AR82 Specimens: Bazenk, Armenia					
	EMPA-Frahm		NAA-MURR		EDXRF-MURR		EMPA-Frahm		NAA-MURR		EDXRF-MURR	
	mean	*st dev*	*mean*	*st dev*	*mean*	*st dev*	*mean*	*st dev*	*mean*	*st dev*	*mean*	*st dev*
SiO_2	76.42	0.36					77.11	0.17				
TiO_2	0.066	0.002			0.067	0.006	0.062	0.002			0.056	0.007
Al_2O_3*	13.14	0.07	13.59	0.64			12.75	0.03	13.43	0.38		
Cr_2O_3	-0.002	0.002					0.000	0.001				
FeO (T)	0.44	0.04	0.46	0.02	0.567	0.040	0.35	0.04	0.55	0.01	0.603	0.029
MnO	0.082	0.002	0.084	0.005	0.060	0.004	0.060	0.006	0.071	0.000	0.047	0.003
MgO	0.040	0.000					0.019	0.012				
CaO	0.566	0.002					0.439	0.022				
Na_2O	4.26	0.05	4.29	0.03			4.17	0.07	4.45	0.13		
K_2O	4.51	0.09	4.25	0.43	4.45	0.11	4.78	0.05	4.24	0.35	4.35	0.17
P_2O_5	0.004	0.001					0.002	0.001				
F	0.003	0.001					0.003	0.001				
SO_3	0.002	0.001					0.002	0.001				
Cl	0.046	0.007	0.034	0.001			0.067	0.007	0.045	0.003		
Zr	81	13	-	-	89	3	86	8	76	3	87	4
Nb	100	8			42	1	96	3			28	2
Ga	37	7			13	1	49	6			12	1
Zn	46	25	33	0	27	2	60	13	36	1	30	3
Ba	58	1	-	-			54	3	-	-		
Ce	61	9	33	3			52	10	31	1		

* The measurement of aluminum in obsidian by NAA is complicated by the abundance of silicon, which produces the same radioisotope, ^{28}Al, under neutron bombardment.

Figure 6.2a and b - EDXRF-MURR Data vs. EMPA Data

a)



b)

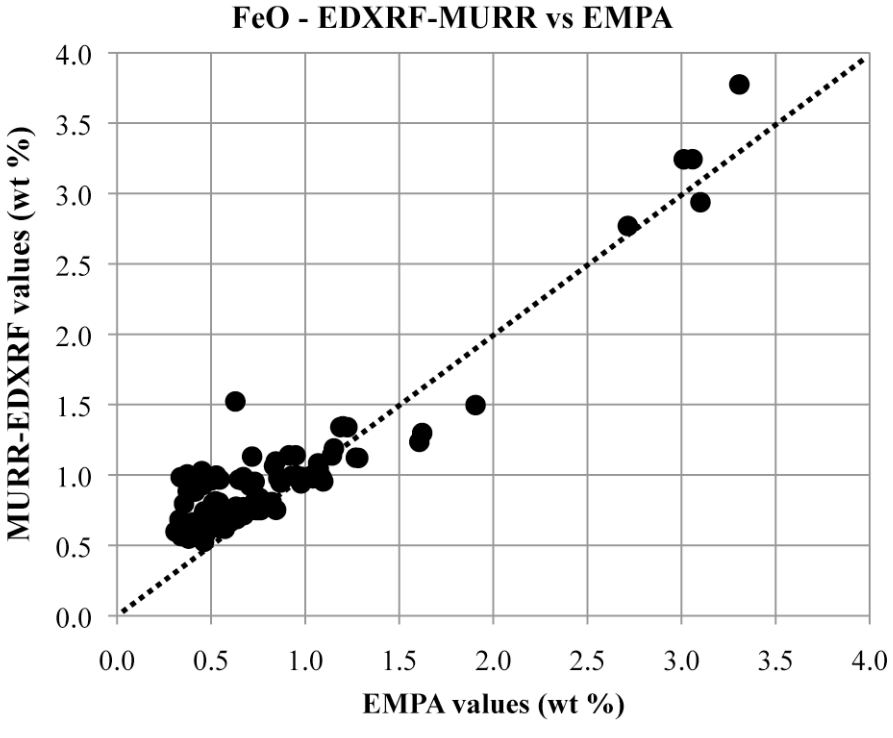
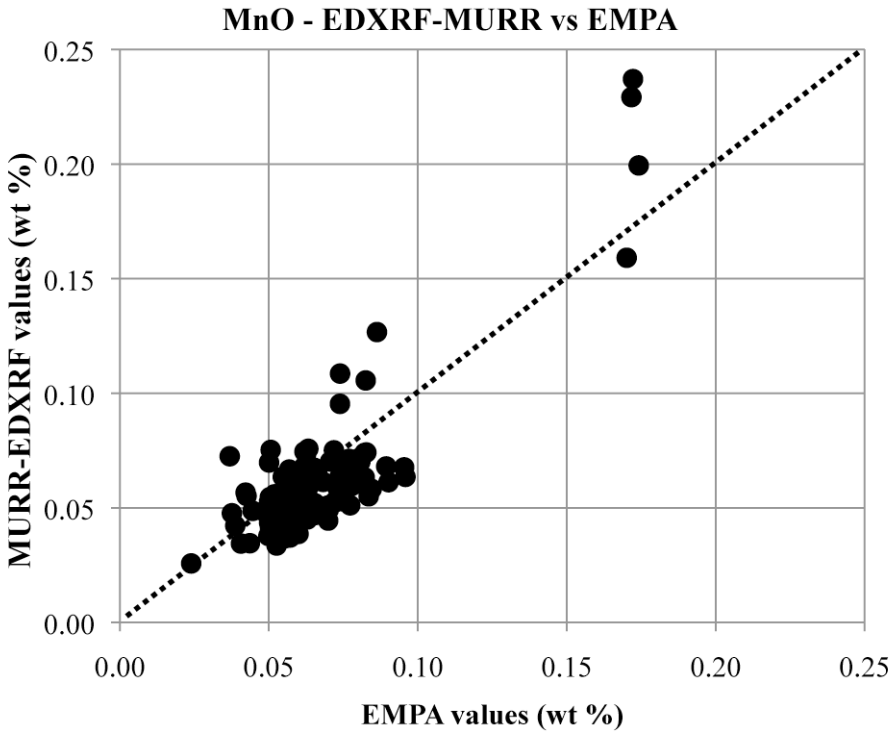


Figure 6.2c and d - EDXRF-MURR Data vs. EMPA Data

c)



d)

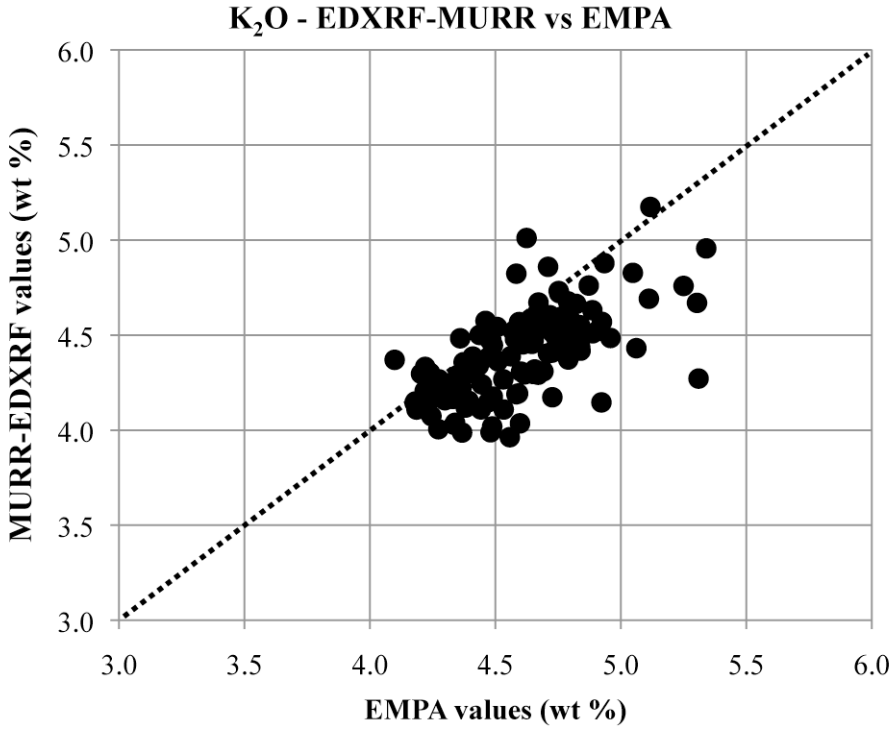
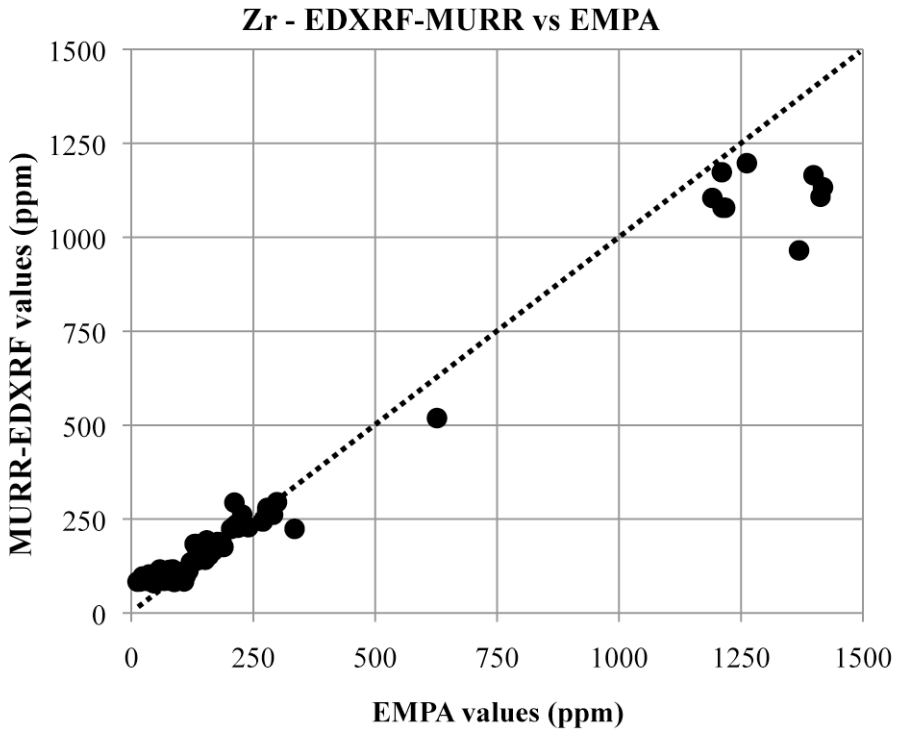
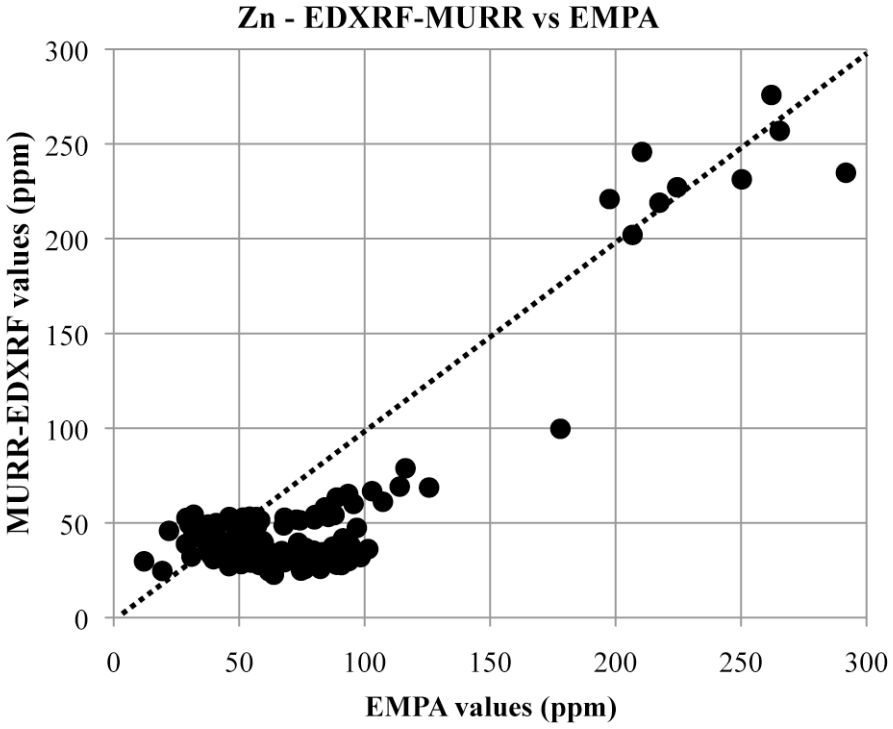


Figure 6.2e and f - EDXRF-MURR Data vs. EMPA Data

e)



f)



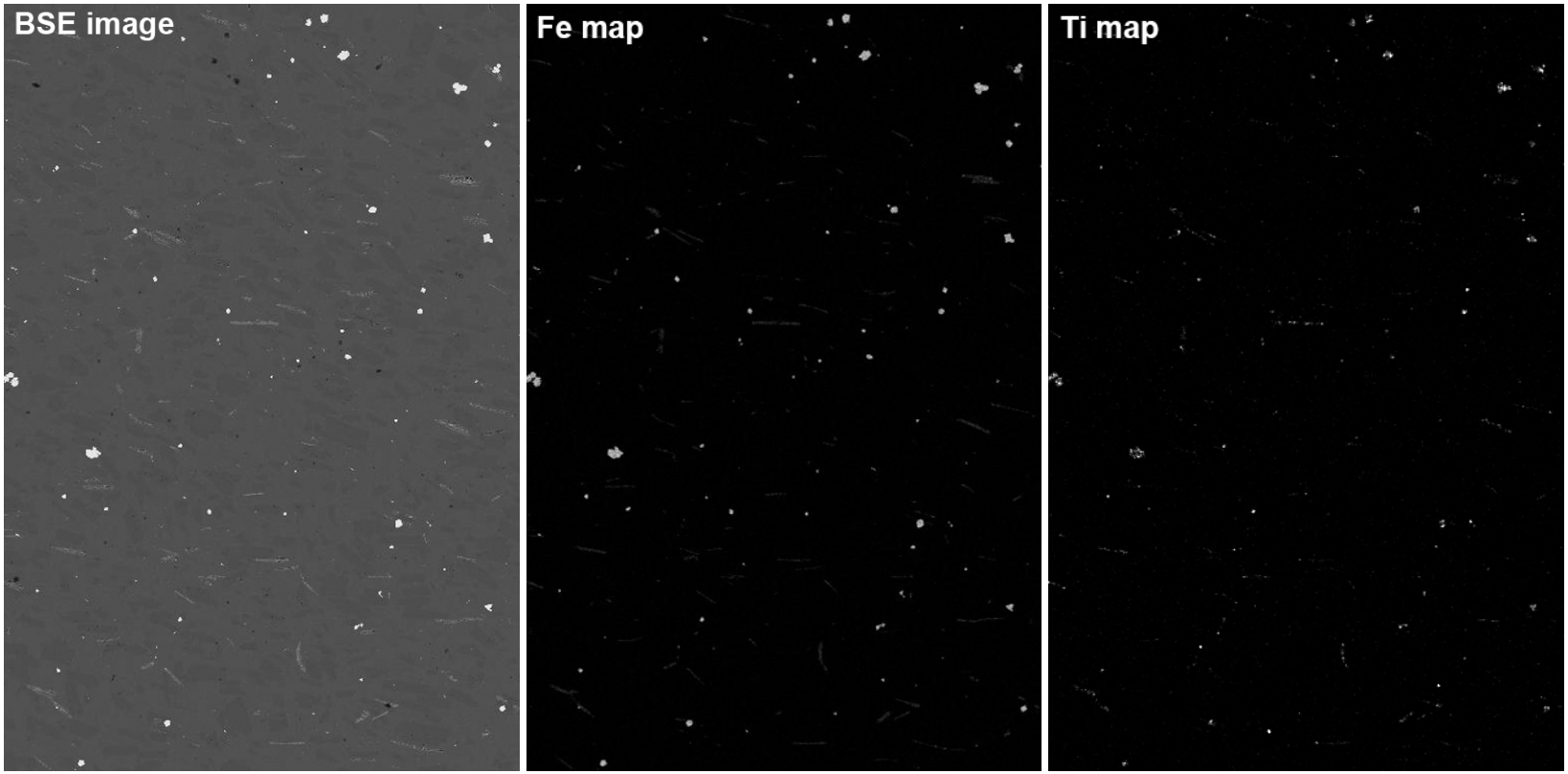


Figure 6.3 - A backscattered-electron (BSE) image and element maps of specimen AR49-sK1 (Fontan, Armenia) reveal the presence of ilmenite ($FeTiO_3$) inclusions. The field of view is 1 × 1.5 mm. The ilmenite inclusions appear white in the BSE image as well as the element maps. The inclusions will contribute to the bulk Fe and Ti contents measured by NAA or XRF.

($FeO(OH) \cdot nH_2O$) -- in most of the obsidian specimens. The presence and abundance of ilmenite and magnetite inclusions may, in addition, affect the Mn measurements because Mn atoms often substitute for Fe atoms in these two minerals.

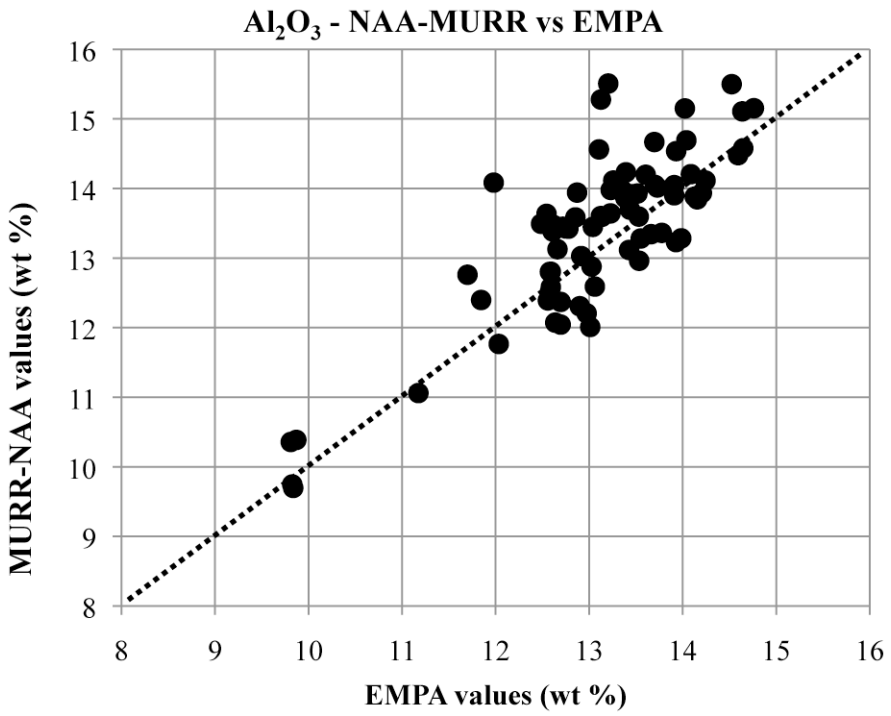
Figures 6.4a to 6.4j reveal how the NAA-MURR and EMPA data correspond, and the dotted line on each graph again represents a 1:1 ratio. Again, the FeO concentrations are frequently greater in the NAA-MURR data due to iron-oxide inclusions in most of the obsidians. The Cl graph shows a calibration issue between the NAA-MURR and EMPA data: the Cl measurements are about 35% relative lower in the NAA-MURR data. Based on the Yellowstone obsidian standard (Table 6.2), the EMPA value for Cl is consistent with the literature values, exhibiting nowhere near 35% error (e.g., 0.100% in my EMPA data would correspond to about 0.065% in "reality" with such error). Unfortunately, Cl is not often reported for obsidian analyses, so I have no other comparison at the moment to resolve this issue. The rest of the NAA-MURR data, though, exhibit excellent agreement with the EMPA data, suggesting both data sets are sufficiently accurate.

6.8 - (Re)Defining Reliability and Validity

I agree with Hughes' (1998) inclusion of reliability and validity in his assessment framework, and these concepts certainly have been previously applied in anthropological and archaeological research (e.g., Landy 1965:17, Brim and Spain 1974:19-23, Pelto and Pelto 1978:33, Baker 1988:244-246, Bernard 1994:38-42, Kuznar 1997:37-38, Madrigal 1998:3-4). Jack Nance (1987:247) even asserts in his chapter titled "Reliability, Validity, and Quantitative Methods in Archaeology" that it is…

Figure 6.4a and b - NAA-MURR Data vs. EMPA Data

a)



b)

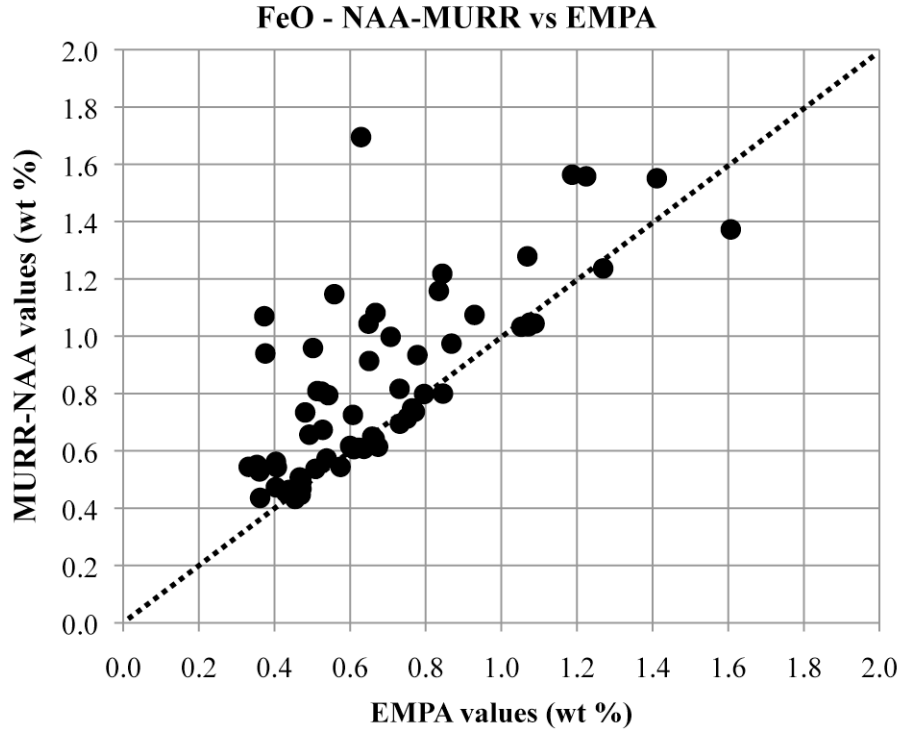
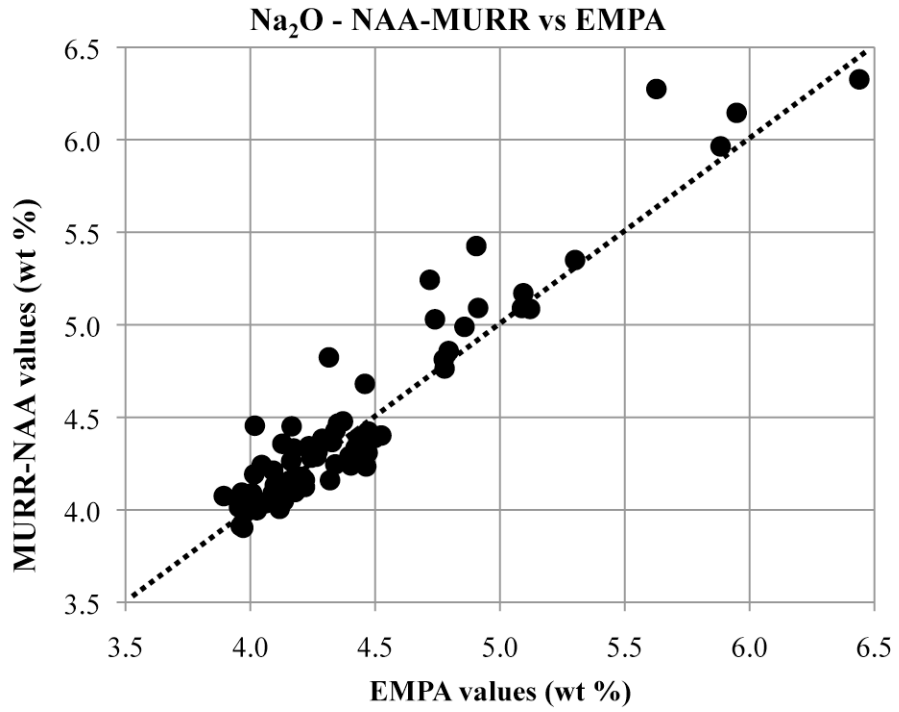


Figure 6.4c and d - NAA-MURR Data vs. EMPA Data

c)



d)

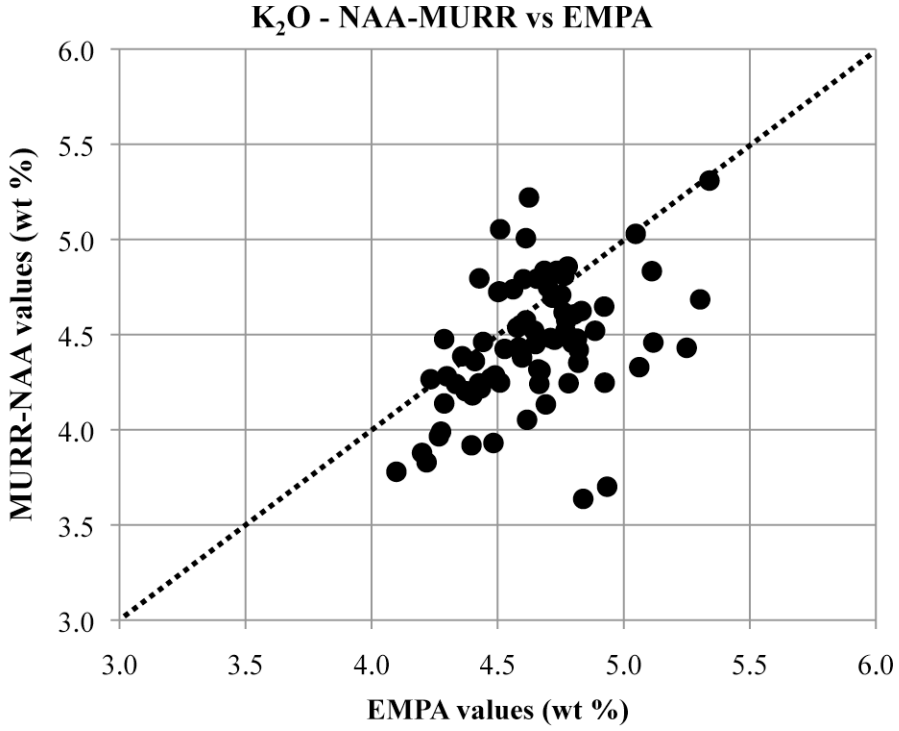
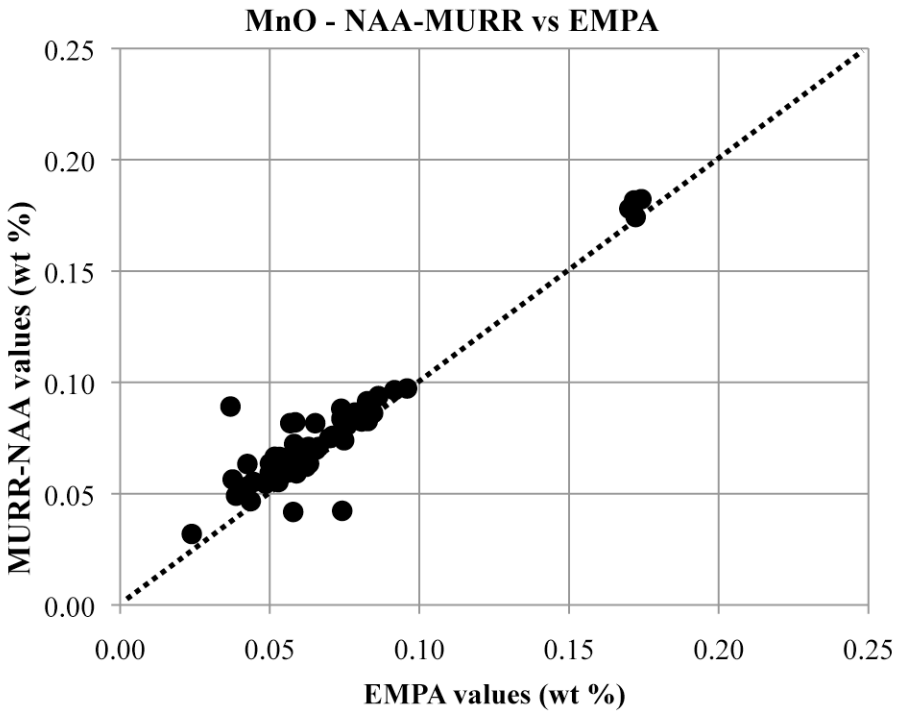


Figure 6.4e and f - NAA-MURR Data vs. EMPA Data

e)



f)

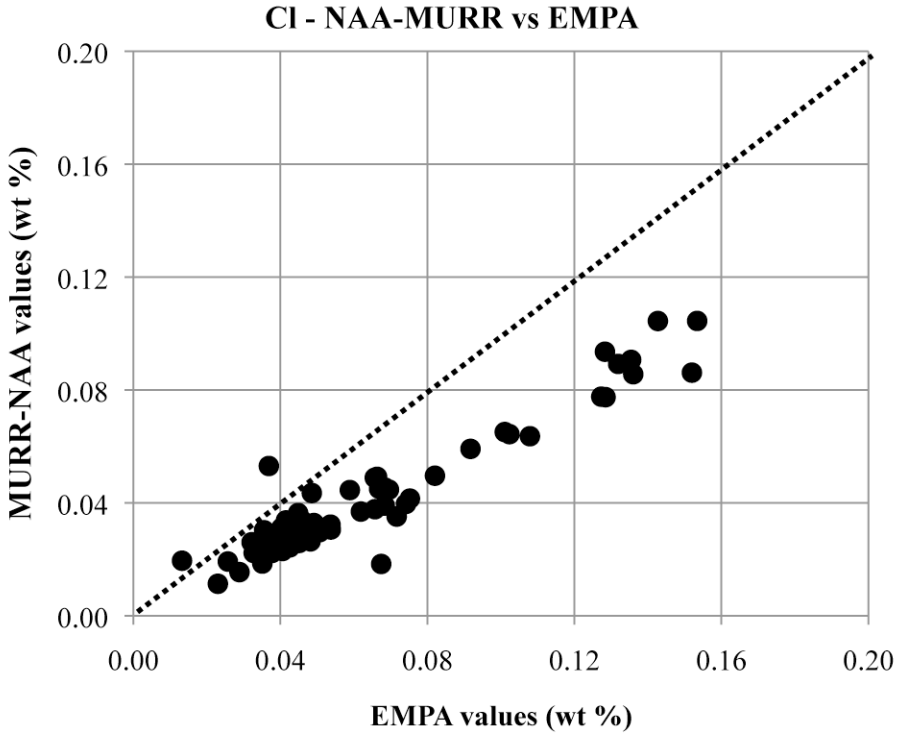
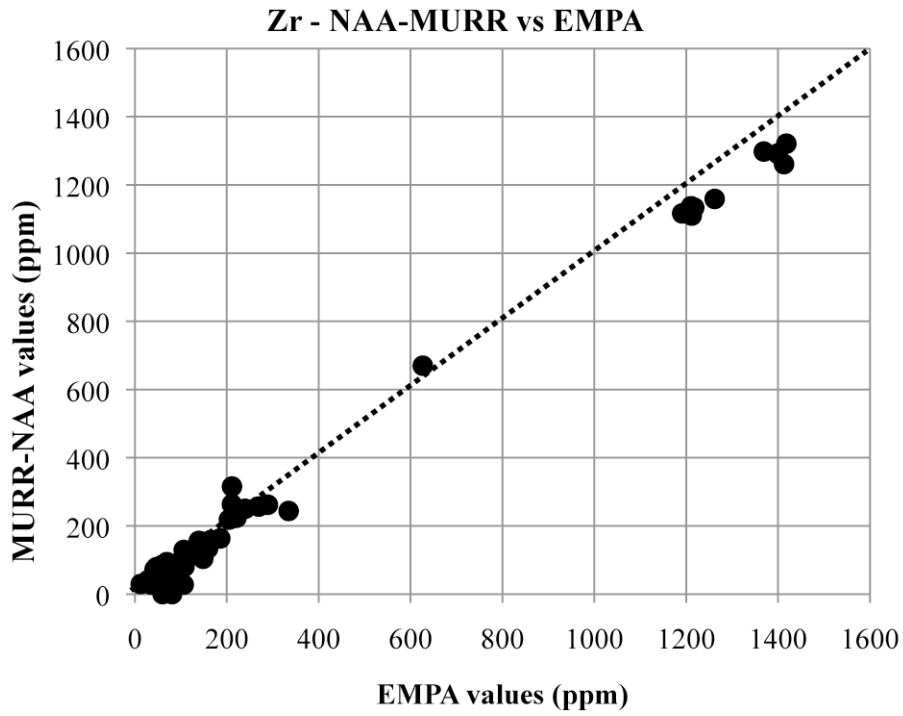


Figure 6.4g and h - NAA-MURR Data vs. EMPA Data

g)



h)

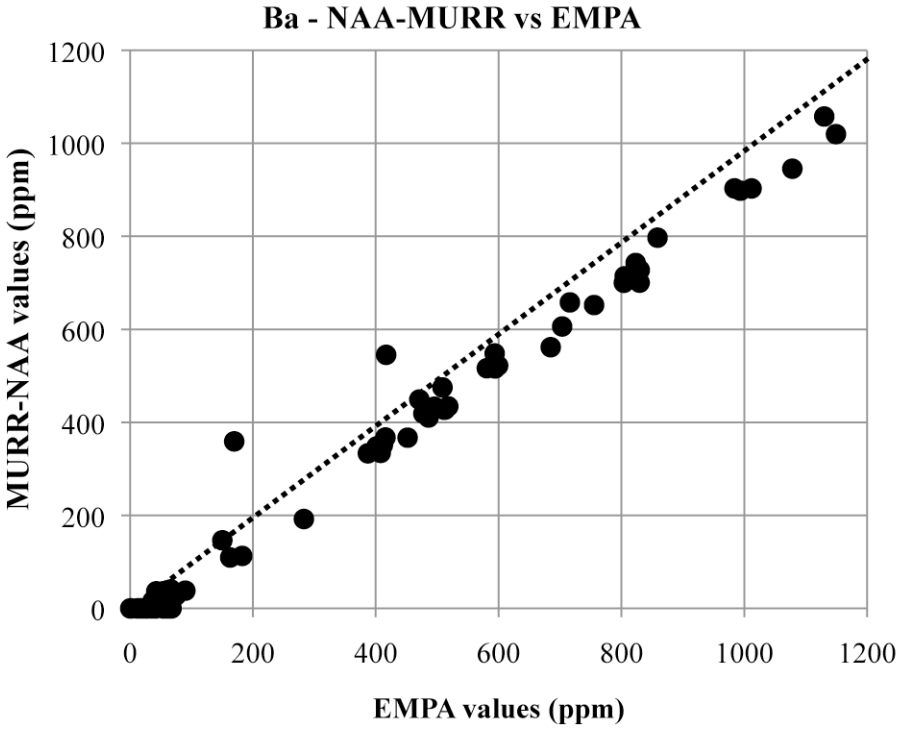
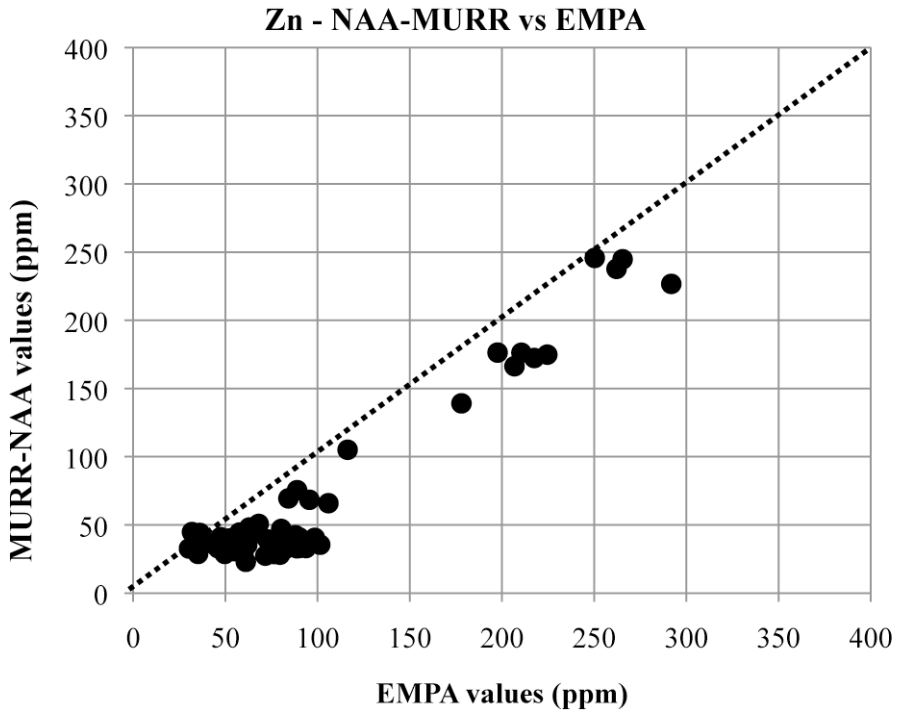
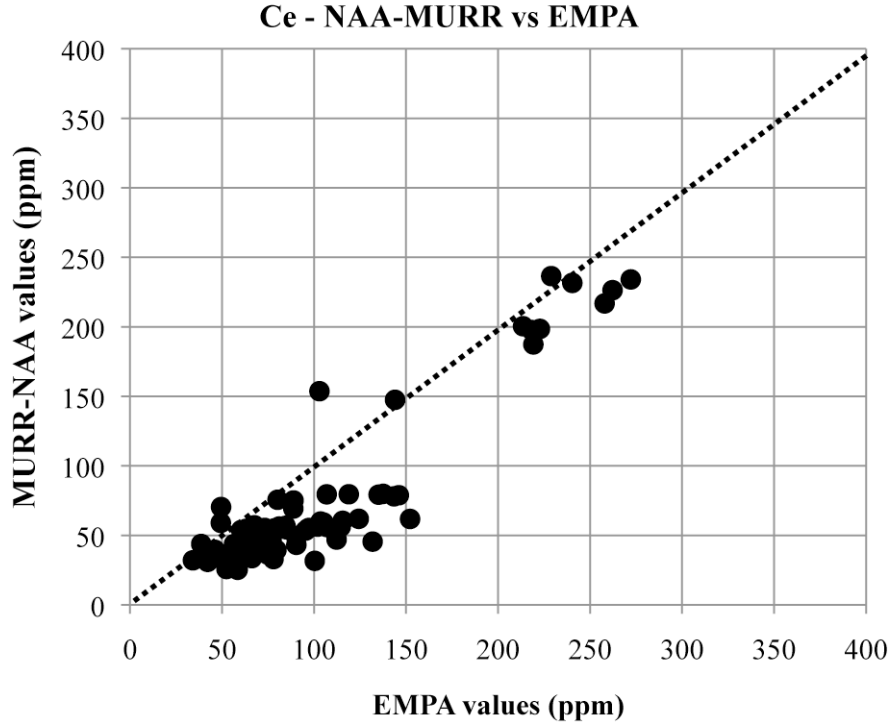


Figure 6.4i and j - NAA-MURR Data vs. EMPA Data

i)



j)



> difficult to overemphasize the importance of these two concepts in archaeology or any science. They relate to our ability to make meaningful observations about the phenomena we study. It is a universal truth of science that if we cannot measure a phenomenon properly, we can never truly understand that phenomenon. Reliability and validity lie at the very heart of the science of prehistory.

I find, however, Hughes' interpretations of reliability and validity to be inconsistent with their traditional meanings in social research. Therefore, Nazaroff et al. (2010), who apply Hughes' framework to evaluate PXRF in Mesoamerica, also use these atypical definitions of reliability and validity. After I review Hughes' conceptions of these terms, I reconsider how reliability and validity, when traditionally defined, apply to sourcing.

6.8.1 - Hughes' Reliability and Validity

Hughes (1998) cites a text by Carmines and Zeller (1979; *Reliability and Validity Assessment*) when he initially defines *reliability* as "the extent to which [the] measuring procedures yield the same results on repeated trials" (108). For geochemical studies, he contends, reliability involves "both precision and accuracy" (108). Hughes then explains the common ways in which precision and accuracy of data are established (i.e., standards, interlaboratory comparisons), as discussed in preceding sections.

After reliability, he moves on to consider validity and contends that, in relation to obsidian sourcing, there are two basic levels of validity. This first validity level, Hughes explains, "concerns the extent to which measurement units are suited to goals of research (i.e., are the units *themselves* valid measures for identifying distinct geochemical varieties of obsidian and for matching artifacts to them?)" (109). One expects that, when he refers to valid "units" for the research, he means suitable conceptions of "source" (as discussed

in Section 4.4), site types (i.e., seasonal camps, farming villages, cities), or some other spatial or temporal unit of analysis. Instead, Hughes discusses only the units in which the obsidian chemical analyses themselves are reported (i.e., reporting the data in comparable units, like weight percent or parts-per-million, rather than ratios or machine-specific units like X-ray counts, just as I discussed earlier in Section 6.1.2).

The "deeper" second level, he argues, "concerns the degree to which geochemical data serve archaeological ends" (109). It is, of course, important that a certain technique yields archaeologically significant, or at least compatible, information. Recall the sixth assumption of sourcing in Wilson and Pollard (2001), that any patterns of raw-material movement can be interpreted in terms of human behaviors such as exchange or territorial mobility. Hughes' formulation of this level really has nothing to do with how a specific technique or approach performs. Instead, it is a broad critique of sourcing. In particular, Hughes criticizes the assumption that obsidian from a distant source is evidence of trade. He writes: "To paraphrase Binford (1989:3), archaeologists do not study trade; they study artifacts... [S]ourcing studies are conducted to inform on such nongeochemical topics, yet they do not speak directly to these issues" (109-110, 111). Really his primary criticism is that trade, direct procurement, and mobility all look archaeologically identical in sourcing studies and that the label of "trade" is often automatically applied to spatial displacement of obsidian. Although Hughes raises legitimate concerns, sourcing studies should hardly be singled out because (1) almost everything in the archaeological record has been moved to where archaeologists eventually recover it, including materials used to build structures,

and (2) archaeologists *never* directly observe past human behaviors. Only at the very end does he bring the discussion back to analytical techniques: "a geologically uninformed (or analytically flawed) chemical analysis can result in a perfect match to an obsidian of absolutely no consequence archaeologically" (1998:113).

6.8.2 - Reconsidering Reliability

As mentioned earlier, I consider Hughes' interpretations of reliability and validity to be atypical. Regarding reliability, Hughes actually starts with a classic definition from Edward Carmines, a political scientist, and Richard Zeller, a statistician: "Fundamentally, *reliability* concerns the extent to which an experiment, test, or any measuring procedure yields the same results on repeated trials" (1979:11; emphasis in original). This is a very typical definition for reliability in the literature -- for example:

- "*Reliability* is the name given to the degree of reproducibility of a measure. If we were able to make repeated, independent, determinations of a measure, we should hope to obtain values that were close together" (Bartholomew 1996:24).
- "*Reliability* refers to whether or not you get the same answer by using an instrument to measure something more than once" (Bernard 1994:38).
- "… *reliability*, in other words, is in turn a measure of the extent to which a measurement remains constant as it is repeated under conditions taken to be constant" (Kaplan 1964:200).
- "A reliable measure is one that, if administered in the same situation, will provide the same result" (Kuznar 1997:37).
- "*Reliability* is the degree to which observations of a study are repeatable. A measuring instrument is reliable if it generates consistent observations at two points in time" (Madrigal 1998:4).

Hughes contends that reliability is comprised of both accuracy and precision. I, however, interpret the definition of Carmines and Zeller to involve only precision. A review of the literature reveals that I am not alone in such an interpretation -- for example:

- "… *validity* is concerned with whether the index measures what it was designed to measure; *reliability*, with the precision with which it does so… Reliability is then equivalent to precision" (Bartholomew 1996:19, 24).

Remember from Section 6.2.1 that NIST separates precision into two parts: repeatability and reproducibility. The former represents "agreement between the results of successive measurements... carried out under the same conditions," while the latter is "closeness of agreement... under changed conditions" (Taylor and Kuyatt 1994). If the observer and/or conditions change or if a period of time passes, reproducibility is involved. Considering these definitions, reliability is analogous to reproducibility -- for example:

- "Accordingly, reliability is often interpreted as a kind of intersubjectivity: the agreement of *different observers* on the measures to be assigned in particular cases. But *changes in the circumstance* of measurement other than the identity of the person making the measurement are also involved in reliability" (Kaplan 1964:200, emphasis added).
- 'Reliability concerns the extent to which measurements are repeatable -- by the same individual using different measures of the same attribute or by different persons using the same measure of an attribute" (Nunnally 1967:172).
- "If *several doctors* use the same thermometer to measure the temperature of the same individual but obtain strikingly dissimilar results, the thermometer is unreliable" (Zeller and Carmines 1980:6, emphasis added).
- "A measuring instrument is said to be reliable according to the degree to which it generates consistent observations *at two points in time*. Or a measure is reliable to the degree that *two different researchers* using the same instrument on the same sample would generate the same observations" (Bohrnstedt and Knoke 1988:14, emphasis added).

- "… reliability means that two procedures yield the same outcome, or the same procedure reapplied over time shows high agreement" (Knoke et al. 2002:14).

Furthermore, many authors consider *reliability* and *accuracy* to be separate (e.g., Kaplan 1964:202-203, Bernard 1994:39) or *validity* and *accuracy* to be equivalent:

- "A synonym for validity is *accuracy*. To the degree that an operation results in observable measures that are accurate representations of a theory's concepts, the resulting measures are said to be *valid*" (Bohrnstedt and Knoke 1988:13).
- "The term 'validity' means the accuracy with which a set of test scores measure what they ought to measure" (Ebel 1965:310).
- "… *validity* refers to the degree to which its operationalization accurately reflects the concept it is intended to measure" (Knoke et al. 2002:13).
- "Valid data are accurate. *Validity* is the degree to which the method for collecting information results in accurate information" (Madrigal 1998:3).

Hence, I consider reliability to be a form of precision, in particular reproducibility. As a result, my reliability assessment of these analytical procedures is, at present, the same as my precision assessment. As others use my procedures and as I use other instruments at different facilities, reproducibility, specifically, will become clearer.

6.8.3 - Reconsidering Validity in Sourcing

I also have problems with Hughes' formulation of validity as it relates to sourcing. Recall that he proposes two levels of validity: (1) the first one, in which a researcher uses "valid" units of measure for their obsidian geochemical data (e.g., weight percent instead of X-ray counts) and (2) a "deeper" level, on which Hughes states that identifying spatial displacement of obsidian is not a "valid" measure of trade because "geochemical data are

directly relevant only to identification of chemical varieties of obsidian and… inferences about distribution mechanisms are essentially nongeochemical in nature" (111). Without focusing on these particulars (e.g., that X-ray counts, on one level, must be equally valid as weight percent because the latter is derived from the former), Hughes sets his levels of validity unreasonably far apart: the first level is too focused on one small detail while the second level is so theoretical that it implicates almost all of archaeology. As Jack Nance (1987) points out, "it is one of the unfortunate truths of archaeology generally that most of the measurements we deal with do not measure the phenomenon they appear to, or at best, they measure the phenomenon imperfectly" (280).

I agree that there are (at least) two types of validity described in the literature, and one is akin to accuracy (as it relates to quantitative data, not the colloquial sense) while a second type is abstract and related to whether one is actually measuring the phenomenon one wishes to measure. Consider these examples of validity and invalidity:

- "If the perforations on a target made by successive shots from a rifle... are all clustered in the bull's-eye, the rifle is also performing validly" (Ebel 1965:310).
- "For example, let us assume that a particular yardstick does not equal 36 inches; instead, the yardstick is 40 inches long. Thus, every time this yardstick is used to determine the height of a person (or object), it systematically underestimates height by 4 inches for every 36 inches. A person who is six feet tall according to this yardstick, for example, is actually six feet eight inches in height. This particular yardstick, in short, provides an *invalid* indication of height" (Carmines and Zeller 1979:13,14; emphasis added).
- "For example, if the shots from a well-anchored rifle hit exactly the some location but not the proper target, the targeting rifle is consistent (and hence reliable) but it did not hit the location that it was supposed to hit *(and hence it is not valid)*" (Zeller and Carmines 1980:77, emphasis added).

These examples all involve accuracy as well as "data" to which, due to systematic error, a correction can be applied (i.e., adjustment to the rifle scope, either subtracting four inches for every yard or cutting the yardstick) to minimize the error and thus become valid. This is one type of validity, and it appears to have been influenced by a focus on measurement error in the early assessment literature in the social sciences.

Compare this accuracy-based validity to the descriptions below:

- "The number of words in a poem... would be readily accepted as a valid measure of the length of the poem. It would not, however, be accepted by most poets or literary critics as a valid measure of the literary merit… [T]o determine how valid a test is, one must compare the reality of what it *does* measure with some ideal conception of what it *ought* to measure" (Ebel 1965:310).
- "'Validity' refers to the degree to which scientific observations actually measure or record what they purport to measure... [W]e all understand the validity of the temperature as measurement by thermometers and the measures of distance we can gauge with yardsticks and rulers" (Pelto and Pelto 1978:33).
- "In a very general sense, any measuring device is valid if it does what it is intended to do. An indicator of some abstract concept is valid to the extent that it measures what it purports to measure... there are almost always theoretical claims being made when one assesses the validity of social science measures. Indeed, strictly speaking, one does not assess the validity of an indicator but rather the use to which is it being put" (Carmines and Zeller 1979:12).
- "... *valid* observations yield satisfactory responses or data. Satisfactory data tell you what you want to know, not something else. Intuitively then, to say that an observation is valid means that the observation doesn't lie to you -- valid observations do not mislead the observer. Put another way, an observation is valid if it measures what you think it measures" (Nance 1987:246).
- "Since a kilogram is equivalent to 2.2 pounds, the scale *is* valid since it is in fact measuring the concept it is intended to measure -- weight. If the second scale had been measuring percent body fat, then it would have been invalid as a measure of weight" (Bohrnstedt and Knoke 1988:13).

This is clearly a different type of validity, one that is conceptual, not quantitative. Under such a conception of validity, one cannot simply apply some sort of correction factor and make an invalid measure valid. Instead, it is concerned with whether or not the variables examined actually correspond to the concept one wished to study.

Zeller and Carmines (1980:77) give an example of both types of validity together, although they do not seem to make the distinction that I have:

> Similarly, a thermometer that gives exactly the same reading for an individual on 10 different occasions is reliable even if it is later discovered that the instrument provided a temperature of 103.2º F for a patient whose actual temperature was 98.6º F. Moreover, such an instrument is reliable but not valid if it is designed to measure blood pressure but it measures body temperature instead.

Note that, according to Hughes, this thermometer would be valid if it was instead marked in degrees Celsius or Kelvin but invalid (on his first level of validity) if its markings were labelled in millimeters rather than "translated" into degrees.

Quite distinctly, in a more recent text *Research Methods in Anthropology*, Bernard (1994) extracts accuracy from validity and considers them separate concepts:

> What if the spring were not calibrated correctly (there was an error at the factory where the scale was built…) and the scale were off?… Suppose it turned out that your scale [readings] were always incorrectly lower by 5 pounds…, then a simple correction formula would be all you'd need in order to feel confident that the data from the instrument were pretty close to the truth… The data from this instrument are valid (it has already been determined that the scale is measuring weight -- exactly what you think it's measuring); the data are reliable (you get the same answer every time you step on it)… But they are not *accurate.* (39, 40)

Bernard, therefore, recognizes validity, reliability, and accuracy as separate concepts. He removes accuracy from validity, which seems to be the current trend in assessment. This

concept-based definition will be the type of validity that I consider, particularly because I have dealt with accuracy in previous sections of this chapter.

6.8.4 - What Constitutes Validity in Sourcing?

Note that one cannot evaluate the validity (using this concept-based definition) of procedures or data alone -- assessment is done in light of a particular phenomenon:

> Validity, in contrast, is *usually* more of a theoretically oriented issue because it inevitably raises the question, 'valid for what purpose?'… The distinction is central to validation because it is quite possible for a measuring instrument to be relatively valid for measuring one kind of phenomenon but entirely invalid for assessing other phenomena. Thus, one validates not the measuring instrument itself but the measuring instrument in relation to the purpose for which it is being used (Carmines and Zeller 1979:16).

Thus, using examples from the previous section, thermometers, yardsticks, and bathroom scales are not inherently valid instruments. Instead, their application to measure a certain phenomenon must be considered: a thermometer is valid for measuring temperature, not wind speed; a yardstick is valid for measuring length, not weight; and a bathroom scale is valid for measuring weight, not body fat. One must select the phenomenon against which one determines the validity of some instrument or procedure.

Hughes (1998) discusses the second-level validity of using obsidian geochemical characterization as an indicator or measure of trade. He sought to assess the data directly in light of human behavior, skipping over the relevant middle-range theory (which is odd for someone who paraphrases Lewis Binford in his argument). Fortunately, Hector Neff, in the very same volume as Hughes (1998), proposes a more reasonable interpretation of

validity in archaeological sourcing: "The instrument is a *valid* indicator to the extent that composition really does measure 'source' as a location in geographic space and not some other concept" (1998:116). Neff considers proximate validity, whereas Hughes jumps to ultimate validity. I follow, at least in this chapter, Neff's formulation of validity: does an analytical technique, when combined with subsequent data analysis, distinguish obsidian sources (i.e., chemical groups) and nondestructively assign artifacts to them.

The best method, of course, to assess the validity of my analytical procedures and subsequent data analyses is to test them using artifacts from known or suspected sources, which I did and discuss in Section 6.3. First, though, I must explain my approach to data analyses because, while the precision, accuracy, and reliability of measurement data may be considered in isolation, validity involves the entire context.

6.9 - Source Discrimination and Artifact Assignment

In obsidian sourcing, there are two basic approaches to source discrimination and subsequent artifact assignment: graphical-based and multivariate-based approaches. The former is abundant and often effective, and the latter, particularly discriminant function analysis, cluster analysis, and principal components analysis, are also rather common but have a number of issues to consider, such as the role of choice and *a priori* knowledge of groups. In addition, some multivariate techniques involve assumptions incongruent with geochemical data in general and, in particular, the presence of multiple obsidian varieties. Transformation of obsidian data is a debated issue as well. Consequently, in recent years,

there has been somewhat of a backlash against multivariate techniques, and the graphical approaches, using unmodified data, have been combined with geochemical knowledge to differentiate obsidian sources and assign artifacts to them.

6.9.1 - Graphical-Based Discrimination and Sourcing

The first, and most common, approach to data analysis is graphical representation of the concentration data for a few elements, often two or three. Shackley (1995) claims that "most involved with archaeological obsidian geochemistry [prefer] to use the fewest variables necessary to discriminate without modifying the data." This often means using scatterplots of two or three elements, in units of either weight percent or ppm, to show the clusters and where the artifacts fall with respect to them. Shackley (1998a) states that "in many cases the bivariate plots may be a more accurate reflection of source heterogeneity, as well as a better media for source assignment" (13). Thus, he maintains, using "simple bivariate plots and central tendency statistics comparing the artefact and geological data is often sufficient to assign artefacts to sources" (2008:198).

Even among studies that measured 20 or more elements, it is typical to see source discrimination and artifact assignments employing one or more two- or three-dimensional scatterplots with the data either in the original units (percent or ppm) or as ratios. Among articles published in the last ten years on Old World obsidian sourcing, studies using two-dimensional scatterplots include: Abbès et al. (2001, Southwestern Asia [hereafter SWA], Y/Zr vs. Nb/Zr) and (2003, SWA, Sr vs. Zr); Bavay et al. (2000, Eastern Africa, Th/Ta vs.

Th/U); Carter and Shackley (2007, SWA, Zn vs. Zr); Bressy et al. (2005, SWA, Zr vs. Y) and (2008, Western Mediterranean [hereafter WM], Zn vs. Ti); Carter et al. (2008, SWA, Zr vs. Zn); Cherry et al. (2007, SWA, La vs. Sc); Constantinescu et al. (2002, Europe and SWA, Ti/Mn vs. Rb/Zr and Ba/Ce vs. Y/Zr); De Francesco et al. (2008, WM, Zr vs. Nb, Sr vs. Zr, Rb/Sr vs. Zr/Y, etc.); Hall and Kimura (2000, Japanese archipelago, Rb vs. Zr, Zr vs. Sr, Y vs. Sr); Khalidi et al. (2009, SWA, Y vs. Zr, Y/Zr vs. Nb/Zr, Zr vs. Ba); Kim et al. (2007, Southeastern Asia, Zr/Fe vs. Rb/Fe); Kuzmin et al. (2002, Russian Far East; Na vs. Mn); Le Bourdonnec et al. (2005b, WM, Ti vs. K, Zn vs. Zr, Zn vs. Ti) and (2005a, WM; Zr/Sr vs. Rb/Sr, Zr vs. Zn); Lugliè et al. (2007, WM, Zr vs. Rb) and (2008, WM, Ca vs. Al, Fe vs. Al); Negash and Shackley (2006, East Africa, Fe vs. Zr, Fe vs. Mn); Negash et al. (2006, East Africa, Fe vs. Mn, Y vs. Zn); Neri (2007, Philippine islands, Zr vs. Sr); Niknami et al. (2010, SWA, Rb vs. Fe, Sr vs. Fe); Phillips and Speakman (2009, Russian Far East, Rb vs. Sr, Zr vs Sr); Poupeau et al. (2000, WM, Zr vs. Rb) and (2005, SWA, Ba vs. Sr); and Reepmeyer and Clark (2010, Fiji, Pb vs. K, Rb/Sr vs. K, etc.)

Three-dimensional scatterplots have also gained popularity in recent years: Carter and Kilikoglou (2006, SWA, Fe vs. Cs vs. Sc); Le Bourdonnec (2010, WM, Sr vs. Zn vs. Zr) and (2008, SWA, Zr/Ga vs. Sr/Ga vs. Rb/Ga); Lugliè et al. (2007, WM, Sr vs. Zn vs. Zr); Nazaroff et al. (2010, Mesoamerica, Rb vs. Zr vs. Sr); Negash and Shackley (2006, East Africa, Fe vs. Zn vs. Zr); Negash et al. (2007, East Africa, Al vs. Fe vs. Ti, Zn vs. Zr vs. Rb); Sanna et al. (2010, Mediterranean, Ca vs. Ti vs. Na); Shackley (1995, Southwest,

Rb vs. Zn vs. Ba), (1998b, Southwest, Zr vs. Y vs. Nb), and (2009, Southwest, Ba vs. Zr vs. Sr, Ba vs. Sr vs. Rb); and Silliman (2005, California, Rb vs. Zr vs. Sr).

Ternary plots are still occasionally used (e.g., Carter et al. 2006 in SWA with Rb vs. Ba vs. Zr; Neri 2007 in the Philippines with Zr vs. Rb vs. Sr; Seelenfreund et al. 2002 in South America with Zr vs. Rb vs. Sr); however, these triangular diagrams were mostly used in prior decades: Anderson et al. (1986, Iowa, Rb vs. Sr vs. Zr, Fe vs. Ti vs. Mn, Ba vs. Ti vs. Mn); Baugh and Nelson (1987, Mesoamerica, Rb vs. Sr vs. Zr, Fe vs. Ti vs. Mn, Ba vs. Ti vs. MnO, Y vs. Zr vs. Nb); Cauvin et al. (1986, SWA, Mn vs. Fe vs. Sc, Mn vs. Na vs. Sc); Bouey (1984, California, Rb vs. Sr vs. Zr); Ferriz (1985, Mesoamerica, Rb vs. Zr vs. Sr); Fornaseri et al. (1975, SWA, Zr vs. Y vs. Rb, Zr vs. Mn vs. Rb); Nelson et al. (1977, Mexico, Sr vs. Zr vs. Rb, Ba vs. Mn vs. Fe); Nelson and Voorhies (1980, Mexico, Ba vs. Mn vs. Fe); and Shackley (1988, American Southwest, Sr vs. Zr vs. Rb, Nb vs. Rb vs. Zr). Ternary plots appear to have largely fallen out of favor because, in part, the three axes should add up to a constant value, normally 1.0 or 100%, and this does not occur for combinations of three trace elements in various obsidian specimens.

Spidergrams have also recently become a popular method to visually represent the fingerprints of obsidian sources, particularly in Old World studies (e.g., Abbès et al. 2001 in SWA; Chabot et al. 2001 in SWA; Bellot-Gurlet and Poupeau 2006 in SWA; Carter et al. 2006 in SWA; Chabot et al. 2001 in SWA; Chataigner et al. 1998 in SWA; Poupeau et al. 2000 in East Africa; Raynal et al. 2005 in East Africa; Reepmeyer and Clark 2010 in Fiji; and Yellin et al. 1996 in SWA). These charts are basically line graphs that show the

abundances of a series of elements relative to some reference, like their abundances in the mantle or meteorites. Spidergrams usually include rare-earth elements (REEs; like Y, Sc, and the lanthanides) and alkali elements (like K, Rb, and Ba).

6.9.2 - Multivariate Discrimination and Sourcing

The other approach to source discrimination and artifact assignment involves the use of multivariate statistical techniques. The most common techniques are: discriminant function analysis (e.g., Anderson et al. 1986 in North America; Baugh and Nelson 1987 in Mesoamerica; Bouey et al. 1990 in California, Keller and Seifried 1990 in the Near East, Braswell and Glascock 1998 in Mesoamerica, Sand and Sheppard 2000 in South Pacific, Le Bourdonnec et al. 2006 in the Mediterranean, Bressy et al. 2008 in the Mediterranean, Eerkens et al. 2008 in California), forms of cluster analysis (e.g., Ambrose et al. 1981 in the South Pacific, Brown 1983 in North America, Blackman 1984 in the Near East, Hatch et al. 1990 in North America, Fralick et al. 1998 in Mesoamerica, and Oddone et al. 2000 in the Near East), and principal components analysis (PCA; e.g., Williams-Thorpe et al. 1984 in Europe and Ericson and Glascock 2004 in California). Discussing the details of these techniques is well beyond the scope of this dissertation, so readers are forwarded to Baxter's *Exploratory Multivariate Analysis in Archaeology* (1994:48-99 for PCA; 140-184 for cluster analysis; 185-218 for discriminant function analysis).

6.9.3 - Issues with the Multivariate Approach

I chose not to use one of the above statistical techniques due, in large part, to their requirements and/or assumptions. For example, I chose not to identify *a priori* groups in the obsidian specimens because I could not assume that the collection areas corresponded to chemical groups (especially because there were specimens with different compositions in individual collection areas, as discussed in Section 6.7.1). Therefore, I could not use discriminant function analysis because group membership must already be known ahead of time (Baxter 1994:14, Baxter and Buck 2000:709, Wilson and Pollard 2001:509-510). I had no valid way to pre-define geochemical groups. Cluster analysis can be used when group membership is not clear (Baxter 1994:14), but many clustering algorithms involve a choice regarding the number of groups present (140). I also did not want to make such a choice and force a structure onto the data. Cluster analysis also requires a choice of the algorithm used, and Wilson and Pollard (2001) contend that "the decision as to which of the many clustering algorithms are employed (e.g., average linkage, Ward's method) can have a profound effect on the nature of the outcome" (510).

I was also wary of the multivariate techniques due to assumptions made about the data set. In most case, a normal distribution for each variable -- that is, each element -- is assumed. Accordingly, bivariate normal distribution is assumed for each set of elements, meaning that the data in a scatterplot of any two elements should fall in a single elliptical cluster. Recall, as discussed in Section 1.2.4, that obsidian has two principal geochemical trends: peralkaline and alkaline/calc-alkaline. As mentioned earlier, alkaline/calc-alkaline

obsidians normally have higher levels of Ba and Sr while peralkaline obsidians have high Zr and Nb contents. In a geographical region in which both calc-alkaline and peralkaline obsidians occur, Sr will not exhibit a normal distribution, for example. Instead, it will be bimodal: one trend for the calc-alkaline obsidian and another for the peralkaline obsidian. Likewise, a scatterplot of, for example, Ba versus Zr would not exhibit a bivariate normal distribution. In a part of the world where only calc-alkaline obsidian occurs, for instance, the assumptions may be valid, but this is not the case in the Near East.

Compositional data pose another problem for several multivariate techniques: for a "complete" analysis of the major and minor elements (what Baxter [1994] terms "fully compositional" data), the sum is constrained to 100% (or, when considering measurement error in EMPA, approximately 99 to 101%). For trace elements (what Baxter [1994] calls "subcompositional" data), there is, at least practically, no such constraint. This constraint on geochemical data and, the subsequent challenge to its statistical analysis, is also noted by Davis (1973:412), Aitchison and Shen (1984: 637), Aitchison (1986:3), Baxter (1989: 48), and Baxter and Buck (2000:718). The problem is that, even for elements that are not truly geochemically correlated, the constraint induces correlations among elements. This affects a variety of multivariate techniques (Baxter 1994:80).

M.S. Shackley recently cautioned that source "assignments based on multivariate statistical measurement do not necessarily represent groupings based on what is occurring in the field" (2002:60). Wilson and Pollard (2001) contend that ceramics "account for the vast majority of all [sourcing] studies" and that they pose "a greater challenge than lithics

in that there is a much greater degree of anthropogenic manipulation of the raw material" and in that they are complex mixtures of materials (511). Therefore, ceramic researchers have dealt with challenges not faced, or often overlooked, in obsidian sourcing. Shackley (2005) explains that the use of multivariate statistical techniques have come under critical review in ceramic sourcing. He notes that such "self-reflection appears to be occurring in ceramic archaeometry but has not yet appeared in obsidian" research (94). Ceramicists in the American Southwest and Aegean (e.g., Day et al. 1996, Tsolakidou et al. 1996) "have begun to question the assumption that group designations based on multivariate statistical analyses… are necessarily the most perspicacious method" to identify meaningful groups (94). In the latter region, petrographic analysis of clay and pottery, considered in light of ethnographic studies of potters, "indicated that multivariate groupings of NAA data were often incorrect with respect to" source (94). Shackley (2005) states that, though ceramics involve alteration in a way that obsidian does not, "the possibility of misassignment using exclusively multivariate analyses may be just as problematic" (94).

6.9.4 - A Compromise Approach and Focus on Geochemistry

Due to the influence of choice on these multivariate statistical techniques, Wilson and Pollard (2001) assert that "all these techniques offer only empirical solutions" (510). Citing the influence of algorithm choice on the results of cluster analysis, they argue that "perhaps because this introduces a measure of personal preference into the analysis, there has been a tendency in recent years to move away from this automated approach, and to

revert to simpler techniques such as bivariate scatter plots, selected on the basis of some geochemical understanding of the systems involved" (501).

Remember, as mentioned in Section 6.1.2, Shackley reported that "most involved with archaeological obsidian geochemistry [prefer] to use the fewest variables necessary to discriminate without modifying the data" (1995). Accordingly, he proposes:

> The best procedure in my opinion is to combine multivariate analyses (i.e., cluster or discriminant analysis), of one must use them, with graphic displays. If the multivariate group assignments do not agree with that observed in the graphic displays (bivariate or trivariate), then it would be advisable to carefully assign the artifacts to sources. (Shackley 2002:60)

This mixed approach -- scatterplots and a simple multivariate technique (a distance-based technique) using carefully selected elements -- was the one that I adopted.

6.9.5 - Two- and Three-Dimensional Scatterplots

In Section 6.9.1, I establish the abundance of two- and three-dimensional plots in obsidian sourcing research. Figures 6.5 to 6.10 are such plots for my EMPA data of the geological specimens and obsidian artifacts. The main geochemical varieties of obsidian are evident in most of these scatterplots (e.g., the two trends in Figure 6.7). Calc-alkaline obsidian has higher concentrations of Ca and alkalis like K and Na, and alkaline obsidian also has high levels of K and Na but lower Ca. Alkaline and calc-alkaline obsidians also tend to have higher levels of Ba. Peralkaline obsidian, on the other hand, is higher in Fe as well as Zr and Nb. Figure 6.11 demonstrates that, while close in composition, Nemrut Dağ obsidians can be differentiated from the peralkaline Bingöl obsidians (often termed

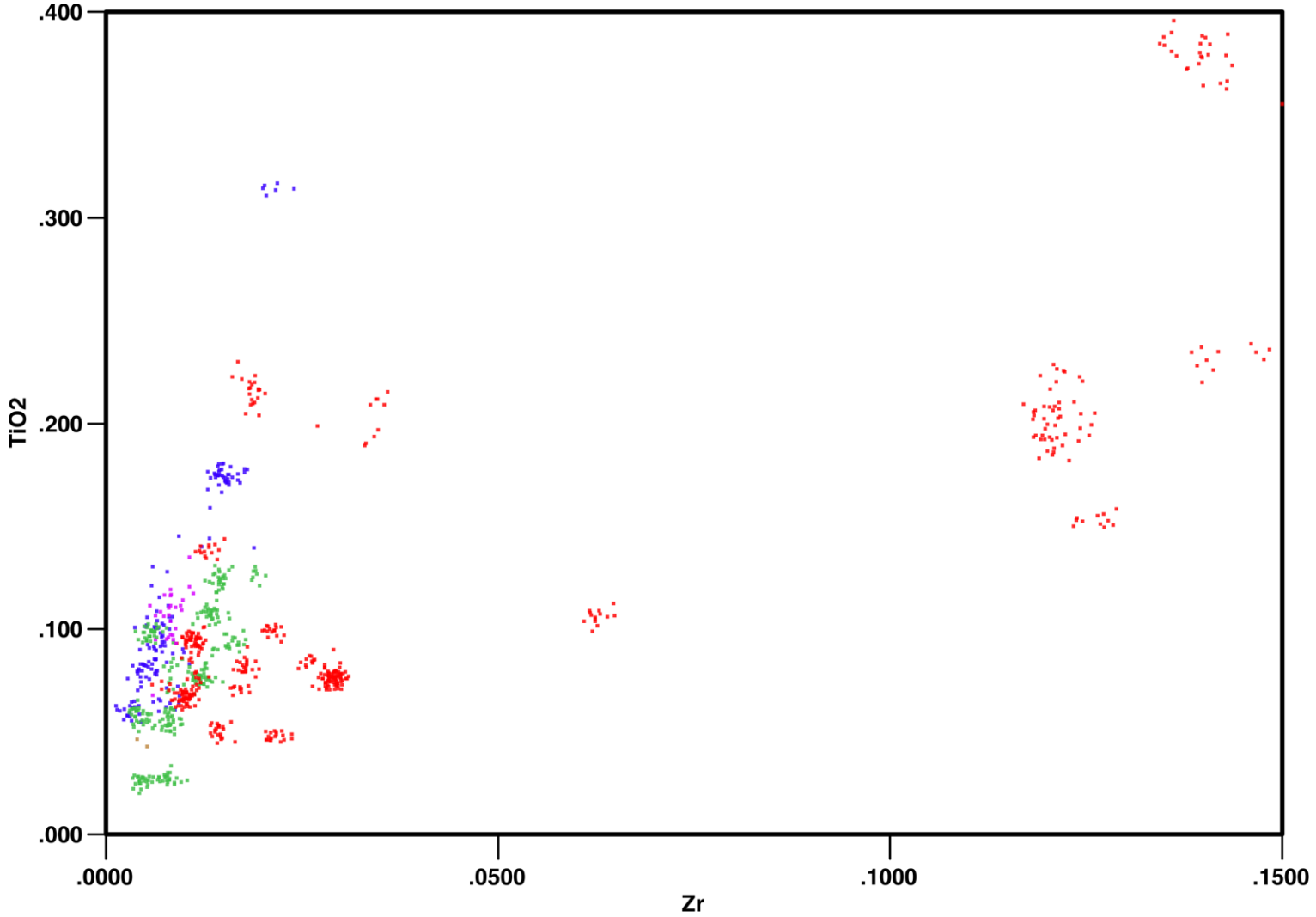


Figure 6.5 - EMPA data for all obsidian specimens; colors coded by region: red = Eastern Anatolia; green = Central Anatolia; brown = the Kabardino-Balkaria Republic of Russia; blue = Armenia; pink = Georgia and Azerbaijan (i.e., the South Caucasus)

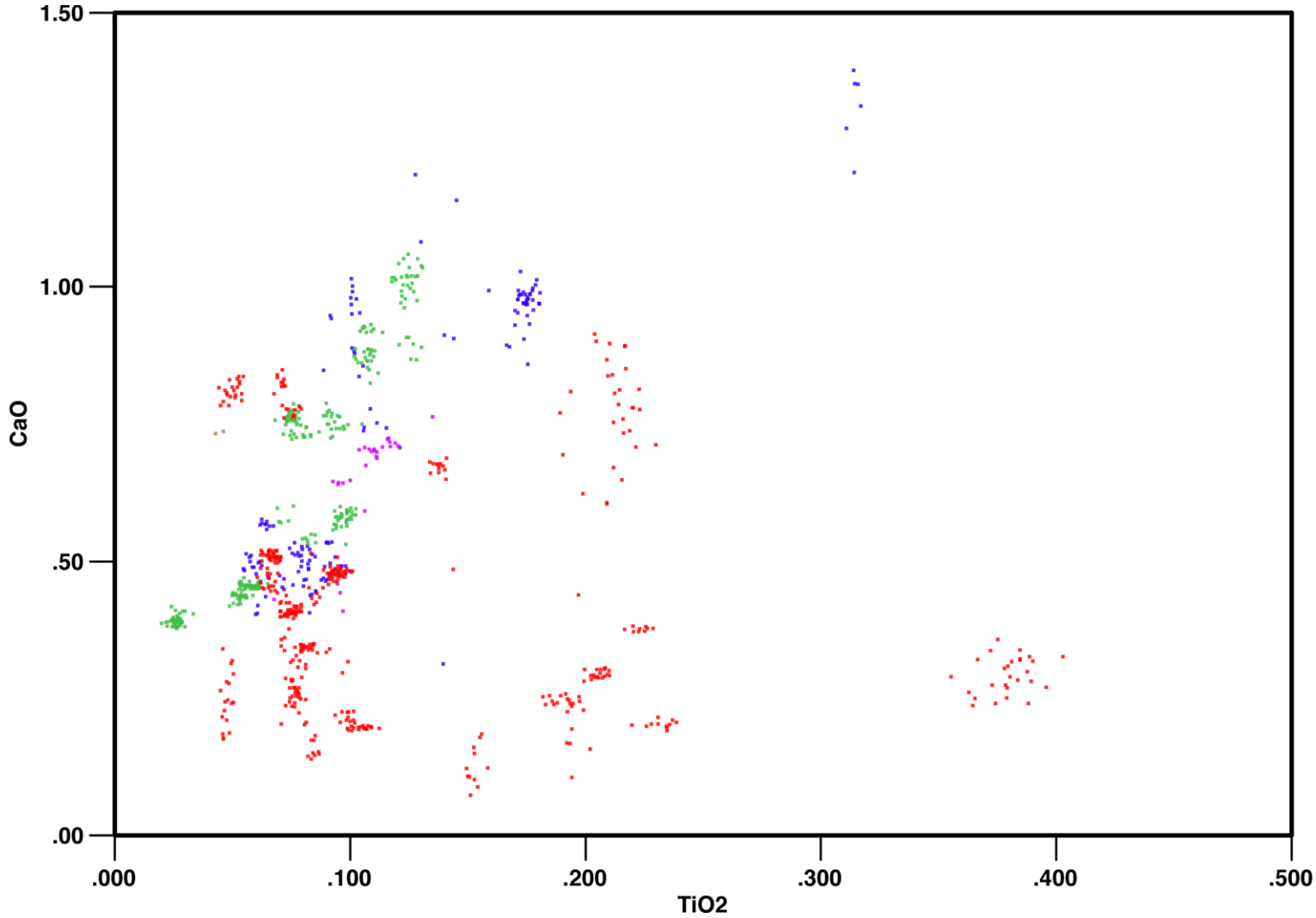


Figure 6.6 - EMPA data for all obsidian specimens; colors coded by region: red = Eastern Anatolia; green = Central Anatolia; brown = the Kabardino-Balkaria Republic of Russia; blue = Armenia; pink = Georgia and Azerbaijan (i.e., the South Caucasus)

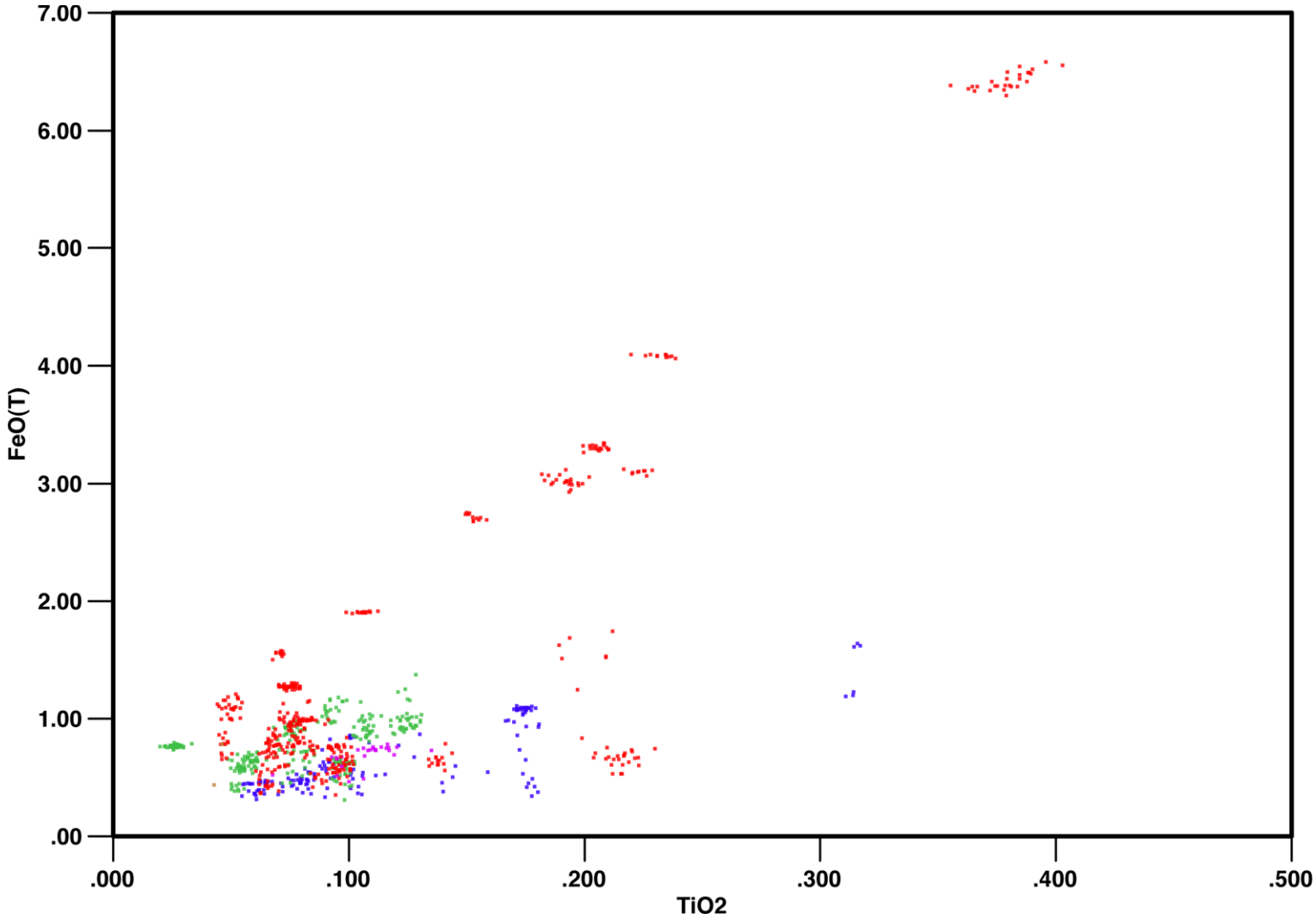


Figure 6.7 - EMPA data for all obsidian specimens; colors coded by region: red = Eastern Anatolia; green = Central Anatolia; brown = the Kabardino-Balkaria Republic of Russia; blue = Armenia; pink = Georgia and Azerbaijan (i.e., the South Caucasus)

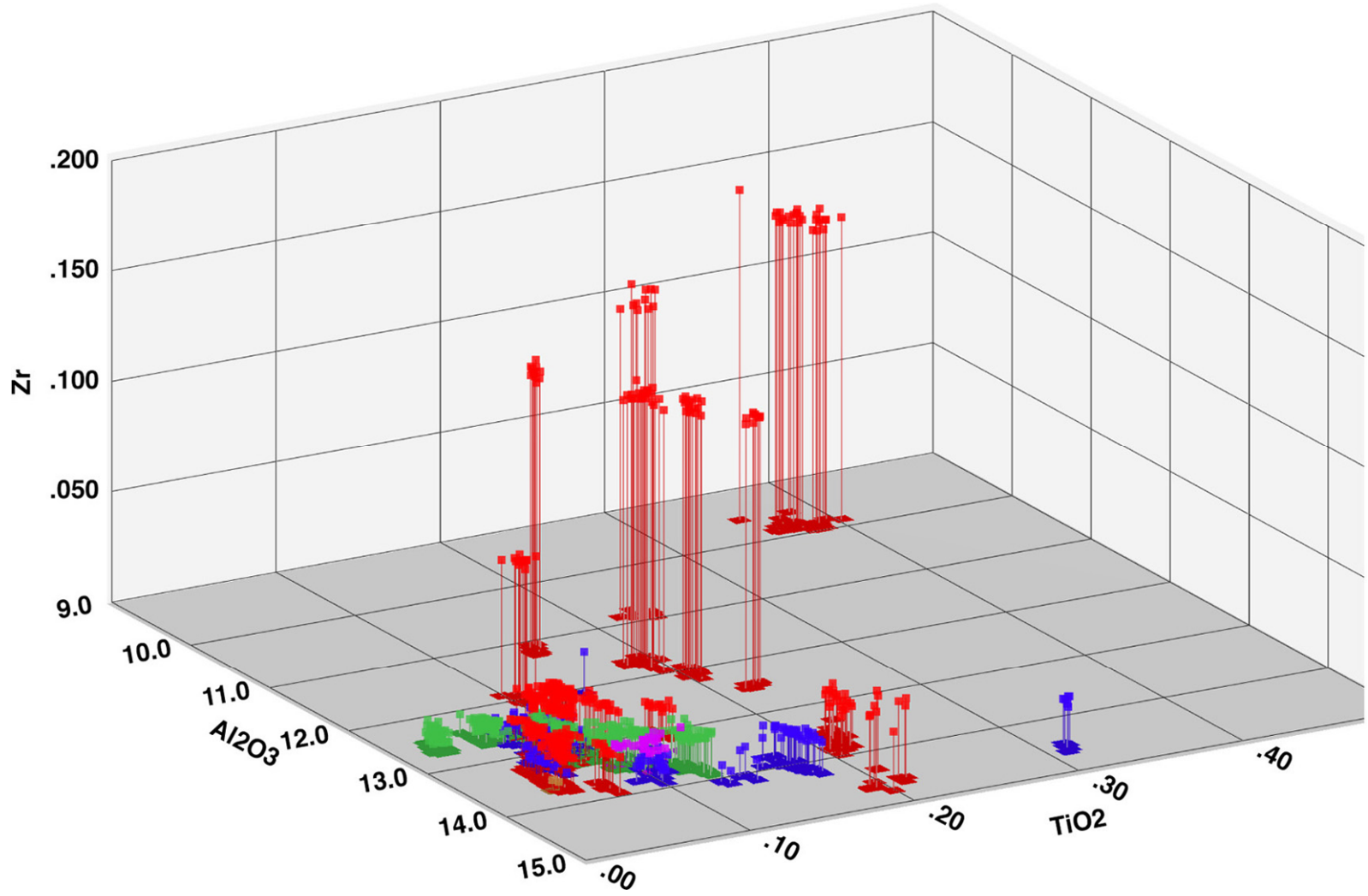


Figure 6.8 - EMPA data for all obsidian specimens; colors coded by region: red = Eastern Anatolia; green = Central Anatolia; brown = the Kabardino-Balkaria Republic of Russia; blue = Armenia; pink = Georgia and Azerbaijan (i.e., the South Caucasus)

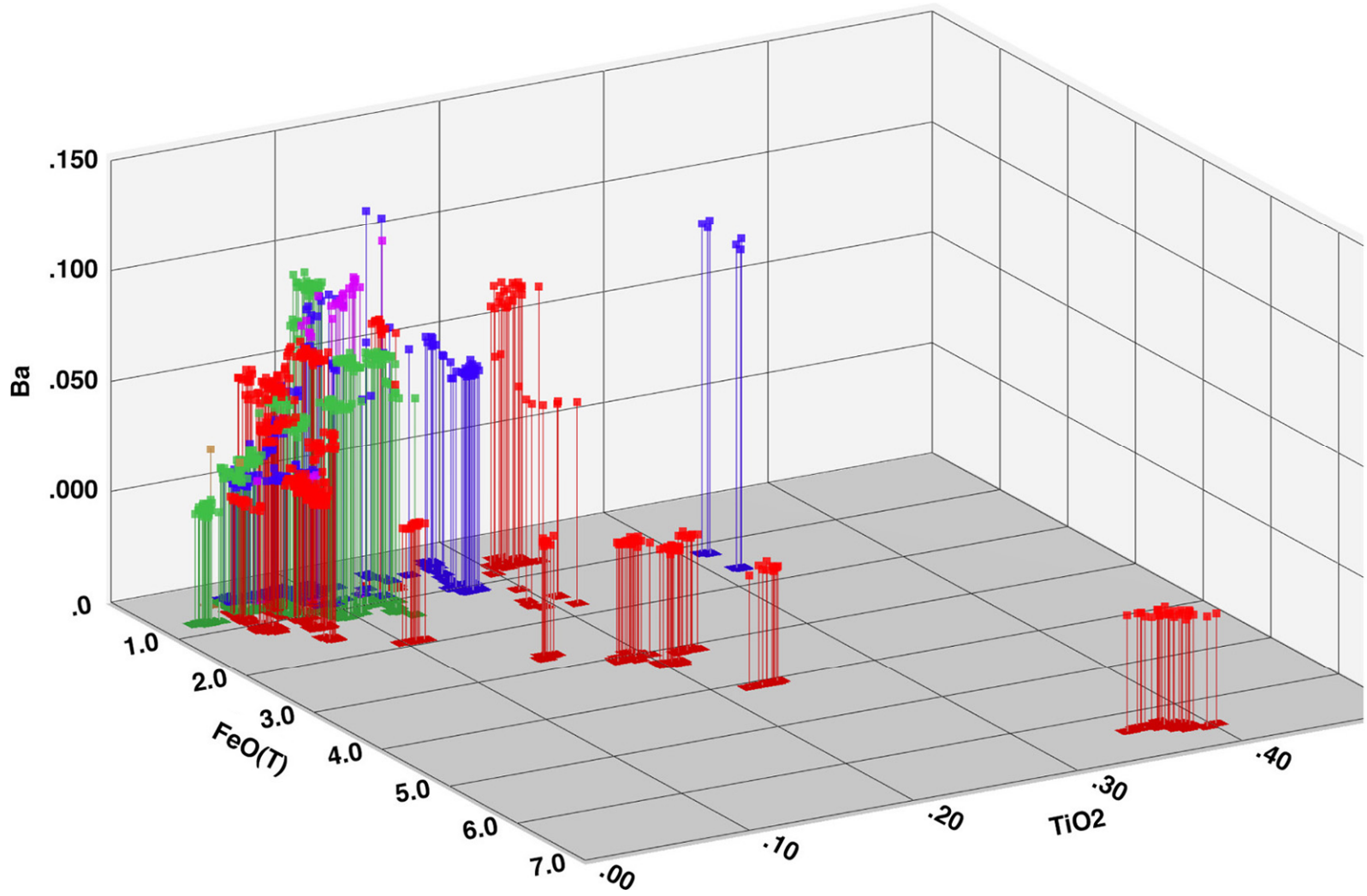


Figure 6.9 - EMPA data for all obsidian specimens; colors coded by region: red = Eastern Anatolia; green = Central Anatolia; brown = the Kabardino-Balkaria Republic of Russia; blue = Armenia; pink = Georgia and Azerbaijan (i.e., the South Caucasus)

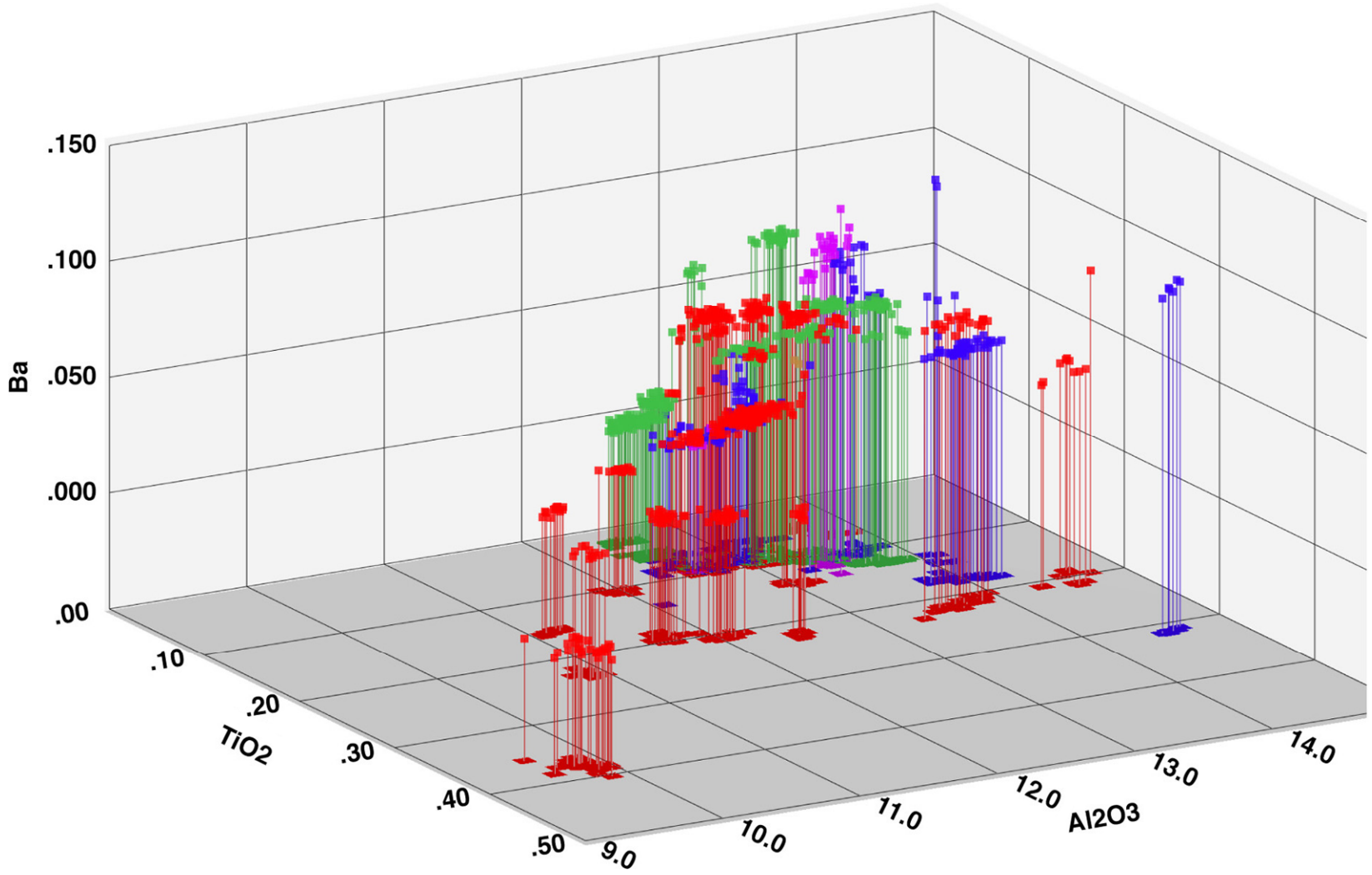


Figure 6.10 - EMPA data for all obsidian specimens; colors coded by region: red = Eastern Anatolia; green = Central Anatolia; brown = the Kabardino-Balkaria Republic of Russia; blue = Armenia; pink = Georgia and Azerbaijan (i.e., the South Caucasus)

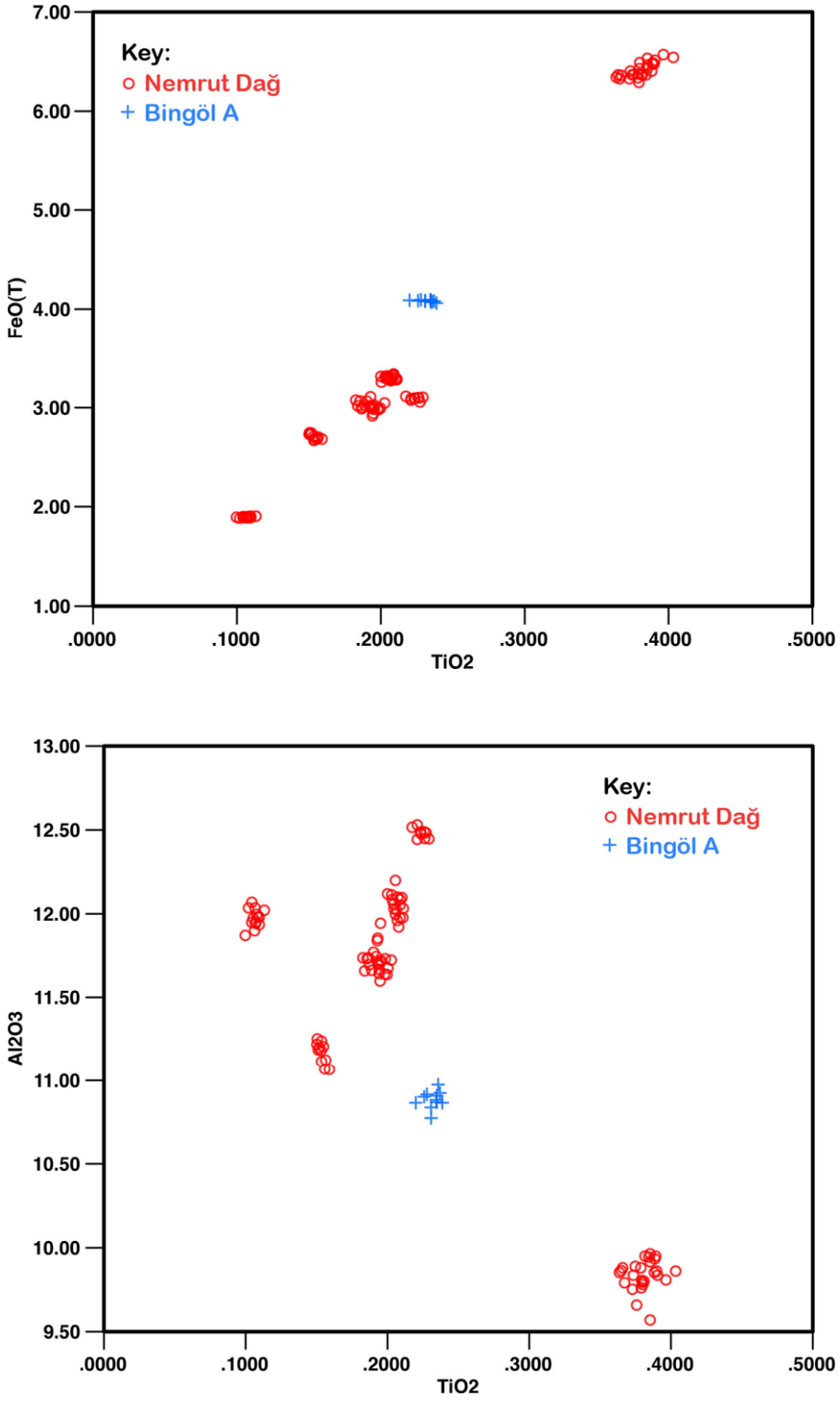


Figure 6.11 - Using major elements (such as Al, Fe, and Ti) and precise analyses, the Nemrut Dağ specimens (red) are clearly separated from the Bingöl A specimens (blue).

"Bingöl A"), a problem in numerous studies (e.g., Renfrew et al. 1966, 1968, *inter alia*; Poidevin 1998:136; Abbès et al. 2001:12, 2003:164; Bellot-Gurlet and Poupeau 2006:3; Carter et al. 2008:900; Khalidi 2009:883; *cf.* Chataigner 1994, 1998). Scatterplots also revealed that, due to the surface hydration and alteration of the artifacts, some elements useful for source discrimination cannot be used for artifact assignment. This is a product of my non-destructive approach to analyzing the artifacts. If I had removed and polished tiny chips from the artifacts, several more elements would have been useful. These plots, therefore, were useful in selecting elements for multivariate analysis.

6.9.6 - Elements for Source Assignment

The two- and three-dimensional scatterplots were especially useful for identifying those elements most effective for distinguishing sources, those measured without enough precision to clearly separate sources, and those most affected by hydration and alteration of the artifacts' surfaces (as discussed in Sections 5.3.3 and 5.3.4). This allowed me to choose critically the elements included in my multivariate data analyses.

As discussed in Section 6.1.1, Hughes (1984) criticized a belief that "the inclusion of larger numbers of variables in discriminant analysis results in a 'better' classification... [I]n fact this is not necessarily the case" (3). Baxter (2003) concurs and claims that there is a bias toward measuring many elements because "one does not know in advance which elements may have discriminatory power" (22). Also, if NAA or XRF, can analyze for 28 elements just as easily as for 10, what harm is there in measuring all 28 elements? Baxter

answers that selecting appropriate variables (i.e., elements) to include in the data analysis then becomes an issue because any one variable "can potentially obscure as well as reveal structure in the data" (2003:22). He asserts that, in sourcing studies, *choice* of "variables to use in analysis is unavoidable" (Baxter and Jackson 2001:253).

There is some validity in measuring as many elements as possible, contend Baxter and Jackson (2001), but "it does not follow that it is necessarily beneficial to use as many measured variables as possible in a statistical analysis" (253). They argue that there is "a distinction between the number of variables measured and the number actually needed in an analysis" and that researchers should use a "subset [of elements] that is 'good' in some sense" (254). Others disagree, like Glascock (1992), who stated about ceramic sourcing: "it is advisable to use the information on all elements having few missing values in order to use the maximum amount of information when generating clusters" (17). This view is, like that of Harbottle (1982) in Section 6.1.1, influenced by taxonomic theories. He even cites the book *Numerical Taxonomy* (1973) by clinical microbiologist Peter H. Sneath and biostatistician Robert R. Sokal, who give the first principle of taxonomy as: "The greater the content of information in the taxa of a classification and the more characters on which it is based, the better a given classification will be" (5). Baxter and Jackson (2001) point out that elements "need not be informative or structure-carrying" and that including such uninstructive elements in multivariate data analyses "can actually obscure the perception of real patterns" (254). In addition, when precision is poor, Baxter (2001) argues that "it is questionable whether the elements so affected should be used in clustering" (138). As

noted in Section 6.1.1, Hughes (1984) made a similar claim: "poorly measured [or] weak [elements]... can actually increase the number of misclassifications" (3).

In the present research, I had to consider two reasons to remove elements from the multivariate analyses: (1) elements measured with poor precision and/or accuracy and (2) elements strongly affected by hydration and chemical alteration of the artifacts' surfaces. With respect to the first criteria, I decided, based on the scatterplots and the accuracy tests earlier in this chapter, that Ga and Nb should not be included. In addition, S and Cr, both from the major-element round, had very low concentrations and, thus, were not measured with sufficient precision to include in the multivariate data analysis.

As for the second criteria, I had an idea what to expect based on the available, but scant, literature. I anticipated that Si would be strongly affected because it is the element directly involved in hydration -- the water breaks Si–O–Si bonds and then forms Si–O–H H–O–Si pairs (Ernsberger 1977, Bartholomew et al. 1980, Yanagisawa et al. 1997). Also I expected that alkalis (Na and K) would have altered concentrations in the surface layers (Friedman et al. 1969:67, Tsong et al. 1978, Patel et al. 1998). Tsong et al. (1978) found near-surface depletion of Ca and Mg but not Al and Si, and Patel et al. (1998) also noted no alteration of Al and Si. Anovitz et al. (1999) reported different alternation patterns for obsidians; however, for most sources, Fe and Ca showed constant concentrations within a few tenths of a micrometer of the surfaces. I also expected that other elements, especially Cl, F, and P, might be highly susceptible to hydration and alteration.

In the end, based chiefly on examination of the scatterplots of both the geological specimens and the artifacts, I decided that eight measured elements -- Ti, Al, Fe, Mn, Ca, Zr, Zn, and Ba -- could be included in my multivariate data analyses.

6.9.7 - Euclidean Distance Measures

As established in Section 6.9.1, two- and three-dimensional scatterplots are quite popular in obsidian sourcing because, with the right elements, they are very effective for source discrimination and artifact assignment. It made sense, then, to use a multivariate technique that could replicate the use of these scatterplots quantitatively and with three or more elements. The Euclidean distance (ED; also called the Euclidean metric or, in older books, the Pythagorean metric) is a straightforward multivariate measure of distance. On a two-dimensional scatterplot, ED is the "straight-line" distance between two data points that one can measure with a ruler or calculate using the Pythagorean theorem. This same concept can be extended to three, four, or even more dimensions.

This is not the first obsidian sourcing study to use an ED-based approach. Barker et al. (2002) explain that, based on four elements (Rb, Zr, Mn, and Fe) measured by XRF, "a Euclidean distance search of the 15,000 obsidian samples in the MURR NAA database was conducted" (106). Other obsidian studies have utilized ED-based techniques as well (e.g., Bustamante et al. 2007 in the Andes, Fralick et al. 1998 in Mexico, Kilikoglou et al. 1997 in the Aegean, and Seelenfreund et al. 2002 in South America). ED-based methods have also been used to source other rocks. For example, Weigand et al. (1977), sourcing

turquoise in Mesoamerica, calculated the ED between specimens and sorted the resulting distance matrix of similarity coefficients (27-28, 30). In their sourcing study of Egyptian basalt, Greenough et al. (2001) found the ED values yielded similar results to those using other techniques, such as cluster analysis (773). Ceramics research has also used similar approaches. For example, studying Sicilian pottery, Barone et al. (2005) explains that ED and nearest neighbor searches were used to identify groups (755).

6.9.8 - A Minimalist Approach to Data Transformation

Before calculating the Euclidean distance matrices, I needed to convert the data so that elemental values, varying over four orders of magnitude, could be compared without major elements (like SiO_2 and Al_2O_3) dominating trace elements (like Nb and Zn, present at ppm-levels). To do this, I transformed the concentrations to have a maximum value of 1 by normalizing to the highest concentration for each element. As a result, my data were transformed (scales equalized) but were not standardized (statistical variances equalized) or converted to a logarithmic scale. Beier and Mommsen (1991, 1994) and Baxter (1995) concluded that it is unnecessary to use logarithmic data except in the presence of extreme outliers. Baxter (2001) claims "the use of untransformed as opposed to logged data is not a critical difference" (138), and he asserts that, when dissimilar results arise between data transformed two different ways (e.g., standardized and logarithmic), "there is no obvious reason for preferring one approach to the other... no single approach can be recommended for data" of this kind (1995:525). Shackley (2005) states that some researchers "are quite

comfortable with normalizing data by normal or other log transformations, elimination of outliers, and reanalysis… although there has been very little critical examination of this technique, particularly in obsidian geochemistry" (12). Thus, I chose the simplest option, keeping in mind the presence of distinct geochemical types of obsidian -- peralkaline and alkine/calc-alkaline -- that might skew a transformation.

Furthermore, I decided not to transform my data from Euclidean distance (ED) to Mahalanobis distance (MD). Dr. Michael Baxter, Professor of Statistical Archaeology at Nottingham Trent University, explains that MD can be applied to transform a data set that contains highly correlated variables (i.e., elements):

> This [correlation] gives rise to an elliptical scatter of points which turns out to be unsuitable for the application of certain common methods of multivariate analysis… Ideally the scatter should be circular, and the idea behind the use of Mahalanobis distance is that such an elliptical scatter is transformed into circularity before analysis… Imagine this to be a solid made of malleable material (such as dough), then in transforming to Mahalanobis distance we are attempting to 'squeeze' this solid into a spherical shape. (1994:80)

These resulting spherical clusters are more compatible with many multivariate techniques than the original ellipsoids, and this transformation also minimizes the "double counting" of correlated variables with ED, which concerns some researchers (Baxter 1994:169). In other words, MD reduces the influence of correlated variables (Jolliffe 1986:77). MD has been used for sourcing ceramics (e.g., Bieber et al. 1976; Harbottle 1976, 1991; Glascock 1992; Beier and Mommsen 1994; Kosakowsky et al. 1999) and obsidian (e.g., Ward 1974 in New Zealand; Glascock 1994 throughout the New World; Shackley 1998a in the North American Southwest; Reepmeyer and Clark 2010 on the Fiji islands).

The MD, though, has a few limitations on its use. For example, bivariate normal distribution is presumed for each pair of elements, so that the data in a scatterplot of any two elements should fall in a single, elongated cluster. This assumption is violated when multiple clusters, or groups, are present in the data. Baxter explains that ED is converted to MD by applying a covariance matrix, which he terms **S**, to the data, and there is only…

> … a single group from which **S** may be calculated. If more than one group exists in the data, then **S** should be calculated as a weighted average of the separate covariance matrices for each group rather than for the data as a whole; this requires, ideally, that groups be of similar shape. This limits the application of Mahalanobis distance in practice since the detection of groups within the data is often the object of the exercise -- they are not known in advance to enable **S** to be calculated. The assumption that groups, even if known, are of similar shape is also often questionable. (1994:81)

Geochemical groups should, therefore, be known ahead of time and taken into account in the calculation of **S**. This, again, requires choice. Furthermore, recall that obsidian in the Near East has two geochemical trends: peralkaline and alkaline/calc-alkaline. In a plot of Ba and Zr, for example, the data will not exhibit a bivariate normal distribution. Instead, the plot will be bimodal: one trend for the alkaline/calc-alkaline obsidian and another for the peralkaline obsidian. The extreme variance due to these two varieties seems likely to cause transformations that do not represent geochemical reality, and it clearly violates the MD assumptions. Regarding such transformations, Shackley (1995:546) warns

> … this would produce 'normaloid' data from generally nonnormal geochemical data. While this has some utility, it often dissolves the very variability (normal or otherwise) that allows one to discriminate sources. While any statistical analysis of the data requiring normality (i.e., many classification analyses) would be enhanced, the sacrifice of variability needed to discriminate may be too great.

Also, for each cluster (i.e., geochemical group), MD requires more cases (i.e., geological specimens) than variables (i.e., elements). In fact, three to five times as many specimens are needed (Baxter and Buck 2000:717, Baxter 2001:135). For only five elements, there is a requirement of 15 to 25 geological specimens per cluster (i.e., source or geochemical group). For ten elements, 30 to 50 specimens are needed. This sample size requirement, unfortunately, was not met for all of the sources in this study. Thus, I decided to use ED, rather than MD, for identifying geological specimen matches to artifacts.

6.9.9 - Using Euclidean Distances to Assign Artifacts to Sources

After I transformed my elemental data, I calculated the ED between each artifact and each of the 900+ obsidian specimens for eight element combinations: (1) Fe, Ti, Ba; (2) Fe, Ti, Zr; (3) Fe, Zr, Ba; (4) Ti, Zr, Ba; (5) Ti, Fe, Zr, Ba; (6) Ti, Fe, Zr, Ba, Zn; (7) Ti, Fe, Mn, Ca, Zr, Ba; and (8) Ti, Al, Fe, Mn, Ca, Zr, Ba. The first four combinations are three-dimensional cases, essentially equivalent to the three-axis scatterplots in Figures 6.8 to 6.10. The final combination, with seven elements, is seven-dimensional. The data for each artifact and specimen (reported in Appendix C) are actually mean values from ten or more analyses. Thus, the EDs were essentially calculated between the centroids for each artifact and specimen. With 900+ geological specimens and 100+ artifacts, the result for each of the eight element combinations was a matrix of over one million ED values. The calculations were conducted using SPSS Version 16.0.2, and the resulting matrices were exported to Microsoft Excel for further calculations and data analysis.

I then conducted a nearest neighbor search of these ED values to discover the ten geological specimens "nearest" to each artifact. Tables 6.18 through 6.21 give examples of the calculated ED values and the nearest neighbors for just four artifacts. Appendix D gives the results for all 98 artifacts from Tell Mozan and eight test artifacts from Georgia, as discussed in the next section. Let us consider a particular artifact: A1 q161-1 f16 k117 in Table 6.18. Based on Fe, Ti, and Ba, the ten "nearest" specimens all came from EA25 at Nemrut Dağ. The same is true for four other element combinations: (i) Fe, Ti, Zr; (ii) Ti, Fe, Zr, Ba; (iii) Ti, Fe, Mn, Ca, Zr, Ba; and (iv) Ti, Al, Fe, Mn, Ca, Zr, Ba. Based on Fe, Zr, and Ba, five of the six "nearest" specimens are from EA25. Based on Ti, Zr, and Ba, the eight "nearest" geological specimens also came from EA25. I am most interested in a stable source assignment (i.e., an artifact is attributed to the same source for multiple combinations of elements), so I consider all eight element combinations. Taken together, 66 of the 80 "nearest" specimens came from EA25, so I consider this collection area to be the "A Rank" match. The other 14 geological specimens came from collection area EA22 at Nemrut Dağ, so I consider it to be the "B Rank" match. Therefore, I quite confidently assigned this artifact to collection area EA25 at Nemrut Dağ.

Let us examine another example: A10 q1194.3 f925 k29 in Table 6.20. Note that, for the first combination of elements (Fe, Ti, and Ba), Bingöl B obsidians constitute the first seven "nearest" geological specimens. Their ED values range from 0.019 to 0.053. The next two specimens are Armenian obsidians from Gutansar, and their values abruptly increase to 0.095 and 0.097. This jump in ED indicates that Bingöl B is a much superior match to the artifact than Gutansar. Consequently, for Fe, Ti, and Ba, Bingöl B is the "A

Table 6.18 - Example of Euclidean Distance Measures and Nearest Neighbors for an Artifact Assigned to Nemrut Dag (EA25)

Artifact: A1 q161-1 f16 k117

A-Rank: **Nemrut Dag (EA25)** **66** ← of the 80 nearest neighbors to this artifact (10 from each of 8 element combinations), 66 are obsidian specimens from collection area EA25
B-Rank: Nemrut Dag (EA22) 14

Elements: Fe, Ti, Ba

A-Rank:	**Nemrut Dag (EA25)**	**10**
B-Rank:	-	-

Specimen	*Location*	*E.D.*
EA25P3	**Nemrut Dag (EA25)**	0.007
EA25R1	**Nemrut Dag (EA25)**	0.012
EA25P1B	**Nemrut Dag (EA25)**	0.015
EA25P1D	**Nemrut Dag (EA25)**	0.016
EA25P1A	**Nemrut Dag (EA25)**	0.018
EA25P2B	**Nemrut Dag (EA25)**	0.019
EA25P1C	**Nemrut Dag (EA25)**	0.023
EA25P2C	**Nemrut Dag (EA25)**	0.026
EA25P2D	**Nemrut Dag (EA25)**	0.026
EA25P2A	**Nemrut Dag (EA25)**	0.027

Elements: Fe, Zr, Ba

A-Rank:	**Nemrut Dag (EA25)**	**5**
B-Rank:	Nemrut Dag (EA22)	5

Specimen	*Location*	*E.D.*
EA25P1D	**Nemrut Dag (EA25)**	0.019
EA25P1A	**Nemrut Dag (EA25)**	0.024
EA25P1B	**Nemrut Dag (EA25)**	0.024
EA22P4	Nemrut Dag (EA22)	0.028
EA25P1C	**Nemrut Dag (EA25)**	0.032
EA25R1	**Nemrut Dag (EA25)**	0.038
EA22P8A	Nemrut Dag (EA22)	0.039
EA22P5B	Nemrut Dag (EA22)	0.040
EA22P6B	Nemrut Dag (EA22)	0.040
EA22P8B	Nemrut Dag (EA22)	0.041

Elements: Ti, Fe, Zr, Ba

A-Rank:	**Nemrut Dag (EA25)**	**10**
B-Rank:	-	-

Specimen	*Location*	*E.D.*
EA25P1D	**Nemrut Dag (EA25)**	0.022
EA25P1B	**Nemrut Dag (EA25)**	0.024
EA25P1A	**Nemrut Dag (EA25)**	0.026
EA25P1C	**Nemrut Dag (EA25)**	0.033
EA25R1	**Nemrut Dag (EA25)**	0.038
EA25P3	**Nemrut Dag (EA25)**	0.042
EA25P2C	**Nemrut Dag (EA25)**	0.046
EA25P2D	**Nemrut Dag (EA25)**	0.049
EA25P2A	**Nemrut Dag (EA25)**	0.053
EA25P2B	**Nemrut Dag (EA25)**	0.053

Elements: Ti, Fe, Mn, Ca, Zr, Ba

A-Rank:	**Nemrut Dag (EA25)**	**10**
B-Rank:	-	-

Specimen	*Location*	*E.D.*
EA25P1A	**Nemrut Dag (EA25)**	0.032
EA25P1C	**Nemrut Dag (EA25)**	0.033
EA25P1B	**Nemrut Dag (EA25)**	0.039
EA25R1	**Nemrut Dag (EA25)**	0.051
EA25P3	**Nemrut Dag (EA25)**	0.052
EA25P1D	**Nemrut Dag (EA25)**	0.055
EA25P2C	**Nemrut Dag (EA25)**	0.057
EA25P2B	**Nemrut Dag (EA25)**	0.061
EA25P2A	**Nemrut Dag (EA25)**	0.062
EA25P2D	**Nemrut Dag (EA25)**	0.064

Elements: Fe, Ti, Zr

A-Rank:	**Nemrut Dag (EA25)**	**10**
B-Rank:	-	-

Specimen	*Location*	*E.D.*
EA25P1B	**Nemrut Dag (EA25)**	0.021
EA25P1D	**Nemrut Dag (EA25)**	0.021
EA25P1A	**Nemrut Dag (EA25)**	0.022
EA25P1C	**Nemrut Dag (EA25)**	0.026
EA25R1	**Nemrut Dag (EA25)**	0.038
EA25P2C	**Nemrut Dag (EA25)**	0.040
EA25P3	**Nemrut Dag (EA25)**	0.042
EA25P2D	**Nemrut Dag (EA25)**	0.044
EA25P2A	**Nemrut Dag (EA25)**	0.048
EA25P2B	**Nemrut Dag (EA25)**	0.051

Elements: Ti, Zr, Ba

A-Rank:	**Nemrut Dag (EA25)**	**8**
B-Rank:	Nemrut Dag (EA22)	2

Specimen	*Location*	*E.D.*
EA25P1D	**Nemrut Dag (EA25)**	0.022
EA25P1B	**Nemrut Dag (EA25)**	0.023
EA25P1A	**Nemrut Dag (EA25)**	0.024
EA25P1C	**Nemrut Dag (EA25)**	0.032
EA25R1	**Nemrut Dag (EA25)**	0.037
EA25P3	**Nemrut Dag (EA25)**	0.042
EA25P2C	**Nemrut Dag (EA25)**	0.046
EA25P2D	**Nemrut Dag (EA25)**	0.049
EA22P2	Nemrut Dag (EA22)	0.050
EA22P6B	Nemrut Dag (EA22)	0.051

Elements: Ti, Fe, Zr, Ba, Zn

A-Rank:	Nemrut Dag (EA22)	7
B-Rank:	**Nemrut Dag (EA25)**	**3**

Specimen	*Location*	*E.D.*
EA25P2C	**Nemrut Dag (EA25)**	0.057
EA22P7A	Nemrut Dag (EA22)	0.073
EA22R1	Nemrut Dag (EA22)	0.080
EA22P1D	Nemrut Dag (EA22)	0.085
EA22P5B	Nemrut Dag (EA22)	0.085
EA22P3	Nemrut Dag (EA22)	0.096
EA22P1C	Nemrut Dag (EA22)	0.106
EA25P1D	**Nemrut Dag (EA25)**	0.107
EA25P1A	**Nemrut Dag (EA25)**	0.108
EA22P7B	Nemrut Dag (EA22)	0.110

Elements: Ti, Al, Fe, Mn, Ca, Zr, Ba

A-Rank:	**Nemrut Dag (EA25)**	**10**
B-Rank:	-	-

Specimen	*Location*	*E.D.*
EA25P1C	**Nemrut Dag (EA25)**	0.043
EA25P1A	**Nemrut Dag (EA25)**	0.046
EA25P1B	**Nemrut Dag (EA25)**	0.047
EA25P1D	**Nemrut Dag (EA25)**	0.059
EA25P3	**Nemrut Dag (EA25)**	0.061
EA25R1	**Nemrut Dag (EA25)**	0.062
EA25P2C	**Nemrut Dag (EA25)**	0.063
EA25P2A	**Nemrut Dag (EA25)**	0.067
EA25P2B	**Nemrut Dag (EA25)**	0.067
EA25P2D	**Nemrut Dag (EA25)**	0.069

Table 6.19 - Example of Euclidean Distance Measures and Nearest Neighbors for an Artifact Assigned to Nemrut Dag (EA22)

Artifact: J1 q276.5 f131 k64

A-Rank: **Nemrut Dag (EA22)** **59** ← of the 80 nearest neighbors to this artifact (10 from each of 8 element combinations), 59 are obsidian specimens from collection area EA22
B-Rank: Nemrut Dag (EA21) 10

Elements: Fe, Ti, Ba

A-Rank:	Nemrut Dag (EA25)	5
B-Rank:	**Nemrut Dag (EA22)**	**5**

Specimen	*Location*	*E.D.*
EA25R2	Nemrut Dag (EA25)	0.064
EA25P2C	**Nemrut Dag (EA22)**	0.068
EA22P7A	**Nemrut Dag (EA22)**	0.070
EA25P2D	Nemrut Dag (EA25)	0.071
EA22P2	**Nemrut Dag (EA22)**	0.072
EA25P1C	Nemrut Dag (EA25)	0.072
EA25P2A	Nemrut Dag (EA25)	0.072
EA22P7B	**Nemrut Dag (EA22)**	0.075
EA22R1	**Nemrut Dag (EA22)**	0.075
EA25P2B	Nemrut Dag (EA25)	0.076

Elements: Fe, Zr, Ba

A-Rank:	**Nemrut Dag (EA22)**	**5**
B-Rank:	Nemrut Dag (EA21)	3

Specimen	*Location*	*E.D.*
EA21P1	Nemrut Dag (EA21)	0.081
EA22P7A	**Nemrut Dag (EA22)**	0.085
EA22P5A	**Nemrut Dag (EA22)**	0.087
EA23P1B	Nemrut Dag (EA23)	0.094
EA22P6A	**Nemrut Dag (EA22)**	0.095
EA22P7B	**Nemrut Dag (EA22)**	0.095
EA21R1A	Nemrut Dag (EA21)	0.096
EA22R1	**Nemrut Dag (EA22)**	0.096
EA23P1A	Nemrut Dag (EA23)	0.096
EA21R1B	Nemrut Dag (EA21)	0.097

Elements: Ti, Fe, Zr, Ba

A-Rank:	**Nemrut Dag (EA22)**	**8**
B-Rank:	Nemrut Dag (EA21)	2

Specimen	*Location*	*E.D.*
EA22P7A	**Nemrut Dag (EA22)**	0.091
EA21P1	Nemrut Dag (EA21)	0.095
EA22P5A	**Nemrut Dag (EA22)**	0.099
EA22R1	**Nemrut Dag (EA22)**	0.102
EA22P7B	**Nemrut Dag (EA22)**	0.103
EA22P6B	**Nemrut Dag (EA22)**	0.104
EA22P8B	**Nemrut Dag (EA22)**	0.105
EA21R1B	Nemrut Dag (EA21)	0.107
EA22P6A	**Nemrut Dag (EA22)**	0.107
EA22P3	**Nemrut Dag (EA22)**	0.108

Elements: Ti, Fe, Mn, Ca, Zr, Ba

A-Rank:	**Nemrut Dag (EA22)**	**8**
B-Rank:	Nemrut Dag (EA21)	2

Specimen	*Location*	*E.D.*
EA22P7B	**Nemrut Dag (EA22)**	0.105
EA21P1	Nemrut Dag (EA21)	0.109
EA22R1	**Nemrut Dag (EA22)**	0.113
EA22P6B	**Nemrut Dag (EA22)**	0.116
EA22P6A	**Nemrut Dag (EA22)**	0.118
EA22P7A	**Nemrut Dag (EA22)**	0.119
EA22P4	**Nemrut Dag (EA22)**	0.120
EA22R2	**Nemrut Dag (EA22)**	0.121
EA21R1B	Nemrut Dag (EA21)	0.122
EA22P1A	**Nemrut Dag (EA22)**	0.125

Elements: Fe, Ti, Zr

A-Rank:	**Nemrut Dag (EA22)**	**8**
B-Rank:	Nemrut Dag (EA21)	2

Specimen	*Location*	*E.D.*
EA22P7A	**Nemrut Dag (EA22)**	0.068
EA22P5A	**Nemrut Dag (EA22)**	0.073
EA22P8B	**Nemrut Dag (EA22)**	0.076
EA21P1	Nemrut Dag (EA21)	0.077
EA21R1B	Nemrut Dag (EA21)	0.077
EA22P3	**Nemrut Dag (EA22)**	0.079
EA22P6A	**Nemrut Dag (EA22)**	0.080
EA22P6B	**Nemrut Dag (EA22)**	0.080
EA22R1	**Nemrut Dag (EA22)**	0.081
EA22P4	**Nemrut Dag (EA22)**	0.082

Elements: Ti, Zr, Ba

A-Rank:	**Nemrut Dag (EA22)**	**9**
B-Rank:	Nemrut Dag (EA21)	1

Specimen	*Location*	*E.D.*
EA22P7A	**Nemrut Dag (EA22)**	0.088
EA21P1	**Nemrut Dag (EA22)**	0.092
EA22P5A	**Nemrut Dag (EA22)**	0.098
EA22R1	**Nemrut Dag (EA22)**	0.098
EA22P7B	**Nemrut Dag (EA22)**	0.101
EA22P6B	**Nemrut Dag (EA22)**	0.103
EA22P8B	**Nemrut Dag (EA22)**	0.104
EA22P6A	**Nemrut Dag (EA22)**	0.105
EA21R1B	Nemrut Dag (EA21)	0.106
EA22P2	**Nemrut Dag (EA22)**	0.106

Elements: Ti, Fe, Zr, Ba, Zn

A-Rank:	**Nemrut Dag (EA22)**	**9**
B-Rank:	Nemrut Dag (EA25)	1

Specimen	*Location*	*E.D.*
EA22P7A	**Nemrut Dag (EA22)**	0.104
EA22R1	**Nemrut Dag (EA22)**	0.116
EA22P5B	**Nemrut Dag (EA22)**	0.122
EA22P3	**Nemrut Dag (EA22)**	0.135
EA22P1D	**Nemrut Dag (EA22)**	0.136
EA25P2C	Nemrut Dag (EA25)	0.139
EA22P1C	**Nemrut Dag (EA22)**	0.146
EA22P7B	**Nemrut Dag (EA22)**	0.146
EA22P6A	**Nemrut Dag (EA22)**	0.163
EA22P8B	**Nemrut Dag (EA22)**	0.163

Elements: Ti, Al, Fe, Mn, Ca, Zr, Ba

A-Rank:	**Nemrut Dag (EA22)**	**7**
B-Rank:	Nemrut Dag (EA21)	2

Specimen	*Location*	*E.D.*
EA22P7B	**Nemrut Dag (EA22)**	0.108
EA21P1	Nemrut Dag (EA21)	0.116
EA22R1	**Nemrut Dag (EA22)**	0.116
EA22P6B	**Nemrut Dag (EA22)**	0.119
EA22P6A	**Nemrut Dag (EA22)**	0.120
EA22P7A	**Nemrut Dag (EA22)**	0.121
EA22P4	**Nemrut Dag (EA22)**	0.122
EA22R2	**Nemrut Dag (EA22)**	0.125
EA25P1C	Nemrut Dag (EA25)	0.126
EA21R1B	Nemrut Dag (EA21)	0.127

Table 6.20 - Example of Euclidean Distance Measures and Nearest Neighbors for an Artifact Assigned to Bingol B

Artifact: A10 q1194.3 f925 k29

A-Rank: **Bingol B** **57** ← of the 80 nearest neighbors to this artifact (10 from each of 8 element combinations), 57 are obsidian specimens from Bingol B
B-Rank: Gutansar 11

Elements: Fe, Ti, Ba

A-Rank:	**Bingol B**	**7**
B-Rank:	Gutansar	2

Specimen	*Location*	*E.D.*
EA52B1	**Bingol B**	0.019
EA52B3	**Bingol B**	0.020
EA52B2	**Bingol B**	0.021
EA56B1	**Bingol B**	0.032
EA53B2	**Bingol B**	0.036
EA53B1	**Bingol B**	0.045
EA54B1	**Bingol B**	0.053
AR06E2A	Gutansar	0.095
AR06E1A	Gutansar	0.097
AR21avH1	Chazencavan	0.097

Elements: Fe, Zr, Ba

A-Rank:	**Bingol B**	**7**
B-Rank:	Erzincan	3

Specimen	*Location*	*E.D.*
EA52B3	**Bingol B**	0.022
EA52B2	**Bingol B**	0.025
EA52B1	**Bingol B**	0.032
EA56B1	**Bingol B**	0.039
EA53B2	**Bingol B**	0.041
EA53B1	**Bingol B**	0.056
EA54B1	**Bingol B**	0.061
EA43R2	Erzincan	0.085
EA44P3	Erzincan	0.086
EA44P2	Erzincan	0.087

Elements: Ti, Fe, Zr, Ba

A-Rank:	**Bingol B**	**7**
B-Rank:	Gutansar	3

Specimen	*Location*	*E.D.*
EA52B3	**Bingol B**	0.029
EA52B2	**Bingol B**	0.030
EA52B1	**Bingol B**	0.034
EA53B2	**Bingol B**	0.044
EA56B1	**Bingol B**	0.044
EA53B1	**Bingol B**	0.058
EA54B1	**Bingol B**	0.062
AR06E3A	Gutansar	0.140
AR30jfL1	Gutansar	0.140
AR06E2A	Gutansar	0.141

Elements: Ti, Fe, Mn, Ca, Zr, Ba

A-Rank:	**Bingol B**	**7**
B-Rank:	Acigol	3

Specimen	*Location*	*E.D.*
EA52B2	**Bingol B**	0.031
EA52B1	**Bingol B**	0.044
EA53B2	**Bingol B**	0.048
EA52B3	**Bingol B**	0.050
EA56B1	**Bingol B**	0.060
EA53B1	**Bingol B**	0.068
EA54B1	**Bingol B**	0.111
CA08R1A	Acigol	0.163
CA08R1C	Acigol	0.169
CA07R2A	Acigol	0.174

Elements: Fe, Ti, Zr

A-Rank:	**Bingol B**	**7**
B-Rank:	Gutansar	2

Specimen	*Location*	*E.D.*
EA52B3	**Bingol B**	0.028
EA52B2	**Bingol B**	0.029
EA53B2	**Bingol B**	0.031
EA52B1	**Bingol B**	0.033
EA53B1	**Bingol B**	0.041
EA56B1	**Bingol B**	0.043
EA54B1	**Bingol B**	0.061
EA66W1	Lake Van	0.117
AR76rB3	Gutansar	0.126
AR06E3A	Gutansar	0.131

Elements: Ti, Zr, Ba

A-Rank:	**Bingol B**	**9**
B-Rank:	Erevan	1

Specimen	*Location*	*E.D.*
EA52B2	**Bingol B**	0.027
EA52B3	**Bingol B**	0.028
EA52B1	**Bingol B**	0.031
EA54B1	**Bingol B**	0.032
EA55B2	**Bingol B**	0.036
EA56B1	**Bingol B**	0.038
EA53B2	**Bingol B**	0.043
EA55B1	**Bingol B**	0.047
EA53B1	**Bingol B**	0.057
AR24jfL1	Erevan	0.109

Elements: Ti, Fe, Zr, Ba, Zn

A-Rank:	**Bingol B**	**6**
B-Rank:	Gutansar	4

Specimen	*Location*	*E.D.*
EA53B1	**Bingol B**	0.126
EA52B1	**Bingol B**	0.169
EA52B3	**Bingol B**	0.182
AR06E2B	Gutansar	0.185
EA54B1	**Bingol B**	0.194
AR11jB1	Gutansar	0.196
EA52B2	**Bingol B**	0.198
AR06E1B	Gutansar	0.213
AR12jB1	Gutansar	0.213
EA56B1	**Bingol B**	0.213

Elements: Ti, Al, Fe, Mn, Ca, Zr, Ba

A-Rank:	**Bingol B**	**7**
B-Rank:	Acigol	3

Specimen	*Location*	*E.D.*
EA52B2	**Bingol B**	0.049
EA53B2	**Bingol B**	0.051
EA52B1	**Bingol B**	0.059
EA52B3	**Bingol B**	0.064
EA56B1	**Bingol B**	0.068
EA53B1	**Bingol B**	0.070
EA54B1	**Bingol B**	0.115
CA08R1A	Acigol	0.166
CA08R1C	Acigol	0.171
CA07R2A	Acigol	0.175

Table 6.21 - Example of Euclidean Distance Measures and Nearest Neighbors for an Artifact Assigned to Komurcu at Gollu Dag

Artifact: A7 q892-1 f261 k12

A-Rank: **Komurcu-Gollu Dag** **76** ← of the 80 nearest neighbors to this artifact (10 from each of 8 element combinations), 76 are obsidian specimens from Komurcu-Gollu Dag
B-Rank: Baksan River 2

Elements: Fe, Ti, Ba

A-Rank:	**Komurcu-Gollu Dag**	**10**
B-Rank:	-	-

Specimen	*Location*	*E.D.*
CA32W4A	**Komurcu-Gollu Dag**	0.011
CA32W4E	**Komurcu-Gollu Dag**	0.011
CA32W1E	**Komurcu-Gollu Dag**	0.012
CA32W4B	**Komurcu-Gollu Dag**	0.014
CA20P4	**Komurcu-Gollu Dag**	0.021
CA20P2	**Komurcu-Gollu Dag**	0.023
CA32W2A	**Komurcu-Gollu Dag**	0.023
CA32W2D	**Komurcu-Gollu Dag**	0.023
CA32W2B	**Komurcu-Gollu Dag**	0.025
CA32W2E	**Komurcu-Gollu Dag**	0.025

Elements: Fe, Zr, Ba

A-Rank:	**Komurcu-Gollu Dag**	**9**
B-Rank:	Baksan River	1

Specimen	*Location*	*E.D.*
CA32W4A	**Komurcu-Gollu Dag**	0.011
CA32W4E	**Komurcu-Gollu Dag**	0.011
CA32W4B	**Komurcu-Gollu Dag**	0.014
CA32W1E	**Komurcu-Gollu Dag**	0.015
KB02jB1	Baksan River	0.016
CA32W2D	**Komurcu-Gollu Dag**	0.023
CA20P2	**Komurcu-Gollu Dag**	0.025
CA32W2A	**Komurcu-Gollu Dag**	0.025
CA32W2E	**Komurcu-Gollu Dag**	0.026
CA32W2B	**Komurcu-Gollu Dag**	0.027

Elements: Ti, Fe, Zr, Ba

A-Rank:	**Komurcu-Gollu Dag**	**10**
B-Rank:	-	-

Specimen	*Location*	*E.D.*
CA32W4E	**Komurcu-Gollu Dag**	0.011
CA32W4A	**Komurcu-Gollu Dag**	0.012
CA32W4B	**Komurcu-Gollu Dag**	0.014
CA32W1E	**Komurcu-Gollu Dag**	0.015
CA32W2A	**Komurcu-Gollu Dag**	0.025
CA32W2D	**Komurcu-Gollu Dag**	0.025
CA32W2E	**Komurcu-Gollu Dag**	0.026
CA32W2B	**Komurcu-Gollu Dag**	0.027
CA20P2	**Komurcu-Gollu Dag**	0.028
CA32W6C	**Komurcu-Gollu Dag**	0.028

Elements: Ti, Fe, Mn, Ca, Zr, Ba

A-Rank:	**Komurcu-Gollu Dag**	**10**
B-Rank:	-	-

Specimen	*Location*	*E.D.*
CA32W4B	**Komurcu-Gollu Dag**	0.020
CA32W1E	**Komurcu-Gollu Dag**	0.026
CA32W4A	**Komurcu-Gollu Dag**	0.028
CA32W6C	**Komurcu-Gollu Dag**	0.029
CA20P2	**Komurcu-Gollu Dag**	0.031
CA32W2D	**Komurcu-Gollu Dag**	0.031
CA32W4D	**Komurcu-Gollu Dag**	0.032
CA32W4E	**Komurcu-Gollu Dag**	0.032
CA32W1D	**Komurcu-Gollu Dag**	0.033
CA32W2E	**Komurcu-Gollu Dag**	0.033

Elements: Fe, Ti, Zr

A-Rank:	**Komurcu-Gollu Dag**	**9**
B-Rank:	Gollu Dag	1

Specimen	*Location*	*E.D.*
CA32W2E	**Komurcu, Gollu Dag**	0.011
CA32W4E	**Komurcu, Gollu Dag**	0.011
CA32W4A	**Komurcu, Gollu Dag**	0.012
CA32W2C	**Komurcu, Gollu Dag**	0.013
CA32W1A	**Komurcu, Gollu Dag**	0.014
CA32W2B	**Komurcu, Gollu Dag**	0.014
CA32W4B	**Komurcu, Gollu Dag**	0.014
CA32W1E	**Komurcu, Gollu Dag**	0.015
CA17R1B	Gollu Dag	0.016
CA32W1B	**Komurcu, Gollu Dag**	0.016

Elements: Ti, Zr, Ba

A-Rank:	**Komurcu-Gollu Dag**	**9**
B-Rank:	Kars-Akbaba Dag	1

Specimen	*Location*	*E.D.*
CA32W4A	**Komurcu-Gollu Dag**	0.005
CA32W4B	**Komurcu-Gollu Dag**	0.005
CA32W4E	**Komurcu-Gollu Dag**	0.005
CA32W1E	**Komurcu-Gollu Dag**	0.010
CA32W6C	**Komurcu-Gollu Dag**	0.021
CA32W2A	**Komurcu-Gollu Dag**	0.023
CA32W2D	**Komurcu-Gollu Dag**	0.023
CA32W2E	**Komurcu-Gollu Dag**	0.023
CA32W2B	**Komurcu-Gollu Dag**	0.026
EA38P2	Kars-Akbaba Dag	0.027

Elements: Ti, Fe, Zr, Ba, Zn

A-Rank:	**Komurcu-Gollu Dag**	**9**
B-Rank:	Baksan River	1

Specimen	*Location*	*E.D.*
CA32W2D	**Komurcu-Gollu Dag**	0.026
CA32W2B	**Komurcu-Gollu Dag**	0.034
CA32W4A	**Komurcu-Gollu Dag**	0.036
CA32W2A	**Komurcu-Gollu Dag**	0.043
CA32W4E	**Komurcu-Gollu Dag**	0.044
KB02jB1	Baksan River	0.044
CA32W4B	**Komurcu-Gollu Dag**	0.052
CA32W4D	**Komurcu-Gollu Dag**	0.053
CA32W6D	**Komurcu-Gollu Dag**	0.058
CA32W1E	**Komurcu-Gollu Dag**	0.059

Elements: Ti, Al, Fe, Mn, Ca, Zr, Ba

A-Rank:	**Komurcu-Gollu Dag**	**10**
B-Rank:	-	-

Specimen	*Location*	*E.D.*
CA32W4B	**Komurcu-Gollu Dag**	0.020
CA32W1E	**Komurcu-Gollu Dag**	0.026
CA32W4A	**Komurcu-Gollu Dag**	0.028
CA32W6C	**Komurcu-Gollu Dag**	0.029
CA20P2	**Komurcu-Gollu Dag**	0.031
CA32W2D	**Komurcu-Gollu Dag**	0.032
CA32W4D	**Komurcu-Gollu Dag**	0.032
CA32W4E	**Komurcu-Gollu Dag**	0.032
CA32W2E	**Komurcu-Gollu Dag**	0.033
CA32W4C	**Komurcu-Gollu Dag**	0.033

Rank" match, and Gutansar is labeled a "B Rank" match. Such a discontinuity in the ED values can be observed in seven of the eight element combinations, and Bingöl B always is the "A Rank" match. Again I am interested in a stable source assignment, so I consider all eight combinations of elements. Taken together, 57 of the 80 "nearest" specimens are from Bingöl B, which I consider to be the "A Rank" match.

We can also examine a third example: A7 q892-1 f261 k12 in Table 6.21. Almost all of the "nearest" specimens came from the Kömürcü source at Göllü Dağ: 76 out of 80. The ten "nearest neighbors" for all eight element combinations include either nine or ten Kömürcü specimens. Hence I consider Kömürcü the "A Rank" match. Only two of 80 specimens came from the Baksan River source in Kabardino-Balkaria, a quite distant "B Rank" match. Thus, I can confidently assign this artifact to the Kömürcü source at Göllü Dağ, over 600 km from Tell Mozan, as discussed in Section 9.2.2.

Most of my artifact assignments follow this procedure: (i) identify the ten "nearest neighbors" to a particular artifact for each of eight element combinations; (ii) identify the most frequent sources listed among the nearest neighbors; and (iii) assign an "A Rank" to the most frequent source and a "B Rank" to the second most frequent source. There were a few exceptions. For some Nemrut Dağ specimens, the choice between EA25 and EA22 was essentially a tie, so I have a "EA25 or EA22" category. As I discuss in Section 7.3.3, there appears to be a previously unknown chemical similarity between Muş and Pasinler obsidians, so I have a "Muş/Pasinler" category for now. Lastly, I used Poidevin's (1998) peralkalinity plot, as discussed in Section 8.1.3, as well as scatterplots to help distinguish Nemrut Dağ and Bingöl A obsidians, as discussed in Section 7.3.1.

6.10 - Assessing Validity with Georgian Artifacts

To evaluate the use of my EMPA data and ED matrices to nondestructively source artifacts, I wanted to analyze artifacts from a known, or very likely, source as a test. I did not, though, have access to obsidian artifacts with firmly established sources. Fortunately Nino Sadradze and Givi Maisuradze of the Institute of Geology in Tbilisi as well as Irina Demetradze of the Ilia Chavchavadze State University in Tbilisi were willing to send me obsidian artifacts from archaeological sites in Georgia. Four artifacts from Sadradze and Maisuradze originated from Anaseuli I (an early Neolithic site in southwestern Georgia), Dzudzuana (a cave site in western Georgia with occupations from the Paleolithic to the Early Bronze Age), and Chachuna (a nature preserve in southeastern Georgia). The four artifacts from Irina Demetradze originated from a Bronze Age tumulus in the Tetritsqaro district. The earthen mound was discovered in 2004 during a survey for the BTC pipeline (then designated site #IV-154) and excavated in 2007 by Guram Mirtskhulava of the Otar Lortkipanidze Archaeological Centre, Georgian National Museum.

The eight obsidian artifacts from four Georgian sites could serve as "test artifacts" because they most likely came from the only source in the country: Chikiani volcano (this source is sometimes known as Paravani Lake or Kojun Dağ, the volcano's Turkish name). To my knowledge, obsidian artifacts have only been sourced at Anaseuli I, and Badalyan et al. (2004) identify the source as Chikiani. Obsidian from the other three sites can be, at least initially, assumed to originate from this source because prior studies have shown the intensive use of Chikiani obsidian at sites in the region (Badalyan et al. 2004:444, Map 2; Chataigner and Barge 2007:3, Figure 2c). Badalyan et al. (2004) points out both the high

quality and accessibility of the Chikiani (Georgian for "the glass that glistens") obsidian: "The Chikiani obsidian is spread everywhere over the dome of the volcano and extends in a large flow to the east. The quality of the obsidian is excellent -- very homogeneous and without inclusions; it is abundant and easy to access" (442). I can attest that many pieces of obsidian from there are extremely clear. It is the only source within the Kura Basin, between the Greater Caucasus mountain range to the north and the Lesser Caucasus range to the south. Its north-south distribution seems restricted by these mountain ranges, but it spread west to the Black Sea and east to the Caspian (443). Badalyan et al. (2004) draw a line from Kobuleti (in Georgia on the Black Sea) to Uchoglan (in central Azerbaijan) and term the area to the north the "Chikiani Zone" (443). After considering the single-source obsidian-procurement model in the Transcaucasus from the Neolithic to the Bronze Age, they conclude that "this model seems to apply during the course of the entire time period considered within one area; namely, at Chikiani" (2004:459).

I analyzed these eight artifacts non-destructively using the conditions discussed in Chapter 5, and I calculated the ED values as described in Section 6.9.9. One example of the results is shown in Table 6.22. The calculations and sources assignments for all eight artifacts are found in Appendix D. In only three instances out of 64 combinations (eight element combinations for eight artifacts) is the "A Rank" not Chikiani. Over 95% of the time Chikiani is the "A Rank" choice. Although this initial test involved obsidian from a single source, it demonstrated that artifacts can be non-destructively sourced this way. In other words, my EMPA and ED methods are valid for obsidian sourcing.

Table 6.22 - Example of Euclidean Distance Measures and Nearest Neighbors for a Georgian Test Artifact

Artifact: Georgia-nS2a, Chachuna

A-Rank: **Chikiani** **61** ← of the 80 nearest neighbors to this artifact (10 from each of 8 element combinations), 61 are obsidian specimens from Chikiani, Georgia
B-Rank: Damlik 3

Elements: Fe, Ti, Ba

A-Rank:	**Chikiani**	**7**
B-Rank:	Damlik	1

Specimen	*Location*	*E.D.*
GE07kM1C	**Chikiani**	0.010
GE11nS4	**Chikiani**	0.010
GE07kM1B	**Chikiani**	0.019
AR60sK1	Damlik	0.021
GE07kM1A	**Chikiani**	0.025
GE02iD1A	**Chikiani**	0.027
GE11nS1	**Chikiani**	0.027
GE05iD1	**Chikiani**	0.031
AR43kM1	Pokr Arteni	0.034
AR29ipS1	Armenia, unknown	0.037

Elements: Fe, Zr, Ba

A-Rank:	**Chikiani**	**7**
B-Rank:	Gollu Dag	2

Specimen	*Location*	*E.D.*
GE11nS4	**Chikiani**	0.009
GE07kM1A	**Chikiani**	0.012
CA21P1	Gollu Dag	0.015
GE07kM1B	**Chikiani**	0.015
GE07kM1C	**Chikiani**	0.019
AR60sK1	Damlik	0.021
GE02iD1A	**Chikiani**	0.021
GE11nS1	**Chikiani**	0.025
GE05iD1	**Chikiani**	0.029
CA21R1B	Gollu Dag	0.030

Elements: Ti, Fe, Zr, Ba

A-Rank:	**Chikiani**	**7**
B-Rank:	Damlik	1

Specimen	*Location*	*E.D.*
GE11nS4	**Chikiani**	0.013
GE07kM1B	**Chikiani**	0.021
GE07kM1C	**Chikiani**	0.021
AR60sK1	Damlik	0.025
GE07kM1A	**Chikiani**	0.025
GE02iD1A	**Chikiani**	0.028
GE11nS1	**Chikiani**	0.028
GE05iD1	**Chikiani**	0.031
AR43kM1	Pokr Arteni	0.036
AR29ipS1	Armenia, unknown	0.037

Elements: Ti, Fe, Mn, Ca, Zr, Ba

A-Rank:	**Chikiani**	**8**
B-Rank:	Damlik	1

Specimen	*Location*	*E.D.*
GE11nS4	**Chikiani**	0.016
GE07kM1B	**Chikiani**	0.021
GE07kM1C	**Chikiani**	0.023
AR60sK1	Damlik	0.026
GE02iD1A	**Chikiani**	0.029
GE11nS1	**Chikiani**	0.030
GE07kM1A	**Chikiani**	0.031
GE05iD1	**Chikiani**	0.032
AR29ipS1	Armenia, unknown	0.039
GE02iD1C	**Chikiani**	0.040

Elements: Fe, Ti, Zr

A-Rank:	**Chikiani**	**10**
B-Rank:	-	-

Specimen	*Location*	*E.D.*
GE11nS6	**Chikiani**	0.001
GE02iD1C	**Chikiani**	0.002
GE01jB1	**Chikiani**	0.009
GE03iD1	**Chikiani**	0.009
GE05iD1	**Chikiani**	0.010
GE02iD1B	**Chikiani**	0.011
GE13nS1	**Chikiani**	0.011
GE13nS2	**Chikiani**	0.011
GE11nS4	**Chikiani**	0.012
GE11nS1	**Chikiani**	0.016

Elements: Ti, Zr, Ba

A-Rank:	**Chikiani**	**5**
B-Rank:	Ttvakar	2

Specimen	*Location*	*E.D.*
AR43kM1	Pokr Arteni	0.012
GE11nS4	**Chikiani**	0.012
AR70rB1	Ttvakar	0.018
AR29ipS1	Unknown	0.019
GE07kM1B	**Chikiani**	0.021
GE07kM1C	**Chikiani**	0.021
AR70rB2	Ttvakar	0.023
AR60sK1	Damlik	0.024
GE07kM1A	**Chikiani**	0.025
GE06iD1	**Chikiani**	0.026

Elements: Ti, Fe, Zr, Ba, Zn

A-Rank:	**Chikiani**	**8**
B-Rank:	Armenia, unknown	1

Specimen	*Location*	*E.D.*
GE07kM1B	**Chikiani**	0.022
GE02iD1A	**Chikiani**	0.033
GE05iD1	**Chikiani**	0.045
GE07kM1A	**Chikiani**	0.045
GE06iD1	**Chikiani**	0.051
AR29ipS1	Armenia, unknown	0.052
GE04iD1	**Chikiani**	0.057
GE07kM1C	**Chikiani**	0.063
AR43kM1	Pokr Arteni	0.069
GE11nS1	**Chikiani**	0.074

Elements: Ti, Al, Fe, Mn, Ca, Zr, Ba

A-Rank:	**Chikiani**	**9**
B-Rank:	Damlik	1

Specimen	*Location*	*E.D.*
GE11nS4	**Chikiani**	0.027
GE07kM1B	**Chikiani**	0.033
GE07kM1C	**Chikiani**	0.035
GE05iD1	**Chikiani**	0.038
GE11nS1	**Chikiani**	0.038
GE02iD1A	**Chikiani**	0.040
AR60sK1	Damlik	0.045
GE02iD1C	**Chikiani**	0.046
GE07kM1A	**Chikiani**	0.048
GE13nS1	**Chikiani**	0.049

6.11 - Summary and Concluding Remarks

Four main concepts of assessment -- precision, accuracy, reliability, and validity -- served as the framework to evaluate my EMPA and data-analysis procedures for sourcing obsidian artifacts non-destructively. My examination of the assessment literature showed that Hughes (1998) and Nazaroff et al. (2010), the only two earlier obsidian studies to use these four concepts, formulated them somewhat atypically. After reviewing the literature, I have attempted to strengthen their application to obsidian sourcing.

Any assessment will be affected by the quality of the data, so the issue of element selection is nontrivial, particularly because there is little consensus on which elements are best to discern sources. Data treatment, before any statistical or data-analysis techniques are applied, is another important issue because it may reduce the long-term usefulness of the data. For example, fully quantitative data are superior to any data reported as element ratios or normalized to 100%. Both practices are largely unacceptable in the geosciences, so they should also be considered unacceptable in obsidian sourcing.

I determined the precision of my EMPA data by analyzing an obsidian specimen from Yellowstone National Park (Smithsonian VG-568, USNM Specimen #72854) over 600 times over a period of 16 months. The results showed that EMPA indeed has enough precision for major and minor elements as well as some trace elements. Reliability is tied to precision, so these two concepts must be considered together.

Assessing the accuracy is difficult because it requires comparison to “true values” that are not actually known. Thus, I took multiple approaches to assess the accuracy: (1)

for the major elements, I analyzed the obsidian standard from Yellowstone National Park as an unknown specimen and compared my data to the published values; (2) for the trace elements, I analyzed two artificial glass standards as unknowns and compared my data to the published values; (3) I participated in an analytical round robin using basalt glass and obtained obsidian from an earlier round robin; and (4) I compared my EMPA data to four different data sets: (i) NAA at the Max Planck Institute, (ii) NAA at MURR, (iii) EDXRF at MURR, and (iv) WDXRF at UWEC. The comparisons, on the whole, exhibit excellent agreement, indicating that my EMPA data are sufficiently accurate.

The validity (using this concept-based definition) of procedures or data cannot be evaluated in a vacuum. Assessment must be done in light of a particular phenomenon, in this case, the ability to assign artifacts to their most likely origins. In addition, data must be assessed together with the data-processing ("statistical") procedures, a wide variety of which is found in the literature. I evaluated the validity of my data and procedures using artifacts almost certainly from Chikiani in Georgia, and all eight artifacts were attributed to that source, highly suggesting my data and procedures are valid.

This chapter concludes my redevelopment and assessment of EMPA for sourcing artifacts non-destructively. The last three chapters of my dissertation are concerned with the sources of the obsidian artifacts from Tell Mozan and the archaeological implications of my findings for Urkesh, the Hurrians, and Northern Mesopotamia.

Part III: Results and Implications

Chapter 7:

The Bronze-Age Obsidian Artifacts of Tell Mozan and Their Sources

> To reintegrate our archaeometric practices within an anthropological archaeology we need to reconsider the fundamentals of what we are seeking to characterise. Traditionally the term 'characterisation study' has come to imply a study of the object's *composition*. On reviewing the obsidian provenancing literature, one rarely comes away with a very clear as to what exactly is being analysed, with only the occasional reference to 'blade' or 'flake', while illustrations are rare in the extreme… I have argued that such an approach is materially reductionist, leading me to develop an alternative model that reintroduces an archaeological sensibility… 'Samples' are reconceptualised as 'artefacts' and are accorded a richer 'character' by considering not only their raw material (source, colour, and texture), but also how they were made, what they looked like, their spatial-temporal contexts, and their prevalence in any given assemblage.
>
> -- Tristan Carter, in prep, "Obsidian Provenance Studies"

In this chapter, I not only present the source assignments for the obsidian artifacts that I analyzed from Bronze-Age Tell Mozan but also address the above criticisms about most sourcing studies. As explained in Chapter 4, the 97 obsidian artifacts that I sourced were classified as "chip debris" and "chunk debris" (based on Rosen 1997:30), but here I have highlighted obsidian artifacts that were recovered with the ones I sourced. I provide some statistics about the prevalence of obsidian and chert tools at Tell Mozan, and I offer an initial assessment of the tool types present as well as observations about the likelihood of obsidian-tool production on-site. First, though, I discuss a 98th artifact that I analyzed

and concluded is actually a fragment of "artificial obsidian," as described in ancient texts. I also discuss three observations based my results: (1) these analyses not only distinguish the Bingöl A and Nemrut Dağ sources clearly but also separate six different compositions of Nemrut Dağ obsidians; (2) the eastern obsidian-bearing lava flows of Meydan Dağ and the western lava flows of Tendürek Dağ overlap to some extent; and (3) the compositions of two rarely studied obsidian sources -- Muş and Pasinler -- are not readily distinguished and must be considered equally probable sources for six of the artifacts. The implications of these obsidian-sourcing results for Northern Mesopotamia in general and Tell Mozan in particular are discussed in Chapter 8 and 9, respectively.

7.1 - An Instance of "Artificial Obsidian"

A total of 98 artifacts from Tell Mozan were approved for export for this research, but only 97 of them were obsidian. One of the exported artifacts, while glassy and black, was found, using chemical analysis, to not be obsidian (or any other rock). The artifact in question, found in southeast corner of the palace complex, appears below:



site unit	lot	feature	square/locus	piece	mass (g)
A10	q541.s1	f245	k26/24	-	1.02

Notice the deep groove with fine striations, which appear tan due to adhered calcareous sediments. There are three such grooves around this artifact. Based on the presence of these grooves, I originally suspected that this object was waste from the production of an

obsidian vessel. I observed an unfinished obsidian vessel in the Metropolitan Museum of Art (Figure 7.1), and it was clear that such vessels were hollowed out by drilling and then breaking out the material that remained between the drilled holes.

The chemical analyses revealed a composition very distinct from that of obsidian: 48% SiO_2, 23% CaO, 10% Al_2O_3, 5.8% FeO, 4.2% MgO, 3.9% K_2O, 1.1% P_2O_5, and 1% Na_2O. Its composition is, instead, similar to those of ancient Mesopotamian glasses. The chemical similarity is shown in Figure 7.2, modified from Henderson (2000: Figure 3.28). The Tell Mozan artifact is, based on the MgO-versus-K_2O plot for ancient glasses, clearly a high-magnesia glass, much like later artifacts from Tell Brak in Syria (circa 1300 BCE), Tell el-Amarna in Egypt (circa 1500-1300 BCE), and Pella in northwestern Jordan (circa 1400-1300 BCE). Notice that all of these examples are from the second millennium, not the third millennium. Henderson (2000) explains that glass was not produced in quantity (that is, enough to make glass vessels) until the second millennium in Mesopotamia (52). He points out, however, that some "small objects of glass, particularly beads, were made in the third millennium" (52), and furthermore, he proposes that "the development of the first glass manufacture [occurred] perhaps in northern Syria" (53).

In Section 2.1.2, I discussed the Chicago Assyrian Dictionary Project (abbreviated CAD), a comprehensive dictionary of terms from Akkadian-language texts, circa the third and second millennia BCE, from various Near Eastern archaeological sites. One of these texts includes the line: "their earrings are of artificial obsidian and gold" (258), and other texts refer to "ornaments of obsidian made in the crucible" (258). Note that a crucible is



Figure 7.1 - An unfinished third-millennium Mesopotamian obsidian vessel in the Metropolitan Museum of Art (catalog #1979.23; photograph by the author).

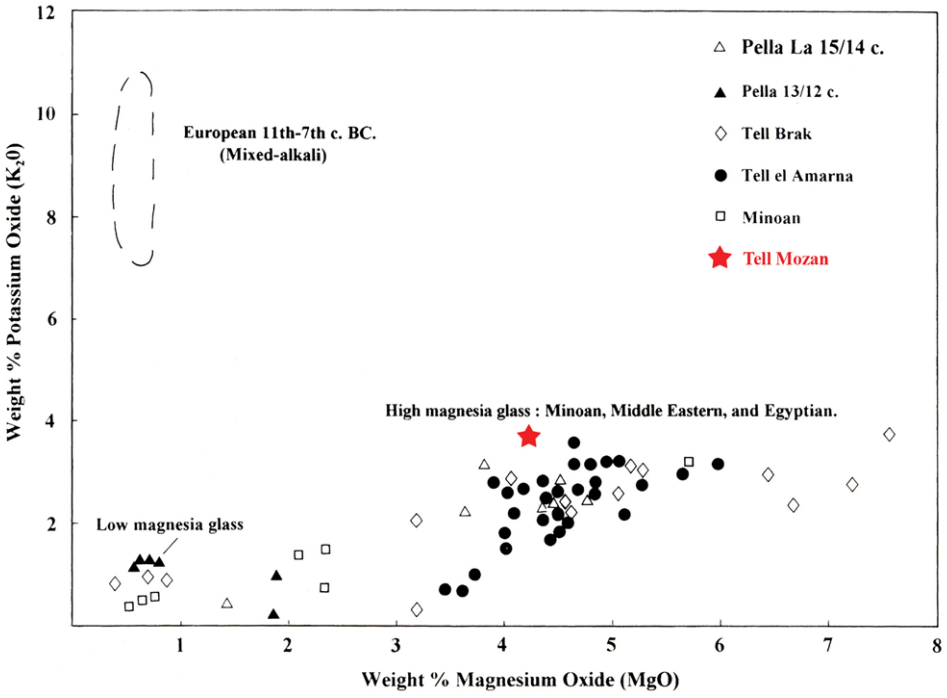


Figure 7.2 - A scatterplot of MgO versus K_2O for various ancient glasses from Henderson (2000: Figure 3.28), to which I have added the "artificial obsidian" from Tell Mozan.

a container used for heating materials to high temperatures, such as smelting ore to make metal or fusing sand, limestone, and soda ash to make glass. There are also references in the texts to another artificial stone: "their wings are of gold [with] lapis lazuli, alabaster, obsidian, and artificial carnelian" (257). It seems that early glass beads were considered, depending on their color, to be artificial versions of stones such as obsidian and carnelian (a reddish-brown variety of chalcedony). This makes sense given, at this time period, the only other glass that these people had previously seen was obsidian.

I suggest, therefore, that this artifact is probably an error or waste from producing an "artificial obsidian" glass bead, showing that such objects actually exist. The grooves might have been intended for inlaying another color of glass to create a striped, or even a twisted, appearance. Stone beads have also been recovered from the palace complex, and I have identified several of which appear to be fashioned of obsidian. This artifact might have been an attempt to produce an "artificial" obsidian bead. As discussed in Chapter 2, Cauvin (1998) and Coqueugniot (1998) contend that stone beads in necklaces were likely selected for symbolic reasons. An attempt to make an artificial stone that combines black "obsidian" with a stone of another color may reflect an endeavor to combine the power or symbolism of both types of stone into a single bead or amulet.

7.2 - Observations on the Obsidian Industry at Tell Mozan

In 2006, I joined the Urkesh expedition for its nineteenth season to participate in the excavations and study the flaked-stone artifacts, focusing on those made of obsidian.

In addition to selecting obsidian artifacts for sourcing, I sought to estimate the quantity of obsidian present, examine its quality, determine the basic tool types (like those discussed in Section 2.1.1), and seek evidence for on-site production activities.

7.2.1 - Quantities of Obsidian and Chert Artifacts

As of the 2006 expedition, over 820 obsidian artifacts have been recovered at Tell Mozan, and I estimate that about 1700 to 1800 chert artifacts have been found. I made no attempt, at this stage, to discern varieties of silica-rich microcrystalline, cryptocrystalline, or microfibrous sedimentary (chert, flint, chalcedony, jasper, and agate) and metamorphic (quartzite) rocks due, in part, to variable definitions for these rocks in the geological and archaeological literature. All of them are classified as "chert" here.

I took measurements on a sample of about 15% of the obsidian and chert artifacts. Based on this sample, I estimate that about 32% of the flaked-stone artifacts are obsidian and about 68% of them are chert. In this sample, the total mass of the obsidian is almost 140 g, and the total mass of the chert is over 2.2 kg. For the obsidian within this sample, the mean artifact mass is 1.1 g, and the median is 0.7 g with a first quartile of 0.5 g and a third quartile of 1.2 g. For the chert, the mean mass is 8.2 g, and the median is 4.5 g with a first quartile of 1.9 g and a third quartile of 9.4 g. Thus, I estimate that the flaked-stone artifacts are, by mass, about 6% obsidian and 94% chert. Furthermore, I estimate that the total mass of all the excavated obsidian artifacts is about 1 kg and the total mass of all the excavated chert artifacts unearthed at Tell Mozan is about 14 kg.

It should be noted, though, that lithic "workshops" have not yet been found at Tell Mozan. The eventual discovery of such workshops at the site could significantly alter the proportions of obsidian and chert. I should also point out that the proportions correspond to a period from the Early Bronze Age to the Late Bronze Age as a whole. When further stratigraphic data become available in the Urkesh Global Record (see Section 7.4), the proportions of chert and obsidian can be parsed better chronologically.

7.2.2 - Obsidian Quality at Tell Mozan

As discussed in Section 1.2.2, obsidian can have varied amounts, sizes, and types of minerals. Even the glassiest obsidians typically contain microscopic (even nanoscale) inclusions that comprise a few tenths of a percent of the volume. In other obsidians, the minerals can be visible to the naked eye and comprise 5 percent (or more) of the volume. In general, in obsidian of sufficient quality for flaked tools ("weapons-grade"), inclusions are microscopic and rare, and as the sizes and/or abundances of the minerals increase, the suitability of the obsidian for flaked stone tools decreases. Accordingly, in some regions, archaeologists have documented preferential use of high-quality obsidian, even when it is more distant (Kamp 1998:149). Obsidian with flow bands (really planes of concentrated inclusions and/or bubbles) should, at least in theory, be undesirable because a crack could deviate from its desired path and propagate along these planes instead.

Much of the obsidian found at Tell Mozan is high quality and either translucent or uniform black. Some blades are so clear that one could read the pages of a book through

them. Other artifacts, though, are fashioned from obsidian of lower quality. Figure 7.3 shows some of the obsidian artifacts with flow bands. These examples reveal that ancient knappers flaked flow-banded obsidian at various angles with respect to the bands, not just in a single orientation (e.g., perpendicular to the bands). Some blades (Figure 7.4) were made of obsidian with minerals, probably feldspars, visible to the naked eye. Pits, caused by small (but not detrimental) deviations in crack propagation, surround these inclusions. A few artifacts (Figure 7.5) were even made of "mottled" obsidian due to either clusters of microscopic minerals or perhaps devitrified and/or perlitic areas.

As noted in Sections 1.2.2 and 1.5, flow bands and abundant mineral inclusions in obsidian can affect the overall (bulk) composition. The presence of these heterogeneities in artifacts supports an approach to obsidian sourcing that treats the material as a mixture, using either sampling equations to calculate representative specimen sizes or a technique that can analyze the glass and mineral components separately.

7.2.3 - Obsidian Tool Types at Tell Mozan

A thorough typology of obsidian tools was beyond the scope of the present study, in part because such a typology should be developed not only in light of both the obsidian and chert tools at Tell Mozan but also to be compatible with various other typologies used throughout the region. I still considered it important, though, to document the basic types of flaked obsidian tools present in the Bronze-Age strata of Tell Mozan.

Based on Section 2.1.1, it should not be surprising that the obsidian flaked-stone tool assemblage at Tell Mozan is dominated by blade-tools, particularly prismatic blades



Figure 7.3 - Examples of flow bands in artifacts all from Area A, the palace complex.



Figure 7.4 - Examples of artifacts containing tiny mineral inclusions that cause small pits on the artifact surfaces during crack propagation, as discussed in Section 5.3.2.

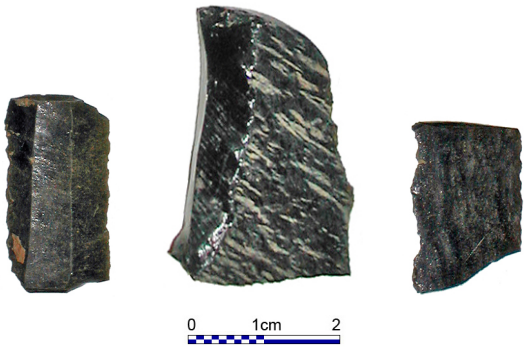


Figure 7.5 - Examples of artifacts made of "mottled" obsidian due to either the presence of microscopic minerals or perhaps devitrified and/or perlitic areas. Such obsidian would commonly be considered low-quality. None of these were found in the palace complex.

and bladelets with trapezoidal cross-sections (Figure 7.6 and Appendix B). Flake-tools, including side and end scrapers, knives, ad-hoc tools, and notched or denticulated flakes, are also common (Figure 7.7). Geometric microliths fashioned from blades, especially trapezes (Figure 7.8) and lunates (7.9), and notches on blades (7.10) were present as well. I also noted a tabular scraper (7.11), a tanged point and a winged point (7.12), transverse points or end scrapers (7.13), borers (7.14), and drills or awls (7.15).

7.2.4 - Ground Obsidian and Platform Preparation

I examined a number of ground-stone obsidian artifacts as well, such as possible fragments of thick-walled obsidian vessels (Figure 7.16). Several artifacts (7.17 to 7.19) seem to have been both flaked and ground. One of them (7.17) is a prismatic blade with dorsal surfaces that were ground flat, and another (7.18) might also have been flaked into its basic shape that then ground flat. There are also obsidian flakes with broad platforms apparently ground flat (7.20). A chert nodule with a ground platform (7.21) suggests that some obsidian cores could also have had ground platforms. Thus, there are multiple links between the flaked- and ground-stone technologies at Tell Mozan.

7.2.5 - Evidence for Production Activities On-Site

As previously mentioned, lithic "workshops" have not yet been discovered at Tell Mozan; however, there is evidence of on-site obsidian tool production activities. There is debris, both chip- (< 2 cm) and chunk-sized (> 2 cm), at the site, but given the brittleness of obsidian, it can be difficult to distinguish production debitage and fragments of broken



Figure 7.6a - Examples of obsidian blade-tools (blades, bladelets, geometrics, etc.) from Tell Mozan, circa 2300-1300 BCE. Appendix B has further examples separated by unit.



Figure 7.6b - Examples of obsidian blade-tools (blades, bladelets, geometrics, etc.) from Tell Mozan, circa 2300-1300 BCE. Appendix B has further examples separated by unit.



Figure 7.6c - Examples of obsidian blade-tools (blades, bladelets, geometrics, etc.) from Tell Mozan, circa 2300-1300 BCE. Appendix B has further examples separated by unit.

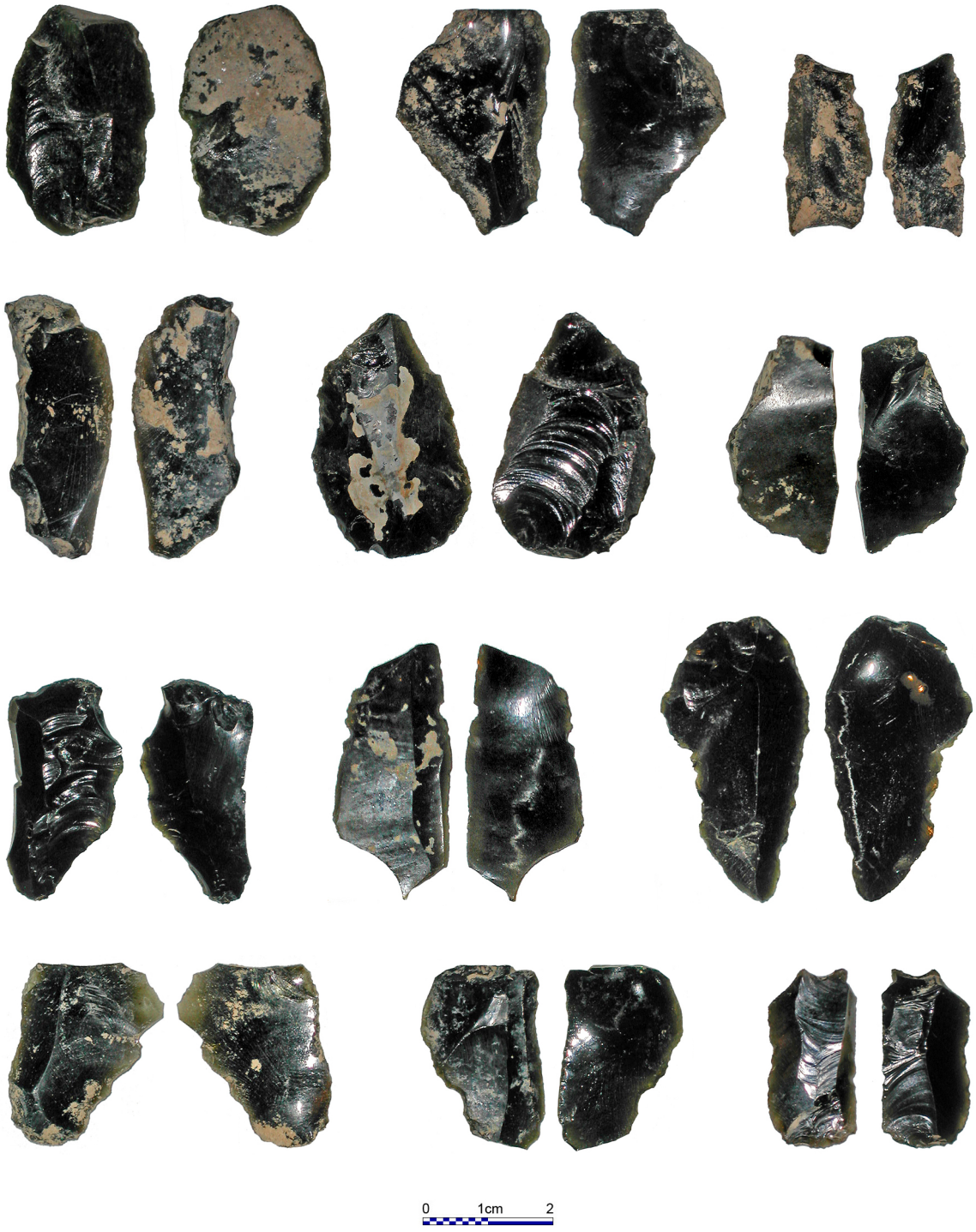


Figure 7.7a - Examples from Tell Mozan of obsidian flake-tools (including side and end scrapers, knives, ad-hoc tools, and notched or denticulated flakes), circa 2300-1300 BCE.



Figure 7.7b - Examples from Tell Mozan of obsidian flake-tools (including side and end scrapers, knives, ad-hoc tools, and notched or denticulated flakes), circa 2300-1300 BCE.



Figure 7.8 - Examples of obsidian trapezes from A7 (left), A10 (center), and J3 (right).



Figure 7.9 - Example of lunates from obsidian blades from A10 (left) and A8 (right).



Figure 7.10 - Examples of notches on blades from A7 (left), A8 (center), and A18 (right).



Figure 7.11 - An obsidian tabular scraper from Unit A9, Feature 98, circa about 2200 BCE -- note that it was apparently ground flat and retouched to give it sharp edges.



Figure 7.12 - Examples of a tanged (left) and a winged (right) obsidian point. Only chert leaf-shaped points have been found so far. Note the red color on the tip of the right point.

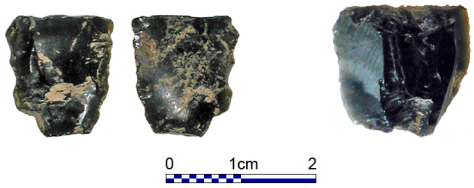


Figure 7.13 - Examples of transverse points or end scrapers from A9 (left) and J1 (right).

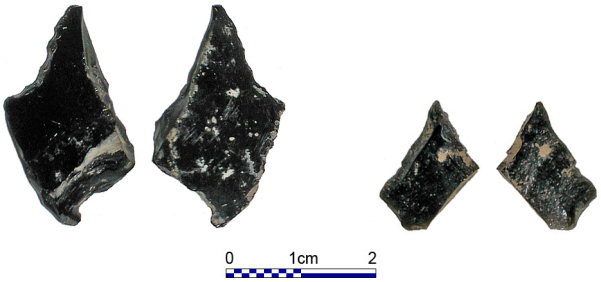


Figure 7.14 - Examples of likely obsidian borers from J2 (left) and A9 (right).



Figure 7.15 - Examples of obsidian drills or awls from H4 (all three).

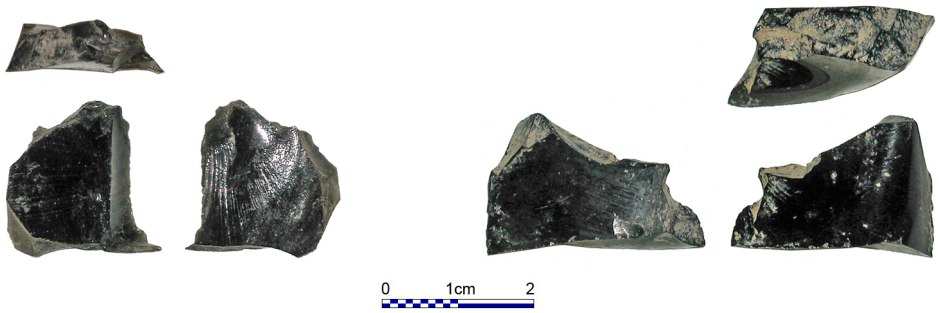


Figure 7.16 - Possible fragments of obsidian vessels from Units A (left) and B (right).



Figure 7.17 - A prismatic blade with its dorsal surfaces subsequently ground flat.



Figure 7.18 - A ground and polished artifact that may have started like the one above.



Figure 7.19 - Examples of other obsidian artifacts with evidence of ground surfaces.

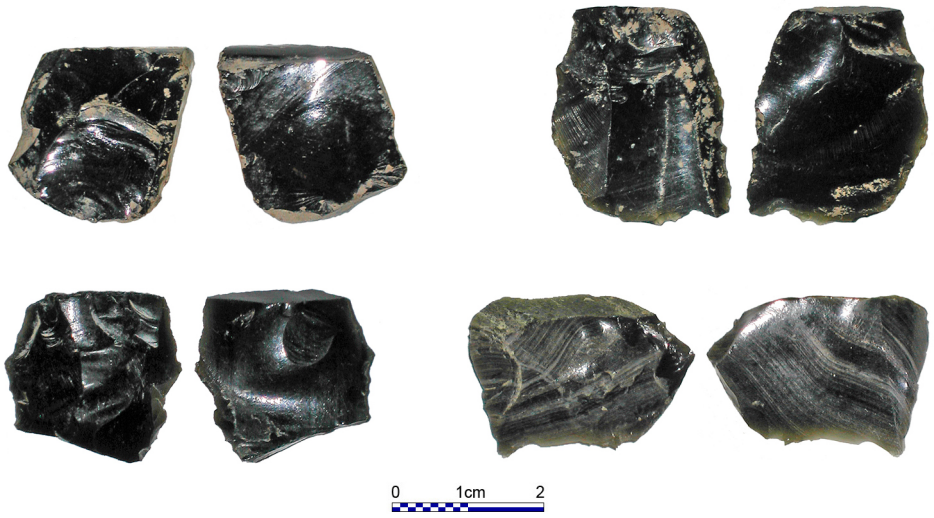


Figure 7.20 - Examples of obsidian flakes from Tell Mozan with ground flat platforms, indicating that some obsidian cores had platforms prepared like the chert core above.



Figure 7.21 - A chert nodule from Tell Mozan with a surface ground flat, apparently to use as a platform so that the nodule can be utilized as a core (Urkesh expedition photo).

or modified tools. More telling is the presence of obsidian flakes with cortex and surfaces original to the obsidian blocks or nodules. Figure 7.23 shows obsidian flakes with cortex, revealing that these outer surfaces were not removed from the transported obsidian pieces until they reached Tell Mozan. In addition, Figure 7.25 shows obsidian artifacts with flat, porous surfaces, like the bubble-rich layers along which obsidian naturally fractures into angular blocks. Figure 7.26 gives examples of apparently mixed flake and blade obsidian cores, either exhausted or discarded, further suggesting lithic production activities at Tell Mozan. All of this evidence, though, does not indicate the tool type.

Figure 7.27 shows a tabular obsidian core, dating to between 2100 and 1800 BCE, for prismatic blade production. Such a core suggests that prismatic obsidian blades were produced at Tell Mozan, but this is not the only evidence. Figure 7.28 shows early-series blades removed from a polyhedral core prior to prismatic-blade production. Such blades are used to initially shape a core, and their removal, likely via pressure flaking, produces the ridges on the dorsal surfaces of prismatic blades. Together, the core and early blades indicate that prismatic blades were produced on site, not imported.

7.3 - Three Findings from the Analytical Results

In subsequent sections, I present my source assignments for 97 obsidian artifacts from Tell Mozan. First, though, I must point out three findings, based on my analyses of the geological specimens, with archaeological implications. There are other findings that, though interesting geologically (e.g., magma fractionation trends), are not relevant to the archaeological interpretations, so these will be discussed elsewhere.



Figure 7.22 - Loose angular and subangular blocks of obsidian (Glass Buttes [top] and Big Obsidian Flow at Newberry Volcano [bottom]; photographs by the author).



Figure 7.23 - Examples from Tell Mozan of decortification flakes from angular (left) and subangular (center and right) obsidian blocks, indicating core reduction occurred on-site.

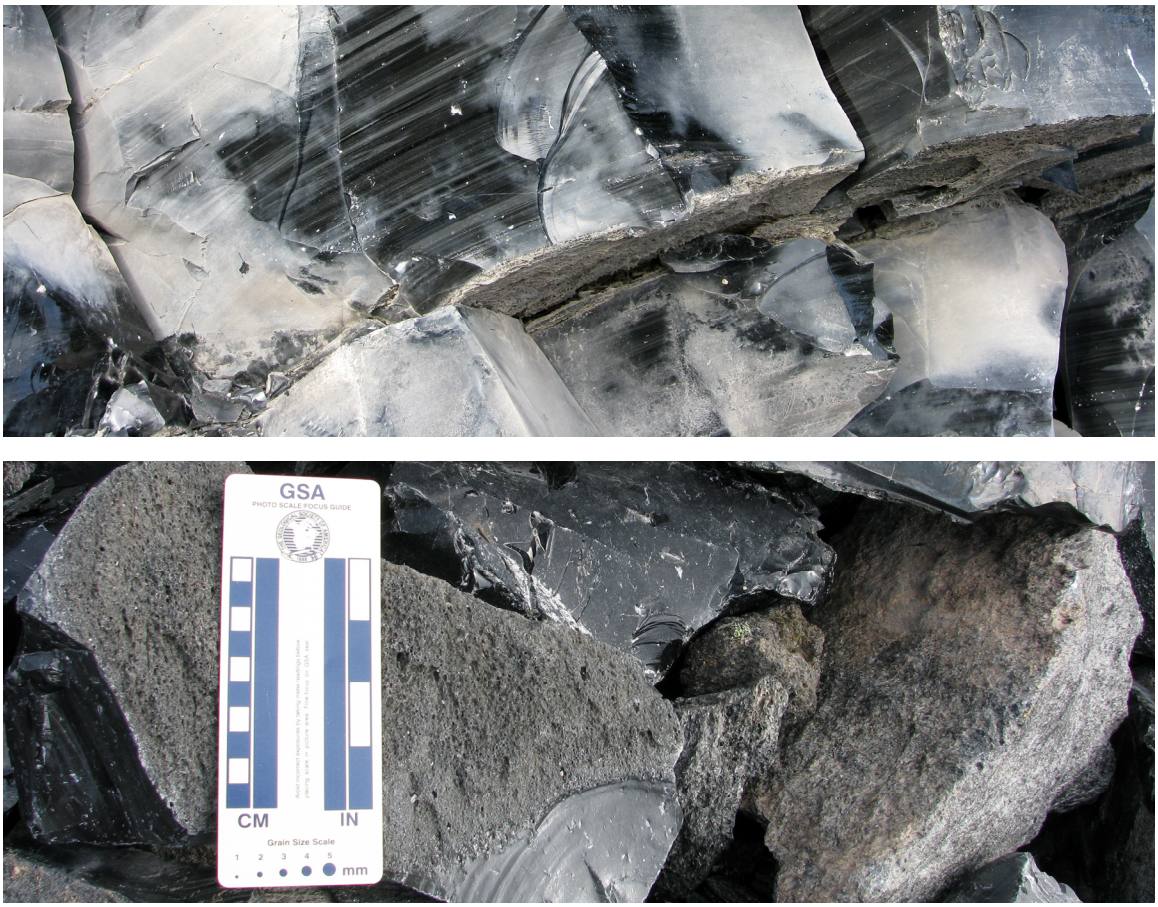


Figure 7.24 - Obsidian can fracture into blocks along weak, porous layers, leaving flat but rough parallel surfaces on the blocks (Newberry Volcano; photographs by the author).



Figure 7.25 - Examples from Tell Mozan of flakes with flat, rough surfaces, indicating that obsidian blocks were brought to the site with porous surfaces like those seen above.



Figure 7.26 - Examples of obsidian blade and flake cores, circa 2300-1300 BCE.



Figure 7.27 - An obsidian blade core from Unit A7, Feature 49, circa 2100-1800 BCE.



Figure 7.28 - Examples from Tell Mozan of probable early-series blades removed from a core prior to prismatic-blade production. The removal of such blades was used to shape a polyhedral core and subsequently produce blades like those shown in Figure 7.27.

7.3.1 - Distinguishing Nemrut Dağ and Bingöl A

As I discuss in Section 2.5.2, there apparently is a magmatic relationship between the two peralkaline obsidian sources in Anatolia -- Bingöl A and Nemrut Dağ -- that often makes it hard to differentiate them. Some authors (e.g., Gratuze et al. 1993, 1995; Abbès et al. 2001, 2003; Le Bourdonnec et al. 2005a; Bellot-Gurlet and Poupeau 2006; Khalidi et al. 2009) even suggest that it is impossible to discern them. Poidevin (1998), though, showed that this claim is incorrect and, given sufficient precision, there are three ways to distinguish Bingöl A and Nemrut Dağ sources. First, he reported the Ba content is higher in the Nemrut Dağ obsidians compared to Bingöl A. Second, a plot of Al_2O_3 versus Fe_2O_3 reveals three chemical clusters: Bingöl A obsidian, pre-caldera Nemrut Dağ obsidian, and post-caldera Nemrut Dağ obsidian. Third, a plot of "peralkalinity" (i.e., a CNK/A versus NK/A plot) shows that a Bingöl A cluster falls between two Nemrut Dağ clusters. Others (e.g., Bressy et al. 2005) have used the type of plot and added a third Nemrut Dağ cluster, called "Nemrut Caldera," which falls close to the Bingöl A cluster.

Figure 7.30 reveals not two or three Nemrut Dağ clusters, but ***six*** clearly distinct clusters: apparently three pre-caldera clusters and three post-caldera clusters. Recall that, at most, four Nemrut Dağ geochemical clusters were identified by Blackman (1984), and most recent studies suggest only one or two, sometimes three, obsidian sources at Nemrut Dağ. My recognition of the six clusters is due to (1) highly precise and accurate analyses for critical elements and (2) very thorough field survey and specimen collection by Rapp and Ercan. Without both components, this would not have been possible. Furthermore,

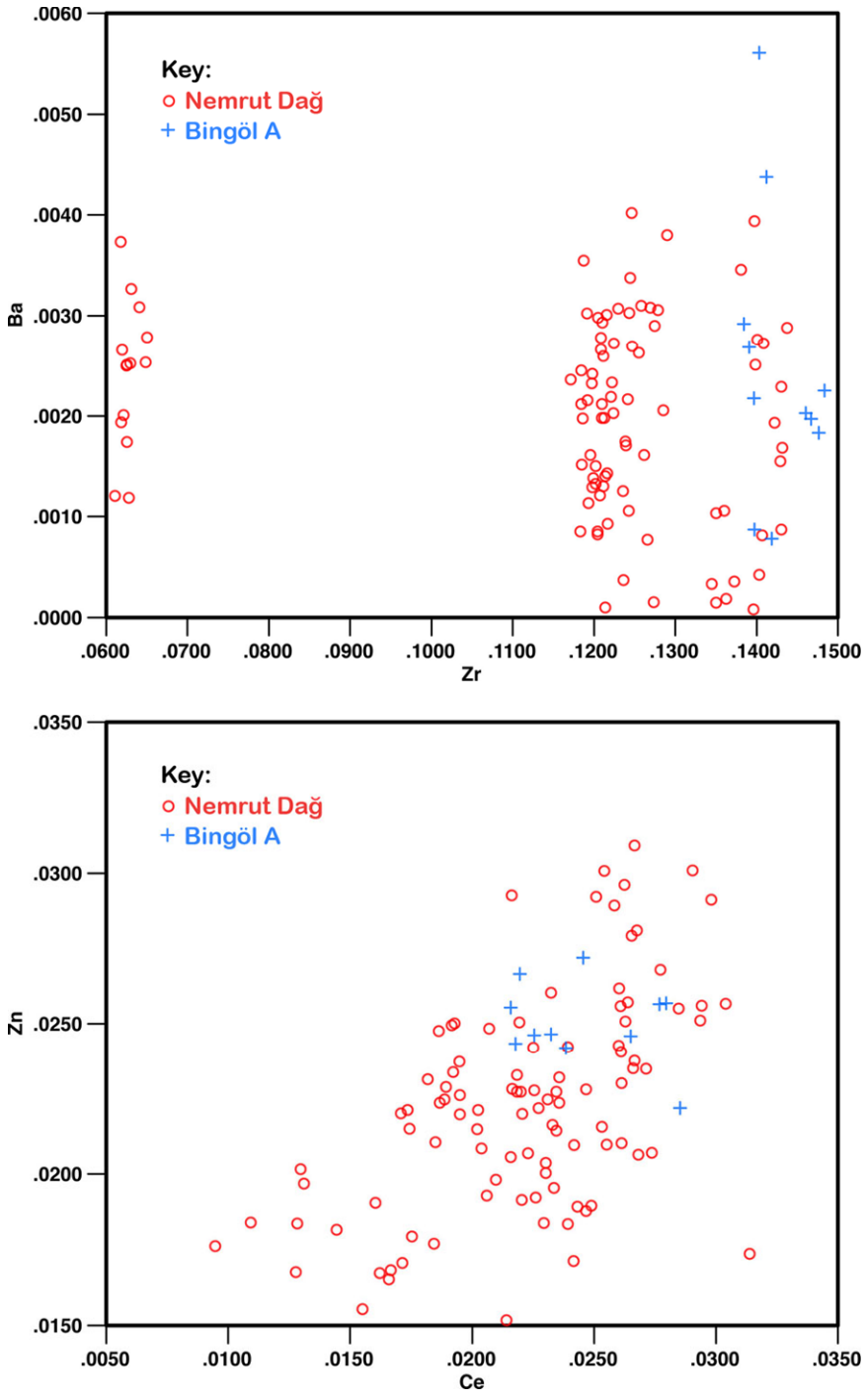


Figure 7.29 - If one only uses trace elements such as Ba vs. Zr (like RDC's famous plot) or Zn vs. Ce, there will only appear to be two or three Nemrut Dağ geochemical clusters (red circles), one of which overlaps with the Bingöl A cluster (blue crosses).

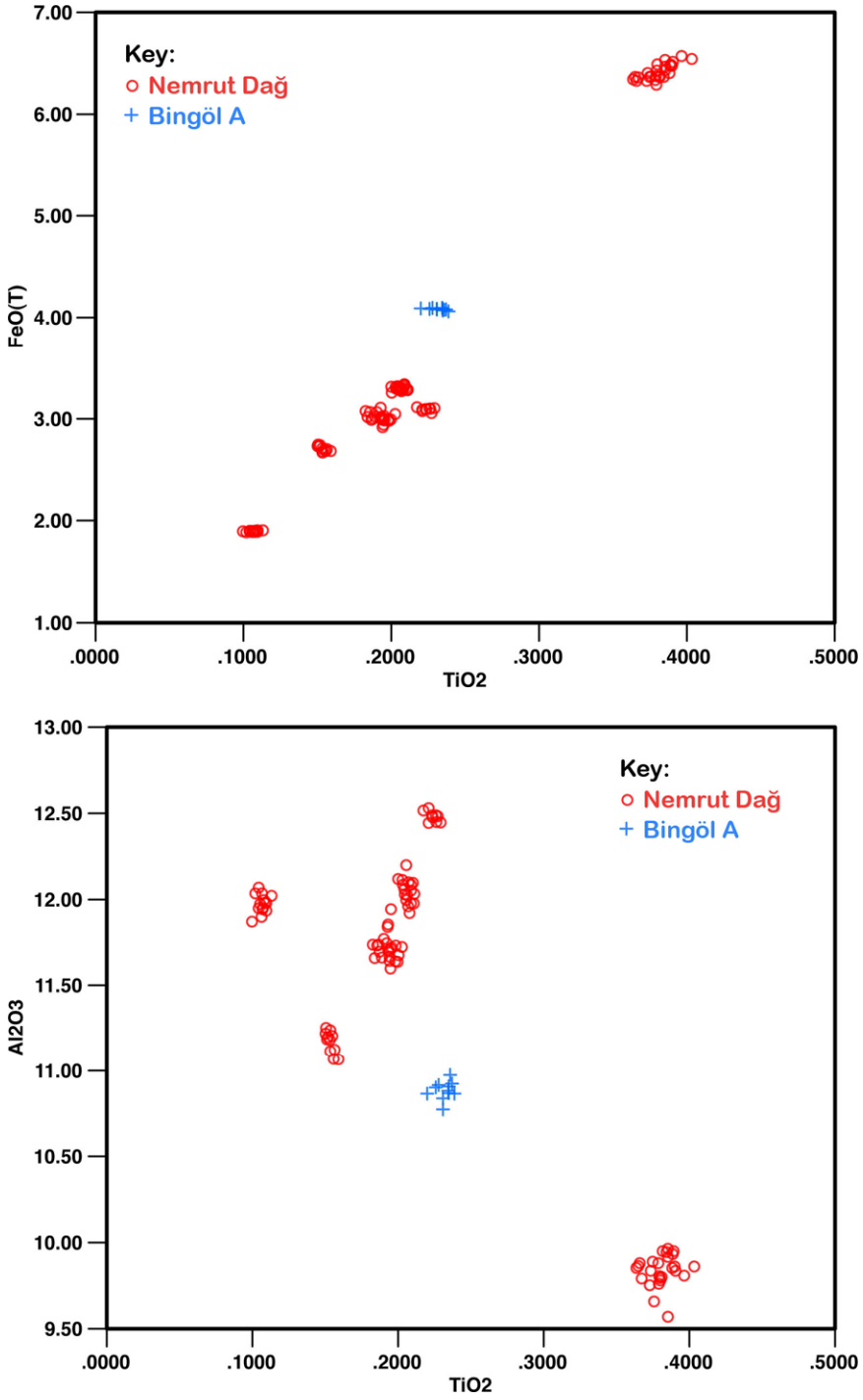


Figure 7.30 - Using major elements (such as Al, Fe, and Ti here), precise analyses, and specimens from eleven collection areas, I reveal ***six*** geochemical clusters among the Nemrut Dağ specimens, all of which are clearly distinguished from Bingöl A.

the Bingöl A obsidians -- two clusters, in fact -- are clearly distinguished from the Nemrut Dağ obsidians. One of these two Bingöl A clusters (EA47) falls close to one of the three Nemrut Dağ clusters but remains distinct. In Chapter 8, I point out, though, that there is a problem with distinguishing the Nemrut Dağ obsidians this way.

The only issue regarding Bingöl A and Nemrut Dağ involved the non-destructive analyses of chemically altered artifact surfaces. Due to alteration of the artifact surfaces, as discussed in Section 5.3.4, it was not clear, based on the Euclidean distances alone, if five artifacts from Tell Mozan originated from Bingöl A and Nemrut Dağ. The Euclidean distances based on Fe, Ti, and Ba indicated that Bingöl A is the correct source, but other element combinations indicated the source was a flow on the eastern shore of the Nemrut Dağ caldera lake (EA24). I used the methods suggested by Poidevin (1998) to determine which of the two sources is the correct one. A "peralkalinity" plot (i.e., a CNK/A versus NK/A plot) as well as scatterplots of Ba, Al, and Fe (plus Ti, which cannot be measured precisely using NAA) indicated that Bingöl A is the correct source.

7.3.2 - A Discovery about Meydan Dağ and Tendürek Dağ

Geological surveys of obsidian-bearing volcanoes in Eastern Anatolia, especially northwest of Lake Van, remain somewhat incomplete. This has been a problem since the work of RDC, who analyzed one obsidian specimen from the British Museum labelled as "Bayezid" (an alternate name for the town of Doğubeyazıd). The volcanic source of this museum specimen has been a subject of much debate. Mount Ararat, immediately to the

northeast, has typically been considered the source; however, two other possibilities have been suggested: Meydan Dağ (also called "Ziyaret" in the literature) and Tendürek Dağ, both of which I discuss in Appendix A. The latter has been particularly neglected in the literature. In fact, in his largely exhaustive compendium of Anatolian obsidian analyses, Poidevin (1998) states that, to the best of his knowledge, no chemical analyses or dates of Tendürek Dağ obsidians have been conducted (143). He even considers a possibility that peralkaline obsidians may occur at Tendürek Dağ, which, if true, could have considerable consequences on the interpretation of prior studies because it is commonly presumed that peralkaline obsidians originate from Nemrut Dağ or Bingöl A (143). In the same volume, Chataigner (1998) suggests that eastern flows of Meydan Dağ could be covering western flows, perhaps with peralkaline obsidians, of Tendürek Dağ (312).

In 1992, Rapp and Ercan collected obsidian specimens from Tendürek Dağ (called "Doğubeyazıd" in their field notes) and Meydan Dağ (I obtained additional Meydan Dağ specimens from a mining company). Unfortunately, the field maps for Tendürek Dağ and Meydan Dağ have since been lost, and their notes about the obsidian collection areas lack details (i.e., from where on the volcanoes they collected obsidian specimens). Therefore, I do not know which obsidian specimens came from, for example, any eastern lava flows of Meydan Dağ volcano or any western lava flows of Tendürek Dağ.

First, and perhaps most important, my analyses show that Tendürek Dağ obsidians are not peralkaline, and Nemrut Dağ and Bingöl A remain the only sources of peralkaline obsidians in the Near East. Another notable discovery, though, is that the specimens from

one Meydan Dağ collection area (EA09) closely match the specimens from the Tendürek Dağ collection areas (see Table 7.1 for data). This strongly suggests that, as Chataigner (1998) thought, the eastern lava flows of Meydan Dağ and the western flows of Tendürek Dağ overlap to some extent. Therefore, at collection area EA09, perhaps Rapp and Ercan thought that they were collecting obsidian from eastern Meydan Dağ flows when, in fact, they were collecting obsidian from western Tendürek Dağ flows.

Consequently, I have reassigned the EA09 specimens to Tendürek Dağ rather than its neighbor Meydan Dağ. This, in fact, changed the assignment of some artifacts in this study from Meydan Dağ to Tendürek Dağ, so this was a notable discovery. Furthermore, it highlights the importance of understanding the potential sources as well as the regional geology whenever a researcher conducts an obsidian-sourcing study.

7.3.3 - Muş, Pasinler, and the Potential for Unknown Sources

Six artifacts from Tell Mozan were assigned to the Muş or Pasinler sources. One artifact (A10 q601.3 f277 k27) had virtually equal probabilities of coming from Muş and Pasinler. Three artifacts are "closest" to the Pasinler specimens, but Muş is a reasonably probable source as well. Similarly, for two artifacts likely from Muş, Pasinler was also a probable source. For two artifacts, Erzincan, nearby Pasinler, was also a possible source. It is possible that non-destructive analyses of chemically altered surfaces contributed to a difficulty in assigning artifacts more conclusively to one of these sources. These sources, though, are little studied, so it is possible that these sources are simply hard to distinguish

Table 7.1 - Comparison of "Meydan Dag" and "Dogubayezid/Tendurek Dag" Geological Specimens

	"Meydan Dag"					"Dogubayezid" (Tendurek Dag)		
	EA07	EA08	EA09	EA10	EA11	EA30	EA31	EA32
SiO_2	75.97	75.87	75.46	75.81	75.81	75.19	75.30	75.42
TiO_2	0.077	0.076	0.076	0.074	0.076	0.074	0.077	0.074
Al_2O_3	13.22	13.15	13.10	13.12	13.16	13.03	13.18	13.20
Cr_2O_3	-	-	-	-	-	-	-	-
FeO(T)	0.978	0.962	1.282	1.025	0.972	1.269	1.259	1.258
MnO	0.052	0.051	0.065	0.057	0.051	0.065	0.064	0.065
MgO	0.020	0.019	0.046	0.030	0.019	0.045	0.043	0.044
CaO	0.277	0.238	0.410	0.349	0.253	0.404	0.407	0.410
Na_2O	4.849	4.706	4.877	4.550	4.815	4.795	4.806	4.830
K_2O	4.588	4.736	4.437	4.658	4.445	4.410	4.456	4.444
P_2O_5	0.005	0.007	0.008	0.006	0.005	0.005	0.008	0.007
F	0.002	0.002	0.002	0.003	0.001	0.002	0.001	0.002
SO_3	0.0010	0.0019	0.0014	0.0019	0.0023	-	0.0036	0.0029
Cl	0.0666	0.0701	0.0704	0.0676	0.0652	0.0619	0.0603	0.0605
Zr	0.0292	0.0288	0.0287	0.0282	0.0294	0.0289	0.0291	0.0293
Nb	0.0099	0.0090	0.0093	0.0088	0.0091	0.0092	0.0084	0.0097
Ga	0.0050	0.0051	0.0049	0.0039	0.0045	0.0056	0.0049	0.0058
Zn	0.0107	0.0095	0.0103	0.0097	0.0108	0.0089	0.0077	0.0086
Ba	0.0078	0.0075	0.0083	0.0093	0.0105	0.0069	0.0066	0.0076
Ce	0.0067	0.0077	0.0060	0.0054	0.0065	0.0089	0.0083	0.0092

using various analytical techniques and that the difficulty is unrecognized in the literature due to a lack of data. As discussed in Appendix A, obsidian sources in the Muş Province and other provinces in northeastern Turkey are rarely studied and poorly understood. The third possibility, therefore, is that these artifacts represent an unknown source, perhaps on the Pasinler Basin or Muş Plain. In these regions, obsidian occurs commonly as rounded blocks, transported by rivers and mudflows, sometimes from unknown eruptions, so there is a possibility of unknown sources buried under recent sediment.

The most conservative interpretation is that these six artifacts originated from one of the Muş sources, either known or unknown, because the Muş Plain is roughly halfway between the Bingöl and Nemrut Dağ sources, both of which I reveal here were exploited at Tell Mozan. The Pasinler Basin is roughly 140 km nearly due north of Muş, through mountainous terrain, so use of obsidian from this source seems less likely. Still the use of obsidian from Pasinler or an unknown source cannot be entirely ruled out. Until further work is done, I ascribe the six artifacts to "Muş/Pasinler" as a compromise.

7.4 - The Urkesh Global Record

In the following sections, I refer extensively to the "Urkesh Global Record" when I discuss the available stratigraphic information for the sourced artifacts. The excavation records for the Urkesh expedition are not published in a traditional book format. Instead, the excavation data and observations are entered into a HTML-based, relational database, called the Urkesh Global Record, for online publication. At present, this database is only

accessible to archaeologists who are part of the Urkesh team; however, the aim is to make the entire database publicly accessible in the near future.

A site unit in the Urkesh Global Record -- for example, A16 -- acts as a volume in an entirely digital series. If I navigate to a feature of interest, such as one that contained a sourced artifact, I can find a description and classification of the feature, photographs, the lots and items contained within the feature, frequencies of the ceramic wares, associations with other features, its locus and elevation, and its stratigraphic and phase assignments. I can even find interpretations of the excavators and, if applicable, a supporting or differing opinion from someone else at the site, like a ceramics expert.

The "volumes" for units more than a few years old are not yet online, but the goal is to make the entirety of the excavation data available eventually. Some units discussed in the following sections are not yet available in the Urkesh Global Record. The delay in publishing the older "volumes" reflects the quantities of data involved. For instance, A16 includes 44,168 excavated sherds, all individually recorded and classified. This unit also has 183,551 records, including 2,939 image files, and half a million hyperlinks among its 27,316 files (Buccellati and Kelly-Buccellati 2007a:22). These data are entered daily on-site in a format that can be automatically processed to generate such links; however, some manual processing is still needed to produce a completed "volume." When available now in the Urkesh Global Record, I provide the contexts for the sourced obsidian artifacts and their stratigraphic assignments. I hope that, in coming years, I will be able to update my interpretations to include such information for artifacts from all units.

7.5 - Sourced Obsidian of Site Area A

Area A of Tell Mozan includes the Royal Palace of Tupkish (discussed in Section 3.6.5), the lower sacral area (including the *âbi* discussed in Section 3.6.6 and the Road to the Netherworld in Section 3.6.7), and subsequent habitations, graves, and accumulations atop them (discussed in Section 3.6.10). For the present research, I analyzed 82 obsidian artifacts from this area of Tell Mozan, and I discuss the results here.

7.5.1 - Sourced Obsidian of Unit A1

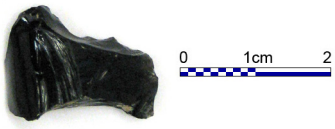
Unit A1 is one part of the original step trench excavated in Area A in 1990, and it includes the service wing of the Royal Palace. The excavation records for A1 are not yet available in the Urkesh Global Record, so I do not yet have precise information about the features from which these artifacts were unearthed or their respective dates. This unit has been fully excavated, from the surface deposits dating to the settlement's abandonment in about 1300 BCE down to the Royal Palace, built circa about 2300 BCE. Thus, at present, these obsidian artifacts can only be dated to between 2300 and 1300 BCE.

7.5.1.1 - Feature 16 of Unit A1



site unit	lot	feature	square/locus	piece	mass (g)
A1	q161.1	f16	k117	-	0.19

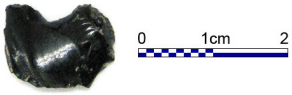
Source Assignment: Nemrut Dağ (EA25), a lava dome in the southeastern portion of the Nemrut Dağ caldera, near or along the shore of the caldera lake.



site unit	lot	feature	square/locus	piece	mass (g)
A1	q342.lw	f16	k117	-	2.20

Source Assignment: Nemrut Dağ (EA25), a lava dome in the southeastern portion of the Nemrut Dağ caldera, near or along the shore of the caldera lake.

7.5.1.2 - Feature 29 of Unit A1



site unit	lot	feature	square/locus	piece	mass (g)
A1	q59.1	f29	k119	-	0.66

Source Assignment: Nemrut Dağ (EA25), a lava dome in the southeastern portion of the Nemrut Dağ caldera, near or along the shore of the caldera lake.

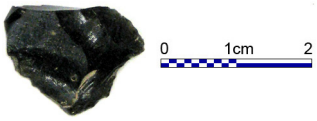
7.5.1.3 - Feature 67 of Unit A1



site unit	lot	feature	square/locus	piece	mass (g)
A1	q264.1	f67	k13	-	1.10

Source Assignment: Nemrut Dağ (EA25), a lava dome in the southeastern portion of the Nemrut Dağ caldera, near or along the shore of the caldera lake.

7.5.1.4 - Feature 606 of Unit A1



site unit	lot	feature	square/locus	piece	mass (g)
A1	q183.1	f606	k?	-	1.04

Source Assignment: Nemrut Dağ (EA25), a lava dome in the southeastern portion of the Nemrut Dağ caldera, near or along the shore of the caldera lake.

7.5.2 - Sourced Obsidian of Unit A2

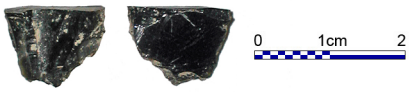
Unit A2 is also a part of the original step trench excavated in Area A in 1990, and the excavation records for A2 are not yet available in the Urkesh Global Record, so I do not yet have detailed information about the features from which the artifacts came or their dates. This unit, though, consists principally of houses and graves from the early second millennium after the Tupkish Royal Palace was abandoned. In particular, this settlement period dates to Phase 4, the first post-Palace settlement circa 2100-2000 BCE, and Phase 5, the second post-Palace settlement circa 2000-1800 BCE. Accordingly, the one sourced artifact from Unit A2 most likely dates to this period between about 2100 and 1800 BCE, during the Middle Bronze Age I and IIA and the Ur III Period.



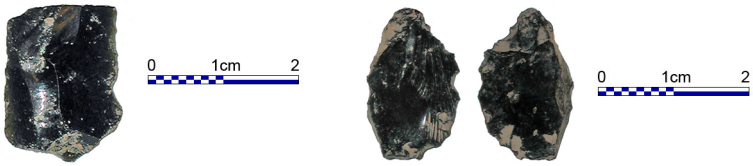
site unit	lot	feature	square/locus	piece	mass (g)
A2	q333.2	f114	k151	-	0.14

Source Assignment: Bingöl B

The same lot (q333) contained the obsidian artifact pictured below, which, given the wide flat surface on its proximal end, appears to be a flake removed while a core preform was being shaped into a core for bladelet production.

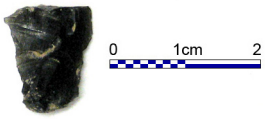


The same feature (f114) in this unit also contained the two artifacts below: a blade (on the left) and perhaps what is best described as a flake-scraper (on the right):



7.5.3 - Sourced Obsidian of Unit A6

Unit A6 is part of the service wing of the Royal Palace (and the later strata above it). In particular, most of A6 is Sector D of the service wing, which is interpreted to be a kitchen (as discussed in Section 3.6.5). The A6 excavation records are not yet available in the Urkesh Global Record, so I do not yet have detailed information about the features or their dates. Like A1, the unit has been fully excavated down to the palace strata, so the artifacts can only be dated, at present, to between 2300 and 1300 BCE.



site unit	lot	feature	square/locus	piece	mass (g)
A6	q386.1	f122	k218	1	0.59

Source Assignment: Tendürek Dağ (“Doğubeyazıd”)



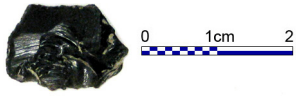
site unit	lot	feature	square/locus	piece	mass (g)
A6	q386.1	f122	k218	2	0.71

Source Assignment: Nemrut Dağ (EA25), a lava dome in the southeastern portion of the Nemrut Dağ caldera, near or along the shore of the caldera lake.



site unit	lot	feature	square/locus	piece	mass (g)
A6	q971.1	f410	k31	-	0.21

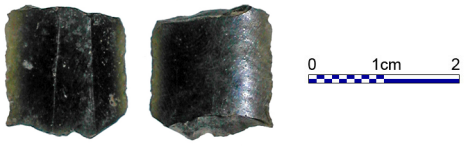
Source Assignment: Bingöl B



site unit	lot	feature	square/locus	piece	mass (g)
A6	q973.1	f412	k31	-	0.63

Source Assignment: Nemrut Dağ (EA25), a lava dome in the southeastern portion of the Nemrut Dağ caldera, near or along the shore of the caldera lake.

The same lot (q973) also included the prismatic blade segment below:

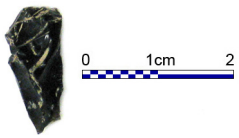


7.5.4 - Sourced Obsidian of Unit A7

Unit A7 is northwest of the service wing of the Royal Palace, and it includes part of the northern service courtyard (noted in Section 3.6.5) and strata from later phases. In

fact, A7 consists mainly of houses and graves from the first half of the second millennium after the Royal Palace was abandoned. In particular, this period dates to Phase 4, the first post-Palace settlement period circa 2100-2000 BCE, and Phase 5, the second post-Palace settlement period circa 2000-1800 BCE. The records for A7 are not yet available in the Urkesh Global Record, so I do not now have information about the features or strata from which the artifacts came or their dates. For now, I assume that artifacts with low feature numbers (e.g., f56, f63, and f69) were unearthed from houses and graves circa 2100-1800 BCE and that artifacts with higher feature numbers (e.g., f465 and f480) most likely came from the northern service courtyard of the Royal Palace. These provisional dates will be adjusted when the A7 records are included in the Urkesh Global Record.

7.5.4.1 - Feature 56 of Unit A7



site unit	lot	feature	square/locus	piece	mass (g)
A7	q287.1	f56	k7	-	0.59

Source Assignment: Nemrut Dağ (EA25), a lava dome in the southeastern portion of the Nemrut Dağ caldera, near or along the shore of the caldera lake.

The same feature (f56) also included the prismatic blade segment below:



7.5.4.2 - Feature 63 of Unit A7



site unit	lot	feature	square/locus	piece	mass (g)
A7	q386.l3	f63	k8	-	0.27

Source Assignment: Bingöl B

The same feature (f63) also included this prismatic blade:



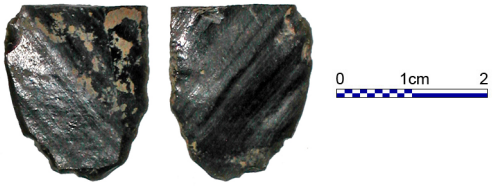
7.5.4.3 - Feature 69 of Unit A7



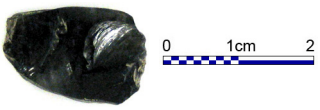
site unit	lot	feature	square/locus	piece	mass (g)
A7	q222.1	f69	k9	-	0.99

Source Assignment: Nemrut Dağ (EA25), a lava dome in the southeastern portion of the Nemrut Dağ caldera, near or along the shore of the caldera lake.

The same lot (q222) included the obsidian artifact pictured below. It appears to be a flake removed form a core preform that was then retouched to use as a scraper.

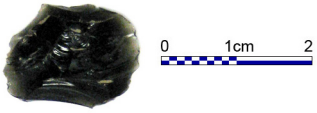


7.5.4.4 - Feature 121 of Unit A7



site unit	lot	feature	square/locus	piece	mass (g)
A7	q350.l2	f121	k13	-	1.91

Source Assignment: Bingöl B



site unit	lot	feature	square/locus	piece	mass (g)
A7	q360.1	f121	k13	1	0.91

Source Assignment: Nemrut Dağ (EA25), a lava dome in the southeastern portion of the Nemrut Dağ caldera, near or along the shore of the caldera lake.



site unit	lot	feature	square/locus	piece	mass (g)
A7	q360.1	f121	k13	2	0.26

Source Assignment: Nemrut Dağ (EA25), a lava dome in the southeastern portion of the Nemrut Dağ caldera, near or along the shore of the caldera lake.



site unit	lot	feature	square/locus	piece	mass (g)
A7	q360.1	f121	k13	3	0.12

Source Assignment: Nemrut Dağ (EA25), a lava dome in the southeastern portion of the Nemrut Dağ caldera, near or along the shore of the caldera lake.



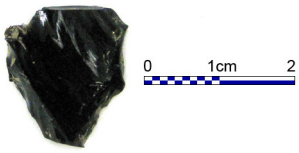
site unit	lot	feature	square/locus	piece	mass (g)
A7	q360.1	f121	k13	4	0.13

Source Assignment: Nemrut Dağ (EA25), a lava dome in the southeastern portion of the Nemrut Dağ caldera, near or along the shore of the caldera lake.

The same feature (f121) also included this prismatic blade:



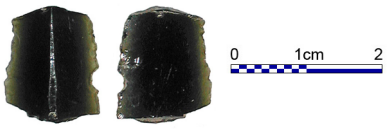
7.5.4.5 - Feature 148 of Unit A7



site unit	lot	feature	square/locus	piece	mass (g)
A7	q602.1	f148	k13	-	1.61

Source Assignment: Nemrut Dağ (EA25), a lava dome in the southeastern portion of the Nemrut Dağ caldera, near or along the shore of the caldera lake.

The same feature (f148) also included this bladelet segment:



7.5.4.6 - Feature 261 of Unit A7



site unit	lot	feature	square/locus	piece	mass (g)
A7	q892.1	f261	k12	-	0.16

Source Assignment: Göllü Dağ - Kömürcü

The same feature (f261) also included this prismatic blade segment:



7.5.4.7 - Feature 465 of Unit A7



site unit	lot	feature	square/locus	piece	mass (g)
A7	q1146.1	f465	k21	-	0.37

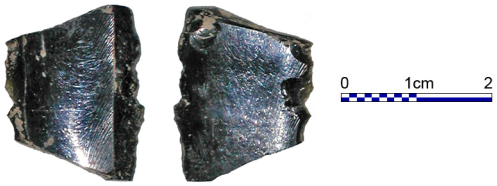
Source Assignment: Tendürek Dağ (“Doğubeyazıd”)



site unit	lot	feature	square/locus	piece	mass (g)
A7	q1150.5	f465	k21	-	0.35

Source Assignment: Bingöl A

The lot (q1150) included this prismatic blade segment, which could also be classified as a geometric microlith, in particular a trapeze (i.e., trapezoid):





site unit	lot	feature	square/locus	piece	mass (g)
A7	q1174.2	f465	k21	-	0.34

Source Assignment: Bingöl A

7.5.4.8 - Feature 480 of Unit A7



site unit	lot	feature	square/locus	piece	mass (g)
A7	q1201.4	f480	k21	-	0.75

Source Assignment: Muş/Pasinler

7.5.5 - Sourced Obsidian of Unit A8

Unit A8 is a fairly small unit that was excavated primarily to investigate the upper strata above the Palace. Like A7, A8 consists mostly of houses and graves from the early second millennium after the Palace had been abandoned. There was scattered occupation

in A8 during Phase 4, the first post-Palace settlement circa 2100-2000 BCE. Later, in Phase 5, the second post-Palace settlement circa 2000-1800 BCE, houses and graves were present on this unit. The excavation records for A8 are not available in the Urkesh Global Record yet, so this one artifact is attributed to between 2100 and 1800 BCE.



site unit	lot	feature	square/locus	piece	mass (g)
A8	q154.1	f58	k9	-	0.77

Source Assignment: Nemrut Dağ (EA25), a lava dome in the southeastern portion of the Nemrut Dağ caldera, near or along the shore of the caldera lake.

7.5.6 - Sourced Obsidian of Unit A9

Unit A9 is north of the service wing of the Royal Palace and immediately east of Unit A7. Consequently, like A7, A9 includes both the northern service courtyard (noted in Section 3.6.5) and strata from later phases (i.e., houses and graves from the first half of the second millennium after the Royal Palace was abandoned). Although the excavation records for A9 are not yet accessible in the Urkesh Global Record, this unit was described and analyzed by Walker (2003), so some feature descriptions are available.

7.5.6.1 - Feature 98 of Unit A9

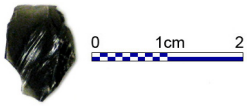
The pebble surface of the Royal Palace service courtyard is overlaid by a series of sediment accumulations, including one labelled feature 98. This particular accumulation

contained over 70 conical cup sherds, and this ceramic type is considered a marker of the Akkadian Period, circa approximately 2200 BCE. Walker (2003) therefore suggests that this feature corresponds to a period when the service courtyard still functioned as an open space but not as part of the Palace, which had been abandoned. The artifacts found in this feature are thus assumed to date roughly to this century.



site unit	lot	feature	square/locus	piece	mass (g)
A9	q376.1	f98	k3	1	0.28

Source Assignment: Nemrut Dağ (EA25), a lava dome in the southeastern portion of the Nemrut Dağ caldera, near or along the shore of the caldera lake.



site unit	lot	feature	square/locus	piece	mass (g)
A9	q376.1	f98	k3	2	0.29

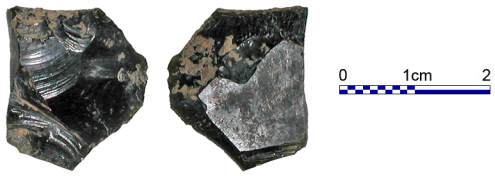
Source Assignment: Nemrut Dağ (EA25), a lava dome in the southeastern portion of the Nemrut Dağ caldera, near or along the shore of the caldera lake.

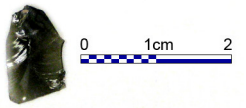


site unit	lot	feature	square/locus	piece	mass (g)
A9	q376.1	f98	k3	3	0.35

Source Assignment: Nemrut Dağ (EA25), a lava dome in the southeastern portion of the Nemrut Dağ caldera, near or along the shore of the caldera lake.

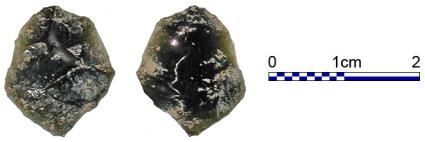
The same lot (q376) also contained the artifact below. It might be a platform preparation flake from an obsidian block that was then reshaped to serve as a scraper.





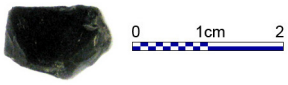
site unit	lot	feature	square/locus	piece	mass (g)
A9	q437.2	f98	k3	-	0.13

Source Assignment: Nemrut Dağ (EA25), a lava dome in the southeastern portion of the Nemrut Dağ caldera, near or along the shore of the caldera lake.



The same lot (q437) also contained two obsidian artifacts above and below. The artifact above is a flake, probably a decortication or platform-preparation flake, without retouch. The artifact below might be a platform preparation flake from a tabular blade-production core, or it could also be an exhausted core reshaped for another use.





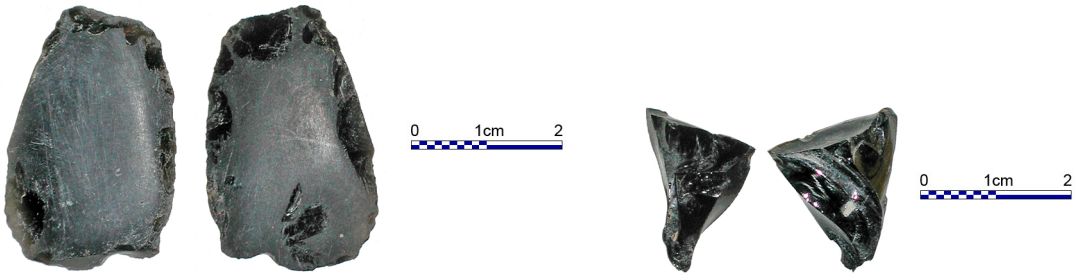
site unit	lot	feature	square/locus	piece	mass (g)
A9	q440.1	f98	k3	1	0.69

Source Assignment: Bingöl B



site unit	lot	feature	square/locus	piece	mass (g)
A9	q440.1	f98	k3	2	0.26

Source Assignment: Nemrut Dağ (EA25), a lava dome in the southeastern portion of the Nemrut Dağ caldera, near or along the shore of the caldera lake.



The same lot (q440) also included the obsidian artifacts above and below. The artifact in the upper left is likely a flake that has been rounded by grounding and retouched along its edges for use as a scraper. The artifact in the upper right might be a platform preparation flake from a tabular blade-production core or something similar. The two artifacts below are fairly undiagnostic debitage just large enough to be classified as chunks.



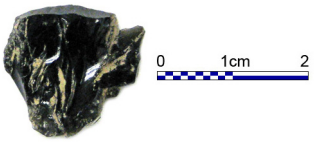


The same feature (f98) also contained the two obsidian artifacts above and the one below. The artifact in the upper left is a flake that, based on its scars, might have been removed from a bladelet core. The artifact in the upper right seems to be a flake that was reshaped to use as a scraper. The artifact below is rather unusual. The dorsal and ventral surfaces are both nearly flat, smooth flake scars, as is one of the sides. The opposite side, though, has been retouched, suggesting it was used as some sort of side scraper.



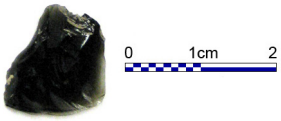
7.5.6.2 - Feature 126 of Unit A9

Feature 126 also dates to a period after the Palace was no longer in use, as it is an accumulation beneath a layer that contains a pit, suggesting scattered occupation.



site unit	lot	feature	square/locus	piece	mass (g)
A9	q454.2	f126	k3	1	1.42

Source Assignment: Nemrut Dağ (EA25), a lava dome in the southeastern portion of the Nemrut Dağ caldera, near or along the shore of the caldera lake.



site unit	lot	feature	square/locus	piece	mass (g)
A9	q454.2	f126	k3	2	0.58

Source Assignment: Nemrut Dağ (EA25), a lava dome in the southeastern portion of the Nemrut Dağ caldera, near or along the shore of the caldera lake.



site unit	lot	feature	square/locus	piece	mass (g)
A9	q454.2	f126	k3	3	0.25

Source Assignment: Nemrut Dağ (EA25), a lava dome in the southeastern portion of the Nemrut Dağ caldera, near or along the shore of the caldera lake.



The same lot (q454) contained these three obsidian artifacts. The artifact above might be a bladelet core. The artifact in the lower left might be part of a core, possibly removed to prepare a new platform. The artifact in the lower right is a flake without retouch.







This lot (q454) also contained two obsidian artifacts above. Both pieces of obsidian seem to be undiagnostic debitage just large enough to be considered chunks. Additional studies of the assemblage may suggest the processes that created such debitage.

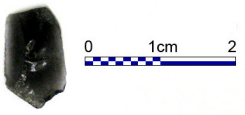
7.5.6.3 - Feature 156 of Unit A9

Feature 156 is an accumulation just above the pebble surface of the palace service courtyard, meaning the feature would have started forming as soon as the pebble surface was no longer being actively maintained, perhaps as soon as its construction around 2300 BCE. Thus these artifacts might have been deposited while service activities for the royal court, perhaps even that of Tupkish, were being carried out in the courtyard.



site unit	lot	feature	square/locus	piece	mass (g)
A9	q463.2	f156	k3	1	1.00

Source Assignment: Göllü Dağ - Kömürcü

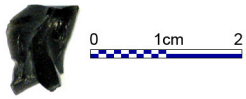


site unit	lot	feature	square/locus	piece	mass (g)
A9	q463.2	f156	k3	2	0.30

Source Assignment: Göllü Dağ - Kömürcü

7.5.6.4 - Feature 247 of Unit A9

Feature 247 is apparently one of the lowest excavated strata in A9. In fact, it sits atop feature 260, which is the lowest in this locus. One of the current excavation goals in Area A is to expose the full horizontal extent of the Tupkish Royal Palace while working to understand the settlement strata above it. Therefore, excavations in this area have not yet explored below the Palace. Accordingly, this feature and its artifacts probably date to around the construction of the Tupkish Royal Palace, circa 2300 BCE.



site unit	lot	feature	square/locus	piece	mass (g)
A9	q693.1	f247	k11	1	0.47

Source Assignment: Nemrut Dağ (EA25), a lava dome in the southeastern portion of the Nemrut Dağ caldera, near or along the shore of the caldera lake.



site unit	lot	feature	square/locus	piece	mass (g)
A9	q693.1	f247	k11	2	1.11

Source Assignment: Nemrut Dağ (EA25), a lava dome in the southeastern portion of the Nemrut Dağ caldera, near or along the shore of the caldera lake.

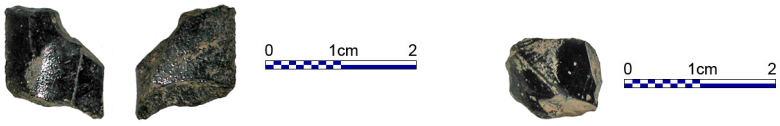


site unit	lot	feature	square/locus	piece	mass (g)
A9	q693.1	f247	k11	3	0.74

Source Assignment: Muş/Pasinler



The same lot (q693) contained the above and below obsidian artifacts. The artifact in the upper left is a prismatic blade with retouch on the ventral and dorsal surfaces. The one in the upper right may be a platform-preparation flake from a core or some other part from a core. The artifact in the lower left is a blade segment, and the artifact in the lower right is fairly undiagnostic debitage small enough to be considered a chip.



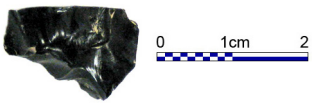
7.5.6.5 - Feature 260 of Unit A9

Feature 260, as noted in the previous section, is the lowest feature excavated in its locus, and it is probably some sort of floor surface. Because excavations in this area have not explored below the Palace levels, this feature and its artifacts probably date to around the construction of the Tupkish Royal Palace, circa 2300 BCE.



site unit	lot	feature	square/locus	piece	mass (g)
A9	q724.1	f260	k11	1	0.94

Source Assignment: Bingöl B



site unit	lot	feature	square/locus	piece	mass (g)
A9	q724.1	f260	k11	2	0.78

Source Assignment: Meydan Dağ

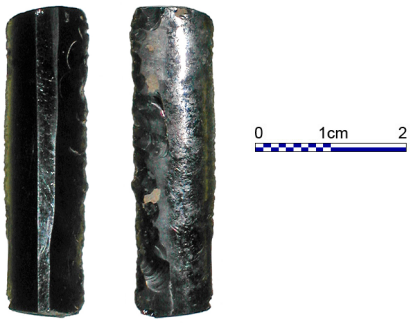
7.5.7 - Sourced Obsidian of Unit A10

Unit A10 is the southeast corner of the Royal Palace complex and the strata above it. In particular, this unit includes Sector C of the Palace, interpreted to be workspaces of the service wing, and the subsequent strata includes houses and graves dating to the early second millennium after the Palace was abandoned. There was only scattered occupation during Phase 4, the first post-Palace settlement circa 2100-2000 BCE, as well as Phase 5, the second post-Palace settlement circa 2000-1800 BCE. The A10 excavation records are not yet accessible in the Urkesh Global Record, so I do not have details about the features or their dates. The unit has, though, been fully excavated down to the palace strata, so the artifacts can simply be dated, at present, to between 2300 and 1300 BCE.



site unit	lot	feature	square/locus	piece	mass (g)
A10	q77.1	f79	k7	-	2.01

Source Assignment: Nemrut Dağ (EA25), a lava dome in the southeastern portion of the Nemrut Dağ caldera, near or along the shore of the caldera lake.



The same lot (q77) also contained the above prismatic blade.

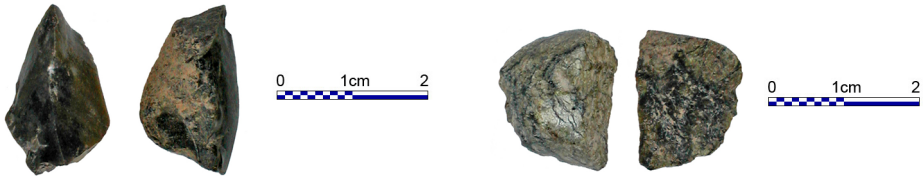


site unit	lot	feature	square/locus	piece	mass (g)
A10	q229.1	f94	k5	-	0.39

Source Assignment: Tendürek Dağ ("Doğubeyazıd")



This same lot (q229) included the obsidian artifacts above and below. The wedge-shaped artifact above has four surfaces that were ground flat. One end is broken, and its original shape and function are not clear. The artifact in the lower left is apparently debitage. The artifact in the lower right has a pumiceous outer "crust" that I have seen on obsidian after a forest fire, so this artifact might also have experienced a fire.



The same feature (f94) also contained the six obsidian artifacts below:



Artifact (a) is a prismatic blade with retouch on both edges, and artifact (e) is a prismatic bladelet. Artifacts (b) and (c) are side scrapers. Artifact (d) appears to be one of the first or second series of blades removed from a core, so it is not as regular as artifacts (a) and (e). Artifact (f) is a small flake probably removed to shape a core. Finding these artifacts in a single feature indicates the obsidian "toolkit" in use at one point in time.



site unit	lot	feature	square/locus	piece	mass (g)
A10	q286.1	f141	k3	-	0.68

Source Assignment: Bingöl B



site unit	lot	feature	square/locus	piece	mass (g)
A10	q601.3	f277	k27	-	0.08

Source Assignment: Muş/Pasinler

This lot (q601) included the artifact below. It appears to be a flake from a core, and there may be deliberate retouch on one side so that it could be used as a scraper.

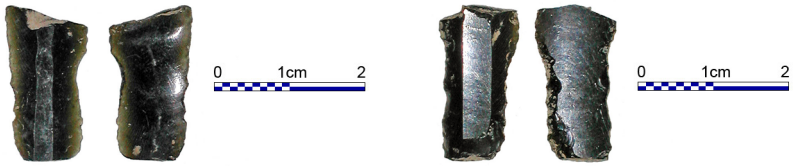




site unit	lot	feature	square/locus	piece	mass (g)
A10	q678.3	f292	k28	-	0.11

Source Assignment: Bingöl B

The same feature (f292) also contained the two prismatic blades below:





site unit	lot	feature	square/locus	piece	mass (g)
A10	q695.1	f300	k28	-	2.00

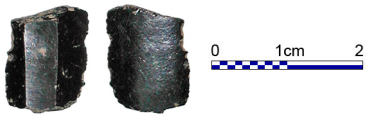
Source Assignment: Bingöl B

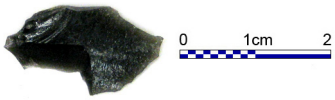


site unit	lot	feature	square/locus	piece	mass (g)
A10	q1081.6	f234	k21	-	1.80

Source Assignment: Nemrut Dağ (EA25), a lava dome in the southeastern portion of the Nemrut Dağ caldera, near or along the shore of the caldera lake.

The same feature (f234) also included the prismatic blade segment below:





site unit	lot	feature	square/locus	piece	mass (g)
A10	q1194.3	f925	k29	-	0.57

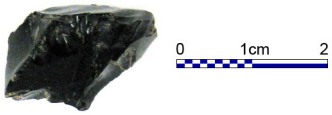
Source Assignment: Bingöl B

7.5.8 - Sourced Obsidian of Unit A14

Unit A14 contains a lower ritual area along the southern edge of the Royal Palace. This area includes the "road to the Netherworld" (discussed in Section 3.6.7) and access to the *abî* (discussed in Section 3.6.7), although not the *abî* itself (which is A12). The *abî* seems to predate the Royal Palace, so it has been suggested that the Palace was built near the *abî* deliberately and that this area was intended to link these two structures (and, thus, the king of Urkesh to the Hurrian deities and religious practices).

7.5.8.1 - Feature 29 of Unit A14

Feature 29 is apparently a recent erosional deposit in a small gully, so the artifacts probably correspond to the later habitation phases. I presume, therefore, that the artifacts likely date to the Mitanni-period habitation at the site, circa 1500 to 1300 BCE.



site unit	lot	feature	square/locus	piece	mass (g)
A14	q244.1	f29	k2	-	2.53

Source Assignment: Nemrut Dağ (EA25), a lava dome in the southeastern portion of the Nemrut Dağ caldera, near or along the shore of the caldera lake.

The same feature (f29) also contained the two obsidian pieces below:

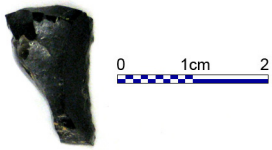


I noticed that these two pieces refit as shown below. It appears that the smaller piece was intended as a platform preparation flake and that the larger one would have been intended as a core. The result must have been unsatisfactory, and both pieces were discarded.



7.5.8.2 - Feature 42 of Unit A14

Feature 42 is part of the later habitation period within this unit, and it corresponds to late Phase 3, the post-imperial Akkadian Period circa 2200-2100 BCE.



site unit	lot	feature	square/locus	piece	mass (g)
A14	q742.2	f42	k12	-	1.33

Source Assignment: Nemrut Dağ (EA22 or EA25), either a lava dome in the northeastern part of the Nemrut Dağ caldera (EA22) or one in the southeastern part of the Nemrut Dağ caldera, near or along the shore of the caldera lake (EA25).

7.5.8.3 - Features 90, 92, and 101 of Unit A14

Features 90, 92, and 101 all seem to be part of small structures built during Phase 4, the first post-Palace settlement circa 2100-2000 BCE, and/or Phase 5, the second post-Palace settlement circa 2000-1800 BCE, in the vicinity of the *abî*.



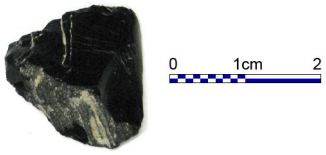
site unit	lot	feature	square/locus	piece	mass (g)
A14	q252.1	f90	k3	-	0.41

Source Assignment: Nemrut Dağ (EA22 or EA25), either a lava dome in the northeastern part of the Nemrut Dağ caldera (EA22) or one in the southeastern part of the Nemrut Dağ caldera, near or along the shore of the caldera lake (EA25).



site unit	lot	feature	square/locus	piece	mass (g)
A14	q265.1	f92	k3	-	2.97

Source Assignment: Bingöl B



site unit	lot	feature	square/locus	piece	mass (g)
A14	q266.1	f92	k3	-	2.08

Source Assignment: Bingöl B



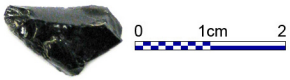
site unit	lot	feature	square/locus	piece	mass (g)
A14	q299.2	f101	k100	-	0.63

Source Assignment: Nemrut Dağ (EA25), a lava dome in the southeastern portion of the Nemrut Dağ caldera, near or along the shore of the caldera lake.

7.5.8.4 - Feature 193 of Unit A14

Feature 193 is an accumulation that covers a pisé (i.e., rammed earth) floor, and it is level with and close to a stone platform in this sacral area. This feature also contained bronze items, grindstones, and restorable ceramic vessels. Based on the stratigraphy and the ceramic sherds, the feature appears to correspond to an early reuse of the service wing

of the Palace. Consequently, the deposition of this feature (and its associated artifacts) is dated to early Phase 3, the post-imperial Akkadian Period, about 2200-2100 BCE. While the formal wing of the Royal Palace became deeply covered by later habitation structures, the service wing was initially reused and remained near the tell surface.



site unit	lot	feature	square/locus	piece	mass (g)
A14	q474.1	f193	k4	-	0.82

Source Assignment: Nemrut Dağ (EA25), a lava dome in the southeastern portion of the Nemrut Dağ caldera, near or along the shore of the caldera lake.

7.5.8.5 - Feature 250 of Unit A14

Feature 250 is an ancient erosional accumulation deposited in a gully that started to form possibly as soon as the Royal Palace was abandoned in Phase 3. Artifacts in this feature, accordingly, originated higher on the tell to the east. Though the feature is gully wash, the artifacts and their deposition may date as early as Phase 3. On the other hand, they could have been deposited here as late as the abandonment of the tell.



site unit	lot	feature	square/locus	piece	mass (g)
A14	q605.2	f250	k23	-	0.27

Source Assignment: Nemrut Dağ (EA25), a lava dome in the southeastern portion of the Nemrut Dağ caldera, near or along the shore of the caldera lake.

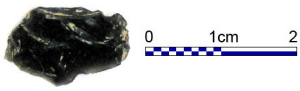


site unit	lot	feature	square/locus	piece	mass (g)
A14	q617.1	f250	k23	-	2.19

Source Assignment: Nemrut Dağ (EA25), a lava dome in the southeastern portion of the Nemrut Dağ caldera, near or along the shore of the caldera lake.

7.5.9 - Sourced Obsidian of Unit A15

Unit A15 is an area east of the *abî* (A12) and south of the formal courtyard paved with flagstone, in A16. It also contains significant accumulations from settlements during the late third and early second millennia. The A15 excavation records are not available in the Urkesh Global Record yet, so I do not have details about these features or their dates. This unit has, though, reached the Palace, so these artifacts can only be dated to between 2300 and 1300 BCE until the records for this unit become accessible. I suspect, however, that some, if not all, of these artifacts date to scattered occupation of this area in Phase 4, the first post-Palace settlement circa 2100-2000 BCE, as well as Phase 5, the second post-Palace settlement circa 2000-1800 BCE. Given the source diversity of the four obsidian artifacts, I am interested to further refine the dates of their features.



site unit	lot	feature	square/locus	piece	mass (g)
A15	q295.2	f108	k92	-	0.53

Source Assignment: Tendürek Dağ (“Doğubeyazıd”)



site unit	lot	feature	square/locus	piece	mass (g)
A15	q734.1	f372	k14	-	2.36

Source Assignment: Nemrut Dağ (EA25), a lava dome in the southeastern portion of the Nemrut Dağ caldera, near or along the shore of the caldera lake.



site unit	lot	feature	square/locus	piece	mass (g)
A15	q752.2	f386	k15	-	2.91

Source Assignment: Muş/Pasinler



site unit	lot	feature	square/locus	piece	mass (g)
A15	q1173.3	f517	k2	-	2.72

Source Assignment: Tendürek Dağ ("Doğubeyazıd")

7.5.10 - Sourced Obsidian of Unit A16

Unit A16 lies east of the service wing of the Royal Palace and is north of A15. It includes the southwestern part of the formal courtyard, which was paved using flagstone. Like A15, this unit also includes copious accumulations from subsequent structures, both houses and graves, built during the late third and early second millennia.

7.5.10.1 - Feature 26 of Unit A16

Feature 26 is most likely an eroded grave that initially consisted of a simple three-walled U-shaped structure. In addition to collapsed brick from these walls, this structure contained human bones, in particular, two mandible pieces and three vertebra. Two large ceramic vessels, known as Khabur ware, were also discovered inside the structure. Based on the stratigraphy and the Khabur-ware ceramics, this grave dates to Phase 5b of the site and the Old Babylonian Period, meaning about 1900-1600 BCE.



site unit	lot	feature	square/locus	piece	mass (g)
A16	q21.1	f26	k5	-	0.11

Source Assignment: Nemrut Dağ (EA25), a lava dome in the southeastern portion of the Nemrut Dağ caldera, near or along the shore of the caldera lake.

7.5.10.2 - Feature 83 of Unit A16

Feature 83 is a thick brickfall layer, dubbed "the great brickfall," across this unit that covers all Phase 5 structures, mainly houses, and includes melted bricks. This period is labelled Phase 5c and dates to approximately 1600 BCE. Artifacts in this feature, thus, most likely would have been present in the houses from Phase 5.



site unit	lot	feature	square/locus	piece	mass (g)
A16	q202.2	f83	k105	-	0.35

Source Assignment: Tendürek Dağ ("Doğubeyazıd")

7.5.10.3 - Feature 208 of Unit A16

Feature 208 is an accumulation on a pavement comprised of sherds and pebbles. It dates to scattered occupation in Phase 4, the first post-Palace settlement period circa 2100-2000 BCE, so this pavement should not be confused with the flagstone courtyard of an earlier phase while the Royal Palace was occupied. In addition to the obsidian artifact below, a stone seal, inscribed with a sun motif, was found in this accumulation.

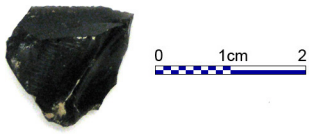


site unit	lot	feature	square/locus	piece	mass (g)
A16	q633.2	f208	k110	-	2.24

Source Assignment: Bingöl B

7.5.11 - Sourced Obsidian of Unit A17

Unit A17 is east of A15, and so far, only the upper second-millennium strata have been excavated. A storehouse for the temple, dating to the Mitanni Period circa roughly 1500-1400 BCE, has been identified in this unit, as have burials, houses, and a possible public building from the Old Babylonian or Khabur Period circa about 1900-1600 BCE. The A17 excavation records are not currently available in the Urkesh Global Record, so I do not have details about this feature or its precise date. Excavations in this unit, though, are limited to the late second-millennium strata, so this obsidian artifact can only be dated to between 1900 and 1300 BCE until the records are accessible.



site unit	lot	feature	square/locus	piece	mass (g)
A17	q231.2	f107	k12	-	1.56

Source Assignment: Bingöl B

7.5.12 - Sourced Obsidian of Unit A18

Unit A18 lies east of A16, and like A17, so far only the upper second-millennium strata have been excavated. A storehouse for the temple, apparently dating to the Mitanni Period circa 1500-1400 BCE, extends from A17 into this unit. During the Khabur Period circa 1900-1600 BCE, there are also burials and a possible open space. The A18 records are not yet available in the Urkesh Global Record, so I do not have information about the features or their dates. Excavations, though, are limited to the second-millennium strata, so the obsidian artifacts can, at present, be dated to about 1900 to 1300 BCE. Eventually, it should be straightforward, using the associated ceramic wares (Khabur versus Nuzi), to identify the Khabur-Period and Mitanni-Period obsidian artifacts.



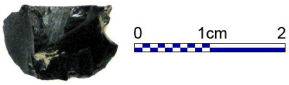
site unit	lot	feature	square/locus	piece	mass (g)
A18	q5.2	f7	k25	-	0.56

Source Assignment: Nemrut Dağ (EA25), a lava dome in the southeastern portion of the Nemrut Dağ caldera, near or along the shore of the caldera lake.



site unit	lot	feature	square/locus	piece	mass (g)
A18	q23.1	f24	k23	-	1.50

Source Assignment: Nemrut Dağ (EA25), a lava dome in the southeastern portion of the Nemrut Dağ caldera, near or along the shore of the caldera lake.



site unit	lot	feature	square/locus	piece	mass (g)
A18	q23.4	f24	k25	-	1.04

Source Assignment: Bingöl B



site unit	lot	feature	square/locus	piece	mass (g)
A18	q35.4	f31	k34	-	0.44

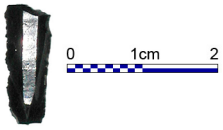
Source Assignment: Muş/Pasinler



site unit	lot	feature	square/locus	piece	mass (g)
A18	q43.3	f44	k26	-	0.65

Source Assignment: Nemrut Dağ (EA25), a lava dome in the southeastern portion of the Nemrut Dağ caldera, near or along the shore of the caldera lake.

This feature (f44) also contained the two obsidian blades below: the prismatic bladelet on the left and the larger blade on the right, which has retouch on both edges and may be one of the first series of blades from a core.







site unit	lot	feature	square/locus	piece	mass (g)
A18	q45.1	f42	k34	-	1.37

Source Assignment: Nemrut Dağ (EA22 or EA25), either a lava dome in the northeastern part of the Nemrut Dağ caldera (EA22) or one in the southeastern part of the Nemrut Dağ caldera, near or along the shore of the caldera lake (EA25).



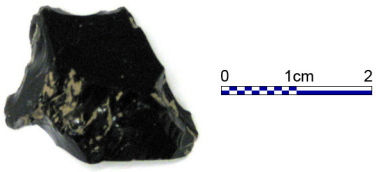
site unit	lot	feature	square/locus	piece	mass (g)
A18	q45.2	f52	k34	-	0.15

Source Assignment: Nemrut Dağ (EA22 or EA25), either a lava dome in the northeastern part of the Nemrut Dağ caldera (EA22) or one in the southeastern part of the Nemrut Dağ caldera, near or along the shore of the caldera lake (EA25).



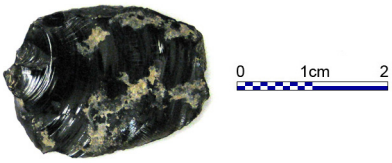
site unit	lot	feature	square/locus	piece	mass (g)
A18	q57.2	f52	k34	-	0.36

Source Assignment: Nemrut Dağ (EA22), a rhyolitic lava dome in the northeastern part of the Nemrut Dağ caldera, away from the caldera lake to the west.



site unit	lot	feature	square/locus	piece	mass (g)
A18	q89.4	f44	k26	-	4.66

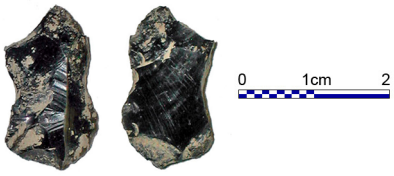
Source Assignment: Nemrut Dağ (EA25), a lava dome in the southeastern portion of the Nemrut Dağ caldera, near or along the shore of the caldera lake.



site unit	lot	feature	square/locus	piece	mass (g)
A18	q249.3	f120	k24	-	3.36

Source Assignment: Nemrut Dağ (EA25), a lava dome in the southeastern portion of the Nemrut Dağ caldera, near or along the shore of the caldera lake.

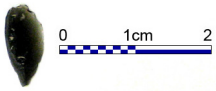
This same feature (f120) included the obsidian artifact below, which appears to be rather undiagnostic debitage just large enough to be classified as a chunk.





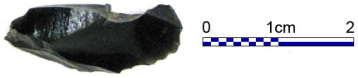
site unit	lot	feature	square/locus	piece	mass (g)
A18	q348.1	f158	k15	-	0.32

Source Assignment: Nemrut Dağ (EA25), a lava dome in the southeastern portion of the Nemrut Dağ caldera, near or along the shore of the caldera lake.



site unit	lot	feature	square/locus	piece	mass (g)
A18	q441.3	f168	k28	-	0.09

Source Assignment: Nemrut Dağ (EA25), a lava dome in the southeastern portion of the Nemrut Dağ caldera, near or along the shore of the caldera lake.



site unit	lot	feature	square/locus	piece	mass (g)
A18	q582.1	f242	k28	-	1.44

Source Assignment: Nemrut Dağ (EA25), a lava dome in the southeastern portion of the Nemrut Dağ caldera, near or along the shore of the caldera lake.

The same feature (f242) also included the obsidian artifact below. It appears to have been a prismatic blade or blade segment that was modified, either retouched or notched, on the edges as well as its distal end. These might, though, be signs of extensive use.





site unit	lot	feature	square/locus	piece	mass (g)
A18	q698.1	f298	k26	-	6.93

Source Assignment: Bingöl A



site unit	lot	feature	square/locus	piece	mass (g)
A18	q746.5	f321	k16	-	7.37

Source Assignment: Nemrut Dağ (EA25), a lava dome in the southeastern portion of the Nemrut Dağ caldera, near or along the shore of the caldera lake.

7.6 - Sourced Obsidian of Site Area B

Area B of Tell Mozan includes the temple (discussed in Section 3.6.1) at the apex of the High Mound. This was one of the first areas excavated, so the Unit B1 excavation records are not yet available in the Urkesh Global Record. Hence, I do not presently have any information about Feature 166, including its date. Recall, however, that the temple's foundations, dated to approximately 2500-2350 BCE, sat just below the current surface of the tell. Therefore, this feature (and its associated artifacts) may be assumed, until further stratigraphic information is available, to date to roughly this period.



site unit	lot	feature	square/locus	piece	mass (g)
B1	q350.i	f166	k?	1	2.59

Source Assignment: Nemrut Dağ (EA25), a lava dome in the southeastern portion of the Nemrut Dağ caldera, near or along the shore of the caldera lake.



site unit	lot	feature	square/locus	piece	mass (g)
B1	q350.i	f166	k?	2	0.42

Source Assignment: Nemrut Dağ (EA25), a lava dome in the southeastern portion of the Nemrut Dağ caldera, near or along the shore of the caldera lake.



site unit	lot	feature	square/locus	piece	mass (g)
B1	q350.i	f166	k?	3	0.14

Source Assignment: Nemrut Dağ (EA25), a lava dome in the southeastern portion of the Nemrut Dağ caldera, near or along the shore of the caldera lake.

7.7 - Sourced Obsidian of Site Area J

Area J includes several features discussed in Chapter 3: the temple terrace and the revetment wall (Section 3.6.2), the monumental staircase (Section 3.6.3), and a plaza that might have stretched from the staircase to the Royal Palace (Section 3.6.4). The area also

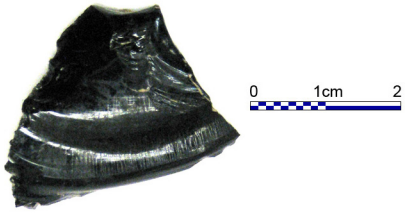
includes features of later habitation phases. As mentioned in Section 3.6.10, occupation in the second millennium BCE was apparently limited to the highest parts of the tell, and Mittani-Period (1500-1400 BCE) habitation encroached on the terrace.

7.7.1 - Sourced Obsidian of Unit J1

Unit J1 includes the plaza area at the southwestern edge of the temple terrace and its revetment wall as well as the late accumulations atop the plaza in this area. The unit is roughly halfway between the monumental staircase in Unit J2 and the anticipated eastern border of the Royal Palace. As previously noted, it is thought that the plaza may connect physically (and, therefore, mentally) the Royal Palace and the monumental staircase, that is, the access point to the temple terrace (and, therefore, the gods).

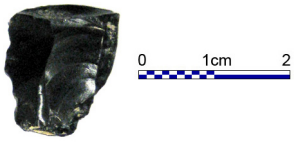
7.7.1.1 - Feature 3 of Unit J1

Feature 3 is an accumulation just below the topsoil, and therefore its contents date to the latest phases of habitation at the site, circa 1300 BCE.



site unit	lot	feature	square/locus	piece	mass (g)
J1	q7.1	f3	k10	1	5.23

Source Assignment: Nemrut Dağ (EA25), a lava dome in the southeastern portion of the Nemrut Dağ caldera, near or along the shore of the caldera lake.



site unit	lot	feature	square/locus	piece	mass (g)
J1	q7.1	f3	k10	2	0.93

Source Assignment: Meydan Dağ

The feature (f3) also included this large prismatic blade with an unusual bend, the edge of which appears to have been either retouched or chipped through use:



7.7.1.2 - Feature 20 of Unit J1

Feature 20 is an accumulation, probably also late in the site's occupational history, but the Urkesh Global Record currently has little information about this feature.



site unit	lot	feature	square/locus	piece	mass (g)
J1	q45.2	f20	k7	-	4.18

Source Assignment: Bingöl B

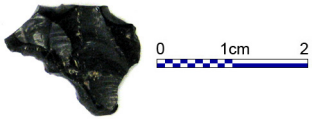


site unit	lot	feature	square/locus	piece	mass (g)
J1	q64.1	f20	k7	-	5.10

Source Assignment: Bingöl A

7.7.1.3 - Feature 131 of Unit J1

Feature 131 is an accumulation, probably a result of occupation during the second millennium, but the Urkesh Global Record currently has little information about it.

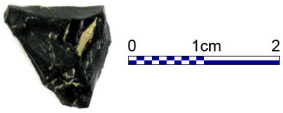


site unit	lot	feature	square/locus	piece	mass (g)
J1	q276.5	f131	k64	-	0.84

Source Assignment: Nemrut Dağ (EA22), a rhyolitic lava dome in the northeastern part of the Nemrut Dağ caldera, away from the caldera lake to the west.

7.7.1.4 - Feature 151 of Unit J1

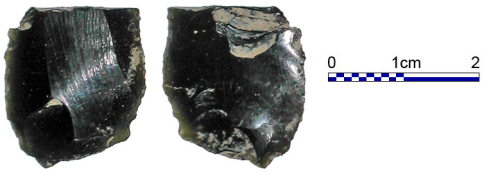
Feature 151 is an accumulation at the interface between the layer that corresponds to the site's abandonment and the latest accumulation layers against the revetment wall of the temple terrace. Consequently, the top of the revetment wall was still visible when this accumulation was deposited. The ceramics in this feature date to the Mitanni Period, so it has been dated to about 1400 BCE, which is also known as the Early-Middle Babylonian Period and the Middle-Assyrian Period in Mesopotamian history.



site unit	lot	feature	square/locus	piece	mass (g)
J1	q344.1	f151	k106	-	0.97

Source Assignment: Bingöl B

This feature (f151) also contained the obsidian artifact below. It appears to be a flake that was removed from a blade core and then reshaped into a flake-scraper.



7.7.2 - Sourced Obsidian of Unit J2

Unit J2 includes the monumental staircase to access the temple terrace as well as subsequent accumulations due to habitation in the second millennium BCE.

7.7.2.1 - Feature 1 of Unit J2

Feature 1 is material from the partial collapse of a trench wall due to erosion and weathering. Artifacts in this feature most likely date to the mid-second millennium.



site unit	lot	feature	square/locus	piece	mass (g)
J2	q58.1	f1	k100	-	1.94

Source Assignment: Muş/Pasinler

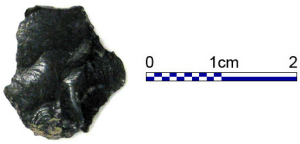
7.7.2.2 - Feature 42 of Unit J2

Feature 42 is the first sediment layer of the tell surface in locus k33 of this unit, so artifacts in this feature likely date to the final phase of habitation circa 1300 BCE.



site unit	lot	feature	square/locus	piece	mass (g)
J2	q87.1	f42	k33	-	3.83

Source Assignment: Nemrut Dağ (EA25), a lava dome in the southeastern portion of the Nemrut Dağ caldera, near or along the shore of the caldera lake.



site unit	lot	feature	square/locus	piece	mass (g)
J2	q99.1	f42	k33	-	1.12

Source Assignment: Bingöl A

7.7.2.3 - Feature 62 of Unit J2

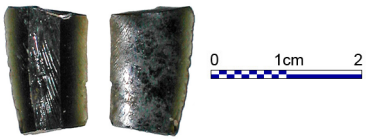
Feature 62 is an accumulation just below the topsoil in this locus, so the artifacts date to the latest phases of habitation at the site, circa 1300 BCE.

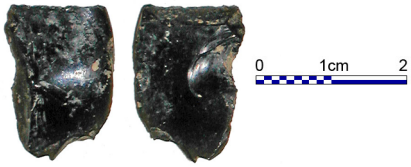


site unit	lot	feature	square/locus	piece	mass (g)
J2	q142.1	f62	k83	-	0.96

Source Assignment: Nemrut Dağ (EA25), a lava dome in the southeastern portion of the Nemrut Dağ caldera, near or along the shore of the caldera lake.

The same feature (f62) also included the two obsidian artifacts below. The artifact on the left is a prismatic blade segment. The artifact on the right appears to be a flake removed from a core (based on the broad, flat striking platform) and then shaped on one edge (at a right angle to the platform) to make a straight-edged scraper.



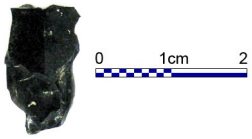


7.7.3 - Sourced Obsidian of Unit J3

Unit J3 lies between J1 and J2, and I excavated in this unit in 2006. In addition to documenting the second-millennium habitation phase in this area, the excavation goals in this unit included further investigating of the terrace, revetment wall, and plaza.

7.7.3.1 - Feature 100 of Unit J3

I excavated Feature 100, an accumulation right below the topsoil in this locus, so the artifacts date to the latest phases of habitation at the site, circa 1300 BCE.



site unit	lot	feature	square/locus	piece	mass (g)
J3	q146.1	f100	k13	-	1.05

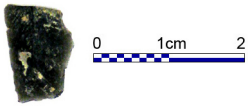
Source Assignment: Nemrut Dağ (EA25), a lava dome in the southeastern portion of the Nemrut Dağ caldera, near or along the shore of the caldera lake.



Figure 7.31 - The author (left), Enrico De Benedictis (center), and one of the local workers, Sawar (right), excavating Feature 100 of Unit J3, from which one of the obsidian artifacts sourced in this study was recovered (Urkesh expedition photograph).

7.7.3.2 - Feature 101 of Unit J3

Feature 101, which I excavated as well, lies within accumulation f100, and it was a conglomerate of stones and laminar soil. The artifacts in the feature most likely date to the latest phases of second-millennium occupation at the site, circa 1300 BCE. It is likely that this feature corresponds to some sort of shallow pit dug into accumulation f100.

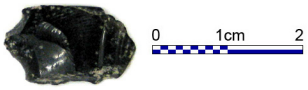


site unit	lot	feature	square/locus	piece	mass (g)
J3	q152.1	f101	k13	-	0.32

Source Assignment: Nemrut Dağ (EA25), a lava dome in the southeastern portion of the Nemrut Dağ caldera, near or along the shore of the caldera lake.

7.7.3.3 - Feature 105 of Unit J3

Feature 105 is the first sediment layer of the surface in locus k22 of this unit, and artifacts in this feature likely date to the final period of habitation. It must be noted that it is also possible that artifacts in this layer, and other superficial layers of the tell, eroded out of older strata from higher parts of the tell or were left by later nomads.



site unit	lot	feature	square/locus	piece	mass (g)
J3	q150.3	f105	k22	-	0.74

Source Assignment: Nemrut Dağ (EA22), a rhyolitic lava dome in the northeastern part of the Nemrut Dağ caldera, away from the caldera lake to the west.

7.8 - Overview of the Results

Tables 7.2 to 7.4 give a summary of my sourcing results by site unit, by source, and by date. Figure 7.32 shows my source assignments on a pie chart, showing that 60% of the sourced artifacts came from one of two locations at Nemrut Dağ, both of which lie within the caldera and on the shore of the caldera lake. Nearly one quarter of the artifacts came from the Bingöl A and B sources. The rest came from Tendürek Dağ (6%), Meydan Dağ (3%), and Muş and/or Pasinler (6%) in Eastern Anatolia and, surprisingly, the widely used Kömürcü source at Göllü Dağ (3%) in Central Anatolia. The presence of Göllü Dağ obsidian at Tell Mozan, which lies on the edge of RDC's supply zone for Nemrut Dağ, is an unexpected, though not unbelievable, discovery. Kömürcü was one of the most widely exchanged obsidian sources in Central Anatolia, but Göllü Dağ and Tell Mozan are about 600 km apart (linearly; much farther via actual travel routes).

The implications of these sourcing results, considered in light of my observations on the obsidian industry of Tell Mozan, for Northern Mesopotamia in general and Urkesh in particular are discussed in Chapters 8 and 9, respectively.

Figure 7.32 - Source Assignments for Bronze-Age Obsidian Artifacts from Tell Mozan

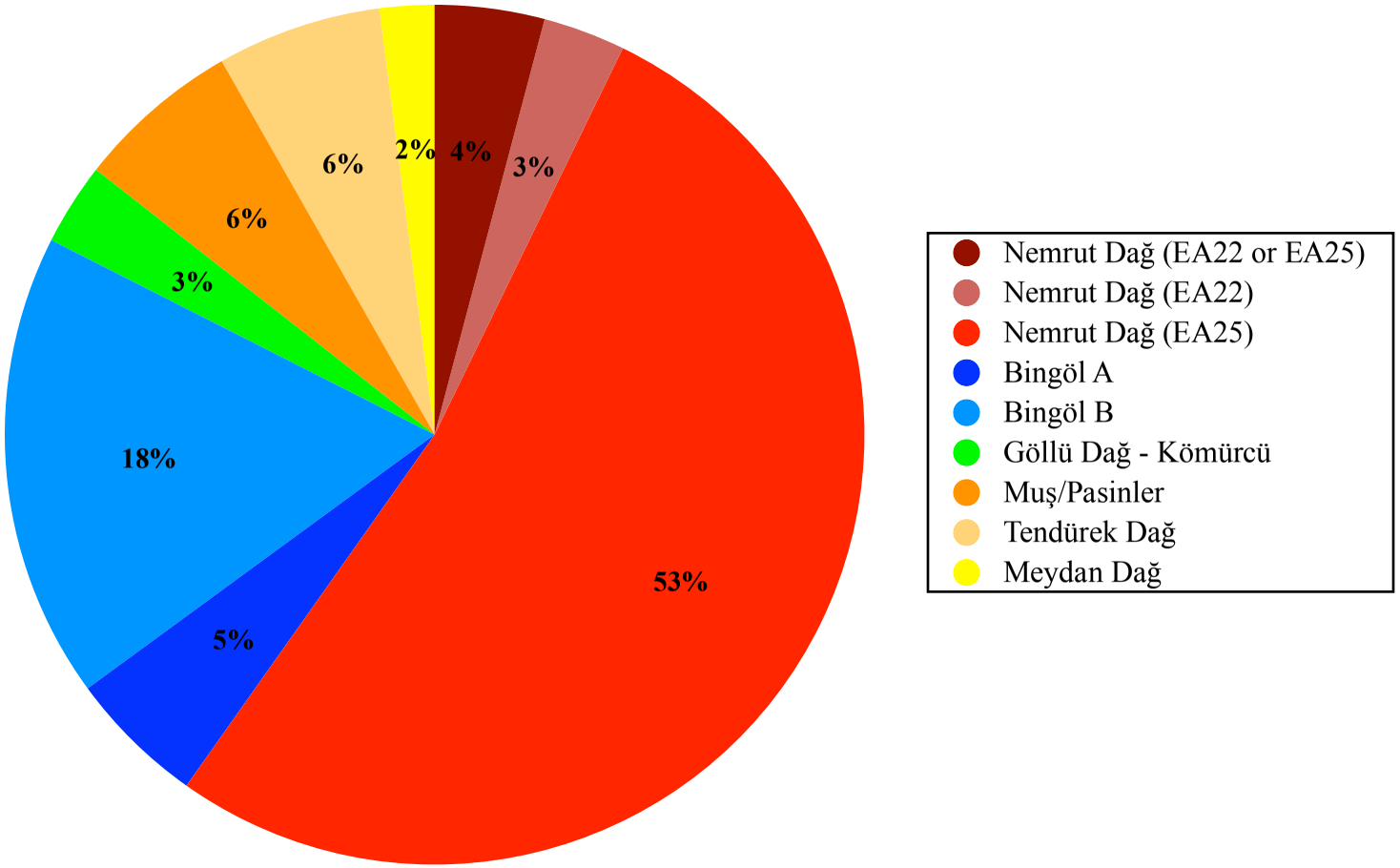


Table 7.2 - Artifact Source Assignments by Unit

Artifact ID	*Estimated Date*	*Source Assignment*
A1 q161.1 f16 k117	2300-1300 BCE	Nemrut Dağ (EA25)
A1 q342.lw f16 k117	2300-1300 BCE	Nemrut Dağ (EA25)
A1 q59.1 f29 k119	2300-1300 BCE	Nemrut Dağ (EA25)
A1 q264.1 f67 k13	2300-1300 BCE	Nemrut Dağ (EA25)
A1 q183.1 f606 k?	2300-1300 BCE	Nemrut Dağ (EA25)
A2 q333.2 f114 k151	2100-1800 BCE	Bingöl B
A6 q386.1 f122 k218 piece 1	2300-1300 BCE	Tendürek Dağ
A6 q386.1 f122 k218 piece 2	2300-1300 BCE	Nemrut Dağ (EA25)
A6 q971.1 f410 k31	2300-1300 BCE	Bingöl B
A6 q973.1 f412 k31	2300-1300 BCE	Nemrut Dağ (EA25)
A7 q287.1 f56 k7	2100-1800 BCE	Nemrut Dağ (EA25)
A7 q386.l3 f63 k8	2100-1800 BCE	Bingöl B
A7 q222.1 f69 k9	2100-1800 BCE	Nemrut Dağ (EA25)
A7 q350.l2 f121 k13	2300-1800 BCE	Bingöl B
A7 q360.1 f121 k13 piece 1	2300-1800 BCE	Nemrut Dağ (EA25)
A7 q360.1 f121 k13 piece 2	2300-1800 BCE	Nemrut Dağ (EA25)
A7 q360.1 f121 k13 piece 3	2300-1800 BCE	Nemrut Dağ (EA25)
A7 q360.1 f121 k13 piece 4	2300-1800 BCE	Nemrut Dağ (EA25)
A7 q602.1 f148 k13	2300-1800 BCE	Nemrut Dağ (EA25)
A7 q892.1 f261 k12	2300-1800 BCE	Göllü Dağ - Kömürcü
A7 q1146.1 f465 k21	2300-2100 BCE	Tendürek Dağ
A7 q1150.5 f465 k21	2300-2100 BCE	Bingöl A
A7 q1174.2 f465 k21	2300-2100 BCE	Bingöl A
A7 q1201.4 f480 k21	2300-2100 BCE	Muş/Pasinler
A8 q154.1 f58 k9	2100-1800 BCE	Nemrut Dağ (EA25)
A9 q376.1 f98 k3 piece 1	2200 BCE	Nemrut Dağ (EA25)
A9 q376.1 f98 k3 piece 2	2200 BCE	Nemrut Dağ (EA25)
A9 q376.1 f98 k3 piece 3	2200 BCE	Nemrut Dağ (EA25)
A9 q437.2 f98 k3	2200 BCE	Nemrut Dağ (EA25)
A9 q440.1 f98 k3 piece 1	2200 BCE	Bingöl B
A9 q440.1 f98 k3 piece 2	2200 BCE	Nemrut Dağ (EA25)
A9 q454.2 f126 k3 piece 1	2200 BCE	Nemrut Dağ (EA25)

Table 7.2 - Artifact Source Assignments by Unit (continued)

Artifact ID	*Estimated Date*	*Source Assignment*
A9 q454.2 f126 k3 piece 2	2200 BCE	Nemrut Dağ (EA25)
A9 q454.2 f126 k3 piece 3	2200 BCE	Nemrut Dağ (EA25)
A9 q463.2 f156 k3 piece 1	2200-2300 BCE	Göllü Dağ - Kömürcü
A9 q463.2 f156 k3 piece 2	2200-2300 BCE	Göllü Dağ - Kömürcü
A9 q693.1 f247 k11 piece 1	2300 BCE	Nemrut Dağ (EA25)
A9 q693.1 f247 k11 piece 2	2300 BCE	Nemrut Dağ (EA25)
A9 q693.1 f247 k11 piece 3	2300 BCE	Muş/Pasinler
A9 q742.1 f260 k11 piece 1	2300 BCE	Bingöl B
A9 q742.1 f260 k11 piece 2	2300 BCE	Meydan Dağ
A10 q77.1 f79 k7	2300-1300 BCE	Nemrut Dağ (EA25)
A10 q229.1 f94 k5	2300-1300 BCE	Tendürek Dağ
A10 q286.1 f141 k3	2300-1300 BCE	Bingöl B
A10 q601.3 f277 k27	2300-1300 BCE	Muş/Pasinler
A10 q678.3 f292 k28	2300-1300 BCE	Bingöl B
A10 q695.1 f300 k28	2300-1300 BCE	Bingöl B
A10 q1081.6 f234 k21	2300-1300 BCE	Nemrut Dağ (EA25)
A10 q1194.3 f925 k29	2300-1300 BCE	Bingöl B
A14 q244.1 f29 k2	1500-1300 BCE	Nemrut Dağ (EA25)
A14 q742.2 f42 k12	2200-2100 BCE	Nemrut Dağ (EA22 or EA25)
A14 q252.1 f90 k3	2100-1800 BCE	Nemrut Dağ (EA22 or EA25)
A14 q265.1 f92 k3	2100-1800 BCE	Bingöl B
A14 q266.1 f92 k3	2100-1800 BCE	Bingöl B
A14 q299.2 f101 k100	2100-1800 BCE	Nemrut Dağ (EA25)
A14 q474.1 f193 k4	2200-2100 BCE	Nemrut Dağ (EA25)
A14 q605.2 f250 k23	2200-1300 BCE	Nemrut Dağ (EA25)
A14 q617.1 f250 k23	2200-1300 BCE	Nemrut Dağ (EA25)
A15 q295.2 f108 k92	2300-1300 BCE	Tendürek Dağ
A15 q734.1 f372 k14	2300-1300 BCE	Nemrut Dağ (EA25)
A15 q752.2 f386 k15	2300-1300 BCE	Muş/Pasinler
A15 q1173.3 f517 k2	2300-1300 BCE	Tendürek Dağ
A16 q21.1 f26 k5	1900-1600 BCE	Nemrut Dağ (EA25)
A16 q202.2 f83 k105	1600 BCE	Tendürek Dağ

Table 7.2 - Artifact Source Assignments by Unit (continued)

Artifact ID	*Estimated Date*	*Source Assignment*
A16 q633.2 f208 k110	2100-2000 BCE	Bingöl B
A17 q231.2 f107 k12	1900-1300 BCE	Bingöl B
A18 q5.2 f7 k25	1900-1300 BCE	Nemrut Dağ (EA25)
A18 q23.1 f24 k23	1900-1300 BCE	Nemrut Dağ (EA25)
A18 q23.4 f24 k25	1900-1300 BCE	Bingöl B
A18 q35.4 f31 k34	1900-1300 BCE	Muş/Pasinler
A18 q43.3 f44 k26	1900-1300 BCE	Nemrut Dağ (EA25)
A18 q45.1 f42 k34	1900-1300 BCE	Nemrut Dağ (EA22 or EA25)
A18 q45.2 f52 k34	1900-1300 BCE	Nemrut Dağ (EA22 or EA25)
A18 q57.2 f52 k34	1900-1300 BCE	Nemrut Dağ (EA22)
A18 q89.4 f44 k26	1900-1300 BCE	Nemrut Dağ (EA25)
A18 q249.3 f120 k24	1900-1300 BCE	Nemrut Dağ (EA25)
A18 q348.1 f158 k15	1900-1300 BCE	Nemrut Dağ (EA25)
A18 q441.3 f168 k28	1900-1300 BCE	Nemrut Dağ (EA25)
A18 q582.1 f242 k28	1900-1300 BCE	Nemrut Dağ (EA25)
A18 q698.1 f298 k26	1900-1300 BCE	Bingöl A
A18 q746.5 f321 k16	1900-1300 BCE	Nemrut Dağ (EA25)
B1 q350.i f166 k? piece 1	2500-2300 BCE	Nemrut Dağ (EA25)
B1 q350.i f166 k? piece 2	2500-2300 BCE	Nemrut Dağ (EA25)
B1 q350.i f166 k? piece 3	2500-2300 BCE	Nemrut Dağ (EA25)
J1 q7.1 f3 k10 piece 1	1300 BCE	Nemrut Dağ (EA25)
J1 q7.1 f3 k10 piece 2	1300 BCE	Meydan Dağ
J1 q45.2 f20 k7	1900-1300 BCE	Bingöl B
J1 q64.1 f20 k7	1900-1300 BCE	Bingöl A
J1 q276.5 f131 k64	1900-1300 BCE	Nemrut Dağ (EA22)
J1 q344.1 f151 k106	1400 BCE	Bingöl B
J2 q58.1 f1 k100	1900-1300 BCE	Muş/Pasinler
J2 q87.1 f42 k33	1400-1300 BCE	Nemrut Dağ (EA25)
J2 q99.1 f42 k33	1400-1300 BCE	Bingöl A
J2 q142.1 f62 k83	1400-1300 BCE	Nemrut Dağ (EA25)
J3 q146.1 f100 k13	1400-1300 BCE	Nemrut Dağ (EA25)
J3 q152.1 f101 k13	1400-1300 BCE	Nemrut Dağ (EA25)
J3 q150.3 f105 k22	1400-1300 BCE	Nemrut Dağ (EA22)

Table 7.3 - Artifact Source Assignments by Source

Artifact ID	*Estimated Date*	*Source Assignment*
A18 q698.1 f298 k26	1900-1300 BCE	Bingöl A
A7 q1150.5 f465 k21	2300-2100 BCE	Bingöl A
A7 q1174.2 f465 k21	2300-2100 BCE	Bingöl A
J1 q64.1 f20 k7	1900-1300 BCE	Bingöl A
J2 q99.1 f42 k33	1400-1300 BCE	Bingöl A
A10 q1194.3 f925 k29	2300-1300 BCE	Bingöl B
A10 q286.1 f141 k3	2300-1300 BCE	Bingöl B
A10 q678.3 f292 k28	2300-1300 BCE	Bingöl B
A10 q695.1 f300 k28	2300-1300 BCE	Bingöl B
A14 q265.1 f92 k3	2100-1800 BCE	Bingöl B
A14 q266.1 f92 k3	2100-1800 BCE	Bingöl B
A16 q633.2 f208 k110	2100-2000 BCE	Bingöl B
A17 q231.2 f107 k12	1900-1300 BCE	Bingöl B
A18 q23.4 f24 k25	1900-1300 BCE	Bingöl B
A2 q333.2 f114 k151	2100-1800 BCE	Bingöl B
A6 q971.1 f410 k31	2300-1300 BCE	Bingöl B
A7 q350.l2 f121 k13	2300-1800 BCE	Bingöl B
A7 q386.l3 f63 k8	2100-1800 BCE	Bingöl B
A9 q440.1 f98 k3 piece 1	2200 BCE	Bingöl B
A9 q742.1 f260 k11 piece 1	2300 BCE	Bingöl B
J1 q344.1 f151 k106	1400 BCE	Bingöl B
J1 q45.2 f20 k7	1900-1300 BCE	Bingöl B
A7 q892.1 f261 k12	2300-1800 BCE	Göllü Dağ - Kömürcü
A9 q463.2 f156 k3 piece 1	2200-2300 BCE	Göllü Dağ - Kömürcü
A9 q463.2 f156 k3 piece 2	2200-2300 BCE	Göllü Dağ - Kömürcü
A9 q742.1 f260 k11 piece 2	2300 BCE	Meydan Dağ
J1 q7.1 f3 k10 piece 2	1300 BCE	Meydan Dağ
A10 q601.3 f277 k27	2300-1300 BCE	Muş/Pasinler
A15 q752.2 f386 k15	2300-1300 BCE	Muş/Pasinler
A18 q35.4 f31 k34	1900-1300 BCE	Muş/Pasinler
A7 q1201.4 f480 k21	2300-2100 BCE	Muş/Pasinler
A9 q693.1 f247 k11 piece 3	2300 BCE	Muş/Pasinler

Table 7.3 - Artifact Source Assignments by Source (continued)

Artifact ID	*Estimated Date*	*Source Assignment*
J2 q58.1 f1 k100	1900-1300 BCE	Muş/Pasinler
A14 q252.1 f90 k3	2100-1800 BCE	Nemrut Dağ (EA22 or EA25)
A14 q742.2 f42 k12	2200-2100 BCE	Nemrut Dağ (EA22 or EA25)
A18 q45.1 f42 k34	1900-1300 BCE	Nemrut Dağ (EA22 or EA25)
A18 q45.2 f52 k34	1900-1300 BCE	Nemrut Dağ (EA22 or EA25)
A18 q57.2 f52 k34	1900-1300 BCE	Nemrut Dağ (EA22)
J1 q276.5 f131 k64	1900-1300 BCE	Nemrut Dağ (EA22)
J3 q150.3 f105 k22	1400-1300 BCE	Nemrut Dağ (EA22)
A1 q161.1 f16 k117	2300-1300 BCE	Nemrut Dağ (EA25)
A1 q183.1 f606 k?	2300-1300 BCE	Nemrut Dağ (EA25)
A1 q264.1 f67 k13	2300-1300 BCE	Nemrut Dağ (EA25)
A1 q342.lw f16 k117	2300-1300 BCE	Nemrut Dağ (EA25)
A1 q59.1 f29 k119	2300-1300 BCE	Nemrut Dağ (EA25)
A10 q1081.6 f234 k21	2300-1300 BCE	Nemrut Dağ (EA25)
A10 q77.1 f79 k7	2300-1300 BCE	Nemrut Dağ (EA25)
A14 q244.1 f29 k2	1500-1300 BCE	Nemrut Dağ (EA25)
A14 q299.2 f101 k100	2100-1800 BCE	Nemrut Dağ (EA25)
A14 q474.1 f193 k4	2200-2100 BCE	Nemrut Dağ (EA25)
A14 q605.2 f250 k23	2200-1300 BCE	Nemrut Dağ (EA25)
A14 q617.1 f250 k23	2200-1300 BCE	Nemrut Dağ (EA25)
A15 q734.1 f372 k14	2300-1300 BCE	Nemrut Dağ (EA25)
A16 q21.1 f26 k5	1900-1600 BCE	Nemrut Dağ (EA25)
A18 q23.1 f24 k23	1900-1300 BCE	Nemrut Dağ (EA25)
A18 q249.3 f120 k24	1900-1300 BCE	Nemrut Dağ (EA25)
A18 q348.1 f158 k15	1900-1300 BCE	Nemrut Dağ (EA25)
A18 q43.3 f44 k26	1900-1300 BCE	Nemrut Dağ (EA25)
A18 q441.3 f168 k28	1900-1300 BCE	Nemrut Dağ (EA25)
A18 q5.2 f7 k25	1900-1300 BCE	Nemrut Dağ (EA25)
A18 q582.1 f242 k28	1900-1300 BCE	Nemrut Dağ (EA25)
A18 q746.5 f321 k16	1900-1300 BCE	Nemrut Dağ (EA25)
A18 q89.4 f44 k26	1900-1300 BCE	Nemrut Dağ (EA25)
A6 q386.1 f122 k218 piece 2	2300-1300 BCE	Nemrut Dağ (EA25)
A6 q973.1 f412 k31	2300-1300 BCE	Nemrut Dağ (EA25)

Table 7.3 - Artifact Source Assignments by Source (continued)

Artifact ID	*Estimated Date*	*Source Assignment*
A7 q222.1 f69 k9	2100-1800 BCE	Nemrut Dağ (EA25)
A7 q287.1 f56 k7	2100-1800 BCE	Nemrut Dağ (EA25)
A7 q360.1 f121 k13 piece 1	2300-1800 BCE	Nemrut Dağ (EA25)
A7 q360.1 f121 k13 piece 2	2300-1800 BCE	Nemrut Dağ (EA25)
A7 q360.1 f121 k13 piece 3	2300-1800 BCE	Nemrut Dağ (EA25)
A7 q360.1 f121 k13 piece 4	2300-1800 BCE	Nemrut Dağ (EA25)
A7 q602.1 f148 k13	2300-1800 BCE	Nemrut Dağ (EA25)
A8 q154.1 f58 k9	2100-1800 BCE	Nemrut Dağ (EA25)
A9 q376.1 f98 k3 piece 1	2200 BCE	Nemrut Dağ (EA25)
A9 q376.1 f98 k3 piece 2	2200 BCE	Nemrut Dağ (EA25)
A9 q376.1 f98 k3 piece 3	2200 BCE	Nemrut Dağ (EA25)
A9 q437.2 f98 k3	2200 BCE	Nemrut Dağ (EA25)
A9 q440.1 f98 k3 piece 2	2200 BCE	Nemrut Dağ (EA25)
A9 q454.2 f126 k3 piece 1	2200 BCE	Nemrut Dağ (EA25)
A9 q454.2 f126 k3 piece 2	2200 BCE	Nemrut Dağ (EA25)
A9 q454.2 f126 k3 piece 3	2200 BCE	Nemrut Dağ (EA25)
A9 q693.1 f247 k11 piece 1	2300 BCE	Nemrut Dağ (EA25)
A9 q693.1 f247 k11 piece 2	2300 BCE	Nemrut Dağ (EA25)
B1 q350.i f166 k? piece 1	2500-2300 BCE	Nemrut Dağ (EA25)
B1 q350.i f166 k? piece 2	2500-2300 BCE	Nemrut Dağ (EA25)
B1 q350.i f166 k? piece 3	2500-2300 BCE	Nemrut Dağ (EA25)
J1 q7.1 f3 k10 piece 1	1300 BCE	Nemrut Dağ (EA25)
J2 q142.1 f62 k83	1400-1300 BCE	Nemrut Dağ (EA25)
J2 q87.1 f42 k33	1400-1300 BCE	Nemrut Dağ (EA25)
J3 q146.1 f100 k13	1400-1300 BCE	Nemrut Dağ (EA25)
J3 q152.1 f101 k13	1400-1300 BCE	Nemrut Dağ (EA25)
A10 q229.1 f94 k5	2300-1300 BCE	Tendürek Dağ
A15 q1173.3 f517 k2	2300-1300 BCE	Tendürek Dağ
A15 q295.2 f108 k92	2300-1300 BCE	Tendürek Dağ
A16 q202.2 f83 k105	1600 BCE	Tendürek Dağ
A6 q386.1 f122 k218 piece 1	2300-1300 BCE	Tendürek Dağ
A7 q1146.1 f465 k21	2300-2100 BCE	Tendürek Dağ

Table 7.4 - Artifact Source Assignments by Period

Artifact ID	*Estimated Date*	*Source Assignment*
B1 q350.i f166 k? piece 1	2500-2300 BCE	Nemrut Dağ (EA25)
B1 q350.i f166 k? piece 2	2500-2300 BCE	Nemrut Dağ (EA25)
B1 q350.i f166 k? piece 3	2500-2300 BCE	Nemrut Dağ (EA25)
A7 q1150.5 f465 k21	2300-2100 BCE	Bingöl A
A7 q1174.2 f465 k21	2300-2100 BCE	Bingöl A
A7 q1201.4 f480 k21	2300-2100 BCE	Muş/Pasinler
A7 q1146.1 f465 k21	2300-2100 BCE	Tendürek Dağ
A7 q350.l2 f121 k13	2300-1800 BCE	Bingöl B
A7 q892.1 f261 k12	2300-1800 BCE	Göllü Dağ - Kömürcü
A7 q360.1 f121 k13 piece 1	2300-1800 BCE	Nemrut Dağ (EA25)
A7 q360.1 f121 k13 piece 2	2300-1800 BCE	Nemrut Dağ (EA25)
A7 q360.1 f121 k13 piece 3	2300-1800 BCE	Nemrut Dağ (EA25)
A7 q360.1 f121 k13 piece 4	2300-1800 BCE	Nemrut Dağ (EA25)
A7 q602.1 f148 k13	2300-1800 BCE	Nemrut Dağ (EA25)
A10 q1194.3 f925 k29	2300-1300 BCE	Bingöl B
A10 q286.1 f141 k3	2300-1300 BCE	Bingöl B
A10 q678.3 f292 k28	2300-1300 BCE	Bingöl B
A10 q695.1 f300 k28	2300-1300 BCE	Bingöl B
A6 q971.1 f410 k31	2300-1300 BCE	Bingöl B
A10 q601.3 f277 k27	2300-1300 BCE	Muş/Pasinler
A15 q752.2 f386 k15	2300-1300 BCE	Muş/Pasinler
A1 q161.1 f16 k117	2300-1300 BCE	Nemrut Dağ (EA25)
A1 q183.1 f606 k?	2300-1300 BCE	Nemrut Dağ (EA25)
A1 q264.1 f67 k13	2300-1300 BCE	Nemrut Dağ (EA25)
A1 q342.lw f16 k117	2300-1300 BCE	Nemrut Dağ (EA25)
A1 q59.1 f29 k119	2300-1300 BCE	Nemrut Dağ (EA25)
A10 q1081.6 f234 k21	2300-1300 BCE	Nemrut Dağ (EA25)
A10 q77.1 f79 k7	2300-1300 BCE	Nemrut Dağ (EA25)
A15 q734.1 f372 k14	2300-1300 BCE	Nemrut Dağ (EA25)
A6 q386.1 f122 k218 piece 2	2300-1300 BCE	Nemrut Dağ (EA25)
A6 q973.1 f412 k31	2300-1300 BCE	Nemrut Dağ (EA25)
A10 q229.1 f94 k5	2300-1300 BCE	Tendürek Dağ

Table 7.4 - Artifact Source Assignments by Period (continued)

Artifact ID	*Estimated Date*	*Source Assignment*
A15 q1173.3 f517 k2	2300-1300 BCE	Tendürek Dağ
A15 q295.2 f108 k92	2300-1300 BCE	Tendürek Dağ
A6 q386.1 f122 k218 piece 1	2300-1300 BCE	Tendürek Dağ
A9 q742.1 f260 k11 piece 1	2300 BCE	Bingöl B
A9 q742.1 f260 k11 piece 2	2300 BCE	Meydan Dağ
A9 q693.1 f247 k11 piece 3	2300 BCE	Muş/Pasinler
A9 q693.1 f247 k11 piece 1	2300 BCE	Nemrut Dağ (EA25)
A9 q693.1 f247 k11 piece 2	2300 BCE	Nemrut Dağ (EA25)
A9 q463.2 f156 k3 piece 1	2200-2300 BCE	Göllü Dağ - Kömürcü
A9 q463.2 f156 k3 piece 2	2200-2300 BCE	Göllü Dağ - Kömürcü
A14 q742.2 f42 k12	2200-2100 BCE	Nemrut Dağ (EA22 or EA25)
A14 q474.1 f193 k4	2200-2100 BCE	Nemrut Dağ (EA25)
A14 q605.2 f250 k23	2200-1300 BCE	Nemrut Dağ (EA25)
A14 q617.1 f250 k23	2200-1300 BCE	Nemrut Dağ (EA25)
A9 q440.1 f98 k3 piece 1	2200 BCE	Bingöl B
A9 q376.1 f98 k3 piece 1	2200 BCE	Nemrut Dağ (EA25)
A9 q376.1 f98 k3 piece 2	2200 BCE	Nemrut Dağ (EA25)
A9 q376.1 f98 k3 piece 3	2200 BCE	Nemrut Dağ (EA25)
A9 q437.2 f98 k3	2200 BCE	Nemrut Dağ (EA25)
A9 q440.1 f98 k3 piece 2	2200 BCE	Nemrut Dağ (EA25)
A9 q454.2 f126 k3 piece 1	2200 BCE	Nemrut Dağ (EA25)
A9 q454.2 f126 k3 piece 2	2200 BCE	Nemrut Dağ (EA25)
A9 q454.2 f126 k3 piece 3	2200 BCE	Nemrut Dağ (EA25)
A16 q633.2 f208 k110	2100-2000 BCE	Bingöl B
A14 q265.1 f92 k3	2100-1800 BCE	Bingöl B
A14 q266.1 f92 k3	2100-1800 BCE	Bingöl B
A2 q333.2 f114 k151	2100-1800 BCE	Bingöl B
A7 q386.l3 f63 k8	2100-1800 BCE	Bingöl B
A14 q252.1 f90 k3	2100-1800 BCE	Nemrut Dağ (EA22 or EA25)
A14 q299.2 f101 k100	2100-1800 BCE	Nemrut Dağ (EA25)
A7 q222.1 f69 k9	2100-1800 BCE	Nemrut Dağ (EA25)
A7 q287.1 f56 k7	2100-1800 BCE	Nemrut Dağ (EA25)
A8 q154.1 f58 k9	2100-1800 BCE	Nemrut Dağ (EA25)

Table 7.4 - Artifact Source Assignments by Period (continued)

Artifact ID	*Estimated Date*	*Source Assignment*
A16 q21.1 f26 k5	1900-1600 BCE	Nemrut Dağ (EA25)
A18 q698.1 f298 k26	1900-1300 BCE	Bingöl A
J1 q64.1 f20 k7	1900-1300 BCE	Bingöl A
A17 q231.2 f107 k12	1900-1300 BCE	Bingöl B
A18 q23.4 f24 k25	1900-1300 BCE	Bingöl B
J1 q45.2 f20 k7	1900-1300 BCE	Bingöl B
A18 q35.4 f31 k34	1900-1300 BCE	Muş/Pasinler
J2 q58.1 f1 k100	1900-1300 BCE	Muş/Pasinler
A18 q45.1 f42 k34	1900-1300 BCE	Nemrut Dağ (EA22 or EA25)
A18 q45.2 f52 k34	1900-1300 BCE	Nemrut Dağ (EA22 or EA25)
A18 q57.2 f52 k34	1900-1300 BCE	Nemrut Dağ (EA22)
J1 q276.5 f131 k64	1900-1300 BCE	Nemrut Dağ (EA22)
A18 q23.1 f24 k23	1900-1300 BCE	Nemrut Dağ (EA25)
A18 q249.3 f120 k24	1900-1300 BCE	Nemrut Dağ (EA25)
A18 q348.1 f158 k15	1900-1300 BCE	Nemrut Dağ (EA25)
A18 q43.3 f44 k26	1900-1300 BCE	Nemrut Dağ (EA25)
A18 q441.3 f168 k28	1900-1300 BCE	Nemrut Dağ (EA25)
A18 q5.2 f7 k25	1900-1300 BCE	Nemrut Dağ (EA25)
A18 q582.1 f242 k28	1900-1300 BCE	Nemrut Dağ (EA25)
A18 q746.5 f321 k16	1900-1300 BCE	Nemrut Dağ (EA25)
A18 q89.4 f44 k26	1900-1300 BCE	Nemrut Dağ (EA25)
A16 q202.2 f83 k105	1600 BCE	Tendürek Dağ
A14 q244.1 f29 k2	1500-1300 BCE	Nemrut Dağ (EA25)
J2 q99.1 f42 k33	1400-1300 BCE	Bingöl A
J3 q150.3 f105 k22	1400-1300 BCE	Nemrut Dağ (EA22)
J2 q142.1 f62 k83	1400-1300 BCE	Nemrut Dağ (EA25)
J2 q87.1 f42 k33	1400-1300 BCE	Nemrut Dağ (EA25)
J3 q146.1 f100 k13	1400-1300 BCE	Nemrut Dağ (EA25)
J3 q152.1 f101 k13	1400-1300 BCE	Nemrut Dağ (EA25)
J1 q344.1 f151 k106	1400 BCE	Bingöl B
J1 q7.1 f3 k10 piece 2	1300 BCE	Meydan Dağ
J1 q7.1 f3 k10 piece 1	1300 BCE	Nemrut Dağ (EA25)

Part III: Results and Implications

Chapter 8:

Implications for Northern Mesopotamia and the Near East

> While working on the flint and obsidian assemblages of Jazirah tell sites… I find that, since the emphasis of research has been, and continues to be, on provenance, many other important aspects of the presence of obsidian remain mysterious… How did the obsidian arrive at the sites? Are we certain that it was imported? Who, exactly, collected the material? Were they the same people as those who brought it to the Jazirah settlements?
>
> -- Lorraine Copeland, 1995, *The Phantom Obsidian Traders of the Jazirah*

In the above quotation, Near Eastern lithics expert Lorraine Copeland raises valid concerns about the interpretation of obsidian sourcing data, particularly within the Jezirah and surrounding region. As I showed in Chapter 2, though, there is still a severe lack of raw data (i.e., sourced obsidian artifacts) for Mesopotamia, even after four decades. For example, prior to my research, in the Bronze-Age Khabur Triangle (my principal area of interest), there were only 32 sourced artifacts from five sites, and only a quarter of those artifacts have been conclusively attributed to one geographical source.

Thus, on one level, I would suggest that Copeland's concern is unfounded because I argue that we, as archaeologists, know less about the distribution of obsidian in the Near East than we think we do, even for the Neolithic. For example, the obsidian distribution

maps of RDC and, more recently, Christine Chataigner and colleagues (Chataigner 1998, Chataigner et al. 1998, and Cauvin and Chataigner 1998) are misleading, in part, because the maps do not show the proportions of obsidians from the various sources. In addition, RDC were unable to differentiate the Bingöl A and Nemrut Dağ obsidians, so their maps reflect this inability. This problem persists with the recent maps as well. Chataigner and her colleagues (Chataigner et al. 1998) produced an obsidian distribution map, spanning from 10,000 to 4000 BCE, from existing data in prior analyses, and they claim to be able to differentiate Bingöl A and Nemrut Dağ obsidians. Their reconstruction is compelling; however, two of the three authors had, that same year (Chataigner 1998, Poidevin 1998), reported that the chemical clusters for Bingöl A and Nemrut Dağ are diffuse and overlap when inter-laboratory data are compiled. Regardless, obsidian distribution maps merely show the farthest occurrences of obsidians and not much more.

Thus, in this chapter, I dispense with such maps and instead plot the abundance of obsidian sources represented at Near Eastern settlements. The resulting plots show more complex structure and trends than the maps, further emphasizing the need for much more raw data (i.e., sourced artifacts) before any economic theory about obsidian exchange and economics in the ancient Near East can be developed and tested.

It must also be noted that the issues raised by Copeland are not limited to obsidian studies. Near Eastern archaeology has a century-long history, and many materials used in ancient Mesopotamia (e.g., metals, various stones, wood, ivory) must have been imported for geographical reasons (e.g., metal ores do not occur in the alluvium between the Tigris

and Euphrates Rivers). It has still been challenging, however, to translate all of these site reports, artifact descriptions, and textual evidence into models of exchange. For example, Moorey (1994) compiled a 414-page volume on Mesopotamian materials and industries, but his "Resource Procurement" section, focusing on exchange routes, is only six pages long. In Algaze's 246-page book *Ancient Mesopotamia at the Dawn of Civilization: The Evolution of an Urban Landscape* (2008), Chapter 6 is "The Evidence for Trade," but it consists of a mere seven pages. The recent 560-page *A Companion to the Ancient Near East*, edited by Snell (2005), is little better: the chapter on "Money and Trade" is just 14 pages. Clearly there are persistent difficulties in reconstructing ancient exchange, even in an area as well studied as Mesopotamia. Thus, we should not be too concerned or critical that obsidian research is still largely focused on data collection.

On another level, however, Copeland is correct in that we should start, even in the absence of regional-scale data, considering questions of how and why people brought the obsidian, either as finished artifacts or unfinished blocks, to these settlements in antiquity. We need not wait until we have sufficient data to investigate regional-scale changes in the cultural landscape from the Neolithic to the Bronze Age. By adding textual evidence and ethnographic accounts to the available, but meager, sourcing data, we can, at least, start to develop questions and hypotheses. Later in this chapter, I offer a few other suggestions, particularly related to the Bingöl and Nemrut Dağ sources. First, though, I highlight my findings from Tell Mozan, as discussed in Chapter 7, that have broader implications for Near Eastern obsidian research, including Copeland's questions.

8.1 - Findings from Tell Mozan with Broader Implications

In the following three sections, I discuss my findings from Tell Mozan that should have broad implications for obsidian studies in the Near East. My findings relate to three topics of widespread interest: (1) if prismatic blades were produced by specialists close to the obsidian sources and then exported throughout Mesopotamia, or if obsidian blocks or cores were instead transported to settlements, where blades were produced on-site; (2) the validity of Gratuze's assumption that peralkaline obsidian should be assigned to Bingöl A when obsidian from Bingöl B has been discovered at a site as well; and (3) if Blackman's (1984) geochemical clusters for Nemrut Dağ (i.e., Nemrut I to IV) and Poidevin's (1998) classifications based on "peralkalinity" (i.e, Nemrut Lake and Nemrut South) can, in fact, be linked to locations on the volcanic landscape of Nemrut Dağ.

8.1.1 - Specialized Blade Production across Mesopotamia?

In Section 2.1.1, I explain that, during the fourth millennium, a type of prismatic blade, called a Canaanean blade, occurred throughout Mesopotamia and the Levant. The long and wide blades have nearly parallel sides and two parallel ridges down their dorsal surfaces, and the result is a cross-section like an isosceles trapezoid. For unclear reasons, the "Canaanean" label tends to describe only chert blades with this form, not very similar obsidian blades, like some of those in Figure 7.6 and Appendix B.

Some have proposed that certain sites were production centers for such blades and that the finished products were distributed to other settlements. For example, Chabot and

Pelegrin (2006) contend that such blades "were crafted by specialists and fragmented into segments and then exported to the villages of Northern Syria and Iraq (for example, 'Atij, Gudeda, Raqa'i, Nusstell, *Mozan*)" (emphasis added). Chabot and Eid (2007) also claim that these blades "were made in specialized workshops, probably in the Anatolian region, and were then sent to northern Mesopotamian agricultural settlements" (23). The result, they argue, was "a specialised distribution network of high-quality tools" and a "network involved in the production of agricultural products throughout northern Mesopotamia and perhaps beyond" (23). This proposal by Chabot and colleagues is based on the recovery of more medial blade segments than proximal or distal blade ends, which they interpret to mean that only finished products are present at the listed sites.

Similarly, as discussed in Section 2.6.3, Reichel (2007) interprets the abundance of obsidian debris found at Tell Hamoukar to be evidence of "a production facility [that] extended far beyond the needs of Hamoukar itself" (65), and he maintains that "its main purpose had to be export" of finished blades produced there (65).

At Tell Mozan, the presence of decortification flakes from obsidian blocks (Figure 7.23) reveals that obsidian core reduction occurred on-site, as do artifacts with flat, rough surfaces in Figure 7.25. Moreover, Figure 7.26 shows examples of mixed blade and flake cores. These artifacts indicate that some sort of lithic production activities occurred at the site, not necessarily prismatic blade production. The presence, though, of a tabular blade core (Figure 7.27) as well as early-series blades (Figure 7.28) removed from a polyhedral obsidian core indicate that prismatic-blade production occurred at Tell Mozan, at least to

some extent. There is similar evidence at Tell Mozan for chert blade production. Hence, the hypothesis of Chabot and his colleagues -- that Canaanean blade production occurred at specialized workshops in southern Anatolia -- should be questioned, at least in the case of Tell Mozan. It should also be doubted that a site like Tell Hamoukar was a production center for prismatic obsidian blades that were utilized throughout Mesopotamia. Instead, two alternative hypotheses should be considered: (1) that Tell Mozan and other sites of its size were indeed blade-production centers with their own specialists but chiefly for their own inhabitants and those in the surrounding settlements, and (2) that specialists travelled from site to site, fashioning prismatic chert and/or obsidian blades for the locals. Clearly, a regional approach, involving detailed lithic studies at Chalcolithic and Bronze-Age sites in Anatolia and Mesopotamia, is necessary to resolve this issue.

8.1.2 - Gratuze's Assumption about Nemrut Dağ and Bingöl

In Section 2.5.2, I mentioned an assumption by Gratuze et al. (1993) to deal with their inability to distinguish between the obsidians from Bingöl A and Nemrut Dağ. They argued that "if, at one archaeological site, we find the artifacts have the two compositions of the Bingöl area, we may suppose that the artifacts come from Bingöl, whereas if only the Bingöl 'A' composition is found, both solutions (Nemrut Dağ and Bingöl) should be retained" (16). In other words, if Bingöl B obsidian is found at a particular site, one may assume the peralkaline obsidian came from Bingöl A. If Bingöl B, though, obsidian does not occur at the site, the peralkaline obsidian may have come from either Nemrut Dağ or

Bingöl A. This assumption was followed in subsequent research explicitly (e.g., Gratuze et al. 1995:503, Khalidi et al. 2009:883) and perhaps implicitly.

My results, however, reveal that the assumption is incorrect at Tell Mozan. There are three features -- A7 f121, A9 f98, and A18 f24 -- that have both Bingöl B and Nemrut Dağ obsidians. In fact, in two of these features, the Bingöl B and Nemrut Dağ obsidians are found within the same artifact lot: A9 f98 lot q440 and A18 f24 lot q23. Other source combinations occur as well. J1 f20 contains both Bingöl A and B obsidians concurrently whereas J2 f42 has Bingöl A and Nemrut Dağ obsidians together.

Thus, this assumption from Gratuze et al. (1993) must be reconsidered, especially for sites within the Khabur Triangle, such as Tell Hamoukar, Tell Brak, and Chagar Bazar. Their assumption, though, may remain valid for archaeological sites along the Upper and Middle Euphrates Valleys. In these regions, Bingöl obsidians may have been more likely utilized due to the potential for their natural transport downstream.

As discussed in Appendix A, although chemically quite similar to the Nemrut Dağ obsidians, Bingöl A obsidians are older, roughly four million years old, and their volcanic source is not clear. Bingöl B obsidians are younger than Bingöl A obsidians, roughly one million years old. Reportedly the obsidian blocks from Bingöl A are frequently about 10 to 25 cm in diameter, and those from Bingöl B can be somewhat larger, as much as 30 cm in diameter. The obsidian blocks from both Bingöl A and B are highly rounded, and their shapes indicate transport by water and mud. Also noteworthy is that Bingöl A obsidians occur near the towns of Orta Düz and Çavuşlar, approximately 20 km apart, and are not

chemically distinguishable. Similarly, Bingöl B obsidians can be found near the towns of Alatepe and Çatak, about 10 km apart, and cannot be distinguished.

These facts, considered together, indicate that the Bingöl A and B obsidians were each erupted during a single event and have since been transported by water and mud 10 to 20 km, possibly much farther. As noted in Section 1.2.3, Shackley (2005) reported that the Rio Grande River transported small nodules from Valles Caldera in New Mexico to Chihuahua, Mexico, a distance greater than 250 km (26). I also mentioned in Section 4.5 that there are areas in the basin around Glass Buttes in Oregon where cobbles from numerous flows can be gathered together. Similar areas, currently undiscovered or buried under recent alluvium, could also exist in the Bingöl region.

Regarding the use of Bingöl obsidians in the Upper Euphrates area, M.-C. Cauvin (1998) reports: "Certainly the people of Cafer [Höyük] could also find obsidian pebbles carried by a tributary of the Euphrates, the Murat, which in its upper reaches, passes not far from the settlement" ("Certes les habitants de Cafer auraient pu également trouver des galets d'obsidienne charriés par un affluent de l'Euphrate, le Murat, qui, dans son cours supérieur, passe non loin des gîtes," 263). She also explains that the Murat and Euphrates Rivers have never been systematically explored for obsidian pebbles. Rivers and streams move stones by traction, that is, by "scooting and rolling" along the bottom (Ritter 2006). She points out that some artifacts at Cafer Höyük bear evidence of water transport while others have cortex that suggests direct procurement (1998:263).

Clearly, further work using techniques capable of distinguishing the Bingöl A and Nemrut Dağ obsidians is needed to assess this assumption. The work of McDaniels et al. (1980) at Abu Hureyra, discussed in Section 8.2.13, also undermines it. Supposedly, the University of Bradford's Groups G1 and G3 correspond to Nemrut Dağ, and their Group G2 corresponds to Bingöl A. If correct, at this site in the Middle Euphrates Valley during the Neolithic, more artifacts (37%) were assigned to Nemrut Dağ than to Bingöl A (10%). Additionally, 28 artifacts were attributed to their Group B2, purportedly Bingöl B. Thus, Gratuze's assumption does not apply to Abu Hureyra, and consequently, we should doubt its veracity for the entire Middle Euphrates Valley during the Neolithic Period, potentially later. One consideration about the collection of Bingöl A versus Nemrut Dağ obsidians at their sources is discussed later in this chapter in Section 8.3.3.

8.1.3 - Peralkalinity and the Nemrut Dağ Sources

In Section 2.5.2, I explained that Poidevin (1998) noted three ways to distinguish Bingöl A and Nemrut Dağ sources using data from prior studies. In a plot of Al_2O_3 versus Fe_2O_3, he reported three clusters: (1) obsidian from the caldera interior ("Nemrut Lake") is high in Fe and low in Al; (2) obsidian from the southern slope ("Nemrut South") is low in Fe and high in Al; and (3) obsidian from Bingöl A that has intermediate amounts of Fe and Al. Based on a CNK/A versus NK/A plot, showing the degree of "peralkalinity," he stated that "Nemrut Lake" obsidians are more peralkaline than "Nemrut South" obsidians and that the Bingöl A obsidians fall between them. Based on this graph, it was proposed

that Blackman's Nemrut III is equivalent to Nemrut Lake and that Blackman's Nemrut I, II, and IV are all equivalent to Nemrut South. Others (e.g., Bressy et al. 2005) have also used the CNK/A versus NK/A plot and added a third Nemrut Dağ cluster, called "Nemrut Caldera," which falls close to the Bingöl A geochemical cluster.

Poidevin's hypothesis appears supported by Pernicka (1992), who used data from other researchers to create a different graph that also essentially showed the peralkalinity of the obsidians. He plotted these data using a graph formulated by Aspinall et al. (1972): Fe / Sc versus (Cs + Ta + Rb/100 + (Th + La + Ce) / 10) / Sc. In this graph, Blackman's Nemrut III is more peralkaline than his Nemrut I and II, which fall with the University of Bradford's G1 cluster. Bradford's G2, interpreted as Bingöl A, falls between them, just as Poidevin (1998) found. Although Bradford's G3 is not shown on Pernicka's plot, Epstein (1977) uses the same type of plot, showing G3 falls between G1 and G2. One is tempted to decide that G3 is equivalent to the "Nemrut Caldera" cluster. I shall assume, therefore, that G1 and G3 represent Nemrut Dağ while G2 represents Bingöl A.

When the necessary elements have been measured, a CNK/A versus NK/A plot is the most popular way to distinguish Bingöl A obsidians from Nemrut Dağ obsidians. My data support such a use of this plot. Figure 8.1 demonstrates that Bingöl A obsidians can be distinguished from all Nemrut Dağ obsidians. It is tempting, however, for researchers to use this plot to determine whether ancient people collected their raw obsidian from the southern slopes of Nemrut Dağ or from one of the sources within the caldera. According to Poidevin (1998), this should be possible. In addition, according to him, artifacts earlier

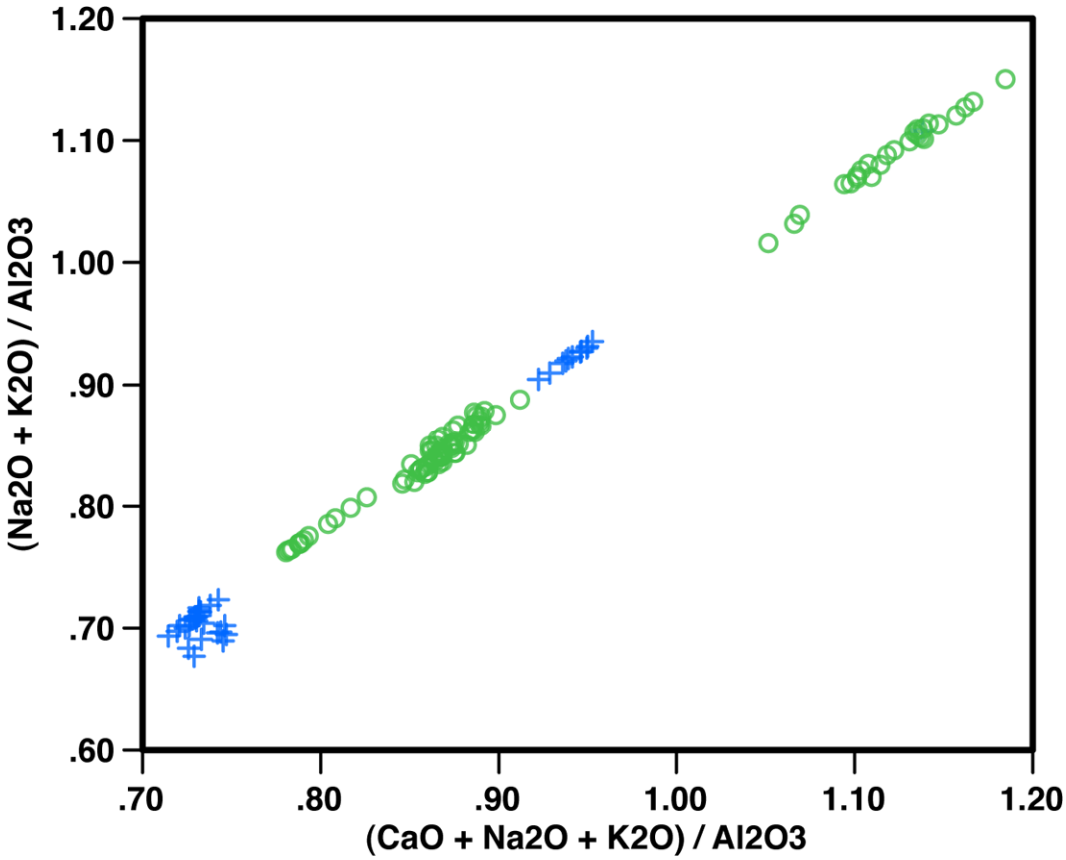


Figure 8.1 - This CNK/A versus NK/A plot demonstrates that Bingöl A and Nemrut Dağ obsidians can indeed be distinguished by their degrees of peralkalinity. Bingöl A and B obsidians are presented by blue crosses, and all Nemrut Dağ obsidians are represented by open green circles. The crosses in the lower left corner are the calc-alkaline Bingöl B specimens, and the crosses in the middle are the peralkaline Bingöl A specimens.

assigned to Blackman's Nemrut III can be retroactively assigned to "Nemrut Lake" in the caldera while those artifacts assigned to Blackman's Nemrut I, II, or IV or Bradford's G1 can be ascribed to "Nemrut South" outside the caldera. In fact, it is shocking that no one, to my knowledge, has yet attempted this. There is great potential to consider behaviors of ancient people when gathering raw materials for use or exchange.

Let us assume, for a moment, that Poidevin (1998) is correct in his identification of "Nemrut Lake" and "Nemrut South" with high and low peralkalinity, respectively. If true, what are the implications for our area of interest? For example, I note in Chapter 2 that Pernicka et al. (1997) sourced one artifact, dating to the third millennium BCE, from Tell Mulla Matar in northeastern Syria. They identify the source as Blackman's Nemrut I. They also sourced 38 obsidian artifacts from five Neolithic Middle-Euphrates sites in Syria, and of the seven artifacts sourced to Nemrut Dağ, all are assigned to Nemrut I, II, or IV. Furthermore, Pernicka (1992) sourced 17 Chacolithic artifacts from Hassek Höyük in Turkey, and he allotted ten of the artifacts to Bingöl B and the other seven to Nemrut I, II, and IV. If Poidevin (1998) is right, based on these (and other) sourcing studies, all of the obsidian from Nemrut Dağ was collected from its southern slopes.

The reality, though, is much more complex, and my analyses show that Poidevin (1998) is not correct. Figure 8.2 is my CNK/A versus NK/A plot of Bingöl A obsidians with one hundred geological specimens from eleven collection areas at Nemrut Dağ. The black open circles represent the Bingöl A obsidians. The rest of the symbols represent the Nemrut Dağ obsidians. The blue circles represent the pre-caldera obsidians on the outer

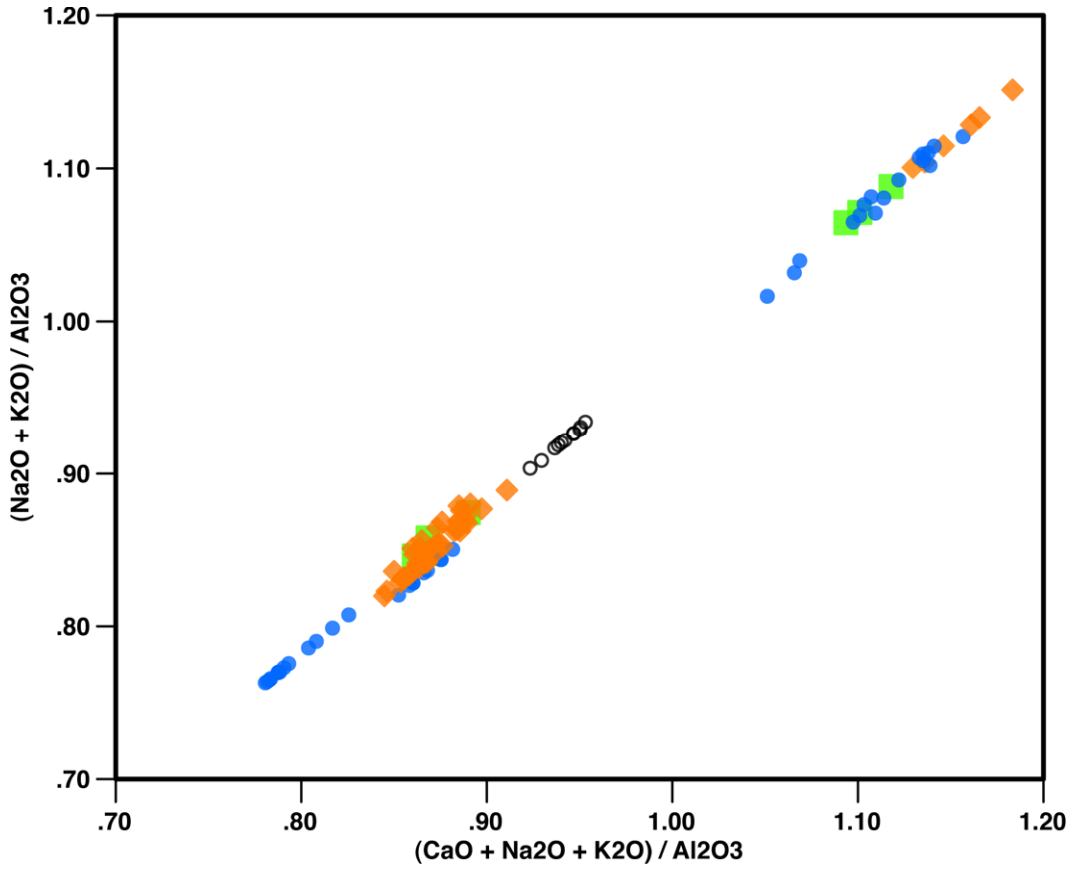


Figure 8.2 - A CNK/A versus NK/A plot of Bingöl A and Nemrut Dağ obsidians. The black open circles represent the Bingöl A specimens. The rest of the symbols represent the Nemrut Dağ specimens. The blue circles represent the pre-caldera obsidians on the outer slopes of the volcano, and the green squares are the pre-caldera obsidians exposed around the inner caldera wall. The orange diamonds represent the post-caldera obsidians within the caldera. Note that all three groups -- pre-caldera obsidians on the slopes, pre-caldera obsidians around the inner rim, and post-caldera obsidians -- all have obsidian flows that are both more and less peralkaline than the Bingöl A obsidians. Therefore, artifacts cannot be assigned to locations on the volcano using their peralkalinity alone.

slopes of the volcano, and the green squares are the pre-caldera obsidians exposed around the inner caldera wall. The orange diamonds represent the post-caldera obsidians within the caldera. Note that all three groups -- pre-caldera obsidians on the slopes, pre-caldera obsidians around the inner rim, and post-caldera obsidians -- all have obsidian flows that are both more and less peralkaline than the Bingöl A obsidians.

Therefore, more peralkaline obsidians (e.g., Nemrut III) cannot be assumed to be post-caldera "Nemrut Lake" obsidians, nor can less peralkaline obsidians (e.g., Nemrut I, II, and IV) be assumed to be pre-caldera "Nemrut South" obsidians. The third "Nemrut Caldera" group could represent either pre-caldera obsidians around the inner rim or post-caldera obsidians. Hence, for the vast majority of obsidian sourcing studies, we can say nothing about where exactly ancient people collected obsidian from Nemrut Dağ: inside or outside the caldera. Recall that most obsidian sourcing studies in the Near East cannot even distinguish between Bingöl A and Nemrut Dağ obsidians. I, though, have identified where Nemrut Dağ obsidian was collected to within a kilometer.

8.2 - Comparative Data from Prior Obsidian Studies

In Section 2.3, I discuss the relative lack of sourced obsidian from post-Neolithic sites in Mesopotamia and the Northern Levant. To consider the sourcing results from Tell Mozan in a proper context, we must compile and evaluate the data (or lack thereof) from those earlier studies. Here I focus on the sourced obsidian artifacts from Bronze-Age and Chalcolithic contexts, but I also discuss a number of Neolithic sites.

This analysis must be conducted here because the four main reviews of Near East obsidian studies end during the Calcholithic: Wright (1969) and Chataigner (1998) end at 3500 BCE; Cauvin and Chataigner (1998) end at 3700 BCE; and Chataigner et al. (1998) end at 4000 BCE. Furthermore, in one article that claims to examine obsidian use during the Neolithic and Bronze Age (Gratuze et al. 1995), the entire Bronze Age is represented by nine artifacts from Ras Shamra on the Mediterranean coast of Syria. Thus there are no existing Bronze-Age obsidian exchange patterns for comparison. Furthermore, these data have not, to my knowledge, been compiled and presented this way.

Parsing and assessing the data from the earlier studies can be challenging because, in some cases, the authors do not actually provide artifact-by-artifact assignments. In one study, in fact, the archaeological sites involved are not even named (Le Bourdonnec et al. 2005a). Furthermore, as noted in Section 2.5.2, an unfortunate variety of nomenclatures have been given to obsidian geochemical clusters. For instance, RDC had one cluster, 4c, for Nemrut Dağ. Wright (1969) reported two chemical clusters in Nemrut Dağ obsidians, which he called Nemrut Dağ-A and -B. Blackman (1984) found as many as four clusters, which he termed Nemrut I, II, III, and IV. Yellin and colleagues also reported two groups labelled NMRD1 and NMRD2. Other schemes followed: G1 and G3 at the University of Bradford, A1 and A2 at C.N.R. Rome, etc. These highly varied nomenclatures are due to the fact that RDC and many later researchers relied primarily on analyses of artifacts, not reference specimens collected from the sources. Some of these nomenclatures have been since abandoned and never definitively linked to actual obsidian sources.

In fact, none of these schemes ever conclusively showed how Bingöl A obsidians fit into, or were differentiated from, the Nemrut Dağ clusters. Only the Bradford scheme appears to have distinguished the Bingöl A (G2) and Nemrut Dağ (G1 and G3) clusters, but confirmation required further analyses of Pernicka et al. (1997), Poidevin (1998), and myself here. In the subsequent sections, I have attempted to "translate" the clusters into the geological sources discussed in Appendix A, but the results are often disappointingly inconclusive, especially regarding Bingöl A and Nemrut Dağ.

8.2.1 - Sourced Obsidian from the Bronze-Age Khabur Triangle

Hall and Shackley (1994) analyzed 21 blades from two sites in northeastern Syria, Tell Hamoukar and Hirbet Tueris, about 90 km southeast of Tell Mozan and at the eastern edge of the Khabur Triangle. These blades were surface finds but, based on the ceramics, probably date to the second millennium BCE. No geological specimens were analyzed in the study, so all assignments were made using published source data. Ten obsidian blades were sourced from Tell Hamoukar. Nine (90%) were assigned to Nemrut Dağ; however, it seems that Bingöl A must also be considered a possible source. One artifact (10%) had an unknown source, but it was similar to an artifact from Zarnaki Tepe north of Lake Van. Hence, it was possibly from either Meydan Dağ or Tendürek Dağ. All eleven blades from Hirbet Tueris were attributed to Nemrut Dağ, and again, Bingöl A should be considered a potential source as well. Taken together, 95% of the obsidian from the two adjacent tells came from the perakaline Nemrut Dağ and/or Bingöl A sources.

Pernicka et al. (1997) sourced a single artifact from Tell Mulla Matar, located near Al Ḥasakah where the Khabur River merges with the Jaghjagh, about 65 km south of Tell Mozan. Therefore, this site sits near the southernmost point of the Khabur Triangle. The artifact was recovered from an Early Bronze Age stratum, and they assigned it to Nemrut Dağ, in particular Blackman's Nemrut I geochemical cluster. Unfortunately, as I showed in Section 8.1.3, the Nemrut I cluster cannot be matched to any specific location on the volcano. Furthermore, Blackman did not have access to any Bingöl A specimens, which most likely would have fallen within his Nemrut Dağ groups. Thus, Blackman's Nemrut groups must all be considered potentially equivalent to Bingöl A.

Chabot et al. (2001) analyzed ten blade fragments from Bronze-Age strata of two sites, Tell Gudeda and Tell 'Atij, both adjacent to Tell Mulla Matar. Four blade fragments from Tell Gudeda were assigned to Bingöl A. Chabot and his colleagues utilized a graph of CNK/A versus NK/A, as discussed in Sections 2.5.2 and 8.1.3, to show conclusively that these artifacts did not come from Nemrut Dağ. From Tell 'Atij, four blade fragments (67%) came from Bingöl A, and two (33%) had an "unknown" source. It is not evident which other obsidian sources, if any, were included in this study, so what could constitute an "unknown source" is not clear. Taken together, 80% of the blade fragments came from Bingöl A, and 20% of them came from some unidentified source.

Thus we have just 32 sourced obsidian artifacts from five Bronze-Age sites in the eastern and southern Khabur Triangle for comparison to Tell Mozan. At Tell Hamoukar, nine obsidian blades were sourced to either Nemrut Dağ or Bingöl A, and one blade came

from an unknown source, perhaps one northeast of Lake Van. At Hirbet Tueris, all eleven blades were sourced to either Nemrut Dağ or Bingöl A. At Tell Mulla Matar, one artifact was assigned to Nemrut Dağ, but Bingöl A is also possible. At Tell Gudeda, four blade fragments were sourced to Bingöl A, not Nemrut Dağ. At Tell ʻAtij, four blade fragments were ascribed to Bingöl A, and two came from an unknown source.

The resulting picture (Figures 8.3 and 8.4) is vague. It is possible that, with the exception of three artifacts (9%) from unknown sources, the rest of them (91%) all came from Bingöl A. This would mean that, during the Bronze Age, settlements in the Khabur Triangle primarily used obsidian from just one source -- Bingöl A -- and that Nemrut Dağ obsidians went unused here. It is possible that a quarter of the artifacts came from Bingöl A and that two-thirds came from Nemrut Dağ. If true, this suggests that, at any particular site, only two obsidian sources, both in Eastern Anatolia, were utilized during the Bronze Age. The other implication, though, would be that nearly all of the obsidian at three sites came from Nemrut Dağ, while most of the obsidian originated from Bingöl A at the other two archaeological sites. Given the proximity of Tell Mulla Matar, Tell Gudeda, and Tell ʻAtij to one another, just a few kilometers apart, it would be quite unusual (but intriguing) if one site (Tell Mulla Matar) used obsidian entirely from Nemrut Dağ while two adjacent sites used obsidian entirely from Bingöl A. A third possibility is that, like at Tell Mozan, a mix of Nemrut Dağ and Bingöl A obsidians was used at the three sites, but there would still be two settlements where Nemrut Dağ obsidians went unused.

Figure 8.3 - Obsidian from Bronze-Age Sites in the Khabur Triangle

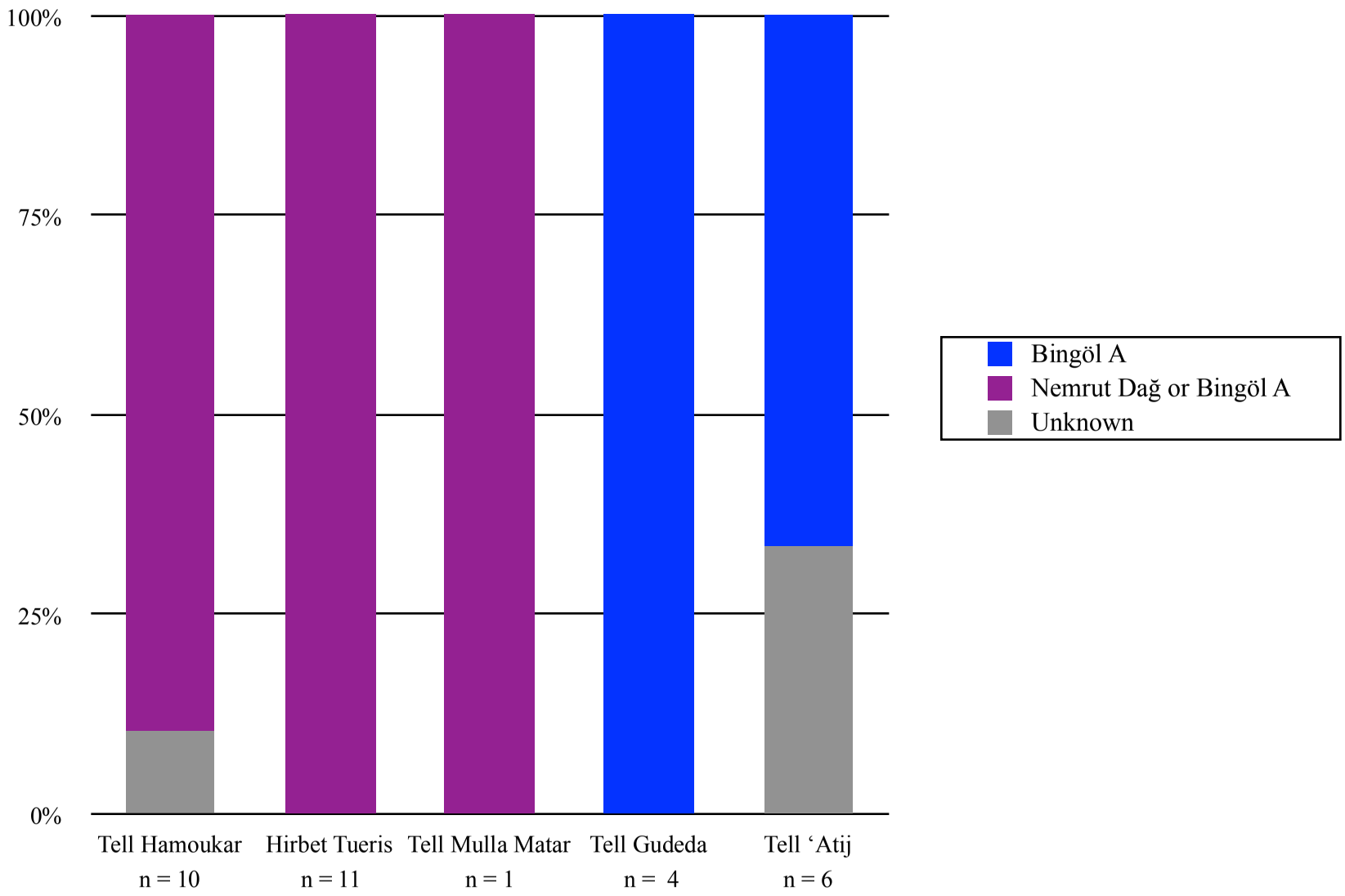
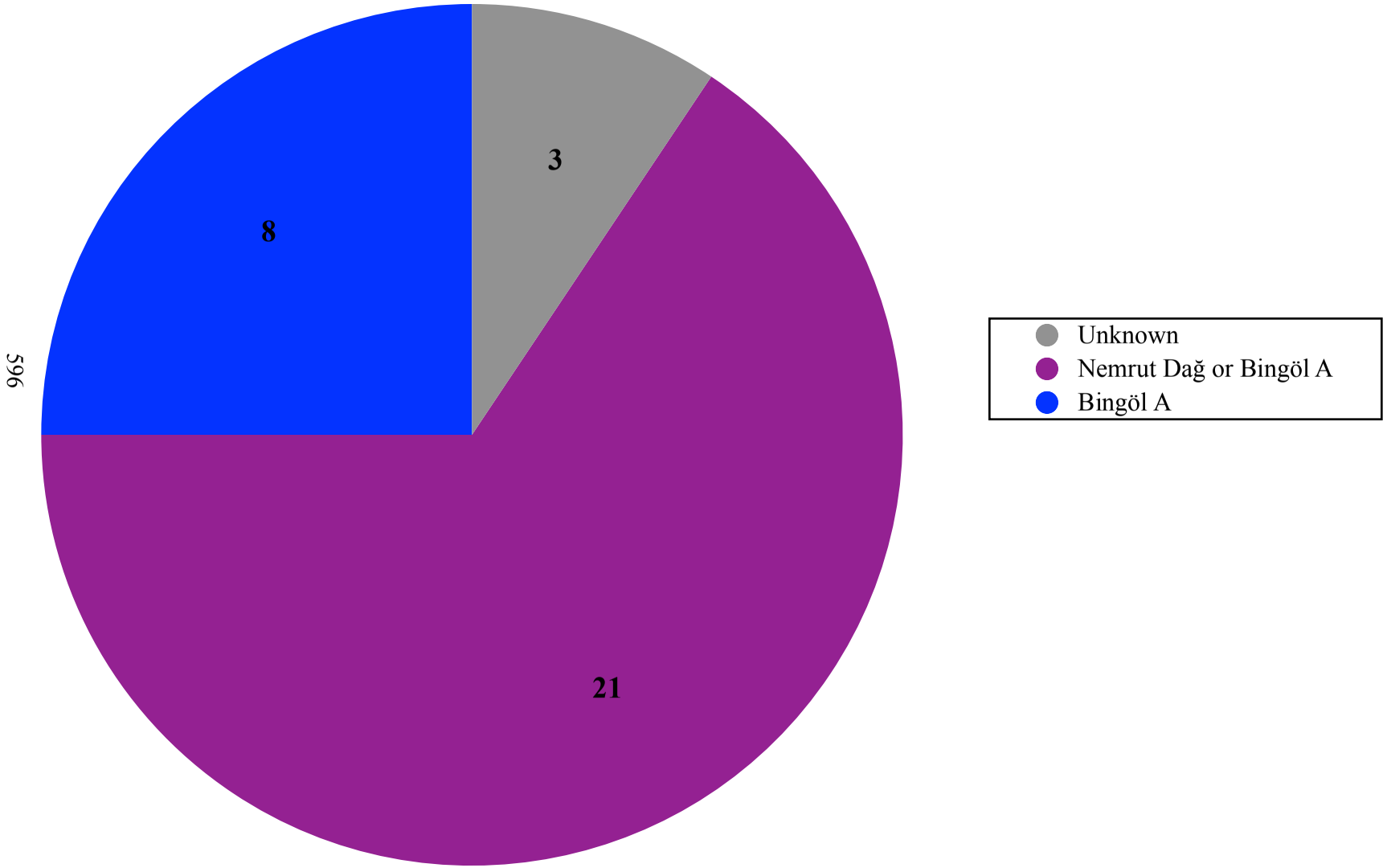


Figure 8.4 - Obsidians at Five Bronze-Age Sites in the Khabur Triangle - n =32



8.2.2 - Sourced Obsidian from Bronze-Age Southern Mesopotamia

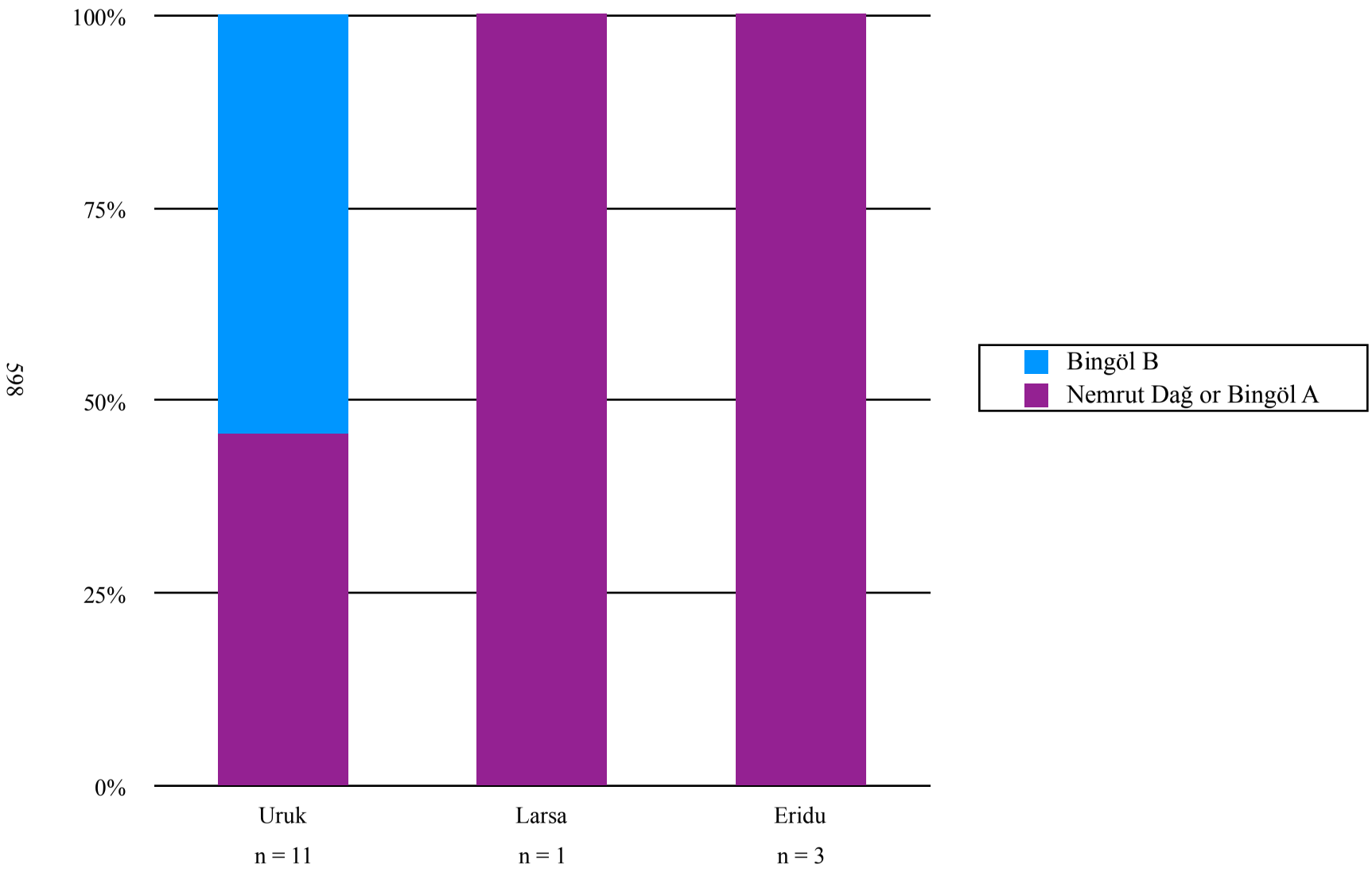
Schneider (1990) analyzed eleven obsidian artifacts (including blades, flakes, and a core) from Uruk, all likely dating from the second half of the fourth millennium. Six of the artifacts (55%) were assigned to RDC's Group 1g, commonly equated with Bingöl B. The other five artifacts (45%), including two blades and the core, were assigned to RDC's peralkaline Group 4c, which includes Nemrut Dağ and Bingöl A.

Gratuze et al. (1993) analyzed a single Middle-Bronze-Age artifact (of unknown type) from Tell as-Senkereh (ancient Larsa) in southeastern Iraq, roughly 25 km southeast of Uruk. This one obsidian artifact was assigned to their Group 1, which is comprised of both Bingöl A and Nemrut Dağ. Notice that this is the article in which Gratuze and his colleagues propose their assumption discussed in Section 8.1.2.

Renfrew et al. (1966) analyzed three artifacts (all blades) from Tell Abu Shahrain (ancient Eridu) also in southeastern Iraq, about 12 km southwest of Ur. The blades came from unstratified contexts, but the settlement reached its height during the late fourth and third millennia BCE, so these blades are presumed to date to this period. All three blades were ascribed to Group 4c, meaning either Bingöl A or Nemrut Dağ.

Hence, these three Bronze-Age cities -- Uruk, Larsa, and Eridu -- in southeastern Iraq, all relatively close, have obsidian assemblages dominated by two, or perhaps three, Eastern Anatolian sources. As in the Khabur Triangle, it is unclear if most of the obsidian came from either Bingöl A or Nemrut Dağ (Figure 8.5). One possibility is that all of the obsidian at these sites came from Bingöl A and Bingöl B. Another possibility is that only

Figure 8.5 - Obsidian from Bronze-Age Sites in Southern Mesopotamia



Nemrut Dağ and Bingöl B obsidians were used here and that the Bingöl A obsidians went unused. A third possible situation is that, like at Tell Mozan, obsidians from Bingöl A and Nemrut Dağ were used together alongside the Bingöl B obsidians.

8.2.3 - Sourced Obsidian from the Bronze-Age Upper Euphrates

Otte and Besnus (1992) analyzed a single artifact from an Early Bronze Age level of Hassek Höyük along the Euphrates. The artifact clearly has a peralkaline composition, and Otte and Besnus assigned it to Bingöl A due to the proximity of those sources. While Nemrut Dağ remains a possible source for the artifact, the proximity of and easy access to the Bingöl region suggests that Bingöl A is the more likely source.

8.2.4 - Sourced Obsidian from the Bronze-Age Northern Levant

Gratuze et al. (1993) sourced nine artifacts (of unknown types) from Late Bronze Age levels (circa 1300 BCE) at Ras Shamra (ancient Ugarit), a city on the Mediterranean coast of northwestern Syria. Six of these artifacts (67%) were ascribed to their Group 3, which is ostensibly the East Kayırlı source of Göllü Dağ. The other three artifacts (33%) were assigned to Group 5, which is Nenezi Dağ, adjacent to Göllü Dağ. Thus, all of their artifacts were ascribed to only two Central Anatolian sources. A complete lack of Eastern Anatolian obsidians differs from RDC's Neolithic patterns, but it is consistent with their post-Neolithic pattern (Renfrew and Dixon 1976; Figure 2.5).

In northern Lebanon, Gratuze (1999) sourced an obsidian chunk from Tell Arqa, a site near Tripoli and the Mediterranean coast. This sizable chunk was recovered with two others during the 1980s in a vineyard. Tell Arqa was inhabited from the Neolithic Period to the Middle Ages, and Gratuze dates the chunk to the Bronze Age for unknown reasons. His analyses indicate that the chunk came from one of the East Göllü Dağ sources, that is, either Komürcü, East Kayırlı, or East Bozköy. Unfortunately, though there are already so few sourced artifacts from the Bronze Age, this chunk must be left out. Thalmann (2006) points out that, in the vineyards around Tell Arqa, grape vines grow on concrete pillars set 1 to 2 meters into the ground. The chunks were churned up with the soil as pits for these pillars were dug, so any dating must be considered highly conjectural. Even if this chunk were included, however, it would not alter the pattern observed at Ras Shamra: during the Bronze Age, unlike the Neolithic, only Central Anatolian obsidian is used in the Northern Levant, and Eastern Anatolian obsidian is no longer found there.

8.2.5 - Sourced Obsidian from Bronze-Age Western Iran

Renfrew et al. (1966) analyzed one Early-Bronze-Age artifact from Susa (near the modern town of Shush) and assigned it to Group 3 with their Bayezıd obsidian specimen, suggesting that either Meydan Dağ or Tendürek Dağ was the source. They also analyzed an Early Bronze Age artifact from Tepe Hasanlu (near Lake Urmia). They attributed it to their Group 4c, which includes the Bingöl A and Nemrut Dağ sources.

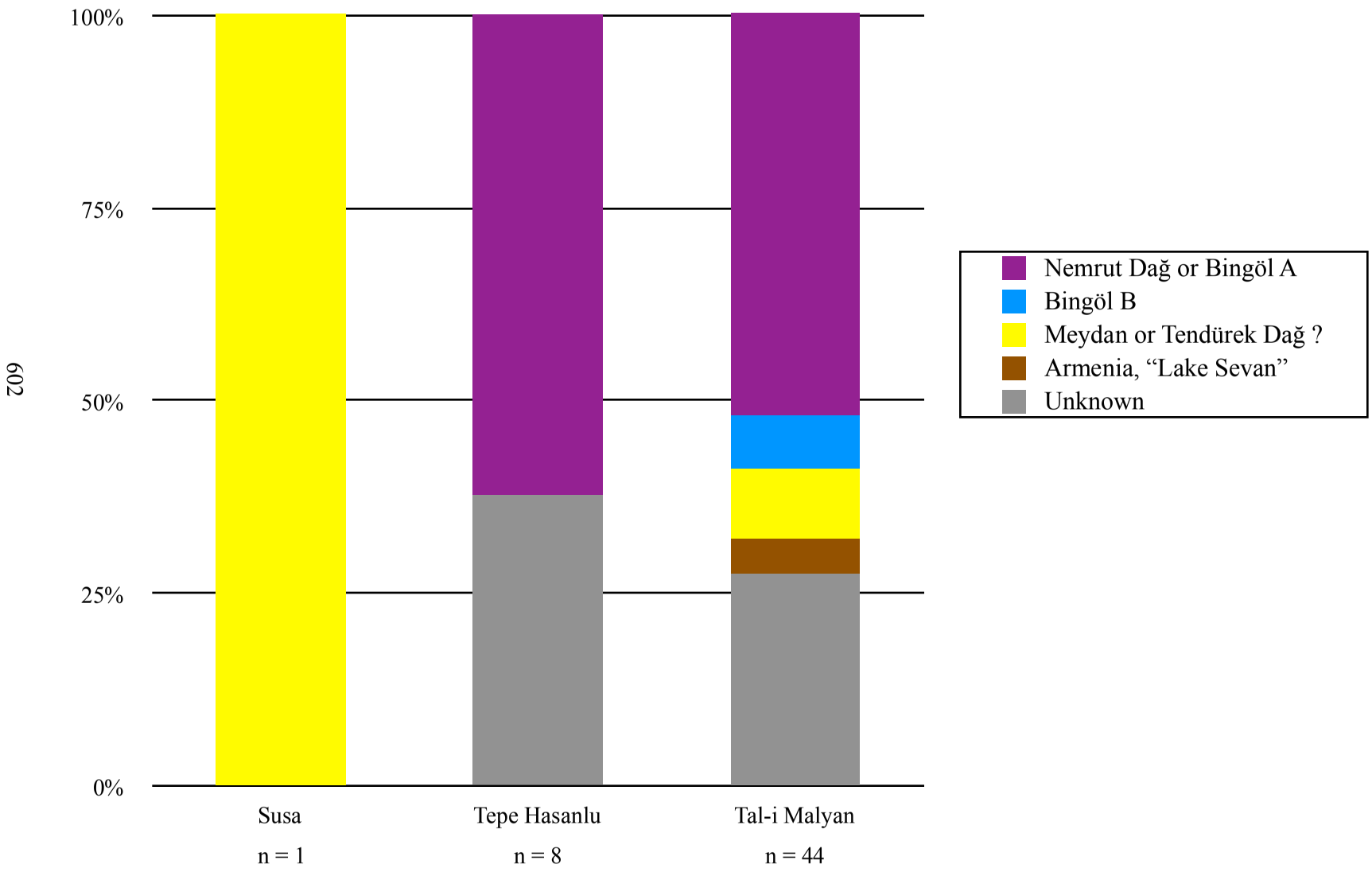
Also at Tepe Hasanlu, Mahdavi and Bovington (1972) sourced seven Bronze-Age artifacts with some highly questionable findings. As I mentioned in Section 4.7.3.7, these

researchers analyzed just five geological specimens, one from each of only five Anatolian source areas, and depend entirely on Mn/Na ratios. They assigned four artifacts to Group E, which included their one Nemrut Dağ specimen. Clearly Mahdavi and Bovington only recognized these four artifacts as peralkaline, and both Nemrut Dağ and Bingöl A must be considered equally probable. The other three artifacts were assigned to Group D, which included their only Hasan Dağ specimen. This attribution is highly unlikely because even sites near Hasan Dağ (e.g., Çatal Hüyük) did not use its obsidians.

Blackman (1984) analyzed 44 Bronze-Age artifacts from Tal-i Malyan (identified as ancient Anshan) in southern Iran. He assigned 23 (52%) of the artifacts to his Nemrut I and II clusters, which Poidevin (1998) erroneously equates to the obsidian flows on the southern slope of Nemrut Dağ. In reality, Blackman's clusters cannot be related to actual locations at Nemrut Dağ, and because he analyzed no Bingöl A obsidians for comparison, Bingöl A should also be considered a likely source. Four artifacts (9%) seemed to match an artifact from Zarnaki Tepe north of Lake Van, meaning that it fits RDC's Group 3 and probably came from either Meydan Dağ or Tendürek Dağ. Three artifacts (7%) matched RDC's Group 1g, now considered to be the Bingöl B source, and two artifacts (5%) were ascribed to "Lake Sevan" in Armenia. The twelve remaining obsidian artifacts (27%) are assigned to three geochemical clusters from unknown sources.

Figure 8.6 summaries the obsidian-sourcing results from these three Bronze-Age sits in western Iran. Tal-i Malyan has the greatest variety of obsidian sources represented in the artifacts. This is most likely, at least in part, a reflection of Blackman's analyses of

Figure 8.6 - Obsidian from Bronze-Age Sites in the Western Iran



44 artifacts, not just a few; however, this variety might also reveal "real" greater access to material and artifacts from different sources. Anshan was a capital of the Elamite culture during the Chalcolithic and Bronze Age, so this city likely served as a "central place" that drew in and redistributed exotic materials like carnelian and lapis lazuli coming from the east. Similar phenomena may also have been at work in Urkesh.

8.2.6 - Sourced Obsidian from the Chalcolithic Khabur Triangle

Cann and Renfrew (1964) sourced two artifacts from Chagar Bazar in the Khabur Triangle but only one from a Chalcolithic context (and the same artifacts were analyzed later by Wright and his colleagues). They assigned this one Chalcolithic artifact to their Group 4c, meaning that it originated from either Bingöl A or Nemrut Dağ. For 45 years, this was the only sourced obsidian artifact from Chacolithic Syria.

As I discuss in Section 2.6.5, Khalidi et al. (2009) analyzed 32 obsidian artifacts from Late Chalcolithic levels of Tell Hamoukar. They assigned 27 artifacts (85%) to the Bingöl A source, but Nemrut Dağ cannot be ruled out as a potential source. Two artifacts (6%) were assigned to the Bingöl B source, and one (3%) was attributed to Meydan Dağ. The remaining two artifacts (6%) came from an "unknown" source.

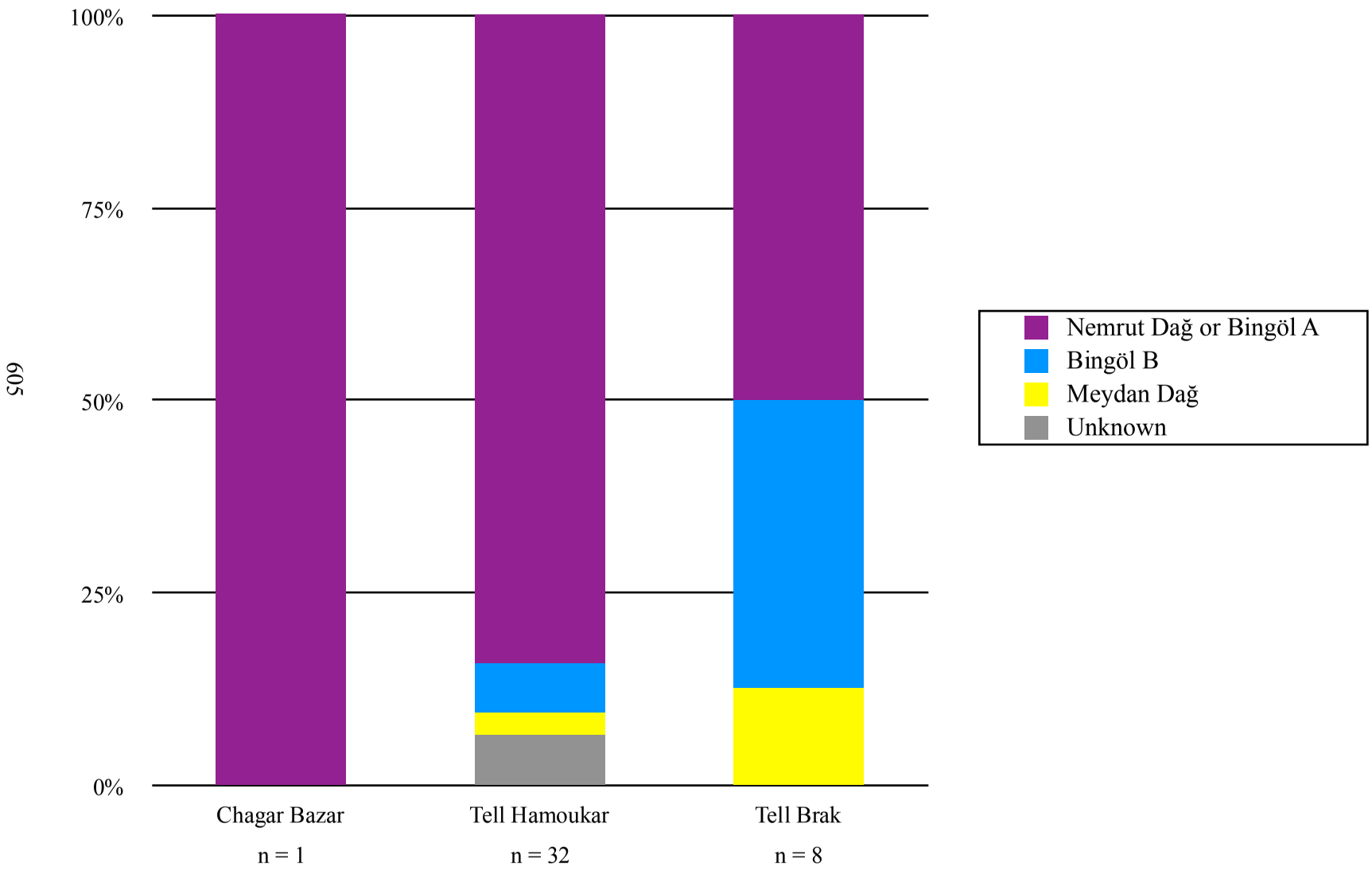
Khalidi and her colleagues also sourced eight Late-Chalcolithic artifacts from Tell Brak (ancient Nagar). They attributed four artifacts (50%) to Bingöl A; however, as with Tell Hamoukar, Nemrut Dağ cannot be ruled out as a likely source. Three artifacts (38%) were assigned to Bingöl B, and one (12%) was ascribed to Meydan Dağ.

Figure 8.7 summarizes the sourcing results from Chalcolithic contexts within the Khabur Triangle. Again the issues are bad reference collections and the use of analytical techniques that cannot differentiate Bingöl A and Nemrut Dağ obsidians. One possibility is that all of the peralkaline obsidians originated from Bingöl A, not Nemrut Dağ. This is the interpretation favored by Khalidi et al. (2009) for Tell Hamoukar and Tell Brak due to the presence of Bingöl B obsidian. The reverse situation -- all of the peralkaline obsidian originated from Nemrut Dağ -- is also a potential. The third possibility is that, like at Tell Mozan during the Bronze Age, Bingöl A and Nemrut Dağ obsidians were used together in the Khabur Triangle during the Chalcolithic. Unfortunately, based on the available data, it is not possible to judge which of these scenarios is closer to reality.

8.2.7 - Sourced Obsidian from Chalcolithic Northern Mespotamia

Outside of the Khabur Triangle, RDC analyzed an obsidian vessel from a tomb at Tepe Gawra in northern Iraq, about 15 km from Mosul. At the time, it was believed that the tomb dated to about 3200 BCE, but later work suggests that its stratum dates to about 3800 BCE, placing it in the Late Chalcolithic. As I discuss in Chapter 2, this was the sole obsidian vessel in the work of RDC, and it is not clear why dozens of obsidian blades and a few cores in the same level were ignored in favor of this bowl. The vessel was ascribed to one of the Acıgöl sources, making it the farthest east occurrence of Central Anatolian obsidian. I consider this finding somewhat of an anomaly as ground- and flaked-obsidian artifacts likely played very different roles in exchange systems.

Figure 8.7 - Obsidian from Chalcolithic Sites in the Khabur Triangle



8.2.8 - Sourced Obsidian from the Chalcolithic Northern Levant

Renfrew et al. (1966) analyzed one Chacolithic artifact from Byblos, a settlement on the Mediterranean coast of Lebanon. They attributed the single artifact to their Group 4c, meaning that it originated from either Bingöl A or Nemrut Dağ.

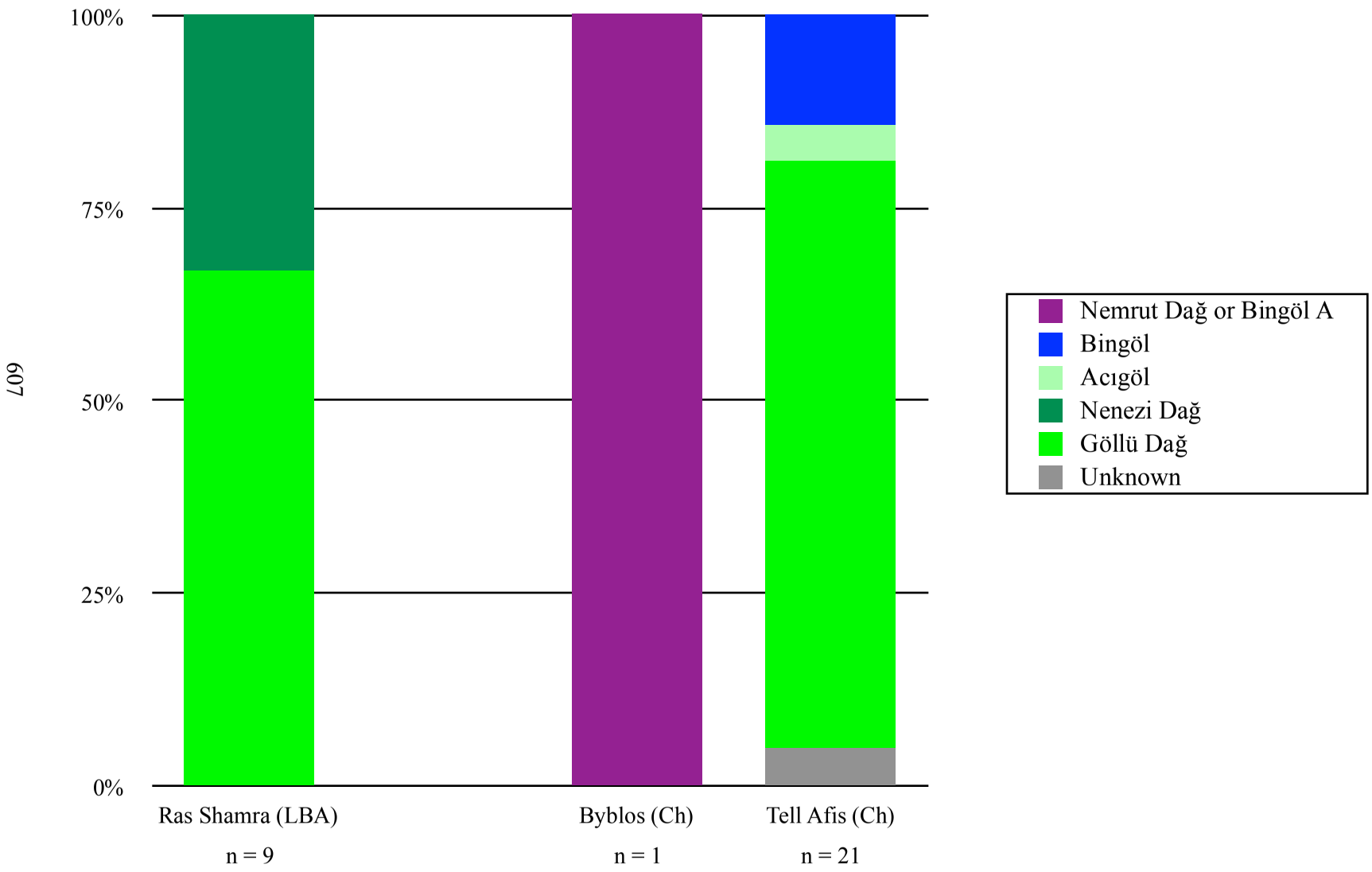
Using fission-track dating, Oddone et al. (2003) sourced 21 artifacts from the Late Chacolithic levels (circa 4000-3500 BCE) of Tell Afis in northwestern Syria, about 45 km southwest of modern Aleppo. They attributed 16 artifacts (76%) to one of the Göllü Dağ sources and one artifact (5%) to Acıgöl, so over 80% of these artifacts came from Central Anatolia. Three artifacts (14%) were attributed to "Bingöl" in Eastern Anatolia. Oddone and colleagues do not identify a particular Bingöl source, but the identification of Bingöl, rather than Nemrut Dağ, is conclusive because their source assignments are based on age, not composition. One artifact (5%) came from an unknown source.

Figure 8.8 summarizes these data from the Bronze Age and Chacolithic Northern Levant. It is fortunate that Oddone and colleagues used fission-track dating to identify obsidian from Bingöl and rule out Nemrut Dağ as a source. This finding lends support to an interpretation that the peralkaline obsidians in the Northern Levant came from Bingöl A, not Nemrut Dağ; however, more such analyses are clearly needed.

8.2.9 - Sourced Obsidian from Chalcolithic Southeastern Turkey

Pernicka (1992) and Otte and Besnus (1992) sourced 17 Chacolithic artifacts from Hassek Höyük in southeastern Turkey. They attributed ten of the artifacts (59%) to their

Figure 8.8 - Obsidian Sources in the Bronze Age and Chacolithic Northern Levant



Group 1, which is Bingöl B. The remaining seven artifacts (41%) were ascribed to either the Nemrut Dağ or Bingöl A sources. Their source assignments are linked to Blackman's groups, which, as I have asserted, have little use. Given the proximity of the Bingöl area, Bingöl A is arguably the more probable source of this obsidian.

8.2.10 - Sourced Obsidian from Chalcolithic Western Iran

Renfrew et al. (1966) analyzed three Chacolithic artifacts from Tal-i-Bakun (just south of Persepolis). They assigned all three to Group 4c, meaning that they came from either the Bingöl A or Nemrut Dağ sources. In addition, they analyzed three Chacolithic artifacts from Pisdeli Tepe (near Tepe Hasanlu). They assigned one artifact to Group 4c, meaning that it came from either Bingöl A or Nemrut Dağ. The other two matched their "Bayezıd" specimen from the British Museum and their Group 3a, suggesting that either Meydan Dağ or Tendürek Dağ was the source of those artifacts.

Mahdavi and Bovington (1972) sourced three Chacolithic artifacts from Susa, two artifacts from Tepe Jaffarabad (near Susa), and five from Marvdasht (near Persepolis). In Section 8.2.5, I explain that, due to inadequate reference specimens and their reliance on Na/Mn ratios, the two researchers have dubious source assignments for their Bronze-Age artifacts. Unfortunately, this trend continues into the Chacolithic, and their results are so questionable that their entire study should be disregarded.

The most recent sourcing research in northwestern Iran is hardly better. Niknami et al. (2010) sourced 60 artifacts from 22 Chacolithic sites in northwestern Iran, but only

three artifacts fall within our area of interest, that is, west of Lake Urmia. Unfortunately, these researchers do not specify the sources of individual artifacts. Even worse, Niknami and his colleagues analyzed only one obsidian specimen from each of three volcanoes in northwestern Iran (and a fourth "obsidian" specimen turned out to be chert). In addition, no obsidian sources outside Iran were included despite prior studies showing that Eastern Anatolian obsidian was widely used in Iran in antiquity.

8.2.11 - A Note about Sourced Obsidian from the Neolithic

Though the relevance of Neolithic obsidian distribution patterns is limited for the research at hand, much greater attention has been paid to sourcing obsidian artifacts from Neolithic contexts, so there is much more sourcing data to consider. These data are worth considering here so long as we keep in mind that Bronze-Age obsidian exchange patterns most likely reflect different human activities (i.e., intensification of agriculture, increased urbanization, and the rise of early empires) compared to the Neolithic.

8.2.12 - Sourced Obsidian from the Neolithic Khabur Triangle

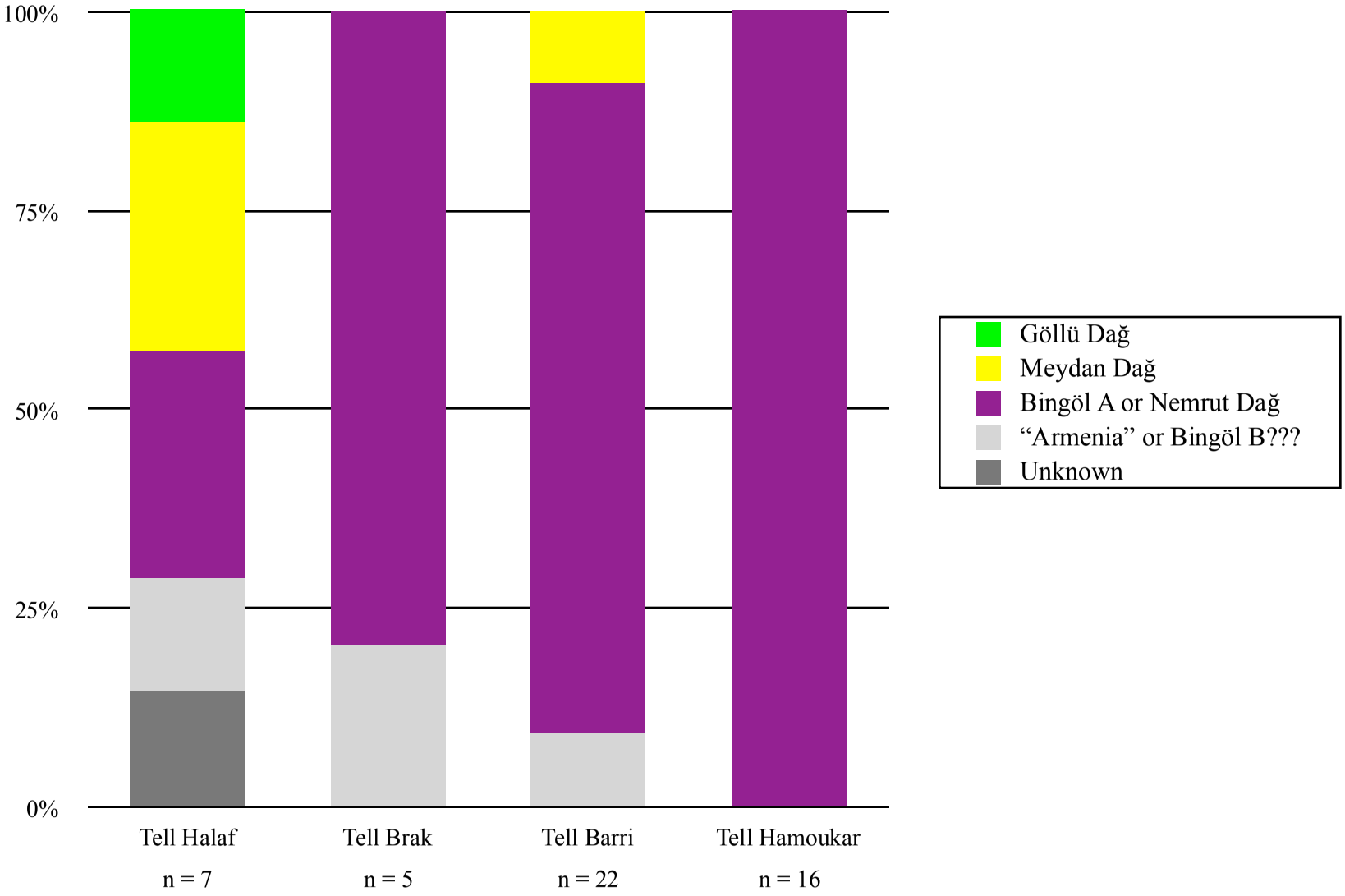
Francaviglia and Palmieri (1998) sourced 50 obsidian artifacts, dating to the Late Neolithic Period from four archaeological sites in the Khabur Triangle. At Tell Barri, 18 artifacts (82%) are attributed to Nemrut Dağ or Bingöl A, two (9%) to "Ziyaret" (that is, Meydan Dağ), and two to "Armenia" (which source is unknown). At Tell Hamoukar, all 16 obsidian artifacts were attributed to Nemrut Dağ and/or Bingöl A. At Tell Halaf, two

artifacts (29%) were attributed to Nemrut Dağ or Bingöl A, two (29%) to "Ziyaret" (that is, Meydan Dağ), one (14%) to one of the Göllü Dağ sources, one (14%) to "Armenia," and one (14%) to an unknown source. At Tell Brak, four artifacts (80%) were assigned to either Nemrut Dağ or Bingöl A, and one (20%) was attributed to "Armenia." It is quite interesting (and suspicious) that no Bingöl B obsidians were identified at these four sites. Given their chemical similarities (e.g., both fall in RDC's Group 1), I highly suspect that the "Armenian" obsidians are really misidentified Bingöl B obsidians.

Figure 8.9 summarizes the data from Francaviglia and Palmieri (1998) for these four contemporaneous Khabur sites. I organized these sites from west to east, revealing the trends along this axis. There is an increasing dependence on obsidian from Bingöl A and/or Nemrut Dağ from west to east. Göllü Dağ is only present at the westernmost site, Tell Halaf, which might have received such obsidian from the Middle Euphrates sites. A decrease in the variety of obsidian sources is also apparent from west to east: five sources are present at Tell Halaf while only one, perhaps two, obsidian sources are present at Tell Hamoukar. Tell Mozan is about 40 km due north of Tell Brak.

From the earlier Halaf Period (circa 6000-5200 BCE), Cann and Renfrew (1964) analyzed an obsidian flake from Chagar Bazar. It matched their Group 3, so Meydan Dağ and Tendürek Dağ are possible sources. Gratuze et al. (1993) sourced eight artifacts from Tell Kashkashok, near Tell Mulla Matar, Tell Gudeda, and Tell 'Atij at the southernmost point of the Khabour Triangle. They ascribed half of the artifacts to their Group 1, which corresponds to Nemrut Dağ and/or Bingöl A, and the other half to their Group 2, which is

Figure 8.9 - Obsidian at Late-Neolithic Khabur-Triangle Sites - West to East - Francaviglia and Palmieri (1998)



Bingöl B. Gratuze and colleagues assumed, given the presence of Bingöl B obsidian, that Bingöl A, not Nemrut Dağ, was the source of the peralkaline obsidians.

Figure 8.10 shows the source data from the Halaf and Ubaid Periods together. At first glance, the source data from Chagar Bazar appears to disrupt the observed west-east trend during the subsequent Ubaid Period; however, the representation of Chagar Bazar by a single flake is almost certainly distorting the result from that site.

8.2.13 - Sourced Obsidian from the Neolithic Middle Euphrates

Pernicka et al. (1997) sourced 38 artifacts from five sites in the Middle Euphrates area, about 200 km southwest of the Khabur Triangle. First, we can consider the results by a site-by-site basis. At Tell Halula, five artifacts (25%) were attributed to Komürcü at Göllü Dağ, one (5%) to a second Göllü Dağ source, one (5%) to Nenezi Dağ, four (20%) to Bingöl B, seven (35%) to Nemrut Dağ and/or Bingöl A, and two (10%) to an unknown source. At Dja'de, three obsidian artifacts (50%) were ascribed to the Komürcü source of East Göllü Dağ, two artifacts (33%) to Bingöl B, and one (17%) to either Nemrut Dağ or Bingöl A. At Jerf el Ahmar, an obsidian artifact was assigned to Komürcü, and at Cheikh Hassan, two artifacts were also assigned to Komürcü. At Mureybet, eight artifacts (80%) were assigned to Komürcü, one (10%) to Bingöl B, and one (10%) to either Nemrut Dağ or Bingöl A. These results are summarized by site in Figure 8.11.

The results from Pernicka et al. (1997) can also be considered by time period. In the PPNA, three artifacts were assigned to the Komürcü source of East Göllü Dağ. In the

Figure 8.10 - Obsidian Sources at Late-Neolithic Khabur-Triangle Sites - West to East

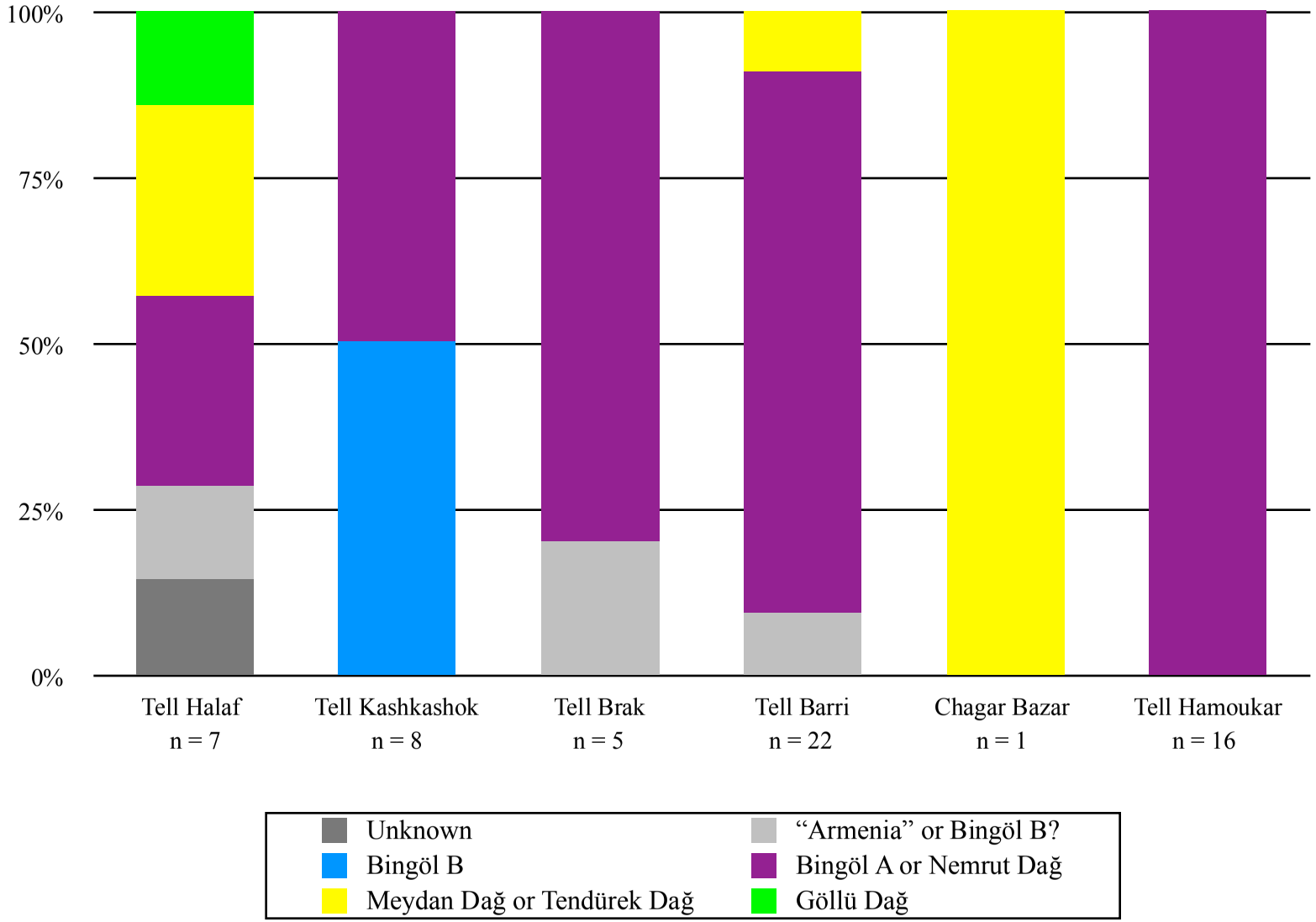
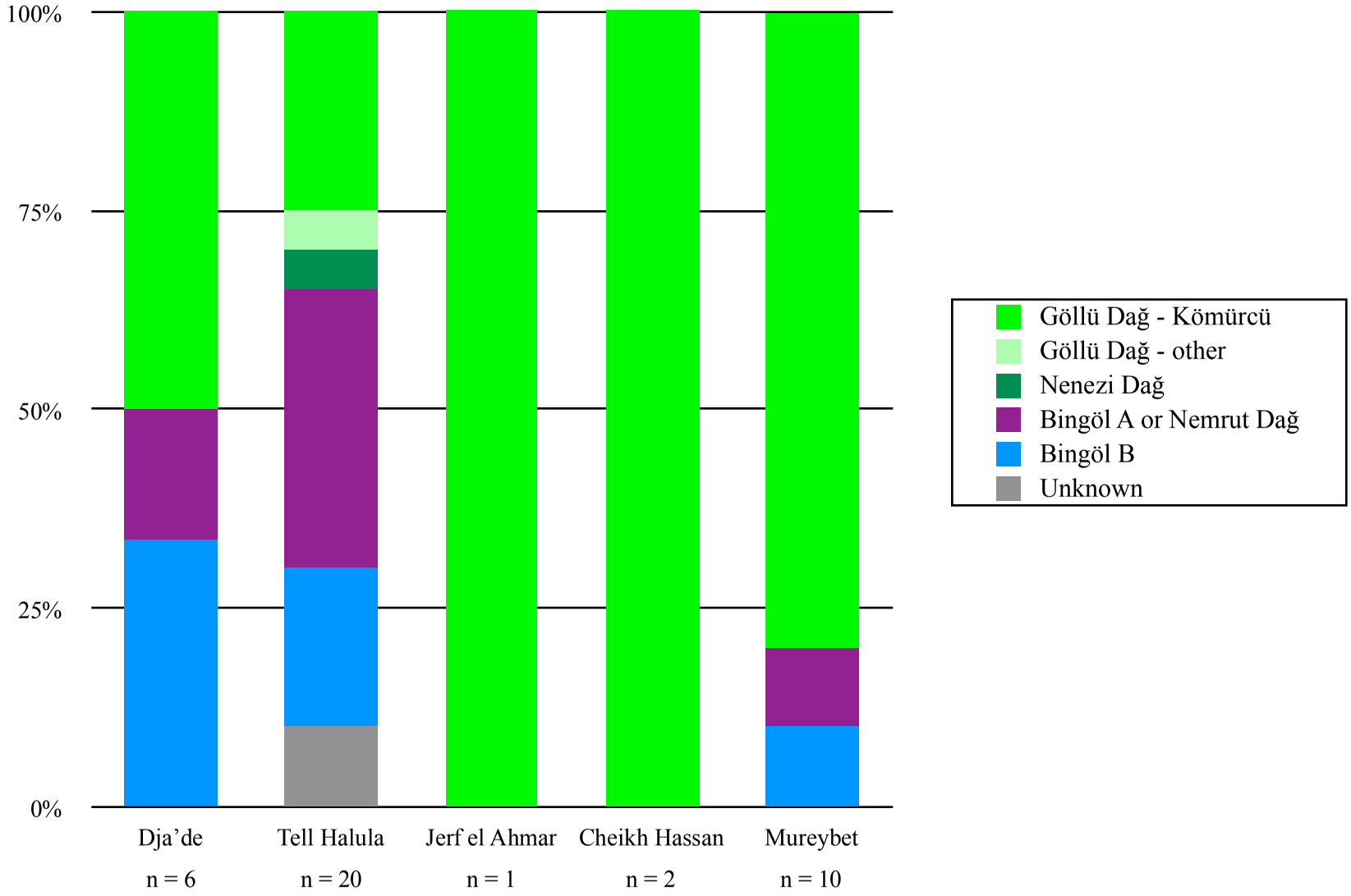


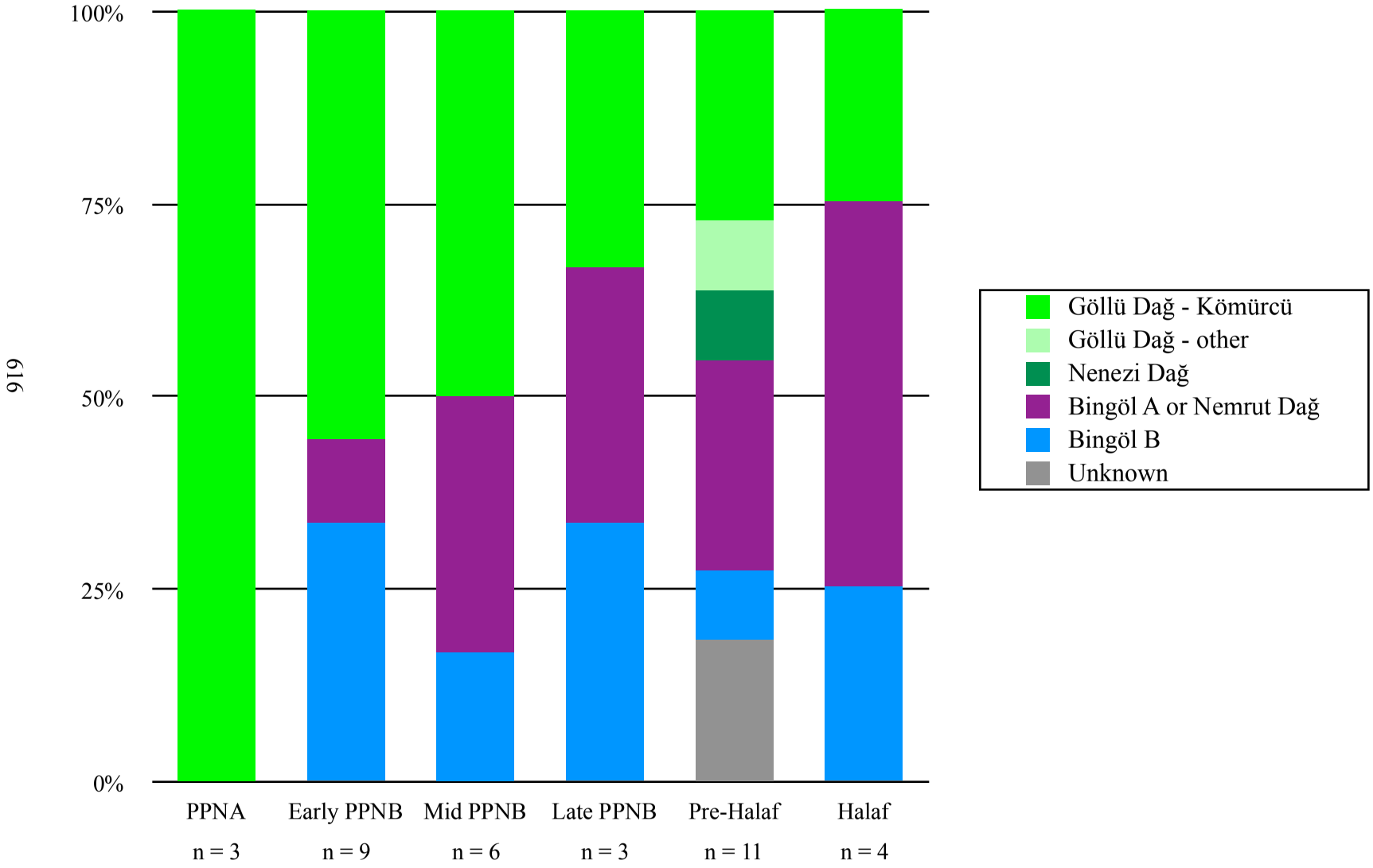
Figure 8.11 - Sources at Neolithic Middle-Euphrates Sites from Pernicka et al. (1997) - By Site: North to South



Early PPNB, five artifacts (56%) were allotted to Komürcü, three (33%) to Bingöl B, and one (11%) to either Nemrut Dağ or Bingöl A. In the Middle PPNB, three artifacts (50%) were assigned to Komürcü, one (17%) to Bingöl B, and two (33%) to either Nemrut Dağ or Bingöl A. In the Late PPNB, one artifact (33%) was assigned to Komürcü, one (33%) to Bingöl B, and one (33%) to Nemrut Dağ or Bingöl A. In the Pre-Halaf, three artifacts (27%) were assigned to Komürcü, one artifact (9%) to a second source at Göllü Dağ, one (9%) to Nenezi Dağ, one (9%) to Bingöl B, three (27%) to either Nemrut Dağ or Bingöl A, and two (19%) to some unknown source. In the Halaf Period, one artifact (25%) was attributed to Komürcü, one artifact (25%) to Bingöl B, and two (50%) to Nemrut Dağ or Bingöl A. See Figure 8.12 for a summary. This graph suggests a decreasing utilization of Komürcü obsidian and an increasing utilization of Bingöl A and/or Nemrut Dağ obsidians with time in the Middle Euphrates region of northern Syria.

Other researchers have also analyzed artifacts from the Middle Euphrates region of Syria. McDaniels et al. (1980) sourced one hundred artifacts from Abu Hureyra. They assigned 24 artifacts (24%) to Group B1, which corresponds to RDC's Group 2b and thus one of the Göllü Dağ sources. Twenty-eight artifacts (28%) were attributed to Group B2, purportedly Bingöl B. Thirty-seven artifacts (37%) were ascribed to Group G1, and ten artifacts (10%) to Group G2. As discussed in Section 8.2, it appears that both Groups G1 and G3 correspond to Nemrut Dağ and that G2 corresponds to Bingöl A. This scheme, developed at the University of Bradford, has been abandoned for 30 years, so there are a

Figure 8.12 - Sources at Neolithic Middle-Euphrates Sites from Pernicka et al. (1997) - By Time



few lingering issues with their assignments. I assume here, though, that their Group G2 does, in fact, accurately correspond to the Bingöl A obsidians.

Gratuze et al. (1993) analyzed 13 artifacts from two sites in the Middle Euphrates region. From PPNA strata at Cheikh Hasan, one artifact (33%) was assigned to Bingöl B, one (33%) to the East Kayırlı source of Göllü Dağ, and one (33%) to an unknown source. From the PPNA and PPNB strata at Mureybet, eight artifacts (80%) were assigned to the East Kayırlı source of Göllü Dağ, one (10%) to Bingöl B, and one (10%) to Nemrut Dağ or Bingöl A. Given the presence of Bingöl B at Mureybet, Gratuze and colleagues argue that Bingöl A, not Nemrut Dağ, is the correct peralkaline source.

Abbès et al. (2001) and (2003) also sourced obsidian from three PPNA and PPNB sites in the Middle Euphrates Valley. At Cheikh Hassan, 14 artifacts (74%) were ascribed to one of the East Göllü Dağ sources, four (21%) to Bingöl B, and one (5%) to Bingöl A or Nemrut Dağ. At Mureybet, 37 artifacts (93%) were attributed to one of the Göllü Dağ sources, and three artifacts (7%) came from Eastern Anatolian sources. At Jerf el Ahmar, 23 artifacts (53%) were assigned to Bingöl B in Eastern Anatolia, and 21 artifacts (47%) came from one of the East Göllü Dağ sources in Central Anatolia.

Figure 8.13 summarizes all the results from these six Neolithic sites in the Middle Euphrates Valley, and Figure 8.14 compiles the data into one pie chart. About half of the obsidian in the Middle Euphrates area came from Nenezi Dağ and the Göllü Dağ sources in Central Anatolia. One quarter came from Bingöl B. At least 4% came from Bingöl A, and at least 15% came from Nemrut Dağ. Bingöl A is usually considered the more likely

Figure 8.13 - Sources at Neolithic Middle-Euphrates Sites - By Site: North to South

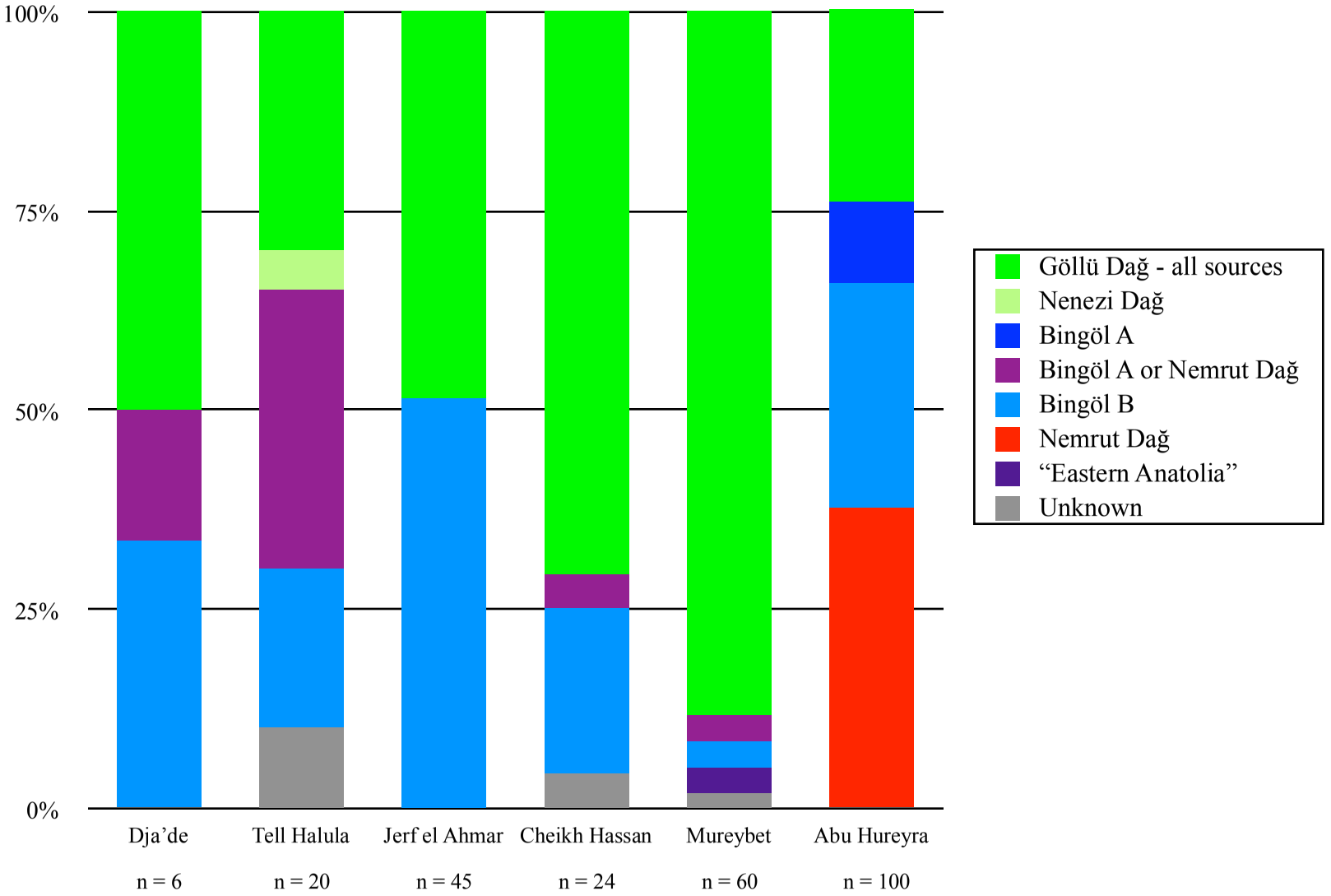
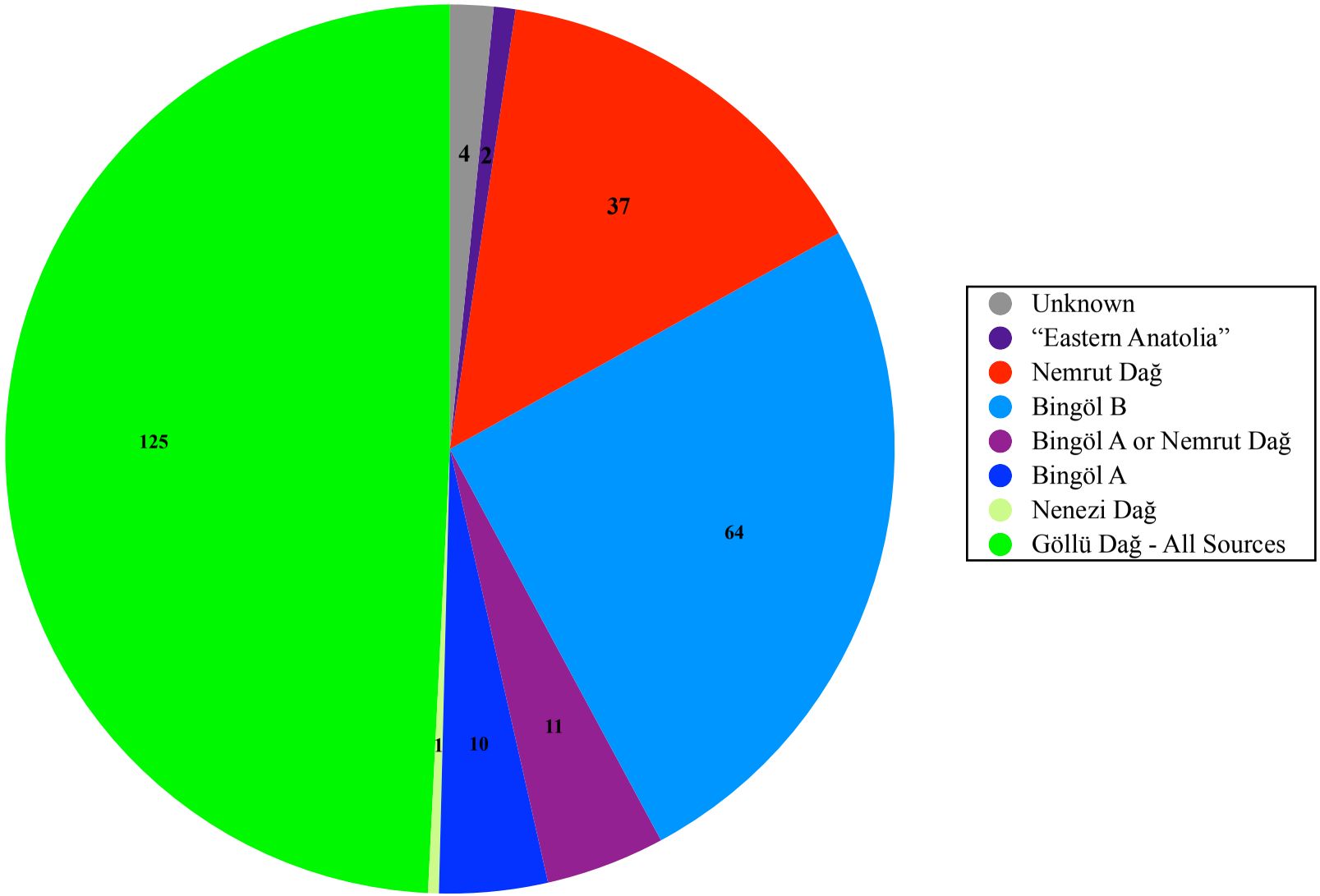


Figure 8.14 - Compiled Sources at Neolithic Middle-Euphrates Sites



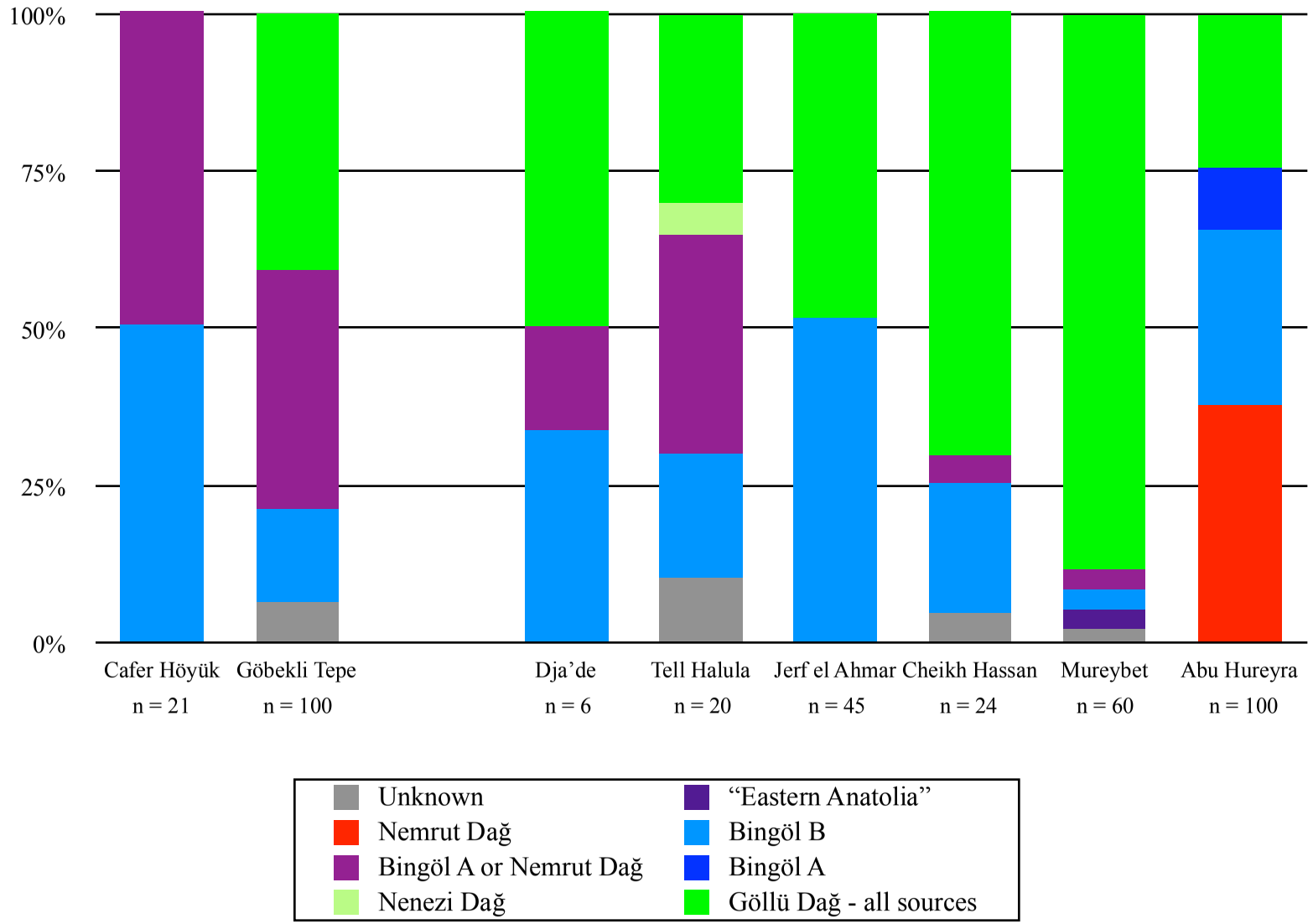
source of peralkaline obsidians here because the Murat River, a principal tributary of the Euphrates, flows near the Bingöl sources, so such obsidians could have been transported via river. If correct, though, the Abu Hureyra results cast doubt on this.

For comparison, in the Upper Euphrates area of southeastern Turkey, Cauvin et al. (1986) sourced 21 artifacts from Cafer Höyük. They ascribed all of them to Bingöl A and B and none to the Göllu Dağ sources. On the other hand, Le Bourdonnec (2008) recently analyzed 100 artifacts from Göbekli Tepe. Forty-one artifacts were assigned to the Göllu Dağ sources, and 15 artifacts were assigned to Bingöl B. Six had unknown sources, and he assigned 38 artifacts to Bingöl A. In both cases, for the peralkaline obsidians, Nemrut Dağ remains, based on their compositions alone, a possible source. Given that the Murat River follows past the Bingöl sources, they conclude that all of the peralkaline obsidian came from this region. This is the interpretation favored by Copeland (1995), who noted that Cafer Höyük lies "relatively near Bingöl, with direct access up the Murat Valley" (6). Figure 8.15 shows these source data for Upper and Middle Euphrates settlements together and suggests their inhabitants used obsidians from similar sources.

8.2.14 - Sourced Obsidian from the Neolithic Northern Levant

Bressy et al. (2005) sourced nine artifacts (circa the Ubaid to Halaf Periods, about 5700 to 4300 BCE) from Tell Kurdu in the Amuq Valley of Turkey, near ancient Antioch and modern Antakya. Three artifacts (33%) are attributed to the East Göllu Dağ sources, three (33%) to Bingöl A or Nemrut Dağ, and one (11%) to Bingöl B. One artifact (11%)

Figure 8.15 - Sources at Neolithic Upper- and Middle-Euphrates Sites - By Site: North to South



is tentatively assigned to "Ziyaret" (Meydan Dağ), and one (11%) is tentatively assigned to Pasinler. This final source assignment is interesting because Bressy et al. (2005) did not analyze any specimens from Muş. Given my challenges in clearly assigning artifacts to either Pasinler or Muş, I would suggest considering Muş, near the Bingöl sources, as another likely source assignment for this particular artifact.

Maeda (2003) analyzed obsidian artifacts from three sites in the El-Rouj Basin in far northwestern Syria. At Tell Abd el-Aziz, one blade (25%) was assigned to one of the East Göllü Dağ sources, one (25%) to Bingöl B, one (25%) to Bingöl A or Nemrut Dağ, and one (25%) to an unknown source. At Tell Aray, 12 artifacts (27%) were assigned to one of the East Göllü Dağ sources, four (9%) to Nenezi Dağ, 13 (30%) to either Bingöl A or Nemrut Dağ, eight (18%) to Bingöl B, and seven (16%) to an unknown source. At Tell el-Kerkh, 323 artifacts (88%) were assigned to the Göllü Dağ sources, 25 (7%) to Nenezi Dağ, ten (3%) to Bingöl B, five (1%) to either Bingöl A or Nemrut Dağ, and four (1%) to an unidentified source. It is worth noting that all of the artifacts from Tell el-Kerkh came from a lithic scatter within a single 5 x 5 m excavation square.

Renfrew et al. (1966) analyzed two obsidian blades from Ras Shamra (Ugarit) on the Mediterranean coast of Syria. A blade from Ubaid Period, circa approximately 5200 to 4000 BCE, was ascribed to their Group 1g, which is Bingöl B. The other blade, dating to the Pre-Pottery Neolithic (PPN), was attributed to Group 3, which is apparently one of the sources northeast of Lake Van. They also analyzed two PPN blades from Tell Ramad in southwestern Syria near Damascus, and both were attributed to Group 4c, meaning the

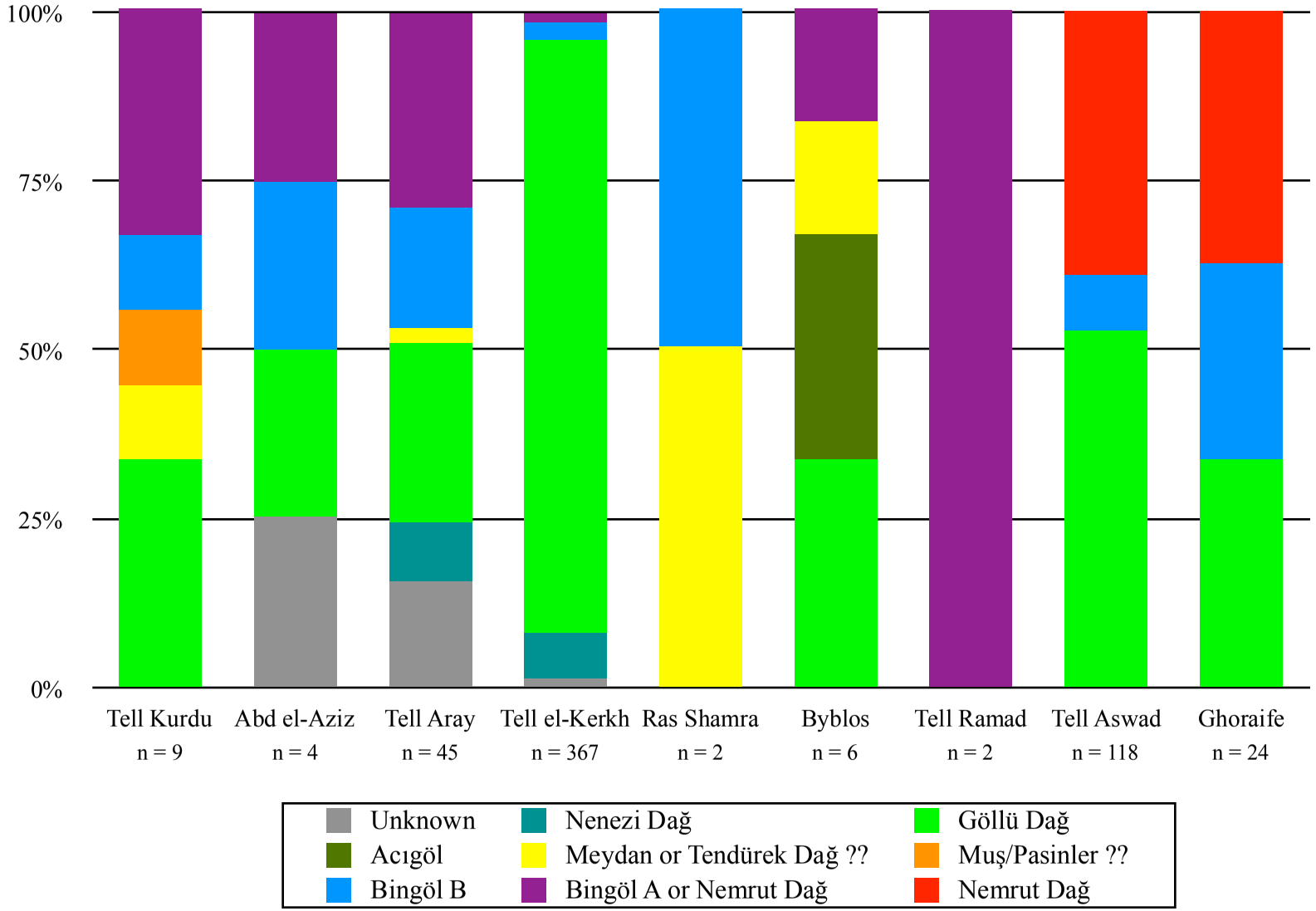
obsidian came from Bingöl A or Nemrut Dağ. In addition, they sourced six artifacts from Byblos in Lebanon. Two artifacts (33%) were assigned to their Group 2b (the Göllü Dağ sources), two artifacts (33%) to their Group 1e-f (the Acıgöl sources), one artifact (17%) to their Group 4c (Bingöl A or Nemrut Dağ), and one artifact (17%) to their Group 3 (the sources north of Lake Van, likely either Meydan or Tendürek Dağ).

Epstein (1977), working at the University of Bradford, analyzed 64 artifacts from Tell Aswad (circa 8000-6500 BCE) in the Damascus basin. Thirty-seven artifacts (58%) were assigned to their Group B1, which is equivalent to RNC's 2b and, therefore, one of the Göllü Dağ sources. Twenty-three artifacts (36%) were assigned to Group G1, which is supposedly Nemrut Dağ. The remaining four (6%) were assigned to Group B2, which supposedly corresponds to RDC's Group 1g and thus Bingöl B.

McDaniels et al. (1980), also at the University of Bradford, analyzed 54 artifacts from Tell Aswad and 24 artifacts from the nearby Ghoraife. At Tell Aswad, 25 artifacts (46%) were assigned to their Group B1, which is equivalent to RNC's 2b and one of the Göllü Dağ sources. Twenty-three artifacts (43%) were attributed to Group G1, which is supposedly Nemrut Dağ. The remaining six artifacts (11%) were assigned to Group B2, which corresponds to Bingöl B. At Ghoraife, eight artifacts (33%) were assigned to their Group B1, the Göllü Dağ sources; nine artifacts (38%) to Group G1, supposedly Nemrut Dağ; and seven artifacts (29%) to Group B2, which is Bingöl B.

Figure 8.16 shows the compiled data from these nine sites in the Northern Levant, listed in order from north to south. This graph suggests that, as distance from the sources

Figure 8.16 - Obsidian Sources in the Neolithic Northern Levant - North to South



increases, the number of sources represented at a site decreases. When it is compared to Figure 8.8, which shows the Bronze-Age and Chalcolithic source data, we have further evidence that, while the Neolithic obsidian distributions can have some similarities to the later distribution patterns, they must not be considered unchanged.

8.2.15 - Sourced Obsidian from Elsewhere in Neolithic Syria

Along the Balikh River, a tributary of the Euphrates roughly between the Middle Euphrates region and the Khabour Triangle, Gratuze et al. (1993) analyzed five obsidian artifacts from PPNB strata at Tell Assouad. Three artifacts (60%) were assigned to their Group 2, which is Bingöl B, and two artifacts (40%) were assigned to Group 1, which is Bingöl A or Nemrut Dağ. Based on the presence of Bingöl B, Gratuze and his colleagues interpret Bingöl A, not Nemrut Dağ, as the correct source of Group 1.

Renfrew et al. (1968) sourced six artifacts, all blades circa about 6000 BCE, from Bouqras in Syria, located in the Euphrates Valley roughly 35 km southeast of Deir ez-Zor. Four artifacts (67%) were assigned to Group 1g, which corresponds to Bingöl B. The last two artifacts (33%) fit their Group 4c, Bingöl A or Nemrut Dağ.

Gratuze et al. (1993) analyzed obsidian from three Neolithic sites near an oasis in the Syrian Desert. From PPNA and PPNB strata at El Kowm, three artifacts (44%) were assigned to either Bingöl A or Nemrut Dağ, one artifact (14%) to Bingöl B, two (28%) to the East Kayırlı source of Göllü Dağ, and one (14%) to the Hotamis Dağ source of East Acıgöl. From PPNB strata at Qdeir, eleven artifacts (44%) were attributed to Bingöl B,

nine (36%) to the East Kayırlı source of Göllü Dağ, and five (25%) to either Bingöl A or Nemrut Dağ. From PPNB levels at Umm el Tlel, five artifacts (63%) were attributed to Bingöl B, and three artifacts (37%) came from an unknown source. These patterns seem consistent with obsidian received from Middle Euphrates sites.

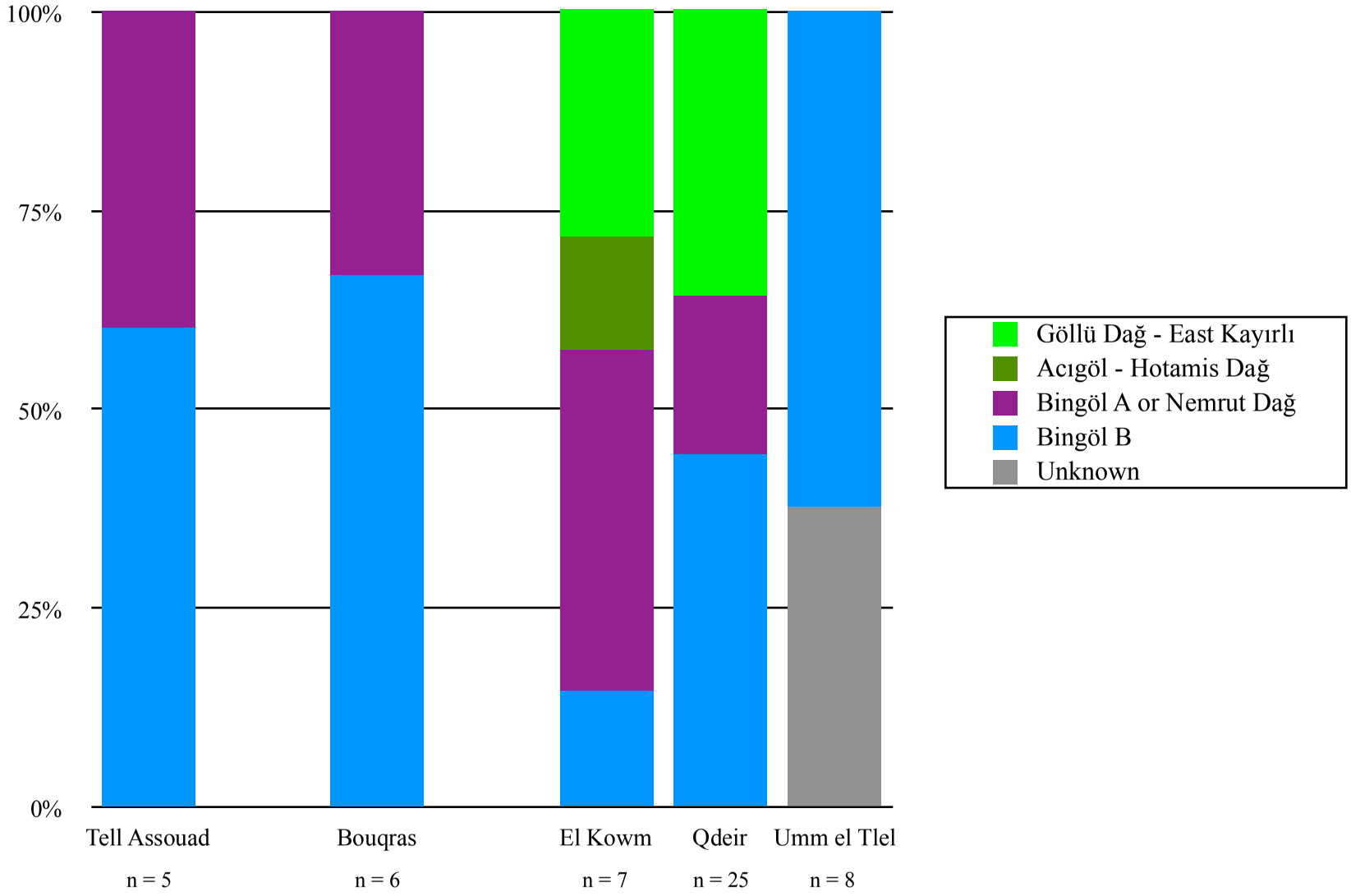
Figure 8.17 summarizes the data for these Syrian sites. It appears that, during the Neolithic at least, Central Anatolian obsidians rarely pass the Middle Euphrates Valley to reach the Balikh River in the Harran Plain, just south of Göbekli Tepe. Central Anatolian obsidians, though, do reach at least two sites in the Syrian Desert, south of the Euphrates. One could assume that the proportion of Bingöl A-to-Nemrut Dağ obsidians would be the same at these five sites as in the Upper and Middle Euphrates areas.

8.2.16 - Sourced Obsidian from in Neolithic Southern Mesopotamia

In northern Iraq, Cann and Renfrew (1964) sourced five Neolithic artifacts (Halaf and Ubaid phases) from Tell Arpachiyah near Mosul. Two artifacts (40%) were assigned to Group 4c, which is Bingöl A or Nemrut Dağ, and two (40%) were ascribed to Group 3, which includes the sources north of Lake Van like Meydan or Tendürek Dağ. One artifact (10%) was ascribed to Group 1, which includes a number of sources, including Bingöl B, which I suspect was a source group not recognized at this point.

Also in Iraq, Renfrew et al. (1966) analyzed nine artifacts from Jarmo (circa about 7000-6000 BCE) and two artifacts from Tell Matarrah (circa 5800-5300 BCE). At Jarmo, four artifacts (44%) were assigned to their Group 4c, which is Bingöl A and Nemrut Dağ,

Figure 8.17 - Obsidian Sources at Various Neolithic Sites in Syria



and five (56%) to their Group 1g, which corresponds to Bingöl B. At Tell Matarrah, both artifacts were ascribed to Group 4c, that is, Bingöl A or Nemrut Dağ.

At Choga Mami (circa 5500-4200 BCE), roughly 100 km northeast of Baghdad, Epstein (1977), working at the University of Bradford, sourced 79 artifacts. Twenty-one artifacts (27%) were assigned to Group B2 (Bingöl B), and one of the artifacts (1%) was ascribed to Group B1 (Göllü Dağ). Forty-one artifacts (52%) were ascribed to Group G1, purportedly Nemrut Dağ, and two artifacts (2%) were assigned to G2, purportedly Bingöl A. Nine artifacts (11%) were assigned to G3, also ostensibly from Nemrut Dağ. The last five artifacts (6%) were assigned to B3 and T1, both unknown.

Francaviglia (1994) analyzed 62 artifacts from Yarim Tepe in northern Iraq. Two artifacts (3%) were assigned to Bingöl B, and 48 artifacts (77%) were attributed to either Bingöl A or Nemrut Dağ. The other twelve artifacts (20%) "*could* be sourced to Central Anatolia" (emphasis added), but this assignment seems uncertain. Given that numerous sources were apparently left out of this study, these last twelve artifacts must be assigned to the "unknown" category. This article is so muddled that his assignments for the other three sites -- Tell Magzalia, Tell Sotto, and Kül Tepe -- are not listed.

In southern Iraq, Gratuze et al. (1993) analyzed five artifacts (circa Ubaid Period, about 5200-4000 BCE) from Tell el-'Oueili. Two artifacts (40%) were attributed to their Group 1, which includes both Bingöl A and Nemrut Dağ, and three artifacts (60%) were assigned to their Group 6, which did not have a known source.

Figure 8.18 summarizes the source data for these six Neolithic sites in Iraq. Only at the northernmost site, Tell Arpachiyah, is obsidian from Meydan Dağ or Tendürek Dağ found, and only one artifact at Choga Mami was (ostensibly) assigned to one of the Göllü Dağ sources. Figure 8.19 shows that half of the artifacts have not been firmly ascribed to a specific source, so conclusions about obsidian use are fleeting.

8.2.17 - Conclusions about the Prior Data

Clearly, one of the largest issues with these prior studies is an inability in most of them to distinguish Bingöl A and Nemrut Dağ obsidians. Only a few sourced artifacts per site also is a major problem in most regions. When displayed as relative proportions, not just as symbols on a map, the existing data indicate much greater complexity in obsidian sources represented as sites than the distribution maps imply. Consequently, I argue that there remains, even after four decades, too few sourced artifacts to test economic models of obsidian exchange. For the research at hand, the value of these earlier data, especially for the Khabur Triangle, lies in comparisons to my data from Tell Mozan. The results of such comparisons are used to consider the two issues about Urkesh and the Hurrians that I raised at the end of Chapter 3 and are the focus of the next chapter.

8.3 - Starting to Address Copeland's Questions

My results from Tell Mozan, when linked with Akkadian textual evidence as well as ethnographic data from around the world, have implications for Near Eastern obsidian studies that start to address some of Lorraine Copeland's questions.

Figure 8.18 - Obsidian Sources at Neolithic Sites in Iraq - North to South

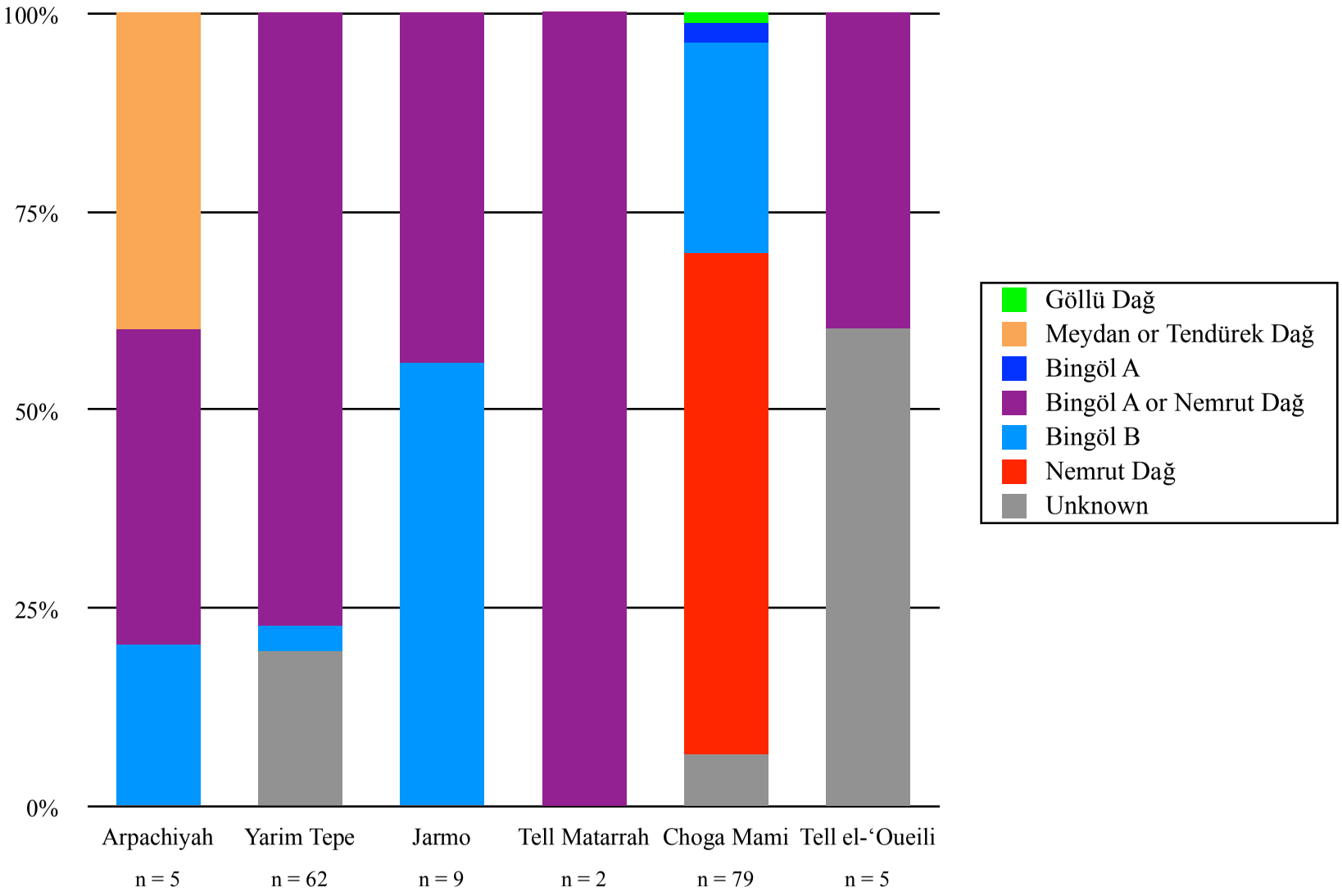
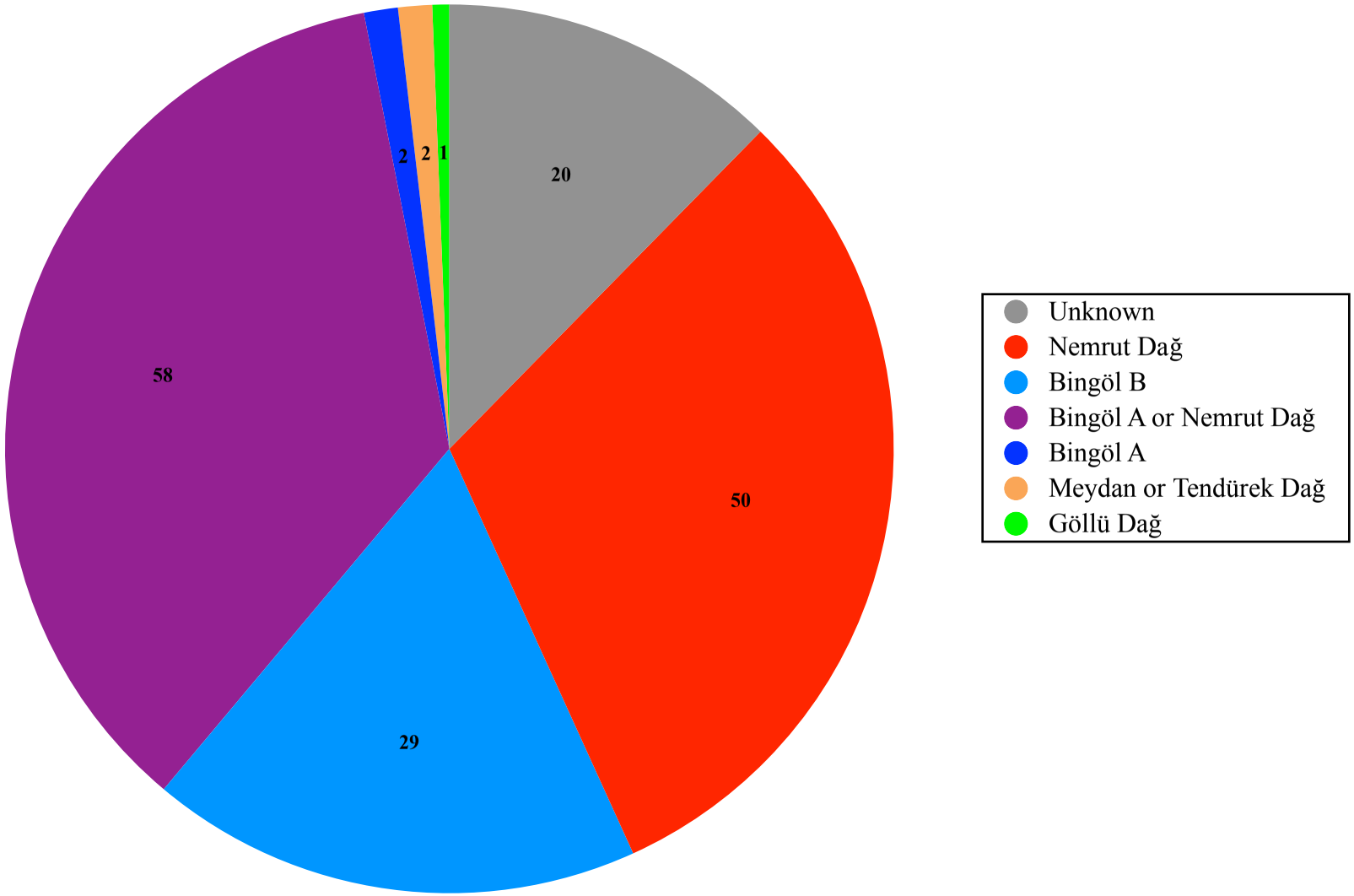


Figure 8.19 - Obsidian Sources at Neolithic Sites in Iraq



8.3.1 - A Note about Approaches to Exchange

I mention at the start of this chapter (and hopefully it is now clear to readers) that there remains insufficient data (i.e., sourced artifacts) to test economic models of obsidian exchange. It would take an entire volume to discuss the varied approaches to the analysis and modeling of exchange systems, so clearly such an overview is well beyond the scope of the chapter. Readers are instead forwarded to Polanyi (1957, 1963), Adams (1974) and the responses that follow, Hodder (1974), Sabloff and Lamberg-Karlovsky (1975) and the papers therein, Earle and Ericson (1977) and the papers therein, Ericson and Earle (1982) and the papers therein, Brumfiel and Earle (1987) and the papers therein, and Dillian and White (2009) and the papers therein for discussions of exchange.

It is worth reviewing, though, three schools of thought in economic anthropology. The first one is formalism. Earle (1982) explains that formalists "investigate the outcome of rational decision making with regard to the choices available to a population" (2), and their approaches follow the formalist school of economic anthropology. Such approaches often use mathematical models, like the fall-off curves of RDC or regression analysis, as a means to predict human behaviors based on a set of assumptions, primarily that humans choose alternatives with maximum utility for the cost and that their choices are rationally made using all available information. Exchange systems are therefore assumed to reflect the maximal utility, and a change in efficiency should also effect a change in the systems. Earle (1982) further explains that "sociopolitical institutions establish constraints in terms of the distribution and value of items. Then, individuals, acting within these institutional

constraints, procure and distribute material in a cost-conscious manner" (2). For instance, Torrence's (1986) analysis of prehistoric obsidian exchange in the Aegean area is focused on efficiency (e.g., "It is important to keep in mind that the types of behavior relevant for monitoring exchange are those that affect *efficiency*," 42).

An alternative is a substantivist approach. Substantivism, as explained by Earle (1982), explores how "economic behavior, including exchange, is embedded in broader social and political institutions" (2). Hodder (1982) similarly explains that substantivist approaches involve "understanding exchange as a part of social process -- functioning to provide essential resources, maintain alliances, or to establish prestige and status" (200). Prominent substantivists include Karl Polanyi (1957) and Marshall Sahlins (1972). This approach typically includes exchange models built on ethnographic data and tested using archaeological data. Cultural phenomena, not maximized efficiency, predominate in the substantivist school. Other factors can include symbolism, social change (such as social ranking and differentiation and the emergence of complex societies or political systems), and flow of information (not only materials). The last factor has long been recognized as an important component in exchange, and it returns us to the discussion in Section 2.2.1 about diffusionism in archaeology during the research of RDC. This is also the basis for using "stylistic" features of artifacts to recognize cultural contacts.

A third approach is culturalism, and its advocates include Stephen Gudeman at the University of Minnesota. Essentially taking substantivism even further, culturalism holds that economic concepts like exchange and profit are cultural constructs and, thus, must be

analyzed as they are conceived by the culture of interest. In other words, anthropologists must study "local models" and "people's own economic construction" rather than merely employing Western economic models (Gudeman 1986:1). For example, in rural Panama, Gudeman showed that the villagers viewed exchange as "exchange of equivalents" rather than a profit-generating enterprise. In addition, he asserts that many cultural phenomena, beyond simple efficiency, affect how individuals conceive of making a living: "Gaining a livelihood might be modeled as a causal and instrumental act, as a natural and inevitable sequence, as a result of supernatural dispositions or as a combination of all these" (1986: 47). He cites, for example, a sacred variety of rice grown by the Iban of Borneo, which is yields a surplus each year but is never exchanged (2001:32-33). Instead, this rice variety is thought to sustain the non-sacred rice varieties that are exchanged. This is reflected in the view of Hodder (1982), who asserted most exchange models are "inadequate because they fail to incorporate the symbolism of the artifacts exchanged" (199).

There is, at present, too little data to formulate a regional-scale economic model -- whether formalist, substantivist, or culturalist -- for Mesopotamia, especially when such a model must include a variety of cultures, not just the Hurrians. All three of these schools of thought, though, emphasize important factors that sourcing alone cannot answer alone: a sense of the value(s) of obsidian, how obsidian might have been transported, and other factors, beyond maximal efficiency, that might have affected peoples' choices in antiquity about which source(s) to use and how to use the gathered obsidian. In the next sections, I

offer a few suggestions, based on both textual evidence and ethnographic accounts, about how such factors might have affected obsidian use in the Near East.

8.3.2 - What is the Value of Obsidian?

Textural evidence indicates that obsidian was valuable in Northern Mesopotamia during the Bronze Age. In Section 2.1.2, I noted that the Chicago Assyrian Dictionary Project (CAD) has assembled a dictionary from Akkadian-language texts, circa the third and second millennia BCE, recovered from Near Eastern archaeological sites. The texts contain references to obsidian as a gift fit for deities and kings. For example, obsidian is included in a list of gifts to Tušratta, a second-millennium king of the Hurrian-controlled Mittani empire (CAD 1962:257). It is also recorded as one of the stones dedicated by the king Sargon to the Akkadian god Marduk (258). Another text describes an offering to the Akkadian god Adad: "in those days I brought [obsidian] from the mountains of Na'iri and placed them in the *hamru*-house of my lord Adad forever" (257-258).

These texts reveal that obsidian had value as a gift to a deity or king, but this does not necessarily translate to "economic" value. There are also texts, however, that indicate obsidian was valuable when exchanged or purchased. For example, a scribe wrote: "as to what the king, our Lord, has written us... obsidian has become expensive" (258). Another relevant text comes from Nuzi, a city in northern Iraq that became Hurrianized during the second millennium BCE. A scribe, in a register of horses, wrote: "one horse (description follows), [personal name] got it for a *surru* stone" (257). We are quite fortunate to have a

Hurrian text, dating to the second millennium BCE, that provides the value of an obsidian block or nodule. Two of the previously mentioned obsidian chunks, found near Tell Arqa in Lebanon, were reportedly 15 and 22 kg in mass and had been transported over 400 km. What size was the piece exchanged for a horse? This is a reason that the sizes of obsidian blocks and nodules at their sources much be investigated.

This Nuzi text suggests that the obsidian "stone" exchanged for a horse was not a finished artifact. The implication is that the obsidian took the form of a block, nodule, or core. Furthermore, it indicates that direct procurement of obsidian was not an option for the Nuzi inhabitants, at least not for everyone, but this is hardly surprising because Nuzi is over 400 km from the nearest sources in Eastern Anatolia. The other text, which states that obsidian has become expensive, supports the notion that, at least within the Akkadian empire, obsidian was not directly procured. The second implication of this text is that the value of obsidian has recently increased, perhaps due to an increase in demand and/or the effort required to gather the obsidian and then transport it. Texts, albeit from a different source, can also provide insight into how obsidian may have been transported in antiquity and who was transporting it from the sources into Mesopotamia.

8.3.3 - Possible Transportation via Rivers

The Greek historian Herodotus, who lived during the fifth century BCE, described the traders from Eastern Anatolia (which he called "Armenia") who travelled the cities of Southern Mesopotamia via the Euphrates and Tigris Rivers:

> The boats which float down the river to Babylon are completely circular in form and made of leather. The Armenians who live upstream from Assyria construct the ribs of the boat out of cut willow branches and stretch around them watertight skins to complete the hull… Then they stuff the entire boat with reeds, fill it with cargo, and release it to drift with the current down the river... These boats are constructed in all sizes, from small to very large… Each boat carries a live donkey; the larger boats hold several donkeys. With these they sail to Babylon, and when they arrive, they sell their cargo and auction off the ribs and reeds from the boats; but they load the skins onto the donkeys and lead them back to Armenia, for it is impossible for them to sail the boats back up the river due to its swift current. This is why the boats are made not of wood but of skins. So they ride the donkeys back to Armenia, and when they arrive, they make other boats in the same way. (Herodotus 1.194, in Strassler and Purvis 2007:105)

The accuracy of Herodotus' various accounts have been questioned as rather fanciful, but there seems little reason to doubt at least the essence of this report. Remains of bitumen-coated reed boats have been discovered throughout Mesopotamia. In the north, remnants of such a boat, dating to the fourth millennium, were found at Hacinebi Tepe in the Upper Euphrates Valley of Turkey (Schwartz 2002). Similar remnants have been documented as far south as Kuwait, dating to the sixth millennium (Crawford 2001). Also, as mentioned in Chapter 3, one Akkadian text included a complaint that beaver dams would sometimes impede shipping on the Euphrates (Landsberger 1934:86).

Evidence of boats in the Upper Euphrates Valley coupled with formalism seems to lend support to the assumption of Gratuze et al. (1993) that, if Bingöl B obsidian is found at a particular site, the peralkaline obsidians may be assigned to Bingöl A. As mentioned in Section 8.2.13, the principal tributary of the Euphrates, the Murat River, flows near the Bingöl sources, so those obsidians could easily have been transported via river. Thus it is often presumed the Upper Euphrates Valley sites engaged in direct collection of Bingöl A

and B obsidians. Not only, it is suggested, could the Bingöl A and B obsidians have been collected within several kilometers of one another, but also the river would have provided food and water for the duration of such a trip. Certainly this would be more efficient than traveling an additional 150 to 200 km east and climbing the sides of a massive volcano to acquire obsidian. The sourcing results from Abu Hureyra in the Middle Euphrates Valley and my results from Tell Mozan in the Khabur Triangle reveal, though, that Bingöl A and Nemrut Dağ obsidians were used synchronically at the two sites.

If additional sourcing research in the Upper and Middle Euphrates regions reveals Bingöl A and Nemrut Dağ obsidians used together, there are two possibilities: (1) people at Upper Euphrates sites did not directly collect some or all of their obsidian and engaged in exchange with groups, perhaps pastoral nomads, farther east, and/or (2) people in these settlements collected obsidian based on other factors, perhaps cultural, beyond the simple maximal utility suggested by formalist economic theory. In the following section, I offer a potential factor, supported by ethnographic and archaeological evidence from elsewhere in the world, that may have played a role in possible preferential exploitation of obsidian from Nemrut Dağ by certain groups in Northern Mesopotamia.

8.3.4 - The Importance of Location

The Bingöl A and B sources and Nemrut Dağ are about 150 km apart linearly (i.e., "as the crow flies"), and accounting for the mountainous terrain, this distance increases to 200 km or more. This corresponds to at least 40 hours by foot. Distinguishing Bingöl A

and Nemrut Dağ obsidians in sourcing studies, though, is about more than increasing the spatial resolution of the raw material's assignment to the landscape. I am also interested in the *experiences* of those who collected obsidian at the source.

Throughout my dissertation, I have often cited M. Steven Shackley as an expert in obsidian sourcing, especially in the American Southwest, and it should be clear to readers by now that I share many of his views on obsidian studies. Regarding gathering obsidian, though, Shackley has taken an essentially formalist view. In the first chapter of his book *Archaeological Obsidian Studies: Method and Theory*, he writes: "stone tool makers are often not concerned with the location from which they procure raw material, only that it be easily procurable" (1998a:6). Later, in his book *Obsidian: Geology and Archaeology in the North American Southwest*, he asserts: "Prehistoric knappers did not care -- indeed no one cared -- where they collected their raw material" (2005:26). Perhaps this is true in the American Southwest; however, ethnographic accounts and archaeological data reveal that the locations where raw materials, such as obsidian and chert, are collected can have important meaning or symbolism that affect collectors' choices.

Regarding obsidian in ancient Mesoamerica, Saunders (2001) states that "mines appear to have been an important physical and metaphysical component of a landscape where individual features were given cosmological significance" (229). Similarly Dillian (2002) found that obsidian from the Glass Mountain lava dome in California was used for different purposes than obsidian from other sources. She writes:

> Ultimately, differential use of Glass Mountain obsidian lies in the context of cultural beliefs, which hold it as a special source to be used exclusively for the

> production of valued objects… while other nearby obsidian was exploited for utilitarian objects… In this sense, the quarry was in itself also an active agent, which gave value to things. It provides evidence for integration of prehistoric belief systems into toolstone procurement and use patterns through the selective use of Glass Mountain obsidian for ceremonial and value objects. (2002:2)

Therefore, the Native American cultures who used Glass Mountain obsidian certainly did care from where it originated, and for some reason, Glass Mountain held a different status than other obsidian sources. This prestige is linked to oral histories and legends about the formation of this lava dome and its obsidian (documented in Hodgson 2007), which dates to about 1100 CE and may indeed have been witnessed. Dillian proposes that witnessing "Glass Mountain's powerful obsidian-forming eruption strongly contributed to the valued status of this obsidian source" (2002:92). She points out that, consequently, "the cultural context of the prehistoric belief system and oral histories about Glass Mountain underlie selective procurement and use of this obsidian source" (92).

Indeed, the selection of lithic material can have important symbolism and cultural meaning. For example, among the Australian Aborigines of Arnhem Land, Taçon (1991) states that quartzite deposits are considered "the petrified remains of the bones of certain Ancestral Beings" (197) while, simultaneously, "the power of Ancestral Beings... created the landscape, including rocky outcrops used as quarries" (194). When tools were made from the remains of Ancestral Beings "powerful and effective pieces would result" (205). Quartzite is associated with Ancestral Beings, Taçon (1989) explains, because it is nearly iridescent, and iridescence is symbolic of life as well as Ancestral Beings. He also notes that a quarry is also "often given heightened significance by associating it with powerful,

dangerous forces" (1991:199). His accounts reveal that lithic materials and their sources can be given cultural meanings that affect their selection and use.

Other times there may be simpler factors involved in the selection of a quarry site, like a workspace with a view. Bradley (2000) studied the acquisition of raw materials for stone axes in Great Britain, and his results refute that maximal utility guided the selection of quarrying sites. He found that, based on their flaking properties, high-quality material in accessible locations went unused while "inaccessible exposures with the same physical characteristics were employed instead" (86). He proposes that the "character of the place seemed at least as important as the qualities of the material" (86-87). He explains:

> … a survey of the entire distribution of the parent rock shows that, contrary to the Principle of Least Effort, people chose to quarry the stone in precisely those areas that were located furthest from the lower ground. They also selected quarry sites overlooking the steepest gradients… the quarries that provided most of the raw material were on narrow edges high up on the face… in locations that were both difficult and dangerous to reach… Taken together, the production sites are among the most remote archaeological monuments anywhere in England [and] are within a short distance of the highest point in the country. (86, 87)

What then was the reason for quarrying in such inaccessible locations? Bradley observes that these formidable sites "commanded enormous views" (86).

The proverb "getting there is half the fun" provides another issue to consider. For example, Hodgson (2007) reports that, for the Wintu Native American tribe in California, mining obsidian had religious components, and the sacrality extended to the journey itself to the obsidian sources at the Glass Mountain lava dome. She writes:

> The Wintu of McCloud River in northern California used obsidian from Glass Mountain. In the summer, two or three men would make a two- to three-day trip

> NE to the quarry. The men fasted throughout the journey, as the act of obtaining obsidian was seen as a semi-religious quest. (307)

This implies that the journeys to and from the obsidian sources, as well as the experiences along the way, can also be significant factors in material selection.

Hodgson's account indicates the potential for a phenomenological approach, like that advocated by Christopher Tilley (1994, 2004), to interpret cultural landscapes. Tilley points out that phenomenology "attempts to reveal the world as it is actually experienced directly by a subject [and] to describe that world as precisely as possible in the manner in which human beings experience it" (2004:1). He argues that such an approach can reveal how people in antiquity interacted with and conceived of the landscapes around them. It asks archaeologists to enter into the physical landscapes and experience them using their own senses. For the Wintu, Glass Mountain and the McCloud River are elements of their cultural landscape, defined by Tilley (1994) as "a set of relational places linked by paths, movements, and narratives… It is invested with powers… and is always sedimented with human significances" (34). Tilley is even interested in rock outcrops' (1994:76-110) and stone monuments' relationships (2004) to cultural landscapes.

Phenomenology is a controversial school of thought in archaeology. We need not, however, subscribe wholesale to the perspectives of existential phenomenologists such as Heidegger or Merleau-Ponty to recognize that, based on ethnographic and archaeological evidence, we must consider symbolism of the landscape as well as the sights, sounds, and smells experienced by those who acquired obsidian at the source. Such factors can affect material selection and how the material was subsequently used.

8.3.5 - Obsidian Sources and their Landscapes

Based on the data that I summarized above, there is a possibility that Nemrut Dağ obsidians predominate at Mesopotamian sites. At least one recent meta-analysis of prior studies (Chataigner et al. 1998) suggests that peralkaline obsidians from Nemrut Dağ, not Bingöl A, reached Southern Mesopotamia, presumably via exchange. I also showed that, like Abu Hureyra in the Middle Euphrates area, obsidians from Bingöl A and Nemrut Dağ were used together at Tell Mozan. This result is contrary to the assumption by Gratuze et al. (1993), which is, in essence, based on maximal utility: if Bingöl B obsidian is found at a site, one can presume that any peralkaline obsidians originated from Bingöl A. In other words, if Bingöl B obsidian was already being gathered, the most efficient place to obtain peralkaline obsidian is Bingöl A. Because Bingöl A and Nemrut Dağ obsidians are found together, maximal efficiency cannot be the only factor involved. Accordingly, I conclude this chapter with a suggestion, albeit a speculative one, about the potential abundance of Nemrut Dağ obsidians at many sites throughout Mesopotamia.

As discussed in earlier sections, Nemrut Dağ is an active stratovolcano that, about 270,000 years ago, experienced a major caldera collapse, creating a circular basin about 7 km (4 miles) by 8 km (5 miles) in diameter. The western half is filled with a lake, and the eastern half has obsidian-bearing lava flows, maars (i.e., craters), and a small lake fed by hot springs. This caldera is the reason that Nemrut Dağ has been called "one of the most spectacular volcanoes of eastern Anatolia" (Yılmaz et al. 1998:175).

Recall Bradley (2000) observed, as noted in the last section, that Neolithic stone-axe quarries in Great Britain had inconvenient, even dangerous, sites but "commanded enormous views [from] within a short distance of the highest point in the country" (86). Consider then the following account from Harry F. B. Lynch, recorded in his 1901 book *Armenia: Travels and Studies*, of his visit to Nemrut Dağ:

> After a short halt, we led our horses up the slope... It was covered with grass, and whole beds of wild pea. These sides of the crater are seamed with deep gullies, which display in section the lava-flows. The dark green obsidian of the uppermost beds was glittering in the sun. A direct ascent of twenty minutes brought us to the surface of a natural terrace... the summit of the circular wall... *The view from this terrace over the landscape of the east is one of the most inspiring that could be conceived.* (300; emphasis added)

He is describing the view looking out to the east, which includes Lake Van, Süphan Dağ, and the northwestern Zagros and eastern Taurus mountain ranges. He then recounts what he saw when looking down into the Nemrut Dağ caldera:

> The ground falls away, and a scene expands before us which Mother Earth, repentant of her orgies, has acted wisely in surrounding with a wall. The whole circumference of the gigantic circle towers around us, the vaulted slopes of the outer sides breaking down with precipitous cliffs, which, in some places, attain a height of over 2000 feet above the rubble at their base. The impression of height and steepness is accentuated by the lighting -- the sun setting behind the crater. The same circumstance increases the weirdness of the vast spaces of the interior, with their multitude of chaotic forms. Flatness is the prevailing characteristic of the bottom of the basin -- but the surface has been blown out by subterranean explosions, or sunk into deep pits, or flooded with viscous lavas, oozing up, and cooling into comb-shaped crags. Here it is a shapeless hill covered with white volcanic dust; there a lava stream, resembling rocks from which the tide has receded, that compels a large circuit from point to point... and the only touch of beauty in this hell of Nature is a little piece of blue... the principal lake. (301)

Lynch offers his perceptions of the caldera interior, something missing from the "clinical"

descriptions of Nemrut Dağ in the geological literature (e.g., Aydar et al. 2003; Karaoğlu et al. 2005; Özdemir et al. 2006, 2007; Ulusoy et al. 2008). This description emphasizes otherworldliness of the place, exhibiting its "weirdness" and chaos.

Lynch also contends that the uniqueness of Nemrut Dağ and its dominance of the physical landscape must draw in travelers out of sheer curiosity:

> The commanding position, the imposing dimensions, the remarkable preservation of the Nimrud crater cannot fail to arouse the curiosity of the traveller, as he sees it from afar or passes it by... it is a startling presence against the sky... such a presence fills the landscape and engrosses the eye. (305).

The result is similar to Molyneaux's (2002) hypothesis that Devils Tower and Obsidian Cliff, both in Wyoming, played wayfinding and cognitive-mapping roles for exchange of obsidian across long distances in North America. Molyneaux claims:

> …the obsidian at Devils Tower and Obsidian Cliff, the two imposing volcanic features at opposite ends of Wyoming, suggest different impacts on the discrete movements of people and resources. Obsidian Cliff exhibits a powerful *centrifugal* effect, as people carried its raw material across vast regions of central North America. Devils Tower exhibits a *centripetal* effect, as it drew -- and continues to draw -- travelers from all directions to its sides. (2002:136)

In this case, one could argue that Nemrut Dağ is simultaneously a conspicuous landmark that draws in travelers (i.e., Molyneaux's centripetal effect) and a source of raw materials that are widely distributed by its visitors (i.e., his centrifugal effect).

In 1978, anthropologist Roger Cribb (1991) conducted an ethnographic study of the Alikanli, a group of Kurdish pastoral nomads who spent summers inside the Nemrut Dağ caldera. Cribb describes approaching the caldera from the shores of Lake Van, that is, from the opposite direction as Lynch's approach (1991:185). He writes:

> Having climbed the 2,000 metres or so from the shores of Lake Van to the rim of the crater of Nemrut Dağ, the traveller is treated to an awesome sight. Below stretches a huge basin surrounded on all sides by precipitous walls. The interior is a tumbled chaos of conical hills, lava flows, depressions and jagged outcroppings of rhyolitic rock and obsidian, its western half drowned by the icy waters of a large semicircular lake... On descending into this lost world, the encircling mountain rim closes off the outside world leaving only the barren moonscape of stony ridges, scree slopes and flat internal drainage basins of alluvial ash...

Cribb's account echoes that of Lynch. Both of them state that "travelers" will experience incredible views of the landscape, and both stress otherworldliness of the caldera interior. Cribb's description of cutting "off the outside world leaving only the barren moonscape" may remind readers of my descriptions in Section 4.5, written completely independently, of the lava flows in the Newberry Volcano caldera. I described the flows as "quasi-lunar landscapes," and about Big Obsidian Flow, I claimed that "when standing between these ridges, the gray, rocky, nearly lifeless surface is all one can see other than sky. It is little exaggeration to say that the surface... seems otherworldly."

I explain in Section 4.5 how my fieldwork at Glass Buttes and Newberry Caldera affected my perception of what constitutes an obsidian "source," but I also point out that I wanted to have the experiences of acquiring obsidian so that I could better understand the experiences of people doing the same in antiquity. My experiences of seeking obsidian at the two places were quite distinct, as I discuss in that section. Almost every sight, sound, and smell was different. For instance, after a little afternoon drizzle at both places, Glass Buttes was filled by the pungent odor of sagebrush while Newberry Caldera had pine and earthy scents. Bald eagles, to which one might ascribe special meaning, may be watched and heard from atop the obsidian-bearing lava flows at Newberry Caldera while there are



Figure 8.20 - The chaotic surface of a lava dome, specifically Big Obsidian Flow at Newberry Volcano, when viewed from the caldera rim (photographs by the author).

none at Glass Buttes. Because bald eagles are symbolic of the United States (e.g., a bald eagle is incorporated into most official seals, including the Great Seal of the United States and the Seal of the President), perhaps one could consider it more "American" to collect obsidian at Newberry. Today, though, one cannot gather obsidian at Newberry because it is ascribed "national significance" and "exceptional value" as a national monument (like Devils Tower), whereas Glass Buttes is simply public land (NPS 2003). Part of its value, no doubt, derives from the spectacular views from the caldera wall, especially the portion known as Paulina Peak at an elevation of more than 2400 m.

Recall Dillian (2002) claims that Native American groups probably witnessed the eruption of Glass Mountain about 1100 CE and that this "contributed to the valued status of this obsidian source" (92). Sediments from the bottom of Lake Van show that Nemrut Dağ erupted ash at least three times during the sixth and fifth millennia: circa 5242 ± 72, 4938 ± 69, and 4055 ± 60 BCE. One or more of these eruptions were certainly witnessed by pastoralists in the area. The last eruption was in April 1692, and Nemrut Dağ remains active. Adjacent to the large caldera lake is a small lake fed by hot springs. One of these springs has a temperature of 58° C (Ulusoy et al. 2008), and others have temperatures of about 34° C (Atasoy et al. 1988, Ulusoy et al. 2008). Lynch (1901) reports that the warm lake is believed by the locals "to possess healing properties" (307). Steam and gas vents are often active on the caldera floor (Yılmaz et al. 1998:177). Any of these factors might have given a special status to Nemrut Dağ, leading to preferential use of its obsidians as well as their occurrence together with Bingöl A and B obsidians.

8.4 - Summary and Concluding Remarks

At the very start of the chapter, I consider Copeland's concerns about the focus of obsidian research in the Near East. I contend that her concerns regarding a current focus on sourcing are, at least in part, unfounded because we have rather few sourced obsidian artifacts from Mesopotamia, particularly for the Chalcolithic Period and the Bronze Age. By presenting what little data we have in plots that emphasize the relative proportions of artifacts from different obsidian sources, it becomes evident that exchange patterns were more complex than the distribution maps imply. These sourcing data will also be useful for comparison in Chapter 9 to my own results from Tell Mozan.

Then I discuss my findings that have broader implications for the Near East. My findings suggest that blocks or cores were transported to Urkesh, where prismatic blades were made on-site. I revealed that Blackman's (1984) chemical clusters for Nemrut Dağ and Poidevin's (1998) classifications based on "peralkalinity" cannot be linked to specific locations on the volcano. In addition, I showed that Gratuze's premise -- that peralkaline obsidian should be assigned to Bingöl A, not Nemrut Dağ, when obsidian from Bingöl B has been found at a site as well -- is not valid. Because this result suggests that maximal efficiency (discussed in the section about approaches to studying exchange) may not have been the determining factor, I offer, based on ethnographic and archaeological evidence, possible influences on the use and exchange of Nemrut Dağ obsidians, such as culturally based symbolism and "arbitrary" factors like impressive views.

Part III: Results and Implications

Chapter 9:

Implications for Urkesh and the Hurrians

> … there in the distance we can see the outer folds of the great Anatolian mountain ranges conjuring up visions of Armenia, Ararat, Van and the lofty Caucasus. As evening set in at Chagar Bazar we could see the lights of Mardin twinkling at us from the hills, fifty miles away. Thence down the precipitous mountain roads, from Urfa, Diyarbakr and elsewhere, in ancient times many a hillman must have set out on his way to the Khabur; warriors, traders, birds of passage, and settlers, all of them seeking their fortunes in the open plains.
>
> -- Max Mallowan, 1947, *Excavations at Brak and Chagar Bazar*

Mallowan here describes the important mountain pass near the town of Mardin in Turkey, a prominent feature of the landscape around Tell Mozan. This is the key route by which the Mesopotamian plains were accessed from the Tur Abdin highlands to the north and vice versa. Urkesh was most likely strategically founded near the pass, which is also most likely how most obsidian (and other mountain resources such as copper) reached the city. In fact, today, there is still evidence in Mardin of obsidian being transported through this pass. An obsidian nodule is embedded in one wall of the Ulu Mosque, and the locals believe that, when touched, the nodule cures certain diseases. Thus the Mardin Pass is an important component of this chapter, particularly regarding a hypothesis about a northern hinterland of Urkesh. Therefore, this pass is discussed here first.

I also discuss the variety of obsidian sources represented among the artifacts from Tell Mozan and the implications for this settlement and its inhabitants, and I point out the significance of Central Anatolian obsidian recovered as far east as Tell Mozan. Temporal and spatial patterns of obsidian source use will also be presented and discussed. I briefly consider other indicators of inter-regional contact and exchange at Urkesh and argue that they cannot provide the same kinds of information as obsidian sourcing. The hypothesis of a Hurrian "homeland" as far northeast as Armenia (or beyond) is considered -- but not supported -- in light of my obsidian data. Regarding the issue of "Nawar," mentioned at the end of Chapter 3, I consider whether my obsidian data, when compared to the earlier data from other Khabur Triangle sites, indicates an extensive mountainous hinterland for Urkesh. The data for Tell Mozan and Tell Brak (likely ancient Nagar) are also compared, with surprising results that suggest some link between to these settlements. It might have been that both Urkesh and Nagar were gateway cities or instead functioned as a gateway-city/central-place pair, a concept defined by Burghardt (1971). The mechanisms for these scenarios, including pastoral nomadism, are considered in each case. Finally, I consider the importance of Nemrut Dağ obsidians, which are the only obsidians found in each site area and for all time periods. The implications of acquiring obsidian from one particular location within the caldera for over a millennia are considered.

9.1 - Urkesh and Ancient Exchange Routes

Figure 9.1 shows how Urkesh sat at the cross-roads of two principal north-south and east-west transportation routes in antiquity. This east-west route ran largely parallel

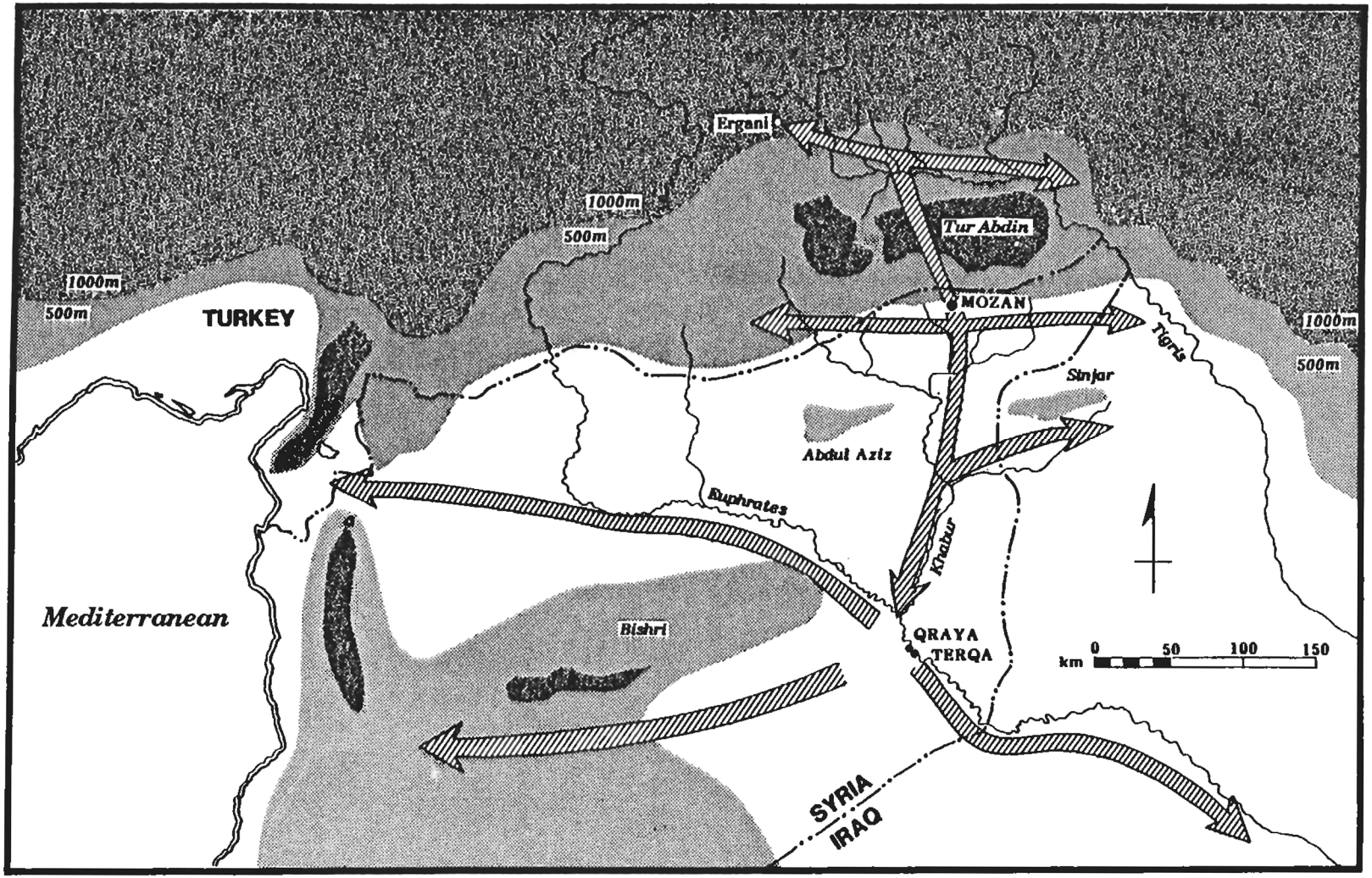


Figure 9.1 - Urkesh at the crossroads of N-S and E-W transportation routes (Buccellati and Kelly-Buccellati 1988, Fig. 2).

to the Tur Abdin and Taurus mountains, along the northern border of the Khabur Triangle and eventually reaching the Northern Levant in the west and the Zagros mountains in the east. My main interest here, though, is the north-south route.

As I noted in Section 3.3, the Tur Abdin, the front range of the Taurus Mountains, fills one's view to the north from Tell Mozan. To the northwest, as seen in Figure 9.2, is the most important mountain pass from Anatolia to Mesopotamia, and it is named for the town that lies directly within the pass: Mardin. The quotation from Max Mallowan at the beginning of this chapter actually refers to this pass. Geographer Louis Dillemann (1962) and archaeologist Guillermo Algaze (1999) -- see Figures 9.3 and 9.4 -- reconstructed the road network of the Roman Empire and illustrate the significance of the Mardin Pass. In fact, Nero's army entered Mesopotamia via the saddle-shaped mountain pass (Henderson 1905:176). Several reconstructions of the Silk Road and the Persian Royal Road also use the Mardin Pass, and both roads likely followed much older routes. Given its prominence on the horizon, this pass must have been used for millennia prior.

In their book *The Archaeology of Syria*, Akkermans and Schwartz (2003) propose that "Mozan's location at the northern edge of the Khabur plains near the Mardin saddle may indicate control of the route [into] eastern Anatolia -- and perhaps an entry point for Hurrian individuals arriving from the highlands to the north" (285-286). Buccellati and Kelly-Buccellati (1988) point out that Tell Mozan, in the alluvial plain just south of the foothills, had a superior location in antiquity to access this mountain pass (26). The pass



Figure 9.2 - The mountain pass near Mardin, Turkey viewed from the ruins of the Tupkish Royal Palace. The modern-day village of Mozan is visible in the lower left, and the town of Amuda is visible in the distance (Urkesh expedition photograph).

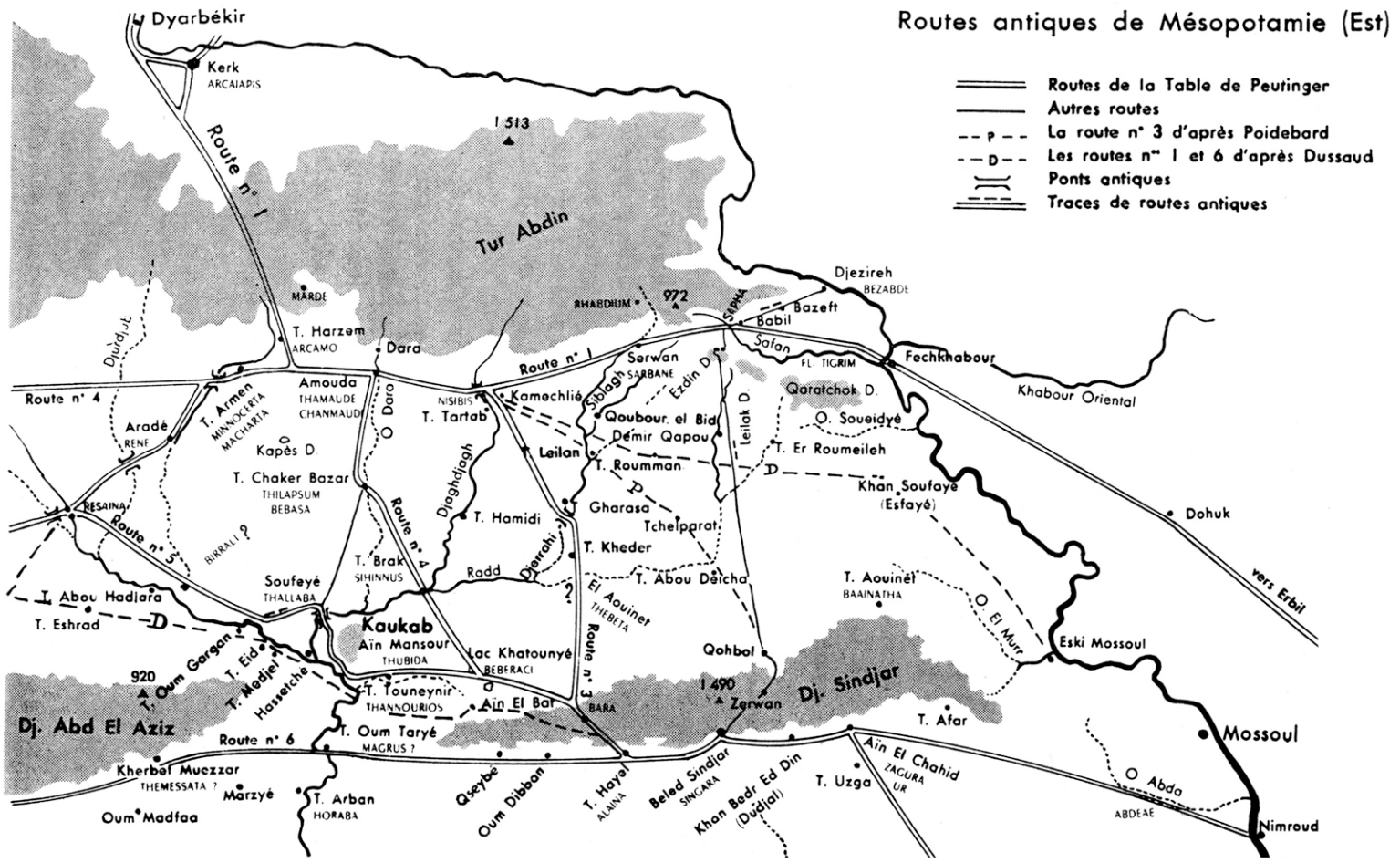


Figure 9.3 - Major transportation routes across the Khabur Triangle reconstructed from Roman itineraries (Dilleman 1962, Figure 18). Tell Mozan lies less than 8 km east of Amuda, the modern Syrian city at the southern side of the Mardin Pass.

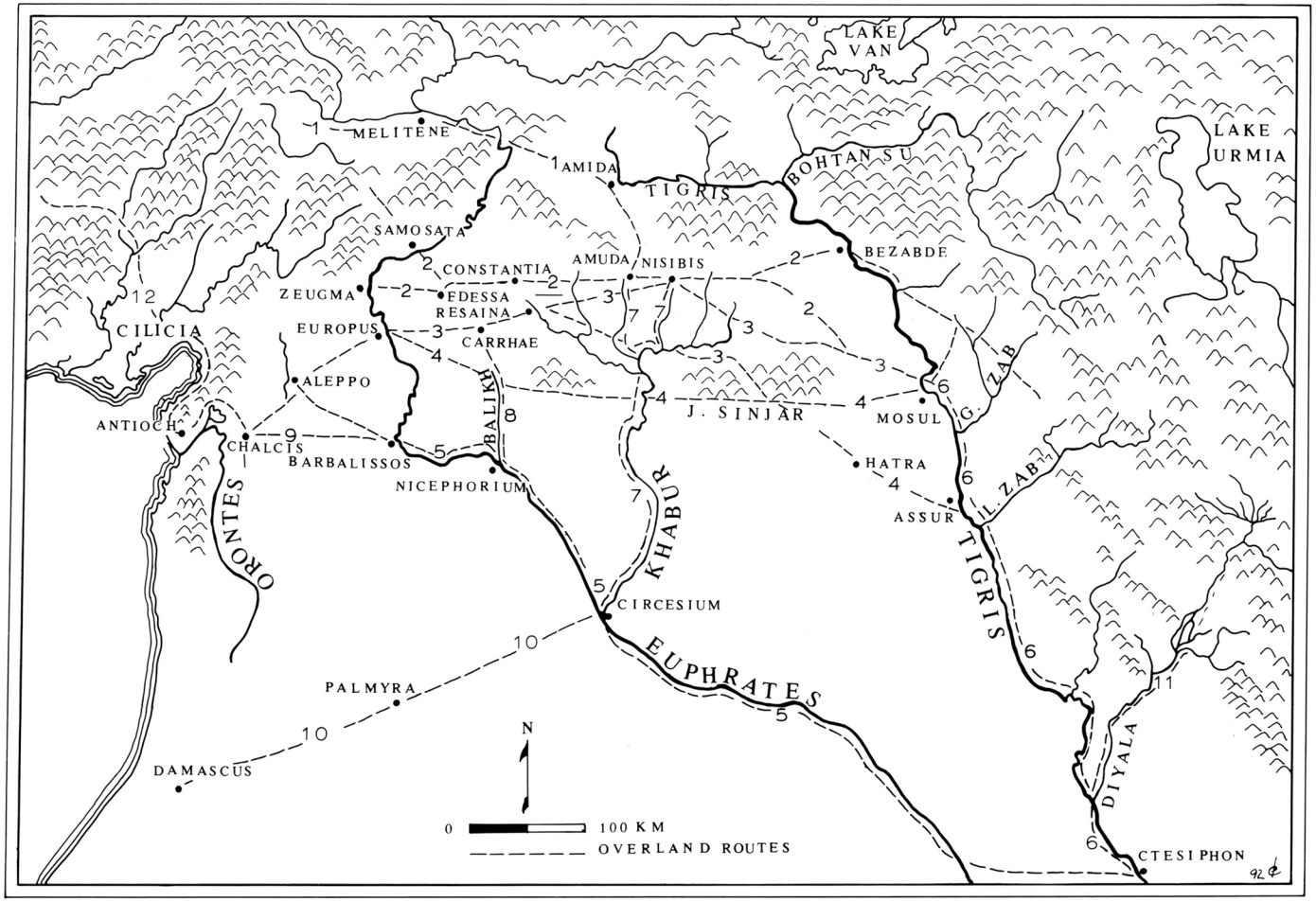


Figure 9.4 - Principal transportation routes across Northern Mesopotamia during the Classical Period (Algaze 1999, Figure 20). Tell Mozan lies less than 8 kilometers east of Amuda, the modern Syrian city at the southern side of the Mardin Pass.

itself, where the town of Mardin (Syriac for "fortress") now lies, experiences more severe temperatures, and water would not have been readily available.

Buccellati (1988) proposes that this conspicuous pass could have served "almost as a visual symbol of an opening to the northern highlands" (38). In addition, he explains a suggestion from Alexis de Morgan, a specialist in the Caucasian and Hurrian languages, about a possible etymology for the name *Urkesh* or *Urkish*. The Hurrian suffix *-is*, which was first recognized by Gelb (1944), might be linked to a Caucasian word for "mountain" while the root *urki* might related to a word for a saddle-shaped cradle. Hence, Buccellati points out: "if so, the name might be a reflection of the saddle-pass of Mardin, one of the most noticeable aspects of the local landscape" (1988:38).

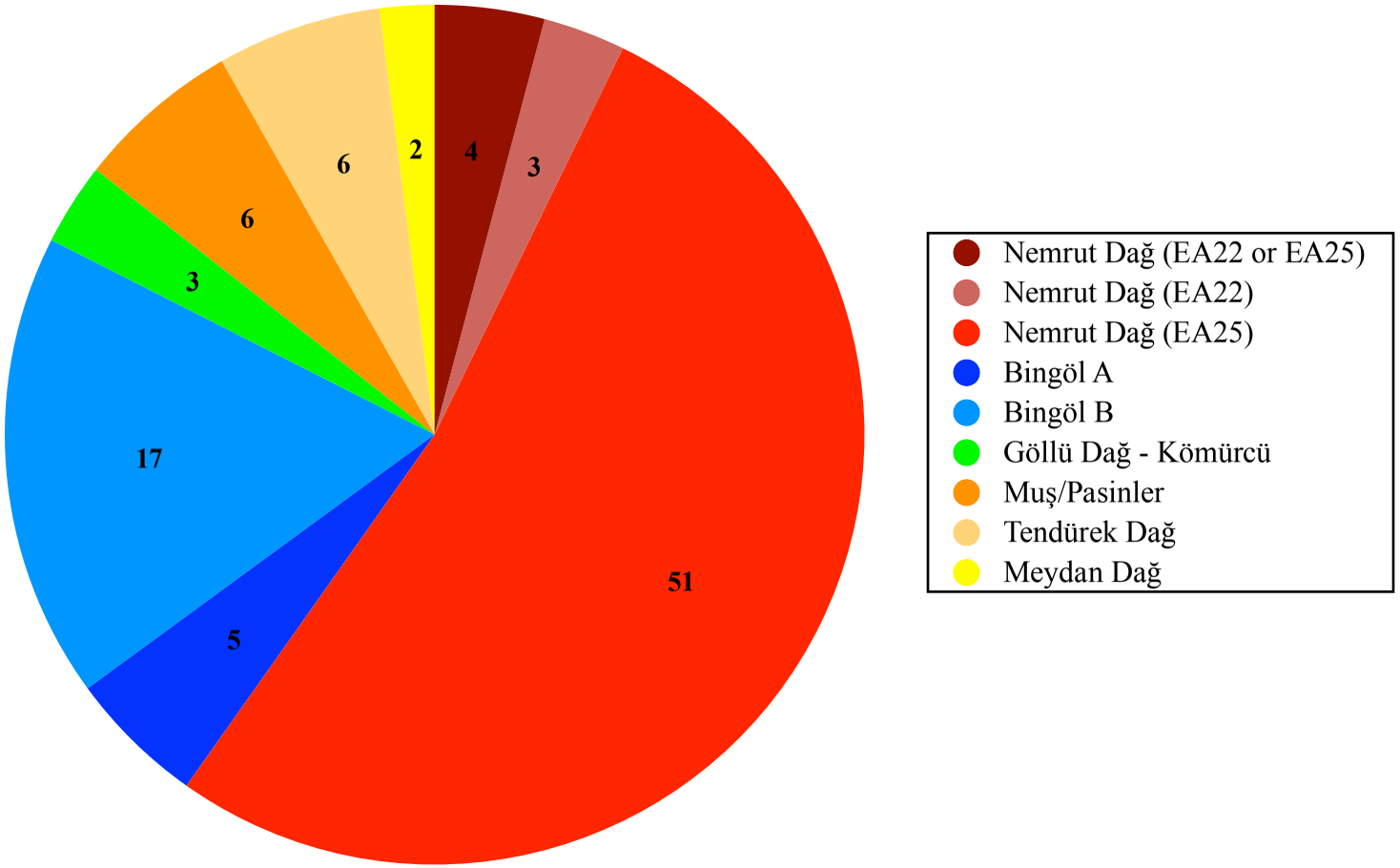
9.2 - Observations on the Obsidian Data

Before applying my obsidian data from Tell Mozan to larger questions regarding Urkesh and the Hurrians, it is worth discussing my results, noting any trends, and briefly considering the implications regarding the site's ancient inhabitants.

9.2.1 - Obsidian Sources at Tell Mozan

After my review in Chapter 8, it should be clear that a relatively large number of sources are represented among the obsidian artifacts at Tell Mozan -- depending on how one defines a "source" of obsidian, there are at least seven or eight sources, maybe even as many as nine. The obsidian sources at Tell Mozan include two intra-caldera flows at

Figure 9.5 - Source Assignments for Bronze-Age Obsidian Artifacts from Tell Mozan



Nemrut Dağ (either one or two sources, depending on one's definition of a "source," as discussed in Section 4.4), the Bingöl A and B sources, Meydan Dağ, Tendürek Dağ, the Kömürcü source of Göllü Dağ, and Muş and/or Pasinler.

Only a handful of sites, mostly during the Neolithic, have obsidians from as many as five or six sources (e.g., Neolithic Tell Halula and Mureybet in the Middle Euphrates, Neolithic Tell Halaf in the Khabur Triangle, Neolithic Choga Mami in Iraq, and Neolithic Tell Kurdu and Tell Aray in the northern Levant). Most sites, though, have obsidian from just one to three sources, including Bronze-Age sites in the Khabur Triangle. Recall that most sourcing studies cannot discern Bingöl A and Nemrut Dağ obsidians, so it is usually unknown if the peralkaline obsidians came from one or two sources. Furthermore, rarely have the individual sources at Nemrut Dağ been recognized.

At least in part, this diversity of identified obsidian sources at Tell Mozan may be a result of studying 97 artifacts, not merely five or ten. I mentioned in Section 2.3.6 that Epstein (1977) analyzed 79 obsidian artifacts from Neolithic Choga Mami, and he found eight different chemical clusters in the data, although some clusters could not be matched to a volcanic source. Consider, though, that Francaviglia and Palmieri (1998) sourced 16 artifacts from Neolithic strata of Tell Hamoukar, and all of them were assigned to Nemrut Dağ and/or Bingöl A, whereas Pernicka et al. (1997) sourced 20 artifacts from Tell Halula and recognized several sources: two Göllü Dağ sources, Nenezi Dağ, Nemrut Dağ and/or Bingöl A, Bingöl B, and an unknown source. Abbès et al. (2001) and (2003) analyzed 44 artifacts from Jerf el Ahmar and found only two sources present, and Maeda (2003) found

five obsidian sources among the 367 artifacts at Tell el-Kerkh. Figure 9.6 shows that the number of sourced artifacts, after a minimum of roughly five or ten, is a poor indicator of the number of obsidian sources one will find among them.

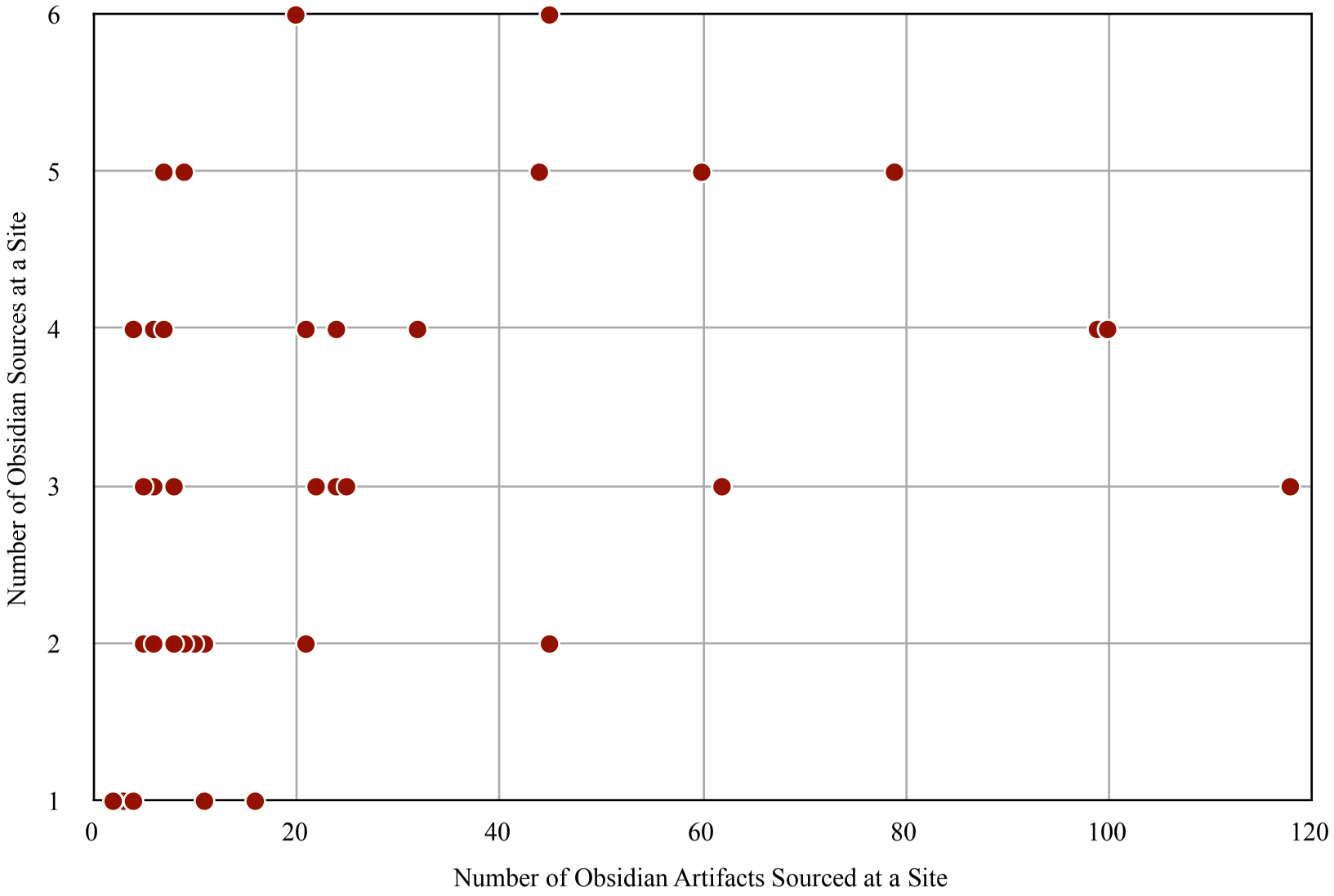
The bottom line is still that, compared to the other archaeological sites considered in Sections 8.2.1 to 8.2.16, there are more (in some cases, many more) obsidian sources represented among the artifacts at Tell Mozan. This will be important later in the chapter when a hypothesis about the hinterland of Urkesh is considered.

About 97% of the sourced artifacts at Tell Mozan came from obsidian sources in Eastern Anatolia. About 60% of the obsidian comes from only two flows at Nemrut Dağ, and both flows lie in its caldera, not on the exterior slopes. Nearly a quarter (23%) of the artifacts originated from both Bingöl sources: 5% from Bingöl A and 18% from Bingöl B. About 8% of the artifacts came from two volcanoes northeast of Lake Van (Meydan Dağ and Tendürek Dağ), and about 6% of the artifacts most likely originated from sources on the Muş Plain, halfway between Nemrut Dağ and the Bingöl sources. The remaining 3% of artifacts came from one source in Central Anatolia: Kömürcü.

9.2.2 - Central Anatolian Obsidian at Tell Mozan

Obsidian from a Central Anatolian source at Tell Mozan was largely unexpected; but it is not unbelievable. It should be noted that I recognized obsidian from not just *any* Central Anatolian sources at Tell Mozan -- these artifacts came from the Kömürcü source of Göllü Dağ, that is, the most intensively used and widely exchanged obsidian in Central

Figure 9.6 - Number of Sourced Artifacts vs Number of Sources Identified at Mesopotamian Sites



Anatolia. As I show in Figure 8.14, nearly half of the sourced artifacts at Neolithic sites in the Middle Euphrates Valley came from the Göllü Dağ sources. In particular, as shown in Figures 8.11 and 8.13, obsidian from Kömürcü is abundant at these sites. Figure 8.12 illustrates that from the PPNA to the Halaf Period, use of Kömürcü obsidian decreased by 75%. If the trend continued through the Chalcolithic and Bronze Age, Kömürcü obsidian may not have even been common at Middle Euphrates sites.

As shown in Figure 8.10, about 14% of the sourced artifacts at Tell Halaf, during the Neolithic, originated from Göllü Dağ. This is the only other settlement in the Khabur Triangle with Göllü Dağ obsidians. To the best of my knowledge, these three Tell Mozan artifacts represent the furtherest east occurrence of Kömürcü obsidian. A single Neolithic artifact from Choga Mami in Iraq was assigned to the University of Bradford's Group B1, corresponding to one of the five obsidian sources at the Göllü Dağ stratovolcano and lava dome complex -- which source, though, is not clear. Recall that the obsidian vessel from Tepe Gawra, sourced by RDC, came from a Central Anatolian source, but it was assigned to one of the seven Acıgöl sources, not the Göllü Dağ sources.

It is worth noting the contexts of the three artifacts from Kömürcü. Two of these artifacts originated from the accumulation directly above a pebble surface of the palace's northern service courtyard. This accumulation would have been forming as soon as the pebble surface was no longer being maintained, maybe as soon as its construction around 2300 BCE or perhaps a bit later, closer to 2250 BCE. Thus these artifacts may have been deposited while service activities for the royal court, maybe even that of Tupkish himself,

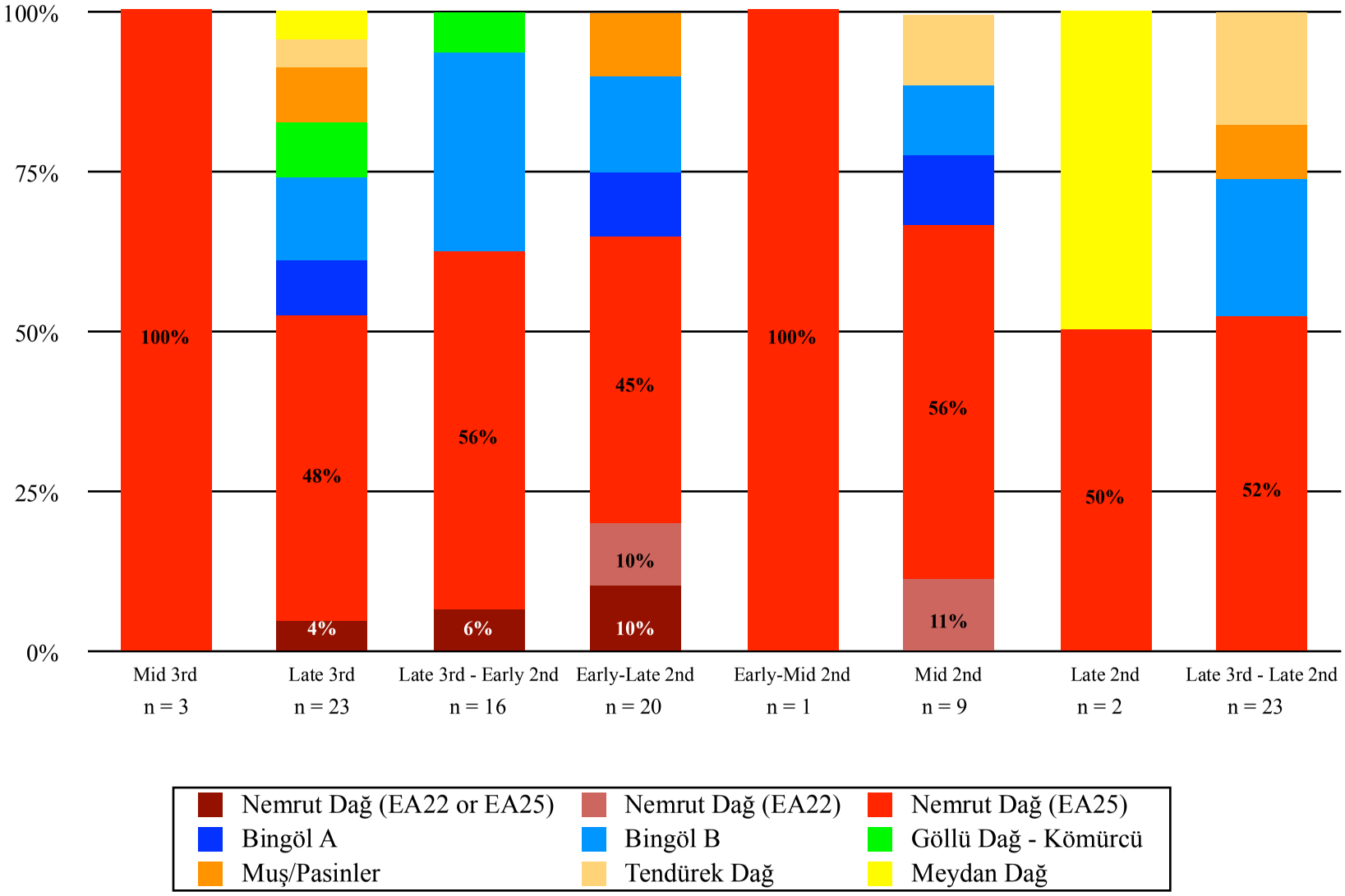
were being conducted in the northern courtyard. The third artifact also comes from a unit (A7) that includes the northern service courtyard and strata from subsequent phases. The stratigraphic data for A7 are not yet available in the Urkesh Global Record, so this artifact cannot be given a date. It may well, though, have come also from the service courtyard and date to around the same period, circa 2300 to 2250 BCE. Did only the royal court of Urkesh have access to Kömürcü obsidian for some reason?

In summary, the Kömürcü obsidian most likely arrived at Tell Mozan via sites in the Middle Euphrates Valley along an east-west exchange route, not directly from Göllü Dağ. All three artifacts were found in Area A, which includes the Royal Palace. At least two artifacts, perhaps all three, were probably used in the northern courtyard, circa 2300 to 2250 BCE, during service activities for the palace. A number of obsidian "workshops" have been discovered near the Komürcü outcrops, and lithic specialists have claimed that these obsidians are of the highest quality. These three artifacts at Tell Mozan are so small that their functions cannot be inferred, so future research should include identifying tools fashioned from Kömürcü obsidian and determining their uses.

9.2.3 - Obsidian Sources by Time

Figure 9.7 shows the obsidian sources represented at Tell Mozan chronologically with the currently available information. This graph will be improved as the stratigraphic data from additional units become available in the Urkesh Global Record. The plot, as-is, does reveal several notable trends. Obsidian from Nemrut Dağ was used throughout the

Figure 9.7 - Source Assignments by Time Period

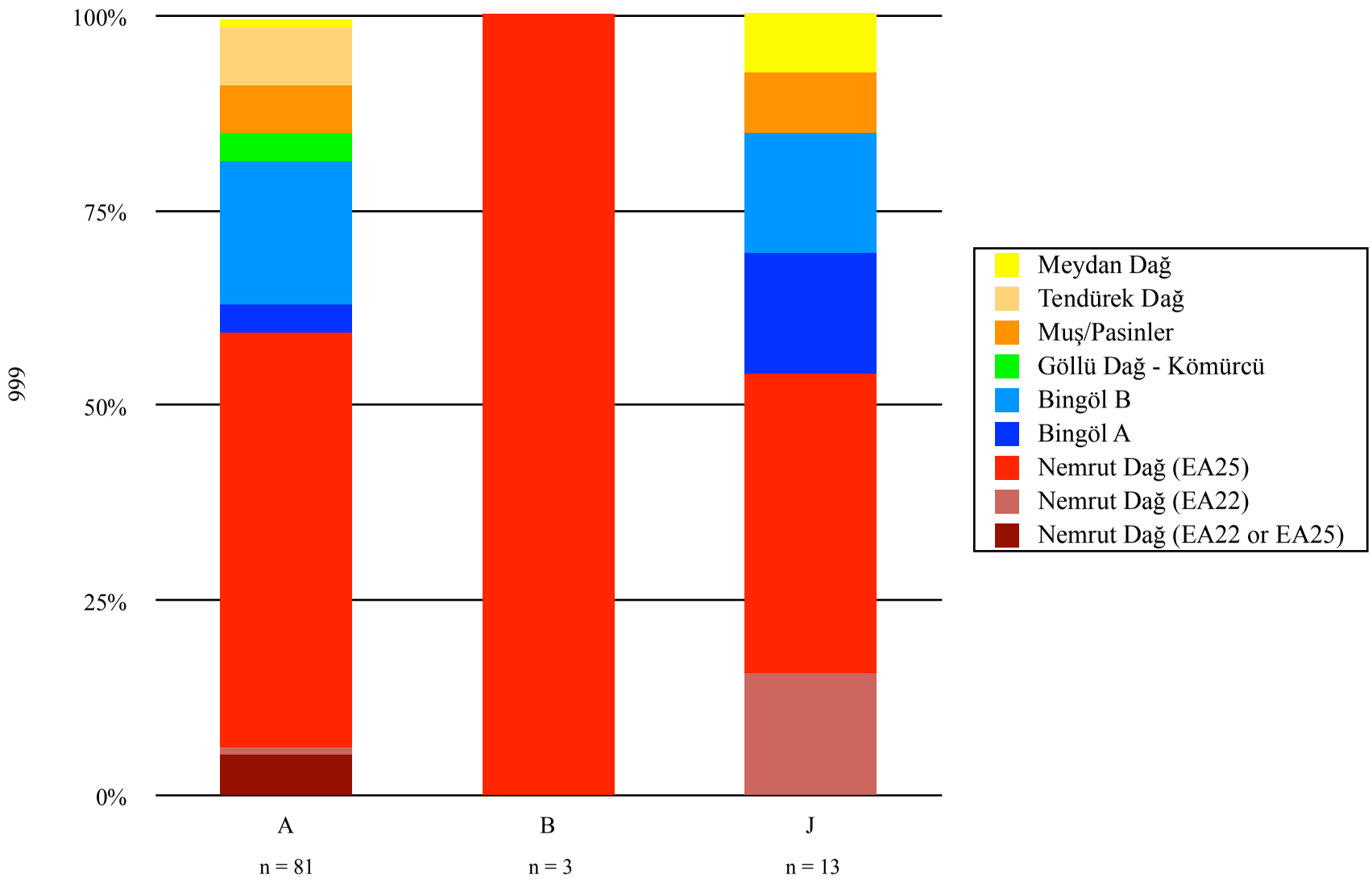


site's occupational history from the mid-third millennium to the late-second millennium, and it comprises at least 50% of the obsidian at any given period. The vast majority of the Nemrut Dağ obsidians came from only one collection area (Rapp and Ercan's EA25), a lava dome in the southeastern portion of the caldera. The only other Nemrut Dağ flow utilized at Tell Mozan is EA22, a lava dome in the northeastern part of the caldera. This secondary source may have only been used during the second millennium. The obsidian from Kömürcü may have been utilized only during the late third millennium. Obsidians from Meydan Dağ, Tendürek Dağ, and the Bingöl sources were used at Tell Mozan from the late-third millennium until the late-second millennium. Overall, however, the use of various obsidian sources at Urkesh seems largely consistent for over one thousand years. As obsidian artifacts are recovered from the Chalcolithic levels of Tell Mozan, it will be interesting to see how earlier patterns of obsidian use compare.

9.2.4 - Obsidian Sources by Site Area

Figure 9.8 illustrates that the obsidian sources represented in Areas A (the palace complex) and J (the plaza and temple terrace), and their proportions, are largely the same. In both areas, for example, over half of the obsidian came from two flows at Nemrut Dağ. There are two notable exceptions: obsidians from Tendürek Dağ and the Kömürcü source of Göllü Dağ are only found in Area A, not J. In Section 9.2.2, I discussed the Kömürcü obsidians and their apparent use in the palace service courtyard, so the obsidian from this source may represent a special case or use related to the palace.

Figure 9.8 - Source Assignments by Site Area



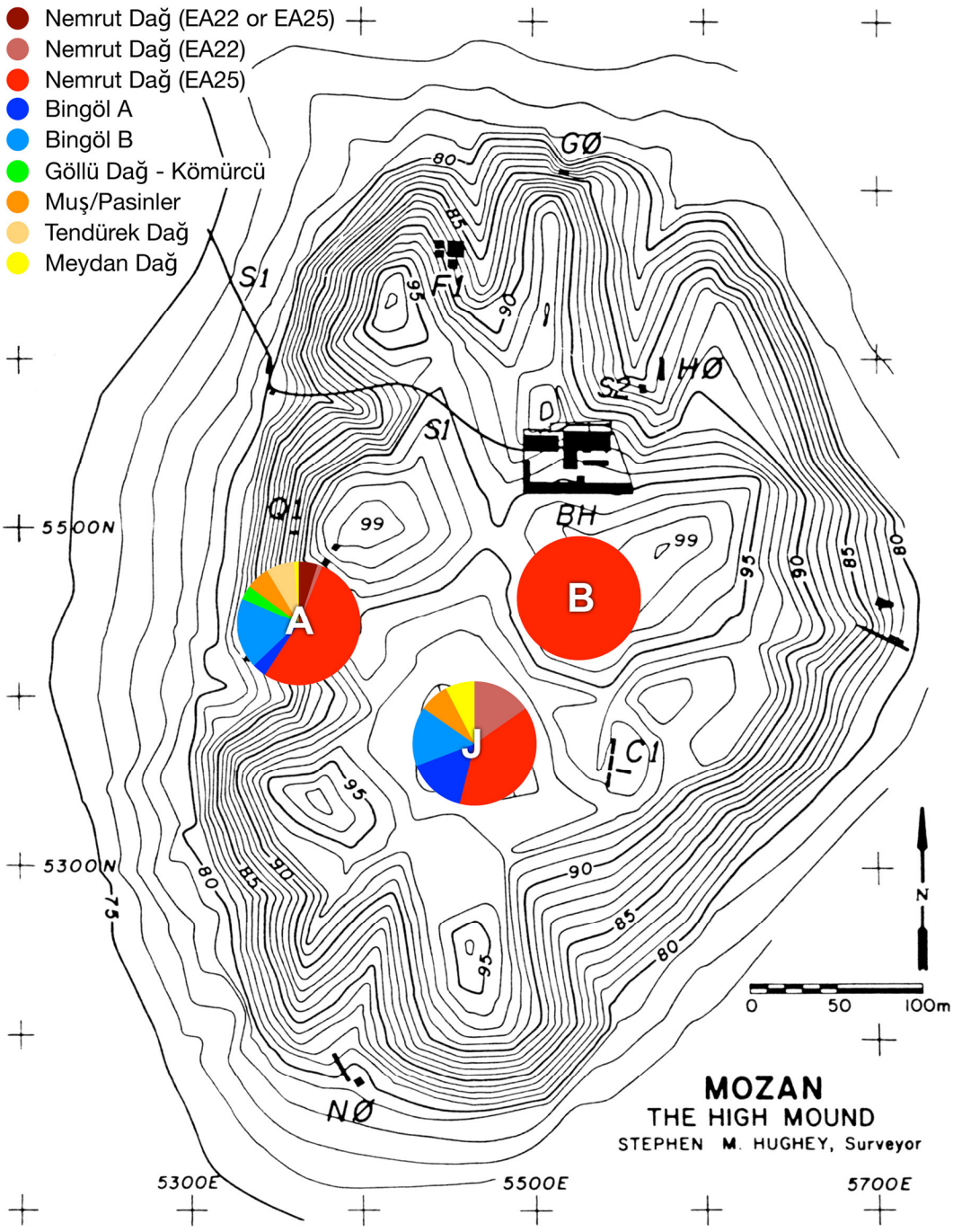


Figure 9.9 - Obsidian sources in three different site areas (A, B, and J) superimposed over a topographic map of Tell Mozan (based on an Urkesh expedition illustration).

Area J does not have any obsidian from Tendürek Dağ, but it does have a greater relative proportion of obsidian from Meydan Dağ. Consequently, the overall proportions of obsidians from these two adjacent volcanoes is almost equal in Areas A and J. Given that Meydan Dağ and Tendürek Dağ are adjacent to one another and that, as I contend in Section 7.3.2, the eastern lava flows of Meydan Dağ and the western flows of Tendürek Dağ overlap to some extent (enough to fool experienced geologists), it is hard to attribute any cultural significance to this difference between Areas A and J.

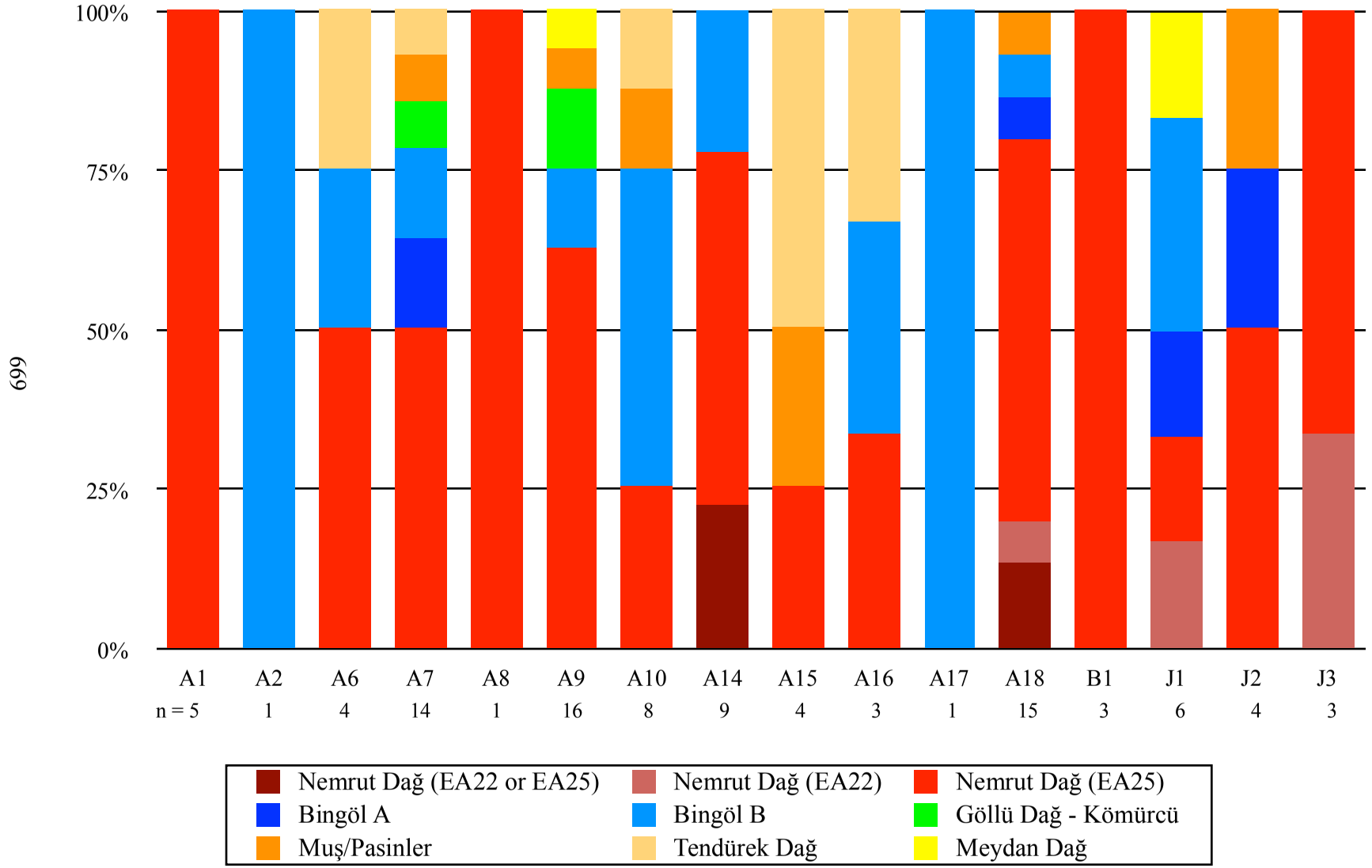
The overall similarities for Areas A and J imply that people living in various parts of ancient Urkesh had similar access to the same obsidian sources in Eastern Turkey. On the other hand, all of the sourced obsidian from Area B (the temple) came from one flow at Nemrut Dağ, but the sample so far only consists of three artifacts.

9.2.5 - Obsidian Sources by Site Unit

When the source data are broken down by site unit, not just area, more complexity is revealed, as shown in Figure 9.10. Figure 9.11 shows the obsidian sources represented in Units B1, J1, J2, and J3. The obsidian sources for the units of Area A are overlaid on a photograph of the excavations (Figure 9.12), a plan of only the Royal Palace (9.13), and a plan with the later second-millennium structures as well (9.14).

Notice that in these figures, for example, there are six distinct sources of obsidian represented in Unit A7, and obsidians from five sources are present in each of three other units: A9, A18, and J1. The graph also suggests that there may have been differential use

Figure 9.10 - Source Assignments by Site Unit



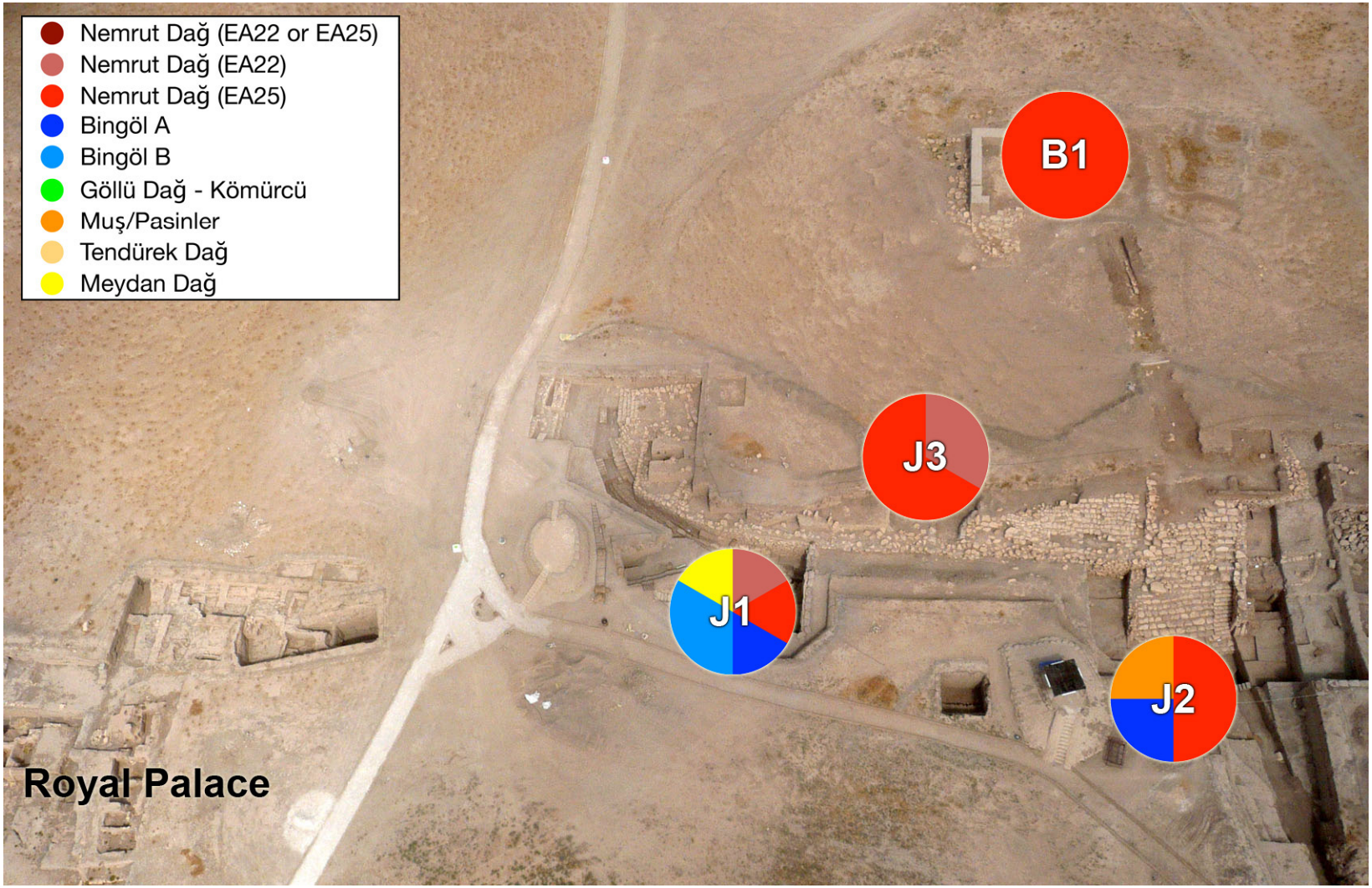


Figure 9.11 - Obsidian sources by unit in Areas J (the terrace and plaza) and B (the temple) (Urkesh expedition photograph).

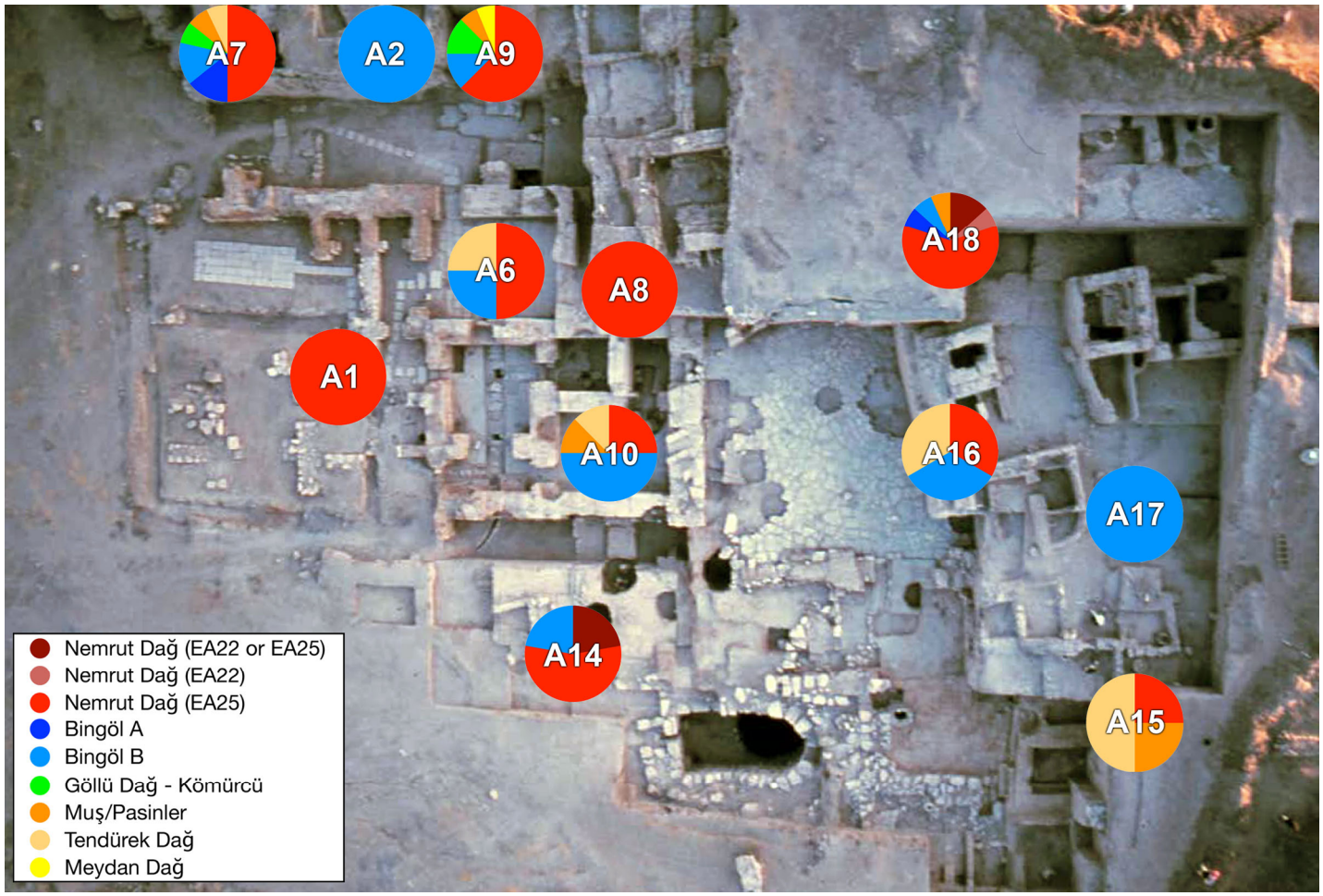


Figure 9.12 - Obsidian sources by unit in Area A superimposed over a photograph of the excavated portions of the Royal Palace and later second-millennium structures (Urkesh expedition photograph); see Figures 9.13 and 9.14 for schematics.

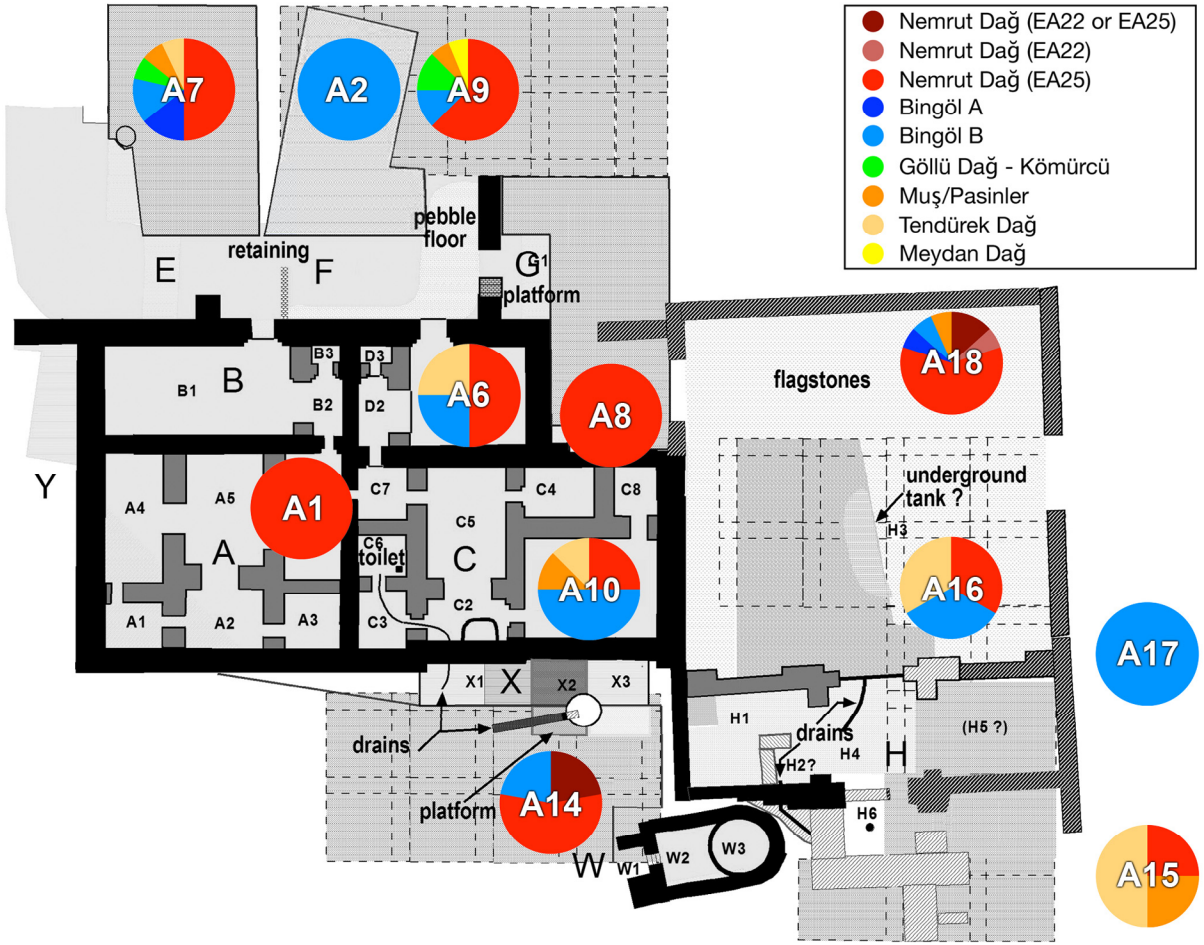


Figure 9.13 - Obsidian sources by unit in Area A superimposed over the Royal Palace, circa the mid-third millennium (based on Urkesh expedition illustrations). Note that the graphs also include artifacts from the late-third and early-second millennia.



Figure 9.14 - Obsidian sources by unit in Area A superimposed over (1) the third-millennium Royal Palace in black and dark cross-hatching and (2) the later second-millennium structures in light gray (based on Urkesh expedition illustrations).

of obsidians spatially in ancient Urkesh. For instance, A7 and A9 apparently have similar source patterns, and both units include the northern service courtyard of the Royal Palace (see Section 3.6.5) and strata from later phases (i.e., houses and graves from the first half of the second millennium after abandonment of the Royal Palace). A18 also represents a courtyard (i.e., the flagstone courtyard of the formal wing), so maybe activities involving obsidian from a variety of sources often occurred in the courtyards.

This plot is of somewhat limited use because it groups together all of the features in a particular unit (e.g., the obsidian artifacts in A16 come from three features -- a tomb, "the great brickfall," and a sherd-and-pebble pavement -- but are grouped together in this graph). Figure 9.15 reveals the differences in obsidian sources within features, emplaced at different times, of Unit A9. This illustration shows, for example, that two of the three artifacts from the Kömürcü source were deposited in a feature without obsidian from any other sources. With further stratigraphic data and sourced artifacts, more graphs linking obsidian sources to site stratigraphy -- such as Figure 9.16 -- will be possible, revealing spatial or temporal patterns at Urkesh that would not have been noticed.

9.3 - Other Evidence of Contact and Exchange at Tell Mozan

Like other Mesopotamian archaeological sites, there is limited evidence of contact and exchange at Tell Mozan. This evidence ranges from reasonably conclusive to highly speculative. In some cases, such as gold artifacts, the raw material does not occur locally but was available from a number of different sources throughout Anatolia and the Zagros

Figure 9.15 - Source Assignments by Feature in Unit A9

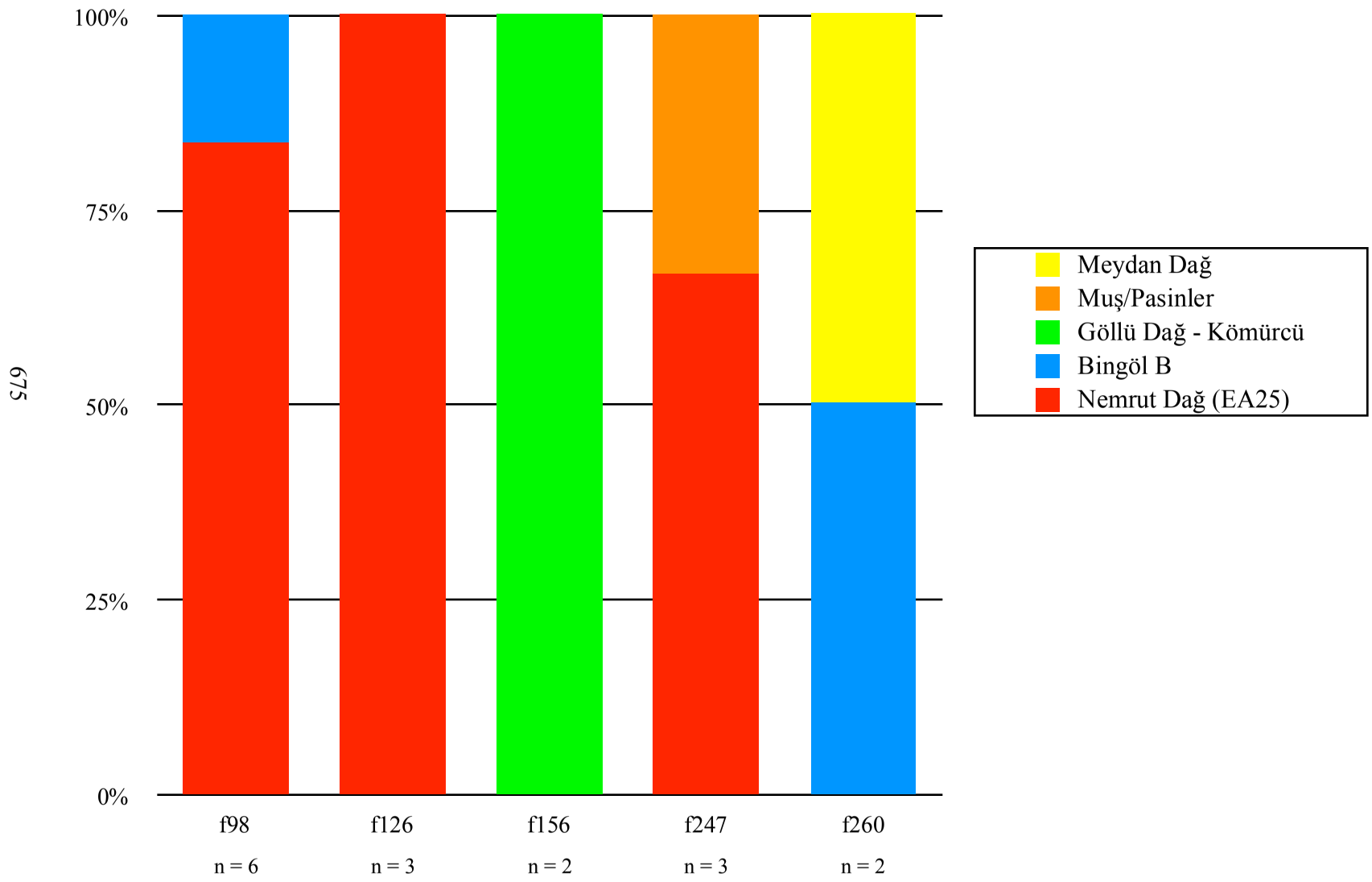
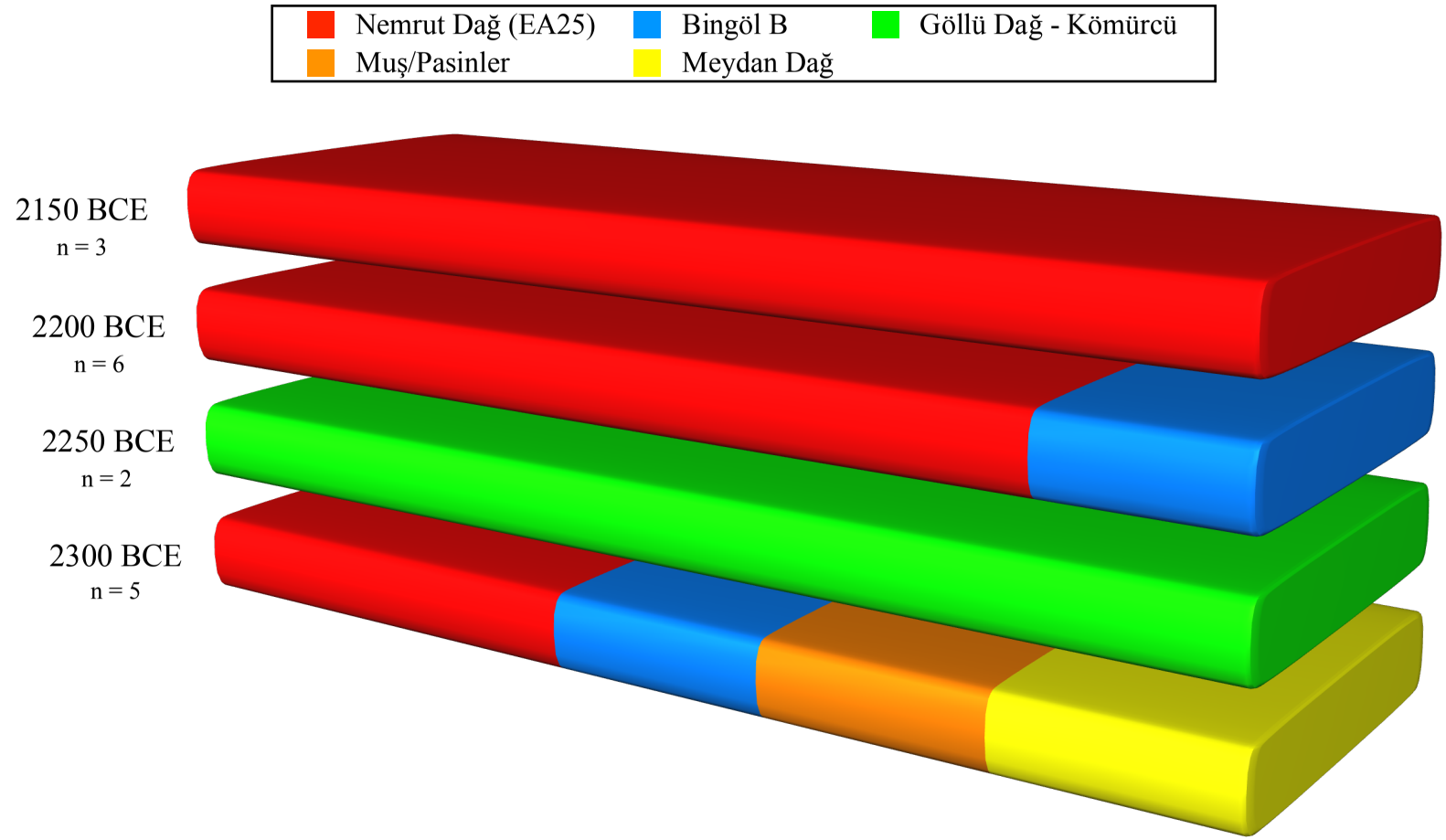


Figure 9.16 - Source Assignments in Unit A9 by Stratigraphy



Mountains. For other artifacts, such as ceramics, it can be hard to establish if items were transported or if the style and/or technology instead dispersed. In the following sections, I briefly review other evidence of long-distance contact and exchange at Tell Mozan. As in Chapter 3, additional information is available in papers online in the Urkesh Electronic Library, part of the expedition's public website: www.urkesh.org.

9.3.1 - Exotic Materials and Items at Tell Mozan

Excavations at Tell Mozan have occasionally uncovered beads of lapis lazuli (see Figure 9.17), and the wife of Tupkish (the *endan* who built the Royal Palace) was named Uqnitum, Akkadian for "lapis lazuli girl." The Badakhshan Province of far northeastern Afghanistan was the exclusive source of this blue stone throughout the Near East, and it was widely circulated for millennia. The routes by which lapis lazuli arrived in Northern Mesopotamia are still not clear. It could have been imported via Southern Mesopotamia, or it may have been transported along a more northerly route near the Caspian Sea. Lapis lazuli certainly was not directly acquired, and these ground-and-polished beads may well have arrived in Northern Mesopotamia in their finished forms.

Most of the other stone resources are more local. The architectural stone used, for example, in the construction of the Tupkish Royal Palace is limestone from the Tur Abdin mountains directly to the north. The sculptures at Tell Mozan, including unfinished ones, suggest these workshops were local (Kelly-Buccellati 1989:151, 1998:38). Vesiculated basalt was also frequently used at Urkesh, primarily for millstones. As I noted in Section



Figure 9.17 - A stone necklace, recovered in Unit A15, with a large bead of lapis lazuli, certainly from the Badakhshan Province of Afghanistan (Urkesh expedition photograph).



Figure 9.18 - An example of a bronze dagger from Unit A16 (shown actual size; Urkesh expedition photograph). Other copper and bronze artifacts include spear points and pins.

3.2, a cinder-cone volcano named Sharat Kovakab lies approximately 60 km south of the site near Al Ḥasakah and Tell Brak, and it is visible from the top of the tell. I suspect that Sharat Kovakab is the most likely source of the vesiculated basalt.

Gold artifacts have been unearthed at Tell Mozan, and either these artifacts or the raw material must have been carried to the site. As noted in the previous section, though, gold occurs in various locations throughout the Near East, and rarely are sourcing studies conducted on precious metals. In Section 3.6.6, I mentioned that silver rings were found in the sacrificial *âbi*. Silver also occurs in a variety of different locations in Anatolia and the Zagros range, but a Hurrian myth offers us some insight. Recall from Section 3.2, the "Song of Silver" myth relates the tale of a young god, Silver, who lives in a mountainous region. Silver learns that his father is Kumarbi, the "father" of Urkesh, where he resides. The young god then travels to Urkesh in search of his father, but Kumarbi is off roaming the highlands. The Hurrians, therefore, knew that silver occurs in the mountains, perhaps even within or quite close to the territory controlled by Urkesh.

Excavations have also unearthed numerous copper and bronze artifacts, including pins, spear points, and daggers (Figure 9.18). In addition, a fragmentary tablet recovered in Unit A1, part of the Royal Palace, is an administrative register that includes an amount of copper. Just through the Mardin pass lie the extensive Ergani copper-sulfide deposits, northeast of Diyarbakır, which apparently supplied copper to much of Mesopotamia since the third millennium BCE. Copper-smelting slag has also been discovered at Tell Mozan.

These facts have lead to the proposal that the Urkesh inhabitants were involved in copper exchange (Buccellati and Kelly-Buccellati 1995b:386, 1997b:60).

Other metals must also have been brought into the Khabur Triangle from Anatolia and the Zagros Mountains. For example, tin was needed for bronze; however, the source of tin in the Bronze-Age Near East remains a topic of debate (e.g., Dayton 1971; Muhly 1979, 1985; Penhallurick 1986; Cierny and Weisgerber 2003; Giumlia-Mair 2003). This issue is commonly known as "the tin problem" thanks to an article titled "The Problem of Tin in the Ancient World" (Dayton 1971) and an edited book titled *The Problem of Early Tin* (Giumlia-Mair and Lo Schiavo 2003). The material for a lead figurine at Tell Mozan must also have come from ore deposits in mountainous regions, but this figurine deserves special attention due to an earlier publication regarding its origin.

9.3.2 - A Lead Figurine at Urkesh from Troy?

Canby (2003) discusses a flat, lead figurine of a woman discovered at Tell Mozan in her article entitled "A Figurine from Urkesh: A 'Darling' from Troy to Mesopotamia." Such figurines are rare, and the initial example was found at Troy, near the Aegean coast. Two of the first known moulds for these figurines also came from western Anatolia, so it was widely held that this region was their origin. Subsequently, additional lead figurines and moulds were found at sites in southeastern Turkey, southern Iraq, the Levant, and the Khabur Triangle, including Tell Mozan and Tell Brak. Thus, Canby (2003) contends that, while the figurines are likely not Anatolian, they are "proof that caravans from far east in Syria travelled as far west as the Aegean coast" (173). She argues:

> It was not the objects that travelled, however; lead had too little value and would have been heavy to carry. It must have been the moulds, designed to make individual trinkets and figurines, that were carried by people going to these far-apart places. A person with such a mould, wherever he happened to be on his journey, could produce a locally popular item almost instantly. (172)

This is merely speculation based on her 1965 article. It appears that lead isotope analyses of these figurines have not been conducted to locate the sources of the lead and determine if, in fact, it was transported long distances. Canby (1965) reports that at least one of the moulds was made of steatite (i.e., soapstone), which can also be sourced (e.g., Allen et al. 1975, Becker 1976, Frison 1982, Moffat, and Buttler, 1986, Truncer et al. 1998), but such work has not been done either. Ultimately, we do not know (1) if the lead figurines were made locally or (2) what moved long distances: lead ore, metallic lead, moulds, figurines, artisans, or some combination of these. Certainly the figurine from Tell Mozan cannot be interpreted as proof of contact with Troy, as implied by the article title.

9.3.3 - The Storehouse of the Royal Palace

In Section 3.6.5, I mentioned the Royal Palace "storehouse" in which more than a thousand *bullae* sealings were found. These clay *bullae* were originally molded around a cord, which was wrapped around a shipping container. Their depositional pattern in this room suggested that shipping containers were opened there and then their contents stored or distributed. Most shipments likely arrived from nearby villages, but some *bullae* have seal impressions thought to represent foreign city-states. Buccellati and Kelly-Buccellati (2001a) point out, in particular, that a seal impression which represents the Akkadian sun deity Šamaš most likely originated in Southern Mesopotamia (22).

Some of the *bullae* sealings indicate the type of shipping container to which they were originally affixed (Buccellati and Kelly-Buccellati 1995a:7). Ceramic jars were the most abundant container, and they ranged from tall and narrow to short and squat. These jars were apparently wrapped in either leather or cloth. A cord was tied around the neck of the jar, and the *bulla* was placed over the knot. On boxes and baskets, the sealing was attached to a peg, and some *bullae* bear impressions of reed baskets. One *bulla* even has the impression from the horn of a gazelle (gazelles, though rare, still live in southeastern Turkey and northern Syria and along the Syria-Jordan border). While the *bullae* remain, the containers are missing, so residue analyses are not possible.

9.3.4 - Influences of the Early Transcaucasian Complex

Two recent papers (Kelly-Buccellati 2005, Buccellati and Kelly-Buccellati 2007c) have highlighted influences of the so-called Early Transcaucasian culture (also sometimes called the Kura-Araxes culture) at ancient Urkesh. We should, to be accurate, refer to the Early Transcaucasian *complex* because it is defined by its material culture (e.g., ceramics, architecture) and had a very wide geographic distribution, including Eastern Anatolia, the Transcaucasus, and the Northern Levant. This complex is not associated with a particular language or ethnic group. It is certainly possible, given its distribution, that this complex is a material culture shared, to various extents, by a series of otherwise distinctive groups, and it likely should not be considered a singular cultural unit with fixed boundaries. This complex is largely restricted to about 3500 to 2000 BCE.

Early Transcaucasian ceramics are painted black and red, typically with geometric designs, and are either burnished or polished, giving them a lustrous appearance. Hearths having anthropomorphic and/or geometric designs are also common features in houses at Early Transcaucasian sites. Both have been recovered, in small quantities, at Tell Mozan. Kelly-Buccellati (2005) reports that, in the first "sixteen campaigns of excavation, only a small amount of Early Transcaucasian pottery has been discovered" (34). The sherds are scarce, but they were found in two important contexts: mid-third-millennium strata of the temple and later third-millennium strata of the Royal Palace (35). She also explains that Early Transcaucasian hearths "are horseshoe shaped with incised and applied decoration, usually anthropomorphic but also with geometric elements" (34). At Tell Mozan, during the Khabur Period, circa the early second millennium, hearths in houses had "decoration very similar to the Early Transcaucasian examples" (34).

Hence, Buccellati and Kelly-Buccellati (2007c) argue that "there was a continuity of contact even if the evidence is scarce" (145), and Kelly-Buccellati (2005) believes that the evidence reveals "complex cultural interactions between the urban Hurrian population of Urkesh and the rural population to its north" (35). Indeed, the sherds and hearths show contact but not necessarily exchange. There are several possible explanations why Early Transcaucasian-type ceramic sherds occur at Urkesh, including: (1) these ceramics were brought to Urkesh for exchange, (2) their *contents* were brought to Urkesh for exchange, or (3) the ceramics were locally manufactured copies of a northern style. Hearths, on the

other hand, would have been made locally, but they could have been made and decorated either by a local or visiting artisan or the homeowners themselves.

Consequently, there is evidence of on-going contact between the people of Urkesh and those of the Early Transcaucasian complex, but the forms of these contacts are yet to be determined. Perhaps the Early Transcaucasian material at Urkesh is an example of the process that led to the expansion of this complex, or it may be an example of material and people moving between neighboring groups. It might also be that there were cultural ties between the Hurrians of Urkesh and the people in the highlands.

9.3.5 - "Invisible" Exchange in Northern Mesopotamia

Many (perhaps even most) of the materials exchanged in Northern Mesopotamia, including at Tell Mozan and other Khabur Triangle sites, are archaeologically invisible or nearly so. Agricultural products are foremost on this list. Paleoclimatological research in the Khabur Triangle, as discussed in Section 3.4, has shown greater water availability during the Early Bronze Age (Deckers 2007, Deckers and Riehl 2007, Riehl et al. 2008), permitting various crops to be grown in the vicinity of Tell Mozan.

As discussed in Section 3.4, two studies have identified the natural and cultivated plants at Tell Mozan. Calvin (1988) recognized remnants of domestic bread wheat, wild barley, and wild einkom, and Riehl (2006) found seeds from bread wheat, emmer wheat, and two-row barley. Legumes were also recognized among the seeds: bitter vetch, grass pea, lentil, chick pea, and bean (Riehl 2000; Deckers and Riehl 2004). In addition, grape

and fig seeds were found, and Riehl (2006) suggests that these seeds represent collection from wild trees in the region. Pistachio and olive trees have also been identified from the charcoal fragments recovered at Tell Mozan (Deckers and Riehl 2004). The assumptions are that the plants grew locally and that they were among the foods (and possible exports) of the locals. Some of these plants, though, may have been imports. Other exported and imported consumables likely included spices, salt, wine, and beer.

Timber likely also would have been an important export from the Khabur Triangle to Southern Mesopotamia. As mentioned in Section 3.4, charcoal fragments indicate the existence of an oak park woodland (Hillman 2000; Deckers and Riehl 2004:343; Deckers 2006), and the piedmont steppe was likely more savanna-like and had light tree coverage (Buccellati and Kelly-Buccellati 2007c). The identified trees include poplar/willow, ash, elm, juniper, and cedar (Deckers and Riehl 2004). Transporting timber would have been as easy as floating logs down seasonal wadis to the Khabur River. As noted in Chapter 8, Herodotus reports that reeds were a commodity in southern cities.

Animal products were also certainly exchanged in Mesopotamia, including wool, leather, oils and fats, and meat (e.g., sheep, pigs, deer, birds, and fish). In Section 3.4, I reported that beaver bones and teeth occur at sites throughout the Syrian Jezireh. Animal furs, like beaver pelts, might also have been exchanged. Other plant and animal products most likely included textiles (including finished garments) and dyes.

Crawford (1973) explains that "cloth and garments of wool played an important part in the export trade" during the third millennium BCE (232). He points out that not

only are textiles perishable but also "the equipment needed for processing them prior to export was also perishable" (232), so there is little evidence left behind of such textile workshops. Wilhelm (1989) points out that, based on the Mitanni-era texts recovered at Nuzi, of the production "activities of the palace, the production of textiles was the most important" (45). He bases his conclusion on a record of the palace slaves, which lists 32 textile workers but only four scribes, three carpenters, three metalsmiths, two potters, and two basket weavers, for example. Therefore, perhaps one of the most important elements of the palace economy is largely archaeologically invisible.

Dalley (1984) discusses what is possibly the most ephemeral imported material of all: ice. Elites at sites like Tell Hariri (ancient Mari) in eastern Syria and Tell al-Rimah in northern Iraq apparently constructed ice-houses, in which ice, collected during winter in the north, was stored for their later use. At Tell Ashara (ancient Terqa) on the Euphrates, the foundation inscription for such a structure was found, which read: "Zimri-Lim... had ice brought and built an ice-house on the bank of the Euphrates at Terqa" (91). There are other texts as well, including one attributed to the Assyrian king Shamshi-Adad, in which he discusses ice brought from a distance of 30 to 60 km (91-92).

In *Early Mesopotamia: Society and Economy at the Dawn of History,* J. Nicholas Postgate (1992) discusses obsidian exchange. He contends that, while sourcing obsidian may be successful at assigning artifacts to their volcanic origins, "one can only speculate at present about the social nature of the obsidian trade and about the possible exchange of other commodities of the time which have not survived" (207). He points out that, based

on later parallels, we may expect that "textiles came upstream in exchange for timber and aromatics from the mountains of Syria and Turkey" (208). Postgate warns, however, "not to place too much faith" in such reconstructions (208).

9.3.6 - Summary of Contact and Exchange Evidence

Most of the prior archaeological evidence for contact and exchange at Tell Mozan is less precise (e.g., gold, silver), originates from a single very close (i.e., copper) or very distant (i.e., lapis lazuli) source, or represents a unique occurrence (i.e., the lead figurine). Furthermore, some of the most frequently exchanged materials in Northern Mesopotamia are archaeologically invisible and are potentially accessible only through written records. Obsidian sourcing offers evidence with high spatial resolution among a series of sources, and obsidian artifacts are abundant and were utilized for millennia. The kind of data that obsidian sourcing can provide is currently unmatched at Tell Mozan.

9.4 - The Existence of a Hurrian "Homeland" to the Northeast

There has been much debate regarding a potential Hurrian "homeland" northeast of Tell Mozan, perhaps centered near Lake Van in Turkey or as far as Armenia, Georgia, or Iran. Many researchers who have ascribed to this hypothesis have also suggested that Hurrian populations also remained in this region, that Hurrians in Northern Mesopotamia maintained (either directly or indirectly) cultural-based ties to their homeland, and/or that there was a series of Hurrian migrations into Mesopotamia. Potentially the origins of the obsidian artifacts at Tell Mozan may or may not support such hypotheses.

9.4.1 - Background of the Debate

As I noted in Section 3.1, our knowledge about the Hurrians is so scattered that authors use words like "mysterious" and "enigmatic" to describe them. Wilhelm (1989) explains that this "fragmentary evidence... has given rise to a variety of assessments and even to rank speculation" (v). The geographical origin of the Hurrians falls into, at best, the former category and, at worst, the latter. Proposed "homelands" have stretched from southeastern Turkey to Iran in the east and to Armenia and Georgia.

Speiser (1953) proposed that "the original home of the Hurrians cannot have been far from the Lake Van district" in southeastern Turkey (325). His reason was that Urkesh probably sat in the Khabur Triangle and that the "geographic center of the people cannot have lain far beyond" (314). Speiser's suggestion has been persistent, and many scholars today cite the region around Lake Van as the Hurrian homeland. In fact, Wilhelm (1989) himself held that the mountainous area south and southeast of Lake Van can be presumed "to have been the oldest homeland of the Hurrians" (41).

Akkermans and Schwartz (2003) argue that the Hurrians probably "originated in the eastern Taurus [in Turkey] or western Zagros highlands [in northwestern Iran]" (285), reflecting another common suggestion. Bernbeck and Pollock (2005) criticize others for "misguided, often racist attempts to identify an ethnically distinct 'Hurrian' culture" (22) while, ironically, reiterating an old proposal that "Hurrian lower classes were ruled by an Indo-Iranian elite" (22) who were supposedly responsible for technological developments like the chariot. von Dassow (2008), though, calls this a "persistent modern myth" and "a

pseudo-historical fantasy" (xix). She traces the origins of this belief and debunks it using textual and archaeological evidence (2008:77-90). Steinkeller (1998) concurs and asserts "there is no shred evidence [for] an Indo-Iranian migration" (98).

The hypothesized Hurrian homeland has also been proposed to lie as far northeast as the Transcaucasia "or beyond" (Stein 1997:126). Such arguments have been primarily linguistically based. Linguists Igor Diakonoff and Sergei Starostin stated that the Hurro-Urartian family has similarities to Northeastern Caucasian languages while others argued that Armenian has loanwords from the Hurro-Urartian languages. Already tenuous, these claims are sometimes advanced as evidence that Hurrians originated in the Transcaucasus mountains, perhaps as far northeast as Georgia or Armenia. Based on fragmented tablets, Steinkeller (1998) believes it quite likely that "their homeland was located somewhere in the Trans-Caucasian region, quite possibly in Armenia" (96). Kammenhuber (1977) even proposes that the Hurrians originated east of the Caspian Sea.

Others dispute such hypotheses about a Hurrian "homeland" outside of Northern Mesopotamia. Benedict (1960) notes that the "belief that the area around Lake Van was an integral part of the Hurrian cultural and political area in the second millennium B.C. rests upon evidence of the most dubious sort" (102). He points out that such notions are based on debunked suggestions regarding a direct cultural link between the Hurrians and the ninth-century-BCE Urartians (i.e., an assumption that the Urartians were direct, lineal descendants of the Hurrians) (101-102). Urartian territory was centered about Lake Van, but that does not mean the same can be presumed of the Hurrians.

Similarly, von Dassow (2008) contends that, although the Hittite texts do not refer to Hurrians until the middle of the second millennium BCE, "there is little reason (and no evidence) for postulating that speakers of Hurrian entered the Near East from elsewhere rather than being indigenous to the area where they are first attested" (71). Amélie Kuhrt (1995) likewise claims that it is most likely "the Hurrians were a cultural-linguistic group *always* located among the foothills and mountains fringing the northern Mesopotamian and Syrian plains" (288). Kuhrt points out that the Hurrians, "as far as we can tell, were from prehistoric times connected with this region -- we do not need to visualise them as a group migrating from somewhere further north or east" (289).

Kuhrt alludes to another common belief tied to the notion of a Hurrian homeland, that the Hurrians were immigrants or invaders who arrived when Hurrian names become visible in textual and glyptic (e.g., seals) records. For example, Stein (1997) claims that occurrences of Hurrian names "indicate a gradual migration from east of the Tigris River in the late third millennium across northern Mesopotamia" (126). Steinkeller (1998) also contends that, at roughly the same time, "there took place a massive migration of Hurrian speaking peoples into northern Mesopotamia" (96). About the emergence of the Mitanni Empire in the second millennium, he favors an explanation involving another "migration of new Hurrian tribes" (97). Wilhelm (1989) proposes two Hurrian migrations during the third millennium BCE followed by "a third, more powerful, incursion" during the second millennium BCE that precipitated the Mitanni Empire (16).

Such hypothesized migrations, especially as formulated by Wilhelm (1989), seem to imply some sort of cultural ties -- either direct or indirect, continuous or intermittent -- maintained between Hurrian immigrants in Northern Mesopotamia and those still living in their homeland. For instance, Wilhelm suggests that the Hurrians were, at least in part, "encouraged by a favourable political situation" to move into Mesopotamia (42), hinting at maintained contact of some form among Hurrian populations. This contact could have possibly taken the form of (1) exchange (of materials and information) among groups of Hurrian pastoral nomads or (2) exchange between transhumant Hurrian pastoral nomads and Hurrian agriculturalists settled in Northern Mesopotamia.

9.4.2 - Formulating a Hypothesis

Given the abundance of obsidian in eastern Turkey and the Transcaucasus region, seeking obsidian from sources in these areas may yield evidence of exchange and contact, either direct or indirect, with these highlands. Obsidian from, for example, the geological sources in far northeastern Turkey, Armenia, Azerbaijan, Georgia, or southeastern Russia could help to identify a Hurrian link to those mountainous regions.

If there were Hurrian migrations into Northern Mesopotamia from the northeast, some, perhaps even many, people would have brought obsidian (either in a raw state or as finished tools and items like beads) with them, appreciating its scarcity. Recall from the Akkadian texts, as discussed in Chapters 2 and 8, that obsidian was valuable and, at least to the Akkadians, had magical abilities. More importantly, obsidian had practical uses as

tools for pastoralists and agriculturalists (noted in Chapter 2). These traits make obsidian useful enough that migrants might have brought it with them.

Furthermore, if Hurrian immigrants in Northern Mesopotamia maintained cultural ties and contacts -- even indirect or intermittent -- with those still living in their homeland, as implied by Wilhelm (1989) and other authors, obsidian from that region may also have entered Northern Mesopotamia via such contact. As noted earlier, this contact could have possibly taken the form of (1) exchange among groups of Hurrian pastoral nomads or (2) exchange between transhumant Hurrian pastoral nomads and Hurrians settled in Northern Mesopotamia. Ethnographic work in eastern Turkey suggests that this proposal is not too far-fetched. Beşikçi (1969) documented the migration routes of Kurdish nomads, several of which exceeded 200 km in a single year (Beşikçi's research and that of Cribb also with the Alikan tribe are discussed later in Sections 9.6.1 and 9.6.2).

At present, the sporadic literature on obsidian sourcing in far northeastern Turkey and the Transcaucasus indicates that these sources do not appear to have been involved in long-distance exchange (unlike the obsidian sources in Central Anatolia and around Lake Van in Eastern Anatolia). For example, as I noted in Chapter 6, there is only one obsidian source in Georgia: Chikiani volcano. Earlier sourcing studies have revealed the intensive use of Chikiani obsidian at sites in Georgia and Armenia, although not Turkey (Badalyan et al. 2004:444; Chataigner and Barge 2007:3). It is the only source in the basin between the Greater Caucasus range to the north and the Lesser Caucasus range to the south. The north-south distribution of Chikiani obsidian was restricted by these mountain ranges, but

it has been reported from the Black Sea in the west to the Caspian in the east. The other sources in the Transcaucasus were used intensively but almost exclusively locally (Barge and Chataigner 2003, Chataigner et al. 2003). To my knowledge, the only reliable report of Transcaucasus obsidians outside their immediate region comes from Blackman (1984; Blackman et al. 1998), who matched almost a third of the artifacts at Tal-i Malyan in Iran to three sources in Armenia: Gutansar, Pokr Arteni, and Sevkar/Satanakar. In general, the Transcaucasus obsidians are extremely rare in Mesopotamia and the Northern Levant, as also shown by my summaries of the existing data in Chapter 8.

Similarly, the obsidian sources in northeastern Turkey beyond the Lake Van area -- Erzincan (Agili Tepe and Degirimen Tepe), Erzurum, Pasinler, Sarıkamış (Çiplak Dağ and Ala Dağ), Kars (Digor, Akbaba Dağ, and Arpacay), and İkizdere (see Appendix A for descriptions) -- seem to have been largely, if not exclusively, used locally. At sites in the Bayburt Plain, for example, Brennan (1996) found obsidian from sources in the area, near Erzurum and Erzincan, that were not used elsewhere in Turkey and beyond. Additionally, my summaries of the existing obsidian data in Chapter 8 show that these sources were not used by the inhabitants of Mesopotamia and the Northern Levant.

Because obsidians in far northeastern Turkey, Armenia, Azerbaijan, Georgia, and southeastern Russia were not exchanged across long distances to the south, the presence of such obsidians at Tell Mozan, one of a very few conclusively Hurrian sites, could help to identify a Hurrian link to those regions. This, in turn, would lend considerable support to a Hurrian homeland in the vicinity. We must keep in mind, of course, that an absence

of Transcaucasus obsidians at Tell Mozan is not evidence against a Transcaucasus origin of the Hurrians. In addition, a Hurrian homeland in southeastern Turkey probably would be difficult to recognize in the obsidian sources at Tell Mozan. As I discussed in Chapter 8, obsidians from the Lake Van region were widely used and transported over a thousand kilometers into Southern Mesopotamia, and they should be entirely expected at a site in Northern Mesopotamia and the Syrian Jezireh like Tell Mozan.

Ideally we could look for Iranian obsidians represented among the artifacts at Tell Mozan, considering the suggestions from some authors regarding Indo-Iranian influences on the Hurrians. As explained, though, in Section 4.7.3.7, I was unable to acquire reliable specimens of Iranian obsidians, and information about Iranian obsidian sources is sparse, incomplete, and contradictory sometimes. When I acquired obsidian specimens from the University of Tabriz in Iran, my analyses revealed that these specimens included artificial glass and obsidian that actually came from Armenia. Unfortunately, others have reported quite similar problems with specimens from Iran (Glascock 2009), which indicates the potential for a pervasive issue in Iranian obsidian studies. Thus, I excluded the "Iranian" specimens from the present study, and for artifacts with unidentified sources, Iran would have been considered a possible source area. Given, however, the weakness of the Indo-Iranian hypothesis and the attribution of all artifacts from Tell Mozan to obsidian sources in Turkey, this should not be considered a serious weakness.

9.4.3 - Comparison to the Obsidian Data

None of the Tell Mozan artifacts were attributed to Armenia, Azerbaijan, Georgia, or southeastern Russia using my sourcing procedures. There is, therefore, no evidence in the obsidian source data for a Hurrian homeland in the Transcaucasus. Similarly, none of the artifacts from Tell Mozan were assigned to the İkizdere, Kars, or Sarıkamış sources in northeastern Turkey near the borders with Armenia and Georgia.

Tendürek Dağ, about 80 km (50 miles) from the Armenian border, was the farthest northeast obsidian source to which I assigned artifacts from Tell Mozan. The six artifacts from this volcano are not, though, convincing evidence for a Hurrian homeland northeast of Lake Van. Tendürek Dağ is one of the likely origins of the "Bayezıd" specimen (from the British Museum) that was analyzed by RDC and was the only geological specimen in their Group 3a. The neighboring Meydan Dağ is another likely source for this specimen, and it also possibly corresponds to one of their Group 3 subgroups. As shown in Chapter 8, obsidians from RDC's Group 3a have been found across Mesopotamia, and apparently Meydan Dağ obsidians have been found at Tell Brak and Hamoukar (Khalidi et al. 2009). Identifications of "Group 3" obsidians must be further refined, but obsidians of Tendürek Dağ and Meydan Dağ are potentially quite widespread. Accordingly, such obsidians are not evidence for a Hurrian homeland in northeastern Anatolia.

The possible assignment, however, of six artifacts from Tell Mozan to Pasinler in northeastern Turkey, about 340 km due north from Tell Mozan, has a greater potential to support a Hurrian homeland in the vicinity. For these artifacts, though, another probable

source is the Muş area, about 200 km north of Tell Mozan and roughly halfway between Bingöl and Nemrut Dağ. It is possible that non-destructive analyses of chemically altered surfaces contributed to this difficulty in assigning the artifacts more conclusively to Muş, Pasinler, or another nearby source. Both areas are little studied, so it is possible that these sources are simply hard to distinguish chemically and that the issue is unrecognized in the literature merely due to a lack of data. A conservative interpretation is that these artifacts originated from one of the Muş sources, either currently known or unknown, because the Muş Plain is between the Bingöl and Nemrut Dağ sources, both of which are represented at Tell Mozan. Pasinler Basin is another 140 km due north through mountainous terrain, so use of obsidian from this source is less likely. Further work is clearly necessary, but at present, the six "Muş/Pasinler" artifacts from Tell Mozan cannot be considered evidence in support of a Hurrian "homeland" within northeastern Turkey.

In summary, other than six artifacts that *might* have come from the Pasinler Basin, there is no evidence in obsidian data to support proposals that a Hurrian homeland existed in far northeastern Turkey or the Transcaucasus. This is not evidence, though, that such a homeland did *not*, in fact, exist in the area -- that is, it does not disprove such suggestions. Instead, the obsidian evidence simply does not support them.

9.5 - *The Debate about "The King of Urkesh and Nawar"*

As noted in Chapter 3, a large copper tablet, first described by Thureau-Dangin in the early twentieth century, bears the inscription of a Hurrian *endan*, Atal-šen, identifying

him as "king of Urkesh and Nawar" (Buccellati and Kelly-Buccellati 2001a:26). Like the copper lion sculptures discussed in Section 3.5, this tablet also reports the dedication of a temple by Atal-šen to Nergal, who, as mentioned in Section 3.6.1, is probably the same as the Hurrian god Kumarbi, the mythical founder of Urkesh. Though the text is Akkadian, the names of the king and his scribe (Šaum-šen) are both Hurrian. This tablet is typically attributed to a few decades before Tiš-atal (and his copper lions).

From the beginning, the location of Nawar was a topic of much debate. Thureau-Dangin proposed that "Nawar" actually referred to the country of "Namar" in the Zagros Mountains in western Iran, implying a sizable empire. Later texts suggested instead that Nawar laid within or near the Khabur Triangle (Wilhelm 2002:175). Today there are two remaining hypotheses regarding the location of Nawar: (1) Nawar is the same as ancient city of Nagar, which is thought to be the nearby site of Tell Brak; and (2) Nawar refers to an Urkesh hinterland along the foothills of the Tur Abdin range and extending north some distance. Wilhelm (2002) argues that, whichever is the case, "Nawar must have played a very important role, because the name of this place appears in numerous Hurrian personal names" (175). In the following sections, I consider these two hypotheses about "Nawar" in light of the obsidian data from Tell Mozan and other sites.

9.5.1 - "Nawar" as Nagar and Tell Brak: Background

Tell Brak has been identified as the ancient city of Nagar in much the same ways that Tell Mozan was identified as Urkesh, as discussed in Section 3.5. Hundreds of seal

impressions and *bullae* found at Tell Brak have a design element that arguably may be an archaic sign that reads Nagar (Oates and Oates 1993:159). A clay bottle stopper bears an inscription with the name Nagar in cuneiform, and a seal impression, originally found by Mallowan, includes the title "sun of the land of Nagar" (159).

In addition, a clay tablet discovered at Tell Brak is a receipt for reeds delivered to "the town of *Nawar* in the district of Ta'idu... received in the presence of Malizzi" (Oates 1987:188; emphasis added). Consequently, Joan and David Oates suggested that "Nagar" and "Nawar" were alternate spellings of the ancient name for Tell Brak (Oates 1987:189; Oates and Oates 1993:161). Similarly Matthews and Eidem (1993) argue that "Nagar" is an older spelling for "Nawar" and that both refer to the same place. They claim that only the oldest references -- texts in the Ebla archives, Old Akkadian administrative texts, and one segment of the inscription of Tiš-atal -- mention "Nagar" (203), and subsequent texts refer instead to "Nawar" (204). Thus, the title "king of Urkesh and Nawar" may describe Tell Mozan in the northern Khabur Triangle and Tell Brak in the south, and it "could well be a logical description for Atal-šen's kingdom" (1993:204).

Others, most notably Salvini (1998), have also argued in favor of Tell Brak being both Nagar and Nawar. The implications, rarely mentioned, are most explicitly noted by Piotr Steinkeller (1998), an Assyriologist at Harvard. He states that, if indeed…

> Atal-šen ruled over two major urban centers, which seem to have been situated at a considerable distance from one another, his must have been a true kingdom. It goes without saying that with this kingdom we cross a critical threshold in the evolution of Hurrian political structures. (95)

In other words, if Atal-šen ruled a territory that included both the cities at Tell Mozan and Tell Brak, his kingdom would have constituted an important step between earlier Hurrian city-states and the later Hurrian-dominated Mitanni empire.

9.5.2 - "Nawar" as a Northern Hinterland: Background

Buccellati and Kelly-Buccellati assert that "Nawar" and "Nagar" are not the same. Their argument is based, in part, on a lack of royal titles in Mesopotamia that specify two cities (Buccellati 1988:33). There is, though, a well documented "pattern, especially in northern Mesopotamia and in western Syria, to include in the royal titulary the name of a city followed by the name of the territory" (33). Accordingly, Atal-šen's title of "king of Urkesh and Nawar" actually refers, as Buccellati (1988) argues, to a city and its territory, not two cities (33). He contends that this title should instead be understood as: Atal-šen, king of the city of Urkesh and the hinterland of Nawar (33).

Consequently, they contend that Nawar refers to an area, not a second city, which encompassed the mountainous region to the north of Urkesh. Nawar is, in their view, an area roughly equivalent to what they call the "Hurrian urban ledge," a strip of land along the Tur Abdin foothills and extending north some distance into the mountains. This area seems to have been the center of Hurrian urbanism. As noted in Section 3.6, Tell Chuera is about the only other third-millennium site that can be argued to be a Hurrian settlement with any confidence. Buccellati and Kelly-Buccellati (2001a) point out that Tell Chuera, like Tell Mozan, lies along the piedmont of the Tur Abdin (26).

This Hurrian "urban ledge" along the Tur Abdin piedmont, in turn, constitutes the southern boundary of an extensive mountainous hinterland, and Urkesh (and perhaps Tell Chuera and other Hurrian cities) controlled access to mountain resources, such as copper, timber, and building stone (Buccellati and Kelly-Buccellati 2001a:26). The identification of a mountainous hinterland for Urkesh relates to some of the evidence I have mentioned of a Hurrian ideological link to the northern highlands. In addition, Buccellati and Kelly-Buccellati (2001a) propose that the inhabitants of Urkesh maintained their cultural ties to the Hurrians living in villages to the north (26-27). They suggest that such ties facilitated access to the mountains and their associated resources "even if the kings exerted no direct administrative or military control over the rural hinterland" (27).

Buccellati (2006) hypothesizes that these urban-hinterland cultural ties may have constituted the foundations of the Hurrian urbanism: "The Hurrian model is based on the principle of ethnic solidarity that transcends the principle of territorial contiguity (central to Sumerian urbanization)" (1). The benefit of such an urban model is that "it could hold together human groups that were not territorially contiguous, but rather separated by the geographical reality of the highlands" (Buccellati and Kelly-Buccellati 2006:30). This form of territoriality, Buccellati and Kelly-Buccellati (2001c) speculate, might have been a reason that the Akkadian king Naram-Sin sought an alliance with Urkesh via marriage of his daughter, Tarlam Agade, to a Hurrian *endan* (69). Their cultural ties to the north, rather than administrative controls, "would have made it difficult for an outsider, such as Naram-Sin, to replace with his own the control of the Urkesh *endans*, and thus an alliance

would have been a wiser political choice" (2000:155). At Tell Brak/Nagar, on the other hand, Naram-Sin apparently commissioned a palace or fortress.

Buccellati and Kelly-Buccellati (1995a) also point out that Tell Brak/Nagar is not as clearly a Hurrian city as Tell Mozan/Urkesh (2). There are some similarities between the two settlements. For example, Kelly-Buccellati (1996) reports that seal "impressions excavated at Brak... exhibit similar stylistic features" to some of those found in the palace at Tell Mozan (247). The seals themselves, though, are distinct, and the title *endan* seems not to have been used at Tell Brak. The architecture also differs (Buccellati 1999:238). Others have noted "differences between the pottery assemblage typical of Tell Mozan and that of Tell Brak" (Kolinski 2007:361). These factors all lead to a belief that Nagar was not Hurrian, at least not in the same way Urkesh was (Buccellati 1999).

9.6 - Considering "Nawar" as a Northern Hinterland

The likelihood of an extensive Urkesh hinterland in the northern highlands can be considered in light of the obsidian source data. We first must hypothesize what processes in an Anatolian hinterland would bring obsidian to a political and religious center such as Urkesh. Then we must consider what effect such processes would have on the sources of obsidian represented among the artifacts at Tell Mozan. Data from the contemporaneous sites, compiled in the previous chapter, will be used for comparison.

9.6.1 - Obsidian Distribution in Southeastern Anatolia

Obsidian from a variety of sources would likely have been transported extensively by nomadic groups in southeastern Anatolia. Wright (1969) was first to hypothesize that pastoral nomads played central roles in the distribution of obsidian during the Neolithic. Nomadism continued in southeastern Turkey and northern Syria into recent times. Yakar (1991) explains that there are "hundreds of ecological niches in Anatolia," many of which are better suited to pastoralism than intensive agriculture (32). He points out that, during the Chalcolithic in southeastern Turkey, agricultural villages were largely restricted to the Upper Euphrates Valley (e.g., Cafer Höyük and Göbekli Tepe), the Balikh Valley, and the confluences of the Tigris and its tributaries (e.g., Çayönü), where the fertile alluvial soils occur (34). One of a few notable exceptions is Tilki Tepe, near the southeastern shore of Lake Van (about the farthest point from any obsidian sources). Sallaberger (2007) shows that, during the third millennium BCE within this area, there was a retreat from urbanism and a return to nomadism. The ceramics also suggest that southeastern Turkey had sparse settlements during the Bronze Age (Burney 1958:164, 168, 193).

In *The Hurrians*, Wilhelm (1989) discusses the likely subsistence practices of "the inhabitants of the mountainous border country" (16). He suggests that highland dwellers could have practiced "many and varied forms of 'mountain nomadism'" supplemented by "exchange and barter with the civilized areas" (16). The archaeological and ethnographic evidence support such a subsistence model being practiced for millennia. Recent surveys in southeastern Turkey by Ur and Hammer (2009), for example, discovered "a variety of

sites and landscape features associated with pastoral nomadic occupation during the last two millennia and possibly earlier" (37). Ashkenazi (1938) recorded that nomads as far as the Harran Plain of southeastern Turkey, just south of Göbekli Tepe, had salt from the Dead Sea, and Crawford (1978) states that, at the same time, nomads in southern Turkey traded salt with the inhabitants of agricultural villages (130).

Crawford (1978) points out, based on historical accounts, that seasonal migrations of several nomadic groups may produce a cross-crossing *de facto* exchange network over long distances (132). Surveys of nomadic groups, conducted in the 1930s during French occupation of Ottoman Syria, mentioned Kurdish shepherds who migrated between Lake Van and the Jebel Sinjar annually. Such a migration would have passed either through or near the Khabur Triangle. Other groups were known to migrate between the Jebel Sinjar and areas near Baghdad. Yet others moved east-west and intersected with the previously mentioned groups, enabling an exchange network among them.

We are also fortunate to have two ethnographic studies of Kurdish shepherds who actually summered their flocks within the Nemrut Dağ caldera: Beşikçi (1969) and Cribb (1991). Beşikçi (1969) migrated with the Alikan tribe and mapped movements of various groups between summer and winter: see Figure 9.19 here. First taking an archaeological approach, Cribb (1991) documented and mapped their dwelling structures, conducted a spatial analysis of their camps, and attempted to reconstruct their demography and social organization (188-195). Subsequently he conducted an ethnographic study of the Alikan tribe, investigating their migratory cycle, tribal and lineage organization, and conceptions

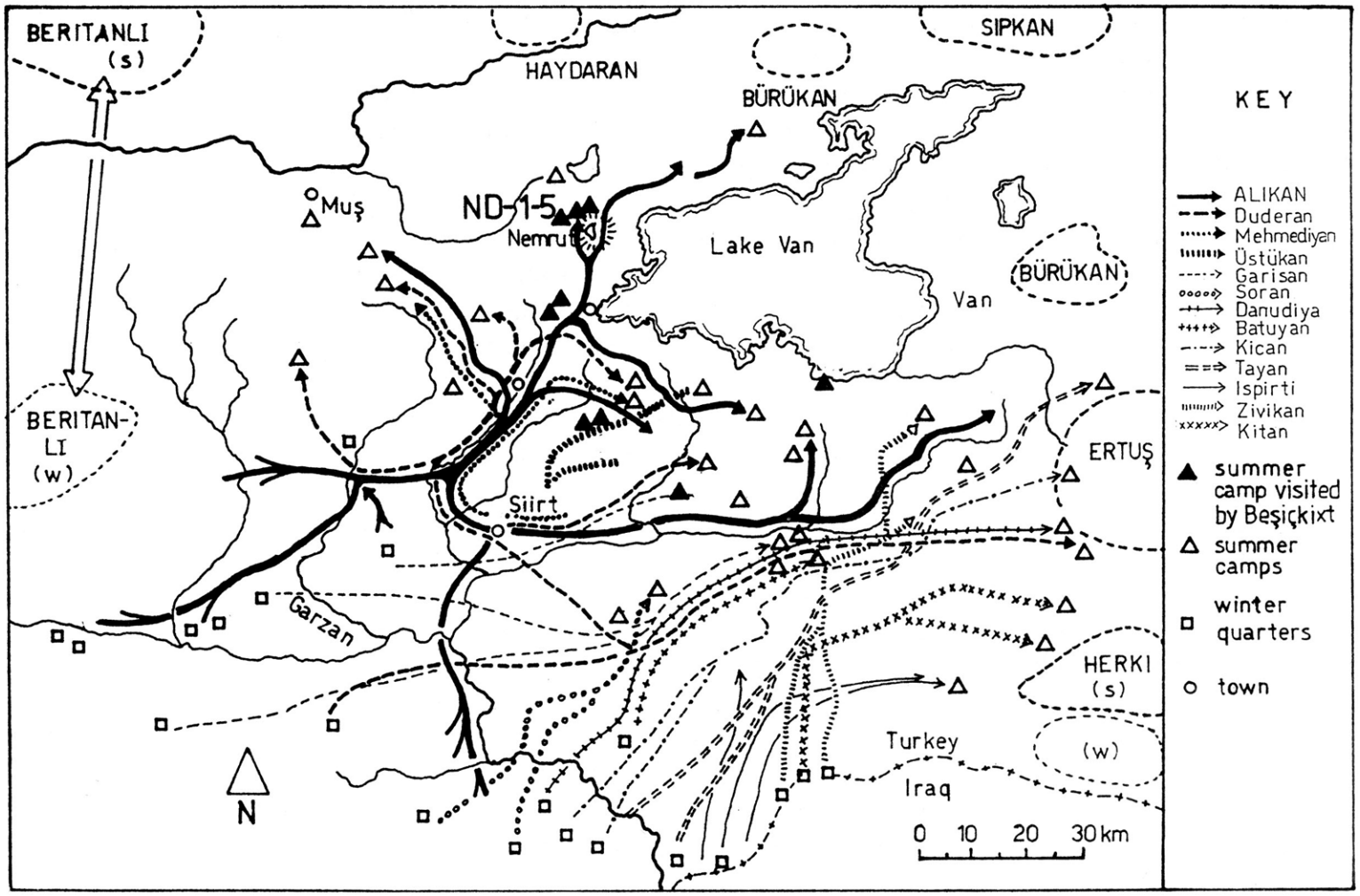


Figure 9.19 - Migration routes of the Alikan and other nomadic tribes across southeastern Turkey and adjacent countries. Note that the Alikan move from Nemrut Dağ to the Tur Abdin foothills. Original map by Beşikçi (1969), redrawn by Cribb (1991).

of wealth and herding, tents and household status, and ranking in camp layout (196-207). Cribb identified several levels of tribal and lineage organization, from confederacy (with other tribes from a common origin in the nineteenth century) and tribe to camp group and tent unit (one extended family or several families) (199). Therefore, it is entirely possible that a number of nomadic groups, each with different migration routes throughout the Tur Abdin highlands and beyond, could all have identified themselves as "Hurrian" on a level roughly equivalent to Cribb's "confederacy" among the Alikan.

Therefore, a *mélange* of obsidians from different sources, transported by nomadic groups during their seasonal migrations, would likely have been present in the Tur Abdin highlands. If Urkesh drew upon a hinterland in the mountainous north, obsidians from a variety of sources should be found at Tell Mozan. If, however, the inhabitants of Urkesh practiced direct procurement or if this city-state exercised control over the nearest source, obsidian from that source should predominate the assemblage.

It is not necessary, though, for the nomads, rather than the inhabitants of farming villages, to have been a Hurrian population. As mentioned previously, during the 1930s, nomads in southeastern Turkey exchanged salt with villagers. Hurrians in the Tur Abdin may have lived in farming villages, and nomads -- perhaps Hurrian, perhaps not -- could have exchanged obsidian with them. In fact, we must consider how obsidians circulating within the northern highlands could have reached the inhabitants of Urkesh, on the other side of the Mardin Pass. This is the topic of the next section.



Figure 9.20 - Modern-day pastoralism in the Khabur Triangle of northeastern Syria. Here a local shepherd guides his flock of sheep and goats across the surface of Tell Mozan (photograph by the author).

9.6.2 - Bringing the Obsidian to Urkesh

There are three ways to explain how a *mélange* of obsidians, the product of varied exchange networks through the highlands, may have reached Urkesh via the Mardin Pass. First, Cribb (1991) documented interactions of an Alikan tribe, which summers within the Nemrut Dağ caldera, with villagers south of the Taurus range during winter:

> During the winter months the tribe is dispersed in small units of two to five tents pitched within or on the outskirts of villages to the south of the Taurus Mountains. Although the villagers have no tribal or kinship connection with the Alikan Aşiret, the wintering nomads become a temporary part of the village community, drawing on its services and land resources and coming under the authority and protection of the village *ağa* [leader] or *kaymakam* [governor]. (198)

These nomads, therefore, become part of a village, and its economy, during winter. Cribb notes that similar phenomena happen, on a smaller scale, at villages along the way:

> … the tribespeople themselves pass through the settlements buying and selling in the local bazaars, visiting mosques, shrines, etc. Stops are made at transit camps on the way for a maximum of five or six days. (198)

Consequently, a wide variety of obsidians could have reached Urkesh as pastoral nomads, perhaps Hurrian themselves, wintered there or somewhere nearby.

A second mechanism for the arrival of varied obsidians at Urkesh could be annual bazaars involving exchange among nomadic and sedentary groups. Crawford (1978), for example, describes two such modern bazaars in Syria and Afghanistan:

> Today, great annual gatherings such as those of the Rwala [clan of the Aniza Bedouins] and others outside Damascus are the occasion for much commercial activity, not only among the Bedu themselves, but also between the long distance travellers and the less mobile sheep and goat herders, who then distribute the surplus of the goods thus acquired to the sedentary population. In Afghanistan there is a similar interaction between the long distance caravaneers and the sheep

> and goat herders at bazaars traditionally held at certain localities outside the settled centres each year. At these bazaars there is a considerable traffic in livestock, especially sheep, as well as in imported goods. (131)

Therefore, bazaars and other economic activities might have occurred at Urkesh, bringing obsidian from a variety of sources to the site. This reflects the quote from Max Mallowan at the start of this chapter: "down the precipitous mountain roads… many a hillman must have set out on his way to the Khabur; warriors, traders, birds of passage and settlers, all of them seeking their fortunes" via the pass (10-11). As the largest settlement in the area, Urkesh was certainly a conspicuous landmark and a magnet that attracted travelers (i.e., Molyneaux's centripetal effect mentioned in Section 8.3.5).

A third possibility is related to the second: as discussed in Chapter 3, Urkesh was a religious center. For example, Urkesh was considered the abode of Kumarbi, the father of the Hurrian deities. The city also had two monumental ritual features: the temple with its extensive terrace and the âbi, where a religious figure consults or appeals to the spirits of the underworld. Perhaps most importantly, there is a public plaza, discussed in Section 3.6.4, where people could gather at the base of the temple. Therefore, it is reasonable to presume that there were festivals at Urkesh, and Hurrians from throughout the hinterland might have travelled to Urkesh as a ceremonial center. This may also be reflected in the tale of Silver's pilgrimage from the mountains to Urkesh.

9.6.3 - Comparison to the Data

As discussed in Section 9.2.1, there is an unusual number of sources represented among the artifacts at Tell Mozan. Depending on one's definition of a "source," there are

at least seven or eight sources, maybe as many as nine, among the studied artifacts alone: two flows at Nemrut Dağ, Bingöl A, Bingöl B, Meydan Dağ, Tendürek Dağ, Kömürcü at Göllü Dağ, and Muş and/or Pasinler. Analyses of further artifacts could reveal even more sources present. Roughly 97% of the sourced artifacts at Tell Mozan came from obsidian sources in Eastern Anatolia, but no single source dominated the assemblage. About 60% of the artifacts came from two flows at Nemrut Dağ, and about 23% of the artifacts came from the Bingöl sources: 5% from A and 18% from B. Roughly 6% came from Tendürek Dağ, 6% likely from a source on the Muş Plain, and 2% from Meydan Dağ. The final 3% originated from a single obsidian source in Central Anatolia.

Earlier studies have reported fewer obsidian sources at other Bronze-Age sites in Mesopotamia, as documented in Chapter 8. Hall and Shackley (1994) found one source at Hirbet Tueris and two sources at Tell Hamoukar. Chabot et al. (2001) reported just one source at Tell Gudeda and two sources at Tell ʻAtij. Schneider (1990) identified only two sources at Uruk, and Renfrew et al. (1966) report one source at Tell Abu Shahrain. Thus, the number of obsidian sources at Tell Mozan is clearly atypical for Mesopotamia during the Bronze Age. There are also fewer obsidian sources at Chalcolithic sites in the Khabur Triangle. Khalidi et al. (2009) recognized four sources in Late Chalcolithic levels of Tell Hamoukar and three sources at Tell Brak during the Chalcolithic. In other words, at least twice as many obsidian sources are present at Tell Mozan.

9.6.4 - Interpretation of the Results

The atypical diversity of sources represented among the obsidian artifacts at Tell Mozan appears to rule out that the inhabitants of Urkesh practiced direct procurement or that the state exercised control over the nearest source. Instead, this *mélange* of sources does support a hypothesis that the Urkesh state and/or inhabitants had access to a greater variety of obsidians, almost entirely from Eastern Anatolian sources within the ranges of pastoral nomads. As a result of migration by nomadic groups -- perhaps Hurrian, perhaps not -- a variety of obsidians were distributed throughout the northern highlands, and these obsidians were brought through the Mardin Pass to Urkesh. This may also mean that the northern highlands served as a hinterland for this city-state. The implications for Urkesh as a "gateway city" are subsequently discussed in Section 9.8.2.

We need not assume that, because Bronze-Age cities like Urkesh seemingly had a palace economy, obsidian exchange was regulated by the state. Wilhelm (1989) explains that a palace economy, as described in the Mitanni-period texts from Nuzi, refers "to the near-monopoly that the palace enjoyed over foreign trade" and its capacity as a center for production activities (44). He emphasizes, in particular, control over exchange of metals and metalworking activities conducted at the palace (44-46), but as mentioned in Section 9.3.5, he concludes that "the production of textiles was the most important" (45). Kuhrt (1995) similarly claims that the palace both controlled exchange of metals and organized the production of finished metal items; however, he notes that the palace apparently "did not play the dominant role in agricultural production" (298). I presume that Urkesh had

a palace (-dominated) economy with respect to certain resources, such as metals, but we cannot state at this point whether obsidian exchange and production activities (e.g., blade production) were, either directly or indirectly, state-controlled.

9.7- Considering "Nawar" as Nagar and Tell Brak

The existence of a direct link between Urkesh and Nagar (or perhaps another city in the Khabur Triangle) may be considered in light of the obsidian data. The proportions of the various obsidian sources represented at Bronze-Age and Chacolithic settlements in northeastern Syria can be compared to those at Urkesh. Notable differences will suggest that obsidian from Urkesh, brought through the Mardin Pass, was not directly exchanged with that site. Similar obsidian source patterns, on the other hand, would lend support to exchange between the two sites. These data should be compared not only for Tell Mozan and Tell Brak but also for other Bronze-Age and Chacolithic cities.

9.7.1 - Formulating and Testing the Hypothesis

If one ruler governed over a kingdom that included Urkesh and Nagar, it follows that imported natural resources might be distributed rather evenly between the two urban centers, especially given the likelihood of a palace economy at these sites. Therefore, if, in fact, Atal-šen was the king of Urkesh and Nawar and there was a link in the resources of Urkesh and Nagar, the obsidian sources represented among the artifacts at Tell Mozan and Tell Brak and their relative proportions should be rather similar. Similar source data

for Tell Mozan and Tell Brak, particularly when compared to other Khabur Triangle sites, would give support to a link between the two settlements. Very distinct source data may indicate that Urkesh and Nagar had different access to obsidians.

At present, the ability to compare my obsidian data from Tell Mozan to data from Tell Brak and the other Bronze-Age and Chacolithic sites is somewhat limited. The vast majority of sourcing studies cannot discern between Nemrut Dağ and Bingöl A obsidians and put them together in an equivalent to RDC's Group 4c. Similarly, nearly all sourcing studies make no distinction between the obsidians of Meydan Dağ and Tendürek Dağ and instead match artifacts to RDC's one "Bayezıd" specimen, part of their Group 3. Thus, to make the comparisons, I must "translate" my sources to reflect these groups, as shown in Figures 9.21 and 9.22. This hinders the comparisons somewhat, and one priority must be using techniques at other sites that can discern these obsidians.

The other limitation, at present, is that obsidian source data are available for only five Bronze-Age sites in the Khabur Triangle: Tell Hamoukar, Hirbet Tueris, Tell Mulla Matar, Tell Gudeda, and Tell 'Atij. There are no data for Bronze-Age strata of Tell Brak. Instead, only data for the Late Chalcolithic levels of Tell Brak, as determined by Khalidi et al. (2009), are available for comparison to my Tell Mozan data. The Late Chalcolithic data for Tell Brak are used here with the understanding that the datasets for the two sites are not contemporaneous. Another priority, to better test the hypothesis at hand, must be acquiring source data from the Bronze-Age strata of Tell Brak.

Figure 9.21 - Obsidian Sources at Khabur Triangle Sites during the Bronze Age

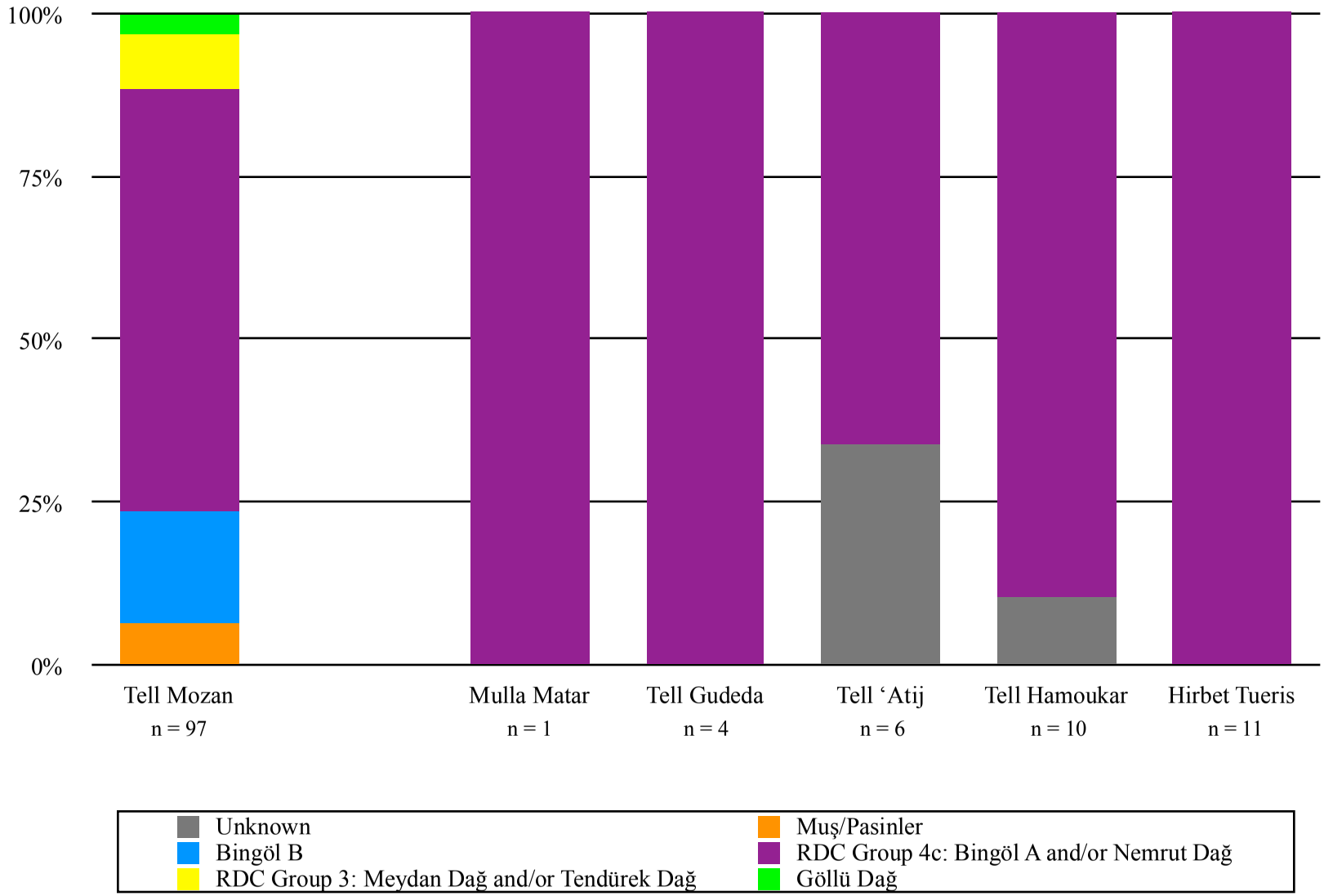
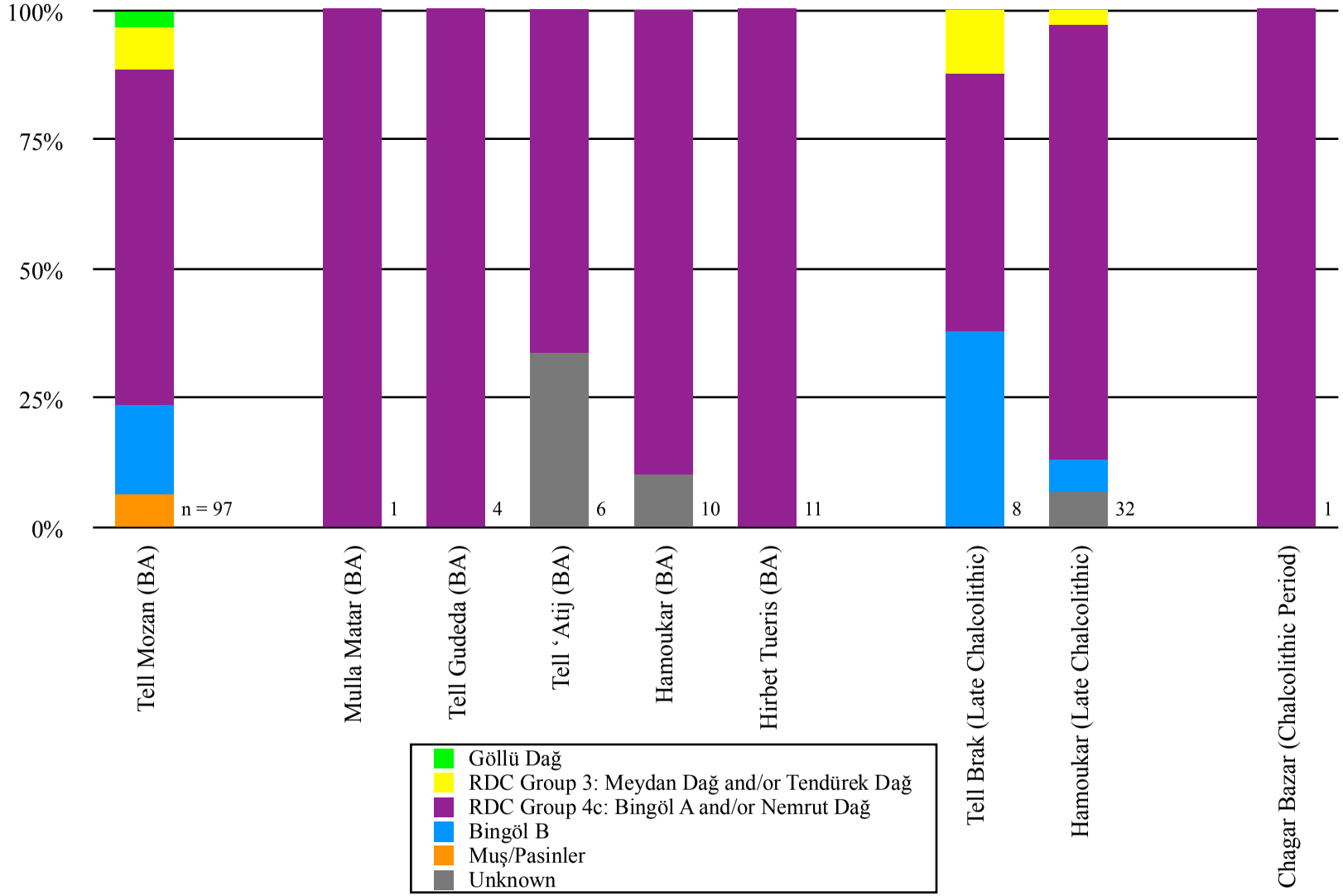


Figure 9.22 - Obsidian Sources at Khabur Triangle Sites - The Bronze Age and Chacolithic Period



9.7.2 - Comparison to the Obsidian Data

Figure 9.22 shows my "translated" obsidian data for Tell Mozan with the existing data for Bronze-Age and Chacolithic settlements in the Khabur Triangle. Clearly there is no match to Tell Mozan among the other Bronze-Age sites. Compared to the Bronze-Age data for Tell Hamoukar, Hirbet Tueris, Tell Mulla Matar, Tell Gudeda, and Tell ʻAtij, the pattern of obsidian sources represented at Tell Mozan is unique.

The data for Tell Brak, in comparison, is a reasonably good fit to the data for Tell Mozan, especially considering that only eight artifacts from Tell Brak were sourced. All three main groups from Tell Mozan are present at Tell Brak: (1) Nemrut Dağ and Bingöl A, (2) Bingöl B, and (3) Meydan Dağ and Tendürek Dağ. The two scarcest groups at Tell Mozan -- Göllü Dağ and Muş/Pasinler -- are not present among the sourced artifacts from Tell Brak, but this is expected given the low number of artifacts analyzed. Provisionally, at least, I would argue that Tell Mozan and Tell Brak are a match.

At first glance, the obsidian source data for Late Chacolithic Tell Hamoukar seem like they might also match the data from Tell Mozan; however, I consider Tell Hamoukar to be a much less likely match than Tell Brak for two reasons. First, Khalidi et al. (2009) explain that their samples, especially that for Tell Hamoukar, are not representative of the entire assemblages and are biased to include diverse obsidians:

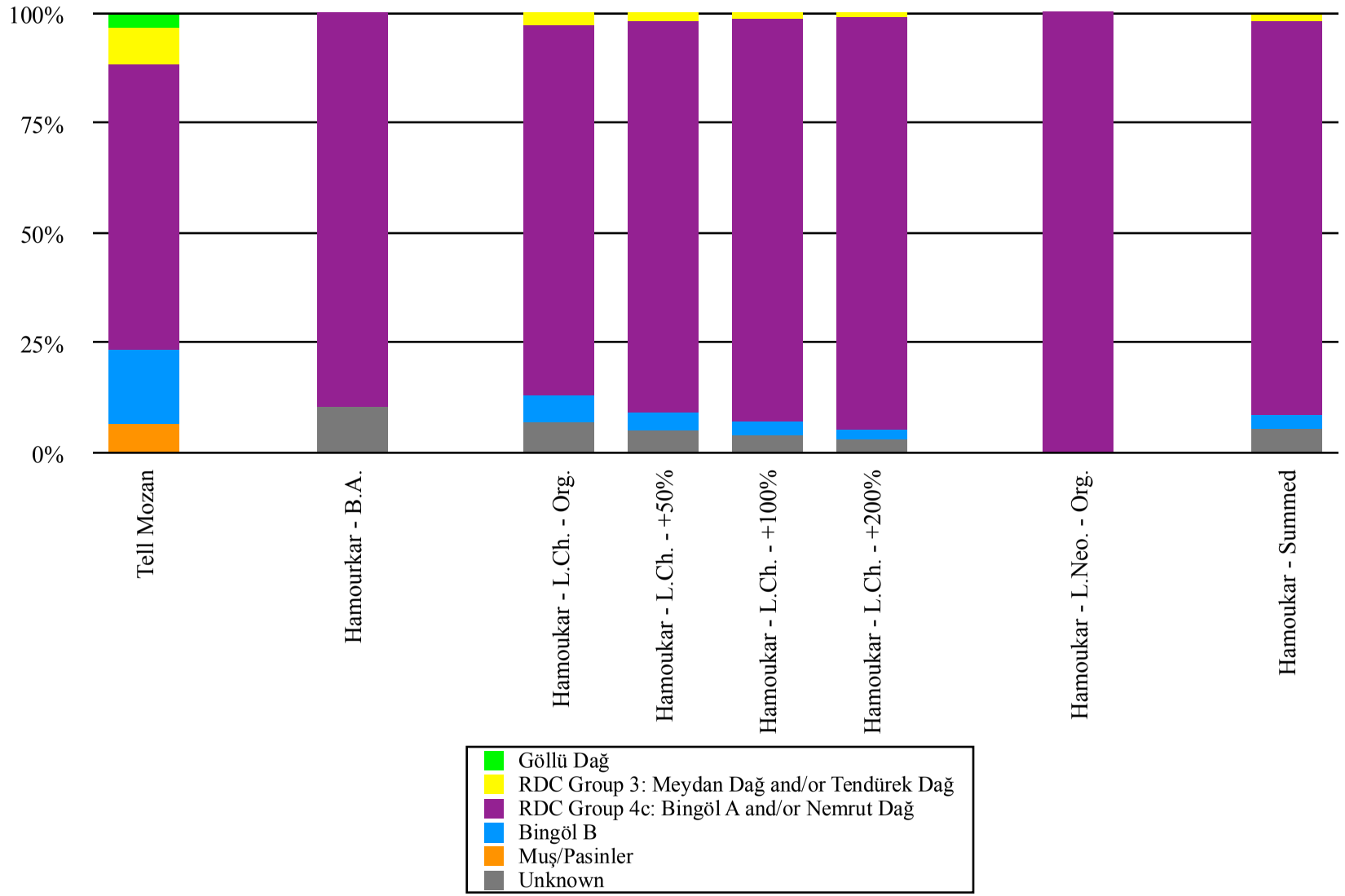
> … the selection aimed towards a diversity of obsidian varieties, despite the fact that peralkaline obsidian predominated at both sites. Because the quantities of obsidian were much higher at Tell Hamoukar, the gamut of small flakes and fragmentary obsidian products (and thus the potential for a greater variety of obsidian) to choose from was larger. (882)

Hence, the source proportions in Khalidi et al. (2009), particularly for Tell Hamoukar, are not representative, and the data consequently exaggerate the abundance of obsidians from scarcely used sources. Even with this distortion, almost 85% of the artifacts analyzed by Khalidi et al. (2009) came from Nemrut Dağ and/or Bingöl A. Depending on how much Khalidi and colleagues undersampled the peralkaline obsidian artifacts at Tell Hamoukar, the actual proportion could be greater than 90% or 95%.

Second, there are also data on obsidian sources at Tell Hamoukar from the Bronze Age and the Late Neolithic Period. These two other datasets show greater deviation from the Tell Mozan source data and reinforce that the actual proportion of peralkaline artifacts at Tell Hamoukar is most certainly closer to 90% or 95%. Recall that Hall and Shackley (1994) sourced ten obsidian blades, likely dating to the Bronze Age, from Tell Hamoukar. Nine (90%) came from Nemrut Dağ and/or Bingöl A, and one blade (10%) came from an unknown source, possibly Meydan Dağ or Tendürek Dağ. From the Late Neolithic strata of Tell Hamoukar, Francaviglia and Palmieri (1998) sourced 16 artifacts and attributed all of them (100%) to Nemrut Dağ and/or Bingöl A. Thus, when sourced artifacts are chosen randomly, the predominance of peralkaline obsidian is evident.

In Figure 9.23, I have attempted to summarize these effects on the source data for Tell Hamoukar. When the data from Khalidi et al. (2009) are even moderately adjusted to account for the undersampling of the peralkaline artifacts, the proportions further increase in deviation from the Tell Mozan data. When the Bronze Age and Late Neolithic data for Tell Brak are considered too, the differences are clear as well.

Figure 9.23 - Comparison of Obsidian Sources at Tell Mozan and Tell Hamoukar

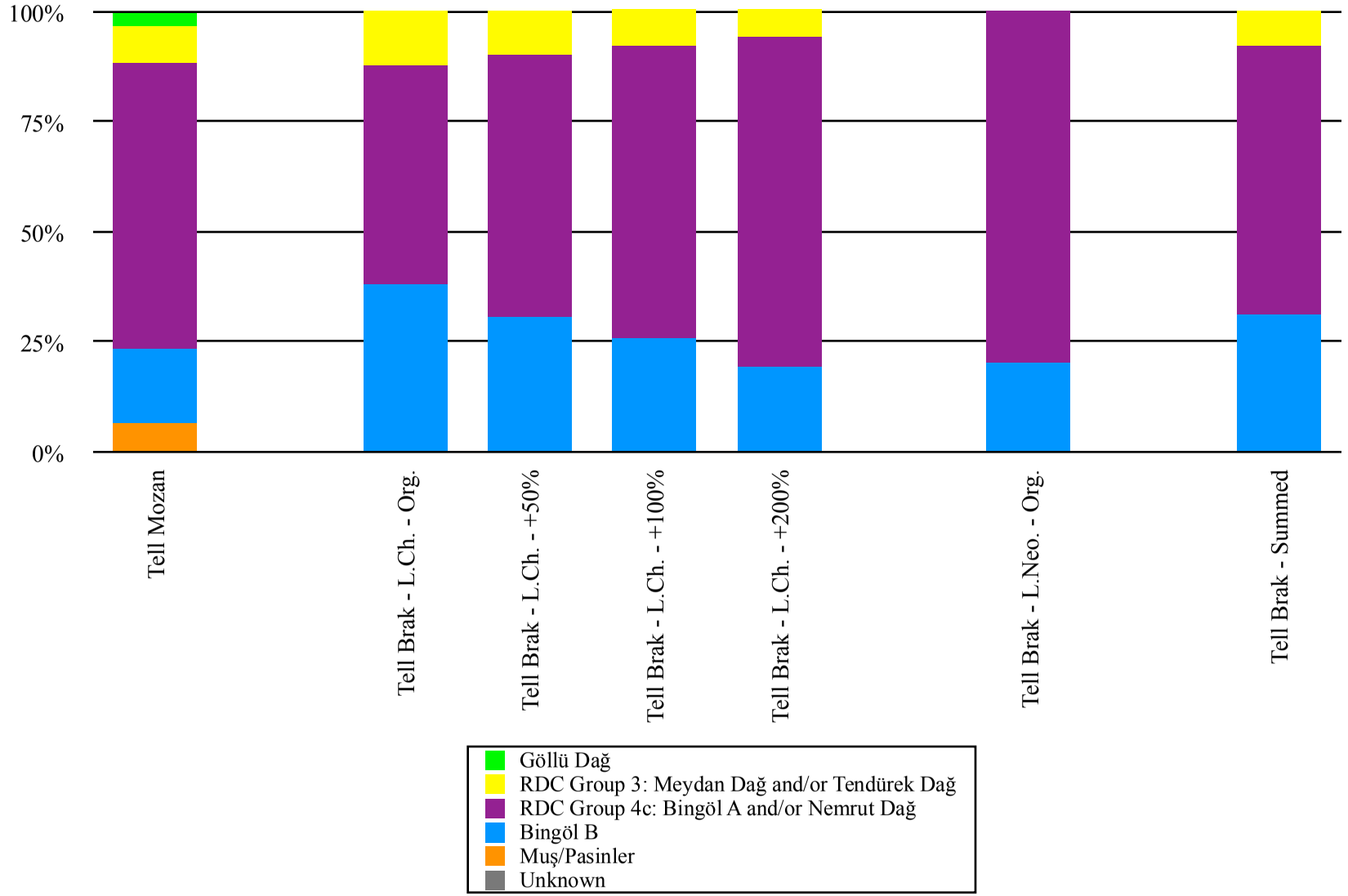


When the same adjustments, though, are made to the Tell Brak data, their fit with the Tell Mozan obsidian source data actually improves, as illustrated in Figure 9.24. This further suggests that Tell Brak is a much more appropriate match to Tell Mozan than Tell Hamourkar. In turn, the similar source patterns at Tell Brak and Tell Mozan give support to the hypothesis that there was an exchange link between the two settlements, perhaps as part of a kingdom or an alliance between Urkesh and Nagar.

9.7.3 - Another Similarity of Urkesh and Nagar

Tell Mozan and Tell Brak have another notable similarity that might also support a link between them. During the so-called "third-millennium urban collapse" in Northern Mesopotamia, many settlements, such as Tell Leilan and Tell Beydar, appear to have been abandoned, or nearly so, for debated reasons. Akkermans and Schwartz (2003) point out the "collapse of the late third millennium had its conspicuous exceptions -- urban centers that thrived in a period traumatic to other communities" (284): Tell Mozan and Tell Brak. These authors inquire: "Why did these two urban centers survive, and not Leilan, Beydar, or Chuera?" (285). They propose the sites' locations (e.g., Tell Mozan near the southern access to the Mardin Pass) played key roles in their survival (286). Other archaeologists have also highlighted the survival of Tell Mozan and Tell Brak after the "collapse" (e.g., Weiss et al. 1993, Oates et al. 2001, Wilkinson 2000, Wilkinson et al. 2007). The general consensus is that most cities were deserted during this "collapse" due to increased aridity straining rain-fed agriculture systems that fed their inhabitants.

Figure 9.24 - Comparison of Obsidian Sources at Tell Mozan and Tell Brak



Another shift happened at roughly the same time. Riehl (2009) reports that hulled emmer wheat (*Triticum turgidum* ssp. *dicoccon*) was a common crop throughout northern Syria during the Early Bronze Age. She explains, though, the crop "virtually disappeared in Syria with the beginning of the Middle Bronze Age, except in the two continuing upper Khabur sites of Tell Brak and Tell Mozan" (100). Riehl (2009) states that, because hulled emmer wheat has lower yields and requires more intensive labor, its continued use at Tell Brak and Tell Mozan suggests that the two cities might have survived due to better water availability and did not endure for "political reasons" alone (111).

Riehl's interpretation of this persistence of hulled emmer wheat at Tell Mozan and Tell Brak is only one scenario. It is also possible that the causality is reversed. This crop might have fallen out of favor at settlements that had been largely abandoned, particularly because there was no longer the labor force needed to support it. Another scenario is that the hulled emmer wheat was not actually grown exclusively at Tell Brak and Tell Mozan. Instead, Tell Brak and Tell Mozan might have had continuing access to this crop while it decreased to near archaeological invisibility at other sites. Special access to a resource or commodity could indicate the importance of Urkesh and Nagar in Bronze-Age exchange throughout the Khabur Triangle. This would also be consistent with Tell Mozan and Tell Brak both serving as "gateway cities" or working together as a gateway-city/central-place pair, which is the topic of my discussion in Section 9.8.2.

9.8 - Implications of the Results Regarding "Nawar"

My obsidian source data from Tell Mozan, when compared to existing data from surrounding sites, suggest that (1) the state and/or inhabitants of Urkesh had access to an unusual variety of obsidians from mostly Eastern Anatolian sources within the ranges of pastoral nomads and (2) the obsidian source pattern at Tell Mozan more closely matches the pattern at Tell Brak than any other post-Neolithic site in the Khabur Triangle, hinting at a possible link between the two settlements. Consequently, it seems equally likely that "Nawar" was a northern hinterland or an alternate name for Tell Brak. One implication is that both places may have had the same name. Another issue is that Tell Brak, regardless of whether it was Nawar, might have played a role in exchange at Tell Mozan if both sites were gateway cities or comprise a gateway/central-place pair.

9.8.1 - Could Both Locations Be "Nawar"?

There is textual evidence that suggests, in fact, Tell Brak and a northern hinterland of Urkesh may both have been known as Nawar. Matthews and Eidem (1993) report that a tablet, recovered at Tell Leilan and dated to about the mid-second millennium, describes a treaty between the kings of Tell Leilan and Kahat. Tell Leilan is about 45 km southeast of Tell Mozan and about 50 km northeast of Tell Brak -- earlier authors (e.g., Weiss 1985: 27) have noted their near equidistance. Kahat is usually identified with Tell Barri, a mere 10 km northeast of Tell Brak. The clay tablet describes the territory of Kahat as spanning "from Nawar to Nawar." Matthews and Eidem (1993) claim that, because ancient Nagar

might also be one "Nawar" and lies south of Tell Barri, "it follows that the second Nawar probably must be located north of Barri," possibly near Al Qamishli (204). They further speculate that perhaps even "the spelling of an original northern Nawar was subsequently applied to a southern place Nagar," that is, Tell Brak (204-205).

There is, in fact, precedence for identical names in Northern Mesopotamia during the Bronze Age. Ristvet (2008) proposes that "Nawar to Nawar" is an instance of "mirror toponymy" as described by Charpin (2003). Based on early- and mid-second-millennium texts, Charpin (2003) discusses cases of twin geographical names. Some of the locations are "mirrored" by the landscape, lying on opposite sides on a mountain or river. In other cases, the two locations are farther apart. Charpin explains the identical names could be due to the movement of people and the use of descriptive terms (e.g., there are two towns in California named Hillside). She suggests, for example, that Amorite migrations during the third and second millennia BCE led to the existence of two territories named Razâma, one area on the northern side of the Jebel Sinjar and one on the southern side. The Sinjar range is the "mirror" in this case. Charpin (2003) reports that there are many other place names in Mesopotamia split between north-south and east-west.

One can conceive of a similar (and contemporaneous) situation in which Hurrians from the northern mountains, which had the name Nawar first, migrated into the southern Khabur Triangle, where a city originally named Nagar came to be known as Nawar. This would fit with the proposals from Matthews and Eidem (1993). These same authors note that, during the late third millennium BCE, the king of Tell Brak was also Hurrian (or had

a Hurrian name). Talpuš-atili had the title "sun of the land of Nagar," as known from seal impressions written in Hurrian, while Tupkish was *endan* of Urkesh. Evidence for a later Hurrian presence at Nagar increases, including a Mitanni palace (Illingworth 1988), texts (Wilhelm 1991), and Mitanni ceramic wares (Oates 1987).

As I noted in Section 3.6.3, Buccellati and Kelly-Buccellati (2007a) propose that, based on the irregular shapes of the terrace and staircase, symmetry "was clearly *not* part of the stylistic preferences of the Hurrians" (3). Their preferences regarding monumental architecture, maybe meant to mimic a mountainous landscape, do not necessarily rule out a sort of geographical symmetry in place names. In fact, Buccellati and Kelly-Buccellati (1997a) documented three Hurrian traditions of mirror imaging and writing in royal seals (88-89). One of these traditions involves pairs of cylinder seals that are mirror images of one another, and another involves seal impressions that may be understood only when the writing is reversed. The third tradition is what they call "epigraphic doublets," which are seals for which the word would have been reversed (and possibly the meanings different) if one read the cuneiform as either Hurrian or Akkadian text. Perhaps, therefore, "mirror toponymy" would be congruent with such Hurrian traditions.

Therefore, in a potential example of mirror toponymy, it is possible that there was one Nawar almost directly due north from Urkesh and a second almost directly due south. The "mirroring" geographical features in this case would be the Mardin Pass in the north and the pass near Al Ḥasakah between the Jebel Abd el Aziz and Jebel Sinjar in the south. Following Charpin (2003), it is possible that the movement of Hurrians could explain the

same names for two locations, and it raises the potential that "Nawar" is a geographically descriptive word for a landscape feature like a mountain pass.

9.8.2 - Urkesh and Nagar as Gateways or a Gateway/Central-Place Pair

The concept of a particular city serving as an access point or "gateway" into some adjoining territory is common in geographical and popular literature. Andrew Burghardt, a geography professor, was the first to rigorously define "gateway cities" and to develop a theory of their development based on modern examples, including Winnipeg, St. Louis, and Minneapolis-St. Paul. Burghardt (1971) explains:

> The word 'gateway' gives a fairly clear image of the unique positional characteristic of a gateway city. It is an entrance into (and necessarily an exit out of) some area. The entrance tends to be narrow and will probably be used by anyone wishing to enter or leave the tributary area 'behind.' The city is in command of the connections between the tributary area and the outside world... an opening through some obstruction is implied. (269)

His theories on "gateway cities" have been used rarely in archaeology (e.g., Hirth 1978 in Formative Mesoamerica, Hodges 1982 in medieval Europe, Algaze 1993 in Uruk-Period Mesopotamia, Kelly 2000 at Cahokia), especially compared to Christaller's older central-place theory. In fact, Burghardt specifically contrasts gateway cities (situated at one end of a tributary area) and central places (situated at the center). He writes:

> Gateway cities… tend to be between differing homogeneous regions. In contrast, the central place, at least in its idealized format, lies within a relatively homogeneous productive region. Although long-distance ties are obviously present, the central place is characterized principally be local trade connections; although local ties are obviously important, the gateway is characterized best by long-distance trade connections. (270)

He furthermore explains that gateway cities are defined, in large part, by their locations at transportation nodes. This is not true for central places because Christaller's formulation includes the assumptions that transportation costs are equal in every direction across a flat landscape. Central-place theory also assumes an even distribution of resources as well as the population. A gateway city, though, is located on or near a boundary, specifically "the boundary (or the zone) between areas of differing intensities or types of production (e.g., ports, humid/arid, fertile/infertile, lowland/upland...)" and "in positions where possess the potentiality of controlling the flows of goods and people" (272, 282).

Kenneth Hirth, a Mesoamerican archaeologist, contends that Burghardt's gateway cities represent actual landscapes more accurately than Christaller's central places:

> Unlike central places, gateway-dendritic networks are based upon the kinds of natural irregularities found in the real world... The central place model is based upon conditions that do not exist in the real world. These include the existence of an isotropic plane with a uniform distribution of population, resources, and purchasing power. The gateway community model on the other hand, sees environmental discontinuities such as natural corridors of trade and communication as important variables in the growth of settlement. In central place analysis these are 'unnatural' anomalies that are thought to distort rather than help explain the pattern of regional settlement. (1978:38, 43)

Thus, in its location on the border of the Tur Abdin mountains and the alluvial plains and near the Mardin Pass, a central place model would be a poor fit for Urkesh. Instead, Tell Mozan is clearly located an obstruction and its main access point.

Burghardt's theories regarding gateway cities are based on modern examples for which there are records on production, transportation, demography, and other important factors. Accordingly, many of his predictions are difficult to establish in antiquity due to

their near archaeological invisibility. Also, as discussed in Section 8.3.1, the relevance of modern economic theories, in the substantivist and culturalist views, to other societies in antiquity is open to debate. A few of his predictions, though, are relevant to the issues at hand. For example, Burghardt claims that hinterlands of gateway cities, on the border of two territories, "usually extend further into the less productive than into the productive area, because competitor cities will not rise as readily in the former as in the latter" (273). This means that, as predicted, the hinterland of Urkesh should have stretched farther into the rural mountains than into the fertile alluvial plains with other urban centers. He also points out that gateway cities grow quickly and "become famous as boom towns" (282). This might also be applicable because, as mentioned in Chapter 3, Urkesh was one of the largest settlements in Syria during the third millennium BCE.

Burghardt's most relevant observation about gateways is that their locations "have have produced a number of twin cities," including Minneapolis-St Paul (285):

> Although it is hazardous to attempt to draw tight distinctions between the two, it does seem that the city closer to the frontier, or to the areas of lower productivity, has been primarily the gateway, whereas its partner (towards the national core region) has been more of a central place... Thus one may distinguish between Fort Worth (gateway) and Dallas (central place), Minneapolis (gateway) and St. Paul (central place), Pest (gateway) and Buda (central place), seventeenth century Bratislava (gateway) and Vienna (central place). (285)

Therefore, a possibility to consider is that Urkesh and Nagar were twin cities (in the sense of their roles in regional exchange). Perhaps these settlements acted as gateway cities, or maybe they instead functioned as a gateway-city/central-place pair.

A few archaeologists have previously proposed, either implicitly or explicitly, that Tell Brak may have functioned as a gateway city (e.g., Algaze 1989, 1993; Wright 2004). Near Eastern archaeologist Harvey Weiss, known primarily for his research at nearby Tell Leilan, was the first to suggest that Tell Brak was such a city:

> Tell Brak might be understood as one of a class of settlements, occurring in a variety of historical and geographical contexts, sometimes labelled 'gateway cities.' Such settlements characteristically control the entrance into a region, command the connections between that region and the 'outside world,' and are often located eccentrically at one end of the region, sometimes at the border between regions defined by different kinds of agricultural production (Burghardt 1971). These characteristics fit the geographical, climatic, and cultural situation of Tell Brak, as we know it, quite well. (1985:26)

For example, Tell Brak lies near the southern limit for reliable rain-fed agriculture, which constitutes a border between more-productive (i.e., dry farming) and less-productive (i.e., irrigation-dependent) regions (although, as discussed in Section 3.4, northeastern Syria was wetter in the third millennium). Its location also suggests that the inhabitants would have been able to control transportation along the Khabur River where "it passes through the 'gates' of the Jebel Abd al-Azziz and the Jebel Sinjar" (27).

Tell Mozan is more clearly an example of a gateway city, as originally claimed by Kelly-Buccellati (1990), who pointed out that Urkesh was…

> … located at a point where the environment changes radically from the fertile north Syrian plains to the mountainous uplands of the southern Taurus; this strong advantage as to site location is emphasized by the fact that Mozan is situated at the outlet of the major pass into the eastern Taurus at Mardin. (126)

She claims that, because gateway cities tend to form in response to developing exchange, Urkesh might have grown in response to an increase in the demand for copper and other

mountain resources in emerging urban centers of the Khabur Triangle.

> we witness at this time the establishment of cultural links between what appear to be predominantly Human (or Proto-Hurrian) populations in northeastern Syria and eastern Anatolia. The flow of goods facilitated by these interregional contacts and stimulated by local and long-distance demands became so complex that mechanisms of resource pooling and redistribution of goods had to be centered in large population areas where goods could be controlled and manipulated on a larger scale. At specific environmentally advantageous points new settlements quickly grew into powerful gateway cities such as Mozan and Chuera, with Brak continuing to control trade in the eastern portion of the Khabur triangle. (126)

In other words, according to Buccellati and Kelly-Buccellati (2007c), ancient Urkesh can be considered "the urban efflorescence of the mountainous north," whereas ancient Nagar seems to have "look[ed] to the south, not the north" (150).

Consequently, it is possible that the similar obsidian source patterns at Tell Mozan and Tell Brak are not a result of a Hurrian kingdom or a political alliance between the two settlements. Instead, Urkesh and Nagar could have been economically linked. It may be that the settlements both served as gateway cities. Tell Mozan lies near the border of the mountains and the fertile alluvial plain, whereas Tell Brak lies near the transition between rain-fed and irrigation-dependent agriculture. In addition, Tell Mozan lies at the outlet of the Mardin Pass, whereas Tell Brak lies near the pass between the Jebel Abd al-Azziz and Jebel Sinjar. Thus, Urkesh served as a gateway between the Tur Abdin highlands and the Khabur Triangle while Nagar may have served as a gateway between the Khabur Triangle and Southern Mesopotamia. Another possibility is that Nagar served as a central place to the gateway city of Urkesh. In this case, which may be archaeologically testable, Urkesh would have been more focused on long-distance exchange while Nagar would have been

more involved in local distribution of the imported resources. In either scenario, Urkesh and Nagar could have been linked not by a kingdom but by their roles -- either similar or different -- in an exchange system across the Khabur Triangle.

9.9 - The Potential Significance of Nemrut Dağ

Over half of the sourced obsidian artifacts (53%) came from one part of a specific within-caldera flow of Nemrut Dağ (i.e., Rapp and Ercan's collection area EA25). These obsidians were collected from a lava dome in the southeastern portion of the caldera, near or along the shore of the lake. Only obsidians from this location were utilized in all three areas of Tell Mozan (A, B, and J) and during all periods from the mid-third to late-second millennium BCE. Therefore, although the inhabitants of Urkesh probably did not directly acquire obsidians from Nemrut Dağ, these obsidians had somewhat a unique status at Tell Mozan, and this volcanic caldera deserves additional attention.

9.9.1 - Identifying the Collection Loci

As I have previously mentioned, most obsidian sourcing studies in the Near East cannot differentiate between Bingöl A and Nemrut Dağ obsidians, the sources for which are more than 150 km apart. I, however, have shown where Nemrut Dağ obsidians were collected to within one kilometer. The obsidian-bearing lava flows of Nemrut Dağ seem to have very similar, but still distinct, compositions that may be distinguished using high-precision chemical analyses. This finding is consistent with that of Laidley and McKay



Figure 9.25 - Nemrut Dağ (right), the Taurus Mountains (center), and the Tur Abdin highlands (left) (Photo ISS022-E-021102, taken 8 January 2010 by the International Space Station crew; the NASA/JSC Gateway to Astronaut Photography of Earth).

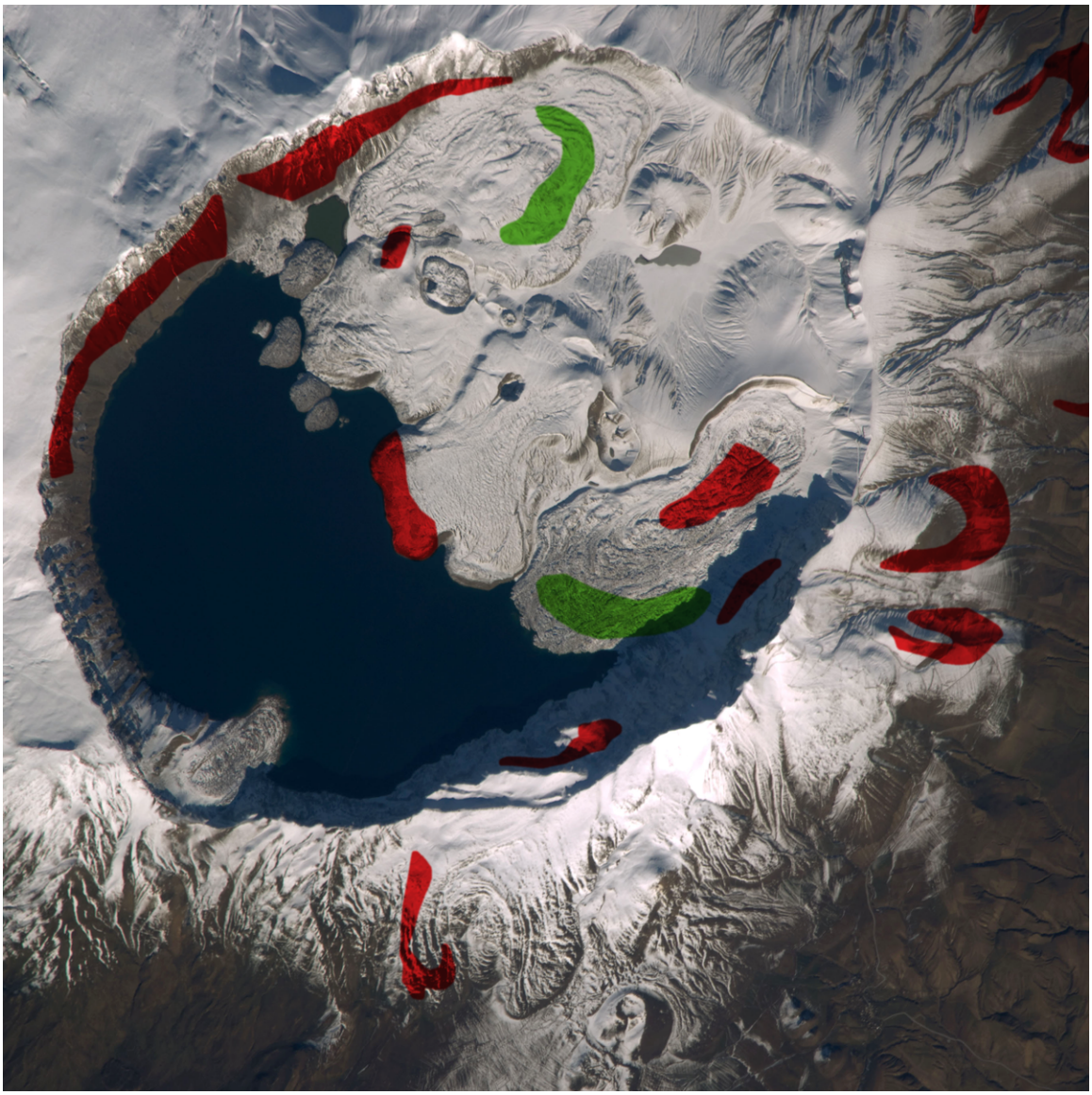


Figure 9.26 - The highlighted locations are the obsidian-bearing features of Nemrut Dağ identified and sampled by Rapp and Ercan. Green represents sources of obsidian found at Tell Mozan (i.e., EA22 and EA25). Red represent sources not found at Tell Mozan. (Based on the survey map of Rapp and Ercan; collection of the author. Background is a composite of Photographs ISS018-E-10205 and -10206 taken by the International Space Station crew; available at the NASA/JSC Gateway to Astronaut Photography of Earth.)

(1971), as mentioned in Section 4.3, at Newberry Volcano. They discovered that the lava flows in the caldera were compositionally similar, due to the same host rock and magma chamber, although still discernible by their chemistries. They also concluded that, while Big Obsidian Flow was homogeneous, two elements -- Mg and Rb -- varied statistically significantly across a transect and that only Zn varied between the lava erupted first and the lava erupted last (338). They explain that "highly precise analyses are necessary" to observe these variations (342). My analyses seem sufficiently precise to identify similar zoning within the southernmost flow in the Nemrut Dağ caldera.

Rapp and Ercan collected specimens from the forward edge of this particular lava flow (i.e., collection area EA25) and from the eruptive center (i.e., collection area EA29) that lies on a fault through the caldera. The obsidian in the lava erupted last (EA29) has a slightly different chemical composition than that erupted first (EA25). This may be due a zoned magma chamber for Nemrut Dağ, the existence of which has proposed by Özdemir et al. (2006:189, 2007:133). It is perhaps more likely that this intra-flow zonation is due to more viscous, slower-moving lava being erupted last. Whatever the mechanism, such zoning within the flow permits identification of the collection locus (or loci): the forward portion of the flow, along or near the shore of the caldera lake.

Collecting obsidian from the forward part of this flow, farther from the entrance to the caldera, could have been preferred for several reasons. First, as mentioned in Section 8.3.4, quarriers have a variety of immaterial reasons for working in one location versus another. Figures 9.27a and b are examples of the landscapes atop rhyolitic lava domes,

and Figures 9.28a and b are examples of the talus slope on the forward edges of domes. Obsidian collectors may simply have preferred working on or near such slopes. Second, these quarriers may have preferred easy access to the caldera lake and the flora and fauna that live on or in the water. Third, higher-quality obsidian may have been exposed along the forward slope but not in the middle of the lava dome. This is consistent with a claim by Hughes and Smith (1993), mentioned in Section 1.2.3, that obsidians formed on the top surface of a lava dome are less uniform (i.e., lower quality) than obsidians formed in an inner shell of the dome (what they call the "basal zone") (31). High-quality obsidians from this inner shell can be exposed on the slope (Figure 9.28a).

This type of precise location information regarding obsidian collection at Nemrut Dağ is, to the best of my knowledge, not available in any prior studies. Consequently, no one has been able to address such procurement questions before.

9.9.2 - Access to Nemrut Dağ and Its Obsidians

Nemrut Dağ is about 200 km (linearly) from Tell Mozan. Accounting for terrain, the distance increases to 250 to 300 km, and travel between Nemrut Dağ and Tell Mozan would take 50 to 60 hours on foot. This distance places Tell Mozan within the border of the 300-km "supply zone" defined by RDC. Recent work, though, in Armenia using GIS modeling suggests that the direct procurement of obsidians occurred only within a radius of approximately 15 hours on foot (Barge and Chataigner 2003:178).



Figures 9.27a and b - Atop a lava dome (Newberry Volcano; author shown for scale).





Figures 9.28a and b - High-quality obsidian from the inner shell of a lava dome may be accessible on its forward talus slope (Newberry Volcano; author shown for scale).

As discussed in Chapter 8, peralkaline obsidians, often attributed to Nemrut Dağ, are found at a variety of Near Eastern sites; however, it is doubtful that the inhabitants of most sites, including Tell Mozan, directly acquired obsidian from Nemrut Dağ. Instead, the obsidians from Nemrut Dağ most likely arrived at these settlements via exchange and nomadic migrations. That does not mean, though, that the inhabitants of Tell Mozan and, for example, Tell Hamoukar acquired Nemrut Dağ obsidians from the same people. This is one of the issues that, hopefully, high-precision sourcing (down to a specific portion of one flow) at Nemrut Dağ could allow archaeologists to investigate.

Knowing precisely from where obsidian, recovered at an archaeological site, was collected at Nemrut Dağ could help to support one of three scenarios. First, it is possible that one group "controlled" access to all of Nemrut Dağ and its obsidians. This would be a local group -- perhaps nomads, perhaps local villagers -- rather than the inhabitants of a settlement more than 200 km away. Second, it is possible that different groups controlled access to different parts of Nemrut Dağ and, therefore, different obsidian flows (e.g, lava flows on the southern flanks of the caldera versus flows inside the caldera). This scenario has the greatest potential for studying the movements and interactions of different groups in antiquity. At Obsidian Cliff in Yellowstone National Park, almost 60 different quarries have been identified on the plateau, and it has been suggested that different groups might have had access to different quarrying loci (Davis et al. 1992).

For the third scenario (or, really, a set of scenarios), we have various ethnographic examples -- the territory might not have been controlled by any one group, or it officially

might have been controlled by one group although access was freely granted to any other group. For example, the Yolngu, Australian Aborigines of Arnhem Land, have a complex code of law (known as the *madayin*) that includes ownership of the land and sea and their associated natural resources, which are important to hunting and gathering groups. Based on her ethnographic work with the Yolngu, Williams (1982) explains that their boundaries "express varying categories of rights, both of users and owners. To request permission to enter, camp on, or use the resources of a particular area is to acknowledge the right of the owners to accede or deny permission" (148). She states, however, that permission rarely was denied to anyone. Similarly, Heizer and Treganza (1971) report:

> The Masut group of the Pomo tribe living around Calpella [in northern California] made the 50-mile trip to Clear Lake to secure magnesite and obsidian from the quarries owned by the other Pomo groups. They had to ask permission to quarry the stone, but did not pay for the privilege. (353)

Hodgson (2007) has a somewhat different take on access to Clear Lake obsidian:

> The... concept of neutral ground occurred in California at the obsidian quarries of Clear Lake in northern California, where any hostile group could meet each other and trouble was forbidden. The system worked out of common consent for the mutual good, as there was no other way to enforce it. (307)

At present, it is impossible to deduce which of these three scenarios most likely existed at Nemrut Dağ during the Bronze Age or any other period. Caution is warranted, however, when interpreting an abundance of Nemrut Dağ obsidians at a particular site as evidence of "control" over the location by inhabitants of that settlement.

9.9.3 - Inspiration for the Lower Sacral Area?

I conclude this chapter with speculation related to a current topic of interest at Tell Mozan: a Hurrian ideological link to the highlands. In Section 3.5, I discuss the Hurrian myth in which Silver lives in the highlands, visits Urkesh in search of his father Kumarbi, and learns that the ancestral god is roaming the mountains. In another Hurrian myth, the half-brother of Silver is Ullikummi, a monstrous stone or lava god, born from a rock cliff (Güterbock 1951). Consequently, some suggest that Hurrian myths involving mountains and volcanoes reflect their suspected origin in the mountainous north.

Recently, it been proposed that the temple terrace at Tell Mozan, which rose over 30 meters above the surrounding agricultural plains, was symbolic of the highlands to the north. Buccellati and Kelly-Buccellati (2007b) suggest that the temple terrace "bears the memory of a volcano" (40), and Buccellati (2009b) speculates that it "echoes... mountain landscapes" and may reflect some sort of "mental template" (5). Their hypothesis is that some of the naturally terraced Tur Abdin mountains may have inspired the temple terrace at Mozan. Indeed, like other arid areas, these mountains include mesas. The horizontally layered rocks of the Tur Abdin have eroded and weathered at different rates: softer layers (such as slate) have worn away, leaving only harder layers (such as limestone, sandstone, and quartzite). The result is a terraced appearance of the mountainside, sometimes called a "cliff-and-bench" topography ("benches" being the flatter portions).

The terrace revetment wall and the stone rings around the terrace could well have been intended to evoke a cliff-and-bench mountainside. Buccellati and Kelly-Buccellati

(2007b) suggest that the terrace's asymmetry and its rough-hewn stones further mimicked the mountains that the inhabitants saw every day. Additionally, the monumental staircase on the south side of the terrace meant that one approached the temple with a mountainous backdrop. Furthermore, as I noted earlier in Section 3.6.2, there is a triangular pattern in the temple terrace wall immediately adjacent to the staircase. Observable from the lower plaza, this pattern is similar to pictograms for "mountain," so Buccellati (2009a) suggests that it may also have been intended to reinforce links to the highlands.

The argument for mountainous symbolism of the temple terrace is compelling. At present, however, there is no analogous case for such symbolism in the lower sacral area, adjacent to the Royal Palace. As discussed in Section 3.6.6, the *âbi* is a large, stone-lined pit, about 5 meters in diameter. The bones of juvenile suids and canids were unearthed in a series of regular deposits, fitting the description of a Hurrian ritual for evoking gods of the underworld. Texts from Hittite archives describe a practice in which one either digs a shallow pit or inscribes a circle in the soil using a pin or dagger, within which piglets and puppies are slaughtered. The *âbi* at Tell Mozan is apparently a monumental construction to contain a long sequence of pits and circles for the Hurrian ritual. During Phase 3, circa about 2200 to 2100 BCE, the *âbi* was covered with a stone corbel arch; however, for the majority of its existence (during Phases 1, 2, 4, and 5), this circular pit apparently had an uncovered top (Buccellati and Kelly-Buccellati 2004:22-25).

I would like to offer, simply for consideration, a highly speculative suggestion for the inspiration of the *âbi*. Recall that Speiser (1953) argues that "the original home of the

Hurrians cannot have been far from the Lake Van district" in Turkey (325), and similarly Wilhelm (1989) contends that the mountainous area south of Lake Van may be assumed "to have been the oldest homeland of the Hurrians" (41). At present, there is insufficient evidence to prove or disprove this hypothesis. My research, though, shows the continuity of obsidian utilization, spanning from at least the mid-third millennium to the late-second millennium, from the Nemrut Dağ caldera near Lake Van. It is probable that Hurrians at Tell Mozan knew of, and had perhaps even seen, Nemrut Dağ.

Perhaps a volcanic crater, maybe even the Nemrut Dağ caldera, inspired this ritual of summoning the gods in a circular pit and, in turn, the *âbi*. Nemrut Dağ is a prominent feature on the landscape near Lake Van, the largest water body for hundreds of kilometers in most directions. Some previously noted features of Nemrut Dağ might have inspired a connection to gods of the underworld. For instance, the caldera is hydrothermally active. Adjacent to the large caldera lake is a small lake fed by hot springs. One of these springs has an average temperature of 58° C (Ulusoy et al. 2008) while others have temperatures of about 34° C (Atasoy et al. 1988, Ulusoy et al. 2008). In addition, steam and gas vents (fumaroles) are frequently active on the caldera floor (Yılmaz et al. 1998:177, Aydar et al. 2003:301). Minor earthquakes are also abundant at Nemrut Dağ. From October 2003 to October 2005, geologists measured more than 130 earthquakes with magnitudes between 1.3 to 4.0 (Ulusoy et al. 2006). Furthermore, Nemrut Dağ is far from extinct. Eruptions last occurred there in 1441, 1597, and 1692 CE, and there is evidence of an ash eruption near the very end of the fifth millennium BCE (Ulusoy et al. 2008).



Figure 9.29 - The stone-lined necromantic pit, known from Hurrian myths as an *âbi*, in the lower sacral area; viewed from the west looking east (Urkesh expedition photograph).



Figure 9.30 - A view of the Nemrut Dağ caldera; viewed from the east looking west (used in compliance with Google Earth's terms of use; ©2010 Google; satellite imagery ©2010 GeoEye and CNES/SPOT; map data ©2010 Basarsoft).

Furthermore, the caldera, compared to others, is especially circular and in-tact. In Lynch's account of his visit to Nemrut Dağ, he writes that "the circle is nowhere broken; the rim of the caldron remains intact" (1901:305). Similarly, Cribb (1991) reports: "On descending into this lost world, the encircling mountain rim closes off the outside world leaving only the barren moonscape of stony ridges… The floor of the crater is an almost perfect circle" (185). Geologists have also commented on its near-circularity (Yılmaz et al. 1998:176) since calderas can be quite irregular and eroded.

Therefore, Nemrut Dağ is an extensive, stone-walled, circular pit in the middle of a mountainous landscape, and it is a place where the ground shakes, hot water seeps from the ground, steam and noxious gas rise from vents, and, on occasion, an eruption may be witnessed. It seems worth entertaining the possibility that the Nemrut Dağ caldera might have inspired Hurrian ritual features like the *âbi*. This proposal, of course, is speculative and, without additional textural evidence, is likely unprovable.

9.10 - Summary and Concluding Remarks

Tell Mozan, situated at the crossroads of east-west and north-south transportation routes, is an ideal location to investigate Bronze-Age obsidian use and distribution across Northern Mesopotamia. In particular, this Hurrian settlement lies at the southern outlet of the Mardin Pass into the Tur Abdin foothills, giving us reason to suspect that Urkesh may have been the ancient equivalent of Burghardt's "gateway city." Other materials found at

Tell Mozan -- from lapis lazuli to gold -- can provide little information about contact and exchange compared to the information that obsidian can offer.

A relatively large number of sources are represented among the obsidian artifacts at Tell Mozan, and this pattern is quite atypical for contemporaneous cities in the Khabur Triangle. While its contemporaries have obsidian from just one to three sources, there are seven to nine obsidian sources (depending how one defines a "source) among the artifacts from Tell Mozan. About 97% of the artifacts came from sources in Eastern Anatolia, and the last 3%, surprisingly, came from the most widely used source in Central Anatolia: the Kömürcü source of Göllü Dağ. About 60% of the obsidian comes from only two flows at Nemrut Dağ, both within the caldera, not on its exterior slopes.

At least two, perhaps even all three, of the Kömürcü obsidian artifacts came from an accumulation directly above the pebble surface of the Royal Palace's northern service courtyard. Dating to roughly 2250 BCE, these artifacts might have been deposited in the courtyard during service activities for the royal court, perhaps even that of Tupkish. This suggests that the royal family may have had special access to Kömürcü obsidian for some reason. This obsidian most likely arrived at Tell Mozan via sites in the Middle Euphrates Valley along an east-west route, not directly from Göllü Dağ. When the obsidian sources are explored with higher spatial resolution (by unit), another pattern emerges: the greatest variety of obsidian sources is found in the units that include palace courtyards, suggesting that obsidians from various sources were most frequently used there.

With the exception of the Kömürcü obsidian artifacts, the sources represented in Areas A (the palace complex) and J (the plaza and temple terrace), and their proportions, are roughly the same. The overall similarities for Areas A and J imply that people living in various parts of Urkesh had similar access to the same sources in Eastern Turkey. On the other hand, all of the sourced obsidian from Area B (the temple) came from one flow at Nemrut Dağ, but the sample so far consists of just three artifacts. That specific flow is also the only obsidian source represented throughout the site's occupational history from the mid-third millennium to the late-second millennium, and it comprises at least 50% of the obsidian at any given period. Overall, however, the use of various obsidian sources at Tell Mozan seems largely consistent for over a thousand years.

The hypothesis of a Hurrian "homeland" as far northeast as Armenia (or beyond) is considered -- but not supported -- in light of my obsidian data. There are no obsidians from far northeastern Turkey, Armenia, Azerbaijan, Georgia, or southeastern Russia that would help to identify a Hurrian link to those regions. Regarding the issue of "Nawar," my source data, when compared to that from other post-Neolithic Khabur sites, suggests that Urkesh had a mountainous hinterland to the north, most likely crossed by groups of pastoral nomads who transported obsidians. The obsidian data for Tell Mozan and Tell Brak, when compared, suggest a link between to these two cities, potentially supporting the hypothesis that ancient Nagar was also known as Nawar. It may have been that both Urkesh and Nagar functioned as "gateway cities" or that these cities instead functioned as

a gateway-city/central-place pair, as described by Burghardt. The mechanisms for these scenarios, including nomadism, are considered in each case.

Finally, I consider the importance of Nemrut Dağ, obsidians from which occur in each site area and for all time periods studied at Tell Mozan. Based on my high-precision data and a thorough collection from Nemrut Dağ, I was able to identify the collection loci at the volcano represented among the artifacts at Tell Mozan. In fact, I identified specific loci down to about a kilometer: most obsidian collected there came from the forward part of a flow in the caldera. Given the other mountainous motifs of the Urkesh monumental architecture, perhaps the Nemrut Dağ caldera even inspired the *âbi*.

Conclusion

In the Introduction, I set forth three main goals for this research. First, I sought to demonstrate a sophisticated approach to obsidian sourcing in the Near East. Nearly every phase of this research exceeds the norm in Mesopotamian obsidian sourcing. It is typical, for example, for recent work to analyze fewer than two dozen geological specimens total from only the four or five sources in Turkey known to RDC. I, on the other hand, had an obsidian reference collection with over 900 geological specimens from dozens of sources in Turkey as well as Armenia, Georgia, Azerbaijan, and the Kabardino-Balkaria Republic. I analyzed a large number of artifacts from one site (n = 98) so that I had a richer data set and could explore spatial and temporal patterns of obsidian use on a site level, rather than jumping to a regional level. I selected a data-analysis approach that (1) is appropriate for a region with both geochemical obsidian varieties and (2) treats each geological specimen individually, rather than "lumping" these specimens into sources at the outset. This latter point is important because I do not consider "sources" to merely be clouds of data points in multivariate space. Instead, sources are places in both physical and mental landscapes while a "collection area" is an emic unit that describes where a geologist or archaeologist gathered obsidian specimens for analysis. Furthermore, I selected an analytical technique that can (1) control for obsidian as a mixture, (2) measure artifacts non-destructively, and (3) distinguish, if critically used, the Nemrut Dağ and Bingöl A obsidians (rather than just ignoring the issue and providing largely ambiguous results).

Consequently, my results exceed those from prior studies. This is most evident in the results from Nemrut Dağ. Recall that, at most, four Nemrut Dağ geochemical clusters were identified by Blackman (1984), and other studies suggest that there are one to three obsidian sources at Nemrut Dağ. My EMPA data, collected from one hundred geological specimens from eleven collection areas at Nemrut Dağ, reveal ***six*** distinct clusters: three for pre-caldera obsidian-bearing lava flows and three for post-caldera flows. I also show that Poidevin's (1998) peralkalinity-based scheme for attributing geochemical clusters to actual locations on the volcano is incorrect. While many recent obsidian sourcing studies in the Near East cannot even distinguish Nemrut Dağ and Bingöl A obsidians, I reveal the collection loci, down to the kilometer, of Nemrut Dağ obsidians found at Tell Mozan. No prior study has been able to show that obsidian was specifically collected at, for example, the forward part of a particular flow in the southeastern portion of the caldera. Given the potential for behavioral interpretations with such precise information regarding collection loci, this advantage of my sourcing approach should be evident.

My second goal was redeveloping EMPA for obsidian sourcing in a new century. A contemporary electron microprobe does not have much in common with the instrument utilized by Merrick and Brown (1984), which output the data onto punch cards. My most important development was non-destructive artifact analyses. All of the previous studies involved removing pieces from the artifacts and polishing them; however, I placed whole artifacts into the microprobe and analyzed their exteriors. There were, though, four main challenges to non-destructive analyses of the artifacts' surfaces.

The first two challenges of non-destructive artifact analyses involve the specimen requirements: an ideal specimen for EMPA has a surface that is (1) flat and normal to the electron beam and (2) highly polished. I minimized the former challenge by identifying small regions on the artifacts' surfaces that were effectively flat and beam-perpendicular. Regarding the latter, the surface of flaked obsidian is quite smooth, and any inclusions or irregular areas can be avoided. The third and fourth challenges involve post-depositional processes that affect the artifacts' surfaces: hydration and chemical alteration. Data about their effects are sparse, even contradictory. For example, reports about the concentration of water in a hydration rind vary from 2% to over 10%. The depth of surface alteration is also difficult to predict, although the latest studies suggest a thickness of just a few tenths of a micrometer. Ultimately I could do nothing to mitigate these two challenges, but two factors worked in my favor: (1) the artifacts dated to the Bronze Age and (2) Tell Mozan lies in a semi-arid steppe on the periphery of the Syrian Desert. When the most seriously altered elements are excluded from the data analysis, my non-destructive surface analyses were adequate, in this situation, for sourcing the obsidian artifacts.

In my redevelopment of EMPA, I also emphasize the role of choice in conducting analyses. On one level, making a stone tool and doing an analysis are similar: one starts with an initial scheme in mind, feedback alters the scheme, the material affects feedback, and actions are affected by one's know-how. These actions form an operational sequence and are informed by the both theoretical and practical "know how" (or *connaissances* and *savoir-faire*, respectively, in the terminology of Pierre Lemonnier).

Equally as important is a rigorous assessment of my data and techniques based on the concepts of precision, accuracy, reliability, and validity. Hughes (1998) called for all four concepts to be included in evaluation of obsidian sourcing techniques, but the use of this framework has been almost nonexistent. Aside from a few one-off uses of the word "reliability" in papers without defining or discussing it, only Nazaroff et al. (2010) apply Hughes' framework in their assessment of PXRF for sourcing obsidian in Mesoamerica. My examination of the literature on evaluation, however, reveals that Hughes (1998) and Nazaroff et al. (2010) formulate reliability and validity atypically, so I have attempted to strengthen the application of these concepts to sourcing research.

My third goal involved using the result of Goals #1 and #2 to establish the sources of obsidian represented among the Bronze-Age artifacts at Tell Mozan. This, though, was only a proximate goal. The ultimate goals for this particular study included (1) exploring spatial and temporal patterns among the obsidian sources used at Urkesh, (2) considering two debated issues regarding Urkesh and its Hurrian inhabitants, and (3) investigating the broader implications for obsidian use in the Bronze-Age Near East.

A surprise during my analytical stage was that one of 98 artifacts from Tell Mozan was not actually obsidian. Instead, its chemical composition is similar to those of ancient Mesopotamian glasses. In particular, it is a high-magnesia glass, rather similar to second-millennium artifacts from Tell Brak and other sites. Glass was not produced in sufficient quantities to make glass vessels until the second millennium BCE, but this fragment dates to the third millennium. Akkadian texts, however, refer to "artificial obsidian" beads and

other ornaments. I suggest, therefore, that the artifact is an error or waste from producing an "artificial obsidian" glass bead, showing that such objects actually exist. The grooves might have been intended for inlaying another color of glass to create a striped, or even a twisted, appearance. Given that Cauvin (1998) and Coqueugniot (1998) state stone beads likely had symbolic meanings, an attempt to make an artificial stone that combines black "obsidian" with a stone of another color may reflect an endeavor to combine the power or symbolism of both types of stone into a single bead or amulet.

As of the 2006 expedition, over 820 obsidian artifacts have been recovered at Tell Mozan, and I estimate that 1700 to 1800 chert artifacts have been found. Thus, one third of the flaked-stone tools are obsidian and two thirds are chert. In general, chert was used to make more robust tools. This is reflected, in part, in the mean masses of the obsidian and chert artifacts: 1.1 g and 8.2 g, respectively. Consequently, the flaked-stone artifacts are, by mass, approximately 6% obsidian and 94% chert. Furthermore, I estimate that the total mass of all the excavated obsidian artifacts, so far, is roughly 1 kg and the total mass of all the excavated chert artifacts at Tell Mozan is roughly 14 kg.

The obsidian assemblage at Tell Mozan is predominated by blade-tools, especially prismatic blades and bladelets with trapezoidal cross-sections. Flake-tools, including side and end scrapers, knives, ad-hoc tools, and notched or denticulated flakes, are common as well. Geometric microliths fashioned from blades, particularly trapezes and lunates, also are present, as are notches on blades. I also noted a tabular scraper, a tanged point and a winged point, transverse points or end scrapers, borers, and drills or awls. Ground-stone

obsidian artifacts are also present, including possible fragments of thick-walled obsidian vessels. Several artifacts seem to have been both flaked and ground -- one is a prismatic blade with dorsal surfaces that were ground flat. Additionally, there are flakes with broad striking platforms that were ground flat. A chert nodule with a ground platform suggests that some obsidian cores could also have had ground platforms.

Lithic workshops have not yet been found at Tell Mozan, but there is evidence of on-site obsidian tool production. There is debris, but given the brittleness of obsidian, it is often difficult to distinguish production debitage and fragments of broken or modified tools. More telling is the presence of obsidian flakes with cortex and surfaces original to the obsidian blocks or nodules. There are obsidian flakes with cortex typical of rounded nodules and others with flat, porous surfaces typical of angular blocks. Mixed flake and blade obsidian cores, either exhausted or discarded, also suggest production activities at Tell Mozan. This evidence, however, does not indicate the tool type. On the other hand, a tabular obsidian core, dating to between 2100 and 1800 BCE, is evidence for prismatic blade production on-site. There are also early-series blades from a polyhedral core. Such blades are used to initially shape a core, and their removal creates the ridges on the dorsal surfaces of prismatic blades. Together, these artifacts indicate that prismatic blades were made at Tell Mozan, not imported from a production center, as others have claimed. This premise should be questioned at other sites in the region as well.

There are also other regional implications of my findings. The most significant is likely that regarding a prevalent assumption initially proposed by Bernard Gratuze of the

CNRS Institut de Recherche sur les Archéomatériaux and colleagues. These researchers assert that "if, at one archaeological site, we find the artifacts have the two compositions of the Bingöl area, we may suppose that the artifacts come from Bingöl, whereas if only the Bingöl 'A' composition is found, both solutions (Nemrut Dağ and Bingöl) should be retained" (Gratuze et al. 1993:16). In other words, if Bingöl B obsidian is identified at a site, Gratuze and his colleagues assume that the peralkaline obsidians came from Bingöl A, not Nemrut Dağ. This presumption stems, of course, from the use of a technique that cannot distinguish these peralkaline obsidian sources, and it continues to be used in new sourcing studies (e.g., Khalidi et al. 2009). Their argument is essentially formalist, and it assumes maximal efficiency in obsidian collection activities.

My results, though, reveal that their assumption is incorrect at Tell Mozan. Three features contain both Bingöl B and Nemrut Dağ obsidians, and in two of them, Bingöl B and Nemrut Dağ obsidians occur in the same artifact lot. Other source combinations are present in other features: Bingöl A and B obsidians occur concurrently, and Bingöl A and Nemrut Dağ obsidians also occur together. This result indicates that maximal efficiency was not the determining factor in obsidian source selection. This fits archaeological and ethnographic evidence elsewhere in the world regarding stone quarrying sites. Based on this other evidence, I speculate on possible influences on the use and exchange of Nemrut Dağ obsidians, such as symbolism and impressive views. This volcano was most likely a conspicuous landmark that drew in travelers (Molyneaux's centripetal effect) as well as a source of widely distributed raw materials (his centrifugal effect).

Tell Mozan is situated at the southern outlet of the Mardin Pass into the Tur Abdin mountains, giving us reason to suspect that Urkesh may have been the ancient equivalent of Burghardt's (1971) "gateway city." Urkesh was most likely strategically founded near the pass, which is almost certainly how most obsidian (and other mountain resources such as copper) reached the city and perhaps much of the Khabur Triangle.

A relatively large number of sources are represented among the obsidian artifacts at Tell Mozan, and this pattern is quite atypical for contemporaneous cities in the Khabur Triangle. While its contemporaries have obsidian from just one to three sources, there are seven to nine obsidian sources (depending how one defines a source) among the artifacts from Tell Mozan. About 97% of the artifacts came from sources in Eastern Anatolia, and in particular, about 60% came from just two Nemrut Dağ flows, both within the caldera, not on its exterior slopes. The last 3% surprisingly originated from the most widely used obsidian source in Central Anatolia: the Kömürcü source of Göllü Dağ.

At least two, perhaps even all three, of the Kömürcü obsidian artifacts came from an accumulation directly above the pebble surface of the Royal Palace's northern service courtyard. Dating to roughly 2250 BCE, these artifacts might have been deposited in the courtyard during service activities for the royal court, perhaps even that of Tupkish. This suggests that the royal family may have had special access to Kömürcü obsidian for some reason. This obsidian most likely arrived at Tell Mozan via sites in the Middle Euphrates Valley along an east-west route, not directly from Göllü Dağ. When the obsidian sources are explored with higher spatial resolution (by unit), another pattern emerges: the greatest

variety of obsidian sources is found in the units that include palace courtyards, suggesting that obsidians from multiple sources were most often used there.

With the exception of the Kömürcü obsidian artifacts, the sources represented in Areas A (the palace complex) and J (the plaza and temple terrace), and their proportions, are roughly the same. The overall similarities for Areas A and J imply that people living in various parts of Urkesh had similar access to the same Eastern Anatolian sources. On the other hand, all of the sourced obsidian from Area B (the temple) came from one flow at Nemrut Dağ, but my sample so far consists of three artifacts. That flow, which lies in the southeastern portion of the caldera, is also the sole source represented throughout the site's occupational history from the mid-third to the late-second millennium BCE, and it comprises at least 50% of the obsidian artifacts at any given time.

The hypothesis of a Hurrian "homeland" as far northeast as Armenia (or beyond) is considered -- but not supported -- in light of my obsidian data. There are no obsidians from Armenia, Azerbaijan, Georgia, or southeastern Russia that would help to identify a Hurrian link to those regions. Similarly, none of the analyzed artifacts were attributed to the İkizdere, Kars, or Sarıkamış sources in far northeastern Turkey near the borders with Armenia and Georgia. Other than six artifacts that *might* have come from Pasinler, there is no evidence in obsidian data to support proposals that a Hurrian homeland existed in either far northeastern Turkey or the Transcaucasus. This is not evidence, however, that such a homeland did *not*, in fact, exist in that region. The obsidian source evidence does not *disprove* such suggestions, but it clearly does not support them.

Regarding the identity of "Nawar," my source data, when compared to the earlier data from other post-Neolithic Khabur Triangle sites, suggests that Urkesh may have had a mountainous hinterland to the north, likely crossed by groups of pastoral nomads given the ethnographic evidence. A *mélange* of obsidians from different sources, transported by nomads during their migrations, would have been present in the Tur Abdin highlands. If Urkesh drew on a mountainous northern hinterland, obsidians from a variety of sources, not just two or three, should be found at Tell Mozan. As noted earlier, an atypical variety of obsidian sources exists at the site, supporting this scenario.

My results, when compared to the extant data for other Khabur Triangle sites, also support a possible link between Tell Mozan and Tell Brak and, hence, potentially support the hypothesis that ancient Nagar was also known as Nawar. The similar obsidian source patterns at Tell Brak and Tell Mozan, especially in comparison to the other sites, hint that there was an exchange link between these two settlements, perhaps as part of a kingdom or an alliance between Urkesh and Nagar. It may even have been that Urkesh and Nagar functioned as dual "gateway cities" or that the two cities instead functioned together as a gateway-city/central-place pair, a situation described by Burghardt.

I considered the importance of Nemrut Dağ because, for over a millennium, much of the obsidian at Tell Mozan was collected from one location near the southeastern shore of the caldera lake. Such precise sourcing is possible only because I fulfilled the first two goals. Future work is needed in this region and period, and as I reveal here, sophisticated approaches to sourcing and appropriate techniques are imperative.

Works Cited

Abbès, F., L. Bellot-Gurlet, C. Bressy, M.-C. Cauvin, B. Gratuze and G. Poupeau
2001 Nouvelles Recherches sur l'Obsidienne de Cheikh Hassan (Vallée de l'Euphrate, Syrie) au Néolithique: PPNA et PPNB Ancien. *Syria* 78:5-17.

Abbès, F., L. Bellot-Gurlet, M. Cauvin, S. Delerue, S. Dubernet, G. Poupeau and D. Stordeur
2003 Provenance of the Jerf el Ahmar (Middle Euphrates Valley, Syria) Obsidians. *Journal of Non-Crystalline Solids* 323(1-3):162-166.

Abrajano, T. A., J. K. Bates and C. D. Byers
1986 Aqueous Corrosion of Natural and Nuclear Waste Glasses. *Journal of Non-Crystalline Solids* 84:251-257.

Acquafredda, P., T. Adriani, S. Lorenzoni and E. Zanettin
1996 Proposal of a Non Destructive Analytical Method by SEM-EDS to Discriminate Mediterranean Obsidian Sources. *Advances in Clay Minerals*:269-271.

Acquafredda, P., T. Andriani, S. Lorenzoni and E. Zanettin
1999 Chemical Characterization of Obsidians from Different Mediterranean Sources by Non-Destructive SEM-EDS Analytical Method. *Journal of Archaeological Science* 26(3):315-325.

Acquafredda, P. and A. Paglionico
2004 SEM-EDS Microanalysis of Microphenocrysts of Mediterranean Obsidians: A Preliminary Approach to Source Discrimination. *European Journal of Mineralogy* 16(3):419-429.

Adams, A. J., E. H. Christiansen, B. J. Kowallis, O. Carranza-Castaneda and W. E. Miller
2006 Contrasting Silicic Magma Series in Miocene-Pliocene Ash Deposits in the San Miguel de Allende Graben, Guanajuato, Mexico. *The Journal of Geology* 114:247-266.

Adams, P.
1984 Glass Corrosion: A Record of the Past? A Predictor of the Future? *Journal of Non-Crystalline Solids* 67: 193-205.

Adams, R. M. C.
1974 Anthropological Perspectives on Ancient Trade. *Current Anthropology* 15(3):239-258.

Aitchison, J.
1986 *The Statistical Analysis of Compositional Data*. Chapman and Hall, London.

Aitchison, J. and S. Shen
1984 Measurement Error in Compositional Data. *Mathematical Geology* 16(6):637-650.

Akkermans, P. A., J. A. K. Boerma, A. T. Clason, S. G. Hill, E. Lohof, C. Meiklejohn, L. M. Miere, G. M. F. Molgot, J. J. Roodenberg, W. Waterbolk-von Rooyen and W. von Zeist
1983 Bouqras Revisited: Preliminary Report on a Project in Eastern Syria. *Proceedings of the Prehistoric Society* 49:335-372.

Akkermans, P. M. M. G. and M. le Mière
1992 The 1988 Excavations at Tell Sabi Abyad, a Later Neolithic Village in Northern Syria. *American Journal of Archaeology* 96(1):1-22.

Akkermans, P. M. M. G., J. J. Rodenberg, M. van Loon and H. T. Waterbolk
1978-9 Tall Buqras. *Archiv fur Orientforschung* 26:152-154.

Akkermans, P. M. M. G. and G. M. Schwartz
2003 *The Archaeology of Syria: From Complex Hunter-Gatherers to Early Urban Societies (c.16,000-300 BC),* Cambridge World Archaeology. Cambridge University Press.

Aksu, A. E., G. Jenner, R. N. Hiscott and E. B. Isler
2008 Occurrence, Stratigraphy and Geochemistry of Late Quaternary Tephra Layers in the Aegean Sea and the Marmara Sea. *Marine Geology* 252:174-192.

Al Isa, K., J. N. Barrandon, B. Gratuze and M. C. Cauvin
1990 Nondestructive Analysis of Obsidian Artefacts Using Nuclear Techniques. The International Symposium on Archaeometry, Heidelberg.

Alfassi, Z. B.
1990 *Activation Analysis, Volumes I and II*. CRC Press, Boca Raton, FL.

Algaze, G.
1989 The Uruk Expansion: Cross-Cultural Exchange in Early Mesopotamian Civilization. *Current Anthropology* 30(5):571-608.

1993 *The Uruk World System: The Dynamics of Expansion of Early Mesopotamian Civilization*. The University of Chicago Press, Chicago.

1999 Trends in the Archaeological Development of the Upper Euphrates Basin of Southeastern Anatolia During the Late Chalcolithic and Early Bronze Ages. In *Archaeology of the Upper Syrian Euphrates, the Tishrin Dam area: Proceedings of the International Symposium held at Barcelona, January 28-30, 1998*, pp. 535-563.

2008 *Ancient Mesopotamia at the Dawn of Civilization: The Evolution of an Urban Landscape*. The University of Chicago Press, Chicago.

Allan, A. S. R., J. A. Baker, L. Carter and R. J. Wysoczanksi
2008 Reconstructing the Quaternary Evolution of the World's Most Active Silicic Volcanic System: Insights from an 1.65 Ma Deep Ocean Tephra Record Sourced from Taupo Volcanic Zone, New Zealand. *Quaternary Science Reviews* 27:2341-2360.

Allen, R. O., H. Luckenbach and C. G. Holland
1975 Application of Instrumental Neutron Activation. Analysis to a Study of Prehistoric Steatite Artifacts and Source Materials. *Archaeometry* 17:69-83.

Altınlı, I. E.
1964 Geology of Eastern and Southeastern Anatolia. *Bulletin of the Minerals Research and Exploration Institute of Turkey* 66:35-76.

Ambrose, W. R., C. Allen, S. O'Connor, M. Spriggs, N. V. Oliveira and C. Reepmey
2009 Possible Obsidian Sources for Artifacts from Timor: Narrowing the Options Using Chemical Data. *Journal of Archaeological Science* 36(3):607-615.

Ambrose, W. R., P. Duerden and J. Bird
1981 An Archaeological Application of PIXE-PIGME Analysis to Admiralty Islands Obsidians. *Nuclear Instruments and Methods* 191(1-3):397-402.

Ambrose, W. R.
1998 Obsidian Hydration Dating at a Recent Age Obsidian Mining Site in Papua, New Guinea. In *Archaeological Obsidian Studies: Method and Theory*, edited by M. S. Shackley, pp. 205-222. Plenum Press, New York.

Ambrose, W. R.
2001 Obsidian Hydration Dating. In *Handbook of Archaeological Sciences*, edited by D. R. Brothwell and A. M. Pollard, pp. 81-92. Wiley.

Ambroz, J. A.
1997 *Characterization of Archaeologically Significant Obsidian Sources in Oregon by Neutron Activation Analysis*, University of Missouri-Columbia.

Ambroz, J. A., M. D. Glascock and C. E. Skinner
2001 Chemical Differentiation of Obsidian within the Glass Buttes Complex, Oregon. *Journal of Archaeological Science* 28(7):741-746.

Ammerman, A. J.
1979 A Study of Obsidian Exchange Networks in Calabria. *World Archaeology* 11(1):95-110.

Ammerman, A. J., A. Cesana and M. Terrani
1990 Neutron Activation Analysis of Obsidian from Two Neolithic Sites in Italy. *Journal of Archaeological Science* 17(2):209-220.

Ammerman, A. J., C. Matessi and L. L. Cavalli-Sforza
1978 Some New Approaches to the Study of the Obsidian Trade in the Mediterranean and Adjacent Areas. In *The Spatial Organisation of Culture*, edited by I. Hodder, pp. 179-196. University of Pittsburgh Press.

Anderson, D., J. Tiffany and F. Nelson
1986 Recent Research on Obsidian from Iowa Archaeological Sites. *American Antiquity* 51(4): 837-852.

Anderson, P.
1998 Using Prehistoric Stone Tools to Harvest Cultivated Wild Cereals: Preliminary Observations of Traces and Impact. In *Industries Lithiques: Tracelogie et Technologie*, edited by S. Beyries, pp. 175-195. vol. BAR International Series 411.

Anderson, P. and J. Chabot
2001 Functional Analysis of Glossed Blades from Northern Mesopotamia in the Early Bronze Age (3000-2500 BC): The Case of Tell 'Atij. In *Journees d'Etude du Groupe de Recherches en Archeometrie du CELAT, 1997-1999*, pp. 257-276.

Anderson, P., J. Chabot and A. van Gijn
2007 The Functional Riddle of 'Glossy' Canaanean Blades and the Near Eastern Threshing Sledge. *Journal of Mediterranean Archaeology* 17(1):87.

Andrefsky, W.
1998 *Lithics: Macroscopic Approaches to Analysis*. 1st ed. Manuals in Archaeology. Cambridge University Press, Cambridge.

2005 *Lithics: Macroscopic Approaches to Analysis*. 2nd ed. Manuals in Archaeology. Cambridge University Press, Cambridge.

Anovitz, L., D. Cole and L. Riciputi
2009 Low-Temperature Isotopic Exchange in Obsidian: Implications for Diffusive Mechanisms. *Geochimica et Cosmochimica Acta* 73:3795-3806.

Anovitz, L. M., J. M. Elam, L. R. Riciputi and D. R. Cole
1999 The Failure of Obsidian Hydration Dating: Sources, Implications, and New Directions. *Journal of Archaeological Science* 26:735-752.

Anovitz, L. M., L. R. Riciputi, D. R. Cole, M. Fayek and J. M. Elam
2006 Obsidian Hydration: A New Paleothermometer. *Geology* 34(7):517-520.

Aoyama, K.
1996 *Exchange, Craft Specialization, and Ancient Maya State Formation: A Study of Chipped Stone Artifacts from the Southeast Maya Lowlands*, University of Pittsburgh.

Aoyama, K., T. Tashiro and M. Glascock
1999 A Pre-Columbian Obsidian Source in San Luis, Honduras: Implications for the Relationship Between Late Classic Maya Political Boundaries and the Boundaries of Obsidian Exchange Networks. *Ancient Mesoamerica* 10(2):237-249.

Arias, A., M. Oddone, G. Bigazzi, A. Di Muro, C. Principe and P. Norelli
2006 New Data for the Characterization of Milos Obsidians. *Journal of Radioanalytical and Nuclear Chemistry* 268(2):371-386.

Arnold, D. E., P. M. Rice, W. A. Jester, W. N. Deutsch, B. K. Lee and R. I. Kirsch
1978 Neutron Activation Analysis of Contemporary Pottery and Pottery Materials from the Valley of Guatemala. In *The Ceramics of Kaminaljuyu*, edited by R. K. Wetherington. vol. 534-586. Penn State University Press, University Park.

Arslan, M., H. Kurt and Y. Kadioglu
1998 Glassy Textures and Emplacement Characteristics of the Tahtayayla Rhyolite-Obsidian Flow, Hasandag (Aksaray) Volcanites, Central Turkey. *Mineralogical Magazine* 62(1):77-78.

Ashkenazi, T.
1938 *Tribus Semi-nomades de la Palestine du Nord: Ouvrage Orné de Six Planches Hors Texte et d'Une Carte Ethnographique*. Études D'ethnographie. Librairie Orientaliste, Geuthner, Paris.

Ashworth, M. and T. P. Abeles
1966 Neutron Activation Analysis and Archaeology. *Nature* 210:9-11.

Aspinall, A., S. Feather and C. Renfrew
1972 Neutron Activation Analysis of Aegean Obsidians. *Nature* 237(5354):333-334.

Astour, M. C.
1968 Two Ugaritic Serpent Charms. *Journal of Near Eastern Studies* 27(1):13-36.

Atasoy, E., N. Terzioğlu and H. C. Mumcuoğlu
1988 *Nemrut Volkanı Jeolojisi ve Jeotermal Olanakları*. T.P.A.O. Research Group Report.

Aufrère, S.
1991 *L'Univers Minéral dans la Pensée Egyptienne*. Institut Francais d'Archeologie Orientale, Cairo.

Aydar, E., A. Gourgaud, I. Ulusoy, F. Digonnet, P. Labazuy, E. Sen, H. Bayhan, T. Kurttas and A. Tolluoglu
2003 Morphological Analysis of Active Mount Nemrut Stratovolcano, Eastern Turkey: Evidences and Possible Impact Areas of Future Eruption. *Journal of Volcanology and Geothermal Research* 123(3-4):301-312.

Badalian, R., G. Bigazzi, M. Cauvin, C. Chataigner, R. Jrbashyan, S. Karapetyan, M. Oddone and J. Poidevin
2001 An International Research Project on Armenian Archaeological Sites: Fission-Track Dating of Obsidians. *Radiation Measurements* 34(1-6):373-378.

Badalyan, R., C. Chataigner and P. Kohl
2004 Trans-Caucasian Obsidian: The Exploitation of the Sources and Their Distribution. In *A View from the Highlands: Archaeological Studies in Honour of Charles Burney*, edited by A. Sagona, pp. 437-465. Ancient Near Eastern Studies.

Bader, N., N. J. Merpert and R. M. Muchaev
1994 Les Importations d'Obsidienne sur les Sites des IXe-VIIe Millénaires B.P. du Djebel Sinjar. *Paléorient* 20(2):6-8.

Bahn, P.
2001 *The Penguin Archaeology Guide*. Penguin.

Bahn, P. and C. Renfrew
2008 *Archaeology: Theories, Methods and Practice*. 5th ed. Thames & Hudson.

Baker, T. L.
1988 *Doing Social Research*. McGraw-Hill.

Balkan-Atli, N., D. Binder and M.-C. Cauvin
1999 Obsidian: Sources, Workshops, and Trade in Central Anatolia. In *Neolithic in Turkey: The Cradle of Civilization, New Discoveries*, pp. 133-145. Ancient Anatolian Civilizations Series. Arkeoloji ve Sanat Yayinlari.

Banterla, G., A. Stanico, M. Terrani and S. Villani
1973 Characterization of Samian Ware Sherds by Means of Neutron Activation Analysis. *Archaeometry* 15:209-220.

Bar-Matthews, M., A. Ayalon and A. Kaufman
1998 Middle to Late Holocene (6500 Yr. Period) Paleoclimate in the Eastern Mediterranean Region from Stable Isotopic Composition of Speleothems from Soreq Cave, Israel. In *Water, Environment, and Society in Time of Climate Change* edited by A. S. Issar and N. Brown, pp. 203-214. Kluer Academic Publishers.

Barge, O. and C. Chataigner
2003 The Procurement of Obsidian: Factors Influencing the Choice of Deposits. *Journal of Non-Crystalline Solids* 323(1-3):172-179.

Barker, A., C. Skinner, M. Shackley, M. Glascock and J. Rogers
2002 Mesoamerican Origin for an Obsidian Scraper from the Precolumbian Southeastern United States. *American Antiquity* 67:103-108.

Barone, G., A. Lo Giudice, P. Mazzoleni, A. Pezzino, D. Barilaro, V. Crupi and M. Triscari
2005 Chemical Characterization and Statistical Multivariate Analysis of Ancient Pottery from Messina, Catania, Lentini and Siracusa (Sicily). *Archaeometry* 47(4):745-762.

Barrett, T. P.
2003 *Tuxtlas Obsidian: Organization and Change in a Regional Craft Industry*, University of New Mexico.

Bartholomew, D. J.
1996 *The Statistical Approach to Social Measurement*. Academic Press, San Diego.

Bartholomew, R. F., B. L. Butler, H. L. Hoover and C. K. Wu
1980 Infrared Spectra of a Water-Containing Glass. *Journal of the Ceramic Chemical Society* 63:481-485.

Bassette, D.
1994 *Geochemische Untersuchungen an Obsidianen Zentralanatoliens, Türkei*, Max Planck Institute.

Bates, J. K., J. T.A. Abrajano, W. L. Ebert, J. J. Mazer and T. J. Gerding
1988 Experimental Hydration Studies of Natural and Synthetic Glasses. In *Materials in Art and Archaeology*, edited by E. Sayer, P. Vandiver, J. Druzik and C. Stevenson, pp. 237. Materials Research Society Symposium.

Baugh, T. and F. Nelson Jr
1987 New Mexico Obsidian Sources and Exchange on the Southern Plains. *Journal of Field Archaeology* 14(3):313-329.

Bavay, L., T. De Putter, B. Adams, J. Navez and L. Andre
2000 The Origin of Obsidian in Predynastic and Early Dynastic Upper Egypt. *Mitteilungen des Deutschen Archäologischen Instituts, Abteilung Kairo* 56:5-20.

Baxter, M. J.
1989 Multivariate Analysis of Data on Glass Compositions: A Methodological Note. *Archaeometry* 31(1):45-53.

1994 *Exploratory Multivariate Analysis in Archaeology* Edinburgh University Press.

1995 Standardization and Transformation in Principal Component Analysis, with Applications to Archaeometry. *Applied Statistics* 44(4):513-527.

2001 Statistical Modelling of Artefact Compositional Data. *Archaeometry* 43(1):131-147.

2003 *Statistics in Archaeology*. Hodder Arnold, London.

Baxter, M. J. and C. E. Buck
2000 Chapter 20: Data Handling and Statistical Analysis. In *Modern Analytical Methods in Art and Archaeology*, edited by E. Ciliberto and G. Spoto, pp. 681-747. Wiley-Interscience.

Baxter, M. J. and C. Jackson
2001 Variable Selection in Artefact Compositional Studies. *Archaeometry* 43(2):253-268.

Bayman, J.
1995 Rethinking "Redistribution" in the Archaeological Record: Obsidian Exchange at the Marana Platform Mound. *Journal of Anthropological Research* 51(1):37-63.

Bayman, J. and M. S. Shackley
1999 Dynamics of Hohokam Obsidian Circulation in the North American Southwest. *Antiquity* 73(282):836-845.

Beale, T.
1973 Early Trade in Highland Iran: A View from a Source Area. *World Archaeology* 5(2):133-148.

Beaman, D. R. and J. A. Isasi
1972 *Electron Beam Microanalysis*. ASTM Technical Publication 506. American Society for Testing and Materials, Philadelphia.

Beck, C. and G. T. Jones
2000 Obsidian Hydration Dating, Past and Present. In *It's About Time: A History of Archaeological Dating in North America*, edited by S. E. Nash. The University of Utah Press, Salt Lake City.

Becker, C.
2005 Small Numbers, Large Potential: New Prehistoric Finds of Elephant and Beaver from the Khabur River/Syria. *Munibe (Antropologia-Arkeologia)* 57:445-456.

Becker, M. J.
1976 Neutron Activation Analysis of Rare Earth Elements in Steatite and Related Rocks: Application to Archaeological Problems throughout the World. *MASCA Newsletter* 12(2):1-2.

Beckhoff, B., B. Kanngießer, N. Langhoff, R. Wedell and H. Wolff
2006 *Handbook of Practical X-Ray Fluorescence Analysis*. Springer.

Beier, T. and H. Mommsen
1991 Modified Mahalanobis Filters for Grouping Pottery by Chemical Composition. *Archaeometry* 36:287-306.

Bellelli, C., F. X. Pereyra and M. Carballido
2006 Obsidian Localization and Circulation in Northwestern Patagonia (Argentina): Sources and Archaeological Record. In *Geomaterials in Cultural Heritage*, edited by M. Maggetti and B. Messiga, pp. 241-255. Special Publications. Geological Society, London.

Bellot-Gurlet, L.
1998 *Caractérisation par Analyse Élémentaire (PIXE et ICP-MS/-AES) d'un Verre Naturel: l'Obsidienne: Application à l'étude de Provenance d'Objets Archéologiques.*

Bellot-Gurlet, L., T. Calligaro, O. Dorighel, J. Dran, G. Poupeau and J. Salomon
1999 PIXE Analysis and Fission Track Dating of Obsidian from South American Prehispanic Cultures (Colombia, Ecuador). In *Nuclear Instruments and Methods in Physics Research Section B: Beam Interactions with Materials and Atoms*, pp. 616-621. vol. 150.

Bellot-Gurlet, L., O. Dorighel and G. Poupeau
2008 Obsidian Provenance Studies in Colombia and Ecuador: Obsidian Sources Revisited. *Journal of Archaeological Science* 35:272-289.

Bellot-Gurlet, L., F.-X. Le Bourdonnec, G. Poupeau and S. Dubernet
2004 Raman Micro-Spectroscopy of Western Mediterranean Obsidian Glass: One Step Towards Provenance Studies? *Journal of Raman Spectroscopy* 35(89):671-677.

Bellot-Gurlet, L. and G. Poupeau
2006 Towards a Non-Destructive Multi-Step Analytical Methodology for the Provenance Determination of Archaeological Obsidians. In *Young Chemists' Workshop on Chemistry for the Conservation of Cultural Heritage: Present and Future Perspectives*, pp. 1-4.

Bellot-Gurlet, L., G. Poupeau, J. Salomon, T. Calligaro, B. Moignard, J. Dran, J. Barrat and L. Pichon
2005 Obsidian Provenance Studies in Archaeology: A Comparison between PIXE, ICP-AES and ICP-MS. *Nuclear Instruments and Methods in Physics Research B* 240(1-2):583-588.

Benedetti-Pichler, A. A.
1956 Theory and Principles of Sampling for Chemical Analysis. In *Physical Methods in Chemical Analysis*, edited by W. G. Berl, pp. 183-217. vol. 3. Academic, New York.

Benedict, W. C.
1960 Urartians and Hurrians. *Journal of the American Oriental Society* 80(2):100-104.

Benitez, A. V.
2006 *Late Classic and Epiclassic Obsidian Procurement and Consumption in the Southeastern Toluca Valley, Central Highland Mexico*, University of Texas at Austin.

Bennett, R. B. and J. M. Dauria
1974 The Application of Energy Dispersive X-Ray Fluorescence Spectroscopy to Determining the Provenience of Obsidian. *International Journal of Applied Radiation and Isotopes* 25:361-71.

Bennyhoff, J. A. and R. F. Heizer
1965 Neutron Activation Analysis of Some Cuicuilco and Teotihuacan Pottery: Archaeological Interpretation of Results. *American Antiquity* 30(3):348-349.

Bernard, H. R.
1994 *Research Methods in Anthropology: Qualitative and Quantitative Approaches*. 2nd ed. AltaMira Press.

Bernbeck, R. and S. Polluck
2005 A Cultural-Historical Framework. In *Archaeologies of the Middle East: Critical Perspectives*, edited by S. Polluck and R. Bernbeck, pp. 11-40. Blackwell Publishing.

Beşikçi, I.
1969 *Gocebe Alikan Aşiret*. Dogan Yayinevi, Ankara.

Best, M. G.
2003 *Igneous and Metamorphic Petrology*. 2nd ed. Blackwell Publishing.

Bettinger, R. L., D. M.G. and R. J. Jackson
1984 Visual Sourcing of Central Eastern Californian Obsidians. In *Obsidian Studies in the Great Basin*, edited by R. E. Hughes, pp. 63-78. Contributions of the University of California Archaeological Research Facility.

Bevan, A.
2007 *Stone Vessels and Values in the Bronze Age Mediterranean*. Cambridge University Press.

Bieber, A. M., D. W. Brooks, G. Harbottle and E. V. Sayre
1976 Application of Multivariate Techniques to Analytical Data on Aegean Ceramics. *Archaeometry* 18:59-74.

Bigazzi, G., T. Ercan, M. Oddone, M. Ozdogan and Z. Yeğingil
1993 Application of Fission Track Dating to Archaeometry: Provenance Studies of Prehistoric Obsidian Artifacts. *International Journal of Radiation Applications and Instrumentation* 22 (Part D):757-762.

Bigazzi, G., M. Oddone and G. RADI
2005 The Italian Obsidian Sources. *Archeometriai Muhely* 1:1–13.

Bigazzi, G., G. Poupeau, Z. Yeğingil and L. Bellot-Gurlet
1998 Provenance Studies of Obsidian Artefacts in Anatolia Using the Fission-Track Dating Method: An Overview. In *L'obsidienne au Proche et Moyen-Orient: Du Volcan à l'Outil*, edited by M.-C. Cauvin, A. Gourgaud, B. Gratuze, N. Arnaud, G. Poupeau, J. L. Poidevin and C. Chataigner, pp. 70-89. BAR International Series.

Bigazzi, G., Z. Yeğingil, T. Ercan, M. Oddone and M. Özdogan
1993 Fission Track Dating Obsidians in Central and Northern Anatolia. *Bulletin of Volcanology* 55(8):588-595.

1994 Provenance Studies of Prehistoric Artifacts in Eastern Anatolian: Interdisciplinary Research Results. *Mineralogica et Petrographica Acta* 37:17-36.

Bigazzi, G., Z. Yeğingil, T. Ercan, M. Oddone and M. Özdogan
1996 The Pisa-Adana Joint Project on Provenance Studies of Prehistoric Obsidian Artifacts: First Results from Eastern Anatolia. *Archaeometry 94: The Proceedings of the 29th International Symposium on Archaeometry; Ankara, 9-14 May 1994*, pp. 521-528.

1997 Age Determination of Obsidian Bearing Volcanics in Eastern Anatolia Using the Fission Track Dating Method. *Geological Bulletin of Turkey* 40(2):57-73.

Binford, L. R.
1965 Archaeological Systematics and the Study of Culture Process. *American Antiquity* 31:203-210.

1967 Smudge Pits and Hide Smoking: The Use of Analogy in Archaeological Reasoning. *American Antiquity* 32(1):1-12.

1989 *Debating Archaeology*. Academic Press, San Diego.

Birks, L. S.
1963 *Electron Probe Microanalysis*. Chemical Analysis 17. John Wiley & Sons, New York.

Biró, T. K. and I. Pozsgai
1984 Obszidian Lelöhely-Azonositas Elektronsugaras Mikroanalizis Segitsegevel (Obsidian Characterization by Electron Microprobe Analysis). *Iparregeszet 2 (Industrial Archaeology II)*, pp. 25-38.

Biró, T. K., I. Pozsgai and A. Vlader
1986 Electron Beam Microanalyses of Obsidian Samples from Geological and Archaeological Sites. *Acta Archaeologica Academiae Scientiarum Hungaricae* 38:257-278.

Bishop, R. L.
1980 Aspects of Ceramic Compositional Modeling. In *Models and Methods in Regional Exchange*, edited by R. E. Fry, pp. 47-66. Society for American Archaeology.

Bishop, R. L. and H. Neff
1987 Compositional Data Analysis in Archaeology. In *Archaeological Chemistry IV*, edited by R. O. Allen, pp. 57-86. American Chemical Society, Advances in Chemistry Series 220, Washington, D.C.

Blackman, M.
1984 Provenance Studies of Middle Eastern Obsidian from Sites in Highland Iran. In *Archaeological Chemistry III*, edited by J. B. Lambert, pp. 19-50.

Blackman, M. J., R. Badalian, Z. Kikodze and P. L. Kohl
1998 Chemical Characterization of Caucasian Obsidian Geological Sources. In *L'obsidienne au Proche et Moyen-Orient: Du Volcan à l'Outil*, edited by M.-C. Cauvin, A. Gourgaud, B. Gratuze, N. Arnaud, G. Poupeau, J. L. Poidevin and C. Chataigner, pp. 205-231. BAR International Series.

Bohn, A. D.
2007 *Scattered Glass: Obsidian Artifact Provenance Patterns in Northwestern Wyoming*, Colorado State University.

Bohrnstedt, G. W. and D. Knoke
1988 *Statistics for Social Data Analysis*. 2nd ed. F. E. Peacock Publishers, Itasca, IL.

Bordet, P.
1972 Le Volcanisme Acide Recent du Dacht-e-Nawar (Afghanistan Central). *Bulletin Volcanologique* 36:289-300.

Bosanquet, R. C.
1904 The Obsidian Trade. In *Excavations at Phylakopi in Melos*, pp. 216-233. British School at Athens.

Bouey, P. D.
1984 Obsidian Studies and Their Implications for Prehistory. *Pacific Coast Archaeological Society Quarterly* 20:55-60.

Bouey, P. D., P. B. Vandiver, J. Druzik and G. S. Wheeler
1990 Recognizing the Limits of Archaeological Applications of Non-Destructive Energy-Dispersive X-Ray Fluorescence Analysis of Obsidians. *Materials Research Society Symposium Proceedings* 185:309-320.

Bouška, V.
1993 *Natural Glasses*. English edition. Ellis Horwood Series in Applied Science and Industrial Technology. Ellis Horwood, New York.

Bower, N. W., S. Faciszewski, S. Renwick and S. Peckham
1986 A Preliminary Analysis of Rio Grande Glazes of the Classic Period Using Scanning Electron Microscopy with X-Ray Fluorescence. *Journal of Field Archaeology* 13:307-315.

Bowman, H., F. Asaro and I. Pearlman
1972 *On the University of Composition in Obsidians and Evidence for Magma Mixing*. University of California, Lawrence Berkeley Lab Report LBL-661.

1973a Composition Variations in Obsidian Sources and the Archaeological Implications. *Archaeometry* 15(1):123-127.

1973b On the Uniformity of Composition in Obsidians and Evidence for Magmatic Mixing. *Journal of Geology* 81(3):312-327.

Bradley, R.
1993 An Interview With Colin Renfrew. *Current Anthropology* 34(1):71-82.

2000 *An Archaeology of Natural Places*. Routledge.

Brandt, S. A., K. J. Weedman and G. Hundie
1996 Gurage Hideworking, Stone-Tool Use, and Social Identity: An Ethnoarchaeological Perspective. In *Essays on Gurage Language and Culture: Dedicated to Wolf Leslau on the Occasion of His 90th Birthday, November 14th, 1996*, pp. 35-51.

Brandt, S. A. and K. J. Weedman
1997 The Ethnoarchaeology of Hideworking and Flake Stone-Tool Use in Southern Ethiopia. In *Ethiopia in Broader Perspective: Papers of the XIIIth International Conference of Ethiopian Studies, Kyoto, 12-17 December 1997*, pp. 351-361.

2002 The Ethnoarchaeology of Hideworking and Stone-Tool Use in Konso, Southern Ethiopia: An Introduction. In *Le Travail Du Cuir de La Prehistoire*, edited by S. Beyries and F. Audoin-Rouzeau, pp. 113-130. APDCA, Antibes.

Braswell, G., J. Clark, K. Aoyama, H. McKillop and M. D. Glascock
2000 Determining the Geological Provenance of Obsidian Artifacts from the Maya Region: A Test of the Efficacy of Visual Sourcing. *Latin American Antiquity* 11(3):269-282.

Braswell, G. and M. D. Glascock
1998 Interpreting Intrasource Variation in the Composition of Obsidian: The Geoarchaeology of San Martin Jilotepeque, Guatemala. *Latin American Antiquity* 9(4):353-369.

2002 The Emergence of Market Economies in the Ancient Maya World: Obsidian Exchange in Terminal Classic Yucatan, Mexico. In *Geochemical Evidence for Long-Distance Exchange*, edited by M. D. Glascock, pp. 33-52. Bergin and Garvey, Westport, Connecticut.

Brennan, P. V.
1996 Obsidian in the Bayburt-Erzurum Area, Eastern Anatolia. *Abr-Nahrain (Supplement Series)* 5:27-36.

Brentjes, B.
1964 Der Syrische Biber. *Zeitschrift für Jagdwissenschaft* 10:183-185.

Bressy, C., A. D'Anna, G. Poupeau, F. Le Bourdonnec, L. Bellot-Gurlet, F. Leandri, P. Tramoni and F. Demouche
2008 Chert and Obsidian Procurement of Three Corsican Sites During the 6th And 5th Millenniums BC. *Comptes Rendus-Palevol* 7(4):237-248.

Bressy, C., G. Poupeau and K. Yener
2005 Cultural Interactions During the Ubaid and Halaf Periods: Tell Kurdu (Amuq Valley, Turkey) Obsidian Sourcing. *Journal of Archaeological Science* 32(10):1560-1565.

Brew, G., M. Barazangi, A. K. Al-Maleh and T. Sawaf
2001 Tectonic and Geologic Evolution of Syria. *GeoArabia* 6(4):573-616.

Brew, G., R. Litak, M. Barazangi and T. Sawaf
1999 Tectonic Evolution of Northeast Syria: Regional Implications and Hydrocarbon Prospects. *GeoArabia* 4(3):289-318.

Brim, J. A. and D. H. Spain
1974 *Research Design in Anthropology: Paradigms and Pragmatics in the Testing of Hypotheses*. Holt, Rinehart, and Winston, New York.

Briois, F., B. Gratuze and J. Guilaine
1997 Obsidiennes du Site Néolithique Précéramique de Shillourokambos (Chypre). *Paléorient* 23(1):95-112.

Bromund, R. H., N. W. Bower and R. H. Smith
1976 Inclusions in Ancient Ceramics: An Approach to the Problem of Sampling for Chemical Analysis. *Archaeometry* 18(2):218-221.

Brooks, C. K., P. Henderson and J. G. Rønsbo
1981 Rare-Earth Partition Between Allanite and Glass in the Obsidian of Sandy Braes, Northern Ireland. *Mineralogical Magazine* 44:157-160.

Brown, F. H., C. Reid and A. Negash
2009 Possible Isotopic Fractionation of Argon in Source Obsidians and Archeological Artifacts from Kulkuletti, Ethiopia. *Journal of Archaeological Science* 36(10):2119-2124.

Brown, P. E.
1983 Tracing Prehistoric Sources of Obsidian. In *Granite Reef: A Study in Desert Archaeology*, edited by P. E. Brown and C. L. Stone, pp. 227-241. Arizona State University.

Brumfiel, E. M. and T. K. Earle
1987 *Specialization, Exchange, and Complex Societies*. Directions in Archaeology. Cambridge University Press.

Buccellati, G.
1988 Scope of the Research. In *Mozan 1: The Soundings of the First Two Seasons*, edited by G. Buccellati and M. Kelly-Buccellati, pp. 29-41. Undena Publications.

1999 Urkesh and the Question of Early Hurrian Urbanism. In *Urbanization and Land Ownership in the Ancient Near East*, edited by M. Hudson, B. A. Levine and B. Levine, pp. 229-250. Peabody Museum of Archaeology and Ethnology.

2000 Urkesh as Tell Mozan: Profiles of the Ancient City. In *Urkesh and the Hurrians: A Volume in Honor of Lloyd Cotsen*, pp. 11-34. Urkesh/Mozan Studies. vol. 3. Undena Publications.

2003 A LU E School Tablet from the Service Quarter of the Royal Palace AP at Urkesh. *Journal of Cuneiform Studies* 55:45-48.

2005a *Tell Mozan/Urkesh: Special Topics*. The International Institute for Mesopotamian Area Studies.

2005b The Monumental Urban Complex at Urkesh: Report on the 16th Season of Excavations, July-September 2003. In *Studies on the Civilization and Culture of Nuzi and the Hurrians*, edited by D. I. Owen and G. Wilhelm, pp. 3-28. CDL Press, Bethesda, Maryland.

2005c *Urkesh 2004: Urkesh @20*. The International Institute for Mesopotamian Area Studies.

2006 *The Discovery of a New Urban Civilization: Urkesh and the Hurrians*. The International Institute for Mesopotamian Area Studies.

2007 *The 2005-2006 Excavations at Tell Mozan, Ancient Urkesh: Recovering a New Civilization*. The International Institute for Mesopotamian Area Studies.

2008a *2007 Excavations at Tell Mozan, Ancient Urkesh and Plans for 2008*. The International Institute for Mesopotamian Area Studies.

2008b *Tell Mozan,Ancient Urkesh - At A Glance*. The International Institute for Mesopotamian Area Studies.

2008c *Final Report on the 21st Season of Excavations at Tell Mozan, Ancient Urkesh*. The International Institute for Mesopotamian Area Studies.

2009a *The Floodwaters of Urkesh*. The International Institute for Mesopotamian Area Studies.

2009b An Architectural "Logogram" at Urkesh? In *Dallo Stirone al Tigri, dal Tevere all'Eufrate: Studi in Onore di Claudio Saporetti*, pp. 23-29. Raffaele Garofalo, Rome.

Buccellati, G. and M. Kelly-Buccellati
1988 *Mozan 1: The Soundings of the First Two Seasons*. Undena Publications.

1995a The Royal Storehouse of Urkesh: The Glyptic Evidence from the Southwestern Wing. *Archiv für Orientforschung* 42-43:1-32.

Buccellati, G. and M. Kelly-Buccellati

1995b Mozan, Tall. In *Reallexikon der Assyriologie: Vorderasiatischen Archäologie*, pp. 386-393. Walter de Gruyter, Belin.

1997a Urkesh: the First Hurrian Capital. *The Biblical Archaeologist* 60(2): 77-96.

1997b Mozan, Tell. In *The Oxford Encyclopedia of Archaeology in the Near East*, edited by E. M. Meyers, pp. 60-63. vol. 4. Oxford University Press.

2000 The Royal Palace of Urkesh: Report on the 12th Season at Tell Mozan/Urkesh: Excavations in Area AA. Mitteilungen der Deutschen Orient-Gesellschaft zu Berlin 132:133-183.

2001a In Search of Hurrian Urkesh: City of Myth. *Archaeology Odyssey* 4:16-27.

2001b *Towards a Functional and Historical Definition of the Royal Palace AP at Urkesh: Report on the 13th Season at Tell Mozan/Urkesh: Excavations in Area AA, June-August 2000*. The International Institute for Mesopotamian Area Studies.

2001c The Royal Palace at Urkesh and the Daughter of Naram-Sin. In *Les Anneles Archelologiques Arabes Syriennes*, pp. 63-69. Ministere de la Culture, Direction Generale des Antiquites et des Musees, Republique Arabe Syrienne.

2002a Tar'am-Agade, Daughter of Naram-Sin, at Urkesh. In *Of Pots and Pans: Papers on the Archaeology and History of Mesopatamia and Syria Presented to David Oates in Honour of His 75th Birthday*, edited by L. Gailani Werr, J. Curtis, H. Martin, A. McMahon, J. Oates and J. Reade, pp. 11-31. NABU Publications, London.

2002b Mozan/Urkesh: A New Capital in the Northern Djezireh. In *Documents d'Archeologie Syrienne I: The Syrian Jezira: Cultural Heritage and Interrelations*, pp. 127-133. Ministere de la Culture, Direction Generale des Antiquites et des Musees, Republique Arabe Syrienne.

2003 Tell Mozan (Ancient Urkesh). In *Art of the First Cities: The Third Millennium B.C. from the Mediterranean to the Indus*, edited by J. Aruz, pp. 224-227. Metropolitan Museum of Art.

2004 *Tell Mozan, Ancient Urkesh: A Self-Guided Tour to the Site*. The International Institute for Mesopotamian Area Studies.

2005a Urkesh as a Hurrian Religious Center. *Studi Micenei ed Egeo-Anatolici* 47:27-59.

2005b *The 2005 season of excavations at Tell Mozan*. The International Institute for Mesopotamian Area Studies.

2006 *The Great Temple Terrace at Urkesh and the Lions of Tish-atal*. The International Institute for Mesopotamian Area Studies.

2007a *The Temple Terrace of Urkesh: From Protoliterate to Mittani*. The International Institute for Mesopotamian Area Studies.

2007b *Site Presentation at Tell Mozan, Ancient Urkesh*. The International Institute for Mesopotamian Area Studies.

2007c Urkesh and the Question of the Hurrian Homeland. *Bulletin of the Georgian National Academy of Sciences* 175(2):141-151.

Buck, B. A.

1982 Ancient Technology in Contemporary Surgery. *Western Journal of Medicine* 136:265-269.

Bunnens, G. L. and A. Roobaert
1988 Tell Shermola (Amouda): Reconnaissance Preliminaire. In *Mozan 1: The Soundings of the First Two Seasons*, edited by G. Buccellati and M. Kelly-Buccellati, pp. 90-92. Undena Publications.

Burger, R., K. Chavez and S. Chavez
2000 Through the Glass Darkly: Prehispanic Obsidian Procurement and Exchange in Southern Peru and Northern Bolivia. *Journal of world prehistory* 14(3):267-362.

Burghardt, A.
1971 A Hypothesis about Gateway Cities. *Annals of the Association of American Geographers* 61(2):269-285.

Burney, C. A.
1958 Eastern Anatolia in the Chalcolithic and Early Bronze Age. *Anatolian Studies* 8:157-209.

1962 The Excavations at Yanik Tepe, Azerbaijan, 1961 Second Preliminary Report. *Iraq* 24:134-152.

Burton, J. H.
1986 *Selected Petrologic Applications of Back-Scattered Electron Imaging*, Arizona State University.

1989 Electron Microscopic Study of Obsidian Artifacts from Waddell Project Sites. In *Settlement, Subsistence, and Specialization in the Northern Periphery: The Waddell Project*, pp. 665-667. vol. 2.

1993 Provenance Determination of Obsidian Artifacts from Shelltown by Back-Scattered Electron Microscopy. In *Shelltown and the Hind Site: A Study of Two Hohokam Craftsman Communities in Southwestern Arizona*, edited by W. S. Marmaduke and R. J. Martnik, pp. B1-B11. vol. 2. Northland Research, Flagstaff.

Burton, J. H. and D. H. Krinsley
1987 Obsidian Provenance Determination by Back-Scattered Electron Imaging. *Nature* 326:585-587.

Bustamante, A., M. Delgado, R. M. Latini and A. V. B. Bellido
2007 Multivariate Analysis in Provenance Studies: Cerrillos Obsidians Case, Peru. *Hyperfine Interactions* 175(1-3):43-48.

CAD (Chicago Assyrian Dictionary)
1962 *Chicago Assyrian Dictionary Project,* Volume 16. The Oriental Institute of the University of Chicago.

Calvin, K. F. and L. Mount-Williams
1988 Samples from the Excavations. In *Mozan 1: The Soundings of the First Two Seasons*, edited by G. Buccellati and M. Kelly-Buccellati, pp. 83-87. Undena Publications.

Canby, J.
1965 Early Bronze 'Trinket' Moulds. *Iraq* 27:42-61.

2003 A Figurine from Urkesh: A "Darling" from Troy to Mesopotamia. *Iraq* 65:171-173.

Cann, J. R.
1983 Petrology of Obsidian Artefacts. In *The Petrology of Archaeological Artefacts*, edited by D. R. C. Kempe and A. P. Harvey, pp. 227-255. Clarendon Press, Oxford.

Cann, J. R., J. E. Dixon and C. Renfrew
1968 The Sources of Saliagos Obsidian. In *Excavations at Saliagos Near Antiparos*, edited by J. D. Evans and C. Renfrew, pp. 105-107. vol. 5. British School at Athens.

1969 Obsidian Analysis and the Obsidian Trade. In *Science in Archaeology: A Survey of Progress and Research, Revised and Expanded Edition*, edited by D. R. Brothwell and E. Higgs, pp. 578-591. Praeger Publishers, New York.

Cann, J. R. and C. Renfrew
1964 The Characterization of Obsidian and its Application to the Mediterranean Region. *Proceedings of the Prehistoric Society* 30:111-133.

Capannesi, G., A. F. Sedda and A. M. Palmieri
1990 Classification of Near East Obsidians Using INAA. The 27th International Symposium on Archaeometry, Heidelberg, Germany.

Carballo, D. M.
2005 *State Political Authority and Obsidian Craft Production at the Moon Pyramid, Teotihuacan, Mexico*, University of California, Los Angeles.

Carmines, E. G. and R. A. Zeller
1979 *Reliability and Validity Assessment*. Quantitative Applications in the Social Sciences. Sage Publications.

Carnes, M. C.
1999 *American National Biography*. Oxford University Press, New York.

Carter, E., M. Hargreaves, N. Kononenko, I. Graham, H. Edwards, B. Swarbrick and R. Torrence
2009 Raman Spectroscopy Applied to Understanding Prehistoric Obsidian Trade in the Pacific Region. *Vibrational Spectroscopy* 50(1):116-124.

Carter, T.
2007 The Theatrics of Technology: Consuming Obsidian in the Early Cycladic Burial Arena. *Archeological Papers of the American Anthropological Association* 17:88-107.

2009 50 Years of Obsidian Sourcing Studies: Successes, Failures and Future Directions. In *Geological Society of America Abstracts with Programs*, pp. 553. vol. 41, Portland, Oregon.

Carter, T., S. Dubernet, R. King, F.-X. Le Bourdonnec, M. Milić, G. Poupeau and M. S. Shackley
2008 Eastern Anatolian Obsidians at Çatalhöyük and the Reconfiguration of Regional Interaction in the Early Ceramic Neolithic. *Antiquity* 82(318):900-909.

Carter, T. and V. Kilikoglou
2006 From Reactor to Royalty? Aegean and Anatolian Obsidians from Quartier Mu, Malia (Crete). *Journal of Mediterranean Archaeology* 20(1):1-29.

Carter, T., G. Poupeau, C. Bressy and N. Pearce
2006 A New Programme of Obsidian Characterization at Çatalhöyük, Turkey. *Journal of Archaeological Science* 33(7):893-909.

Carter, T. and M. S. Shackley
2007 Sourcing Obsidian from Neolithic Catalhoyuk (Turkey) Using Energy Dispersive X-Ray Fluorescence. *Archaeometry* 49(3):437-454.

Castro, J.
1999 *Textural and Structural Development of Obsidian Lavas*, University of Oregon.

Castro, J., K. Cashman and M. Manga
2003 A Technique for Measuring 3D Crystal-Size Distributions of Prismatic Microlites in Obsidian. *American Mineralogist* 88(8-9):1230-1240.

Castro, J., D. Dingwell, A. Nichols and K. Hess
2004 Petrologic and Dynamic Importance of Flow Banding in Obsidian Lavas. American Geophysical Union Annual Meeting, San Francisco.

Castro, J., M. Manga and K. Cashman
2002 Dynamics of Obsidian Flows Inferred from Microstructures: Insights from Microlite Preferred Orientations. *Earth and Planetary Science Letters* 199:211-226.

Castro, J. M. and C. Mercer
2004 Microlite Textures and Volatile Contents of Obsidian from the Inyo Volcanic Chain, California. *Geophysical Research Letters* 31(18):1-4.

Cauvin, J.
1998 La Signification Symbolique de L'obsidienne. In *L'obsidienne au Proche et Moyen-Orient: Du Volcan à l'Outil*, edited by M.-C. Cauvin, A. Gourgaud, B. Gratuze, N. Arnaud, G. Poupeau, J. L. Poidevin and C. Chataigner, pp. 379-382. BAR International Series.

Cauvin, M.-C.
1991 L'obsidienne au Levant Prehistorique: Provenance et Fonction. *Cahiers de l'Euphrate* 5-6:163-190.

1998 L'obsidienne: Données Récentes Provenant de Sites-Habitats Néolithiques. In *L'obsidienne au Proche et Moyen-Orient: Du Volcan à l'Outil*, edited by M. C. Cauvin, A. Gourgaud, B. Gratuze, N. Arnaud, G. Poupeau, J. L. Poidevin and C. Chataigner, pp. 259-271. BAR International Series.

Cauvin, M.-C., N. Balkan, Y. Besnus and F. Saroglu
1986 Origine de l'Obsidienne de Cafer Höyük (Turquie): Premiers Résultats. *Paléorient* 12(2): 89-97.

Cauvin, M.-C. and C. Chataigner
1994 Possible Relationships Between Geochemical Groups of Obsidian from the Near East. In *Archaeometry 94: The Proceedings of the 29th International Symposium on Archaeometry; Ankara, 9-14 May 1994*, pp. 529-533.

1998 Distribution de l'Obsidienne dans les Sites Archéologiques du Proche et du Moyen Orient (Par Phase Chronologique). In *L'obsidienne au Proche et Moyen-Orient: Du Volcan à l'Outil*, edited by M. C. Cauvin, A. Gourgaud, B. Gratuze, N. Arnaud, G. Poupeau, J. L. Poidevin and C. Chataigner, pp. 325-350. BAR International Series.

Chabot, J. and P. Eid
2007 Stone Tools from a Bronze Age Village (Tell Nusstell, Syria) in their Wider Context. *Berytus: Archaeological Studies* L:7-36.

Chabot, J. and J. Pelegrin
2006 Two Examples of Lithic Industries Employing Pressure Flaking with a Lever: Recent Research from Northern Mesopotamia (Syria, Irak) and Southern Caucasus (Armenia). UISPP / IUPPS, XV Congress / XV Congrès, Université de Lisbonne.

Chabot, J., J.-L. Poidevin, C. Chataigner and M. Fortin
2001 Caracterisation et Provenance des Artefacts en Obsidienne de Tell 'Atij et de Tell Gudeda (III Millenaire, Syrie). *Cahiers d'Acheologie du CELAT* 10(1):241-256.

Charlton, C. L. O.
1993 Obsidian as Jewelry: Lapidary Production in Aztec Otumba, Mexico. *Ancient Mesoamerica* 4:231-243.

Charpin, D.
2003 La « Toponymie en Miroir » dans le Proche-Orient Amorrite. *Revue d'Assyriologie et d'Archéologie Orientale* 97:3-34.

Chataigner, C.
1994 Les Propriétés Géochimiques des Obsidiennes et la Distinction des Sources de Bingöl et du Nemrut Dag. *Paléorient* 20(2):9-17.

1998 Sources des Artefacts du Proche Orient D'aprés Leur Caractérisation Géochimique. In *L'obsidienne au Proche et Moyen-Orient: Du Volcan à l'Outil*, edited by M.-C. Cauvin, A. Gourgaud, B. Gratuze, N. Arnaud, G. Poupeau, J. L. Poidevin and C. Chataigner, pp. 273-324. BAR International Series.

Chataigner, C., R. Badalian, G. Bigazzi and M.-C. Cauvin
2003 Provenance Studies of Obsidian Artefacts from Armenian Archaeological Sites Using the Fission-Track Dating Method. *Journal of Non-Crystalline Solids* 323:172-179.

Chataigner, C. and O. Barge
2007 Quantitative Approach to the Diffusion of Obsidian in the Ancient Northern Near East. Conference on Computer Applications and Quantitative Methods in Archaeology (CAA), Berlin, Germany.

Chataigner, C., J. Poidevin and N. Arnaud
1998 Turkish Occurrences of Obsidian and Use by Prehistoric Peoples in the Near East from 14,000 to 6000 BP. *Journal of Volcanology and Geothermal Research* 85(1-4):517-537.

Chen, S., Y. Bai, G. Lin and X. Han
2005 Variations in Life-Form Composition and Foliar Carbon Isotope Discrimination Among Eight Plant Communities Under Different Soil Moisture Conditions in the Xilin River Basin, Inner Mongolia, China. *Ecological Research* 20:167-176.

Chernicoff, S. and H. A. Fox
1997 *Essentials of Geology*. Worth Publishers, New York.

Cherry, J. F., E. Z. Faro and R. Badalyan
2007 Obsidian Studies in Southern Armenia: Work by the Vorotan Project in 2005-2006. Archaeological Institute of America Annual Meeting.

Christie, A.
1946 *Come, Tell Me How You Live*. Dodd, Mead & Company.

Cierny, J. and G. Weisgerber
2003 The Bronze Age Tin Mines in Central Asia. In *The Problem of Early Tin*, edited by A. Giumlia-Mair and F. Lo Schiavo, pp. 23-31. Archaeopress, Oxford.

Clark, J. D. and H. Kurashina
1981 A Study of the Work of a Modern Tanner in Ethiopia and its Relevance for Archaeological Interpretation. In *Modern Material Culture: The Archaeology of Us*, edited by R. A. Gould and M. B. Schiffer, pp. 303-343. Academic Press.

Clark, J. G. D.
1952 *Prehistoric Europe: The Economic Basis*. Stanford University Press.

1965 Traffic in Stone Axe and Adze Blades. *Economic History Review* 18(1):1-28.

Clark, J. J.
2001 *Tracking Prehistoric Migrations: Pueblo Settlers among the Tonto Basin Hohokam*. Anthropological Papers 65. University of Arizona Press, Tucson.

Collins, B. J.
2004 A Channel to the Underworld in Syria. *Near Eastern Archaeology* 67(1):54-56.

Conde, G., P. D. Ihinger and E. Frahm
2009a Water in Anatolian Obsidian: Factors Influencing Hydrous Species Concentrations with Implications for Sourcing and Dating of Artifacts. In *Geological Society of America, Abstracts with Programs*, pp. 554. vol. 41, Portland, Oregon.

2009b Water Speciation in Anatolian Obsidian: Quenched Magmatic Water versus Low-Temperature Hydration. The 19th V.M. Goldschmidt Conference, Davos, Switzerland.

2009c Water Speciation in Anatolian Obsidian: Quenched Magmatic Water versus Low-Temperature Hydration. University of Wisconsin-Eau Claire Student Research Day.

Conde, G., J. Sisko, P. D. Ihinger and E. Frahm
2008 Obsidian Hydration Dating of Archaeological Artifacts from the Middle East: Characterizing Compositional Variations of Potential Volcanic Sources. University of Wisconsin-Eau Claire Student Research Day.

Constantinescu, B., R. Bugoi and G. Sziki
2002 Obsidian Provenance Studies of Transylvania's Neolithic Tools Using PIXE, Micro-PIXE and XRF. *Nuclear Instruments and Methods in Physics Research B* 189:373-377.

Coote, G. E. and P. Nistor
1982 Depth Profiles of Sodium in Obsidian by the Resonant Nuclear Reaction Method: A Potential Dating Method. In *Archaeometry: An Australian Perspective*, edited by W. Ambrose and P. Duerden. The Australian National University Press.

Copeland, L.
1989 The Flint and Obsidian Artifacts of Tell Sabi Abyad. In *Excavations at Tell Sabi Abyad: Prehistoric Investigations in the Balikh Valley, Northern Syria*, edited by P. M. M. G. Akkermans, pp. 237-284. vol. 468. BAR International Series.

1995 The Phantom Obsidian Traders of the Jazirah. *Neo-Lithics: A Newsletter of Southwest Asian Lithics Research* 1:5-6.

1996 The Flint and Obsidian Industries. In *Tell Sabi Abyad: The Late Neolithic Settlement: Report on the Excavations of the University of Amsterdam (1988) and the National Museum of Antiquities Leiden (1991-1993) in Syria, Volume 2*, edited by P. M. M. G. Akkermans, pp. 285-338. Nederlands Historisch-Archaeologisch Institute.

Coqueugniot, É.
1998 L'obsidienne en Méditerranée Orientale aux Époques Post-Néolithiques. In *L'Obsidienne au Proche et Moyen Orient: Du Volcan l'Outil*, edited by M.-C. Cauvin, A. Gourgaud, B. Gratauze, N. Arnaud, G. Poupeau, J. L. Poidevin and C. Chataigner, pp. 351-361. British Archaeological Reports. Maison de l'Orient Méditerranéen, Archaeopress, Oxford.

Cornaggio-Castiglioni, O., F. Fussi and G. D'Agnolo
1962 Indagini Sulla Provenienza dell'Ossidiana in uso Nelle Industrie Preistoriche Italiane. Parte Prima: Problematica e Techniche di Indagine. *Atti della Societa Italiana di Scienze Naturali e del Museo Civico di Storia Naturale di Milano* 101:12-19.

1963 Indagini Sulla Provenienza dell'Ossidiana Utilizzata Nelle Industrie Preistoriche del Mediterraneo Occidentale. *Atti della Societa Italiana di Scienze Naturali e del Museo Civico di Storia Naturale di Milano* 102:310-322.

Coskunsu, G.
2007 Obsidian Assemblage of Mezraa Teleilat: Evidence of Cultural and Chronological Continuation from Late Pre-Pottery Neolithic to Pottery Neolithic. *Neo-Lithics* 2:36-43.

Cotterell, B. and J. Kamminga
1987 The Formation of Flakes. *American Antiquity* 52(4):675-708.

Courty, M.-A.
1994 Le Cadre Paléogéographique des Occupations Humaines dans le Bassin du Haut-Khabur (Syrie du Nord-Est): Premiers Résultats. *Paléorient* 20(1):21-59.

Craig, N., R. Speakman, R. Popelka-Filcoff, M. Glascock, J. Robertson, M. Shackley and M. Aldenderfer
2007 Comparison of XRF and PXRF for Analysis of Archaeological Obsidian from Southern Perú. *Journal of Archaeological Science* 34(12):2012-2024.

Crawford, H.
1973 Mesopotamia's Invisible Exports in the Third Millennium BC. *World Archaeology* 5(2): 232-241.

1978 The Mechanics of the Obsidian Trade: A Suggestion. *Antiquity* 52:129-132

1991 *Sumer and the Sumerians*. Cambridge University Press.

2001 The British Archaeological Expedition to Kuwait. *British School of Archaeology in Iraq Newsletter* 7:6.

Cribb, R.
1991 *Nomads in Archaeology*. New Studies in Archaeology. Cambridge University Press.

Dalley, S.
1984 *Mari and Karana: Two Old Babylonian Cities*. Longman Group, London.

Daraban, L., C. Comsa, O. Cozar, V. Simon, V. Znamirovschi, I. Ghiurca, M. Salagean and A. Pantelica
2002 Obsidian Provenance Studies. In *Archaeometry 98: Proceedings of the 31st Symposium, Budapest, 1998 April 26-May 3*, edited by E. Jerem and K. T. Biró, pp. 705-707. BAR International Series 1043.

Darling, J. A.
1998 *Obsidian Distribution and Exchange in the North-Central Frontier of Mesoamerica.* University of Michigan.

Darvill, T.
2008 *Concise Oxford Dictionary of Archaeology*. 2nd ed. Oxford University Press.

Davis, L., S. Aaberg and A. Johnson
1992 Archaeological Fieldwork at Yellowstone's Obsidian Cliff. *Park Science* 12(2):26-27.

Davis, R. S. and L. Dupree
1977 Prehistoric Survey in Central Afghanistan. *Journal of Field Archaeology* 4(2):139-148.

Day, P. M., N. J. Brodie and V. Kilikoglou
1996 The Presumption of Local Provenance and Other Deadly Sins. The 30th International Symposium on Archaeometry, Urbana.

Dayton, J. E.
1971 The Problem of Tin in the Ancient World. *World Archaeology* 3(1):49-70.

de B. Pereira, C., N. Miekeley, G. Poupeau and I. Küchler
2001 Determination of Minor and Trace Elements in Obsidian Rock Samples and Archaeological Artifacts By Laser Ablation Inductively Coupled Plasma Mass Spectrometry Using Synthetic Obsidian Standards. *Spectrochimica Acta Part B: Atomic Spectroscopy* 56(10):1927-1940.

De Francesco, A. M., G. M. Crisci and M. Bocci
2008 Non-Destructive Analytic Method Using XRF For Determination of Provenance of Archaeological Obsidians from the Mediterranean Area: A Comparison with Traditional XRF Methods. *Archaeometry* 50(2):337-350.

de Morgan, J. J.
1927 *Prehistoire Orientale III*. Geuthner, Paris.

De Soete, D., R. Gijbels and J. Hoste
1972 *Neutron Activation Analysis*. John Wiley and Sons, New York, NY.

Deckers, K.
2006 *Northeastern Syrian Archaeological Sites in their Environmental Context: A Fluvial Geoarchaeological Survey*. Ältere Urgeschichte und Quartärökologie website.

2007 The Ancient River. In *The Temple Terrace of Urkesh: From Protoliterate to Mittani*, edited by G. Buccellati and M. Kelly-Buccellati, pp. 24-26. The International Institute for Mesopotamian Area Studies.

Deckers, K. and S. Riehl
2004 The Development of Economy and Environment from the Bronze Age to the Early Iron Age in Northern Syria and the Levant. A Case-Study from the Upper Khabur Region. *Antiquity (Online project gallery)* 78(302).

2007 Fluvial Environmental Contexts for Archaeological Sites in the Upper Khabur Basin (Northeastern Syria). *Quaternary Research* 67:337-348.

Decourt, J.-C.
1998 L'obsidienne dans les Sources Anciennes: Notes Sur L'Historie du mot et L'Utilisation de la Roches Dans L'Antiquité. In *L'obsidienne au Proche et Moyen-Orient: Du Volcan à l'Outil*, edited by M.-C. Cauvin, A. Gourgaud, B. Gratauze, N. Arnaud, G. Poupeau, J. L. Poidevin and C. Chataigner, pp. 363-377. British Archaeological Reports. Maison de l'Orient Méditerranéen, Archaeopress, Oxford.

Dillemann, L.
1962 *Haute Mésopotamie Orientale et Pays Adjacents: Contribution a la Géographie Historique de la Région, du Ve s. Avant l'ère Chrétienne au VIe s. de Cette Ère*. Institut Français d'Archéologie de Beyrouth, Bibliothèque Archéologique et Historique. Paul Geuthner, Paris.

Dillian, C. D.
2002 *More Than Toolstone: Differential Utilization of Glass Mountain Obsidian*, University of California-Berkeley.

2004 Sourcing Belief: Using Obsidian Sourcing to Understand Prehistoric Ideology in Northeastern California, U.S.A. *Mediterranean Archaeology and Archaeometry Abstracts*. vol. 4.

2007 Archaeology of Fire and Glass: Cultural Adoption of Glass Mountain in Obsidian. In *Under the Shadow: The Cultural Impacts of Volcanic Eruptions*, edited by J. Grattan and R. Torrence, pp. 253-273. Left Coast Press, Walnut Creek, California.

Dillian, C. D., C. A. Bello and M. S. Shackley
2006 Long Distance Exchange? The Case of an Obsidian Projectile Point from the University of Pennsylvania Museum. *Pennsylvania Archaeologist* 76(2):41-47.

Dillian, C. D. and C. L. White
2009 Introduction: Perspectives on Trade and Exchange. In *Trade and Exchange: Archaeological Studies from History and Prehistory*, edited by C. D. Dillian and C. L. White, pp. 3-16. Springer.

Dixon, J., J. Cann and C. Renfrew
1968 Obsidian and the Origins of Trade. *Scientific American* 218(3):38-46.

Dixon, J. E.
1976 Obsidian Characterization Studies in the Mediterranean and Near East. In *Advances in Obsidian Glass Studies: archaeological and geochemical perspectives*, edited by R. E. Taylor. Noyes Press, Park Ridge, New Jersey.

Donovan, J. J., D. A. Wark and M. J. Jercinovic
2007 Improved EPMA Trace Element Accuracy Using a Matrix Iterated Quantitative Blank Correction. American Geophysical Union Annual Meeting, San Francisco.

Doremus, R.
2000 Diffusion of Water in Rhyolite Glass: Diffusion–Reaction Model. *Journal of Non-Crystalline Solids* 261(1-3):101-107.

Doremus, R. H.
1975 Interdiffusion of Hydrogen and Alkali Ions in a Glass Surface. *Journal of Non-Crystalline Solids* 19:137–144.

1979 Chemical Durability of Glass. In *Treatise on Materials Science and Technology*, edited by M. Tomozawa and R. H. Doremus, pp. 41–69. vol. 17. Academic Press, New York.

Dostal, J. and M. Zerbi
1978 Geochemistry of the Savalan Volcano (Northwestern Iran). *Chemical Geology* 22:31-42.

Draucker, A., D. Baron, R. Horton and R. Yohe
2002 Trace Element Characterization of Distinct Obsidian Flows within the Coso Volcanic Field, California By Laser Ablation ICP/MS and Archaeological Implications. Geological Society of America Annual Meeting, Denver.

Draucker, A.
2007 *Geochemical Characterization of Obsidian Subsources from the Coso Range, California Using Laser Ablation Inductively Coupled Plasma Mass Spectrometry as a Tool for Archaeological Investigations*. California State University, Bakersfield.

Drower, M. S.
1973 Chapter 10: Syria c. 1550-1400 B.C. In *The Cambridge Ancient History Volume 2: The Middle East and the Aegean Region, c.1800-1380 BC*, edited by I. E. S. Edwards, C. J. Gadd, N. G. L. Hammond and E. Sollberger, pp. 417-525. Cambridge University Press.

Duranni, S., M. T. Khan and C. Renfrew
1971 Obsidian Source Identification by Fission Track Analysis. *Nature* 233:242-252.

Duttine, M., G. Villeneuve, G. Poupeau, A. Rossi and R. Scorzelli
2003 Electron Spin Resonance of Fe3+ Ion in Obsidians from Mediterranean Islands: Application to Provenance Studies. *Journal of Non-Crystalline Solids* 323(1-3):193-199.

Earle, T. K.
1982 The Ecology and Politics of Primitive Valuables. In *Culture and Ecology: Eclectic Perspectives*, edited by J. G. Kennedy and R. B. Edgerton, pp. 65-83. AAAS Special Pub. 15.

Earle, T. K. and J. E. Ericson
1977 *Exchange Systems in Prehistory*. Studies in Archaeology. Academic Press, New York.

Eastwood, W. J., N. J. G. Pearce, J. A. Westgate, W. T. Perkins, H. F. Lamb and N. Roberts
1999 Geochemistry of Santorini Tephra in Lake Sediments from Southwest Turkey. *Global and Planetary Change* 21:17-29.

Ebel, R. L.
1965 *Measuring Educational Achievement*. Prentice-Hall, Englewood Cliffs, New Jersey.

Eden, D. N., A. S. Palmer, S. J. Cronin, M. Marden and K. R. Berryman
2001 Dating the Culmination of River Aggradation at the End of the Last Glaciation Using Distal Tephra Compositions, Eastern North Island, New Zealand. *Geomorphology* 38:133-151.

Edwards, T. W. D., W. Graf, P. Trimborn, W. Stichler, J. Lipp and H. D. Payer
2000 δ13C Response Surface Resolves Humidity and Temperature Signals in Trees. *Geochimica and Cosmochimica Acta* 64(2):161-167.

Eerkens, J. and J. Rosenthal
2004 Are Obsidian Subsources Meaningful Units of Analysis?: Temporal and Spatial Patterning of Subsources in the Coso Volcanic Field, Southeastern California. *Journal of Archaeological Science* 31(1):21-29.

Eerkens, J., A. Spurling and M. Gras
2008 Measuring Prehistoric Mobility Strategies Based on Obsidian Geochemical and Technological Signatures in the Owens Valley, California. *Journal of Archaeological Science* 35(3):668-680.

Ehleringer, J. R.
1989 Carbon Isotope Ratios and Physiological Processes in Aridland Plants. In *Stable Isotopes in Ecological Research*, edited by P. W. Rundel, J. R. Ehleringer and K. A. Nagy, pp. 41-54. Springer, Heidelberg.

1993 Carbon and Water Relations in Desert Plants: An Isotopic Perspective. In *Stable Isotopes and Plant Carbon-Water Relations*, edited by J. R. Ehleringer, A. E. Hall and G. D. Farquhar, pp. 155-172. Academic Press, San Diego, CA.

Ehmann, W. D. and D. E. Vance
1991 *Radiochemistry and Nuclear Methods of Analysis*. John Wiley and Sons, New York, NY.

Epstein, S.
1977 *The Trade in Near Eastern Obsidians*, University of Cambridge.

Ercan, T., F. Saroglu and I. Kuscu
1994 Features of Obsidian Beds Formed by Volcanic Activity in Anatolia since 25 Million Years BP. In *The 29th International Symposium on Archaeometry; Ankara, 9-14 May 1994*.

1995 Features of Obsidian Beds Formed by the Activity of the Volcanoes in Anatolia since 25 Million Years B.P. *The Proceedings of the 29th International Symposium on Archaeometry, 1994 May 9-14, Ankara, Turkey*, pp. 505-513.

Ercan, T., S. Tokel, A. Akbasli, T. Yildirim, A. Fisekci, Y. Selvi, M. Olmez, B. Can, J. I. Matsuda, T. Ui, T. Fujitani and K. Notsu
1990 Origin and Evolution of the Cenozoic Rocks around Hasan Dagi and Karaca (Central Anatolia). *Jeom Derg (Bulletin of Geomorphology)* 18:39-54.

Ercan, T., Z. Yeğingil and G. Bigazzi
1989 Obsidian, Definition, Characteristics and Distribution in Anatolia: Geochemical Features of Central Anatolian Obsidians. *Bulletin of Geomorphology (Jeomorfoloji Bergisi)* 17:71-83.

Ericson, J. E.
1975 New Results in Obsidian Hydration Dating. *World Archaeology*:151-159.

Ericson, J. E. and T. K. Earle
1982 *Contexts for Prehistoric Exchange*. Studies in Archaeology. Academic Press, New York.

Ericson, J. E. and M. D. Glascock
2004 Subsource Characterization: Obsidian Utilization of Subsources of the Coso Volcanic Field, Coso Junction, California, USA. *Geoarchaeology* 19(8):779-805.

Ericson, J. E., J. D. Mackenzie and R. Berger
1976 Physics and Chemistry of the Hydration Process in Obsidians: Theoretical Implications. In *Advances in Obsidian Glass Studies: Archaeological and Geochemical Perspectives*, edited by R. E. Taylor, pp. 25-45. Noyes Press, Park Ridge, New Jersey.

Ernsberger, F. M.
1977 Molecular Water in Glass. *Journal of the American Ceramic Society* 60(1-2):91-92.

Evans, C. and B. J. Meggers
1960 A New Dating Method Using Obsidian: An Archaeological Evaluation of the New Method. *American Antiquity* 25(4):523-537.

Farquhar, G. D., J. R. Ehleringer and K. T. Hubick
1989 Carbon Isotope Discrimination and Photosynthesis. *Annual Review of Plant Physiology and Plant Molecular Biology* 40:503-537.

Faure, P.
1987 *Parfums et Aromates de l'Antiquite*. Nouvelles Etudes Historiques. Fayard, Paris.

Federman, A. N. and S. N. Carey
1980 Electron Microprobe Correlation of Tephra Layers from Eastern Mediterranean Abyssal Sediments and the Island of Santorini. *Quaternary Research* 13:160-171.

Feinberg, J., C. Johnson and E. Frahm
2009 A Database of Obsidian Magnetic Properties for Archaeological Sourcing. In *Geological Society of America Abstracts with Programs*, pp. 553. vol. 41, Portland, Oregon.

Ferretti, M.
2000 X-ray Fluorescence Applications for the Study and Conservation of Cultural Heritage. In *Radiation in Art and Archeometry*, edited by D. C. Creagh and D. A. Bradley, pp. 285-297. Elsevier Science.

Ferriz, H.
1985 Caltonac, A Prehispanic Obsidian-Mining Center in Eastern Mexico?: A Preliminary Report. *Journal of Field Archaeology* 12(3):363-370.

Filippakis, S. E., A. P. Grimanis and B. Perdikatsis
1981 X-ray and Neutron Activation Analysis of Obsidian Artifacts from Kitsos Cave. In *Science and Archaeology*, edited by R. H. Brill, pp. 21-26. vol. 23. The MIT Press.

Fink, J. H.
1987 The Emplacement of Silicic Domes and Lava Flows. Geological Society of America, Special Paper 212.

Fink, J. H. and C. R. Manley
1987 Origin of Pumiceous and Glassy Textures in Rhyolite Flows and Domes. *The Emplacement of Silicic Domes and Lava Flows*, Geological Society of America Special Paper 212, pp. 77-88.

Foit, F. F., D. G. Gavin and F. S. Hu
2004 The Tephra Stratigraphy of Two Lakes in South-Central British Columbia, Canada and its Implications for Mid-Late Holocene Volcanic Activity at Glacier Peak and Mount St. Helens, Washington, USA. *Canadian Journal of Earth Sciences* 41:1401-1410.

Ford, B. A. and G. A. Cox
1988 Electron Probe Micro-Analysis of Soil Corroded Glass. *Institute of Physics Conference Series* 2(93):523.

Fornaseri, M., L. Malpieri, A. M. Palmieri and A. Taddeucci
1975 Analyses of Obsidians from the Late Chalcolithic Levels of Arslantepe (Malatya). *Paléorient* 3(1):231-246.

Frahm, E.
2002 *The Potential of Electron Microprobe Analysis in Provenance Studies of North American Native Copper Artifacts*. University of Minnesota.

2007 An Evaluation of Portable X-Ray Fluorescence for Artifact Sourcing in the Field: Can A Handheld Device Differentiate Anatolian Obsidian Sources? In *Geological Society of America Abstracts with Programs*, pp. 29. vol. 39, Denver, Colorado.

2009 Exploring Glass and Mineral Components of Obsidian with Electron Microprobe Analysis and the Implications for Archaeological Sourcing and Dating (or: Treating Obsidian Like the Mixture It Is). In *Geological Society of America Abstracts with Programs*, pp. 552. vol. 41, Portland, Oregon.

Fralick, P., J. Stewart and A. MacWilliams
1998 Geochemistry of West-Central Chihuahua Obsidian Nodules and Implications for the Derivation of Obsidian Artefacts. *Journal of Archaeological Science* 25(10):1023-1038.

Francaviglia, V.
1984 Characterization of Mediterranean Obsidian Sources by Classical Petrochemical Methods. *Preistoria Alpina* 20:311-332.

1985 In Search of the Ancient Arabian Obsidian Sources. *East and West* 35:373.

1988 Ancient Obsidian Sources on Pantelleria (Italy). *Journal of Archaeological Science* 15(2): 109-122.

1990 Characterization of Mediterranean Obsidian Sources by Classical Petrochemical Methods. *Preistoria Alpina* 20:311-332.

1994 L'origine des Outils en Obsidienne de Tell Magzalia, Tell Sotto, Yarim Tepe et Kül Tepe, Iraq. *Paléorient* 20(2):18-31.

1995 Discriminating Between Mediterranean Obsidians. In *Proceedings of the Egyptian-Italian Seminar on 'Geosciences and Archaeology in the Mediterranean Countries'*, pp. 381-398. Geological Survey of Egypt. vol. 70.

Francaviglia, V. and A. M. Palmieri
1998 Analisi di Ossidiane dell'Area del Habur (Giazira Settentrionale). In *Tell Barri/Kahat 2: Relazione Sulle Campagne 1980-1993 a Tell Barri/Kahat, nel Bacino del Habur (Siria)*, edited by P. E. Pecorella, pp. 335-344. CNR, Rome.

Freestone, I. C.
1982 Applications and Potential of Electron Probe Microanalysis in Technological and Provenance Investigations of Ancient Ceramics. *Archaeometry* 24(2):99-116.

French, C.
2003 *Geoarchaeology in Action: Studies in Soil Micromorphology and Landscape Evolution*. Routledge, New York.

Friedlander, G., J. W. Kennedy, E. S. Macias and J. M. Miller
1981 *Nuclear and Radiochemistry*. John Wiley and Sons, New York, NY.

Friedman, I. and W. D. Long
1976 Hydration Rate of Obsidian. *Science* 191:347-352.

Friedman, I. and R. L. Smith
1960 A New Dating Method Using Obsidian: Part I. The Development of the Technique. *American Antiquity* 25:476-493.

Friedman, I., R. L. Smith and D. Clark
1969 Obsidian Dating. In *Science in Archaeology: A Survey of Progress and Research, Revised and Expanded Edition*, edited by D. R. Brothwell and E. Higgs. Praeger Publishers, New York.

Friedman, I., R. L. Smith and W. D. Long
1966 Hydration of Natural Glass and Formation of Perlite. *Geological Society of America Bulletin* 77:323-328.

Frison, G. C.
1982 Sources of Steatite and Methods of Prehistoric Procurement and Use in Wyoming. *Plains Anthropologist* 27(98):273-286.

Froggatt, P. C.
1983 Toward a Comprehensive Upper Quaternary Tephra and Ignimbrite Stratigraphy in New Zealand Using Electron Microprobe Analysis of Glass Shards. *Quaternary Research* 19:188-200.

Gale, N. H.
1981 Mediterranean Obsidian Source Characterization by Strontium Isotope Analysis. *Archaeometry* 23:41-51.

Gallagher, J.
1974 The Preparation of Hides with Stone-Tools in South Central Ethiopia. *Journal of Ethiopian Studies* 12:177-182.

1977 Contemporary Stone Tools in Ethiopia: Implications for Archaeology. *Journal of Field Archaeology* 4(4):407-414.

Garstang, J.
1953 *Prehistoric Mersin: Yümük Tepe in Southern Turkey: The Neilson Expedition in Cilicia*. Clarendon Press, Oxford.

Gelb, I. J.
1944 *Hurrians and Subarians*. University of Chicago Press.

Georgiadis, M.
2008 The Obsidian in the Aegean Beyond Melos: An Outlook from Yali. *Oxford Journal of Archaeology* 27(2):101–117.

Gibson, M.
2000 Hamoukar: Early City in Northeastern Syria. *The Oriental Institute News and Notes* 166:1-8.

Gibson, M., J. Franke, T. Wilkinson and J. Ur
2002 First Season of Syrian-American Investigations at Hamoukar, Hasekeh Province. *Iraq* 64:45-68.

Gimeno, D.
2003 Devitrification of Natural Rhyolitic Obsidian Glasses: Petrographic and Microstructural Study (SEM+ EDS) of Recent (Lipari Island) and Ancient (Sarrabus, SE Sardinia) Samples. *Journal of Non-Crystalline Solids* 323(1-3):84-90.

Giumlia-Mair, A.
2003 Iron Age Tin in the Oriental Alps. In *The Problem of Early Tin*, edited by A. Giumlia-Mair and F. Lo Schiavo, pp. 93-108. Archaeopress, Oxford.

Giumlia-Mair, A. and F. Lo Schiavo
2003 *The Problem of Early Tin*. Archaeopress, Oxford.

Glascock, M. D.
1992 Characterization of Archaeological Ceramics at MURR by Neutron Activation Analysis and Multivariate Statistics. In *Chemical Characterization of Ceramic Pastes in Archaeology*, edited by H. Neff, pp. 11-26. Prehistory Press, Madison.

1994 New World Obsidian: Recent Investigations. In *Archaeometry of Pre-Columbian Sites and Artifacts*, edited by D. A. Scott and P. Meyers. Getty Trust Publications.

1996 A Report of the IAOS Annual Meeting. *Bulletin of the International Association for Obsidian Studies* 17:2.

Glascock, M. D.
1999 An Inter-Laboratory Comparison of Element Compositions for Two Obsidian Sources. *International Association for Obsidian Studies Bulletin* 23(Winter):13-25.

2002 Archaeology, Geology, and Geochemistry of Obsidian for Provenance Research. Geological Society of America Annual Meeting, Denver.

2009 Provenance Studies on Obsidian Artifacts from Early Neolithic Iran. In *Geological Society of America Abstracts with Programs*, pp. 553. vol. 41, Portland, Oregon.

Glascock, M. D., A. Beyin and C. E. M.
2008 X-ray Fluorescence and Neutron Activation Analysis of Obsidian from the Red Sea Coast of Eritrea. *Bulletin of International Association for Obsidian Studies* 38:6-10.

Glascock, M. D., G. Braswell and R. H. Cobean
1998 A Systematic Approach to Obsidian Source Characterization. In *Archaeological Obsidian Studies: Method and Theory*, edited by M. S. Shackley, pp. 15-65. Society for Archaeological Sciences.

Glascock, M. D., R. Kunselman and D. Wolfman
1999 Intrasource Chemical Differentiation of Obsidian in the Jemez Mountains and Taos Plateau, New Mexico. *Journal of Archaeological Science* 26(8):861-868.

Glascock, M. D., R. Speakman and H. Neff
2007 Archaeometry at the University of Missouri Research Reactor and the Provenance of Obsidian Artefacts in North America. *Archaeometry* 49(2):343-357.

Godfrey-Smith, D. I., J. Kronfeld, A. Strull and J. D'Auria
1993 Obsidian Provenancing and Magmatic Fractionation in Central Oregon. *Geoarchaeology* 8(5): 385-394.

Godfrey-Smith, D. I. and N. Haywood
1984 Obsidian Sources in Ontario Prehistory. *Ontario Archaeology* 41:29-35.

Goetze, A.
1953 An Old Babylonian Itinerary. *Journal of Cuneiform Studies* 7(2):51-72.

Goffer, Z.
2007 *Archaeological Chemistry*. 2nd ed. Chemical Analysis: A Series of Monographs on Analytical Chemistry and Its Applications. Wiley-Interscience.

Goldstein, J. I.
1967 Distribution of Germanium in the Metallic Phases of Some Iron Meteorites. *Journal of Geophysical Research* 72(18):4689-4696.

Goldstein, J. I., D. E. Newberry, P. Echlin, D. C. Joy, C. Fiori and E. Lifshin
1981 *Scanning Electron Microscopy and X-ray Microanalysis: A Text for Biologists, Materials Scientists, and Geologists*. 1st ed. Plenum Press, New York.

Goldstein, J. I., D. E. Newberry, P. Echlin, D. C. Joy, A. D. Romig, C. E. Lyman, C. Fiori and E. Lifshin
1992 *Scanning Electron Microscopy and X-ray Microanalysis: A Text for Biologists, Materials Scientists, and Geologists*. 2nd ed. Plenum Press, New York.

Goldstein, J.I., D. E. Newbury, D. C. Joy, C. E. Lyman, P. Echlin, E. Lifshin, L. Sawyer and J. R. Michael
2003 *Scanning Electron Microscopy and X-ray Microanalysis*. 3rd ed. Springer, New York.

Gonnermann, H. and M. Manga
2005 Flow Banding in Obsidian: A Record of Evolving Textural Heterogeneity During Magma Deformation. *Earth and Planetary Science Letters* 236(1-2):135-147.

Gopher, A., R. Barkai and O. Marder
1998 Cultural Contacts in the Neolithic Period: Anatolian Obsidians in the Southern Levant. *Prehistoire d'Anatolie, Genese de Deux Mondes* 85:641-650.

Gordus, A. A., W. C. Fink, M. E. Hill, J. C. Purdy and T. R. Wilcox
1967 Identification of the Geologic Origins of Archaeological Artifacts: An Automated Method of Na and Mn Neutron Activation Analysis. *Archaeometry* 10:87-96.

Gordus. A. A, J. B. Griffin and G. A. Wright
1971 Activation Analysis Identification of the Geologic Origins of Prehistoric Obsidian Artifacts. In *Science and Archaeology*, edited by R. H. Brill, pp. 222-234. The MIT Press, Cambridge.

Gordus, A. A., G. A. Wright and J. B. Griffin
1968 Obsidian Sources Characterized by Neutron-Activation Analysis. *Science* 161(3839):382-384.

Gorelick, L. and A. Gwinnett
1990 The Ancient Near Eastern Cylinder Seal as Social Emblem and Status Symbol. *Journal of Near Eastern Studies* 49(1):45-56.

Gourgaud, A.
1998 Géologie de L'obsidienne. In *L'obsidienne au Proche et Moyen-Orient: Du Volcan à l'Outil*, edited by M. C. Cauvin, A. Gourgaud, B. Gratauze, N. Arnaud, G. Poupeau, J. L. Poidevin and C. Chataigner, pp. 15-29. British Archaeological Reports. Maison de l'Orient Méditerranéen, Archaeopress, Oxford.

Gourichon, L. and D. Helmer
2004 Exploitation du Petit Gibier dans le Moyen Euphrate Syrien du XIIe au IXe Millénaires av. In *Petit Animaux et Sociétés Humaines: Du Complément Alimentaire aux Ressources Utilitaires*, edited by J. P. Brugal and J. Desse. XXIVe Rencontres Internationales d'Archéologie et d'Histoire d'Antibes. Editions APDCA, Antibes.

Gratuze, B.
1999 Obsidian Characterization by Laser Ablation ICP-MS and its Application to Prehistoric Trade in the Mediterranean and the Near East: Sources and Distribution of Obsidian within the Aegean and Anatolia. *Journal of Archaeological Science* 26(8):869-881.

Gratuze, B., J. Barrandon, K. Al Isa and M.-C. Cauvin
1993 Non-destructive Analysis of Obsidian Artefacts Using Nuclear Techniques: Investigation of Provenance of Near Eastern artefacts. *Archaeometry* 35(1):11-21.

1995 Obsidian Trade in the Near East in Neolithic and Bronze-Age Times. *PACT* 45:499-506.

Green, R. C.
1998 A 1990s Perspective on Method and Theory in Archaeological Volcanic Glass Studies. In *Archaeological Obsidian Studies: Method and Theory*, edited by M. S. Shackley, pp. 223-235. Plenum Press, New York.

Greenough, J., M. Gorton and L. Mallory-Greenough
2001 The Major- and Trace-Element Whole-Rock Fingerprints of Egyptian Basalts and the Provenance of Egyptian artefacts. *Geoarchaeology* 16(7):655-657.

Griffen, W. B.
1969 *Culture Change and Shifting Populations in Central Northern Mexico*. Anthropological Papers of the University of Arizona 13. University of Arizona Press, Tucson.

Griffin, J. B., A. A. Gordus and G. Wright
1969 Identification of the Sources of Hopewellian Obsidian in the Middle West. *American Antiquity* 34(1):1-14.

Gudeman, S.
1986 *Economics as Culture: Models and Metaphors of Livelihood*. Routledge, London.

2001 *The Anthropology of Economy: Community, Market, and Culture*. Wiley-Blackwell.

Guterbock, H. G.
1951 The Song of Ullikummi Revised Text of the Hittite Version of a Hurrian Myth. *Journal of Cuneiform Studies* 5(4):135-161.

Hall, E. T.
1971 Two Examples of the Use of Chemical Analysis in the Solution of Archaeological Problems. In *Science and Archaeology*, edited by R. H. Brill, pp. 156-164. MIT Press, Cambridge.

Hall, M.E. and H. Kimura
2002 Quantitative EDXRF Studies of Obsidian Sources in Northern Hokkaido. *Journal of Archaeological Science* 29(3):259-266.

Hall, M. E. and M. S. Shackley
1994 An Energy Dispersive X-Ray Fluorescence Study of Some Near Eastern Obsidians. *Al-Rafidan* 15:25-32.

Hallam, B. R., S. E. Warren and C. Renfrew
1976 Obsidian in the Western Mediterranean: Characterisation by Neutron Activation Analysis and Optical Emission Spectroscopy. *Proceedings of the Prehistoric Society* 42:85-110.

Hammo, N. B.
1984 Characterization of Some Iraqi Obsidian Archaeological Samples. *Baghdad: Directorate General of Antiquities* 43:239-242.

Hammond, N.
1972 Obsidian Trade Routes in the Mayan Area. *Science* 178(4065):1092-1093.

Hancock, R. G. V. and T. Carter
2010 How Reliable are Our Published Archaeometric Analyses? Effects of Analytical Techniques Through Time on the Elemental Analysis of Obsidians. *Journal of Archaeological Science* 37(2):243-250.

Hang, T., S. Wastegard, S. Veski and A. Heinsalu
2006 First Discovery of Cryptotephra in Holocene Peat Deposits of Estonia, Eastern Baltic. *Boreas* 35:644-649.

Hanson, B., J. W. Delano and D. J. Lindstrom
1996 High-Precision Analysis of Hydrous Rhyolitic Glass Inclusions in Quartz Phenocrysts Using the Electron Microprobe and INAA. *American Mineralogist* 81:1249-1262.

Harbottle, G.
1970 Neutron Activation Analysis of Sherds from Knossos and Mycenae. *Archaeometry* 12:23-34.

Harbottle, G.
1976 Activation Analysis in Archaeology. In *Radiochemistry: A Specialist Periodical Report*, edited by G. W. A. Newton, pp. 33-72. The Chemical Society, London.

1982 Chemical Characterization in Archaeology. In *Contexts for Prehistoric Exchange*, edited by J. Ericson and T. K. Earle, pp. 13-51. Academic Press, New York.

1991 The Efficiencies and Error-Rates in Euclidean Mahalanobis Searches in Hypergeometries of Archaeological Ceramic Compositions. *Archaeometry '90: Proceedings of the International Archaeometry Symposium*, pp. 413-424.

Hatch, J. W., J. W. Michels, C. M. Stevenson, B. E. Scheetz and R. A. Geidel
1990 Hopewell Obsidian Studies: Behavioral Implications of Recent Sourcing and Dating Research. *American Antiquity* 55(3):461-479.

Heizer, R. F., H. Williams and J. Graham
1965 Notes on Mesoamerican Obsidians and Their Significance in Archaeological Studies. *Contributions of the University of California Archaeological Research Facility* 1:94-103.

Heizer, R. F. and A. E. Treganza
1971 Mines and Quarries of the Indians of California. In *The California Indians*, edited by R. F. Heizer and M. Whipple, pp. 346- 359. University of California Press, Berkeley.

Henderson, B. W.
1905 *The Life and Principate of the Emperor Nero*. Methuen & Company, London.

Henderson, J.
2000 *The Science and Archaeology of Materials: An Investigation of Inorganic Materials*. Routledge, London.

Herz, N.
2001 Sourcing Lithic Artifacts by Instrumental Analysis. In *Earth Sciences and Archaeology*, edited by P. Goldberg, V. T. Holliday and C. R. Ferring, pp. 449-469. Kluwer Academic, New York.

Herz, N. and E. G. Garrison
1998 *Geological Methods for Archaeology*. Oxford University Press, Oxford.

Hess, S. C.
1997 *Rocks, Range, and Renfrew: Using Distance-decay Effects to Study Late Pre-Mazama Period Obsidian Acquisition and Mobility in Oregon and Washington*, Washington State University.

Heyden, D.
1988 Black Magic: Obsidian in Symbolism and Metaphor. In *Smoke and Mist: Mesoamerican Studies in Memory of Thelma D. Sullivan*, edited by J. K. Josserand and K. Dakin, pp. 217-236. BAR International Series. Oxford.

Hillman, G. C.
2000 Abu Hureyra 1: The Epipalaeolithic. In *Village on the Euphrates: From Foraging to Farming at Abu Hureyra*, edited by M. T. Moore, G. C. Hillman and A. J. Legge, pp. 327-398. Oxford University Press.

Hirth, K. G.
1978 Interregional Trade and the Formation of Prehistoric Gateway Communities. *American Antiquity* 43(1):35-45.

Hirth, K. G.
2006 *Obsidian Craft Production in Ancient Central Mexico: Archaeological Research at Xochicalco*. The University of Utah Press, Salt Lake City.

Hirth, K. G. and B. Andrews
2002 *Pathways to Prismatic Blades: A Study in Mesoamerican Obsidian Core-Blade Technology*. Mongraphs 45. The Cotsen Institute of Archaeology, University of California-Los Angeles.

Hodder, I.
1974 Regression Analysis of Some Trade and Marketing Patterns. *World Archaeology* 6:172-189.

1982 The Social Context of Production and Exchange. In *Contexts for Prehistoric Exchange*, edited by J. E. Ericson and T. K. Earle, pp. 173-211. Academic Press, New York.

Hodder, I. and C. Orton
1976 *Spatial Analysis in Archaeology*. New Studies in Archaeology. Cambridge University Press.

Hodges, R.
1982 The Evolution of Gateway Communities. In *Ranking, Resource, and Exchange: Aspects of the Archaeology of Early European Society*, edited by C. Renfrew and S. Shennan, pp. 117-123. Cambridge University Press.

Hodgson, S. F.
2007 Obsidian: Sacred Glass from the California Sky. In *Myth and Geology*, edited by L. Piccardi and W. B. Masse, pp. 295-313. Special Publications. Geological Society, London.

Hoffner, H. A.
1990 *Hurrians Myths*. Writings from the Ancient World 2. Scholars Press, Atlanta.

Hole, F.
2009 Drivers of Unsustainable Land Use in the Semi-Arid Khabur River Basin, Syria. *Geographical Research* 47(1):4-14.

Hughes, M.
1991 Tracing to Source. In *Science and the Past*, edited by S. Bowman, pp. 99-116. British Museum Press.

Hughes, R. E.
1984 *Obsidian Studies in the Great Basin.* Contributions of the University of California Archaeological Research Facility. vol. 45. University of California.

1988 The Coso Volcanic Field Reexamined: Implications for Obsidian Sourcing and Hydration Dating Research. *Geoarchaeology* 3(4):253-265.

1992 Another Look at Hopewell Obsidian Studies. *American Antiquity* 57(3):515-523.

1994 Intrasource Chemical Variability of Artefact-Quality Obsidians from the Casa Diablo Area, California. *Journal of Archaeological Science* 21(2):263-271.

1998 On Reliability, Validity, and Scale in Obsidian Sourcing Research. In *Unit Issues in Archaeology: Measuring Time, Space, and Material*, edited by A. F. Ramenofsky and A. Steffen, pp. 103-114. University of Utah Press.

Hughes, R. E. and R. L. Smith
1993 Archaeology, Geology, and Geochemistry of Obsidian Provenance Studies. In *Effects of Scale on Archaeological and Geological Perspectives*, edited by J. K. Stein and A. R. Linse, pp. 79-91. GSA Special Paper. vol. 283. Geological Society of America, Boulder, Colorado.

Hunt, J. and P. Hill
2001 Tephrachronological Implications of Beam Size: Sample-Size Effects in Electron Microprobe Analysis of Glass Shards. *Journal of Quaternary Science* 16(2):105-117.

Huntley, D. J. and D. C. Bailey
1978 Obsidian Source Identification by Thermoluminescence. *Archaeometry* 20:159-170.

Hurcombe, L. M.
1992 *Use Wear Analysis and Obsidian: Theory, Experiments, and Results*. Sheffield Archaeological Monographs 4. J.R. Collis Publications.

IAEA (International Atomic Energy Agency)
2003 *Nuclear Analytical Techniques in Archaeological Investigations*. Technical Reports Series, International Atomic Energy Agency.

Iddings, J. P.
1886 Obsidian Cliff, Yellowstone National Park. *United States Geological Survey, Seventh Annual Report of the Director of the U.S. Geological Survey.* Washington, D.C.

Illingworth, N. J. J.
1988 Inscriptions from Tell Brak 1986. *Iraq* 50:87-108.

Inizan, M.-L., M. Reduron-Ballinger, H. Roche and J. Tixier
1999 *Technology and Terminology of Knapped Stone*. Préhistoire de la Pierre Taillée. Cercle de Recherches et d'Etudes Prehist, Nanterre.

Innocenti, F., P. Manetti, R. Mazzuoli, G. Pasquarè and L. Villari
1982 Anatolia and North-Western Iran. In *Andesites: Orogenic Andesites and Related Rocks*, edited by R. S. Thorpe, pp. 327-349. John Wiley & Sons.

Izuho, M. and H. Sato
2007 Archaeological Obsidian Studies in Hokkaido, Japan: Retrospect and Prospects. *Indo-Pacific Prehistory Association Bulletin* 27:114-121.

James, M. A., J. Bailey and J. M. D'Auria
1996 A Volcanic Glass Library for the Pacific Northwest: Problems and Prospects. *Canadian Journal of Archaeology* 20:93-122.

Jarosewich, E., J. A. Nelen and J. A. Norberg
1980 Reference Samples for Electron Microprobe Analysis. *Geostandards Newsletter* 4:43-47.

Jenkins, R.
1999 *X-Ray Fluorescence Spectrometry*. 2nd ed. Chemical Analysis: A Series of Monographs on Analytical Chemistry and Its Applications. Wiley-Interscience.

Jezek, P. and D. Noble
1978 Natural Hydration and Ion Exchange of Obsidian: An Electron Microprobe Study. *American Mineralogist* 63(3-4):266-273.

Johnson, C., J. Feinberg and E. Frahm
2009 Comparing Magnetic Properties and Geochemical Measurements of Obsidian. In *Geological Society of America Abstracts with Programs*, pp. 679. vol. 41, Portland.

Johnson, R. A. and F. H. Stross
1965 Laboratory-Scale Instrumental Neutron Activation for Archaeological Analysis. *American Antiquity* 30(3):345-347.

Jolliffe, I. T.
1986 *Principal Component Analysis*. Springer-Verlag, New York.

Jones, M., P. J. Sheppard and D. G. Sutton
1997 Soil Temperature and Obsidian Hydration Dating: A Clarification of Variables Affecting Accuracy. *Journal of Archaeological Science* 24:505-516.

Jones, M., D. G. Sutton, G. Jones and C. McLeod
1995 Measuring Soil Temperature for Obsidian Hydration Dating in Northern New Zealand. *Archaeology in New Zealand* 38:9-16.

Kammenhuber, A.
1977 Die Arier im Vorderen und die Historischen Wohnsitze der Hurriter. *Orientalia* 46:129-144.

Kamp, K. A.
1998 *Life in the Pueblo: Understanding the Past Through Archaeology*. Waveland Press.

Kaplan, A.
1964 *The Conduct of Inquiry: Methodology for Behavioral Science*. Chandler Publishing Company, San Francisco.

Karaolu, Ö., Y. Özdemr, A. Ü. Tolluolu, M. Karabiyikolu and O. K. J.-L. Froger
2005 Stratigraphy of the Volcanic Products Around Nemrut Caldera: Implications for Reconstruction of the Caldera Formation. *Turkish Journal of Earth Sciences* 14:123-143.

Kasper, K.
2005 *Obsidian Sources in Transcaucasia and Their Exploitation in the Bronze Age*. TU Bergakademie Freiberg website.

Kasper, K., E. Pernicka and P. Kohl
2004 Neutronenaktivierungsanalyse zur Herkunftsbestimmung Archäologischer Obsidianartefakte aus Aserbaidschan. In *Archäometrie und Denkmalpflege 2004, Jahrestagung in den Reiss-Engelhorn Museen Mannheim, 6-9 Oktober 2004*.

Kayani, P. and G. McDonnell
1996 An Assessment of Back-Scattered Electron Petrography as a Method for Distinguishing Mediterranean Obsidians. *Archaeometry* 38(1):43-58.

Keisch, B.
1972 *The Atomic Fingerprint: Neutron Activation Analysis*. USERDA-Technical Information Center, Washington, DC.

Keller, J., E. Djerbashian, E. Pernicka, S. Karapetian and V. Nasedkin
1996 Armenian and Caucasian Obsidian Occurrences as Sources for the Neolithic Trade: Volcanological Setting and Chemical Characteristics. In *Archaeometry 94: The Proceedings of the 29th International Symposium on Archaeometry; Ankara, 9-14 May 1994*, pp. 69-86.

Keller, J. and C. Seifried
1990 The Present Status of Obsidian Source Identification in Anatolia and the Near East. *PACT 25: Volcanology and Archaeology, Proceedings of the European Workshops of Ravello* 25:57-87.

Kelly, J. E.
2000 Cahokia and its Role as a Gateway Center in Interregional Exchange. In *Cahokia and the Hinterlands: Middle Mississippian Cultures of the Midwest*, edited by T. E. Emerson and R. B. Lewis, pp. 61-82. University of Illinois Press.

Kelly-Buccellati, M.
1988 The High Mound: Introduction and Surface Collection. In *Mozan 1: The Soundings of the First Two Seasons*, edited by G. Buccellati and M. Kelly-Buccellati. Undena Publications.

1989 A New Third Millennium Sculpture from Mozan. In *Essays in Ancient Civilization Presented to Helene Kantor*, edited by A. Leonard and B. Williams, pp. 149-154. The Oriental Institute.

1990 Trade in Metals in the Third Millennium: Northeastern Syria and Eastern Anatolia. In *Resurrecting the Past: A Joint Tribute to Adnan Bounni*, edited by P. Matthiae, M. Van Loon and H. Weiss, pp. 117-130. Nederlands Instituut voor het Nabije Oosten.

1996 Nuzi Viewed from Urkesh, Urkesh Viewed from Nuzi: Stock Elements and Framing Devices in Northern Syro-Mesopotamia. In *Studies on the Civilization and Culture of Nuzi and the Hurrians*, edited by D.I. Owen and G. Wilhelm, pp. 247-268. vol. 8. CDL Press, Bethesda.

1998 The Workshops of Urkesh. In *Urkesh and the Hurrians: A Volume in Honor of Lloyd Cotsen*, pp. 35-50. Urkesh/Mozan Studies. vol. 3. Undena Publications.

2005 Urkesh and the North: Recent Discoveries. In *Studies on the Civilization and Culture of Nuzi and the Hurrians*, edited by D. I. Owen and G. Wilhelm, pp. 29-40. CDL Press, Bethesda.

Kempe, D. R. C. and J. A. Templeman
1983 Techniques. In *The Petrology of Archaeological Artifacts*, edited by D. R. C. Kempe and A. P. Harvey, pp. 26-52. Clarendon Press, Oxford.

Khademi, F., S. C. Phillips and M. Safari
2007 WDXRF Spectroscopy of Obsidian Tools in the Northwest of Iran. *International Association for Obsidian Studies Bulletin* 37:3-6.

Khalidi, L.
2009 Holocene Obsidian Exchange in the Red Sea Region. In *The Evolution of Human Populations in Arabia: Paleoenvironments, Prehistory, and Genetics*, edited by M. D. Petraglia and J. I. Rose, pp. 279-291. Springer.

Khalidi, L., B. Gratuze and S. Boucetta
2009 Provenance of Obsidian Excavated from Late Chalcolithic Levels at the Sites of Tell Hamoukar and Tell Brak, Syria. *Archaeometry* 51(6): 879-893.

Kilikoglou, V., Y. Bassiakos, R. Doonan and J. Stratis
1997 NAA and ICP Analysis of Obsidian from Central Europe and the Aegean: Source Characterisation and Provenance Determination. *Journal of Radioanalytical and Nuclear Chemistry* 216(1):87-93.

Kilikoglou, V., Y. Bassiakos, A. Grimanis, K. Souvatzis, A. Pilali-Papasteriou, A. Papanthimou-Papaefthimiou
1996 Carpathian Obsidian in Macedonia, Greece. *Journal of Archaeological Science* 23:343-349.

Kim, J., D. Kim, M. Youn, C. Yun, G. Park, H. Woo, M.-Y. Hong and G. Lee
2007 PIXE Provenancing of Obsidian Artefacts from Paleolithic Sites in Korea. *Indo-Pacific Prehistory Association Bulletin* 27:122-128.

Kingery, W. D.
1996 *Learning from Things: Method and Theory of Material Culture Studies*. Smithsonian Institution Press, Washington.

Kipfer, B. A.
2000 *Encyclopedic Dictionary of Archaeology*. Springer.

Kloess, G., S. Schorr, G. Kloess and M. Tovar
2006 *Study of Crystalline Phases (Microlites) in Natural Obsidian*. BENC Experimental Report.

Knoke, D., G. W. Bornstedt and A. P. Mee
2002 *Statistics for Social Data Analysis*. 4th ed. Thomson Wadsworth, Belmont, California.

Kohl, P.
1978 The Balance of Trade in Southwestern Asia in the Mid-Third Millennium BC. *Current Anthropology* 19(3):463.

Kolars, J. F. and W. A. Mitchell
1991 *The Euphrates River and the Southeast Anatolia Development Project*. Southern Illinois University Press, Illinois.

Kosakowsky, L., F. Belli and H. Neff
1999 Late Preclassic Ceramic Industries of Pacific Guatemala and El Salvador: The Pacific Coast as Core, Not Periphery. *Journal of Field Archaeology* 26(4):377-390.

Kramer, C.
1977 Pots and People. In *Mountains and Lowlands: Essays in the Archaeology of Greater Mesopotamia*, edited by L. D. Levine and T. C. Young, pp. 91-112. Bibliotheca Mesopotamica. vol. 7. Undena Publications.

Kratcher, A.
2001 Standard Choice for the Electron Microprobe: Making the Right Compromise. *Microscopy Today,* September 2001:22.

Kratochvil, B. and J. K. Taylor
1981 Sampling for Chemical Analysis. *Analytical Chemistry* 53:924-938.

Kroeber, A. L.
1940 Stimulus Diffusion. *American Anthropologist* 42:1-20.

Kruger, P.
1971 *Principles of Activation Analysis*. Wiley Interscience, New York, NY.

Kunselman, R.
1994 Prehistoric Obsidian Utilization in the Central Rocky Mountains: the Lookingbill Site 48FR308. *The Wyoming Archaeologist* 40:1-17.

Kurt, A.
1995 *The Ancient Near East c. 3000-330 BC, Volume One*. Routledge History of the Ancient World. Routledge, London.

Kuzmin, Y., M. D. Glascock and H. Sato
2002 Sources of Archaeological Obsidian on Sakhalin Island (Russian Far East). *Journal of Archaeological Science* 29(7):741-749.

Kuzmin, Y. V.
2006 Recent Studies of Obsidian Exchange Networks in Prehistoric Northeast Asia. In *Archaeology in Northeast Asia: On the Pathway to Bering Strait*, edited by D. E. Dumond and R. L. Bland, pp. 61-71. University of Oregon, Eugene.

Kuzmin, Y. V. and M. D. Glascock
1997 Two Islands in the Ocean: Prehistoric Obsidian Exchange between Sakhalin and Hokkaido, Northeast Asia. *Journal of Island and Coastal Archaeology* 2:99-120.

Kuzmin, Y. V., A. V. Tabarev, V. L. Popov, M. D. Glascock and M. S. Shackley
1999 Geochemical Source Analysis of Archaeological Obsidian in Primorye (Russian Far East). *Current Research in the Pleistocene* 16:97-99.

Kuznar, L. A.
1997 *Reclaiming a Scientific Anthropology*. AltaMira Press.

Kyle, P. R. and P. A. Jezek
1978 Compositions of Three Tephra Layers from the Byrd Station Ice Core, Antarctica. *Journal of Volcanology and Geothermal Research* 4:225-232.

Laidley, R. A.
1968 X-Ray Fluorescence of Rock Samples as Applied to Geological Problems. *Applied Spectroscopy* 22(5):420-422.

Laidley, R.A. and D. McKay
1971 Geochemical Examination of Obsidians from Newberry Caldera, Oregon. *Contributions to Mineralogy and Petrology* 30(4):336-342.

Landsberger, B.
1934 *Die Fauna des Alten Mesopotamien nach der 14. Tafel der Serie Hara-ra = Hubullu.* Abhandlungen Philologisch-Historische Klasse Sächsische Akademie der Wissenschaften.

Landy, D.
1965 *Tropical Childhood: Cultural Transmission and Learning in a Rural Puerto Rican Village*. Researches in the Social, Cultural and Behavioral Sciences. Harper & Row, New York.

Lazzari, M.
2005 The Texture of Things: Objects, People and Social Spaces in NW Argentina. In *Archaeologies of Materiality*, edited by L. Meskell, pp. 126-161. Blackwell, Oxford.

2006 *Traveling Things and the Production of Social Spaces: An Archaeological Study of Circulation and Value in North Western Argentina*, Columbia University.

Lazzari, M., L. P. Domingorena, M. C. Scattolin, L. Cecil, M. D. Glascock and R. J. Speakman
2009 Ancient Social Landscapes of Northwestern Argentina: Preliminary Results of an Integrated Approach to Obsidian and Ceramic Provenance. *Journal of Archaeological Science* 36(9): 1955-1964.

Le Bourdonnec, F.-X.
2008 *Towards A Materiality of Pilgrimage?: Characterizing Obsidian from Neolithic Göbekli Tepe (Urfa Region, SE Turkey)*. Report on the Project EU-ARTECH 07.

Le Bourdonnec, F.-X., J.-M. Bontempi, N. Marini, S. Mazet, P. F. Neuville, G. Poupeau and J. Sicurani
2010 SEM-EDS Characterization of Western Mediterranean Obsidians and the Neolithic Site of A Fuata (Corsica). *Journal of Archaeological Science* 37(1):92-106.

Le Bourdonnec, F.-X., S. Delerue, S. Dubernet, P. Moretto, T. Calligaro, J. Dran and G. Poupeau
2005a PIXE Characterization of Western Mediterranean and Anatolian Obsidians and Neolithic Provenance Studies. *Nuclear Instruments and Methods in Physics Research B* 240(1-2): 595-599.

Le Bourdonnec, F.-X., C. Lugliè, S. Dubernet, M. Bohn and G. Poupeau
2005b Monte Arci (Sardinia) Obsidians: New Geochemical Data from Electron Microprobe and Ion Beam Analysis. In *Le vie dell'Ossidiana nel Mediterraneo ed in Europa*, pp. 129-140.

Le Bourdonnec, F.-X., G. Poupeau and C. Luglie
2006 SEM–EDS Analysis of Western Mediterranean Obsidians: A New Tool for Neolithic Provenance Studies. *Comptes Rendus-Géoscience* 338(16):1150-1157.

2010 The Monte Arci (Sardinia, Western Mediterranean) Obsidians: Characterization by Multivariate Analysis from SEM-EDS, EMP-WDS and PIXE Elemental Compositions. In *L'ossidiana del Monte Arci nel Mediterraneo. Nuovi Apporti Sulla Diffusione, sui Sistemi di Produzione e Sulla Loro Cronologia, Atti del 5° Convegno Internazionale (Pau, Italia, 27-29 Giugno 2008)*, pp. 13-28.

Leach, B. F. and G. E. Hamel
1984 The Influence of Archaeological Soil Temperatures on Obsidian Dating in New Zealand. *New Zealand Journal of Science* 27:399-408.

Leakey, M. D.
1971 *Olduvai Gorge. Volume 3. Excavations in Beds I and II, 1960-1963*. Cambridge University Press, Cambridge.

Lees, G. J. and R. A. Roach
1993 A Preliminary Volcanological and Petrochemical Survey of the Late Precambrian Calc-Alkaline Volcanic Succession of Eastern Jersey, Channel Islands. *Proceedings of the Ussher Society* 8:145-150.

Legge, A. J. and P. A. Rowley-Conway
1986 The Beaver (*Castor fiber L.*) in the Tigris-Euphrates Basin. *Journal of Archaeological Science* 13:469-476.

Lewenstein, S.
1981 Mesoamerican Obsidian Blades: An Experimental Approach to Function. *Journal of Field Archaeology* 8(2):175-188.

Lifshin, E. and R. Gauvin
2001 Minimizing Errors in Electron Microprobe Analysis. *Microscopy & Microanalysis* 7(2): 168-177.

Long, J. V. P.
1995 Microanalysis from 1950 to the 1990s. In *Microprobe Techniques in the Earth Sciences*, edited by P. J. Potts, J. F. Bowles, S. J. Reed and R. Cave, pp. 1-48. The Mineralogical Society Series. Chapman & Hall.

Longworth, G. and S. E. Warren
1979 The Application of Mössbauer Spectroscopy to the Characterisation of Western Mediterranean Obsidian. *Journal of Archaeological Science* 61:179-193.

Lugliè, C., F. Le Bourdonnec, G. Poupeau, E. Atzeni, S. Dubernet, P. Moretto and L. Serani
2007 Early Neolithic Obsidians in Sardinia (Western Mediterranean): The Su Carroppu Case. *Journal of Archaeological Science* 34(3):428-439.

Lugliè, C., F. Le Bourdonnec, G. Poupeau, C. Congia, P. Moretto, T. Calligaro, I. Sanna and S. Dubernet
2008 Obsidians in the Rio Saboccu (Sardinia, Italy) Campsite: Provenance, Reduction and Relations with the Wider Early Neolithic Tyrrhenian Area. *Comptes Rendus-Palevol* 7(4): 249-258.

Lynch, H. F. B.
1901 *Armenia, Travels and Studies: Volume 2. The Turkish Provinces*. Longmans, Green, and Company, London.

Lynch, J. and Y. L. Wolfe
1997 "Old" Scalpel for New Faces. *Prevention* 49(12):128.

Ma, C., J. Gresh, G. Rossman, G. Ulmer and E. Vicenzi
2001 Micro-Analytical Study of the Optical Properties of Rainbow and Sheen Obsidians. *Canadian Mineralogist* 39(1):57-71

Ma, C., G. Rossman and J. Miller
2007 The Origin of Color in "Fire" Obsidian. *Canadian Mineralogist* 45(3):551-557

Madrigal, L.
1998 *Statistics for Anthropology*. Cambridge University Press.

Maeda, O.
2003 Prehistoric Obsidian Distribution in the Rouj Basin. In *Archaeology of the Rouj Basin - Volume 1: Regional Study of the Transition from Village to City in Northwest Syria*, pp. 167-184. vol. 1.

Mahdavi, A. and C. Bovington
1972 Neutron Activation Analysis of Some Obsidian Samples from Geological and Archaeological Sites. *Iran* 10:148-151.

Mallowan, M. E. L.
1947 Excavations at Brak and Chagar Bazar. *Iraq* 9:1-259.

Manga, M.
1998 Orientation Distribution of Microlites in Obsidian. *Journal of Volcanology and Geothermal Research* 86(1-4):107-115.

Manga, M., J. Castro, K. V. Cashman and M. Loewenberg
1998 Rheology of Bubble-Bearing Magmas. *Journal of Volcanology and Geothermal Research* 87:15-28.

Mark, H. and J. Workman
2003 *Statistics in Spectroscopy*. 2nd ed. Elsevier Academic Press.

Martinetto, P.
1996 *Sur la Provenance de l'Obsidienne de Quelques Sites Archdologiques des IXe-VIIIe Milldnaires B.P. de la Haute Vallde de l'Euphrate: Une Approche par ICP/AES-MS*. Memoire de DESS, Universite de Bordeaux III.

Matthews, D. and J. Eidem
1993 Tell Brak and Nagar. *Iraq* 55:201-207.

Matthews, R. and H. Fazeli
2004 Copper and Complexity: Iran and Mesopotamia in the Fourth Millennium BC. *Iran* 42:61-75.

Mazer, J. J., J. K. Bates, C. M. Stevenson and J. P. Bradley
1992 Obsidians and Tektites: Natural Analogues for Water Diffusion in Nuclear Waste Glass. *Materials Research Society Symposium Proceedings* 257:513-520.

McCorriston, J.
1992 The Halaf Environment and Human Activities in the Khabur Drainage, Syria. *Journal of Field Archaeology* 19(3):315-333.

McCorriston, J. and S. Weisberg
2002 Spatial and Temporal Variation in Mesopotamian Agricultural Practices in the Khabur Basin, Syrian Jazira. *Journal of Archaeological Science* 29(5):485-498.

McDaniels, J., S. E. Warren and A. M. T. Moore
1980 New Investigations of Obsidian from Some Neolithic Sites in the Near East. In *Proceedings of the 16th International Symposium of Archaeometry and Archaeological Prospection*, pp. 1-19.

Mehringer, P. J., J. C. Sheppard and F. F. Foit
1984 The Age of Glacier Peak Tephra in West-Central Montana. *Quaternary Research* 21:36-41.

Mellaart, J.
1970 *Excavations at Hacılar*. Edinburgh University Press.

Mellars, P.
1996 *The Neanderthal Legacy: An Archaeological Perspective from Western Europe*. Princeton University Press, Princeton, New Jersey.

Merpert, N. Y. and R. M. Munchaev
1993 Yarimtepe I. In *Early Stages in the Evolution of Mesopotamian Civilization*, edited by N. Yoffee and J. J. Clark, pp. 73-114. University of Arizona Press, Tucson.

Merrick, H. and F. Brown
1984 Rapid Chemical Characterization of Obsidian Artifacts by Electron Microprobe Analysis. *Archaeometry* 26(2):230-236.

Merrick, H., F. Brown and W. Nash
1994 Use and Movement of Obsidian in the Early and Middle Stone Ages of Kenya and Northern Tanzania. In *Society, Culture, and Technology in Africa*, edited by S. T. Childs, pp. 29–44. Masca Research Papers in Science and Archaeology.

Michels, J. W.
1971 The Colonial Obsidian Industry of the Valley of Mexico. In *Science and Archaeology*, edited by R. H. Brill, pp. 251-271. The MIT Press, Cambridge.

1982 Bulk Element Composition Versus Trace Element Composition in the Reconstruction of an Obsidian Source System. *Journal of Archaeological Science* 9:113-123.

Mignon, M. R.
1993 *Dictionary of Concepts in Archaeology*. Greenwood Press.

Miller, J. M., R. J. Williams and G. D. Farquhar
2001 Carbon Isotope Discrimination by a Sequence of Eucalyptus Species Along a Subcontinental Rainfall Gradient in Australia. *Functional Ecology* 15:222-232.

Millet, A. and H. Catling
1966 Composition and Provenance: A Challenge. *Archaeometry* 9:92-97.

Moens, L., A. v. Bohlen and P. Vandenabeele
2000 X-ray Fluorescence. In *Modern Analytical Methods in Art and Archaeology* edited by E. Ciliberto and G. Spoto, pp. 55-80. Wiley-Interscience.

Moffat, D. and S. J. Butler
1986 Rare Earth Element Distribution Patterns in Shetland Steatite: Consequences for Artefact Provenancing Studies. *Archaeometry* 28:101–115.

Moholy-Nagy, H.
2003 Source Attribution and the Utilization of Obsidian in the Maya Area. *Latin American Antiquity* 14(3):301-310.

Moholy-Nagy, H. and F. W. Nelson
1990 New Data on Sources of Obsidian Artifacts from Tikal, Gatemala. *Ancient Mesoamerica* 1:71-80.

Molyneaux, B. L.
2002 Exploring the Landscapes of Long-Distance Exchange: Evidence from Obsidian Cliffs and Devils Tower, Wyoming. In *Geochemical Evidence for Long-Distance Exchange*, edited by M. D. Glascock, pp. 133-152. Bergin and Garvey, Westport, Connecticut.

Moorey, P. R. S.
1994 *Ancient Mesopotamian Materials and Industries: The Archaeological Evidence*. Clarendon Press, Oxford.

Morgan, L. E., P. R. Renne, R. E. Taylor and G. Woldegabriel
2009 Archaeological Age Constraints from Extrusion Ages of Obsidian: Examples from the Middle Awash, Ethiopia. *Quaternary Geochronology* 4(3):193-203.

Mortensen, P.
1973 A Sequence of Samarran Flint and Obsidian Tools from Choga Mami. *Iraq* 35(1):37-55.

Moyer, A.
2008a Mirrors as Artifacts and Agents in Mortuary Contexts. 73rd Annual Meeting of the Society for American Archaeology, Vancouver, British Columbia.

2008b Reflected Glory: Mirrors, Power, and Prestige in Iron Age Eurasia. The 41st Annual Chacmool Conference. Chacmool Archaeological Association and the Department of Archaeology, University of Calgary.

Mueller, J. W.
1975 *Sampling in Archaeology*. University of Arizona Press, Tucson.

Muhly, J. D.
1979 The Evidence for Sources of and Trade in Bronze Age Tin. In *The Search for Ancient Tin*, edited by A. D. Franklin, J. S. Olin and T. A. Wertime, pp. 43-48. A seminar organized by Theodore A. Wertime and held at the Smithsonian Institution and the National Bureau of Standards, Washington D.C. March 14-15, 1977.

1985 Sources of Tin and the Beginnings of Bronze Metallurgy. *Journal of American Archaeology* 89(2):275-291.

Muir, I., F. Hivernel and J. Scoon
1976 Obsidians from the Melka-Konture Prehistoric Site, Ethiopia. *Journal of Archaeological Science* 3:211-217.

Murilloa, G., R. Policroniadesa, D. Tenorioa, B. Méndeza, E. Andradeb, J. C. Pinedab, E. P. Zavalab and J. L. Torres
1998 Analysis of Mexican Obsidians by IBA Techniques. *Nuclear Instruments and Methods in Physics Research Section B: Beam Interactions with Materials and Atoms* 136-138:888-892.

Mysen, B. and P. Richet
2005 *Silicate Glasses and Melts: Properties and Structure*. Developments in Geochemistry. Elsevier, Amsterdam.

Nance, J. D.
1987 Reliability, Validity, and Quantitative Methods in Archaeology. In *Quantitative Research in Archaeology: Progress and Prospects*, edited by M. S. Aldenderfer, pp. 244-293. Sage Publications, Newberry Park.

Nandris, J.
1975 A Re-Consideration of the South-East European Sources of Archaeological Obsidian. *Bulletin of the Institute of Archaeology* 12:71-94.

Nazaroff, A. J., K. M. Prufer and B. L. Drake
2010 Assessing the Applicability of Portable X-ray Fluorescence Spectrometry for Obsidian Provenance Research in the Maya Lowlands. *Journal of Archaeological Science* 37:885-895.

Neff, H.
1998 Units in Chemistry-Based Ceramic Provenance Investigations. In *Unit Issues in Archaeology: Measuring Time, Space, and Material*, edited by A. F. Ramenofsky and A. Steffen, pp. 115-127. University of Utah Press.

2000 Neutron Activation Analysis for Provenance Determination in Archaeology. In *Modern Analytical Methods in Art and Archaeology*, edited by E. Ciliberto and G. Spoto, pp. 81-134, Wiley-Interscience.

Neff, H., R. Bishop and E. Sayre
1988 A Simulation Approach to the Problem of Tempering in Compositional Studies of Archaeological Ceramics. *Journal of Archaeological Science* 15:159–172.

1989 More Observations on the Problem of Tempering in Compositional Studies of Archaeological Ceramics. *Journal of Archaeological Science* 16:57-69.

Negash, A., M. Alene, F. Brown, B. Nash and M. Shackley
2007 Geochemical Sources for the Terminal Pleistocene/Early Holocene Obsidian Artifacts of the Site of Beseka, Central Ethiopia. *Journal of Archaeological Science* 34(8):1205-1210.

Negash, A. and M. Shackley
2006 Geochemical Provenance of Obsidian Artefacts from the MSA Site of Porc Epic, Ethiopia. *Archaeometry* 48(1):1-12.

Negash, A., M. Steven Shackley and M. Alene
2006 Source Provenance of Obsidian Artifacts from the Early Stone Age (ESA) Site of Melka Konture, Ethiopia. *Journal of Archaeological Science* 33(12):1647-1650.

Nelson, D. E., J. M. D'Auria and R. B. Bennett
1975 Characterization of Pacific Northwest Coast Obsidian by X-ray Fluorescence Analysis. *Archaeometry* 17:85-97.

Nelson, F., K. Nielson, N. Mangelson, M. Hill and R. Matheny
1977 Preliminary Studies of the Trace Element Composition of Obsidian Artifacts from Northern Campeche, Mexico. *American Antiquity* 42(2):209-225.

Nelson, F. and B. Voorhies
1980 Trace Element Analysis of Obsidian Artifacts from Three Shell Midden Sites in the Littoral Zone, Chiapas, Mexico. *American Antiquity* 45(3):540-550.

Neri, L. A. M.
2007 Philippine Obsidian and its Archaeological Applications. *Bulletin of the Indo-Pacific Prehistory Association* 27:154-162.

Neri, L. A. M., J. R. Ferguson and M. D. Glascock
2009 Obsidian Sourcing in Philippine Archaeology. In *Geological Society of America Abstracts with Programs*, pp. 553. vol. 41, Portland.

Nicolaysen, K. P.
2009 Provenance of Obsidian Fragments Recovered from Adak Island, Central Aleutian Islands: Evidence for Long-Distance Transport. In *Geological Society of America Abstracts with Programs*, pp. 553. vol. 41, Portland.

Nielsen, C. H. and H. Sigurdsson
1981 Quantitative Methods of Electron Microprobe Analysis of Sodium in Natural and Synthetic Glasses. *American Mineralogist* 66:547-552.

Nielson, K. K., N. W. Hill, N. F. Mangelson and F. W. Nelson
1976 Elemental Analysis of Obsidian Artefacts by Proton Particle-Induced X-Ray Emission. *Analytical Chemistry* 48:1947-1953.

Niknami, K. A., A. C. Amirkhiz and M. D. Glascock
2010 Provenance Studies of Chalcolithic Obsidian Artefacts from Near Lake Urmia, Northwestern Iran Using WDXRF Analysis. *Archaeometry* 52(1):19-30.

Nishiaki, Y.
1990 Corner-Thinned Blades: A New Obsidian Tool Type from a Pottery Neolithic Mound in the Khabur Basin, Syria. *Bulletin of the American Schools of Oriental Research* 280:5-14.

1993 Anatolian Obsidian and the Neolithic Obsidian Industries of North Syria: A Preliminary Review. In *Essays on Anatolian Archaeology*, edited by T. Mikasa, pp. 140-160. Verlag.

2000 *Lithic Technology of Neolithic Syria*. BAR International Series 840.

2003 Chronological Developments of the Chalcolithic Flaked Stone Industries at Tell Kosak Shamali. In *Tell Kosak Shamali: The Archaeological Investigations on the Upper Euphrates, Syria, Vol. 2. Chalcolithic Technology and Subsistence*, edited by Y. Nishiaki and T. Matsutani, pp. 15-106. Oxbow Books.

Norris, S. M.
2002 *Political Economy of the Aztec Empire: A Regional Analysis of Obsidian Craft Production in the Provinces of Huaxtepec and Cuauhnahuac, Morelos, Mexico*, Harvard University.

NPS (National Park Service)
2003 Criteria for Parklands, National Park Service, U.S. Department of the Interior.

Nunnally, J. C.
1967 *Psychometric Theory*. McGraw Hill, New York.

Oates, D. and J. Oates
1993 Excavations at Tell Brak 1992-93. *Iraq* 55:155-199.

Oates, D., J. Oates and H. McDonald
2001 *Excavations at Tell Brak 2: Nagar in the Third Millennium BC*. McDonald Institute Monograph, Cambridge.

Oates, J.
1987 A Note on 'Ubaid and Mitanni Pottery from Tell Brak. *Iraq* 49:193-198.

Oddone, M., G. Bigazzi, Y. Keheyan and S. Meloni
2000 Characterisation of Armenian Obsidians: Implications for Raw Material Supply for Prehistoric Artifacts. *Journal of Radioanaytical and Nuclear Chemistry* 243(3):673-682.

Oddone, M., C. De Gregorio, S. Mazzoni and G. Bigazzi
2003 Provenance Studies of Obsidian Artefacts from the Tell Afis Site (Syria) Using the Fission-Track Dating Method. Revue d'Archéométrie conference.

Oddone, M., Z. Yeğingil, G. Bigazzi, T. Ercan and M. Özdogan
1997 Chemical Characterisations of Anatolian Obsidians by Instrumental and Epithermal Neutron Activation Analysis. *Journal of Radioanalytical and Nuclear Chemistry* 224(1):27-38.

Ogburn, D., S. Connell and C. Gifford
2008 Provisioning of the Inka Army in Wartime: Obsidian Procurement in Pambamarca, Ecuador. *Journal of Archaeological Science* 36:740-751.

Ohring, M.
1995 *Engineering Materials Science*. Academic Press.

Okuno, M., H. Iwatsuki and T. Matsumoto
1996 Structural Analysis of an Obsidian by X-ray Diffraction Method. *European Journal of Mineralogy* 8(6):1257-1264.

Olanca, K.
1994 *Géochimie des Laves Quaternaires de Cappadoce (Turquie): Les Appareils Monogeniques*, Blaise Pascal.

Olin, J. S. and E. V. Sayre
1971 Compositional Categories of Some English and American Pottery of the American Colonial Period. In *Science and Archaeology*, edited by R. H. Brill, pp. 196-209. The MIT Press, Cambridge.

Otte, M. and Y. Besnus
1992 Analyses Chimiques Multi-Elementaires d'Objets Archaeologiques en Obsidienne de Hassek Hoyuk. *Istanbuler Forschungen* 38:132-134.

Özdemir, Y., Ö. Karaoğlu, A. Tolluoğlu and N. Güleç
2006 Volcanostratigraphy and Petrogenesis of the Nemrut Stratovolcano (East Anatolian High Plateau): The Most Recent Post-Collisional Volcanism in Turkey. *Chemical Geology* 226(3-4):189-211.

Özdemir, Y., Ö. Karaoğlu, A. Ü. Tolluoğlu and N. Güleç
2007 Reply to Discussion by Evren Çubukçu, Erkan Aydar and Alain Gourgaud of "Volcanostratigraphy and Petrogenesis of the Nemrut Stratovolcano (East Anatolian High Plateau): The Most Recent Post Collisional Volcanism in Turkey" by Y. Özdemir, Ö. Karaoğlu, A.Ü. Tolluoğlu and N. Güleç. *Chemical Geology* 245:130-134.

Özdoğan, M.
1994 Obsidian in Anatolia: An Archaeological Perspective on the Status of the Research. In *Archaeometry 94: The Proceedings of the 29th International Symposium on Archaeometry; Ankara, 9-14 May 1994*, pp. 423-431.

Özgür, N. and A. Bilgin
1990 Geochemistry, Genesis, and Economic Importance of the Sarikamis/Kars Perlite and Obsidian. *Jeomorfoloji Dergisi* 18:25-38.

Pantona, C. G.
1976 AES Compositional Profiles of Mobile Ions in the Surface Region of Glass. *Journal of Vacuum Science Technology* 13(1):414.

Park, R. J.
2010 *A Culture of Convenience? Obsidian Source Selection in Yellowstone National Park*, University of Saskatchewan.

Parker, H. C., L. V. Kim, N. B. Suiter, S. Carlson, T. D. Lorentzen, T. B. Malek, G. S. Johnson, H. B. DeFrance, E. A. Ostrander and L. Kruglyak
2004 Genetic Structure of the Purebred Domestic Dog. *Science* 304(5674):1160-1164.

Patel, S., R. Hedges and J. Kilner
1998 Surface Analysis of Archaeological Obsidian by SIMS. *Journal of Archaeological Science* 25(10):1047-1054.

Payne, R., J. Blackford and J. van der Plicht
2008 Using Cryptotephras to Extend Regional Tephrochronologies: An Example from Southeast Alaska and Implications for Hazard Assessment. *Quaternary Research* 69:42-55.

Payne, S.
1975 The Year's Work. *Anatolian Studies* 25:3-14.

Peet, T. E.
1909 *The Stone and Bronze Ages in Italy and Sicily*, Oxford.

Pelto, P. J. and G. H. Pelto
1978 *Anthropological Research: The Structure of Inquiry*. 2nd ed. Cambridge University Press.

Penhallurick, R. D.
1986 *Tin in Antiquity: Its Mining and Trade Throughout the Ancient World with Particular Reference to Cornwall*. The Institute of Metals, London.

Perlman, I. and F. Asaro
1969 Pottery Analysis by Neutron Activation. *Archaeometry* 11:21-52.

Pernicka, E.
1992 Herkenftsbestimmung Spaturukzeitlicher Obsidianfunde vom Hassek Hoyuk. *Istanbuler Forschungen* 38:124-131.

1996 Analyse Eines Prädynastischen Obsidianmessers aus Unterägypten. In *Interregional Contacts in the Later Prehistory of Northeastern Africa*, edited by L. Krzyżaniak, K. Kroeper and M. Kobusiewicz, pp. 286-289. Poznań Archaeological Museum.

Pernicka, E., J. Keller and M.-C. Cauvin
1997 Obsidian from Anatolian Sources in the Neolithic of the Middle Euphrates Region (Syria). *Paléorient* 23(1):113-122.

Pernicka, E., J. Keller, G. Rapp and T. Ercan
1996 Provenance of Late Neolithic and Early Bronze Age Obsidian Artifacts from the Troad. In *Archaeometry 94: The Proceedings of the 29th International Symposium on Archaeometry; Ankara, 9-14 May 1994*, pp. 515-519.

Phillips, S. and R. Speakman
2009 Initial Source Evaluation of Archaeological Obsidian from the Kuril Islands of the Russian Far East Using Portable XRF. *Journal of Archaeological Science* 36(6):1256-1263.

Pinhasi, R., B. Gasparian, K. Wilkinson, R. Bailey, G. Bar-Oz, A. Bruch, C. Chataigner, D. Hoffmann, R. Hovsepyan, S. Nahapetyan, A. W. G. Pike, D. Schreve and M. Stephens
2008 Hovk 1 and the Middle and Upper Paleolithic of Armenia: A Preliminary Framework. *Journal of Human Evolution* 55(5):803-816.

Piperno, M., C. Collina, R. Gallotti, J.-P. Raynal, G. Kieffer, F.-X. Le Bourdonnec, G. Poupeau and D. Geraads
2009 Obsidian Exploitation and Utilization during the Oldowan at Melka Kunture (Ethiopia). In *Interdisciplinary Approaches to the Oldowan*, edited by E. Hovers and D. R. Braun, pp. 111-128. Springer Netherlands.

Poidevin, J.-L.
1998 Les Gisements d'Obsidienne de Turquie et de Transcaucasie: Géologie, Géochimie et Chronométrie. In *L'obsidienne au Proche et Moyen-Orient: Du vVolcan à l'Outil*, edited by M.-C. Cauvin, A. Gourgaud, B. Gratauze, N. Arnaud, G. Poupeau, J. L. Poidevin and C. Chataigner, pp. 105-167. British Archaeological Reports. Maison de l'Orient Méditerranéen, Archaeopress, Oxford.

Polanyi, K.
1957 Marketless Trading in Hammurabi's Time. In *Trade and Market in the Early Empires*, edited by K. Polanyi, C. M. Arensberg and H. W. Pearson, pp. 12-26. Henry Regnery, Chicago.

1963 Ports of Trade in Early Societies. *Journal of Economic History* 23(1):30-45.

Pollard, A. M., C. M. Batt, B. Stern and S. M. M. Young
2007 *Analytical Chemistry in Archaeology*. Cambridge Manuals in Archaeology. Cambridge University Press.

Pollard, A. M. and C. Heron
1996 *Archaeological Chemistry*. 1st ed. RSC Publishing, Cambridge.

2008 *Archaeological Chemistry*. 2nd ed. RSC Publishing, Cambridge.

Ponomarev, L. I.
1993 *The Quantum Dice*. 2nd ed. Taylor & Francis.

Postgate, J. N.
1992 *Early Mesopotamia: Society and Economy at the Dawn of History*. Routledge.

Potts, P. J., M. Thompson, S. Wilson and P. Webb
2005 G-Probe-2: An International Proficiency Test for Microbeam Laboratories - Report on Round 2 / May 2005 (NKT-1G Basaltic Glass).

Potts, T.
1993 Patterns of Trade in Third-Millennium BC Mesopotamia and Iran. *World Archaeology* 24(3): 379-402.

Poupeau, G., L. Bellot-Gurlet, V. Brisotto and O. Dorighel
2000 Nouvelles Donnees sur la Provenance de l'Obsidienne des Sites Neolithiques du Sud-Est de la France. *Earth and Planetary Sciences* 330:297-303.

Poupeau, G., S. Delerue, T. Carter, C. d. B. Pereira, N. Miekeley and L. Bellot-Gurlet
2005 How Homogeneous is the "East Göllü Dağ" (Cappadocia, Turkey) Obsidian "Source" Composition? *IAOS Bulletin* 32:3-7.

Poupeau, G., G. Kieffer, J.-P. Raynal, A. Milton and S. Delerue
2004 Trace Element Geochemistry in Balchit Obsidian (Upper Awash, Ethiopia). In *Studies on the Early Paleolithic site of Melka Kunture, Ethiopia*, edited by J. Chavaillon and M. Piperno, pp. 103-110. Istituto Italiano di Preistoria e Protostoria, Florence.

Pullar, J., J. Yellin and I. Perlman
1986 Source of Obsidian from Tepe Abdul Hosein as Determined by Neutron Activation Analysis. In *Proceedings of the 24th International Archaeometry Symposium*, pp. 389-401.

Rafifar, J.
1991 Obsidian and Early Cultural Contact in Iran. *Majallah-'i Bastan'shinasi va Tarikh* 5(2):14-26.

Randle, K., L. Barfield and B. Bagolini
1993 Recent Italian Obsidian Analyses. *Journal of Archaeological Science* 20:503-503.

Rapp, G. R.
2002 *Archaeomineralogy*. Springer-Verlag.

Rapp, G. R., J. Allert, V.Vitali, Z. Jing and E. Henrickson
2000 *Determining Geologic Sources of Artifact Copper: Source Characterization Using Trace Element Patterns*. University Press of America.

Rapp, G. R. and C. L. Hill
1998 *Geoarchaeology: The Earth-Science Approach to Archaeological Interpretation*. Yale University Press, New Haven.

Rasic, J. T., C. Houlette, N. Slobodina, J. Reuther, V. Florey and R. J. Speakman
1990 A Twelve Thousand Year History of Obsidian Prospecting in Eastern Beringia. In *Geological Society of America Abstracts with Programs,*, pp. 679. vol. 41, Portland.

Raynal, J., G. Poupeau, G. Kieffer and M. Piperno
2005 Balchit Obsidian (Upper Awash, Ethiopia). Colloque du GMPCA, Archéométrie 2005, INSTN-CEA, Saclay, 19-22 Avril 2005.

Reed, S. J. B.
1993 *Electron Microprobe Analysis*. 2nd ed. Cambridge University Press.

1996 *Electron Microprobe Analysis and Scanning Electron Microscopy in Geology*. 1st ed. Cambridge University Press.

2005 *Electron Microprobe Analysis and Scanning Electron Microscopy in Geology*. 2nd ed. Cambridge University Press.

Reepmeyer, C. and G. Clark
2010 Post-Colonization Interaction Between Vanuatu and Fiji Reconsidered: The Re-Analysis of Obsidian from Lakeba Island, Fiji. *Archaeometry* 52(1):1-18.

Reichel, C. D.
2006 Hamoukar. *The Oriental Institute Annual Report 2005-2006*:65-77.

2006 Urbanism and Warfare: The 2005 Hamoukar, Syria, Excavations. *The Oriental Institute News and Notes* 189.

2007 Hamoukar. *The Oriental Institute Annual Report 2006-2007*:59-68.

Renfrew, C.
1969 Trade and Culture Process in European Prehistory. *Current Anthropology* 10(2/3):151-169.

1970 Trace Element Analysis of Obsidian and Early Neolithic Trade. In *International Congress of Prehistoric and Protohistoric Sciences VII*, pp. 92-94. vol. 7.

1972 *The Emergence of Civilization*. Methuen, London.

1975 Trade as Action at a Distance. In *Ancient Civilization and Trade*, edited by J. A. Sabloff and C. C. Lamberg-Karlovsky, pp. 3-60. University of New Mexico Press.

Renfrew, C., J. Cann and J. Dixon
1965 Obsidian in the Aegean. *Annual of the British School at Athens* 60:225-247.

Renfrew, C. and J. Dixon
1976 Obsidian in Western Asia: A Review. *Problems in Economics and Social Archaeology* 42:137-150.

Renfrew, C., J. Dixon and J. Cann
1966 Obsidian and Early Cultural Contact in the Near East. *Proceedings of the Prehistoric Society* 2:30-72.

1968 Further Analysis of Near Eastern Obsidians. *Proceedings of the Prehistoric Society* 34:319-331.

Rice, P. M.
1978 Clear Answers to Vague Questions: Some Assumptions of Provenience Studies of Pottery. In *The Ceramics of Kaminaljuyu*, edited by R. K. Wetherington, pp. 511-542. Penn State University Press, University Park.

Riciputi, L., J. M. Elam, L. M. Anovitz and D. R. Cole
2002 Obsidian Diffusion Dating by Secondary Ion Mass Spectrometry: A Test Using Results from Mound 65, Chalco, Mexico. *Journal of Archaeological Science* 29(10):1055-1075.

Ridings, R.
1991 Obsidian Hydration Dating: The Effects of Mean Exponential Ground Temperature and Depth of Artifact Recovery. *Journal of Field Archaeology* 18:77-85.

1996 Where in the World Does Obsidian Hydration Dating Work? *American Antiquity* 61:136-148.

Riehl, S.
2000 Erste Ergebnisse der Archäobotanischen Untersuchungen am Tall Mozan/Urkeš. *Mitteilungen der Deutschen Orient-Gesellschaft zu Berlin* 132:229-238.

2006 *Tell Mozan - Early and Middle Bronze Age Economy and Ecology in Northern Syria*. Ältere Urgeschichte und Quartärökologie website.

Riehl, S.
2009 Archaeobotanical Evidence for the Interrelationship of Agricultural Decision-Making and Climate Change in the Ancient Near East. *Quaternary International* 197:93-114.

Riehl, S., K. E. Pustovoytov, S. Hotchkiss and R. A. Bryson
2008 Local Holocene Environmental Indicators in Upper Mesopotamia: Pedogenic Carbonate Record vs. Archaeobotanical Data and Archaeoclimatological Models. *Quaternary International* 209:154-163.

Ristvet, L.
2008 Legal and Archaeological Territories of the Second Millennium BC in Northern Mesopotamia. *Antiquity* 82:585-599.

Ritter, M. E.
2006 The Physical Environment: An Introduction to Physical Geography: The Geologic Work of Streams. http://www.uwsp.edu/geo/faculty/ritter/geog101/textbook/title_page.html.

Roaf, M.
1990 *Cultural Atlas of Mesopotamia and the Ancient Near East*. Facts on File.

Rollinson, H.
1993 *Using Geochemical Data: Evaluation, Presentation, Interpretation*. Prentice Hall, Harlow.

Rosania, C. N., M. T. Boulanger, K. T. Biró, S. Ryzhov, G. Trnka and M. D. Glascock
2008 Revisiting Carpathian Obsidian. *Antiquity [online project gallery]* 82(318).

Rosen, A. M.
1986 *Cities of Clay: The Geoarchaeology of Tells*. Prehistoric Archaeology and Ecology. The University of Chicago Press, Chicago.

Rosen, S. A.
1997 *Lithics after the Stone Age: A Handbook of Stone Tools from the Levant*. AltaMira Press.

Rosen, S.A., R. Tykot and M. Gottesman
2005 Long Distance Trinket Trade: Early Bronze Age Obsidian from the Negev. *Journal of Archaeological Science* 32(5):775-784.

Ross, C. S. and R. L. Smith
1955 Water and Other Volatiles in Volcanic Glasses. *American Mineralogist* 40:1071-1089.

Roth, B.
2000 Obsidian Source Characterization and Hunter–Gatherer Mobility: An Example from the Tucson Basin. *Journal of Archaeological Science* 27(4):305-314.

Rothman, M.
2002 *Tepe Gawra: The Evolution of a Small Prehistoric Center in Northern Iraq*. Monograph 112. University of Pennsylvania Museum, Philadelphia.

Rowe, M. C.
2008 *Catalog of Mount St. Helens 2004-2005 Tephra Samples with Major-and Trace-element Geochemistry*. Volcano Hazards Program, U.S. Geological Survey.

Rózsa, P., Z. Elekes, G. Szöőr, A. Simon, J. Simulak, I. Uzonyi and Á. Kiss
2003 Phenocrysts in Obsidian Glasses. *Journal of Radioanalytical and Nuclear Chemistry* 256(2): 329-337.

Rózsa, P., Z. Elekes, G. Szöőr, A. Simon and I. Uzonyi
2003 *Mapping Minerals in Obsidian Glasses by Using Micro-PIXE Technique*. Acta Mineralogica-Petrographica, Abstract Series 1, Szeged.

Rózsa, P., G. Szöőr, Z. Elekes, B. Gratuze, I. Uzonyi and Á. Z. Kiss
2006 Comparative Geochemical Studies of Obsidian Samples from Various Localities. *Acta Geologica Hungarica* 49(1):73-87.

Rubio, G.
2008 Hurrian Literature: Correction to "Who Were the Humans?". *Archaeology* 61(5).

Russell, I. C.
1905 Preliminary Report on the Geology and Water Resources of Central Oregon. *U.S. Geology Survey Bulletin* 252:49.

Sabloff, J. A. and C. C. Lamberg-Karlovsky
1975 *Trade and Ancient Civilizations*. University of New Mexico Press.

Sahlins, M.
1972 *Stone Age Economics*. Aldine de Gruyter, New York.

Sallaberger, W.
2007 From Urban Culture to Nomadism: A History of Upper Mesopotamia inthe Late Third Millennium. In *Sociétés Humaines et Changement Climatique à la Fin du Troisième Millénaire: Une Crise a-t-elle eu Lieu en Haute Mésopotamie?*, edited by C. Kuzucuoğlu and C. Marro, pp. 417-456. vol. 19. Varia Anatolica, Istanbul.

Salvini, M.
1998 The Earliest Evidences of the Hurrians Before the Formation of the Reign of Mittanni. In *Urkesh and the Hurrians, Studies in Honour of Lloyd Costen*, edited by G. Buccellati and M. Kelly-Buccellati, pp. 99-115. Undena Publications.

Sand, C. and P. Sheppard
2000 Long Distance Prehistoric Obsidian Imports in New Caledonia: Characteristics and Meaning. *Comptes Rendus de l'Academie des Sciences - Series IIA - Earth and Planetary Science* 331(3):235-243.

Sanna, I., F.-X. Le Bourdonnec, G. Poupeau and C. Luglie
2010 Ossidiane non sarde in Sardegna. Analisi di un rinvenimento subacqueo nel Porto di Cagliari. In *L'ossidiana del Monte Arci nel Mediterraneo. Nuovi Apporti Sulla Diffusione, sui Sistemi di Produzione e Sulla Loro Cronologia, Atti del 5° Convegno Internazionale*.

Santley, R., T. Barrett, M. D. Glascock and H. Neff
2001 Pre-Hispanic Obsidian Procurement in the Tuxtla Mountains, Southern Veracruz, Mexico. *Ancient Mesoamerica* 12(1):49-63.

Saunders, N.
2001 A Dark Light: Reflections on Obsidian in Mesoamerica. *World Archaeology* 33:220-236.

Sayre, E., R. Dodson and D. Thompson
1957 Neutron Activation Study of Mediterranean Potsherds. *American Journal of Archaeology* 61(1):35-41.

Schmidbauer, E., E. Mosheim and N. Semioschkina
1986 Magnetization and 57 Fe Mössbauer Study of Obsidians. *Physics and Chemistry of Minerals* 13(4):256-261.

Schneider, G.
1989 A Technological Study of North-Mesopotamian Stone Ware. *World Archaeology* 21(1):30-50.

1990 Herkunft von Obsidianartefakten in Uruk. *Baghdader Mitteilungen* 21:67-72.

1992 Analysis of Eastern Anatolian Obsidian Using X-ray Fluorescence. In *Archaeometry 92: The Proceedings of the 28th International Symposium on Archaeometry; Los Angeles, California, 23-27 March 1992*, pp. 131.

1994 Analysis of Obsidian from Sites in Central-Anatolia and Northern Syria by X-Ray Fluorescence. Archaeometry 94: The 29th International Symposium on Archaeometry, Ankara, 9-14 May 1994.

Schreiner, M., M. Grasserbauer and P. March
1988 Quantitative NRA and SIMS Depth Profiling of Hydrogen in Naturally Weathered Medieval Glass. *Fresenius' Journal of Analytical Chemistry* 331:428.

Schreiner, M., G. Stingeder and M. Grasserbauer
1984 Quantitative Characterization of Surface Layers on Corroded Medieval Glass with SIMS. *Fresenius' Journal of Analytical Chemistry* 319:600.

Schroder, S.-A.
2002 A Synthesis of Previous Studies that Explored the Effects of Fire on Obsidian: Where We've Been and Where We're Going. In *The Effects of Fire and Heat on Obsidian*, edited by J. Loyd, T. Origer and D. Fredrickson, pp. 5-10. Papers presented in "The Effects of Fire/Heat on Obsidian" at the 33rd Annual Meeting of the Society for California Archaeology, 1999 Sacramento, California.

Schwartz, M.
2002 Early Evidence of Reed Boats from Southeast Anatolia. *Antiquity* 76(293):617–618.

Scorzelli, B. R., S. Petrick, A. M. Rossi, G. Poupeau and G. Bigazzi
2001 Obsidian Archaeological Artefacts Provenance Studies in the Western Mediterranean Basin: An Approach by Mossbauer Spectroscopy and Electron Paramagnetic Resonance. *Comptes Rendus de l'Académie des Sciences - Series IIA - Earth and Planetary Science* 332(12): 769-776.

Scott, M. J. and M. J. Scott
1982 Obsidian Surgical Blades: Modern Use of a Stone Age Implement. *The Journal of Dermatologic Surgery and Oncology* 8(12):1050-1052.

Scott, V. D., G. Love and S. J. B. Reed
1995 *Quantitative Electron-Probe Microanalysis*. 2nd ed. Physics and its Applications. Ellis Horwood, New York.

Seelenfreund, A., J. Miranda, M. Dinator and J. Morales
2002 The Provenance of Archaeological Obsidian Artifacts from Northern Chile Determined by Source-Induced X-Ray Fluorescence. *Journal of Radioanalytical and Nuclear Chemistry* 251(1):15-19.

Shackley, M. S.
1988 Sources of Archaeological Obsidian in the Southwest: An Archaeological, Petrological, and Geochemical Study. *American Antiquity* 53(4):752-772.

1992 The Upper Gila River Gravels as an Archaeological Source Region: Implications for Models of Exchange and Interaction. *Geoarchaeology* 7:315-326.

Shackley, M. S.
1995 Sources Of Archaeological Obsidian in the Greater American Southwest: An Update and Quantitative Analysis. *American Antiquity* 60(3):531-551.

1998a *Archaeological Obsidian Studies: Method and Theory* Springer.

1998b Geochemical Differentiation and Prehistoric Procurement of Obsidian in the Mount Taylor Volcanic Field, Northwest New Mexico. *Journal of Archaeological Science* 25:1073-1082.

2002 More than Exchange: Pre-Ceramic through Ceramic Period Obsidian Studies in the Greater North American Southwest. In *Geochemical Evidence for Long-Distance Exchange*, edited by M.D. Glascock, pp. 53-87. Bergin and Garvey, Wesport, Connecticut.

2005 *Obsidian: Geology and Archaeology in the North American Southwest*. University of Arizona.

2008a A Short History of Obsidian Studies and X-Ray Fluorescence Spectrometry at Berkeley. Berkeley Archaeological XRF Laboratory website.

2008b Archaeological Petrology and the Archaeometry of Lithic Materials. *Archaeometry* 50(2): 194-215.

2009 Intersource and Intrasource Geochemical Variability in Two Newly Discovered Archaeological Obsidian Sources in the Southern Great Basin. *Journal of California and Great Basin Anthropology* 16(1):118-129.

Shackley, M. S. and C. Dillian
2002 Thermal and Environmental Effects on Obsidian Geochemistry: Experimental and Archaeological Evidence. *The Effects of Fire and Heat on Obsidian.* BLM, Bishop, CA.

Shackley, M. S., J. R. Hyland and M. de la Luz Gutierrez
1996 Mass Production and Procurement at Valle del Azufre: A Unique Archaeological Obsidian Source in Baja California Sur. *American Antiquity* 61:718-731.

Shane, P., V. Smith and I. Nairn
2003 Biotite Composition as a Tool for the Identification of Quaternary Tephra Beds. *Quaternary Research* 59:262-270.

Shaw, D. M.
2006 *Trace Elements in Magmas: A Theoretical Treatment*. Cambridge University Press.

Sheets, P.
1989 Dawn of a New Stone Age in Eye Surgery. In *Applying Anthropology: An Introductory Reader*, edited by A. Poloefsky and P. J. Brown, pp. 113-115. Mayfield, Mountain View, CA.

Shelford, P., F. Hodson, M. E. Cosgrove, S. E. Warren and C. Renfrew
1982 The Obsidian Trade. In *An Island Polity: The Archaeology of Exploitation in Melos*, edited by C. Renfrew and J. M. Wagstaff, pp. 182-221. Cambridge University Press.

Shepard, A. O.
1966 Problems in Pottery Analysis. *American Antiquity* 31:870-871.

Sidrys, R. V.
1976 Classic Maya Obsidian Trade. *American Antiquity* 41(4):449-464.

Silliman, S.
2005 Obsidian Studies and the Archaeology of 19th-Century California. *Journal of Field Archaeology* 30(1):75-94.

Skinner, C. E.
1995 Obsidian Characterization Studies. In *Archaeological Investigations, PGT-PG&E Pipeline Expansion Project, Idaho, Washington, Oregon, and California, Volume V: Technical Studies*, edited by R. U. Bryson, C. E. Skinner and R. M. Pettigrew, pp. 4.1-4.54. Report prepared for Pacific Gas Transmission Company, Portland, Oregon, by INFOTEC Research, Inc., Fresno, California, and Far Western Anthropological Research Group, Davis, California.

2010 Lab Field Work Projects. Northwest Research Obsidian Studies Laboratory website.

Skinner, C. E., A. C. Bennet-Rogers and J. J. Thatcher
1999 Obsidian Studies of Two Possible Wealth Blade Fragments from the Umpqua/Eden Site (35-DO-83), Central Orgen Coast: Results of X-Ray Fluorescence and Obsidian Hydration Analysis. *Current Archaeological Happenings in Oregon* 24(2):17-23.

Smith, D. G. W. and J. A. Westgate
1969 Electron Probe Technique for Characterizing Pyroclastic Deposits. *Earth and Planetary Science Letters* 5:313-319.

Smith, H. W., R. Okazaki and C. R. Knowles
1977 Electron Microprobe Data for Tephra Attributed to Glacier Peak, Washington. *Quaternary Research* 7:197-206.

Smith, R. and G. V. James
1981 *The Sampling of Bulk Materials*. Royal Society of Chemistry, London.

Sneath, P. H. A. and R. R. Sokal
1973 *Numerical Taxonomy: The Principles and Practice of Numerical Classification*. W. H. Freeman & Company.

Snell, D. C.
2005 *A Companion to the Ancient Near East*. Blackwell Companions to the Ancient World. Blackwell Publishing.

Speiser, E.
1953 The Hurrian Participation in the Civilizations of Mesopotamia, Syria, and Palestine. *Cahiers d'Histoire Mondiale* 1/2:311-327.

Spray, J. and D. Rae
1995 Quantitative Electron-Microprobe Analysis of Alkali Silicate Glasses: A Review and User Guide. *Canadian Mineralogist* 33:323-332.

Squier, E. G. and E. H. Davis
1847 *Ancient Monuments of the Mississippi Valley*. Smithsonian Contributions to Knowledge.

Steen-McIntyre, V.
1985 Tephrachronology and Its Application to Archaeology. In *Archaeological Geology*, edited by G. Rapp and J. Gifford, pp. 265-302. Yale University Press, New Haven.

Stein, D. L.
1984 Khabur Ware and Nuzi Ware: Their Origin, Relationship and Significance. *Assur* 4(1):1-65.

1997 Hurrians. In *The Oxford Encyclopedia of Archaeology in the Near East*, edited by E. M. Meyers, pp. 126-130. Oxford University Press.

Steinkeller, P.
1998 The Historical Background of Urkesh and the Hurrian Beginnings in Northern Mesopotamia. In *Urkesh and the Hurrians, Studies in Honour of Lloyd Costen*, edited by G. Buccellati and M. Kelly-Buccellati, pp. 75-98. Undena Publications.

Stephens, J. L.
1843 *Incidents of Travel in Yucatan*. Harper & Brothers.

Stern, C.
2002 Obsidian Sources and Distribution in Southernmost Patagonia, South America. Geological Society of America Annual Meeting, Denver.

Stevenson, C. M., J. J. Mazer and B. E. Scheetz
1998 Laboratory Obsidian Hydration Rates: Theory, Method, and Application. In *Archaeological Obsidian Studies: Method and Theory*, edited by M. S. Shackley, pp. 181-204. Advances in Archaeological and Museum Science. Plenum Press, New York.

Stevenson, C. M. and M. O. McCurry
1990 Chemical Characterization and Hydration Rate Development for New Mexican Obsidian Sources. *Geoarchaeology* 5:149-170.

Stevenson, C. M., P. Sheppard, D. Sutton and W. Ambrose
1996 Advances in the Hydration Dating of New Zealand Obsidian. *Journal of Archaeological Science* 23(2):233-242.

Stewart, S., G. Cernicchiaro, R. Scorzelli, G. Poupeau, P. Acquafredda and A. De Francesco
2003 Magnetic Properties and 57Fe Mössbauer Spectroscopy of Mediterranean Prehistoric Obsidians for Provenance Studies. *Journal of Non-Crystalline Solids* 323(1-3):188-192.

Strassler, R. B. and A. L. Purvis
2007 *The Landmark Herodotus*. Pantheon.

Streck, M. and S. Wacaster
2006 Plagioclase and Pyroxene Hosted Melt Inclusions in Basaltic Andesites of the Current Eruption of Arenal Volcano, Costa Rica. *Journal of Volcanology and Geothermal Research* 157(1-3):236-253.

Stross, F. H., D. P. Stevenson, J. R. Weaver and G. Wyld
1971 Analysis of American Obsidians by X-ray Fluorescence and Neutron Activation Analysis. In *Science and Archaeology*, edited by R. H. Brill, pp. 210-221. The MIT Press, Cambridge.

Summerhayes, G.
1997 Losing Your Temper: The Effect of Mineral Inclusions on Pottery Analyses. *Archaeology in Oceania* 32(1):108-117.

Summerhayes, G., J. R. Bird, R. Fullagar, C. Gosden, J. Specht and R. Torrence
1998 Application of PIXE-PIGME to Archaeological Analysis of Changing Patterns of Obsidian Use in West New Britain, Papua New Guinea. In *Archaeological Obsidian Studies: Method and Theory*, edited by M. S. Shackley, pp. 129-158. Plenum Press, New York.

Swanson, S., M. Naney, H. Westrich and J. Eichelberger
1989 Crystallization History of Obsidian Dome, Inyo Domes, California. *Bulletin of Volcanology* 51(3):161-176.

Taçon, P. S. C.
1989 *From Rainbow Snakes to 'X-Ray' Fish: The Nature of the Recent Rock Painting Tradition of Western Arnhem Land, Australia*, Australian National University.

1991 The Power of Stone: Symbolic Aspects of Stone Use and Tool Development in Western Arnhem Land, Australia. *Antiquity* 65:192-207.

Takase, K.
2004 Hide Processing of Oxen and Koryak: An Ethnoarchaeological Survey in Kamchatka Peninsula, Russia. *Busshitsu Bunka: Kokogaku Minzokugaku Kenkyu* 77:57-84.

Taliaferro, M. S., B. A. Schriever and M. S. Shackley
2009 Obsidian Procurement, Least Cost Path Analysis, and Social Interaction in the Mimbres Area of Southwestern New Mexico. *Journal of Archaeological Science* 37(3):536-548.

Taube, K. A.
1991 Obsidian Polyhedral Cores and Prismatic Blades in the Writing and Art of Ancient Mexico. *Ancient Mesoamerica* 2:61-70.

Taylor, B. N. and C. E. Kuyatt
1994 Guidelines for Evaluating and Expressing the Uncertainty of NIST Measurement Results. NIST Technical Note 1297.

Taylor, J. R.
1996 *Introduction to Error Analysis: The Study of Uncertainties in Physical Measurements*. 2nd ed. University Science Books.

Tenorio, D., A. Cabral, B. Bosch, M. Jiménez-Reyes and S. Bulbulian
1998 Differences in Colored Obsidians from Sierra de Pachua, Mexico. *Journal of Archaeological Science* 25:229-234.

Thalmann, J.
2006 L'obsidienne à Tell Arqa, Nord du Liban: Une Escale sur une Route Commerciale? (Obsidian at Tell Arqa, North Lebanon: A Stop-Over Point on a Trade Route?) *Baghdader Mitteilungen* 37:575-592.

Thomas, H. H.
1923 The Source of the Stones of Stonehenge. *Antiquaries Journal* 3:239-260.

Thompson-Miragliuolo, J.
1988 The Outer City: Introduction and Surface Collection. In *Mozan 1: The Soundings of the First Two Seasons*, edited by G. Buccellati and M. Kelly-Buccellati, pp. 49-56. Undena Publications.

Thorpe, O., S. Warren and J. Nandris
1984 The Distribution and Provenance of Archaeological Obsidian in Central and Eastern Europe. *Journal of Archaeological Science* 11(3):183-212.

Tilley, C.
1994 *A Phenomenology of Landscape: Places, Paths, and Monuments*. Explorations in Anthropology. Berg Publishers.

2004 *The Materiality of Stone: Explorations in Landscape Phenomenology*. Berg Publishers.

Todd, I. A.
1980 *The Prehistory of Central Anatolia I: The Neolithic Period*. Coronet Books.

Torrence, R.
1986 *Production and Exchange of Stone Tools: Prehistoric Obsidian in the Aegean*. New Studies in Archaeology. Cambridge University Press, Cambridge.

2004 Now You See It, Now You Don't: Changing Obsidian Source Use in the Willaumez Peninsula, Papua New Guinea. In *Explaining Social Change: Studies in Honour of Colin Renfrew*, edited by J. Cherry, C. Scarre and S. Shennan, pp. 115-125. McDonald Institute, Cambridge.

Torrence, R., P. Swadling, N. Kononenko, W. Ambrose, P. Rath and M. D. Glascock
2009 Mid-Holocene Social Interaction in Melanesia: New Evidence from Hammer-Dressed Obsidian Stemmed Tools. *Asian Perspectives* 48(1):119-148.

Toya, T. and A. Kato
1983 *Practical Techniques for Microprobe Analysis*. JEOL Training Center.

Tremaine, K. J. and D. A. Fredrickson
1988 Induced Obsidian Hydration Experiments: An Investigation in Relative Dating. *Materials Research Society Symposium Proceedings* 123:271-278.

Tripcevich, N.
2007 *Quarries, Caravans, and Routes to Complexity: Prehispanic Obsidian in the South-Central Andes*, University of California, Santa Barbara.

2009 Exotic Goods, Chivay Obsidian, and Sociopolitical Change in the South-Central Andes. In *Trade and Exchange: Archaeological Studies from History and Prehistory*, edited by C. D. Dillian and C. L. White, pp. 59-73. Springer.

Truncer, J., M. D. Glascock and H. Neff
1998 Steatite Source Characterization in Eastern North America: New Results Using Instrumental Neutron Activation Analysis. *Archaeometry* 40:23-44.

Tryon, C., M. Logan, D. Mouralis and S. Kuhn
2009 Building a Tephrostratigraphic Framework for the Paleolithic of Central Anatolia, Turkey. *Journal of Archaeological Science* 36:637-652.

Tsolakidou, A., R. Day, E. Kiriatzi and Kihkoglou.V.
1996 Group Therapy in Crete: A Comparison Between Analyses by NAA and Petrographic Thin Section of Early Bronze Age Pottery from Knossos. The 30th International Symposium on Archaeometry, Urbana.

Tsong, I., C. Houser, N. Yusef and R. Messier
1978 Obsidian Hydration Profiles Measured by Sputter-Induced Optical Emission. *Science* 201(4353):339-341.

Tykot, R. H.
1995 *Prehistoric Trade in the Western Mediterranean: The Sources and Distribution of Sardinian Obsidian*, Harvard University.

1996 Obsidian Procurement and Distribution in the Central and Western Mediterranean. *Journal of Mediterranean Archaeology* 9(1):39-82.

1997 Characterization of the Monte Arci (Sardinia) Obsidian Sources. *Journal of Archaeological Science* 24(5):467-479.

Tykot, R. H.
1998 Mediterranean Islands and Multiple Flows: The Sources and Exploitation of Sardinian Obsidian. In *Archaeological Obsidian Studies: Method and Theory*, edited by M. S. Shackley, pp. 67-81. Society for Archaeological Sciences.

2002 Chemical Fingerprinting and Source Tracing of Obsidian: The Central Mediterranean Trade in Black Gold. *Accounts of Chemical Research* 35(8):618-627.

2004 Scientific Methods and Applications to Archaeological Provenance Studies. In *Proceedings of the International School of Physics "Enrico Fermi" Course CLIV*, edited by M. Martini, M. Milazzo and M. Piacentini, pp. 407-422. IOS Press, Amsterdam.

Tykot, R. H. and A. Ammerman
1997 New Directions in Central Mediterranean Obsidian Studies. *Antiquity* 71:1000-1006.

Tykot, R. H. and S. Chia
1997 Long-Distance Obsidian Trade in Indonesia. In *Materials Issues in Art and Archaeology V: Materials Research Society Symposium Proceedings Volume 462*, edited by P. B. Vandiver, J. R. Druzik, J. F. Merkel and J. Stewart, pp. 175-180.

Uerpmann, H. P. and M. Uerpmann
2007 Archaeo-zoological Work. In *The Temple Terrace of Urkesh: From Protoliterate to Mittani*, edited by G. Buccellati and M. Kelly-Buccellati, pp. 26-30. The International Institute for Mesopotamian Area Studies.

Ulusoy, I., P. Labazuy, E. Aydar, O. Ersoy and E. Çubukçu
2008 Structure of the Nemrut Caldera (Eastern Anatolia, Turkey) and Associated Hydrothermal Fluid Circulation. *Journal of Volcanology and Geothermal Research* 174:269-283.

Ur, J.
2002 Surface Collection and Offsite Studies at Tell Hamoukar, 1999. *Iraq* 64:15-43.

Ur, J. and E. Hammer
2009 Pastoral Nomads of the 2nd and 3rd Millennia A.D. on the Upper Tigris River, Turkey: The Hirbenterdon Tepe Survey. *Journal of Field Archaeology* 34:37-56.

Ur, J. A., P. Karsgaard and J. Oates
2007 Early Urban Development in the Near East. *Science* 317:1188.

Van De Mieroop, M.
2007 *A History of the Ancient Near East ca. 3000-323 BC*. 2nd ed. Blackwell History of the Ancient World. Blackwell Publishing.

Vargo, B. A., R. H. Tykot, J. Bliss, V. Colella, M. Tosi and S. Tusa
2001 The Characterization of Obsidian from Pantelleria (Italy): The Archaeological Significance of Multiple Island Sources. Society for American Archaeology Annual Meeting, New Orleans.

Vasquez, C., H. G. Nami and A. E. Rapalini
2001 Magnetic Sourcing of Obsidians in Southern South America: Some Successes and Doubts. *Journal of Archaeological Science* 28(6):613-618.

Vedder, J. F.
2005 The Obsidian Mirrors of Çatalhöyük. In *Changing Materialities at Çatalhöyük: Reports from the 1995-1999 Seasons*, edited by I. Hodder, pp. 597-619. McDonald Institute Monographs and BIAA, Cambridge.

Verhoeven, M.
1999 Traces and Spaces: Microwear Analysis and Spatial Context of Later Neolithic Flint Tools from Tell Sabi Abyad, Syria. *Paléorient* 25(2):147-166.

Vila, E.
1998 *L'Explotation des Animaux en Mésopotamie Aux IVe et IIIe Millénaires Avant J.-C.* Monographie de CRA 21, Paris.

Vogel, N., S. Nomade, A. Negash and P. Renne
2006 Forensic 40Ar/39Ar dating: A Provenance Study of Middle Stone Age Obsidian Artifacts from Ethiopia. *Journal of Archaeological Science* 33(12):1749-1765.

Vogel, W.
1971 *Structure and Crystallization of Glasses*. Pergamon Press, Oxford.

von Dassow, E.
2008 *State and Society in the Late Bronze Age Alalah under the Mittani Empire*. Studies on the Civilization and Culture of Nuzi and the Hurrians 17. CDL Press, Bethesda, Maryland.

Vreeken, W. J., J. A. Westgate and B. V. Alloway
1992 Geomorphic Significance of Miocene Rhyolitic Tephra Beds from the Cypress Hills, Saskatchewan, Canada. *Quaternary International* 13/14:23-28.

Wada, K.
2009 Petrologic Model of Shirataki Obsidian, Northern Hokkaido, Japan: Its Structure, Composition and the Origin. In *Geological Society of America Abstracts with Programs*, pp. 553. vol. 41, Portland.

Wada, K., M. Mukai and O. Takeda
2003 Chemical Compositions of Obsidian Glasses Determined by EPMA: The Origin of Obsidians from the Remains at the Mouth of Tokoro River, Eastern Hokkaido. *Reports of Taisetsuzan Institute of Science, Hokkaido University of Education* 37:59-70.

Wainwright, G. A.
1927 Obsidian. *Ancient Egypt* 3:77-93.

Walker, G. W., G. B. Dalrymple and M. A. Lanphere
1974 Index to Potassium-Argon Ages of Cenozoic Volcanic Rocks of Oregon. *U.S. Geological Survey, Field Studies Map* MF-569.

Walker, J.
2003 *Stratigraphic Analysis of the Unit A9 Excavations at Tell Mozan, Syria*. University of Missouri-Columbia.

Wang, G., J. Han, L. Zhou, X. Xiong and Z. Wu
2005 Carbon Isotope Ratios of Plants and Occurrences of C4 Species under Different Soil Moisture Regimes in Arid Region of Northwest China. *Physiologia Plantarum* 125:74-81.

Ward, G.
1974 Comparison of Source and Artifact Characterization Data Using a Generalized Distance Measure. *American Antiquity* 39(3):473-477.

Waters, A.
1927 A Structural and Petrographic Study of the Glass Buttes, Lake County, Oregon. *The Journal of Geology* 35(5):441-452.

Webb, S. L.
1997 *Silicate Melts*. Springer, Berlin.

Weber, J. A.
1997 Faunal Remains from Tell es-Sweyhat and Tell Hajji Ibrahim. *MASCA Research Papers in Science and Archaeology* 14:133-168.

Weedman, K.
2005 Gender and Stone Tools: An Ethnographic Study of the Konso and Gamo Hideworkers of Southern Ethiopia. In *Gender and Hide Production*, edited by L. Frink and K. Weedman, pp. 175–196. AltaMira Press.

Weedman-Arthur, K. J.
2008 The Gamo Hideworkers of Southwestern Ethiopia and Cross-Cultural Comparisons. *Anthropozoologica* 43(1):67-98.

Weigand, P. C., G. Harbottle and E. V. Sayre
1977 Turquoise Sources and Source Analysis: Mesoamerica and the Southwestern USA. In *Exchange Systems in Prehistory: Studies in Archaeology*, edited by T. K. Earle and J. E. Ericson, pp. 15-34. Academic Press, New York.

Weisler, M. I.
1990 Sources and Sourcing of Volcanic Glass in Hawai'i: Implications for Exchange Studies. *Archaeology in Oceania* 25:16-23.

Weisler, M. I. and D. A. Clague
1998 Characterisation of Archaeological Volcanic Glass from Oceania: The Utility of Three Techniques. In *Archaeological Obsidian Studies: Method and Theory*, edited by M. S. Shackley, pp. 103-128. Society for Archaeological Sciences.

Weiss, H.
1985 Rediscovering: Tell Leilan on the Habur Plains of Syria. *The Biblical Archaeologist* 48(1): 5-34.

1994 Archaeology in Syria. *American Journal of Archaeology* 98(1):101-158.

Weiss, H., M. Courty, W. Wetterstrom, F. Guichard, L. Senior, R. Meadow and A. Curnow
1993 The Genesis and Collapse of Third Millennium North Mesopotamian Civilization. *Science* 261(5124):995-1004.

Wheeler, M. E. and D. W. Clark
1977 Elemental Characterization of Obsidian from the Koyukuk River, Alaska, by Atomic Absorption Spectrophotometry. *Archaeometry* 18:15-31.

White, A. F.
1984 Weathering Characteristics of Natural Glass and Influences on Associated Water Chemistry. *Journal of Non-Crystalline Solids* 67:225-244.

Whittaker, J. C.
1994 *Flintknapping: Making and Understanding Stone Tools*. University of Texas Press, Austin.

Wilford, J. N.
2007 *Ruins in Northern Syria Bear the Scars of a City's Final Battle*. The New York Times, 2007 January 16.

Wilhelm, G.
1989 *The Hurrians*. Aris & Phillips.

1991 A Hurrian Letter from Tell Brak. *Iraq* 53:159-168.

2002 Hurrian Participation in the Bronze Age Civilization of Syria: Recent Results and Perspectives of Research. In *Documents D'archeologie Syrienne I: The Syrian Jezira Cultural Heritage And Interrelations: Proceedings of the International Conference held in Deir ez-Zor, April 22-25, 1996*, edited by M. Al-Maqdissi, M. A. Karim, A. Al-Azm and M. D. Al-Khoury, pp. 173-180. Ministerede la Culture, Direction Generale des Antiquites et des Musees, Republique Arabe Syrienne.

Wilkinson, T. J.
2000 Regional Approaches to Mesopotamian Archaeology: The Contribution of Archaeological Surveys. *Journal of Archaeological Research* 8(3):219-267.

Wilkinson, T. J., J. H. Christiansen, J. Ur, M. Widell and M. Altaweel
2007 Urbanization within a Dynamic Environment: Modeling Bronze Age Communities in Upper Mesopotamia. *American Anthropologist* 109(1):52-68.

Wilkinson, T. J., C. French, W. Matthews and J. Oates
2001 Geoarchaeology, Landscape, and the Region. In *Excavations at Tell Brak: Vol 2. Nagar in the Third Millennium BC*, edited by D. Oates, J. Oates and H. McDonald. British School of Archaeology in Iraq, London.

Williams, N. M.
1982 A Boundary is to Cross: Observations on Yolngu Boundaries and Permission. In *Resource Managers: North American and Australian Hunter-Gatherers*, edited by N. M. Williams and E. S. Hunn. AAAS Selected Symposium. Westview Press, Boulder, Colorado.

Williams-Thorpe, O.
1995 Obsidian in the Mediterranean and the Near East: A Provenancing Success Story. *Archaeometry* 37:217-248.

Williams-Thorpe, O., S. E. Warren and J. Nandris
1984 The Distribution and Provenance of Archaeological Obsidian in Central and Eastern Europe. *Journal of Archaeological Science* 11:183-212.

Wilson, A.
1978 Elemental Analysis of Pottery in the Study of Its Provenance: A Review. *Journal of Archaeological Science* 5(3):219-236.

Wilson, L. and A. M. Pollard
2001 The Provenance Hypothesis. In *Handbook of Archaeological Sciences*, edited by D. R. Brothwell and A. M. Pollard, pp. 507-517. John Wiley and Sons, Chichester.

Wood, C. A. and J. Kienle
1990 *Volcanoes of North America: The United States and Canada*. Cambridge University Press.

Wright, G. and A. Gordus
1969 Distribution and Utilization of Obsidian from Lake Van Sources Between 7500 and 3500 BC. *American Journal of Archaeology* 73(1):75-77.

Wright, G. A.
1969 *Obsidian Analyses and Prehistoric Near Eastern Trade: 7500 to 3500 B.C.* Anthropological Papers, Museum of Anthropology, University of Michigan 37.

Wright, H.
2004 The Earliest Bronze Age in Southwest Asia (3100-2700 BC). Session: Civilizations as Dynamic Networks. European Conference on Complex Systems, Paris.

Yacobaccio, H., P. Escola, F. Pereyra, M. Lazzari and M. Glascock
2004 Quest for Ancient Routes: Obsidian Sourcing Research in Northwestern Argentina. *Journal of Archaeological Science* 31(2):193-204.

Yakar, J.
1991 *Prehistoric Anatolia: The Neolithic Transformation and the Early Chalcolithic Period*. Institute of Archaeology, Tel Aviv University.

Yanagisawa, N., K. Fujimoto, S. Nakashima, Y. Kurata and N. Sanada
1997 Micro FF-IR Study of the Hydration-Layer During Dissolution of Silica Glass. *Geochimica et Cosmochimica Acta* 61:1165-1170.

Yanev, Y., S. Todorova, J.-M. Bardintzeff and R. Pichon
1997 Andesitic Obsidian from the Dambalak Oligocene Volcano (Eastern Rhodopes). *Comptes-Rendus de l'Académie Bulgare des Sciences* 50(7):41-44.

Yeğingil, Z., G. Bigazzi, M. Ozdogan, M. Oddone and T. Ercan
1990 Provenance Studies of Obsidian Artifacts from North-West Anatolia using the FT Dating Method. In *Proceedings of the 12th International Symposium on Excavations, Surveys, and Archaeometry*, pp. 73-86, Ankara, Turkey.

Yeğingil, Z., G. Bigazzi, G. Poupeau and L. Bellot- Gurlet
1998 Provenance Studies of Obsidian Artefacts in Anatolia: The Contribution of the Fission Track Analyses. In *"Light on Top of the Black Hill": Studies presented to Halet Cambel*, edited by G. Arsebük, M. J. Mellink and W. Schirmer, pp. 823-844. Ege Yayinlari, Istanbul.

Yellin, J.
1995 Trace eLement Characteristics of Central Anatolian Obsidian Flows and their Relevance to Pre-History. *Israel Journal of Chemistry* 35(2):175-190.

Yellin, J., T. Levy and Y. Rowan
1996 New Evidence on Prehistoric Trade Routes: The Obsidian Evidence from Gilat, Israel. *Journal of Field Archaeology* 23(3):361-368.

Yılmaz, Y., Y. Güner and F. Şaroğlu
1998 Geology of the Quaternary Volcanic Centres of the East Anatolia. *Journal of Volcanology and Geothermal Research* 85(1-4):173-210.

Yılmaz, Y., F. Saroglu and Y. Guner
1987 Initiation of the Neo-Magmatism in East Anatolia. *Tectonophysics* 134:177-199.

Zallen, R.
1998 *The Physics of Amorphous Solids*. Wiley, New York.

Zarins, J.
1990 Obsidian and the Red Sea Trade: Prehistoric Aspects. In *South Asian Archaeology 1987: Proceedings of the Ninth International Conference of the Association of South Asian Archaeologists in Western Eouope*, edited by M. Taddei, pp. 509-541. Istituto Italiano per il Medio ed Estremo Oriente, Rome.

Zeitlin, R. N.
1982 Toward a More Comprehensive Model of Interregional Commodity Distribution: Political Variables and Prehistoric Obsidian Procurement in Mesoamerica. *American Antiquity* 47(2): 260-275.

Zeller, R. A. and E. G. Carmines
1980 *Measurement in the Social Sciences: The Link Between Theory and Data*. Cambridge University Press, London.

Zhang, Y., R. Belcher, P. Ihinger, L. Wang, Z. Xu and S. Newman
1997 New Calibration of Infrared Measurement of Dissolved Water in Rhyolitic Glasses. *Geochimica et Cosmochimica Acta* 61(15):3089-3100.

Zielinski, R., P. Lipman and H. Millard
1977 Minor-Element Abundances in Obsidian, Perlite, and Felsite of Calc-Alkalic Rhyolites. *American Mineralogist* 62(5-6):426-437.

Zohary, M.
1973 *Geobotanical Foundations of the Middle East*. Geobotanica Selecta. G. Fischer, Stuttgart.

Zotov, N.
2003 Structure of Natural Volcanic Glasses: Diffraction Versus Spectroscopic Perspective. *Journal of Non-Crystalline Solids* 323(1-3):1-6.

Appendix A - Obsidian Sources in the Near East

Dozens of obsidian "sources" (I discussed this term in Chapter 4) exist in Turkey and the Transcaucasus (Georgia, Russia, Armenia, and Azerbaijan). I briefly discuss here the principal sources in this region. Such information is important for obsidian sourcing because, as Inizan et al. (1999:25) asserts, meaningful conclusions for sourcing research also requires knowledge about the nature of the possible sources:

> What is the geological context of occurrence? Is the raw material locally rare, or abundant? Is there only one sort of raw material, or are there several varieties? Is the raw material easy, or on the contrary difficult, to collect or extract? What is its quality, in what shapes and sizes does it occur? Could it be easily transported?

Ideally, such information is known not only about those sources used in antiquity but also about the sources that seem not to have been used. Consequently, I endeavored to gather what information I could about these sources. Furthermore, in Chapter 4, I discuss some fieldwork that I did in Oregon at two volcanoes, one analogous to Göllü Dağ (i.e., Glass Buttes) and another analogous to Nemrut Dağ (i.e., Newberry Caldera).

As should be clear from the previous chapters, differing terminology is a problem: Çiftlik/Göllü Dağ, Ziyaret/Meydan Dağ, Kalatepe/Komürcü, Birtlikeler/Kayırlı, and so on. Todd (1980) reports that Güneydağ, an area of Acigöl, is also called Güneydağ Tepe, Göl Dağ, and Güneş Dağ (30). I shall use standard or common terms whenever possible, but there is little or no consensus on some of these source names.

I also make no attempt to connect these sources to the RDC chemical groups (i.e., 1e-f, 2b, 3a, 4c, etc.). This numbering scheme, based on the clusters on their scatterplots

of Ba versus Zr and other elements, was provisionally adequate when it was thought that there were only four to six obsidian sources in the Near East. In the 1970s, it should have been clear that their numbering scheme was untenable. Renfrew and Dixon (1976) report revisions to Group 3 and its subdivisions 3a, 3b, 3c, 3d, including the need for additional subdivisions, like 3a' , 3a'', and 3c' (139). Furthermore, obsidian sources hundreds, even thousands, of kilometers apart were part of the same chemical group (e.g., Group 1e-f for Acigöl and a suspected source near Lake Van). Today, with dozens of Near East obsidian sources known, the RDC numbering scheme is obsolete.

The following descriptions have been assembled from a wide variety of studies, in particular: Arslan et al. (1998), Badalian et al. (2001), Badalyan et al. (2004), Balkan-Atli et al. (1999), Bigazzi et al. (1993a, 1993b, 1996, 1997), Blackman et al. (1998), Brennan (1996), Cauvin and Chataigner (1998), Cauvin (1991, 1998a, 1998b), Chataigner (1998), Chataigner et al. (1998), Ercan et al. (1989, 1994), Gopher et al. (1998), Gourgaud (1998), Keller and Seifried (1990), Keller et al. (1996), Özdoğan (1994), Özgür and Bilgin (1990), Poidevin (1998), Williams-Thorpe (1995), Wright (1969), and Yellin (1995). The field notes from researchers who sent me obsidian specimens, including George "Rip" Rapp of the University of Minnesota-Duluth, Tuncay Ercan of the General Directorate of Mineral Research and Exploration, Giulio Bigazzi at the Institute of Geochronology and Isotope Geochemistry in Pisa, and John Whittaker of Grinnell College, further contributed to my knowledge of these obsidian sources, particularly those in Turkey. In addition, geological maps and satellite images were useful in my studies of these sources.

A.1 - Central Anatolian Sources

Acıgöl is a volcanic complex within multiple lava domes, largely contained in an extensive caldera. RDC analyzed obsidian from one flow within this complex; however, since that time, at least two phases of volcanism have been identified: ancient volcanism related to faulting, and younger volcanism within the caldera after it formed. Three main source areas, defined both geochemically and geographically, occur within this complex: East Acıgöl ante-caldera, East Acıgöl post-caldera, and West Acıgöl. The name "Acıgöl," therefore, is vague and corresponds to a variety of obsidian sources.

The East Acıgöl ante-caldera sources are ***White Tuffs Hotamis Dağ (WTHD)*** and ***Bogazköy***. The WTHD obsidians originate from lava flows that predate this caldera and are largely covered by white-colored tuff, that is, consolidated volcanic ash. The ash also contains glassy fragments and blocks of obsidian, though often small and fractured. The flow-ridges from this viscous flow are still apparent as dips on the surface. The "Acıgöl" obsidian analyzed by RDC appears to have come from this particular source. Bogazköy is similar to WTHD, but this lava flow, exposed in a valley near the village of Bogazköy, is geochemically distinct, indicating a separate ancient eruption. The Bogazköy obsidian reportedly has abundant mineral spherules and microfractures.

The only (at present) East Acıgöl post-caldera source is ***Hotamis Dağ***, a massive volcanic dome located near WTHD within the caldera. This is the largest rhyolitic dome in the vicinity, and it has at least three lobes. Like most domes, the outer shell is mainly pumice and crystalline rhyolite, but obsidian is accessible at several spots, particularly on

the northwest slope and in the landslide debris on the southern slope. The obsidian from Hotamis Dağ has been reported to fracture somewhat irregularly, making it less desirable for fashioning flaked-stone tools. The name "Hotamis Dağ" has been applied to both the ancient WTHD source and the younger lava dome described here.

The West Acıgöl sources are ***Korudağ***, ***Güneydağ***, ***Kalecitepe***, and ***Acıgöl-maar***. The Acıgöl-maar is a shallow volcanic crater most likely produced by a phreatomagmatic eruption, that is, an explosion due to contact between groundwater and hot magma, and a lake recently filled the crater. The crater walls are comprised largely of pyroclastics (ash, lapilli, volcanic bombs, and other volcanic materials), and obsidian chunks occur in those levels. The other three sources -- Korudağ, Güneydağ, Kalecitepe -- are all rhyolitic lava domes and seem geochemically related to the Acıgöl-maar, possibly due to the formations being volcanically linked. Korudağ has several outcrops that might be distinct flows, but this is not certain. The largest outcrops occur on its northeast slope, and the obsidian was reported to be of moderate quality, having a few small mineral spherules. Higher quality obsidian in useful-sized pieces can be found in tuffs on its northeastern and western sides of the dome. Obsidian blocks similarly occur in the pyroclastic deposits around the other two domes, Güneydağ and Kalecitepe. It has been suggested that the lava domes are not truly the sources of this obsidian and that their pyroclastic deposits merely contain blocks of obsidian strewn about during the eruption of the Acıgöl-maar.

Göllü Dağ (called Çiftlik by RDC and other early researchers) is a stratovolcano with a lava dome complex, about a dozen kilometers in diameter, and there are multiple

geochemically distinct obsidian deposits on its flanks. The obsidians here are among the oldest known in Central Anatolia, dated to 1.0 to 1.5 million years old, highly eroded and dissected by channels from streams and springs. The obsidian sources of the complex are often divided into two classes: East Göllü Dağ, consisting of ***Komürcü***, ***East Kayırlı***, and ***East Bozköy***, and West Göllü Dağ, consisting of ***Kayırlı Village*** and ***North Bozköy***. The naming scheme for these sources unfortunately varies quite a bit.

Obsidians from the East Göllü Dağ sources appear to have been the most widely distributed in the western Near East for millennia, and lithic specialists' experiments have indicated that these obsidians are of the highest quality in Central Anatolia. A number of obsidian "workshops" have been discovered near the Komürcü and East Kayırlı outcrops. On the northeastern side of Göllü Dağ, obsidian occurs quite abundantly at various places around Komürcü village. The obsidian quality varies from excellent to moderate, and its sizes range from small pebbles to blocks over 25 cm in diameter. The obsidian is banded in some outcrops, and perlitic (i.e., hydrated) in others. It is not yet clear if there are one or more domes here or if there was a fault-related eruption. East Kayırlı is more clearly a lava dome, and the obsidian layers, as thick as 50 cm, are exposed around the dome edges or where cut by a small stream bed. Because the Komürcü and East Kayırlı obsidians are difficult to distinguish geochemically, they are frequently grouped together. East Bozköy, a source exposed by a valley on the southern side of Göllü Dağ, seems chemically related to Komürcü and East Kayırlı, so it is usually grouped with them.

Obsidians from the West Göllü Dağ sources were apparently much more rare in antiquity. North Bozköy is a small lava dome, and obsidian has been exposed by erosion at the junction of two valleys cut by streams. Obsidian outcrops are present, as are loose blocks of useful quality and size. Reportedly some parts of this obsidian flow have small mineral spherules, reducing its usefulness for flaked tools. West of the village of Kayırlı, a large stream has exposed large blocks of white pumice, grey perlite, and black obsidian. The North Bozköy and Kayırlı Village obsidians cannot be discerned chemically, so they are ordinarily grouped together as "West Göllü Dağ."

Nenezi Dağ lies northwest of Gollü Dag, and it is a large, isolated lava dome with obsidian exposed along its western slopes, mostly by streams. Obsidian workshops have been found on this western flank and attest to use of this source in antiquity. The dome is tall, rising 500 meters (1600 feet) above the plains. The obsidians' colors reportedly vary, from matte gray and shiny black to blue-tinted and mottled red.

Hasan Dağ is a large stratovolcano, more than 3200 meters (10,500 feet) tall, that lies on the Konya Plain, southwest of Gollü Dag. Its two peaks are a result of at least one caldera-forming eruption. Its obsidian, poorly known and possibly generated by several distinct eruptions, apparently was not widely distributed in the ancient Near East despite its proximity to Çatal Höyük and other Neolithic sites. The volcano has not been entirely surveyed for obsidian, demonstrating that its sources are difficult to access. According to field notes and maps from Rapp and Ercan, obsidian is known to occur in the pyroclastic deposits, primarily ash, on the western and southern flanks. This obsidian may have been

produced by a lava dome that was destroyed by a caldera-forming eruption, scattering the broken fragments throughout the ash deposits. Geological maps show similar deposits on the northeastern flank, so obsidian pieces may also occur there. The obsidian colors vary reportedly from greenish black to reddish brown, and some obsidian has flow banding or feldspar crystals, indicating that it might not be useful for tools.

Çatkoy is a small village several kilometers north of the Acıgöl volcanic complex, but no lava dome or outcrops are apparent here. Instead, stream beds have exposed small pieces of obsidian within pyroclastic deposits. There are a few possibilities for the origin of this material. Obsidian may have been part of a rhyolitic lava dome that was destroyed by the formation of the extensive caldera, and fragments were strewn about. It could also be related to the Acıgöl-maar eruption. A third possibility is that these small pieces come from one or more Acıgöl sources and were transported by erosion. This last possibility is discussed further in Chapters 4 and, with some evidence, in Chapter 6.

A.2 - Eastern Anatolian Sources

Nemrut Dağ is an active stratovolcano (the last reported volcanic activity was 400 years ago), and about 270,000 years ago, it experienced a major caldera collapse, creating a circular basin about 7 km (4 miles) by 8 km (5 miles) in diameter. The western half of the caldera is filled with a lake, and the eastern half is covered by subsequent lava domes and flows. Obsidian in the caldera has been dated to 24,000 ± 14,000 and 34,000 ± 6000 years old, making it among the youngest in the Near East. This impressive caldera is the

reason that Nemrut Dağ has been called "one of the most spectacular volcanoes of eastern Anatolia" (Yılmaz et al. 1998:175). This is one of two peralkaline obsidian sources in the Near East, and its obsidian was widely distributed. There is, quite unfortunately, another archaeologically significant mountain named "Nemrut Dağ" in Turkey, one known for its huge statues, part of what is interpreted as a first-century-BCE tomb. In this dissertation, all references to "Nemrut Dağ" refer to the volcanic caldera.

Soon after the work of RDC, it was recognized, at least analytically, that obsidian with more than one chemical composition exists at Nemrut Dağ (e.g., Nemrut Dağ A and B in Wright 1969). It was eventually hypothesized that these two obsidian compositions corresponded to two distinct periods of volcanism: before and after the caldera formation. There is little to no consensus about terminology; however, the term "***Nemrut Lake***" has been used to describe the post-caldera obsidians while "***Nemrut South***" describes the pre-caldera obsidians. A third category, termed "***Nemrut Caldera***," also has been recognized. These terms, though, must be considered provisional, and they are misleading because, as I show in Chapter 8, Poidevin's (1998) scheme is incorrect.

Nemrut Caldera refers, as best I can determine, to an obsidian layer that predates the caldera and, after the explosion, became exposed in the stratigraphic sequence of the caldera wall. The problem, though, is that there seems to be more than one such layer of obsidian. A thin layer, two or three meters thick, near the top of the caldera wall appears to circle much of the caldera. A second layer, as much as 50 meters thick, is lower in the

wall and is exposed primarily on the northern and southern sides. It is unclear how these layers compare or which is intended to be the Nemrut Caldera source.

Nemrut South refers to obsidian in rhyolitic flows, which also predate the caldera, exposed in multiple locations on the southern flank of the volcano. These flows may not correspond to a single eruption. Obsidian exposed on the eastern flank of the volcano is commonly considered part of the Nemrut South source, but the geological maps suggest otherwise. It is unclear how these flows related exactly to the Nemrut Caldera obsidians: some of these flows may also be represented in the caldera wall. Some of this obsidian is perlitic and "crumbly" due to microfractures. It appears that most analyzed specimens of "Nemrut Dağ" obsidian originate from the Nemrut South exposures.

Nemrut Lake refers to obsidian that occurs within the caldera, but there are many overlapping flows, domes, and maars on the caldera floor. Some of this volcanic activity is linked to a fault running North-Southeast through the caldera. At least four flows and domes in the caldera are rhyolitic and obsidian-bearing, possibly more. Obsidian pieces could also be present in pyroclastic deposits within the caldera. Nemrut Dağ, particularly the obsidians in its caldera, are discussed in Chapters 2 and 7 through 9. I must reiterate, however, that the nomenclature is misleading because Poidevin's (1998) scheme, linking the degree of peralkalinity to location on the volcano, is incorrect.

Bingöl A is the commonly used term for a set of peralkaline obsidian sources near the city of Bingöl, namely Orta Düz and Çavuşlar. Although chemically quite similar to the Nemrut Dağ obsidians, the Bingöl A obsidians are older, about four million years old,

and their volcanic source is unclear. The obsidian blocks are highly rounded, about 10 to 25 cm in diameter, and their shapes indicate transport by water or mud. These obsidians are dark green or gray and often exhibit flow bands. Analytically the Bingöl A obsidians are frequently lumped together with the similar Nemrut Dağ obsidians.

Bingöl B is the term for calcalkaline obsidian sources also near the city of Bingöl, namely Alatepe and Çatak. These obsidians are younger than Bingöl A obsidians, about one million years old. Their origins are also relatively unclear, and obsidian from Alatepe and Çatak cannot be chemically differentiated. These blocks are also highly rounded but a bit larger, as much as 30 cm in diameter. Their shapes also indicate movement by water or mudflows. These obsidians are reportedly more variable in appearance, often black or gray, sometimes brown or red, occasionally exhibiting flow bands. This suggests that the obsidian originated from the upper shell of a rhyolitic lava dome.

Muş is a largely unknown obsidian locality described by Yılmaz et al. (1987) and Ercan et al. (1995) as well as Bigazzi and colleagues (Bigazzi et al. 1996:552, 1997:66). Near the city of Muş, roughly halfway between the Bingöl and Nemrut Dağ source areas, are two obsidian sources. One deposit is located near the village of Mercimekkale, and a second deposit, sometimes called Ziyaret Tepe, is about 15 km northwest of Muş. These two sources may possibly be somehow related to the Bingöl B sources.

Süphan Dağ lies east of Nemrut Dağ and north of Lake Van. After Mount Ararat, Süphan Dağ, a stratovolcano, is the tallest mountain in Turkey, over 4000 meters (13,300 feet) in elevation. Its summit was destroyed by a caldera, which, in turn, has been largely

filled by a dome, comprised of rhyolitic and dacitic lavas, about 2 kilometers in diameter. This entire structure lies within an even larger, older caldera, and a number of domes and cones occur on the mountainsides. Obsidian exists in numerous locations at Süphan Dağ, including the northern and southwestern slopes and the caldera. Many of these obsidians contain mineral inclusions, particularly plagioclase, occasionally sufficiently large to see with the unaided eye. The inclusions make the obsidian less useful for flaked-stone tools, and Süphan Dağ obsidians do not seem to have been widely utilized.

Meydan Dağ lies to the east of Süphan Dağ and also north of Lake Van, and it is another stratovolcano with caldera at its summit. There are also several volcanic craters, including named ones: Zamak Dağ and Ziyaret Tepe (not the same as the "Ziyaret Tepe" near Muş). In fact, Meydan Dağ is sometimes called "Ziyaret" in the literature. Its flows seem to overlay somewhat with those of Tendürek Dağ to the east. Meydan Dağ is one of the possible origins of the "Bayezid" specimen analyzed by RDC.

Tendürek Dağ lies east of Meydan Dağ, northeast of Lake Van, and southwest of the city of Dogubeyazıt and Mount Ararat. It is a shield volcano with twin peaks, about 6 kilometers apart, and a lake-filled crater at the summit. Obsidian occurs north-northeast of the western peak and due north of the eastern peak, possibly elsewhere. Tendürek Dağ is another potential source of RDC's "Bayezid" obsidian specimen.

A.3 - Northeastern Anatolian Sources

The obsidian sources north of the Lake Van region have not been studied nearly as much as those in Central Anatolia, and geological information about them is rare. In fact,

it is possible that there are obsidian sources yet to be discovered. These problems date to the original work of RDC: they analyzed a British Museum specimen labelled as "Kars," after the Erzurum-Kars Plateau, a broad volcanic field across northeastern Turkey. Many of these sources are part of the same or similar geological features.

The entire ***Kars*** Province has abundant Pleistocene tuffs and pyroclastic deposits, called ignimbrites, that contain isolated blocks of obsidian. Three obsidian sources near the city of Kars are known as ***Kars-Digor*** (near the city of Digor and Yağlıca Köyü, about 40 kilometers southeast of Kars), ***Kars-Akbaba Dağ*** (about 15 kilometers south of Kars), and ***Kars-Arpacay*** (near Akuzum village, 55 kilometers east of Kars).

Adjacent to Kars is the ***Erzurum*** Province. It is probable that obsidian blocks are present in pyroclastic deposit throughout the province, and most domes in this region are dacitic and intrusive, not rhyolitic and extrusive. The most prominent obsidian source is near the village of Tambura, about 20 kilometers southwest of the town of Erzurum. The slopes and crater of a cinder cone here contains blocks of obsidian.

The ***Erzincan*** Province has at least two volcanic domes with obsidian: ***Agili Tepe*** (near Keleriç, 30 kilometers east of Erzincan city) and ***Degirimen Tepe*** (near Kertah Köy village and Kaban Tepe, 20 kilometers east of Erzincan). Volcanism here appears related to the North Anatolian Fault between the Anatolian and Eurasian Plates.

The ***Pasinler*** Basin is geologically similar to the Erzurum-Kars Plateau. Obsidian likely occurs in pyroclastic deposits here and, after erosion, in river valleys. The primary

source may be a lava dome, known locally as Hasanbabu Dağ, northwest of Tizgi village and its associated pyroclastic deposits, produced by an explosive eruption.

The ***Sarıkamış*** district of Kars Province is rather poorly understood geologically, but there are two generations of obsidian, which differ in age by about one million years. One source is ***Çiplak Dağ*** near Mescitli village, and the other is ***Ala Dağ*** near Sehitemin. Obsidian pieces from the two sources can also be found in stream beds.

In the ***İkizdere*** District of Rize Province is Haros Dağ, a rhyolitic lava dome with an area of about four square kilometers. Obsidian occurs among the folds of pumice and rhyolite, and it is reported to be mostly black but occasionally red. Accounts suggest that this source is not easily accessible and, thus, possibly went unused.

A.4 - Transcaucasian Sources

In comparison to Anatolia, the Transcaucasus region has had much less attention until recently. One of the reasons is that, as former Soviet republics, these countries were largely inaccessible until 1991. A few systematic studies in this region have showed that Transcaucasian obsidians principally remained in the region and were not exchanged over great distances, like those from Anatolia, most likely for geographical reasons (Blackman et al. 1998, Barge and Chataigner 2003, and Chataigner et al. 2003).

Azerbaijan has only one main obsidian source: the ***Kel'bedzhar*** volcano, which is also known in the literature as Kechel Dağ and Merkasar. Georgia also has a single major obsidian source: ***Chikiani*** volcano (also called the Paravani Lake source and Kojun Dağ,

its Turkish name). Obsidian is accessible on the northern slope of this volcano, the name of which means "glass that glistens" in Georgian, and pebbles of obsidian occur along the banks of the nearby Khrami River. Obsidian from this source is often nearly clear, and it is reportedly abundant. Another obsidian source occurs across the Georgian border into Russia, in particular, the Kabardino-Balkaria Republic. It is known as the ***Baksan River*** source, and this obsidian derives from the eastern slopes of Mount Elbrus stratovolcano, the highest mountain of the Caucasus Range (5600 meters; 18,400 ft).

Renfrew et al. (1966) analyzed only one specimen from the British Museum that had "Erevan," that is, the Armenian capital Yerevan, listed as its origin. Armenia, though, actually has over twenty obsidian-bearing volcanoes. Unfortunately, reliable descriptions of these volcanoes, much less their obsidian outcrops, is sparse. Much of the geological literature is only written in Russian and, to a lesser extent, Armenian and has never been translated. Dixon (1976) pointed out that the "extent of our basic geological knowledge decreases from west to east through the... obsidian source" areas from the Mediterranean to the Transcaucasus (289), and this holds true still today. The Central Anatolian sources are better understood than the Eastern Anatolian sources, which, in turn, are better known than the Transcaucasian Sources. Problems that existed decades ago in Central Anatolia, such as a variety of source names, are present in Armenia now. For example, the Yeni-Ël source has also been called Kechut (after the volcanic massif), Amasia (after the district), Ashotsk (after the region), Sizevit (after a nearby village), Agvorik (after another nearby village), and Javakheti (after the mountain range) in various studies.

Over 150 specimens of Armenian obsidians were included in the research at hand; however, until additional source descriptions are available, readers are forwarded to a few articles coauthored by Armenian geologists. Badalian et al. (2001) discuss fission-track dating of obsidians from 18 different Armenian sources, but their descriptions are mainly limited to area, elevation, and fission-track dates. Badalyan et al. (2004) report on these sources in somewhat greater detail (note the different transliteration of the same author's name). Keller et al. (1996) describe their analyses of 13 volcanic complexes with at least 17 different obsidian sources, and the article includes copies of geological maps from the 1960s and early 1970s. Others have recently analyzed or dated Armenian obsidians (e.g., Oddone et al. 2000; Chataigner et al. 2003; Kasper et al. 2004; Kasper 2005; Chataigner and Barge 2007; Cherry et al. 2007), but their source descriptions are minimal (also note that all of these references date to the past ten years). A list of all the Armenian obsidian sources included in the present research can be found in Table 4.1.



Figure B.1 - Examples of obsidian blade-tools (blades, segments, etc.) from A1.



Figure B.2 - Examples of obsidian blade-tools (blades, segments, etc.) from A2.



Figure B.3 - Examples of obsidian blade-tools (blades, segments, etc.) from A5.



Figure B.4 - Examples of obsidian blade-tools (blades, segments, etc.) from A6.



Figure B.5 - Obsidian artifacts recovered together from a single feature in unit A5 (lot q30-L-1). Unit A5 includes Sector A of the Royal Palace and the later accumulations above it. This "toolkit" includes obsidian blade-tools and flake-tools.



Figure B.6 - Examples of obsidian blade-tools (blades, segments, etc.) from A7.



Figure B.7 - Examples of obsidian blade-tools (blades, segments, etc.) from A8.



Figure B.8 - Examples of obsidian blade-tools (blades, segments, etc.) from A9.

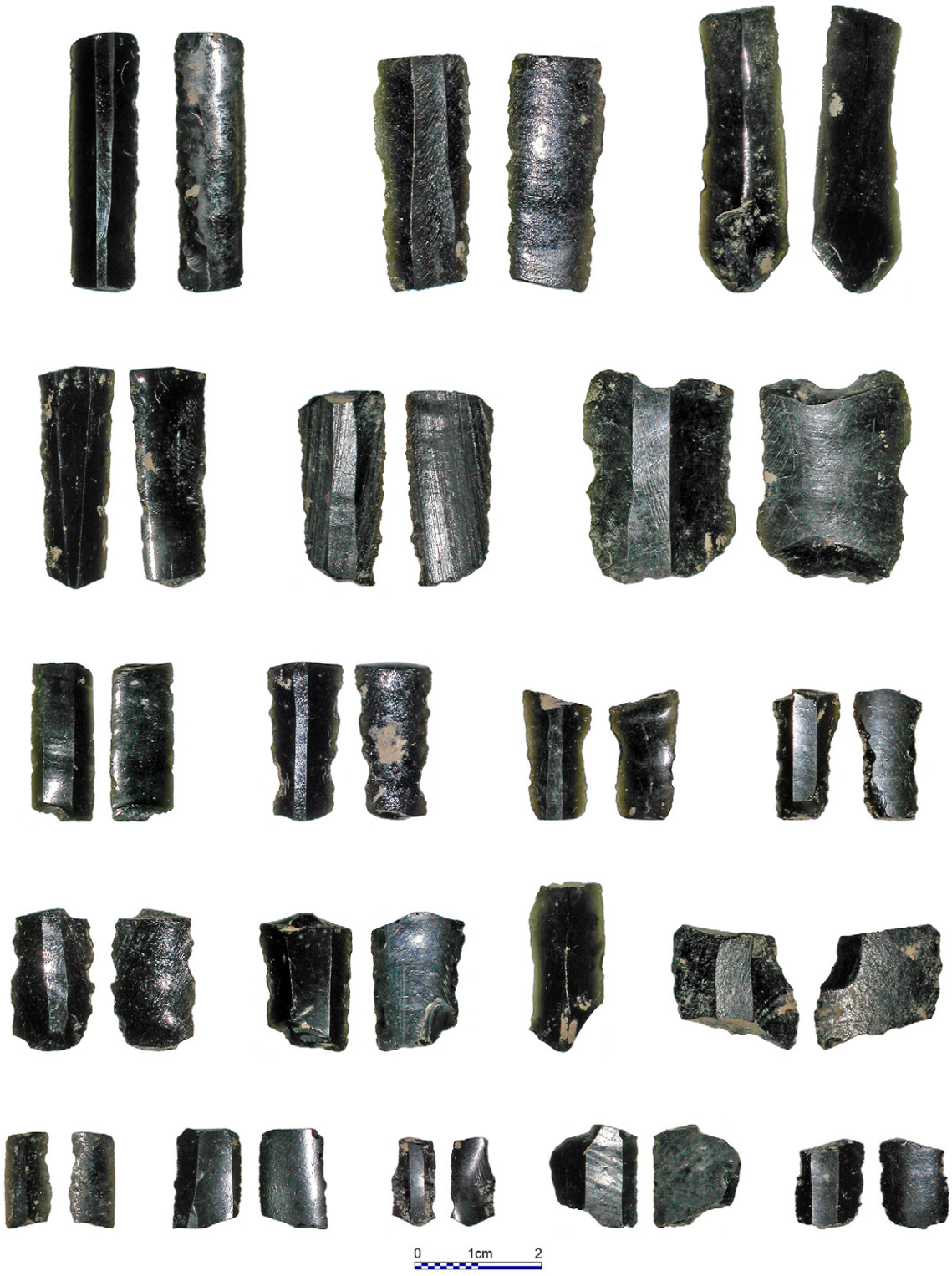


Figure B.9 - Examples of obsidian blade-tools (blades, segments, etc.) from A10.

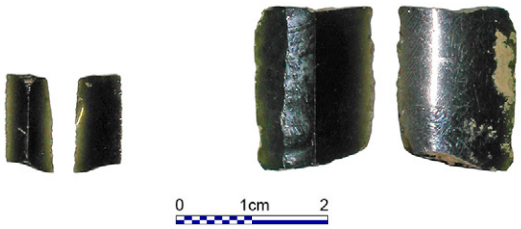


Figure B.10 - Examples of obsidian blade-tools (blades, segments, etc.) from A11.



Figure B.11 - Examples of obsidian blade-tools (blades, segments, etc.) from A12, which includes the *âbi* -- some of these blades may have been used to slaughter juvenile suids and canids in a Hurrian religious ritual known from texts, as discussed in Section 3.6.6.



Figure B.12 - Examples of obsidian blade-tools (blades, segments, etc.) from A13.



Figure B.13 - Examples of obsidian blade-tools (blades, segments, etc.) from A14.



Figure B.14 - Examples of obsidian blade-tools (blades, segments, etc.) from A15.

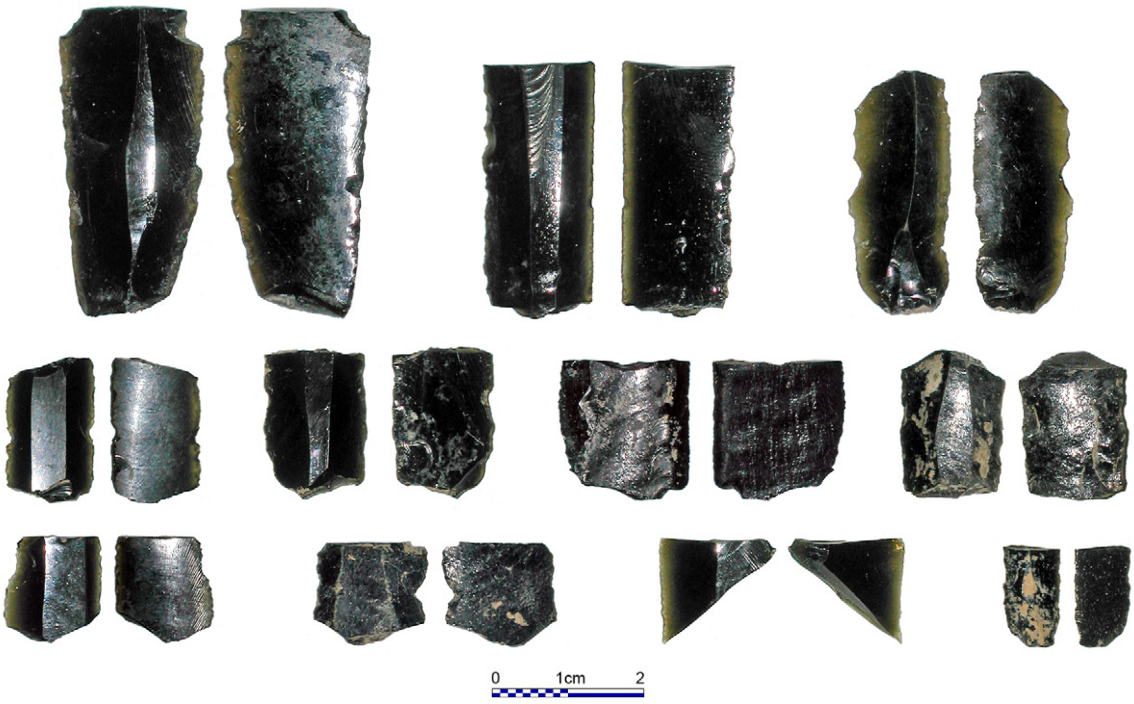


Figure B.15 - Examples of obsidian blade-tools (blades, segments, etc.) from A16.



Figure B.16 - Examples of obsidian blade-tools (blades, segments, etc.) from A17.



Figure B.17 - Examples of obsidian blade-tools (blades, segments, etc.) from A18.

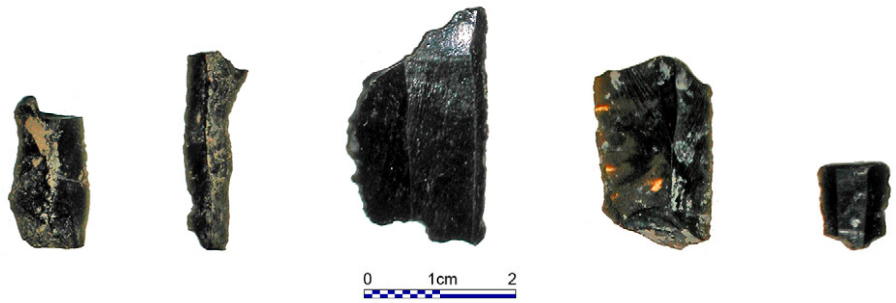


Figure B.18 - Examples of obsidian blade-tools (blades, segments, etc.) from B1.



Figure B.19 - Examples of obsidian blade-tools (blades, segments, etc.) from B2.



Figure B.20 - Obsidian blades from B3 (left) and B5 (center and right).



Figure B.21 - Examples of obsidian blade-tools (blades, segments, etc.) from B4.

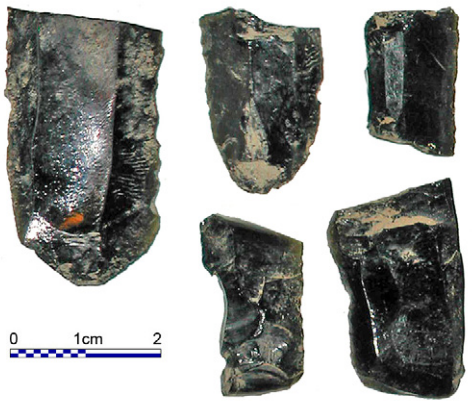


Figure B.22 - Obsidian artifacts recovered together from a single feature in Unit B1 (lot q5-L). Unit B1 includes the temple at the apex of the High Mound.



Figure B.23 - Obsidian artifacts recovered together from a single feature in Unit B1 (lot q19-L). Unit B1 includes the temple at the apex of the High Mound.

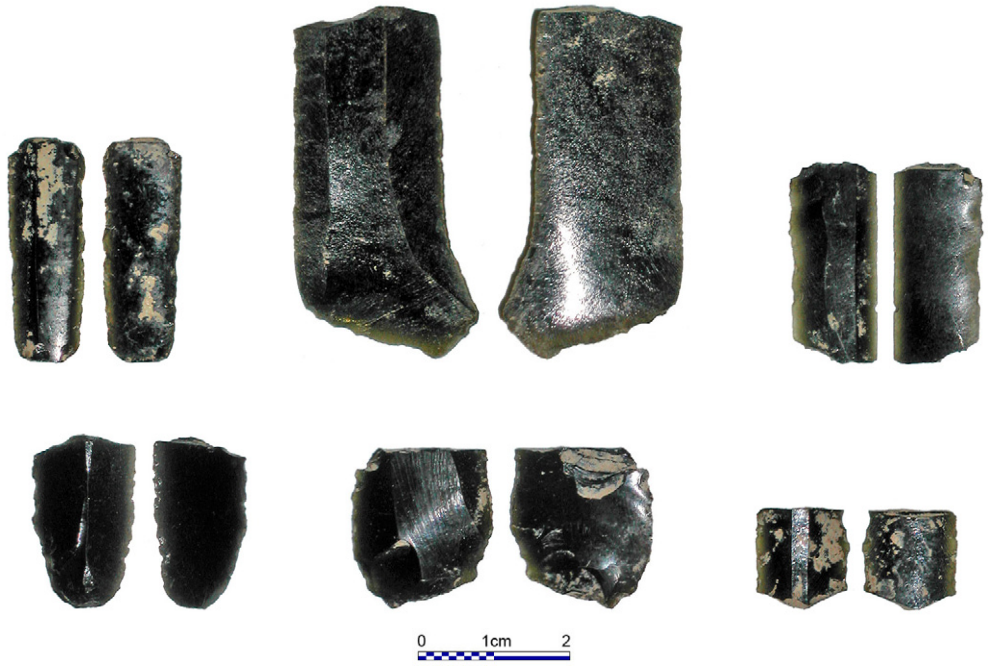


Figure B.24 - Examples of obsidian blade-tools (blades, segments, etc.) from J1.



Figure B.25 - Examples of obsidian blade-tools (blades, segments, etc.) from J3.



Figure B.26 - Examples of obsidian blade-tools (blades, segments, etc.) from J2.



Figure B.27 - Examples of chert blades from Unit A7 (Urkesh expedition photographs).



Figure B.28 - Examples of chert blades from Unit A9 (Urkesh expedition photographs).



Figure B.29 - Examples of chert blades from Unit A10 (Urkesh expedition photographs).

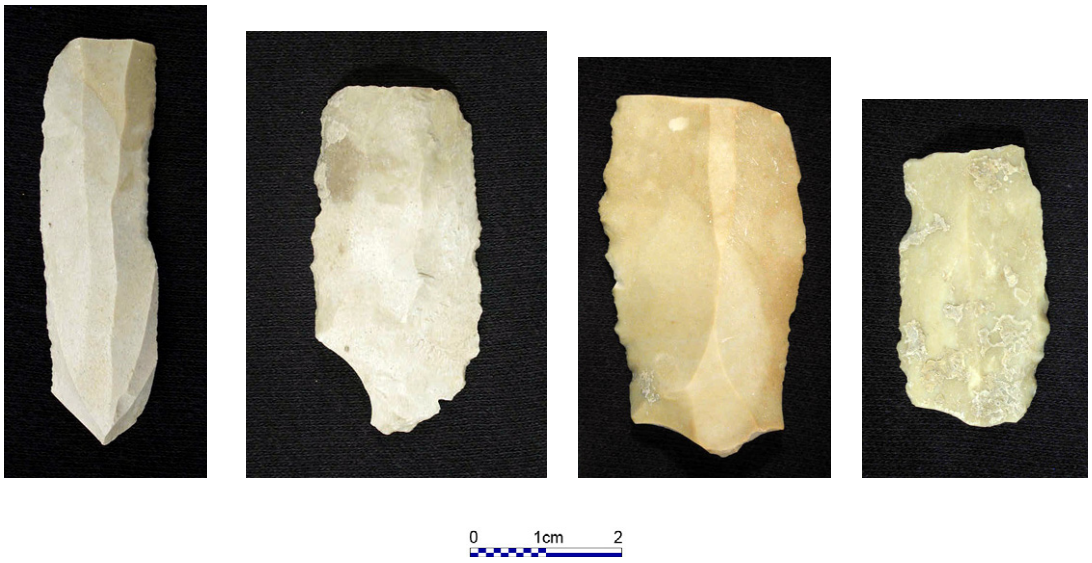


Figure B.30 - Examples of chert blades from Unit A14 (Urkesh expedition photographs).



Figure B.31 - Chert blades and a flake from Unit A2 (Urkesh expedition photographs).

Appendix C: Electron Microprobe Analysis Data of Geological Specimens and Artifacts

Table C.1 - Major-Element Analyses of Geological Specimens (mean of *n* analyses; weight percent)

Specimen	n	SiO_2	TiO_2	Al_2O3	Cr_2O_3	FeO(T)	MnO	MgO	CaO	Na_2O	K_2O	P_2O_5	F	SO_3	Cl	Total
AR01-E1	20	76.69	0.092	13.06	-	0.491	0.068	0.062	0.535	4.083	4.702	0.007	0.004	0.002	0.037	99.84
AR02-E1	20	76.91	0.084	13.11	-	0.359	0.074	0.050	0.513	4.172	4.639	0.008	0.002	0.001	0.041	99.96
AR03-E1	20	76.71	0.078	13.15	0.002	0.478	0.077	0.048	0.509	4.150	4.584	0.008	0.002	0.002	0.052	99.85
AR04-E1	10	76.62	0.082	13.02	0.001	0.438	0.073	0.055	0.528	4.186	4.757	0.007	0.006	0.001	0.044	99.82
AR04-E2	10	76.89	0.074	13.18	-	0.490	0.076	0.048	0.524	4.248	4.533	0.008	0.001	0.002	0.047	100.11
AR05-E1A	10	76.81	0.076	13.03	0.001	0.433	0.080	0.049	0.535	4.198	4.767	0.004	0.003	0.004	0.048	100.04
AR05-E1B	10	76.61	0.080	13.09	-	0.447	0.069	0.053	0.527	4.097	4.759	0.010	0.004	0.004	0.043	99.79
AR05-E1C	10	76.39	0.079	13.12	-	0.451	0.073	0.049	0.511	4.190	4.677	0.012	0.002	0.007	0.046	99.61
AR06-E1A	10	74.33	0.176	13.98	-	1.093	0.076	0.211	0.978	4.317	4.235	0.036	0.001	0.003	0.040	99.48
AR06-E1B	10	74.57	0.175	13.96	-	1.089	0.080	0.210	0.968	4.403	4.162	0.031	0.005	-	0.042	99.69
AR06-E1C	10	74.65	0.171	14.00	-	1.106	0.077	0.210	0.977	4.365	4.255	0.033	0.003	0.002	0.039	99.89
AR06-E2A	20	74.65	0.177	13.99	0.004	1.091	0.076	0.219	0.987	4.389	4.230	0.037	0.003	0.008	0.039	99.90
AR06-E2B	20	74.63	0.174	14.05	0.002	1.091	0.079	0.217	0.990	4.292	4.255	0.036	0.003	0.008	0.037	99.86
AR06-E2C	10	74.74	0.179	13.94	-	1.088	0.075	0.211	1.013	4.371	4.234	0.030	0.003	0.004	0.040	99.93
AR06-E3A	20	74.63	0.175	13.99	-	1.074	0.077	0.215	0.981	4.384	4.245	0.029	0.003	0.003	0.037	99.85
AR06-E3B	20	74.56	0.175	13.94	0.001	1.083	0.076	0.214	0.975	4.381	4.240	0.037	0.003	0.005	0.040	99.73
AR06-E3C	20	74.53	0.172	14.03	-	1.076	0.077	0.216	0.984	4.436	4.249	0.033	0.004	0.004	0.036	99.84
AR07-jB1	10	75.64	0.101	13.87	0.004	0.838	0.060	0.158	0.991	4.304	4.325	0.020	0.002	-	0.044	100.36
AR07-jB2	10	75.46	0.101	13.87	-	0.834	0.059	0.152	1.014	4.310	4.310	0.021	0.004	-	0.048	100.18
AR08-jB1	10	75.14	0.103	13.81	-	0.840	0.062	0.156	0.978	4.331	4.341	0.023	0.004	0.002	0.045	99.84
AR08-jB2	10	75.51	0.101	13.90	-	0.856	0.060	0.157	0.968	4.369	4.291	0.017	0.004	0.002	0.048	100.29
AR09-jB1	20	76.35	0.062	13.35	-	0.390	0.091	0.038	0.499	4.116	4.844	0.005	0.003	0.003	0.044	99.80
AR10-jB1	10	76.32	0.058	13.20	0.001	0.382	0.089	0.029	0.500	4.124	4.839	0.013	0.003	0.006	0.041	99.60
AR11-jB1	10	74.94	0.177	14.06	0.001	1.087	0.077	0.210	0.987	4.465	4.236	0.038	0.001	-	0.038	100.32
AR12-jB1	10	74.51	0.175	14.06	0.002	1.096	0.077	0.208	0.986	4.373	4.265	0.034	0.001	0.003	0.042	99.83
AR13-jB1	10	75.89	0.102	13.63	-	0.485	0.051	0.099	0.882	4.152	4.516	0.019	0.001	0.001	0.047	99.87
AR14-jB1	10	76.10	0.104	13.62	-	0.366	0.042	0.060	0.837	4.115	4.658	0.015	0.002	-	0.052	99.97
AR15-jB1	20	75.16	0.179	14.10	0.001	0.420	0.063	0.143	1.003	4.417	4.297	0.035	0.003	-	0.038	99.86
AR16-jB1	20	72.89	0.314	14.56	-	1.612	0.060	0.373	1.371	4.292	4.347	0.063	0.005	0.003	0.040	99.94

Table C.1 - Major-Element Analyses of Geological Specimens (mean of *n* analyses; weight percent)

Specimen	n	SiO_2	TiO_2	Al_2O3	Cr_2O_3	FeO(T)	MnO	MgO	CaO	Na_2O	K_2O	P_2O_5	F	SO_3	Cl	Total
AR17-jB1	20	72.71	0.316	14.48	0.003	1.638	0.060	0.368	1.371	4.229	4.379	0.065	0.003	-	0.041	99.66
AR18-avH1	20	76.61	0.090	12.90	-	0.575	0.066	0.064	0.535	4.007	4.602	0.010	0.003	0.005	0.045	99.51
AR19-avH1	20	76.99	0.090	13.01	-	0.332	0.063	0.059	0.534	4.090	4.700	0.012	0.003	0.004	0.042	99.93
AR20-avH1	10	76.85	0.091	12.97	-	0.406	0.061	0.058	0.533	4.060	4.752	0.013	0.003	0.002	0.041	99.85
AR21-avH1	10	74.73	0.175	13.93	0.001	1.071	0.081	0.200	0.968	4.341	4.267	0.036	0.001	0.003	0.038	99.85
AR22-avH1	10	74.72	0.174	13.78	-	1.075	0.083	0.202	0.971	4.351	4.275	0.035	0.002	0.001	0.036	99.70
AR23-ipS1	10	75.27	0.056	13.14	-	0.442	0.101	0.049	0.513	4.174	4.427	0.010	0.002	0.002	0.019	98.21
AR23-jfL1	10	75.51	0.058	13.24	0.001	0.443	0.099	0.050	0.511	4.207	4.528	0.008	0.003	0.011	0.021	98.69
AR24-ipS1	10	74.76	0.170	13.86	-	0.970	0.079	0.198	0.930	4.298	4.277	0.034	0.003	-	0.040	99.62
AR24-jfL1	10	75.03	0.175	14.01	-	0.932	0.069	0.185	0.948	4.382	4.329	0.037	0.003	0.005	0.038	100.14
AR25-ipS1	10	75.88	0.059	13.27	0.001	0.442	0.104	0.050	0.490	4.216	4.614	0.007	-	0.004	0.015	99.15
AR25-jfL1	20	76.15	0.061	13.33	0.001	0.342	0.107	0.051	0.405	4.063	5.011	0.006	0.002	0.001	0.020	99.55
AR26-ipS1	10	76.12	0.062	12.95	0.002	0.453	0.077	0.039	0.567	4.200	4.500	-	0.001	0.001	0.042	99.02
AR26-jfL1	20	76.05	0.062	12.98	-	0.467	0.081	0.040	0.570	4.205	4.528	0.002	0.002	0.001	0.045	99.03
AR27-ipS1	10	75.50	0.101	13.82	0.002	0.408	0.052	0.088	0.951	4.319	4.316	0.021	-	-	0.042	99.62
AR27-jfL1	20	75.23	0.104	13.82	-	0.420	0.052	0.087	0.953	4.281	4.365	0.022	0.003	-	0.047	99.38
AR28-ipS1	10	74.83	0.145	14.15	0.001	0.594	0.050	0.188	1.159	4.302	4.333	0.047	0.002	-	0.045	99.84
AR29-ipS1	10	75.46	0.106	13.59	0.003	0.538	0.055	0.116	0.744	4.236	4.577	0.018	0.001	0.003	0.033	99.47
AR30-ipS1	10	74.19	0.170	13.86	-	1.079	0.075	0.210	0.957	4.303	4.275	0.035	0.003	-	0.036	99.20
AR30-jfL1	20	74.74	0.172	13.93	-	1.079	0.077	0.198	0.986	4.421	4.280	0.031	0.004	0.007	0.039	99.96
AR31-ipS1	10	76.02	0.055	13.13	-	0.437	0.091	0.043	0.483	4.346	4.312	0.008	-	0.003	0.042	98.97
AR31-jfL1	20	76.04	0.057	13.25	-	0.450	0.092	0.043	0.508	4.386	4.425	0.003	0.003	0.004	0.044	99.30
AR32-ipS1	10	76.73	0.072	13.10	-	0.376	0.078	0.047	0.468	4.205	4.381	0.009	0.003	-	0.047	99.51
AR32-jfL1	20	76.73	0.076	13.13	0.001	0.426	0.079	0.046	0.457	4.259	4.644	0.009	0.002	0.006	0.049	99.92
AR33-ipS1	10	77.03	0.089	12.84	0.002	0.627	0.058	0.052	0.490	4.216	4.786	0.001	0.001	-	0.067	100.26
AR33-ipS2A	10	76.86	0.096	12.77	-	0.632	0.057	0.048	0.492	4.182	4.652	0.001	0.002	0.003	0.070	99.87
AR33-ipS2B	10	76.74	0.094	12.76	-	0.615	0.058	0.049	0.486	4.199	4.739	0.004	-	0.001	0.066	99.81
AR33-ipS2C	10	76.82	0.100	12.75	-	0.615	0.055	0.047	0.482	4.232	4.761	0.006	0.001	-	0.063	99.93
AR34-ipS1	10	76.74	0.090	12.64	-	0.600	0.054	0.043	0.464	4.091	4.725	0.004	0.003	-	0.066	99.52

Table C.1 - Major-Element Analyses of Geological Specimens (mean of *n* analyses; weight percent)

Specimen	n	SiO_2	TiO_2	Al_2O3	Cr_2O_3	FeO(T)	MnO	MgO	CaO	Na_2O	K_2O	P_2O_5	F	SO_3	Cl	Total
AR35-ipS1A	10	76.83	0.097	12.75	-	0.608	0.054	0.045	0.491	4.154	4.621	0.005	0.002	0.002	0.064	99.72
AR35-ipS1B	10	76.67	0.098	12.61	0.002	0.594	0.047	0.049	0.492	4.140	4.771	0.004	0.001	0.005	0.071	99.55
AR35-ipS1C	10	76.50	0.092	12.39	0.004	0.629	0.057	0.049	0.496	4.182	4.760	0.003	0.003	0.002	0.069	99.23
AR36-ipS1A	10	76.78	0.085	12.74	0.001	0.531	0.060	0.032	0.444	4.288	4.710	-	0.003	-	0.069	99.74
AR36-ipS1B	20	76.35	0.084	12.65	-	0.537	0.055	0.033	0.440	4.291	4.663	0.002	0.002	0.004	0.071	99.18
AR36-ipS1C	20	76.35	0.083	12.70	-	0.546	0.059	0.035	0.438	4.286	4.683	0.002	0.002	0.004	0.069	99.26
AR37-ipS1A	20	76.68	0.082	12.51	-	0.482	0.051	0.040	0.495	3.913	4.873	0.001	0.002	0.002	0.048	99.18
AR37-ipS1B	20	76.95	0.082	12.50	0.001	0.475	0.054	0.039	0.487	3.993	4.861	0.002	0.001	-	0.047	99.49
AR37-ipS1C	20	77.02	0.079	12.58	0.001	0.466	0.054	0.037	0.490	3.995	4.882	0.002	0.004	0.004	0.048	99.66
AR37-ipS2A	10	77.04	0.082	12.38	-	0.442	0.053	0.037	0.486	4.005	4.614	-	0.003	0.004	0.038	99.19
AR37-ipS2B	10	76.91	0.079	12.66	0.002	0.494	0.054	0.039	0.500	3.963	4.849	0.001	0.002	0.003	0.049	99.61
AR37-ipS2C	10	76.90	0.083	12.64	-	0.468	0.051	0.043	0.502	3.925	4.810	0.001	0.002	0.004	0.042	99.47
AR38-ipS1A	10	76.57	0.071	12.64	0.004	0.450	0.072	0.025	0.453	4.159	4.843	0.006	0.004	0.004	0.069	99.37
AR38-ipS1B	10	76.54	0.065	12.50	-	0.449	0.070	0.027	0.472	4.195	4.816	0.008	0.005	-	0.068	99.22
AR38-ipS1C	10	76.56	0.072	12.59	0.002	0.418	0.065	0.023	0.448	4.191	4.852	-	0.004	0.002	0.067	99.29
AR39-ipS1	10	75.86	0.059	13.11	-	0.444	0.093	0.044	0.489	4.213	4.414	0.006	0.002	-	0.041	98.77
AR40-rlS1	10	74.48	0.178	14.19	0.001	1.102	0.074	0.210	0.997	4.454	4.262	0.036	0.003	0.004	0.041	100.04
AR41-sK1	10	76.44	0.077	13.16	-	0.471	0.077	0.049	0.512	4.257	4.631	0.011	0.001	0.002	0.041	99.73
AR41-sK2	10	76.47	0.075	13.09	-	0.471	0.074	0.049	0.515	4.181	4.594	0.009	0.004	0.001	0.041	99.58
AR42-kM1	10	76.37	0.080	12.86	0.002	0.458	0.072	0.055	0.522	4.203	4.651	0.007	0.002	0.005	0.037	99.33
AR42-kM2	10	76.27	0.085	12.88	-	0.476	0.070	0.053	0.509	4.156	4.671	0.007	0.001	0.002	0.040	99.22
AR43-kM1	10	75.69	0.115	13.52	-	0.524	0.050	0.101	0.743	4.244	4.617	0.018	0.003	-	0.040	99.67
AR44-sK1	10	75.28	0.180	14.24	0.001	0.373	0.057	0.116	0.970	4.525	4.288	0.038	0.001	0.003	0.043	100.12
AR45-kM1	10	75.14	0.175	14.16	0.001	0.649	0.075	0.194	0.972	4.499	4.288	0.036	0.005	0.004	0.033	100.23
AR46-sK1	10	74.81	0.180	14.21	-	0.929	0.065	0.157	0.969	4.488	4.218	0.034	0.003	0.006	0.041	100.11
AR47-kM1	20	73.89	0.174	13.88	0.001	1.042	0.068	0.190	0.970	4.450	4.253	0.032	0.006	0.003	0.039	99.00
AR47-kM2	20	73.70	0.171	13.84	0.001	1.072	0.078	0.210	0.977	4.370	4.178	0.031	0.006	0.006	0.038	98.68
AR47-kM3	20	74.10	0.175	13.96	0.001	1.050	0.073	0.193	0.968	4.460	4.180	0.033	0.005	0.002	0.042	99.24
AR47-kM4	20	73.93	0.177	13.94	0.001	1.070	0.080	0.210	0.993	4.448	4.186	0.030	0.004	0.007	0.039	99.11

Table C.1 - Major-Element Analyses of Geological Specimens (mean of *n* analyses; weight percent)

Specimen	n	SiO_2	TiO_2	Al_2O3	Cr_2O_3	FeO(T)	MnO	MgO	CaO	Na_2O	K_2O	P_2O_5	F	SO_3	Cl	Total
AR47-kM5	20	74.08	0.174	13.93	0.005	1.032	0.074	0.190	0.970	4.433	4.204	0.032	0.003	0.007	0.041	99.17
AR48-sK1	10	74.76	0.130	14.13	-	0.868	0.050	0.167	1.082	4.018	4.839	0.032	0.002	0.005	0.044	100.12
AR49-sK1	10	77.84	0.139	12.08	-	0.456	0.075	0.046	0.312	3.355	5.310	0.035	0.002	-	0.042	99.69
AR50-sK1	10	75.42	0.168	13.98	-	0.984	0.082	0.168	0.891	4.468	4.382	0.036	0.005	0.004	0.043	100.63
AR50-sK2	10	75.47	0.167	13.78	0.001	0.978	0.077	0.181	0.893	4.352	4.339	0.035	0.005	0.004	0.040	100.32
AR51-sK1	10	76.81	0.064	13.04	-	0.471	0.075	0.042	0.573	4.170	4.612	0.009	0.004	-	0.043	99.91
AR52-sK1	10	76.81	0.064	13.11	-	0.452	0.079	0.041	0.567	4.269	4.691	0.004	-	-	0.047	100.13
AR53-kM1	10	76.73	0.121	13.26	0.002	0.771	0.075	0.117	0.708	4.218	4.578	0.016	0.003	0.003	0.035	100.64
AR54-kM1	10	77.34	0.065	13.23	-	0.430	0.085	0.043	0.559	4.403	4.561	0.005	0.002	0.003	0.041	100.76
AR55-sK1	10	77.01	0.063	13.20	-	0.469	0.074	0.040	0.576	4.315	4.510	0.004	0.002	-	0.049	100.31
AR56-sK1	10	77.28	0.085	12.85	-	0.509	0.058	0.029	0.446	4.128	4.761	0.005	0.002	0.004	0.072	100.23
AR57-sK1	10	77.11	0.092	12.70	0.002	0.637	0.056	0.045	0.478	4.177	4.833	0.006	0.005	0.002	0.075	100.21
AR58-sK1	10	77.40	0.060	12.72	0.001	0.361	0.060	0.009	0.403	4.046	5.062	-	0.003	0.004	0.068	100.20
AR59-kM1	10	75.80	0.101	13.91	0.003	0.542	0.057	0.142	1.002	4.340	4.396	0.020	0.003	-	0.045	100.36
AR60-sK1	30	75.48	0.109	13.66	-	0.796	0.059	0.120	0.778	4.422	4.442	0.012	0.003	0.002	0.066	99.95
AR61-sK1	30	77.14	0.078	12.62	0.001	0.404	0.056	0.037	0.481	4.117	4.665	0.004	0.002	0.001	0.054	99.66
AR62-sK1	30	73.12	0.314	14.59	-	1.224	0.043	0.223	1.209	4.327	4.427	0.068	0.005	0.002	0.040	99.60
AR63-kM1	30	73.08	0.311	14.64	-	1.187	0.051	0.296	1.290	4.419	4.473	0.071	0.004	0.006	0.041	99.87
AR64-sK1	30	75.26	0.140	14.04	0.001	0.376	0.042	0.119	0.912	4.464	4.490	0.019	0.003	0.009	0.074	99.95
AR65-E1	10	75.07	0.181	14.14	0.005	0.952	0.066	0.177	0.990	4.353	4.220	0.028	0.005	0.004	0.041	100.24
AR66-rB1	20	73.05	0.314	14.54	-	1.200	0.055	0.323	1.395	4.390	4.484	0.067	0.003	0.004	0.037	99.86
AR66-rB2	20	72.85	0.317	14.51	0.003	1.622	0.064	0.356	1.330	4.405	4.367	0.064	0.004	0.003	0.045	99.94
AR67-rB1	10	76.38	0.055	13.29	0.003	0.342	0.090	0.037	0.487	4.160	4.758	0.005	-	0.006	0.045	99.66
AR67-rB2	10	76.39	0.061	13.16	-	0.381	0.089	0.039	0.498	4.094	4.726	0.006	0.002	0.005	0.041	99.49
AR67-rB3	10	76.43	0.060	13.24	0.001	0.363	0.095	0.028	0.477	4.090	4.906	0.009	0.003	0.004	0.041	99.74
AR68-rB1	10	76.73	0.083	12.98	0.001	0.540	0.070	0.051	0.522	4.122	4.652	0.012	0.004	0.007	0.044	99.82
AR68-rB2	10	77.02	0.078	13.06	-	0.525	0.073	0.051	0.516	4.153	4.578	0.010	-	0.002	0.048	100.11
AR68-rB3	10	76.75	0.070	13.08	0.004	0.356	0.074	0.048	0.475	4.125	4.747	0.003	-	0.004	0.041	99.78
AR68-rB4	10	76.58	0.080	13.05	-	0.369	0.068	0.042	0.467	4.090	4.740	0.004	0.002	0.005	0.038	99.54

Table C.1 - Major-Element Analyses of Geological Specimens (mean of *n* analyses; weight percent)

Specimen	n	SiO_2	TiO_2	Al_2O3	Cr_2O_3	FeO(T)	MnO	MgO	CaO	Na_2O	K_2O	P_2O_5	F	SO_3	Cl	Total
AR68-rB5	10	76.56	0.094	12.99	-	0.500	0.070	0.059	0.508	4.073	4.667	0.009	0.002	-	0.048	99.58
AR68-rB6	10	76.48	0.080	12.91	-	0.481	0.074	0.051	0.455	3.961	4.888	0.007	0.003	-	0.041	99.43
AR68-rB7	10	76.49	0.081	13.02	-	0.573	0.072	0.053	0.467	4.026	4.709	0.007	0.002	-	0.049	99.55
AR69-rB1	10	75.75	0.102	13.58	0.001	0.568	0.052	0.106	0.879	4.137	4.481	0.011	0.003	0.003	0.049	99.72
AR69-rB2	10	75.75	0.101	13.57	-	0.520	0.050	0.103	0.888	4.084	4.531	0.017	0.005	0.003	0.055	99.68
AR69-rB3	10	75.53	0.106	13.66	-	0.356	0.050	0.094	0.856	4.072	4.571	0.014	0.001	0.002	0.057	99.37
AR70-rB1	10	75.57	0.111	13.72	-	0.517	0.050	0.116	0.753	4.327	4.533	0.011	0.003	0.002	0.064	99.78
AR70-rB2	10	75.59	0.106	13.74	-	0.510	0.050	0.115	0.738	4.265	4.471	0.018	0.002	0.002	0.032	99.64
AR71-rB1	10	75.37	0.144	14.02	-	0.502	0.045	0.141	0.906	4.471	4.506	0.021	0.004	0.003	0.082	100.22
AR72-rB1	10	74.61	0.159	13.93	-	0.546	0.057	0.201	0.993	4.355	4.446	0.033	0.005	0.003	0.028	99.36
AR72-rB2	10	74.51	0.128	14.07	0.004	0.671	0.052	0.230	1.205	4.241	4.297	0.034	0.003	0.003	0.051	99.49
AR72-rB3	10	74.87	0.089	13.80	0.002	0.735	0.062	0.126	0.848	4.181	4.557	0.013	0.001	0.005	0.049	99.33
AR73-rB1	10	75.52	0.100	13.70	-	0.846	0.054	0.151	0.980	4.235	4.299	0.025	0.003	0.002	0.049	99.96
AR74-rB1	10	74.92	0.092	13.79	-	0.633	0.059	0.151	0.948	4.237	4.393	0.018	0.002	0.011	0.042	99.29
AR74-rB2	10	74.71	0.092	13.78	-	0.822	0.058	0.151	0.942	4.237	4.373	0.022	0.003	0.014	0.044	99.25
AR75-rB1	10	76.84	0.062	13.46	0.007	0.455	0.096	0.039	0.492	4.470	4.360	0.002	0.002	0.001	0.041	100.33
AR76-rB1	10	74.71	0.171	14.04	0.002	0.857	0.073	0.211	0.994	4.481	4.261	0.031	0.002	0.004	0.039	99.87
AR76-rB2	10	74.35	0.173	14.11	-	1.094	0.077	0.219	0.986	4.436	4.235	0.035	0.002	0.005	0.037	99.76
AR76-rB3	10	74.47	0.171	14.01	-	1.083	0.071	0.211	0.953	4.472	4.271	0.028	0.002	-	0.040	99.78
AR77-rB1	10	74.86	0.175	14.17	-	0.416	0.050	0.066	0.859	4.371	4.598	0.029	0.004	0.002	0.037	99.64
AR77-rB2	10	74.98	0.174	14.03	-	0.528	0.063	0.109	0.905	4.563	4.330	0.027	0.004	0.001	0.037	99.76
AR77-rB3	20	74.53	0.172	14.06	-	0.731	0.062	0.199	1.028	4.484	4.273	0.030	0.003	0.002	0.031	99.61
AR78-rB1	20	74.86	0.178	14.09	-	0.339	0.060	0.133	0.976	4.479	4.365	0.032	0.003	0.003	0.033	99.55
AR78-rB2	20	75.02	0.176	14.14	0.003	0.451	0.062	0.139	0.932	4.184	4.958	0.030	0.005	0.003	0.036	100.15
AR78-rB3	20	74.91	0.178	14.18	-	0.486	0.063	0.139	0.958	4.510	4.487	0.029	0.004	0.004	0.032	99.98
AR79-rB1	20	76.52	0.067	13.22	-	0.462	0.084	0.040	0.565	4.325	4.433	0.005	0.003	0.002	0.040	99.77
AR79-rB2	10	76.72	0.064	13.11	-	0.391	0.080	0.040	0.568	4.218	4.605	0.003	0.004	0.003	0.054	99.86
AR79-rB3	10	76.03	0.066	13.08	-	0.462	0.082	0.041	0.564	4.250	4.490	0.003	0.003	0.002	0.044	99.12
AR80-rB1	20	77.46	0.083	12.92	-	0.404	0.053	0.018	0.406	4.319	4.656	0.004	0.004	-	0.068	100.39

Table C.1 - Major-Element Analyses of Geological Specimens (mean of *n* analyses; weight percent)

Specimen	n	SiO_2	TiO_2	Al_2O3	Cr_2O_3	FeO(T)	MnO	MgO	CaO	Na_2O	K_2O	P_2O_5	F	SO_3	Cl	Total
AR81-rB1	20	76.74	0.088	12.80	-	0.595	0.056	0.041	0.467	4.143	4.723	0.003	0.002	0.002	0.068	99.73
AR81-rB2	20	76.94	0.090	12.73	0.001	0.547	0.060	0.042	0.468	4.104	4.754	0.002	0.001	0.002	0.056	99.80
AR81-rB3	20	76.98	0.089	12.86	-	0.572	0.054	0.045	0.469	4.151	4.838	0.001	0.005	0.001	0.062	100.13
AR82-rB1	20	76.93	0.061	12.74	0.002	0.311	0.054	0.008	0.419	4.093	4.790	0.001	0.002	0.003	0.070	99.48
AR82-rB2	20	77.23	0.062	12.73	-	0.391	0.066	0.032	0.463	4.233	4.727	0.002	0.004	0.001	0.058	100.00
AR82-rB3	20	77.19	0.064	12.78	-	0.358	0.060	0.017	0.435	4.170	4.827	0.003	0.003	0.003	0.072	99.98
AZ01-jB1	20	76.92	0.068	12.90	-	0.519	0.071	0.033	0.430	4.375	4.508	-	0.003	0.002	0.056	99.89
AZ02-kM1	20	77.30	0.097	12.61	-	0.674	0.062	0.049	0.409	4.016	4.820	0.004	0.001	0.003	0.051	100.09
AZ03-kM1	20	77.03	0.095	12.66	-	0.665	0.060	0.048	0.459	4.168	4.710	0.003	0.002	0.003	0.059	99.97
AZ04-kM1	20	76.87	0.096	12.58	-	0.653	0.057	0.048	0.443	3.894	5.112	-	0.003	-	0.042	99.79
CA01-P1	10	75.92	0.026	12.54	-	0.754	0.073	0.012	0.379	4.230	4.310	0.002	0.004	-	0.073	98.33
CA01-R1	10	75.36	0.073	12.94	0.001	0.912	0.051	0.067	0.764	4.100	4.873	0.008	0.001	0.001	0.124	99.27
CA02-P1	10	74.95	0.090	13.15	-	1.107	0.057	0.099	0.788	4.328	4.651	0.015	0.003	-	0.125	99.36
CA02-R1-A	10	76.12	0.029	12.57	-	0.772	0.070	0.012	0.409	4.129	4.359	-	0.003	0.002	0.080	98.55
CA02-R1-B	10	76.16	0.030	12.60	-	0.762	0.074	0.012	0.409	4.028	4.303	0.008	0.001	-	0.081	98.46
CA03-P1	10	75.41	0.078	13.16	-	0.980	0.055	0.070	0.761	4.118	4.704	0.009	0.004	0.004	0.120	99.47
CA03-R1-A	10	75.58	0.077	13.15	-	0.975	0.054	0.069	0.767	3.911	4.534	0.008	0.003	0.002	0.118	99.25
CA03-R1-B	10	75.96	0.082	13.16	-	0.905	0.051	0.066	0.746	4.023	4.523	0.008	0.002	0.003	0.126	99.65
CA03-R2	10	75.79	0.080	13.13	0.001	0.903	0.052	0.064	0.731	4.158	4.811	0.008	-	-	0.129	99.86
CA04-P1	10	75.35	0.077	13.01	0.001	0.728	0.050	0.061	0.758	3.361	5.944	0.003	-	0.002	0.100	99.45
CA04-R1-A	10	75.48	0.075	13.05	0.004	0.610	0.047	0.058	0.730	2.957	6.030	0.002	0.006	-	0.102	99.15
CA04-R1-B	10	75.46	0.083	13.12	0.001	0.532	0.047	0.064	0.731	2.965	6.038	0.008	0.003	0.006	0.105	99.16
CA04-R1-C	10	75.63	0.083	13.05	-	0.629	0.045	0.057	0.728	3.031	5.961	0.010	0.003	0.004	0.092	99.31
CA04-R1-D	10	75.60	0.081	13.12	0.001	0.582	0.049	0.059	0.745	3.022	5.962	0.011	0.001	-	0.096	99.33
CA04-R2-A	10	75.53	0.075	13.04	-	0.452	0.044	0.056	0.723	2.942	6.077	0.007	0.001	-	0.100	99.04
CA04-R2-B	10	75.58	0.076	13.05	0.001	0.551	0.046	0.060	0.733	2.971	6.046	0.007	0.001	0.002	0.113	99.23
CA04-R2-C	10	75.72	0.074	13.13	-	0.535	0.052	0.063	0.772	3.107	5.870	0.002	0.006	-	0.103	99.43
CA04-R2-D	10	75.59	0.080	13.03	-	0.513	0.045	0.055	0.727	3.062	6.041	0.010	0.004	0.007	0.096	99.26
CA04-R2-E	10	75.57	0.081	12.90	-	0.642	0.050	0.066	0.727	3.056	6.018	0.008	0.003	0.007	0.099	99.23

Table C.1 - Major-Element Analyses of Geological Specimens (mean of *n* analyses; weight percent)

Specimen	n	SiO_2	TiO_2	Al_2O3	Cr_2O_3	FeO(T)	MnO	MgO	CaO	Na_2O	K_2O	P_2O_5	F	SO_3	Cl	Total
CA04-R2-F	10	75.71	0.076	12.96	-	0.650	0.048	0.060	0.756	3.070	5.958	0.004	0.001	0.007	0.104	99.41
CA05-P1	10	75.57	0.094	13.41	-	0.971	0.051	0.061	0.742	4.272	4.520	0.015	0.002	-	0.126	99.83
CA05-P2	10	75.53	0.093	13.40	0.002	0.962	0.049	0.055	0.729	4.330	4.523	0.014	0.001	0.002	0.125	99.81
CA05-P3	10	75.38	0.087	13.32	-	0.968	0.052	0.059	0.736	4.129	4.565	0.009	0.003	0.005	0.125	99.44
CA05-R1-A	10	75.51	0.091	13.31	0.001	1.010	0.051	0.066	0.750	4.323	4.583	0.012	0.004	0.004	0.130	99.84
CA05-R1-B	10	75.59	0.092	13.21	-	0.977	0.049	0.051	0.725	4.238	4.613	0.016	0.004	-	0.133	99.70
CA05-R1-C	10	75.60	0.094	13.47	-	0.976	0.054	0.059	0.755	4.221	4.554	0.015	0.005	0.002	0.126	99.93
CA05-R2-A	10	75.26	0.090	13.33	-	1.062	0.054	0.064	0.772	4.209	4.550	0.012	-	0.003	0.138	99.55
CA05-R2-B	10	75.61	0.089	13.49	-	1.016	0.056	0.075	0.766	4.257	4.567	0.018	0.005	-	0.129	100.07
CA05-R3-A	10	75.16	0.092	13.39	0.001	1.074	0.055	0.078	0.770	4.089	4.614	0.016	0.008	0.004	0.133	99.49
CA05-R3-B	10	75.21	0.091	13.50	0.001	1.060	0.060	0.082	0.775	4.101	4.654	0.010	0.006	0.005	0.127	99.68
CA05-R3-C	10	75.34	0.090	13.47	-	1.079	0.053	0.073	0.766	4.232	4.601	0.018	0.003	0.001	0.134	99.87
CA05-R4A	10	75.48	0.092	13.46	-	1.163	0.059	0.089	0.764	4.076	4.608	0.019	0.003	-	0.127	99.93
CA05-R4B	10	75.26	0.096	13.35	-	1.181	0.055	0.092	0.764	4.074	4.617	0.015	0.002	-	0.121	99.63
CA05-R4C	10	75.34	0.097	13.44	-	1.146	0.055	0.085	0.747	4.177	4.595	0.013	0.002	-	0.125	99.82
CA05-R4D	10	75.74	0.099	13.49	-	1.155	0.060	0.090	0.750	4.172	4.623	0.014	0.002	0.002	0.133	100.33
CA05-R4E	10	75.06	0.105	13.30	-	1.142	0.053	0.086	0.751	4.011	4.607	0.016	0.004	0.006	0.127	99.26
CA05-R5A	10	74.68	0.097	13.57	-	1.147	0.058	0.088	0.742	3.975	4.475	0.017	0.002	-	0.124	98.97
CA05-R5B	10	74.43	0.095	13.46	0.004	1.094	0.059	0.093	0.766	4.072	4.498	0.014	0.002	0.001	0.125	98.71
CA05-R5C	10	75.09	0.096	13.54	0.001	1.066	0.056	0.077	0.742	4.192	4.641	0.018	0.002	0.001	0.121	99.64
CA05-R5D	10	74.84	0.092	13.52	0.003	1.157	0.052	0.083	0.741	4.112	4.651	0.015	0.001	-	0.127	99.39
CA05-R5E	10	74.92	0.090	13.54	-	1.038	0.052	0.076	0.750	4.178	4.599	0.012	0.004	0.003	0.119	99.38
CA06-P1	10	75.56	0.073	13.10	0.001	0.858	0.054	0.065	0.749	3.798	4.675	0.007	0.005	-	0.117	99.06
CA06-P2	10	75.92	0.068	13.17	0.002	0.923	0.049	0.069	0.757	3.928	4.617	0.009	0.002	-	0.123	99.64
CA06-P3	10	76.05	0.079	13.22	-	0.895	0.045	0.065	0.748	4.019	4.606	0.007	0.001	-	0.113	99.84
CA06-P4	10	75.83	0.075	13.14	-	0.899	0.055	0.068	0.759	4.017	4.621	0.008	-	0.001	0.113	99.59
CA06-P5-A	10	75.65	0.073	13.12	-	0.871	0.054	0.070	0.755	3.973	4.622	0.005	0.003	0.003	0.125	99.33
CA06-P5-B	10	75.53	0.077	13.06	-	0.849	0.047	0.069	0.749	4.125	4.613	0.011	0.001	0.002	0.115	99.24
CA06-P5-C	10	75.50	0.076	13.12	0.007	0.868	0.052	0.073	0.758	4.167	4.573	0.005	0.004	0.001	0.120	99.32

Table C.1 - Major-Element Analyses of Geological Specimens (mean of *n* analyses; weight percent)

Specimen	n	SiO_2	TiO_2	Al_2O3	Cr_2O_3	FeO(T)	MnO	MgO	CaO	Na_2O	K_2O	P_2O_5	F	SO_3	Cl	Total
CA06-P6	10	76.02	0.073	13.24	-	0.927	0.055	0.066	0.756	4.043	4.624	0.008	0.004	-	0.113	99.92
CA06-P7-A	10	75.19	0.077	13.14	-	0.877	0.049	0.068	0.760	4.054	4.579	0.006	0.004	-	0.121	98.92
CA06-P7-B	10	75.81	0.077	13.14	-	0.831	0.046	0.065	0.726	4.168	4.622	0.013	0.006	0.002	0.118	99.62
CA06-P8-A	10	75.89	0.078	13.32	-	0.922	0.053	0.066	0.773	3.923	4.547	0.011	0.002	0.001	0.120	99.71
CA06-P8-B	10	75.62	0.074	13.29	-	0.926	0.052	0.067	0.763	4.077	4.602	0.003	0.001	-	0.126	99.61
CA06-R1	10	75.72	0.073	13.22	-	0.928	0.051	0.067	0.760	4.072	4.601	0.005	0.003	0.001	0.131	99.63
CA06-R2-A	10	75.79	0.074	13.19	0.001	0.871	0.051	0.065	0.765	4.134	4.544	0.011	0.005	-	0.122	99.62
CA06-R2-B	10	75.72	0.076	13.26	-	0.950	0.055	0.066	0.787	3.946	4.569	0.006	0.002	0.003	0.126	99.56
CA06-R3-A	10	75.70	0.077	13.16	-	0.855	0.050	0.070	0.752	4.197	4.604	0.007	0.003	0.001	0.149	99.63
CA06-R3-B	10	75.74	0.075	13.15	-	0.814	0.047	0.064	0.738	3.843	4.925	0.004	-	-	0.123	99.53
CA07-P1	10	74.49	0.128	13.92	-	1.374	0.062	0.141	0.975	4.372	4.340	0.022	0.004	-	0.114	99.95
CA07-R1	10	74.69	0.127	13.86	0.001	1.015	0.044	0.048	0.896	4.006	4.505	0.028	0.002	-	0.132	99.36
CA07-R2-A	10	74.46	0.130	13.88	-	0.970	0.044	0.054	0.890	4.317	4.566	0.025	0.003	-	0.144	99.48
CA07-R2-B	10	74.65	0.128	13.88	-	0.940	0.043	0.047	0.867	4.360	4.567	0.020	0.002	0.003	0.141	99.64
CA08-P1	10	76.22	0.026	12.63	-	0.797	0.067	0.015	0.410	4.053	4.379	0.002	0.003	-	0.087	98.69
CA08-P2	10	76.08	0.025	12.58	0.003	0.736	0.065	0.012	0.381	4.217	4.219	0.003	0.002	0.002	0.079	98.40
CA08-R1-A	10	74.28	0.126	13.63	-	1.157	0.045	0.087	0.868	4.296	4.471	0.023	0.008	-	0.142	99.13
CA08-R1-B	10	74.21	0.121	13.57	0.003	1.227	0.054	0.107	0.895	4.321	4.451	0.026	0.003	0.002	0.139	99.12
CA08-R1-C	10	74.12	0.125	13.68	-	1.166	0.041	0.086	0.908	4.401	4.434	0.026	0.002	0.001	0.143	99.13
CA08-R1-D	10	74.13	0.124	13.74	-	1.252	0.064	0.119	0.908	4.463	4.423	0.023	0.003	0.002	0.139	99.39
CA09-P1	10	76.70	0.027	12.48	-	0.755	0.072	0.012	0.382	4.134	4.398	0.003	0.001	-	0.074	99.04
CA09-P2	10	75.87	0.028	12.53	-	0.757	0.072	0.011	0.390	4.161	4.424	0.001	0.004	-	0.077	98.32
CA09-P3	10	76.33	0.029	12.61	0.001	0.773	0.068	0.012	0.390	4.250	4.437	0.003	0.003	-	0.075	98.98
CA09-R1	10	75.98	0.072	12.92	-	0.451	0.046	0.052	0.732	2.997	6.041	0.008	-	-	0.114	99.41
CA09-R2-A	10	76.24	0.025	12.58	-	0.772	0.071	0.011	0.384	4.373	4.370	0.004	0.003	0.005	0.073	98.91
CA09-R2-B	10	76.27	0.026	12.64	-	0.765	0.073	0.012	0.390	4.294	4.403	0.004	0.002	-	0.072	98.96
CA09-R2-C	10	76.39	0.026	12.53	0.001	0.773	0.068	0.013	0.392	4.115	4.461	0.003	0.004	-	0.072	98.85
CA09-R2-D	10	76.62	0.028	12.58	-	0.759	0.067	0.013	0.387	4.194	4.425	-	0.001	0.006	0.080	99.16
CA10-P1	10	76.47	0.024	12.53	-	0.765	0.069	0.012	0.417	4.223	4.452	-	0.002	-	0.087	99.05

Table C.1 - Major-Element Analyses of Geological Specimens (mean of *n* analyses; weight percent)

Specimen	n	SiO_2	TiO_2	Al_2O3	Cr_2O_3	FeO(T)	MnO	MgO	CaO	Na_2O	K_2O	P_2O_5	F	SO_3	Cl	Total
CA10-R1-A	10	76.00	0.033	12.44	-	0.788	0.074	0.014	0.404	4.109	4.400	0.003	0.003	-	0.086	98.35
CA10-R1-B	10	75.89	0.028	12.46	0.001	0.777	0.065	0.015	0.406	4.091	4.435	-	0.005	-	0.089	98.27
CA10-R1-C	10	75.87	0.027	12.52	0.002	0.784	0.066	0.015	0.401	4.111	4.402	-	0.003	-	0.087	98.29
CA10-R2	10	76.07	0.027	12.52	-	0.782	0.069	0.014	0.395	4.150	4.368	-	0.003	-	0.085	98.49
CA11-P1	10	76.54	0.030	12.64	-	0.753	0.061	0.012	0.381	4.138	4.484	0.007	0.003	-	0.069	99.12
CA11-P2	10	76.34	0.025	12.60	-	0.755	0.069	0.013	0.383	4.155	4.472	0.004	0.002	0.003	0.074	98.89
CA11-R1	10	76.47	0.026	12.59	-	0.743	0.069	0.014	0.388	4.250	4.398	0.002	0.003	-	0.076	99.03
CA12-P1	10	75.86	0.074	13.19	-	0.946	0.050	0.075	0.770	4.160	4.558	0.012	0.002	-	0.114	99.81
CA12-R1-A	10	75.76	0.076	13.16	-	0.883	0.052	0.075	0.776	4.144	4.580	0.008	0.002	0.007	0.135	99.66
CA12-R1-B	10	75.77	0.074	13.18	-	0.952	0.054	0.071	0.758	4.138	4.616	0.010	0.001	-	0.130	99.75
CA12-R2-A	10	75.50	0.076	13.16	0.001	0.920	0.056	0.069	0.775	4.098	4.630	0.010	0.003	0.001	0.118	99.41
CA12-R2-B	10	75.91	0.078	13.12	-	0.950	0.052	0.071	0.783	4.017	4.582	0.008	0.002	-	0.125	99.69
CA13-P1	10	76.35	0.024	12.48	-	0.758	0.073	0.011	0.381	4.111	4.405	0.003	0.002	0.002	0.085	98.69
CA13-R1	10	76.30	0.026	12.45	-	0.762	0.073	0.012	0.378	4.245	4.356	0.005	0.002	-	0.080	98.69
CA14-P1	10	76.73	0.076	12.84	-	0.702	0.059	0.053	0.601	4.126	4.525	0.003	0.005	-	0.130	99.85
CA14-P2	10	76.46	0.069	12.79	-	0.692	0.053	0.052	0.598	4.095	4.541	0.005	0.004	-	0.134	99.49
CA14-R1-A	10	76.55	0.071	12.66	-	0.733	0.059	0.058	0.571	3.983	4.498	0.013	0.004	0.004	0.137	99.34
CA14-R1-B	10	76.83	0.074	12.79	-	0.716	0.057	0.057	0.574	3.974	4.524	0.006	-	-	0.142	99.74
CA15-P1	10	77.04	0.053	12.64	-	0.593	0.059	0.030	0.436	4.006	4.662	0.003	0.004	0.002	0.093	99.61
CA15-R1-A	10	76.99	0.052	12.54	-	0.431	0.062	0.028	0.422	3.916	4.720	0.003	0.001	0.004	0.085	99.25
CA15-R1-B	10	77.18	0.050	12.56	-	0.420	0.059	0.029	0.424	4.002	4.728	0.003	0.003	-	0.076	99.53
CA15-R2	10	77.37	0.050	12.68	-	0.443	0.058	0.029	0.439	3.988	4.691	0.005	0.002	-	0.077	99.83
CA16-P1	10	76.67	0.056	12.57	-	0.649	0.061	0.030	0.433	3.229	5.929	0.001	0.005	0.002	0.099	99.74
CA16-R1	10	76.45	0.050	12.54	-	0.642	0.064	0.033	0.443	3.090	6.000	0.001	0.003	-	0.097	99.41
CA16-R2	10	75.97	0.049	12.39	-	0.652	0.063	0.029	0.418	3.130	5.962	0.004	0.001	0.002	0.096	98.77
CA17-P1	10	76.77	0.057	12.53	-	0.662	0.062	0.036	0.455	3.875	4.598	0.006	0.002	-	0.094	99.14
CA17-P2	10	76.73	0.053	12.47	-	0.442	0.064	0.028	0.423	3.097	5.882	0.006	0.002	-	0.088	99.29
CA17-R1-A	10	76.97	0.057	12.53	-	0.676	0.064	0.035	0.454	3.886	4.635	0.011	0.002	-	0.098	99.42
CA17-R1-B	10	77.03	0.056	12.59	0.002	0.678	0.058	0.036	0.456	3.939	4.708	0.003	-	0.003	0.101	99.66

Table C.1 - Major-Element Analyses of Geological Specimens (mean of *n* analyses; weight percent)

Specimen	n	SiO_2	TiO_2	Al_2O3	Cr_2O_3	FeO(T)	MnO	MgO	CaO	Na_2O	K_2O	P_2O_5	F	SO_3	Cl	Total
CA18-P1	10	76.87	0.054	12.57	-	0.539	0.061	0.030	0.441	3.140	5.826	0.008	0.004	0.003	0.101	99.65
CA18-P2	20	77.21	0.053	12.54	0.001	0.395	0.064	0.029	0.428	3.808	5.068	0.007	0.002	-	0.088	99.69
CA18-R1	10	76.93	0.052	12.59	0.004	0.382	0.060	0.027	0.441	3.001	5.936	0.008	0.002	0.001	0.095	99.53
CA18-R2	10	77.07	0.056	12.60	-	0.402	0.060	0.027	0.437	2.960	6.078	0.006	0.004	-	0.089	99.79
CA18-R3-A	10	76.52	0.050	12.49	0.001	0.399	0.062	0.027	0.441	3.024	5.995	0.003	0.003	0.003	0.093	99.11
CA18-R3-B	10	76.75	0.053	12.57	-	0.383	0.055	0.024	0.431	2.930	6.001	0.004	0.003	0.002	0.092	99.30
CA19-P1	20	76.73	0.055	12.56	-	0.574	0.065	0.030	0.456	4.133	4.677	0.006	0.001	-	0.100	99.39
CA19-R1-A	10	77.05	0.053	12.60	0.002	0.613	0.060	0.033	0.461	3.967	4.515	0.005	0.003	-	0.104	99.47
CA19-R1-B	10	77.19	0.059	12.65	-	0.536	0.067	0.031	0.454	3.969	4.578	0.014	-	0.003	0.103	99.65
CA19-R2-A	10	76.99	0.053	12.60	-	0.594	0.059	0.033	0.459	3.985	4.587	0.008	0.005	-	0.105	99.48
CA19-R2-B	10	76.98	0.056	12.64	-	0.554	0.061	0.032	0.453	3.972	4.562	0.009	0.002	-	0.108	99.43
CA19-R2-C	10	76.74	0.054	12.65	-	0.598	0.060	0.034	0.458	3.942	4.643	0.007	0.002	-	0.106	99.30
CA19-R3-A	10	76.88	0.054	12.59	-	0.596	0.062	0.033	0.463	3.946	4.627	0.008	0.002	-	0.097	99.36
CA19-R3-B	10	76.64	0.055	12.59	-	0.651	0.062	0.032	0.470	3.958	4.657	0.011	0.001	-	0.099	99.23
CA19-R3-C	10	77.12	0.056	12.69	0.005	0.570	0.062	0.032	0.457	3.863	4.692	0.006	0.001	-	0.095	99.65
CA19-R3-D	10	76.99	0.061	12.64	-	0.577	0.062	0.032	0.460	3.863	4.658	0.009	0.001	-	0.101	99.45
CA20-P1-A	10	77.05	0.061	12.62	-	0.703	0.060	0.035	0.451	3.948	4.635	0.007	0.005	-	0.109	99.69
CA20-P1-B	10	77.16	0.058	12.48	0.001	0.684	0.057	0.040	0.454	3.895	4.562	0.008	0.001	0.001	0.100	99.51
CA20-P2	20	76.75	0.053	12.50	-	0.695	0.054	0.036	0.449	4.169	4.595	0.008	0.003	-	0.105	99.41
CA20-P3	20	76.89	0.058	12.56	-	0.711	0.059	0.037	0.450	4.083	4.614	0.007	0.002	0.004	0.123	99.59
CA20-P4	20	76.94	0.061	12.60	0.001	0.714	0.061	0.035	0.451	4.107	4.608	0.006	0.004	0.001	0.100	99.70
CA20-R1-A	10	76.82	0.061	12.56	0.003	0.665	0.063	0.035	0.451	4.077	4.612	0.004	0.002	-	0.095	99.45
CA20-R1-B	10	77.04	0.059	12.64	0.002	0.692	0.063	0.035	0.450	4.075	4.642	0.004	0.002	-	0.098	99.80
CA21-P1	10	76.64	0.081	12.69	-	0.719	0.051	0.062	0.542	3.960	4.532	0.007	0.002	0.002	0.139	99.42
CA21-P2	10	76.65	0.084	12.73	-	0.738	0.045	0.062	0.549	3.867	4.394	0.012	0.003	0.005	0.151	99.29
CA21-R1-A	10	76.34	0.082	12.67	-	0.718	0.050	0.062	0.532	3.791	4.539	0.004	-	0.001	0.141	98.93
CA21-R1-B	10	76.73	0.082	12.75	-	0.718	0.046	0.060	0.538	3.733	4.525	0.008	0.001	-	0.134	99.32
CA21-R2-A	10	76.45	0.086	12.61	-	0.686	0.048	0.060	0.534	3.941	4.534	0.004	0.005	0.002	0.123	99.09
CA21-R2-B	10	76.59	0.080	12.66	-	0.716	0.053	0.061	0.541	3.915	4.510	0.013	0.003	-	0.136	99.28

Table C.1 - Major-Element Analyses of Geological Specimens (mean of *n* analyses; weight percent)

Specimen	n	SiO_2	TiO_2	Al_2O3	Cr_2O_3	FeO(T)	MnO	MgO	CaO	Na_2O	K_2O	P_2O_5	F	SO_3	Cl	Total
CA21-R2-C	10	76.66	0.085	12.67	-	0.730	0.053	0.060	0.548	3.819	4.578	0.009	0.004	0.004	0.136	99.36
CA22-P1	10	75.03	0.109	13.58	-	1.039	0.065	0.108	0.932	4.026	4.615	0.013	0.004	0.004	0.193	99.72
CA22-P2	20	75.19	0.110	13.55	-	1.021	0.066	0.107	0.923	4.129	4.579	0.010	0.002	-	0.195	99.89
CA22-P3	20	74.94	0.114	13.51	0.001	1.023	0.061	0.108	0.917	4.147	4.532	0.011	-	-	0.190	99.56
CA22-R1	10	75.20	0.106	13.57	0.001	0.972	0.061	0.105	0.926	4.211	4.384	0.012	0.002	-	0.192	99.75
CA22-R2-A	10	74.80	0.107	13.43	-	0.983	0.064	0.108	0.917	4.219	4.600	0.007	0.001	0.001	0.186	99.43
CA22-R2-B	10	74.79	0.109	13.49	-	1.001	0.067	0.108	0.920	4.305	4.356	0.013	0.001	0.005	0.185	99.34
CA22-R2-C	10	74.94	0.105	13.54	-	0.995	0.067	0.108	0.924	4.236	4.560	0.009	0.002	0.002	0.186	99.67
CA22-R2-D	10	74.91	0.104	13.42	-	0.980	0.066	0.109	0.919	4.125	4.667	0.018	0.001	-	0.194	99.51
CA22-R2-E	10	74.97	0.106	13.43	-	1.022	0.065	0.108	0.928	4.284	4.385	0.004	0.006	0.001	0.187	99.50
CA23-P1	20	75.13	0.109	13.50	-	0.804	0.061	0.072	0.825	4.118	4.738	0.011	0.002	0.003	0.175	99.55
CA23-P2-A	10	74.96	0.102	13.44	0.004	0.859	0.056	0.084	0.873	4.038	4.568	0.009	0.002	0.003	0.179	99.17
CA23-P2-B	10	74.96	0.103	13.53	-	0.845	0.059	0.073	0.862	4.165	4.609	0.011	0.001	-	0.174	99.40
CA23-P2-C	10	74.93	0.109	13.47	-	0.888	0.061	0.093	0.881	4.153	4.617	0.007	0.003	0.003	0.177	99.38
CA23-P2-D	10	74.90	0.112	13.49	-	0.850	0.054	0.075	0.843	4.110	4.605	0.012	-	-	0.178	99.23
CA23-P3-A	10	75.15	0.105	13.52	0.002	0.825	0.056	0.079	0.861	3.992	4.508	0.010	-	0.004	0.176	99.29
CA23-P3-B	10	76.00	0.070	12.61	-	0.817	0.056	0.051	0.573	3.907	4.392	0.008	0.002	0.001	0.140	98.62
CA23-P4-A	10	75.09	0.107	13.51	0.001	0.856	0.060	0.085	0.854	4.109	4.629	0.013	0.003	0.003	0.179	99.49
CA23-P4-B	10	75.25	0.108	13.55	-	0.901	0.064	0.097	0.887	4.276	4.537	0.012	0.002	-	0.189	99.87
CA23-P5-A	10	75.07	0.102	13.50	0.001	0.851	0.058	0.082	0.869	4.197	4.597	0.013	0.002	-	0.172	99.51
CA23-P5-B	10	75.21	0.110	13.42	0.002	0.895	0.061	0.086	0.873	4.145	4.508	0.012	-	-	0.187	99.51
CA23-R1-A	10	75.15	0.109	13.48	-	0.882	0.059	0.082	0.866	3.948	4.591	0.006	-	0.005	0.186	99.37
CA23-R1-B	10	75.26	0.108	13.52	-	0.860	0.054	0.077	0.849	4.048	4.589	0.006	-	-	0.173	99.54
CA23-R2-A	10	75.34	0.107	13.55	-	0.844	0.055	0.084	0.865	4.095	4.532	0.013	0.001	-	0.170	99.66
CA23-R2-B	10	75.46	0.107	13.56	0.003	0.836	0.061	0.085	0.865	4.254	4.597	0.013	0.004	0.002	0.161	100.00
CA23-R2-C	10	75.50	0.109	13.47	-	0.874	0.063	0.086	0.886	3.945	4.633	0.010	0.001	-	0.174	99.75
CA24-P1	20	75.21	0.110	13.43	0.001	0.940	0.066	0.096	0.884	4.118	4.504	0.008	0.001	0.003	0.183	99.55
CA24-P2	20	75.19	0.107	13.38	-	0.923	0.063	0.090	0.872	4.189	4.540	0.011	0.001	0.005	0.188	99.56
CA24-R1-A	10	74.84	0.102	13.32	-	0.928	0.061	0.095	0.887	4.076	4.601	0.017	0.003	-	0.185	99.11

Table C.1 - Major-Element Analyses of Geological Specimens (mean of *n* analyses; weight percent)

Specimen	n	SiO_2	TiO_2	Al_2O3	Cr_2O_3	FeO(T)	MnO	MgO	CaO	Na_2O	K_2O	P_2O_5	F	SO_3	Cl	Total
CA24-R1-B	10	74.81	0.106	13.38	-	0.904	0.060	0.092	0.881	4.192	4.568	0.007	0.002	-	0.174	99.18
CA24-R1-C	10	74.79	0.108	13.37	-	0.944	0.065	0.094	0.876	4.184	4.568	0.011	0.003	0.004	0.182	99.20
CA24-R1-D	10	74.78	0.108	13.32	0.002	0.916	0.061	0.093	0.887	3.982	4.626	0.008	-	-	0.177	98.96
CA25-P1	30	74.88	0.122	13.69	0.002	0.992	0.060	0.122	1.017	4.245	4.475	0.018	0.002	0.001	0.194	99.83
CA25-P2	30	74.51	0.123	13.70	-	0.924	0.060	0.100	0.962	4.268	4.420	0.014	0.001	0.003	0.182	99.27
CA25-R1-A	10	75.00	0.123	13.71	0.001	0.901	0.067	0.119	1.003	4.290	4.438	0.020	0.003	0.001	0.182	99.85
CA25-R1-B	10	74.90	0.118	13.76	-	0.935	0.061	0.117	1.010	4.258	4.480	0.016	0.001	-	0.194	99.85
CA25-R1-C	10	74.91	0.126	13.78	-	0.951	0.060	0.123	1.020	4.159	4.466	0.024	0.001	-	0.187	99.80
CA25-R1-D	10	74.90	0.125	13.65	-	0.987	0.061	0.132	1.035	4.268	4.398	0.017	0.001	0.003	0.187	99.76
CA25-R2-A	20	74.77	0.122	13.56	0.002	0.914	0.062	0.102	0.971	4.235	4.461	0.016	0.001	0.005	0.204	99.43
CA25-R2-B	20	74.70	0.122	13.65	-	0.927	0.063	0.112	0.983	4.285	4.498	0.019	0.002	0.001	0.198	99.56
CA26-P1	30	74.82	0.127	13.77	-	0.921	0.058	0.120	0.991	4.272	4.531	0.016	0.002	-	0.192	99.82
CA26-R1-A	10	74.37	0.125	13.59	-	0.915	0.063	0.120	1.018	3.853	4.972	0.018	0.005	-	0.194	99.24
CA26-R1-B	10	74.68	0.119	13.71	-	0.878	0.061	0.126	1.017	4.182	4.435	0.020	-	-	0.174	99.40
CA26-R1-C	10	74.71	0.119	13.74	0.008	0.868	0.061	0.122	1.013	4.156	4.468	0.015	0.001	0.001	0.164	99.45
CA26-R1-D	10	74.83	0.124	13.76	-	0.907	0.061	0.127	1.021	4.017	4.681	0.016	0.002	0.002	0.183	99.73
CA26-R2-A	10	74.88	0.126	13.73	-	0.940	0.060	0.128	1.006	4.272	4.398	0.021	0.004	0.002	0.198	99.77
CA26-R2-B	10	74.46	0.129	13.77	-	0.936	0.064	0.124	1.020	4.147	4.577	0.020	-	-	0.201	99.45
CA26-R3-A	10	74.62	0.130	13.71	0.002	0.986	0.063	0.133	1.038	4.176	4.713	0.017	-	-	0.194	99.79
CA26-R3-B	10	74.80	0.128	13.76	-	0.920	0.068	0.127	1.019	3.913	4.916	0.014	0.003	0.006	0.195	99.87
CA27-P1	20	74.74	0.122	13.73	-	0.982	0.060	0.105	0.992	4.276	4.433	0.018	0.002	0.002	0.190	99.65
CA27-P2	20	75.19	0.124	13.75	-	0.885	0.060	0.095	0.978	4.279	4.490	0.017	0.001	0.003	0.187	100.06
CA27-R1-A	10	74.32	0.123	13.57	-	1.019	0.067	0.131	1.051	4.226	4.513	0.017	0.003	0.006	0.192	99.24
CA27-R1-B	10	74.82	0.118	13.53	-	0.986	0.059	0.123	1.017	4.123	4.491	0.017	0.005	0.003	0.167	99.46
CA27-R1-C	10	74.60	0.121	13.65	-	1.010	0.063	0.127	1.043	4.154	4.514	0.019	-	-	0.184	99.49
CA27-R1-D	10	74.61	0.125	13.70	-	1.040	0.062	0.138	1.059	4.131	4.475	0.019	0.001	0.002	0.173	99.54
CA27-R2-A	10	74.75	0.131	13.79	0.001	1.031	0.061	0.129	1.035	4.225	4.484	0.022	0.001	-	0.189	99.84
CA27-R2-B	10	75.20	0.129	13.84	-	1.013	0.064	0.133	1.051	4.241	4.412	0.017	0.001	0.001	0.192	100.30
CA27-R3	30	74.59	0.125	13.72	0.001	1.001	0.063	0.122	1.003	4.266	4.483	0.016	0.002	-	0.182	99.57

Table C.1 - Major-Element Analyses of Geological Specimens (mean of *n* analyses; weight percent)

Specimen	n	SiO_2	TiO_2	Al_2O3	Cr_2O_3	FeO(T)	MnO	MgO	CaO	Na_2O	K_2O	P_2O_5	F	SO_3	Cl	Total
CA27-R4	30	74.93	0.125	13.77	-	1.004	0.063	0.123	0.997	4.276	4.457	0.014	0.002	-	0.181	99.94
CA28-P1	20	76.76	0.095	13.24	-	0.636	0.052	0.119	0.582	4.169	4.151	0.027	0.001	0.001	0.087	99.92
CA28-P2	20	76.47	0.099	13.20	0.002	0.594	0.053	0.119	0.576	4.199	4.213	0.030	0.001	0.001	0.081	99.64
CA28-P3	20	77.14	0.093	13.16	-	0.486	0.052	0.114	0.558	4.146	4.223	0.030	0.002	0.002	0.082	100.09
CA28-P4	20	77.09	0.100	13.10	-	0.420	0.052	0.119	0.582	4.195	4.202	0.031	0.002	0.004	0.086	99.98
CA28-P5	20	77.02	0.094	13.27	-	0.630	0.056	0.116	0.566	4.235	4.232	0.029	0.002	0.003	0.084	100.33
CA28-R1-A	10	76.65	0.099	13.14	-	0.639	0.051	0.120	0.565	3.981	4.341	0.028	0.002	0.005	0.098	99.72
CA28-R1-B	10	76.94	0.094	13.18	-	0.623	0.053	0.120	0.560	3.927	4.214	0.024	0.003	-	0.090	99.82
CA29-P1-A	10	76.64	0.093	13.06	0.004	0.658	0.047	0.122	0.592	4.032	4.111	0.027	0.005	0.001	0.084	99.48
CA29-P1-B	10	76.59	0.099	13.12	-	0.613	0.047	0.122	0.587	4.164	4.088	0.034	0.003	0.001	0.084	99.55
CA29-P1-C	10	76.59	0.096	13.04	-	0.625	0.054	0.123	0.600	4.024	4.133	0.026	0.007	0.003	0.084	99.40
CA29-P2-A	10	76.78	0.097	13.23	0.002	0.642	0.049	0.125	0.584	4.088	4.031	0.027	0.002	0.002	0.085	99.73
CA29-P2-B	10	76.86	0.095	13.21	0.002	0.634	0.050	0.127	0.579	4.109	4.086	0.033	0.004	0.002	0.091	99.88
CA29-P3-A	10	76.65	0.099	13.17	0.001	0.597	0.047	0.125	0.590	4.185	4.059	0.029	0.007	0.001	0.088	99.64
CA29-P3-B	10	76.93	0.102	13.20	-	0.612	0.054	0.125	0.585	4.170	4.107	0.030	0.002	0.008	0.085	100.01
CA29-P4	10	76.74	0.101	13.20	-	0.618	0.054	0.121	0.590	4.129	4.060	0.029	0.001	0.003	0.082	99.74
CA29-P5-A	20	76.80	0.093	13.12	-	0.578	0.051	0.121	0.567	4.213	4.182	0.027	0.003	0.007	0.089	99.85
CA29-P5-B	20	76.68	0.099	13.20	0.001	0.631	0.050	0.127	0.592	4.191	4.133	0.030	0.004	0.002	0.102	99.84
CA29-P6	20	77.05	0.096	13.00	-	0.609	0.052	0.119	0.587	4.286	4.169	0.031	0.002	0.002	0.086	100.09
CA29-R1	10	76.51	0.102	13.25	-	0.632	0.055	0.121	0.596	4.181	4.127	0.035	-	0.001	0.089	99.69
CA29-R2	10	76.58	0.100	13.20	-	0.630	0.050	0.117	0.597	4.140	4.174	0.028	0.004	0.002	0.086	99.70
CA30-P1	20	77.06	0.101	13.20	0.002	0.429	0.050	0.118	0.585	4.213	4.141	0.028	0.002	0.001	0.091	100.02
CA30-P2	20	76.85	0.094	13.15	-	0.473	0.053	0.118	0.581	4.133	4.137	0.034	0.003	0.002	0.091	99.72
CA30-P3	10	77.05	0.098	13.19	0.002	0.305	0.052	0.109	0.531	3.973	4.666	0.028	0.003	0.004	0.089	100.10
CA30-P4	20	77.14	0.099	13.21	-	0.529	0.053	0.122	0.594	4.184	4.152	0.032	0.002	0.003	0.096	100.22
CA30-P5	10	76.90	0.099	13.31	-	0.604	0.051	0.123	0.592	4.234	4.164	0.030	0.005	0.004	0.077	100.19
CA30-R1-A	20	76.86	0.099	13.14	0.002	0.567	0.052	0.125	0.578	4.241	4.056	0.030	0.003	-	0.090	99.85
CA30-R1-B	20	76.93	0.099	13.21	-	0.524	0.054	0.124	0.571	4.243	4.058	0.033	0.003	0.003	0.086	99.94
CA30-R2-A	20	76.66	0.095	13.14	-	0.464	0.054	0.124	0.575	4.272	4.057	0.028	0.002	0.004	0.092	99.56

Table C.1 - Major-Element Analyses of Geological Specimens (mean of *n* analyses; weight percent)

Specimen	n	SiO_2	TiO_2	Al_2O3	Cr_2O_3	FeO(T)	MnO	MgO	CaO	Na_2O	K_2O	P_2O_5	F	SO_3	Cl	Total
CA30-R2-B	20	77.12	0.098	13.20	-	0.438	0.052	0.124	0.574	4.255	4.099	0.031	0.003	0.004	0.086	100.08
CA31-P1	20	77.16	0.096	13.23	0.003	0.518	0.053	0.120	0.581	4.109	4.174	0.031	0.004	0.001	0.079	100.16
CA31-P2	20	77.28	0.101	13.20	-	0.533	0.050	0.122	0.577	4.200	4.195	0.029	0.002	0.003	0.082	100.37
CA31-R1	9	76.89	0.096	13.19	-	0.619	0.054	0.118	0.564	4.179	4.154	0.027	-	0.004	0.084	99.98
CA32-W1A	10	76.05	0.061	12.51	0.002	0.634	0.058	0.034	0.457	3.995	4.665	0.006	0.003	-	0.103	98.58
CA32-W1B	20	76.65	0.061	12.57	-	0.636	0.058	0.036	0.456	3.972	4.629	0.008	0.001	-	0.102	99.18
CA32-W1C	10	76.63	0.061	12.65	0.002	0.643	0.062	0.035	0.457	4.008	4.681	0.007	0.003	-	0.098	99.34
CA32-W1D	10	76.59	0.055	12.49	-	0.623	0.056	0.036	0.450	3.937	4.675	0.003	0.002	-	0.106	99.02
CA32-W1E	20	76.38	0.060	12.54	-	0.637	0.060	0.037	0.450	4.022	4.649	0.009	0.003	0.001	0.103	98.95
CA32-W2A	10	76.38	0.061	12.46	0.003	0.637	0.061	0.036	0.464	4.011	4.623	0.003	-	-	0.103	98.84
CA32-W2B	10	77.02	0.057	12.65	-	0.665	0.060	0.036	0.463	4.049	4.628	0.005	0.005	0.003	0.102	99.75
CA32-W2C	10	76.39	0.060	12.49	-	0.647	0.055	0.036	0.456	3.863	4.610	0.006	0.002	0.002	0.104	98.72
CA32-W2D	10	76.62	0.065	12.66	-	0.649	0.060	0.032	0.459	3.952	4.652	0.005	0.002	-	0.114	99.27
CA32-W2E	10	76.46	0.060	12.59	-	0.644	0.060	0.036	0.455	3.969	4.639	0.006	0.003	-	0.113	99.04
CA32-W3A	10	76.37	0.059	12.64	-	0.569	0.058	0.029	0.437	3.932	4.632	0.006	0.002	-	0.096	98.83
CA32-W3B	20	76.29	0.055	12.49	-	0.554	0.060	0.028	0.436	3.930	4.656	0.007	0.002	-	0.100	98.61
CA32-W3C	20	76.74	0.053	12.55	0.003	0.564	0.062	0.028	0.435	4.025	4.627	0.006	0.001	0.002	0.096	99.19
CA32-W3D	20	76.44	0.055	12.53	-	0.584	0.064	0.028	0.434	3.949	4.679	0.002	0.001	-	0.099	98.86
CA32-W3E	20	76.53	0.052	12.54	0.002	0.576	0.061	0.029	0.433	3.962	4.630	0.006	0.001	-	0.100	98.91
CA32-W4A	20	76.87	0.059	12.53	0.001	0.642	0.061	0.038	0.454	3.955	4.589	0.003	0.002	0.002	0.106	99.31
CA32-W4B	20	76.67	0.058	12.59	-	0.624	0.059	0.035	0.451	3.995	4.713	0.010	0.001	-	0.099	99.30
CA32-W4C	10	76.71	0.058	12.51	0.002	0.633	0.057	0.034	0.456	4.040	4.672	0.001	0.001	0.002	0.105	99.28
CA32-W4D	10	76.62	0.059	12.59	0.002	0.631	0.057	0.032	0.454	3.995	4.525	0.006	0.002	0.001	0.103	99.08
CA32-W4E	20	76.83	0.058	12.61	0.001	0.644	0.062	0.036	0.456	3.974	4.738	0.005	0.003	0.002	0.098	99.51
CA32-W5A	10	76.70	0.050	12.57	-	0.578	0.062	0.028	0.438	3.911	4.690	0.009	0.003	0.001	0.094	99.13
CA32-W5B	10	76.82	0.056	12.52	0.002	0.589	0.066	0.027	0.438	4.073	4.672	0.003	0.001	0.003	0.098	99.37
CA32-W5C	20	76.68	0.052	12.56	-	0.555	0.064	0.029	0.438	3.989	4.659	0.006	0.003	-	0.096	99.13
CA32-W5D	20	76.66	0.056	12.57	-	0.563	0.060	0.029	0.433	4.025	4.571	0.007	0.002	-	0.106	99.07
CA32-W5E	20	76.55	0.054	12.55	-	0.580	0.064	0.029	0.437	4.008	4.680	0.003	0.002	-	0.102	99.06

Table C.1 - Major-Element Analyses of Geological Specimens (mean of *n* analyses; weight percent)

Specimen	n	SiO_2	TiO_2	Al_2O3	Cr_2O_3	FeO(T)	MnO	MgO	CaO	Na_2O	K_2O	P_2O_5	F	SO_3	Cl	Total
CA32-W6A	20	76.64	0.057	12.55	-	0.597	0.060	0.036	0.456	4.000	4.621	0.005	0.001	0.003	0.105	99.13
CA32-W6B	10	76.98	0.054	12.54	-	0.560	0.055	0.033	0.455	3.997	4.681	0.007	-	0.001	0.102	99.47
CA32-W6C	10	76.95	0.060	12.61	0.005	0.589	0.058	0.034	0.453	3.954	4.597	0.005	0.001	0.002	0.100	99.42
CA32-W6D	10	76.98	0.054	12.58	-	0.580	0.058	0.036	0.448	3.983	4.631	0.010	0.003	0.002	0.102	99.47
CA32-W6E	20	76.72	0.060	12.54	-	0.598	0.060	0.036	0.456	3.959	4.627	0.004	0.001	-	0.113	99.18
CA33-W1A	20	76.15	0.024	12.62	-	0.770	0.072	0.012	0.394	4.224	4.376	0.005	0.001	0.007	0.072	98.73
CA33-W1B	10	76.07	0.026	12.63	-	0.757	0.070	0.009	0.386	4.112	4.392	0.001	0.002	0.003	0.066	98.52
CA33-W1C	20	76.04	0.028	12.55	-	0.764	0.065	0.012	0.389	4.141	4.402	0.003	0.002	-	0.069	98.47
CA33-W1D	20	75.70	0.028	12.58	-	0.769	0.069	0.011	0.395	4.105	4.383	0.004	0.003	-	0.066	98.11
CA33-W1E	20	75.98	0.029	12.55	0.002	0.764	0.070	0.011	0.389	4.175	4.285	0.005	0.002	-	0.066	98.33
CA33-W2A	20	76.02	0.026	12.57	0.001	0.767	0.070	0.013	0.394	4.069	4.411	0.004	0.002	0.002	0.080	98.43
CA33-W2B	10	76.17	0.025	12.54	-	0.771	0.070	0.009	0.390	4.314	4.300	0.004	-	-	0.067	98.66
CA33-W2C	20	76.09	0.025	12.62	0.003	0.773	0.068	0.011	0.393	4.238	4.404	0.002	0.002	-	0.067	98.69
CA33-W2D	10	75.51	0.026	12.49	-	0.765	0.072	0.007	0.391	4.130	4.395	0.003	0.001	-	0.068	97.85
CA33-W2E	10	76.13	0.023	12.69	-	0.754	0.071	0.013	0.390	4.245	4.364	0.003	0.001	0.001	0.066	98.76
CA33-W3A	20	76.22	0.024	12.47	-	0.764	0.071	0.011	0.392	4.105	4.419	-	0.002	-	0.070	98.55
CA33-W3B	10	75.79	0.028	12.59	0.001	0.767	0.076	0.010	0.390	4.106	4.396	0.006	0.001	0.002	0.071	98.24
CA33-W3C	20	75.99	0.026	12.56	-	0.757	0.068	0.009	0.385	4.166	4.353	0.006	0.001	-	0.070	98.39
CA33-W3D	10	76.00	0.027	12.68	-	0.760	0.069	0.012	0.397	4.212	4.410	0.001	0.002	0.007	0.066	98.64
CA33-W3E	20	75.69	0.027	12.63	-	0.752	0.066	0.012	0.389	4.155	4.352	-	0.003	-	0.070	98.15
CA33-W4A	10	75.41	0.025	12.49	0.001	0.757	0.072	0.014	0.398	4.200	4.397	0.003	0.002	0.006	0.063	97.83
CA33-W4B	20	76.15	0.028	12.59	0.002	0.764	0.066	0.011	0.389	4.094	4.367	0.001	0.002	0.002	0.072	98.54
CA33-W4C	10	75.38	0.028	12.57	0.002	0.762	0.073	0.010	0.389	4.231	4.398	-	0.002	0.005	0.064	97.91
CA33-W4D	20	75.93	0.028	12.60	-	0.760	0.068	0.011	0.383	4.169	4.353	0.005	0.002	-	0.067	98.38
CA33-W4E	10	75.85	0.022	12.55	-	0.765	0.071	0.008	0.382	4.137	4.412	0.002	0.001	-	0.070	98.27
CA33-W5A	10	75.96	0.028	12.69	0.002	0.769	0.070	0.011	0.394	4.214	4.341	0.006	0.001	0.003	0.066	98.56
CA33-W5B	20	76.16	0.027	12.66	-	0.774	0.068	0.012	0.396	4.169	4.380	-	0.001	-	0.068	98.72
CA33-W5C	20	75.81	0.022	12.61	-	0.764	0.069	0.011	0.388	4.222	4.290	0.003	0.001	0.005	0.072	98.26
CA33-W5D	20	75.84	0.026	12.58	-	0.769	0.071	0.012	0.389	4.225	4.402	0.001	0.003	-	0.066	98.38

Table C.1 - Major-Element Analyses of Geological Specimens (mean of *n* analyses; weight percent)

Specimen	n	SiO_2	TiO_2	Al_2O3	Cr_2O_3	FeO(T)	MnO	MgO	CaO	Na_2O	K_2O	P_2O_5	F	SO_3	Cl	Total
CA33-W5E	10	76.10	0.020	12.66	-	0.760	0.071	0.010	0.387	4.177	4.337	0.003	0.002	0.005	0.067	98.59
EA01-P1	20	76.86	0.093	12.78	-	0.540	0.033	0.065	0.484	4.077	4.682	0.010	0.003	0.002	0.015	99.64
EA01-P2	20	77.05	0.090	12.83	0.002	0.467	0.034	0.063	0.478	3.857	4.711	0.009	0.003	-	0.017	99.61
EA01-P3	20	77.05	0.096	12.77	0.001	0.562	0.034	0.065	0.475	3.985	4.659	0.008	0.002	-	0.014	99.72
EA01-P4	20	77.05	0.094	12.85	-	0.541	0.037	0.065	0.476	4.035	4.661	0.009	0.005	-	0.016	99.83
EA01-R1	20	77.02	0.095	12.80	0.002	0.556	0.035	0.066	0.474	4.163	4.708	0.011	0.003	0.001	0.016	99.95
EA01-R2-A	10	76.77	0.093	12.68	-	0.587	0.037	0.064	0.481	4.056	4.649	0.012	-	-	0.017	99.45
EA01-R2-B	10	77.09	0.093	12.71	-	0.610	0.034	0.066	0.479	4.045	4.658	0.011	0.004	-	0.014	99.82
EA02-P1-A	10	76.82	0.097	12.72	0.002	0.447	0.038	0.063	0.472	4.243	4.683	0.006	0.004	-	0.017	99.61
EA02-P1-B	10	76.74	0.091	12.58	-	0.652	0.036	0.064	0.472	4.001	4.672	0.012	0.001	0.003	0.016	99.34
EA02-P2	10	76.26	0.096	12.65	-	0.549	0.030	0.063	0.488	4.083	4.688	0.011	0.001	-	0.020	98.94
EA02-P3	10	76.72	0.091	12.73	-	0.572	0.036	0.068	0.490	4.137	4.670	0.010	0.003	0.002	0.013	99.54
EA02-P4	10	76.70	0.095	12.57	-	0.580	0.034	0.064	0.507	4.088	4.665	0.012	-	0.002	0.014	99.33
EA02-R1	10	76.72	0.095	12.74	0.004	0.658	0.032	0.070	0.491	4.009	4.672	0.006	0.002	0.002	0.014	99.51
EA02-R2-A	10	76.95	0.096	12.71	-	0.560	0.034	0.066	0.485	4.071	4.570	0.008	0.003	0.001	0.015	99.57
EA02-R2-B	10	77.11	0.098	12.72	0.001	0.561	0.039	0.069	0.480	4.155	4.634	0.011	0.002	0.002	0.017	99.90
EA03-P1-A	10	76.91	0.098	12.59	-	0.600	0.042	0.064	0.482	3.994	4.613	0.010	0.002	0.007	0.022	99.44
EA03-P1-B	10	76.96	0.095	12.75	0.001	0.530	0.043	0.064	0.468	4.055	4.596	0.008	0.002	0.001	0.020	99.60
EA03-P2-A	10	76.85	0.091	12.66	-	0.528	0.038	0.060	0.458	3.996	4.665	0.014	0.002	-	0.028	99.39
EA03-P2-B	10	77.01	0.094	12.69	0.002	0.575	0.046	0.061	0.475	3.932	4.656	0.015	0.006	0.003	0.023	99.58
EA03-P3	10	76.83	0.096	12.74	0.002	0.562	0.044	0.065	0.487	4.101	4.643	0.013	0.002	-	0.022	99.60
EA03-P4	10	76.92	0.101	12.71	-	0.558	0.040	0.066	0.481	4.147	4.660	0.009	0.003	0.001	0.027	99.73
EA03-P5	10	76.99	0.096	12.85	-	0.491	0.036	0.057	0.478	4.197	4.613	0.009	0.004	0.005	0.031	99.86
EA03-R1	10	76.84	0.099	12.57	-	0.648	0.045	0.064	0.485	4.051	4.630	0.008	0.003	-	0.023	99.47
EA04-P1	10	76.83	0.095	12.74	-	0.777	0.039	0.067	0.478	4.046	4.658	0.014	0.002	0.004	0.020	99.77
EA04-P2	10	76.52	0.091	12.80	-	0.755	0.038	0.066	0.478	4.011	4.642	0.008	0.002	-	0.022	99.44
EA04-R1-A	20	76.84	0.091	12.78	-	0.757	0.043	0.060	0.467	4.079	4.622	0.010	0.002	-	0.022	99.77
EA04-R1-B	20	77.16	0.093	12.66	-	0.732	0.039	0.063	0.464	4.114	4.592	0.008	0.001	0.002	0.020	99.95
EA04-R2	10	76.59	0.101	12.73	-	0.758	0.044	0.062	0.482	4.063	4.612	0.006	-	0.002	0.022	99.48

Table C.1 - Major-Element Analyses of Geological Specimens (mean of *n* analyses; weight percent)

Specimen	n	SiO_2	TiO_2	Al_2O3	Cr_2O_3	FeO(T)	MnO	MgO	CaO	Na_2O	K_2O	P_2O_5	F	SO_3	Cl	Total
EA04-R3	10	76.62	0.092	12.77	0.001	0.756	0.039	0.064	0.483	4.032	4.641	0.007	0.002	0.006	0.021	99.54
EA04-R4A	10	76.40	0.096	12.78	-	0.763	0.040	0.064	0.475	4.007	4.607	0.010	0.004	0.003	0.022	99.27
EA04-R4B	10	76.57	0.093	12.78	-	0.752	0.043	0.064	0.469	4.068	4.514	0.014	0.002	0.001	0.021	99.40
EA04-R4C	10	76.77	0.092	12.68	0.001	0.750	0.039	0.065	0.479	4.057	4.638	0.009	0.004	-	0.021	99.61
EA04-R4D	10	76.29	0.093	12.74	0.003	0.737	0.042	0.063	0.476	4.026	4.517	0.012	0.002	-	0.017	99.02
EA04-R4E	10	76.65	0.096	12.82	-	0.743	0.038	0.059	0.475	4.088	4.647	0.015	0.001	0.002	0.024	99.66
EA04-R5A	10	76.69	0.095	12.82	-	0.773	0.038	0.064	0.477	4.025	4.551	0.007	0.001	0.004	0.024	99.56
EA04-R5B	10	76.50	0.098	12.74	0.001	0.759	0.041	0.061	0.479	4.058	4.628	0.009	0.001	-	0.027	99.40
EA04-R5C	10	76.73	0.092	12.76	-	0.766	0.042	0.063	0.475	4.003	4.655	0.009	0.001	-	0.023	99.62
EA04-R5D	10	76.62	0.095	12.60	0.003	0.763	0.045	0.063	0.474	4.057	4.639	0.011	0.004	-	0.023	99.39
EA04-R5E	10	76.32	0.098	12.74	-	0.774	0.042	0.062	0.476	3.950	4.600	0.008	0.001	0.005	0.025	99.10
EA05-P1	20	77.02	0.097	12.81	-	0.581	0.042	0.063	0.480	4.060	4.625	0.006	0.001	0.001	0.023	99.81
EA05-P2	10	76.91	0.098	12.59	-	0.624	0.041	0.065	0.471	3.901	4.604	0.003	0.003	-	0.023	99.33
EA05-R1	10	76.92	0.092	12.66	-	0.647	0.039	0.064	0.473	4.056	4.614	0.004	0.002	-	0.020	99.60
EA05-R2	10	76.86	0.089	12.73	-	0.450	0.042	0.064	0.484	3.907	4.684	0.011	-	-	0.020	99.35
EA06-P1	20	76.90	0.095	12.77	0.002	0.768	0.039	0.066	0.482	4.037	4.540	0.010	0.005	-	0.017	99.73
EA06-P2	20	76.55	0.095	12.71	-	0.770	0.044	0.067	0.482	4.031	4.514	0.010	0.001	-	0.019	99.29
EA06-R1	20	76.74	0.095	12.67	-	0.764	0.039	0.067	0.486	3.996	4.624	0.010	0.004	-	0.018	99.51
EA07-P1	20	75.98	0.078	13.22	-	0.952	0.051	0.016	0.259	4.880	4.492	0.007	0.002	-	0.066	100.01
EA07-P2	20	75.69	0.077	13.12	-	0.981	0.051	0.022	0.270	4.648	4.838	0.006	0.002	0.003	0.070	99.78
EA07-P3	10	76.04	0.077	13.26	-	0.996	0.053	0.019	0.260	4.902	4.568	0.006	0.002	-	0.062	100.25
EA07-P4	10	75.75	0.074	13.21	-	0.938	0.043	0.017	0.243	4.812	4.571	0.004	0.002	-	0.067	99.73
EA07-R1	10	76.06	0.078	13.30	-	1.046	0.057	0.028	0.306	4.983	4.536	0.007	-	-	0.068	100.47
EA07-R2	10	76.10	0.073	13.12	-	1.014	0.053	0.023	0.286	4.895	4.531	0.003	0.001	-	0.064	100.16
EA07-R3	10	76.18	0.081	13.31	-	0.920	0.056	0.017	0.311	4.824	4.579	0.005	0.001	0.006	0.069	100.36
EA08-P1	20	75.76	0.075	13.12	-	0.961	0.050	0.019	0.254	4.691	4.725	0.008	0.004	-	0.070	99.74
EA08-P2	20	75.92	0.075	13.19	-	0.972	0.053	0.020	0.235	4.711	4.685	0.007	0.002	0.004	0.076	99.95
EA08-R1	20	75.94	0.078	13.14	0.002	0.952	0.051	0.018	0.223	4.717	4.799	0.006	-	0.002	0.065	99.99
EA09-P1-A	20	75.58	0.078	13.10	-	1.281	0.065	0.045	0.418	4.889	4.470	0.007	0.001	-	0.070	100.00

Table C.1 - Major-Element Analyses of Geological Specimens (mean of *n* analyses; weight percent)

Specimen	n	SiO_2	TiO_2	Al_2O3	Cr_2O_3	FeO(T)	MnO	MgO	CaO	Na_2O	K_2O	P_2O_5	F	SO_3	Cl	Total
EA09-P1-B	20	75.95	0.077	13.15	-	1.273	0.067	0.047	0.416	4.936	4.428	0.005	0.003	0.003	0.076	100.43
EA09-P1-C	20	75.76	0.076	13.12	-	1.273	0.068	0.045	0.419	4.877	4.480	0.006	0.003	0.001	0.073	100.20
EA09-P1-D	20	75.80	0.079	13.13	-	1.267	0.066	0.045	0.422	4.788	4.473	0.009	0.002	-	0.070	100.15
EA09-P2	20	75.51	0.079	13.14	-	1.275	0.062	0.046	0.416	4.838	4.414	0.006	0.003	0.002	0.070	99.86
EA09-R1	20	75.42	0.075	13.17	0.001	1.274	0.063	0.046	0.412	4.879	4.448	0.007	0.001	0.002	0.072	99.87
EA09-R2A	20	75.22	0.076	13.13	0.001	1.275	0.065	0.046	0.410	4.878	4.392	0.009	0.002	0.001	0.068	99.57
EA09-R2B	10	75.40	0.077	13.04	-	1.301	0.069	0.047	0.413	4.951	4.433	0.010	0.001	0.004	0.085	99.84
EA09-R2C	20	75.40	0.070	13.13	0.001	1.277	0.059	0.046	0.408	4.841	4.453	0.009	0.001	-	0.070	99.76
EA09-R2D	20	75.00	0.075	13.10	-	1.274	0.065	0.045	0.408	4.819	4.435	0.005	0.002	0.002	0.071	99.30
EA09-R2E	10	75.69	0.078	13.12	-	1.299	0.061	0.047	0.408	4.951	4.448	0.006	0.002	0.003	0.068	100.17
EA09-R3A	10	75.26	0.073	13.08	-	1.291	0.064	0.044	0.405	4.936	4.435	0.009	0.001	-	0.062	99.66
EA09-R3B	10	75.56	0.077	13.09	0.001	1.290	0.060	0.047	0.404	4.884	4.456	0.012	0.001	-	0.067	99.96
EA09-R3C	20	75.27	0.074	13.15	-	1.275	0.067	0.046	0.411	4.786	4.404	0.007	0.001	0.002	0.067	99.56
EA09-R3D	10	75.51	0.076	13.01	-	1.301	0.069	0.046	0.404	4.904	4.387	0.009	0.002	0.002	0.071	99.79
EA09-R3E	10	75.07	0.076	12.98	-	1.287	0.074	0.047	0.396	4.882	4.432	0.007	0.004	0.006	0.065	99.33
EA10-P1	10	75.81	0.077	13.12	-	1.020	0.056	0.026	0.328	4.629	4.620	0.006	0.001	0.002	0.064	99.76
EA10-P2	10	75.67	0.071	13.01	0.002	1.057	0.056	0.031	0.357	4.435	4.889	0.003	0.004	0.007	0.067	99.66
EA10-P3	10	75.52	0.072	13.12	-	1.128	0.059	0.035	0.360	4.446	4.489	0.006	0.003	0.003	0.071	99.32
EA10-P4	10	76.01	0.071	13.13	-	0.992	0.058	0.032	0.345	4.508	4.619	0.005	0.003	-	0.070	99.84
EA10-R1-A	20	75.73	0.074	13.16	0.001	1.045	0.056	0.034	0.377	4.579	4.664	0.007	0.002	0.001	0.061	99.79
EA10-R1-B	20	76.20	0.079	13.18	-	0.945	0.054	0.029	0.335	4.665	4.673	0.006	0.002	0.001	0.066	100.23
EA10-R2	10	75.70	0.072	13.15	0.004	0.989	0.057	0.027	0.337	4.586	4.653	0.011	0.004	0.002	0.074	99.66
EA11-P1	20	75.83	0.078	13.22	0.001	1.013	0.050	0.021	0.269	4.886	4.459	0.003	-	0.004	0.064	99.90
EA11-R1	20	76.06	0.077	13.17	0.001	0.940	0.050	0.017	0.253	4.844	4.444	0.006	0.002	0.004	0.065	99.94
EA11-R2	20	75.54	0.073	13.09	-	0.965	0.052	0.018	0.236	4.716	4.432	0.005	0.002	-	0.067	99.20
EA12-P1	20	76.05	0.068	13.24	-	0.714	0.023	0.015	0.463	3.882	5.072	0.017	0.002	0.002	0.025	99.57
EA12-P2	20	76.16	0.069	13.30	-	0.777	0.024	0.016	0.442	3.911	5.102	0.016	0.004	0.003	0.024	99.85
EA12-R1-A	20	75.97	0.066	13.23	-	0.756	0.029	0.021	0.446	3.869	5.119	0.017	0.002	0.003	0.020	99.55
EA12-R1-B	20	76.03	0.065	13.23	-	0.791	0.029	0.023	0.478	3.876	5.122	0.018	0.002	-	0.019	99.69

Table C.1 - Major-Element Analyses of Geological Specimens (mean of *n* analyses; weight percent)

Specimen	n	SiO_2	TiO_2	Al_2O3	Cr_2O_3	FeO(T)	MnO	MgO	CaO	Na_2O	K_2O	P_2O_5	F	SO_3	Cl	Total
EA13-P1	20	76.13	0.069	13.23	-	0.770	0.024	0.021	0.478	3.882	5.112	0.015	0.002	-	0.016	99.76
EA13-P2	20	75.98	0.065	13.27	0.001	0.790	0.028	0.023	0.452	3.868	5.164	0.017	0.004	0.002	0.033	99.70
EA13-R1	20	75.80	0.065	13.18	-	0.715	0.022	0.012	0.487	3.865	5.099	0.016	0.002	-	0.022	99.28
EA13-R2	20	75.78	0.066	13.23	-	0.797	0.026	0.022	0.469	3.863	5.078	0.014	0.002	0.002	0.022	99.38
EA14-P1-A	10	76.23	0.063	13.04	-	0.367	0.022	0.024	0.516	3.901	4.988	0.021	0.003	0.002	0.035	99.21
EA14-P1-B	10	76.55	0.062	13.28	-	0.365	0.031	0.028	0.500	3.792	4.956	0.013	0.002	-	0.022	99.60
EA14-P2	10	76.43	0.065	13.36	-	0.468	0.027	0.028	0.507	4.145	4.873	0.018	0.001	0.005	0.032	99.95
EA14-P3	10	76.25	0.068	13.29	0.003	0.441	0.023	0.028	0.512	4.162	4.951	0.015	0.002	0.003	0.021	99.77
EA14-P4	10	76.38	0.062	13.25	-	0.441	0.025	0.031	0.512	4.061	4.965	0.017	0.005	0.005	0.024	99.78
EA14-P5	10	76.21	0.065	13.30	0.001	0.423	0.026	0.035	0.511	3.955	4.861	0.017	0.002	0.002	0.017	99.42
EA14-R1	10	76.54	0.069	13.33	-	0.563	0.032	0.034	0.520	4.186	4.803	0.015	0.002	-	0.019	100.11
EA15-P1	10	76.51	0.065	13.26	0.002	0.433	0.024	0.031	0.518	3.967	4.951	0.023	0.002	-	0.023	99.81
EA15-P2	10	76.45	0.067	13.23	0.001	0.426	0.029	0.034	0.519	3.878	4.962	0.016	0.004	-	0.020	99.63
EA15-P3	10	76.23	0.062	12.98	-	0.514	0.025	0.032	0.520	3.960	4.977	0.018	-	-	0.034	99.36
EA15-R1-A	10	76.46	0.070	13.21	-	0.383	0.025	0.029	0.502	3.887	4.959	0.016	0.003	0.008	0.020	99.57
EA15-R1-B	10	76.48	0.066	13.19	-	0.423	0.027	0.029	0.503	3.835	4.919	0.017	0.005	0.003	0.019	99.52
EA15-R2	10	76.51	0.066	13.21	-	0.406	0.025	0.028	0.518	3.882	4.943	0.015	0.003	-	0.020	99.63
EA16-P1-A	10	76.66	0.063	13.01	-	0.607	0.031	0.028	0.450	3.694	4.987	0.017	0.001	-	0.019	99.56
EA16-P1-B	10	76.81	0.062	12.96	0.001	0.481	0.023	0.028	0.461	3.970	5.032	0.013	0.004	0.002	0.026	99.88
EA16-P2-A	10	76.57	0.066	12.99	-	0.677	0.023	0.026	0.477	3.799	4.995	0.017	0.002	-	0.021	99.67
EA16-P2-B	10	76.52	0.066	13.11	-	0.566	0.028	0.027	0.470	3.775	4.994	0.016	0.002	-	0.020	99.59
EA16-P2-C	10	76.79	0.061	13.06	-	0.555	0.026	0.024	0.471	3.623	5.010	0.018	0.001	-	0.022	99.66
EA16-R1-A	10	76.64	0.063	12.98	-	0.546	0.025	0.027	0.452	3.951	4.950	0.018	0.003	0.001	0.019	99.67
EA16-R1-B	10	76.51	0.066	13.02	-	0.727	0.029	0.025	0.455	3.806	5.012	0.016	0.002	-	0.020	99.69
EA16-R2-A	10	76.37	0.068	12.88	-	0.667	0.027	0.025	0.446	3.770	5.001	0.017	0.002	0.004	0.020	99.30
EA16-R2-B	10	76.80	0.068	13.16	-	0.542	0.024	0.025	0.455	3.786	5.015	0.018	0.003	-	0.024	99.92
EA16-R3	10	76.44	0.062	13.00	-	0.702	0.030	0.025	0.488	3.835	4.997	0.011	0.005	-	0.019	99.61
EA17-P1-A	10	76.16	0.069	13.21	-	0.704	0.021	0.016	0.508	3.720	4.966	0.025	0.002	0.002	0.034	99.44
EA17-P1-B	10	76.32	0.070	13.32	-	0.674	0.025	0.013	0.507	3.803	4.819	0.016	0.005	-	0.024	99.60

Table C.1 - Major-Element Analyses of Geological Specimens (mean of *n* analyses; weight percent)

Specimen	n	SiO_2	TiO_2	Al_2O3	Cr_2O_3	FeO(T)	MnO	MgO	CaO	Na_2O	K_2O	P_2O_5	F	SO_3	Cl	Total
EA17-P1-C	10	76.30	0.063	13.28	0.002	0.712	0.025	0.019	0.512	3.900	4.946	0.022	0.005	0.004	0.021	99.81
EA17-P1-D	10	76.13	0.070	13.24	0.001	0.780	0.024	0.020	0.501	3.986	4.792	0.016	0.003	-	0.025	99.59
EA17-P1-E	10	76.22	0.068	13.32	-	0.764	0.027	0.017	0.504	3.905	4.874	0.014	0.002	-	0.025	99.74
EA17-P1-F	10	76.21	0.066	13.28	-	0.915	0.022	0.022	0.508	3.823	4.879	0.013	0.001	-	0.025	99.76
EA17-P2-A	10	76.24	0.069	13.24	-	0.842	0.024	0.020	0.498	3.982	4.861	0.020	0.002	-	0.025	99.82
EA17-P2-B	10	76.24	0.068	13.22	0.005	0.766	0.023	0.019	0.498	3.798	4.863	0.019	0.006	-	0.017	99.54
EA17-P2-C	10	76.13	0.071	13.19	-	1.004	0.026	0.026	0.508	3.816	4.888	0.019	0.004	-	0.021	99.70
EA17-P2-D	10	76.35	0.066	13.29	0.001	0.727	0.022	0.015	0.513	3.640	4.902	0.018	0.003	-	0.020	99.56
EA17-P3-A	10	75.89	0.066	13.21	-	0.814	0.022	0.016	0.507	3.778	4.889	0.014	0.001	0.001	0.021	99.24
EA17-P3-B	10	76.14	0.068	13.19	-	0.858	0.018	0.021	0.508	3.757	4.888	0.019	0.004	0.004	0.027	99.50
EA17-P3-C	10	76.23	0.066	13.29	-	0.783	0.022	0.013	0.502	3.769	4.862	0.015	0.003	-	0.019	99.57
EA17-P4	10	76.05	0.067	13.07	-	0.699	0.024	0.013	0.509	3.667	4.936	0.018	0.002	-	0.028	99.08
EA17-P5	10	75.92	0.066	13.29	0.003	0.828	0.029	0.023	0.521	3.881	4.923	0.019	0.002	-	0.033	99.54
EA17-R1	10	76.01	0.069	13.23	-	0.831	0.026	0.019	0.508	3.835	4.897	0.014	0.005	0.003	0.019	99.47
EA17-R2-A	10	75.68	0.069	13.19	-	0.859	0.024	0.016	0.506	3.686	4.920	0.011	0.003	-	0.023	98.99
EA17-R2-B	10	76.24	0.070	13.22	0.001	0.780	0.022	0.017	0.508	3.844	4.937	0.015	0.002	-	0.020	99.68
EA18-P1	10	76.35	0.065	13.24	-	0.669	0.025	0.018	0.511	4.021	4.880	0.019	0.002	-	0.019	99.82
EA18-R1	10	75.73	0.067	13.14	-	0.810	0.024	0.021	0.515	3.923	4.868	0.015	0.002	-	0.019	99.14
EA19-P1	10	75.76	0.069	13.24	-	0.908	0.026	0.021	0.518	3.832	4.924	0.018	0.003	-	0.018	99.34
EA19-R1	10	75.88	0.068	13.19	-	0.876	0.032	0.022	0.507	3.821	4.937	0.009	0.003	0.004	0.021	99.38
EA20-P1	10	71.51	0.378	9.77	0.002	6.385	0.172	0.007	0.274	5.475	5.162	0.018	0.002	0.014	0.148	99.31
EA20-P2	10	71.64	0.379	9.80	0.002	6.441	0.175	0.009	0.269	5.575	4.867	0.014	0.002	0.031	0.157	99.36
EA20-R1	10	71.48	0.389	9.87	0.003	6.484	0.169	0.004	0.281	5.830	4.745	0.014	0.002	0.024	0.155	99.45
EA21-P1	10	74.46	0.194	11.95	-	3.036	0.073	0.001	0.106	5.035	5.226	0.001	0.001	0.001	0.146	100.23
EA21-P2	10	73.91	0.192	11.84	-	3.117	0.074	0.001	0.168	5.148	5.218	0.004	0.002	0.002	0.137	99.81
EA21-R1-A	10	73.86	0.202	11.73	-	3.055	0.075	0.003	0.158	4.657	5.274	0.005	0.003	0.004	0.132	99.16
EA21-R1-B	10	74.02	0.192	11.86	-	3.025	0.074	0.002	0.226	4.781	5.280	0.009	0.001	0.002	0.130	99.60
EA22-P1-A	10	74.32	0.198	11.74	-	2.986	0.067	0.001	0.245	5.016	5.120	0.005	0.003	0.002	0.138	99.83
EA22-P1-B	10	74.36	0.194	11.60	-	2.948	0.075	0.002	0.194	4.801	5.276	0.002	0.002	0.009	0.153	99.62

Table C.1 - Major-Element Analyses of Geological Specimens (mean of *n* analyses; weight percent)

Specimen	n	SiO_2	TiO_2	Al_2O3	Cr_2O_3	FeO(T)	MnO	MgO	CaO	Na_2O	K_2O	P_2O_5	F	SO_3	Cl	Total
EA22-P1-C	10	74.17	0.195	11.73	-	2.991	0.073	0.002	0.241	4.999	5.124	0.004	0.001	0.001	0.134	99.66
EA22-P1-D	10	74.27	0.192	11.75	-	3.010	0.070	0.003	0.257	4.976	5.216	0.008	-	0.004	0.143	99.90
EA22-P2	10	74.27	0.182	11.74	-	3.082	0.076	0.002	0.253	4.833	5.159	0.004	0.001	0.004	0.130	99.74
EA22-P3	10	74.37	0.192	11.71	-	3.018	0.075	0.001	0.248	4.704	5.198	0.005	0.002	0.005	0.130	99.66
EA22-P4	10	74.34	0.193	11.65	-	2.928	0.071	0.002	0.167	4.727	5.008	-	0.003	-	0.128	99.21
EA22-P5-A	10	73.82	0.193	11.67	-	2.997	0.077	0.001	0.240	5.104	5.128	0.008	0.003	0.003	0.143	99.39
EA22-P5-B	10	73.80	0.197	11.64	-	3.003	0.082	0.002	0.253	5.190	5.164	0.007	0.004	-	0.131	99.48
EA22-P6-A	10	74.04	0.194	11.72	-	3.013	0.072	0.001	0.235	5.049	5.127	0.007	0.002	0.001	0.125	99.59
EA22-P6-B	10	74.39	0.186	11.74	-	2.996	0.072	-	0.245	4.786	5.142	0.004	0.002	0.001	0.128	99.70
EA22-P7-A	10	74.16	0.183	11.67	-	3.026	0.077	0.002	0.238	4.941	5.115	0.003	0.006	-	0.132	99.55
EA22-P7-B	10	74.48	0.188	11.67	-	3.032	0.067	0.001	0.241	4.780	5.070	0.005	0.002	0.001	0.130	99.67
EA22-P8-A	10	74.24	0.199	11.64	-	3.000	0.081	0.001	0.228	4.833	5.085	0.003	0.001	-	0.128	99.45
EA22-P8-B	10	74.31	0.187	11.70	-	3.010	0.077	0.001	0.238	4.863	5.119	0.001	0.002	0.003	0.123	99.63
EA22-P9	10	74.44	0.193	11.71	-	3.023	0.075	0.002	0.247	5.055	4.935	0.003	-	-	0.126	99.80
EA22-R1	10	74.55	0.185	11.74	-	3.072	0.072	0.001	0.254	4.824	5.049	-	0.005	0.004	0.128	99.88
EA22-R2	10	74.62	0.189	11.78	0.005	3.075	0.071	0.002	0.255	4.944	5.080	0.004	0.005	0.001	0.126	100.15
EA23-P1-A	10	73.15	0.217	12.52	0.002	3.121	0.081	0.005	0.376	5.130	5.356	0.004	0.005	0.004	0.102	100.08
EA23-P1-B	10	73.15	0.223	12.48	-	3.102	0.081	0.006	0.377	5.118	5.424	0.007	0.004	0.008	0.101	100.08
EA23-P2	10	72.88	0.226	12.49	-	3.067	0.077	0.008	0.378	5.062	5.271	0.003	0.003	0.004	0.099	99.57
EA23-P3	10	72.95	0.226	12.45	-	3.110	0.085	0.008	0.380	4.903	5.422	0.009	0.001	0.004	0.107	99.66
EA23-P4	10	73.22	0.220	12.45	0.003	3.085	0.085	0.008	0.382	4.879	5.345	-	0.001	0.005	0.104	99.79
EA23-R1-A	10	72.92	0.229	12.45	-	3.114	0.078	0.004	0.377	4.995	5.331	0.007	0.001	0.008	0.102	99.62
EA23-R1-B	10	72.95	0.225	12.49	-	3.108	0.092	0.006	0.373	5.358	5.276	0.003	0.002	0.012	0.099	100.00
EA23-R2-A	10	73.35	0.220	12.54	0.003	3.096	0.082	0.006	0.372	5.148	5.331	0.007	0.002	0.008	0.097	100.27
EA23-R2-B	10	73.44	0.223	12.50	-	3.101	0.082	0.007	0.372	5.250	5.304	0.003	0.002	0.012	0.098	100.39
EA24-P1-A	10	73.59	0.206	12.03	-	3.289	0.083	0.003	0.287	5.533	4.837	0.004	0.003	0.001	0.131	100.00
EA24-P1-B	10	73.61	0.209	12.10	0.003	3.308	0.089	0.003	0.293	5.489	4.708	0.006	0.001	0.002	0.129	99.96
EA24-P1-C	10	73.63	0.206	12.10	0.002	3.301	0.083	0.001	0.302	5.228	4.804	-	0.001	0.001	0.129	99.79
EA24-P2-A	10	73.64	0.204	12.03	-	3.297	0.086	-	0.288	5.491	4.724	0.011	0.002	0.007	0.130	99.91

Table C.1 - Major-Element Analyses of Geological Specimens (mean of *n* analyses; weight percent)

Specimen	n	SiO_2	TiO_2	Al_2O3	Cr_2O_3	FeO(T)	MnO	MgO	CaO	Na_2O	K_2O	P_2O_5	F	SO_3	Cl	Total
EA24-P2-B	10	73.79	0.202	12.12	0.001	3.321	0.087	0.001	0.291	5.330	4.738	0.003	0.004	0.006	0.125	100.01
EA24-P3	10	73.90	0.210	11.98	-	3.289	0.090	0.001	0.301	5.245	4.800	0.001	0.002	0.002	0.127	99.95
EA24-P4	10	74.05	0.210	12.04	-	3.293	0.087	0.001	0.291	5.464	4.798	0.008	0.002	-	0.127	100.37
EA24-P5-A	10	73.26	0.208	11.98	-	3.347	0.088	0.002	0.304	5.304	4.780	0.002	0.003	0.005	0.133	99.42
EA24-P5-B	10	73.51	0.205	12.00	0.003	3.302	0.084	0.005	0.303	5.162	4.934	-	0.002	0.002	0.134	99.65
EA24-P6-A	10	73.30	0.208	12.06	-	3.343	0.088	0.002	0.305	5.194	4.691	0.003	0.003	0.004	0.128	99.32
EA24-P6-B	10	73.97	0.208	12.09	-	3.327	0.089	0.001	0.290	5.297	4.755	0.002	0.002	0.005	0.126	100.16
EA24-P7	10	73.76	0.206	11.97	0.001	3.281	0.088	0.001	0.295	5.264	4.711	0.004	0.001	0.003	0.122	99.71
EA24-P8-A	10	73.65	0.204	12.07	-	3.328	0.083	-	0.293	5.316	4.766	0.004	0.001	0.001	0.132	99.84
EA24-P8-B	10	73.80	0.203	12.09	-	3.301	0.085	0.002	0.284	5.090	4.858	0.007	0.001	0.008	0.129	99.86
EA24-P9-A	10	73.75	0.199	12.12	-	3.320	0.082	0.002	0.281	5.434	4.780	0.002	0.004	0.001	0.130	100.11
EA24-P9-B	10	74.04	0.205	12.20	0.001	3.323	0.082	0.003	0.290	5.388	4.761	0.004	0.003	0.005	0.129	100.44
EA24-R1	10	73.69	0.200	11.68	0.001	3.265	0.085	0.002	0.303	5.044	4.791	0.004	0.005	0.006	0.127	99.20
EA24-R2	10	73.82	0.207	11.93	-	3.292	0.094	0.001	0.287	5.146	4.765	0.005	0.004	-	0.124	99.67
EA25-P1-A	10	75.38	0.153	11.12	-	2.689	0.053	-	0.149	4.571	4.889	0.009	0.001	0.001	0.138	99.16
EA25-P1-B	10	75.55	0.154	11.21	-	2.708	0.051	-	0.088	4.722	5.013	-	0.002	0.002	0.132	99.64
EA25-P1-C	10	75.46	0.153	11.19	-	2.715	0.056	-	0.160	4.644	4.830	0.001	0.004	0.004	0.134	99.35
EA25-P1-D	10	75.72	0.150	11.26	-	2.753	0.047	-	0.108	4.682	4.896	0.003	0.001	0.004	0.141	99.76
EA25-P2-A	10	75.51	0.153	11.24	0.003	2.676	0.050	-	0.102	4.802	4.820	0.002	0.001	0.004	0.141	99.50
EA25-P2-B	10	75.48	0.151	11.19	-	2.739	0.051	-	0.106	4.791	4.879	0.001	0.004	0.007	0.142	99.55
EA25-P2-C	10	75.40	0.151	11.20	0.002	2.748	0.050	-	0.073	4.806	5.039	-	0.002	0.005	0.135	99.62
EA25-P2-D	10	75.49	0.150	11.23	0.003	2.740	0.049	-	0.121	4.856	4.974	0.002	0.006	0.008	0.142	99.77
EA25-P3	10	75.44	0.156	11.13	-	2.710	0.051	-	0.185	4.719	4.986	-	0.001	0.001	0.129	99.51
EA25-R1	10	75.47	0.155	11.08	-	2.691	0.050	-	0.178	4.719	4.901	0.002	0.002	0.002	0.125	99.37
EA25-R2	10	75.50	0.158	11.07	0.003	2.692	0.049	-	0.123	4.825	4.919	0.001	0.003	0.004	0.130	99.48
EA26-P1-A	10	76.18	0.107	12.00	0.001	1.901	0.041	0.002	0.194	4.640	4.614	-	-	0.001	0.101	99.78
EA26-P1-B	10	76.60	0.106	12.04	0.001	1.899	0.038	0.001	0.194	4.617	4.579	0.004	0.003	-	0.102	100.18
EA26-P2-A	10	75.89	0.106	11.95	-	1.911	0.040	0.004	0.195	4.572	4.585	0.003	0.001	-	0.106	99.36
EA26-P2-B	10	76.11	0.112	12.03	-	1.915	0.041	0.003	0.194	4.604	4.594	0.001	0.003	0.001	0.104	99.71

Table C.1 - Major-Element Analyses of Geological Specimens (mean of *n* analyses; weight percent)

Specimen	n	SiO_2	TiO_2	Al_2O3	Cr_2O_3	FeO(T)	MnO	MgO	CaO	Na_2O	K_2O	P_2O_5	F	SO_3	Cl	Total
EA26-R1-A	10	76.04	0.109	11.94	-	1.915	0.044	0.006	0.198	4.579	4.619	-	0.003	0.002	0.115	99.57
EA26-R1-B	10	76.14	0.109	11.99	0.001	1.902	0.038	0.003	0.197	4.981	4.603	0.003	-	0.002	0.118	100.08
EA26-R2-A	10	75.76	0.107	11.96	-	1.899	0.037	-	0.193	4.676	4.574	0.002	0.001	-	0.107	99.31
EA26-R2-B	10	75.67	0.104	11.95	-	1.911	0.037	0.003	0.197	4.624	4.588	0.002	-	0.004	0.104	99.20
EA26-R2-C	10	75.87	0.105	11.98	0.001	1.901	0.036	0.002	0.198	4.562	4.609	-	0.001	0.003	0.107	99.38
EA26-R2-D	10	75.93	0.108	11.99	-	1.911	0.036	0.004	0.199	4.813	4.615	-	-	0.002	0.105	99.71
EA26-R3-A	10	75.81	0.099	11.88	-	1.905	0.042	0.002	0.195	5.039	4.562	0.005	0.001	-	0.113	99.65
EA26-R3-B	10	76.14	0.101	12.04	0.001	1.897	0.036	0.001	0.196	4.955	4.570	-	0.001	0.001	0.108	100.05
EA26-R3-C	10	75.95	0.106	11.90	0.002	1.902	0.037	0.002	0.200	4.610	4.568	0.005	0.003	0.002	0.113	99.40
EA26-R3-D	10	76.30	0.104	12.07	-	1.904	0.037	0.002	0.193	4.793	4.584	0.002	0.004	0.002	0.110	100.11
EA27-P1	10	71.64	0.385	9.92	0.004	6.546	0.172	0.004	0.320	6.228	4.725	0.009	0.004	0.034	0.133	100.13
EA27-P2	10	71.51	0.379	9.78	0.003	6.499	0.174	0.004	0.308	5.745	5.161	0.005	0.002	0.024	0.151	99.75
EA27-R1	10	71.67	0.380	9.80	-	6.384	0.170	0.006	0.289	5.872	4.917	0.009	0.002	0.020	0.144	99.67
EA28-P1	10	72.01	0.379	9.81	-	6.300	0.168	0.007	0.250	6.531	4.036	0.013	0.002	0.020	0.106	99.63
EA28-P2-A	10	72.00	0.396	9.81	0.001	6.583	0.179	0.006	0.270	7.370	2.841	0.014	0.003	0.023	0.135	99.64
EA28-P2-B	10	71.95	0.390	9.84	0.003	6.524	0.179	0.007	0.318	6.816	3.350	0.010	0.004	0.023	0.119	99.54
EA28-P2-C	10	72.29	0.403	9.86	-	6.554	0.177	0.006	0.326	7.343	2.693	0.012	0.002	0.027	0.128	99.83
EA28-P3-A	10	71.80	0.388	9.86	-	6.417	0.180	0.006	0.299	5.954	4.596	0.005	0.001	0.016	0.141	99.66
EA28-P3-B	10	71.89	0.378	9.88	-	6.348	0.176	0.005	0.304	5.997	4.539	0.010	0.001	0.026	0.140	99.70
EA28-P4-A	10	71.71	0.384	9.95	0.002	6.377	0.167	0.003	0.283	6.276	4.728	0.010	0.001	0.026	0.141	100.06
EA28-P4-B	10	71.92	0.381	9.96	0.002	6.377	0.170	0.006	0.317	6.169	4.600	0.014	0.002	0.027	0.141	100.08
EA28-P5-A	10	71.63	0.385	9.57	-	6.443	0.172	0.007	0.338	5.944	4.616	0.010	0.001	0.023	0.117	99.26
EA28-P5-B	10	71.95	0.388	9.94	-	6.493	0.173	0.009	0.240	6.866	3.890	0.010	-	0.019	0.100	100.08
EA28-R1	10	70.92	0.375	9.66	0.001	6.381	0.175	0.006	0.357	5.791	4.564	0.007	0.004	0.022	0.134	98.40
EA28-R2	10	70.92	0.372	9.76	-	6.340	0.174	0.007	0.337	6.217	4.728	0.010	0.003	0.026	0.138	99.04
EA29-R1-A	10	71.65	0.384	9.97	0.001	6.477	0.168	0.006	0.322	6.178	5.300	0.009	0.004	0.019	0.151	100.64
EA29-R1-B	10	71.93	0.389	9.95	-	6.495	0.169	0.007	0.326	5.977	5.301	0.011	0.002	0.026	0.157	100.74
EA29-R2	10	71.47	0.367	9.80	-	6.374	0.176	0.003	0.321	5.817	5.237	0.012	0.002	0.022	0.143	99.74
EA30-P1	20	74.80	0.072	12.89	-	1.269	0.065	0.045	0.403	4.732	4.376	0.006	0.003	-	0.064	98.73

Table C.1 - Major-Element Analyses of Geological Specimens (mean of *n* analyses; weight percent)

Specimen	n	SiO_2	TiO_2	Al_2O3	Cr_2O_3	FeO(T)	MnO	MgO	CaO	Na_2O	K_2O	P_2O_5	F	SO_3	Cl	Total
EA30-P2	20	75.08	0.072	12.96	-	1.280	0.066	0.047	0.400	4.780	4.438	0.002	-	-	0.063	99.19
EA30-R1	20	75.30	0.074	13.09	-	1.265	0.068	0.044	0.404	4.859	4.395	0.005	0.003	-	0.059	99.57
EA30-R2-A	20	74.91	0.074	13.05	0.002	1.268	0.064	0.046	0.405	4.791	4.428	0.001	0.002	-	0.066	99.11
EA30-R2-B	20	75.10	0.071	13.03	0.001	1.273	0.062	0.045	0.399	4.774	4.422	0.004	0.001	0.002	0.066	99.25
EA30-R3A	20	75.34	0.079	13.04	-	1.262	0.066	0.043	0.409	4.760	4.432	0.006	0.003	-	0.060	99.50
EA30-R3B	20	75.29	0.074	13.09	-	1.268	0.066	0.046	0.404	4.840	4.410	0.003	0.002	-	0.060	99.55
EA30-R3C	20	75.29	0.073	13.09	-	1.263	0.070	0.045	0.404	4.838	4.427	0.008	0.002	-	0.058	99.58
EA30-R3D	20	75.29	0.079	12.99	-	1.257	0.064	0.043	0.409	4.773	4.445	0.005	0.002	-	0.060	99.42
EA30-R3E	20	75.44	0.073	13.01	-	1.250	0.064	0.043	0.402	4.841	4.399	0.007	0.003	-	0.061	99.59
EA30-R3F	20	75.26	0.070	12.99	-	1.287	0.066	0.045	0.399	4.737	4.387	0.007	0.002	-	0.063	99.32
EA30-R3G	20	75.14	0.076	13.08	-	1.290	0.064	0.045	0.407	4.811	4.358	0.005	0.002	-	0.062	99.34
EA31-P1	20	75.06	0.076	13.16	-	1.246	0.064	0.043	0.407	4.769	4.458	0.010	0.001	0.004	0.060	99.36
EA31-R1	20	75.55	0.077	13.19	-	1.271	0.065	0.043	0.406	4.843	4.455	0.007	0.002	0.003	0.061	99.97
EA32-P1	20	75.38	0.071	13.19	-	1.269	0.065	0.043	0.409	4.790	4.387	0.008	0.003	0.003	0.061	99.67
EA32-R1	20	75.32	0.074	13.22	0.001	1.252	0.065	0.045	0.410	4.836	4.479	0.007	0.001	0.001	0.059	99.77
EA32-R2	20	75.56	0.078	13.20	-	1.255	0.063	0.044	0.412	4.864	4.467	0.005	0.001	0.005	0.061	100.02
EA33-P1-A	20	76.35	0.079	12.61	-	0.969	0.043	0.039	0.348	4.105	4.839	0.006	0.002	0.005	0.046	99.44
EA33-P1-B	20	76.66	0.079	12.68	0.004	0.984	0.045	0.040	0.336	4.221	4.876	0.006	0.001	0.004	0.049	99.98
EA33-P2-A	20	76.27	0.080	12.57	-	0.987	0.047	0.038	0.341	4.163	4.872	0.005	0.001	-	0.051	99.42
EA33-P2-B	20	76.59	0.084	12.71	0.001	1.002	0.046	0.039	0.346	4.094	4.868	0.006	0.002	-	0.051	99.84
EA33-P3	10	76.71	0.081	12.60	-	0.986	0.047	0.041	0.343	4.259	4.780	0.003	0.001	-	0.050	99.90
EA33-P4	10	76.60	0.082	12.67	-	0.993	0.044	0.037	0.338	4.261	4.813	0.005	0.002	-	0.049	99.89
EA33-P5	10	76.75	0.080	12.65	0.002	0.981	0.043	0.037	0.339	4.263	4.826	0.012	0.001	-	0.048	100.04
EA33-P6	10	76.77	0.091	12.64	-	0.989	0.044	0.040	0.340	4.213	4.852	0.003	0.002	0.001	0.050	100.04
EA33-P7	10	76.38	0.077	12.70	-	0.987	0.044	0.040	0.343	4.207	4.897	0.006	0.001	-	0.051	99.73
EA33-P8	10	75.73	0.085	12.51	-	0.991	0.042	0.042	0.349	4.148	4.875	0.003	-	0.005	0.053	98.84
EA33-R1	10	76.81	0.086	12.49	-	0.985	0.043	0.039	0.333	4.219	4.831	0.005	0.001	-	0.046	99.89
EA34-P1	10	76.35	0.082	12.72	-	0.982	0.042	0.038	0.344	4.273	4.822	0.003	0.003	0.003	0.047	99.71
EA34-P2	20	76.20	0.081	12.63	-	1.000	0.042	0.039	0.344	4.130	4.968	0.008	0.002	0.003	0.052	99.49

Table C.1 - Major-Element Analyses of Geological Specimens (mean of *n* analyses; weight percent)

Specimen	n	SiO_2	TiO_2	Al_2O3	Cr_2O_3	FeO(T)	MnO	MgO	CaO	Na_2O	K_2O	P_2O_5	F	SO_3	Cl	Total
EA34-P3	20	76.24	0.080	12.69	-	0.982	0.041	0.041	0.347	4.231	4.824	0.005	0.001	0.002	0.053	99.54
EA34-P4	20	75.29	0.077	13.16	0.001	1.243	0.061	0.043	0.401	4.833	4.425	0.011	0.001	-	0.060	99.61
EA34-P5	20	75.39	0.074	13.09	0.001	1.235	0.065	0.044	0.399	4.791	4.373	0.007	0.003	-	0.066	99.54
EA34-R1	10	76.56	0.079	12.47	0.001	0.992	0.048	0.041	0.347	4.213	4.852	0.003	0.002	0.001	0.046	99.66
EA34-R2	10	76.29	0.083	12.68	-	0.985	0.048	0.038	0.348	4.201	4.820	0.005	0.001	-	0.048	99.54
EA35-P1	10	76.43	0.080	12.68	-	0.978	0.044	0.038	0.345	4.260	4.840	0.004	0.002	-	0.046	99.74
EA35-P2	10	76.50	0.079	12.74	-	0.980	0.042	0.039	0.342	4.251	4.883	0.006	0.002	-	0.047	99.91
EA35-P3	20	76.63	0.084	12.71	-	0.986	0.043	0.039	0.342	4.220	4.707	0.006	0.003	-	0.049	99.82
EA35-R1	10	76.52	0.084	12.82	-	1.007	0.044	0.041	0.349	4.183	4.758	0.006	0.002	0.005	0.050	99.87
EA35-R2	20	76.46	0.084	12.72	-	0.988	0.044	0.040	0.338	4.197	4.807	0.004	0.004	-	0.052	99.73
EA36-P1-A	20	74.88	0.204	13.85	0.002	0.668	0.049	0.181	0.914	4.753	4.040	0.037	0.003	0.001	0.011	99.59
EA36-P1-B	20	75.06	0.217	13.85	-	0.680	0.054	0.165	0.891	4.660	4.186	0.036	0.002	-	0.011	99.82
EA36-P1-C	20	74.93	0.210	13.86	0.003	0.673	0.052	0.159	0.896	4.618	4.160	0.043	0.002	0.001	0.010	99.62
EA36-P1-D	20	75.30	0.214	13.67	-	0.651	0.044	0.125	0.812	4.516	4.288	0.037	0.002	-	0.013	99.67
EA36-P2	20	75.06	0.223	13.67	-	0.665	0.043	0.141	0.814	4.418	4.292	0.036	0.004	-	0.010	99.38
EA36-P3	20	75.65	0.230	13.34	0.001	0.741	0.055	0.186	0.713	4.278	4.416	0.037	0.002	-	0.010	99.65
EA36-P4-A	20	74.90	0.205	13.98	-	0.705	0.051	0.178	0.901	4.640	4.190	0.039	0.004	0.002	0.009	99.80
EA36-P4-B	20	75.29	0.210	13.74	-	0.752	0.054	0.168	0.838	4.574	4.090	0.035	0.004	-	0.013	99.76
EA36-R1	20	74.88	0.217	13.86	-	0.690	0.050	0.164	0.893	4.610	4.187	0.038	0.004	0.001	0.009	99.61
EA36-R2	20	75.59	0.216	13.54	0.001	0.606	0.045	0.145	0.735	4.254	4.477	0.042	0.003	-	0.008	99.66
EA36-R3A	20	74.75	0.220	13.56	-	0.734	0.054	0.183	0.780	4.259	4.517	0.039	0.003	-	0.013	99.12
EA36-R3B	20	75.07	0.223	13.64	0.002	0.603	0.057	0.171	0.777	4.364	4.507	0.039	0.002	0.001	0.029	99.49
EA36-R3C	20	74.59	0.220	13.60	-	0.721	0.064	0.217	0.780	4.287	4.561	0.036	0.001	0.001	0.020	99.10
EA36-R3D	20	74.90	0.217	13.73	-	0.704	0.052	0.168	0.851	4.439	4.309	0.034	0.003	0.001	0.008	99.42
EA36-R3E-A	20	75.01	0.214	13.57	-	0.683	0.055	0.172	0.786	4.308	4.514	0.040	0.002	0.004	0.019	99.38
EA36-R3E-B	20	75.08	0.209	13.90	-	0.659	0.054	0.186	0.867	4.576	4.243	0.039	0.002	0.002	0.024	99.85
EA36-R4A	20	75.23	0.219	13.59	-	0.629	0.052	0.164	0.739	4.381	4.404	0.038	0.003	-	0.011	99.46
EA36-R4B	20	75.07	0.216	13.68	-	0.527	0.048	0.138	0.760	4.428	4.416	0.040	0.003	-	0.017	99.35
EA36-R4C	20	75.23	0.221	13.47	-	0.664	0.055	0.191	0.709	4.330	4.536	0.035	0.002	-	0.011	99.46

Table C.1 - Major-Element Analyses of Geological Specimens (mean of *n* analyses; weight percent)

Specimen	n	SiO_2	TiO_2	Al_2O3	Cr_2O_3	FeO(T)	MnO	MgO	CaO	Na_2O	K_2O	P_2O_5	F	SO_3	Cl	Total
EA36-R4D	20	75.09	0.212	13.77	-	0.653	0.046	0.136	0.806	4.456	4.357	0.037	0.004	-	0.012	99.58
EA36-R4E	20	74.65	0.212	13.89	-	0.605	0.052	0.164	0.840	4.491	4.343	0.036	0.003	-	0.010	99.30
EA37-P1	20	76.44	0.138	12.95	0.003	0.604	0.037	0.087	0.662	4.108	4.357	0.017	0.002	-	0.047	99.45
EA37-P2	20	76.06	0.134	13.00	-	0.594	0.037	0.087	0.661	4.150	4.317	0.018	0.003	-	0.047	99.10
EA37-P3	20	76.11	0.134	12.97	-	0.653	0.039	0.105	0.682	4.125	4.390	0.015	0.002	0.001	0.048	99.27
EA37-P4	20	76.30	0.138	12.96	-	0.611	0.038	0.097	0.674	4.183	4.351	0.016	0.002	-	0.048	99.41
EA37-P5-A	20	76.40	0.140	13.02	-	0.665	0.040	0.108	0.674	4.142	4.418	0.015	0.002	-	0.050	99.67
EA37-P5-B	20	76.48	0.140	13.06	-	0.613	0.038	0.084	0.667	4.174	4.429	0.016	0.002	0.001	0.052	99.75
EA37-P6-A	20	76.41	0.138	12.98	-	0.639	0.038	0.094	0.669	4.200	4.421	0.017	0.003	-	0.049	99.66
EA37-P6-B	20	76.70	0.141	13.09	0.001	0.558	0.032	0.068	0.650	4.229	4.369	0.016	0.001	0.004	0.049	99.91
EA37-P7-A	20	76.52	0.137	13.08	0.002	0.669	0.038	0.097	0.677	4.207	4.379	0.016	0.002	0.002	0.048	99.87
EA37-P7-B	20	76.51	0.138	13.07	0.002	0.642	0.036	0.101	0.679	4.172	4.331	0.017	0.001	0.001	0.050	99.75
EA37-P8	20	76.53	0.135	12.99	-	0.622	0.041	0.097	0.678	4.206	4.334	0.015	0.002	-	0.047	99.70
EA37-R1	10	76.32	0.137	13.11	-	0.670	0.043	0.111	0.677	4.204	4.340	0.016	0.003	0.002	0.049	99.69
EA37-R2	10	76.23	0.141	13.16	0.001	0.784	0.039	0.123	0.689	4.242	4.326	0.020	0.002	0.003	0.050	99.81
EA38-P1	20	77.20	0.074	12.61	-	0.601	0.058	0.065	0.424	4.122	4.320	0.008	0.002	0.002	0.044	99.54
EA38-P2	20	77.32	0.070	12.63	0.002	0.588	0.057	0.064	0.423	4.164	4.370	0.007	0.001	-	0.039	99.74
EA38-P3	10	77.10	0.073	12.80	-	0.605	0.059	0.066	0.438	4.176	4.412	0.009	0.002	-	0.040	99.78
EA38-P4	20	77.19	0.073	12.59	-	0.591	0.060	0.064	0.424	4.104	4.409	0.011	0.003	0.004	0.038	99.56
EA38-R1	20	77.16	0.071	12.58	0.001	0.589	0.062	0.065	0.427	4.187	4.382	0.013	0.001	-	0.040	99.57
EA39-P1-A	20	76.01	0.081	12.87	-	0.837	0.062	0.013	0.202	4.768	4.680	0.006	0.001	-	0.038	99.57
EA39-P1-B	20	76.30	0.083	12.87	-	0.762	0.054	0.009	0.173	4.769	4.662	0.003	0.001	-	0.036	99.72
EA39-P2-A	20	76.21	0.084	12.87	-	0.729	0.054	0.009	0.150	4.779	4.649	0.001	0.002	0.002	0.035	99.57
EA39-P2-B	20	76.45	0.084	12.92	-	0.806	0.054	0.008	0.138	4.759	4.637	0.003	0.002	0.004	0.038	99.90
EA39-P3	20	76.06	0.085	12.82	-	0.728	0.057	0.007	0.146	4.771	4.676	0.002	0.001	0.003	0.037	99.40
EA39-P4	20	76.20	0.085	12.86	-	0.774	0.058	0.013	0.173	4.690	4.692	-	0.002	0.002	0.039	99.59
EA39-P5	20	76.18	0.082	12.89	0.002	0.690	0.051	0.009	0.144	4.763	4.656	0.003	0.001	-	0.035	99.50
EA39-P6-A	20	76.36	0.087	12.85	-	0.754	0.058	0.008	0.148	4.785	4.647	0.004	0.003	0.003	0.035	99.74
EA39-P6-B	20	76.69	0.087	12.98	-	0.763	0.057	0.010	0.153	4.898	4.654	0.002	0.001	0.002	0.037	100.33

Table C.1 - Major-Element Analyses of Geological Specimens (mean of *n* analyses; weight percent)

Specimen	n	SiO_2	TiO_2	Al_2O3	Cr_2O_3	FeO(T)	MnO	MgO	CaO	Na_2O	K_2O	P_2O_5	F	SO_3	Cl	Total
EA39-R1	20	76.76	0.085	12.80	0.002	0.699	0.053	0.011	0.182	4.816	4.629	0.004	0.001	0.002	0.034	100.08
EA39-R2	10	76.42	0.081	12.99	-	0.669	0.062	0.015	0.206	4.774	4.532	0.003	0.003	-	0.037	99.79
EA40-P1	20	75.62	0.098	13.01	-	0.608	0.061	0.009	0.210	4.705	4.659	0.008	0.001	-	0.037	99.02
EA40-R1	10	75.71	0.100	13.03	-	0.616	0.063	0.008	0.208	4.830	4.642	0.011	0.002	0.002	0.036	99.25
EA40-R2-A	10	75.91	0.094	13.14	-	0.712	0.060	0.015	0.219	4.796	4.530	0.009	0.003	0.003	0.040	99.53
EA40-R2-B	10	76.25	0.097	13.29	0.005	0.677	0.062	0.015	0.226	4.838	4.653	0.004	0.004	0.003	0.037	100.16
EA40-R3A	10	75.84	0.099	13.15	-	0.672	0.059	0.012	0.225	4.803	4.662	0.009	-	0.001	0.038	99.57
EA40-R3B	10	75.80	0.101	13.16	0.001	0.572	0.052	0.006	0.199	4.785	4.670	0.006	0.002	-	0.035	99.39
EA40-R3C	20	75.60	0.101	13.00	0.002	0.565	0.053	0.005	0.191	4.755	4.641	0.011	-	-	0.037	98.96
EA40-R3D	10	75.70	0.102	13.19	-	0.610	0.058	0.008	0.205	4.789	4.524	0.010	-	-	0.033	99.22
EA40-R3E	10	75.68	0.099	12.99	-	0.506	0.049	0.003	0.192	4.742	4.645	0.014	0.001	-	0.037	98.96
EA40-R4A	10	75.99	0.101	13.13	-	0.639	0.054	0.010	0.210	4.813	4.566	0.007	0.002	0.002	0.034	99.57
EA40-R4B	10	75.89	0.099	13.13	0.002	0.651	0.058	0.014	0.224	4.781	4.645	0.009	0.001	-	0.035	99.54
EA40-R4C	10	75.56	0.101	13.16	-	0.675	0.059	0.012	0.227	4.781	4.657	0.006	0.001	0.003	0.038	99.28
EA40-R4D	10	75.71	0.096	13.16	-	0.604	0.061	0.011	0.206	4.739	4.664	0.008	0.002	-	0.042	99.31
EA40-R4E	10	75.88	0.099	13.23	0.004	0.699	0.060	0.016	0.215	4.740	4.579	0.010	0.002	-	0.038	99.57
EA41-P1	20	75.88	0.074	13.16	-	0.755	0.048	0.064	0.777	3.887	4.921	0.008	0.002	-	0.105	99.68
EA41-R1	10	75.75	0.073	13.24	-	0.712	0.052	0.065	0.778	4.003	4.794	0.008	0.003	-	0.113	99.58
EA42-P1-A	10	75.68	0.072	13.17	0.001	0.732	0.052	0.066	0.762	4.061	4.728	0.010	0.002	0.002	0.107	99.44
EA42-P1-B	10	75.81	0.071	13.14	0.002	0.761	0.047	0.066	0.784	3.859	4.820	0.004	0.002	-	0.119	99.49
EA42-P2-A	10	75.91	0.079	13.22	0.002	0.792	0.050	0.068	0.782	4.137	4.596	0.004	-	-	0.111	99.76
EA42-P2-B	10	76.07	0.076	13.23	-	0.699	0.048	0.067	0.764	4.040	4.685	0.006	-	-	0.104	99.79
EA42-P3-A	10	75.92	0.076	13.22	-	0.709	0.049	0.065	0.764	4.097	4.679	0.007	0.001	0.001	0.103	99.69
EA42-P3-B	10	75.49	0.076	13.21	-	0.764	0.053	0.066	0.768	4.029	4.698	0.004	0.002	0.002	0.113	99.27
EA42-P4	10	75.64	0.077	13.16	-	0.764	0.054	0.068	0.776	4.015	4.637	0.006	0.002	0.002	0.114	99.32
EA42-R1	10	75.58	0.079	13.28	-	0.807	0.051	0.068	0.778	4.023	4.712	0.006	-	-	0.105	99.49
EA43-P1	10	73.52	0.069	13.68	0.004	1.560	0.047	0.050	0.840	4.328	4.796	0.022	-	-	0.109	99.03
EA43-P2-A	10	73.90	0.072	13.71	-	1.549	0.054	0.047	0.820	4.253	4.658	0.017	0.002	0.001	0.107	99.19
EA43-P2-B	10	73.80	0.072	13.94	-	1.571	0.052	0.051	0.831	4.340	4.764	0.017	0.003	0.002	0.116	99.55

Table C.1 - Major-Element Analyses of Geological Specimens (mean of *n* analyses; weight percent)

Specimen	n	SiO_2	TiO_2	Al_2O3	Cr_2O_3	FeO(T)	MnO	MgO	CaO	Na_2O	K_2O	P_2O_5	F	SO_3	Cl	Total
EA43-P3	10	73.59	0.071	13.83	-	1.579	0.050	0.058	0.849	4.361	4.796	0.017	0.004	-	0.105	99.31
EA43-R1	10	74.06	0.068	13.82	0.005	1.502	0.055	0.044	0.806	4.271	4.756	0.017	0.001	0.001	0.110	99.51
EA43-R2	10	73.56	0.069	13.82	0.002	1.562	0.053	0.049	0.835	4.287	4.646	0.020	0.003	0.002	0.103	99.00
EA44-P1	10	73.87	0.071	13.85	-	1.547	0.053	0.046	0.827	4.269	4.704	0.016	0.002	0.001	0.102	99.36
EA44-P2	20	73.95	0.071	13.69	-	1.555	0.055	0.047	0.819	4.268	4.740	0.019	0.002	-	0.103	99.32
EA44-P3	20	73.91	0.071	13.82	-	1.564	0.055	0.050	0.826	4.219	4.733	0.020	0.003	0.002	0.103	99.37
EA44-R1	10	73.63	0.072	13.74	-	1.529	0.051	0.046	0.820	4.219	4.774	0.020	0.001	0.003	0.103	99.01
EA45-P1-A	10	74.83	0.054	13.55	-	1.087	0.039	0.021	0.806	4.243	4.541	0.014	0.003	-	0.103	99.29
EA45-P1-B	10	75.31	0.051	13.66	-	1.092	0.040	0.021	0.803	4.275	4.637	0.010	0.001	0.003	0.103	100.01
EA45-P1-C	10	75.15	0.051	13.61	-	1.073	0.040	0.022	0.798	4.209	4.621	0.008	-	0.001	0.100	99.69
EA45-P1-D	10	75.18	0.052	13.66	-	1.099	0.040	0.023	0.817	4.293	4.695	0.016	0.001	-	0.103	99.98
EA45-P2-A	10	74.68	0.048	13.72	-	1.094	0.041	0.020	0.803	4.274	4.705	0.011	0.003	-	0.096	99.50
EA45-P2-B	10	75.51	0.048	13.72	-	1.153	0.044	0.023	0.808	4.203	4.693	0.013	0.001	0.002	0.103	100.32
EA45-P2-C	10	75.11	0.047	13.71	-	1.157	0.040	0.025	0.811	4.123	4.661	0.015	0.003	0.004	0.100	99.80
EA45-P3	10	75.39	0.045	13.67	0.004	1.105	0.042	0.021	0.784	4.094	4.663	0.011	0.001	-	0.103	99.94
EA45-P4	10	75.06	0.055	13.58	0.003	1.138	0.043	0.028	0.837	4.339	4.661	0.009	0.001	-	0.097	99.85
EA45-R1-A	10	74.40	0.053	13.61	-	1.169	0.044	0.028	0.828	4.082	4.704	0.014	0.002	0.005	0.103	99.04
EA45-R1-B	10	75.01	0.053	13.71	-	1.182	0.042	0.029	0.837	4.180	4.700	0.012	-	0.003	0.108	99.87
EA45-R2-A	10	74.59	0.051	13.40	0.001	1.082	0.032	0.022	0.811	4.232	4.602	0.012	0.001	-	0.103	98.93
EA45-R2-B	10	74.42	0.049	13.61	-	1.182	0.044	0.029	0.831	4.240	4.662	0.006	0.002	0.001	0.115	99.19
EA46-P1-A	10	74.84	0.044	13.61	0.001	1.122	0.044	0.026	0.816	4.187	4.553	0.014	0.002	-	0.109	99.37
EA46-P1-B	10	75.12	0.052	13.76	-	1.207	0.045	0.027	0.833	4.299	4.684	0.015	0.001	-	0.110	100.15
EA46-P1-C	10	75.34	0.053	13.66	-	1.169	0.042	0.028	0.823	4.266	4.638	0.018	0.004	-	0.108	100.15
EA46-P2	10	74.95	0.050	13.60	0.003	1.086	0.041	0.026	0.818	4.258	4.666	0.009	0.001	0.001	0.110	99.62
EA46-P3	10	75.07	0.049	13.62	-	1.118	0.043	0.022	0.801	4.309	4.638	0.013	0.002	-	0.109	99.80
EA46-P4	10	75.68	0.046	13.73	-	1.084	0.043	0.022	0.791	4.294	4.702	0.013	0.006	-	0.112	100.53
EA46-P5	10	74.94	0.048	13.43	-	1.036	0.041	0.017	0.784	4.295	4.645	0.011	0.001	-	0.110	99.36
EA46-R1	10	75.03	0.054	13.64	0.002	1.006	0.041	0.019	0.793	4.230	4.679	0.015	0.001	0.002	0.097	99.61
EA47-R1	10	71.67	0.355	9.56	-	6.386	0.175	0.003	0.289	5.867	4.722	0.011	0.004	0.016	0.173	99.23

Table C.1 - Major-Element Analyses of Geological Specimens (mean of *n* analyses; weight percent)

Specimen	n	SiO_2	TiO_2	Al_2O3	Cr_2O_3	FeO(T)	MnO	MgO	CaO	Na_2O	K_2O	P_2O_5	F	SO_3	Cl	Total
EA48-P1-A	10	73.63	0.239	10.87	0.003	4.062	0.093	-	0.206	5.460	4.611	0.004	0.004	0.007	0.140	99.32
EA48-P1-B	10	74.01	0.236	10.97	-	4.077	0.095	-	0.202	5.351	4.571	0.003	-	0.004	0.135	99.66
EA48-P2-A	10	73.82	0.237	10.92	-	4.081	0.092	-	0.210	5.372	4.563	0.005	0.005	0.008	0.137	99.46
EA48-P2-B	10	73.78	0.235	10.91	-	4.070	0.097	-	0.196	5.473	4.578	0.007	0.002	0.003	0.139	99.49
EA48-P2-C	10	74.17	0.228	10.91	0.005	4.094	0.091	0.001	0.203	5.521	4.550	0.004	0.003	0.006	0.141	99.93
EA48-P3	10	74.15	0.235	10.87	-	4.091	0.094	-	0.190	5.573	4.590	-	0.003	-	0.141	99.93
EA48-P4	10	73.71	0.226	10.90	-	4.086	0.091	-	0.199	5.525	4.501	0.004	0.001	0.004	0.140	99.38
EA48-P5	10	73.65	0.220	10.87	0.001	4.093	0.095	-	0.201	5.581	4.539	0.003	0.002	-	0.139	99.39
EA48-R1	10	73.74	0.231	10.84	-	4.082	0.095	-	0.215	5.497	4.581	0.008	0.001	-	0.133	99.42
EA48-R2-A	10	73.42	0.231	10.77	-	4.084	0.094	0.001	0.203	5.505	4.488	0.008	0.002	0.010	0.131	98.95
EA48-R2-B	10	73.67	0.234	10.88	-	4.097	0.099	-	0.198	5.489	4.497	0.004	-	0.004	0.135	99.31
EA49-P1	10	75.48	0.079	13.16	0.004	0.980	0.057	0.028	0.318	4.470	4.745	0.009	0.003	-	0.067	99.40
EA49-R1	10	75.25	0.075	13.00	0.003	0.958	0.048	0.025	0.315	4.532	4.596	0.006	0.003	-	0.064	98.88
EA49-R2	10	75.58	0.076	13.14	-	0.943	0.058	0.026	0.320	4.582	4.691	0.007	0.002	0.001	0.069	99.49
EA50-P1-A	10	75.79	0.075	13.07	-	0.898	0.044	0.018	0.251	4.498	4.959	0.007	0.002	-	0.065	99.68
EA50-P1-B	10	75.63	0.076	13.14	-	0.776	0.044	0.014	0.241	4.605	4.765	0.011	0.002	-	0.058	99.36
EA50-P1-C	10	76.16	0.077	13.18	-	0.768	0.044	0.018	0.235	4.610	4.798	0.007	-	0.002	0.065	99.96
EA50-P2-A	10	75.10	0.076	12.96	0.002	0.854	0.046	0.021	0.269	4.396	4.800	0.007	0.003	-	0.069	98.61
EA50-P2-B	10	75.76	0.080	13.07	0.005	0.890	0.048	0.024	0.288	4.532	4.584	0.005	-	-	0.068	99.35
EA50-P2-C	10	75.55	0.078	12.99	-	0.801	0.044	0.017	0.257	4.386	4.948	0.003	0.002	-	0.061	99.14
EA50-P3-A	10	75.62	0.075	13.10	0.003	0.920	0.049	0.021	0.281	4.597	4.697	0.006	0.003	-	0.062	99.43
EA50-P3-B	10	75.82	0.075	13.18	-	0.939	0.048	0.023	0.284	4.586	4.748	0.007	0.002	0.001	0.065	99.78
EA50-P4-A	10	75.59	0.079	13.15	0.001	0.795	0.043	0.015	0.249	4.405	4.975	0.008	0.004	-	0.062	99.37
EA50-P4-B	10	75.72	0.081	13.11	-	0.792	0.044	0.019	0.248	4.406	4.950	0.004	0.001	0.001	0.065	99.44
EA50-P4-C	10	75.72	0.077	13.22	-	0.846	0.048	0.018	0.266	4.430	4.915	0.008	0.004	0.001	0.061	99.61
EA50-P4-D	10	75.81	0.076	13.23	0.001	0.895	0.053	0.024	0.284	4.554	4.620	0.007	0.003	-	0.065	99.63
EA50-P5	10	75.98	0.074	13.13	0.003	0.791	0.042	0.019	0.269	4.520	4.774	0.006	0.001	0.001	0.069	99.69
EA50-P6	10	75.55	0.078	13.08	-	0.821	0.051	0.019	0.263	4.508	4.774	0.007	0.001	0.004	0.068	99.23
EA50-R1-A	10	75.77	0.078	13.21	-	0.838	0.047	0.018	0.252	4.538	4.734	0.011	-	0.001	0.074	99.57

Table C.1 - Major-Element Analyses of Geological Specimens (mean of *n* analyses; weight percent)

Specimen	n	SiO_2	TiO_2	Al_2O3	Cr_2O_3	FeO(T)	MnO	MgO	CaO	Na_2O	K_2O	P_2O_5	F	SO_3	Cl	Total
EA50-R1-B	10	75.90	0.071	13.21	0.001	0.855	0.040	0.013	0.203	4.509	4.955	0.005	0.002	-	0.064	99.83
EA51-P1	10	76.75	0.088	12.69	-	0.478	0.037	0.065	0.452	3.956	4.576	0.008	0.002	-	0.019	99.12
EA51-R1	10	77.15	0.094	12.69	-	0.349	0.037	0.060	0.463	4.135	4.631	0.010	0.005	-	0.017	99.64
EA52-B1	10	72.34	0.194	14.65	-	1.685	0.037	0.164	0.810	4.810	5.294	0.023	0.001	0.009	0.072	100.08
EA52-B2	10	72.66	0.190	14.64	-	1.513	0.040	0.150	0.694	4.886	5.313	0.024	0.002	0.003	0.060	100.18
EA52-B3	10	72.40	0.189	14.66	-	1.623	0.034	0.150	0.771	4.878	5.303	0.030	0.002	-	0.070	100.11
EA53-B1	10	72.59	0.209	14.33	0.003	1.520	0.035	0.101	0.605	4.417	5.382	0.017	0.003	-	0.081	99.30
EA53-B2	10	72.59	0.209	14.35	-	1.530	0.038	0.106	0.607	4.554	5.354	0.026	0.003	-	0.074	99.44
EA54-B1	10	73.43	0.197	14.55	0.003	1.244	0.025	0.051	0.439	4.780	5.470	0.021	0.002	-	0.068	100.29
EA55-B1	10	73.24	0.215	14.57	-	0.530	0.022	0.073	0.649	4.859	5.366	0.021	0.002	0.001	0.063	99.61
EA55-B2	10	73.72	0.212	14.64	-	0.532	0.023	0.103	0.671	4.869	5.322	0.024	0.003	0.004	0.068	100.18
EA56-B1	10	72.63	0.212	14.55	0.005	1.744	0.034	0.176	0.754	4.711	5.142	0.024	0.002	0.001	0.061	100.05
EA57-B1	10	75.27	0.050	13.63	-	0.698	0.038	-	0.243	5.261	4.501	-	0.006	-	0.088	99.78
EA58-B1	10	75.57	0.048	13.36	-	0.663	0.034	0.001	0.247	5.206	4.406	0.002	0.003	-	0.090	99.63
EA59-B1	10	74.92	0.049	13.26	-	0.797	0.035	-	0.186	5.109	4.326	0.001	0.004	0.004	0.094	98.78
EA60-B1-A	10	75.25	0.048	13.24	0.002	0.880	0.039	0.001	0.280	5.103	4.535	-	0.001	-	0.077	99.46
EA60-B1-B	10	75.72	0.050	13.20	-	0.991	0.047	0.002	0.294	5.108	4.448	0.002	0.005	-	0.073	99.93
EA60-B2	10	75.57	0.050	13.35	-	0.997	0.041	-	0.319	4.954	4.377	-	0.004	-	0.082	99.74
EA61-B1	10	75.22	0.046	13.46	-	0.687	0.030	-	0.177	5.231	4.425	0.006	0.002	0.001	0.090	99.37
EA61-B2	10	75.15	0.050	13.61	-	1.000	0.045	0.001	0.240	5.010	4.542	0.001	0.004	0.002	0.093	99.75
EA62-Y1-A	10	75.17	0.048	13.37	0.002	0.782	0.033	0.001	0.210	5.261	4.435	0.005	0.004	0.007	0.094	99.43
EA62-Y1-B	10	75.40	0.047	13.43	0.005	0.787	0.037	-	0.243	5.231	4.428	0.004	0.003	0.002	0.093	99.71
EA62-Y1-C	10	75.49	0.047	13.47	-	0.831	0.039	-	0.228	5.181	4.455	0.001	0.005	0.001	0.094	99.84
EA62-Y1-D	10	75.48	0.046	13.48	-	0.782	0.036	0.001	0.216	5.262	4.367	-	0.002	0.002	0.098	99.77
EA62-Y2-A	10	74.43	0.046	13.33	0.001	0.993	0.049	-	0.340	5.178	4.453	0.004	0.001	-	0.093	98.91
EA62-Y2-B	10	74.82	0.050	13.29	-	0.997	0.042	-	0.313	5.248	4.442	0.004	0.002	-	0.094	99.29
EA62-Y3-A	10	75.22	0.046	13.46	-	0.654	0.031	-	0.176	5.201	4.520	-	0.002	0.001	0.100	99.41
EA62-Y3-B	10	75.13	0.045	13.50	0.003	0.863	0.041	0.001	0.264	5.322	4.430	0.003	0.003	-	0.098	99.71
EA62-Y4	10	75.27	0.049	13.45	0.004	0.805	0.036	-	0.277	5.161	4.488	0.006	0.004	0.003	0.099	99.66

Table C.1 - Major-Element Analyses of Geological Specimens (mean of *n* analyses; weight percent)

Specimen	n	SiO_2	TiO_2	Al_2O3	Cr_2O_3	FeO(T)	MnO	MgO	CaO	Na_2O	K_2O	P_2O_5	F	SO_3	Cl	Total
EA62-Y5	10	75.16	0.046	13.24	0.001	0.706	0.027	-	0.185	5.173	4.496	0.002	0.003	-	0.100	99.13
EA63-E1A	10	77.05	0.086	12.56	0.003	0.490	0.046	0.052	0.442	3.878	4.640	0.008	0.002	-	0.016	99.28
EA63-E1B	10	77.06	0.087	12.67	-	0.524	0.045	0.057	0.434	3.949	4.677	0.005	0.002	-	0.017	99.53
EA63-E1C	10	76.95	0.084	12.58	-	0.532	0.043	0.057	0.433	4.000	4.704	0.010	0.001	-	0.033	99.43
EA63-E1D	10	77.10	0.086	12.57	-	0.500	0.044	0.054	0.425	4.030	4.660	0.007	0.003	-	0.028	99.51
EA63-E1E	10	76.97	0.085	12.56	0.001	0.415	0.040	0.048	0.421	3.917	4.671	0.013	0.002	-	0.020	99.17
EA64-E1A	10	71.88	0.374	9.89	0.004	6.378	0.169	0.005	0.240	6.041	4.921	0.012	0.002	0.027	0.157	100.10
EA64-E1B	10	71.42	0.373	9.84	-	6.416	0.167	0.005	0.274	5.708	5.051	0.007	0.002	0.026	0.154	99.45
EA64-E1C	10	71.53	0.364	9.87	0.002	6.376	0.177	0.008	0.236	5.836	5.124	0.011	0.002	0.021	0.151	99.71
EA64-E1D	10	71.64	0.363	9.86	-	6.355	0.170	0.006	0.260	5.983	4.969	0.009	0.001	0.028	0.152	99.80
EA64-E1E	10	71.69	0.365	9.89	0.001	6.340	0.167	0.005	0.250	5.851	5.174	0.011	-	0.025	0.146	99.91
EA65-W1	10	75.93	0.097	13.36	-	0.718	0.072	0.033	0.297	4.795	4.583	0.006	0.002	-	0.031	99.92
EA65-W2	10	75.60	0.099	13.35	0.003	0.838	0.078	0.043	0.317	4.755	4.610	0.005	0.002	0.004	0.033	99.74
EA66-W1	10	73.88	0.199	14.76	-	0.835	0.083	0.110	0.624	5.088	4.650	0.023	0.004	0.003	0.029	100.29
EA67-W1	10	76.38	0.144	13.06	-	0.707	0.024	0.057	0.485	4.134	4.886	0.008	0.002	0.004	0.026	99.92
EA68-SX1	30	75.55	0.083	13.27	-	1.142	0.063	0.049	0.452	4.966	4.408	0.008	0.002	-	0.040	100.04
EA68-SX2	20	75.52	0.083	13.28	-	1.153	0.063	0.047	0.515	4.938	4.350	0.007	0.004	0.002	0.047	100.01
EA69-SX1	20	75.61	0.090	13.17	-	0.949	0.054	0.029	0.334	4.915	4.461	0.004	0.003	0.002	0.068	99.69
EA69-SX2	20	75.55	0.081	12.92	-	0.914	0.049	0.022	0.305	4.953	4.431	0.006	0.003	-	0.061	99.30
GE01-jB1	10	75.98	0.116	13.58	-	0.783	0.061	0.111	0.725	3.939	4.672	0.026	0.003	0.004	0.036	100.04
GE02-iD1A	10	76.04	0.106	13.52	-	0.748	0.056	0.102	0.708	4.035	4.730	0.024	0.001	-	0.039	100.11
GE02-iD1B	10	76.26	0.110	13.61	-	0.757	0.058	0.101	0.705	4.010	4.793	0.025	0.002	0.009	0.041	100.48
GE02-iD1C	20	75.86	0.116	13.46	-	0.747	0.056	0.106	0.723	3.963	4.770	0.027	0.001	0.006	0.038	99.87
GE03-iD1	20	75.90	0.119	13.42	0.001	0.691	0.054	0.094	0.716	3.919	4.773	0.023	0.003	0.003	0.039	99.75
GE04-iD1	20	75.91	0.107	13.47	0.002	0.680	0.054	0.091	0.676	4.007	4.745	0.023	0.002	0.003	0.037	99.80
GE05-iD1	20	75.93	0.111	13.43	-	0.733	0.056	0.101	0.700	3.971	4.745	0.023	0.003	0.002	0.041	99.85
GE06-iD1	20	76.30	0.106	13.39	0.002	0.485	0.053	0.067	0.592	3.843	5.084	0.024	0.003	0.001	0.040	99.99
GE07-kM1A	10	75.80	0.104	13.65	-	0.732	0.054	0.096	0.704	4.021	4.738	0.023	0.002	0.006	0.041	99.97
GE07-kM1B	10	75.75	0.108	13.50	-	0.731	0.058	0.100	0.704	3.992	4.819	0.019	0.004	0.008	0.038	99.83

Table C.1 - Major-Element Analyses of Geological Specimens (mean of *n* analyses; weight percent)

Specimen	n	SiO_2	TiO_2	Al_2O3	Cr_2O_3	FeO(T)	MnO	MgO	CaO	Na_2O	K_2O	P_2O_5	F	SO_3	Cl	Total
GE07-kM1C	10	75.45	0.111	13.51	-	0.732	0.056	0.098	0.692	3.902	4.760	0.019	0.003	0.004	0.039	99.37
GE08-rB1	20	75.87	0.097	13.44	-	0.592	0.056	0.085	0.643	3.991	4.805	0.024	0.004	0.001	0.040	99.65
GE08-rB2	20	76.04	0.100	13.43	-	0.463	0.055	0.086	0.648	3.963	4.802	0.020	0.004	-	0.037	99.65
GE09-nS1	20	75.86	0.135	13.39	-	0.731	0.049	0.119	0.763	3.961	4.769	0.026	0.003	-	0.036	99.85
GE10-nS1	20	75.88	0.095	13.39	0.001	0.659	0.063	0.084	0.640	4.026	4.822	0.022	0.003	-	0.042	99.73
GE11-nS1	10	75.91	0.109	13.46	-	0.734	0.056	0.105	0.701	4.011	4.794	0.021	0.004	0.003	0.038	99.95
GE11-nS2	10	75.65	0.120	13.44	-	0.756	0.055	0.107	0.711	3.954	4.721	0.022	0.003	-	0.037	99.58
GE11-nS3	10	75.63	0.117	13.41	-	0.727	0.055	0.105	0.710	3.993	4.777	0.021	0.005	0.003	0.045	99.61
GE11-nS4	10	75.87	0.111	13.45	0.003	0.730	0.059	0.100	0.688	3.971	4.789	0.023	0.004	0.003	0.042	99.85
GE11-nS5	20	75.71	0.093	13.44	-	0.671	0.058	0.088	0.646	4.051	4.766	0.020	0.003	0.005	0.042	99.59
GE11-nS6	20	75.46	0.117	13.36	-	0.754	0.054	0.110	0.718	3.940	4.807	0.027	0.005	0.003	0.032	99.39
GE12-nS1	20	75.80	0.095	13.43	-	0.510	0.058	0.081	0.644	4.046	4.799	0.016	0.002	0.003	0.030	99.52
GE13-nS1	20	75.63	0.110	13.42	-	0.743	0.057	0.106	0.701	3.912	4.754	0.023	0.002	-	0.039	99.50
GE13-nS2	20	75.76	0.114	13.48	-	0.758	0.054	0.111	0.709	3.941	4.760	0.022	0.004	0.001	0.036	99.76
KB01-jB1	10	76.53	0.043	13.69	0.005	0.437	0.063	0.056	0.734	4.143	4.423	0.020	-	0.001	0.027	100.17
KB02-jB1	10	76.14	0.046	13.70	-	0.781	0.073	0.058	0.737	4.060	4.386	0.019	0.001	0.010	0.029	100.04

Total: 11,779 major-element analyses

Note: When the mean concentration value was below 10 ppm, the value was replaced by a "-" to denote that it was below the minimum detection limits; the dash does not indicate unmeasured values.

Table C.2 - Trace-Element Analyses of Specimens (mean of *n* analyses; ppm)

Specimen	n	Zr	Nb	Ga	Zn	Ba	Ce
AR01-E1	20	54	66	44	66	413	54
AR02-E1	20	55	70	52	80	142	32
AR03-E1	20	41	69	45	87	163	29
AR04-E1	10	34	80	47	87	220	52
AR04-E2	10	45	77	50	102	157	30
AR05-E1A	10	51	50	47	116	163	23
AR05-E1B	10	42	38	45	106	205	47
AR05-E1C	10	40	54	46	100	194	46
AR06-E1A	10	139	59	44	72	483	105
AR06-E1B	20	143	68	39	92	497	65
AR06-E1C	20	154	79	43	92	507	100
AR06-E2A	20	144	68	41	85	477	75
AR06-E2B	20	153	75	42	103	489	72
AR06-E2C	20	142	72	42	86	492	84
AR06-E3A	20	157	71	42	79	489	87
AR06-E3B	10	145	65	31	65	481	92
AR06-E3C	10	153	75	38	61	483	67
AR07-jB1	10	51	66	46	66	564	83
AR07-jB2	10	66	56	42	60	587	57
AR08-jB1	10	72	48	37	63	553	95
AR08-jB2	10	67	74	32	71	573	91
AR09-jB1	10	37	63	54	106	58	29
AR10-jB1	10	27	72	46	96	63	69
AR11-jB1	10	130	64	40	102	493	96
AR12-jB1	10	148	58	37	91	487	90
AR13-jB1	10	74	65	46	42	723	98
AR14-jB1	10	83	53	41	91	748	78
AR15-jB1	10	159	54	42	83	496	78
AR16-jB1	10	201	58	40	86	965	163
AR17-jB1	20	202	54	39	78	946	111
AR18-avH1	20	62	56	47	62	408	80
AR19-avH1	20	43	52	46	85	416	46
AR20-avH1	20	55	61	52	87	402	72
AR21-avH1	20	139	75	46	73	471	85
AR22-avH1	20	134	79	41	68	478	63
AR23-ipS1	10	23	109	41	90	35	38
AR23-jfL1	10	28	79	36	71	17	48
AR24-ipS1	10	144	77	46	85	479	67
AR24-jfL1	10	156	74	41	62	463	80
AR25-ipS1	10	31	91	-	67	30	63
AR25-jfL1	10	15	90	51	100	15	64
AR26-ipS1	10	34	71	39	89	25	56
AR26-jfL1	10	42	84	37	84	23	90

Table C.2 - Trace-Element Analyses of Specimens (mean of *n* analyses; ppm)

Specimen	n	Zr	Nb	Ga	Zn	Ba	Ce
AR27-ipS1	10	64	61	44	95	593	124
AR27-jfL1	10	66	51	39	81	591	64
AR28-ipS1	20	93	47	31	77	649	96
AR29-ipS1	20	80	55	40	79	814	94
AR30-ipS1	20	157	58	46	62	491	84
AR30-jfL1	20	152	69	40	77	473	106
AR31-ipS1	20	33	74	44	89	59	33
AR31-jfL1	20	31	67	44	81	56	50
AR32-ipS1	10	45	78	47	75	120	72
AR32-jfL1	10	28	89	46	64	132	31
AR33-ipS1	10	64	57	45	76	48	103
AR33-ipS2A	10	71	57	39	72	58	98
AR33-ipS2B	10	72	65	47	60	55	106
AR33-ipS2C	10	81	76	42	103	54	75
AR34-ipS1	10	64	87	43	82	66	73
AR35-ipS1A	10	73	61	45	100	58	67
AR35-ipS1B	10	70	74	47	87	66	80
AR35-ipS1C	10	61	75	60	94	67	76
AR36-ipS1A	20	64	72	42	92	39	60
AR36-ipS1B	20	77	72	42	82	31	78
AR36-ipS1C	20	59	77	51	98	41	61
AR37-ipS1A	20	51	73	43	91	19	45
AR37-ipS1B	20	48	66	41	103	20	69
AR37-ipS1C	20	64	75	45	87	23	76
AR37-ipS2A	10	49	70	50	71	38	93
AR37-ipS2B	10	46	59	38	42	30	60
AR37-ipS2C	10	47	71	44	84	39	46
AR38-ipS1A	10	78	86	44	89	57	45
AR38-ipS1B	10	70	84	51	94	43	50
AR38-ipS1C	10	92	90	44	99	24	66
AR39-ipS1	10	43	64	45	59	75	39
AR40-rlS1	10	148	84	36	87	517	94
AR41-sK1	10	44	76	34	99	171	57
AR41-sK2	10	56	103	51	98	155	75
AR42-kM1	10	66	65	29	93	285	53
AR42-kM2	10	63	64	51	83	281	57
AR43-kM1	10	68	64	40	72	805	152
AR44-sK1	10	144	56	41	49	518	102
AR45-kM1	20	140	76	42	57	495	78
AR46-sK1	20	149	83	42	32	513	115
AR47-kM1	20	150	100	24	54	487	86
AR47-kM2	20	155	78	46	57	484	99
AR47-kM3	20	144	67	17	57	475	111

Table C.2 - Trace-Element Analyses of Specimens (mean of *n* analyses; ppm)

Specimen	n	Zr	Nb	Ga	Zn	Ba	Ce
AR47-kM4	20	145	67	37	41	501	103
AR47-kM5	10	140	52	41	80	483	84
AR48-sK1	10	60	36	41	54	599	76
AR49-sK1	10	189	54	31	97	326	112
AR50-sK1	10	130	73	47	54	454	98
AR50-sK2	10	148	70	42	51	455	121
AR51-sK1	10	33	67	54	82	35	43
AR52-sK1	10	60	89	50	81	13	100
AR53-kM1	10	59	66	39	90	387	105
AR54-kM1	10	36	84	49	77	27	78
AR55-sK1	10	31	83	34	75	23	34
AR56-sK1	20	62	70	44	79	42	74
AR57-sK1	20	75	72	44	89	68	75
AR58-sK1	20	68	75	45	89	27	55
AR59-kM1	20	62	62	37	45	594	132
AR60-sK1	20	64	57	45	50	830	124
AR61-sK1	20	63	68	45	77	11	75
AR62-sK1	10	240	19	36	80	1012	138
AR63-kM1	10	205	33	28	68	994	146
AR64-sK1	10	122	73	39	35	1149	144
AR65-E1	10	150	79	40	46	496	120
AR66-rB1	10	216	26	38	74	977	120
AR66-rB2	10	219	46	38	52	991	150
AR67-rB1	10	45	82	44	73	73	48
AR67-rB2	10	23	92	40	45	72	70
AR67-rB3	10	18	88	44	84	81	39
AR68-rB1	10	44	38	51	73	244	75
AR68-rB2	10	65	75	49	51	225	72
AR68-rB3	10	40	71	56	57	184	82
AR68-rB4	10	58	56	51	64	256	16
AR68-rB5	10	75	75	46	47	420	82
AR68-rB6	10	42	42	49	56	301	58
AR68-rB7	10	54	69	46	58	320	78
AR69-rB1	10	52	53	46	12	755	116
AR69-rB2	10	37	67	46	41	753	108
AR69-rB3	10	52	62	39	38	759	98
AR70-rB1	10	80	45	40	31	832	100
AR70-rB2	10	85	66	41	39	828	131
AR71-rB1	10	132	33	45	60	1130	107
AR72-rB1	10	133	88	43	56	524	177
AR72-rB2	10	78	35	36	45	618	76
AR72-rB3	10	72	58	40	40	639	83
AR73-rB1	10	63	64	35	39	581	77

Table C.2 - Trace-Element Analyses of Specimens (mean of *n* analyses; ppm)

Specimen	n	Zr	Nb	Ga	Zn	Ba	Ce
AR74-rB1	10	70	71	34	39	604	74
AR74-rB2	10	72	69	38	54	599	96
AR75-rB1	10	13	74	52	67	90	59
AR76-rB1	20	157	105	33	22	502	114
AR76-rB2	20	156	101	45	41	520	94
AR76-rB3	20	171	91	44	29	511	105
AR77-rB1	20	168	88	40	31	511	88
AR77-rB2	20	161	88	34	36	516	113
AR77-rB3	20	168	90	37	41	508	91
AR78-rB1	10	180	85	37	38	521	108
AR78-rB2	10	177	113	39	30	540	118
AR78-rB3	10	177	89	32	58	508	72
AR79-rB1	10	94	91	44	51	60	52
AR79-rB2	10	82	106	38	68	58	70
AR79-rB3	10	68	103	30	19	57	61
AR80-rB1	10	106	92	49	76	62	90
AR81-rB1	10	85	101	50	79	84	104
AR81-rB2	10	98	103	41	39	95	69
AR81-rB3	10	99	99	45	77	98	73
AR82-rB1	10	88	95	44	72	57	41
AR82-rB2	10	77	94	48	46	54	54
AR82-rB3	10	93	100	55	62	50	60
AZ01-jB1	20	60	63	44	93	43	44
AZ02-kM1	20	82	70	29	91	57	81
AZ03-kM1	20	63	66	48	94	43	49
AZ04-kM1	20	80	64	46	101	47	68
CA01-P1	10	80	65	47	88	36	-
CA01-R1	10	121	71	50	92	343	72
CA02-P1	10	143	55	64	37	435	119
CA02-R1-A	10	75	76	49	81	53	-
CA02-R1-B	10	82	99	50	73	37	-
CA03-P1	10	110	83	59	54	374	126
CA03-R1-A	10	112	85	43	56	362	55
CA03-R1-B	10	107	87	47	41	376	48
CA03-R2	10	125	69	57	60	384	53
CA04-P1	10	112	87	58	78	393	76
CA04-R1-A	20	133	93	50	89	386	92
CA04-R1-B	10	127	77	43	91	411	43
CA04-R1-C	10	128	90	54	68	389	69
CA04-R1-D	10	126	86	56	73	403	48
CA04-R2-A	10	128	78	43	100	388	50
CA04-R2-B	10	140	83	56	86	390	74
CA04-R2-C	10	149	92	50	78	396	78

Table C.2 - Trace-Element Analyses of Specimens (mean of *n* analyses; ppm)

Specimen	n	Zr	Nb	Ga	Zn	Ba	Ce
CA04-R2-D	10	122	73	48	82	387	60
CA04-R2-E	10	128	87	54	96	397	39
CA04-R2-F	10	124	83	37	112	381	90
CA05-P1	10	161	84	51	69	459	32
CA05-P2	10	156	81	48	56	442	86
CA05-P3	10	136	73	51	52	450	61
CA05-R1-A	10	154	74	54	64	455	90
CA05-R1-B	10	152	93	33	69	457	47
CA05-R1-C	10	169	85	43	29	456	98
CA05-R2-A	20	158	79	46	57	456	82
CA05-R2-B	20	170	76	48	57	437	114
CA05-R3-A	10	176	80	57	51	443	107
CA05-R3-B	10	157	63	62	80	469	112
CA05-R3-C	10	137	86	47	67	465	71
CA05-R4A	10	167	83	60	81	458	91
CA05-R4B	10	165	77	43	58	445	76
CA05-R4C	10	151	93	43	35	446	82
CA05-R4D	10	176	73	42	52	462	129
CA05-R4E	10	158	87	45	73	461	66
CA05-R5A	10	154	72	43	70	447	43
CA05-R5B	10	178	76	49	54	427	66
CA05-R5C	10	162	80	48	61	450	65
CA05-R5D	10	169	73	36	68	460	104
CA05-R5E	10	138	55	38	47	444	75
CA06-P1	10	119	64	43	77	371	47
CA06-P2	10	113	56	37	55	346	89
CA06-P3	10	105	75	43	47	365	73
CA06-P4	10	111	79	44	27	335	67
CA06-P5-A	20	125	75	53	43	368	95
CA06-P5-B	20	120	75	51	69	379	78
CA06-P5-C	20	131	77	47	70	362	46
CA06-P6	10	125	77	55	39	359	82
CA06-P7-A	20	128	70	56	55	369	86
CA06-P7-B	20	121	69	46	48	365	58
CA06-P8-A	20	116	66	38	66	341	67
CA06-P8-B	20	121	88	45	54	332	64
CA06-R1	10	99	78	64	67	371	52
CA06-R2-A	20	114	88	46	52	353	91
CA06-R2-B	20	120	75	45	-	366	32
CA06-R3-A	20	118	75	42	33	336	75
CA06-R3-B	20	115	72	45	81	352	80
CA07-P1	10	191	69	48	24	482	114
CA07-R1	10	192	73	32	40	493	100

Table C.2 - Trace-Element Analyses of Specimens (mean of *n* analyses; ppm)

Specimen	n	Zr	Nb	Ga	Zn	Ba	Ce
CA07-R2-A	20	190	75	48	63	475	111
CA07-R2-B	20	188	74	44	47	487	98
CA08-P1	10	73	94	30	48	-	54
CA08-P2	10	79	98	26	42	10	70
CA08-R1-A	20	204	70	42	56	473	98
CA08-R1-B	20	196	81	36	55	471	111
CA08-R1-C	20	187	70	45	62	486	115
CA08-R1-D	20	186	81	35	52	469	87
CA09-P1	10	81	94	40	-	10	101
CA09-P2	10	77	86	46	42	10	47
CA09-P3	10	79	96	35	31	-	26
CA09-R1	10	129	94	39	71	338	103
CA09-R2-A	20	87	88	46	47	-	54
CA09-R2-B	20	81	102	53	52	-	49
CA09-R2-C	20	78	99	49	60	-	43
CA09-R2-D	20	75	95	53	51	-	61
CA10-P1	20	78	100	45	31	-	60
CA10-R1-A	20	83	90	42	57	-	56
CA10-R1-B	20	68	92	46	54	-	87
CA10-R1-C	20	66	90	46	58	-	70
CA10-R2	10	90	79	28	36	-	69
CA11-P1	20	79	101	49	27	-	39
CA11-P2	20	96	87	49	37	-	35
CA11-R1	20	69	97	49	40	-	34
CA12-P1	10	136	82	51	18	309	133
CA12-R1-A	20	119	82	51	43	347	110
CA12-R1-B	20	121	76	50	45	352	103
CA12-R2-A	20	113	82	56	52	339	73
CA12-R2-B	20	125	79	51	54	346	99
CA13-P1	10	87	90	35	59	-	75
CA13-R1	10	104	86	40	46	-	75
CA14-P1	10	82	68	64	43	461	108
CA14-P2	10	78	83	48	47	488	122
CA14-R1-A	20	86	77	46	47	451	105
CA14-R1-B	20	80	76	49	36	433	90
CA15-P1	10	80	83	48	27	88	41
CA15-R1-A	20	72	88	56	42	67	68
CA15-R1-B	20	71	91	57	35	89	70
CA15-R2	10	82	103	54	14	67	82
CA16-P1	10	94	86	56	49	94	80
CA16-R1	10	77	105	47	68	92	85
CA16-R2	10	88	94	61	45	95	37
CA17-P1	10	78	81	46	17	166	80

Table C.2 - Trace-Element Analyses of Specimens (mean of *n* analyses; ppm)

Specimen	n	Zr	Nb	Ga	Zn	Ba	Ce
CA17-P2	10	79	111	58	34	92	86
CA17-R1-A	20	82	91	50	34	167	91
CA17-R1-B	20	73	72	44	29	164	80
CA18-P1	20	82	107	54	78	104	79
CA18-P2	10	82	96	50	-	79	77
CA18-R1	10	87	88	53	87	99	92
CA18-R2	10	80	115	67	66	83	75
CA18-R3-A	20	82	82	59	93	108	61
CA18-R3-B	20	95	94	53	86	99	88
CA19-P1	10	86	81	51	25	147	80
CA19-R1-A	20	76	82	52	34	126	61
CA19-R1-B	20	75	93	45	23	140	92
CA19-R2-A	20	63	83	52	35	149	100
CA19-R2-B	20	86	82	47	29	145	71
CA19-R2-C	20	80	80	44	19	125	110
CA19-R3-A	10	97	85	52	67	143	117
CA19-R3-B	10	69	100	51	48	149	83
CA19-R3-C	10	96	93	43	41	131	78
CA19-R3-D	10	87	101	38	30	150	40
CA20-P1-A	20	83	90	45	39	172	49
CA20-P1-B	20	79	79	36	18	166	47
CA20-P2	10	78	87	41	25	187	60
CA20-P3	10	84	82	41	16	179	85
CA20-P4	10	82	91	47	19	184	52
CA20-R1-A	20	76	86	43	21	180	55
CA20-R1-B	20	81	83	49	47	176	81
CA21-P1	10	84	69	45	-	793	74
CA21-P2	10	83	61	38	22	703	116
CA21-R1-A	20	91	67	45	40	755	67
CA21-R1-B	20	74	79	43	28	775	89
CA21-R2-A	20	86	69	44	38	772	99
CA21-R2-B	20	81	65	46	43	766	103
CA21-R2-C	20	98	85	49	55	776	106
CA22-P1	10	131	80	50	28	590	81
CA22-P2	10	138	72	34	24	590	111
CA22-P3	10	141	75	53	17	602	48
CA22-R1	10	134	83	34	45	600	107
CA22-R2-A	10	132	76	37	72	596	75
CA22-R2-B	10	140	71	55	68	584	112
CA22-R2-C	10	117	66	46	80	611	107
CA22-R2-D	10	135	75	50	12	601	69
CA22-R2-E	10	143	67	42	32	576	61
CA23-P1	10	124	80	45	31	581	88

Table C.2 - Trace-Element Analyses of Specimens (mean of *n* analyses; ppm)

Specimen	n	Zr	Nb	Ga	Zn	Ba	Ce
CA23-P2-A	10	132	81	45	48	605	84
CA23-P2-B	10	144	80	48	36	598	73
CA23-P2-C	10	136	81	49	44	580	95
CA23-P2-D	10	129	84	37	41	601	31
CA23-P3-A	10	136	77	54	67	601	108
CA23-P3-B	10	80	77	46	27	490	42
CA23-P4-A	10	117	72	46	45	603	78
CA23-P4-B	10	134	76	51	21	600	60
CA23-P5-A	10	140	93	41	16	589	116
CA23-P5-B	10	130	75	39	31	600	58
CA23-R1-A	10	134	78	50	24	601	124
CA23-R1-B	10	121	78	44	29	604	82
CA23-R2-A	10	141	75	45	59	592	88
CA23-R2-B	10	134	68	49	44	601	61
CA23-R2-C	10	142	88	45	57	601	86
CA24-P1	10	127	72	56	35	584	99
CA24-P2	10	133	74	47	51	576	121
CA24-R1-A	10	111	85	56	-	603	98
CA24-R1-B	10	129	71	45	28	606	56
CA24-R1-C	10	128	80	54	32	586	63
CA24-R1-D	10	156	110	77	62	638	93
CA25-P1	10	150	68	44	26	603	99
CA25-P2	10	132	74	44	48	597	91
CA25-R1-A	10	146	91	48	59	606	71
CA25-R1-B	10	141	84	56	60	625	48
CA25-R1-C	10	151	67	51	50	613	92
CA25-R1-D	10	144	68	58	-	611	107
CA25-R2-A	10	144	70	51	39	607	61
CA25-R2-B	10	136	65	48	77	610	40
CA26-P1	10	139	69	43	10	604	76
CA26-R1-A	10	149	88	55	46	622	46
CA26-R1-B	10	144	79	54	61	621	90
CA26-R1-C	10	149	63	48	54	589	62
CA26-R1-D	10	145	95	65	68	584	51
CA26-R2-A	10	137	87	47	38	590	96
CA26-R2-B	10	144	91	38	35	605	88
CA26-R3-A	10	162	96	37	37	606	48
CA26-R3-B	10	145	90	52	38	606	79
CA27-P1	10	150	66	46	24	618	79
CA27-P2	10	127	69	32	32	613	96
CA27-R1-A	10	144	86	54	48	582	66
CA27-R1-B	10	141	67	40	79	583	77
CA27-R1-C	10	149	76	33	89	585	56

Table C.2 - Trace-Element Analyses of Specimens (mean of *n* analyses; ppm)

Specimen	n	Zr	Nb	Ga	Zn	Ba	Ce
CA27-R1-D	10	153	70	54	41	609	89
CA27-R2-A	10	139	81	47	32	576	62
CA27-R2-B	10	157	88	50	59	609	47
CA27-R3	10	146	83	44	52	624	78
CA27-R4	10	149	73	52	29	620	52
CA28-P1	10	41	66	54	30	923	112
CA28-P2	10	63	63	35	19	901	43
CA28-P3	10	63	76	43	57	907	30
CA28-P4	10	78	63	46	38	929	119
CA28-P5	10	52	72	53	36	904	49
CA28-R1-A	10	60	79	40	37	893	-
CA28-R1-B	10	52	70	46	27	892	13
CA29-P1-A	10	86	79	43	56	874	47
CA29-P1-B	10	38	88	41	40	874	12
CA29-P1-C	10	65	80	57	49	885	10
CA29-P2-A	10	62	69	43	17	892	23
CA29-P2-B	10	50	50	29	-	921	62
CA29-P3-A	10	73	64	48	34	889	23
CA29-P3-B	10	54	69	43	-	898	42
CA29-P4	10	68	46	46	42	890	61
CA29-P5-A	10	47	82	41	26	901	45
CA29-P5-B	10	58	72	37	62	898	53
CA29-P6	10	56	61	42	38	901	39
CA29-R1	10	64	70	58	46	917	97
CA29-R2	10	66	77	41	24	921	32
CA30-P1	10	49	67	43	14	891	-
CA30-P2	10	57	54	39	57	880	44
CA30-P3	10	48	69	50	-	901	60
CA30-P4	10	62	65	47	15	901	22
CA30-P5	10	60	60	47	-	906	93
CA30-R1-A	10	59	78	35	39	891	-
CA30-R1-B	10	58	72	37	34	878	23
CA30-R2-A	10	52	62	35	18	897	54
CA30-R2-B	10	49	75	49	19	875	-
CA31-P1	10	55	63	38	11	873	50
CA31-P2	10	52	71	41	-	867	33
CA31-R1	10	56	73	51	27	899	69
CA32-W1A	20	42	65	94	60	163	27
CA32-W1B	10	37	65	115	67	168	48
CA32-W1C	10	33	62	94	30	149	43
CA32-W1D	10	56	63	93	65	174	43
CA32-W1E	20	39	64	99	64	215	59
CA32-W2A	20	36	61	98	71	186	27

Table C.2 - Trace-Element Analyses of Specimens (mean of *n* analyses; ppm)

Specimen	n	Zr	Nb	Ga	Zn	Ba	Ce
CA32-W2B	10	37	49	96	88	181	32
CA32-W2C	10	41	76	99	69	162	29
CA32-W2D	10	40	74	102	79	186	41
CA32-W2E	10	48	62	109	54	182	68
CA32-W3A	20	52	69	93	76	122	44
CA32-W3B	10	48	50	98	74	83	16
CA32-W3C	20	47	57	93	49	82	-
CA32-W3D	10	39	59	109	59	72	-
CA32-W3E	10	36	64	94	42	89	-
CA32-W4A	20	47	68	91	71	211	63
CA32-W4B	20	57	62	101	67	214	87
CA32-W4C	10	33	43	104	54	176	30
CA32-W4D	10	30	60	114	69	179	55
CA32-W4E	20	54	53	99	69	207	63
CA32-W5A	10	42	78	104	62	98	-
CA32-W5B	10	46	73	103	59	65	60
CA32-W5C	10	60	52	95	64	93	26
CA32-W5D	10	52	74	92	38	95	51
CA32-W5E	10	42	56	88	59	97	37
CA32-W6A	10	38	75	93	56	166	19
CA32-W6B	10	35	72	91	60	165	57
CA32-W6C	10	38	77	96	53	188	45
CA32-W6D	10	52	61	105	69	171	40
CA32-W6E	10	30	50	113	37	168	55
CA33-W1A	10	37	68	93	102	44	45
CA33-W1B	20	43	69	89	71	-	50
CA33-W1C	20	41	89	99	63	11	57
CA33-W1D	20	46	71	92	71	32	42
CA33-W1E	20	36	67	94	63	13	20
CA33-W2A	20	42	78	86	68	16	41
CA33-W2B	20	44	75	86	61	16	32
CA33-W2C	10	59	68	100	76	28	54
CA33-W2D	10	48	78	95	73	25	29
CA33-W2E	20	53	78	90	77	13	36
CA33-W3A	10	53	72	78	31	32	53
CA33-W3B	10	68	68	110	84	12	77
CA33-W3C	10	52	77	92	90	19	-
CA33-W3D	10	50	81	94	99	21	61
CA33-W3E	10	34	87	83	80	24	61
CA33-W4A	10	43	75	89	76	20	39
CA33-W4B	10	55	72	102	99	30	50
CA33-W4C	10	61	86	96	88	38	45
CA33-W4D	10	40	96	80	86	36	-

Table C.2 - Trace-Element Analyses of Specimens (mean of *n* analyses; ppm)

Specimen	n	Zr	Nb	Ga	Zn	Ba	Ce
CA33-W4E	10	35	78	86	85	28	58
CA33-W5A	10	48	76	92	70	-	30
CA33-W5B	10	45	84	87	57	21	19
CA33-W5C	10	45	54	85	64	16	82
CA33-W5D	10	54	64	73	94	16	37
CA33-W5E	10	42	61	89	79	-	41
EA01-P1	10	101	69	58	75	591	141
EA01-P2	20	122	76	50	50	615	101
EA01-P3	10	109	97	56	60	584	108
EA01-P4	10	103	90	63	72	597	67
EA01-R1	10	109	78	56	47	590	52
EA01-R2-A	10	90	74	62	54	582	112
EA01-R2-B	10	114	89	57	32	626	100
EA02-P1-A	10	104	86	55	54	627	106
EA02-P1-B	10	120	78	59	57	629	92
EA02-P2	10	98	65	64	60	602	130
EA02-P3	10	117	84	52	69	591	90
EA02-P4	10	108	82	68	64	616	102
EA02-R1	10	107	83	54	59	600	87
EA02-R2-A	10	115	73	61	42	615	109
EA02-R2-B	10	111	82	53	38	589	114
EA03-P1-A	10	103	77	65	15	604	110
EA03-P1-B	10	102	77	57	-	588	111
EA03-P2-A	10	102	69	53	58	579	58
EA03-P2-B	10	103	79	57	32	590	84
EA03-P3	10	108	77	70	49	593	89
EA03-P4	10	124	72	40	72	576	94
EA03-P5	10	98	77	65	48	571	144
EA03-R1	10	106	66	56	60	575	80
EA04-P1	10	121	72	54	76	596	88
EA04-P2	20	109	64	54	42	599	137
EA04-R1-A	20	114	71	60	48	593	107
EA04-R1-B	20	124	68	60	45	614	109
EA04-R2	10	126	70	61	77	625	127
EA04-R3	10	102	79	52	76	612	122
EA04-R4A	20	119	74	55	62	596	84
EA04-R4B	20	123	77	59	50	596	102
EA04-R4C	20	117	75	52	43	576	65
EA04-R4D	20	115	80	48	36	595	86
EA04-R4E	20	116	84	50	65	587	65
EA04-R5A	10	127	91	57	79	597	49
EA04-R5B	20	109	65	57	60	593	116
EA04-R5C	10	119	72	51	69	615	87

Table C.2 - Trace-Element Analyses of Specimens (mean of *n* analyses; ppm)

Specimen	n	Zr	Nb	Ga	Zn	Ba	Ce
EA04-R5D	10	119	74	54	47	628	117
EA04-R5E	20	112	63	61	62	598	89
EA05-P1	20	109	88	57	44	584	77
EA05-P2	20	118	82	55	45	583	81
EA05-R1	10	113	88	43	65	613	84
EA05-R2	10	119	86	58	60	571	96
EA06-P1	10	115	74	42	66	602	39
EA06-P2	10	107	92	56	43	595	63
EA06-R1	10	114	86	39	60	609	46
EA07-P1	10	300	101	53	108	102	87
EA07-P2	10	288	97	58	123	55	121
EA07-P3	10	285	95	52	95	66	70
EA07-P4	10	294	100	54	112	53	70
EA07-R1	10	299	104	42	108	87	65
EA07-R2	10	301	95	48	120	97	11
EA07-R3	10	279	100	47	83	86	42
EA08-P1	10	293	96	46	83	61	90
EA08-P2	10	285	86	56	112	69	105
EA08-R1	10	285	87	51	91	94	36
EA09-P1-A	10	295	89	52	94	68	83
EA09-P1-B	10	297	93	54	119	54	51
EA09-P1-C	10	271	97	49	138	48	72
EA09-P1-D	10	291	86	57	98	45	85
EA09-P2	20	292	83	45	97	87	35
EA09-R1	10	284	97	46	90	116	49
EA09-R2A	10	277	94	50	117	94	24
EA09-R2B	20	287	81	49	75	92	63
EA09-R2C	20	281	91	48	105	98	61
EA09-R2D	10	292	109	54	111	70	92
EA09-R2E	10	288	99	44	85	82	44
EA09-R3A	10	292	94	39	110	100	43
EA09-R3B	10	284	87	50	82	95	37
EA09-R3C	10	291	98	50	107	100	75
EA09-R3D	10	276	99	47	102	79	67
EA09-R3E	10	290	96	52	121	93	80
EA10-P1	10	295	86	35	83	82	45
EA10-P2	10	300	84	43	90	112	17
EA10-P3	10	284	91	43	129	91	66
EA10-P4	20	272	95	33	92	93	75
EA10-R1-A	20	280	85	41	89	90	54
EA10-R1-B	20	283	87	43	89	82	52
EA10-R2	10	263	89	33	110	103	68
EA11-P1	10	302	88	43	97	102	66

Table C.2 - Trace-Element Analyses of Specimens (mean of *n* analyses; ppm)

Specimen	n	Zr	Nb	Ga	Zn	Ba	Ce
EA11-R1	10	285	90	57	109	92	88
EA11-R2	10	294	96	37	118	122	42
EA12-P1	10	97	91	47	21	525	51
EA12-P2	10	103	82	51	42	568	64
EA12-R1-A	20	104	65	49	53	519	11
EA12-R1-B	20	100	69	51	62	525	41
EA13-P1	20	98	77	47	39	553	74
EA13-P2	10	119	88	50	97	530	66
EA13-R1	10	96	79	45	36	551	23
EA13-R2	10	97	81	56	52	549	35
EA14-P1-A	20	96	68	49	52	495	127
EA14-P1-B	20	92	71	54	55	495	122
EA14-P2	10	106	59	61	42	493	61
EA14-P3	10	102	71	51	31	537	49
EA14-P4	10	89	64	52	51	502	29
EA14-P5	10	93	74	62	33	505	103
EA14-R1	10	92	80	61	29	503	81
EA15-P1	10	85	66	63	19	498	81
EA15-P2	10	107	73	56	56	510	-
EA15-P3	10	105	73	57	65	500	68
EA15-R1-A	20	95	72	51	53	504	113
EA15-R1-B	20	101	79	47	64	492	85
EA15-R2	10	99	72	60	28	536	77
EA16-P1-A	20	102	84	60	49	433	49
EA16-P1-B	20	100	69	61	63	437	69
EA16-P2-A	20	99	70	53	67	465	88
EA16-P2-B	20	94	75	48	65	455	107
EA16-P2-C	20	97	59	43	68	433	91
EA16-R1-A	20	113	75	61	33	449	21
EA16-R1-B	20	102	77	60	64	453	66
EA16-R2-A	20	110	70	53	58	439	71
EA16-R2-B	20	110	80	57	33	450	105
EA16-R3	10	107	73	45	22	439	60
EA17-P1-A	20	100	79	64	47	520	34
EA17-P1-B	20	98	81	60	47	510	66
EA17-P1-C	20	104	82	58	44	520	48
EA17-P1-D	20	116	70	55	52	514	46
EA17-P1-E	20	107	64	55	40	513	97
EA17-P1-F	20	103	82	49	35	511	79
EA17-P2-A	20	103	62	52	76	502	88
EA17-P2-B	20	97	69	52	54	505	103
EA17-P2-C	20	102	70	50	74	492	134
EA17-P2-D	20	98	79	53	79	505	97

Table C.2 - Trace-Element Analyses of Specimens (mean of *n* analyses; ppm)

Specimen	n	Zr	Nb	Ga	Zn	Ba	Ce
EA17-P3-A	20	107	70	43	24	502	76
EA17-P3-B	20	113	65	51	17	514	91
EA17-P3-C	20	99	69	53	28	511	77
EA17-P4	10	107	75	55	-	500	63
EA17-P5	10	88	75	71	84	511	67
EA17-R1	10	88	79	68	55	518	48
EA17-R2-A	20	112	77	52	28	523	50
EA17-R2-B	20	110	74	56	37	533	48
EA18-P1	10	84	86	51	30	521	48
EA18-R1	10	107	72	51	66	513	66
EA19-P1	10	103	71	54	34	512	-
EA19-R1	10	106	75	50	27	488	82
EA20-P1	10	1396	123	-	243	40	239
EA20-P2	10	1428	145	15	293	16	216
EA20-R1	10	1430	149	26	261	17	232
EA21-P1	10	1186	120	12	204	36	230
EA21-P2	10	1206	124	-	193	12	206
EA21-R1-A	20	1182	126	-	201	-	230
EA21-R1-B	20	1192	119	11	193	11	226
EA22-P1-A	20	1242	141	18	215	30	202
EA22-P1-B	20	1254	127	30	206	26	216
EA22-P1-C	20	1223	133	20	238	27	194
EA22-P1-D	20	1240	123	16	248	22	186
EA22-P2	10	1228	135	39	184	31	229
EA22-P3	10	1197	121	25	241	13	261
EA22-P4	10	1203	112	33	210	-	255
EA22-P5-A	20	1183	137	28	210	21	241
EA22-P5-B	20	1198	127	24	251	14	219
EA22-P6-A	20	1194	126	-	228	16	225
EA22-P6-B	20	1209	142	26	225	21	231
EA22-P7-A	20	1190	138	23	250	30	193
EA22-P7-B	20	1209	130	23	234	29	192
EA22-P8-A	20	1210	132	36	207	13	223
EA22-P8-B	20	1201	126	23	228	13	220
EA22-P9	10	1212	127	22	190	14	248
EA22-R1	10	1207	147	12	249	28	207
EA22-R2	10	1220	136	-	229	22	189
EA23-P1-A	20	1204	159	-	225	30	188
EA23-P1-B	20	1191	142	-	229	22	216
EA23-P2	10	1212	138	-	172	-	241
EA23-P3	10	1221	147	-	174	23	313
EA23-P4	10	1212	140	-	184	20	239
EA23-R1-A	20	1209	159	-	207	20	268

Table C.2 - Trace-Element Analyses of Specimens (mean of *n* analyses; ppm)

Specimen	n	Zr	Nb	Ga	Zn	Ba	Ce
EA23-R1-B	20	1223	146	-	233	20	218
EA23-R2-A	20	1245	154	-	222	40	227
EA23-R2-B	20	1241	138	-	216	11	253
EA24-P1-A	20	1183	130	53	224	25	235
EA24-P1-B	20	1170	141	64	224	24	186
EA24-P1-C	20	1185	127	63	220	20	170
EA24-P2-A	20	1184	136	69	232	15	235
EA24-P2-B	20	1197	137	54	190	24	243
EA24-P3	10	1215	118	54	192	14	220
EA24-P4	10	1235	139	64	207	-	273
EA24-P5-A	20	1210	113	59	231	26	261
EA24-P5-B	20	1243	129	50	215	34	234
EA24-P6-A	20	1196	127	62	211	23	185
EA24-P6-B	20	1203	140	66	228	-	246
EA24-P7	10	1207	132	61	152	27	214
EA24-P8-A	20	1217	122	61	215	-	174
EA24-P8-B	20	1214	137	57	221	30	173
EA24-P9-A	20	1257	128	67	232	31	181
EA24-P9-B	20	1261	140	69	198	16	209
EA24-R1	10	1201	150	60	177	15	184
EA24-R2	10	1215	136	56	220	-	220
EA25-P1-A	20	1237	128	45	228	18	234
EA25-P1-B	20	1238	132	55	226	17	195
EA25-P1-C	20	1246	129	38	217	27	233
EA25-P1-D	20	1234	129	55	228	13	218
EA25-P2-A	20	1278	121	40	209	31	204
EA25-P2-B	20	1284	122	56	220	21	195
EA25-P2-C	20	1268	127	55	250	31	191
EA25-P2-D	20	1273	118	45	221	29	202
EA25-P3	10	1272	118	39	211	-	261
EA25-R1	10	1265	123	49	196	-	233
EA25-R2	10	1289	110	57	188	38	246
EA26-P1-A	20	630	133	63	156	33	155
EA26-P1-B	20	640	119	64	166	31	166
EA26-P2-A	20	649	133	65	176	28	94
EA26-P2-B	20	647	128	68	184	25	128
EA26-R1-A	20	617	134	74	184	37	109
EA26-R1-B	20	628	114	72	197	25	131
EA26-R2-A	20	619	140	69	191	27	160
EA26-R2-B	20	624	139	63	182	18	144
EA26-R2-C	20	624	143	72	168	25	162
EA26-R2-D	20	617	129	62	171	19	171
EA26-R3-A	20	620	130	64	169	20	166

Table C.2 - Trace-Element Analyses of Specimens (mean of *n* analyses; ppm)

Specimen	n	Zr	Nb	Ga	Zn	Ba	Ce
EA26-R3-B	20	627	141	63	168	12	127
EA26-R3-C	20	623	128	63	180	25	175
EA26-R3-D	15	609	138	72	202	12	129
EA27-P1	20	1396	132	-	243	-	260
EA27-P2	20	1406	143	-	262	-	260
EA27-R1	20	1395	141	-	281	-	267
EA28-P1	20	1365	114	-	238	-	266
EA28-P2-A	30	1362	122	-	255	-	284
EA28-P2-B	30	1359	110	-	251	11	293
EA28-P2-C	30	1372	123	-	235	-	271
EA28-P3-A	30	1402	119	-	251	-	262
EA28-P3-B	30	1398	116	-	235	-	266
EA28-P4-A	30	1349	122	-	256	10	261
EA28-P4-B	30	1359	116	-	257	-	264
EA28-P5-A	30	1344	117	-	257	-	304
EA28-P5-B	30	1349	115	-	256	-	294
EA28-R1	10	1394	136	-	242	-	225
EA28-R2	20	1378	133	-	268	-	277
EA29-R1-A	20	1408	144	43	309	27	266
EA29-R1-B	20	1397	140	49	291	25	298
EA29-R2	20	1429	144	14	301	-	290
EA30-P1	10	280	105	69	92	70	116
EA30-P2	10	294	94	66	84	67	53
EA30-R1	10	280	86	58	117	51	55
EA30-R2-A	20	284	94	54	98	78	90
EA30-R2-B	20	281	72	50	94	79	156
EA30-R3A	10	295	105	53	86	62	103
EA30-R3B	10	299	90	51	91	82	42
EA30-R3C	10	282	92	44	73	60	97
EA30-R3D	10	305	94	61	78	78	57
EA30-R3E	10	296	89	55	87	74	87
EA30-R3F	10	285	89	50	84	62	101
EA30-R3G	10	293	95	56	84	62	109
EA31-P1	20	300	90	51	93	66	57
EA31-R1	10	283	78	48	62	67	108
EA32-P1	20	292	97	53	91	66	85
EA32-R1	20	295	99	57	80	83	87
EA32-R2	10	291	95	64	85	80	104
EA33-P1-A	20	178	100	65	42	20	99
EA33-P1-B	20	174	92	55	36	22	98
EA33-P2-A	10	169	84	53	82	28	139
EA33-P2-B	10	191	85	47	60	28	134
EA33-P3	20	176	83	42	108	62	62

Table C.2 - Trace-Element Analyses of Specimens (mean of *n* analyses; ppm)

Specimen	n	Zr	Nb	Ga	Zn	Ba	Ce
EA33-P4	10	174	109	54	81	37	67
EA33-P5	10	195	108	58	56	51	42
EA33-P6	10	181	89	57	60	48	84
EA33-P7	20	191	78	45	54	57	97
EA33-P8	20	180	84	48	56	89	50
EA33-R1	10	177	114	45	85	42	78
EA34-P1	10	179	81	57	65	52	106
EA34-P2	10	178	98	66	41	33	73
EA34-P3	20	187	100	48	50	62	110
EA34-P4	20	291	94	44	127	103	88
EA34-P5	20	295	78	53	93	115	75
EA34-R1	10	178	113	56	87	36	64
EA34-R2	10	180	102	44	43	58	144
EA35-P1	10	162	99	43	50	49	57
EA35-P2	20	173	84	41	83	64	84
EA35-P3	20	171	102	47	65	70	90
EA35-R1	10	167	85	47	38	50	86
EA35-R2	20	180	93	49	75	41	84
EA36-P1-A	20	195	84	-	48	677	57
EA36-P1-B	20	195	77	-	29	689	53
EA36-P1-C	20	190	72	-	15	682	64
EA36-P1-D	20	203	80	-	38	660	97
EA36-P2	10	161	65	-	89	745	41
EA36-P3	10	168	81	-	32	743	47
EA36-P4-A	20	178	79	-	34	675	72
EA36-P4-B	20	187	82	-	36	678	96
EA36-R1	10	182	77	-	56	720	48
EA36-R2	10	196	69	-	47	728	22
EA36-R3A	10	190	73	-	34	721	44
EA36-R3B	20	190	83	-	37	750	89
EA36-R3C	10	183	80	-	58	745	20
EA36-R3D	20	184	73	-	64	761	83
EA36-R3E-A	20	183	80	-	47	695	69
EA36-R3E-B	20	185	75	-	40	689	74
EA36-R4A	20	186	80	-	56	757	85
EA36-R4B	20	195	79	-	84	748	73
EA36-R4C	10	173	69	-	30	740	32
EA36-R4D	20	194	76	-	47	730	79
EA36-R4E	10	186	90	-	77	705	23
EA37-P1	20	125	78	40	15	691	23
EA37-P2	10	128	67	46	25	682	42
EA37-P3	20	142	79	38	25	700	47
EA37-P4	10	119	70	34	40	699	43

Table C.2 - Trace-Element Analyses of Specimens (mean of *n* analyses; ppm)

Specimen	n	Zr	Nb	Ga	Zn	Ba	Ce
EA37-P5-A	10	131	68	51	51	664	50
EA37-P5-B	10	121	80	42	48	654	53
EA37-P6-A	20	114	77	48	50	655	95
EA37-P6-B	20	132	72	43	-	663	56
EA37-P7-A	20	135	76	46	28	653	73
EA37-P7-B	20	144	65	44	50	637	67
EA37-P8	20	126	65	43	31	698	61
EA37-R1	10	121	70	41	44	692	32
EA37-R2	10	139	54	32	61	661	17
EA38-P1	20	71	90	42	20	233	20
EA38-P2	20	80	82	38	23	225	47
EA38-P3	10	82	77	42	65	225	33
EA38-P4	10	59	64	26	27	235	-
EA38-R1	20	71	76	38	35	232	27
EA39-P1-A	10	246	90	55	101	64	52
EA39-P1-B	10	263	106	59	110	54	111
EA39-P2-A	20	263	100	52	58	50	113
EA39-P2-B	20	249	102	52	78	46	69
EA39-P3	20	266	95	44	66	90	37
EA39-P4	20	265	79	45	97	83	39
EA39-P5	10	255	88	49	52	108	48
EA39-P6-A	20	260	99	55	94	54	46
EA39-P6-B	20	262	92	55	76	44	56
EA39-R1	10	256	80	43	91	67	73
EA39-R2	10	256	99	47	65	110	59
EA40-P1	20	212	91	45	101	175	30
EA40-R1	10	209	95	50	127	192	62
EA40-R2-A	20	223	89	55	71	137	76
EA40-R2-B	20	218	87	58	86	130	66
EA40-R3A	20	214	94	48	93	173	84
EA40-R3B	20	217	82	45	80	174	41
EA40-R3C	20	224	94	46	92	176	31
EA40-R3D	20	216	92	40	84	187	52
EA40-R3E	20	202	97	52	78	178	-
EA40-R4A	20	206	80	54	97	178	42
EA40-R4B	20	206	81	46	70	161	58
EA40-R4C	20	205	96	49	74	172	50
EA40-R4D	20	206	85	40	72	173	55
EA40-R4E	10	200	79	57	106	169	54
EA41-P1	20	121	84	62	39	364	81
EA41-R1	20	116	67	54	36	346	86
EA42-P1-A	10	111	73	43	72	331	66
EA42-P1-B	10	118	71	63	95	331	83

Table C.2 - Trace-Element Analyses of Specimens (mean of *n* analyses; ppm)

Specimen	n	Zr	Nb	Ga	Zn	Ba	Ce
EA42-P2-A	20	113	76	55	75	344	111
EA42-P2-B	20	103	72	55	30	325	121
EA42-P3-A	20	115	77	47	62	332	109
EA42-P3-B	20	118	78	52	49	335	71
EA42-P4	10	131	108	51	41	354	-
EA42-R1	20	115	78	57	24	369	59
EA43-P1	10	183	85	50	40	374	88
EA43-P2-A	10	182	69	51	70	354	82
EA43-P2-B	10	164	82	34	63	376	120
EA43-P3	20	159	88	44	54	430	81
EA43-R1	10	162	72	41	72	431	52
EA43-R2	10	173	76	50	45	428	38
EA44-P1	10	163	90	38	29	403	65
EA44-P2	10	172	74	48	49	404	47
EA44-P3	20	171	89	46	78	412	82
EA44-R1	10	171	84	36	76	428	63
EA45-P1-A	20	135	89	47	47	398	128
EA45-P1-B	20	141	77	43	75	397	129
EA45-P1-C	20	150	73	49	60	387	107
EA45-P1-D	20	144	80	43	78	396	100
EA45-P2-A	20	136	70	49	56	394	116
EA45-P2-B	20	146	81	45	53	400	131
EA45-P2-C	20	148	66	36	68	416	80
EA45-P3	10	165	85	44	44	408	71
EA45-P4	10	160	74	46	30	406	90
EA45-R1-A	10	133	83	36	51	404	129
EA45-R1-B	10	144	73	40	34	406	125
EA45-R2-A	10	139	85	34	103	400	121
EA45-R2-B	10	146	80	36	31	420	141
EA46-P1-A	20	142	72	41	59	430	115
EA46-P1-B	20	149	70	45	35	422	67
EA46-P1-C	20	144	87	39	53	432	92
EA46-P2	10	139	80	37	43	431	99
EA46-P3	10	133	81	40	63	425	102
EA46-P4	10	147	77	41	60	401	126
EA46-P5	10	143	76	51	67	382	71
EA46-R1	10	142	65	44	32	438	108
EA47-R1	10	1500	139	41	279	30	236
EA48-P1-A	20	1460	138	58	247	20	232
EA48-P1-B	20	1483	138	58	272	23	246
EA48-P2-A	20	1397	136	52	243	22	218
EA48-P2-B	20	1384	137	58	255	29	216
EA48-P2-C	20	1391	147	54	242	27	238

Table C.2 - Trace-Element Analyses of Specimens (mean of *n* analyses; ppm)

Specimen	n	Zr	Nb	Ga	Zn	Ba	Ce
EA48-P3	10	1418	151	58	267	-	220
EA48-P4	10	1412	130	60	246	44	265
EA48-P5	10	1398	124	63	257	-	277
EA48-R1	10	1403	142	53	257	56	280
EA48-R2-A	20	1476	138	62	246	18	226
EA48-R2-B	20	1467	143	60	222	20	285
EA49-P1	10	284	107	46	89	64	90
EA49-R1	10	301	75	30	86	82	64
EA49-R2	10	293	107	42	120	87	134
EA50-P1-A	20	283	98	45	94	77	96
EA50-P1-B	20	299	105	40	115	83	74
EA50-P1-C	20	291	91	45	111	84	100
EA50-P2-A	20	306	97	42	119	78	67
EA50-P2-B	20	293	89	40	124	75	94
EA50-P2-C	20	300	94	51	115	72	69
EA50-P3-A	20	288	98	47	101	71	97
EA50-P3-B	20	284	98	41	97	70	74
EA50-P4-A	20	297	105	50	100	80	84
EA50-P4-B	20	298	93	56	85	82	101
EA50-P4-C	20	309	106	42	114	79	83
EA50-P4-D	20	307	93	45	105	81	44
EA50-P5	10	287	95	52	65	81	106
EA50-P6	10	279	93	46	95	74	47
EA50-R1-A	20	274	96	45	83	77	79
EA50-R1-B	20	296	94	46	72	75	89
EA51-P1	10	109	75	46	64	595	72
EA51-R1	10	109	59	47	35	579	70
EA52-B1	10	342	77	52	89	417	95
EA52-B2	10	332	80	57	79	417	105
EA52-B3	10	330	81	61	85	417	66
EA53-B1	10	355	81	51	106	373	113
EA53-B2	10	337	68	50	65	385	59
EA54-B1	10	347	72	50	83	422	95
EA55-B1	10	359	86	59	79	423	99
EA55-B2	10	344	96	55	39	418	98
EA56-B1	10	346	85	58	76	415	99
EA57-B1	10	224	121	43	142	-	58
EA58-B1	10	225	140	52	139	23	63
EA59-B1	10	217	144	44	136	-	56
EA60-B1-A	20	208	142	49	143	36	80
EA60-B1-B	20	215	140	34	149	27	56
EA60-B2	10	204	149	38	82	13	101
EA61-B1	10	205	138	43	126	13	124

Table C.2 - Trace-Element Analyses of Specimens (mean of *n* analyses; ppm)

Specimen	n	Zr	Nb	Ga	Zn	Ba	Ce
EA61-B2	10	217	141	53	107	35	82
EA62-Y1-A	10	216	150	48	152	28	10
EA62-Y1-B	10	211	133	38	134	34	10
EA62-Y1-C	10	237	137	46	134	40	-
EA62-Y1-D	10	210	141	40	130	26	22
EA62-Y2-A	20	204	130	49	125	25	35
EA62-Y2-B	20	210	140	42	113	33	46
EA62-Y3-A	20	209	148	44	129	25	36
EA62-Y3-B	20	223	133	49	141	43	30
EA62-Y4	10	237	137	47	139	31	40
EA62-Y5	10	227	130	55	121	27	45
EA63-E1A	10	97	76	53	43	535	42
EA63-E1B	10	118	80	37	65	487	73
EA63-E1C	10	110	79	51	32	534	42
EA63-E1D	10	109	84	51	72	502	100
EA63-E1E	10	107	82	33	62	486	62
EA64-E1A	10	1436	152	18	301	29	254
EA64-E1B	10	1380	141	-	296	35	262
EA64-E1C	10	1400	134	-	290	28	258
EA64-E1D	10	1429	130	-	280	23	265
EA64-E1E	10	1421	132	-	293	19	251
EA65-W1	10	227	86	45	114	163	96
EA65-W2	10	215	74	44	98	202	65
EA66-W1	10	270	60	40	96	804	119
EA67-W1	10	151	89	41	58	412	85
EA68-SX1	10	279	90	42	94	123	34
EA68-SX2	10	299	82	42	126	124	91
EA69-SX1	10	291	68	45	107	128	57
EA69-SX2	20	279	80	44	93	126	86
GE01-jB1	10	74	61	53	96	939	90
GE02-iD1A	10	74	32	52	95	837	99
GE02-iD1B	10	81	43	46	73	878	107
GE02-iD1C	10	82	53	44	70	861	64
GE03-iD1	10	83	35	44	88	926	62
GE04-iD1	10	80	57	43	99	754	45
GE05-iD1	10	83	44	49	80	849	92
GE06-iD1	10	63	31	52	96	828	60
GE07-kM1A	10	83	34	52	101	827	58
GE07-kM1B	10	70	19	52	92	826	99
GE07-kM1C	10	56	50	45	72	816	61
GE08-rB1	10	85	61	43	55	688	70
GE08-rB2	20	89	74	48	60	719	43
GE09-nS1	20	106	66	46	52	1078	104

Table C.2 - Trace-Element Analyses of Specimens (mean of *n* analyses; ppm)

Specimen	n	Zr	Nb	Ga	Zn	Ba	Ce
GE10-nS1	20	86	75	45	60	685	70
GE11-nS1	20	96	77	48	69	842	73
GE11-nS2	20	107	65	46	66	893	103
GE11-nS3	20	112	69	43	44	895	117
GE11-nS4	10	95	62	47	53	808	98
GE11-nS5	10	89	66	52	56	710	82
GE11-nS6	10	83	70	46	69	921	82
GE12-nS1	10	77	65	49	53	712	101
GE13-nS1	10	89	66	52	29	867	79
GE13-nS2	20	98	59	39	74	895	112
KB01-jB1	10	52	38	50	52	209	53
KB02-jB1	10	40	62	51	72	201	82

Total: 12,785 trace-element analyses

Note: When the mean concentration value was below 10 ppm, the value was replaced by a "-" to denote that it was below the detection limits; the dash does not indicate unmeasured values.

Table C.3 - Major-Element Analyses of Artifacts (mean of *n* analyses; weight percent)

Artifact	n	SiO_2	TiO_2	Al_2O3	Cr_2O_3	FeO(T)	MnO	MgO	CaO	Na_2O	K_2O	P_2O_5	F	SO_3	Cl	Total
A1 q161-1 f16 k117	10	74.69	0.157	11.60	-	2.753	0.056	-	0.210	5.479	4.578	0.002	0.003	0.002	0.119	99.65
A1 q183-1 f606 k?	10	75.14	0.168	11.33	-	2.686	0.054	0.019	0.213	4.905	4.745	0.015	0.003	0.005	0.164	99.45
A1 q264-1 f67 k13	10	75.01	0.152	11.19	-	2.695	0.054	0.015	0.184	4.472	5.185	0.005	0.001	0.004	0.146	99.11
A1 q342-lw f16 k117	10	73.82	0.150	11.11	-	2.653	0.052	0.018	0.191	4.310	5.257	0.010	0.003	0.005	0.142	97.72
A1 q59-1 f29 k119	10	74.13	0.152	11.24	0.003	2.730	0.058	0.066	0.210	4.349	5.210	0.013	0.002	0.009	0.209	98.38
A10 q1081-6 f234 k21	20	72.54	0.153	10.89	-	2.653	0.053	0.031	0.489	3.658	5.402	0.008	0.002	0.004	0.135	96.02
A10 q1194.3 f925 k29	10	70.54	0.200	14.08	0.003	1.590	0.042	0.147	0.690	3.858	6.327	0.027	0.002	-	0.092	97.60
A10 q229-1 f94 k5	10	74.33	0.081	13.10	-	1.273	0.069	0.047	0.401	4.699	4.445	0.007	0.002	0.001	0.059	98.52
A10 q286-1 f141 k3	10	68.21	0.194	14.06	-	1.700	0.035	0.186	0.716	4.096	5.978	0.035	-	0.005	0.112	95.32
A10 q541-s1 f245 k26/24	10	48.21	0.584	10.33	0.035	5.812	0.117	4.194	22.849	0.996	3.897	1.126	0.065	0.197	0.165	98.58
A10 q601.3 f277 k27	10	72.30	0.069	13.97	0.001	0.842	0.031	0.032	0.482	3.858	5.811	0.022	0.003	-	0.103	97.52
A10 q678.3 f292 k28	20	70.29	0.199	13.99	-	1.644	0.035	0.178	0.695	3.556	6.485	0.037	0.001	0.005	0.084	97.20
A10 q695.1 f300 k28	10	70.67	0.196	14.06	0.002	1.720	0.039	0.211	0.788	4.101	6.405	0.037	0.002	0.007	0.085	98.33
A10 q77-1 f79 k7	10	74.71	0.157	11.37	-	2.699	0.054	0.015	0.196	4.749	4.980	0.011	0.003	0.005	0.139	99.09
A14 q244-1 f29 k2	10	72.93	0.158	10.84	-	2.660	0.057	0.025	0.199	3.347	6.624	0.011	0.002	0.013	0.149	97.02
A14 q252-1 f90 k3	10	75.11	0.159	11.44	0.002	2.716	0.050	0.042	0.192	4.359	5.374	0.011	0.001	0.006	0.138	99.60
A14 q265-1 f92 k3	10	68.02	0.198	13.47	-	1.672	0.037	0.143	0.710	3.426	6.371	0.023	0.003	-	0.060	94.13
A14 q266-1 f92 k3	10	70.90	0.204	14.16	-	1.341	0.026	0.106	0.574	3.600	6.658	0.040	0.001	0.007	0.103	97.73
A14 q299.2 f101 k100	10	74.86	0.155	11.21	-	2.697	0.056	0.001	0.190	4.528	5.139	-	0.004	0.002	0.128	98.96
A14 q474.1 f193 k4	10	74.29	0.153	11.23	-	2.704	0.057	0.013	0.191	4.424	5.271	0.006	0.002	0.009	0.129	98.49
A14 q605-2 f250 k23	10	71.64	0.151	10.68	-	2.744	0.054	0.288	0.249	3.430	5.901	0.037	0.004	0.003	0.215	95.40
A14 q617-1 f250 k23	10	74.45	0.160	11.15	0.001	2.655	0.054	0.033	0.245	4.338	5.107	0.008	0.003	0.013	0.177	98.39
A14 q742-2 f42 k12	10	71.90	0.158	10.63	-	2.950	0.055	0.253	0.683	4.346	5.843	0.032	0.002	0.012	0.244	97.11
A15 q1173-3 f517 k2	10	72.96	0.068	12.75	-	1.226	0.062	0.053	0.348	3.894	5.521	0.018	0.003	0.006	0.087	96.99
A15 q295.2 f108 k92	30	71.89	0.077	12.60	0.002	1.234	0.062	0.045	0.408	4.061	5.237	0.009	0.002	0.003	0.079	95.71
A15 q734-1 f372 k14	10	72.52	0.156	10.67	0.001	2.641	0.060	0.013	0.214	4.090	5.154	0.005	0.003	0.005	0.150	95.68
A15 q752-2 f386 k15	10	71.49	0.071	13.68	0.002	1.212	0.038	0.059	0.565	3.912	5.433	0.016	0.002	0.002	0.099	96.58
A16 q202-2 f83 k105	10	71.61	0.081	12.54	0.002	1.255	0.063	0.078	0.401	3.914	5.943	0.018	0.002	0.008	0.079	95.99
A16 q21.1 f26 k5	10	73.88	0.157	11.14	-	2.718	0.058	0.008	0.204	3.572	5.746	0.005	0.004	0.006	0.119	97.62

Table C.3 - Major-Element Analyses of Artifacts (mean of *n* analyses; weight percent)

Artifact	n	SiO_2	TiO_2	Al_2O3	Cr_2O_3	FeO(T)	MnO	MgO	CaO	Na_2O	K_2O	P_2O_5	F	SO_3	Cl	Total
A16 q633-2 f208 k110	40	68.44	0.196	13.61	-	1.735	0.033	0.292	0.643	3.679	6.440	0.051	0.003	0.013	0.193	95.33
A17 q231-2 f107 k12	10	70.54	0.194	13.82	-	1.741	0.038	0.261	0.758	3.725	6.364	0.086	0.003	0.013	0.136	97.68
A18 q23-1 f24 k23	40	71.61	0.156	10.80	0.001	2.692	0.051	0.103	0.275	4.593	6.834	0.027	0.002	0.007	0.192	97.34
A18 q23-4 f24 k25	10	68.13	0.175	13.55	-	1.787	0.031	0.190	0.680	3.403	6.262	0.032	0.003	0.003	0.117	94.36
A18 q249-3 f120 k24	10	73.43	0.155	10.89	-	2.687	0.054	0.046	0.204	3.912	5.440	0.014	0.002	0.005	0.142	96.98
A18 q348-1 f158 k15	10	72.56	0.139	10.64	0.001	2.720	0.054	0.016	0.179	4.396	5.049	0.012	0.003	0.002	0.174	95.94
A18 q35-4 f31 k34	10	71.93	0.063	13.70	0.002	0.878	0.030	0.089	0.456	3.780	5.637	0.020	0.004	0.006	0.101	96.69
A18 q43-3 f44 k26	10	74.41	0.160	11.24	-	2.713	0.055	0.038	0.214	4.277	5.316	0.006	0.004	0.008	0.180	98.62
A18 q441.3 f168 k28	10	71.49	0.157	10.67	0.006	2.766	0.056	0.069	0.231	4.169	5.091	0.026	0.004	0.006	0.138	94.88
A18 q45-1 f42 k34	10	71.18	0.138	10.35	0.004	2.706	0.057	0.272	0.560	3.157	6.387	0.095	0.005	0.020	0.188	95.12
A18 q45.2 f52 k34	10	70.71	0.156	10.73	0.001	2.861	0.058	0.303	0.459	3.699	5.281	0.061	0.006	0.034	0.171	94.53
A18 q5-2 f7 k25	10	72.97	0.146	11.03	-	2.749	0.056	0.066	0.204	4.141	5.175	0.017	0.001	0.002	0.129	96.68
A18 q57.2 f52 k34	10	70.23	0.162	11.07	-	2.842	0.057	0.336	0.325	3.299	5.796	0.068	0.003	0.021	0.381	94.58
A18 q582-1 f242 k28	10	71.76	0.150	10.76	-	2.731	0.052	0.012	0.195	3.988	5.224	0.004	-	0.011	0.135	95.02
A18 q698-1 f298 k26	25	72.17	0.207	10.42	-	3.954	0.074	0.111	0.210	5.200	4.659	0.023	0.004	0.011	0.262	97.31
A18 q746.5 f321 k16	25	74.09	0.151	11.11	-	2.694	0.054	0.016	0.204	4.619	4.852	0.013	0.003	0.010	0.137	97.95
A18 q89-4 f44 k26	10	72.46	0.156	10.68	-	2.657	0.056	0.008	0.206	4.021	5.105	0.004	0.001	0.001	0.137	95.49
A2 q333.2 f114 k151	10	70.50	0.203	14.05	-	1.724	0.032	0.183	0.710	4.053	6.066	0.034	0.005	0.009	0.071	97.64
A6 q386-1 f122 k218 piece 1	10	71.42	0.098	13.32	0.001	1.746	0.067	0.392	0.413	4.146	4.725	0.015	0.001	0.032	0.156	96.53
A6 q386-1 f122 k218 piece 2	15	73.49	0.154	11.09	-	2.779	0.055	0.013	0.201	4.358	5.159	0.008	0.003	0.008	0.124	97.44
A6 q971.1 f410 k31	10	70.98	0.208	14.13	-	1.675	0.035	0.155	0.637	3.667	6.271	0.024	0.002	0.001	0.065	97.84
A6 q973-1 f412 k31	10	72.58	0.149	10.77	-	2.735	0.055	0.072	0.200	3.882	5.328	0.016	0.001	0.007	0.148	95.95
A7 q1146.1 f465 k21	10	73.19	0.078	12.59	-	1.225	0.064	0.062	0.405	3.790	5.658	0.010	0.003	0.005	0.074	97.15
A7 q1150.5 f465 k21	10	73.43	0.203	10.67	0.001	3.826	0.073	0.116	0.215	5.366	4.648	0.030	0.003	0.006	0.308	98.89
A7 q1174.2 f465 k21	10	71.03	0.196	10.96	-	3.808	0.078	0.036	0.260	4.406	4.892	0.023	0.002	0.011	0.247	95.94
A7 q1201.4 f480 k21	10	70.86	0.071	13.41	-	1.328	0.038	0.163	0.538	3.390	6.044	0.038	0.003	0.013	0.139	96.04
A7 q222-1 f69 k9	10	72.46	0.150	10.87	-	2.624	0.055	0.017	0.308	4.550	5.369	0.005	0.006	0.002	0.146	96.56
A7 q287-1 f56 k7	10	73.36	0.153	10.96	0.001	2.706	0.054	0.020	0.197	3.764	5.919	0.008	0.002	0.005	0.150	97.30
A7 q350-l2 f121 k13	10	70.26	0.194	14.17	-	1.787	0.041	0.254	0.743	4.113	5.814	0.048	0.002	0.015	0.117	97.56

Table C.3 - Major-Element Analyses of Artifacts (mean of *n* analyses; weight percent)

Artifact	n	SiO_2	TiO_2	Al_2O3	Cr_2O_3	FeO(T)	MnO	MgO	CaO	Na_2O	K_2O	P_2O_5	F	SO_3	Cl	Total
A7 q360-1 f121 k13 piece 1	10	74.50	0.153	11.40	-	2.714	0.054	0.006	0.199	4.526	5.120	0.007	0.001	0.003	0.120	98.80
A7 q360-1 f121 k13 piece 2	10	72.48	0.151	10.99	0.002	2.712	0.051	0.004	0.187	4.304	4.974	0.002	0.003	0.008	0.134	96.00
A7 q360-1 f121 k13 piece 3	10	72.28	0.151	10.82	-	2.672	0.049	0.004	0.188	4.261	4.972	-	0.002	-	0.137	95.53
A7 q360-1 f121 k13 piece 4	10	73.87	0.152	11.01	0.002	2.699	0.048	0.007	0.189	4.462	5.001	0.001	0.003	0.004	0.135	97.58
A7 q386-l3 f63 k8	10	69.12	0.193	13.88	-	1.769	0.038	0.205	0.850	5.388	7.154	0.049	0.006	0.009	0.115	98.78
A7 q602-1 f148 k13	10	73.50	0.157	11.11	-	2.673	0.053	0.009	0.191	4.405	4.947	0.006	0.004	0.005	0.130	97.19
A7 q892-1 f261 k12	10	76.28	0.060	12.59	0.001	0.712	0.057	0.051	0.441	3.404	5.375	0.009	0.003	0.007	0.093	99.08
A8 q154-1 f58 k9	10	72.55	0.154	10.98	0.003	2.726	0.054	0.005	0.197	4.129	5.140	0.003	0.003	0.008	0.138	96.10
A9 q376.1 f98 k3 piece 1	15	72.68	0.152	11.49	-	2.793	0.055	0.002	0.186	4.441	4.902	0.004	0.002	-	0.110	96.81
A9 q376.1 f98 k3 piece 2	10	73.27	0.152	10.81	-	2.680	0.050	0.009	0.214	4.502	4.949	0.018	0.003	0.007	0.143	96.80
A9 q376.1 f98 k3 piece 3	15	72.66	0.158	10.49	0.001	2.753	0.054	0.026	0.192	4.380	5.159	0.007	0.004	0.006	0.132	96.02
A9 q437.2 f98 k3	10	73.83	0.157	10.94	-	2.662	0.051	0.003	0.183	4.288	5.050	0.006	0.001	0.001	0.128	97.30
A9 q440.1 f98 k3 piece 1	10	70.45	0.200	13.75	0.006	1.505	0.030	0.100	0.656	3.624	6.330	0.024	0.002	-	0.084	96.76
A9 q440.1 f98 k3 piece 2	10	74.02	0.153	10.94	-	2.697	0.054	0.015	0.200	4.585	4.854	0.008	0.002	0.010	0.132	97.67
A9 q454.2 f126 k3 piece 1	10	71.42	0.147	10.65	0.002	2.696	0.056	-	0.192	3.816	5.057	0.003	0.002	0.006	0.147	94.19
A9 q454.2 f126 k3 piece 2	10	73.69	0.152	10.98	-	2.696	0.053	0.003	0.179	4.362	5.029	0.002	0.004	-	0.137	97.29
A9 q454.2 f126 k3 piece 3	10	74.18	0.154	11.18	-	2.695	0.058	0.002	0.198	4.614	5.044	0.004	0.004	0.003	0.120	98.25
A9 q463.2 f156 k3 piece 1	10	73.17	0.058	12.66	0.003	0.708	0.057	0.052	0.438	2.879	5.585	0.005	0.004	0.003	0.100	95.72
A9 q463.2 f156 k3 piece 2	15	73.83	0.061	12.28	0.001	0.754	0.058	0.075	0.443	3.035	5.590	0.023	0.003	0.005	0.093	96.25
A9 q693.1 f247 k11 piece 1	10	73.45	0.151	11.23	0.004	2.705	0.057	-	0.196	4.723	4.825	0.006	0.005	0.002	0.142	97.50
A9 q693.1 f247 k11 piece 2	10	74.95	0.158	11.24	0.003	2.708	0.052	0.003	0.188	4.937	4.852	0.006	0.002	0.003	0.121	99.22
A9 q693.1 f247 k11 piece 3	10	72.43	0.063	13.57	0.003	0.781	0.026	0.023	0.472	4.060	5.570	0.024	0.004	0.005	0.135	97.16
A9 q724.1 f260 k11 piece 1	10	69.91	0.192	13.79	-	1.707	0.040	0.161	0.699	3.643	6.556	0.031	0.003	0.007	0.126	96.87
A9 q724.1 f260 k11 piece 2	10	73.47	0.078	12.58	0.001	1.072	0.052	0.042	0.339	3.516	6.028	0.014	0.001	0.003	0.062	97.25
B1 q350-i f166 k? piece 1	15	72.21	0.155	10.29	0.001	2.706	0.054	0.032	0.216	4.784	4.976	0.012	0.004	0.008	0.157	95.60
B1 q350-i f166 k? piece 2	10	71.18	0.151	10.34	0.002	2.764	0.054	0.050	0.232	4.369	4.937	0.018	0.002	0.012	0.144	94.26
B1 q350-i f166 k? piece 3	10	74.42	0.156	11.21	0.001	2.698	0.055	0.003	0.196	4.815	5.148	0.002	0.004	0.007	0.118	98.83
J1 q276.5 f131 k64	10	72.15	0.165	11.33	0.003	2.901	0.063	0.212	0.316	4.369	5.252	0.071	0.005	0.037	0.252	97.13
J1 q344.1 f151 k106	10	70.01	0.212	14.02	-	1.926	0.038	0.411	0.866	3.930	5.437	0.129	0.005	0.022	0.109	97.11

Table C.3 - Major-Element Analyses of Artifacts (mean of *n* analyses; weight percent)

Artifact	n	SiO_2	TiO_2	Al_2O3	Cr_2O_3	FeO(T)	MnO	MgO	CaO	Na_2O	K_2O	P_2O_5	F	SO_3	Cl	Total
J1 q45-2 f20 k7	10	70.76	0.192	14.32	0.001	1.752	0.037	0.221	0.646	4.134	6.165	0.031	0.001	0.006	0.115	98.38
J1 q64-1 f20 k7	15	72.57	0.209	10.60	-	3.831	0.074	0.022	0.234	4.553	5.388	0.011	0.004	0.010	0.213	97.71
J1 q7-1 f3 k10 piece 1	15	71.36	0.159	10.25	-	2.758	0.054	0.053	0.224	4.156	5.481	0.017	0.002	0.013	0.189	94.71
J1 q7-1 f3 k10 piece 2	10	72.08	0.081	12.29	0.001	0.908	0.053	0.043	0.424	3.633	5.960	0.004	0.001	0.004	0.079	95.56
J2 q142-1 f62 k83	10	74.03	0.153	10.58	-	2.624	0.052	0.132	0.224	4.178	5.113	0.021	0.002	0.007	0.199	97.31
J2 q58-1 f1 k100	10	71.83	0.068	13.54	-	1.013	0.034	0.068	0.548	3.569	6.346	0.028	0.004	0.004	0.107	97.16
J2 q87-1 f42 k33	10	73.24	0.157	10.92	0.005	2.700	0.054	0.016	0.189	4.178	5.423	0.010	0.003	0.009	0.138	97.04
J2 q99-1 f42 k33	10	72.75	0.215	10.83	-	3.844	0.073	0.157	0.232	3.424	6.994	0.017	0.002	0.012	0.312	98.86
J3 q146.1 f100 k13	10	73.97	0.151	10.98	0.004	2.695	0.055	0.030	0.209	2.817	7.187	0.008	0.002	0.002	0.150	98.26
J3 q150.3 f105 k22	10	74.15	0.162	11.10	-	2.711	0.054	0.037	0.198	4.164	5.609	0.009	0.002	0.007	0.153	98.35
J3 q152.1 f101 k13	40	72.41	0.157	10.94	-	2.790	0.057	0.126	0.237	3.450	5.970	0.019	0.001	0.010	0.178	96.35
Georgian archaeological artifacts:																
Georgia-nS1, Anaseuli	10	72.12	0.105	12.83	0.005	0.752	0.058	0.098	0.695	3.580	4.819	0.034	0.005	0.018	0.050	95.17
Georgia-nS2a, Chachuna	10	74.70	0.117	13.12	0.004	0.746	0.058	0.105	0.773	4.116	4.797	0.033	0.007	0.007	0.046	98.63
Georgia-nS2b, Chachuna	10	75.02	0.117	13.06	-	0.803	0.053	0.129	0.742	3.848	4.847	0.028	0.005	0.005	0.040	98.69
Georgia-nS3, Dzudzuana	10	73.41	0.111	12.96	-	0.738	0.052	0.107	0.720	3.859	4.770	0.022	0.005	0.012	0.047	96.81
Georgia-iD1, Tetritsqaro	10	74.48	0.111	13.62	-	0.734	0.054	0.108	0.668	4.065	4.636	0.025	0.004	-	0.057	98.57
Georgia-iD2, Tetritsqaro	10	72.65	0.116	12.92	-	0.716	0.054	0.095	0.702	3.780	4.776	0.027	0.003	0.012	0.130	95.98
Georgia-iD3, Tetritsqaro	10	74.48	0.108	13.12	0.002	0.685	0.049	0.105	0.700	4.073	4.689	0.031	0.003	0.014	0.160	98.22
Georgia-iD4, Tetritsqaro	10	71.71	0.111	12.53	-	0.601	0.060	0.097	0.633	3.503	4.963	0.038	0.006	0.010	0.160	94.42

Table C.4 - Trace-Element Analyses of Artifacts (mean of *n* analyses; ppm)

Artifact	n	Zr	Nb	Ga	Zn	Ba	Ce
A1 q161-1 f16 k117	15	1210	91	32	260	-	239
A1 q183-1 f606 k?	15	1204	91	47	240	10	202
A1 q264-1 f67 k13	15	1225	94	46	231	45	195
A1 q342-lw f16 k117	15	1229	93	44	229	-	221
A1 q59-1 f29 k119	15	1246	115	40	262	-	214
A10 q1081-6 f234 k21	70	1124	84	61	275	77	182
A10 q1194.3 f925 k29	15	300	49	114	140	425	118
A10 q229-1 f94 k5	15	255	100	107	120	83	52
A10 q286-1 f141 k3	15	257	42	159	131	411	73
A10 q541-s1 f245 k26/24	20	95	56	-	35	334	79
A10 q601.3 f277 k27	15	172	46	100	187	67	92
A10 q678.3 f292 k28	15	295	81	57	128	435	74
A10 q695.1 f300 k28	15	288	34	40	124	390	101
A10 q77-1 f79 k7	15	1292	90	52	248	56	209
A14 q244-1 f29 k2	15	1198	111	50	254	-	231
A14 q252-1 f90 k3	15	1069	79	49	231	30	174
A14 q265-1 f92 k3	15	307	47	43	124	410	76
A14 q266-1 f92 k3	15	324	32	33	165	418	66
A14 q299.2 f101 k100	15	1120	91	112	263	-	172
A14 q474.1 f193 k4	15	1175	85	80	213	18	170
A14 q605-2 f250 k23	15	1074	87	37	230	-	216
A14 q617-1 f250 k23	15	1184	98	50	254	23	226
A14 q742-2 f42 k12	15	1164	87	86	249	90	177
A15 q1173-3 f517 k2	15	287	33	40	147	119	78
A15 q295.2 f108 k92	15	246	69	86	149	82	52
A15 q734-1 f372 k14	15	1232	83	46	238	-	203
A15 q752-2 f386 k15	50	190	48	36	212	99	107
A16 q202-2 f83 k105	15	279	76	36	161	58	90
A16 q21.1 f26 k5	15	1117	92	105	234	32	195
A16 q633-2 f208 k110	15	271	26	56	137	381	77
A17 q231-2 f107 k12	15	289	35	42	105	407	145
A18 q23-1 f24 k23	50	1146	104	98	280	19	223
A18 q23-4 f24 k25	15	290	32	31	138	471	97
A18 q249-3 f120 k24	15	1106	89	57	237	-	202
A18 q348-1 f158 k15	15	1219	73	48	250	46	233
A18 q35-4 f31 k34	15	197	63	32	172	45	101
A18 q43-3 f44 k26	15	1235	100	44	254	-	208
A18 q441.3 f168 k28	15	1186	85	104	239	35	197
A18 q45-1 f42 k34	25	937	65	34	258	206	188
A18 q45.2 f52 k34	15	1121	91	113	265	33	198
A18 q5-2 f7 k25	15	1112	49	50	233	48	151
A18 q57.2 f52 k34	15	1063	81	68	258	44	143

Table C.4 - Trace-Element Analyses of Artifacts (mean of *n* analyses; ppm)

Artifact	n	Zr	Nb	Ga	Zn	Ba	Ce
A18 q582-1 f242 k28	15	1191	87	45	240	-	196
A18 q698-1 f298 k26	70	1119	84	18	271	37	198
A18 q746.5 f321 k16	50	1246	114	53	229	22	194
A18 q89-4 f44 k26	15	1193	93	56	256	-	238
A2 q333.2 f114 k151	15	277	66	84	105	414	93
A6 q386-1 f122 k218 piece 1	15	263	56	29	203	118	88
A6 q386-1 f122 k218 piece 2	15	1252	96	47	226	37	226
A6 q971.1 f410 k31	15	307	49	84	109	402	87
A6 q973-1 f412 k31	15	1142	100	112	259	41	207
A7 q1146.1 f465 k21	15	268	78	42	153	71	104
A7 q1150.5 f465 k21	15	1150	95	98	265	39	241
A7 q1174.2 f465 k21	15	1143	100	61	246	25	181
A7 q1201.4 f480 k21	15	173	71	138	170	52	92
A7 q222-1 f69 k9	15	1153	100	105	218	35	211
A7 q287-1 f56 k7	15	1215	117	89	218	25	171
A7 q350-l2 f121 k13	15	275	65	74	128	395	104
A7 q360-1 f121 k13 piece 1	15	1272	98	39	251	25	217
A7 q360-1 f121 k13 piece 2	15	1259	97	44	245	17	217
A7 q360-1 f121 k13 piece 3	15	1278	100	40	262	24	225
A7 q360-1 f121 k13 piece 4	15	1233	107	40	242	26	251
A7 q386-l3 f63 k8	15	302	50	22	133	375	84
A7 q602-1 f148 k13	15	1175	94	96	227	33	213
A7 q892-1 f261 k12	15	53	51	124	82	211	20
A8 q154-1 f58 k9	15	1146	94	61	241	20	143
A9 q376.1 f98 k3 piece 1	15	1226	84	41	236	26	199
A9 q376.1 f98 k3 piece 2	15	1194	97	104	232	20	182
A9 q376.1 f98 k3 piece 3	15	1198	77	43	207	48	209
A9 q437.2 f98 k3	15	1245	95	128	261	-	196
A9 q440.1 f98 k3 piece 1	15	309	46	38	127	421	75
A9 q440.1 f98 k3 piece 2	15	1212	81	45	241	25	200
A9 q454.2 f126 k3 piece 1	15	1161	85	54	257	25	187
A9 q454.2 f126 k3 piece 2	15	1243	87	44	259	31	218
A9 q454.2 f126 k3 piece 3	15	1249	96	35	233	22	205
A9 q463.2 f156 k3 piece 1	15	81	54	37	88	193	25
A9 q463.2 f156 k3 piece 2	20	62	42	31	103	262	54
A9 q693.1 f247 k11 piece 1	15	1133	73	51	234	42	210
A9 q693.1 f247 k11 piece 2	15	1175	64	43	207	22	196
A9 q693.1 f247 k11 piece 3	15	166	64	38	156	61	67
A9 q724.1 f260 k11 piece 1	15	317	51	47	99	451	82
A9 q724.1 f260 k11 piece 2	15	250	64	52	126	118	75
B1 q350-i f166 k? piece 1	15	1215	92	33	243	43	185
B1 q350-i f166 k? piece 2	15	1242	101	50	203	18	215

Table C.4 - Trace-Element Analyses of Artifacts (mean of *n* analyses; ppm)

Artifact	**n**	**Zr**	**Nb**	**Ga**	**Zn**	**Ba**	**Ce**
B1 q350-i f166 k? piece 3	15	1120	60	51	189	26	167
J1 q276.5 f131 k64	15	1104	103	67	266	107	162
J1 q344.1 f151 k106	15	249	48	94	175	431	67
J1 q45-2 f20 k7	15	306	38	45	117	429	103
J1 q64-1 f20 k7	15	1052	53	33	297	132	173
J1 q7-1 f3 k10 piece 1	50	1254	88	47	248	33	209
J1 q7-1 f3 k10 piece 2	50	255	60	39	205	114	59
J2 q142-1 f62 k83	15	1200	87	51	245	-	173
J2 q58-1 f1 k100	15	182	58	48	146	95	109
J2 q87-1 f42 k33	100	1204	87	43	248	-	196
J2 q99-1 f42 k33	15	1096	69	44	295	-	213
J3 q146.1 f100 k13	30	1136	91	111	246	89	183
J3 q150.3 f105 k22	15	1023	92	122	276	21	206
J3 q152.1 f101 k13	15	1123	86	86	229	27	168
Georgian archaeological artifacts:							
Georgia-nS1, Anaseuli	30	83	54	41	66	722	105
Georgia-nS2a, Chachuna	15	84	82	35	90	812	92
Georgia-nS2b, Chachuna	15	98	47	53	62	922	114
Georgia-nS3, Dzudzuana	15	90	58	38	48	836	106
Georgia-iD1, Tetritsqaro	15	68	56	21	74	793	79
Georgia-iD2, Tetritsqaro	15	89	56	33	86	891	105
Georgia-iD3, Tetritsqaro	15	93	55	39	92	838	125
Georgia-iD4, Tetritsqaro	15	97	46	23	80	800	99

Note: When the mean concentration value was below 10 ppm, the value was replaced by a "-" to denote that it was below the detection limits; the dash does not indicate unmeasured values.

Appendix D: Source Assignments based on Euclidean Distances

Table D.1 - Source Assignments of Artifacts based on Euclidean Distance to Centroids of Geological Specimens

Artifact: A1 q161-1 f16 k117

A-Rank: **Nemrut Dag (EA25)** **66**
B-Rank: Nemrut Dag (EA22) 14

Elements: Fe, Ti, Ba

A-Rank:	Nemrut Dag (EA25)	10
B-Rank:	-	-

Specimen	*Location*	*E.D.*
EA25P3	Nemrut Dag (EA25)	0.007
EA25R1	Nemrut Dag (EA25)	0.012
EA25P1B	Nemrut Dag (EA25)	0.015
EA25P1D	Nemrut Dag (EA25)	0.016
EA25P1A	Nemrut Dag (EA25)	0.018
EA25P2B	Nemrut Dag (EA25)	0.019
EA25P1C	Nemrut Dag (EA25)	0.023
EA25P2C	Nemrut Dag (EA25)	0.026
EA25P2D	Nemrut Dag (EA25)	0.026
EA25P2A	Nemrut Dag (EA25)	0.027

Elements: Fe, Zr, Ba

A-Rank:	Nemrut Dag (EA25)	5
B-Rank:	Nemrut Dag (EA22)	5

Specimen	*Location*	*E.D.*
EA25P1D	Nemrut Dag (EA25)	0.019
EA25P1A	Nemrut Dag (EA25)	0.024
EA25P1B	Nemrut Dag (EA25)	0.024
EA22P4	Nemrut Dag (EA22)	0.028
EA25P1C	Nemrut Dag (EA25)	0.032
EA25R1	Nemrut Dag (EA25)	0.038
EA22P8A	Nemrut Dag (EA22)	0.039
EA22P5B	Nemrut Dag (EA22)	0.040
EA22P6B	Nemrut Dag (EA22)	0.040
EA22P8B	Nemrut Dag (EA22)	0.041

Elements: Ti, Fe, Zr, Ba

A-Rank:	Nemrut Dag (EA25)	10
B-Rank:	-	-

Specimen	*Location*	*E.D.*
EA25P1D	Nemrut Dag (EA25)	0.022
EA25P1B	Nemrut Dag (EA25)	0.024
EA25P1A	Nemrut Dag (EA25)	0.026
EA25P1C	Nemrut Dag (EA25)	0.033
EA25R1	Nemrut Dag (EA25)	0.038
EA25P3	Nemrut Dag (EA25)	0.042
EA25P2C	Nemrut Dag (EA25)	0.046
EA25P2D	Nemrut Dag (EA25)	0.049
EA25P2A	Nemrut Dag (EA25)	0.053
EA25P2B	Nemrut Dag (EA25)	0.053

Elements: Ti, Fe, Mn, Ca, Zr, Ba

A-Rank:	Nemrut Dag (EA25)	10
B-Rank:	-	-

Specimen	*Location*	*E.D.*
EA25P1A	Nemrut Dag (EA25)	0.032
EA25P1C	Nemrut Dag (EA25)	0.033
EA25P1B	Nemrut Dag (EA25)	0.039
EA25R1	Nemrut Dag (EA25)	0.051
EA25P3	Nemrut Dag (EA25)	0.052
EA25P1D	Nemrut Dag (EA25)	0.055
EA25P2C	Nemrut Dag (EA25)	0.057
EA25P2B	Nemrut Dag (EA25)	0.061
EA25P2A	Nemrut Dag (EA25)	0.062
EA25P2D	Nemrut Dag (EA25)	0.064

Elements: Fe, Ti, Zr

A-Rank:	Nemrut Dag (EA25)	10
B-Rank:	-	-

Specimen	*Location*	*E.D.*
EA25P1B	Nemrut Dag (EA25)	0.021
EA25P1D	Nemrut Dag (EA25)	0.021
EA25P1A	Nemrut Dag (EA25)	0.022
EA25P1C	Nemrut Dag (EA25)	0.026
EA25R1	Nemrut Dag (EA25)	0.038
EA25P2C	Nemrut Dag (EA25)	0.040
EA25P3	Nemrut Dag (EA25)	0.042
EA25P2D	Nemrut Dag (EA25)	0.044
EA25P2A	Nemrut Dag (EA25)	0.048
EA25P2B	Nemrut Dag (EA25)	0.051

Elements: Ti, Zr, Ba

A-Rank:	Nemrut Dag (EA25)	8
B-Rank:	Nemrut Dag (EA22)	2

Specimen	*Location*	*E.D.*
EA25P1D	Nemrut Dag (EA25)	0.022
EA25P1B	Nemrut Dag (EA25)	0.023
EA25P1A	Nemrut Dag (EA25)	0.024
EA25P1C	Nemrut Dag (EA25)	0.032
EA25R1	Nemrut Dag (EA25)	0.037
EA25P3	Nemrut Dag (EA25)	0.042
EA25P2C	Nemrut Dag (EA25)	0.046
EA25P2D	Nemrut Dag (EA25)	0.049
EA22P2	Nemrut Dag (EA22)	0.050
EA22P6B	Nemrut Dag (EA22)	0.051

Elements: Ti, Fe, Zr, Ba, Zn

A-Rank:	Nemrut Dag (EA22)	7
B-Rank:	Nemrut Dag (EA25)	3

Specimen	*Location*	*E.D.*
EA25P2C	Nemrut Dag (EA25)	0.057
EA22P7A	Nemrut Dag (EA22)	0.073
EA22R1	Nemrut Dag (EA22)	0.080
EA22P1D	Nemrut Dag (EA22)	0.085
EA22P5B	Nemrut Dag (EA22)	0.085
EA22P3	Nemrut Dag (EA22)	0.096
EA22P1C	Nemrut Dag (EA22)	0.106
EA25P1D	Nemrut Dag (EA25)	0.107
EA25P1A	Nemrut Dag (EA25)	0.108
EA22P7B	Nemrut Dag (EA22)	0.110

Elements: Ti, Al, Fe, Mn, Ca, Zr, Ba

A-Rank:	Nemrut Dag (EA25)	10
B-Rank:	-	-

Specimen	*Location*	*E.D.*
EA25P1C	Nemrut Dag (EA25)	0.043
EA25P1A	Nemrut Dag (EA25)	0.046
EA25P1B	Nemrut Dag (EA25)	0.047
EA25P1D	Nemrut Dag (EA25)	0.059
EA25P3	Nemrut Dag (EA25)	0.061
EA25R1	Nemrut Dag (EA25)	0.062
EA25P2C	Nemrut Dag (EA25)	0.063
EA25P2A	Nemrut Dag (EA25)	0.067
EA25P2B	Nemrut Dag (EA25)	0.067
EA25P2D	Nemrut Dag (EA25)	0.069

Table D.1 - Source Assignments of Artifacts based on Euclidean Distance to Centroids of Geological Specimens

Artifact: A1 q183-1 f606 k?

A-Rank: **Nemrut Dag (EA25)** **59**
B-Rank: Nemrut Dag (EA22) 21

Elements: Fe, Ti, Ba

A-Rank:	Nemrut Dag (EA25)	10
B-Rank:	-	-

Specimen	*Location*	*E.D.*
EA25P3	Nemrut Dag (EA25)	0.023
EA25R1	Nemrut Dag (EA25)	0.023
EA25P1B	Nemrut Dag (EA25)	0.025
EA25P1A	Nemrut Dag (EA25)	0.027
EA25R2	Nemrut Dag (EA25)	0.028
EA25P1C	Nemrut Dag (EA25)	0.030
EA25P2A	Nemrut Dag (EA25)	0.031
EA25P2B	Nemrut Dag (EA25)	0.032
EA25P1D	Nemrut Dag (EA25)	0.033
EA25P2C	Nemrut Dag (EA25)	0.035

Elements: Fe, Zr, Ba

A-Rank:	Nemrut Dag (EA25)	7
B-Rank:	Nemrut Dag (EA22)	3

Specimen	*Location*	*E.D.*
EA25P1A	Nemrut Dag (EA25)	0.023
EA25P1D	Nemrut Dag (EA25)	0.023
EA25P1B	Nemrut Dag (EA25)	0.024
EA25P1C	Nemrut Dag (EA25)	0.031
EA22P4	Nemrut Dag (EA22)	0.037
EA25R1	Nemrut Dag (EA25)	0.040
EA25P3	Nemrut Dag (EA25)	0.046
EA25P2C	Nemrut Dag (EA25)	0.047
EA22P5B	Nemrut Dag (EA22)	0.048
EA22P6B	Nemrut Dag (EA22)	0.048

Elements: Ti, Fe, Zr, Ba

A-Rank:	Nemrut Dag (EA25)	7
B-Rank:	Nemrut Dag (EA22)	3

Specimen	*Location*	*E.D.*
EA25P1B	Nemrut Dag (EA25)	0.034
EA25P1A	Nemrut Dag (EA25)	0.035
EA25P1D	Nemrut Dag (EA25)	0.039
EA25P1C	Nemrut Dag (EA25)	0.041
EA25R1	Nemrut Dag (EA25)	0.046
EA25P3	Nemrut Dag (EA25)	0.051
EA25P2C	Nemrut Dag (EA25)	0.055
EA22P4	Nemrut Dag (EA22)	0.057
EA22P6B	Nemrut Dag (EA22)	0.057
EA25P2A	Nemrut Dag (EA22)	0.058

Elements: Ti, Fe, Mn, Ca, Zr, Ba

A-Rank:	Nemrut Dag (EA25)	10
B-Rank:	-	-

Specimen	*Location*	*E.D.*
EA25P1A	Nemrut Dag (EA25)	0.036
EA25P1B	Nemrut Dag (EA25)	0.039
EA25P1C	Nemrut Dag (EA25)	0.042
EA25R1	Nemrut Dag (EA25)	0.051
EA25P1D	Nemrut Dag (EA25)	0.054
EA25P3	Nemrut Dag (EA25)	0.054
EA25P2C	Nemrut Dag (EA25)	0.059
EA25P2A	Nemrut Dag (EA25)	0.062
EA25P2B	Nemrut Dag (EA25)	0.065
EA25P2D	Nemrut Dag (EA25)	0.066

Elements: Fe, Ti, Zr

A-Rank:	Nemrut Dag (EA25)	8
B-Rank:	Nemrut Dag (EA22)	2

Specimen	*Location*	*E.D.*
EA25P1B	Nemrut Dag (EA25)	0.033
EA25P1A	Nemrut Dag (EA25)	0.034
EA25P1D	Nemrut Dag (EA25)	0.038
EA25P1C	Nemrut Dag (EA25)	0.039
EA25R1	Nemrut Dag (EA25)	0.046
EA25P3	Nemrut Dag (EA25)	0.050
EA25P2C	Nemrut Dag (EA25)	0.053
EA22P6B	Nemrut Dag (EA22)	0.056
EA25P2A	Nemrut Dag (EA25)	0.056
EA22P4	Nemrut Dag (EA22)	0.057

Elements: Ti, Zr, Ba

A-Rank:	Nemrut Dag (EA22)	7
B-Rank:	Nemrut Dag (EA25)	3

Specimen	*Location*	*E.D.*
EA22P6B	Nemrut Dag (EA22)	0.032
EA22P7A	Nemrut Dag (EA22)	0.032
EA22P8B	Nemrut Dag (EA22)	0.032
EA22R1	Nemrut Dag (EA22)	0.032
EA22P2	Nemrut Dag (EA22)	0.033
EA25P1B	Nemrut Dag (EA25)	0.034
EA25P1A	Nemrut Dag (EA25)	0.035
EA22P7B	Nemrut Dag (EA22)	0.037
EA25P1D	Nemrut Dag (EA25)	0.037
818.EA22K 2	Nemrut Dag (EA22)	0.039

Elements: Ti, Fe, Zr, Ba, Zn

A-Rank:	Nemrut Dag (EA22)	6
B-Rank:	Nemrut Dag (EA25)	4

Specimen	*Location*	*E.D.*
EA25P1A	Nemrut Dag (EA25)	0.053
EA25P1B	Nemrut Dag (EA25)	0.055
EA25P1D	Nemrut Dag (EA25)	0.056
EA25P2C	Nemrut Dag (EA25)	0.063
EA22P3	Nemrut Dag (EA22)	0.065
EA22P7B	Nemrut Dag (EA22)	0.067
EA22P1C	Nemrut Dag (EA22)	0.068
EA22P7A	Nemrut Dag (EA22)	0.069
EA22P8B	Nemrut Dag (EA22)	0.071
EA22R1	Nemrut Dag (EA22)	0.072

Elements: Ti, Al, Fe, Mn, Ca, Zr, Ba

A-Rank:	Nemrut Dag (EA25)	10
B-Rank:	-	-

Specimen	*Location*	*E.D.*
EA25P1A	Nemrut Dag (EA25)	0.039
EA25P1B	Nemrut Dag (EA25)	0.039
EA25P1C	Nemrut Dag (EA25)	0.043
EA25R1	Nemrut Dag (EA25)	0.054
EA25P1D	Nemrut Dag (EA25)	0.055
EA25P3	Nemrut Dag (EA25)	0.056
EA25P2C	Nemrut Dag (EA25)	0.060
EA25P2A	Nemrut Dag (EA25)	0.062
EA25P2B	Nemrut Dag (EA25)	0.066
EA25P2D	Nemrut Dag (EA25)	0.066

Table D.1 - Source Assignments of Artifacts based on Euclidean Distance to Centroids of Geological Specimens

Artifact: A1 q264-1 f67 k13

A-Rank: **Nemrut Dag (EA25)** **79**
B-Rank: Nemrut Dag (EA22) 1

Elements: Fe, Ti, Ba

A-Rank:	Nemrut Dag (EA25)	10
B-Rank:	-	-

Specimen	*Location*	*E.D.*
EA25P2A	Nemrut Dag (EA25)	0.012
EA25R2	Nemrut Dag (EA25)	0.012
EA25P1C	Nemrut Dag (EA25)	0.014
EA25P2C	Nemrut Dag (EA25)	0.014
EA25P2D	Nemrut Dag (EA25)	0.015
EA25P2B	Nemrut Dag (EA25)	0.020
EA25P1A	Nemrut Dag (EA25)	0.022
EA25P1B	Nemrut Dag (EA25)	0.022
EA25P1D	Nemrut Dag (EA25)	0.027
EA25R1	Nemrut Dag (EA25)	0.030

Elements: Fe, Zr, Ba

A-Rank:	Nemrut Dag (EA25)	10
B-Rank:	-	-

Specimen	*Location*	*E.D.*
EA25P1C	Nemrut Dag (EA25)	0.020
EA25P1A	Nemrut Dag (EA25)	0.023
EA25P1B	Nemrut Dag (EA25)	0.024
EA25P1D	Nemrut Dag (EA25)	0.028
EA25P2C	Nemrut Dag (EA25)	0.032
EA25P2D	Nemrut Dag (EA25)	0.035
EA25P2A	Nemrut Dag (EA25)	0.037
EA25R1	Nemrut Dag (EA25)	0.039
EA25R2	Nemrut Dag (EA25)	0.043
EA25P2B	Nemrut Dag (EA25)	0.044

Elements: Ti, Fe, Zr, Ba

A-Rank:	Nemrut Dag (EA25)	10
B-Rank:	-	-

Specimen	*Location*	*E.D.*
EA25P1C	Nemrut Dag (EA25)	0.020
EA25P1A	Nemrut Dag (EA25)	0.023
EA25P1B	Nemrut Dag (EA25)	0.024
EA25P1D	Nemrut Dag (EA25)	0.028
EA25P2C	Nemrut Dag (EA25)	0.032
EA25P2D	Nemrut Dag (EA25)	0.035
EA25P2A	Nemrut Dag (EA25)	0.037
EA25R1	Nemrut Dag (EA25)	0.040
EA25P2B	Nemrut Dag (EA25)	0.044
EA25R2	Nemrut Dag (EA25)	0.044

Elements: Ti, Fe, Mn, Ca, Zr, Ba

A-Rank:	Nemrut Dag (EA25)	10
B-Rank:	-	-

Specimen	*Location*	*E.D.*
EA25P1C	Nemrut Dag (EA25)	0.022
EA25P1A	Nemrut Dag (EA25)	0.025
EA25P1B	Nemrut Dag (EA25)	0.031
EA25P2C	Nemrut Dag (EA25)	0.039
EA25P2A	Nemrut Dag (EA25)	0.043
EA25P2D	Nemrut Dag (EA25)	0.046
EA25R1	Nemrut Dag (EA25)	0.046
EA25P1D	Nemrut Dag (EA25)	0.048
EA25P2B	Nemrut Dag (EA25)	0.048
EA25P3	Nemrut Dag (EA25)	0.051

Elements: Fe, Ti, Zr

A-Rank:	Nemrut Dag (EA25)	10
B-Rank:	-	-

Specimen	*Location*	*E.D.*
EA25P1A	Nemrut Dag (EA25)	0.008
EA25P1B	Nemrut Dag (EA25)	0.010
EA25P1D	Nemrut Dag (EA25)	0.011
EA25P1C	Nemrut Dag (EA25)	0.014
EA25R1	Nemrut Dag (EA25)	0.027
EA25P2C	Nemrut Dag (EA25)	0.030
EA25P3	Nemrut Dag (EA25)	0.032
EA25P2D	Nemrut Dag (EA25)	0.033
EA25P2A	Nemrut Dag (EA25)	0.035
EA25P2B	Nemrut Dag (EA25)	0.040

Elements: Ti, Zr, Ba

A-Rank:	Nemrut Dag (EA25)	10
B-Rank:	-	-

Specimen	*Location*	*E.D.*
EA25P1C	Nemrut Dag (EA25)	0.020
EA25P1A	Nemrut Dag (EA25)	0.023
EA25P1B	Nemrut Dag (EA25)	0.024
EA25P1D	Nemrut Dag (EA25)	0.026
EA25P2C	Nemrut Dag (EA25)	0.031
EA25P2D	Nemrut Dag (EA25)	0.035
EA25P2A	Nemrut Dag (EA25)	0.037
EA25R1	Nemrut Dag (EA25)	0.040
EA25P2B	Nemrut Dag (EA25)	0.044
EA25R2	Nemrut Dag (EA25)	0.044

Elements: Ti, Fe, Zr, Ba, Zn

A-Rank:	Nemrut Dag (EA25)	9
B-Rank:	Nemrut Dag (EA22)	1

Specimen	*Location*	*E.D.*
EA25P1A	Nemrut Dag (EA25)	0.026
EA25P1B	Nemrut Dag (EA25)	0.028
EA25P1D	Nemrut Dag (EA25)	0.030
EA25P2D	Nemrut Dag (EA25)	0.047
EA25P1C	Nemrut Dag (EA25)	0.050
EA25P2B	Nemrut Dag (EA25)	0.057
EA25P2C	Nemrut Dag (EA25)	0.069
EA22P6B	Nemrut Dag (EA22)	0.080
EA25P2A	Nemrut Dag (EA25)	0.081
EA25P3	Nemrut Dag (EA25)	0.081

Elements: Ti, Al, Fe, Mn, Ca, Zr, Ba

A-Rank:	Nemrut Dag (EA25)	10
B-Rank:	-	-

Specimen	*Location*	*E.D.*
EA25P1C	Nemrut Dag (EA25)	0.022
EA25P1A	Nemrut Dag (EA25)	0.025
EA25P1B	Nemrut Dag (EA25)	0.031
EA25P2C	Nemrut Dag (EA25)	0.039
EA25P2A	Nemrut Dag (EA25)	0.043
EA25P2D	Nemrut Dag (EA25)	0.046
EA25R1	Nemrut Dag (EA25)	0.047
EA25P1D	Nemrut Dag (EA25)	0.048
EA25P2B	Nemrut Dag (EA25)	0.048
EA25P3	Nemrut Dag (EA25)	0.051

Table D.1 - Source Assignments of Artifacts based on Euclidean Distance to Centroids of Geological Specimens

Artifact: A1 q342-lw f16 k117

A-Rank: **Nemrut Dag (EA25)** **79**
B-Rank: Nemrut Dag (EA22) 1

Elements: Fe, Ti, Ba

A-Rank:	Nemrut Dag (EA25)	10
B-Rank:	-	-

Specimen	*Location*	*E.D.*
EA25R1	Nemrut Dag (EA25)	0.011
EA25P1A	Nemrut Dag (EA25)	0.013
EA25P3	Nemrut Dag (EA25)	0.013
EA25P1B	Nemrut Dag (EA25)	0.015
EA25P1D	Nemrut Dag (EA25)	0.017
EA25P2B	Nemrut Dag (EA25)	0.019
EA25P1C	Nemrut Dag (EA25)	0.021
EA25P2A	Nemrut Dag (EA25)	0.022
EA25P2D	Nemrut Dag (EA25)	0.024
EA25P2C	Nemrut Dag (EA25)	0.026

Elements: Fe, Zr, Ba

A-Rank:	Nemrut Dag (EA25)	10
B-Rank:	-	-

Specimen	*Location*	*E.D.*
EA25P1A	Nemrut Dag (EA25)	0.014
EA25P1B	Nemrut Dag (EA25)	0.015
EA25P1D	Nemrut Dag (EA25)	0.017
EA25P1C	Nemrut Dag (EA25)	0.024
EA25R1	Nemrut Dag (EA25)	0.025
EA25P3	Nemrut Dag (EA25)	0.030
EA25P2C	Nemrut Dag (EA25)	0.037
EA25P2D	Nemrut Dag (EA25)	0.038
EA25P2A	Nemrut Dag (EA25)	0.039
EA25P2B	Nemrut Dag (EA25)	0.041

Elements: Ti, Fe, Zr, Ba

A-Rank:	Nemrut Dag (EA25)	10
B-Rank:	-	-

Specimen	*Location*	*E.D.*
EA25P1A	Nemrut Dag (EA25)	0.014
EA25P1B	Nemrut Dag (EA25)	0.016
EA25P1D	Nemrut Dag (EA25)	0.017
EA25P1C	Nemrut Dag (EA25)	0.024
EA25R1	Nemrut Dag (EA25)	0.026
EA25P3	Nemrut Dag (EA25)	0.032
EA25P2C	Nemrut Dag (EA25)	0.037
EA25P2D	Nemrut Dag (EA25)	0.038
EA25P2A	Nemrut Dag (EA25)	0.039
EA25P2B	Nemrut Dag (EA25)	0.041

Elements: Ti, Fe, Mn, Ca, Zr, Ba

A-Rank:	Nemrut Dag (EA25)	10
B-Rank:	-	-

Specimen	*Location*	*E.D.*
EA25P1A	Nemrut Dag (EA25)	0.016
EA25P1B	Nemrut Dag (EA25)	0.018
EA25R1	Nemrut Dag (EA25)	0.028
EA25P1D	Nemrut Dag (EA25)	0.031
EA25P1C	Nemrut Dag (EA25)	0.032
EA25P3	Nemrut Dag (EA25)	0.032
EA25P2C	Nemrut Dag (EA25)	0.038
EA25P2A	Nemrut Dag (EA25)	0.040
EA25P2B	Nemrut Dag (EA25)	0.042
EA25P2D	Nemrut Dag (EA25)	0.042

Elements: Fe, Ti, Zr

A-Rank:	Nemrut Dag (EA25)	10
B-Rank:	-	-

Specimen	*Location*	*E.D.*
EA25P1A	Nemrut Dag (EA25)	0.009
EA25P1B	Nemrut Dag (EA25)	0.012
EA25P1C	Nemrut Dag (EA25)	0.015
EA25P1D	Nemrut Dag (EA25)	0.016
EA25R1	Nemrut Dag (EA25)	0.026
EA25P2C	Nemrut Dag (EA25)	0.030
EA25P3	Nemrut Dag (EA25)	0.031
EA25P2D	Nemrut Dag (EA25)	0.032
EA25P2A	Nemrut Dag (EA25)	0.033
EA25P2B	Nemrut Dag (EA25)	0.039

Elements: Ti, Zr, Ba

A-Rank:	Nemrut Dag (EA25)	10
B-Rank:	-	-

Specimen	*Location*	*E.D.*
EA25P1D	Nemrut Dag (EA25)	0.008
EA25P1A	Nemrut Dag (EA25)	0.013
EA25P1B	Nemrut Dag (EA25)	0.014
EA25P1C	Nemrut Dag (EA25)	0.022
EA25R1	Nemrut Dag (EA25)	0.025
EA25P3	Nemrut Dag (EA25)	0.030
EA25P2C	Nemrut Dag (EA25)	0.034
EA25P2D	Nemrut Dag (EA25)	0.036
EA25P2A	Nemrut Dag (EA25)	0.039
EA25P2B	Nemrut Dag (EA25)	0.039

Elements: Ti, Fe, Zr, Ba, Zn

A-Rank:	Nemrut Dag (EA25)	9
B-Rank:	Nemrut Dag (EA22)	1

Specimen	*Location*	*E.D.*
EA25P1A	Nemrut Dag (EA25)	0.015
EA25P1B	Nemrut Dag (EA25)	0.018
EA25P1D	Nemrut Dag (EA25)	0.018
EA25P2D	Nemrut Dag (EA25)	0.045
EA25P1C	Nemrut Dag (EA25)	0.047
EA25P2B	Nemrut Dag (EA25)	0.050
EA25P3	Nemrut Dag (EA25)	0.067
EA25P2A	Nemrut Dag (EA25)	0.076
EA25P2C	Nemrut Dag (EA25)	0.077
EA22P6B	Nemrut Dag (EA22)	0.084

Elements: Ti, Al, Fe, Mn, Ca, Zr, Ba

A-Rank:	Nemrut Dag (EA25)	10
B-Rank:	-	-

Specimen	*Location*	*E.D.*
EA25P1A	Nemrut Dag (EA25)	0.016
EA25P1B	Nemrut Dag (EA25)	0.019
EA25R1	Nemrut Dag (EA25)	0.028
EA25P1D	Nemrut Dag (EA25)	0.032
EA25P3	Nemrut Dag (EA25)	0.032
EA25P1C	Nemrut Dag (EA25)	0.033
EA25P2C	Nemrut Dag (EA25)	0.039
EA25P2A	Nemrut Dag (EA25)	0.041
EA25P2B	Nemrut Dag (EA25)	0.042
EA25P2D	Nemrut Dag (EA25)	0.042

Table D.1 - Source Assignments of Artifacts based on Euclidean Distance to Centroids of Geological Specimens

Artifact: A1 q59-1 f29 k119

A-Rank: **Nemrut Dag (EA25)** **74**
B-Rank: Nemrut Dag (EA22) 6

Elements: Fe, Ti, Ba

A-Rank:	Nemrut Dag (EA25)	10
B-Rank:	-	-

Specimen	*Location*	*E.D.*
EA25P3	Nemrut Dag (EA25)	0.010
EA25R1	Nemrut Dag (EA25)	0.015
EA25P1D	Nemrut Dag (EA25)	0.017
EA25P1B	Nemrut Dag (EA25)	0.020
EA25P1A	Nemrut Dag (EA25)	0.021
EA25P2B	Nemrut Dag (EA25)	0.023
EA25P1C	Nemrut Dag (EA25)	0.028
EA25P2D	Nemrut Dag (EA25)	0.029
EA25P2A	Nemrut Dag (EA25)	0.031
EA25P2C	Nemrut Dag (EA25)	0.031

Elements: Fe, Zr, Ba

A-Rank:	Nemrut Dag (EA25)	10
B-Rank:	-	-

Specimen	*Location*	*E.D.*
EA25P1D	Nemrut Dag (EA25)	0.018
EA25R1	Nemrut Dag (EA25)	0.018
EA25P3	Nemrut Dag (EA25)	0.019
EA25P1B	Nemrut Dag (EA25)	0.021
EA25P1A	Nemrut Dag (EA25)	0.022
EA25P1C	Nemrut Dag (EA25)	0.028
EA25P2B	Nemrut Dag (EA25)	0.034
EA25P2C	Nemrut Dag (EA25)	0.034
EA25P2D	Nemrut Dag (EA25)	0.034
EA25P2A	Nemrut Dag (EA25)	0.038

Elements: Ti, Fe, Zr, Ba

A-Rank:	Nemrut Dag (EA25)	10
B-Rank:	-	-

Specimen	*Location*	*E.D.*
EA25P1D	Nemrut Dag (EA25)	0.019
EA25R1	Nemrut Dag (EA25)	0.019
EA25P3	Nemrut Dag (EA25)	0.020
EA25P1B	Nemrut Dag (EA25)	0.021
EA25P1A	Nemrut Dag (EA25)	0.022
EA25P1C	Nemrut Dag (EA25)	0.028
EA25P2B	Nemrut Dag (EA25)	0.034
EA25P2C	Nemrut Dag (EA25)	0.034
EA25P2D	Nemrut Dag (EA25)	0.035
EA25P2A	Nemrut Dag (EA25)	0.038

Elements: Ti, Fe, Mn, Ca, Zr, Ba

A-Rank:	Nemrut Dag (EA25)	10
B-Rank:	-	-

Specimen	*Location*	*E.D.*
EA25P1C	Nemrut Dag (EA25)	0.030
EA25P1A	Nemrut Dag (EA25)	0.036
EA25P1B	Nemrut Dag (EA25)	0.045
EA25P3	Nemrut Dag (EA25)	0.045
EA25R1	Nemrut Dag (EA25)	0.048
EA25P2B	Nemrut Dag (EA25)	0.052
EA25P2C	Nemrut Dag (EA25)	0.055
EA25P2A	Nemrut Dag (EA25)	0.057
EA25P2D	Nemrut Dag (EA25)	0.061
EA25P1D	Nemrut Dag (EA25)	0.063

Elements: Fe, Ti, Zr

A-Rank:	Nemrut Dag (EA25)	10
B-Rank:	-	-

Specimen	*Location*	*E.D.*
EA25P1C	Nemrut Dag (EA25)	0.002
EA25P1B	Nemrut Dag (EA25)	0.007
EA25P1A	Nemrut Dag (EA25)	0.009
EA25P1D	Nemrut Dag (EA25)	0.009
EA25P2C	Nemrut Dag (EA25)	0.015
EA25R1	Nemrut Dag (EA25)	0.015
EA25P2D	Nemrut Dag (EA25)	0.019
EA25P3	Nemrut Dag (EA25)	0.019
EA25P2A	Nemrut Dag (EA25)	0.023
EA25P2B	Nemrut Dag (EA25)	0.025

Elements: Ti, Zr, Ba

A-Rank:	Nemrut Dag (EA25)	10
B-Rank:	-	-

Specimen	*Location*	*E.D.*
EA25P1D	Nemrut Dag (EA25)	0.018
EA25R1	Nemrut Dag (EA25)	0.018
EA25P3	Nemrut Dag (EA25)	0.020
EA25P1A	Nemrut Dag (EA25)	0.021
EA25P1B	Nemrut Dag (EA25)	0.021
EA25P1C	Nemrut Dag (EA25)	0.027
EA25P2B	Nemrut Dag (EA25)	0.034
EA25P2C	Nemrut Dag (EA25)	0.034
EA25P2D	Nemrut Dag (EA25)	0.034
EA25P2A	Nemrut Dag (EA25)	0.037

Elements: Ti, Fe, Zr, Ba, Zn

A-Rank:	Nemrut Dag (EA22)	6
B-Rank:	Nemrut Dag (EA25)	4

Specimen	*Location*	*E.D.*
EA25P2C	Nemrut Dag (EA25)	0.052
EA22P7A	Nemrut Dag (EA22)	0.093
EA22P1D	Nemrut Dag (EA22)	0.095
EA22R1	Nemrut Dag (EA22)	0.096
EA22P5B	Nemrut Dag (EA22)	0.102
EA22P3	Nemrut Dag (EA22)	0.113
EA25P1D	Nemrut Dag (EA25)	0.113
EA25P1A	Nemrut Dag (EA25)	0.114
EA25P1B	Nemrut Dag (EA25)	0.117
EA22P1C	Nemrut Dag (EA22)	0.119

Elements: Ti, Al, Fe, Mn, Ca, Zr, Ba

A-Rank:	Nemrut Dag (EA25)	10
B-Rank:	-	-

Specimen	*Location*	*E.D.*
EA25P1C	Nemrut Dag (EA25)	0.031
EA25P1A	Nemrut Dag (EA25)	0.037
EA25P1B	Nemrut Dag (EA25)	0.045
EA25P3	Nemrut Dag (EA25)	0.046
EA25R1	Nemrut Dag (EA25)	0.049
EA25P2B	Nemrut Dag (EA25)	0.052
EA25P2C	Nemrut Dag (EA25)	0.055
EA25P2A	Nemrut Dag (EA25)	0.057
EA25P2D	Nemrut Dag (EA25)	0.061
EA25P1D	Nemrut Dag (EA25)	0.063

Table D.1 - Source Assignments of Artifacts based on Euclidean Distance to Centroids of Geological Specimens

Artifact: A10 q1081-6 f234 k21

A-Rank: **Nemrut Dag (EA25)** **46**
B-Rank: Nemrut Dag (EA22) 29

Elements: Fe, Ti, Ba

A-Rank:	Nemrut Dag (EA25)	10
B-Rank:	-	-

Specimen	*Location*	*E.D.*
EA25R2	Nemrut Dag (EA25)	0.033
EA25P2A	Nemrut Dag (EA25)	0.036
EA25P2C	Nemrut Dag (EA25)	0.039
EA25P1C	Nemrut Dag (EA25)	0.040
EA25P2D	Nemrut Dag (EA25)	0.040
EA25P2B	Nemrut Dag (EA25)	0.046
EA25P1A	Nemrut Dag (EA25)	0.047
EA25P1B	Nemrut Dag (EA25)	0.048
EA25P1D	Nemrut Dag (EA25)	0.053
EA25R1	Nemrut Dag (EA25)	0.055

Elements: Fe, Zr, Ba

A-Rank:	Nemrut Dag (EA22)	8
B-Rank:	Nemrut Dag (EA21)	2

Specimen	*Location*	*E.D.*
EA21P1	Nemrut Dag (EA21)	0.078
EA22P5A	Nemrut Dag (EA22)	0.079
EA22P7A	Nemrut Dag (EA22)	0.081
EA22P4	Nemrut Dag (EA22)	0.086
EA22P6A	Nemrut Dag (EA22)	0.086
EA22P5B	Nemrut Dag (EA22)	0.088
EA22P6B	Nemrut Dag (EA22)	0.088
EA21R1B	Nemrut Dag (EA21)	0.089
EA22P3	Nemrut Dag (EA22)	0.089
EA22P7B	Nemrut Dag (EA22)	0.089

Elements: Ti, Fe, Zr, Ba

A-Rank:	Nemrut Dag (EA25)	5
B-Rank:	Nemrut Dag (EA22)	4

Specimen	*Location*	*E.D.*
EA25P1A	Nemrut Dag (EA25)	0.089
EA25P1B	Nemrut Dag (EA25)	0.090
EA25P1C	Nemrut Dag (EA25)	0.090
EA25P1D	Nemrut Dag (EA25)	0.090
EA22P7A	Nemrut Dag (EA22)	0.096
EA25P2C	Nemrut Dag (EA25)	0.103
EA22P5A	Nemrut Dag (EA22)	0.105
EA22P6B	Nemrut Dag (EA22)	0.105
EA21P1	Nemrut Dag (EA21)	0.106
EA22P8B	Nemrut Dag (EA22)	0.107

Elements: Ti, Fe, Mn, Ca, Zr, Ba

A-Rank:	Nemrut Dag (EA25)	10
B-Rank:	-	-

Specimen	*Location*	*E.D.*
EA25P1A	Nemrut Dag (EA25)	0.090
EA25P1B	Nemrut Dag (EA25)	0.092
EA25P1C	Nemrut Dag (EA25)	0.093
EA25P1D	Nemrut Dag (EA25)	0.098
EA25P2C	Nemrut Dag (EA25)	0.106
EA25P2A	Nemrut Dag (EA25)	0.111
EA25P2D	Nemrut Dag (EA25)	0.111
EA25R1	Nemrut Dag (EA25)	0.111
EA25P3	Nemrut Dag (EA25)	0.117
EA25P2B	Nemrut Dag (EA25)	0.118

Elements: Fe, Ti, Zr

A-Rank:	Nemrut Dag (EA22)	5
B-Rank:	Nemrut Dag (EA25)	4

Specimen	*Location*	*E.D.*
EA25P1A	Nemrut Dag (EA25)	0.099
EA25P1D	Nemrut Dag (EA25)	0.099
EA25P1B	Nemrut Dag (EA25)	0.100
EA22P7A	Nemrut Dag (EA22)	0.103
EA25P1C	Nemrut Dag (EA25)	0.106
EA22P5A	Nemrut Dag (EA22)	0.108
EA22P8B	Nemrut Dag (EA22)	0.110
EA21R1B	Nemrut Dag (EA21)	0.112
EA22P4	Nemrut Dag (EA22)	0.112
EA22P6B	Nemrut Dag (EA22)	0.112

Elements: Ti, Zr, Ba

A-Rank:	Nemrut Dag (EA22)	5
B-Rank:	Nemrut Dag (EA25)	4

Specimen	*Location*	*E.D.*
EA22P7A	Nemrut Dag (EA22)	0.078
EA22R1	Nemrut Dag (EA22)	0.087
EA21P1	Nemrut Dag (EA21)	0.089
EA25P1A	Nemrut Dag (EA25)	0.089
EA25P1B	Nemrut Dag (EA25)	0.089
EA25P1D	Nemrut Dag (EA25)	0.089
EA25P1C	Nemrut Dag (EA25)	0.090
EA22P5A	Nemrut Dag (EA22)	0.091
EA22P6B	Nemrut Dag (EA22)	0.091
EA22P7B	Nemrut Dag (EA22)	0.091

Elements: Ti, Fe, Zr, Ba, Zn

A-Rank:	Nemrut Dag (EA22)	7
B-Rank:	Nemrut Dag (EA25)	3

Specimen	*Location*	*E.D.*
EA22P7A	Nemrut Dag (EA22)	0.125
EA25P2C	Nemrut Dag (EA25)	0.132
EA22R1	Nemrut Dag (EA22)	0.137
EA22P5B	Nemrut Dag (EA22)	0.140
EA22P1D	Nemrut Dag (EA22)	0.151
EA22P3	Nemrut Dag (EA22)	0.157
EA22P1C	Nemrut Dag (EA22)	0.168
EA22P7B	Nemrut Dag (EA22)	0.171
EA25P1A	Nemrut Dag (EA25)	0.177
EA25P1D	Nemrut Dag (EA25)	0.178

Elements: Ti, Al, Fe, Mn, Ca, Zr, Ba

A-Rank:	Nemrut Dag (EA25)	10
B-Rank:	-	-

Specimen	*Location*	*E.D.*
EA25P1A	Nemrut Dag (EA25)	0.092
EA25P1B	Nemrut Dag (EA25)	0.095
EA25P1C	Nemrut Dag (EA25)	0.095
EA25P1D	Nemrut Dag (EA25)	0.101
EA25P2C	Nemrut Dag (EA25)	0.109
EA25R1	Nemrut Dag (EA25)	0.111
EA25P2D	Nemrut Dag (EA25)	0.113
EA25P2A	Nemrut Dag (EA25)	0.114
EA25P3	Nemrut Dag (EA25)	0.118
EA25R2	Nemrut Dag (EA25)	0.119

Table D.1 - Source Assignments of Artifacts based on Euclidean Distance to Centroids of Geological Specimens

Artifact: A10 q1194.3 f925 k29

A-Rank: **Bingol B** **57**
B-Rank: Gutansar 11

Elements: Fe, Ti, Ba

A-Rank: Bingol B 7
B-Rank: Gutansar 2

Specimen	*Location*	*E.D.*
EA52B1	Bingol B	0.019
EA52B3	Bingol B	0.020
EA52B2	Bingol B	0.021
EA56B1	Bingol B	0.032
EA53B2	Bingol B	0.036
EA53B1	Bingol B	0.045
EA54B1	Bingol B	0.053
AR06E2A	Gutansar	0.095
AR06E1A	Gutansar	0.097
AR21avH1	Chazencavan	0.097

Elements: Fe, Zr, Ba

A-Rank: Bingol B 7
B-Rank: Erzincan 3

Specimen	*Location*	*E.D.*
EA52B3	Bingol B	0.022
EA52B2	Bingol B	0.025
EA52B1	Bingol B	0.032
EA56B1	Bingol B	0.039
EA53B2	Bingol B	0.041
EA53B1	Bingol B	0.056
EA54B1	Bingol B	0.061
EA43R2	Erzincan	0.085
EA44P3	Erzincan	0.086
EA44P2	Erzincan	0.087

Elements: Ti, Fe, Zr, Ba

A-Rank: Bingol B 7
B-Rank: Gutansar 3

Specimen	*Location*	*E.D.*
EA52B3	Bingol B	0.029
EA52B2	Bingol B	0.030
EA52B1	Bingol B	0.034
EA53B2	Bingol B	0.044
EA56B1	Bingol B	0.044
EA53B1	Bingol B	0.058
EA54B1	Bingol B	0.062
AR06E3A	Gutansar	0.140
AR30jfL1	Gutansar	0.140
AR06E2A	Gutansar	0.141

Elements: Ti, Fe, Mn, Ca, Zr, Ba

A-Rank: Bingol B 7
B-Rank: Acigol 3

Specimen	*Location*	*E.D.*
EA52B2	Bingol B	0.031
EA52B1	Bingol B	0.044
EA53B2	Bingol B	0.048
EA52B3	Bingol B	0.050
EA56B1	Bingol B	0.060
EA53B1	Bingol B	0.068
EA54B1	Bingol B	0.111
CA08R1A	Acigol	0.163
CA08R1C	Acigol	0.169
CA07R2A	Acigol	0.174

Elements: Fe, Ti, Zr

A-Rank: Bingol B 7
B-Rank: Gutansar 2

Specimen	*Location*	*E.D.*
EA52B3	Bingol B	0.028
EA52B2	Bingol B	0.029
EA53B2	Bingol B	0.031
EA52B1	Bingol B	0.033
EA53B1	Bingol B	0.041
EA56B1	Bingol B	0.043
EA54B1	Bingol B	0.061
EA66W1	Lake Van	0.117
AR76rB3	Gutansar	0.126
AR06E3A	Gutansar	0.131

Elements: Ti, Zr, Ba

A-Rank: Bingol B 9
B-Rank: Erevan 1

Specimen	*Location*	*E.D.*
EA52B2	Bingol B	0.027
EA52B3	Bingol B	0.028
EA52B1	Bingol B	0.031
EA54B1	Bingol B	0.032
EA55B2	Bingol B	0.036
EA56B1	Bingol B	0.038
EA53B2	Bingol B	0.043
EA55B1	Bingol B	0.047
EA53B1	Bingol B	0.057
AR24jfL1	Erevan	0.109

Elements: Ti, Fe, Zr, Ba, Zn

A-Rank: Bingol B 6
B-Rank: Gutansar 4

Specimen	*Location*	*E.D.*
EA53B1	Bingol B	0.126
EA52B1	Bingol B	0.169
EA52B3	Bingol B	0.182
AR06E2B	Gutansar	0.185
EA54B1	Bingol B	0.194
AR11jB1	Gutansar	0.196
EA52B2	Bingol B	0.198
AR06E1B	Gutansar	0.213
AR12jB1	Gutansar	0.213
EA56B1	Bingol B	0.213

Elements: Ti, Al, Fe, Mn, Ca, Zr, Ba

A-Rank: Bingol B 7
B-Rank: Acigol 3

Specimen	*Location*	*E.D.*
EA52B2	Bingol B	0.049
EA53B2	Bingol B	0.051
EA52B1	Bingol B	0.059
EA52B3	Bingol B	0.064
EA56B1	Bingol B	0.068
EA53B1	Bingol B	0.070
EA54B1	Bingol B	0.115
CA08R1A	Acigol	0.166
CA08R1C	Acigol	0.171
CA07R2A	Acigol	0.175

Table D.1 - Source Assignments of Artifacts based on Euclidean Distance to Centroids of Geological Specimens

Artifact: A10 q229-1 f94 k5

A-Rank: **Tendurek Dag** **69**
B-Rank: Kars-Arpacay 4

Elements: Fe, Ti, Ba

A-Rank:	Tendurek Dag	10
B-Rank:	-	-

Specimen	*Location*	*E.D.*
EA09P2	Tendurek Dag	0.005
EA30R3D	Tendurek Dag	0.006
EA32R2	Tendurek Dag	0.006
EA09R2E	Tendurek Dag	0.007
EA09R2B	Tendurek Dag	0.011
EA09R3D	Tendurek Dag	0.011
EA09R3B	Tendurek Dag	0.012
EA09R3E	Tendurek Dag	0.012
EA30R3B	Tendurek Dag	0.012
EA09P1A	Tendurek Dag	0.013

Elements: Fe, Zr, Ba

A-Rank:	Tendurek Dag	10
B-Rank:	-	-

Specimen	*Location*	*E.D.*
EA09R3D	Tendurek Dag	0.015
EA09R2A	Tendurek Dag	0.017
EA30R2B	Tendurek Dag	0.018
EA30P1	Tendurek Dag	0.019
EA30R2A	Tendurek Dag	0.020
EA09R2C	Tendurek Dag	0.021
EA09R3B	Tendurek Dag	0.021
EA09R2E	Tendurek Dag	0.022
EA31R1	Tendurek Dag	0.022
EA09R2B	Tendurek Dag	0.023

Elements: Ti, Fe, Zr, Ba

A-Rank:	Tendurek Dag	10
B-Rank:	-	-

Specimen	*Location*	*E.D.*
EA09R3D	Tendurek Dag	0.018
EA09R2A	Tendurek Dag	0.019
EA09R2E	Tendurek Dag	0.023
EA09R3B	Tendurek Dag	0.023
EA30R2A	Tendurek Dag	0.023
EA31R1	Tendurek Dag	0.023
EA09R2B	Tendurek Dag	0.024
EA09P2	Tendurek Dag	0.025
EA30P1	Tendurek Dag	0.025
EA30R2B	Tendurek Dag	0.025

Elements: Ti, Fe, Mn, Ca, Zr, Ba

A-Rank:	Tendurek Dag	10
B-Rank:	-	-

Specimen	*Location*	*E.D.*
EA09R3D	Tendurek Dag	0.018
EA09R2B	Tendurek Dag	0.024
EA09R2A	Tendurek Dag	0.029
EA09P1C	Tendurek Dag	0.031
EA30R3C	Tendurek Dag	0.031
EA31R1	Tendurek Dag	0.031
EA09R3C	Tendurek Dag	0.033
EA30R1	Tendurek Dag	0.034
EA30P1	Tendurek Dag	0.035
EA30R2A	Tendurek Dag	0.035

Elements: Fe, Ti, Zr

A-Rank:	Tendurek Dag	10
B-Rank:	-	-

Specimen	*Location*	*E.D.*
EA09P1C	Tendurek Dag	0.014
EA09R3D	Tendurek Dag	0.017
EA09R2A	Tendurek Dag	0.018
EA31R1	Tendurek Dag	0.020
EA09R3B	Tendurek Dag	0.021
EA30R1	Tendurek Dag	0.021
EA09R1	Tendurek Dag	0.022
EA09R2B	Tendurek Dag	0.023
EA09R2E	Tendurek Dag	0.023
EA30P1	Tendurek Dag	0.023

Elements: Ti, Zr, Ba

A-Rank:	Kars-Arpacay	4
B-Rank:	Tendurek Dag	2

Specimen	*Location*	*E.D.*
EA39P4	Kars-Arpacay	0.009
EA39P3	Kars-Arpacay	0.011
EA39R1	Kars-Arpacay	0.014
EA50R1A	Bingol	0.015
EA07R3	Meydan Dag	0.016
EA39P1A	Kars-Arpacay	0.016
EA09R3D	Tendurek Dag	0.017
EA09R2A	Tendurek Dag	0.019
EA10R1B	Meydan Dag	0.019
EA50P6	Bingol	0.019

Elements: Ti, Fe, Zr, Ba, Zn

A-Rank:	Tendurek Dag	7
B-Rank:	Meydan Dag	2

Specimen	*Location*	*E.D.*
EA09R2A	Tendurek Dag	0.022
EA09R3E	Tendurek Dag	0.027
EA30R1	Tendurek Dag	0.034
EA09P1B	Tendurek Dag	0.037
EA34P4	Pasinler	0.037
EA09R2D	Tendurek Dag	0.041
EA09R3A	Tendurek Dag	0.045
EA10P3	Meydan Dag	0.045
EA68SX2	Meydan Dag	0.051
EA09R3C	Tendurek Dag	0.052

Elements: Ti, Al, Fe, Mn, Ca, Zr, Ba

A-Rank:	Tendurek Dag	10
B-Rank:	-	-

Specimen	*Location*	*E.D.*
EA09R3D	Tendurek Dag	0.019
EA09R2B	Tendurek Dag	0.024
EA09R2A	Tendurek Dag	0.030
EA09P1C	Tendurek Dag	0.031
EA30R3C	Tendurek Dag	0.031
EA31R1	Tendurek Dag	0.032
EA09R3C	Tendurek Dag	0.033
EA30R1	Tendurek Dag	0.034
EA30R2A	Tendurek Dag	0.035
EA30R3A	Tendurek Dag	0.035

Table D.1 - Source Assignments of Artifacts based on Euclidean Distance to Centroids of Geological Specimens

Artifact: A10 q286-1 f141 k3

A-Rank: **Bingol B** **54**
B-Rank: Gutansar 12

Elements: Fe, Ti, Ba

A-Rank: Bingol B 7
B-Rank: Gutansar 2

Specimen	*Location*	*E.D.*
EA52B1	Bingol B	0.005
EA52B3	Bingol B	0.015
EA52B2	Bingol B	0.030
EA56B1	Bingol B	0.031
EA53B2	Bingol B	0.042
EA53B1	Bingol B	0.048
EA54B1	Bingol B	0.070
AR06E2A	Gutansar	0.110
AR21avH1	Chazencavan	0.111
AR06E1A	Gutansar	0.113

Elements: Fe, Zr, Ba

A-Rank: Bingol B 5
B-Rank: Erzincan 5

Specimen	*Location*	*E.D.*
EA52B3	Bingol B	0.050
EA52B1	Bingol B	0.057
EA52B2	Bingol B	0.057
EA56B1	Bingol B	0.060
EA43P1	Erzincan	0.061
EA44P2	Erzincan	0.061
EA44P3	Erzincan	0.061
EA43R2	Erzincan	0.062
EA53B2	Bingol B	0.063
EA44R1	Erzincan	0.064

Elements: Ti, Fe, Zr, Ba

A-Rank: Bingol B 7
B-Rank: Gutansar 3

Specimen	*Location*	*E.D.*
EA52B3	Bingol B	0.051
EA52B1	Bingol B	0.057
EA52B2	Bingol B	0.058
EA56B1	Bingol B	0.067
EA53B2	Bingol B	0.068
EA53B1	Bingol B	0.081
EA54B1	Bingol B	0.092
AR30jfL1	Gutansar	0.133
AR06E2A	Gutansar	0.134
AR06E2B	Gutansar	0.135

Elements: Ti, Fe, Mn, Ca, Zr, Ba

A-Rank: Bingol B 7
B-Rank: Acigol 3

Specimen	*Location*	*E.D.*
EA52B3	Bingol B	0.051
EA52B1	Bingol B	0.058
EA52B2	Bingol B	0.064
EA56B1	Bingol B	0.067
EA53B2	Bingol B	0.070
EA53B1	Bingol B	0.081
EA54B1	Bingol B	0.108
CA08R1A	Acigol	0.166
CA08R1C	Acigol	0.166
CA07R2A	Acigol	0.177

Elements: Fe, Ti, Zr

A-Rank: Bingol B 7
B-Rank: Gutansar 2

Specimen	*Location*	*E.D.*
EA52B3	Bingol B	0.051
EA52B1	Bingol B	0.057
EA52B2	Bingol B	0.058
EA53B2	Bingol B	0.064
EA56B1	Bingol B	0.067
EA53B1	Bingol B	0.075
EA54B1	Bingol B	0.092
AR76rB3	Gutansar	0.117
AR06E1C	Gutansar	0.120
AR40rlS1	Erevan	0.120

Elements: Ti, Zr, Ba

A-Rank: Bingol B 9
B-Rank: Erevan 1

Specimen	*Location*	*E.D.*
EA52B2	Bingol B	0.050
EA52B3	Bingol B	0.050
EA52B1	Bingol B	0.057
EA54B1	Bingol B	0.061
EA53B2	Bingol B	0.063
EA55B2	Bingol B	0.065
EA56B1	Bingol B	0.067
EA53B1	Bingol B	0.076
EA55B1	Bingol B	0.078
AR24jfL1	Erevan	0.085

Elements: Ti, Fe, Zr, Ba, Zn

A-Rank: Bingol B 5
B-Rank: Gutansar 5

Specimen	*Location*	*E.D.*
EA53B1	Bingol B	0.115
EA52B1	Bingol B	0.148
EA52B3	Bingol B	0.159
AR06E2B	Gutansar	0.163
AR11jB1	Gutansar	0.173
EA52B2	Bingol B	0.177
EA54B1	Bingol B	0.180
AR12jB1	Gutansar	0.188
AR06E1B	Gutansar	0.189
AR06E1C	Gutansar	0.190

Elements: Ti, Al, Fe, Mn, Ca, Zr, Ba

A-Rank: Bingol B 7
B-Rank: Acigol 3

Specimen	*Location*	*E.D.*
EA52B3	Bingol B	0.065
EA52B1	Bingol B	0.070
EA53B2	Bingol B	0.073
EA52B2	Bingol B	0.075
EA56B1	Bingol B	0.075
EA53B1	Bingol B	0.083
EA54B1	Bingol B	0.113
CA08R1A	Acigol	0.168
CA08R1C	Acigol	0.168
CA07R2A	Acigol	0.177

Table D.1 - Source Assignments of Artifacts based on Euclidean Distance to Centroids of Geological Specimens

Artifact: A10 q541-s1 f245 k26/24

A-Rank: n.a. - glass*
B-Rank:

Elements: Fe, Ti, Ba

A-Rank: n.a. - glass*
B-Rank:

Specimen	*Location*	*E.D.*
EA28P2C	Nemrut Dag	0.420
EA29R1B	Nemrut Dag	0.426
EA20R1	Nemrut Dag	0.428
EA20P1	Nemrut Dag	0.430
EA28P2A	Nemrut Dag	0.430
EA29R1A	Nemrut Dag	0.430
EA28P2B	Nemrut Dag	0.432
EA28P3A	Nemrut Dag	0.434
EA28P4A	Nemrut Dag	0.435
EA28P5B	Nemrut Dag	0.437

Elements: Fe, Zr, Ba

A-Rank: n.a. - glass*
B-Rank:

Specimen	*Location*	*E.D.*
EA56B1	Bingol	0.643
EA43P2B	Erzincan	0.647
EA43P1	Erzincan	0.649
EA43P3	Erzincan	0.649
EA43P2A	Erzincan	0.650
EA44P3	Erzincan	0.650
EA44P2	Erzincan	0.651
EA43R2	Erzincan	0.652
EA44P1	Erzincan	0.652
EA52B1	Bingol	0.652

Elements: Ti, Fe, Zr, Ba

A-Rank: n.a. - glass*
B-Rank:

Specimen	*Location*	*E.D.*
EA56B1	Bingol	0.906
AR17jB1	Sizevit Yeni-el	0.921
EA53B2	Bingol	0.929
AR16jB1	Sizevit Yeni-el	0.932
EA53B1	Bingol	0.932
EA52B1	Bingol	0.933
AR66rB2	Aghvorik	0.941
EA28P5A	Nemrut Dag	0.941
EA28P4A	Nemrut Dag	0.942
EA28P5B	Nemrut Dag	0.943

Elements: Ti, Fe, Mn, Ca, Zr, Ba

A-Rank: n.a. - glass*
B-Rank:

Specimen	*Location*	*E.D.*
AR17jB1	Sizevit Yeni-el	1.354
AR16jB1	Sizevit Yeni-el	1.361
AR66rB2	Aghvorik	1.364
EA28P4A	Nemrut Dag	1.393
EA28P5A	Nemrut Dag	1.397
AR66rB1	Aghvorik	1.402
EA28P4B	Nemrut Dag	1.402
EA28P5B	Nemrut Dag	1.402
EA56B1	Bingol	1.402
AR22avH1	Varik/Dar-Alages	1.406

Elements: Fe, Ti, Zr

A-Rank: n.a. - glass*
B-Rank:

Specimen	*Location*	*E.D.*
AR17jB1	Sizevit Yeni-el	0.786
AR66rB2	Aghvorik	0.788
AR16jB1	Sizevit Yeni-el	0.791
AR62sK1	Sizevit Yeni-el	0.842
AR66rB1	Aghvorik	0.843
AR63kM1	Aghvorik	0.847
EA56B1	Bingol	0.903
EA28P5A	Nemrut Dag	0.905
EA28P5B	Nemrut Dag	0.907
EA28P4A	Nemrut Dag	0.908

Elements: Ti, Zr, Ba

A-Rank: n.a. - glass*
B-Rank:

Specimen	*Location*	*E.D.*
EA55B1	Bingol	0.659
EA55B2	Bingol	0.662
EA56B1	Bingol	0.662
EA53B2	Bingol	0.663
EA53B1	Bingol	0.666
AR17jB1	Sizevit Yeni-el	0.668
AR16jB1	Sizevit Yeni-el	0.680
EA36P1D	Kars-Digor	0.686
EA36P3	Kars-Digor	0.687
EA54B1	Bingol	0.687

Elements: Ti, Fe, Zr, Ba, Zn

A-Rank: n.a. - glass*
B-Rank:

Specimen	*Location*	*E.D.*
EA56B1	Bingol	0.915
AR17jB1	Sizevit Yeni-el	0.931
EA53B2	Bingol	0.934
AR66rB2	Aghvorik	0.943
AR16jB1	Sizevit Yeni-el	0.947
EA52B1	Bingol	0.949
EA52B3	Bingol	0.957
EA53B1	Bingol	0.959
EA52B2	Bingol	0.964
EA54B1	Bingol	0.989

Elements: Ti, Al, Fe, Mn, Ca, Zr, Ba

A-Rank: n.a. - glass*
B-Rank:

Specimen	*Location*	*E.D.*
AR17jB1	Sizevit Yeni-el	1.382
AR16jB1	Sizevit Yeni-el	1.390
AR66rB2	Aghvorik	1.393
EA28P4A	Nemrut Dag	1.393
EA28P5A	Nemrut Dag	1.398
EA28P5B	Nemrut Dag	1.402
EA28P4B	Nemrut Dag	1.403
EA28P1	Nemrut Dag	1.408
EA28P2C	Nemrut Dag	1.408
EA64E1B	Nemrut Dag	1.408

* Note the relatively large Euclidean distances, which indicate that none of the nearest neighbors are matches to this artifact.

Table D.1 - Source Assignments of Artifacts based on Euclidean Distance to Centroids of Geological Specimens

Artifact: A10 q601.3 f277 k27

A-Rank: **Pasinler** **38**
B-Rank: **Mus** **27**

Elements: Fe, Ti, Ba

A-Rank:	Bingol B	10
B-Rank:	-	-

Specimen	*Location*	*E.D.*
EA50R1B	Bingol B	0.008
EA50P1A	Bingol B	0.015
EA50P2A	Bingol B	0.015
EA50P3A	Bingol B	0.016
EA50P4C	Bingol B	0.016
EA50P5	Bingol B	0.016
EA50P6	Bingol B	0.016
EA50P2C	Bingol B	0.017
EA50P3B	Bingol B	0.018
EA50P4D	Bingol B	0.018

Elements: Fe, Zr, Ba

A-Rank:	Pasinler	10
B-Rank:	-	-

Specimen	*Location*	*E.D.*
EA35P2	Pasinler	0.021
EA33P3	Pasinler	0.022
EA35P3	Pasinler	0.022
EA34R2	Pasinler	0.023
EA34P3	Pasinler	0.024
EA34P1	Pasinler	0.025
EA35P1	Pasinler	0.026
EA33P6	Pasinler	0.027
EA33P7	Pasinler	0.027
EA33P5	Pasinler	0.029

Elements: Ti, Fe, Zr, Ba

A-Rank:	Pasinler	10
B-Rank:	-	-

Specimen	*Location*	*E.D.*
EA35P2	Pasinler	0.027
EA33P3	Pasinler	0.030
EA33P7	Pasinler	0.030
EA34P3	Pasinler	0.030
EA35P1	Pasinler	0.032
EA34P1	Pasinler	0.033
EA34R2	Pasinler	0.033
EA35P3	Pasinler	0.033
EA33P5	Pasinler	0.035
EA34R1	Pasinler	0.038

Elements: Ti, Fe, Mn, Ca, Zr, Ba

A-Rank:	Mus	7
B-Rank:	Pasinler	3

Specimen	*Location*	*E.D.*
EA62Y1A	Mus	0.060
EA34P3	Pasinler	0.064
EA62Y3A	Mus	0.065
EA62Y1B	Mus	0.066
EA61B1	Mus	0.067
EA62Y1D	Mus	0.067
EA34P1	Pasinler	0.069
EA35P2	Pasinler	0.069
EA60B1A	Mus	0.069
EA58B1	Mus	0.070

Elements: Fe, Ti, Zr

A-Rank:	Pasinler	8
B-Rank:	Hotamis Dag	2

Specimen	*Location*	*E.D.*
EA33P1A	Pasinler	0.026
EA33P1B	Pasinler	0.027
EA35P2	Pasinler	0.027
EA33P7	Pasinler	0.028
EA33P2A	Pasinler	0.029
EA34R1	Pasinler	0.029
EA35P1	Pasinler	0.029
CA06P5C	Hotamis Dag	0.030
CA12P1	Hotamis Dag	0.030
EA33P3	Pasinler	0.030

Elements: Ti, Zr, Ba

A-Rank:	Pasinler	10
B-Rank:	-	-

Specimen	*Location*	*E.D.*
EA35P2	Pasinler	0.017
EA33P7	Pasinler	0.020
EA33P3	Pasinler	0.021
EA34P3	Pasinler	0.022
EA35P1	Pasinler	0.024
EA34R2	Pasinler	0.025
EA35P3	Pasinler	0.025
EA34P1	Pasinler	0.026
EA33P5	Pasinler	0.027
EA35R1	Pasinler	0.029

Elements: Ti, Fe, Zr, Ba, Zn

A-Rank:	Mus	10
B-Rank:	-	-

Specimen	*Location*	*E.D.*
EA62Y1A	Mus	0.126
EA60B1B	Mus	0.135
EA60B1A	Mus	0.151
EA62Y3B	Mus	0.159
EA57B1	Mus	0.165
EA62Y4	Mus	0.168
EA58B1	Mus	0.170
EA59B1	Mus	0.180
EA62Y1B	Mus	0.180
EA62Y1C	Mus	0.182

Elements: Ti, Al, Fe, Mn, Ca, Zr, Ba

A-Rank:	Mus	10
B-Rank:	-	-

Specimen	*Location*	*E.D.*
EA62Y1A	Mus	0.072
EA62Y3A	Mus	0.074
EA62Y1D	Mus	0.075
EA61B1	Mus	0.076
EA62Y1B	Mus	0.076
EA62Y4	Mus	0.079
EA58B1	Mus	0.081
EA60B1A	Mus	0.084
EA62Y1C	Mus	0.084
EA62Y5	Mus	0.086

Table D.1 - Source Assignments of Artifacts based on Euclidean Distance to Centroids of Geological Specimens

Artifact: A10 q687.5 f292 k28

A-Rank: **Bingol B** **57**
B-Rank: Gutansar 11

Elements: Fe, Ti, Ba

A-Rank: Bingol B 7
B-Rank: Gutansar 2

Specimen	*Location*	*E.D.*
EA52B1	Bingol B	0.018
EA52B3	Bingol B	0.022
EA52B2	Bingol B	0.028
EA56B1	Bingol B	0.031
EA53B2	Bingol B	0.047
EA53B1	Bingol B	0.055
EA54B1	Bingol B	0.062
AR06E2A	Gutansar	0.098
AR06E1A	Gutansar	0.100
AR21avH1	Chazencavan	0.100

Elements: Fe, Zr, Ba

A-Rank: Bingol B 7
B-Rank: Erzincan 3

Specimen	*Location*	*E.D.*
EA52B3	Bingol B	0.028
EA52B2	Bingol B	0.034
EA52B1	Bingol B	0.035
EA56B1	Bingol B	0.040
EA53B2	Bingol B	0.051
EA53B1	Bingol B	0.066
EA54B1	Bingol B	0.071
EA43R2	Erzincan	0.083
EA44P3	Erzincan	0.085
EA44R1	Erzincan	0.085

Elements: Ti, Fe, Zr, Ba

A-Rank: Bingol B 7
B-Rank: Gutansar 3

Specimen	*Location*	*E.D.*
EA52B3	Bingol B	0.032
EA52B1	Bingol B	0.036
EA52B2	Bingol B	0.037
EA56B1	Bingol B	0.046
EA53B2	Bingol B	0.054
EA53B1	Bingol B	0.068
EA54B1	Bingol B	0.071
AR06E3A	Gutansar	0.139
AR30jfL1	Gutansar	0.139
AR06E2A	Gutansar	0.140

Elements: Ti, Fe, Mn, Ca, Zr, Ba

A-Rank: Bingol B 7
B-Rank: Acigol 3

Specimen	*Location*	*E.D.*
EA52B3	Bingol B	0.032
EA52B1	Bingol B	0.038
EA56B1	Bingol B	0.046
EA52B2	Bingol B	0.047
EA53B2	Bingol B	0.058
EA53B1	Bingol B	0.068
EA54B1	Bingol B	0.090
CA08R1A	Acigol	0.171
CA08R1C	Acigol	0.171
CA07R2A	Acigol	0.181

Elements: Fe, Ti, Zr

A-Rank: Bingol B 7
B-Rank: Gutansar 2

Specimen	*Location*	*E.D.*
EA52B3	Bingol B	0.029
EA52B1	Bingol B	0.033
EA52B2	Bingol B	0.035
EA53B2	Bingol B	0.037
EA56B1	Bingol B	0.043
EA53B1	Bingol B	0.048
EA54B1	Bingol B	0.070
EA66W1	Lake Van	0.124
AR76rB3	Gutansar	0.128
AR06E3A	Gutansar	0.132

Elements: Ti, Zr, Ba

A-Rank: Bingol B 9
B-Rank: Erevan 1

Specimen	*Location*	*E.D.*
EA52B2	Bingol B	0.031
EA52B3	Bingol B	0.032
EA52B1	Bingol B	0.036
EA54B1	Bingol B	0.036
EA55B2	Bingol B	0.042
EA56B1	Bingol B	0.044
EA53B2	Bingol B	0.052
EA55B1	Bingol B	0.052
EA53B1	Bingol B	0.065
AR24jfL1	Erevan	0.103

Elements: Ti, Fe, Zr, Ba, Zn

A-Rank: Bingol B 6
B-Rank: Gutansar 4

Specimen	*Location*	*E.D.*
EA53B1	Bingol B	0.100
EA52B1	Bingol B	0.132
EA52B3	Bingol B	0.144
EA54B1	Bingol B	0.161
AR06E2B	Gutansar	0.162
EA52B2	Bingol B	0.162
AR11jB1	Gutansar	0.173
EA56B1	Bingol B	0.176
AR12jB1	Gutansar	0.185
AR06E1B	Gutansar	0.186

Elements: Ti, Al, Fe, Mn, Ca, Zr, Ba

A-Rank: Bingol B 7
B-Rank: Acigol 3

Specimen	*Location*	*E.D.*
EA52B3	Bingol B	0.055
EA52B1	Bingol B	0.058
EA56B1	Bingol B	0.060
EA53B2	Bingol B	0.062
EA52B2	Bingol B	0.064
EA53B1	Bingol B	0.072
EA54B1	Bingol B	0.097
CA08R1A	Acigol	0.172
CA08R1C	Acigol	0.173
CA07R2A	Acigol	0.181

Table D.1 - Source Assignments of Artifacts based on Euclidean Distance to Centroids of Geological Specimens

Artifact: A10 q695.1 f300 k28

A-Rank: **Bingol B** **56**
B-Rank: Gutansar 11

Elements: Fe, Ti, Ba

A-Rank:	Bingol B	7
B-Rank:	Gutansar	2

Specimen	*Location*	*E.D.*
EA52B1	Bingol B	0.022
EA52B3	Bingol B	0.029
EA56B1	Bingol B	0.033
EA53B2	Bingol B	0.036
EA52B2	Bingol B	0.039
EA53B1	Bingol B	0.040
EA54B1	Bingol B	0.077
AR06E2A	Gutansar	0.122
AR21avH1	Chazencavan	0.123
AR30jfL1	Gutansar	0.124

Elements: Fe, Zr, Ba

A-Rank:	Bingol B	6
B-Rank:	Erzincan	4

Specimen	*Location*	*E.D.*
EA52B3	Bingol B	0.038
EA52B1	Bingol B	0.042
EA53B2	Bingol B	0.044
EA56B1	Bingol B	0.044
EA52B2	Bingol B	0.048
EA53B1	Bingol B	0.056
EA43P1	Erzincan	0.075
EA43P2A	Erzincan	0.081
EA44P2	Erzincan	0.082
EA44P3	Erzincan	0.083

Elements: Ti, Fe, Zr, Ba

A-Rank:	Bingol B	7
B-Rank:	Gutansar	3

Specimen	*Location*	*E.D.*
EA52B3	Bingol B	0.040
EA52B1	Bingol B	0.042
EA52B2	Bingol B	0.049
EA53B2	Bingol B	0.049
EA56B1	Bingol B	0.051
EA53B1	Bingol B	0.060
EA54B1	Bingol B	0.086
AR30jfL1	Gutansar	0.154
AR06E2A	Gutansar	0.155
AR06E2B	Gutansar	0.157

Elements: Ti, Fe, Mn, Ca, Zr, Ba

A-Rank:	Bingol B	7
B-Rank:	Acigol	3

Specimen	*Location*	*E.D.*
EA52B1	Bingol B	0.045
EA52B2	Bingol B	0.049
EA52B3	Bingol B	0.049
EA53B2	Bingol B	0.050
EA56B1	Bingol B	0.058
EA53B1	Bingol B	0.064
EA54B1	Bingol B	0.117
CA08R1A	Acigol	0.175
CA08R1C	Acigol	0.180
CA07R2A	Acigol	0.188

Elements: Fe, Ti, Zr

A-Rank:	Bingol B	7
B-Rank:	Gutansar	2

Specimen	*Location*	*E.D.*
EA52B3	Bingol B	0.034
EA52B1	Bingol B	0.037
EA52B2	Bingol B	0.044
EA56B1	Bingol B	0.047
EA53B2	Bingol B	0.049
EA53B1	Bingol B	0.058
EA54B1	Bingol B	0.082
AR76rB3	Gutansar	0.132
EA66W1	Lake Van	0.135
AR06E1C	Gutansar	0.136

Elements: Ti, Zr, Ba

A-Rank:	Bingol B	9
B-Rank:	Erevan	1

Specimen	*Location*	*E.D.*
EA52B2	Bingol B	0.037
EA52B3	Bingol B	0.037
EA53B2	Bingol B	0.039
EA52B1	Bingol B	0.042
EA54B1	Bingol B	0.047
EA53B1	Bingol B	0.051
EA55B2	Bingol B	0.051
EA56B1	Bingol B	0.051
EA55B1	Bingol B	0.063
AR24jfL1	Erevan	0.111

Elements: Ti, Fe, Zr, Ba, Zn

A-Rank:	Bingol B	6
B-Rank:	Gutansar	4

Specimen	*Location*	*E.D.*
EA53B1	Bingol B	0.084
EA52B1	Bingol B	0.121
EA52B3	Bingol B	0.134
EA52B2	Bingol B	0.153
EA54B1	Bingol B	0.157
EA56B1	Bingol B	0.164
AR06E2B	Gutansar	0.172
AR11jB1	Gutansar	0.182
AR12jB1	Gutansar	0.191
AR06E1B	Gutansar	0.193

Elements: Ti, Al, Fe, Mn, Ca, Zr, Ba

A-Rank:	Bingol B	7
B-Rank:	Acigol	3

Specimen	*Location*	*E.D.*
EA53B2	Bingol B	0.053
EA52B1	Bingol B	0.060
EA52B2	Bingol B	0.063
EA52B3	Bingol B	0.064
EA56B1	Bingol B	0.066
EA53B1	Bingol B	0.067
EA54B1	Bingol B	0.122
CA08R1A	Acigol	0.177
CA08R1C	Acigol	0.182
CA07R2A	Acigol	0.188

Table D.1 - Source Assignments of Artifacts based on Euclidean Distance to Centroids of Geological Specimens

Artifact: A10 q77-1 f79 k7

A-Rank: **Nemrut Dag (EA25)** **76**
B-Rank: Nemrut Dag (EA22) 4

Elements: Fe, Ti, Ba

A-Rank:	Nemrut Dag (EA25)	10
B-Rank:	-	-

Specimen	*Location*	*E.D.*
EA25R2	Nemrut Dag (EA25)	0.014
EA25P2A	Nemrut Dag (EA25)	0.022
EA25P2C	Nemrut Dag (EA25)	0.023
EA25P1C	Nemrut Dag (EA25)	0.024
EA25P2D	Nemrut Dag (EA25)	0.026
EA25P1A	Nemrut Dag (EA25)	0.031
EA25P1B	Nemrut Dag (EA25)	0.031
EA25P2B	Nemrut Dag (EA25)	0.031
EA25P1D	Nemrut Dag (EA25)	0.037
EA25R1	Nemrut Dag (EA25)	0.038

Elements: Fe, Zr, Ba

A-Rank:	Nemrut Dag (EA25)	10
B-Rank:	-	-

Specimen	*Location*	*E.D.*
EA25R2	Nemrut Dag (EA25)	0.014
EA25P2A	Nemrut Dag (EA25)	0.022
EA25P2D	Nemrut Dag (EA25)	0.025
EA25P2C	Nemrut Dag (EA25)	0.027
EA25P2B	Nemrut Dag (EA25)	0.029
EA25P1C	Nemrut Dag (EA25)	0.038
EA25R1	Nemrut Dag (EA25)	0.042
EA25P3	Nemrut Dag (EA25)	0.045
EA25P1A	Nemrut Dag (EA25)	0.047
EA25P1B	Nemrut Dag (EA25)	0.047

Elements: Ti, Fe, Zr, Ba

A-Rank:	Nemrut Dag (EA25)	10
B-Rank:	-	-

Specimen	*Location*	*E.D.*
EA25R2	Nemrut Dag (EA25)	0.014
EA25P2A	Nemrut Dag (EA25)	0.024
EA25P2C	Nemrut Dag (EA25)	0.028
EA25P2D	Nemrut Dag (EA25)	0.029
EA25P2B	Nemrut Dag (EA25)	0.031
EA25P1C	Nemrut Dag (EA25)	0.039
EA25R1	Nemrut Dag (EA25)	0.042
EA25P3	Nemrut Dag (EA25)	0.045
EA25P1B	Nemrut Dag (EA25)	0.047
EA25P1A	Nemrut Dag (EA25)	0.048

Elements: Ti, Fe, Mn, Ca, Zr, Ba

A-Rank:	Nemrut Dag (EA25)	10
B-Rank:	-	-

Specimen	*Location*	*E.D.*
EA25P2A	Nemrut Dag (EA25)	0.033
EA25R2	Nemrut Dag (EA25)	0.035
EA25P2B	Nemrut Dag (EA25)	0.036
EA25P2C	Nemrut Dag (EA25)	0.037
EA25P1C	Nemrut Dag (EA25)	0.040
EA25P2D	Nemrut Dag (EA25)	0.042
EA25R1	Nemrut Dag (EA25)	0.048
EA25P1A	Nemrut Dag (EA25)	0.049
EA25P3	Nemrut Dag (EA25)	0.049
EA25P1B	Nemrut Dag (EA25)	0.051

Elements: Fe, Ti, Zr

A-Rank:	Nemrut Dag (EA25)	10
B-Rank:	-	-

Specimen	*Location*	*E.D.*
EA25R2	Nemrut Dag (EA25)	0.003
EA25P2A	Nemrut Dag (EA25)	0.013
EA25P2B	Nemrut Dag (EA25)	0.014
EA25P3	Nemrut Dag (EA25)	0.014
EA25R1	Nemrut Dag (EA25)	0.018
EA25P2D	Nemrut Dag (EA25)	0.019
EA25P2C	Nemrut Dag (EA25)	0.021
EA25P1C	Nemrut Dag (EA25)	0.032
EA25P1B	Nemrut Dag (EA25)	0.036
EA25P1A	Nemrut Dag (EA25)	0.037

Elements: Ti, Zr, Ba

A-Rank:	Nemrut Dag (EA25)	10
B-Rank:	-	-

Specimen	*Location*	*E.D.*
EA25R2	Nemrut Dag (EA25)	0.014
EA25P2A	Nemrut Dag (EA25)	0.023
EA25P2C	Nemrut Dag (EA25)	0.027
EA25P2D	Nemrut Dag (EA25)	0.028
EA25P2B	Nemrut Dag (EA25)	0.030
EA25P1C	Nemrut Dag (EA25)	0.039
EA25R1	Nemrut Dag (EA25)	0.042
EA25P3	Nemrut Dag (EA25)	0.045
EA25P1B	Nemrut Dag (EA25)	0.047
EA25P1A	Nemrut Dag (EA25)	0.048

Elements: Ti, Fe, Zr, Ba, Zn

A-Rank:	Nemrut Dag (EA25)	6
B-Rank:	Nemrut Dag (EA22)	4

Specimen	*Location*	*E.D.*
EA25P2C	Nemrut Dag (EA25)	0.029
EA25P1A	Nemrut Dag (EA25)	0.082
EA25P1B	Nemrut Dag (EA25)	0.084
EA25P1D	Nemrut Dag (EA25)	0.085
EA22P1D	Nemrut Dag (EA22)	0.087
EA25P2D	Nemrut Dag (EA25)	0.090
EA25P2B	Nemrut Dag (EA25)	0.095
EA22R1	Nemrut Dag (EA22)	0.096
EA22P7A	Nemrut Dag (EA22)	0.097
EA22P1C	Nemrut Dag (EA22)	0.099

Elements: Ti, Al, Fe, Mn, Ca, Zr, Ba

A-Rank:	Nemrut Dag (EA25)	10
B-Rank:	-	-

Specimen	*Location*	*E.D.*
EA25P2A	Nemrut Dag (EA25)	0.034
EA25P2B	Nemrut Dag (EA25)	0.038
EA25P2C	Nemrut Dag (EA25)	0.039
EA25R2	Nemrut Dag (EA25)	0.041
EA25P1C	Nemrut Dag (EA25)	0.042
EA25P2D	Nemrut Dag (EA25)	0.043
EA25P1A	Nemrut Dag (EA25)	0.051
EA25P1B	Nemrut Dag (EA25)	0.052
EA25P3	Nemrut Dag (EA25)	0.052
EA25R1	Nemrut Dag (EA25)	0.052

Table D.1 - Source Assignments of Artifacts based on Euclidean Distance to Centroids of Geological Specimens

Artifact: A14 q244-1 f29 k2

A-Rank: **Nemrut Dag (EA25)** **66**
B-Rank: Nemrut Dag (EA22) 14

Elements: Fe, Ti, Ba

A-Rank:	Nemrut Dag (EA25)	10
B-Rank:	-	-

Specimen	*Location*	*E.D.*
EA25P3	Nemrut Dag (EA25)	0.012
EA25R1	Nemrut Dag (EA25)	0.015
EA25P1A	Nemrut Dag (EA25)	0.023
EA25P1B	Nemrut Dag (EA25)	0.023
EA25P1D	Nemrut Dag (EA25)	0.026
EA25P2B	Nemrut Dag (EA25)	0.029
EA25P1C	Nemrut Dag (EA25)	0.031
EA25P2A	Nemrut Dag (EA25)	0.032
EA25P2D	Nemrut Dag (EA25)	0.035
EA25P2C	Nemrut Dag (EA25)	0.036

Elements: Fe, Zr, Ba

A-Rank:	Nemrut Dag (EA25)	6
B-Rank:	Nemrut Dag (EA22)	4

Specimen	*Location*	*E.D.*
EA25P1D	Nemrut Dag (EA25)	0.033
EA25P1A	Nemrut Dag (EA25)	0.034
EA25P1B	Nemrut Dag (EA25)	0.034
EA22P4	Nemrut Dag (EA22)	0.043
EA25P1C	Nemrut Dag (EA25)	0.043
EA25R1	Nemrut Dag (EA25)	0.046
EA25P3	Nemrut Dag (EA25)	0.051
EA22P5B	Nemrut Dag (EA22)	0.055
EA22P8A	Nemrut Dag (EA22)	0.055
EA22P8B	Nemrut Dag (EA22)	0.056

Elements: Ti, Fe, Zr, Ba

A-Rank:	Nemrut Dag (EA25)	10
B-Rank:	-	-

Specimen	*Location*	*E.D.*
EA25P1A	Nemrut Dag (EA25)	0.035
EA25P1B	Nemrut Dag (EA25)	0.035
EA25P1D	Nemrut Dag (EA25)	0.035
EA25P1C	Nemrut Dag (EA25)	0.044
EA25R1	Nemrut Dag (EA25)	0.047
EA25P3	Nemrut Dag (EA25)	0.051
EA25P2C	Nemrut Dag (EA25)	0.059
EA25P2D	Nemrut Dag (EA25)	0.061
EA25P2A	Nemrut Dag (EA25)	0.062
EA25P2B	Nemrut Dag (EA25)	0.064

Elements: Ti, Fe, Mn, Ca, Zr, Ba

A-Rank:	Nemrut Dag (EA25)	10
B-Rank:	-	-

Specimen	*Location*	*E.D.*
EA25P1A	Nemrut Dag (EA25)	0.043
EA25P1C	Nemrut Dag (EA25)	0.045
EA25P1B	Nemrut Dag (EA25)	0.050
EA25R1	Nemrut Dag (EA25)	0.061
EA25P3	Nemrut Dag (EA25)	0.062
EA25P1D	Nemrut Dag (EA25)	0.066
EA25P2C	Nemrut Dag (EA25)	0.071
EA25P2A	Nemrut Dag (EA25)	0.073
EA25P2B	Nemrut Dag (EA25)	0.073
EA25P2D	Nemrut Dag (EA25)	0.077

Elements: Fe, Ti, Zr

A-Rank:	Nemrut Dag (EA25)	10
B-Rank:	-	-

Specimen	*Location*	*E.D.*
EA25P1A	Nemrut Dag (EA25)	0.028
EA25P1B	Nemrut Dag (EA25)	0.028
EA25P1D	Nemrut Dag (EA25)	0.031
EA25P1C	Nemrut Dag (EA25)	0.034
EA25R1	Nemrut Dag (EA25)	0.045
EA25P2C	Nemrut Dag (EA25)	0.050
EA25P3	Nemrut Dag (EA25)	0.050
EA25P2D	Nemrut Dag (EA25)	0.053
EA25P2A	Nemrut Dag (EA25)	0.054
EA25P2B	Nemrut Dag (EA25)	0.060

Elements: Ti, Zr, Ba

A-Rank:	Nemrut Dag (EA25)	6
B-Rank:	Nemrut Dag (EA22)	4

Specimen	*Location*	*E.D.*
EA25P1D	Nemrut Dag (EA25)	0.032
EA25P1B	Nemrut Dag (EA25)	0.034
EA25P1A	Nemrut Dag (EA25)	0.035
EA25P1C	Nemrut Dag (EA25)	0.043
EA25R1	Nemrut Dag (EA25)	0.047
EA25P3	Nemrut Dag (EA25)	0.050
EA22P8B	Nemrut Dag (EA22)	0.052
EA22P7A	Nemrut Dag (EA22)	0.053
EA22P6B	Nemrut Dag (EA22)	0.054
EA22P2	Nemrut Dag (EA22)	0.055

Elements: Ti, Fe, Zr, Ba, Zn

A-Rank:	Nemrut Dag (EA22)	6
B-Rank:	Nemrut Dag (EA25)	4

Specimen	*Location*	*E.D.*
EA25P2C	Nemrut Dag (EA25)	0.060
EA22P7A	Nemrut Dag (EA22)	0.078
EA22R1	Nemrut Dag (EA22)	0.085
EA22P5B	Nemrut Dag (EA22)	0.088
EA22P1D	Nemrut Dag (EA22)	0.089
EA22P3	Nemrut Dag (EA22)	0.092
EA25P1A	Nemrut Dag (EA25)	0.092
EA25P1D	Nemrut Dag (EA25)	0.093
EA25P1B	Nemrut Dag (EA25)	0.096
EA22P1C	Nemrut Dag (EA22)	0.102

Elements: Ti, Al, Fe, Mn, Ca, Zr, Ba

A-Rank:	Nemrut Dag (EA25)	10
B-Rank:	-	-

Specimen	*Location*	*E.D.*
EA25P1A	Nemrut Dag (EA25)	0.047
EA25P1C	Nemrut Dag (EA25)	0.051
EA25P1B	Nemrut Dag (EA25)	0.056
EA25R1	Nemrut Dag (EA25)	0.063
EA25P3	Nemrut Dag (EA25)	0.065
EA25P1D	Nemrut Dag (EA25)	0.072
EA25P2C	Nemrut Dag (EA25)	0.075
EA25P2B	Nemrut Dag (EA25)	0.077
EA25P2A	Nemrut Dag (EA25)	0.078
EA25P2D	Nemrut Dag (EA25)	0.081

Table D.1 - Source Assignments of Artifacts based on Euclidean Distance to Centroids of Geological Specimens

Artifact: A14 q252-1 f90 k3

A-Rank: **Nemrut Dag (EA22)** **35**
B-Rank: **Nemrut Dag (EA25)** **33**

Elements: Fe, Ti, Ba

A-Rank:	Nemrut Dag (EA25)	10
B-Rank:	-	-

Specimen	*Location*	*E.D.*
EA25R2	Nemrut Dag (EA25)	0.007
EA25P1C	Nemrut Dag (EA25)	0.012
EA25P2A	Nemrut Dag (EA25)	0.013
EA25P1B	Nemrut Dag (EA25)	0.014
EA25P1A	Nemrut Dag (EA25)	0.015
EA25P2C	Nemrut Dag (EA25)	0.015
EA25P2B	Nemrut Dag (EA25)	0.017
EA25P2D	Nemrut Dag (EA25)	0.017
EA25R1	Nemrut Dag (EA25)	0.019
EA25P1D	Nemrut Dag (EA25)	0.022

Elements: Fe, Zr, Ba

A-Rank:	Nemrut Dag (EA22)	7
B-Rank:	Nemrut Dag (EA21)	3

Specimen	*Location*	*E.D.*
EA22P5A	Nemrut Dag (EA22)	0.087
EA21P1	Nemrut Dag (EA21)	0.092
EA21R1A	Nemrut Dag (EA21)	0.093
EA22P7A	Nemrut Dag (EA22)	0.094
EA21R1B	Nemrut Dag (EA21)	0.095
EA22P6A	Nemrut Dag (EA22)	0.096
EA22P4	Nemrut Dag (EA22)	0.097
EA22P5B	Nemrut Dag (EA22)	0.097
EA22P3	Nemrut Dag (EA22)	0.098
EA22P8B	Nemrut Dag (EA22)	0.099

Elements: Ti, Fe, Zr, Ba

A-Rank:	Nemrut Dag (EA22)	7
B-Rank:	Nemrut Dag (EA21)	2

Specimen	*Location*	*E.D.*
EA22P7A	Nemrut Dag (EA22)	0.102
EA22P5A	Nemrut Dag (EA22)	0.105
EA21P1	Nemrut Dag (EA21)	0.110
EA22P8B	Nemrut Dag (EA22)	0.110
EA21R1B	Nemrut Dag (EA21)	0.111
EA22P6B	Nemrut Dag (EA22)	0.112
EA25P1D	Nemrut Dag (EA25)	0.112
EA22P3	Nemrut Dag (EA22)	0.113
EA22P4	Nemrut Dag (EA22)	0.113
EA22P6A	Nemrut Dag (EA22)	0.113

Elements: Ti, Fe, Mn, Ca, Zr, Ba

A-Rank:	Nemrut Dag (EA25)	10
B-Rank:	-	-

Specimen	*Location*	*E.D.*
EA25P1D	Nemrut Dag (EA25)	0.113
EA25P1A	Nemrut Dag (EA25)	0.114
EA25P1B	Nemrut Dag (EA25)	0.114
EA25P1C	Nemrut Dag (EA25)	0.123
EA25R1	Nemrut Dag (EA25)	0.132
EA25P2C	Nemrut Dag (EA25)	0.133
EA25P2D	Nemrut Dag (EA25)	0.137
EA25P3	Nemrut Dag (EA25)	0.138
EA25P2A	Nemrut Dag (EA25)	0.140
EA25P2B	Nemrut Dag (EA25)	0.145

Elements: Fe, Ti, Zr

A-Rank:	Nemrut Dag (EA22)	7
B-Rank:	Nemrut Dag (EA21)	2

Specimen	*Location*	*E.D.*
EA22P7A	Nemrut Dag (EA22)	0.102
EA22P5A	Nemrut Dag (EA22)	0.105
EA22P8B	Nemrut Dag (EA22)	0.109
EA21P1	Nemrut Dag (EA21)	0.110
EA21R1B	Nemrut Dag (EA21)	0.110
EA25P1D	Nemrut Dag (EA25)	0.111
EA22P3	Nemrut Dag (EA22)	0.112
EA22P4	Nemrut Dag (EA22)	0.112
EA22P6A	Nemrut Dag (EA22)	0.112
EA22P6B	Nemrut Dag (EA22)	0.112

Elements: Ti, Zr, Ba

A-Rank:	Nemrut Dag (EA22)	7
B-Rank:	Nemrut Dag (EA21)	3

Specimen	*Location*	*E.D.*
EA22P7A	Nemrut Dag (EA22)	0.090
EA22P5A	Nemrut Dag (EA22)	0.096
EA21P1	Nemrut Dag (EA21)	0.098
EA21R1B	Nemrut Dag (EA21)	0.100
EA22P8B	Nemrut Dag (EA22)	0.100
EA22R1	Nemrut Dag (EA22)	0.102
EA22P3	Nemrut Dag (EA22)	0.103
EA22P6A	Nemrut Dag (EA22)	0.103
EA22P6B	Nemrut Dag (EA22)	0.104
EA21R1A	Nemrut Dag (EA21)	0.106

Elements: Ti, Fe, Zr, Ba, Zn

A-Rank:	Nemrut Dag (EA22)	7
B-Rank:	Nemrut Dag (EA25)	3

Specimen	*Location*	*E.D.*
EA22P8B	Nemrut Dag (EA22)	0.110
EA22P6A	Nemrut Dag (EA22)	0.113
EA25P1D	Nemrut Dag (EA25)	0.113
EA22P6B	Nemrut Dag (EA22)	0.114
EA25P1A	Nemrut Dag (EA25)	0.114
EA25P1B	Nemrut Dag (EA25)	0.114
EA22P7B	Nemrut Dag (EA22)	0.116
EA22P3	Nemrut Dag (EA22)	0.117
EA22P7A	Nemrut Dag (EA22)	0.120
EA22P5A	Nemrut Dag (EA22)	0.125

Elements: Ti, Al, Fe, Mn, Ca, Zr, Ba

A-Rank:	Nemrut Dag (EA25)	10
B-Rank:	-	-

Specimen	*Location*	*E.D.*
EA25P1D	Nemrut Dag (EA25)	0.114
EA25P1B	Nemrut Dag (EA25)	0.115
EA25P1A	Nemrut Dag (EA25)	0.116
EA25P1C	Nemrut Dag (EA25)	0.124
EA25P2C	Nemrut Dag (EA25)	0.134
EA25R1	Nemrut Dag (EA25)	0.134
EA25P2D	Nemrut Dag (EA25)	0.138
EA25P3	Nemrut Dag (EA25)	0.139
EA25P2A	Nemrut Dag (EA25)	0.140
EA25P2B	Nemrut Dag (EA25)	0.146

Table D.1 - Source Assignments of Artifacts based on Euclidean Distance to Centroids of Geological Specimens

Artifact: A14 q265-1 f92 k3

A-Rank: **Bingol B** **57**
B-Rank: Gutansar 11

Elements: Fe, Ti, Ba

A-Rank: Bingol B 7
B-Rank: Gutansar 2

Specimen	*Location*	*E.D.*
EA52B1	Bingol B	0.009
EA52B3	Bingol B	0.017
EA56B1	Bingol B	0.027
EA52B2	Bingol B	0.028
EA53B2	Bingol B	0.035
EA53B1	Bingol B	0.042
EA54B1	Bingol B	0.066
AR06E2A	Gutansar	0.109
AR21avH1	Chazencavan	0.110
AR06E1A	Gutansar	0.111

Elements: Fe, Zr, Ba

A-Rank: Bingol B 7
B-Rank: Erzincan 3

Specimen	*Location*	*E.D.*
EA52B3	Bingol B	0.018
EA52B1	Bingol B	0.024
EA56B1	Bingol B	0.029
EA52B2	Bingol B	0.030
EA53B2	Bingol B	0.035
EA53B1	Bingol B	0.049
EA54B1	Bingol B	0.071
EA43P1	Erzincan	0.089
EA43R2	Erzincan	0.092
EA44P2	Erzincan	0.092

Elements: Ti, Fe, Zr, Ba

A-Rank: Bingol B 7
B-Rank: Gutansar 3

Specimen	*Location*	*E.D.*
EA52B3	Bingol B	0.023
EA52B1	Bingol B	0.025
EA52B2	Bingol B	0.032
EA56B1	Bingol B	0.037
EA53B2	Bingol B	0.041
EA53B1	Bingol B	0.053
EA54B1	Bingol B	0.071
AR30jfL1	Gutansar	0.152
AR06E2A	Gutansar	0.154
AR06E2B	Gutansar	0.154

Elements: Ti, Fe, Mn, Ca, Zr, Ba

A-Rank: Bingol B 7
B-Rank: Acigol 3

Specimen	*Location*	*E.D.*
EA52B1	Bingol B	0.026
EA52B3	Bingol B	0.027
EA52B2	Bingol B	0.037
EA56B1	Bingol B	0.040
EA53B2	Bingol B	0.042
EA53B1	Bingol B	0.053
EA54B1	Bingol B	0.097
CA08R1A	Acigol	0.175
CA08R1C	Acigol	0.179
CA07R2A	Acigol	0.187

Elements: Fe, Ti, Zr

A-Rank: Bingol B 7
B-Rank: Gutansar 2

Specimen	*Location*	*E.D.*
EA52B3	Bingol B	0.022
EA52B1	Bingol B	0.024
EA52B2	Bingol B	0.032
EA53B2	Bingol B	0.035
EA56B1	Bingol B	0.037
EA53B1	Bingol B	0.044
EA54B1	Bingol B	0.070
EA66W1	Lake Van	0.130
AR76rB3	Gutansar	0.135
AR06E3A	Gutansar	0.140

Elements: Ti, Zr, Ba

A-Rank: Bingol B 9
B-Rank: Erevan 1

Specimen	*Location*	*E.D.*
EA52B2	Bingol B	0.021
EA52B3	Bingol B	0.022
EA52B1	Bingol B	0.025
EA54B1	Bingol B	0.028
EA53B2	Bingol B	0.034
EA55B2	Bingol B	0.035
EA56B1	Bingol B	0.036
EA53B1	Bingol B	0.047
EA55B1	Bingol B	0.047
AR24jfL1	Erevan	0.116

Elements: Ti, Fe, Zr, Ba, Zn

A-Rank: Bingol B 6
B-Rank: Gutansar 4

Specimen	*Location*	*E.D.*
EA53B1	Bingol B	0.080
EA52B1	Bingol B	0.117
EA52B3	Bingol B	0.130
EA52B2	Bingol B	0.148
EA54B1	Bingol B	0.150
EA56B1	Bingol B	0.161
AR06E2B	Gutansar	0.169
AR11jB1	Gutansar	0.180
AR12jB1	Gutansar	0.188
AR06E1B	Gutansar	0.191

Elements: Ti, Al, Fe, Mn, Ca, Zr, Ba

A-Rank: Bingol B 7
B-Rank: Acigol 3

Specimen	*Location*	*E.D.*
EA53B2	Bingol B	0.073
EA53B1	Bingol B	0.079
EA52B1	Bingol B	0.084
EA56B1	Bingol B	0.084
EA52B3	Bingol B	0.085
EA52B2	Bingol B	0.087
EA54B1	Bingol B	0.122
CA08R1A	Acigol	0.176
CA08R1C	Acigol	0.179
CA07R2A	Acigol	0.189

Table D.1 - Source Assignments of Artifacts based on Euclidean Distance to Centroids of Geological Specimens

Artifact: A14 q266-1 f92 k3

A-Rank: **Bingol B** **62**
B-Rank: Gutansar 10

Elements: Fe, Ti, Ba

A-Rank:	Bingol B	7
B-Rank:	Gutansar	2

Specimen	*Location*	*E.D.*
EA54B1	Bingol B	0.019
EA52B2	Bingol B	0.035
EA53B2	Bingol B	0.040
EA53B1	Bingol B	0.045
EA52B3	Bingol B	0.050
EA52B1	Bingol B	0.055
EA56B1	Bingol B	0.063
AR06E2A	Gutansar	0.076
AR21avH1	Chazencavan	0.076
AR06E1A	Gutansar	0.080

Elements: Fe, Zr, Ba

A-Rank:	Bingol B	7
B-Rank:	Acigol	3

Specimen	*Location*	*E.D.*
EA54B1	Bingol B	0.022
EA52B2	Bingol B	0.027
EA53B2	Bingol B	0.040
EA52B3	Bingol B	0.043
EA53B1	Bingol B	0.049
EA52B1	Bingol B	0.054
EA56B1	Bingol B	0.063
CA08R1A	Acigol	0.095
CA08R1B	Acigol	0.096
CA08R1D	Acigol	0.101

Elements: Ti, Fe, Zr, Ba

A-Rank:	Bingol B	9
B-Rank:	Gutansar	1

Specimen	*Location*	*E.D.*
EA54B1	Bingol B	0.025
EA52B2	Bingol B	0.035
EA53B2	Bingol B	0.041
EA52B3	Bingol B	0.050
EA53B1	Bingol B	0.050
EA52B1	Bingol B	0.056
EA56B1	Bingol B	0.064
EA55B2	Bingol B	0.124
EA55B1	Bingol B	0.127
AR06E3A	Gutansar	0.140

Elements: Ti, Fe, Mn, Ca, Zr, Ba

A-Rank:	Bingol B	9
B-Rank:	Lake Van	1

Specimen	*Location*	*E.D.*
EA54B1	Bingol B	0.026
EA52B3	Bingol B	0.067
EA53B1	Bingol B	0.071
EA53B2	Bingol B	0.078
EA56B1	Bingol B	0.079
EA52B1	Bingol B	0.081
EA52B2	Bingol B	0.084
EA55B2	Bingol B	0.126
EA55B1	Bingol B	0.129
EA67W1	Lake Van	0.183

Elements: Fe, Ti, Zr

A-Rank:	Bingol B	8
B-Rank:	Gutansar	1

Specimen	*Location*	*E.D.*
EA54B1	Bingol B	0.025
EA53B2	Bingol B	0.031
EA52B2	Bingol B	0.035
EA53B1	Bingol B	0.035
EA52B3	Bingol B	0.050
EA52B1	Bingol B	0.056
EA56B1	Bingol B	0.064
EA66W1	Lake Van	0.085
AR76rB3	Gutansar	0.123
EA55B2	Bingol B	0.124

Elements: Ti, Zr, Ba

A-Rank:	Bingol B	9
B-Rank:	Erevan	1

Specimen	*Location*	*E.D.*
EA55B2	Bingol B	0.019
EA54B1	Bingol B	0.020
EA56B1	Bingol B	0.020
EA52B1	Bingol B	0.022
EA52B2	Bingol B	0.024
EA52B3	Bingol B	0.026
EA53B2	Bingol B	0.029
EA55B1	Bingol B	0.031
EA53B1	Bingol B	0.042
AR24jfL1	Erevan	0.127

Elements: Ti, Fe, Zr, Ba, Zn

A-Rank:	Bingol B	5
B-Rank:	Gutansar	5

Specimen	*Location*	*E.D.*
EA53B1	Bingol B	0.199
AR06E2B	Gutansar	0.246
EA52B1	Bingol B	0.253
AR11jB1	Gutansar	0.256
EA52B3	Bingol B	0.265
EA54B1	Bingol B	0.266
AR06E1B	Gutansar	0.278
AR06E1C	Gutansar	0.279
AR12jB1	Gutansar	0.279
EA52B2	Bingol B	0.279

Elements: Ti, Al, Fe, Mn, Ca, Zr, Ba

A-Rank:	Bingol B	9
B-Rank:	Acigol	1

Specimen	*Location*	*E.D.*
EA54B1	Bingol B	0.037
EA53B1	Bingol B	0.072
EA52B3	Bingol B	0.075
EA53B2	Bingol B	0.079
EA56B1	Bingol B	0.083
EA52B1	Bingol B	0.087
EA52B2	Bingol B	0.090
EA55B2	Bingol B	0.130
EA55B1	Bingol B	0.132
CA08R1C	Acigol	0.196

Table D.1 - Source Assignments of Artifacts based on Euclidean Distance to Centroids of Geological Specimens

Artifact: A14 q299.2 f101 k100

A-Rank: **Nemrut Dag (EA25)** **44**
B-Rank: Nemrut Dag (EA22) 30

Elements: Fe, Ti, Ba

A-Rank:	Nemrut Dag (EA25)	10
B-Rank:	-	-

Specimen	*Location*	*E.D.*
EA25R1	Nemrut Dag (EA25)	0.002
EA25P3	Nemrut Dag (EA25)	0.004
EA25P1B	Nemrut Dag (EA25)	0.009
EA25P1A	Nemrut Dag (EA25)	0.010
EA25P1D	Nemrut Dag (EA25)	0.013
EA25P2B	Nemrut Dag (EA25)	0.015
EA25P1C	Nemrut Dag (EA25)	0.017
EA25P2A	Nemrut Dag (EA25)	0.020
EA25P2D	Nemrut Dag (EA25)	0.021
EA25P2C	Nemrut Dag (EA25)	0.022

Elements: Fe, Zr, Ba

A-Rank:	Nemrut Dag (EA22)	7
B-Rank:	Nemrut Dag (EA21)	3

Specimen	*Location*	*E.D.*
EA22P5A	Nemrut Dag (EA22)	0.063
EA22P4	Nemrut Dag (EA22)	0.066
EA21R1A	Nemrut Dag (EA21)	0.068
EA21R1B	Nemrut Dag (EA21)	0.069
EA22P6A	Nemrut Dag (EA22)	0.069
EA22P5B	Nemrut Dag (EA22)	0.070
EA21P1	Nemrut Dag (EA21)	0.071
EA22P3	Nemrut Dag (EA22)	0.071
EA22P7A	Nemrut Dag (EA22)	0.071
EA22P8B	Nemrut Dag (EA22)	0.072

Elements: Ti, Fe, Zr, Ba

A-Rank:	Nemrut Dag (EA22)	5
B-Rank:	Nemrut Dag (EA25)	4

Specimen	*Location*	*E.D.*
EA25P1D	Nemrut Dag (EA25)	0.077
EA25P1A	Nemrut Dag (EA25)	0.079
EA25P1B	Nemrut Dag (EA25)	0.079
EA25P1C	Nemrut Dag (EA25)	0.085
EA22P7A	Nemrut Dag (EA22)	0.086
EA22P8B	Nemrut Dag (EA22)	0.090
EA22P5A	Nemrut Dag (EA22)	0.091
EA22P6B	Nemrut Dag (EA22)	0.092
EA22P4	Nemrut Dag (EA22)	0.093
EA21R1B	Nemrut Dag (EA21)	0.094

Elements: Ti, Fe, Mn, Ca, Zr, Ba

A-Rank:	Nemrut Dag (EA25)	10
B-Rank:	-	-

Specimen	*Location*	*E.D.*
EA25P1A	Nemrut Dag (EA25)	0.081
EA25P1B	Nemrut Dag (EA25)	0.084
EA25P1C	Nemrut Dag (EA25)	0.085
EA25P1D	Nemrut Dag (EA25)	0.092
EA25R1	Nemrut Dag (EA25)	0.102
EA25P2C	Nemrut Dag (EA25)	0.106
EA25P3	Nemrut Dag (EA25)	0.106
EA25P2A	Nemrut Dag (EA25)	0.112
EA25P2D	Nemrut Dag (EA25)	0.112
EA25P2B	Nemrut Dag (EA25)	0.114

Elements: Fe, Ti, Zr

A-Rank:	Nemrut Dag (EA22)	5
B-Rank:	Nemrut Dag (EA25)	4

Specimen	*Location*	*E.D.*
EA25P1D	Nemrut Dag (EA25)	0.077
EA25P1A	Nemrut Dag (EA25)	0.078
EA25P1B	Nemrut Dag (EA25)	0.079
EA22P7A	Nemrut Dag (EA22)	0.084
EA25P1C	Nemrut Dag (EA25)	0.084
EA22P5A	Nemrut Dag (EA22)	0.090
EA22P8B	Nemrut Dag (EA22)	0.090
EA22P6B	Nemrut Dag (EA22)	0.092
EA22P4	Nemrut Dag (EA22)	0.093
EA21R1B	Nemrut Dag (EA21)	0.094

Elements: Ti, Zr, Ba

A-Rank:	Nemrut Dag (EA22)	6
B-Rank:	Nemrut Dag (EA25)	3

Specimen	*Location*	*E.D.*
EA22P7A	Nemrut Dag (EA22)	0.070
EA22P8B	Nemrut Dag (EA22)	0.076
EA25P1D	Nemrut Dag (EA25)	0.077
EA22P5A	Nemrut Dag (EA22)	0.079
EA22R1	Nemrut Dag (EA22)	0.079
EA25P1A	Nemrut Dag (EA25)	0.079
EA25P1B	Nemrut Dag (EA25)	0.079
EA21R1B	Nemrut Dag (EA21)	0.080
EA22P6B	Nemrut Dag (EA22)	0.080
EA22P3	Nemrut Dag (EA22)	0.082

Elements: Ti, Fe, Zr, Ba, Zn

A-Rank:	Nemrut Dag (EA22)	7
B-Rank:	Nemrut Dag (EA25)	3

Specimen	*Location*	*E.D.*
EA22P7A	Nemrut Dag (EA22)	0.095
EA22P5B	Nemrut Dag (EA22)	0.108
EA22R1	Nemrut Dag (EA22)	0.108
EA25P2C	Nemrut Dag (EA25)	0.110
EA22P3	Nemrut Dag (EA22)	0.119
EA22P1D	Nemrut Dag (EA22)	0.123
EA22P1C	Nemrut Dag (EA22)	0.136
EA22P7B	Nemrut Dag (EA22)	0.136
EA25P1D	Nemrut Dag (EA25)	0.138
EA25P1A	Nemrut Dag (EA25)	0.139

Elements: Ti, Al, Fe, Mn, Ca, Zr, Ba

A-Rank:	Nemrut Dag (EA25)	10
B-Rank:	-	-

Specimen	*Location*	*E.D.*
EA25P1A	Nemrut Dag (EA25)	0.081
EA25P1B	Nemrut Dag (EA25)	0.084
EA25P1C	Nemrut Dag (EA25)	0.086
EA25P1D	Nemrut Dag (EA25)	0.092
EA25R1	Nemrut Dag (EA25)	0.102
EA25P2C	Nemrut Dag (EA25)	0.106
EA25P3	Nemrut Dag (EA25)	0.106
EA25P2A	Nemrut Dag (EA25)	0.112
EA25P2D	Nemrut Dag (EA25)	0.112
EA25P2B	Nemrut Dag (EA25)	0.114

Table D.1 - Source Assignments of Artifacts based on Euclidean Distance to Centroids of Geological Specimens

Artifact: A14 q474.1 f193 k4

A-Rank: **Nemrut Dag (EA25)** **66**
B-Rank: Nemrut Dag (EA22) 13

Elements: Fe, Ti, Ba

A-Rank:	Nemrut Dag (EA25)	10
B-Rank:	-	-

Specimen	*Location*	*E.D.*
EA25P1A	Nemrut Dag (EA25)	0.002
EA25P1B	Nemrut Dag (EA25)	0.002
EA25P1C	Nemrut Dag (EA25)	0.007
EA25P2B	Nemrut Dag (EA25)	0.007
EA25R1	Nemrut Dag (EA25)	0.009
EA25P1D	Nemrut Dag (EA25)	0.010
EA25P2A	Nemrut Dag (EA25)	0.011
EA25P2D	Nemrut Dag (EA25)	0.012
EA25P2C	Nemrut Dag (EA25)	0.013
EA25P3	Nemrut Dag (EA25)	0.014

Elements: Fe, Zr, Ba

A-Rank:	Nemrut Dag (EA22)	5
B-Rank:	Nemrut Dag (EA25)	4

Specimen	*Location*	*E.D.*
EA22P4	Nemrut Dag (EA22)	0.040
EA25P1D	Nemrut Dag (EA25)	0.040
EA25P1A	Nemrut Dag (EA25)	0.042
EA25P1B	Nemrut Dag (EA25)	0.042
EA22P5A	Nemrut Dag (EA22)	0.045
EA22P5B	Nemrut Dag (EA22)	0.048
EA25P1C	Nemrut Dag (EA25)	0.048
EA22P6A	Nemrut Dag (EA22)	0.049
EA21R1B	Nemrut Dag (EA21)	0.050
EA22P3	Nemrut Dag (EA22)	0.050

Elements: Ti, Fe, Zr, Ba

A-Rank:	Nemrut Dag (EA25)	9
B-Rank:	Nemrut Dag (EA22)	1

Specimen	*Location*	*E.D.*
EA25P1D	Nemrut Dag (EA25)	0.041
EA25P1A	Nemrut Dag (EA25)	0.042
EA25P1B	Nemrut Dag (EA25)	0.042
EA25P1C	Nemrut Dag (EA25)	0.048
EA25R1	Nemrut Dag (EA25)	0.060
EA25P2C	Nemrut Dag (EA25)	0.063
EA25P3	Nemrut Dag (EA25)	0.066
EA25P2D	Nemrut Dag (EA25)	0.067
EA25P2A	Nemrut Dag (EA25)	0.069
EA22P7A	Nemrut Dag (EA22)	0.072

Elements: Ti, Fe, Mn, Ca, Zr, Ba

A-Rank:	Nemrut Dag (EA25)	10
B-Rank:	-	-

Specimen	*Location*	*E.D.*
EA25P1A	Nemrut Dag (EA25)	0.048
EA25P1C	Nemrut Dag (EA25)	0.048
EA25P1B	Nemrut Dag (EA25)	0.054
EA25P1D	Nemrut Dag (EA25)	0.067
EA25R1	Nemrut Dag (EA25)	0.071
EA25P2C	Nemrut Dag (EA25)	0.074
EA25P3	Nemrut Dag (EA25)	0.075
EA25P2A	Nemrut Dag (EA25)	0.079
EA25P2B	Nemrut Dag (EA25)	0.080
EA25P2D	Nemrut Dag (EA25)	0.080

Elements: Fe, Ti, Zr

A-Rank:	Nemrut Dag (EA25)	9
B-Rank:	Nemrut Dag (EA22)	1

Specimen	*Location*	*E.D.*
EA25P1D	Nemrut Dag (EA25)	0.040
EA25P1A	Nemrut Dag (EA25)	0.041
EA25P1B	Nemrut Dag (EA25)	0.042
EA25P1C	Nemrut Dag (EA25)	0.047
EA25R1	Nemrut Dag (EA25)	0.060
EA25P2C	Nemrut Dag (EA25)	0.062
EA25P3	Nemrut Dag (EA25)	0.065
EA25P2D	Nemrut Dag (EA25)	0.066
EA25P2A	Nemrut Dag (EA25)	0.069
EA22P7A	Nemrut Dag (EA22)	0.072

Elements: Ti, Zr, Ba

A-Rank:	Nemrut Dag (EA25)	5
B-Rank:	Nemrut Dag (EA22)	5

Specimen	*Location*	*E.D.*
EA25P1D	Nemrut Dag (EA25)	0.040
EA25P1A	Nemrut Dag (EA25)	0.042
EA25P1B	Nemrut Dag (EA25)	0.042
EA25P1C	Nemrut Dag (EA25)	0.048
EA22P7A	Nemrut Dag (EA22)	0.053
EA22R1	Nemrut Dag (EA22)	0.059
EA22P6B	Nemrut Dag (EA22)	0.060
EA22P8B	Nemrut Dag (EA22)	0.060
EA25R1	Nemrut Dag (EA25)	0.060
EA22P2	Nemrut Dag (EA22)	0.061

Elements: Ti, Fe, Zr, Ba, Zn

A-Rank:	Nemrut Dag (EA25)	9
B-Rank:	Nemrut Dag (EA22)	1

Specimen	*Location*	*E.D.*
EA25P1C	Nemrut Dag (EA25)	0.049
EA25P1B	Nemrut Dag (EA25)	0.060
EA25P1D	Nemrut Dag (EA25)	0.062
EA25P1A	Nemrut Dag (EA25)	0.063
EA25P3	Nemrut Dag (EA25)	0.067
EA25P2A	Nemrut Dag (EA25)	0.071
EA25P2D	Nemrut Dag (EA25)	0.072
EA25P2B	Nemrut Dag (EA25)	0.077
EA22P4	Nemrut Dag (EA22)	0.080
EA25R1	Nemrut Dag (EA25)	0.082

Elements: Ti, Al, Fe, Mn, Ca, Zr, Ba

A-Rank:	Nemrut Dag (EA25)	10
B-Rank:	-	-

Specimen	*Location*	*E.D.*
EA25P1A	Nemrut Dag (EA25)	0.048
EA25P1C	Nemrut Dag (EA25)	0.048
EA25P1B	Nemrut Dag (EA25)	0.054
EA25P1D	Nemrut Dag (EA25)	0.067
EA25R1	Nemrut Dag (EA25)	0.072
EA25P2C	Nemrut Dag (EA25)	0.074
EA25P3	Nemrut Dag (EA25)	0.075
EA25P2A	Nemrut Dag (EA25)	0.079
EA25P2B	Nemrut Dag (EA25)	0.080
EA25P2D	Nemrut Dag (EA25)	0.080

Table D.1 - Source Assignments of Artifacts based on Euclidean Distance to Centroids of Geological Specimens

Artifact: A14 q605-2 f250 k23

A-Rank: **Nemrut Dag (EA25)** **40**
B-Rank: Nemrut Dag (EA22) 30

Elements: Fe, Ti, Ba

A-Rank:	Nemrut Dag (EA25)	10
B-Rank:	-	-

Specimen	*Location*	*E.D.*
EA25P1D	Nemrut Dag (EA25)	0.009
EA25P3	Nemrut Dag (EA25)	0.010
EA25R1	Nemrut Dag (EA25)	0.012
EA25P1B	Nemrut Dag (EA25)	0.015
EA25P2B	Nemrut Dag (EA25)	0.015
EA25P1A	Nemrut Dag (EA25)	0.016
EA25P1C	Nemrut Dag (EA25)	0.021
EA25P2D	Nemrut Dag (EA25)	0.022
EA25P2C	Nemrut Dag (EA25)	0.023
EA25P2A	Nemrut Dag (EA25)	0.026

Elements: Fe, Zr, Ba

A-Rank:	Nemrut Dag (EA22)	7
B-Rank:	Nemrut Dag (EA21)	3

Specimen	*Location*	*E.D.*
EA22P5A	Nemrut Dag (EA22)	0.084
EA21R1A	Nemrut Dag (EA21)	0.086
EA21R1B	Nemrut Dag (EA21)	0.090
EA21P1	Nemrut Dag (EA21)	0.091
EA22P4	Nemrut Dag (EA22)	0.091
EA22P6A	Nemrut Dag (EA22)	0.091
EA22P7A	Nemrut Dag (EA22)	0.091
EA22P3	Nemrut Dag (EA22)	0.092
EA22P5B	Nemrut Dag (EA22)	0.092
EA22P8B	Nemrut Dag (EA22)	0.094

Elements: Ti, Fe, Zr, Ba

A-Rank:	Nemrut Dag (EA22)	6
B-Rank:	Nemrut Dag (EA25)	3

Specimen	*Location*	*E.D.*
EA22P7A	Nemrut Dag (EA22)	0.107
EA25P1D	Nemrut Dag (EA25)	0.107
EA25P1A	Nemrut Dag (EA25)	0.110
EA25P1B	Nemrut Dag (EA25)	0.110
EA22P5A	Nemrut Dag (EA22)	0.111
EA22P8B	Nemrut Dag (EA22)	0.112
EA21R1B	Nemrut Dag (EA21)	0.114
EA22P6B	Nemrut Dag (EA22)	0.115
EA22P3	Nemrut Dag (EA22)	0.116
EA22P4	Nemrut Dag (EA22)	0.116

Elements: Ti, Fe, Mn, Ca, Zr, Ba

A-Rank:	Nemrut Dag (EA25)	9
B-Rank:	Nemrut Dag (EA22)	1

Specimen	*Location*	*E.D.*
EA25P1A	Nemrut Dag (EA25)	0.111
EA25P1B	Nemrut Dag (EA25)	0.112
EA25P1D	Nemrut Dag (EA25)	0.114
EA25P1C	Nemrut Dag (EA25)	0.117
EA25R1	Nemrut Dag (EA25)	0.130
EA25P2C	Nemrut Dag (EA25)	0.134
EA25P3	Nemrut Dag (EA25)	0.134
EA25P2D	Nemrut Dag (EA25)	0.138
EA22P7B	Nemrut Dag (EA22)	0.140
EA25P2A	Nemrut Dag (EA25)	0.140

Elements: Fe, Ti, Zr

A-Rank:	Nemrut Dag (EA25)	4
B-Rank:	Nemrut Dag (EA22)	4

Specimen	*Location*	*E.D.*
EA22P7A	Nemrut Dag (EA22)	0.104
EA25P1D	Nemrut Dag (EA25)	0.107
EA25P1A	Nemrut Dag (EA25)	0.109
EA22P5A	Nemrut Dag (EA22)	0.110
EA25P1B	Nemrut Dag (EA25)	0.110
EA22P8B	Nemrut Dag (EA22)	0.112
EA21P1	Nemrut Dag (EA21)	0.114
EA21R1B	Nemrut Dag (EA21)	0.114
EA22P6B	Nemrut Dag (EA22)	0.115
EA25P1C	Nemrut Dag (EA25)	0.115

Elements: Ti, Zr, Ba

A-Rank:	Nemrut Dag (EA22)	7
B-Rank:	Nemrut Dag (EA21)	2

Specimen	*Location*	*E.D.*
EA22P7A	Nemrut Dag (EA22)	0.098
EA22P5A	Nemrut Dag (EA22)	0.104
EA22P8B	Nemrut Dag (EA22)	0.104
EA21R1B	Nemrut Dag (EA21)	0.106
EA25P1D	Nemrut Dag (EA25)	0.107
EA21P1	Nemrut Dag (EA21)	0.108
EA22P3	Nemrut Dag (EA22)	0.108
EA22R1	Nemrut Dag (EA22)	0.108
EA22P6B	Nemrut Dag (EA22)	0.109
EA22P6A	Nemrut Dag (EA22)	0.110

Elements: Ti, Fe, Zr, Ba, Zn

A-Rank:	Nemrut Dag (EA22)	6
B-Rank:	Nemrut Dag (EA25)	4

Specimen	*Location*	*E.D.*
EA25P1D	Nemrut Dag (EA25)	0.107
EA25P1A	Nemrut Dag (EA25)	0.110
EA25P1B	Nemrut Dag (EA25)	0.111
EA22P8B	Nemrut Dag (EA22)	0.112
EA22P6B	Nemrut Dag (EA22)	0.116
EA22P6A	Nemrut Dag (EA22)	0.117
EA22P3	Nemrut Dag (EA22)	0.121
EA22P7B	Nemrut Dag (EA22)	0.121
EA25P1C	Nemrut Dag (EA25)	0.124
EA22P7A	Nemrut Dag (EA22)	0.125

Elements: Ti, Al, Fe, Mn, Ca, Zr, Ba

A-Rank:	Nemrut Dag (EA25)	10
B-Rank:	-	-

Specimen	*Location*	*E.D.*
EA25P1A	Nemrut Dag (EA25)	0.115
EA25P1B	Nemrut Dag (EA25)	0.118
EA25P1D	Nemrut Dag (EA25)	0.121
EA25P1C	Nemrut Dag (EA25)	0.122
EA25R1	Nemrut Dag (EA25)	0.133
EA25P2C	Nemrut Dag (EA25)	0.138
EA25P3	Nemrut Dag (EA25)	0.138
EA25P2D	Nemrut Dag (EA25)	0.143
EA25P2A	Nemrut Dag (EA25)	0.145
EA25P2B	Nemrut Dag (EA25)	0.146

Table D.1 - Source Assignments of Artifacts based on Euclidean Distance to Centroids of Geological Specimens

Artifact: A14 q617-1 f250 k23

A-Rank: **Nemrut Dag (EA25)** **62**
B-Rank: Nemrut Dag (EA22) 18

Elements: Fe, Ti, Ba

A-Rank:	Nemrut Dag (EA25)	10
B-Rank:	-	-

Specimen	*Location*	*E.D.*
EA25R2	Nemrut Dag (EA25)	0.013
EA25P1A	Nemrut Dag (EA25)	0.014
EA25P1B	Nemrut Dag (EA25)	0.014
EA25P2A	Nemrut Dag (EA25)	0.014
EA25P1C	Nemrut Dag (EA25)	0.016
EA25R1	Nemrut Dag (EA25)	0.016
EA25P3	Nemrut Dag (EA25)	0.020
EA25P2B	Nemrut Dag (EA25)	0.021
EA25P2C	Nemrut Dag (EA25)	0.022
EA25P2D	Nemrut Dag (EA25)	0.023

Elements: Fe, Zr, Ba

A-Rank:	Nemrut Dag (EA25)	5
B-Rank:	Nemrut Dag (EA22)	5

Specimen	*Location*	*E.D.*
EA25P1A	Nemrut Dag (EA25)	0.036
EA25P1B	Nemrut Dag (EA25)	0.037
EA25P1D	Nemrut Dag (EA25)	0.038
EA25P1C	Nemrut Dag (EA25)	0.042
EA22P4	Nemrut Dag (EA22)	0.045
EA22P5A	Nemrut Dag (EA22)	0.052
EA22P5B	Nemrut Dag (EA22)	0.054
EA22P6B	Nemrut Dag (EA22)	0.054
EA22P6A	Nemrut Dag (EA22)	0.055
EA25R1	Nemrut Dag (EA25)	0.055

Elements: Ti, Fe, Zr, Ba

A-Rank:	Nemrut Dag (EA25)	9
B-Rank:	Nemrut Dag (EA22)	1

Specimen	*Location*	*E.D.*
EA25P1A	Nemrut Dag (EA25)	0.038
EA25P1B	Nemrut Dag (EA25)	0.039
EA25P1D	Nemrut Dag (EA25)	0.041
EA25P1C	Nemrut Dag (EA25)	0.044
EA25R1	Nemrut Dag (EA25)	0.056
EA25P2C	Nemrut Dag (EA25)	0.060
EA25P3	Nemrut Dag (EA25)	0.062
EA25P2A	Nemrut Dag (EA25)	0.064
EA25P2D	Nemrut Dag (EA25)	0.064
EA22P7A	Nemrut Dag (EA22)	0.069

Elements: Ti, Fe, Mn, Ca, Zr, Ba

A-Rank:	Nemrut Dag (EA25)	10
B-Rank:	-	-

Specimen	*Location*	*E.D.*
EA25P1A	Nemrut Dag (EA25)	0.039
EA25P1B	Nemrut Dag (EA25)	0.042
EA25P1C	Nemrut Dag (EA25)	0.046
EA25P1D	Nemrut Dag (EA25)	0.054
EA25R1	Nemrut Dag (EA25)	0.059
EA25P2C	Nemrut Dag (EA25)	0.063
EA25P3	Nemrut Dag (EA25)	0.064
EA25P2A	Nemrut Dag (EA25)	0.067
EA25P2D	Nemrut Dag (EA25)	0.069
EA25P2B	Nemrut Dag (EA25)	0.071

Elements: Fe, Ti, Zr

A-Rank:	Nemrut Dag (EA25)	9
B-Rank:	Nemrut Dag (EA22)	1

Specimen	*Location*	*E.D.*
EA25P1A	Nemrut Dag (EA25)	0.038
EA25P1B	Nemrut Dag (EA25)	0.038
EA25P1D	Nemrut Dag (EA25)	0.040
EA25P1C	Nemrut Dag (EA25)	0.044
EA25R1	Nemrut Dag (EA25)	0.055
EA25P2C	Nemrut Dag (EA25)	0.060
EA25P3	Nemrut Dag (EA25)	0.060
EA25P2D	Nemrut Dag (EA25)	0.063
EA25P2A	Nemrut Dag (EA25)	0.064
EA22P7A	Nemrut Dag (EA22)	0.069

Elements: Ti, Zr, Ba

A-Rank:	Nemrut Dag (EA25)	5
B-Rank:	Nemrut Dag (EA22)	5

Specimen	*Location*	*E.D.*
EA25P1A	Nemrut Dag (EA25)	0.038
EA25P1B	Nemrut Dag (EA25)	0.038
EA25P1D	Nemrut Dag (EA25)	0.038
EA22P7A	Nemrut Dag (EA25)	0.040
EA25P1C	Nemrut Dag (EA25)	0.043
EA22R1	Nemrut Dag (EA22)	0.045
EA22P6B	Nemrut Dag (EA22)	0.047
EA22P2	Nemrut Dag (EA22)	0.048
EA22P8B	Nemrut Dag (EA22)	0.048
EA22P7B	Nemrut Dag (EA22)	0.051

Elements: Ti, Fe, Zr, Ba, Zn

A-Rank:	Nemrut Dag (EA22)	6
B-Rank:	Nemrut Dag (EA25)	4

Specimen	*Location*	*E.D.*
EA25P2C	Nemrut Dag (EA25)	0.061
EA22P7A	Nemrut Dag (EA22)	0.070
EA22R1	Nemrut Dag (EA22)	0.080
EA22P5B	Nemrut Dag (EA22)	0.084
EA22P1D	Nemrut Dag (EA22)	0.087
EA22P3	Nemrut Dag (EA22)	0.090
EA25P1A	Nemrut Dag (EA25)	0.094
EA25P1D	Nemrut Dag (EA25)	0.095
EA25P1B	Nemrut Dag (EA25)	0.097
EA22P1C	Nemrut Dag (EA22)	0.098

Elements: Ti, Al, Fe, Mn, Ca, Zr, Ba

A-Rank:	Nemrut Dag (EA25)	10
B-Rank:	-	-

Specimen	*Location*	*E.D.*
EA25P1A	Nemrut Dag (EA25)	0.039
EA25P1B	Nemrut Dag (EA25)	0.042
EA25P1C	Nemrut Dag (EA25)	0.046
EA25P1D	Nemrut Dag (EA25)	0.055
EA25R1	Nemrut Dag (EA25)	0.059
EA25P2C	Nemrut Dag (EA25)	0.063
EA25P3	Nemrut Dag (EA25)	0.064
EA25P2A	Nemrut Dag (EA25)	0.067
EA25P2D	Nemrut Dag (EA25)	0.069
EA25P2B	Nemrut Dag (EA25)	0.072

Table D.1 - Source Assignments of Artifacts based on Euclidean Distance to Centroids of Geological Specimens

Artifact: A14 q742-2 f42 k12

A-Rank: **Nemrut Dag (EA22)** **38**
B-Rank: Nemrut Dag (EA25) 35

Elements: Fe, Ti, Ba

A-Rank:	Nemrut Dag (EA25)	7
B-Rank:	Nemrut Dag (EA22)	3

Specimen	*Location*	*E.D.*
EA25R2	Nemrut Dag (EA25)	0.056
EA25P2C	Nemrut Dag (EA25)	0.057
EA25P2D	Nemrut Dag (EA25)	0.059
EA25P1C	Nemrut Dag (EA25)	0.062
EA25P2A	Nemrut Dag (EA25)	0.063
EA22P7A	Nemrut Dag (EA22)	0.064
EA22P2	Nemrut Dag (EA22)	0.065
EA25P2B	Nemrut Dag (EA25)	0.065
EA25P1B	Nemrut Dag (EA25)	0.068
EA22R1	Nemrut Dag (EA22)	0.069

Elements: Fe, Zr, Ba

A-Rank:	Nemrut Dag (EA22)	7
B-Rank:	Nemrut Dag (EA23)	2

Specimen	*Location*	*E.D.*
EA21P1	Nemrut Dag (EA21)	0.047
EA22P7A	Nemrut Dag (EA22)	0.051
EA22P5A	Nemrut Dag (EA22)	0.056
EA22P7B	Nemrut Dag (EA22)	0.058
EA22R1	Nemrut Dag (EA22)	0.059
EA23P1A	Nemrut Dag (EA23)	0.060
EA23P1B	Nemrut Dag (EA23)	0.061
EA22P6A	Nemrut Dag (EA22)	0.062
EA22P6B	Nemrut Dag (EA22)	0.062
EA22P1C	Nemrut Dag (EA22)	0.063

Elements: Ti, Fe, Zr, Ba

A-Rank:	Nemrut Dag (EA22)	7
B-Rank:	Nemrut Dag (EA25)	2

Specimen	*Location*	*E.D.*
EA22P7A	Nemrut Dag (EA22)	0.066
EA22R1	Nemrut Dag (EA22)	0.075
EA21P1	Nemrut Dag (EA21)	0.077
EA22P7B	Nemrut Dag (EA22)	0.077
EA22P2	Nemrut Dag (EA22)	0.078
EA22P6B	Nemrut Dag (EA22)	0.078
EA22P8B	Nemrut Dag (EA22)	0.081
EA22P5A	Nemrut Dag (EA22)	0.082
EA25P1C	Nemrut Dag (EA25)	0.082
EA25P1D	Nemrut Dag (EA25)	0.083

Elements: Ti, Fe, Mn, Ca, Zr, Ba

A-Rank:	Nemrut Dag (EA25)	9
B-Rank:	Nemrut Dag (EA22)	1

Specimen	*Location*	*E.D.*
EA25P1C	Nemrut Dag (EA25)	0.085
EA25P1A	Nemrut Dag (EA25)	0.090
EA25P1B	Nemrut Dag (EA25)	0.092
EA25P1D	Nemrut Dag (EA25)	0.098
EA25P2C	Nemrut Dag (EA25)	0.098
EA22P7B	Nemrut Dag (EA22)	0.103
EA25P2D	Nemrut Dag (EA25)	0.104
EA25P2A	Nemrut Dag (EA25)	0.106
EA25R1	Nemrut Dag (EA25)	0.108
EA25P2B	Nemrut Dag (EA25)	0.109

Elements: Fe, Ti, Zr

A-Rank:	Nemrut Dag (EA22)	7
B-Rank:	Nemrut Dag (EA25)	2

Specimen	*Location*	*E.D.*
EA22P7A	Nemrut Dag (EA22)	0.047
EA22P8B	Nemrut Dag (EA22)	0.055
EA22P6B	Nemrut Dag (EA22)	0.056
EA22R1	Nemrut Dag (EA22)	0.057
EA25P1D	Nemrut Dag (EA25)	0.057
EA22P7B	Nemrut Dag (EA22)	0.060
EA21R1B	Nemrut Dag (EA21)	0.062
EA22P2	Nemrut Dag (EA22)	0.062
EA22P5A	Nemrut Dag (EA22)	0.062
EA25P1B	Nemrut Dag (EA25)	0.062

Elements: Ti, Zr, Ba

A-Rank:	Nemrut Dag (EA22)	5
B-Rank:	Nemrut Dag (EA25)	4

Specimen	*Location*	*E.D.*
EA22P7A	Nemrut Dag (EA22)	0.065
EA22R1	Nemrut Dag (EA22)	0.072
EA25P1C	Nemrut Dag (EA25)	0.074
EA22P2	Nemrut Dag (EA22)	0.075
EA21P1	Nemrut Dag (EA21)	0.076
EA22P7B	Nemrut Dag (EA22)	0.076
EA25P1A	Nemrut Dag (EA25)	0.076
EA25P1B	Nemrut Dag (EA25)	0.076
EA22P6B	Nemrut Dag (EA22)	0.078
EA25P1D	Nemrut Dag (EA25)	0.078

Elements: Ti, Fe, Zr, Ba, Zn

A-Rank:	Nemrut Dag (EA22)	9
B-Rank:	Nemrut Dag (EA25)	1

Specimen	*Location*	*E.D.*
EA22P7A	Nemrut Dag (EA22)	0.067
EA22R1	Nemrut Dag (EA22)	0.075
EA25P2C	Nemrut Dag (EA25)	0.090
EA22P3	Nemrut Dag (EA22)	0.091
EA22P7B	Nemrut Dag (EA22)	0.091
EA22P5B	Nemrut Dag (EA22)	0.093
EA22P1D	Nemrut Dag (EA22)	0.094
EA22P1C	Nemrut Dag (EA22)	0.096
EA22P8B	Nemrut Dag (EA22)	0.107
EA22R2	Nemrut Dag (EA22)	0.107

Elements: Ti, Al, Fe, Mn, Ca, Zr, Ba

A-Rank:	Nemrut Dag (EA25)	10
B-Rank:	-	-

Specimen	*Location*	*E.D.*
EA25P1C	Nemrut Dag (EA25)	0.093
EA25P1A	Nemrut Dag (EA25)	0.096
EA25P1B	Nemrut Dag (EA25)	0.100
EA25P2C	Nemrut Dag (EA25)	0.105
EA25P1D	Nemrut Dag (EA25)	0.107
EA25P2D	Nemrut Dag (EA25)	0.111
EA25R1	Nemrut Dag (EA25)	0.112
EA25P2A	Nemrut Dag (EA25)	0.114
EA25R2	Nemrut Dag (EA25)	0.114
EA25P2B	Nemrut Dag (EA25)	0.115

Table D.1 - Source Assignments of Artifacts based on Euclidean Distance to Centroids of Geological Specimens

Artifact: A15 q1173-3 f517 k2

A-Rank: **Tendurek Dag** **49**
B-Rank: Meydan Dag 11

Elements: Fe, Ti, Ba

A-Rank: Tendurek Dag 7
B-Rank: Pasinler 2

Specimen	*Location*	*E.D.*
EA34P5	Pasinler	0.010
EA09R1	Tendurek Dag	0.014
EA09R2C	Tendurek Dag	0.018
EA09R3C	Tendurek Dag	0.019
EA09R3A	Tendurek Dag	0.020
EA34P4	Pasinler	0.020
EA09R2A	Tendurek Dag	0.025
EA09R3B	Tendurek Dag	0.026
EA09R3E	Tendurek Dag	0.026
EA10P2	Meydan Dag	0.027

Elements: Fe, Zr, Ba

A-Rank: Tendurek Dag 6
B-Rank: Pasinler 2

Specimen	*Location*	*E.D.*
EA34P5	Pasinler	0.007
EA09R1	Tendurek Dag	0.008
EA34P4	Pasinler	0.013
EA68SX1	Meydan Dag	0.014
EA68SX2	Meydan Dag	0.014
EA09R3C	Tendurek Dag	0.017
EA09R2C	Tendurek Dag	0.018
EA09R3A	Tendurek Dag	0.018
EA09R2A	Tendurek Dag	0.022
EA09R3B	Tendurek Dag	0.022

Elements: Ti, Fe, Zr, Ba

A-Rank: Tendurek Dag 8
B-Rank: Pasinler 2

Specimen	*Location*	*E.D.*
EA34P5	Pasinler	0.012
EA09R1	Tendurek Dag	0.014
EA09R2C	Tendurek Dag	0.019
EA09R3A	Tendurek Dag	0.020
EA09R3C	Tendurek Dag	0.020
EA34P4	Pasinler	0.020
EA09R2A	Tendurek Dag	0.026
EA09R3B	Tendurek Dag	0.026
EA09R3E	Tendurek Dag	0.026
EA09R2B	Tendurek Dag	0.028

Elements: Ti, Fe, Mn, Ca, Zr, Ba

A-Rank: Tendurek Dag 5
B-Rank: Meydan Dag 3

Specimen	*Location*	*E.D.*
EA09R1	Tendurek Dag	0.016
EA34P4	Pasinler	0.021
EA34P5	Pasinler	0.021
EA09R3A	Tendurek Dag	0.023
EA09R2C	Tendurek Dag	0.025
EA09R3B	Tendurek Dag	0.028
EA68SX1	Meydan Dag	0.030
EA09R2A	Tendurek Dag	0.031
EA68SX2	Meydan Dag	0.031
EA10P3	Meydan Dag	0.032

Elements: Fe, Ti, Zr

A-Rank: Tendurek Dag 9
B-Rank: Meydan Dag 1

Specimen	*Location*	*E.D.*
EA32P1	Tendurek Dag	0.008
EA09R2C	Tendurek Dag	0.010
EA30R2B	Tendurek Dag	0.010
EA30R3C	Tendurek Dag	0.010
EA30R3E	Tendurek Dag	0.010
EA30R3F	Tendurek Dag	0.010
EA30P1	Tendurek Dag	0.011
EA32R1	Tendurek Dag	0.011
EA34P5	Pasinler	0.011
EA30P2	Tendurek Dag	0.012

Elements: Ti, Zr, Ba

A-Rank: Meydan Dag 4
B-Rank: Tendurek Dag 4

Specimen	*Location*	*E.D.*
EA11R2	Meydan Dag	0.009
EA10P2	Meydan Dag	0.011
EA09R1	Tendurek Dag	0.012
EA34P5	Pasinler	0.012
EA09R2C	Tendurek Dag	0.017
EA09R3A	Tendurek Dag	0.017
EA09R3C	Tendurek Dag	0.018
EA34P4	Pasinler	0.020
EA07R2	Meydan Dag	0.021
EA10R2	Meydan Dag	0.021

Elements: Ti, Fe, Zr, Ba, Zn

A-Rank: Meydan Dag 4
B-Rank: Tendurek Dag 3

Specimen	*Location*	*E.D.*
EA10P3	Meydan Dag	0.064
EA09P1C	Tendurek Dag	0.066
EA34P4	Pasinler	0.068
EA68SX2	Meydan Dag	0.075
EA09R3E	Tendurek Dag	0.089
EA07R2	Meydan Dag	0.095
EA50P2B	Bingol	0.099
EA60B1B	Mus	0.099
EA07P2	Meydan Dag	0.101
EA09R2A	Tendurek Dag	0.101

Elements: Ti, Al, Fe, Mn, Ca, Zr, Ba

A-Rank: Tendurek Dag 7
B-Rank: Pasinler 2

Specimen	*Location*	*E.D.*
EA34P5	Pasinler	0.031
EA09R3A	Tendurek Dag	0.032
EA09R1	Tendurek Dag	0.033
EA34P4	Pasinler	0.034
EA09R2C	Tendurek Dag	0.036
EA09R3B	Tendurek Dag	0.037
EA30R2B	Tendurek Dag	0.038
EA09R2A	Tendurek Dag	0.040
EA10P3	Meydan Dag	0.040
EA09P2	Tendurek Dag	0.042

Table D.1 - Source Assignments of Artifacts based on Euclidean Distance to Centroids of Geological Specimens

Artifact: A15 q295.2 f108 k92

A-Rank: **Tendurek Dag** **61**
B-Rank: Mus 5

Elements: Fe, Ti, Ba

A-Rank:	Tendurek Dag	10
B-Rank:	-	-

Specimen	*Location*	*E.D.*
EA32R2	Tendurek Dag	0.004
EA30R3B	Tendurek Dag	0.006
EA30R3D	Tendurek Dag	0.006
EA32R1	Tendurek Dag	0.006
EA30R2A	Tendurek Dag	0.008
EA09P2	Tendurek Dag	0.009
EA09R2E	Tendurek Dag	0.010
EA30R3E	Tendurek Dag	0.010
EA09R3D	Tendurek Dag	0.011
EA09R2A	Tendurek Dag	0.012

Elements: Fe, Zr, Ba

A-Rank:	Tendurek Dag	10
B-Rank:	-	-

Specimen	*Location*	*E.D.*
EA09R2A	Tendurek Dag	0.023
EA09R3D	Tendurek Dag	0.023
EA30R2B	Tendurek Dag	0.024
EA30P1	Tendurek Dag	0.025
EA30R2A	Tendurek Dag	0.026
EA09R2C	Tendurek Dag	0.028
EA09R3B	Tendurek Dag	0.028
EA31R1	Tendurek Dag	0.028
EA09R2B	Tendurek Dag	0.030
EA09R2E	Tendurek Dag	0.030

Elements: Ti, Fe, Zr, Ba

A-Rank:	Tendurek Dag	10
B-Rank:	-	-

Specimen	*Location*	*E.D.*
EA09R2A	Tendurek Dag	0.023
EA09R3D	Tendurek Dag	0.023
EA30P1	Tendurek Dag	0.026
EA30R2A	Tendurek Dag	0.026
EA30R2B	Tendurek Dag	0.026
EA09R3B	Tendurek Dag	0.028
EA31R1	Tendurek Dag	0.028
EA09R2B	Tendurek Dag	0.030
EA09R2C	Tendurek Dag	0.030
EA09R2E	Tendurek Dag	0.030

Elements: Ti, Fe, Mn, Ca, Zr, Ba

A-Rank:	Tendurek Dag	9
B-Rank:	Pasinler	1

Specimen	*Location*	*E.D.*
EA30R2B	Tendurek Dag	0.026
EA09R2A	Tendurek Dag	0.028
EA30R2A	Tendurek Dag	0.028
EA30P1	Tendurek Dag	0.029
EA09R2E	Tendurek Dag	0.030
EA32R2	Tendurek Dag	0.030
EA09R3B	Tendurek Dag	0.031
EA09P2	Tendurek Dag	0.032
EA31R1	Tendurek Dag	0.033
EA34P4	Pasinler	0.034

Elements: Fe, Ti, Zr

A-Rank:	Tendurek Dag	10
B-Rank:	-	-

Specimen	*Location*	*E.D.*
EA09P1C	Tendurek Dag	0.018
EA09R2A	Tendurek Dag	0.022
EA09R3D	Tendurek Dag	0.023
EA30R1	Tendurek Dag	0.024
EA30P1	Tendurek Dag	0.025
EA30R3C	Tendurek Dag	0.025
EA31R1	Tendurek Dag	0.025
EA09R1	Tendurek Dag	0.026
EA30R2A	Tendurek Dag	0.026
EA30R2B	Tendurek Dag	0.026

Elements: Ti, Zr, Ba

A-Rank:	Kars-Arpacay	4
B-Rank:	Meydan Dag	3

Specimen	*Location*	*E.D.*
EA39P1A	Kars-Arpacay	0.016
EA39P4	Kars-Arpacay	0.018
EA50R1A	Bingol	0.019
EA09R3D	Tendurek Dag	0.020
EA39P3	Kars-Arpacay	0.020
EA39R1	Kars-Arpacay	0.020
EA10P4	Meydan Dag	0.022
EA10R2	Meydan Dag	0.022
EA07R3	Meydan Dag	0.023
EA09R2A	Tendurek Dag	0.023

Elements: Ti, Fe, Zr, Ba, Zn

A-Rank:	Mus	5
B-Rank:	Tendurek Dag	2

Specimen	*Location*	*E.D.*
EA09P1C	Tendurek Dag	0.048
EA10P3	Meydan Dag	0.071
EA60B1B	Mus	0.075
EA34P4	Pasinler	0.079
EA60B1A	Mus	0.088
EA62Y3B	Mus	0.089
EA68SX2	Meydan Dag	0.091
EA62Y4	Mus	0.096
EA09R3E	Tendurek Dag	0.097
EA62Y1A	Mus	0.097

Elements: Ti, Al, Fe, Mn, Ca, Zr, Ba

A-Rank:	Tendurek Dag	10
B-Rank:	-	-

Specimen	*Location*	*E.D.*
EA30P1	Tendurek Dag	0.035
EA30R2B	Tendurek Dag	0.039
EA30R2A	Tendurek Dag	0.042
EA30R3E	Tendurek Dag	0.045
EA09R2A	Tendurek Dag	0.046
EA09R2E	Tendurek Dag	0.046
EA09R3B	Tendurek Dag	0.046
EA09P2	Tendurek Dag	0.048
EA30R3F	Tendurek Dag	0.048
EA09R2D	Tendurek Dag	0.049

Table D.1 - Source Assignments of Artifacts based on Euclidean Distance to Centroids of Geological Specimens

Artifact: A15 q734-1 f372 k14

A-Rank: **Nemrut Dag (EA25)** **77**
B-Rank: Nemrut Dag (EA22) 3

Elements: Fe, Ti, Ba

A-Rank:	Nemrut Dag (EA25)	10
B-Rank:	-	-

Specimen	*Location*	*E.D.*
EA25P3	Nemrut Dag (EA25)	0.014
EA25R1	Nemrut Dag (EA25)	0.017
EA25P1A	Nemrut Dag (EA25)	0.024
EA25P1B	Nemrut Dag (EA25)	0.025
EA25P1D	Nemrut Dag (EA25)	0.027
EA25P2B	Nemrut Dag (EA25)	0.031
EA25P1C	Nemrut Dag (EA25)	0.033
EA25P2A	Nemrut Dag (EA25)	0.034
EA25P2D	Nemrut Dag (EA25)	0.037
EA25P2C	Nemrut Dag (EA25)	0.038

Elements: Fe, Zr, Ba

A-Rank:	Nemrut Dag (EA25)	10
B-Rank:	-	-

Specimen	*Location*	*E.D.*
EA25P1A	Nemrut Dag (EA25)	0.024
EA25P1B	Nemrut Dag (EA25)	0.025
EA25P1D	Nemrut Dag (EA25)	0.025
EA25R1	Nemrut Dag (EA25)	0.027
EA25P3	Nemrut Dag (EA25)	0.030
EA25P1C	Nemrut Dag (EA25)	0.033
EA25P2C	Nemrut Dag (EA25)	0.044
EA25P2D	Nemrut Dag (EA25)	0.044
EA25P2A	Nemrut Dag (EA25)	0.045
EA25P2B	Nemrut Dag (EA25)	0.045

Elements: Ti, Fe, Zr, Ba

A-Rank:	Nemrut Dag (EA25)	10
B-Rank:	-	-

Specimen	*Location*	*E.D.*
EA25P1A	Nemrut Dag (EA25)	0.025
EA25P1B	Nemrut Dag (EA25)	0.025
EA25P1D	Nemrut Dag (EA25)	0.027
EA25R1	Nemrut Dag (EA25)	0.027
EA25P3	Nemrut Dag (EA25)	0.030
EA25P1C	Nemrut Dag (EA25)	0.034
EA25P2A	Nemrut Dag (EA25)	0.045
EA25P2C	Nemrut Dag (EA25)	0.045
EA25P2B	Nemrut Dag (EA25)	0.046
EA25P2D	Nemrut Dag (EA25)	0.046

Elements: Ti, Fe, Mn, Ca, Zr, Ba

A-Rank:	Nemrut Dag (EA25)	10
B-Rank:	-	-

Specimen	*Location*	*E.D.*
EA25P1C	Nemrut Dag (EA25)	0.041
EA25P1A	Nemrut Dag (EA25)	0.047
EA25P1B	Nemrut Dag (EA25)	0.056
EA25P3	Nemrut Dag (EA25)	0.059
EA25R1	Nemrut Dag (EA25)	0.061
EA25P2B	Nemrut Dag (EA25)	0.068
EA25P2A	Nemrut Dag (EA25)	0.070
EA25P2C	Nemrut Dag (EA25)	0.070
EA25P1D	Nemrut Dag (EA25)	0.075
EA25P2D	Nemrut Dag (EA25)	0.076

Elements: Fe, Ti, Zr

A-Rank:	Nemrut Dag (EA25)	10
B-Rank:	-	-

Specimen	*Location*	*E.D.*
EA25P1A	Nemrut Dag (EA25)	0.010
EA25P1B	Nemrut Dag (EA25)	0.012
EA25P1C	Nemrut Dag (EA25)	0.016
EA25P1D	Nemrut Dag (EA25)	0.020
EA25R1	Nemrut Dag (EA25)	0.023
EA25P3	Nemrut Dag (EA25)	0.029
EA25P2C	Nemrut Dag (EA25)	0.030
EA25P2A	Nemrut Dag (EA25)	0.032
EA25P2D	Nemrut Dag (EA25)	0.033
EA25P2B	Nemrut Dag (EA25)	0.039

Elements: Ti, Zr, Ba

A-Rank:	Nemrut Dag (EA25)	10
B-Rank:	-	-

Specimen	*Location*	*E.D.*
EA25P1D	Nemrut Dag (EA25)	0.022
EA25P1A	Nemrut Dag (EA25)	0.023
EA25P1B	Nemrut Dag (EA25)	0.023
EA25R1	Nemrut Dag (EA25)	0.026
EA25P3	Nemrut Dag (EA25)	0.029
EA25P1C	Nemrut Dag (EA25)	0.032
EA25P2C	Nemrut Dag (EA25)	0.042
EA25P2D	Nemrut Dag (EA25)	0.043
EA25P2B	Nemrut Dag (EA25)	0.044
EA25P2A	Nemrut Dag (EA25)	0.045

Elements: Ti, Fe, Zr, Ba, Zn

A-Rank:	Nemrut Dag (EA25)	7
B-Rank:	Nemrut Dag (EA22)	3

Specimen	*Location*	*E.D.*
EA25P1A	Nemrut Dag (EA25)	0.042
EA25P1D	Nemrut Dag (EA25)	0.044
EA25P1B	Nemrut Dag (EA25)	0.045
EA25P2C	Nemrut Dag (EA25)	0.059
EA25P2D	Nemrut Dag (EA25)	0.070
EA25P2B	Nemrut Dag (EA25)	0.074
EA25P1C	Nemrut Dag (EA25)	0.077
EA22P8B	Nemrut Dag (EA22)	0.088
EA22P7B	Nemrut Dag (EA22)	0.089
EA22P1C	Nemrut Dag (EA22)	0.090

Elements: Ti, Al, Fe, Mn, Ca, Zr, Ba

A-Rank:	Nemrut Dag (EA25)	10
B-Rank:	-	-

Specimen	*Location*	*E.D.*
EA25P1C	Nemrut Dag (EA25)	0.054
EA25P1A	Nemrut Dag (EA25)	0.056
EA25P1B	Nemrut Dag (EA25)	0.067
EA25P3	Nemrut Dag (EA25)	0.067
EA25R1	Nemrut Dag (EA25)	0.067
EA25P2B	Nemrut Dag (EA25)	0.076
EA25P2C	Nemrut Dag (EA25)	0.079
EA25P2A	Nemrut Dag (EA25)	0.080
EA25P1D	Nemrut Dag (EA25)	0.085
EA25P2D	Nemrut Dag (EA25)	0.085

Table D.1 - Source Assignments of Artifacts based on Euclidean Distance to Centroids of Geological Specimens

Artifact: A15 q752-2 f386 k15

A-Rank: **Pasinler** **54**
B-Rank: **Mus** **14**

Elements: Fe, Ti, Ba

A-Rank:	Tendurek Dag	7
B-Rank:	Pasinler	2

Specimen	*Location*	*E.D.*
EA09R2C	Tendurek Dag	0.010
EA09R3C	Tendurek Dag	0.011
EA09R3A	Tendurek Dag	0.012
EA34P4	Pasinler	0.012
EA09R2A	Tendurek Dag	0.013
EA10P3	Meydan Dag	0.014
EA34P5	Pasinler	0.014
EA09R3E	Tendurek Dag	0.015
EA32R1	Tendurek Dag	0.015
EA09R3B	Tendurek Dag	0.016

Elements: Fe, Zr, Ba

A-Rank:	Pasinler	10
B-Rank:	-	-

Specimen	*Location*	*E.D.*
EA33P8	Pasinler	0.035
EA35P3	Pasinler	0.043
EA34P3	Pasinler	0.045
EA33P3	Pasinler	0.046
EA35P2	Pasinler	0.046
EA33P7	Pasinler	0.047
EA34R2	Pasinler	0.048
EA33P5	Pasinler	0.051
EA34P1	Pasinler	0.051
EA35R1	Pasinler	0.052

Elements: Ti, Fe, Zr, Ba

A-Rank:	Pasinler	10
B-Rank:	-	-

Specimen	*Location*	*E.D.*
EA33P8	Pasinler	0.042
EA33P7	Pasinler	0.048
EA34P3	Pasinler	0.048
EA35P2	Pasinler	0.048
EA35P3	Pasinler	0.048
EA33P3	Pasinler	0.049
EA34R2	Pasinler	0.052
EA33P5	Pasinler	0.054
EA34P1	Pasinler	0.055
EA35R1	Pasinler	0.057

Elements: Ti, Fe, Mn, Ca, Zr, Ba

A-Rank:	Pasinler	10
B-Rank:	-	-

Specimen	*Location*	*E.D.*
EA33P8	Pasinler	0.049
EA34P3	Pasinler	0.052
EA35P2	Pasinler	0.055
EA35P3	Pasinler	0.057
EA33P7	Pasinler	0.060
EA34P1	Pasinler	0.060
EA33P5	Pasinler	0.061
EA35R1	Pasinler	0.067
EA35P1	Pasinler	0.068
EA34P2	Pasinler	0.069

Elements: Fe, Ti, Zr

A-Rank:	Pasinler	7
B-Rank:	Bogazkoy	2

Specimen	*Location*	*E.D.*
EA33P7	Pasinler	0.036
EA45P4	Erzincan	0.036
EA34P2	Pasinler	0.037
EA34R1	Pasinler	0.037
EA34P3	Pasinler	0.038
CA05R5D	Bogazkoy	0.039
EA33P1B	Pasinler	0.039
EA33P2B	Pasinler	0.039
EA33P5	Pasinler	0.039
CA05R4A	Bogazkoy	0.040

Elements: Ti, Zr, Ba

A-Rank:	Pasinler	10
B-Rank:	-	-

Specimen	*Location*	*E.D.*
EA33P8	Pasinler	0.026
EA34P3	Pasinler	0.033
EA35P2	Pasinler	0.033
EA33P7	Pasinler	0.034
EA35P3	Pasinler	0.034
EA33P3	Pasinler	0.035
EA34R2	Pasinler	0.039
EA33P5	Pasinler	0.041
EA34P1	Pasinler	0.042
EA35P1	Pasinler	0.046

Elements: Ti, Fe, Zr, Ba, Zn

A-Rank:	Mus	9
B-Rank:	Tendurek Dag	1

Specimen	*Location*	*E.D.*
EA60B1B	Mus	0.216
EA62Y1A	Mus	0.216
EA60B1A	Mus	0.238
EA62Y3B	Mus	0.244
EA09P1C	Tendurek Dag	0.249
EA62Y4	Mus	0.255
EA57B1	Mus	0.257
EA58B1	Mus	0.262
EA62Y1C	Mus	0.268
EA62Y1B	Mus	0.269

Elements: Ti, Al, Fe, Mn, Ca, Zr, Ba

A-Rank:	Mus	5
B-Rank:	Pasinler	5

Specimen	*Location*	*E.D.*
EA62Y2B	Mus	0.081
EA35P2	Pasinler	0.084
EA61B2	Mus	0.084
EA34P3	Pasinler	0.085
EA35P3	Pasinler	0.087
EA34P1	Pasinler	0.088
EA60B1A	Mus	0.088
EA35R1	Pasinler	0.089
EA60B2	Mus	0.089
EA62Y3B	Mus	0.089

Table D.1 - Source Assignments of Artifacts based on Euclidean Distance to Centroids of Geological Specimens

Artifact: A16 q202-2 f83 k105

A-Rank: **Tendurek Dag** **64**
B-Rank: Meydan Dag 6

Elements: Fe, Ti, Ba

A-Rank:	Tendurek Dag	10
B-Rank:	-	-

Specimen	*Location*	*E.D.*
EA30R3A	Tendurek Dag	0.004
EA09P1B	Tendurek Dag	0.008
EA31R1	Tendurek Dag	0.009
EA09P1A	Tendurek Dag	0.010
EA30R3G	Tendurek Dag	0.010
EA31P1	Tendurek Dag	0.010
EA09P1D	Tendurek Dag	0.011
EA09P1C	Tendurek Dag	0.012
EA09R2D	Tendurek Dag	0.013
EA30R1	Tendurek Dag	0.013

Elements: Fe, Zr, Ba

A-Rank:	Tendurek Dag	10
B-Rank:	-	-

Specimen	*Location*	*E.D.*
EA30R3C	Tendurek Dag	0.003
EA30R1	Tendurek Dag	0.006
EA30R3F	Tendurek Dag	0.007
EA31R1	Tendurek Dag	0.008
EA09P1C	Tendurek Dag	0.010
EA30P1	Tendurek Dag	0.010
EA30R3A	Tendurek Dag	0.011
EA30R3G	Tendurek Dag	0.011
EA32P1	Tendurek Dag	0.011
EA09P1B	Tendurek Dag	0.013

Elements: Ti, Fe, Zr, Ba

A-Rank:	Tendurek Dag	10
B-Rank:	-	-

Specimen	*Location*	*E.D.*
EA31R1	Tendurek Dag	0.009
EA30R3A	Tendurek Dag	0.011
EA09P1C	Tendurek Dag	0.013
EA09P1D	Tendurek Dag	0.013
EA30R1	Tendurek Dag	0.013
EA09P1B	Tendurek Dag	0.014
EA30R3C	Tendurek Dag	0.014
EA30R3G	Tendurek Dag	0.014
EA09P1A	Tendurek Dag	0.015
EA09R2D	Tendurek Dag	0.016

Elements: Ti, Fe, Mn, Ca, Zr, Ba

A-Rank:	Tendurek Dag	10
B-Rank:	-	-

Specimen	*Location*	*E.D.*
EA30R3G	Tendurek Dag	0.014
EA31R1	Tendurek Dag	0.016
EA09P1A	Tendurek Dag	0.017
EA31P1	Tendurek Dag	0.017
EA09R2D	Tendurek Dag	0.018
EA09P1D	Tendurek Dag	0.019
EA30P1	Tendurek Dag	0.020
EA32R2	Tendurek Dag	0.020
EA30R2A	Tendurek Dag	0.021
EA30R3A	Tendurek Dag	0.021

Elements: Fe, Ti, Zr

A-Rank:	Tendurek Dag	10
B-Rank:	-	-

Specimen	*Location*	*E.D.*
EA31R1	Tendurek Dag	0.007
EA09P1D	Tendurek Dag	0.009
EA09R2A	Tendurek Dag	0.009
EA09R3B	Tendurek Dag	0.009
EA32R2	Tendurek Dag	0.009
EA09P1C	Tendurek Dag	0.010
EA09P2	Tendurek Dag	0.010
EA09R2E	Tendurek Dag	0.010
EA09R1	Tendurek Dag	0.011
EA09R2B	Tendurek Dag	0.011

Elements: Ti, Zr, Ba

A-Rank:	Tendurek Dag	4
B-Rank:	Meydan Dag	4

Specimen	*Location*	*E.D.*
8EA49P1	Bingol	0.007
EA31R1	Tendurek Dag	0.009
EA07P2	Meydan Dag	0.010
EA07P3	Meydan Dag	0.011
EA30R3A	Tendurek Dag	0.011
EA09P1C	Tendurek Dag	0.012
EA39P1B	Kars-Arpacay	0.012
EA08P1	Meydan Dag	0.013
EA08P2	Meydan Dag	0.013
EA09P1D	Tendurek Dag	0.013

Elements: Ti, Fe, Zr, Ba, Zn

A-Rank:	Mus	6
B-Rank:	Meydan Dag	2

Specimen	*Location*	*E.D.*
EA09P1C	Tendurek Dag	0.076
EA60B1B	Mus	0.090
EA62Y1A	Mus	0.107
EA10P3	Meydan Dag	0.109
EA60B1A	Mus	0.112
EA62Y3B	Mus	0.114
EA34P4	Pasinler	0.117
EA62Y4	Mus	0.119
EA62Y1C	Mus	0.127
EA68SX2	Meydan Dag	0.127

Elements: Ti, Al, Fe, Mn, Ca, Zr, Ba

A-Rank:	Tendurek Dag	10
B-Rank:	-	-

Specimen	*Location*	*E.D.*
EA30P1	Tendurek Dag	0.031
EA30P2	Tendurek Dag	0.039
EA30R3D	Tendurek Dag	0.039
EA30R3E	Tendurek Dag	0.039
EA30R3G	Tendurek Dag	0.039
EA30R2A	Tendurek Dag	0.040
EA30R3A	Tendurek Dag	0.040
EA30R3F	Tendurek Dag	0.040
EA30R2B	Tendurek Dag	0.041
EA09P1A	Tendurek Dag	0.042

Table D.1 - Source Assignments of Artifacts based on Euclidean Distance to Centroids of Geological Specimens

Artifact: A16 q21.1 f26 k5

A-Rank: **Nemrut Dag (EA25)** **39**
B-Rank: Nemrut Dag (EA22) 30

Elements: Fe, Ti, Ba

A-Rank:	Nemrut Dag (EA25)	10
B-Rank:	-	-

Specimen	*Location*	*E.D.*
EA25R2	Nemrut Dag (EA25)	0.006
EA25P1C	Nemrut Dag (EA25)	0.009
EA25P2A	Nemrut Dag (EA25)	0.010
EA25P2C	Nemrut Dag (EA25)	0.012
EA25P1B	Nemrut Dag (EA25)	0.013
EA25P1A	Nemrut Dag (EA25)	0.014
EA25P2D	Nemrut Dag (EA25)	0.014
EA25P2B	Nemrut Dag (EA25)	0.015
EA25R1	Nemrut Dag (EA25)	0.020
EA25P1D	Nemrut Dag (EA25)	0.021

Elements: Fe, Zr, Ba

A-Rank:	Nemrut Dag (EA22)	7
B-Rank:	Nemrut Dag (EA21)	3

Specimen	*Location*	*E.D.*
EA22P5A	Nemrut Dag (EA22)	0.062
EA21P1	Nemrut Dag (EA21)	0.067
EA22P4	Nemrut Dag (EA22)	0.068
EA22P7A	Nemrut Dag (EA22)	0.068
EA22P6A	Nemrut Dag (EA22)	0.069
EA21R1A	Nemrut Dag (EA21)	0.070
EA21R1B	Nemrut Dag (EA21)	0.070
EA22P5B	Nemrut Dag (EA22)	0.071
EA22P3	Nemrut Dag (EA22)	0.072
EA22P8B	Nemrut Dag (EA22)	0.073

Elements: Ti, Fe, Zr, Ba

A-Rank:	Nemrut Dag (EA25)	4
B-Rank:	Nemrut Dag (EA22)	4

Specimen	*Location*	*E.D.*
EA22P7A	Nemrut Dag (EA22)	0.081
EA25P1D	Nemrut Dag (EA25)	0.081
EA25P1A	Nemrut Dag (EA25)	0.082
EA25P1B	Nemrut Dag (EA25)	0.082
EA25P1C	Nemrut Dag (EA25)	0.086
EA22P5A	Nemrut Dag (EA22)	0.087
EA22P8B	Nemrut Dag (EA22)	0.088
EA22P6B	Nemrut Dag (EA22)	0.089
EA21P1	Nemrut Dag (EA21)	0.092
EA21R1B	Nemrut Dag (EA21)	0.092

Elements: Ti, Fe, Mn, Ca, Zr, Ba

A-Rank:	Nemrut Dag (EA25)	8
B-Rank:	Nemrut Dag (EA22)	2

Specimen	*Location*	*E.D.*
EA25P1A	Nemrut Dag (EA25)	0.087
EA25P1C	Nemrut Dag (EA25)	0.087
EA25P1B	Nemrut Dag (EA25)	0.092
EA25P1D	Nemrut Dag (EA25)	0.102
EA22P7B	Nemrut Dag (EA22)	0.106
EA25R1	Nemrut Dag (EA25)	0.110
EA25P2C	Nemrut Dag (EA25)	0.111
EA25P3	Nemrut Dag (EA25)	0.114
EA22P4	Nemrut Dag (EA22)	0.115
EA25P2A	Nemrut Dag (EA25)	0.117

Elements: Fe, Ti, Zr

A-Rank:	Nemrut Dag (EA22)	6
B-Rank:	Nemrut Dag (EA25)	3

Specimen	*Location*	*E.D.*
EA25P1D	Nemrut Dag (EA25)	0.079
EA22P7A	Nemrut Dag (EA22)	0.081
EA25P1A	Nemrut Dag (EA25)	0.081
EA25P1B	Nemrut Dag (EA25)	0.081
EA25P1C	Nemrut Dag (EA25)	0.086
EA22P5A	Nemrut Dag (EA22)	0.087
EA22P8B	Nemrut Dag (EA22)	0.087
EA22P6B	Nemrut Dag (EA22)	0.089
EA22P4	Nemrut Dag (EA22)	0.090
EA21R1B	Nemrut Dag (EA21)	0.091

Elements: Ti, Zr, Ba

A-Rank:	Nemrut Dag (EA22)	7
B-Rank:	Nemrut Dag (EA21)	2

Specimen	*Location*	*E.D.*
EA22P7A	Nemrut Dag (EA22)	0.066
EA22P5A	Nemrut Dag (EA22)	0.076
EA22P8B	Nemrut Dag (EA22)	0.076
EA22R1	Nemrut Dag (EA22)	0.076
EA21P1	Nemrut Dag (EA21)	0.078
EA21R1B	Nemrut Dag (EA21)	0.079
EA22P6B	Nemrut Dag (EA22)	0.079
EA22P3	Nemrut Dag (EA22)	0.081
EA22P7B	Nemrut Dag (EA22)	0.081
EA25P1A	Nemrut Dag (EA25)	0.081

Elements: Ti, Fe, Zr, Ba, Zn

A-Rank:	Nemrut Dag (EA22)	6
B-Rank:	Nemrut Dag (EA25)	4

Specimen	*Location*	*E.D.*
EA25P1D	Nemrut Dag (EA25)	0.083
EA25P1A	Nemrut Dag (EA25)	0.084
EA25P1B	Nemrut Dag (EA25)	0.085
EA22P8B	Nemrut Dag (EA22)	0.091
EA22P6B	Nemrut Dag (EA22)	0.094
EA22P7B	Nemrut Dag (EA22)	0.094
EA22P3	Nemrut Dag (EA22)	0.096
EA22P6A	Nemrut Dag (EA22)	0.096
EA22P7A	Nemrut Dag (EA22)	0.097
EA25P1C	Nemrut Dag (EA25)	0.103

Elements: Ti, Al, Fe, Mn, Ca, Zr, Ba

A-Rank:	Nemrut Dag (EA25)	10
B-Rank:	-	-

Specimen	*Location*	*E.D.*
EA25P1A	Nemrut Dag (EA25)	0.087
EA25P1C	Nemrut Dag (EA25)	0.087
EA25P1B	Nemrut Dag (EA25)	0.092
EA25P1D	Nemrut Dag (EA25)	0.102
EA25R1	Nemrut Dag (EA25)	0.110
EA25P2C	Nemrut Dag (EA25)	0.111
EA22P7B	Nemrut Dag (EA22)	0.112
EA25P3	Nemrut Dag (EA25)	0.114
EA25P2A	Nemrut Dag (EA25)	0.117
EA25P2D	Nemrut Dag (EA25)	0.118

Table D.1 - Source Assignments of Artifacts based on Euclidean Distance to Centroids of Geological Specimens

Artifact: A16 q633-2 f208 k110

A-Rank: **Bingol B** **56**
B-Rank: Gutansar 10

Elements: Fe, Ti, Ba

A-Rank: Bingol B 7
B-Rank: Gutansar 2

Specimen	*Location*	*E.D.*
EA52B1	Bingol B	0.029
EA52B3	Bingol B	0.035
EA56B1	Bingol B	0.038
EA53B2	Bingol B	0.039
EA53B1	Bingol B	0.040
EA52B2	Bingol B	0.045
EA54B1	Bingol B	0.081
AR06E2A	Gutansar	0.128
AR21avH1	Chazencavan	0.128
AR30jfL1	Gutansar	0.130

Elements: Fe, Zr, Ba

A-Rank: Bingol B 6
B-Rank: Erzincan 4

Specimen	*Location*	*E.D.*
EA52B3	Bingol B	0.051
EA53B2	Bingol B	0.054
EA52B1	Bingol B	0.056
EA56B1	Bingol B	0.057
EA52B2	Bingol B	0.060
EA43P1	Erzincan	0.065
EA53B1	Bingol B	0.065
EA43P2A	Erzincan	0.069
EA44P2	Erzincan	0.073
EA44P3	Erzincan	0.075

Elements: Ti, Fe, Zr, Ba

A-Rank: Bingol B 7
B-Rank: Gutansar 2

Specimen	*Location*	*E.D.*
EA52B3	Bingol B	0.053
EA52B1	Bingol B	0.056
EA53B2	Bingol B	0.058
EA52B2	Bingol B	0.061
EA56B1	Bingol B	0.063
EA53B1	Bingol B	0.069
EA54B1	Bingol B	0.096
AR30jfL1	Gutansar	0.152
AR06E2A	Gutansar	0.153
AR21avH1	Chazencavan	0.155

Elements: Ti, Fe, Mn, Ca, Zr, Ba

A-Rank: Bingol B 7
B-Rank: Acigol 3

Specimen	*Location*	*E.D.*
EA52B3	Bingol B	0.054
EA52B1	Bingol B	0.061
EA56B1	Bingol B	0.064
EA53B2	Bingol B	0.066
EA53B1	Bingol B	0.071
EA52B2	Bingol B	0.073
EA54B1	Bingol B	0.105
CA08R1A	Acigol	0.186
CA08R1C	Acigol	0.186
CA07R2A	Acigol	0.196

Elements: Fe, Ti, Zr

A-Rank: Bingol B 7
B-Rank: Gutansar 2

Specimen	*Location*	*E.D.*
EA52B3	Bingol B	0.044
EA52B1	Bingol B	0.048
EA52B2	Bingol B	0.054
EA56B1	Bingol B	0.057
EA53B2	Bingol B	0.058
EA53B1	Bingol B	0.069
EA54B1	Bingol B	0.090
AR76rB3	Gutansar	0.127
AR06E1C	Gutansar	0.130
AR40rlS1	Erevan	0.130

Elements: Ti, Zr, Ba

A-Rank: Bingol B 9
B-Rank: Erevan 1

Specimen	*Location*	*E.D.*
EA52B2	Bingol B	0.050
EA52B3	Bingol B	0.050
EA53B2	Bingol B	0.050
EA52B1	Bingol B	0.055
EA54B1	Bingol B	0.060
EA53B1	Bingol B	0.061
EA55B2	Bingol B	0.063
EA56B1	Bingol B	0.063
EA55B1	Bingol B	0.075
AR24jfL1	Erevan	0.106

Elements: Ti, Fe, Zr, Ba, Zn

A-Rank: Bingol B 6
B-Rank: Gutansar 4

Specimen	*Location*	*E.D.*
EA53B1	Bingol B	0.123
EA52B1	Bingol B	0.165
EA52B3	Bingol B	0.178
AR06E2B	Gutansar	0.191
EA52B2	Bingol B	0.196
EA54B1	Bingol B	0.198
AR11jB1	Gutansar	0.201
EA56B1	Bingol B	0.208
AR12jB1	Gutansar	0.216
AR06E1B	Gutansar	0.217

Elements: Ti, Al, Fe, Mn, Ca, Zr, Ba

A-Rank: Bingol B 7
B-Rank: Acigol 3

Specimen	*Location*	*E.D.*
EA53B2	Bingol B	0.083
EA53B1	Bingol B	0.086
EA52B3	Bingol B	0.089
EA56B1	Bingol B	0.090
EA52B1	Bingol B	0.093
EA52B2	Bingol B	0.101
EA54B1	Bingol B	0.123
CA08R1A	Acigol	0.186
CA08R1C	Acigol	0.186
CA07R2A	Acigol	0.197

Table D.1 - Source Assignments of Artifacts based on Euclidean Distance to Centroids of Geological Specimens

Artifact: A17 q231-2 f107 k12

A-Rank: **Bingol B** **57**
B-Rank: Gutansar 11

Elements: Fe, Ti, Ba

A-Rank:	Bingol B	7
B-Rank:	Gutansar	2

Specimen	*Location*	*E.D.*
EA52B1	Bingol B	0.011
EA52B3	Bingol B	0.021
EA56B1	Bingol B	0.031
EA52B2	Bingol B	0.036
EA53B2	Bingol B	0.044
EA53B1	Bingol B	0.050
EA54B1	Bingol B	0.076
AR06E2A	Gutansar	0.117
AR21avH1	Chazencavan	0.118
AR06E1A	Gutansar	0.119

Elements: Fe, Zr, Ba

A-Rank:	Bingol B	6
B-Rank:	Erzincan	4

Specimen	*Location*	*E.D.*
EA52B3	Bingol B	0.034
EA52B1	Bingol B	0.037
EA56B1	Bingol B	0.039
EA52B2	Bingol B	0.045
EA53B2	Bingol B	0.048
EA53B1	Bingol B	0.061
EA43P1	Erzincan	0.080
EA44P2	Erzincan	0.083
EA44P3	Erzincan	0.083
EA43R2	Erzincan	0.084

Elements: Ti, Fe, Zr, Ba

A-Rank:	Bingol B	7
B-Rank:	Gutansar	3

Specimen	*Location*	*E.D.*
EA52B3	Bingol B	0.035
EA52B1	Bingol B	0.037
EA52B2	Bingol B	0.046
EA56B1	Bingol B	0.049
EA53B2	Bingol B	0.055
EA53B1	Bingol B	0.066
EA54B1	Bingol B	0.086
AR30jfL1	Gutansar	0.150
AR06E2A	Gutansar	0.152
AR06E3A	Gutansar	0.152

Elements: Ti, Fe, Mn, Ca, Zr, Ba

A-Rank:	Bingol B	7
B-Rank:	Acigol	3

Specimen	*Location*	*E.D.*
EA52B1	Bingol B	0.039
EA52B3	Bingol B	0.042
EA52B2	Bingol B	0.047
EA56B1	Bingol B	0.053
EA53B2	Bingol B	0.055
EA53B1	Bingol B	0.069
EA54B1	Bingol B	0.114
CA08R1A	Acigol	0.171
CA08R1C	Acigol	0.174
CA07R2A	Acigol	0.184

Elements: Fe, Ti, Zr

A-Rank:	Bingol B	7
B-Rank:	Gutansar	3

Specimen	*Location*	*E.D.*
EA52B3	Bingol B	0.034
EA52B1	Bingol B	0.036
EA52B2	Bingol B	0.045
EA56B1	Bingol B	0.048
EA53B2	Bingol B	0.052
EA53B1	Bingol B	0.061
EA54B1	Bingol B	0.085
AR76rB3	Gutansar	0.133
AR76rB2	Gutansar	0.137
AR06E1C	Gutansar	0.138

Elements: Ti, Zr, Ba

A-Rank:	Bingol B	9
B-Rank:	Erevan	1

Specimen	*Location*	*E.D.*
EA52B2	Bingol B	0.030
EA52B3	Bingol B	0.030
EA52B1	Bingol B	0.036
EA54B1	Bingol B	0.041
EA53B2	Bingol B	0.044
EA55B2	Bingol B	0.048
EA56B1	Bingol B	0.049
EA53B1	Bingol B	0.057
EA55B1	Bingol B	0.060
AR24jfL1	Erevan	0.104

Elements: Ti, Fe, Zr, Ba, Zn

A-Rank:	Bingol B	7
B-Rank:	Gutansar	3

Specimen	*Location*	*E.D.*
EA52B1	Bingol B	0.064
EA53B1	Bingol B	0.066
EA52B3	Bingol B	0.075
EA52B2	Bingol B	0.095
EA56B1	Bingol B	0.107
EA54B1	Bingol B	0.111
EA53B2	Bingol B	0.140
AR06E2B	Gutansar	0.153
AR12jB1	Gutansar	0.160
AR11jB1	Gutansar	0.163

Elements: Ti, Al, Fe, Mn, Ca, Zr, Ba

A-Rank:	Bingol B	7
B-Rank:	Acigol	3

Specimen	*Location*	*E.D.*
EA53B2	Bingol B	0.066
EA52B1	Bingol B	0.068
EA52B3	Bingol B	0.071
EA52B2	Bingol B	0.073
EA56B1	Bingol B	0.073
EA53B1	Bingol B	0.077
EA54B1	Bingol B	0.124
CA08R1A	Acigol	0.171
CA08R1C	Acigol	0.175
CA07R2A	Acigol	0.184

Table D.1 - Source Assignments of Artifacts based on Euclidean Distance to Centroids of Geological Specimens

Artifact: A18 q23-1 f24 k23

A-Rank: **Nemrut Dag (EA25)** **49**
B-Rank: Nemrut Dag (EA22) 26

Elements: Fe, Ti, Ba

A-Rank:	Nemrut Dag (EA25)	10
B-Rank:	-	-

Specimen	*Location*	*E.D.*
EA25P1B	Nemrut Dag (EA25)	0.004
EA25P1A	Nemrut Dag (EA25)	0.005
EA25P1C	Nemrut Dag (EA25)	0.009
EA25R1	Nemrut Dag (EA25)	0.009
EA25P2A	Nemrut Dag (EA25)	0.011
EA25P2B	Nemrut Dag (EA25)	0.011
EA25P3	Nemrut Dag (EA25)	0.014
EA25P1D	Nemrut Dag (EA25)	0.015
EA25P2C	Nemrut Dag (EA25)	0.015
EA25P2D	Nemrut Dag (EA25)	0.015

Elements: Fe, Zr, Ba

A-Rank:	Nemrut Dag (EA22)	6
B-Rank:	Nemrut Dag (EA21)	3

Specimen	*Location*	*E.D.*
EA22P4	Nemrut Dag (EA22)	0.053
EA22P5A	Nemrut Dag (EA22)	0.053
EA21R1B	Nemrut Dag (EA21)	0.059
EA22P5B	Nemrut Dag (EA22)	0.059
EA22P6A	Nemrut Dag (EA22)	0.059
EA22P7A	Nemrut Dag (EA22)	0.059
EA21P1	Nemrut Dag (EA21)	0.060
EA22P3	Nemrut Dag (EA22)	0.060
EA25P1D	Nemrut Dag (EA25)	0.060
EA21R1A	Nemrut Dag (EA21)	0.061

Elements: Ti, Fe, Zr, Ba

A-Rank:	Nemrut Dag (EA25)	5
B-Rank:	Nemrut Dag (EA22)	5

Specimen	*Location*	*E.D.*
EA25P1A	Nemrut Dag (EA25)	0.061
EA25P1B	Nemrut Dag (EA25)	0.061
EA25P1D	Nemrut Dag (EA25)	0.061
EA25P1C	Nemrut Dag (EA25)	0.067
EA22P7A	Nemrut Dag (EA22)	0.076
EA25R1	Nemrut Dag (EA25)	0.079
EA22P8B	Nemrut Dag (EA22)	0.080
EA22P6B	Nemrut Dag (EA22)	0.081
EA22P4	Nemrut Dag (EA22)	0.083
EA22P5A	Nemrut Dag (EA22)	0.083

Elements: Ti, Fe, Mn, Ca, Zr, Ba

A-Rank:	Nemrut Dag (EA25)	10
B-Rank:	-	-

Specimen	*Location*	*E.D.*
EA25P1A	Nemrut Dag (EA25)	0.062
EA25P1B	Nemrut Dag (EA25)	0.062
EA25P1D	Nemrut Dag (EA25)	0.064
EA25P1C	Nemrut Dag (EA25)	0.073
EA25R1	Nemrut Dag (EA25)	0.080
EA25P2C	Nemrut Dag (EA25)	0.083
EA25P3	Nemrut Dag (EA25)	0.085
EA25P2D	Nemrut Dag (EA25)	0.087
EA25P2A	Nemrut Dag (EA25)	0.089
EA25P2B	Nemrut Dag (EA25)	0.093

Elements: Fe, Ti, Zr

A-Rank:	Nemrut Dag (EA25)	6
B-Rank:	Nemrut Dag (EA22)	4

Specimen	*Location*	*E.D.*
EA25P1D	Nemrut Dag (EA25)	0.060
EA25P1A	Nemrut Dag (EA25)	0.061
EA25P1B	Nemrut Dag (EA25)	0.061
EA25P1C	Nemrut Dag (EA25)	0.067
EA22P7A	Nemrut Dag (EA22)	0.075
EA25R1	Nemrut Dag (EA25)	0.079
EA22P8B	Nemrut Dag (EA22)	0.080
EA22P6B	Nemrut Dag (EA22)	0.081
EA25P2C	Nemrut Dag (EA25)	0.082
EA22P4	Nemrut Dag (EA22)	0.083

Elements: Ti, Zr, Ba

A-Rank:	Nemrut Dag (EA25)	5
B-Rank:	Nemrut Dag (EA22)	4

Specimen	*Location*	*E.D.*
EA22P7A	Nemrut Dag (EA25)	0.056
EA25P1D	Nemrut Dag (EA25)	0.060
EA25P1A	Nemrut Dag (EA25)	0.061
EA25P1B	Nemrut Dag (EA25)	0.061
EA22P8B	Nemrut Dag (EA22)	0.064
EA22R1	Nemrut Dag (EA22)	0.065
EA22P6B	Nemrut Dag (EA22)	0.066
EA25P1C	Nemrut Dag (EA25)	0.067
EA22P5A	Nemrut Dag (EA22)	0.069
EA21R1B	Nemrut Dag (EA21)	0.070

Elements: Ti, Fe, Zr, Ba, Zn

A-Rank:	Nemrut Dag (EA22)	7
B-Rank:	Nemrut Dag (EA25)	3

Specimen	*Location*	*E.D.*
EA22P7A	Nemrut Dag (EA22)	0.122
EA25P2C	Nemrut Dag (EA25)	0.128
EA22P5B	Nemrut Dag (EA22)	0.132
EA22R1	Nemrut Dag (EA22)	0.133
EA22P1D	Nemrut Dag (EA22)	0.144
EA22P3	Nemrut Dag (EA22)	0.153
EA22P1C	Nemrut Dag (EA22)	0.167
EA22P7B	Nemrut Dag (EA22)	0.172
EA25P1A	Nemrut Dag (EA25)	0.180
EA25P1D	Nemrut Dag (EA25)	0.180

Elements: Ti, Al, Fe, Mn, Ca, Zr, Ba

A-Rank:	Nemrut Dag (EA25)	10
B-Rank:	-	-

Specimen	*Location*	*E.D.*
EA25P1A	Nemrut Dag (EA25)	0.066
EA25P1B	Nemrut Dag (EA25)	0.068
EA25P1D	Nemrut Dag (EA25)	0.071
EA25P1C	Nemrut Dag (EA25)	0.077
EA25R1	Nemrut Dag (EA25)	0.082
EA25P2C	Nemrut Dag (EA25)	0.088
EA25P3	Nemrut Dag (EA25)	0.088
EA25P2D	Nemrut Dag (EA25)	0.092
EA25P2A	Nemrut Dag (EA25)	0.094
EA25P2B	Nemrut Dag (EA25)	0.097

Table D.1 - Source Assignments of Artifacts based on Euclidean Distance to Centroids of Geological Specimens

Artifact: A18 q23-4 f24 k25

A-Rank: **Bingol B** **52**
B-Rank: Gutansar 13

Elements: Fe, Ti, Ba

A-Rank: Bingol B 7
B-Rank: Gutansar 2

Specimen	*Location*	*E.D.*
EA52B3	Bingol B	0.055
EA52B1	Bingol B	0.056
EA52B2	Bingol B	0.065
EA56B1	Bingol B	0.077
EA53B2	Bingol B	0.098
EA54B1	Bingol B	0.098
CA07P1	Acigol	0.102
EA53B1	Bingol B	0.105
AR06E1A	Gutansar	0.106
AR06E2A	Gutansar	0.106

Elements: Fe, Zr, Ba

A-Rank: Bingol B 6
B-Rank: Erzincan 3

Specimen	*Location*	*E.D.*
EA52B3	Bingol B	0.056
EA52B1	Bingol B	0.057
EA56B1	Bingol B	0.058
EA52B2	Bingol B	0.065
EA53B2	Bingol B	0.084
CA07P1	Acigol	0.092
EA43R2	Erzincan	0.092
EA44R1	Erzincan	0.095
EA53B1	Bingol B	0.097
EA43P3	Erzincan	0.098

Elements: Ti, Fe, Zr, Ba

A-Rank: Bingol B 7
B-Rank: Acigol 2

Specimen	*Location*	*E.D.*
EA52B3	Bingol B	0.061
EA52B1	Bingol B	0.066
EA52B2	Bingol B	0.071
EA56B1	Bingol B	0.086
EA53B2	Bingol B	0.103
EA54B1	Bingol B	0.106
EA53B1	Bingol B	0.113
CA07P1	Acigol	0.121
AR76rB3	Gutansar	0.137
CA08R1D	Acigol	0.138

Elements: Ti, Fe, Mn, Ca, Zr, Ba

A-Rank: Bingol B 7
B-Rank: Acigol 3

Specimen	*Location*	*E.D.*
EA52B3	Bingol B	0.063
EA52B1	Bingol B	0.072
EA52B2	Bingol B	0.085
EA56B1	Bingol B	0.087
EA53B2	Bingol B	0.109
EA54B1	Bingol B	0.112
EA53B1	Bingol B	0.115
CA08R1C	Acigol	0.155
CA08R1A	Acigol	0.160
CA07R1	Acigol	0.173

Elements: Fe, Ti, Zr

A-Rank: Bingol B 7
B-Rank: Gutansar 2

Specimen	*Location*	*E.D.*
EA52B3	Bingol B	0.044
EA52B1	Bingol B	0.050
EA52B2	Bingol B	0.057
EA56B1	Bingol B	0.074
EA53B2	Bingol B	0.077
EA53B1	Bingol B	0.083
EA54B1	Bingol B	0.098
CA07P1	Acigol	0.121
AR76rB3	Gutansar	0.133
AR06E1C	Gutansar	0.138

Elements: Ti, Zr, Ba

A-Rank: Bingol B 6
B-Rank: Gutansar 4

Specimen	*Location*	*E.D.*
EA52B3	Bingol B	0.056
EA52B2	Bingol B	0.057
EA52B1	Bingol B	0.064
EA54B1	Bingol B	0.066
AR78rB3	Gutansar	0.081
AR78rB1	Gutansar	0.083
EA55B2	Bingol B	0.084
AR76rB3	Gutansar	0.085
AR77rB3	Gutansar	0.086
EA56B1	Bingol B	0.086

Elements: Ti, Fe, Zr, Ba, Zn

A-Rank: Bingol B 5
B-Rank: Gutansar 5

Specimen	*Location*	*E.D.*
EA53B1	Bingol B	0.154
EA52B1	Bingol B	0.172
AR06E2B	Gutansar	0.181
EA52B3	Bingol B	0.183
AR11jB1	Gutansar	0.192
EA52B2	Bingol B	0.202
AR06E1C	Gutansar	0.205
EA54B1	Bingol B	0.206
AR06E1B	Gutansar	0.207
AR12jB1	Gutansar	0.208

Elements: Ti, Al, Fe, Mn, Ca, Zr, Ba

A-Rank: Bingol B 7
B-Rank: Acigol 3

Specimen	*Location*	*E.D.*
EA52B3	Bingol B	0.098
EA52B1	Bingol B	0.103
EA56B1	Bingol B	0.111
EA52B2	Bingol B	0.112
EA53B2	Bingol B	0.122
EA53B1	Bingol B	0.127
EA54B1	Bingol B	0.131
CA08R1C	Acigol	0.156
CA08R1A	Acigol	0.160
CA07R1	Acigol	0.174

Table D.1 - Source Assignments of Artifacts based on Euclidean Distance to Centroids of Geological Specimens

Artifact: A18 q249-3 f120 k24

A-Rank: **Nemrut Dag (EA25)** **41**
B-Rank: Nemrut Dag (EA22) 30

Elements: Fe, Ti, Ba

A-Rank:	Nemrut Dag (EA25)	10
B-Rank:	-	-

Specimen	*Location*	*E.D.*
EA25R1	Nemrut Dag (EA25)	0.001
EA25P1B	Nemrut Dag (EA25)	0.007
EA25P3	Nemrut Dag (EA25)	0.007
EA25P1A	Nemrut Dag (EA25)	0.008
EA25P1D	Nemrut Dag (EA25)	0.014
EA25P2B	Nemrut Dag (EA25)	0.014
EA25P1C	Nemrut Dag (EA25)	0.015
EA25P2A	Nemrut Dag (EA25)	0.018
EA25P2D	Nemrut Dag (EA25)	0.020
EA25P2C	Nemrut Dag (EA25)	0.021

Elements: Fe, Zr, Ba

A-Rank:	Nemrut Dag (EA22)	7
B-Rank:	Nemrut Dag (EA21)	3

Specimen	*Location*	*E.D.*
EA22P5A	Nemrut Dag (EA22)	0.070
EA22P4	Nemrut Dag (EA22)	0.074
EA21R1A	Nemrut Dag (EA21)	0.076
EA21R1B	Nemrut Dag (EA21)	0.077
EA22P6A	Nemrut Dag (EA22)	0.077
EA21P1	Nemrut Dag (EA21)	0.078
EA22P5B	Nemrut Dag (EA22)	0.078
EA22P7A	Nemrut Dag (EA22)	0.078
EA22P3	Nemrut Dag (EA22)	0.079
EA22P8B	Nemrut Dag (EA22)	0.080

Elements: Ti, Fe, Zr, Ba

A-Rank:	Nemrut Dag (EA22)	5
B-Rank:	Nemrut Dag (EA25)	4

Specimen	*Location*	*E.D.*
EA25P1D	Nemrut Dag (EA25)	0.087
EA25P1A	Nemrut Dag (EA25)	0.088
EA25P1B	Nemrut Dag (EA25)	0.088
EA22P7A	Nemrut Dag (EA22)	0.091
EA25P1C	Nemrut Dag (EA25)	0.094
EA22P5A	Nemrut Dag (EA22)	0.096
EA22P8B	Nemrut Dag (EA22)	0.096
EA22P4	Nemrut Dag (EA22)	0.099
EA22P6B	Nemrut Dag (EA22)	0.099
EA21R1B	Nemrut Dag (EA21)	0.100

Elements: Ti, Fe, Mn, Ca, Zr, Ba

A-Rank:	Nemrut Dag (EA25)	10
B-Rank:	-	-

Specimen	*Location*	*E.D.*
EA25P1A	Nemrut Dag (EA25)	0.088
EA25P1B	Nemrut Dag (EA25)	0.090
EA25P1C	Nemrut Dag (EA25)	0.095
EA25P1D	Nemrut Dag (EA25)	0.095
EA25R1	Nemrut Dag (EA25)	0.108
EA25P2C	Nemrut Dag (EA25)	0.112
EA25P3	Nemrut Dag (EA25)	0.113
EA25P2D	Nemrut Dag (EA25)	0.117
EA25P2A	Nemrut Dag (EA25)	0.118
EA25P2B	Nemrut Dag (EA25)	0.121

Elements: Fe, Ti, Zr

A-Rank:	Nemrut Dag (EA22)	5
B-Rank:	Nemrut Dag (EA25)	4

Specimen	*Location*	*E.D.*
EA25P1D	Nemrut Dag (EA25)	0.086
EA25P1A	Nemrut Dag (EA25)	0.087
EA25P1B	Nemrut Dag (EA25)	0.088
EA22P7A	Nemrut Dag (EA22)	0.090
EA25P1C	Nemrut Dag (EA25)	0.094
EA22P5A	Nemrut Dag (EA22)	0.096
EA22P8B	Nemrut Dag (EA22)	0.097
EA22P6B	Nemrut Dag (EA22)	0.098
EA22P4	Nemrut Dag (EA22)	0.099
EA21R1B	Nemrut Dag (EA21)	0.100

Elements: Ti, Zr, Ba

A-Rank:	Nemrut Dag (EA22)	6
B-Rank:	Nemrut Dag (EA21)	2

Specimen	*Location*	*E.D.*
EA22P7A	Nemrut Dag (EA22)	0.076
EA22P8B	Nemrut Dag (EA22)	0.083
EA22P5A	Nemrut Dag (EA22)	0.084
EA21R1B	Nemrut Dag (EA21)	0.086
EA22R1	Nemrut Dag (EA22)	0.086
EA25P1D	Nemrut Dag (EA25)	0.086
EA22P6B	Nemrut Dag (EA22)	0.087
EA21P1	Nemrut Dag (EA21)	0.088
EA22P3	Nemrut Dag (EA22)	0.088
EA25P1A	Nemrut Dag (EA25)	0.088

Elements: Ti, Fe, Zr, Ba, Zn

A-Rank:	Nemrut Dag (EA22)	7
B-Rank:	Nemrut Dag (EA25)	3

Specimen	*Location*	*E.D.*
EA25P1D	Nemrut Dag (EA25)	0.092
EA25P1A	Nemrut Dag (EA25)	0.093
EA25P1B	Nemrut Dag (EA25)	0.095
EA22P7A	Nemrut Dag (EA22)	0.101
EA22P8B	Nemrut Dag (EA22)	0.101
EA22P3	Nemrut Dag (EA22)	0.102
EA22P7B	Nemrut Dag (EA22)	0.105
EA22P6A	Nemrut Dag (EA22)	0.106
EA22P6B	Nemrut Dag (EA22)	0.106
EA22R1	Nemrut Dag (EA22)	0.110

Elements: Ti, Al, Fe, Mn, Ca, Zr, Ba

A-Rank:	Nemrut Dag (EA25)	10
B-Rank:	-	-

Specimen	*Location*	*E.D.*
EA25P1A	Nemrut Dag (EA25)	0.090
EA25P1B	Nemrut Dag (EA25)	0.093
EA25P1C	Nemrut Dag (EA25)	0.097
EA25P1D	Nemrut Dag (EA25)	0.098
EA25R1	Nemrut Dag (EA25)	0.109
EA25P2C	Nemrut Dag (EA25)	0.114
EA25P3	Nemrut Dag (EA25)	0.114
EA25P2D	Nemrut Dag (EA25)	0.119
EA25P2A	Nemrut Dag (EA25)	0.121
EA25P2B	Nemrut Dag (EA25)	0.123

Table D.1 - Source Assignments of Artifacts based on Euclidean Distance to Centroids of Geological Specimens

Artifact: A18 q348-1 f158 k15

A-Rank: **Nemrut Dag (EA25)** **73**
B-Rank: Nemrut Dag (EA22) 7

Elements: Fe, Ti, Ba

A-Rank:	Nemrut Dag (EA25)	10
B-Rank:	-	-

Specimen	*Location*	*E.D.*
EA25P2D	Nemrut Dag (EA25)	0.023
EA25P2C	Nemrut Dag (EA25)	0.025
EA25P2A	Nemrut Dag (EA25)	0.027
EA25P1C	Nemrut Dag (EA25)	0.028
EA25P2B	Nemrut Dag (EA25)	0.028
EA25P1A	Nemrut Dag (EA25)	0.033
EA25P1D	Nemrut Dag (EA25)	0.033
EA25R2	Nemrut Dag (EA25)	0.034
EA25P1B	Nemrut Dag (EA25)	0.035
EA25R1	Nemrut Dag (EA25)	0.041

Elements: Fe, Zr, Ba

A-Rank:	Nemrut Dag (EA25)	8
B-Rank:	Nemrut Dag (EA22)	2

Specimen	*Location*	*E.D.*
EA25P1C	Nemrut Dag (EA25)	0.023
EA25P1A	Nemrut Dag (EA25)	0.026
EA25P1B	Nemrut Dag (EA25)	0.026
EA25P1D	Nemrut Dag (EA25)	0.028
EA25P2C	Nemrut Dag (EA25)	0.035
EA25P2D	Nemrut Dag (EA25)	0.039
EA25P2A	Nemrut Dag (EA25)	0.042
EA25R1	Nemrut Dag (EA25)	0.043
EA22P1C	Nemrut Dag (EA22)	0.044
EA22P4	Nemrut Dag (EA22)	0.044

Elements: Ti, Fe, Zr, Ba

A-Rank:	Nemrut Dag (EA25)	10
B-Rank:	-	-

Specimen	*Location*	*E.D.*
EA25P1C	Nemrut Dag (EA25)	0.033
EA25P1D	Nemrut Dag (EA25)	0.034
EA25P1A	Nemrut Dag (EA25)	0.035
EA25P1B	Nemrut Dag (EA25)	0.037
EA25P2C	Nemrut Dag (EA25)	0.041
EA25P2D	Nemrut Dag (EA25)	0.043
EA25P2A	Nemrut Dag (EA25)	0.048
EA25R1	Nemrut Dag (EA25)	0.051
EA25P2B	Nemrut Dag (EA25)	0.052
EA25P3	Nemrut Dag (EA25)	0.058

Elements: Ti, Fe, Mn, Ca, Zr, Ba

A-Rank:	Nemrut Dag (EA25)	10
B-Rank:	-	-

Specimen	*Location*	*E.D.*
EA25P1C	Nemrut Dag (EA25)	0.034
EA25P1A	Nemrut Dag (EA25)	0.036
EA25P1B	Nemrut Dag (EA25)	0.042
EA25P2C	Nemrut Dag (EA25)	0.047
EA25P1D	Nemrut Dag (EA25)	0.052
EA25P2D	Nemrut Dag (EA25)	0.052
EA25P2A	Nemrut Dag (EA25)	0.053
EA25P2B	Nemrut Dag (EA25)	0.055
EA25R1	Nemrut Dag (EA25)	0.056
EA25P3	Nemrut Dag (EA25)	0.061

Elements: Fe, Ti, Zr

A-Rank:	Nemrut Dag (EA25)	10
B-Rank:	-	-

Specimen	*Location*	*E.D.*
EA25P1D	Nemrut Dag (EA25)	0.022
EA25P1A	Nemrut Dag (EA25)	0.027
EA25P1B	Nemrut Dag (EA25)	0.029
EA25P1C	Nemrut Dag (EA25)	0.029
EA25P2C	Nemrut Dag (EA25)	0.039
EA25P2D	Nemrut Dag (EA25)	0.040
EA25R1	Nemrut Dag (EA25)	0.042
EA25P2A	Nemrut Dag (EA25)	0.046
EA25P3	Nemrut Dag (EA25)	0.046
EA25P2B	Nemrut Dag (EA25)	0.048

Elements: Ti, Zr, Ba

A-Rank:	Nemrut Dag (EA25)	10
B-Rank:	-	-

Specimen	*Location*	*E.D.*
EA25P1C	Nemrut Dag (EA25)	0.033
EA25P1D	Nemrut Dag (EA25)	0.034
EA25P1A	Nemrut Dag (EA25)	0.035
EA25P1B	Nemrut Dag (EA25)	0.037
EA25P2C	Nemrut Dag (EA25)	0.041
EA25P2D	Nemrut Dag (EA25)	0.043
EA25P2A	Nemrut Dag (EA25)	0.047
EA25R1	Nemrut Dag (EA25)	0.051
EA25P2B	Nemrut Dag (EA25)	0.052
EA25P3	Nemrut Dag (EA25)	0.058

Elements: Ti, Fe, Zr, Ba, Zn

A-Rank:	Nemrut Dag (EA25)	5
B-Rank:	Nemrut Dag (EA22)	5

Specimen	*Location*	*E.D.*
EA25P2C	Nemrut Dag (EA25)	0.041
EA25P1D	Nemrut Dag (EA25)	0.080
EA25P1A	Nemrut Dag (EA25)	0.081
EA25P1B	Nemrut Dag (EA25)	0.085
EA22P7A	Nemrut Dag (EA22)	0.092
EA22R1	Nemrut Dag (EA22)	0.097
EA25P2D	Nemrut Dag (EA25)	0.102
EA22P1D	Nemrut Dag (EA22)	0.103
EA22P3	Nemrut Dag (EA22)	0.110
EA22P7B	Nemrut Dag (EA22)	0.110

Elements: Ti, Al, Fe, Mn, Ca, Zr, Ba

A-Rank:	Nemrut Dag (EA25)	10
B-Rank:	-	-

Specimen	*Location*	*E.D.*
EA25P1A	Nemrut Dag (EA25)	0.049
EA25P1C	Nemrut Dag (EA25)	0.050
EA25P1B	Nemrut Dag (EA25)	0.057
EA25P2C	Nemrut Dag (EA25)	0.061
EA25R1	Nemrut Dag (EA25)	0.063
EA25P2D	Nemrut Dag (EA25)	0.066
EA25P1D	Nemrut Dag (EA25)	0.067
EA25P2A	Nemrut Dag (EA25)	0.067
EA25P2B	Nemrut Dag (EA25)	0.067
EA25P3	Nemrut Dag (EA25)	0.069

Table D.1 - Source Assignments of Artifacts based on Euclidean Distance to Centroids of Geological Specimens

Artifact: A18 q35-4 f31 k34

A-Rank: **Mus** **60**
B-Rank: **Pasinler** **15**

Elements: Fe, Ti, Ba

A-Rank:	Mus	5
B-Rank:	Meydan Dag	3

Specimen	*Location*	*E.D.*
EA07P4	Meydan Dag	0.023
EA60B1A	Mus	0.027
EA08P1	Meydan Dag	0.028
EA50R1B	Bingol	0.028
EA62Y1C	Mus	0.029
EA62Y4	Mus	0.029
EA07P2	Meydan Dag	0.030
EA50P3A	Bingol	0.030
EA60B1B	Mus	0.030
EA61B2	Mus	0.030

Elements: Fe, Zr, Ba

A-Rank:	Pasinler	7
B-Rank:	Mus	3

Specimen	*Location*	*E.D.*
EA60B1A	Mus	0.010
EA33P5	Pasinler	0.016
EA62Y3B	Mus	0.018
EA33P7	Pasinler	0.019
EA62Y1B	Mus	0.019
EA33P6	Pasinler	0.020
EA33R1	Pasinler	0.021
EA34P1	Pasinler	0.021
EA35R2	Pasinler	0.021
EA34P3	Pasinler	0.022

Elements: Ti, Fe, Zr, Ba

A-Rank:	Mus	7
B-Rank:	Pasinler	3

Specimen	*Location*	*E.D.*
EA60B1A	Mus	0.028
EA33P7	Pasinler	0.031
EA62Y2B	Mus	0.031
EA60B1B	Mus	0.033
EA61B2	Mus	0.033
EA62Y1B	Mus	0.033
EA33P5	Pasinler	0.034
EA62Y1A	Mus	0.035
EA62Y3B	Mus	0.035
EA34R1	Pasinler	0.036

Elements: Ti, Fe, Mn, Ca, Zr, Ba

A-Rank:	Mus	10
B-Rank:	-	-

Specimen	*Location*	*E.D.*
EA62Y1A	Mus	0.041
EA61B1	Mus	0.049
EA62Y3A	Mus	0.050
EA62Y5	Mus	0.050
EA62Y1D	Mus	0.052
EA58B1	Mus	0.053
EA59B1	Mus	0.054
EA62Y4	Mus	0.054
EA62Y1B	Mus	0.055
EA60B1A	Mus	0.058

Elements: Fe, Ti, Zr

A-Rank:	Mus	8
B-Rank:	Pasinler	2

Specimen	*Location*	*E.D.*
EA60B1A	Mus	0.027
EA33P7	Pasinler	0.029
EA60B2	Mus	0.029
EA59B1	Mus	0.030
EA60B1B	Mus	0.030
EA62Y2B	Mus	0.030
EA61B2	Mus	0.032
EA62Y1A	Mus	0.032
EA62Y1B	Mus	0.032
EA33P1A	Pasinler	0.034

Elements: Ti, Zr, Ba

A-Rank:	Mus	7
B-Rank:	Pasinler	3

Specimen	*Location*	*E.D.*
EA33P7	Pasinler	0.026
EA62Y2B	Mus	0.026
EA61B2	Mus	0.027
EA60B1A	Mus	0.028
EA60B1B	Mus	0.028
EA62Y1B	Mus	0.030
EA33P5	Pasinler	0.031
EA62Y1A	Mus	0.031
EA34R1	Pasinler	0.032
EA60B2	Mus	0.033

Elements: Ti, Fe, Zr, Ba, Zn

A-Rank:	Mus	10
B-Rank:	-	-

Specimen	*Location*	*E.D.*
EA62Y1A	Mus	0.073
EA60B1B	Mus	0.080
EA60B1A	Mus	0.098
EA62Y3B	Mus	0.106
EA57B1	Mus	0.112
EA62Y4	Mus	0.114
EA58B1	Mus	0.118
EA59B1	Mus	0.126
EA62Y1B	Mus	0.128
EA62Y1C	Mus	0.129

Elements: Ti, Al, Fe, Mn, Ca, Zr, Ba

A-Rank:	Mus	10
B-Rank:	-	-

Specimen	*Location*	*E.D.*
EA62Y1A	Mus	0.046
EA61B1	Mus	0.052
EA62Y3A	Mus	0.053
EA62Y1D	Mus	0.054
EA62Y4	Mus	0.056
EA58B1	Mus	0.058
EA62Y1B	Mus	0.058
EA62Y5	Mus	0.059
EA59B1	Mus	0.062
EA60B1A	Mus	0.066

Table D.1 - Source Assignments of Artifacts based on Euclidean Distance to Centroids of Geological Specimens

Artifact: A18 q43-3 f44 k26

A-Rank: **Nemrut Dag (EA25)** **73**
B-Rank: Nemrut Dag (EA22) 7

Elements: Fe, Ti, Ba

A-Rank:	Nemrut Dag (EA25)	10
B-Rank:	-	-

Specimen	*Location*	*E.D.*
EA25P3	Nemrut Dag (EA25)	0.017
EA25R1	Nemrut Dag (EA25)	0.022
EA25P1B	Nemrut Dag (EA25)	0.029
EA25P1A	Nemrut Dag (EA25)	0.030
EA25P1D	Nemrut Dag (EA25)	0.030
EA25P2B	Nemrut Dag (EA25)	0.034
EA25P1C	Nemrut Dag (EA25)	0.037
EA25P2A	Nemrut Dag (EA25)	0.040
EA25P2C	Nemrut Dag (EA25)	0.041
EA25P2D	Nemrut Dag (EA25)	0.041

Elements: Fe, Zr, Ba

A-Rank:	Nemrut Dag (EA25)	9
B-Rank:	Nemrut Dag (EA22)	1

Specimen	*Location*	*E.D.*
EA25P1D	Nemrut Dag (EA25)	0.025
EA25P1A	Nemrut Dag (EA25)	0.028
EA25P1B	Nemrut Dag (EA25)	0.028
EA25R1	Nemrut Dag (EA25)	0.028
EA25P3	Nemrut Dag (EA25)	0.029
EA25P1C	Nemrut Dag (EA25)	0.036
EA22P4	Nemrut Dag (EA22)	0.044
EA25P2C	Nemrut Dag (EA25)	0.044
EA25P2B	Nemrut Dag (EA25)	0.045
EA25P2D	Nemrut Dag (EA25)	0.045

Elements: Ti, Fe, Zr, Ba

A-Rank:	Nemrut Dag (EA25)	10
B-Rank:	-	-

Specimen	*Location*	*E.D.*
EA25P1B	Nemrut Dag (EA25)	0.029
EA25R1	Nemrut Dag (EA25)	0.029
EA25P1A	Nemrut Dag (EA25)	0.030
EA25P1D	Nemrut Dag (EA25)	0.030
EA25P3	Nemrut Dag (EA25)	0.030
EA25P1C	Nemrut Dag (EA25)	0.038
EA25P2B	Nemrut Dag (EA25)	0.047
EA25P2C	Nemrut Dag (EA25)	0.047
EA25P2D	Nemrut Dag (EA25)	0.048
EA25P2A	Nemrut Dag (EA25)	0.049

Elements: Ti, Fe, Mn, Ca, Zr, Ba

A-Rank:	Nemrut Dag (EA25)	10
B-Rank:	-	-

Specimen	*Location*	*E.D.*
EA25P1A	Nemrut Dag (EA25)	0.033
EA25P1B	Nemrut Dag (EA25)	0.037
EA25P1C	Nemrut Dag (EA25)	0.038
EA25P3	Nemrut Dag (EA25)	0.038
EA25R1	Nemrut Dag (EA25)	0.039
EA25P1D	Nemrut Dag (EA25)	0.052
EA25P2B	Nemrut Dag (EA25)	0.052
EA25P2C	Nemrut Dag (EA25)	0.054
EA25P2A	Nemrut Dag (EA25)	0.056
EA25P2D	Nemrut Dag (EA25)	0.059

Elements: Fe, Ti, Zr

A-Rank:	Nemrut Dag (EA25)	10
B-Rank:	-	-

Specimen	*Location*	*E.D.*
EA25P1B	Nemrut Dag (EA25)	0.010
EA25P1A	Nemrut Dag (EA25)	0.012
EA25P1C	Nemrut Dag (EA25)	0.014
EA25P1D	Nemrut Dag (EA25)	0.018
EA25R1	Nemrut Dag (EA25)	0.022
EA25P3	Nemrut Dag (EA25)	0.025
EA25P2C	Nemrut Dag (EA25)	0.027
EA25P2A	Nemrut Dag (EA25)	0.031
EA25P2D	Nemrut Dag (EA25)	0.031
EA25P2B	Nemrut Dag (EA25)	0.036

Elements: Ti, Zr, Ba

A-Rank:	Nemrut Dag (EA25)	10
B-Rank:	-	-

Specimen	*Location*	*E.D.*
EA25P1B	Nemrut Dag (EA25)	0.029
EA25P1D	Nemrut Dag (EA25)	0.029
EA25R1	Nemrut Dag (EA25)	0.029
EA25P1A	Nemrut Dag (EA25)	0.030
EA25P3	Nemrut Dag (EA25)	0.030
EA25P1C	Nemrut Dag (EA25)	0.038
EA25P2C	Nemrut Dag (EA25)	0.046
EA25P2B	Nemrut Dag (EA25)	0.047
EA25P2D	Nemrut Dag (EA25)	0.048
EA25P2A	Nemrut Dag (EA25)	0.049

Elements: Ti, Fe, Zr, Ba, Zn

A-Rank:	Nemrut Dag (EA22)	6
B-Rank:	Nemrut Dag (EA25)	4

Specimen	*Location*	*E.D.*
EA25P2C	Nemrut Dag (EA25)	0.049
EA22P1D	Nemrut Dag (EA22)	0.080
EA22P7A	Nemrut Dag (EA22)	0.080
EA22R1	Nemrut Dag (EA22)	0.082
EA22P5B	Nemrut Dag (EA22)	0.086
EA22P3	Nemrut Dag (EA22)	0.091
EA25P1A	Nemrut Dag (EA25)	0.091
EA25P1D	Nemrut Dag (EA25)	0.091
EA25P1B	Nemrut Dag (EA25)	0.094
EA22P1C	Nemrut Dag (EA22)	0.098

Elements: Ti, Al, Fe, Mn, Ca, Zr, Ba

A-Rank:	Nemrut Dag (EA25)	10
B-Rank:	-	-

Specimen	*Location*	*E.D.*
EA25P1A	Nemrut Dag (EA25)	0.034
EA25P1B	Nemrut Dag (EA25)	0.037
EA25P3	Nemrut Dag (EA25)	0.038
EA25P1C	Nemrut Dag (EA25)	0.039
EA25R1	Nemrut Dag (EA25)	0.041
EA25P1D	Nemrut Dag (EA25)	0.052
EA25P2B	Nemrut Dag (EA25)	0.052
EA25P2C	Nemrut Dag (EA25)	0.054
EA25P2A	Nemrut Dag (EA25)	0.056
EA25P2D	Nemrut Dag (EA25)	0.059

Table D.1 - Source Assignments of Artifacts based on Euclidean Distance to Centroids of Geological Specimens

Artifact: A18 q441.3 f168 k28

A-Rank: **Nemrut Dag (EA25)** **58**
B-Rank: Nemrut Dag (EA22) 21

Elements: Fe, Ti, Ba

A-Rank:	Nemrut Dag (EA25)	10
B-Rank:	-	-

Specimen	*Location*	*E.D.*
EA25P2C	Nemrut Dag (EA25)	0.010
EA25P1C	Nemrut Dag (EA25)	0.012
EA25R2	Nemrut Dag (EA25)	0.012
EA25P2D	Nemrut Dag (EA25)	0.014
EA25P2A	Nemrut Dag (EA25)	0.016
EA25P2B	Nemrut Dag (EA25)	0.016
EA25P1B	Nemrut Dag (EA25)	0.017
EA25P1A	Nemrut Dag (EA25)	0.019
EA25P1D	Nemrut Dag (EA25)	0.021
EA25R1	Nemrut Dag (EA25)	0.024

Elements: Fe, Zr, Ba

A-Rank:	Nemrut Dag (EA22)	6
B-Rank:	Nemrut Dag (EA25)	3

Specimen	*Location*	*E.D.*
EA22P4	Nemrut Dag (EA22)	0.034
EA22P5A	Nemrut Dag (EA22)	0.037
EA25P1D	Nemrut Dag (EA25)	0.037
EA25P1B	Nemrut Dag (EA25)	0.038
EA25P1A	Nemrut Dag (EA25)	0.039
EA22P5B	Nemrut Dag (EA22)	0.040
EA22P6B	Nemrut Dag (EA22)	0.040
EA22P7A	Nemrut Dag (EA22)	0.040
EA21P1	Nemrut Dag (EA21)	0.041
EA22P6A	Nemrut Dag (EA22)	0.041

Elements: Ti, Fe, Zr, Ba

A-Rank:	Nemrut Dag (EA25)	8
B-Rank:	Nemrut Dag (EA22)	2

Specimen	*Location*	*E.D.*
EA25P1D	Nemrut Dag (EA25)	0.038
EA25P1A	Nemrut Dag (EA25)	0.039
EA25P1B	Nemrut Dag (EA25)	0.039
EA25P1C	Nemrut Dag (EA25)	0.042
EA25P2C	Nemrut Dag (EA25)	0.055
EA25R1	Nemrut Dag (EA25)	0.058
EA22P7A	Nemrut Dag (EA22)	0.060
EA25P2D	Nemrut Dag (EA25)	0.060
EA25P2A	Nemrut Dag (EA25)	0.063
EA22P6B	Nemrut Dag (EA22)	0.064

Elements: Ti, Fe, Mn, Ca, Zr, Ba

A-Rank:	Nemrut Dag (EA25)	10
B-Rank:	-	-

Specimen	*Location*	*E.D.*
EA25P1C	Nemrut Dag (EA25)	0.042
EA25P1A	Nemrut Dag (EA25)	0.044
EA25P1B	Nemrut Dag (EA25)	0.049
EA25P1D	Nemrut Dag (EA25)	0.063
EA25P2C	Nemrut Dag (EA25)	0.065
EA25R1	Nemrut Dag (EA25)	0.067
EA25P3	Nemrut Dag (EA25)	0.070
EA25P2A	Nemrut Dag (EA25)	0.071
EA25P2D	Nemrut Dag (EA25)	0.072
EA25P2B	Nemrut Dag (EA25)	0.073

Elements: Fe, Ti, Zr

A-Rank:	Nemrut Dag (EA25)	8
B-Rank:	Nemrut Dag (EA22)	2

Specimen	*Location*	*E.D.*
EA25P1D	Nemrut Dag (EA25)	0.034
EA25P1B	Nemrut Dag (EA25)	0.036
EA25P1A	Nemrut Dag (EA25)	0.037
EA25P1C	Nemrut Dag (EA25)	0.041
EA25R1	Nemrut Dag (EA25)	0.054
EA25P2C	Nemrut Dag (EA25)	0.056
EA25P3	Nemrut Dag (EA25)	0.058
EA25P2D	Nemrut Dag (EA25)	0.059
EA22P7A	Nemrut Dag (EA22)	0.060
EA22P6B	Nemrut Dag (EA22)	0.063

Elements: Ti, Zr, Ba

A-Rank:	Nemrut Dag (EA25)	5
B-Rank:	Nemrut Dag (EA22)	5

Specimen	*Location*	*E.D.*
EA25P1A	Nemrut Dag (EA25)	0.037
EA25P1B	Nemrut Dag (EA25)	0.038
EA25P1D	Nemrut Dag (EA25)	0.038
EA25P1C	Nemrut Dag (EA25)	0.041
EA22P7A	Nemrut Dag (EA22)	0.046
EA22R1	Nemrut Dag (EA22)	0.050
EA22P2	Nemrut Dag (EA22)	0.052
EA22P6B	Nemrut Dag (EA22)	0.054
EA22P8B	Nemrut Dag (EA22)	0.055
EA25P2C	Nemrut Dag (EA25)	0.055

Elements: Ti, Fe, Zr, Ba, Zn

A-Rank:	Nemrut Dag (EA22)	6
B-Rank:	Nemrut Dag (EA25)	4

Specimen	*Location*	*E.D.*
EA25P1D	Nemrut Dag (EA25)	0.053
EA25P1A	Nemrut Dag (EA25)	0.054
EA25P1B	Nemrut Dag (EA25)	0.056
EA25P2C	Nemrut Dag (EA25)	0.066
EA22P7A	Nemrut Dag (EA22)	0.071
EA22P7B	Nemrut Dag (EA22)	0.071
EA22P3	Nemrut Dag (EA22)	0.075
EA22R1	Nemrut Dag (EA22)	0.075
EA22P8B	Nemrut Dag (EA22)	0.076
EA22P1C	Nemrut Dag (EA22)	0.078

Elements: Ti, Al, Fe, Mn, Ca, Zr, Ba

A-Rank:	Nemrut Dag (EA25)	10
B-Rank:	-	-

Specimen	*Location*	*E.D.*
EA25P1A	Nemrut Dag (EA25)	0.053
EA25P1C	Nemrut Dag (EA25)	0.055
EA25P1B	Nemrut Dag (EA25)	0.061
EA25R1	Nemrut Dag (EA25)	0.072
EA25P1D	Nemrut Dag (EA25)	0.074
EA25P2C	Nemrut Dag (EA25)	0.074
EA25P3	Nemrut Dag (EA25)	0.077
EA25P2A	Nemrut Dag (EA25)	0.081
EA25P2B	Nemrut Dag (EA25)	0.081
EA25P2D	Nemrut Dag (EA25)	0.081

Table D.1 - Source Assignments of Artifacts based on Euclidean Distance to Centroids of Geological Specimens

Artifact: A18 q45-1 f42 k34

A-Rank: **Nemrut Dag (EA25) 31**
B-Rank: **Nemrut Dag (EA22) 31**

Elements: Fe, Ti, Ba

A-Rank:	Nemrut Dag (EA25)	10
B-Rank:	-	-

Specimen	*Location*	*E.D.*
EA25R2	Nemrut Dag (EA25)	0.136
EA25P2C	Nemrut Dag (EA25)	0.139
EA25P2A	Nemrut Dag (EA25)	0.140
EA25P2D	Nemrut Dag (EA25)	0.140
EA25P1C	Nemrut Dag (EA25)	0.142
EA25P2B	Nemrut Dag (EA25)	0.147
EA25P1A	Nemrut Dag (EA25)	0.150
EA25P1B	Nemrut Dag (EA25)	0.150
EA25P1D	Nemrut Dag (EA25)	0.153
EA25R1	Nemrut Dag (EA25)	0.158

Elements: Fe, Zr, Ba

A-Rank:	Nemrut Dag (EA22)	5
B-Rank:	Nemrut Dag (EA21)	3

Specimen	*Location*	*E.D.*
EA21P1	Nemrut Dag (EA21)	0.219
EA22P5A	Nemrut Dag (EA22)	0.223
EA22P7A	Nemrut Dag (EA22)	0.223
EA24P1B	Nemrut Dag (EA24)	0.230
EA21R1A	Nemrut Dag (EA21)	0.231
EA23P1B	Nemrut Dag (EA23)	0.231
EA22P6A	Nemrut Dag (EA22)	0.232
EA21R1B	Nemrut Dag (EA21)	0.233
EA22P5B	Nemrut Dag (EA22)	0.234
EA22P7B	Nemrut Dag (EA22)	0.234

Elements: Ti, Fe, Zr, Ba

A-Rank:	Nemrut Dag (EA22)	6
B-Rank:	Nemrut Dag (EA25)	3

Specimen	*Location*	*E.D.*
EA22P7A	Nemrut Dag (EA22)	0.236
EA21P1	Nemrut Dag (EA21)	0.239
EA22P5A	Nemrut Dag (EA22)	0.242
EA22R1	Nemrut Dag (EA22)	0.247
EA22P7B	Nemrut Dag (EA22)	0.248
EA22P6B	Nemrut Dag (EA22)	0.250
EA22P8B	Nemrut Dag (EA22)	0.250
EA25P1A	Nemrut Dag (EA25)	0.250
EA25P1C	Nemrut Dag (EA25)	0.250
EA25P1D	Nemrut Dag (EA25)	0.250

Elements: Ti, Fe, Mn, Ca, Zr, Ba

A-Rank:	Nemrut Dag (EA25)	5
B-Rank:	Nemrut Dag (EA22)	4

Specimen	*Location*	*E.D.*
EA25P1A	Nemrut Dag (EA25)	0.251
EA25P1C	Nemrut Dag (EA25)	0.251
EA25P1B	Nemrut Dag (EA25)	0.253
EA21P1	Nemrut Dag (EA21)	0.256
EA22P7B	Nemrut Dag (EA22)	0.256
EA25P1D	Nemrut Dag (EA25)	0.256
EA22P7A	Nemrut Dag (EA22)	0.262
EA22R1	Nemrut Dag (EA22)	0.262
EA25P2C	Nemrut Dag (EA25)	0.264
EA22P6A	Nemrut Dag (EA22)	0.265

Elements: Fe, Ti, Zr

A-Rank:	Nemrut Dag (EA22)	5
B-Rank:	Nemrut Dag (EA25)	3

Specimen	*Location*	*E.D.*
EA22P7A	Nemrut Dag (EA22)	0.184
EA22P5A	Nemrut Dag (EA22)	0.187
EA25P1D	Nemrut Dag (EA25)	0.190
EA21P1	Nemrut Dag (EA21)	0.191
EA21R1B	Nemrut Dag (EA21)	0.192
EA22P8B	Nemrut Dag (EA22)	0.192
EA25P1A	Nemrut Dag (EA25)	0.193
EA22P6A	Nemrut Dag (EA22)	0.194
EA25P1B	Nemrut Dag (EA25)	0.194
EA22P3	Nemrut Dag (EA22)	0.195

Elements: Ti, Zr, Ba

A-Rank:	Nemrut Dag (EA22)	5
B-Rank:	Nemrut Dag (EA21)	2

Specimen	*Location*	*E.D.*
EA22P7A	Nemrut Dag (EA22)	0.231
EA21P1	Nemrut Dag (EA21)	0.233
EA22P5A	Nemrut Dag (EA22)	0.238
EA22R1	Nemrut Dag (EA22)	0.241
EA22P7B	Nemrut Dag (EA22)	0.243
EA24P1B	Nemrut Dag (EA24)	0.243
EA26P2B	Nemrut Dag (EA26)	0.243
EA26P2A	Nemrut Dag (EA26)	0.244
EA21R1B	Nemrut Dag (EA21)	0.246
EA22P6A	Nemrut Dag (EA22)	0.246

Elements: Ti, Fe, Zr, Ba, Zn

A-Rank:	Nemrut Dag (EA22)	8
B-Rank:	Nemrut Dag (EA25)	2

Specimen	*Location*	*E.D.*
EA22P7A	Nemrut Dag (EA22)	0.237
EA22R1	Nemrut Dag (EA22)	0.249
EA22P5B	Nemrut Dag (EA22)	0.256
EA22P3	Nemrut Dag (EA22)	0.258
EA22P7B	Nemrut Dag (EA22)	0.260
EA25P2C	Nemrut Dag (EA25)	0.262
EA22P1C	Nemrut Dag (EA22)	0.267
EA22P6A	Nemrut Dag (EA22)	0.269
EA22P8B	Nemrut Dag (EA22)	0.269
EA25P1A	Nemrut Dag (EA25)	0.269

Elements: Ti, Al, Fe, Mn, Ca, Zr, Ba

A-Rank:	Nemrut Dag (EA25)	8
B-Rank:	Nemrut Dag (EA22)	2

Specimen	*Location*	*E.D.*
EA25P1A	Nemrut Dag (EA25)	0.257
EA25P1C	Nemrut Dag (EA25)	0.257
EA25P1B	Nemrut Dag (EA25)	0.260
EA25P1D	Nemrut Dag (EA25)	0.263
EA25P2C	Nemrut Dag (EA25)	0.270
EA22P7B	Nemrut Dag (EA22)	0.271
EA25P2D	Nemrut Dag (EA25)	0.275
EA25P2A	Nemrut Dag (EA25)	0.276
EA22P7A	Nemrut Dag (EA22)	0.277
EA25R1	Nemrut Dag (EA25)	0.277

Table D.1 - Source Assignments of Artifacts based on Euclidean Distance to Centroids of Geological Specimens

Artifact: A18 q45.2 f52 k34

A-Rank: **Nemrut Dag (EA25)** **35**
B-Rank: **Nemrut Dag (EA22)** **31**

Elements: Fe, Ti, Ba

A-Rank:	Nemrut Dag (EA25)	10
B-Rank:	-	-

Specimen	*Location*	*E.D.*
EA25P2C	Nemrut Dag (EA25)	0.019
EA25P2D	Nemrut Dag (EA25)	0.021
EA25P1C	Nemrut Dag (EA25)	0.023
EA25P2B	Nemrut Dag (EA25)	0.023
EA25P1D	Nemrut Dag (EA25)	0.025
EA25P1B	Nemrut Dag (EA25)	0.026
EA25R2	Nemrut Dag (EA25)	0.026
EA25P1A	Nemrut Dag (EA25)	0.029
EA25P2A	Nemrut Dag (EA25)	0.029
EA25R1	Nemrut Dag (EA25)	0.033

Elements: Fe, Zr, Ba

A-Rank:	Nemrut Dag (EA22)	7
B-Rank:	Nemrut Dag (EA21)	3

Specimen	*Location*	*E.D.*
EA22P5A	Nemrut Dag (EA22)	0.047
EA21P1	Nemrut Dag (EA21)	0.051
EA22P7A	Nemrut Dag (EA22)	0.053
EA21R1A	Nemrut Dag (EA21)	0.054
EA21R1B	Nemrut Dag (EA21)	0.056
EA22P6A	Nemrut Dag (EA22)	0.056
EA22P5B	Nemrut Dag (EA22)	0.057
EA22P3	Nemrut Dag (EA22)	0.058
EA22P4	Nemrut Dag (EA22)	0.059
EA22P8B	Nemrut Dag (EA22)	0.060

Elements: Ti, Fe, Zr, Ba

A-Rank:	Nemrut Dag (EA22)	5
B-Rank:	Nemrut Dag (EA25)	3

Specimen	*Location*	*E.D.*
EA22P7A	Nemrut Dag (EA22)	0.070
EA25P1D	Nemrut Dag (EA25)	0.079
EA22P5A	Nemrut Dag (EA22)	0.080
EA22P8B	Nemrut Dag (EA22)	0.080
EA22P6B	Nemrut Dag (EA22)	0.081
EA22R1	Nemrut Dag (EA22)	0.082
EA25P1B	Nemrut Dag (EA25)	0.082
EA21P1	Nemrut Dag (EA21)	0.083
EA25P1A	Nemrut Dag (EA25)	0.083
EA21R1B	Nemrut Dag (EA21)	0.084

Elements: Ti, Fe, Mn, Ca, Zr, Ba

A-Rank:	Nemrut Dag (EA25)	5
B-Rank:	Nemrut Dag (EA22)	5

Specimen	*Location*	*E.D.*
EA25P1C	Nemrut Dag (EA25)	0.088
EA25P1A	Nemrut Dag (EA25)	0.089
EA25P1B	Nemrut Dag (EA25)	0.092
EA22P7B	Nemrut Dag (EA22)	0.100
EA25P1D	Nemrut Dag (EA25)	0.100
EA25P2C	Nemrut Dag (EA25)	0.110
EA25R1	Nemrut Dag (EA25)	0.110
EA22P4	Nemrut Dag (EA22)	0.113
EA22P6B	Nemrut Dag (EA22)	0.114
EA22R1	Nemrut Dag (EA22)	0.114

Elements: Fe, Ti, Zr

A-Rank:	Nemrut Dag (EA22)	5
B-Rank:	Nemrut Dag (EA25)	3

Specimen	*Location*	*E.D.*
EA22P7A	Nemrut Dag (EA22)	0.070
EA22P8B	Nemrut Dag (EA22)	0.078
EA25P1D	Nemrut Dag (EA25)	0.078
EA22P5A	Nemrut Dag (EA22)	0.079
EA22P6B	Nemrut Dag (EA22)	0.081
EA25P1B	Nemrut Dag (EA25)	0.081
EA21R1B	Nemrut Dag (EA21)	0.082
EA22R1	Nemrut Dag (EA22)	0.082
EA25P1A	Nemrut Dag (EA25)	0.082
EA21P1	Nemrut Dag (EA21)	0.083

Elements: Ti, Zr, Ba

A-Rank:	Nemrut Dag (EA22)	5
B-Rank:	Nemrut Dag (EA25)	3

Specimen	*Location*	*E.D.*
EA22P7A	Nemrut Dag (EA22)	0.066
EA22P8B	Nemrut Dag (EA22)	0.076
EA22R1	Nemrut Dag (EA22)	0.076
EA22P5A	Nemrut Dag (EA22)	0.077
EA22P6B	Nemrut Dag (EA22)	0.078
EA25P1D	Nemrut Dag (EA25)	0.078
EA21P1	Nemrut Dag (EA21)	0.079
EA25P1A	Nemrut Dag (EA25)	0.079
EA25P1B	Nemrut Dag (EA25)	0.079
EA21R1B	Nemrut Dag (EA21)	0.080

Elements: Ti, Fe, Zr, Ba, Zn

A-Rank:	Nemrut Dag (EA22)	8
B-Rank:	Nemrut Dag (EA25)	2

Specimen	*Location*	*E.D.*
EA22P7A	Nemrut Dag (EA22)	0.085
EA22R1	Nemrut Dag (EA22)	0.098
EA22P5B	Nemrut Dag (EA22)	0.102
EA25P2C	Nemrut Dag (EA25)	0.111
EA22P3	Nemrut Dag (EA22)	0.115
EA22P1D	Nemrut Dag (EA22)	0.117
EA22P7B	Nemrut Dag (EA22)	0.131
EA22P1C	Nemrut Dag (EA22)	0.132
EA22P8B	Nemrut Dag (EA22)	0.145
EA25P1D	Nemrut Dag (EA25)	0.145

Elements: Ti, Al, Fe, Mn, Ca, Zr, Ba

A-Rank:	Nemrut Dag (EA25)	9
B-Rank:	Nemrut Dag (EA22)	1

Specimen	*Location*	*E.D.*
EA25P1A	Nemrut Dag (EA25)	0.093
EA25P1C	Nemrut Dag (EA25)	0.093
EA25P1B	Nemrut Dag (EA25)	0.098
EA25P1D	Nemrut Dag (EA25)	0.106
EA25R1	Nemrut Dag (EA25)	0.113
EA25P2C	Nemrut Dag (EA25)	0.114
EA25P3	Nemrut Dag (EA25)	0.117
EA22P7B	Nemrut Dag (EA22)	0.119
EA25P2D	Nemrut Dag (EA25)	0.121
EA25P2A	Nemrut Dag (EA25)	0.122

Table D.1 - Source Assignments of Artifacts based on Euclidean Distance to Centroids of Geological Specimens

Artifact: A18 q5-2 f7 k25

A-Rank: **Nemrut Dag (EA25)** **48**
B-Rank: Nemrut Dag (EA22) 28

Elements: Fe, Ti, Ba

A-Rank:	Nemrut Dag (EA25)	10
B-Rank:	-	-

Specimen	*Location*	*E.D.*
EA25P2C	Nemrut Dag (EA25)	0.016
EA25P2D	Nemrut Dag (EA25)	0.016
EA25P1C	Nemrut Dag (EA25)	0.021
EA25P2A	Nemrut Dag (EA25)	0.021
EA25P2B	Nemrut Dag (EA25)	0.023
EA25R2	Nemrut Dag (EA25)	0.024
EA25P1A	Nemrut Dag (EA25)	0.028
EA25P1B	Nemrut Dag (EA25)	0.029
EA25P1D	Nemrut Dag (EA25)	0.029
EA25R1	Nemrut Dag (EA25)	0.036

Elements: Fe, Zr, Ba

A-Rank:	Nemrut Dag (EA22)	7
B-Rank:	Nemrut Dag (EA21)	3

Specimen	*Location*	*E.D.*
EA22P5A	Nemrut Dag (EA22)	0.064
EA21P1	Nemrut Dag (EA21)	0.066
EA22P7A	Nemrut Dag (EA22)	0.068
EA22P6A	Nemrut Dag (EA22)	0.072
EA21R1A	Nemrut Dag (EA21)	0.073
EA21R1B	Nemrut Dag (EA21)	0.073
EA22P4	Nemrut Dag (EA22)	0.073
EA22P5B	Nemrut Dag (EA22)	0.074
EA22P3	Nemrut Dag (EA22)	0.075
EA22P8B	Nemrut Dag (EA22)	0.076

Elements: Ti, Fe, Zr, Ba

A-Rank:	Nemrut Dag (EA25)	5
B-Rank:	Nemrut Dag (EA22)	5

Specimen	*Location*	*E.D.*
EA25P1D	Nemrut Dag (EA25)	0.086
EA25P1A	Nemrut Dag (EA25)	0.088
EA25P1B	Nemrut Dag (EA25)	0.089
EA25P1C	Nemrut Dag (EA25)	0.091
EA22P7A	Nemrut Dag (EA22)	0.094
EA22P6B	Nemrut Dag (EA22)	0.103
EA22P8B	Nemrut Dag (EA22)	0.103
EA22P5A	Nemrut Dag (EA22)	0.104
EA22R1	Nemrut Dag (EA22)	0.105
EA25P2C	Nemrut Dag (EA25)	0.105

Elements: Ti, Fe, Mn, Ca, Zr, Ba

A-Rank:	Nemrut Dag (EA25)	10
B-Rank:	-	-

Specimen	*Location*	*E.D.*
EA25P1A	Nemrut Dag (EA25)	0.090
EA25P1C	Nemrut Dag (EA25)	0.091
EA25P1B	Nemrut Dag (EA25)	0.093
EA25P1D	Nemrut Dag (EA25)	0.099
EA25P2C	Nemrut Dag (EA25)	0.110
EA25R1	Nemrut Dag (EA25)	0.113
EA25P2D	Nemrut Dag (EA25)	0.115
EA25P2A	Nemrut Dag (EA25)	0.117
EA25P3	Nemrut Dag (EA25)	0.118
EA25P2B	Nemrut Dag (EA25)	0.120

Elements: Fe, Ti, Zr

A-Rank:	Nemrut Dag (EA25)	5
B-Rank:	Nemrut Dag (EA22)	5

Specimen	*Location*	*E.D.*
EA25P1D	Nemrut Dag (EA25)	0.082
EA25P1A	Nemrut Dag (EA25)	0.085
EA25P1B	Nemrut Dag (EA25)	0.085
EA25P1C	Nemrut Dag (EA25)	0.090
EA22P7A	Nemrut Dag (EA22)	0.093
EA22P8B	Nemrut Dag (EA22)	0.100
EA22P5A	Nemrut Dag (EA22)	0.102
EA22P6B	Nemrut Dag (EA22)	0.102
EA22R1	Nemrut Dag (EA22)	0.104
EA25P2C	Nemrut Dag (EA25)	0.104

Elements: Ti, Zr, Ba

A-Rank:	Nemrut Dag (EA22)	5
B-Rank:	Nemrut Dag (EA25)	4

Specimen	*Location*	*E.D.*
EA22P7A	Nemrut Dag (EA22)	0.083
EA25P1D	Nemrut Dag (EA25)	0.086
EA25P1A	Nemrut Dag (EA25)	0.088
EA25P1B	Nemrut Dag (EA25)	0.089
EA25P1C	Nemrut Dag (EA25)	0.091
EA22R1	Nemrut Dag (EA22)	0.093
EA22P8B	Nemrut Dag (EA22)	0.095
EA22P5A	Nemrut Dag (EA22)	0.096
EA22P6B	Nemrut Dag (EA22)	0.096
EA21P1	Nemrut Dag (EA21)	0.097

Elements: Ti, Fe, Zr, Ba, Zn

A-Rank:	Nemrut Dag (EA22)	6
B-Rank:	Nemrut Dag (EA25)	4

Specimen	*Location*	*E.D.*
EA25P1D	Nemrut Dag (EA25)	0.088
EA25P1A	Nemrut Dag (EA25)	0.090
EA25P1B	Nemrut Dag (EA25)	0.091
EA22P8B	Nemrut Dag (EA22)	0.105
EA25P1C	Nemrut Dag (EA25)	0.106
EA22P6B	Nemrut Dag (EA22)	0.107
EA22P7B	Nemrut Dag (EA22)	0.107
EA22P7A	Nemrut Dag (EA22)	0.109
EA22P6A	Nemrut Dag (EA22)	0.111
EA22P3	Nemrut Dag (EA22)	0.112

Elements: Ti, Al, Fe, Mn, Ca, Zr, Ba

A-Rank:	Nemrut Dag (EA25)	10
B-Rank:	-	-

Specimen	*Location*	*E.D.*
EA25P1A	Nemrut Dag (EA25)	0.090
EA25P1C	Nemrut Dag (EA25)	0.092
EA25P1B	Nemrut Dag (EA25)	0.094
EA25P1D	Nemrut Dag (EA25)	0.100
EA25P2C	Nemrut Dag (EA25)	0.110
EA25R1	Nemrut Dag (EA25)	0.113
EA25P2D	Nemrut Dag (EA25)	0.116
EA25P2A	Nemrut Dag (EA25)	0.118
EA25P3	Nemrut Dag (EA25)	0.118
EA25P2B	Nemrut Dag (EA25)	0.121

Table D.1 - Source Assignments of Artifacts based on Euclidean Distance to Centroids of Geological Specimens

Artifact: A18 q57.2 f52 k34

A-Rank: **Nemrut Dag (EA22)** **47**
B-Rank: Nemrut Dag (EA25) 17

Elements: Fe, Ti, Ba

A-Rank:	Nemrut Dag (EA25)	10
B-Rank:	-	-

Specimen	*Location*	*E.D.*
EA25R2	Nemrut Dag (EA25)	0.024
EA25P2C	Nemrut Dag (EA25)	0.025
EA25P1C	Nemrut Dag (EA25)	0.028
EA25P2D	Nemrut Dag (EA25)	0.028
EA25P2A	Nemrut Dag (EA25)	0.031
EA25P2B	Nemrut Dag (EA25)	0.031
EA25P1B	Nemrut Dag (EA25)	0.032
EA25P1D	Nemrut Dag (EA25)	0.034
EA25P1A	Nemrut Dag (EA25)	0.035
EA25R1	Nemrut Dag (EA25)	0.038

Elements: Fe, Zr, Ba

A-Rank:	Nemrut Dag (EA22)	6
B-Rank:	Nemrut Dag (EA21)	3

Specimen	*Location*	*E.D.*
EA22P5A	Nemrut Dag (EA22)	0.085
EA21P1	Nemrut Dag (EA21)	0.087
EA21R1A	Nemrut Dag (EA21)	0.090
EA22P7A	Nemrut Dag (EA22)	0.090
EA21R1B	Nemrut Dag (EA21)	0.094
EA22P6A	Nemrut Dag (EA22)	0.094
EA22P3	Nemrut Dag (EA22)	0.096
EA22P5B	Nemrut Dag (EA22)	0.096
EA23P1B	Nemrut Dag (EA23)	0.096
EA22P4	Nemrut Dag (EA22)	0.098

Elements: Ti, Fe, Zr, Ba

A-Rank:	Nemrut Dag (EA22)	8
B-Rank:	Nemrut Dag (EA21)	2

Specimen	*Location*	*E.D.*
EA22P7A	Nemrut Dag (EA22)	0.097
EA22P5A	Nemrut Dag (EA22)	0.101
EA21P1	Nemrut Dag (EA21)	0.104
EA21R1B	Nemrut Dag (EA21)	0.107
EA22P8B	Nemrut Dag (EA22)	0.107
EA22P6A	Nemrut Dag (EA22)	0.109
EA22P3	Nemrut Dag (EA22)	0.110
EA22P6B	Nemrut Dag (EA22)	0.110
EA22R1	Nemrut Dag (EA22)	0.110
EA22P4	Nemrut Dag (EA22)	0.112

Elements: Ti, Fe, Mn, Ca, Zr, Ba

A-Rank:	Nemrut Dag (EA22)	5
B-Rank:	Nemrut Dag (EA25)	4

Specimen	*Location*	*E.D.*
EA25P1A	Nemrut Dag (EA25)	0.124
EA25P1C	Nemrut Dag (EA25)	0.125
EA22P7B	Nemrut Dag (EA22)	0.126
EA25P1B	Nemrut Dag (EA25)	0.126
EA25P1D	Nemrut Dag (EA25)	0.131
EA21P1	Nemrut Dag (EA21)	0.135
EA22P4	Nemrut Dag (EA22)	0.136
EA22P6A	Nemrut Dag (EA22)	0.137
EA22R1	Nemrut Dag (EA22)	0.138
EA22P6B	Nemrut Dag (EA22)	0.139

Elements: Fe, Ti, Zr

A-Rank:	Nemrut Dag (EA22)	7
B-Rank:	Nemrut Dag (EA21)	3

Specimen	*Location*	*E.D.*
EA22P7A	Nemrut Dag (EA22)	0.096
EA22P5A	Nemrut Dag (EA22)	0.100
EA21P1	Nemrut Dag (EA21)	0.103
EA21R1B	Nemrut Dag (EA21)	0.105
EA22P8B	Nemrut Dag (EA22)	0.105
EA22P3	Nemrut Dag (EA22)	0.107
EA22P6A	Nemrut Dag (EA22)	0.107
EA22P6B	Nemrut Dag (EA22)	0.108
EA22P4	Nemrut Dag (EA22)	0.109
EA21R1A	Nemrut Dag (EA21)	0.110

Elements: Ti, Zr, Ba

A-Rank:	Nemrut Dag (EA22)	8
B-Rank:	Nemrut Dag (EA21)	2

Specimen	*Location*	*E.D.*
EA22P7A	Nemrut Dag (EA22)	0.093
EA22P5A	Nemrut Dag (EA22)	0.098
EA21P1	Nemrut Dag (EA21)	0.099
EA21R1B	Nemrut Dag (EA21)	0.104
EA22P8B	Nemrut Dag (EA22)	0.104
EA22R1	Nemrut Dag (EA22)	0.105
EA22P3	Nemrut Dag (EA22)	0.106
EA22P6A	Nemrut Dag (EA22)	0.106
EA22P6B	Nemrut Dag (EA22)	0.107
EA22P7B	Nemrut Dag (EA22)	0.108

Elements: Ti, Fe, Zr, Ba, Zn

A-Rank:	Nemrut Dag (EA22)	9
B-Rank:	Nemrut Dag (EA25)	1

Specimen	*Location*	*E.D.*
EA22P7A	Nemrut Dag (EA22)	0.100
EA22R1	Nemrut Dag (EA22)	0.114
EA22P5B	Nemrut Dag (EA22)	0.116
EA22P3	Nemrut Dag (EA22)	0.123
EA22P1D	Nemrut Dag (EA22)	0.136
EA22P7B	Nemrut Dag (EA22)	0.136
EA22P1C	Nemrut Dag (EA22)	0.140
EA25P2C	Nemrut Dag (EA25)	0.141
EA22P8B	Nemrut Dag (EA22)	0.145
EA22P6A	Nemrut Dag (EA22)	0.146

Elements: Ti, Al, Fe, Mn, Ca, Zr, Ba

A-Rank:	Nemrut Dag (EA25)	6
B-Rank:	Nemrut Dag (EA22)	4

Specimen	*Location*	*E.D.*
EA25P1A	Nemrut Dag (EA25)	0.124
EA25P1B	Nemrut Dag (EA25)	0.126
EA25P1C	Nemrut Dag (EA25)	0.126
EA22P7B	Nemrut Dag (EA22)	0.132
EA25P1D	Nemrut Dag (EA25)	0.132
EA22P4	Nemrut Dag (EA22)	0.142
EA22P6A	Nemrut Dag (EA22)	0.144
EA22R1	Nemrut Dag (EA22)	0.145
EA25P2C	Nemrut Dag (EA25)	0.145
EA25R1	Nemrut Dag (EA25)	0.145

Table D.1 - Source Assignments of Artifacts based on Euclidean Distance to Centroids of Geological Specimens

Artifact: A18 q582-1 f242 k28

A-Rank: **Nemrut Dag (EA25)** **68**
B-Rank: Nemrut Dag (EA22) 11

Elements: Fe, Ti, Ba

A-Rank:	Nemrut Dag (EA25)	10
B-Rank:	-	-

Specimen	*Location*	*E.D.*
EA25P3	Nemrut Dag (EA25)	0.014
EA25P1D	Nemrut Dag (EA25)	0.018
EA25R1	Nemrut Dag (EA25)	0.018
EA25P1A	Nemrut Dag (EA25)	0.023
EA25P1B	Nemrut Dag (EA25)	0.023
EA25P2B	Nemrut Dag (EA25)	0.024
EA25P1C	Nemrut Dag (EA25)	0.030
EA25P2D	Nemrut Dag (EA25)	0.031
EA25P2C	Nemrut Dag (EA25)	0.032
EA25P2A	Nemrut Dag (EA25)	0.033

Elements: Fe, Zr, Ba

A-Rank:	Nemrut Dag (EA22)	5
B-Rank:	Nemrut Dag (EA25)	4

Specimen	*Location*	*E.D.*
EA22P4	Nemrut Dag (EA22)	0.034
EA25P1D	Nemrut Dag (EA25)	0.034
EA25P1A	Nemrut Dag (EA25)	0.038
EA25P1B	Nemrut Dag (EA25)	0.038
EA22P5B	Nemrut Dag (EA22)	0.046
EA22P3	Nemrut Dag (EA22)	0.047
EA22P8A	Nemrut Dag (EA22)	0.047
EA22P8B	Nemrut Dag (EA22)	0.047
EA25P1C	Nemrut Dag (EA25)	0.047
EA21R1B	Nemrut Dag (EA21)	0.048

Elements: Ti, Fe, Zr, Ba

A-Rank:	Nemrut Dag (EA25)	10
B-Rank:	-	-

Specimen	*Location*	*E.D.*
EA25P1D	Nemrut Dag (EA25)	0.034
EA25P1A	Nemrut Dag (EA25)	0.039
EA25P1B	Nemrut Dag (EA25)	0.039
EA25P1C	Nemrut Dag (EA25)	0.047
EA25R1	Nemrut Dag (EA25)	0.052
EA25P3	Nemrut Dag (EA25)	0.056
EA25P2C	Nemrut Dag (EA25)	0.061
EA25P2D	Nemrut Dag (EA25)	0.063
EA25P2A	Nemrut Dag (EA25)	0.067
EA25P2B	Nemrut Dag (EA25)	0.067

Elements: Ti, Fe, Mn, Ca, Zr, Ba

A-Rank:	Nemrut Dag (EA25)	10
B-Rank:	-	-

Specimen	*Location*	*E.D.*
EA25P1A	Nemrut Dag (EA25)	0.039
EA25P1B	Nemrut Dag (EA25)	0.040
EA25P1D	Nemrut Dag (EA25)	0.044
EA25P1C	Nemrut Dag (EA25)	0.051
EA25R1	Nemrut Dag (EA25)	0.053
EA25P3	Nemrut Dag (EA25)	0.057
EA25P2C	Nemrut Dag (EA25)	0.062
EA25P2D	Nemrut Dag (EA25)	0.065
EA25P2B	Nemrut Dag (EA25)	0.067
EA25P2A	Nemrut Dag (EA25)	0.068

Elements: Fe, Ti, Zr

A-Rank:	Nemrut Dag (EA25)	10
B-Rank:	-	-

Specimen	*Location*	*E.D.*
EA25P1D	Nemrut Dag (EA25)	0.029
EA25P1A	Nemrut Dag (EA25)	0.032
EA25P1B	Nemrut Dag (EA25)	0.032
EA25P1C	Nemrut Dag (EA25)	0.037
EA25P2C	Nemrut Dag (EA25)	0.051
EA25R1	Nemrut Dag (EA25)	0.051
EA25P2D	Nemrut Dag (EA25)	0.055
EA25P3	Nemrut Dag (EA25)	0.055
EA25P2A	Nemrut Dag (EA25)	0.059
EA25P2B	Nemrut Dag (EA25)	0.062

Elements: Ti, Zr, Ba

A-Rank:	Nemrut Dag (EA25)	8
B-Rank:	Nemrut Dag (EA22)	2

Specimen	*Location*	*E.D.*
EA25P1D	Nemrut Dag (EA25)	0.034
EA25P1A	Nemrut Dag (EA25)	0.038
EA25P1B	Nemrut Dag (EA25)	0.039
EA25P1C	Nemrut Dag (EA25)	0.047
EA25R1	Nemrut Dag (EA25)	0.052
EA25P3	Nemrut Dag (EA25)	0.056
EA25P2C	Nemrut Dag (EA25)	0.060
EA25P2D	Nemrut Dag (EA25)	0.063
EA22P7A	Nemrut Dag (EA22)	0.066
EA22P8B	Nemrut Dag (EA22)	0.066

Elements: Ti, Fe, Zr, Ba, Zn

A-Rank:	Nemrut Dag (EA25)	6
B-Rank:	Nemrut Dag (EA22)	4

Specimen	*Location*	*E.D.*
EA25P1D	Nemrut Dag (EA25)	0.053
EA25P1A	Nemrut Dag (EA25)	0.056
EA25P1B	Nemrut Dag (EA25)	0.059
EA25P2C	Nemrut Dag (EA25)	0.068
EA22P7A	Nemrut Dag (EA22)	0.086
EA22P3	Nemrut Dag (EA22)	0.087
EA25P2D	Nemrut Dag (EA25)	0.087
EA22P8B	Nemrut Dag (EA22)	0.088
EA22P7B	Nemrut Dag (EA22)	0.089
EA25P1C	Nemrut Dag (EA25)	0.089

Elements: Ti, Al, Fe, Mn, Ca, Zr, Ba

A-Rank:	Nemrut Dag (EA25)	10
B-Rank:	-	-

Specimen	*Location*	*E.D.*
EA25P1A	Nemrut Dag (EA25)	0.046
EA25P1B	Nemrut Dag (EA25)	0.050
EA25P1D	Nemrut Dag (EA25)	0.055
EA25R1	Nemrut Dag (EA25)	0.058
EA25P1C	Nemrut Dag (EA25)	0.059
EA25P3	Nemrut Dag (EA25)	0.062
EA25P2C	Nemrut Dag (EA25)	0.069
EA25P2B	Nemrut Dag (EA25)	0.073
EA25P2D	Nemrut Dag (EA25)	0.073
EA25P2A	Nemrut Dag (EA25)	0.075

Table D.1 - Source Assignments of Artifacts based on Euclidean Distance to Centroids of Geological Specimens

Artifact: A18 q698-1 f298 k26

A-Rank: Nemrut Dag (EA24) 58
B-Rank: **Bingol A*** **10**

Elements: Fe, Ti, Ba

A-Rank:	**Bingol A***	**10**
B-Rank:	-	-

Specimen	*Location*	*E.D.*
EA48P5	Bingol A	0.038
EA48P4	Bingol A	0.039
EA48P2C	Bingol A	0.043
EA48R1	Bingol A	0.048
EA48R2A	Bingol A	0.049
EA48P2B	Bingol A	0.052
EA48R2B	Bingol A	0.054
EA48P1B	Bingol A	0.055
EA48P2A	Bingol A	0.057
EA48P3	Bingol A	0.057

Elements: Fe, Zr, Ba

A-Rank:	Nemrut Dag (EA24)	10
B-Rank:	-	-

Specimen	*Location*	*E.D.*
EA24P1B	Nemrut Dag (EA24)	0.104
EA24P6A	Nemrut Dag (EA24)	0.107
EA24P1C	Nemrut Dag (EA24)	0.109
EA24P1A	Nemrut Dag (EA24)	0.110
EA24P2A	Nemrut Dag (EA24)	0.110
EA24P2B	Nemrut Dag (EA24)	0.110
EA24P5A	Nemrut Dag (EA24)	0.111
EA24P6B	Nemrut Dag (EA24)	0.113
EA24P7	Nemrut Dag (EA24)	0.118
EA24P8B	Nemrut Dag (EA24)	0.118

Elements: Ti, Fe, Zr, Ba

A-Rank:	Nemrut Dag (EA24)	10
B-Rank:	-	-

Specimen	*Location*	*E.D.*
EA24P1B	Nemrut Dag (EA24)	0.105
EA24P6A	Nemrut Dag (EA24)	0.107
EA24P1C	Nemrut Dag (EA24)	0.109
EA24P1A	Nemrut Dag (EA24)	0.110
EA24P2A	Nemrut Dag (EA24)	0.110
EA24P2B	Nemrut Dag (EA24)	0.110
EA24P5A	Nemrut Dag (EA24)	0.111
EA24P6B	Nemrut Dag (EA24)	0.113
EA24P7	Nemrut Dag (EA24)	0.118
EA24P8B	Nemrut Dag (EA24)	0.118

Elements: Ti, Fe, Mn, Ca, Zr, Ba

A-Rank:	Nemrut Dag (EA24)	10
B-Rank:	-	-

Specimen	*Location*	*E.D.*
EA24P1A	Nemrut Dag (EA24)	0.120
EA24P1C	Nemrut Dag (EA24)	0.120
EA24P2A	Nemrut Dag (EA24)	0.128
EA24P8A	Nemrut Dag (EA24)	0.129
EA24P6A	Nemrut Dag (EA24)	0.130
EA24P1B	Nemrut Dag (EA24)	0.131
EA24P2B	Nemrut Dag (EA24)	0.132
EA24P5A	Nemrut Dag (EA24)	0.133
EA24P8B	Nemrut Dag (EA24)	0.133
EA24R1	Nemrut Dag (EA24)	0.134

Elements: Fe, Ti, Zr

A-Rank:	Nemrut Dag (EA24)	10
B-Rank:	-	-

Specimen	*Location*	*E.D.*
EA24P1B	Nemrut Dag (EA24)	0.105
EA24P6A	Nemrut Dag (EA24)	0.108
EA24P1C	Nemrut Dag (EA24)	0.110
EA24P2A	Nemrut Dag (EA24)	0.110
EA24P1A	Nemrut Dag (EA24)	0.111
EA24P2B	Nemrut Dag (EA24)	0.111
EA24P5A	Nemrut Dag (EA24)	0.112
EA24P6B	Nemrut Dag (EA24)	0.112
EA24P8A	Nemrut Dag (EA24)	0.117
EA24P7	Nemrut Dag (EA24)	0.120

Elements: Ti, Zr, Ba

A-Rank:	Nemrut Dag (EA24)	6
B-Rank:	Nemrut Dag (EA21)	2

Specimen	*Location*	*E.D.*
EA24P1B	Nemrut Dag (EA24)	0.036
EA24P1A	Nemrut Dag (EA24)	0.044
EA24P1C	Nemrut Dag (EA24)	0.046
EA24P2A	Nemrut Dag (EA24)	0.046
EA21R1A	Nemrut Dag (EA21)	0.048
EA21P1	Nemrut Dag (EA21)	0.049
EA22P5A	Nemrut Dag (EA22)	0.050
EA24P6A	Nemrut Dag (EA24)	0.052
EA24P2B	Nemrut Dag (EA24)	0.053
EA22P6A	Nemrut Dag (EA22)	0.057

Elements: Ti, Fe, Zr, Ba, Zn

A-Rank:	Nemrut Dag (EA22)	5
B-Rank:	Nemrut Dag (EA24)	5

Specimen	*Location*	*E.D.*
EA22R1	Nemrut Dag (EA22)	0.167
EA24P2A	Nemrut Dag (EA24)	0.167
EA22P7A	Nemrut Dag (EA22)	0.168
EA22P5B	Nemrut Dag (EA22)	0.169
EA24P5A	Nemrut Dag (EA24)	0.171
EA24P6B	Nemrut Dag (EA24)	0.178
EA22P1D	Nemrut Dag (EA22)	0.183
EA22P3	Nemrut Dag (EA22)	0.183
EA24P1B	Nemrut Dag (EA24)	0.185
EA24P9A	Nemrut Dag (EA24)	0.185

Elements: Ti, Al, Fe, Mn, Ca, Zr, Ba

A-Rank:	Nemrut Dag (EA24)	7
B-Rank:	Nemrut Dag (EA21)	3

Specimen	*Location*	*E.D.*
EA24R1	Nemrut Dag (EA24)	0.159
EA24P1A	Nemrut Dag (EA24)	0.163
EA24P1C	Nemrut Dag (EA24)	0.166
EA24P2A	Nemrut Dag (EA24)	0.169
EA21R1A	Nemrut Dag (EA21)	0.170
EA24P5A	Nemrut Dag (EA24)	0.170
EA24P6A	Nemrut Dag (EA24)	0.171
EA24P8A	Nemrut Dag (EA24)	0.171
EA21P2	Nemrut Dag (EA21)	0.173
EA24P1B	Nemrut Dag (EA21)	0.174

* "Bingol A" is the correct source based on the CNK/A vs. NK/A peralkalinity plot and scatterplots of critical elements identified by Poidevin (1998): Al, Fe, and Ba plus Ti.

Table D.1 - Source Assignments of Artifacts based on Euclidean Distance to Centroids of Geological Specimens

Artifact: A18 q746.5 f321 k16

A-Rank: **Nemrut Dag (EA25)** **79**
B-Rank: Nemrut Dag (EA22) 1

Elements: Fe, Ti, Ba

A-Rank:	Nemrut Dag (EA25)	10
B-Rank:	-	-

Specimen	*Location*	*E.D.*
EA25P1A	Nemrut Dag (EA25)	0.005
EA25P1C	Nemrut Dag (EA25)	0.006
EA25P1B	Nemrut Dag (EA25)	0.007
EA25P2B	Nemrut Dag (EA25)	0.007
EA25P2A	Nemrut Dag (EA25)	0.008
EA25P2D	Nemrut Dag (EA25)	0.009
EA25P2C	Nemrut Dag (EA25)	0.011
EA25P1D	Nemrut Dag (EA25)	0.012
EA25R1	Nemrut Dag (EA25)	0.013
EA25P3	Nemrut Dag (EA25)	0.018

Elements: Fe, Zr, Ba

A-Rank:	Nemrut Dag (EA25)	10
B-Rank:	-	-

Specimen	*Location*	*E.D.*
EA25P1C	Nemrut Dag (EA25)	0.005
EA25P1A	Nemrut Dag (EA25)	0.007
EA25P1B	Nemrut Dag (EA25)	0.007
EA25P1D	Nemrut Dag (EA25)	0.014
EA25R1	Nemrut Dag (EA25)	0.017
EA25P2C	Nemrut Dag (EA25)	0.018
EA25P2D	Nemrut Dag (EA25)	0.020
EA25P2A	Nemrut Dag (EA25)	0.022
EA25P3	Nemrut Dag (EA25)	0.024
EA25P2B	Nemrut Dag (EA25)	0.026

Elements: Ti, Fe, Zr, Ba

A-Rank:	Nemrut Dag (EA25)	10
B-Rank:	-	-

Specimen	*Location*	*E.D.*
EA25P1C	Nemrut Dag (EA25)	0.006
EA25P1A	Nemrut Dag (EA25)	0.008
EA25P1B	Nemrut Dag (EA25)	0.009
EA25P1D	Nemrut Dag (EA25)	0.014
EA25P2C	Nemrut Dag (EA25)	0.018
EA25R1	Nemrut Dag (EA25)	0.018
EA25P2D	Nemrut Dag (EA25)	0.020
EA25P2A	Nemrut Dag (EA25)	0.023
EA25P3	Nemrut Dag (EA25)	0.025
EA25P2B	Nemrut Dag (EA25)	0.026

Elements: Ti, Fe, Mn, Ca, Zr, Ba

A-Rank:	Nemrut Dag (EA25)	10
B-Rank:	-	-

Specimen	*Location*	*E.D.*
EA25P1C	Nemrut Dag (EA25)	0.010
EA25P1A	Nemrut Dag (EA25)	0.012
EA25P1B	Nemrut Dag (EA25)	0.021
EA25R1	Nemrut Dag (EA25)	0.029
EA25P2C	Nemrut Dag (EA25)	0.030
EA25P2A	Nemrut Dag (EA25)	0.032
EA25P2B	Nemrut Dag (EA25)	0.032
EA25P3	Nemrut Dag (EA25)	0.032
EA25P2D	Nemrut Dag (EA25)	0.036
EA25P1D	Nemrut Dag (EA25)	0.042

Elements: Fe, Ti, Zr

A-Rank:	Nemrut Dag (EA25)	10
B-Rank:	-	-

Specimen	*Location*	*E.D.*
EA25P1C	Nemrut Dag (EA25)	0.004
EA25P1A	Nemrut Dag (EA25)	0.007
EA25P1B	Nemrut Dag (EA25)	0.008
EA25P1D	Nemrut Dag (EA25)	0.012
EA25R1	Nemrut Dag (EA25)	0.015
EA25P2C	Nemrut Dag (EA25)	0.017
EA25P2D	Nemrut Dag (EA25)	0.019
EA25P3	Nemrut Dag (EA25)	0.019
EA25P2A	Nemrut Dag (EA25)	0.022
EA25P2B	Nemrut Dag (EA25)	0.026

Elements: Ti, Zr, Ba

A-Rank:	Nemrut Dag (EA25)	10
B-Rank:	-	-

Specimen	*Location*	*E.D.*
EA25P1C	Nemrut Dag (EA25)	0.005
EA25P1A	Nemrut Dag (EA25)	0.008
EA25P1B	Nemrut Dag (EA25)	0.009
EA25P1D	Nemrut Dag (EA25)	0.011
EA25P2C	Nemrut Dag (EA25)	0.016
EA25R1	Nemrut Dag (EA25)	0.018
EA25P2D	Nemrut Dag (EA25)	0.019
EA25P2A	Nemrut Dag (EA25)	0.022
EA25P2B	Nemrut Dag (EA25)	0.025
EA25P3	Nemrut Dag (EA25)	0.025

Elements: Ti, Fe, Zr, Ba, Zn

A-Rank:	Nemrut Dag (EA25)	9
B-Rank:	Nemrut Dag (EA22)	1

Specimen	*Location*	*E.D.*
EA25P1A	Nemrut Dag (EA25)	0.009
EA25P1B	Nemrut Dag (EA25)	0.012
EA25P1D	Nemrut Dag (EA25)	0.015
EA25P2D	Nemrut Dag (EA25)	0.032
EA25P2B	Nemrut Dag (EA25)	0.039
EA25P1C	Nemrut Dag (EA25)	0.040
EA25P3	Nemrut Dag (EA25)	0.065
EA25P2A	Nemrut Dag (EA25)	0.069
EA25P2C	Nemrut Dag (EA25)	0.070
EA22P6B	Nemrut Dag (EA22)	0.081

Elements: Ti, Al, Fe, Mn, Ca, Zr, Ba

A-Rank:	Nemrut Dag (EA25)	10
B-Rank:	-	-

Specimen	*Location*	*E.D.*
EA25P1C	Nemrut Dag (EA25)	0.011
EA25P1A	Nemrut Dag (EA25)	0.012
EA25P1B	Nemrut Dag (EA25)	0.023
EA25P2C	Nemrut Dag (EA25)	0.030
EA25R1	Nemrut Dag (EA25)	0.030
EA25P3	Nemrut Dag (EA25)	0.032
EA25P2A	Nemrut Dag (EA25)	0.033
EA25P2B	Nemrut Dag (EA25)	0.033
EA25P2D	Nemrut Dag (EA25)	0.037
EA25P1D	Nemrut Dag (EA25)	0.043

Table D.1 - Source Assignments of Artifacts based on Euclidean Distance to Centroids of Geological Specimens

Artifact: A18 q89-4 f44 k26

A-Rank: **Nemrut Dag (EA25)** **67**
B-Rank: Nemrut Dag (EA22) 13

Elements: Fe, Ti, Ba

A-Rank:	Nemrut Dag (EA25)	10
B-Rank:	-	-

Specimen	*Location*	*E.D.*
EA25P3	Nemrut Dag (EA25)	0.009
EA25R1	Nemrut Dag (EA25)	0.010
EA25P1A	Nemrut Dag (EA25)	0.018
EA25P1B	Nemrut Dag (EA25)	0.018
EA25P1D	Nemrut Dag (EA25)	0.022
EA25P2B	Nemrut Dag (EA25)	0.024
EA25P1C	Nemrut Dag (EA25)	0.026
EA25P2A	Nemrut Dag (EA25)	0.027
EA25P2D	Nemrut Dag (EA25)	0.030
EA25P2C	Nemrut Dag (EA25)	0.031

Elements: Fe, Zr, Ba

A-Rank:	Nemrut Dag (EA25)	6
B-Rank:	Nemrut Dag (EA22)	4

Specimen	*Location*	*E.D.*
EA25P1D	Nemrut Dag (EA25)	0.033
EA25P1A	Nemrut Dag (EA25)	0.034
EA25P1B	Nemrut Dag (EA25)	0.035
EA22P4	Nemrut Dag (EA22)	0.043
EA25P1C	Nemrut Dag (EA25)	0.043
EA25R1	Nemrut Dag (EA25)	0.049
EA22P5B	Nemrut Dag (EA22)	0.054
EA25P3	Nemrut Dag (EA25)	0.054
EA22P5A	Nemrut Dag (EA22)	0.055
EA22P8A	Nemrut Dag (EA22)	0.055

Elements: Ti, Fe, Zr, Ba

A-Rank:	Nemrut Dag (EA25)	10
B-Rank:	-	-

Specimen	*Location*	*E.D.*
EA25P1A	Nemrut Dag (EA25)	0.034
EA25P1B	Nemrut Dag (EA25)	0.035
EA25P1D	Nemrut Dag (EA25)	0.035
EA25P1C	Nemrut Dag (EA25)	0.044
EA25R1	Nemrut Dag (EA25)	0.049
EA25P3	Nemrut Dag (EA25)	0.054
EA25P2C	Nemrut Dag (EA25)	0.059
EA25P2D	Nemrut Dag (EA25)	0.061
EA25P2A	Nemrut Dag (EA25)	0.063
EA25P2B	Nemrut Dag (EA25)	0.065

Elements: Ti, Fe, Mn, Ca, Zr, Ba

A-Rank:	Nemrut Dag (EA25)	10
B-Rank:	-	-

Specimen	*Location*	*E.D.*
EA25P1A	Nemrut Dag (EA25)	0.038
EA25P1B	Nemrut Dag (EA25)	0.044
EA25P1C	Nemrut Dag (EA25)	0.044
EA25R1	Nemrut Dag (EA25)	0.057
EA25P1D	Nemrut Dag (EA25)	0.058
EA25P3	Nemrut Dag (EA25)	0.060
EA25P2C	Nemrut Dag (EA25)	0.066
EA25P2A	Nemrut Dag (EA25)	0.069
EA25P2B	Nemrut Dag (EA25)	0.070
EA25P2D	Nemrut Dag (EA25)	0.072

Elements: Fe, Ti, Zr

A-Rank:	Nemrut Dag (EA25)	10
B-Rank:	-	-

Specimen	*Location*	*E.D.*
EA25P1A	Nemrut Dag (EA25)	0.030
EA25P1B	Nemrut Dag (EA25)	0.031
EA25P1D	Nemrut Dag (EA25)	0.033
EA25P1C	Nemrut Dag (EA25)	0.037
EA25R1	Nemrut Dag (EA25)	0.048
EA25P2C	Nemrut Dag (EA25)	0.053
EA25P3	Nemrut Dag (EA25)	0.053
EA25P2D	Nemrut Dag (EA25)	0.056
EA25P2A	Nemrut Dag (EA25)	0.057
EA25P2B	Nemrut Dag (EA25)	0.063

Elements: Ti, Zr, Ba

A-Rank:	Nemrut Dag (EA25)	7
B-Rank:	Nemrut Dag (EA22)	3

Specimen	*Location*	*E.D.*
EA25P1D	Nemrut Dag (EA25)	0.032
EA25P1A	Nemrut Dag (EA25)	0.034
EA25P1B	Nemrut Dag (EA25)	0.034
EA25P1C	Nemrut Dag (EA25)	0.043
EA25R1	Nemrut Dag (EA25)	0.048
EA22P7A	Nemrut Dag (EA22)	0.053
EA25P3	Nemrut Dag (EA25)	0.053
EA22P8B	Nemrut Dag (EA22)	0.054
EA22P6B	Nemrut Dag (EA22)	0.056
EA22R1	Nemrut Dag (EA22)	0.056

Elements: Ti, Fe, Zr, Ba, Zn

A-Rank:	Nemrut Dag (EA22)	6
B-Rank:	Nemrut Dag (EA25)	4

Specimen	*Location*	*E.D.*
EA25P2C	Nemrut Dag (EA25)	0.062
EA22P7A	Nemrut Dag (EA22)	0.079
EA22R1	Nemrut Dag (EA22)	0.087
EA22P5B	Nemrut Dag (EA22)	0.091
EA22P1D	Nemrut Dag (EA22)	0.093
EA22P3	Nemrut Dag (EA22)	0.097
EA25P1A	Nemrut Dag (EA25)	0.098
EA25P1D	Nemrut Dag (EA25)	0.099
EA25P1B	Nemrut Dag (EA25)	0.102
EA22P1C	Nemrut Dag (EA22)	0.107

Elements: Ti, Al, Fe, Mn, Ca, Zr, Ba

A-Rank:	Nemrut Dag (EA25)	10
B-Rank:	-	-

Specimen	*Location*	*E.D.*
EA25P1A	Nemrut Dag (EA25)	0.048
EA25P1C	Nemrut Dag (EA25)	0.055
EA25P1B	Nemrut Dag (EA25)	0.057
EA25R1	Nemrut Dag (EA25)	0.063
EA25P3	Nemrut Dag (EA25)	0.067
EA25P1D	Nemrut Dag (EA25)	0.070
EA25P2C	Nemrut Dag (EA25)	0.075
EA25P2B	Nemrut Dag (EA25)	0.078
EA25P2A	Nemrut Dag (EA25)	0.079
EA25P2D	Nemrut Dag (EA25)	0.081

Table D.1 - Source Assignments of Artifacts based on Euclidean Distance to Centroids of Geological Specimens

Artifact: A2 q333.2 f114 k151

A-Rank: **Bingol B** **57**
B-Rank: Gutansar 10

Elements: Fe, Ti, Ba

A-Rank: Bingol B 7
B-Rank: Gutansar 2

Specimen	*Location*	*E.D.*
EA56B1	Bingol B	0.016
EA52B1	Bingol B	0.017
EA52B3	Bingol B	0.028
EA52B2	Bingol B	0.038
EA53B2	Bingol B	0.039
EA53B1	Bingol B	0.046
EA54B1	Bingol B	0.074
AR06E2A	Gutansar	0.117
AR21avH1	Chazencavan	0.118
AR06E1A	Gutansar	0.119

Elements: Fe, Zr, Ba

A-Rank: Bingol B 6
B-Rank: Erzincan 4

Specimen	*Location*	*E.D.*
EA52B3	Bingol B	0.039
EA52B1	Bingol B	0.044
EA56B1	Bingol B	0.046
EA52B2	Bingol B	0.048
EA53B2	Bingol B	0.055
EA53B1	Bingol B	0.069
EA43P1	Erzincan	0.074
EA43R2	Erzincan	0.075
EA44P2	Erzincan	0.075
EA44P3	Erzincan	0.075

Elements: Ti, Fe, Zr, Ba

A-Rank: Bingol B 7
B-Rank: Gutansar 3

Specimen	*Location*	*E.D.*
EA52B3	Bingol B	0.045
EA52B1	Bingol B	0.047
EA56B1	Bingol B	0.049
EA52B2	Bingol B	0.053
EA53B2	Bingol B	0.056
EA53B1	Bingol B	0.069
EA54B1	Bingol B	0.087
AR06E2A	Gutansar	0.147
AR30jfL1	Gutansar	0.147
AR06E2B	Gutansar	0.148

Elements: Ti, Fe, Mn, Ca, Zr, Ba

A-Rank: Bingol B 7
B-Rank: Acigol 3

Specimen	*Location*	*E.D.*
EA52B3	Bingol B	0.046
EA56B1	Bingol B	0.050
EA52B1	Bingol B	0.052
EA53B2	Bingol B	0.064
EA52B2	Bingol B	0.067
EA53B1	Bingol B	0.071
EA54B1	Bingol B	0.097
CA08R1C	Acigol	0.185
CA08R1A	Acigol	0.186
CA07R2A	Acigol	0.195

Elements: Fe, Ti, Zr

A-Rank: Bingol B 7
B-Rank: Gutansar 2

Specimen	*Location*	*E.D.*
EA52B3	Bingol B	0.045
EA52B1	Bingol B	0.046
EA56B1	Bingol B	0.049
EA53B2	Bingol B	0.051
EA52B2	Bingol B	0.053
EA53B1	Bingol B	0.061
EA54B1	Bingol B	0.087
AR76rB3	Gutansar	0.132
AR06E3A	Gutansar	0.135
AR40rlS1	Erevan	0.135

Elements: Ti, Zr, Ba

A-Rank: Bingol B 9
B-Rank: Erevan 1

Specimen	*Location*	*E.D.*
EA52B2	Bingol B	0.042
EA52B3	Bingol B	0.042
EA52B1	Bingol B	0.046
EA53B2	Bingol B	0.047
EA55B2	Bingol B	0.047
EA54B1	Bingol B	0.048
EA56B1	Bingol B	0.049
EA55B1	Bingol B	0.059
EA53B1	Bingol B	0.062
AR24jfL1	Erevan	0.101

Elements: Ti, Fe, Zr, Ba, Zn

A-Rank: Bingol B 7
B-Rank: Gutansar 3

Specimen	*Location*	*E.D.*
EA53B1	Bingol B	0.069
EA52B1	Bingol B	0.070
EA52B3	Bingol B	0.080
EA52B2	Bingol B	0.098
EA56B1	Bingol B	0.107
EA54B1	Bingol B	0.112
EA53B2	Bingol B	0.140
AR06E2B	Gutansar	0.148
AR12jB1	Gutansar	0.155
AR11jB1	Gutansar	0.158

Elements: Ti, Al, Fe, Mn, Ca, Zr, Ba

A-Rank: Bingol B 7
B-Rank: Acigol 3

Specimen	*Location*	*E.D.*
EA56B1	Bingol B	0.061
EA52B3	Bingol B	0.062
EA52B1	Bingol B	0.066
EA53B2	Bingol B	0.067
EA53B1	Bingol B	0.074
EA52B2	Bingol B	0.078
EA54B1	Bingol B	0.103
CA08R1C	Acigol	0.186
CA08R1A	Acigol	0.188
CA07R2A	Acigol	0.196

Table D.1 - Source Assignments of Artifacts based on Euclidean Distance to Centroids of Geological Specimens

Artifact: A6 q386-1 f122 k218 piece 1

A-Rank: **Tendurek Dag** **50**
B-Rank: Nemrut Dag (EA26) 12

Elements: Fe, Ti, Ba

A-Rank:	Nemrut Dag (EA26)	8
B-Rank:	Tendurek Dag	2

Specimen	*Location*	*E.D.*
EA26R1A	Nemrut Dag (EA26)	0.071
EA26P1A	Nemrut Dag (EA26)	0.072
EA26P1B	Nemrut Dag (EA26)	0.073
EA26P2A	Nemrut Dag (EA26)	0.076
EA26R2A	Nemrut Dag (EA26)	0.077
EA26R2C	Nemrut Dag (EA26)	0.077
EA26R3C	Nemrut Dag (EA26)	0.078
EA09R2B	Tendurek Dag	0.079
EA26R1B	Nemrut Dag (EA26)	0.079
EA09R3B	Tendurek Dag	0.080

Elements: Fe, Zr, Ba

A-Rank:	Tendurek Dag	10
B-Rank:	-	-

Specimen	*Location*	*E.D.*
EA09R2B	Tendurek Dag	0.072
EA09R1	Tendurek Dag	0.073
EA09R3A	Tendurek Dag	0.073
EA09R3B	Tendurek Dag	0.073
EA09R2C	Tendurek Dag	0.074
EA09R2A	Tendurek Dag	0.075
EA09R2E	Tendurek Dag	0.075
EA09R3C	Tendurek Dag	0.075
EA09R3D	Tendurek Dag	0.075
EA09R3E	Tendurek Dag	0.075

Elements: Ti, Fe, Zr, Ba

A-Rank:	Tendurek Dag	10
B-Rank:	-	-

Specimen	*Location*	*E.D.*
EA09R2B	Tendurek Dag	0.081
EA09R3B	Tendurek Dag	0.082
EA09R1	Tendurek Dag	0.083
EA09R2E	Tendurek Dag	0.083
EA09P2	Tendurek Dag	0.084
EA09R2A	Tendurek Dag	0.084
EA09R3D	Tendurek Dag	0.084
EA09R3E	Tendurek Dag	0.084
EA09R3A	Tendurek Dag	0.085
EA09R3C	Tendurek Dag	0.086

Elements: Ti, Fe, Mn, Ca, Zr, Ba

A-Rank:	Tendurek Dag	10
B-Rank:	-	-

Specimen	*Location*	*E.D.*
EA09R2B	Tendurek Dag	0.082
EA09R2A	Tendurek Dag	0.084
EA09R1	Tendurek Dag	0.085
EA09R3D	Tendurek Dag	0.085
EA09R3A	Tendurek Dag	0.086
EA09R3C	Tendurek Dag	0.086
EA09P2	Tendurek Dag	0.088
EA09R2E	Tendurek Dag	0.088
EA09R3B	Tendurek Dag	0.089
EA09P1A	Tendurek Dag	0.091

Elements: Fe, Ti, Zr

A-Rank:	Tendurek Dag	8
B-Rank:	Erzincan	2

Specimen	*Location*	*E.D.*
EA43P2A	Erzincan	0.076
EA09R2B	Tendurek Dag	0.078
EA09R2E	Tendurek Dag	0.078
EA09R3D	Tendurek Dag	0.078
EA43P1	Erzincan	0.078
EA09R3B	Tendurek Dag	0.079
EA09P1C	Tendurek Dag	0.081
EA09P2	Tendurek Dag	0.081
EA09R3E	Tendurek Dag	0.081
EA30R3G	Tendurek Dag	0.081

Elements: Ti, Zr, Ba

A-Rank:	Kars-Arpacay	6
B-Rank:	Meydan Dag	4

Specimen	*Location*	*E.D.*
EA69SX1	Meydan Dag	0.025
EA39P5	Kars-Arpacay	0.029
EA68SX1	Meydan Dag	0.029
EA39R2	Kars-Arpacay	0.030
EA40R2A	Kars-Arpacay	0.031
EA39P3	Kars-Arpacay	0.032
EA40R2B	Kars-Arpacay	0.032
EA69SX2	Meydan Dag	0.032
EA68SX2	Meydan Dag	0.035
EA39P4	Kars-Arpacay	0.036

Elements: Ti, Fe, Zr, Ba, Zn

A-Rank:	Nemrut Dag (EA26)	4
B-Rank:	Mus	3

Specimen	*Location*	*E.D.*
EA09P1C	Tendurek Dag	0.232
EA60B1B	Mus	0.237
EA26R3D	Nemrut Dag (EA26)	0.247
EA62Y1A	Mus	0.249
EA26R2A	Nemrut Dag (EA26)	0.252
EA26R1A	Nemrut Dag (EA26)	0.253
EA26R1B	Nemrut Dag (EA26)	0.257
EA10P3	Meydan Dag	0.261
EA34P4	Pasinler	0.261
EA60B1A	Mus	0.261

Elements: Ti, Al, Fe, Mn, Ca, Zr, Ba

A-Rank:	Tendurek Dag	10
B-Rank:	-	-

Specimen	*Location*	*E.D.*
EA09R2B	Tendurek Dag	0.084
EA09R2A	Tendurek Dag	0.085
EA09R1	Tendurek Dag	0.086
EA09R3C	Tendurek Dag	0.087
EA09R3D	Tendurek Dag	0.087
EA09R3A	Tendurek Dag	0.088
EA09P2	Tendurek Dag	0.089
EA09R2E	Tendurek Dag	0.089
EA09R3B	Tendurek Dag	0.091
EA31R1	Tendurek Dag	0.091

Table D.1 - Source Assignments of Artifacts based on Euclidean Distance to Centroids of Geological Specimens

Artifact: A6 q386-1 f122 k218 piece 2

A-Rank: **Nemrut Dag (EA25)** **78**
B-Rank: Nemrut Dag (EA22) 2

Elements: Fe, Ti, Ba

A-Rank:	Nemrut Dag (EA25)	10
B-Rank:	-	-

Specimen	*Location*	*E.D.*
EA25P2C	Nemrut Dag (EA25)	0.008
EA25P2D	Nemrut Dag (EA25)	0.011
EA25P1C	Nemrut Dag (EA25)	0.013
EA25P2B	Nemrut Dag (EA25)	0.015
EA25R2	Nemrut Dag (EA25)	0.016
EA25P2A	Nemrut Dag (EA25)	0.017
EA25P1B	Nemrut Dag (EA25)	0.019
EA25P1A	Nemrut Dag (EA25)	0.021
EA25P1D	Nemrut Dag (EA25)	0.021
EA25R1	Nemrut Dag (EA25)	0.027

Elements: Fe, Zr, Ba

A-Rank:	Nemrut Dag (EA25)	10
B-Rank:	-	-

Specimen	*Location*	*E.D.*
EA25P2C	Nemrut Dag (EA25)	0.012
EA25P1C	Nemrut Dag (EA25)	0.013
EA25P2D	Nemrut Dag (EA25)	0.016
EA25P1B	Nemrut Dag (EA25)	0.021
EA25P1A	Nemrut Dag (EA25)	0.023
EA25P1D	Nemrut Dag (EA25)	0.023
EA25P2A	Nemrut Dag (EA25)	0.024
EA25P2B	Nemrut Dag (EA25)	0.026
EA22P1B	Nemrut Dag (EA22)	0.027
EA25R1	Nemrut Dag (EA25)	0.028

Elements: Ti, Fe, Zr, Ba

A-Rank:	Nemrut Dag (EA25)	10
B-Rank:	-	-

Specimen	*Location*	*E.D.*
EA25P1C	Nemrut Dag (EA25)	0.013
EA25P2C	Nemrut Dag (EA25)	0.013
EA25P2D	Nemrut Dag (EA25)	0.018
EA25P1B	Nemrut Dag (EA25)	0.021
EA25P1A	Nemrut Dag (EA25)	0.023
EA25P1D	Nemrut Dag (EA25)	0.024
EA25P2A	Nemrut Dag (EA25)	0.024
EA25P2B	Nemrut Dag (EA25)	0.026
EA25R1	Nemrut Dag (EA25)	0.028
EA25R2	Nemrut Dag (EA25)	0.029

Elements: Ti, Fe, Mn, Ca, Zr, Ba

A-Rank:	Nemrut Dag (EA25)	10
B-Rank:	-	-

Specimen	*Location*	*E.D.*
EA25P1C	Nemrut Dag (EA25)	0.014
EA25P1A	Nemrut Dag (EA25)	0.026
EA25P2C	Nemrut Dag (EA25)	0.029
EA25P1B	Nemrut Dag (EA25)	0.031
EA25P2B	Nemrut Dag (EA25)	0.034
EA25P2A	Nemrut Dag (EA25)	0.035
EA25P2D	Nemrut Dag (EA25)	0.038
EA25R1	Nemrut Dag (EA25)	0.038
EA25P3	Nemrut Dag (EA25)	0.040
EA25R2	Nemrut Dag (EA25)	0.045

Elements: Fe, Ti, Zr

A-Rank:	Nemrut Dag (EA25)	10
B-Rank:	-	-

Specimen	*Location*	*E.D.*
EA25P1C	Nemrut Dag (EA25)	0.011
EA25P2C	Nemrut Dag (EA25)	0.012
EA25P1B	Nemrut Dag (EA25)	0.014
EA25P1D	Nemrut Dag (EA25)	0.014
EA25R1	Nemrut Dag (EA25)	0.016
EA25P1A	Nemrut Dag (EA25)	0.017
EA25P2D	Nemrut Dag (EA25)	0.017
EA25P3	Nemrut Dag (EA25)	0.017
EA25P2A	Nemrut Dag (EA25)	0.023
EA25P2B	Nemrut Dag (EA25)	0.023

Elements: Ti, Zr, Ba

A-Rank:	Nemrut Dag (EA25)	10
B-Rank:	-	-

Specimen	*Location*	*E.D.*
EA25P1C	Nemrut Dag (EA25)	0.009
EA25P2C	Nemrut Dag (EA25)	0.012
EA25P2D	Nemrut Dag (EA25)	0.017
EA25P1A	Nemrut Dag (EA25)	0.018
EA25P1B	Nemrut Dag (EA25)	0.018
EA25P2A	Nemrut Dag (EA25)	0.018
EA25P1D	Nemrut Dag (EA25)	0.023
EA25R1	Nemrut Dag (EA25)	0.024
EA25P2B	Nemrut Dag (EA25)	0.026
EA25R2	Nemrut Dag (EA25)	0.026

Elements: Ti, Fe, Zr, Ba, Zn

A-Rank:	Nemrut Dag (EA25)	8
B-Rank:	Nemrut Dag (EA22)	2

Specimen	*Location*	*E.D.*
EA25P1B	Nemrut Dag (EA25)	0.021
EA25P1A	Nemrut Dag (EA25)	0.023
EA25P2D	Nemrut Dag (EA25)	0.023
EA25P1D	Nemrut Dag (EA25)	0.024
EA25P2B	Nemrut Dag (EA25)	0.032
EA25P1C	Nemrut Dag (EA25)	0.033
EA25P3	Nemrut Dag (EA25)	0.060
EA25P2A	Nemrut Dag (EA25)	0.061
EA22P6B	Nemrut Dag (EA22)	0.072
EA22P8B	Nemrut Dag (EA22)	0.077

Elements: Ti, Al, Fe, Mn, Ca, Zr, Ba

A-Rank:	Nemrut Dag (EA25)	10
B-Rank:	-	-

Specimen	*Location*	*E.D.*
EA25P1C	Nemrut Dag (EA25)	0.016
EA25P1A	Nemrut Dag (EA25)	0.026
EA25P2C	Nemrut Dag (EA25)	0.030
EA25P1B	Nemrut Dag (EA25)	0.032
EA25P2B	Nemrut Dag (EA25)	0.035
EA25P2A	Nemrut Dag (EA25)	0.037
EA25R1	Nemrut Dag (EA25)	0.038
EA25P2D	Nemrut Dag (EA25)	0.039
EA25P3	Nemrut Dag (EA25)	0.040
EA25R2	Nemrut Dag (EA25)	0.045

Table D.1 - Source Assignments of Artifacts based on Euclidean Distance to Centroids of Geological Specimens

Artifact: A6 q971.1 f410 k31

A-Rank: **Bingol B** **62**
B-Rank: Gutansar 10

Elements: Fe, Ti, Ba

A-Rank: Bingol B 7
B-Rank: Gutansar 2

Specimen	*Location*	*E.D.*
EA56B1	Bingol B	0.016
EA53B2	Bingol B	0.026
EA52B1	Bingol B	0.027
EA53B1	Bingol B	0.033
EA52B3	Bingol B	0.035
EA52B2	Bingol B	0.041
EA54B1	Bingol B	0.070
AR06E2A	Gutansar	0.119
AR21avH1	Chazencavan	0.120
AR06E1A	Gutansar	0.122

Elements: Fe, Zr, Ba

A-Rank: Bingol B 7
B-Rank: Erzincan 3

Specimen	*Location*	*E.D.*
EA52B3	Bingol B	0.021
EA52B1	Bingol B	0.026
EA56B1	Bingol B	0.030
EA52B2	Bingol B	0.032
EA53B2	Bingol B	0.033
EA53B1	Bingol B	0.046
EA54B1	Bingol B	0.072
EA43P1	Erzincan	0.087
EA44P2	Erzincan	0.092
EA44P3	Erzincan	0.092

Elements: Ti, Fe, Zr, Ba

A-Rank: Bingol B 7
B-Rank: Gutansar 3

Specimen	*Location*	*E.D.*
EA56B1	Bingol B	0.031
EA53B2	Bingol B	0.033
EA52B1	Bingol B	0.036
EA52B3	Bingol B	0.039
EA52B2	Bingol B	0.044
EA53B1	Bingol B	0.046
EA54B1	Bingol B	0.075
AR06E2A	Gutansar	0.161
AR30jfL1	Gutansar	0.161
AR06E3A	Gutansar	0.162

Elements: Ti, Fe, Mn, Ca, Zr, Ba

A-Rank: Bingol B 9
B-Rank: Acigol 1

Specimen	*Location*	*E.D.*
EA56B1	Bingol B	0.031
EA53B2	Bingol B	0.037
EA52B1	Bingol B	0.038
EA52B3	Bingol B	0.039
EA53B1	Bingol B	0.046
EA52B2	Bingol B	0.052
EA54B1	Bingol B	0.093
EA55B2	Bingol B	0.189
EA55B1	Bingol B	0.192
CA08R1A	Acigol	0.193

Elements: Fe, Ti, Zr

A-Rank: Bingol B 7
B-Rank: Gutansar 2

Specimen	*Location*	*E.D.*
EA56B1	Bingol B	0.029
EA53B2	Bingol B	0.030
EA52B1	Bingol B	0.034
EA52B3	Bingol B	0.037
EA53B1	Bingol B	0.040
EA52B2	Bingol B	0.042
EA54B1	Bingol B	0.073
EA66W1	Lake Van	0.131
AR76rB3	Gutansar	0.142
AR06E3A	Gutansar	0.147

Elements: Ti, Zr, Ba

A-Rank: Bingol B 9
B-Rank: Erevan 1

Specimen	*Location*	*E.D.*
EA53B2	Bingol B	0.024
EA55B2	Bingol B	0.028
EA56B1	Bingol B	0.029
EA52B1	Bingol B	0.036
EA52B2	Bingol B	0.036
EA54B1	Bingol B	0.036
EA52B3	Bingol B	0.038
EA53B1	Bingol B	0.039
EA55B1	Bingol B	0.041
AR24jfL1	Erevan	0.125

Elements: Ti, Fe, Zr, Ba, Zn

A-Rank: Bingol B 7
B-Rank: Gutansar 3

Specimen	*Location*	*E.D.*
EA53B1	Bingol B	0.047
EA52B1	Bingol B	0.075
EA52B3	Bingol B	0.088
EA52B2	Bingol B	0.106
EA54B1	Bingol B	0.112
EA56B1	Bingol B	0.112
EA53B2	Bingol B	0.146
AR06E2B	Gutansar	0.164
AR12jB1	Gutansar	0.173
AR11jB1	Gutansar	0.175

Elements: Ti, Al, Fe, Mn, Ca, Zr, Ba

A-Rank: Bingol B 9
B-Rank: Acigol 1

Specimen	*Location*	*E.D.*
EA53B2	Bingol B	0.040
EA56B1	Bingol B	0.042
EA53B1	Bingol B	0.048
EA52B1	Bingol B	0.052
EA52B3	Bingol B	0.053
EA52B2	Bingol B	0.062
EA54B1	Bingol B	0.098
EA55B2	Bingol B	0.192
EA55B1	Bingol B	0.195
CA08R1A	Acigol	0.196

Table D.1 - Source Assignments of Artifacts based on Euclidean Distance to Centroids of Geological Specimens

Artifact: A6 q973-1 f412 k31

A-Rank: **Nemrut Dag (EA25)** **52**
B-Rank: Nemrut Dag (EA22) 25

Elements: Fe, Ti, Ba

A-Rank:	Nemrut Dag (EA25)	10
B-Rank:	-	-

Specimen	*Location*	*E.D.*
EA25P2C	Nemrut Dag (EA25)	0.009
EA25P2D	Nemrut Dag (EA25)	0.009
EA25P1C	Nemrut Dag (EA25)	0.013
EA25P2A	Nemrut Dag (EA25)	0.014
EA25P2B	Nemrut Dag (EA25)	0.016
EA25R2	Nemrut Dag (EA25)	0.018
EA25P1A	Nemrut Dag (EA25)	0.021
EA25P1B	Nemrut Dag (EA25)	0.021
EA25P1D	Nemrut Dag (EA25)	0.022
EA25R1	Nemrut Dag (EA25)	0.029

Elements: Fe, Zr, Ba

A-Rank:	Nemrut Dag (EA22)	7
B-Rank:	Nemrut Dag (EA21)	3

Specimen	*Location*	*E.D.*
EA22P5A	Nemrut Dag (EA22)	0.051
EA21P1	Nemrut Dag (EA21)	0.054
EA22P7A	Nemrut Dag (EA22)	0.055
EA22P4	Nemrut Dag (EA22)	0.056
EA22P6A	Nemrut Dag (EA22)	0.058
EA22P5B	Nemrut Dag (EA22)	0.059
EA21R1B	Nemrut Dag (EA21)	0.060
EA21R1A	Nemrut Dag (EA21)	0.061
EA22P3	Nemrut Dag (EA22)	0.061
EA22P8B	Nemrut Dag (EA22)	0.061

Elements: Ti, Fe, Zr, Ba

A-Rank:	Nemrut Dag (EA25)	7
B-Rank:	Nemrut Dag (EA22)	3

Specimen	*Location*	*E.D.*
EA25P1D	Nemrut Dag (EA25)	0.065
EA25P1A	Nemrut Dag (EA25)	0.067
EA25P1B	Nemrut Dag (EA25)	0.067
EA25P1C	Nemrut Dag (EA25)	0.070
EA22P7A	Nemrut Dag (EA22)	0.081
EA25P2C	Nemrut Dag (EA25)	0.084
EA25R1	Nemrut Dag (EA25)	0.087
EA22P6B	Nemrut Dag (EA22)	0.088
EA25P2D	Nemrut Dag (EA25)	0.088
EA22P8B	Nemrut Dag (EA22)	0.089

Elements: Ti, Fe, Mn, Ca, Zr, Ba

A-Rank:	Nemrut Dag (EA25)	10
B-Rank:	-	-

Specimen	*Location*	*E.D.*
EA25P1A	Nemrut Dag (EA25)	0.068
EA25P1B	Nemrut Dag (EA25)	0.070
EA25P1C	Nemrut Dag (EA25)	0.071
EA25P1D	Nemrut Dag (EA25)	0.077
EA25P2C	Nemrut Dag (EA25)	0.088
EA25R1	Nemrut Dag (EA25)	0.090
EA25P2D	Nemrut Dag (EA25)	0.093
EA25P2A	Nemrut Dag (EA25)	0.095
EA25P3	Nemrut Dag (EA25)	0.095
EA25P2B	Nemrut Dag (EA25)	0.098

Elements: Fe, Ti, Zr

A-Rank:	Nemrut Dag (EA25)	7
B-Rank:	Nemrut Dag (EA22)	3

Specimen	*Location*	*E.D.*
EA25P1D	Nemrut Dag (EA25)	0.061
EA25P1A	Nemrut Dag (EA25)	0.064
EA25P1B	Nemrut Dag (EA25)	0.065
EA25P1C	Nemrut Dag (EA25)	0.070
EA22P7A	Nemrut Dag (EA22)	0.080
EA25R1	Nemrut Dag (EA25)	0.083
EA25P2C	Nemrut Dag (EA25)	0.084
EA22P6B	Nemrut Dag (EA22)	0.087
EA22P8B	Nemrut Dag (EA22)	0.087
EA25P2D	Nemrut Dag (EA25)	0.087

Elements: Ti, Zr, Ba

A-Rank:	Nemrut Dag (EA25)	5
B-Rank:	Nemrut Dag (EA22)	5

Specimen	*Location*	*E.D.*
EA25P1D	Nemrut Dag (EA25)	0.065
EA22P7A	Nemrut Dag (EA25)	0.067
EA25P1A	Nemrut Dag (EA25)	0.067
EA25P1B	Nemrut Dag (EA25)	0.067
EA25P1C	Nemrut Dag (EA25)	0.070
EA22R1	Nemrut Dag (EA22)	0.076
EA22P6B	Nemrut Dag (EA22)	0.079
EA22P8B	Nemrut Dag (EA22)	0.079
EA22P2	Nemrut Dag (EA22)	0.081
EA22P7B	Nemrut Dag (EA22)	0.081

Elements: Ti, Fe, Zr, Ba, Zn

A-Rank:	Nemrut Dag (EA22)	7
B-Rank:	Nemrut Dag (EA25)	3

Specimen	*Location*	*E.D.*
EA22P7A	Nemrut Dag (EA22)	0.085
EA25P2C	Nemrut Dag (EA25)	0.089
EA22R1	Nemrut Dag (EA22)	0.097
EA22P5B	Nemrut Dag (EA22)	0.105
EA22P3	Nemrut Dag (EA22)	0.112
EA22P1D	Nemrut Dag (EA22)	0.114
EA25P1D	Nemrut Dag (EA25)	0.121
EA25P1A	Nemrut Dag (EA25)	0.122
EA22P7B	Nemrut Dag (EA22)	0.123
EA22P1C	Nemrut Dag (EA22)	0.125

Elements: Ti, Al, Fe, Mn, Ca, Zr, Ba

A-Rank:	Nemrut Dag (EA25)	10
B-Rank:	-	-

Specimen	*Location*	*E.D.*
EA25P1A	Nemrut Dag (EA25)	0.072
EA25P1C	Nemrut Dag (EA25)	0.076
EA25P1B	Nemrut Dag (EA25)	0.077
EA25P1D	Nemrut Dag (EA25)	0.084
EA25R1	Nemrut Dag (EA25)	0.092
EA25P2C	Nemrut Dag (EA25)	0.093
EA25P2D	Nemrut Dag (EA25)	0.098
EA25P3	Nemrut Dag (EA25)	0.098
EA25P2A	Nemrut Dag (EA25)	0.100
EA25P2B	Nemrut Dag (EA25)	0.102

Table D.1 - Source Assignments of Artifacts based on Euclidean Distance to Centroids of Geological Specimens

Artifact: A7 q1146.1 f465 k21

A-Rank: **Tendurek Dag** **60**
B-Rank: Meydan Dag 6

Elements: Fe, Ti, Ba

A-Rank:	Tendurek Dag	10
B-Rank:	-	-

Specimen	*Location*	*E.D.*
EA31P1	Tendurek Dag	0.006
EA30R3D	Tendurek Dag	0.008
EA31R1	Tendurek Dag	0.008
EA09P1A	Tendurek Dag	0.009
EA09R2D	Tendurek Dag	0.009
EA30R3A	Tendurek Dag	0.009
EA32R2	Tendurek Dag	0.009
EA30R2A	Tendurek Dag	0.010
EA30R3E	Tendurek Dag	0.010
EA30P1	Tendurek Dag	0.012

Elements: Fe, Zr, Ba

A-Rank:	Tendurek Dag	10
B-Rank:	-	-

Specimen	*Location*	*E.D.*
EA30P1	Tendurek Dag	0.010
EA31R1	Tendurek Dag	0.012
EA30R2A	Tendurek Dag	0.013
EA30R2B	Tendurek Dag	0.013
EA09R3D	Tendurek Dag	0.014
EA30R3C	Tendurek Dag	0.014
EA30R3F	Tendurek Dag	0.016
EA09R2D	Tendurek Dag	0.017
EA32P1	Tendurek Dag	0.017
EA32R2	Tendurek Dag	0.017

Elements: Ti, Fe, Zr, Ba

A-Rank:	Tendurek Dag	10
B-Rank:	-	-

Specimen	*Location*	*E.D.*
EA31R1	Tendurek Dag	0.012
EA30P1	Tendurek Dag	0.014
EA09R3D	Tendurek Dag	0.015
EA30R2A	Tendurek Dag	0.015
EA30R3C	Tendurek Dag	0.017
EA32R2	Tendurek Dag	0.017
EA09R2D	Tendurek Dag	0.018
EA30R2B	Tendurek Dag	0.018
EA09R2E	Tendurek Dag	0.019
EA09P1A	Tendurek Dag	0.020

Elements: Ti, Fe, Mn, Ca, Zr, Ba

A-Rank:	Tendurek Dag	10
B-Rank:	-	-

Specimen	*Location*	*E.D.*
EA30P1	Tendurek Dag	0.015
EA30R2A	Tendurek Dag	0.015
EA31R1	Tendurek Dag	0.015
EA09R2D	Tendurek Dag	0.018
EA32R2	Tendurek Dag	0.018
EA09P1A	Tendurek Dag	0.020
EA30R2B	Tendurek Dag	0.020
EA30R3E	Tendurek Dag	0.021
EA30R3G	Tendurek Dag	0.021
EA09R2A	Tendurek Dag	0.022

Elements: Fe, Ti, Zr

A-Rank:	Tendurek Dag	10
B-Rank:	-	-

Specimen	*Location*	*E.D.*
EA09P1C	Tendurek Dag	0.008
EA09R2A	Tendurek Dag	0.010
EA30R1	Tendurek Dag	0.012
EA31R1	Tendurek Dag	0.012
EA09R3D	Tendurek Dag	0.013
EA09R1	Tendurek Dag	0.014
EA30P1	Tendurek Dag	0.014
EA30R2A	Tendurek Dag	0.014
EA30R3C	Tendurek Dag	0.014
EA09R3B	Tendurek Dag	0.015

Elements: Ti, Zr, Ba

A-Rank:	Bingol B	4
B-Rank:	Meydan Dag	3

Specimen	*Location*	*E.D.*
EA50R1A	Bingol	0.006
EA50P6	Bingol	0.007
EA09R3D	Tendurek Dag	0.009
EA31R1	Tendurek Dag	0.010
EA07P3	Meydan Dag	0.012
EA08P2	Meydan Dag	0.012
EA49P1	Bingol	0.012
EA50P3B	Bingol	0.012
EA10R1B	Meydan Dag	0.013
EA30P1	Tendurek Dag	0.013

Elements: Ti, Fe, Zr, Ba, Zn

A-Rank:	Mus	5
B-Rank:	Meydan Dag	3

Specimen	*Location*	*E.D.*
EA09P1C	Tendurek Dag	0.053
EA60B1B	Mus	0.078
EA10P3	Meydan Dag	0.081
EA34P4	Pasinler	0.090
EA60B1A	Mus	0.094
EA62Y3B	Mus	0.095
EA62Y1A	Mus	0.098
EA62Y4	Mus	0.101
EA68SX2	Meydan Dag	0.101
EA07P2	Meydan Dag	0.106

Elements: Ti, Al, Fe, Mn, Ca, Zr, Ba

A-Rank:	Tendurek Dag	10
B-Rank:	-	-

Specimen	*Location*	*E.D.*
EA30P1	Tendurek Dag	0.025
EA30R2A	Tendurek Dag	0.034
EA30P2	Tendurek Dag	0.036
EA30R2B	Tendurek Dag	0.036
EA30R3E	Tendurek Dag	0.036
EA30R3F	Tendurek Dag	0.037
EA30R3D	Tendurek Dag	0.038
EA09R2D	Tendurek Dag	0.039
EA30R3A	Tendurek Dag	0.039
EA30R3G	Tendurek Dag	0.039

Table D.1 - Source Assignments of Artifacts based on Euclidean Distance to Centroids of Geological Specimens

Artifact: A7 q1150.5 f465 k21

A-Rank: Nemrut Dag (EA24) 60
B-Rank: **Bingol A*** **10**

Elements: Fe, Ti, Ba

A-Rank:	**Bingol A***	**10**
B-Rank:	-	-

Specimen	*Location*	*E.D.*
EA48P5	Bingol A	0.055
EA48P4	Bingol A	0.056
EA48P2C	Bingol A	0.060
EA48R1	Bingol A	0.063
EA48R2A	Bingol A	0.064
EA48P2B	Bingol A	0.066
EA48P1B	Bingol A	0.069
EA48R2B	Bingol A	0.070
EA48P2A	Bingol A	0.071
EA48P3	Bingol A	0.072

Elements: Fe, Zr, Ba

A-Rank:	Nemrut Dag (EA24)	10
B-Rank:	-	-

Specimen	*Location*	*E.D.*
EA24P6A	Nemrut Dag (EA24)	0.080
EA24P1B	Nemrut Dag (EA24)	0.081
EA24P2B	Nemrut Dag (EA24)	0.083
EA24P1C	Nemrut Dag (EA24)	0.084
EA24P5A	Nemrut Dag (EA24)	0.084
EA24P1A	Nemrut Dag (EA24)	0.085
EA24P2A	Nemrut Dag (EA24)	0.085
EA24P6B	Nemrut Dag (EA24)	0.087
EA24P8B	Nemrut Dag (EA24)	0.091
EA24P7	Nemrut Dag (EA24)	0.092

Elements: Ti, Fe, Zr, Ba

A-Rank:	Nemrut Dag (EA24)	10
B-Rank:	-	-

Specimen	*Location*	*E.D.*
EA24P6A	Nemrut Dag (EA24)	0.081
EA24P1B	Nemrut Dag (EA24)	0.082
EA24P2B	Nemrut Dag (EA24)	0.084
EA24P5A	Nemrut Dag (EA24)	0.084
EA24P1A	Nemrut Dag (EA24)	0.085
EA24P1C	Nemrut Dag (EA24)	0.085
EA24P2A	Nemrut Dag (EA24)	0.085
EA24P6B	Nemrut Dag (EA24)	0.088
EA24P8B	Nemrut Dag (EA24)	0.091
EA24P7	Nemrut Dag (EA24)	0.092

Elements: Ti, Fe, Mn, Ca, Zr, Ba

A-Rank:	Nemrut Dag (EA24)	9
B-Rank:	Nemrut Dag (EA21)	1

Specimen	*Location*	*E.D.*
EA24P1A	Nemrut Dag (EA24)	0.102
EA24P1C	Nemrut Dag (EA24)	0.102
EA24P8A	Nemrut Dag (EA24)	0.109
EA24P2A	Nemrut Dag (EA24)	0.112
EA24P8B	Nemrut Dag (EA24)	0.113
EA24P6A	Nemrut Dag (EA24)	0.114
EA24P2B	Nemrut Dag (EA24)	0.115
EA24R1	Nemrut Dag (EA24)	0.115
EA24P5A	Nemrut Dag (EA24)	0.116
EA21P2	Nemrut Dag (EA21)	0.117

Elements: Fe, Ti, Zr

A-Rank:	Nemrut Dag (EA24)	10
B-Rank:	-	-

Specimen	*Location*	*E.D.*
EA24P6A	Nemrut Dag (EA24)	0.080
EA24P1B	Nemrut Dag (EA24)	0.081
EA24P1C	Nemrut Dag (EA24)	0.083
EA24P2B	Nemrut Dag (EA24)	0.083
EA24P2A	Nemrut Dag (EA24)	0.084
EA24P5A	Nemrut Dag (EA24)	0.084
EA24P6B	Nemrut Dag (EA24)	0.084
EA24P1A	Nemrut Dag (EA24)	0.085
EA24P8A	Nemrut Dag (EA24)	0.088
EA24P8B	Nemrut Dag (EA24)	0.090

Elements: Ti, Zr, Ba

A-Rank:	Nemrut Dag (EA24)	6
B-Rank:	Nemrut Dag (EA21)	2

Specimen	*Location*	*E.D.*
EA24P1B	Nemrut Dag (EA24)	0.021
EA24P1A	Nemrut Dag (EA24)	0.025
EA21P1	Nemrut Dag (EA21)	0.028
EA24P1C	Nemrut Dag (EA24)	0.029
EA24P2A	Nemrut Dag (EA24)	0.029
EA22P5A	Nemrut Dag (EA22)	0.030
EA21R1A	Nemrut Dag (EA21)	0.032
EA24P2B	Nemrut Dag (EA24)	0.033
EA24P6A	Nemrut Dag (EA24)	0.034
EA22P6A	Nemrut Dag (EA22)	0.038

Elements: Ti, Fe, Zr, Ba, Zn

A-Rank:	Nemrut Dag (EA22)	5
B-Rank:	Nemrut Dag (EA24)	5

Specimen	*Location*	*E.D.*
EA22R1	Nemrut Dag (EA22)	0.135
EA24P2A	Nemrut Dag (EA24)	0.136
EA22P7A	Nemrut Dag (EA22)	0.137
EA22P5B	Nemrut Dag (EA22)	0.139
EA24P5A	Nemrut Dag (EA24)	0.140
EA24P6B	Nemrut Dag (EA24)	0.147
EA22P1D	Nemrut Dag (EA22)	0.150
EA22P3	Nemrut Dag (EA22)	0.151
EA24P9A	Nemrut Dag (EA24)	0.151
EA24P1B	Nemrut Dag (EA24)	0.156

Elements: Ti, Al, Fe, Mn, Ca, Zr, Ba

A-Rank:	Nemrut Dag (EA24)	6
B-Rank:	Nemrut Dag (EA21)	2

Specimen	*Location*	*E.D.*
EA24R1	Nemrut Dag (EA24)	0.134
EA24P1A	Nemrut Dag (EA24)	0.137
EA24P1C	Nemrut Dag (EA24)	0.141
EA21P2	Nemrut Dag (EA21)	0.142
EA21R1A	Nemrut Dag (EA21)	0.142
EA22R1	Nemrut Dag (EA22)	0.144
EA24P8A	Nemrut Dag (EA24)	0.144
EA24P2A	Nemrut Dag (EA24)	0.145
EA24P5A	Nemrut Dag (EA24)	0.146
EA22P6A	Nemrut Dag (EA22)	0.147

* "Bingol A" is the correct source based on the CNK/A vs. NK/A peralkalinity plot and scatterplots of critical elements identified by Poidevin (1998): Al, Fe, and Ba plus Ti.

Table D.1 - Source Assignments of Artifacts based on Euclidean Distance to Centroids of Geological Specimens

Artifact: A7 q1174.2 f465 k21

A-Rank: Nemrut Dag (EA24) 72
B-Rank: **Bingol A*** **4**

Elements: Fe, Ti, Ba

A-Rank:	**Bingol A***	**4**
B-Rank:	Nemrut Dag (EA24)	6

Specimen	*Location*	*E.D.*
EA48P5	Bingol A	0.061
EA48P4	Bingol A	0.068
EA48P2C	Bingol A	0.070
EA24P5A	Nemrut Dag (EA24)	0.073
EA24P6A	Nemrut Dag (EA24)	0.074
EA48R2A	Bingol A	0.074
EA24P2B	Nemrut Dag (EA24)	0.075
EA24P9A	Nemrut Dag (EA24)	0.075
EA24P9B	Nemrut Dag (EA24)	0.076
EA24P6B	Nemrut Dag (EA24)	0.077

Elements: Fe, Zr, Ba

A-Rank:	Nemrut Dag (EA24)	10
B-Rank:	-	-

Specimen	*Location*	*E.D.*
EA24P1B	Nemrut Dag (EA24)	0.078
EA24P6A	Nemrut Dag (EA24)	0.079
EA24P1C	Nemrut Dag (EA24)	0.082
EA24P2B	Nemrut Dag (EA24)	0.082
EA24P1A	Nemrut Dag (EA24)	0.083
EA24P2A	Nemrut Dag (EA24)	0.083
EA24P5A	Nemrut Dag (EA24)	0.083
EA24P6B	Nemrut Dag (EA24)	0.084
EA24P8A	Nemrut Dag (EA24)	0.090
EA24P7	Nemrut Dag (EA24)	0.091

Elements: Ti, Fe, Zr, Ba

A-Rank:	Nemrut Dag (EA24)	10
B-Rank:	-	-

Specimen	*Location*	*E.D.*
EA24P1B	Nemrut Dag (EA24)	0.081
EA24P6A	Nemrut Dag (EA24)	0.082
EA24P2B	Nemrut Dag (EA24)	0.083
EA24P1C	Nemrut Dag (EA24)	0.084
EA24P2A	Nemrut Dag (EA24)	0.084
EA24P1A	Nemrut Dag (EA24)	0.085
EA24P5A	Nemrut Dag (EA24)	0.086
EA24P6B	Nemrut Dag (EA24)	0.087
EA24P8A	Nemrut Dag (EA24)	0.091
EA24P8B	Nemrut Dag (EA24)	0.091

Elements: Ti, Fe, Mn, Ca, Zr, Ba

A-Rank:	Nemrut Dag (EA24)	10
B-Rank:	-	-

Specimen	*Location*	*E.D.*
EA24P1A	Nemrut Dag (EA24)	0.089
EA24P1C	Nemrut Dag (EA24)	0.089
EA24P2A	Nemrut Dag (EA24)	0.094
EA24P8A	Nemrut Dag (EA24)	0.095
EA24P2B	Nemrut Dag (EA24)	0.097
EA24P6A	Nemrut Dag (EA24)	0.097
EA24P8B	Nemrut Dag (EA24)	0.099
EA24R1	Nemrut Dag (EA24)	0.099
EA24P1B	Nemrut Dag (EA24)	0.100
EA24P5A	Nemrut Dag (EA24)	0.100

Elements: Fe, Ti, Zr

A-Rank:	Nemrut Dag (EA24)	10
B-Rank:	-	-

Specimen	*Location*	*E.D.*
EA24P1B	Nemrut Dag (EA24)	0.081
EA24P6A	Nemrut Dag (EA24)	0.082
EA24P2A	Nemrut Dag (EA24)	0.083
EA24P2B	Nemrut Dag (EA24)	0.083
EA24P1C	Nemrut Dag (EA24)	0.084
EA24P1A	Nemrut Dag (EA24)	0.085
EA24P5A	Nemrut Dag (EA24)	0.086
EA24P6B	Nemrut Dag (EA24)	0.086
EA24P8A	Nemrut Dag (EA24)	0.089
EA24P8B	Nemrut Dag (EA24)	0.091

Elements: Ti, Zr, Ba

A-Rank:	Nemrut Dag (EA24)	4
B-Rank:	Nemrut Dag (EA21)	3

Specimen	*Location*	*E.D.*
EA22P5A	Nemrut Dag (EA22)	0.027
EA21P1	Nemrut Dag (EA21)	0.030
EA24P1B	Nemrut Dag (EA24)	0.030
EA21R1A	Nemrut Dag (EA21)	0.031
EA24P2A	Nemrut Dag (EA24)	0.031
EA24P1A	Nemrut Dag (EA24)	0.032
EA24P1C	Nemrut Dag (EA24)	0.034
EA21R1B	Nemrut Dag (EA21)	0.035
EA22P6A	Nemrut Dag (EA22)	0.035
EA22P3	Nemrut Dag (EA22)	0.037

Elements: Ti, Fe, Zr, Ba, Zn

A-Rank:	Nemrut Dag (EA24)	7
B-Rank:	Nemrut Dag (EA22)	2

Specimen	*Location*	*E.D.*
EA24P2A	Nemrut Dag (EA24)	0.095
EA24P5A	Nemrut Dag (EA24)	0.099
EA24P6B	Nemrut Dag (EA24)	0.104
EA24P1B	Nemrut Dag (EA24)	0.108
EA24P1A	Nemrut Dag (EA24)	0.111
EA24P9A	Nemrut Dag (EA24)	0.116
EA24P1C	Nemrut Dag (EA24)	0.118
EA22R1	Nemrut Dag (EA22)	0.121
EA24P8B	Bingol A	0.121
EA22P7A	Nemrut Dag (EA22)	0.126

Elements: Ti, Al, Fe, Mn, Ca, Zr, Ba

A-Rank:	Nemrut Dag (EA24)	10
B-Rank:	-	-

Specimen	*Location*	*E.D.*
EA24R1	Nemrut Dag (EA24)	0.111
EA24P1A	Nemrut Dag (EA24)	0.115
EA24P1C	Nemrut Dag (EA24)	0.118
EA24P2A	Nemrut Dag (EA24)	0.119
EA24P8A	Nemrut Dag (EA24)	0.121
EA24P5A	Nemrut Dag (EA24)	0.122
EA24P6A	Nemrut Dag (EA24)	0.122
EA24P2B	Nemrut Dag (EA24)	0.125
EA24P1B	Nemrut Dag (EA24)	0.126
EA24P8B	Nemrut Dag (EA24)	0.126

* "Bingol A" is the correct source based on the CNK/A vs. NK/A peralkalinity plot and scatterplots of critical elements identified by Poidevin (1998): Al, Fe, and Ba plus Ti.

Table D.1 - Source Assignments of Artifacts based on Euclidean Distance to Centroids of Geological Specimens

Artifact: A7 q1201.4 f480 k21

A-Rank: **Pasinler** **48**
B-Rank: **Mus** **11**

Elements: Fe, Ti, Ba

A-Rank:	Tendurek Dag	10
B-Rank:	-	-

Specimen	*Location*	*E.D.*
EA30R3F	Tendurek Dag	0.010
EA30R1	Tendurek Dag	0.011
EA30R3C	Tendurek Dag	0.012
EA09P1C	Tendurek Dag	0.013
EA09P1B	Tendurek Dag	0.014
EA30P2	Tendurek Dag	0.014
EA30R3G	Tendurek Dag	0.014
EA32P1	Tendurek Dag	0.014
EA30P1	Tendurek Dag	0.017
EA09P1D	Tendurek Dag	0.018

Elements: Fe, Zr, Ba

A-Rank:	Pasinler	10
B-Rank:	-	-

Specimen	*Location*	*E.D.*
EA35R1	Pasinler	0.049
EA33P4	Pasinler	0.052
EA33P6	Pasinler	0.052
EA34P2	Pasinler	0.052
EA33P3	Pasinler	0.053
EA33P7	Pasinler	0.053
EA33R1	Pasinler	0.053
EA34P1	Pasinler	0.053
EA34R1	Pasinler	0.053
EA34R2	Pasinler	0.053

Elements: Ti, Fe, Zr, Ba

A-Rank:	Pasinler	10
B-Rank:	-	-

Specimen	*Location*	*E.D.*
EA33P7	Pasinler	0.054
EA35R1	Pasinler	0.054
EA34P2	Pasinler	0.055
EA34R1	Pasinler	0.055
EA33P3	Pasinler	0.056
EA33P4	Pasinler	0.056
EA34P1	Pasinler	0.056
EA34P3	Pasinler	0.056
EA35P1	Pasinler	0.056
EA35P2	Pasinler	0.056

Elements: Ti, Fe, Mn, Ca, Zr, Ba

A-Rank:	Pasinler	10
B-Rank:	-	-

Specimen	*Location*	*E.D.*
EA34P3	Pasinler	0.059
EA34P1	Pasinler	0.060
EA34P2	Pasinler	0.060
EA35P2	Pasinler	0.060
EA33P5	Pasinler	0.063
EA33P7	Pasinler	0.063
EA35P3	Pasinler	0.064
EA35R1	Pasinler	0.064
EA35P1	Pasinler	0.065
EA35R2	Pasinler	0.065

Elements: Fe, Ti, Zr

A-Rank:	Erzincan	10
B-Rank:	-	-

Specimen	*Location*	*E.D.*
EA43R1	Erzincan	0.028
EA44R1	Erzincan	0.031
EA43P2A	Erzincan	0.034
EA44P1	Erzincan	0.034
EA44P2	Erzincan	0.034
EA43P1	Erzincan	0.036
EA43R2	Erzincan	0.036
EA44P3	Erzincan	0.036
EA43P2B	Erzincan	0.037
EA43P3	Erzincan	0.039

Elements: Ti, Zr, Ba

A-Rank:	Pasinler	10
B-Rank:	-	-

Specimen	*Location*	*E.D.*
EA33P7	Pasinler	0.016
EA35P2	Pasinler	0.017
EA35P1	Pasinler	0.018
EA33P3	Pasinler	0.020
EA34P1	Pasinler	0.020
EA34R1	Pasinler	0.020
EA34P3	Pasinler	0.021
EA33P5	Pasinler	0.022
EA34R2	Pasinler	0.022
EA33P4	Pasinler	0.023

Elements: Ti, Fe, Zr, Ba, Zn

A-Rank:	Mus	9
B-Rank:	Tendurek Dag	1

Specimen	*Location*	*E.D.*
EA60B1B	Mus	0.097
EA62Y1A	Mus	0.114
EA60B1A	Mus	0.121
EA09P1C	Tendurek Dag	0.123
EA62Y3B	Mus	0.130
EA62Y4	Mus	0.141
EA57B1	Mus	0.147
EA59B1	Mus	0.151
EA62Y1B	Mus	0.152
EA62Y1C	Mus	0.152

Elements: Ti, Al, Fe, Mn, Ca, Zr, Ba

A-Rank:	Pasinler	8
B-Rank:	Mus	2

Specimen	*Location*	*E.D.*
EA62Y2B	Mus	0.073
EA60B2	Mus	0.074
EA34P1	Pasinler	0.076
EA35P2	Pasinler	0.076
EA35R1	Pasinler	0.076
EA34P3	Pasinler	0.077
EA33P7	Pasinler	0.080
EA34P2	Pasinler	0.080
EA35P3	Pasinler	0.080
EA35R2	Pasinler	0.080

Table D.1 - Source Assignments of Artifacts based on Euclidean Distance to Centroids of Geological Specimens

Artifact: A7 q222-1 f69 k9

A-Rank: **Nemrut Dag (EA25)** **64**
B-Rank: Nemrut Dag (EA22) 10

Elements: Fe, Ti, Ba

A-Rank:	Nemrut Dag (EA25)	10
B-Rank:	-	-

Specimen	*Location*	*E.D.*
EA25P2A	Nemrut Dag (EA25)	0.010
EA25P1C	Nemrut Dag (EA25)	0.016
EA25P1A	Nemrut Dag (EA25)	0.018
EA25P2D	Nemrut Dag (EA25)	0.018
EA25R2	Nemrut Dag (EA25)	0.018
EA25P2C	Nemrut Dag (EA25)	0.019
EA25P1B	Nemrut Dag (EA25)	0.020
EA25P2B	Nemrut Dag (EA25)	0.021
EA25R1	Nemrut Dag (EA25)	0.025
EA25P1D	Nemrut Dag (EA25)	0.026

Elements: Fe, Zr, Ba

A-Rank:	Nemrut Dag (EA22)	5
B-Rank:	Nemrut Dag (EA25)	4

Specimen	*Location*	*E.D.*
EA25P1A	Nemrut Dag (EA25)	0.059
EA25P1B	Nemrut Dag (EA25)	0.060
EA25P1D	Nemrut Dag (EA25)	0.060
EA22P4	Nemrut Dag (EA22)	0.061
EA22P5A	Nemrut Dag (EA22)	0.061
EA25P1C	Nemrut Dag (EA25)	0.064
EA21P1	Nemrut Dag (EA21)	0.066
EA22P7A	Nemrut Dag (EA22)	0.066
EA22P5B	Nemrut Dag (EA22)	0.067
EA22P6A	Nemrut Dag (EA22)	0.067

Elements: Ti, Fe, Zr, Ba

A-Rank:	Nemrut Dag (EA25)	9
B-Rank:	Nemrut Dag (EA22)	1

Specimen	*Location*	*E.D.*
EA25P1A	Nemrut Dag (EA25)	0.059
EA25P1B	Nemrut Dag (EA25)	0.060
EA25P1D	Nemrut Dag (EA25)	0.060
EA25P1C	Nemrut Dag (EA25)	0.064
EA25R1	Nemrut Dag (EA25)	0.078
EA25P2C	Nemrut Dag (EA25)	0.079
EA25P2D	Nemrut Dag (EA25)	0.082
EA25P2A	Nemrut Dag (EA25)	0.084
EA25P3	Nemrut Dag (EA25)	0.085
EA22P7A	Nemrut Dag (EA22)	0.087

Elements: Ti, Fe, Mn, Ca, Zr, Ba

A-Rank:	Nemrut Dag (EA25)	10
B-Rank:	-	-

Specimen	*Location*	*E.D.*
EA25P1A	Nemrut Dag (EA25)	0.060
EA25P1C	Nemrut Dag (EA25)	0.064
EA25P1B	Nemrut Dag (EA25)	0.065
EA25P1D	Nemrut Dag (EA25)	0.074
EA25R1	Nemrut Dag (EA25)	0.083
EA25P2C	Nemrut Dag (EA25)	0.084
EA25P2A	Nemrut Dag (EA25)	0.088
EA25P3	Nemrut Dag (EA25)	0.088
EA25P2D	Nemrut Dag (EA25)	0.089
EA25P2B	Nemrut Dag (EA25)	0.093

Elements: Fe, Ti, Zr

A-Rank:	Nemrut Dag (EA25)	9
B-Rank:	Nemrut Dag (EA22)	1

Specimen	*Location*	*E.D.*
EA25P1A	Nemrut Dag (EA25)	0.057
EA25P1D	Nemrut Dag (EA25)	0.057
EA25P1B	Nemrut Dag (EA25)	0.059
EA25P1C	Nemrut Dag (EA25)	0.064
EA25R1	Nemrut Dag (EA25)	0.076
EA25P2C	Nemrut Dag (EA25)	0.079
EA25P3	Nemrut Dag (EA25)	0.081
EA25P2D	Nemrut Dag (EA25)	0.082
EA25P2A	Nemrut Dag (EA25)	0.084
EA22P7A	Nemrut Dag (EA22)	0.087

Elements: Ti, Zr, Ba

A-Rank:	Nemrut Dag (EA22)	6
B-Rank:	Nemrut Dag (EA25)	4

Specimen	*Location*	*E.D.*
EA25P1D	Nemrut Dag (EA25)	0.057
EA25P1A	Nemrut Dag (EA25)	0.058
EA25P1B	Nemrut Dag (EA25)	0.059
EA22P7A	Nemrut Dag (EA22)	0.062
EA25P1C	Nemrut Dag (EA25)	0.062
EA22R1	Nemrut Dag (EA22)	0.070
EA22P8B	Nemrut Dag (EA22)	0.072
EA22P6B	Nemrut Dag (EA22)	0.073
EA22P2	Nemrut Dag (EA22)	0.074
EA22P7B	Nemrut Dag (EA22)	0.075

Elements: Ti, Fe, Zr, Ba, Zn

A-Rank:	Nemrut Dag (EA25)	8
B-Rank:	Nemrut Dag (EA22)	2

Specimen	*Location*	*E.D.*
EA25P1C	Nemrut Dag (EA25)	0.064
EA25P1A	Nemrut Dag (EA25)	0.066
EA25P1B	Nemrut Dag (EA25)	0.066
EA25P1D	Nemrut Dag (EA25)	0.068
EA25P2D	Nemrut Dag (EA25)	0.083
EA25P2A	Nemrut Dag (EA25)	0.089
EA25P3	Nemrut Dag (EA25)	0.089
EA25P2B	Nemrut Dag (EA25)	0.090
EA22P6B	Nemrut Dag (EA22)	0.095
EA22P8B	Nemrut Dag (EA22)	0.098

Elements: Ti, Al, Fe, Mn, Ca, Zr, Ba

A-Rank:	Nemrut Dag (EA25)	10
B-Rank:	-	-

Specimen	*Location*	*E.D.*
EA25P1A	Nemrut Dag (EA25)	0.063
EA25P1C	Nemrut Dag (EA25)	0.068
EA25P1B	Nemrut Dag (EA25)	0.069
EA25P1D	Nemrut Dag (EA25)	0.078
EA25R1	Nemrut Dag (EA25)	0.084
EA25P2C	Nemrut Dag (EA25)	0.087
EA25P3	Nemrut Dag (EA25)	0.090
EA25P2A	Nemrut Dag (EA25)	0.092
EA25P2D	Nemrut Dag (EA25)	0.092
EA25P2B	Nemrut Dag (EA25)	0.095

Table D.1 - Source Assignments of Artifacts based on Euclidean Distance to Centroids of Geological Specimens

Artifact: A7 q287-1 f56 k7

A-Rank: **Nemrut Dag (EA25)** **78**
B-Rank: Nemrut Dag (EA22) 2

Elements: Fe, Ti, Ba

A-Rank:	Nemrut Dag (EA25)	10
B-Rank:	-	-

Specimen	*Location*	*E.D.*
EA25P1C	Nemrut Dag (EA25)	0.003
EA25P1A	Nemrut Dag (EA25)	0.006
EA25P1B	Nemrut Dag (EA25)	0.006
EA25P2A	Nemrut Dag (EA25)	0.006
EA25P2B	Nemrut Dag (EA25)	0.008
EA25P2C	Nemrut Dag (EA25)	0.009
EA25P2D	Nemrut Dag (EA25)	0.009
EA25P1D	Nemrut Dag (EA25)	0.013
EA25R1	Nemrut Dag (EA25)	0.014
EA25R2	Nemrut Dag (EA25)	0.014

Elements: Fe, Zr, Ba

A-Rank:	Nemrut Dag (EA25)	9
B-Rank:	Nemrut Dag (EA22)	1

Specimen	*Location*	*E.D.*
EA25P1A	Nemrut Dag (EA25)	0.016
EA25P1B	Nemrut Dag (EA25)	0.017
EA25P1D	Nemrut Dag (EA25)	0.018
EA25P1C	Nemrut Dag (EA25)	0.020
EA25P2C	Nemrut Dag (EA25)	0.036
EA25R1	Nemrut Dag (EA25)	0.036
EA22P4	Nemrut Dag (EA22)	0.037
EA25P2D	Nemrut Dag (EA25)	0.039
EA25P2A	Nemrut Dag (EA25)	0.042
EA25P3	Nemrut Dag (EA25)	0.042

Elements: Ti, Fe, Zr, Ba

A-Rank:	Nemrut Dag (EA25)	10
B-Rank:	-	-

Specimen	*Location*	*E.D.*
EA25P1A	Nemrut Dag (EA25)	0.016
EA25P1B	Nemrut Dag (EA25)	0.017
EA25P1D	Nemrut Dag (EA25)	0.019
EA25P1C	Nemrut Dag (EA25)	0.021
EA25P2C	Nemrut Dag (EA25)	0.036
EA25R1	Nemrut Dag (EA25)	0.036
EA25P2D	Nemrut Dag (EA25)	0.040
EA25P2A	Nemrut Dag (EA25)	0.042
EA25P3	Nemrut Dag (EA25)	0.043
EA25P2B	Nemrut Dag (EA25)	0.047

Elements: Ti, Fe, Mn, Ca, Zr, Ba

A-Rank:	Nemrut Dag (EA25)	10
B-Rank:	-	-

Specimen	*Location*	*E.D.*
EA25P1A	Nemrut Dag (EA25)	0.017
EA25P1C	Nemrut Dag (EA25)	0.023
EA25P1B	Nemrut Dag (EA25)	0.024
EA25P1D	Nemrut Dag (EA25)	0.041
EA25R1	Nemrut Dag (EA25)	0.041
EA25P2C	Nemrut Dag (EA25)	0.042
EA25P3	Nemrut Dag (EA25)	0.046
EA25P2A	Nemrut Dag (EA25)	0.047
EA25P2D	Nemrut Dag (EA25)	0.048
EA25P2B	Nemrut Dag (EA25)	0.049

Elements: Fe, Ti, Zr

A-Rank:	Nemrut Dag (EA25)	10
B-Rank:	-	-

Specimen	*Location*	*E.D.*
EA25P1A	Nemrut Dag (EA25)	0.015
EA25P1B	Nemrut Dag (EA25)	0.015
EA25P1D	Nemrut Dag (EA25)	0.016
EA25P1C	Nemrut Dag (EA25)	0.021
EA25R1	Nemrut Dag (EA25)	0.034
EA25P2C	Nemrut Dag (EA25)	0.036
EA25P3	Nemrut Dag (EA25)	0.038
EA25P2D	Nemrut Dag (EA25)	0.040
EA25P2A	Nemrut Dag (EA25)	0.042
EA25P2B	Nemrut Dag (EA25)	0.047

Elements: Ti, Zr, Ba

A-Rank:	Nemrut Dag (EA25)	10
B-Rank:	-	-

Specimen	*Location*	*E.D.*
EA25P1A	Nemrut Dag (EA25)	0.016
EA25P1B	Nemrut Dag (EA25)	0.017
EA25P1D	Nemrut Dag (EA25)	0.017
EA25P1C	Nemrut Dag (EA25)	0.020
EA25P2C	Nemrut Dag (EA25)	0.036
EA25R1	Nemrut Dag (EA25)	0.036
EA25P2D	Nemrut Dag (EA25)	0.039
EA25P2A	Nemrut Dag (EA25)	0.042
EA25P3	Nemrut Dag (EA25)	0.043
EA25P2B	Nemrut Dag (EA25)	0.046

Elements: Ti, Fe, Zr, Ba, Zn

A-Rank:	Nemrut Dag (EA25)	9
B-Rank:	Nemrut Dag (EA22)	1

Specimen	*Location*	*E.D.*
EA25P1C	Nemrut Dag (EA25)	0.021
EA25P1B	Nemrut Dag (EA25)	0.032
EA25P1A	Nemrut Dag (EA25)	0.035
EA25P1D	Nemrut Dag (EA25)	0.036
EA25P2D	Nemrut Dag (EA25)	0.041
EA25P2B	Nemrut Dag (EA25)	0.047
EA25P3	Nemrut Dag (EA25)	0.049
EA25P2A	Nemrut Dag (EA25)	0.052
EA22P6B	Nemrut Dag (EA22)	0.075
EA25R1	Nemrut Dag (EA25)	0.080

Elements: Ti, Al, Fe, Mn, Ca, Zr, Ba

A-Rank:	Nemrut Dag (EA25)	10
B-Rank:	-	-

Specimen	*Location*	*E.D.*
EA25P1A	Nemrut Dag (EA25)	0.021
EA25P1C	Nemrut Dag (EA25)	0.028
EA25P1B	Nemrut Dag (EA25)	0.029
EA25R1	Nemrut Dag (EA25)	0.042
EA25P2C	Nemrut Dag (EA25)	0.045
EA25P1D	Nemrut Dag (EA25)	0.046
EA25P3	Nemrut Dag (EA25)	0.047
EA25P2A	Nemrut Dag (EA25)	0.051
EA25P2B	Nemrut Dag (EA25)	0.052
EA25P2D	Nemrut Dag (EA25)	0.052

Table D.1 - Source Assignments of Artifacts based on Euclidean Distance to Centroids of Geological Specimens

Artifact: A7 q350-l2 f121 k13

A-Rank: **Bingol B** **56**
B-Rank: Gutansar 12

Elements: Fe, Ti, Ba

A-Rank: Bingol B 7
B-Rank: Gutansar 2

Specimen	*Location*	*E.D.*
EA52B1	Bingol B	0.023
EA52B3	Bingol B	0.032
EA56B1	Bingol B	0.034
EA52B2	Bingol B	0.046
EA53B2	Bingol B	0.047
EA53B1	Bingol B	0.051
EA54B1	Bingol B	0.085
AR06E2A	Gutansar	0.127
AR21avH1	Chazencavan	0.128
AR06E1A	Gutansar	0.130

Elements: Fe, Zr, Ba

A-Rank: Bingol B 6
B-Rank: Erzincan 4

Specimen	*Location*	*E.D.*
EA52B3	Bingol B	0.048
EA52B1	Bingol B	0.050
EA56B1	Bingol B	0.050
EA53B2	Bingol B	0.057
EA52B2	Bingol B	0.059
EA53B1	Bingol B	0.069
EA43P1	Erzincan	0.072
EA44P2	Erzincan	0.077
EA44P3	Erzincan	0.078
EA43P2A	Erzincan	0.079

Elements: Ti, Fe, Zr, Ba

A-Rank: Bingol B 7
B-Rank: Gutansar 3

Specimen	*Location*	*E.D.*
EA52B3	Bingol B	0.048
EA52B1	Bingol B	0.050
EA52B2	Bingol B	0.059
EA56B1	Bingol B	0.059
EA53B2	Bingol B	0.063
EA53B1	Bingol B	0.074
EA54B1	Bingol B	0.098
AR30jfL1	Gutansar	0.153
AR06E2A	Gutansar	0.154
AR06E2B	Gutansar	0.156

Elements: Ti, Fe, Mn, Ca, Zr, Ba

A-Rank: Bingol B 7
B-Rank: Acigol 3

Specimen	*Location*	*E.D.*
EA52B1	Bingol B	0.056
EA52B2	Bingol B	0.060
EA52B3	Bingol B	0.061
EA53B2	Bingol B	0.065
EA56B1	Bingol B	0.069
EA53B1	Bingol B	0.080
EA54B1	Bingol B	0.132
CA08R1A	Acigol	0.172
CA08R1C	Acigol	0.178
CA08R1B	Acigol	0.186

Elements: Fe, Ti, Zr

A-Rank: Bingol B 7
B-Rank: Gutansar 2

Specimen	*Location*	*E.D.*
EA52B3	Bingol B	0.045
EA52B1	Bingol B	0.047
EA56B1	Bingol B	0.056
EA52B2	Bingol B	0.057
EA53B2	Bingol B	0.062
EA53B1	Bingol B	0.072
EA54B1	Bingol B	0.096
AR76rB3	Gutansar	0.133
AR06E1C	Gutansar	0.137
AR40rlS1	Erevan	0.137

Elements: Ti, Zr, Ba

A-Rank: Bingol B 9
B-Rank: Erevan 1

Specimen	*Location*	*E.D.*
EA52B2	Bingol B	0.042
EA52B3	Bingol B	0.042
EA52B1	Bingol B	0.048
EA53B2	Bingol B	0.049
EA54B1	Bingol B	0.053
EA55B2	Bingol B	0.058
EA56B1	Bingol B	0.058
EA53B1	Bingol B	0.061
EA55B1	Bingol B	0.070
AR24jfL1	Erevan	0.101

Elements: Ti, Fe, Zr, Ba, Zn

A-Rank: Bingol B 6
B-Rank: Gutansar 4

Specimen	*Location*	*E.D.*
EA53B1	Bingol B	0.103
EA52B1	Bingol B	0.136
EA52B3	Bingol B	0.149
EA52B2	Bingol B	0.168
EA54B1	Bingol B	0.175
AR06E2B	Gutansar	0.176
EA56B1	Bingol B	0.179
AR11jB1	Gutansar	0.186
AR12jB1	Gutansar	0.197
AR06E1B	Gutansar	0.199

Elements: Ti, Al, Fe, Mn, Ca, Zr, Ba

A-Rank: Bingol B 7
B-Rank: Acigol 3

Specimen	*Location*	*E.D.*
EA52B1	Bingol B	0.065
EA53B2	Bingol B	0.066
EA52B2	Bingol B	0.068
EA52B3	Bingol B	0.070
EA56B1	Bingol B	0.074
EA53B1	Bingol B	0.081
EA54B1	Bingol B	0.135
CA08R1A	Acigol	0.176
CA08R1C	Acigol	0.181
CA07R2A	Acigol	0.188

Table D.1 - Source Assignments of Artifacts based on Euclidean Distance to Centroids of Geological Specimens

Artifact: A7 q360-1 f121 k13 piece 1

A-Rank: **Nemrut Dag (EA25)** **76**
B-Rank: Nemrut Dag (EA22) 4

Elements: Fe, Ti, Ba

A-Rank:	Nemrut Dag (EA25)	10
B-Rank:	-	-

Specimen	*Location*	*E.D.*
EA25P1C	Nemrut Dag (EA25)	0.002
EA25P2B	Nemrut Dag (EA25)	0.006
EA25P1A	Nemrut Dag (EA25)	0.007
EA25P1B	Nemrut Dag (EA25)	0.007
EA25P2A	Nemrut Dag (EA25)	0.007
EA25P2C	Nemrut Dag (EA25)	0.007
EA25P2D	Nemrut Dag (EA25)	0.007
EA25P1D	Nemrut Dag (EA25)	0.012
EA25R1	Nemrut Dag (EA25)	0.015
EA25R2	Nemrut Dag (EA25)	0.015

Elements: Fe, Zr, Ba

A-Rank:	Nemrut Dag (EA25)	10
B-Rank:	-	-

Specimen	*Location*	*E.D.*
EA25P2D	Nemrut Dag (EA25)	0.005
EA25P2C	Nemrut Dag (EA25)	0.007
EA25P2A	Nemrut Dag (EA25)	0.008
EA25P2B	Nemrut Dag (EA25)	0.009
EA25R1	Nemrut Dag (EA25)	0.015
EA25R2	Nemrut Dag (EA25)	0.016
EA25P1C	Nemrut Dag (EA25)	0.018
EA25P3	Nemrut Dag (EA25)	0.018
EA25P1A	Nemrut Dag (EA25)	0.024
EA25P1B	Nemrut Dag (EA25)	0.024

Elements: Ti, Fe, Zr, Ba

A-Rank:	Nemrut Dag (EA25)	10
B-Rank:	-	-

Specimen	*Location*	*E.D.*
EA25P2D	Nemrut Dag (EA25)	0.007
EA25P2A	Nemrut Dag (EA25)	0.008
EA25P2C	Nemrut Dag (EA25)	0.008
EA25P2B	Nemrut Dag (EA25)	0.010
EA25R1	Nemrut Dag (EA25)	0.015
EA25P1C	Nemrut Dag (EA25)	0.018
EA25R2	Nemrut Dag (EA25)	0.018
EA25P3	Nemrut Dag (EA25)	0.019
EA25P1A	Nemrut Dag (EA25)	0.024
EA25P1B	Nemrut Dag (EA25)	0.024

Elements: Ti, Fe, Mn, Ca, Zr, Ba

A-Rank:	Nemrut Dag (EA25)	10
B-Rank:	-	-

Specimen	*Location*	*E.D.*
EA25P2B	Nemrut Dag (EA25)	0.019
EA25P1C	Nemrut Dag (EA25)	0.021
EA25P2A	Nemrut Dag (EA25)	0.021
EA25P2C	Nemrut Dag (EA25)	0.022
EA25P1A	Nemrut Dag (EA25)	0.025
EA25P3	Nemrut Dag (EA25)	0.025
EA25R1	Nemrut Dag (EA25)	0.025
EA25P2D	Nemrut Dag (EA25)	0.028
EA25P1B	Nemrut Dag (EA25)	0.029
EA25R2	Nemrut Dag (EA25)	0.034

Elements: Fe, Ti, Zr

A-Rank:	Nemrut Dag (EA25)	10
B-Rank:	-	-

Specimen	*Location*	*E.D.*
EA25P2C	Nemrut Dag (EA25)	0.006
EA25P3	Nemrut Dag (EA25)	0.006
EA25P2A	Nemrut Dag (EA25)	0.007
EA25P2D	Nemrut Dag (EA25)	0.007
EA25R1	Nemrut Dag (EA25)	0.007
EA25P2B	Nemrut Dag (EA25)	0.009
EA25R2	Nemrut Dag (EA25)	0.016
EA25P1C	Nemrut Dag (EA25)	0.017
EA25P1B	Nemrut Dag (EA25)	0.023
EA25P1A	Nemrut Dag (EA25)	0.024

Elements: Ti, Zr, Ba

A-Rank:	Nemrut Dag (EA25)	10
B-Rank:	-	-

Specimen	*Location*	*E.D.*
EA25P2A	Nemrut Dag (EA25)	0.006
EA25P2C	Nemrut Dag (EA25)	0.006
EA25P2D	Nemrut Dag (EA25)	0.006
EA25P2B	Nemrut Dag (EA25)	0.009
EA25R1	Nemrut Dag (EA25)	0.015
EA25P1C	Nemrut Dag (EA25)	0.018
EA25R2	Nemrut Dag (EA25)	0.018
EA25P3	Nemrut Dag (EA25)	0.019
EA25P1A	Nemrut Dag (EA25)	0.024
EA25P1B	Nemrut Dag (EA25)	0.024

Elements: Ti, Fe, Zr, Ba, Zn

A-Rank:	Nemrut Dag (EA25)	6
B-Rank:	Nemrut Dag (EA22)	4

Specimen	*Location*	*E.D.*
EA25P2C	Nemrut Dag (EA25)	0.009
EA25P1A	Nemrut Dag (EA25)	0.080
EA25P1D	Nemrut Dag (EA25)	0.081
EA25P1B	Nemrut Dag (EA25)	0.083
EA22P1D	Nemrut Dag (EA22)	0.084
EA22P7A	Nemrut Dag (EA22)	0.089
EA22R1	Nemrut Dag (EA22)	0.089
EA25P2D	Nemrut Dag (EA25)	0.096
EA22P1C	Nemrut Dag (EA22)	0.100
EA25P2B	Nemrut Dag (EA25)	0.100

Elements: Ti, Al, Fe, Mn, Ca, Zr, Ba

A-Rank:	Nemrut Dag (EA25)	10
B-Rank:	-	-

Specimen	*Location*	*E.D.*
EA25P2B	Nemrut Dag (EA25)	0.023
EA25P2A	Nemrut Dag (EA25)	0.024
EA25P1C	Nemrut Dag (EA25)	0.025
EA25P2C	Nemrut Dag (EA25)	0.025
EA25P2D	Nemrut Dag (EA25)	0.030
EA25P1A	Nemrut Dag (EA25)	0.031
EA25P1B	Nemrut Dag (EA25)	0.031
EA25P3	Nemrut Dag (EA25)	0.031
EA25R1	Nemrut Dag (EA25)	0.033
EA25R2	Nemrut Dag (EA25)	0.041

Table D.1 - Source Assignments of Artifacts based on Euclidean Distance to Centroids of Geological Specimens

Artifact: A7 q360-1 f121 k13 piece 2

A-Rank: **Nemrut Dag (EA25)** **77**
B-Rank: Nemrut Dag (EA22) 3

Elements: Fe, Ti, Ba

A-Rank:	Nemrut Dag (EA25)	10
B-Rank:	-	-

Specimen	*Location*	*E.D.*
EA25P1A	Nemrut Dag (EA25)	0.005
EA25P1B	Nemrut Dag (EA25)	0.005
EA25P2B	Nemrut Dag (EA25)	0.005
EA25P1D	Nemrut Dag (EA25)	0.007
EA25P1C	Nemrut Dag (EA25)	0.008
EA25P2D	Nemrut Dag (EA25)	0.011
EA25R1	Nemrut Dag (EA25)	0.011
EA25P2A	Nemrut Dag (EA25)	0.012
EA25P2C	Nemrut Dag (EA25)	0.012
EA25P3	Nemrut Dag (EA25)	0.015

Elements: Fe, Zr, Ba

A-Rank:	Nemrut Dag (EA25)	10
B-Rank:	-	-

Specimen	*Location*	*E.D.*
EA25R1	Nemrut Dag (EA25)	0.009
EA25P1C	Nemrut Dag (EA25)	0.012
EA25P1B	Nemrut Dag (EA25)	0.014
EA25P2C	Nemrut Dag (EA25)	0.014
EA25P2D	Nemrut Dag (EA25)	0.014
EA25P1A	Nemrut Dag (EA25)	0.015
EA25P3	Nemrut Dag (EA25)	0.015
EA25P2A	Nemrut Dag (EA25)	0.017
EA25P2B	Nemrut Dag (EA25)	0.017
EA25P1D	Nemrut Dag (EA25)	0.018

Elements: Ti, Fe, Zr, Ba

A-Rank:	Nemrut Dag (EA25)	10
B-Rank:	-	-

Specimen	*Location*	*E.D.*
EA25R1	Nemrut Dag (EA25)	0.011
EA25P1C	Nemrut Dag (EA25)	0.012
EA25P2C	Nemrut Dag (EA25)	0.014
EA25P2D	Nemrut Dag (EA25)	0.014
EA25P1A	Nemrut Dag (EA25)	0.015
EA25P1B	Nemrut Dag (EA25)	0.015
EA25P2B	Nemrut Dag (EA25)	0.017
EA25P3	Nemrut Dag (EA25)	0.017
EA25P1D	Nemrut Dag (EA25)	0.018
EA25P2A	Nemrut Dag (EA25)	0.018

Elements: Ti, Fe, Mn, Ca, Zr, Ba

A-Rank:	Nemrut Dag (EA25)	10
B-Rank:	-	-

Specimen	*Location*	*E.D.*
EA25R1	Nemrut Dag (EA25)	0.012
EA25P2C	Nemrut Dag (EA25)	0.015
EA25P1B	Nemrut Dag (EA25)	0.016
EA25P3	Nemrut Dag (EA25)	0.017
EA25P2A	Nemrut Dag (EA25)	0.018
EA25P2B	Nemrut Dag (EA25)	0.018
EA25P2D	Nemrut Dag (EA25)	0.018
EA25P1A	Nemrut Dag (EA25)	0.019
EA25P1D	Nemrut Dag (EA25)	0.027
EA25P1C	Nemrut Dag (EA25)	0.030

Elements: Fe, Ti, Zr

A-Rank:	Nemrut Dag (EA25)	10
B-Rank:	-	-

Specimen	*Location*	*E.D.*
EA25P2C	Nemrut Dag (EA25)	0.008
EA25P1C	Nemrut Dag (EA25)	0.009
EA25R1	Nemrut Dag (EA25)	0.009
EA25P2D	Nemrut Dag (EA25)	0.011
EA25P3	Nemrut Dag (EA25)	0.012
EA25P2A	Nemrut Dag (EA25)	0.014
EA25P1A	Nemrut Dag (EA25)	0.015
EA25P1B	Nemrut Dag (EA25)	0.015
EA25P2B	Nemrut Dag (EA25)	0.017
EA25P1D	Nemrut Dag (EA25)	0.018

Elements: Ti, Zr, Ba

A-Rank:	Nemrut Dag (EA25)	10
B-Rank:	-	-

Specimen	*Location*	*E.D.*
EA25R1	Nemrut Dag (EA25)	0.011
EA25P1C	Nemrut Dag (EA25)	0.012
EA25P2C	Nemrut Dag (EA25)	0.012
EA25P2D	Nemrut Dag (EA25)	0.014
EA25P1A	Nemrut Dag (EA25)	0.015
EA25P1B	Nemrut Dag (EA25)	0.015
EA25P1D	Nemrut Dag (EA25)	0.017
EA25P2A	Nemrut Dag (EA25)	0.017
EA25P2B	Nemrut Dag (EA25)	0.017
EA25P3	Nemrut Dag (EA25)	0.017

Elements: Ti, Fe, Zr, Ba, Zn

A-Rank:	Nemrut Dag (EA25)	7
B-Rank:	Nemrut Dag (EA22)	3

Specimen	*Location*	*E.D.*
EA25P2C	Nemrut Dag (EA25)	0.021
EA25P1A	Nemrut Dag (EA25)	0.059
EA25P1D	Nemrut Dag (EA25)	0.059
EA25P1B	Nemrut Dag (EA25)	0.062
EA25P2D	Nemrut Dag (EA25)	0.077
EA25P2B	Nemrut Dag (EA25)	0.082
EA22P1D	Nemrut Dag (EA22)	0.084
EA22P7A	Nemrut Dag (EA22)	0.088
EA22R1	Nemrut Dag (EA22)	0.088
EA25P1C	Nemrut Dag (EA25)	0.092

Elements: Ti, Al, Fe, Mn, Ca, Zr, Ba

A-Rank:	Nemrut Dag (EA25)	10
B-Rank:	-	-

Specimen	*Location*	*E.D.*
EA25R1	Nemrut Dag (EA25)	0.013
EA25P3	Nemrut Dag (EA25)	0.019
EA25P1A	Nemrut Dag (EA25)	0.021
EA25P2C	Nemrut Dag (EA25)	0.021
EA25P1B	Nemrut Dag (EA25)	0.022
EA25P2B	Nemrut Dag (EA25)	0.022
EA25P2D	Nemrut Dag (EA25)	0.024
EA25P2A	Nemrut Dag (EA25)	0.025
EA25P1D	Nemrut Dag (EA25)	0.032
EA25R2	Nemrut Dag (EA25)	0.032

Table D.1 - Source Assignments of Artifacts based on Euclidean Distance to Centroids of Geological Specimens

Artifact: A7 q360-1 f121 k13 piece 3

A-Rank: **Nemrut Dag (EA25)** **74**
B-Rank: Nemrut Dag (EA22) 6

Elements: Fe, Ti, Ba

A-Rank:	Nemrut Dag (EA25)	10
B-Rank:	-	-

Specimen	*Location*	*E.D.*
EA25P1A	Nemrut Dag (EA25)	0.006
EA25P2A	Nemrut Dag (EA25)	0.006
EA25P1C	Nemrut Dag (EA25)	0.007
EA25P1B	Nemrut Dag (EA25)	0.009
EA25P2B	Nemrut Dag (EA25)	0.011
EA25P2D	Nemrut Dag (EA25)	0.012
EA25P2C	Nemrut Dag (EA25)	0.013
EA25R1	Nemrut Dag (EA25)	0.014
EA25P1D	Nemrut Dag (EA25)	0.015
EA25R2	Nemrut Dag (EA25)	0.017

Elements: Fe, Zr, Ba

A-Rank:	Nemrut Dag (EA25)	10
B-Rank:	-	-

Specimen	*Location*	*E.D.*
EA25P2A	Nemrut Dag (EA25)	0.005
EA25P2B	Nemrut Dag (EA25)	0.011
EA25P2D	Nemrut Dag (EA25)	0.012
EA25R2	Nemrut Dag (EA25)	0.014
EA25P2C	Nemrut Dag (EA25)	0.015
EA25R1	Nemrut Dag (EA25)	0.016
EA25P3	Nemrut Dag (EA25)	0.019
EA25P1C	Nemrut Dag (EA25)	0.023
EA25P1A	Nemrut Dag (EA25)	0.028
EA25P1B	Nemrut Dag (EA25)	0.028

Elements: Ti, Fe, Zr, Ba

A-Rank:	Nemrut Dag (EA25)	10
B-Rank:	-	-

Specimen	*Location*	*E.D.*
EA25P2A	Nemrut Dag (EA25)	0.006
EA25P2B	Nemrut Dag (EA25)	0.011
EA25P2D	Nemrut Dag (EA25)	0.012
EA25P2C	Nemrut Dag (EA25)	0.015
EA25R1	Nemrut Dag (EA25)	0.017
EA25R2	Nemrut Dag (EA25)	0.018
EA25P3	Nemrut Dag (EA25)	0.020
EA25P1C	Nemrut Dag (EA25)	0.023
EA25P1A	Nemrut Dag (EA25)	0.028
EA25P1B	Nemrut Dag (EA25)	0.028

Elements: Ti, Fe, Mn, Ca, Zr, Ba

A-Rank:	Nemrut Dag (EA25)	10
B-Rank:	-	-

Specimen	*Location*	*E.D.*
EA25P2A	Nemrut Dag (EA25)	0.008
EA25P2D	Nemrut Dag (EA25)	0.013
EA25P2B	Nemrut Dag (EA25)	0.015
EA25P2C	Nemrut Dag (EA25)	0.016
EA25R1	Nemrut Dag (EA25)	0.017
EA25R2	Nemrut Dag (EA25)	0.019
EA25P3	Nemrut Dag (EA25)	0.022
EA25P1B	Nemrut Dag (EA25)	0.030
EA25P1A	Nemrut Dag (EA25)	0.034
EA25P1D	Nemrut Dag (EA25)	0.035

Elements: Fe, Ti, Zr

A-Rank:	Nemrut Dag (EA25)	10
B-Rank:	-	-

Specimen	*Location*	*E.D.*
EA25P2A	Nemrut Dag (EA25)	0.002
EA25P3	Nemrut Dag (EA25)	0.010
EA25P2B	Nemrut Dag (EA25)	0.011
EA25P2D	Nemrut Dag (EA25)	0.011
EA25R1	Nemrut Dag (EA25)	0.011
EA25P2C	Nemrut Dag (EA25)	0.013
EA25R2	Nemrut Dag (EA25)	0.014
EA25P1C	Nemrut Dag (EA25)	0.022
EA25P1A	Nemrut Dag (EA25)	0.028
EA25P1B	Nemrut Dag (EA25)	0.028

Elements: Ti, Zr, Ba

A-Rank:	Nemrut Dag (EA25)	10
B-Rank:	-	-

Specimen	*Location*	*E.D.*
EA25P2B	Nemrut Dag (EA25)	0.005
EA25P2A	Nemrut Dag (EA25)	0.006
EA25P2D	Nemrut Dag (EA25)	0.006
EA25P2C	Nemrut Dag (EA25)	0.009
EA25R1	Nemrut Dag (EA25)	0.017
EA25R2	Nemrut Dag (EA25)	0.018
EA25P3	Nemrut Dag (EA25)	0.019
EA25P1C	Nemrut Dag (EA25)	0.022
EA25P1A	Nemrut Dag (EA25)	0.028
EA25P1B	Nemrut Dag (EA25)	0.028

Elements: Ti, Fe, Zr, Ba, Zn

A-Rank:	Nemrut Dag (EA22)	6
B-Rank:	Nemrut Dag (EA25)	4

Specimen	*Location*	*E.D.*
EA25P2C	Nemrut Dag (EA25)	0.042
EA22P1D	Nemrut Dag (EA22)	0.100
EA22P7A	Nemrut Dag (EA22)	0.103
EA22R1	Nemrut Dag (EA22)	0.105
EA22P5B	Nemrut Dag (EA22)	0.114
EA25P1A	Nemrut Dag (EA25)	0.115
EA25P1D	Nemrut Dag (EA25)	0.116
EA25P1B	Nemrut Dag (EA25)	0.118
EA22P1C	Nemrut Dag (EA22)	0.124
EA22P3	Nemrut Dag (EA22)	0.124

Elements: Ti, Al, Fe, Mn, Ca, Zr, Ba

A-Rank:	Nemrut Dag (EA25)	10
B-Rank:	-	-

Specimen	*Location*	*E.D.*
EA25R1	Nemrut Dag (EA25)	0.025
EA25R2	Nemrut Dag (EA25)	0.026
EA25P2A	Nemrut Dag (EA25)	0.030
EA25P2B	Nemrut Dag (EA25)	0.030
EA25P3	Nemrut Dag (EA25)	0.030
EA25P2C	Nemrut Dag (EA25)	0.031
EA25P2D	Nemrut Dag (EA25)	0.031
EA25P1A	Nemrut Dag (EA25)	0.039
EA25P1B	Nemrut Dag (EA25)	0.040
EA25P1D	Nemrut Dag (EA25)	0.046

Table D.1 - Source Assignments of Artifacts based on Euclidean Distance to Centroids of Geological Specimens

Artifact: A7 q360-1 f121 k13 piece 4

A-Rank: **Nemrut Dag (EA25)** **77**
B-Rank: Nemrut Dag (EA22) 3

Elements: Fe, Ti, Ba

A-Rank:	Nemrut Dag (EA25)	10
B-Rank:	-	-

Specimen	*Location*	*E.D.*
EA25P1C	Nemrut Dag (EA25)	0.003
EA25P2A	Nemrut Dag (EA25)	0.005
EA25P1A	Nemrut Dag (EA25)	0.007
EA25P1B	Nemrut Dag (EA25)	0.008
EA25P2B	Nemrut Dag (EA25)	0.008
EA25P2C	Nemrut Dag (EA25)	0.008
EA25P2D	Nemrut Dag (EA25)	0.008
EA25P1D	Nemrut Dag (EA25)	0.014
EA25R1	Nemrut Dag (EA25)	0.015
EA25R2	Nemrut Dag (EA25)	0.015

Elements: Fe, Zr, Ba

A-Rank:	Nemrut Dag (EA25)	10
B-Rank:	-	-

Specimen	*Location*	*E.D.*
EA25P1A	Nemrut Dag (EA25)	0.007
EA25P1B	Nemrut Dag (EA25)	0.008
EA25P1C	Nemrut Dag (EA25)	0.009
EA25P1D	Nemrut Dag (EA25)	0.013
EA25P2C	Nemrut Dag (EA25)	0.025
EA25R1	Nemrut Dag (EA25)	0.025
EA25P2D	Nemrut Dag (EA25)	0.028
EA25P2A	Nemrut Dag (EA25)	0.030
EA25P3	Nemrut Dag (EA25)	0.032
EA25P2B	Nemrut Dag (EA25)	0.035

Elements: Ti, Fe, Zr, Ba

A-Rank:	Nemrut Dag (EA25)	10
B-Rank:	-	-

Specimen	*Location*	*E.D.*
EA25P1A	Nemrut Dag (EA25)	0.008
EA25P1B	Nemrut Dag (EA25)	0.009
EA25P1C	Nemrut Dag (EA25)	0.009
EA25P1D	Nemrut Dag (EA25)	0.014
EA25P2C	Nemrut Dag (EA25)	0.025
EA25R1	Nemrut Dag (EA25)	0.026
EA25P2D	Nemrut Dag (EA25)	0.028
EA25P2A	Nemrut Dag (EA25)	0.030
EA25P3	Nemrut Dag (EA25)	0.033
EA25P2B	Nemrut Dag (EA25)	0.035

Elements: Ti, Fe, Mn, Ca, Zr, Ba

A-Rank:	Nemrut Dag (EA25)	10
B-Rank:	-	-

Specimen	*Location*	*E.D.*
EA25P1D	Nemrut Dag (EA25)	0.015
EA25P1B	Nemrut Dag (EA25)	0.018
EA25P1A	Nemrut Dag (EA25)	0.027
EA25P2C	Nemrut Dag (EA25)	0.028
EA25P2D	Nemrut Dag (EA25)	0.028
EA25R1	Nemrut Dag (EA25)	0.028
EA25P2A	Nemrut Dag (EA25)	0.033
EA25P3	Nemrut Dag (EA25)	0.036
EA25P2B	Nemrut Dag (EA25)	0.039
EA25R2	Nemrut Dag (EA25)	0.040

Elements: Fe, Ti, Zr

A-Rank:	Nemrut Dag (EA25)	10
B-Rank:	-	-

Specimen	*Location*	*E.D.*
EA25P1A	Nemrut Dag (EA25)	0.003
EA25P1B	Nemrut Dag (EA25)	0.005
EA25P1C	Nemrut Dag (EA25)	0.009
EA25P1D	Nemrut Dag (EA25)	0.009
EA25R1	Nemrut Dag (EA25)	0.022
EA25P2C	Nemrut Dag (EA25)	0.025
EA25P3	Nemrut Dag (EA25)	0.027
EA25P2D	Nemrut Dag (EA25)	0.028
EA25P2A	Nemrut Dag (EA25)	0.030
EA25P2B	Nemrut Dag (EA25)	0.035

Elements: Ti, Zr, Ba

A-Rank:	Nemrut Dag (EA25)	10
B-Rank:	-	-

Specimen	*Location*	*E.D.*
EA25P1A	Nemrut Dag (EA25)	0.007
EA25P1C	Nemrut Dag (EA25)	0.008
EA25P1B	Nemrut Dag (EA25)	0.009
EA25P1D	Nemrut Dag (EA25)	0.011
EA25P2C	Nemrut Dag (EA25)	0.024
EA25R1	Nemrut Dag (EA25)	0.026
EA25P2D	Nemrut Dag (EA25)	0.027
EA25P2A	Nemrut Dag (EA25)	0.030
EA25P3	Nemrut Dag (EA25)	0.033
EA25P2B	Nemrut Dag (EA25)	0.034

Elements: Ti, Fe, Zr, Ba, Zn

A-Rank:	Nemrut Dag (EA25)	7
B-Rank:	Nemrut Dag (EA22)	3

Specimen	*Location*	*E.D.*
EA25P2C	Nemrut Dag (EA25)	0.035
EA25P1A	Nemrut Dag (EA25)	0.047
EA25P1D	Nemrut Dag (EA25)	0.049
EA25P1B	Nemrut Dag (EA25)	0.051
EA25P2D	Nemrut Dag (EA25)	0.072
EA25P2B	Nemrut Dag (EA25)	0.079
EA25P1C	Nemrut Dag (EA25)	0.082
EA22P7A	Nemrut Dag (EA22)	0.083
EA22R1	Nemrut Dag (EA22)	0.084
EA22P1D	Nemrut Dag (EA22)	0.085

Elements: Ti, Al, Fe, Mn, Ca, Zr, Ba

A-Rank:	Nemrut Dag (EA25)	10
B-Rank:	-	-

Specimen	*Location*	*E.D.*
EA25P1B	Nemrut Dag (EA25)	0.023
EA25P1D	Nemrut Dag (EA25)	0.023
EA25P1A	Nemrut Dag (EA25)	0.028
EA25R1	Nemrut Dag (EA25)	0.029
EA25P2C	Nemrut Dag (EA25)	0.031
EA25P2D	Nemrut Dag (EA25)	0.032
EA25P2A	Nemrut Dag (EA25)	0.036
EA25P3	Nemrut Dag (EA25)	0.037
EA25R2	Nemrut Dag (EA25)	0.040
EA25P2B	Nemrut Dag (EA25)	0.041

Table D.1 - Source Assignments of Artifacts based on Euclidean Distance to Centroids of Geological Specimens

Artifact: A7 q386-l3 f63 k8

A-Rank: **Bingol B** **57**
B-Rank: Gutansar 10

Elements: Fe, Ti, Ba

A-Rank: Bingol B 7
B-Rank: Gutansar 2

Specimen	*Location*	*E.D.*
EA52B1	Bingol B	0.035
EA52B3	Bingol B	0.040
EA56B1	Bingol B	0.045
EA53B2	Bingol B	0.046
EA53B1	Bingol B	0.047
EA52B2	Bingol B	0.051
EA54B1	Bingol B	0.088
AR06E2A	Gutansar	0.133
AR21avH1	Chazencavan	0.133
AR30jfL1	Gutansar	0.135

Elements: Fe, Zr, Ba

A-Rank: Bingol B 7
B-Rank: Erzincan 3

Specimen	*Location*	*E.D.*
EA56B1	Bingol B	0.043
EA52B1	Bingol B	0.044
EA52B3	Bingol B	0.044
EA53B2	Bingol B	0.044
EA53B1	Bingol B	0.052
EA52B2	Bingol B	0.055
EA43P1	Erzincan	0.085
EA43P2A	Erzincan	0.088
EA54B1	Bingol	0.093
EA44P2	Erzincan	0.095

Elements: Ti, Fe, Zr, Ba

A-Rank: Bingol B 7
B-Rank: Gutansar 2

Specimen	*Location*	*E.D.*
EA52B1	Bingol B	0.044
EA52B3	Bingol B	0.044
EA53B2	Bingol B	0.052
EA56B1	Bingol B	0.054
EA52B2	Bingol B	0.055
EA53B1	Bingol B	0.059
EA54B1	Bingol B	0.093
AR30jfL1	Gutansar	0.168
CA07P1	Acigol	0.168
AR06E2A	Gutansar	0.170

Elements: Ti, Fe, Mn, Ca, Zr, Ba

A-Rank: Bingol B 7
B-Rank: Acigol 3

Specimen	*Location*	*E.D.*
EA52B1	Bingol B	0.045
EA52B3	Bingol B	0.050
EA53B2	Bingol B	0.053
EA52B2	Bingol B	0.056
EA56B1	Bingol B	0.058
EA53B1	Bingol B	0.062
EA54B1	Bingol B	0.119
CA08R1A	Acigol	0.183
CA08R1C	Acigol	0.189
CA07R2A	Acigol	0.197

Elements: Fe, Ti, Zr

A-Rank: Bingol B 7
B-Rank: Gutansar 2

Specimen	*Location*	*E.D.*
EA52B1	Bingol B	0.030
EA52B3	Bingol B	0.030
EA52B2	Bingol B	0.044
EA56B1	Bingol B	0.044
EA53B2	Bingol B	0.051
EA53B1	Bingol B	0.059
EA54B1	Bingol B	0.085
AR76rB3	Gutansar	0.141
EA66W1	Lake Van	0.144
AR76rB2	Gutansar	0.145

Elements: Ti, Zr, Ba

A-Rank: Bingol B 9
B-Rank: Erevan 1

Specimen	*Location*	*E.D.*
EA53B2	Bingol B	0.037
EA52B3	Bingol B	0.038
EA52B2	Bingol B	0.039
EA52B1	Bingol B	0.042
EA53B1	Bingol B	0.045
EA54B1	Bingol B	0.048
EA56B1	Bingol B	0.054
EA55B2	Bingol B	0.055
EA55B1	Bingol B	0.066
AR24jfL1	Erevan	0.123

Elements: Ti, Fe, Zr, Ba, Zn

A-Rank: Bingol B 6
B-Rank: Gutansar 4

Specimen	*Location*	*E.D.*
EA53B1	Bingol B	0.107
EA52B1	Bingol B	0.150
EA52B3	Bingol B	0.163
EA52B2	Bingol B	0.182
EA54B1	Bingol B	0.186
EA56B1	Bingol B	0.193
AR06E2B	Gutansar	0.198
AR11jB1	Gutansar	0.208
AR12jB1	Gutansar	0.220
AR06E1B	Gutansar	0.222

Elements: Ti, Al, Fe, Mn, Ca, Zr, Ba

A-Rank: Bingol B 7
B-Rank: Acigol 3

Specimen	*Location*	*E.D.*
EA53B2	Bingol B	0.062
EA52B1	Bingol B	0.069
EA53B1	Bingol B	0.069
EA52B3	Bingol B	0.072
EA56B1	Bingol B	0.074
EA52B2	Bingol B	0.076
EA54B1	Bingol B	0.128
CA08R1A	Acigol	0.184
CA08R1C	Acigol	0.189
CA07R2A	Acigol	0.197

Table D.1 - Source Assignments of Artifacts based on Euclidean Distance to Centroids of Geological Specimens

Artifact: A7 q602-1 f148 k13

A-Rank: **Nemrut Dag (EA25)** **63**
B-Rank: Nemrut Dag (EA22) 17

Elements: Fe, Ti, Ba

A-Rank:	Nemrut Dag (EA25)	10
B-Rank:	-	-

Specimen	*Location*	*E.D.*
EA25R2	Nemrut Dag (EA25)	0.006
EA25P2A	Nemrut Dag (EA25)	0.007
EA25P1C	Nemrut Dag (EA25)	0.011
EA25P1A	Nemrut Dag (EA25)	0.014
EA25P1B	Nemrut Dag (EA25)	0.014
EA25P2C	Nemrut Dag (EA25)	0.015
EA25P2D	Nemrut Dag (EA25)	0.016
EA25P2B	Nemrut Dag (EA25)	0.017
EA25R1	Nemrut Dag (EA25)	0.020
EA25P1D	Nemrut Dag (EA25)	0.023

Elements: Fe, Zr, Ba

A-Rank:	Nemrut Dag (EA22)	6
B-Rank:	Nemrut Dag (EA25)	4

Specimen	*Location*	*E.D.*
EA25P1A	Nemrut Dag (EA25)	0.043
EA25P1B	Nemrut Dag (EA25)	0.044
EA25P1D	Nemrut Dag (EA25)	0.044
EA22P4	Nemrut Dag (EA22)	0.047
EA25P1C	Nemrut Dag (EA25)	0.048
EA22P5A	Nemrut Dag (EA22)	0.050
EA22P5B	Nemrut Dag (EA22)	0.054
EA22P6A	Nemrut Dag (EA22)	0.055
EA22P6B	Nemrut Dag (EA22)	0.055
EA22P7A	Nemrut Dag (EA22)	0.055

Elements: Ti, Fe, Zr, Ba

A-Rank:	Nemrut Dag (EA25)	9
B-Rank:	Nemrut Dag (EA22)	1

Specimen	*Location*	*E.D.*
EA25P1A	Nemrut Dag (EA25)	0.044
EA25P1B	Nemrut Dag (EA25)	0.044
EA25P1D	Nemrut Dag (EA25)	0.046
EA25P1C	Nemrut Dag (EA25)	0.048
EA25R1	Nemrut Dag (EA25)	0.063
EA25P2C	Nemrut Dag (EA25)	0.064
EA25P2D	Nemrut Dag (EA25)	0.067
EA25P2A	Nemrut Dag (EA25)	0.069
EA25P3	Nemrut Dag (EA25)	0.070
EA22P7A	Nemrut Dag (EA22)	0.071

Elements: Ti, Fe, Mn, Ca, Zr, Ba

A-Rank:	Nemrut Dag (EA25)	10
B-Rank:	-	-

Specimen	*Location*	*E.D.*
EA25P1A	Nemrut Dag (EA25)	0.044
EA25P1B	Nemrut Dag (EA25)	0.046
EA25P1C	Nemrut Dag (EA25)	0.051
EA25P1D	Nemrut Dag (EA25)	0.055
EA25P2C	Nemrut Dag (EA25)	0.065
EA25R1	Nemrut Dag (EA25)	0.065
EA25P2A	Nemrut Dag (EA25)	0.070
EA25P3	Nemrut Dag (EA25)	0.070
EA25P2D	Nemrut Dag (EA25)	0.071
EA25P2B	Nemrut Dag (EA25)	0.075

Elements: Fe, Ti, Zr

A-Rank:	Nemrut Dag (EA25)	9
B-Rank:	Nemrut Dag (EA22)	1

Specimen	*Location*	*E.D.*
EA25P1A	Nemrut Dag (EA25)	0.042
EA25P1B	Nemrut Dag (EA25)	0.043
EA25P1D	Nemrut Dag (EA25)	0.043
EA25P1C	Nemrut Dag (EA25)	0.048
EA25R1	Nemrut Dag (EA25)	0.060
EA25P2C	Nemrut Dag (EA25)	0.064
EA25P3	Nemrut Dag (EA25)	0.065
EA25P2D	Nemrut Dag (EA25)	0.067
EA25P2A	Nemrut Dag (EA25)	0.069
EA22P7A	Nemrut Dag (EA22)	0.071

Elements: Ti, Zr, Ba

A-Rank:	Nemrut Dag (EA25)	5
B-Rank:	Nemrut Dag (EA22)	5

Specimen	*Location*	*E.D.*
EA25P1A	Nemrut Dag (EA25)	0.044
EA25P1B	Nemrut Dag (EA25)	0.044
EA25P1D	Nemrut Dag (EA25)	0.044
EA22P7A	Nemrut Dag (EA25)	0.047
EA25P1C	Nemrut Dag (EA25)	0.048
EA22R1	Nemrut Dag (EA22)	0.053
EA22P2	Nemrut Dag (EA22)	0.056
EA22P6B	Nemrut Dag (EA22)	0.056
EA22P8B	Nemrut Dag (EA22)	0.056
EA22P7B	Nemrut Dag (EA22)	0.059

Elements: Ti, Fe, Zr, Ba, Zn

A-Rank:	Nemrut Dag (EA25)	6
B-Rank:	Nemrut Dag (EA22)	4

Specimen	*Location*	*E.D.*
EA25P1A	Nemrut Dag (EA25)	0.044
EA25P1B	Nemrut Dag (EA25)	0.044
EA25P1D	Nemrut Dag (EA25)	0.046
EA25P1C	Nemrut Dag (EA25)	0.059
EA25P2D	Nemrut Dag (EA25)	0.070
EA22P6B	Nemrut Dag (EA22)	0.075
EA22P8B	Nemrut Dag (EA22)	0.076
EA25P2B	Nemrut Dag (EA25)	0.078
EA22P7B	Nemrut Dag (EA22)	0.083
EA22P6A	Nemrut Dag (EA22)	0.085

Elements: Ti, Al, Fe, Mn, Ca, Zr, Ba

A-Rank:	Nemrut Dag (EA25)	10
B-Rank:	-	-

Specimen	*Location*	*E.D.*
EA25P1A	Nemrut Dag (EA25)	0.044
EA25P1B	Nemrut Dag (EA25)	0.046
EA25P1C	Nemrut Dag (EA25)	0.051
EA25P1D	Nemrut Dag (EA25)	0.056
EA25R1	Nemrut Dag (EA25)	0.065
EA25P2C	Nemrut Dag (EA25)	0.066
EA25P3	Nemrut Dag (EA25)	0.070
EA25P2A	Nemrut Dag (EA25)	0.071
EA25P2D	Nemrut Dag (EA25)	0.071
EA25P2B	Nemrut Dag (EA25)	0.076

Table D.1 - Source Assignments of Artifacts based on Euclidean Distance to Centroids of Geological Specimens

Artifact: A7 q892-1 f261 k12

A-Rank: **Komurcu-Gollu Dag** **76**
B-Rank: Baksan River 2

Elements: Fe, Ti, Ba

A-Rank:	Komurcu-Gollu Dag	10
B-Rank:	-	-

Specimen	*Location*	*E.D.*
CA32W4A	Komurcu-Gollu Dag	0.011
CA32W4E	Komurcu-Gollu Dag	0.011
CA32W1E	Komurcu-Gollu Dag	0.012
CA32W4B	Komurcu-Gollu Dag	0.014
CA20P4	Komurcu-Gollu Dag	0.021
CA20P2	Komurcu-Gollu Dag	0.023
CA32W2A	Komurcu-Gollu Dag	0.023
CA32W2D	Komurcu-Gollu Dag	0.023
CA32W2B	Komurcu-Gollu Dag	0.025
CA32W2E	Komurcu-Gollu Dag	0.025

Elements: Fe, Zr, Ba

A-Rank:	Komurcu-Gollu Dag	9
B-Rank:	Baksan River	1

Specimen	*Location*	*E.D.*
CA32W4A	Komurcu-Gollu Dag	0.011
CA32W4E	Komurcu-Gollu Dag	0.011
CA32W4B	Komurcu-Gollu Dag	0.014
CA32W1E	Komurcu-Gollu Dag	0.015
KB02jB1	Baksan River	0.016
CA32W2D	Komurcu-Gollu Dag	0.023
CA20P2	Komurcu-Gollu Dag	0.025
CA32W2A	Komurcu-Gollu Dag	0.025
CA32W2E	Komurcu-Gollu Dag	0.026
CA32W2B	Komurcu-Gollu Dag	0.027

Elements: Ti, Fe, Zr, Ba

A-Rank:	Komurcu-Gollu Dag	10
B-Rank:	-	-

Specimen	*Location*	*E.D.*
CA32W4E	Komurcu-Gollu Dag	0.011
CA32W4A	Komurcu-Gollu Dag	0.012
CA32W4B	Komurcu-Gollu Dag	0.014
CA32W1E	Komurcu-Gollu Dag	0.015
CA32W2A	Komurcu-Gollu Dag	0.025
CA32W2D	Komurcu-Gollu Dag	0.025
CA32W2E	Komurcu-Gollu Dag	0.026
CA32W2B	Komurcu-Gollu Dag	0.027
CA20P2	Komurcu-Gollu Dag	0.028
CA32W6C	Komurcu-Gollu Dag	0.028

Elements: Ti, Fe, Mn, Ca, Zr, Ba

A-Rank:	Komurcu-Gollu Dag	10
B-Rank:	-	-

Specimen	*Location*	*E.D.*
CA32W4B	Komurcu-Gollu Dag	0.020
CA32W1E	Komurcu-Gollu Dag	0.026
CA32W4A	Komurcu-Gollu Dag	0.028
CA32W6C	Komurcu-Gollu Dag	0.029
CA20P2	Komurcu-Gollu Dag	0.031
CA32W2D	Komurcu-Gollu Dag	0.031
CA32W4D	Komurcu-Gollu Dag	0.032
CA32W4E	Komurcu-Gollu Dag	0.032
CA32W1D	Komurcu-Gollu Dag	0.033
CA32W2E	Komurcu-Gollu Dag	0.033

Elements: Fe, Ti, Zr

A-Rank:	Komurcu-Gollu Dag	9
B-Rank:	Gollu Dag	1

Specimen	*Location*	*E.D.*
CA32W2E	Komurcu, Gollu Dag	0.011
CA32W4E	Komurcu, Gollu Dag	0.011
CA32W4A	Komurcu, Gollu Dag	0.012
CA32W2C	Komurcu, Gollu Dag	0.013
CA32W1A	Komurcu, Gollu Dag	0.014
CA32W2B	Komurcu, Gollu Dag	0.014
CA32W4B	Komurcu, Gollu Dag	0.014
CA32W1E	Komurcu, Gollu Dag	0.015
CA17R1B	Gollu Dag	0.016
CA32W1B	Komurcu, Gollu Dag	0.016

Elements: Ti, Zr, Ba

A-Rank:	Komurcu-Gollu Dag	9
B-Rank:	Kars-Akbaba Dag	1

Specimen	*Location*	*E.D.*
CA32W4A	Komurcu-Gollu Dag	0.005
CA32W4B	Komurcu-Gollu Dag	0.005
CA32W4E	Komurcu-Gollu Dag	0.005
CA32W1E	Komurcu-Gollu Dag	0.010
CA32W6C	Komurcu-Gollu Dag	0.021
CA32W2A	Komurcu-Gollu Dag	0.023
CA32W2D	Komurcu-Gollu Dag	0.023
CA32W2E	Komurcu-Gollu Dag	0.023
CA32W2B	Komurcu-Gollu Dag	0.026
EA38P2	Kars-Akbaba Dag	0.027

Elements: Ti, Fe, Zr, Ba, Zn

A-Rank:	Komurcu-Gollu Dag	9
B-Rank:	Baksan River	1

Specimen	*Location*	*E.D.*
CA32W2D	Komurcu-Gollu Dag	0.026
CA32W2B	Komurcu-Gollu Dag	0.034
CA32W4A	Komurcu-Gollu Dag	0.036
CA32W2A	Komurcu-Gollu Dag	0.043
CA32W4E	Komurcu-Gollu Dag	0.044
KB02jB1	Baksan River	0.044
CA32W4B	Komurcu-Gollu Dag	0.052
CA32W4D	Komurcu-Gollu Dag	0.053
CA32W6D	Komurcu-Gollu Dag	0.058
CA32W1E	Komurcu-Gollu Dag	0.059

Elements: Ti, Al, Fe, Mn, Ca, Zr, Ba

A-Rank:	Komurcu-Gollu Dag	10
B-Rank:	-	-

Specimen	*Location*	*E.D.*
CA32W4B	Komurcu-Gollu Dag	0.020
CA32W1E	Komurcu-Gollu Dag	0.026
CA32W4A	Komurcu-Gollu Dag	0.028
CA32W6C	Komurcu-Gollu Dag	0.029
CA20P2	Komurcu-Gollu Dag	0.031
CA32W2D	Komurcu-Gollu Dag	0.032
CA32W4D	Komurcu-Gollu Dag	0.032
CA32W4E	Komurcu-Gollu Dag	0.032
CA32W2E	Komurcu-Gollu Dag	0.033
CA32W4C	Komurcu-Gollu Dag	0.033

Table D.1 - Source Assignments of Artifacts based on Euclidean Distance to Centroids of Geological Specimens

Artifact: A8 q154-1 f58 k9

A-Rank: **Nemrut Dag (EA25)** **52**
B-Rank: Nemrut Dag (EA22) 24

Elements: Fe, Ti, Ba

A-Rank:	Nemrut Dag (EA25)	10
B-Rank:	-	-

Specimen	*Location*	*E.D.*
EA25P1B	Nemrut Dag (EA25)	0.004
EA25P1A	Nemrut Dag (EA25)	0.006
EA25P1C	Nemrut Dag (EA25)	0.006
EA25P2B	Nemrut Dag (EA25)	0.006
EA25P1D	Nemrut Dag (EA25)	0.010
EA25P2C	Nemrut Dag (EA25)	0.010
EA25P2D	Nemrut Dag (EA25)	0.010
EA25P2A	Nemrut Dag (EA25)	0.011
EA25R1	Nemrut Dag (EA25)	0.011
EA25P3	Nemrut Dag (EA25)	0.015

Elements: Fe, Zr, Ba

A-Rank:	Nemrut Dag (EA22)	7
B-Rank:	Nemrut Dag (EA21)	3

Specimen	*Location*	*E.D.*
EA22P5A	Nemrut Dag (EA22)	0.048
EA22P4	Nemrut Dag (EA22)	0.050
EA22P6A	Nemrut Dag (EA22)	0.054
EA21P1	Nemrut Dag (EA21)	0.055
EA21R1B	Nemrut Dag (EA21)	0.055
EA22P5B	Nemrut Dag (EA22)	0.055
EA22P7A	Nemrut Dag (EA22)	0.055
EA21R1A	Nemrut Dag (EA21)	0.056
EA22P3	Nemrut Dag (EA22)	0.056
EA22P8B	Nemrut Dag (EA22)	0.057

Elements: Ti, Fe, Zr, Ba

A-Rank:	Nemrut Dag (EA25)	6
B-Rank:	Nemrut Dag (EA22)	4

Specimen	*Location*	*E.D.*
EA25P1D	Nemrut Dag (EA25)	0.060
EA25P1A	Nemrut Dag (EA25)	0.061
EA25P1B	Nemrut Dag (EA25)	0.061
EA25P1C	Nemrut Dag (EA25)	0.067
EA22P7A	Nemrut Dag (EA22)	0.075
EA22P8B	Nemrut Dag (EA22)	0.080
EA25R1	Nemrut Dag (EA25)	0.080
EA22P6B	Nemrut Dag (EA22)	0.081
EA25P2C	Nemrut Dag (EA25)	0.082
EA22P5A	Nemrut Dag (EA22)	0.083

Elements: Ti, Fe, Mn, Ca, Zr, Ba

A-Rank:	Nemrut Dag (EA25)	10
B-Rank:	-	-

Specimen	*Location*	*E.D.*
EA25P1A	Nemrut Dag (EA25)	0.062
EA25P1B	Nemrut Dag (EA25)	0.064
EA25P1C	Nemrut Dag (EA25)	0.067
EA25P1D	Nemrut Dag (EA25)	0.071
EA25R1	Nemrut Dag (EA25)	0.083
EA25P2C	Nemrut Dag (EA25)	0.085
EA25P3	Nemrut Dag (EA25)	0.088
EA25P2D	Nemrut Dag (EA25)	0.090
EA25P2A	Nemrut Dag (EA25)	0.091
EA25P2B	Nemrut Dag (EA25)	0.094

Elements: Fe, Ti, Zr

A-Rank:	Nemrut Dag (EA25)	8
B-Rank:	Nemrut Dag (EA22)	2

Specimen	*Location*	*E.D.*
EA25P1D	Nemrut Dag (EA25)	0.059
EA25P1A	Nemrut Dag (EA25)	0.061
EA25P1B	Nemrut Dag (EA25)	0.061
EA25P1C	Nemrut Dag (EA25)	0.067
EA22P7A	Nemrut Dag (EA25)	0.074
EA22P8B	Nemrut Dag (EA25)	0.080
EA25R1	Nemrut Dag (EA25)	0.080
EA22P6B	Nemrut Dag (EA22)	0.081
EA25P2C	Nemrut Dag (EA25)	0.082
EA22P5A	Nemrut Dag (EA22)	0.083

Elements: Ti, Zr, Ba

A-Rank:	Nemrut Dag (EA22)	5
B-Rank:	Nemrut Dag (EA25)	4

Specimen	*Location*	*E.D.*
EA22P7A	Nemrut Dag (EA22)	0.059
EA25P1D	Nemrut Dag (EA25)	0.059
EA25P1A	Nemrut Dag (EA25)	0.061
EA25P1B	Nemrut Dag (EA25)	0.061
EA22P8B	Nemrut Dag (EA22)	0.067
EA22R1	Nemrut Dag (EA22)	0.067
EA25P1C	Nemrut Dag (EA25)	0.067
EA22P6B	Nemrut Dag (EA22)	0.069
EA22P5A	Nemrut Dag (EA22)	0.072
EA21R1B	Nemrut Dag (EA21)	0.073

Elements: Ti, Fe, Zr, Ba, Zn

A-Rank:	Nemrut Dag (EA22)	6
B-Rank:	Nemrut Dag (EA25)	4

Specimen	*Location*	*E.D.*
EA25P1D	Nemrut Dag (EA25)	0.074
EA25P1A	Nemrut Dag (EA25)	0.075
EA25P1B	Nemrut Dag (EA25)	0.077
EA22P7A	Nemrut Dag (EA22)	0.081
EA22P3	Nemrut Dag (EA22)	0.087
EA25P2C	Nemrut Dag (EA25)	0.087
EA22P7B	Nemrut Dag (EA22)	0.089
EA22R1	Nemrut Dag (EA22)	0.089
EA22P8B	Nemrut Dag (EA22)	0.091
EA22P6B	Nemrut Dag (EA22)	0.096

Elements: Ti, Al, Fe, Mn, Ca, Zr, Ba

A-Rank:	Nemrut Dag (EA25)	10
B-Rank:	-	-

Specimen	*Location*	*E.D.*
EA25P1A	Nemrut Dag (EA25)	0.062
EA25P1B	Nemrut Dag (EA25)	0.066
EA25P1C	Nemrut Dag (EA25)	0.069
EA25P1D	Nemrut Dag (EA25)	0.073
EA25R1	Nemrut Dag (EA25)	0.083
EA25P2C	Nemrut Dag (EA25)	0.086
EA25P3	Nemrut Dag (EA25)	0.088
EA25P2D	Nemrut Dag (EA25)	0.092
EA25P2A	Nemrut Dag (EA25)	0.093
EA25P2B	Nemrut Dag (EA25)	0.095

Table D.1 - Source Assignments of Artifacts based on Euclidean Distance to Centroids of Geological Specimens

Artifact: A9 q376.1 f98 k3 piece 1

A-Rank: **Nemrut Dag (EA25)** **73**
B-Rank: Nemrut Dag (EA22) 7

Elements: Fe, Ti, Ba

A-Rank:	Nemrut Dag (EA25)	10
B-Rank:	-	-

Specimen	*Location*	*E.D.*
EA25P2C	Nemrut Dag (EA25)	0.008
EA25P2B	Nemrut Dag (EA25)	0.010
EA25P2D	Nemrut Dag (EA25)	0.010
EA25P1C	Nemrut Dag (EA25)	0.012
EA25P1D	Nemrut Dag (EA25)	0.013
EA25P1B	Nemrut Dag (EA25)	0.015
EA25P1A	Nemrut Dag (EA25)	0.017
EA25P2A	Nemrut Dag (EA25)	0.018
EA25R2	Nemrut Dag (EA25)	0.021
EA25R1	Nemrut Dag (EA25)	0.022

Elements: Fe, Zr, Ba

A-Rank:	Nemrut Dag (EA25)	6
B-Rank:	Nemrut Dag (EA22)	4

Specimen	*Location*	*E.D.*
EA25P1D	Nemrut Dag (EA25)	0.013
EA25P1B	Nemrut Dag (EA25)	0.017
EA25P1C	Nemrut Dag (EA25)	0.018
EA25P1A	Nemrut Dag (EA25)	0.019
EA22P4	Nemrut Dag (EA22)	0.029
EA25P2C	Nemrut Dag (EA25)	0.029
EA22P1B	Nemrut Dag (EA22)	0.030
EA22P1C	Nemrut Dag (EA22)	0.030
EA22P1A	Nemrut Dag (EA22)	0.032
EA25P2D	Nemrut Dag (EA25)	0.032

Elements: Ti, Fe, Zr, Ba

A-Rank:	Nemrut Dag (EA25)	10
B-Rank:	-	-

Specimen	*Location*	*E.D.*
EA25P1D	Nemrut Dag (EA25)	0.014
EA25P1B	Nemrut Dag (EA25)	0.017
EA25P1C	Nemrut Dag (EA25)	0.018
EA25P1A	Nemrut Dag (EA25)	0.019
EA25P2C	Nemrut Dag (EA25)	0.029
EA25P2D	Nemrut Dag (EA25)	0.033
EA25R1	Nemrut Dag (EA25)	0.034
EA25P2A	Nemrut Dag (EA25)	0.039
EA25P3	Nemrut Dag (EA25)	0.039
EA25P2B	Nemrut Dag (EA25)	0.040

Elements: Ti, Fe, Mn, Ca, Zr, Ba

A-Rank:	Nemrut Dag (EA25)	10
B-Rank:	-	-

Specimen	*Location*	*E.D.*
EA25P1C	Nemrut Dag (EA25)	0.018
EA25P1A	Nemrut Dag (EA25)	0.022
EA25P1B	Nemrut Dag (EA25)	0.027
EA25P2C	Nemrut Dag (EA25)	0.039
EA25R1	Nemrut Dag (EA25)	0.042
EA25P1D	Nemrut Dag (EA25)	0.044
EA25P2B	Nemrut Dag (EA25)	0.045
EA25P3	Nemrut Dag (EA25)	0.045
EA25P2A	Nemrut Dag (EA25)	0.046
EA25P2D	Nemrut Dag (EA25)	0.046

Elements: Fe, Ti, Zr

A-Rank:	Nemrut Dag (EA25)	10
B-Rank:	-	-

Specimen	*Location*	*E.D.*
EA25P1D	Nemrut Dag (EA25)	0.009
EA25P1B	Nemrut Dag (EA25)	0.015
EA25P1A	Nemrut Dag (EA25)	0.017
EA25P1C	Nemrut Dag (EA25)	0.018
EA25P2C	Nemrut Dag (EA25)	0.029
EA25R1	Nemrut Dag (EA25)	0.031
EA25P2D	Nemrut Dag (EA25)	0.033
EA25P3	Nemrut Dag (EA25)	0.034
EA25P2A	Nemrut Dag (EA25)	0.039
EA25P2B	Nemrut Dag (EA25)	0.040

Elements: Ti, Zr, Ba

A-Rank:	Nemrut Dag (EA25)	10
B-Rank:	-	-

Specimen	*Location*	*E.D.*
EA25P1A	Nemrut Dag (EA25)	0.010
EA25P1B	Nemrut Dag (EA25)	0.011
EA25P1D	Nemrut Dag (EA25)	0.012
EA25P1C	Nemrut Dag (EA25)	0.013
EA25P2C	Nemrut Dag (EA25)	0.028
EA25R1	Nemrut Dag (EA25)	0.030
EA25P2D	Nemrut Dag (EA25)	0.032
EA25P2A	Nemrut Dag (EA25)	0.035
EA25P3	Nemrut Dag (EA25)	0.037
EA25P2B	Nemrut Dag (EA25)	0.039

Elements: Ti, Fe, Zr, Ba, Zn

A-Rank:	Nemrut Dag (EA25)	7
B-Rank:	Nemrut Dag (EA22)	3

Specimen	*Location*	*E.D.*
EA25P1D	Nemrut Dag (EA25)	0.031
EA25P1A	Nemrut Dag (EA25)	0.033
EA25P1B	Nemrut Dag (EA25)	0.035
EA25P2C	Nemrut Dag (EA25)	0.053
EA25P2D	Nemrut Dag (EA25)	0.057
EA25P1C	Nemrut Dag (EA25)	0.065
EA25P2B	Nemrut Dag (EA25)	0.065
EA22P7B	Nemrut Dag (EA22)	0.072
EA22P6B	Nemrut Dag (EA22)	0.075
EA22P8B	Nemrut Dag (EA22)	0.075

Elements: Ti, Al, Fe, Mn, Ca, Zr, Ba

A-Rank:	Nemrut Dag (EA25)	10
B-Rank:	-	-

Specimen	*Location*	*E.D.*
EA25P1C	Nemrut Dag (EA25)	0.027
EA25P1A	Nemrut Dag (EA25)	0.033
EA25P1B	Nemrut Dag (EA25)	0.033
EA25P2C	Nemrut Dag (EA25)	0.043
EA25P1D	Nemrut Dag (EA25)	0.046
EA25P2A	Nemrut Dag (EA25)	0.049
EA25P2B	Nemrut Dag (EA25)	0.049
EA25P2D	Nemrut Dag (EA25)	0.049
EA25P3	Nemrut Dag (EA25)	0.051
EA25R1	Nemrut Dag (EA25)	0.051

Table D.1 - Source Assignments of Artifacts based on Euclidean Distance to Centroids of Geological Specimens

Artifact: A9 q376.1 f98 k3 piece 2

A-Rank: **Nemrut Dag (EA25) 70**
B-Rank: Nemrut Dag (EA22) 10

Elements: Fe, Ti, Ba

A-Rank:	Nemrut Dag (EA25)	10
B-Rank:	-	-

Specimen	*Location*	*E.D.*
EA25P1A	Nemrut Dag (EA25)	0.003
EA25P1B	Nemrut Dag (EA25)	0.006
EA25P1C	Nemrut Dag (EA25)	0.008
EA25P2A	Nemrut Dag (EA25)	0.008
EA25P2B	Nemrut Dag (EA25)	0.009
EA25R1	Nemrut Dag (EA25)	0.011
EA25P1D	Nemrut Dag (EA25)	0.013
EA25P2D	Nemrut Dag (EA25)	0.013
EA25P2C	Nemrut Dag (EA25)	0.014
EA25P3	Nemrut Dag (EA25)	0.016

Elements: Fe, Zr, Ba

A-Rank:	Nemrut Dag (EA25)	5
B-Rank:	Nemrut Dag (EA22)	5

Specimen	*Location*	*E.D.*
EA25P1A	Nemrut Dag (EA25)	0.029
EA25P1B	Nemrut Dag (EA25)	0.030
EA25P1D	Nemrut Dag (EA25)	0.030
EA25P1C	Nemrut Dag (EA25)	0.035
EA22P4	Nemrut Dag (EA22)	0.039
EA25R1	Nemrut Dag (EA25)	0.048
EA22P5A	Nemrut Dag (EA22)	0.049
EA22P5B	Nemrut Dag (EA22)	0.049
EA22P6B	Nemrut Dag (EA22)	0.049
EA22P8A	Nemrut Dag (EA22)	0.050

Elements: Ti, Fe, Zr, Ba

A-Rank:	Nemrut Dag (EA25)	10
B-Rank:	-	-

Specimen	*Location*	*E.D.*
EA25P1A	Nemrut Dag (EA25)	0.029
EA25P1B	Nemrut Dag (EA25)	0.030
EA25P1D	Nemrut Dag (EA25)	0.030
EA25P1C	Nemrut Dag (EA25)	0.035
EA25R1	Nemrut Dag (EA25)	0.048
EA25P2C	Nemrut Dag (EA25)	0.051
EA25P2D	Nemrut Dag (EA25)	0.054
EA25P3	Nemrut Dag (EA25)	0.055
EA25P2A	Nemrut Dag (EA25)	0.056
EA25P2B	Nemrut Dag (EA25)	0.061

Elements: Ti, Fe, Mn, Ca, Zr, Ba

A-Rank:	Nemrut Dag (EA25)	10
B-Rank:	-	-

Specimen	*Location*	*E.D.*
EA25P1B	Nemrut Dag (EA25)	0.031
EA25P1A	Nemrut Dag (EA25)	0.032
EA25P1D	Nemrut Dag (EA25)	0.035
EA25P1C	Nemrut Dag (EA25)	0.046
EA25R1	Nemrut Dag (EA25)	0.048
EA25P2C	Nemrut Dag (EA25)	0.051
EA25P2D	Nemrut Dag (EA25)	0.055
EA25P3	Nemrut Dag (EA25)	0.055
EA25P2A	Nemrut Dag (EA25)	0.057
EA25P2B	Nemrut Dag (EA25)	0.061

Elements: Fe, Ti, Zr

A-Rank:	Nemrut Dag (EA25)	10
B-Rank:	-	-

Specimen	*Location*	*E.D.*
EA25P1A	Nemrut Dag (EA25)	0.029
EA25P1D	Nemrut Dag (EA25)	0.029
EA25P1B	Nemrut Dag (EA25)	0.030
EA25P1C	Nemrut Dag (EA25)	0.035
EA25R1	Nemrut Dag (EA25)	0.048
EA25P2C	Nemrut Dag (EA25)	0.050
EA25P3	Nemrut Dag (EA25)	0.053
EA25P2D	Nemrut Dag (EA25)	0.054
EA25P2A	Nemrut Dag (EA25)	0.056
EA25P2B	Nemrut Dag (EA25)	0.061

Elements: Ti, Zr, Ba

A-Rank:	Nemrut Dag (EA25)	8
B-Rank:	Nemrut Dag (EA22)	2

Specimen	*Location*	*E.D.*
EA25P1D	Nemrut Dag (EA25)	0.028
EA25P1A	Nemrut Dag (EA25)	0.029
EA25P1B	Nemrut Dag (EA25)	0.030
EA25P1C	Nemrut Dag (EA25)	0.035
EA25R1	Nemrut Dag (EA25)	0.048
EA25P2C	Nemrut Dag (EA25)	0.050
EA22P7A	Nemrut Dag (EA22)	0.053
EA25P2D	Nemrut Dag (EA25)	0.053
EA25P3	Nemrut Dag (EA25)	0.054
EA22P2	Nemrut Dag (EA22)	0.056

Elements: Ti, Fe, Zr, Ba, Zn

A-Rank:	Nemrut Dag (EA25)	7
B-Rank:	Nemrut Dag (EA22)	3

Specimen	*Location*	*E.D.*
EA25P1A	Nemrut Dag (EA25)	0.032
EA25P1D	Nemrut Dag (EA25)	0.033
EA25P1B	Nemrut Dag (EA25)	0.035
EA25P1C	Nemrut Dag (EA25)	0.061
EA25P2D	Nemrut Dag (EA25)	0.064
EA25P2B	Nemrut Dag (EA25)	0.072
EA25P2C	Nemrut Dag (EA25)	0.077
EA22P6B	Nemrut Dag (EA22)	0.079
EA22P8B	Nemrut Dag (EA22)	0.079
EA22P7B	Nemrut Dag (EA22)	0.083

Elements: Ti, Al, Fe, Mn, Ca, Zr, Ba

A-Rank:	Nemrut Dag (EA25)	10
B-Rank:	-	-

Specimen	*Location*	*E.D.*
EA25P1A	Nemrut Dag (EA25)	0.039
EA25P1B	Nemrut Dag (EA25)	0.041
EA25P1D	Nemrut Dag (EA25)	0.046
EA25R1	Nemrut Dag (EA25)	0.052
EA25P1C	Nemrut Dag (EA25)	0.053
EA25P2C	Nemrut Dag (EA25)	0.058
EA25P3	Nemrut Dag (EA25)	0.059
EA25P2D	Nemrut Dag (EA25)	0.062
EA25P2A	Nemrut Dag (EA25)	0.064
EA25P2B	Nemrut Dag (EA25)	0.066

Table D.1 - Source Assignments of Artifacts based on Euclidean Distance to Centroids of Geological Specimens

Artifact: A9 q376.1 f98 k3 piece 3

A-Rank: **Nemrut Dag (EA25)** **66**
B-Rank: Nemrut Dag (EA22) 13

Elements: Fe, Ti, Ba

A-Rank:	Nemrut Dag (EA25)	10
B-Rank:	-	-

Specimen	*Location*	*E.D.*
EA25R2	Nemrut Dag (EA25)	0.012
EA25P2C	Nemrut Dag (EA25)	0.018
EA25P1C	Nemrut Dag (EA25)	0.020
EA25P2A	Nemrut Dag (EA25)	0.020
EA25P2D	Nemrut Dag (EA25)	0.021
EA25P2B	Nemrut Dag (EA25)	0.025
EA25P1B	Nemrut Dag (EA25)	0.026
EA25P1A	Nemrut Dag (EA25)	0.027
EA25P1D	Nemrut Dag (EA25)	0.031
EA25R1	Nemrut Dag (EA25)	0.033

Elements: Fe, Zr, Ba

A-Rank:	Nemrut Dag (EA22)	5
B-Rank:	Nemrut Dag (EA25)	4

Specimen	*Location*	*E.D.*
EA25P1C	Nemrut Dag (EA25)	0.036
EA25P1A	Nemrut Dag (EA25)	0.037
EA25P1B	Nemrut Dag (EA25)	0.037
EA25P1D	Nemrut Dag (EA25)	0.037
EA22P4	Nemrut Dag (EA22)	0.041
EA22P1C	Nemrut Dag (EA22)	0.043
EA22P6B	Nemrut Dag (EA22)	0.043
EA22P5A	Nemrut Dag (EA22)	0.044
EA22P7A	Nemrut Dag (EA22)	0.044
EA21P1	Nemrut Dag (EA21)	0.045

Elements: Ti, Fe, Zr, Ba

A-Rank:	Nemrut Dag (EA25)	9
B-Rank:	Nemrut Dag (EA22)	1

Specimen	*Location*	*E.D.*
EA25P1B	Nemrut Dag (EA25)	0.037
EA25P1C	Nemrut Dag (EA25)	0.037
EA25P1A	Nemrut Dag (EA25)	0.038
EA25P1D	Nemrut Dag (EA25)	0.039
EA25P2C	Nemrut Dag (EA25)	0.050
EA25P2D	Nemrut Dag (EA25)	0.054
EA25R1	Nemrut Dag (EA25)	0.055
EA25P2A	Nemrut Dag (EA25)	0.057
EA22P7A	Nemrut Dag (EA22)	0.062
EA25P2B	Nemrut Dag (EA25)	0.062

Elements: Ti, Fe, Mn, Ca, Zr, Ba

A-Rank:	Nemrut Dag (EA25)	10
B-Rank:	-	-

Specimen	*Location*	*E.D.*
EA25P1A	Nemrut Dag (EA25)	0.038
EA25P1C	Nemrut Dag (EA25)	0.039
EA25P1B	Nemrut Dag (EA25)	0.040
EA25P1D	Nemrut Dag (EA25)	0.053
EA25P2C	Nemrut Dag (EA25)	0.053
EA25R1	Nemrut Dag (EA25)	0.059
EA25P2A	Nemrut Dag (EA25)	0.060
EA25P2D	Nemrut Dag (EA25)	0.060
EA25P2B	Nemrut Dag (EA25)	0.064
EA25P3	Nemrut Dag (EA25)	0.064

Elements: Fe, Ti, Zr

A-Rank:	Nemrut Dag (EA25)	10
B-Rank:	-	-

Specimen	*Location*	*E.D.*
EA25P1D	Nemrut Dag (EA25)	0.027
EA25P1B	Nemrut Dag (EA25)	0.028
EA25P1A	Nemrut Dag (EA25)	0.029
EA25P1C	Nemrut Dag (EA25)	0.034
EA25R1	Nemrut Dag (EA25)	0.046
EA25P2C	Nemrut Dag (EA25)	0.048
EA25P3	Nemrut Dag (EA25)	0.050
EA25P2D	Nemrut Dag (EA25)	0.052
EA25P2A	Nemrut Dag (EA25)	0.055
EA25P2B	Nemrut Dag (EA25)	0.059

Elements: Ti, Zr, Ba

A-Rank:	Nemrut Dag (EA25)	5
B-Rank:	Nemrut Dag (EA22)	5

Specimen	*Location*	*E.D.*
EA25P1A	Nemrut Dag (EA25)	0.036
EA25P1B	Nemrut Dag (EA25)	0.037
EA25P1C	Nemrut Dag (EA25)	0.037
EA25P1D	Nemrut Dag (EA25)	0.039
EA22P7A	Nemrut Dag (EA22)	0.046
EA22P2	Nemrut Dag (EA22)	0.048
EA22R1	Nemrut Dag (EA22)	0.049
EA25P2C	Nemrut Dag (EA25)	0.050
EA22P6B	Nemrut Dag (EA22)	0.053
EA22P7B	Nemrut Dag (EA22)	0.054

Elements: Ti, Fe, Zr, Ba, Zn

A-Rank:	Nemrut Dag (EA25)	8
B-Rank:	Nemrut Dag (EA22)	2

Specimen	*Location*	*E.D.*
EA25P1C	Nemrut Dag (EA25)	0.049
EA25P2A	Nemrut Dag (EA25)	0.057
EA25P3	Nemrut Dag (EA25)	0.063
EA25R1	Nemrut Dag (EA25)	0.066
EA25P2D	Nemrut Dag (EA25)	0.071
EA25P1B	Nemrut Dag (EA25)	0.073
EA22P4	Nemrut Dag (EA22)	0.074
EA22P5A	Nemrut Dag (EA22)	0.076
EA25P1A	Nemrut Dag (EA25)	0.076
EA25P2B	Nemrut Dag (EA25)	0.076

Elements: Ti, Al, Fe, Mn, Ca, Zr, Ba

A-Rank:	Nemrut Dag (EA25)	10
B-Rank:	-	-

Specimen	*Location*	*E.D.*
EA25P1A	Nemrut Dag (EA25)	0.057
EA25P1C	Nemrut Dag (EA25)	0.061
EA25P1B	Nemrut Dag (EA25)	0.063
EA25R1	Nemrut Dag (EA25)	0.071
EA25P2C	Nemrut Dag (EA25)	0.072
EA25P1D	Nemrut Dag (EA25)	0.074
EA25P3	Nemrut Dag (EA25)	0.077
EA25P2D	Nemrut Dag (EA25)	0.078
EA25R2	Nemrut Dag (EA25)	0.078
EA25P2A	Nemrut Dag (EA25)	0.079

Table D.1 - Source Assignments of Artifacts based on Euclidean Distance to Centroids of Geological Specimens

Artifact: A9 q437.2 f98 k3

A-Rank: **Nemrut Dag (EA25)** **74**
B-Rank: Nemrut Dag (EA22) 6

Elements: Fe, Ti, Ba

A-Rank:	Nemrut Dag (EA25)	10
B-Rank:	-	-

Specimen	*Location*	*E.D.*
EA25R1	Nemrut Dag (EA25)	0.006
EA25P3	Nemrut Dag (EA25)	0.008
EA25P1A	Nemrut Dag (EA25)	0.013
EA25P1B	Nemrut Dag (EA25)	0.013
EA25P1D	Nemrut Dag (EA25)	0.019
EA25P2B	Nemrut Dag (EA25)	0.020
EA25P1C	Nemrut Dag (EA25)	0.021
EA25P2A	Nemrut Dag (EA25)	0.022
EA25P2C	Nemrut Dag (EA25)	0.026
EA25P2D	Nemrut Dag (EA25)	0.026

Elements: Fe, Zr, Ba

A-Rank:	Nemrut Dag (EA25)	10
B-Rank:	-	-

Specimen	*Location*	*E.D.*
EA25P1A	Nemrut Dag (EA25)	0.012
EA25P1B	Nemrut Dag (EA25)	0.013
EA25R1	Nemrut Dag (EA25)	0.014
EA25P1D	Nemrut Dag (EA25)	0.017
EA25P1C	Nemrut Dag (EA25)	0.019
EA25P3	Nemrut Dag (EA25)	0.020
EA25P2C	Nemrut Dag (EA25)	0.029
EA25P2D	Nemrut Dag (EA25)	0.029
EA25P2A	Nemrut Dag (EA25)	0.030
EA25P2B	Nemrut Dag (EA25)	0.031

Elements: Ti, Fe, Zr, Ba

A-Rank:	Nemrut Dag (EA25)	10
B-Rank:	-	-

Specimen	*Location*	*E.D.*
EA25P1A	Nemrut Dag (EA25)	0.014
EA25P1B	Nemrut Dag (EA25)	0.014
EA25R1	Nemrut Dag (EA25)	0.014
EA25P3	Nemrut Dag (EA25)	0.020
EA25P1C	Nemrut Dag (EA25)	0.021
EA25P1D	Nemrut Dag (EA25)	0.021
EA25P2C	Nemrut Dag (EA25)	0.030
EA25P2A	Nemrut Dag (EA25)	0.031
EA25P2D	Nemrut Dag (EA25)	0.032
EA25P2B	Nemrut Dag (EA25)	0.033

Elements: Ti, Fe, Mn, Ca, Zr, Ba

A-Rank:	Nemrut Dag (EA25)	10
B-Rank:	-	-

Specimen	*Location*	*E.D.*
EA25P1B	Nemrut Dag (EA25)	0.014
EA25R1	Nemrut Dag (EA25)	0.015
EA25P1A	Nemrut Dag (EA25)	0.017
EA25P3	Nemrut Dag (EA25)	0.020
EA25P1D	Nemrut Dag (EA25)	0.029
EA25P2A	Nemrut Dag (EA25)	0.031
EA25P2C	Nemrut Dag (EA25)	0.031
EA25P1C	Nemrut Dag (EA25)	0.033
EA25P2B	Nemrut Dag (EA25)	0.033
EA25P2D	Nemrut Dag (EA25)	0.034

Elements: Fe, Ti, Zr

A-Rank:	Nemrut Dag (EA25)	10
B-Rank:	-	-

Specimen	*Location*	*E.D.*
EA25P1A	Nemrut Dag (EA25)	0.010
EA25P1B	Nemrut Dag (EA25)	0.010
EA25P1C	Nemrut Dag (EA25)	0.011
EA25R1	Nemrut Dag (EA25)	0.014
EA25P3	Nemrut Dag (EA25)	0.019
EA25P1D	Nemrut Dag (EA25)	0.020
EA25P2C	Nemrut Dag (EA25)	0.022
EA25P2A	Nemrut Dag (EA25)	0.023
EA25P2D	Nemrut Dag (EA25)	0.026
EA25R2	Nemrut Dag (EA25)	0.030

Elements: Ti, Zr, Ba

A-Rank:	Nemrut Dag (EA25)	10
B-Rank:	-	-

Specimen	*Location*	*E.D.*
EA25P1B	Nemrut Dag (EA25)	0.012
EA25P1A	Nemrut Dag (EA25)	0.013
EA25R1	Nemrut Dag (EA25)	0.014
EA25P1D	Nemrut Dag (EA25)	0.015
EA25P1C	Nemrut Dag (EA25)	0.019
EA25P3	Nemrut Dag (EA25)	0.019
EA25P2C	Nemrut Dag (EA25)	0.027
EA25P2D	Nemrut Dag (EA25)	0.030
EA25P2A	Nemrut Dag (EA25)	0.031
EA25P2B	Nemrut Dag (EA25)	0.031

Elements: Ti, Fe, Zr, Ba, Zn

A-Rank:	Nemrut Dag (EA22)	6
B-Rank:	Nemrut Dag (EA25)	4

Specimen	*Location*	*E.D.*
EA25P2C	Nemrut Dag (EA25)	0.047
EA22P7A	Nemrut Dag (EA22)	0.089
EA22P1D	Nemrut Dag (EA22)	0.091
EA22R1	Nemrut Dag (EA22)	0.093
EA22P5B	Nemrut Dag (EA22)	0.098
EA22P3	Nemrut Dag (EA22)	0.109
EA25P1A	Nemrut Dag (EA25)	0.109
EA25P1D	Nemrut Dag (EA25)	0.110
EA25P1B	Nemrut Dag (EA25)	0.113
EA22P1C	Nemrut Dag (EA22)	0.114

Elements: Ti, Al, Fe, Mn, Ca, Zr, Ba

A-Rank:	Nemrut Dag (EA25)	10
B-Rank:	-	-

Specimen	*Location*	*E.D.*
EA25R1	Nemrut Dag (EA25)	0.018
EA25P1A	Nemrut Dag (EA25)	0.021
EA25P1B	Nemrut Dag (EA25)	0.023
EA25P3	Nemrut Dag (EA25)	0.024
EA25P2C	Nemrut Dag (EA25)	0.036
EA25P1C	Nemrut Dag (EA25)	0.037
EA25P1D	Nemrut Dag (EA25)	0.037
EA25P2A	Nemrut Dag (EA25)	0.037
EA25P2B	Nemrut Dag (EA25)	0.037
EA25P2D	Nemrut Dag (EA25)	0.039

Table D.1 - Source Assignments of Artifacts based on Euclidean Distance to Centroids of Geological Specimens

Artifact: A9 q440.1 f98 k3 piece 1

A-Rank: **Bingol B** **61**
B-Rank: Gutansar 11

Elements: Fe, Ti, Ba

A-Rank: Bingol B 7
B-Rank: Gutansar 2

Specimen	*Location*	*E.D.*
EA52B2	Bingol B	0.017
EA52B3	Bingol B	0.026
EA52B1	Bingol B	0.030
EA53B2	Bingol B	0.033
EA54B1	Bingol B	0.040
EA53B1	Bingol B	0.041
EA56B1	Bingol B	0.042
AR06E2A	Gutansar	0.087
AR21avH1	Chazencavan	0.088
AR06E1A	Gutansar	0.090

Elements: Fe, Zr, Ba

A-Rank: Bingol B 7
B-Rank: Erzincan 3

Specimen	*Location*	*E.D.*
EA52B2	Bingol B	0.015
EA52B3	Bingol B	0.023
EA53B2	Bingol B	0.034
EA52B1	Bingol B	0.035
EA56B1	Bingol B	0.044
EA54B1	Bingol B	0.047
EA53B1	Bingol B	0.049
EA43P1	Erzincan	0.092
EA43R2	Erzincan	0.092
EA44P2	Erzincan	0.092

Elements: Ti, Fe, Zr, Ba

A-Rank: Bingol B 7
B-Rank: Gutansar 3

Specimen	*Location*	*E.D.*
EA52B2	Bingol B	0.023
EA52B3	Bingol B	0.030
EA52B1	Bingol B	0.037
EA53B2	Bingol B	0.038
EA54B1	Bingol B	0.047
EA56B1	Bingol B	0.048
EA53B1	Bingol B	0.051
AR30jfL1	Gutansar	0.138
AR06E3A	Gutansar	0.139
AR06E2A	Gutansar	0.140

Elements: Ti, Fe, Mn, Ca, Zr, Ba

A-Rank: Bingol B 9
B-Rank: Acigol 1

Specimen	*Location*	*E.D.*
EA52B3	Bingol B	0.039
EA52B1	Bingol B	0.054
EA54B1	Bingol B	0.055
EA56B1	Bingol B	0.055
EA53B1	Bingol B	0.060
EA53B2	Bingol B	0.060
EA52B2	Bingol B	0.061
EA55B2	Bingol B	0.156
EA55B1	Bingol B	0.159
CA08R1C	Acigol	0.181

Elements: Fe, Ti, Zr

A-Rank: Bingol B 7
B-Rank: Gutansar 2

Specimen	*Location*	*E.D.*
EA52B2	Bingol B	0.023
EA53B2	Bingol B	0.025
EA52B3	Bingol B	0.030
EA53B1	Bingol B	0.034
EA52B1	Bingol B	0.037
EA54B1	Bingol B	0.047
EA56B1	Bingol B	0.048
EA66W1	Lake Van	0.105
AR76rB3	Gutansar	0.123
AR06E3A	Gutansar	0.128

Elements: Ti, Zr, Ba

A-Rank: Bingol B 9
B-Rank: Erevan 1

Specimen	*Location*	*E.D.*
EA52B2	Bingol B	0.023
EA52B3	Bingol B	0.024
EA52B1	Bingol B	0.025
EA54B1	Bingol B	0.026
EA55B2	Bingol B	0.031
EA56B1	Bingol B	0.032
EA53B2	Bingol B	0.037
EA55B1	Bingol B	0.042
EA53B1	Bingol B	0.051
AR24jfL1	Erevan	0.115

Elements: Ti, Fe, Zr, Ba, Zn

A-Rank: Bingol B 6
B-Rank: Gutansar 4

Specimen	*Location*	*E.D.*
EA53B1	Bingol B	0.086
EA52B1	Bingol B	0.129
EA52B3	Bingol B	0.141
EA54B1	Bingol B	0.149
EA52B2	Bingol	0.156
AR06E2B	Gutansar	0.161
AR11jB1	Gutansar	0.173
EA56B1	Bingol B	0.173
AR12jB1	Gutansar	0.183
AR06E1B	Gutansar	0.185

Elements: Ti, Al, Fe, Mn, Ca, Zr, Ba

A-Rank: Bingol B 9
B-Rank: Acigol 1

Specimen	*Location*	*E.D.*
EA53B1	Bingol B	0.072
EA52B3	Bingol B	0.073
EA53B2	Bingol B	0.073
EA54B1	Bingol B	0.077
EA56B1	Bingol B	0.078
EA52B1	Bingol B	0.081
EA52B2	Bingol B	0.086
EA55B2	Bingol B	0.167
EA55B1	Bingol B	0.169
CA08R1C	Acigol	0.181

Table D.1 - Source Assignments of Artifacts based on Euclidean Distance to Centroids of Geological Specimens

Artifact: A9 q440.1 f98 k3 piece 2

A-Rank: **Nemrut Dag (EA25)** **76**
B-Rank: Nemrut Dag (EA22) 4

Elements: Fe, Ti, Ba

A-Rank:	Nemrut Dag (EA25)	10
B-Rank:	-	-

Specimen	*Location*	*E.D.*
EA25P1C	Nemrut Dag (EA25)	0.003
EA25P2A	Nemrut Dag (EA25)	0.005
EA25P1A	Nemrut Dag (EA25)	0.006
EA25P1B	Nemrut Dag (EA25)	0.007
EA25P2B	Nemrut Dag (EA25)	0.008
EA25P2C	Nemrut Dag (EA25)	0.009
EA25P2D	Nemrut Dag (EA25)	0.009
EA25P1D	Nemrut Dag (EA25)	0.014
EA25R1	Nemrut Dag (EA25)	0.014
EA25R2	Nemrut Dag (EA25)	0.014

Elements: Fe, Zr, Ba

A-Rank:	Nemrut Dag (EA25)	9
B-Rank:	Nemrut Dag (EA22)	1

Specimen	*Location*	*E.D.*
EA25P1A	Nemrut Dag (EA25)	0.018
EA25P1B	Nemrut Dag (EA25)	0.018
EA25P1D	Nemrut Dag (EA25)	0.020
EA25P1C	Nemrut Dag (EA25)	0.023
EA22P4	Nemrut Dag (EA22)	0.038
EA25P2C	Nemrut Dag (EA25)	0.038
EA25R1	Nemrut Dag (EA25)	0.038
EA25P2D	Nemrut Dag (EA25)	0.041
EA25P2A	Nemrut Dag (EA25)	0.044
EA25P3	Nemrut Dag (EA25)	0.044

Elements: Ti, Fe, Zr, Ba

A-Rank:	Nemrut Dag (EA25)	10
B-Rank:	-	-

Specimen	*Location*	*E.D.*
EA25P1A	Nemrut Dag (EA25)	0.018
EA25P1B	Nemrut Dag (EA25)	0.019
EA25P1D	Nemrut Dag (EA25)	0.020
EA25P1C	Nemrut Dag (EA25)	0.023
EA25P2C	Nemrut Dag (EA25)	0.038
EA25R1	Nemrut Dag (EA25)	0.038
EA25P2D	Nemrut Dag (EA25)	0.042
EA25P2A	Nemrut Dag (EA25)	0.044
EA25P3	Nemrut Dag (EA25)	0.045
EA25P2B	Nemrut Dag (EA25)	0.049

Elements: Ti, Fe, Mn, Ca, Zr, Ba

A-Rank:	Nemrut Dag (EA25)	10
B-Rank:	-	-

Specimen	*Location*	*E.D.*
EA25P1A	Nemrut Dag (EA25)	0.020
EA25P1C	Nemrut Dag (EA25)	0.024
EA25P1B	Nemrut Dag (EA25)	0.027
EA25P1D	Nemrut Dag (EA25)	0.044
EA25R1	Nemrut Dag (EA25)	0.044
EA25P2C	Nemrut Dag (EA25)	0.045
EA25P3	Nemrut Dag (EA25)	0.048
EA25P2A	Nemrut Dag (EA25)	0.049
EA25P2D	Nemrut Dag (EA25)	0.051
EA25P2B	Nemrut Dag (EA25)	0.052

Elements: Fe, Ti, Zr

A-Rank:	Nemrut Dag (EA25)	10
B-Rank:	-	-

Specimen	*Location*	*E.D.*
EA25P1A	Nemrut Dag (EA25)	0.017
EA25P1B	Nemrut Dag (EA25)	0.018
EA25P1D	Nemrut Dag (EA25)	0.018
EA25P1C	Nemrut Dag (EA25)	0.023
EA25R1	Nemrut Dag (EA25)	0.036
EA25P2C	Nemrut Dag (EA25)	0.038
EA25P3	Nemrut Dag (EA25)	0.040
EA25P2D	Nemrut Dag (EA25)	0.042
EA25P2A	Nemrut Dag (EA25)	0.044
EA25P2B	Nemrut Dag (EA25)	0.049

Elements: Ti, Zr, Ba

A-Rank:	Nemrut Dag (EA25)	10
B-Rank:	-	-

Specimen	*Location*	*E.D.*
EA25P1A	Nemrut Dag (EA25)	0.018
EA25P1D	Nemrut Dag (EA25)	0.018
EA25P1B	Nemrut Dag (EA25)	0.019
EA25P1C	Nemrut Dag (EA25)	0.022
EA25P2C	Nemrut Dag (EA25)	0.038
EA25R1	Nemrut Dag (EA25)	0.038
EA25P2D	Nemrut Dag (EA25)	0.041
EA25P2A	Nemrut Dag (EA25)	0.044
EA25P3	Nemrut Dag (EA25)	0.045
EA25P2B	Nemrut Dag (EA25)	0.048

Elements: Ti, Fe, Zr, Ba, Zn

A-Rank:	Nemrut Dag (EA25)	7
B-Rank:	Nemrut Dag (EA22)	3

Specimen	*Location*	*E.D.*
EA25P1A	Nemrut Dag (EA25)	0.047
EA25P1D	Nemrut Dag (EA25)	0.048
EA25P2C	Nemrut Dag (EA25)	0.048
EA25P1B	Nemrut Dag (EA25)	0.051
EA25P2D	Nemrut Dag (EA25)	0.076
EA22P7A	Nemrut Dag (EA22)	0.080
EA22P7B	Nemrut Dag (EA22)	0.082
EA25P1C	Nemrut Dag (EA25)	0.082
EA22R1	Nemrut Dag (EA22)	0.083
EA25P2B	Nemrut Dag (EA25)	0.083

Elements: Ti, Al, Fe, Mn, Ca, Zr, Ba

A-Rank:	Nemrut Dag (EA25)	10
B-Rank:	-	-

Specimen	*Location*	*E.D.*
EA25P1A	Nemrut Dag (EA25)	0.023
EA25P1C	Nemrut Dag (EA25)	0.029
EA25P1B	Nemrut Dag (EA25)	0.032
EA25R1	Nemrut Dag (EA25)	0.045
EA25P2C	Nemrut Dag (EA25)	0.048
EA25P1D	Nemrut Dag (EA25)	0.049
EA25P3	Nemrut Dag (EA25)	0.050
EA25P2A	Nemrut Dag (EA25)	0.054
EA25P2B	Nemrut Dag (EA25)	0.055
EA25P2D	Nemrut Dag (EA25)	0.055

Table D.1 - Source Assignments of Artifacts based on Euclidean Distance to Centroids of Geological Specimens

Artifact: A9 q454.2 f126 k3 piece 1

A-Rank: **Nemrut Dag (EA25)** **61**
B-Rank: Nemrut Dag (EA22) 17

Elements: Fe, Ti, Ba

A-Rank:	Nemrut Dag (EA25)	10
B-Rank:	-	-

Specimen	*Location*	*E.D.*
EA25P2D	Nemrut Dag (EA25)	0.009
EA25P1C	Nemrut Dag (EA25)	0.010
EA25P2B	Nemrut Dag (EA25)	0.010
EA25P1A	Nemrut Dag (EA25)	0.012
EA25P2A	Nemrut Dag (EA25)	0.012
EA25P2C	Nemrut Dag (EA25)	0.012
EA25P1B	Nemrut Dag (EA25)	0.014
EA25P1D	Nemrut Dag (EA25)	0.014
EA25R1	Nemrut Dag (EA25)	0.020
EA25R2	Nemrut Dag (EA25)	0.023

Elements: Fe, Zr, Ba

A-Rank:	Nemrut Dag (EA22)	5
B-Rank:	Nemrut Dag (EA25)	3

Specimen	*Location*	*E.D.*
EA22P4	Nemrut Dag (EA22)	0.047
EA22P5A	Nemrut Dag (EA22)	0.048
EA25P1D	Nemrut Dag (EA25)	0.050
EA25P1A	Nemrut Dag (EA25)	0.051
EA25P1B	Nemrut Dag (EA25)	0.052
EA22P5B	Nemrut Dag (EA22)	0.053
EA22P6A	Nemrut Dag (EA22)	0.053
EA22P7A	Nemrut Dag (EA22)	0.054
EA21P1	Nemrut Dag (EA21)	0.055
EA21R1B	Nemrut Dag (EA21)	0.055

Elements: Ti, Fe, Zr, Ba

A-Rank:	Nemrut Dag (EA25)	9
B-Rank:	Nemrut Dag (EA22)	1

Specimen	*Location*	*E.D.*
EA25P1D	Nemrut Dag (EA25)	0.051
EA25P1A	Nemrut Dag (EA25)	0.052
EA25P1B	Nemrut Dag (EA25)	0.053
EA25P1C	Nemrut Dag (EA25)	0.057
EA25P2C	Nemrut Dag (EA25)	0.072
EA25R1	Nemrut Dag (EA25)	0.072
EA25P2D	Nemrut Dag (EA25)	0.075
EA25P3	Nemrut Dag (EA25)	0.078
EA25P2A	Nemrut Dag (EA25)	0.079
EA22P7A	Nemrut Dag (EA22)	0.082

Elements: Ti, Fe, Mn, Ca, Zr, Ba

A-Rank:	Nemrut Dag (EA25)	10
B-Rank:	-	-

Specimen	*Location*	*E.D.*
EA25P1A	Nemrut Dag (EA25)	0.056
EA25P1C	Nemrut Dag (EA25)	0.057
EA25P1B	Nemrut Dag (EA25)	0.062
EA25P1D	Nemrut Dag (EA25)	0.072
EA25P2C	Nemrut Dag (EA25)	0.080
EA25R1	Nemrut Dag (EA25)	0.080
EA25P3	Nemrut Dag (EA25)	0.084
EA25P2A	Nemrut Dag (EA25)	0.086
EA25P2D	Nemrut Dag (EA25)	0.086
EA25P2B	Nemrut Dag (EA25)	0.088

Elements: Fe, Ti, Zr

A-Rank:	Nemrut Dag (EA25)	9
B-Rank:	Nemrut Dag (EA22)	1

Specimen	*Location*	*E.D.*
EA25P1D	Nemrut Dag (EA25)	0.050
EA25P1A	Nemrut Dag (EA25)	0.052
EA25P1B	Nemrut Dag (EA25)	0.053
EA25P1C	Nemrut Dag (EA25)	0.058
EA25R1	Nemrut Dag (EA25)	0.071
EA25P2C	Nemrut Dag (EA25)	0.072
EA25P2D	Nemrut Dag (EA25)	0.075
EA25P3	Nemrut Dag (EA25)	0.076
EA25P2A	Nemrut Dag (EA25)	0.079
EA22P7A	Nemrut Dag (EA22)	0.082

Elements: Ti, Zr, Ba

A-Rank:	Nemrut Dag (EA25)	6
B-Rank:	Nemrut Dag (EA22)	4

Specimen	*Location*	*E.D.*
EA25P1D	Nemrut Dag (EA25)	0.050
EA25P1A	Nemrut Dag (EA25)	0.052
EA25P1B	Nemrut Dag (EA25)	0.053
EA25P1C	Nemrut Dag (EA25)	0.057
EA22P7A	Nemrut Dag (EA22)	0.065
EA22R1	Nemrut Dag (EA22)	0.072
EA25P2C	Nemrut Dag (EA25)	0.072
EA25R1	Nemrut Dag (EA25)	0.072
EA22P6B	Nemrut Dag (EA22)	0.074
EA22P8B	Nemrut Dag (EA22)	0.074

Elements: Ti, Fe, Zr, Ba, Zn

A-Rank:	Nemrut Dag (EA22)	6
B-Rank:	Nemrut Dag (EA25)	4

Specimen	*Location*	*E.D.*
EA25P2C	Nemrut Dag (EA25)	0.076
EA22P7A	Nemrut Dag (EA22)	0.085
EA22R1	Nemrut Dag (EA22)	0.096
EA22P5B	Nemrut Dag (EA22)	0.104
EA25P1D	Nemrut Dag (EA25)	0.108
EA22P1D	Nemrut Dag (EA22)	0.109
EA22P3	Nemrut Dag (EA22)	0.109
EA25P1A	Nemrut Dag (EA25)	0.109
EA25P1B	Nemrut Dag (EA25)	0.112
EA22P7B	Nemrut Dag (EA22)	0.119

Elements: Ti, Al, Fe, Mn, Ca, Zr, Ba

A-Rank:	Nemrut Dag (EA25)	10
B-Rank:	-	-

Specimen	*Location*	*E.D.*
EA25P1A	Nemrut Dag (EA25)	0.065
EA25P1C	Nemrut Dag (EA25)	0.068
EA25P1B	Nemrut Dag (EA25)	0.073
EA25P1D	Nemrut Dag (EA25)	0.083
EA25R1	Nemrut Dag (EA25)	0.085
EA25P2C	Nemrut Dag (EA25)	0.089
EA25P3	Nemrut Dag (EA25)	0.090
EA25P2A	Nemrut Dag (EA25)	0.095
EA25P2B	Nemrut Dag (EA25)	0.095
EA25P2D	Nemrut Dag (EA25)	0.095

Table D.1 - Source Assignments of Artifacts based on Euclidean Distance to Centroids of Geological Specimens

Artifact: A9 q454.2 f126 k3 piece 2

A-Rank: **Nemrut Dag (EA25)** **74**
B-Rank: Nemrut Dag (EA22) 6

Elements: Fe, Ti, Ba

A-Rank:	Nemrut Dag (EA25)	10
B-Rank:	-	-

Specimen	*Location*	*E.D.*
EA25P2A	Nemrut Dag (EA25)	0.003
EA25P1C	Nemrut Dag (EA25)	0.004
EA25P2C	Nemrut Dag (EA25)	0.008
EA25P2D	Nemrut Dag (EA25)	0.008
EA25P1A	Nemrut Dag (EA25)	0.011
EA25P1B	Nemrut Dag (EA25)	0.011
EA25P2B	Nemrut Dag (EA25)	0.011
EA25R2	Nemrut Dag (EA25)	0.012
EA25P1D	Nemrut Dag (EA25)	0.017
EA25R1	Nemrut Dag (EA25)	0.019

Elements: Fe, Zr, Ba

A-Rank:	Nemrut Dag (EA25)	10
B-Rank:	-	-

Specimen	*Location*	*E.D.*
EA25P1C	Nemrut Dag (EA25)	0.005
EA25P1A	Nemrut Dag (EA25)	0.011
EA25P1B	Nemrut Dag (EA25)	0.011
EA25P1D	Nemrut Dag (EA25)	0.018
EA25P2C	Nemrut Dag (EA25)	0.018
EA25P2D	Nemrut Dag (EA25)	0.021
EA25P2A	Nemrut Dag (EA25)	0.023
EA25R1	Nemrut Dag (EA25)	0.023
EA25P2B	Nemrut Dag (EA25)	0.029
EA25P3	Nemrut Dag (EA25)	0.030

Elements: Ti, Fe, Zr, Ba

A-Rank:	Nemrut Dag (EA25)	10
B-Rank:	-	-

Specimen	*Location*	*E.D.*
EA25P1C	Nemrut Dag (EA25)	0.005
EA25P1A	Nemrut Dag (EA25)	0.011
EA25P1B	Nemrut Dag (EA25)	0.012
EA25P1D	Nemrut Dag (EA25)	0.018
EA25P2C	Nemrut Dag (EA25)	0.018
EA25P2D	Nemrut Dag (EA25)	0.022
EA25P2A	Nemrut Dag (EA25)	0.023
EA25R1	Nemrut Dag (EA25)	0.024
EA25P2B	Nemrut Dag (EA25)	0.029
EA25P3	Nemrut Dag (EA25)	0.031

Elements: Ti, Fe, Mn, Ca, Zr, Ba

A-Rank:	Nemrut Dag (EA25)	10
B-Rank:	-	-

Specimen	*Location*	*E.D.*
EA25P1A	Nemrut Dag (EA25)	0.011
EA25P1B	Nemrut Dag (EA25)	0.015
EA25P1C	Nemrut Dag (EA25)	0.019
EA25P2C	Nemrut Dag (EA25)	0.023
EA25P2A	Nemrut Dag (EA25)	0.027
EA25R1	Nemrut Dag (EA25)	0.027
EA25P2D	Nemrut Dag (EA25)	0.030
EA25P2B	Nemrut Dag (EA25)	0.031
EA25P3	Nemrut Dag (EA25)	0.032
EA25P1D	Nemrut Dag (EA25)	0.034

Elements: Fe, Ti, Zr

A-Rank:	Nemrut Dag (EA25)	10
B-Rank:	-	-

Specimen	*Location*	*E.D.*
EA25P1A	Nemrut Dag (EA25)	0.004
EA25P1C	Nemrut Dag (EA25)	0.004
EA25P1B	Nemrut Dag (EA25)	0.005
EA25P1D	Nemrut Dag (EA25)	0.011
EA25R1	Nemrut Dag (EA25)	0.015
EA25P2C	Nemrut Dag (EA25)	0.019
EA25P3	Nemrut Dag (EA25)	0.020
EA25P2D	Nemrut Dag (EA25)	0.022
EA25P2A	Nemrut Dag (EA25)	0.024
EA25P2B	Nemrut Dag (EA25)	0.028

Elements: Ti, Zr, Ba

A-Rank:	Nemrut Dag (EA25)	10
B-Rank:	-	-

Specimen	*Location*	*E.D.*
EA25P1C	Nemrut Dag (EA25)	0.004
EA25P1A	Nemrut Dag (EA25)	0.011
EA25P1B	Nemrut Dag (EA25)	0.012
EA25P1D	Nemrut Dag (EA25)	0.016
EA25P2C	Nemrut Dag (EA25)	0.017
EA25P2D	Nemrut Dag (EA25)	0.021
EA25P2A	Nemrut Dag (EA25)	0.023
EA25R1	Nemrut Dag (EA25)	0.024
EA25P2B	Nemrut Dag (EA25)	0.029
EA25P3	Nemrut Dag (EA25)	0.031

Elements: Ti, Fe, Zr, Ba, Zn

A-Rank:	Nemrut Dag (EA22)	6
B-Rank:	Nemrut Dag (EA25)	4

Specimen	*Location*	*E.D.*
EA25P2C	Nemrut Dag (EA25)	0.035
EA22P7A	Nemrut Dag (EA22)	0.086
EA22P1D	Nemrut Dag (EA22)	0.090
EA22R1	Nemrut Dag (EA22)	0.090
EA22P5B	Nemrut Dag (EA22)	0.100
EA25P1A	Nemrut Dag (EA25)	0.102
EA25P1D	Nemrut Dag (EA25)	0.103
EA25P1B	Nemrut Dag (EA25)	0.106
EA22P3	Nemrut Dag (EA22)	0.108
EA22P1C	Nemrut Dag (EA22)	0.111

Elements: Ti, Al, Fe, Mn, Ca, Zr, Ba

A-Rank:	Nemrut Dag (EA25)	10
B-Rank:	-	-

Specimen	*Location*	*E.D.*
EA25P1A	Nemrut Dag (EA25)	0.015
EA25P1B	Nemrut Dag (EA25)	0.022
EA25P1C	Nemrut Dag (EA25)	0.023
EA25P2C	Nemrut Dag (EA25)	0.027
EA25R1	Nemrut Dag (EA25)	0.028
EA25P2A	Nemrut Dag (EA25)	0.032
EA25P2B	Nemrut Dag (EA25)	0.034
EA25P2D	Nemrut Dag (EA25)	0.034
EA25P3	Nemrut Dag (EA25)	0.034
EA25P1D	Nemrut Dag (EA25)	0.039

Table D.1 - Source Assignments of Artifacts based on Euclidean Distance to Centroids of Geological Specimens

Artifact: A9 q454.2 f126 k3 piece 3

A-Rank: **Nemrut Dag (EA25)** **79**
B-Rank: Nemrut Dag (EA22) 1

Elements: Fe, Ti, Ba

A-Rank:	Nemrut Dag (EA25)	10
B-Rank:	-	-

Specimen	*Location*	*E.D.*
EA25P1A	Nemrut Dag (EA25)	0.004
EA25P1B	Nemrut Dag (EA25)	0.004
EA25P1C	Nemrut Dag (EA25)	0.005
EA25P2A	Nemrut Dag (EA25)	0.008
EA25P2B	Nemrut Dag (EA25)	0.009
EA25P2D	Nemrut Dag (EA25)	0.011
EA25R1	Nemrut Dag (EA25)	0.011
EA25P2C	Nemrut Dag (EA25)	0.012
EA25P1D	Nemrut Dag (EA25)	0.013
EA25R2	Nemrut Dag (EA25)	0.015

Elements: Fe, Zr, Ba

A-Rank:	Nemrut Dag (EA25)	10
B-Rank:	-	-

Specimen	*Location*	*E.D.*
EA25P1C	Nemrut Dag (EA25)	0.005
EA25P1B	Nemrut Dag (EA25)	0.008
EA25P1A	Nemrut Dag (EA25)	0.009
EA25P1D	Nemrut Dag (EA25)	0.015
EA25R1	Nemrut Dag (EA25)	0.015
EA25P2C	Nemrut Dag (EA25)	0.016
EA25P2D	Nemrut Dag (EA25)	0.018
EA25P2A	Nemrut Dag (EA25)	0.021
EA25P3	Nemrut Dag (EA25)	0.022
EA25P2B	Nemrut Dag (EA25)	0.024

Elements: Ti, Fe, Zr, Ba

A-Rank:	Nemrut Dag (EA25)	10
B-Rank:	-	-

Specimen	*Location*	*E.D.*
EA25P1C	Nemrut Dag (EA25)	0.006
EA25P1B	Nemrut Dag (EA25)	0.008
EA25P1A	Nemrut Dag (EA25)	0.009
EA25R1	Nemrut Dag (EA25)	0.015
EA25P1D	Nemrut Dag (EA25)	0.016
EA25P2C	Nemrut Dag (EA25)	0.017
EA25P2D	Nemrut Dag (EA25)	0.020
EA25P2A	Nemrut Dag (EA25)	0.021
EA25P3	Nemrut Dag (EA25)	0.023
EA25P2B	Nemrut Dag (EA25)	0.025

Elements: Ti, Fe, Mn, Ca, Zr, Ba

A-Rank:	Nemrut Dag (EA25)	10
B-Rank:	-	-

Specimen	*Location*	*E.D.*
EA25P1C	Nemrut Dag (EA25)	0.015
EA25P1A	Nemrut Dag (EA25)	0.032
EA25P1B	Nemrut Dag (EA25)	0.042
EA25P2B	Nemrut Dag (EA25)	0.047
EA25P2C	Nemrut Dag (EA25)	0.048
EA25P3	Nemrut Dag (EA25)	0.048
EA25R1	Nemrut Dag (EA25)	0.048
EA25P2A	Nemrut Dag (EA25)	0.049
EA25P2D	Nemrut Dag (EA25)	0.056
EA25R2	Nemrut Dag (EA25)	0.062

Elements: Fe, Ti, Zr

A-Rank:	Nemrut Dag (EA25)	10
B-Rank:	-	-

Specimen	*Location*	*E.D.*
EA25P1C	Nemrut Dag (EA25)	0.004
EA25P1A	Nemrut Dag (EA25)	0.008
EA25P1B	Nemrut Dag (EA25)	0.008
EA25R1	Nemrut Dag (EA25)	0.011
EA25P1D	Nemrut Dag (EA25)	0.015
EA25P2C	Nemrut Dag (EA25)	0.016
EA25P3	Nemrut Dag (EA25)	0.016
EA25P2D	Nemrut Dag (EA25)	0.019
EA25P2A	Nemrut Dag (EA25)	0.020
EA25P2B	Nemrut Dag (EA25)	0.025

Elements: Ti, Zr, Ba

A-Rank:	Nemrut Dag (EA25)	10
B-Rank:	-	-

Specimen	*Location*	*E.D.*
EA25P1C	Nemrut Dag (EA25)	0.005
EA25P1B	Nemrut Dag (EA25)	0.008
EA25P1A	Nemrut Dag (EA25)	0.009
EA25P1D	Nemrut Dag (EA25)	0.014
EA25P2C	Nemrut Dag (EA25)	0.015
EA25R1	Nemrut Dag (EA25)	0.015
EA25P2D	Nemrut Dag (EA25)	0.018
EA25P2A	Nemrut Dag (EA25)	0.020
EA25P3	Nemrut Dag (EA25)	0.023
EA25P2B	Nemrut Dag (EA25)	0.024

Elements: Ti, Fe, Zr, Ba, Zn

A-Rank:	Nemrut Dag (EA25)	9
B-Rank:	Nemrut Dag (EA22)	1

Specimen	*Location*	*E.D.*
EA25P1A	Nemrut Dag (EA25)	0.020
EA25P1B	Nemrut Dag (EA25)	0.023
EA25P1D	Nemrut Dag (EA25)	0.024
EA25P2D	Nemrut Dag (EA25)	0.042
EA25P2B	Nemrut Dag (EA25)	0.048
EA25P1C	Nemrut Dag (EA25)	0.053
EA25P2C	Nemrut Dag (EA25)	0.057
EA25P3	Nemrut Dag (EA25)	0.076
EA22P6B	Nemrut Dag (EA22)	0.081
EA25P2A	Nemrut Dag (EA25)	0.081

Elements: Ti, Al, Fe, Mn, Ca, Zr, Ba

A-Rank:	Nemrut Dag (EA25)	10
B-Rank:	-	-

Specimen	*Location*	*E.D.*
EA25P1C	Nemrut Dag (EA25)	0.015
EA25P1A	Nemrut Dag (EA25)	0.032
EA25P1B	Nemrut Dag (EA25)	0.042
EA25P2B	Nemrut Dag (EA25)	0.047
EA25P2C	Nemrut Dag (EA25)	0.048
EA25P3	Nemrut Dag (EA25)	0.048
EA25R1	Nemrut Dag (EA25)	0.048
EA25P2A	Nemrut Dag (EA25)	0.049
EA25P2D	Nemrut Dag (EA25)	0.056
EA25R2	Nemrut Dag (EA25)	0.062

Table D.1 - Source Assignments of Artifacts based on Euclidean Distance to Centroids of Geological Specimens

Artifact: A9 q463.2 f156 k3 piece 1

A-Rank: **Komurcu-Gollu Dag** **64**
B-Rank: Gollu Dag-other 10

Elements: Fe, Ti, Ba

A-Rank:	Komurcu-Gollu Dag	10
B-Rank:	-	-

Specimen	*Location*	*E.D.*
CA20P4	Komurcu-Gollu Dag	0.009
CA20P2	Komurcu-Gollu Dag	0.010
CA20P3	Komurcu-Gollu Dag	0.011
CA32W2B	Komurcu-Gollu Dag	0.011
CA20R1A	Komurcu-Gollu Dag	0.013
CA32W2A	Komurcu-Gollu Dag	0.013
CA20R1B	Komurcu-Gollu Dag	0.014
CA32W2E	Komurcu-Gollu Dag	0.014
CA32W4E	Komurcu-Gollu Dag	0.015
CA32W2D	Komurcu-Gollu Dag	0.016

Elements: Fe, Zr, Ba

A-Rank:	Komurcu-Gollu Dag	8
B-Rank:	Gollu Dag	2

Specimen	*Location*	*E.D.*
CA20P2	Komurcu-Gollu Dag	0.006
CA20P4	Komurcu-Gollu Dag	0.007
CA20P3	Komurcu-Gollu Dag	0.011
CA20R1A	Komurcu-Gollu Dag	0.013
CA20R1B	Komurcu-Gollu Dag	0.014
CA20P1A	Komurcu-Gollu Dag	0.016
CA17R1A	Gollu Dag	0.021
CA20P1B	Komurcu-Gollu Dag	0.021
CA17P1	Gollu Dag	0.023
CA32W4E	Komurcu-Gollu Dag	0.023

Elements: Ti, Fe, Zr, Ba

A-Rank:	Komurcu-Gollu Dag	8
B-Rank:	Gollu Dag	2

Specimen	*Location*	*E.D.*
CA20P4	Komurcu-Gollu Dag	0.009
CA20P2	Komurcu-Gollu Dag	0.010
CA20P3	Komurcu-Gollu Dag	0.011
CA20R1A	Komurcu-Gollu Dag	0.014
CA20R1B	Komurcu-Gollu Dag	0.014
CA20P1A	Komurcu-Gollu Dag	0.018
CA17R1A	Gollu Dag	0.021
CA20P1B	Komurcu-Gollu Dag	0.021
CA17P1	Gollu Dag	0.023
CA32W4E	Komurcu-Gollu Dag	0.023

Elements: Ti, Fe, Mn, Ca, Zr, Ba

A-Rank:	Komurcu-Gollu Dag	9
B-Rank:	Gollu Dag	1

Specimen	*Location*	*E.D.*
CA20P2	Komurcu-Gollu Dag	0.018
CA20P3	Komurcu-Gollu Dag	0.018
CA20P1B	Komurcu-Gollu Dag	0.021
CA20P1A	Komurcu-Gollu Dag	0.023
CA17R1B	Gollu Dag	0.024
CA20P4	Komurcu-Gollu Dag	0.024
CA32W1D	Komurcu-Gollu Dag	0.027
CA32W4B	Komurcu-Gollu Dag	0.029
CA32W2E	Komurcu-Gollu Dag	0.032
CA32W6D	Komurcu-Gollu Dag	0.033

Elements: Fe, Ti, Zr

A-Rank:	Komurcu-Golludag	7
B-Rank:	Golludag	3

Specimen	*Location*	*E.D.*
CA20P3	Komurcu, Golludag	0.002
CA20P1B	Komurcu, Golludag	0.004
CA20R1B	Komurcu, Golludag	0.004
CA17R1A	Golludag	0.005
CA20P1A	Komurcu, Golludag	0.006
CA20P4	Komurcu, Golludag	0.006
CA17P1	Golludag	0.007
CA17R1B	Golludag	0.008
CA20P2	Komurcu, Golludag	0.009
CA20R1A	Komurcu, Golludag	0.009

Elements: Ti, Zr, Ba

A-Rank:	Komurcu-Gollu Dag	8
B-Rank:	Gollu Dag	2

Specimen	*Location*	*E.D.*
CA20P4	Komurcu-Gollu Dag	0.009
CA20P2	Komurcu-Gollu Dag	0.010
CA20P3	Komurcu-Gollu Dag	0.011
CA20R1A	Komurcu-Gollu Dag	0.012
CA20R1B	Komurcu-Gollu Dag	0.014
CA20P1A	Komurcu-Gollu Dag	0.018
CA17R1A	Gollu Dag	0.020
CA20P1B	Komurcu-Gollu Dag	0.021
CA32W4E	Komurcu-Gollu Dag	0.021
CA17P1	Gollu Dag	0.022

Elements: Ti, Fe, Zr, Ba, Zn

A-Rank:	Komurcu-Gollu Dag	5
B-Rank:	Hrazdan Cluster	2

Specimen	*Location*	*E.D.*
CA32W2B	Komurcu-Gollu Dag	0.031
CA32W2D	Komurcu-Gollu Dag	0.042
AR03E1	Hrazdan Cluster	0.061
CA32W4A	Komurcu-Gollu Dag	0.061
CA32W2A	Komurcu-Gollu Dag	0.064
KB02jB1	Baksan River	0.064
CA32W4E	Komurcu-Gollu Dag	0.066
AR41sK1	Pokr Arteni	0.067
AR41sK2	Pokr Arteni	0.067
AR04E1	Hrazdan Cluster	0.070

Elements: Ti, Al, Fe, Mn, Ca, Zr, Ba

A-Rank:	Komurcu-Gollu Dag	9
B-Rank:	Gollu Dag	1

Specimen	*Location*	*E.D.*
CA20P3	Komurcu-Gollu Dag	0.019
CA20P2	Komurcu-Gollu Dag	0.021
CA20P1A	Komurcu-Gollu Dag	0.023
CA20P1B	Komurcu-Gollu Dag	0.024
CA20P4	Komurcu-Gollu Dag	0.024
CA17R1B	Gollu Dag	0.025
CA32W1D	Komurcu-Gollu Dag	0.029
CA32W4B	Komurcu-Gollu Dag	0.029
CA32W2E	Komurcu-Gollu Dag	0.032
CA32W6D	Komurcu-Gollu Dag	0.034

Table D.1 - Source Assignments of Artifacts based on Euclidean Distance to Centroids of Geological Specimens

Artifact: A9 q463.2 f156 k3 piece 2

A-Rank: Kars-Akbaba Dag 31
B-Rank: **Komurcu-Gollu Dag** **25**

Elements: Fe, Ti, Ba

A-Rank:	Kars-Akbaba Dag	5
B-Rank:	Komurcu-Gollu Dag	4

Specimen	*Location*	*E.D.*
EA38P4	Kars-Akbaba Dag	0.038
EA38R1	Kars-Akbaba Dag	0.038
EA38P1	Kars-Akbaba Dag	0.040
CA32W1E	Komurcu-Gollu Dag	0.041
EA38P2	Kars-Akbaba Dag	0.042
EA38P3	Kars-Akbaba Dag	0.042
CA32W4B	Komurcu-Gollu Dag	0.043
CA32W4A	Komurcu-Gollu Dag	0.044
CA32W4E	Komurcu-Gollu Dag	0.047
AR68rB1	Pokr Arteni	0.051

Elements: Fe, Zr, Ba

A-Rank:	Kars-Akbaba Dag	5
B-Rank:	Komurcu-Gollu Dag	3

Specimen	*Location*	*E.D.*
EA38P1	Kars-Akbaba Dag	0.033
EA38P4	Kars-Akbaba Dag	0.033
EA38R1	Kars-Akbaba Dag	0.035
AR68rB1	Pokr Arteni	0.037
EA38P3	Kars-Akbaba Dag	0.039
EA38P2	Kars-Akbaba Dag	0.040
CA32W4B	Komurcu-Gollu Dag	0.043
CA32W1E	Komurcu-Gollu Dag	0.044
AR42kM2	Pokr Arteni	0.045
CA32W4A	Komurcu-Gollu Dag	0.045

Elements: Ti, Fe, Zr, Ba

A-Rank:	Kars-Akbaba Dag	5
B-Rank:	Komurcu-Gollu Dag	4

Specimen	*Location*	*E.D.*
EA38P4	Kars-Akbaba Dag	0.038
EA38R1	Kars-Akbaba Dag	0.039
EA38P1	Kars-Akbaba Dag	0.040
CA32W4B	Komurcu-Gollu Dag	0.043
EA38P2	Kars-Akbaba Dag	0.043
CA32W1E	Komurcu-Gollu Dag	0.044
EA38P3	Kars-Akbaba Dag	0.044
CA32W4A	Komurcu-Gollu Dag	0.045
CA32W4E	Komurcu-Gollu Dag	0.047
AR68rB1	Pokr Arteni	0.053

Elements: Ti, Fe, Mn, Ca, Zr, Ba

A-Rank:	Kars-Akbaba Dag	5
B-Rank:	Komurcu-Gollu Dag	5

Specimen	*Location*	*E.D.*
EA38P1	Kars-Akbaba Dag	0.040
EA38P4	Kars-Akbaba Dag	0.041
CA32W4B	Komurcu-Gollu Dag	0.043
EA38R1	Kars-Akbaba Dag	0.043
EA38P2	Kars-Akbaba Dag	0.044
EA38P3	Kars-Akbaba Dag	0.044
CA32W1E	Komurcu-Gollu Dag	0.046
CA32W4A	Komurcu-Gollu Dag	0.048
CA32W4E	Komurcu-Gollu Dag	0.052
CA32W2D	Komurcu-Gollu Dag	0.064

Elements: Fe, Ti, Zr

A-Rank:	Komurcu-Golludag	7
B-Rank:	Golludag	3

Specimen	*Location*	*E.D.*
CA20P4	Komurcu, Golludag	0.015
CA17R1B	Golludag	0.016
CA20P1A	Komurcu, Golludag	0.016
CA20P1B	Komurcu, Golludag	0.016
CA20R1A	Komurcu, Golludag	0.016
CA20R1B	Komurcu, Golludag	0.016
CA20P3	Komurcu, Golludag	0.017
CA32W4E	Komurcu, Golludag	0.018
CA14P2	Bozkoy, Golludag	0.019
CA17P1	Golludag	0.019

Elements: Ti, Zr, Ba

A-Rank:	Kars-Akbaba Dag	6
B-Rank:	Komurcu-Gollu Dag	2

Specimen	*Location*	*E.D.*
EA38P4	Kars-Akbaba Dag	0.029
EA38R1	Kars-Akbaba Dag	0.029
AR68rB4	Pokr Arteni	0.033
EA38P1	Kars-Akbaba Dag	0.033
EA38P2	Kars-Akbaba Dag	0.035
AR42kM1	Pokr Arteni	0.036
CA32W4B	Komurcu-Gollu Dag	0.038
EA38P3	Kars-Akbaba Dag	0.038
CA32W1E	Komurcu-Gollu Dag	0.040
AR68rB1	Kars-Akbaba Dag	0.041

Elements: Ti, Fe, Zr, Ba, Zn

A-Rank:	Hrazdan Cluster	4
B-Rank:	Pokr Arteni	3

Specimen	*Location*	*E.D.*
AR42kM1	Pokr Arteni	0.066
EA42P1B	Erzurum	0.072
AR05E1B	Hrazdan Cluster	0.074
AR05E1C	Hrazdan Cluster	0.079
CA32W2B	Komurcu-Gollu Dag	0.082
AR04E1	Hrazdan Cluster	0.087
CA01R1	Catkoy	0.088
AR41sK1	Pokr Arteni	0.089
AR42kM2	Pokr Arteni	0.089
AR04E2	Hrazdan Cluster	0.095

Elements: Ti, Al, Fe, Mn, Ca, Zr, Ba

A-Rank:	Kars-Akbaba Dag	5
B-Rank:	Komurcu-Gollu Dag	5

Specimen	*Location*	*E.D.*
EA38P1	Kars-Akbaba Dag	0.046
EA38P4	Kars-Akbaba Dag	0.046
CA32W4B	Komurcu-Gollu Dag	0.048
EA38R1	Kars-Akbaba Dag	0.048
CA32W1E	Komurcu-Gollu Dag	0.049
EA38P2	Kars-Akbaba Dag	0.050
CA32W4A	Komurcu-Gollu Dag	0.051
CA32W4E	Komurcu-Gollu Dag	0.056
EA38P3	Kars-Akbaba Dag	0.056
CA20P2	Komurcu-Gollu Dag	0.067

Table D.1 - Source Assignments of Artifacts based on Euclidean Distance to Centroids of Geological Specimens

Artifact: A9 q693.1 f247 k11 piece 1

A-Rank: **Nemrut Dag (EA25)** **50**
B-Rank: Nemrut Dag (EA22) 26

Elements: Fe, Ti, Ba

A-Rank:	Nemrut Dag (EA25)	10
B-Rank:	-	-

Specimen	*Location*	*E.D.*
EA25P2A	Nemrut Dag (EA25)	0.010
EA25P2C	Nemrut Dag (EA25)	0.011
EA25P1C	Nemrut Dag (EA25)	0.012
EA25P2D	Nemrut Dag (EA25)	0.012
EA25R2	Nemrut Dag (EA25)	0.013
EA25P2B	Nemrut Dag (EA25)	0.018
EA25P1A	Nemrut Dag (EA25)	0.020
EA25P1B	Nemrut Dag (EA25)	0.020
EA25P1D	Nemrut Dag (EA25)	0.024
EA25R1	Nemrut Dag (EA25)	0.028

Elements: Fe, Zr, Ba

A-Rank:	Nemrut Dag (EA22)	7
B-Rank:	Nemrut Dag (EA21)	3

Specimen	*Location*	*E.D.*
EA22P5A	Nemrut Dag (EA22)	0.058
EA21P1	Nemrut Dag (EA21)	0.062
EA22P4	Nemrut Dag (EA22)	0.063
EA22P7A	Nemrut Dag (EA22)	0.063
EA22P6A	Nemrut Dag (EA22)	0.065
EA22P5B	Nemrut Dag (EA22)	0.066
EA21R1B	Nemrut Dag (EA21)	0.067
EA21R1A	Nemrut Dag (EA21)	0.068
EA22P3	Nemrut Dag (EA22)	0.068
EA22P8B	Nemrut Dag (EA22)	0.068

Elements: Ti, Fe, Zr, Ba

A-Rank:	Nemrut Dag (EA25)	6
B-Rank:	Nemrut Dag (EA22)	4

Specimen	*Location*	*E.D.*
EA25P1A	Nemrut Dag (EA25)	0.072
EA25P1D	Nemrut Dag (EA25)	0.072
EA25P1B	Nemrut Dag (EA25)	0.073
EA25P1C	Nemrut Dag (EA25)	0.076
EA22P7A	Nemrut Dag (EA22)	0.083
EA22P6B	Nemrut Dag (EA22)	0.091
EA25P2C	Nemrut Dag (EA25)	0.091
EA22P8B	Nemrut Dag (EA22)	0.092
EA25R1	Nemrut Dag (EA25)	0.092
EA22P5A	Nemrut Dag (EA22)	0.093

Elements: Ti, Fe, Mn, Ca, Zr, Ba

A-Rank:	Nemrut Dag (EA25)	10
B-Rank:	-	-

Specimen	*Location*	*E.D.*
EA25P1A	Nemrut Dag (EA25)	0.076
EA25P1C	Nemrut Dag (EA25)	0.076
EA25P1B	Nemrut Dag (EA25)	0.081
EA25P1D	Nemrut Dag (EA25)	0.090
EA25P2C	Nemrut Dag (EA25)	0.099
EA25R1	Nemrut Dag (EA25)	0.100
EA25P2A	Nemrut Dag (EA25)	0.104
EA25P2D	Nemrut Dag (EA25)	0.105
EA25P3	Nemrut Dag (EA25)	0.105
EA25P2B	Nemrut Dag (EA25)	0.108

Elements: Fe, Ti, Zr

A-Rank:	Nemrut Dag (EA25)	6
B-Rank:	Nemrut Dag (EA22)	4

Specimen	*Location*	*E.D.*
EA25P1D	Nemrut Dag (EA25)	0.068
EA25P1A	Nemrut Dag (EA25)	0.069
EA25P1B	Nemrut Dag (EA25)	0.070
EA25P1C	Nemrut Dag (EA25)	0.075
EA22P7A	Nemrut Dag (EA22)	0.083
EA25R1	Nemrut Dag (EA25)	0.088
EA22P8B	Nemrut Dag (EA22)	0.089
EA22P6B	Nemrut Dag (EA22)	0.090
EA25P2C	Nemrut Dag (EA25)	0.090
EA22P5A	Nemrut Dag (EA22)	0.092

Elements: Ti, Zr, Ba

A-Rank:	Nemrut Dag (EA22)	5
B-Rank:	Nemrut Dag (EA25)	4

Specimen	*Location*	*E.D.*
EA22P7A	Nemrut Dag (EA22)	0.068
EA25P1D	Nemrut Dag (EA25)	0.071
EA25P1A	Nemrut Dag (EA25)	0.072
EA25P1B	Nemrut Dag (EA25)	0.073
EA25P1C	Nemrut Dag (EA25)	0.076
EA22R1	Nemrut Dag (EA22)	0.077
EA22P8B	Nemrut Dag (EA22)	0.079
EA22P6B	Nemrut Dag (EA22)	0.080
EA21P1	Nemrut Dag (EA21)	0.082
EA22P5A	Nemrut Dag (EA22)	0.082

Elements: Ti, Fe, Zr, Ba, Zn

A-Rank:	Nemrut Dag (EA22)	6
B-Rank:	Nemrut Dag (EA25)	4

Specimen	*Location*	*E.D.*
EA25P1A	Nemrut Dag (EA25)	0.075
EA25P1D	Nemrut Dag (EA25)	0.075
EA25P1B	Nemrut Dag (EA25)	0.077
EA22P8B	Nemrut Dag (EA22)	0.094
EA25P1C	Nemrut Dag (EA25)	0.094
EA22P6B	Nemrut Dag (EA22)	0.096
EA22P7B	Nemrut Dag (EA22)	0.096
EA22P7A	Nemrut Dag (EA22)	0.099
EA22P3	Nemrut Dag (EA22)	0.100
EA22P6A	Nemrut Dag (EA22)	0.101

Elements: Ti, Al, Fe, Mn, Ca, Zr, Ba

A-Rank:	Nemrut Dag (EA25)	10
B-Rank:	-	-

Specimen	*Location*	*E.D.*
EA25P1A	Nemrut Dag (EA25)	0.077
EA25P1C	Nemrut Dag (EA25)	0.077
EA25P1B	Nemrut Dag (EA25)	0.081
EA25P1D	Nemrut Dag (EA25)	0.090
EA25P2C	Nemrut Dag (EA25)	0.099
EA25R1	Nemrut Dag (EA25)	0.101
EA25P2A	Nemrut Dag (EA25)	0.104
EA25P2D	Nemrut Dag (EA25)	0.105
EA25P3	Nemrut Dag (EA25)	0.105
EA25P2B	Nemrut Dag (EA25)	0.108

Table D.1 - Source Assignments of Artifacts based on Euclidean Distance to Centroids of Geological Specimens

Artifact: A9 q693.1 f247 k11 piece 2

A-Rank: **Nemrut Dag (EA25)** **61**
B-Rank: Nemrut Dag (EA22) 18

Elements: Fe, Ti, Ba

A-Rank:	Nemrut Dag (EA25)	10
B-Rank:	-	-

Specimen	*Location*	*E.D.*
EA25P1B	Nemrut Dag (EA25)	0.007
EA25P1A	Nemrut Dag (EA25)	0.009
EA25P1C	Nemrut Dag (EA25)	0.010
EA25P2A	Nemrut Dag (EA25)	0.012
EA25R1	Nemrut Dag (EA25)	0.012
EA25P2B	Nemrut Dag (EA25)	0.013
EA25R2	Nemrut Dag (EA25)	0.013
EA25P2C	Nemrut Dag (EA25)	0.014
EA25P1D	Nemrut Dag (EA25)	0.016
EA25P2D	Nemrut Dag (EA25)	0.016

Elements: Fe, Zr, Ba

A-Rank:	Nemrut Dag (EA22)	6
B-Rank:	Nemrut Dag (EA25)	4

Specimen	*Location*	*E.D.*
EA22P4	Nemrut Dag (EA22)	0.040
EA25P1D	Nemrut Dag (EA25)	0.041
EA25P1A	Nemrut Dag (EA25)	0.042
EA25P1B	Nemrut Dag (EA25)	0.042
EA22P5A	Nemrut Dag (EA22)	0.044
EA25P1C	Nemrut Dag (EA25)	0.047
EA22P5B	Nemrut Dag (EA22)	0.048
EA22P6A	Nemrut Dag (EA22)	0.048
EA22P6B	Nemrut Dag (EA22)	0.049
EA22P8B	Nemrut Dag (EA22)	0.049

Elements: Ti, Fe, Zr, Ba

A-Rank:	Nemrut Dag (EA25)	8
B-Rank:	Nemrut Dag (EA22)	2

Specimen	*Location*	*E.D.*
EA25P1A	Nemrut Dag (EA25)	0.043
EA25P1B	Nemrut Dag (EA25)	0.043
EA25P1D	Nemrut Dag (EA25)	0.043
EA25P1C	Nemrut Dag (EA25)	0.048
EA25R1	Nemrut Dag (EA25)	0.061
EA25P2C	Nemrut Dag (EA25)	0.064
EA22P7A	Nemrut Dag (EA22)	0.066
EA25P2D	Nemrut Dag (EA25)	0.067
EA25P3	Nemrut Dag (EA25)	0.067
EA22P6B	Nemrut Dag (EA22)	0.069

Elements: Ti, Fe, Mn, Ca, Zr, Ba

A-Rank:	Nemrut Dag (EA25)	10
B-Rank:	-	-

Specimen	*Location*	*E.D.*
EA25P1A	Nemrut Dag (EA25)	0.043
EA25P1B	Nemrut Dag (EA25)	0.043
EA25P1D	Nemrut Dag (EA25)	0.051
EA25P1C	Nemrut Dag (EA25)	0.052
EA25R1	Nemrut Dag (EA25)	0.062
EA25P2C	Nemrut Dag (EA25)	0.065
EA25P3	Nemrut Dag (EA25)	0.067
EA25P2A	Nemrut Dag (EA25)	0.070
EA25P2D	Nemrut Dag (EA25)	0.070
EA25P2B	Nemrut Dag (EA25)	0.074

Elements: Fe, Ti, Zr

A-Rank:	Nemrut Dag (EA25)	8
B-Rank:	Nemrut Dag (EA22)	2

Specimen	*Location*	*E.D.*
EA25P1A	Nemrut Dag (EA25)	0.042
EA25P1B	Nemrut Dag (EA25)	0.042
EA25P1D	Nemrut Dag (EA25)	0.042
EA25P1C	Nemrut Dag (EA25)	0.048
EA25R1	Nemrut Dag (EA25)	0.060
EA25P2C	Nemrut Dag (EA25)	0.063
EA25P3	Nemrut Dag (EA25)	0.065
EA22P7A	Nemrut Dag (EA22)	0.066
EA25P2D	Nemrut Dag (EA25)	0.067
EA22P6B	Nemrut Dag (EA22)	0.069

Elements: Ti, Zr, Ba

A-Rank:	Nemrut Dag (EA22)	6
B-Rank:	Nemrut Dag (EA25)	4

Specimen	*Location*	*E.D.*
EA25P1D	Nemrut Dag (EA25)	0.042
EA25P1A	Nemrut Dag (EA25)	0.043
EA25P1B	Nemrut Dag (EA25)	0.043
EA22P7A	Nemrut Dag (EA22)	0.045
EA25P1C	Nemrut Dag (EA25)	0.048
EA22R1	Nemrut Dag (EA22)	0.051
EA22P8B	Nemrut Dag (EA22)	0.053
EA22P6B	Nemrut Dag (EA22)	0.054
EA22P2	Nemrut Dag (EA22)	0.055
EA22P7B	Nemrut Dag (EA22)	0.057

Elements: Ti, Fe, Zr, Ba, Zn

A-Rank:	Nemrut Dag (EA25)	7
B-Rank:	Nemrut Dag (EA22)	2

Specimen	*Location*	*E.D.*
EA25P1C	Nemrut Dag (EA25)	0.057
EA25P3	Nemrut Dag (EA25)	0.068
EA25P2A	Nemrut Dag (EA25)	0.070
EA25R1	Nemrut Dag (EA25)	0.071
EA22P4	Nemrut Dag (EA22)	0.074
EA22P5A	Nemrut Dag (EA22)	0.076
EA25P1B	Nemrut Dag (EA25)	0.076
EA25P1A	Nemrut Dag (EA25)	0.079
EA25P1D	Nemrut Dag (EA25)	0.079
EA21P1	Nemrut Dag (EA21)	0.082

Elements: Ti, Al, Fe, Mn, Ca, Zr, Ba

A-Rank:	Nemrut Dag (EA25)	10
B-Rank:	-	-

Specimen	*Location*	*E.D.*
EA25P1B	Nemrut Dag (EA25)	0.043
EA25P1A	Nemrut Dag (EA25)	0.044
EA25P1D	Nemrut Dag (EA25)	0.051
EA25P1C	Nemrut Dag (EA25)	0.052
EA25R1	Nemrut Dag (EA25)	0.063
EA25P2C	Nemrut Dag (EA25)	0.065
EA25P3	Nemrut Dag (EA25)	0.068
EA25P2A	Nemrut Dag (EA25)	0.070
EA25P2D	Nemrut Dag (EA25)	0.070
EA25P2B	Nemrut Dag (EA25)	0.074

Table D.1 - Source Assignments of Artifacts based on Euclidean Distance to Centroids of Geological Specimens

Artifact: A9 q693.1 f247 k11 piece 3

A-Rank: **Mus** **32**
B-Rank: **Pasinler** **28**

Elements: Fe, Ti, Ba

A-Rank:	Bingol B	10
B-Rank:	-	-

Specimen	*Location*	*E.D.*
EA50R1B	Bingol B	0.021
EA50P5	Bingol B	0.024
EA50P2C	Bingol B	0.027
EA50P6	Bingol B	0.027
EA50P1B	Bingol B	0.028
EA50P2A	Bingol B	0.028
EA50P1A	Bingol B	0.029
EA50P1C	Bingol B	0.029
EA50P4C	Bingol B	0.029
EA50R1A	Bingol B	0.030

Elements: Fe, Zr, Ba

A-Rank:	Pasinler	10
B-Rank:	-	-

Specimen	*Location*	*E.D.*
EA35P1	Pasinler	0.031
EA35P2	Pasinler	0.031
EA33P3	Pasinler	0.032
EA34R2	Pasinler	0.032
EA35P3	Pasinler	0.032
EA34P1	Pasinler	0.033
EA34P3	Pasinler	0.034
EA33P6	Pasinler	0.035
EA33R1	Pasinler	0.035
EA33P7	Pasinler	0.036

Elements: Ti, Fe, Zr, Ba

A-Rank:	Pasinler	8
B-Rank:	Mus	2

Specimen	*Location*	*E.D.*
EA35P2	Pasinler	0.041
EA33P7	Pasinler	0.042
EA35P1	Pasinler	0.043
EA33P3	Pasinler	0.044
EA34P3	Pasinler	0.044
EA34P1	Pasinler	0.046
EA60B1A	Mus	0.046
EA62Y1B	Mus	0.046
EA33P5	Pasinler	0.047
EA34R1	Pasinler	0.047

Elements: Ti, Fe, Mn, Ca, Zr, Ba

A-Rank:	Mus	10
B-Rank:	-	-

Specimen	*Location*	*E.D.*
EA62Y5	Mus	0.060
EA61B1	Mus	0.063
EA62Y3A	Mus	0.063
EA62Y1A	Mus	0.065
EA58B1	Mus	0.073
EA62Y1D	Mus	0.077
EA62Y1B	Mus	0.080
EA59B1	Mus	0.081
EA62Y4	Mus	0.083
EA60B1A	Mus	0.086

Elements: Fe, Ti, Zr

A-Rank:	Hotamis Dag	5
B-Rank:	Erzurum	3

Specimen	*Location*	*E.D.*
5EA13P2	Suphan Dag	0.032
EA42P4	Erzurum	0.033
CA06P5C	Hotamis Dag	0.034
CA06P5A	Hotamis Dag	0.035
EA17P1D	Suphan Dag	0.035
EA41P1	Erzurum	0.035
EA42P1B	Erzurum	0.035
CA06P1	Hotamis Dag	0.037
CA06P7A	Hotamis Dag	0.037
CA12P1	Hotamis Dag	0.037

Elements: Ti, Zr, Ba

A-Rank:	Pasinler	10
B-Rank:	-	-

Specimen	*Location*	*E.D.*
EA35P2	Pasinler	0.028
EA33P7	Pasinler	0.029
EA35P1	Pasinler	0.030
EA33P3	Pasinler	0.031
EA34P3	Pasinler	0.032
EA34P1	Pasinler	0.034
EA34R1	Pasinler	0.035
EA34R2	Pasinler	0.035
EA33P5	Pasinler	0.036
EA35P3	Pasinler	0.036

Elements: Ti, Fe, Zr, Ba, Zn

A-Rank:	Mus	10
B-Rank:	-	-

Specimen	*Location*	*E.D.*
EA62Y1A	Mus	0.051
EA60B1B	Mus	0.061
EA60B1A	Mus	0.063
EA62Y3B	Mus	0.071
EA58B1	Mus	0.081
EA62Y4	Mus	0.081
EA57B1	Mus	0.083
EA62Y1B	Mus	0.085
EA59B1	Mus	0.092
EA62Y1C	Mus	0.092

Elements: Ti, Al, Fe, Mn, Ca, Zr, Ba

A-Rank:	Mus	10
B-Rank:	-	-

Specimen	*Location*	*E.D.*
EA61B1	Mus	0.063
EA62Y3A	Mus	0.063
EA62Y5	Mus	0.064
EA62Y1A	Mus	0.066
EA58B1	Mus	0.074
EA62Y1D	Mus	0.077
EA62Y1B	Mus	0.080
EA59B1	Mus	0.083
EA62Y4	Mus	0.083
EA60B1A	Mus	0.088

Table D.1 - Source Assignments of Artifacts based on Euclidean Distance to Centroids of Geological Specimens

Artifact: A9 q742.1 f260 k11 piece 1

A-Rank: **Bingol B** **58**
B-Rank: Gutansar 11

Elements: Fe, Ti, Ba

A-Rank:	Bingol B	7
B-Rank:	Gutansar	3

Specimen	*Location*	*E.D.*
EA52B1	Bingol B	0.027
EA52B3	Bingol B	0.030
EA52B2	Bingol B	0.040
EA56B1	Bingol B	0.045
EA53B2	Bingol B	0.066
EA53B1	Bingol B	0.073
EA54B1	Bingol B	0.074
AR06E2A	Gutansar	0.099
AR06E1A	Gutansar	0.100
AR12jB1	Gutansar	0.101

Elements: Fe, Zr, Ba

A-Rank:	Bingol B	7
B-Rank:	Erzincan	2

Specimen	*Location*	*E.D.*
EA52B3	Bingol B	0.031
EA52B1	Bingol B	0.032
EA56B1	Bingol B	0.035
EA52B2	Bingol B	0.041
EA53B2	Bingol B	0.060
EA53B1	Bingol B	0.072
EA54B1	Bingol B	0.077
EA43R2	Erzincan	0.100
CA07P1	Acigol	0.101
EA44R1	Erzincan	0.103

Elements: Ti, Fe, Zr, Ba

A-Rank:	Bingol B	7
B-Rank:	Gutansar	2

Specimen	*Location*	*E.D.*
EA52B3	Bingol B	0.031
EA52B1	Bingol B	0.032
EA52B2	Bingol B	0.041
EA56B1	Bingol B	0.049
EA53B2	Bingol B	0.067
EA54B1	Bingol B	0.077
EA53B1	Bingol B	0.078
AR76rB3	Gutansar	0.148
AR06E3A	Gutansar	0.149
CA07P1	Acigol	0.149

Elements: Ti, Fe, Mn, Ca, Zr, Ba

A-Rank:	Bingol B	7
B-Rank:	Acigol	3

Specimen	*Location*	*E.D.*
EA52B1	Bingol B	0.037
EA52B2	Bingol B	0.041
EA52B3	Bingol B	0.044
EA56B1	Bingol B	0.057
EA53B2	Bingol B	0.067
EA53B1	Bingol B	0.081
EA54B1	Bingol B	0.112
CA08R1A	Acigol	0.164
CA08R1C	Acigol	0.168
CA07R2A	Acigol	0.178

Elements: Fe, Ti, Zr

A-Rank:	Bingol B	7
B-Rank:	Gutansar	2

Specimen	*Location*	*E.D.*
EA52B3	Bingol B	0.016
EA52B1	Bingol B	0.017
EA52B2	Bingol B	0.031
EA56B1	Bingol B	0.040
EA53B2	Bingol B	0.042
EA53B1	Bingol B	0.048
EA54B1	Bingol B	0.074
EA66W1	Lake Van	0.137
AR76rB3	Gutansar	0.140
AR06E1C	Gutansar	0.146

Elements: Ti, Zr, Ba

A-Rank:	Bingol B	9
B-Rank:	Gutansar	1

Specimen	*Location*	*E.D.*
EA52B2	Bingol B	0.028
EA52B3	Bingol B	0.029
EA52B1	Bingol B	0.032
EA54B1	Bingol B	0.032
EA55B2	Bingol B	0.046
EA56B1	Bingol B	0.048
EA55B1	Bingol B	0.054
EA53B2	Bingol B	0.061
EA53B1	Bingol B	0.072
AR78rB3	Gutansar	0.106

Elements: Ti, Fe, Zr, Ba, Zn

A-Rank:	Bingol B	7
B-Rank:	Gutansar	3

Specimen	*Location*	*E.D.*
EA52B1	Bingol B	0.046
EA52B3	Bingol B	0.056
EA52B2	Bingol B	0.076
EA53B1	Bingol B	0.080
EA56B1	Bingol B	0.090
EA54B1	Bingol B	0.092
EA53B2	Bingol B	0.128
AR06E2B	Gutansar	0.151
AR06E1C	Gutansar	0.154
AR12jB1	Gutansar	0.154

Elements: Ti, Al, Fe, Mn, Ca, Zr, Ba

A-Rank:	Bingol B	7
B-Rank:	Acigol	3

Specimen	*Location*	*E.D.*
EA52B1	Bingol B	0.068
EA52B2	Bingol B	0.070
EA52B3	Bingol B	0.073
EA53B2	Bingol B	0.077
EA56B1	Bingol B	0.077
EA53B1	Bingol B	0.089
EA54B1	Bingol B	0.123
CA08R1A	Acigol	0.164
CA08R1C	Acigol	0.168
CA07R2A	Acigol	0.178

Table D.1 - Source Assignments of Artifacts based on Euclidean Distance to Centroids of Geological Specimens

Artifact: A9 q742.1 f260 k11 piece 2

A-Rank: **Meydan Dag** **68**
B-Rank: Tendurek Dag 5

Elements: Fe, Ti, Ba

A-Rank:	Meydan Dag	10
B-Rank:	-	-

Specimen	*Location*	*E.D.*
EA10P2	Meydan Dag	0.014
EA68SX1	Meydan Dag	0.014
EA11P1	Meydan Dag	0.016
EA68SX2	Meydan Dag	0.016
EA11R2	Meydan Dag	0.019
EA10R2	Meydan Dag	0.020
EA07R2	Meydan Dag	0.021
EA07P1	Meydan Dag	0.022
EA10R1A	Meydan Dag	0.023
EA07R1	Meydan Dag	0.025

Elements: Fe, Zr, Ba

A-Rank:	Meydan Dag	10
B-Rank:	-	-

Specimen	*Location*	*E.D.*
EA10R2	Meydan Dag	0.019
EA68SX1	Meydan Dag	0.022
EA10P4	Meydan Dag	0.028
EA10R1A	Meydan Dag	0.030
EA69SX2	Meydan Dag	0.031
EA10P3	Meydan Dag	0.032
EA10P2	Meydan Dag	0.034
EA11R2	Meydan Dag	0.034
EA69SX1	Meydan Dag	0.034
EA08R1	Meydan Dag	0.035

Elements: Ti, Fe, Zr, Ba

A-Rank:	Meydan Dag	10
B-Rank:	-	-

Specimen	*Location*	*E.D.*
EA10R2	Meydan Dag	0.022
EA68SX1	Meydan Dag	0.024
EA10P4	Meydan Dag	0.030
EA10R1A	Meydan Dag	0.031
EA69SX2	Meydan Dag	0.032
EA10P3	Meydan Dag	0.034
EA08R1	Meydan Dag	0.035
EA11R2	Meydan Dag	0.035
EA10P2	Meydan Dag	0.036
EA68SX2	Meydan Dag	0.036

Elements: Ti, Fe, Mn, Ca, Zr, Ba

A-Rank:	Meydan Dag	10
B-Rank:	-	-

Specimen	*Location*	*E.D.*
EA69SX2	Meydan Dag	0.034
EA10R2	Meydan Dag	0.035
EA11R2	Meydan Dag	0.035
EA08R1	Meydan Dag	0.036
EA10R1A	Meydan Dag	0.039
EA11P1	Meydan Dag	0.039
EA11R1	Meydan Dag	0.039
EA07P1	Meydan Dag	0.040
EA07R2	Meydan Dag	0.041
EA69SX1	Meydan Dag	0.041

Elements: Fe, Ti, Zr

A-Rank:	Meydan Dag	9
B-Rank:	Bingol B	1

Specimen	*Location*	*E.D.*
EA10R2	Meydan Dag	0.018
EA10R1A	Meydan Dag	0.022
EA10P4	Meydan Dag	0.023
EA68SX1	Meydan Dag	0.023
EA07P3	Meydan Dag	0.026
EA10P3	Meydan Dag	0.026
EA49P1	Bingol B	0.027
EA08P2	Meydan Dag	0.028
EA07P2	Meydan Dag	0.029
EA10R1B	Meydan Dag	0.029

Elements: Ti, Zr, Ba

A-Rank:	Meydan Dag	4
B-Rank:	Tendurek Dag	3

Specimen	*Location*	*E.D.*
EA39R2	Kars-Arpacay	0.009
EA39P5	Kars-Arpacay	0.011
EA10R2	Meydan Dag	0.018
EA68SX1	Meydan Dag	0.021
EA69SX2	Meydan Dag	0.021
EA09R1	Tendurek Dag	0.023
EA09R2A	Tendurek Dag	0.026
EA39P3	Kars-Arpacay	0.027
EA10P4	Meydan Dag	0.028
EA09R2C	Tendurek Dag	0.029

Elements: Ti, Fe, Zr, Ba, Zn

A-Rank:	Meydan Dag	5
B-Rank:	Tendurek Dag	2

Specimen	*Location*	*E.D.*
EA10P3	Meydan Dag	0.035
EA68SX2	Meydan Dag	0.036
EA34P4	Pasinler	0.040
EA07R2	Meydan Dag	0.044
EA11R2	Meydan Dag	0.044
EA49R2	Bingol B	0.047
EA09R2A	Tendurek Dag	0.050
EA09R3E	Tendurek Dag	0.050
EA50P2B	Bingol B	0.053
EA10R2	Meydan Dag	0.057

Elements: Ti, Al, Fe, Mn, Ca, Zr, Ba

A-Rank:	Meydan Dag	10
B-Rank:	-	-

Specimen	*Location*	*E.D.*
EA69SX2	Meydan Dag	0.041
EA11R2	Meydan Dag	0.049
EA08R1	Meydan Dag	0.052
EA10P2	Meydan Dag	0.052
EA10R2	Meydan Dag	0.052
EA07R2	Meydan Dag	0.055
EA10R1A	Meydan Dag	0.056
EA11R1	Meydan Dag	0.056
EA11P1	Meydan Dag	0.058
EA69SX1	Meydan Dag	0.058

Table D.1 - Source Assignments of Artifacts based on Euclidean Distance to Centroids of Geological Specimens

Artifact: B1 q350-i f166 k? piece 1

A-Rank: **Nemrut Dag (EA25)** **72**
B-Rank: Nemrut Dag (EA22) 8

Elements: Fe, Ti, Ba

A-Rank:	Nemrut Dag (EA25)	10
B-Rank:	-	-

Specimen	*Location*	*E.D.*
EA25R2	Nemrut Dag (EA25)	0.007
EA25P2A	Nemrut Dag (EA25)	0.012
EA25P1C	Nemrut Dag (EA25)	0.014
EA25P2C	Nemrut Dag (EA25)	0.014
EA25P2D	Nemrut Dag (EA25)	0.016
EA25P1B	Nemrut Dag (EA25)	0.020
EA25P2B	Nemrut Dag (EA25)	0.020
EA25P1A	Nemrut Dag (EA25)	0.021
EA25P1D	Nemrut Dag (EA25)	0.027
EA25R1	Nemrut Dag (EA25)	0.028

Elements: Fe, Zr, Ba

A-Rank:	Nemrut Dag (EA25)	8
B-Rank:	Nemrut Dag (EA22)	2

Specimen	*Location*	*E.D.*
EA25P1C	Nemrut Dag (EA25)	0.024
EA25P1A	Nemrut Dag (EA25)	0.025
EA25P1B	Nemrut Dag (EA25)	0.025
EA25P1D	Nemrut Dag (EA25)	0.028
EA25P2C	Nemrut Dag (EA25)	0.037
EA25P2D	Nemrut Dag (EA25)	0.041
EA25P2A	Nemrut Dag (EA25)	0.043
EA25R1	Nemrut Dag (EA25)	0.043
EA22P4	Nemrut Dag (EA22)	0.044
EA22P1C	Nemrut Dag (EA22)	0.045

Elements: Ti, Fe, Zr, Ba

A-Rank:	Nemrut Dag (EA25)	10
B-Rank:	-	-

Specimen	*Location*	*E.D.*
EA25P1C	Nemrut Dag (EA25)	0.024
EA25P1A	Nemrut Dag (EA25)	0.025
EA25P1B	Nemrut Dag (EA25)	0.026
EA25P1D	Nemrut Dag (EA25)	0.029
EA25P2C	Nemrut Dag (EA25)	0.038
EA25P2D	Nemrut Dag (EA25)	0.042
EA25P2A	Nemrut Dag (EA25)	0.043
EA25R1	Nemrut Dag (EA25)	0.043
EA25P2B	Nemrut Dag (EA25)	0.050
EA25P3	Nemrut Dag (EA25)	0.050

Elements: Ti, Fe, Mn, Ca, Zr, Ba

A-Rank:	Nemrut Dag (EA25)	10
B-Rank:	-	-

Specimen	*Location*	*E.D.*
EA25P1C	Nemrut Dag (EA25)	0.026
EA25P1A	Nemrut Dag (EA25)	0.027
EA25P1B	Nemrut Dag (EA25)	0.032
EA25P2C	Nemrut Dag (EA25)	0.044
EA25P1D	Nemrut Dag (EA25)	0.048
EA25R1	Nemrut Dag (EA25)	0.048
EA25P2A	Nemrut Dag (EA25)	0.049
EA25P2D	Nemrut Dag (EA25)	0.051
EA25P2B	Nemrut Dag (EA25)	0.053
EA25P3	Nemrut Dag (EA25)	0.053

Elements: Fe, Ti, Zr

A-Rank:	Nemrut Dag (EA25)	10
B-Rank:	-	-

Specimen	*Location*	*E.D.*
EA25P1A	Nemrut Dag (EA25)	0.015
EA25P1B	Nemrut Dag (EA25)	0.015
EA25P1D	Nemrut Dag (EA25)	0.017
EA25P1C	Nemrut Dag (EA25)	0.021
EA25R1	Nemrut Dag (EA25)	0.033
EA25P2C	Nemrut Dag (EA25)	0.037
EA25P3	Nemrut Dag (EA25)	0.038
EA25P2D	Nemrut Dag (EA25)	0.040
EA25P2A	Nemrut Dag (EA25)	0.043
EA25P2B	Nemrut Dag (EA25)	0.047

Elements: Ti, Zr, Ba

A-Rank:	Nemrut Dag (EA25)	9
B-Rank:	Nemrut Dag (EA22)	1

Specimen	*Location*	*E.D.*
EA25P1C	Nemrut Dag (EA25)	0.024
EA25P1A	Nemrut Dag (EA25)	0.025
EA25P1B	Nemrut Dag (EA25)	0.025
EA25P1D	Nemrut Dag (EA25)	0.029
EA25P2C	Nemrut Dag (EA25)	0.037
EA25P2D	Nemrut Dag (EA25)	0.041
EA25P2A	Nemrut Dag (EA25)	0.043
EA25R1	Nemrut Dag (EA25)	0.043
EA22P2	Nemrut Dag (EA22)	0.047
EA25P2B	Nemrut Dag (EA25)	0.050

Elements: Ti, Fe, Zr, Ba, Zn

A-Rank:	Nemrut Dag (EA25)	5
B-Rank:	Nemrut Dag (EA22)	5

Specimen	*Location*	*E.D.*
EA25P2C	Nemrut Dag (EA25)	0.044
EA25P1A	Nemrut Dag (EA25)	0.056
EA25P1D	Nemrut Dag (EA25)	0.058
EA25P1B	Nemrut Dag (EA25)	0.059
EA22P7A	Nemrut Dag (EA22)	0.075
EA22R1	Nemrut Dag (EA22)	0.078
EA22P7B	Nemrut Dag (EA22)	0.081
EA25P2D	Nemrut Dag (EA25)	0.081
EA22P1D	Nemrut Dag (EA22)	0.082
EA22P1C	Nemrut Dag (EA22)	0.083

Elements: Ti, Al, Fe, Mn, Ca, Zr, Ba

A-Rank:	Nemrut Dag (EA25)	10
B-Rank:	-	-

Specimen	*Location*	*E.D.*
EA25P1A	Nemrut Dag (EA25)	0.063
EA25P1C	Nemrut Dag (EA25)	0.066
EA25P1B	Nemrut Dag (EA25)	0.070
EA25R1	Nemrut Dag (EA25)	0.072
EA25P2C	Nemrut Dag (EA25)	0.076
EA25P3	Nemrut Dag (EA25)	0.078
EA25R2	Nemrut Dag (EA25)	0.079
EA25P2A	Nemrut Dag (EA25)	0.081
EA25P2B	Nemrut Dag (EA25)	0.081
EA25P1D	Nemrut Dag (EA25)	0.082

Table D.1 - Source Assignments of Artifacts based on Euclidean Distance to Centroids of Geological Specimens

Artifact: B1 q350-i f166 k? piece 2

A-Rank: **Nemrut Dag (EA25)** **80**
B-Rank: - -

Elements: Fe, Ti, Ba

A-Rank: Nemrut Dag (EA25) 10
B-Rank: - -

Specimen	*Location*	*E.D.*
EA25P2B	Nemrut Dag (EA25)	0.004
EA25P1D	Nemrut Dag (EA25)	0.005
EA25P1B	Nemrut Dag (EA25)	0.010
EA25P2C	Nemrut Dag (EA25)	0.010
EA25P2D	Nemrut Dag (EA25)	0.010
EA25P1C	Nemrut Dag (EA25)	0.011
EA25P1A	Nemrut Dag (EA25)	0.012
EA25R1	Nemrut Dag (EA25)	0.015
EA25P2A	Nemrut Dag (EA25)	0.017
EA25P3	Nemrut Dag (EA25)	0.017

Elements: Fe, Zr, Ba

A-Rank: Nemrut Dag (EA25) 10
B-Rank: - -

Specimen	*Location*	*E.D.*
EA25P1D	Nemrut Dag (EA25)	0.007
EA25P1B	Nemrut Dag (EA25)	0.009
EA25P1C	Nemrut Dag (EA25)	0.010
EA25P1A	Nemrut Dag (EA25)	0.012
EA25P2C	Nemrut Dag (EA25)	0.020
EA25R1	Nemrut Dag (EA25)	0.020
EA25P2D	Nemrut Dag (EA25)	0.023
EA25P3	Nemrut Dag (EA25)	0.025
EA25P2B	Nemrut Dag (EA25)	0.028
EA25P2A	Nemrut Dag (EA25)	0.029

Elements: Ti, Fe, Zr, Ba

A-Rank: Nemrut Dag (EA25) 10
B-Rank: - -

Specimen	*Location*	*E.D.*
EA25P1D	Nemrut Dag (EA25)	0.007
EA25P1B	Nemrut Dag (EA25)	0.010
EA25P1C	Nemrut Dag (EA25)	0.011
EA25P1A	Nemrut Dag (EA25)	0.012
EA25P2C	Nemrut Dag (EA25)	0.020
EA25R1	Nemrut Dag (EA25)	0.022
EA25P2D	Nemrut Dag (EA25)	0.023
EA25P3	Nemrut Dag (EA25)	0.027
EA25P2B	Nemrut Dag (EA25)	0.028
EA25P2A	Nemrut Dag (EA25)	0.029

Elements: Ti, Fe, Mn, Ca, Zr, Ba

A-Rank: Nemrut Dag (EA25) 10
B-Rank: - -

Specimen	*Location*	*E.D.*
EA25P1A	Nemrut Dag (EA25)	0.014
EA25P1C	Nemrut Dag (EA25)	0.015
EA25P1B	Nemrut Dag (EA25)	0.020
EA25P2C	Nemrut Dag (EA25)	0.029
EA25R1	Nemrut Dag (EA25)	0.030
EA25P3	Nemrut Dag (EA25)	0.032
EA25P2B	Nemrut Dag (EA25)	0.033
EA25P2A	Nemrut Dag (EA25)	0.036
EA25P2D	Nemrut Dag (EA25)	0.036
EA25P1D	Nemrut Dag (EA25)	0.037

Elements: Fe, Ti, Zr

A-Rank: Nemrut Dag (EA25) 10
B-Rank: - -

Specimen	*Location*	*E.D.*
EA25P1D	Nemrut Dag (EA25)	0.006
EA25P1C	Nemrut Dag (EA25)	0.008
EA25P1B	Nemrut Dag (EA25)	0.010
EA25P1A	Nemrut Dag (EA25)	0.012
EA25P2C	Nemrut Dag (EA25)	0.017
EA25R1	Nemrut Dag (EA25)	0.020
EA25P2D	Nemrut Dag (EA25)	0.021
EA25P3	Nemrut Dag (EA25)	0.023
EA25P2A	Nemrut Dag (EA25)	0.028
EA25P2B	Nemrut Dag (EA25)	0.028

Elements: Ti, Zr, Ba

A-Rank: Nemrut Dag (EA25) 10
B-Rank: - -

Specimen	*Location*	*E.D.*
EA25P1A	Nemrut Dag (EA25)	0.005
EA25P1B	Nemrut Dag (EA25)	0.006
EA25P1D	Nemrut Dag (EA25)	0.007
EA25P1C	Nemrut Dag (EA25)	0.008
EA25R1	Nemrut Dag (EA25)	0.018
EA25P2C	Nemrut Dag (EA25)	0.020
EA25P2D	Nemrut Dag (EA25)	0.023
EA25P3	Nemrut Dag (EA25)	0.025
EA25P2A	Nemrut Dag (EA25)	0.026
EA25P2B	Nemrut Dag (EA25)	0.028

Elements: Ti, Fe, Zr, Ba, Zn

A-Rank: Nemrut Dag (EA25) 10
B-Rank: - -

Specimen	*Location*	*E.D.*
EA25R1	Nemrut Dag (EA25)	0.032
EA25P2A	Nemrut Dag (EA25)	0.035
EA25P3	Nemrut Dag (EA25)	0.036
EA25P1C	Nemrut Dag (EA25)	0.045
EA25P2B	Nemrut Dag (EA25)	0.062
EA25R2	Nemrut Dag (EA25)	0.062
EA25P2D	Nemrut Dag (EA25)	0.064
EA25P1B	Nemrut Dag (EA25)	0.076
EA25P1D	Nemrut Dag (EA25)	0.079
EA25P1A	Nemrut Dag (EA25)	0.080

Elements: Ti, Al, Fe, Mn, Ca, Zr, Ba

A-Rank: Nemrut Dag (EA25) 10
B-Rank: - -

Specimen	*Location*	*E.D.*
EA25P1A	Nemrut Dag (EA25)	0.055
EA25R1	Nemrut Dag (EA25)	0.058
EA25P1C	Nemrut Dag (EA25)	0.060
EA25P3	Nemrut Dag (EA25)	0.062
EA25P1B	Nemrut Dag (EA25)	0.063
EA25P2C	Nemrut Dag (EA25)	0.066
EA25P2B	Nemrut Dag (EA25)	0.067
EA25P2D	Nemrut Dag (EA25)	0.070
EA25R2	Nemrut Dag (EA25)	0.070
EA25P2A	Nemrut Dag (EA25)	0.071

Table D.1 - Source Assignments of Artifacts based on Euclidean Distance to Centroids of Geological Specimens

Artifact: B1 q350-i f166 k? piece 3

A-Rank: **Nemrut Dag (EA25)** **41**
B-Rank: Nemrut Dag (EA22) 26

Elements: Fe, Ti, Ba

A-Rank:	Nemrut Dag (EA25)	10
B-Rank:	-	-

Specimen	*Location*	*E.D.*
EA25P1C	Nemrut Dag (EA25)	0.007
EA25P1B	Nemrut Dag (EA25)	0.008
EA25P2A	Nemrut Dag (EA25)	0.008
EA25P1A	Nemrut Dag (EA25)	0.009
EA25R2	Nemrut Dag (EA25)	0.010
EA25P2B	Nemrut Dag (EA25)	0.012
EA25P2C	Nemrut Dag (EA25)	0.012
EA25P2D	Nemrut Dag (EA25)	0.014
EA25R1	Nemrut Dag (EA25)	0.014
EA25P1D	Nemrut Dag (EA25)	0.017

Elements: Fe, Zr, Ba

A-Rank:	Nemrut Dag (EA22)	7
B-Rank:	Nemrut Dag (EA21)	3

Specimen	*Location*	*E.D.*
EA22P5A	Nemrut Dag (EA22)	0.062
EA22P4	Nemrut Dag (EA22)	0.067
EA21P1	Nemrut Dag (EA21)	0.068
EA22P7A	Nemrut Dag (EA22)	0.068
EA22P6A	Nemrut Dag (EA22)	0.069
EA21R1A	Nemrut Dag (EA21)	0.070
EA21R1B	Nemrut Dag (EA21)	0.070
EA22P5B	Nemrut Dag (EA22)	0.070
EA22P3	Nemrut Dag (EA22)	0.071
EA22P8B	Nemrut Dag (EA22)	0.072

Elements: Ti, Fe, Zr, Ba

A-Rank:	Nemrut Dag (EA22)	5
B-Rank:	Nemrut Dag (EA25)	4

Specimen	*Location*	*E.D.*
EA25P1D	Nemrut Dag (EA25)	0.078
EA25P1A	Nemrut Dag (EA25)	0.079
EA25P1B	Nemrut Dag (EA25)	0.079
EA22P7A	Nemrut Dag (EA22)	0.082
EA25P1C	Nemrut Dag (EA25)	0.084
EA22P5A	Nemrut Dag (EA22)	0.089
EA22P8B	Nemrut Dag (EA22)	0.089
EA22P6B	Nemrut Dag (EA22)	0.090
EA22P4	Nemrut Dag (EA22)	0.092
EA21R1B	Nemrut Dag (EA21)	0.093

Elements: Ti, Fe, Mn, Ca, Zr, Ba

A-Rank:	Nemrut Dag (EA25)	10
B-Rank:	-	-

Specimen	*Location*	*E.D.*
EA25P1A	Nemrut Dag (EA25)	0.080
EA25P1B	Nemrut Dag (EA25)	0.082
EA25P1C	Nemrut Dag (EA25)	0.084
EA25P1D	Nemrut Dag (EA25)	0.089
EA25R1	Nemrut Dag (EA25)	0.101
EA25P2C	Nemrut Dag (EA25)	0.103
EA25P3	Nemrut Dag (EA25)	0.106
EA25P2D	Nemrut Dag (EA25)	0.108
EA25P2A	Nemrut Dag (EA25)	0.109
EA25P2B	Nemrut Dag (EA25)	0.112

Elements: Fe, Ti, Zr

A-Rank:	Nemrut Dag (EA22)	5
B-Rank:	Nemrut Dag (EA25)	4

Specimen	*Location*	*E.D.*
EA25P1D	Nemrut Dag (EA25)	0.077
EA25P1A	Nemrut Dag (EA25)	0.078
EA25P1B	Nemrut Dag (EA25)	0.079
EA22P7A	Nemrut Dag (EA22)	0.082
EA25P1C	Nemrut Dag (EA25)	0.084
EA22P5A	Nemrut Dag (EA22)	0.089
EA22P8B	Nemrut Dag (EA22)	0.089
EA22P6B	Nemrut Dag (EA22)	0.090
EA22P4	Nemrut Dag (EA22)	0.091
EA21R1B	Nemrut Dag (EA21)	0.093

Elements: Ti, Zr, Ba

A-Rank:	Nemrut Dag (EA22)	5
B-Rank:	Nemrut Dag (EA25)	3

Specimen	*Location*	*E.D.*
EA22P7A	Nemrut Dag (EA22)	0.066
EA22P8B	Nemrut Dag (EA22)	0.075
EA22P5A	Nemrut Dag (EA22)	0.076
EA22R1	Nemrut Dag (EA22)	0.076
EA22P6B	Nemrut Dag (EA22)	0.078
EA25P1D	Nemrut Dag (EA25)	0.078
EA21P1	Nemrut Dag (EA21)	0.079
EA21R1B	Nemrut Dag (EA21)	0.079
EA25P1A	Nemrut Dag (EA25)	0.079
EA25P1B	Nemrut Dag (EA25)	0.079

Elements: Ti, Fe, Zr, Ba, Zn

A-Rank:	Nemrut Dag (EA21)	4
B-Rank:	Nemrut Dag (EA22)	4

Specimen	*Location*	*E.D.*
EA21R1B	Nemrut Dag (EA21)	0.094
EA25R1	Nemrut Dag (EA25)	0.100
EA22P9	Nemrut Dag (EA22)	0.101
EA22P2	Nemrut Dag (EA22)	0.104
EA21P1	Nemrut Dag (EA21)	0.106
EA21P2	Nemrut Dag (EA21)	0.107
EA21R1A	Nemrut Dag (EA21)	0.111
EA22P5A	Nemrut Dag (EA22)	0.111
EA25R2	Nemrut Dag (EA25)	0.113
EA22P4	Nemrut Dag (EA22)	0.115

Elements: Ti, Al, Fe, Mn, Ca, Zr, Ba

A-Rank:	Nemrut Dag (EA25)	10
B-Rank:	-	-

Specimen	*Location*	*E.D.*
EA25P1A	Nemrut Dag (EA25)	0.080
EA25P1B	Nemrut Dag (EA25)	0.082
EA25P1C	Nemrut Dag (EA25)	0.084
EA25P1D	Nemrut Dag (EA25)	0.089
EA25R1	Nemrut Dag (EA25)	0.101
EA25P2C	Nemrut Dag (EA25)	0.103
EA25P3	Nemrut Dag (EA25)	0.106
EA25P2D	Nemrut Dag (EA25)	0.108
EA25P2A	Nemrut Dag (EA25)	0.109
EA25P2B	Nemrut Dag (EA25)	0.112

Table D.1 - Source Assignments of Artifacts based on Euclidean Distance to Centroids of Geological Specimens

Artifact: J1 q276.5 f131 k64

A-Rank: **Nemrut Dag (EA22)** **59**
B-Rank: Nemrut Dag (EA21) 10

Elements: Fe, Ti, Ba

A-Rank:	Nemrut Dag (EA25)	5
B-Rank:	Nemrut Dag (EA22)	5

Specimen	*Location*	*E.D.*
EA25R2	Nemrut Dag (EA25)	0.064
EA25P2C	Nemrut Dag (EA22)	0.068
EA22P7A	Nemrut Dag (EA22)	0.070
EA25P2D	Nemrut Dag (EA25)	0.071
EA22P2	Nemrut Dag (EA22)	0.072
EA25P1C	Nemrut Dag (EA25)	0.072
EA25P2A	Nemrut Dag (EA25)	0.072
EA22P7B	Nemrut Dag (EA22)	0.075
EA22R1	Nemrut Dag (EA22)	0.075
EA25P2B	Nemrut Dag (EA25)	0.076

Elements: Fe, Zr, Ba

A-Rank:	Nemrut Dag (EA22)	5
B-Rank:	Nemrut Dag (EA21)	3

Specimen	*Location*	*E.D.*
EA21P1	Nemrut Dag (EA21)	0.081
EA22P7A	Nemrut Dag (EA22)	0.085
EA22P5A	Nemrut Dag (EA22)	0.087
EA23P1B	Nemrut Dag (EA23)	0.094
EA22P6A	Nemrut Dag (EA22)	0.095
EA22P7B	Nemrut Dag (EA22)	0.095
EA21R1A	Nemrut Dag (EA21)	0.096
EA22R1	Nemrut Dag (EA22)	0.096
EA23P1A	Nemrut Dag (EA23)	0.096
EA21R1B	Nemrut Dag (EA21)	0.097

Elements: Ti, Fe, Zr, Ba

A-Rank:	Nemrut Dag (EA22)	8
B-Rank:	Nemrut Dag (EA21)	2

Specimen	*Location*	*E.D.*
EA22P7A	Nemrut Dag (EA22)	0.091
EA21P1	Nemrut Dag (EA21)	0.095
EA22P5A	Nemrut Dag (EA22)	0.099
EA22R1	Nemrut Dag (EA22)	0.102
EA22P7B	Nemrut Dag (EA22)	0.103
EA22P6B	Nemrut Dag (EA22)	0.104
EA22P8B	Nemrut Dag (EA22)	0.105
EA21R1B	Nemrut Dag (EA21)	0.107
EA22P6A	Nemrut Dag (EA22)	0.107
EA22P3	Nemrut Dag (EA22)	0.108

Elements: Ti, Fe, Mn, Ca, Zr, Ba

A-Rank:	Nemrut Dag (EA22)	8
B-Rank:	Nemrut Dag (EA21)	2

Specimen	*Location*	*E.D.*
EA22P7B	Nemrut Dag (EA22)	0.105
EA21P1	Nemrut Dag (EA21)	0.109
EA22R1	Nemrut Dag (EA22)	0.113
EA22P6B	Nemrut Dag (EA22)	0.116
EA22P6A	Nemrut Dag (EA22)	0.118
EA22P7A	Nemrut Dag (EA22)	0.119
EA22P4	Nemrut Dag (EA22)	0.120
EA22R2	Nemrut Dag (EA22)	0.121
EA21R1B	Nemrut Dag (EA21)	0.122
EA22P1A	Nemrut Dag (EA22)	0.125

Elements: Fe, Ti, Zr

A-Rank:	Nemrut Dag (EA22)	8
B-Rank:	Nemrut Dag (EA21)	2

Specimen	*Location*	*E.D.*
EA22P7A	Nemrut Dag (EA22)	0.068
EA22P5A	Nemrut Dag (EA22)	0.073
EA22P8B	Nemrut Dag (EA22)	0.076
EA21P1	Nemrut Dag (EA21)	0.077
EA21R1B	Nemrut Dag (EA21)	0.077
EA22P3	Nemrut Dag (EA22)	0.079
EA22P6A	Nemrut Dag (EA22)	0.080
EA22P6B	Nemrut Dag (EA22)	0.080
EA22R1	Nemrut Dag (EA22)	0.081
EA22P4	Nemrut Dag (EA22)	0.082

Elements: Ti, Zr, Ba

A-Rank:	Nemrut Dag (EA22)	9
B-Rank:	Nemrut Dag (EA21)	1

Specimen	*Location*	*E.D.*
EA22P7A	Nemrut Dag (EA22)	0.088
EA21P1	Nemrut Dag (EA22)	0.092
EA22P5A	Nemrut Dag (EA22)	0.098
EA22R1	Nemrut Dag (EA22)	0.098
EA22P7B	Nemrut Dag (EA22)	0.101
EA22P6B	Nemrut Dag (EA22)	0.103
EA22P8B	Nemrut Dag (EA22)	0.104
EA22P6A	Nemrut Dag (EA22)	0.105
EA21R1B	Nemrut Dag (EA21)	0.106
EA22P2	Nemrut Dag (EA22)	0.106

Elements: Ti, Fe, Zr, Ba, Zn

A-Rank:	Nemrut Dag (EA22)	9
B-Rank:	Nemrut Dag (EA25)	1

Specimen	*Location*	*E.D.*
EA22P7A	Nemrut Dag (EA22)	0.104
EA22R1	Nemrut Dag (EA22)	0.116
EA22P5B	Nemrut Dag (EA22)	0.122
EA22P3	Nemrut Dag (EA22)	0.135
EA22P1D	Nemrut Dag (EA22)	0.136
EA25P2C	Nemrut Dag (EA25)	0.139
EA22P1C	Nemrut Dag (EA22)	0.146
EA22P7B	Nemrut Dag (EA22)	0.146
EA22P6A	Nemrut Dag (EA22)	0.163
EA22P8B	Nemrut Dag (EA22)	0.163

Elements: Ti, Al, Fe, Mn, Ca, Zr, Ba

A-Rank:	Nemrut Dag (EA22)	7
B-Rank:	Nemrut Dag (EA21)	2

Specimen	*Location*	*E.D.*
EA22P7B	Nemrut Dag (EA22)	0.108
EA21P1	Nemrut Dag (EA21)	0.116
EA22R1	Nemrut Dag (EA22)	0.116
EA22P6B	Nemrut Dag (EA22)	0.119
EA22P6A	Nemrut Dag (EA22)	0.120
EA22P7A	Nemrut Dag (EA22)	0.121
EA22P4	Nemrut Dag (EA22)	0.122
EA22R2	Nemrut Dag (EA22)	0.125
EA25P1C	Nemrut Dag (EA25)	0.126
EA21R1B	Nemrut Dag (EA21)	0.127

Table D.1 - Source Assignments of Artifacts based on Euclidean Distance to Centroids of Geological Specimens

Artifact: J1 q344.1 f151 k106

A-Rank: **Bingol B** **52**
B-Rank: Gutansar 13

Elements: Fe, Ti, Ba

A-Rank:	Bingol B	7
B-Rank:	Gutansar	3

Specimen	*Location*	*E.D.*
EA56B1	Bingol B	0.030
EA52B1	Bingol B	0.049
EA52B3	Bingol B	0.061
EA53B2	Bingol B	0.070
EA52B2	Bingol B	0.073
EA53B1	Bingol B	0.077
EA54B1	Bingol B	0.107
AR06E2A	Gutansar	0.145
AR06E1A	Gutansar	0.146
AR06E2C	Gutansar	0.147

Elements: Fe, Zr, Ba

A-Rank:	Erzincan	7
B-Rank:	Bingol B	3

Specimen	*Location*	*E.D.*
EA56B1	Bingol B	0.071
EA52B3	Bingol B	0.072
EA52B1	Bingol B	0.073
EA43R2	Erzincan	0.075
EA44P3	Erzincan	0.077
EA44P2	Erzincan	0.079
EA43P3	Erzincan	0.080
EA44R1	Erzincan	0.080
EA43P1	Erzincan	0.084
EA44P1	Erzincan	0.084

Elements: Ti, Fe, Zr, Ba

A-Rank:	Bingol B	7
B-Rank:	Gutansar	3

Specimen	*Location*	*E.D.*
EA56B1	Bingol B	0.071
EA52B1	Bingol B	0.079
EA52B3	Bingol B	0.082
EA52B2	Bingol B	0.092
EA53B2	Bingol B	0.092
EA53B1	Bingol B	0.104
EA54B1	Bingol B	0.125
AR06E2A	Gutansar	0.161
AR12jB1	Gutansar	0.162
AR06E2B	Gutansar	0.163

Elements: Ti, Fe, Mn, Ca, Zr, Ba

A-Rank:	Bingol B	7
B-Rank:	Acigol	3

Specimen	*Location*	*E.D.*
EA56B1	Bingol B	0.075
EA52B1	Bingol B	0.080
EA52B3	Bingol B	0.085
EA52B2	Bingol B	0.092
EA53B2	Bingol B	0.092
EA53B1	Bingol B	0.106
EA54B1	Bingol B	0.146
CA08R1A	Acigol	0.197
CA08R1C	Acigol	0.198
CA07R2A	Acigol	0.210

Elements: Fe, Ti, Zr

A-Rank:	Bingol B	7
B-Rank:	Gutansar	2

Specimen	*Location*	*E.D.*
EA56B1	Bingol B	0.070
EA52B1	Bingol B	0.078
EA52B3	Bingol B	0.081
EA53B2	Bingol B	0.084
EA52B2	Bingol B	0.091
EA53B1	Bingol B	0.094
EA54B1	Bingol B	0.125
AR40rlS1	Erevan	0.154
AR76rB3	Gutansar	0.155
AR06E1C	Gutansar	0.156

Elements: Ti, Zr, Ba

A-Rank:	Bingol B	9
B-Rank:	Erevan	1

Specimen	*Location*	*E.D.*
EA55B2	Bingol B	0.064
EA56B1	Bingol B	0.066
EA52B2	Bingol B	0.067
EA52B3	Bingol B	0.067
EA53B2	Bingol B	0.069
EA52B1	Bingol B	0.070
EA54B1	Bingol B	0.071
EA55B1	Bingol B	0.074
EA53B1	Bingol B	0.084
AR24jfL1	Erevan	0.092

Elements: Ti, Fe, Zr, Ba, Zn

A-Rank:	Bingol B	5
B-Rank:	Gutansar	5

Specimen	*Location*	*E.D.*
EA53B1	Bingol B	0.248
AR06E2B	Gutansar	0.284
EA52B1	Bingol B	0.290
AR11jB1	Gutansar	0.291
EA52B3	Bingol B	0.304
AR06E1B	Gutansar	0.315
AR06E1C	Gutansar	0.316
AR12jB1	Gutansar	0.317
EA54B1	Bingol B	0.322
EA52B2	Bingol B	0.323

Elements: Ti, Al, Fe, Mn, Ca, Zr, Ba

A-Rank:	Bingol B	7
B-Rank:	Acigol	3

Specimen	*Location*	*E.D.*
EA56B1	Bingol B	0.083
EA52B1	Bingol B	0.091
EA52B3	Bingol B	0.095
EA53B2	Bingol B	0.095
EA52B2	Bingol B	0.102
EA53B1	Bingol B	0.108
EA54B1	Bingol B	0.151
CA08R1A	Acigol	0.199
CA08R1C	Acigol	0.199
CA07R2A	Acigol	0.210

Table D.1 - Source Assignments of Artifacts based on Euclidean Distance to Centroids of Geological Specimens

Artifact: J1 q45-2 f20 k7

A-Rank:	**Bingol B**	**57**
B-Rank:	Gutansar	10

Elements: Fe, Ti, Ba

A-Rank:	Bingol B	7
B-Rank:	Gutansar	2

Specimen	*Location*	*E.D.*
EA52B1	Bingol B	0.014
EA52B3	Bingol B	0.022
EA56B1	Bingol B	0.035
EA52B2	Bingol B	0.038
EA53B2	Bingol B	0.056
EA53B1	Bingol B	0.063
EA54B1	Bingol B	0.078
AR06E2A	Gutansar	0.111
AR06E1A	Gutansar	0.112
AR21avH1	Chazencavan	0.112

Elements: Fe, Zr, Ba

A-Rank:	Bingol B	7
B-Rank:	Erzincan	3

Specimen	*Location*	*E.D.*
EA52B3	Bingol B	0.027
EA52B1	Bingol B	0.028
EA56B1	Bingol B	0.029
EA52B2	Bingol B	0.041
EA53B2	Bingol B	0.053
EA53B1	Bingol B	0.065
EA54B1	Bingol B	0.082
EA43R2	Erzincan	0.094
EA44P3	Erzincan	0.095
EA44P2	Erzincan	0.096

Elements: Ti, Fe, Zr, Ba

A-Rank:	Bingol B	7
B-Rank:	Gutansar	2

Specimen	*Location*	*E.D.*
EA52B1	Bingol B	0.028
EA52B3	Bingol B	0.028
EA52B2	Bingol B	0.041
EA56B1	Bingol B	0.044
EA53B2	Bingol B	0.060
EA53B1	Bingol B	0.071
EA54B1	Bingol B	0.083
CA07P1	Acigol	0.151
AR06E3A	Gutansar	0.153
AR30jfL1	Gutansar	0.153

Elements: Ti, Fe, Mn, Ca, Zr, Ba

A-Rank:	Bingol B	7
B-Rank:	Acigol	3

Specimen	*Location*	*E.D.*
EA52B1	Bingol B	0.029
EA52B3	Bingol B	0.033
EA52B2	Bingol B	0.044
EA56B1	Bingol B	0.047
EA53B2	Bingol B	0.060
EA53B1	Bingol B	0.072
EA54B1	Bingol B	0.107
CA08R1A	Acigol	0.171
CA08R1C	Acigol	0.173
CA07R2A	Acigol	0.184

Elements: Fe, Ti, Zr

A-Rank:	Bingol B	7
B-Rank:	Gutansar	2

Specimen	*Location*	*E.D.*
EA52B1	Bingol B	0.026
EA52B3	Bingol B	0.026
EA52B2	Bingol B	0.040
EA56B1	Bingol B	0.043
EA53B2	Bingol B	0.049
EA53B1	Bingol B	0.056
EA54B1	Bingol B	0.082
AR76rB3	Gutansar	0.140
EA66W1	Lake Van	0.142
AR76rB2	Gutansar	0.145

Elements: Ti, Zr, Ba

A-Rank:	Bingol B	9
B-Rank:	Erevan	1

Specimen	*Location*	*E.D.*
EA52B3	Bingol B	0.019
EA52B2	Bingol B	0.020
EA52B1	Bingol B	0.026
EA54B1	Bingol B	0.029
EA55B2	Bingol B	0.043
EA56B1	Bingol B	0.044
EA53B2	Bingol B	0.050
EA55B1	Bingol B	0.053
EA53B1	Bingol B	0.062
AR24jfL1	Erevan	0.108

Elements: Ti, Fe, Zr, Ba, Zn

A-Rank:	Bingol B	6
B-Rank:	Gutansar	4

Specimen	*Location*	*E.D.*
EA53B1	Bingol B	0.080
EA52B1	Bingol B	0.095
EA52B3	Bingol B	0.109
EA52B2	Bingol B	0.129
EA54B1	Bingol B	0.137
EA56B1	Bingol B	0.141
AR06E2B	Gutansar	0.161
AR11jB1	Gutansar	0.172
AR12jB1	Gutansar	0.176
AR06E1C	Gutansar	0.178

Elements: Ti, Al, Fe, Mn, Ca, Zr, Ba

A-Rank:	Bingol B	7
B-Rank:	Acigol	3

Specimen	*Location*	*E.D.*
EA52B1	Bingol B	0.037
EA52B3	Bingol B	0.040
EA52B2	Bingol B	0.049
EA56B1	Bingol B	0.050
EA53B2	Bingol B	0.060
EA53B1	Bingol B	0.072
EA54B1	Bingol B	0.108
CA08R1A	Acigol	0.177
CA08R1C	Acigol	0.179
CA07R2A	Acigol	0.187

Table D.1 - Source Assignments of Artifacts based on Euclidean Distance to Centroids of Geological Specimens

Artifact: J1 q64-1 f20 k7

A-Rank: Nemrut Dag (EA24) 55
B-Rank: **Bingol A*** **10**

Elements: Fe, Ti, Ba

A-Rank:	**Bingol A***	**10**
B-Rank:	-	-

Specimen	*Location*	*E.D.*
EA48R1	Bingol A	0.080
EA48P4	Bingol A	0.084
EA48P2C	Bingol A	0.097
EA48P2B	Bingol A	0.099
EA48P1B	Bingol A	0.104
EA48R2A	Bingol A	0.104
EA48P2A	Bingol A	0.106
EA48P5	Bingol A	0.106
EA48R2B	Bingol A	0.106
EA48P1A	Bingol A	0.107

Elements: Fe, Zr, Ba

A-Rank:	Nemrut Dag (EA24)	10
B-Rank:	-	-

Specimen	*Location*	*E.D.*
EA24P1B	Nemrut Dag (EA24)	0.140
EA24P1A	Nemrut Dag (EA24)	0.147
EA24P6A	Nemrut Dag (EA24)	0.148
EA24P1C	Nemrut Dag (EA24)	0.149
EA24P2A	Nemrut Dag (EA24)	0.150
EA24P2B	Nemrut Dag (EA24)	0.150
EA24P5A	Nemrut Dag (EA24)	0.153
EA24P7	Nemrut Dag (EA24)	0.157
EA24P8B	Nemrut Dag (EA24)	0.157
EA24P6B	Nemrut Dag (EA24)	0.159

Elements: Ti, Fe, Zr, Ba

A-Rank:	Nemrut Dag (EA24)	10
B-Rank:	-	-

Specimen	*Location*	*E.D.*
EA24P1B	Nemrut Dag (EA24)	0.140
EA24P1A	Nemrut Dag (EA24)	0.147
EA24P6A	Nemrut Dag (EA24)	0.148
EA24P1C	Nemrut Dag (EA24)	0.149
EA24P2B	Nemrut Dag (EA24)	0.150
EA24P2A	Nemrut Dag (EA24)	0.151
EA24P5A	Nemrut Dag (EA24)	0.153
EA24P7	Nemrut Dag (EA24)	0.157
EA24P8B	Nemrut Dag (EA24)	0.157
EA24P6B	Nemrut Dag (EA24)	0.159

Elements: Ti, Fe, Mn, Ca, Zr, Ba

A-Rank:	Nemrut Dag (EA24)	10
B-Rank:	-	-

Specimen	*Location*	*E.D.*
EA24P1A	Nemrut Dag (EA24)	0.156
EA24P1C	Nemrut Dag (EA24)	0.158
EA24P1B	Nemrut Dag (EA24)	0.163
EA24P2A	Nemrut Dag (EA24)	0.166
EA24P6A	Nemrut Dag (EA24)	0.167
EA24P2B	Nemrut Dag (EA24)	0.168
EA21P1	Nemrut Dag (EA24)	0.170
EA24P8B	Nemrut Dag (EA24)	0.170
EA24P5A	Nemrut Dag (EA24)	0.171
EA24R1	Nemrut Dag (EA24)	0.173

Elements: Fe, Ti, Zr

A-Rank:	Nemrut Dag (EA24)	10
B-Rank:	-	-

Specimen	*Location*	*E.D.*
EA24P1B	Nemrut Dag (EA24)	0.112
EA24P1A	Nemrut Dag (EA24)	0.120
EA24P1C	Nemrut Dag (EA24)	0.120
EA24P2A	Nemrut Dag (EA24)	0.120
EA24P6A	Nemrut Dag (EA24)	0.121
EA24P2B	Nemrut Dag (EA24)	0.124
EA24P6B	Nemrut Dag (EA24)	0.126
EA24P5A	Nemrut Dag (EA24)	0.128
EA24R1	Nemrut Dag (EA24)	0.132
EA24P7	Nemrut Dag (EA24)	0.133

Elements: Ti, Zr, Ba

A-Rank:	Nemrut Dag (EA24)	6
B-Rank:	Nemrut Dag (EA22)	2

Specimen	*Location*	*E.D.*
EA24P1B	Nemrut Dag (EA24)	0.116
EA21P1	Nemrut Dag (EA21)	0.119
EA24P1A	Nemrut Dag (EA24)	0.121
EA24P1C	Nemrut Dag (EA24)	0.125
EA22P5A	Nemrut Dag (EA22)	0.126
EA24P2A	Nemrut Dag (EA24)	0.127
EA24P6A	Nemrut Dag (EA24)	0.128
EA22P7A	Nemrut Dag (EA22)	0.129
EA23P1B	Nemrut Dag (EA23)	0.129
EA24P2B	Nemrut Dag (EA24)	0.129

Elements: Ti, Fe, Zr, Ba, Zn

A-Rank:	Nemrut Dag (EA22)	7
B-Rank:	Nemrut Dag (EA24)	3

Specimen	*Location*	*E.D.*
EA22P7A	Nemrut Dag (EA22)	0.233
EA22P5B	Nemrut Dag (EA22)	0.238
EA22R1	Nemrut Dag (EA22)	0.238
EA22P1D	Nemrut Dag (EA22)	0.254
EA24P2A	Nemrut Dag (EA24)	0.258
EA22P3	Nemrut Dag (EA22)	0.259
EA24P5A	Nemrut Dag (EA24)	0.264
EA22P1C	Nemrut Dag (EA22)	0.271
EA24P6B	Nemrut Dag (EA24)	0.273
EA22P7B	Nemrut Dag (EA22)	0.274

Elements: Ti, Al, Fe, Mn, Ca, Zr, Ba

A-Rank:	Nemrut Dag (EA24)	6
B-Rank:	Nemrut Dag (EA21)	2

Specimen	*Location*	*E.D.*
EA24P1A	Nemrut Dag (EA24)	0.183
EA24P1C	Nemrut Dag (EA24)	0.188
EA24R1	Nemrut Dag (EA24)	0.188
EA21R1A	Nemrut Dag (EA21)	0.192
EA24P1B	Nemrut Dag (EA24)	0.192
EA24P2A	Nemrut Dag (EA24)	0.192
EA21P1	Nemrut Dag (EA21)	0.193
EA22P7A	Nemrut Dag (EA24)	0.193
EA22P5A	Nemrut Dag (EA22)	0.194
EA24P6A	Nemrut Dag (EA24)	0.194

* "Bingol A" is the correct source based on the CNK/A vs. NK/A peralkalinity plot and scatterplots of critical elements identified by Poidevin (1998): Al, Fe, and Ba plus Ti.

Table D.1 - Source Assignments of Artifacts based on Euclidean Distance to Centroids of Geological Specimens

Artifact: J1 q7-1 f3 k10 piece 1

A-Rank: **Nemrut Dag (EA25)** **74**
B-Rank: Nemrut Dag (EA22) 6

Elements: Fe, Ti, Ba

A-Rank:	Nemrut Dag (EA25)	10
B-Rank:	-	-

Specimen	*Location*	*E.D.*
EA25R2	Nemrut Dag (EA25)	0.011
EA25P1C	Nemrut Dag (EA25)	0.013
EA25P2C	Nemrut Dag (EA25)	0.013
EA25P2A	Nemrut Dag (EA25)	0.016
EA25P2D	Nemrut Dag (EA25)	0.016
EA25P1B	Nemrut Dag (EA25)	0.017
EA25P2B	Nemrut Dag (EA25)	0.017
EA25P1A	Nemrut Dag (EA25)	0.019
EA25P1D	Nemrut Dag (EA25)	0.022
EA25R1	Nemrut Dag (EA25)	0.023

Elements: Fe, Zr, Ba

A-Rank:	Nemrut Dag (EA25)	10
B-Rank:	-	-

Specimen	*Location*	*E.D.*
EA25P2C	Nemrut Dag (EA25)	0.009
EA25P1C	Nemrut Dag (EA25)	0.010
EA25P2D	Nemrut Dag (EA25)	0.013
EA25P1B	Nemrut Dag (EA25)	0.018
EA25P1A	Nemrut Dag (EA25)	0.019
EA25P2A	Nemrut Dag (EA25)	0.020
EA25P1D	Nemrut Dag (EA25)	0.021
EA25P2B	Nemrut Dag (EA25)	0.022
EA25R1	Nemrut Dag (EA25)	0.023
EA25R2	Nemrut Dag (EA25)	0.025

Elements: Ti, Fe, Zr, Ba

A-Rank:	Nemrut Dag (EA25)	10
B-Rank:	-	-

Specimen	*Location*	*E.D.*
EA25P1C	Nemrut Dag (EA25)	0.014
EA25P2C	Nemrut Dag (EA25)	0.016
EA25P1B	Nemrut Dag (EA25)	0.020
EA25P2D	Nemrut Dag (EA25)	0.021
EA25P1A	Nemrut Dag (EA25)	0.022
EA25P2A	Nemrut Dag (EA25)	0.023
EA25R1	Nemrut Dag (EA25)	0.024
EA25R2	Nemrut Dag (EA25)	0.025
EA25P1D	Nemrut Dag (EA25)	0.026
EA25P2B	Nemrut Dag (EA25)	0.026

Elements: Ti, Fe, Mn, Ca, Zr, Ba

A-Rank:	Nemrut Dag (EA25)	10
B-Rank:	-	-

Specimen	*Location*	*E.D.*
EA25P1C	Nemrut Dag (EA25)	0.019
EA25P1A	Nemrut Dag (EA25)	0.022
EA25P1B	Nemrut Dag (EA25)	0.025
EA25P2C	Nemrut Dag (EA25)	0.025
EA25P2A	Nemrut Dag (EA25)	0.029
EA25P2B	Nemrut Dag (EA25)	0.030
EA25R1	Nemrut Dag (EA25)	0.031
EA25P2D	Nemrut Dag (EA25)	0.033
EA25P3	Nemrut Dag (EA25)	0.033
EA25R2	Nemrut Dag (EA25)	0.038

Elements: Fe, Ti, Zr

A-Rank:	Nemrut Dag (EA25)	10
B-Rank:	-	-

Specimen	*Location*	*E.D.*
EA25P1C	Nemrut Dag (EA25)	0.014
EA25R1	Nemrut Dag (EA25)	0.014
EA25P1B	Nemrut Dag (EA25)	0.015
EA25P3	Nemrut Dag (EA25)	0.015
EA25P2C	Nemrut Dag (EA25)	0.016
EA25P1A	Nemrut Dag (EA25)	0.018
EA25P1D	Nemrut Dag (EA25)	0.020
EA25P2D	Nemrut Dag (EA25)	0.020
EA25P2A	Nemrut Dag (EA25)	0.023
EA25P2B	Nemrut Dag (EA25)	0.025

Elements: Ti, Zr, Ba

A-Rank:	Nemrut Dag (EA25)	10
B-Rank:	-	-

Specimen	*Location*	*E.D.*
EA25P1C	Nemrut Dag (EA25)	0.013
EA25P2C	Nemrut Dag (EA25)	0.016
EA25P1B	Nemrut Dag (EA25)	0.018
EA25P1A	Nemrut Dag (EA25)	0.019
EA25P2A	Nemrut Dag (EA25)	0.019
EA25P2D	Nemrut Dag (EA25)	0.020
EA25R1	Nemrut Dag (EA25)	0.022
EA25R2	Nemrut Dag (EA25)	0.023
EA25P1D	Nemrut Dag (EA25)	0.026
EA25P2B	Nemrut Dag (EA25)	0.026

Elements: Ti, Fe, Zr, Ba, Zn

A-Rank:	Nemrut Dag (EA22)	6
B-Rank:	Nemrut Dag (EA25)	4

Specimen	*Location*	*E.D.*
EA25P2C	Nemrut Dag (EA25)	0.017
EA22P1D	Nemrut Dag (EA22)	0.069
EA25P1A	Nemrut Dag (EA25)	0.070
EA25P1D	Nemrut Dag (EA25)	0.071
EA22P7A	Nemrut Dag (EA22)	0.073
EA22R1	Nemrut Dag (EA22)	0.073
EA25P1B	Nemrut Dag (EA25)	0.073
EA22P1C	Nemrut Dag (EA22)	0.082
EA22P3	Nemrut Dag (EA22)	0.084
EA22P7B	Nemrut Dag (EA22)	0.085

Elements: Ti, Al, Fe, Mn, Ca, Zr, Ba

A-Rank:	Nemrut Dag (EA25)	10
B-Rank:	-	-

Specimen	*Location*	*E.D.*
EA25P1A	Nemrut Dag (EA25)	0.063
EA25R1	Nemrut Dag (EA25)	0.064
EA25P1C	Nemrut Dag (EA25)	0.067
EA25R2	Nemrut Dag (EA25)	0.067
EA25P3	Nemrut Dag (EA25)	0.068
EA25P1B	Nemrut Dag (EA25)	0.070
EA25P2C	Nemrut Dag (EA25)	0.070
EA25P2B	Nemrut Dag (EA25)	0.071
EA25P2A	Nemrut Dag (EA25)	0.074
EA25P2D	Nemrut Dag (EA25)	0.074

Table D.1 - Source Assignments of Artifacts based on Euclidean Distance to Centroids of Geological Specimens

Artifact: J1 q7-1 f3 k10 piece 2

A-Rank: **Meydan Dag** **54**
B-Rank: Mus 9

Elements: Fe, Ti, Ba

A-Rank: Meydan Dag 9
B-Rank: Pasinler 1

Specimen	*Location*	*E.D.*
EA69SX2	Meydan Dag	0.009
EA07P1	Meydan Dag	0.012
EA11R2	Meydan Dag	0.017
EA08R1	Meydan Dag	0.018
EA11P1	Meydan Dag	0.019
EA11R1	Meydan Dag	0.019
EA69SX1	Meydan Dag	0.020
EA10R2	Meydan Dag	0.021
EA07R3	Meydan Dag	0.022
EA33P8	Pasinler	0.024

Elements: Fe, Zr, Ba

A-Rank: Meydan Dag 10
B-Rank: - -

Specimen	*Location*	*E.D.*
EA10R2	Meydan Dag	0.016
EA69SX2	Meydan Dag	0.018
EA10P4	Meydan Dag	0.024
EA08R1	Meydan Dag	0.026
EA07R3	Meydan Dag	0.027
EA11R1	Meydan Dag	0.027
EA69SX1	Meydan Dag	0.027
EA11R2	Meydan Dag	0.028
EA07P1	Meydan Dag	0.032
EA10R1B	Meydan Dag	0.032

Elements: Ti, Fe, Zr, Ba

A-Rank: Meydan Dag 10
B-Rank: - -

Specimen	*Location*	*E.D.*
EA69SX2	Meydan Dag	0.018
EA10R2	Meydan Dag	0.022
EA07R3	Meydan Dag	0.027
EA08R1	Meydan Dag	0.027
EA11R1	Meydan Dag	0.028
EA10P4	Meydan Dag	0.029
EA11R2	Meydan Dag	0.031
EA69SX1	Meydan Dag	0.031
EA07P1	Meydan Dag	0.032
EA10R1B	Meydan Dag	0.032

Elements: Ti, Fe, Mn, Ca, Zr, Ba

A-Rank: Meydan Dag 9
B-Rank: Kars-Arpacay 1

Specimen	*Location*	*E.D.*
EA69SX2	Meydan Dag	0.027
EA10R2	Meydan Dag	0.030
EA07R3	Meydan Dag	0.031
EA08R1	Meydan Dag	0.031
EA69SX1	Meydan Dag	0.032
EA10R1B	Meydan Dag	0.033
EA11R2	Meydan Dag	0.033
EA11R1	Meydan Dag	0.034
EA07P1	Meydan Dag	0.035
EA39P5	Kars-Arpacay	0.037

Elements: Fe, Ti, Zr

A-Rank: Meydan Dag 6
B-Rank: Kars-Arpacay 2

Specimen	*Location*	*E.D.*
EA39P1A	Kars-Arpacay	0.012
EA07R3	Meydan Dag	0.016
EA69SX2	Meydan Dag	0.016
EA39P2B	Kars-Arpacay	0.017
EA50R1A	Bingol	0.017
EA10R1B	Meydan Dag	0.020
EA10R2	Meydan Dag	0.020
EA50P6	Bingol	0.021
EA08R1	Meydan Dag	0.022
EA11R1	Meydan Dag	0.022

Elements: Ti, Zr, Ba

A-Rank: Meydan Dag 4
B-Rank: Tendurek Dag 3

Specimen	*Location*	*E.D.*
EA39R2	Kars-Arpacay	0.003
EA39P5	Kars-Arpacay	0.005
EA10R2	Meydan Dag	0.018
EA68SX1	Meydan Dag	0.018
EA69SX2	Meydan Dag	0.018
EA09R1	Tendurek Dag	0.022
EA39P3	Kars-Arpacay	0.022
EA09R2A	Tendurek Dag	0.023
EA09R3B	Tendurek Dag	0.025
EA08R1	Meydan Dag	0.026

Elements: Ti, Fe, Zr, Ba, Zn

A-Rank: Mus 9
B-Rank: Tendurek Dag 1

Specimen	*Location*	*E.D.*
EA62Y1A	Mus	0.195
EA60B1B	Mus	0.202
EA60B1A	Mus	0.220
EA62Y3B	Mus	0.223
EA09P1C	Tendurek Dag	0.230
EA62Y4	Mus	0.231
EA57B1	Mus	0.233
EA58B1	Mus	0.236
EA62Y1C	Mus	0.245
EA62Y1B	Mus	0.248

Elements: Ti, Al, Fe, Mn, Ca, Zr, Ba

A-Rank: Kars-Arpacay 5
B-Rank: Meydan Dag 5

Specimen	*Location*	*E.D.*
EA69SX2	Meydan Dag	0.050
EA39P5	Kars-Arpacay	0.055
EA39P3	Kars-Arpacay	0.056
EA39P4	Kars-Arpacay	0.061
EA39R1	Kars-Arpacay	0.061
EA11R2	Meydan Dag	0.063
EA08R1	Meydan Dag	0.065
EA10R2	Meydan Dag	0.065
EA10P2	Meydan Dag	0.066
EA39P1B	Kars-Arpacay	0.067

Table D.1 - Source Assignments of Artifacts based on Euclidean Distance to Centroids of Geological Specimens

Artifact: J2 q142-1 f62 k83

A-Rank: **Nemrut Dag (EA25)** **71**
B-Rank: Nemrut Dag (EA22) 9

Elements: Fe, Ti, Ba

A-Rank:	Nemrut Dag (EA25)	10
B-Rank:	-	-

Specimen	*Location*	*E.D.*
EA25P3	Nemrut Dag (EA25)	0.016
EA25R1	Nemrut Dag (EA25)	0.017
EA25P1A	Nemrut Dag (EA25)	0.023
EA25P1B	Nemrut Dag (EA25)	0.024
EA25P1D	Nemrut Dag (EA25)	0.026
EA25P2B	Nemrut Dag (EA25)	0.029
EA25P1C	Nemrut Dag (EA25)	0.031
EA25P2A	Nemrut Dag (EA25)	0.032
EA25P2D	Nemrut Dag (EA25)	0.035
EA25P2C	Nemrut Dag (EA25)	0.037

Elements: Fe, Zr, Ba

A-Rank:	Nemrut Dag (EA25)	8
B-Rank:	Nemrut Dag (EA22)	2

Specimen	*Location*	*E.D.*
EA25P1A	Nemrut Dag (EA25)	0.034
EA25P1B	Nemrut Dag (EA25)	0.035
EA25P1D	Nemrut Dag (EA25)	0.035
EA25P1C	Nemrut Dag (EA25)	0.044
EA25R1	Nemrut Dag (EA25)	0.046
EA22P4	Nemrut Dag (EA22)	0.048
EA25P3	Nemrut Dag (EA25)	0.051
EA25P2C	Nemrut Dag (EA25)	0.058
EA22P5B	Nemrut Dag (EA22)	0.060
EA22P8A	Nemrut Dag (EA22)	0.060

Elements: Ti, Fe, Zr, Ba

A-Rank:	Nemrut Dag (EA25)	10
B-Rank:	-	-

Specimen	*Location*	*E.D.*
EA25P1A	Nemrut Dag (EA25)	0.034
EA25P1B	Nemrut Dag (EA25)	0.035
EA25P1D	Nemrut Dag (EA25)	0.035
EA25P1C	Nemrut Dag (EA25)	0.044
EA25R1	Nemrut Dag (EA25)	0.046
EA25P3	Nemrut Dag (EA25)	0.051
EA25P2C	Nemrut Dag (EA25)	0.058
EA25P2D	Nemrut Dag (EA25)	0.060
EA25P2A	Nemrut Dag (EA25)	0.061
EA25P2B	Nemrut Dag (EA25)	0.063

Elements: Ti, Fe, Mn, Ca, Zr, Ba

A-Rank:	Nemrut Dag (EA25)	10
B-Rank:	-	-

Specimen	*Location*	*E.D.*
EA25P1A	Nemrut Dag (EA25)	0.035
EA25P1B	Nemrut Dag (EA25)	0.036
EA25P1D	Nemrut Dag (EA25)	0.043
EA25R1	Nemrut Dag (EA25)	0.047
EA25P1C	Nemrut Dag (EA25)	0.049
EA25P3	Nemrut Dag (EA25)	0.051
EA25P2C	Nemrut Dag (EA25)	0.059
EA25P2A	Nemrut Dag (EA25)	0.062
EA25P2D	Nemrut Dag (EA25)	0.062
EA25P2B	Nemrut Dag (EA25)	0.064

Elements: Fe, Ti, Zr

A-Rank:	Nemrut Dag (EA25)	10
B-Rank:	-	-

Specimen	*Location*	*E.D.*
EA25P1A	Nemrut Dag (EA25)	0.027
EA25P1B	Nemrut Dag (EA25)	0.028
EA25P1D	Nemrut Dag (EA25)	0.030
EA25P1C	Nemrut Dag (EA25)	0.034
EA25R1	Nemrut Dag (EA25)	0.045
EA25P2C	Nemrut Dag (EA25)	0.049
EA25P3	Nemrut Dag (EA25)	0.050
EA25P2D	Nemrut Dag (EA25)	0.052
EA25P2A	Nemrut Dag (EA25)	0.053
EA25P2B	Nemrut Dag (EA25)	0.059

Elements: Ti, Zr, Ba

A-Rank:	Nemrut Dag (EA25)	8
B-Rank:	Nemrut Dag (EA22)	2

Specimen	*Location*	*E.D.*
EA25P1D	Nemrut Dag (EA25)	0.029
EA25P1A	Nemrut Dag (EA25)	0.032
EA25P1B	Nemrut Dag (EA25)	0.033
EA25P1C	Nemrut Dag (EA25)	0.041
EA25R1	Nemrut Dag (EA25)	0.045
EA25P3	Nemrut Dag (EA25)	0.049
EA25P2C	Nemrut Dag (EA25)	0.055
EA25P2D	Nemrut Dag (EA25)	0.057
EA22P7A	Nemrut Dag (EA22)	0.060
EA22P8B	Nemrut Dag (EA22)	0.060

Elements: Ti, Fe, Zr, Ba, Zn

A-Rank:	Nemrut Dag (EA25)	5
B-Rank:	Nemrut Dag (EA22)	5

Specimen	*Location*	*E.D.*
EA25P2C	Nemrut Dag (EA25)	0.060
EA25P1A	Nemrut Dag (EA25)	0.066
EA25P1D	Nemrut Dag (EA25)	0.066
EA25P1B	Nemrut Dag (EA25)	0.070
EA22P7A	Nemrut Dag (EA22)	0.088
EA22P3	Nemrut Dag (EA22)	0.093
EA22R1	Nemrut Dag (EA22)	0.093
EA22P1D	Nemrut Dag (EA22)	0.096
EA25P2D	Nemrut Dag (EA25)	0.097
EA22P7B	Nemrut Dag (EA22)	0.098

Elements: Ti, Al, Fe, Mn, Ca, Zr, Ba

A-Rank:	Nemrut Dag (EA25)	10
B-Rank:	-	-

Specimen	*Location*	*E.D.*
EA25P1A	Nemrut Dag (EA25)	0.051
EA25P1B	Nemrut Dag (EA25)	0.056
EA25R1	Nemrut Dag (EA25)	0.058
EA25P1D	Nemrut Dag (EA25)	0.063
EA25P3	Nemrut Dag (EA25)	0.063
EA25P1C	Nemrut Dag (EA25)	0.065
EA25P2C	Nemrut Dag (EA25)	0.073
EA25P2A	Nemrut Dag (EA25)	0.076
EA25P2B	Nemrut Dag (EA25)	0.076
EA25P2D	Nemrut Dag (EA25)	0.076

Table D.1 - Source Assignments of Artifacts based on Euclidean Distance to Centroids of Geological Specimens

Artifact: J2 q58-1 f1 k100

A-Rank: **Pasinler** **51**
B-Rank: **Mus** **16**

Elements: Fe, Ti, Ba

A-Rank:	Meydan Dag	9
B-Rank:	Bingol	1

Specimen	*Location*	*E.D.*
EA10P4	Meydan Dag	0.006
EA07R2	Meydan Dag	0.009
EA10R2	Meydan Dag	0.011
EA10R1A	Meydan Dag	0.012
EA10P2	Meydan Dag	0.016
EA49R1	Bingol	0.018
EA07R1	Meydan Dag	0.019
EA10P1	Meydan Dag	0.019
EA10P3	Meydan Dag	0.019
EA11P1	Meydan Dag	0.019

Elements: Fe, Zr, Ba

A-Rank:	Pasinler	10
B-Rank:	-	-

Specimen	*Location*	*E.D.*
EA33P8	Pasinler	0.006
EA35P3	Pasinler	0.021
EA33P3	Pasinler	0.026
EA34P3	Pasinler	0.026
EA35P2	Pasinler	0.026
EA34R2	Pasinler	0.029
EA33P7	Pasinler	0.031
EA34P1	Pasinler	0.034
EA33P5	Pasinler	0.036
EA33P6	Pasinler	0.037

Elements: Ti, Fe, Zr, Ba

A-Rank:	Pasinler	10
B-Rank:	-	-

Specimen	*Location*	*E.D.*
EA33P8	Pasinler	0.030
EA35P2	Pasinler	0.032
EA33P7	Pasinler	0.034
EA34P3	Pasinler	0.034
EA33P3	Pasinler	0.035
EA35P3	Pasinler	0.035
EA34R2	Pasinler	0.039
EA33P5	Pasinler	0.042
EA34P1	Pasinler	0.042
EA35P1	Pasinler	0.044

Elements: Ti, Fe, Mn, Ca, Zr, Ba

A-Rank:	Pasinler	9
B-Rank:	Mus	1

Specimen	*Location*	*E.D.*
EA33P8	Pasinler	0.051
EA34P3	Pasinler	0.051
EA35P2	Pasinler	0.054
EA34P1	Pasinler	0.059
EA35P3	Pasinler	0.059
EA33P5	Pasinler	0.063
EA33P7	Pasinler	0.063
EA34P2	Pasinler	0.069
EA60B1A	Mus	0.069
EA35P1	Pasinler	0.070

Elements: Fe, Ti, Zr

A-Rank:	Pasinler	10
B-Rank:	-	-

Specimen	*Location*	*E.D.*
EA33P7	Pasinler	0.017
EA34R1	Pasinler	0.020
EA33P1A	Pasinler	0.021
EA33P1B	Pasinler	0.021
EA35P2	Pasinler	0.021
EA34P3	Pasinler	0.022
EA33P2A	Pasinler	0.023
EA34P2	Pasinler	0.023
EA33P3	Pasinler	0.024
EA33P5	Pasinler	0.024

Elements: Ti, Zr, Ba

A-Rank:	Pasinler	10
B-Rank:	-	-

Specimen	*Location*	*E.D.*
EA33P8	Pasinler	0.030
EA35P2	Pasinler	0.032
EA33P7	Pasinler	0.034
EA34P3	Pasinler	0.034
EA35P3	Pasinler	0.034
EA33P3	Pasinler	0.035
EA34R2	Pasinler	0.039
EA33P5	Pasinler	0.041
EA34P1	Pasinler	0.042
EA35P1	Pasinler	0.044

Elements: Ti, Fe, Zr, Ba, Zn

A-Rank:	Mus	8
B-Rank:	Tendurek Dag	1

Specimen	*Location*	*E.D.*
EA60B1A	Mus	0.064
EA60B1B	Mus	0.066
EA62Y3B	Mus	0.068
EA62Y1A	Mus	0.078
EA62Y4	Mus	0.080
EA62Y1B	Mus	0.082
EA62Y1C	Mus	0.083
EA09P1C	Tendurek Dag	0.086
EA10P3	Meydan Dag	0.089
EA58B1	Mus	0.092

Elements: Ti, Al, Fe, Mn, Ca, Zr, Ba

A-Rank:	Mus	8
B-Rank:	Pasinler	2

Specimen	*Location*	*E.D.*
EA60B1A	Mus	0.072
EA62Y1B	Mus	0.075
EA62Y2B	Mus	0.076
EA34P3	Pasinler	0.077
EA35P2	Pasinler	0.077
EA62Y1A	Mus	0.078
EA62Y1C	Mus	0.078
EA62Y3B	Mus	0.078
EA62Y1D	Mus	0.079
EA62Y4	Mus	0.079

Table D.1 - Source Assignments of Artifacts based on Euclidean Distance to Centroids of Geological Specimens

Artifact: J2 q87-1 f42 k33

A-Rank: **Nemrut Dag (EA25)** **67**
B-Rank: Nemrut Dag (EA22) 13

Elements: Fe, Ti, Ba

A-Rank:	Nemrut Dag (EA25)	10
B-Rank:	-	-

Specimen	*Location*	*E.D.*
EA25P3	Nemrut Dag (EA25)	0.013
EA25R1	Nemrut Dag (EA25)	0.018
EA25P1A	Nemrut Dag (EA25)	0.026
EA25P1B	Nemrut Dag (EA25)	0.026
EA25P1D	Nemrut Dag (EA25)	0.026
EA25P2B	Nemrut Dag (EA25)	0.030
EA25P1C	Nemrut Dag (EA25)	0.034
EA25P2A	Nemrut Dag (EA25)	0.037
EA25P2D	Nemrut Dag (EA25)	0.037
EA25P2C	Nemrut Dag (EA25)	0.038

Elements: Fe, Zr, Ba

A-Rank:	Nemrut Dag (EA25)	6
B-Rank:	Nemrut Dag (EA22)	4

Specimen	*Location*	*E.D.*
EA25P1D	Nemrut Dag (EA25)	0.031
EA25P1A	Nemrut Dag (EA25)	0.034
EA25P1B	Nemrut Dag (EA25)	0.034
EA22P4	Nemrut Dag (EA22)	0.039
EA25P1C	Nemrut Dag (EA25)	0.043
EA25R1	Nemrut Dag (EA25)	0.044
EA25P3	Nemrut Dag (EA25)	0.047
EA22P5B	Nemrut Dag (EA22)	0.051
EA22P8A	Nemrut Dag (EA22)	0.051
EA22P8B	Nemrut Dag (EA22)	0.052

Elements: Ti, Fe, Zr, Ba

A-Rank:	Nemrut Dag (EA25)	10
B-Rank:	-	-

Specimen	*Location*	*E.D.*
EA25P1D	Nemrut Dag (EA25)	0.033
EA25P1B	Nemrut Dag (EA25)	0.034
EA25P1A	Nemrut Dag (EA25)	0.035
EA25P1C	Nemrut Dag (EA25)	0.044
EA25R1	Nemrut Dag (EA25)	0.044
EA25P3	Nemrut Dag (EA25)	0.047
EA25P2C	Nemrut Dag (EA25)	0.057
EA25P2D	Nemrut Dag (EA25)	0.059
EA25P2A	Nemrut Dag (EA25)	0.061
EA25P2B	Nemrut Dag (EA25)	0.061

Elements: Ti, Fe, Mn, Ca, Zr, Ba

A-Rank:	Nemrut Dag (EA25)	10
B-Rank:	-	-

Specimen	*Location*	*E.D.*
EA25P1A	Nemrut Dag (EA25)	0.035
EA25P1B	Nemrut Dag (EA25)	0.038
EA25P1C	Nemrut Dag (EA25)	0.045
EA25P1D	Nemrut Dag (EA25)	0.049
EA25R1	Nemrut Dag (EA25)	0.049
EA25P3	Nemrut Dag (EA25)	0.050
EA25P2C	Nemrut Dag (EA25)	0.060
EA25P2B	Nemrut Dag (EA25)	0.063
EA25P2A	Nemrut Dag (EA25)	0.064
EA25P2D	Nemrut Dag (EA25)	0.065

Elements: Fe, Ti, Zr

A-Rank:	Nemrut Dag (EA25)	10
B-Rank:	-	-

Specimen	*Location*	*E.D.*
EA25P1A	Nemrut Dag (EA25)	0.023
EA25P1B	Nemrut Dag (EA25)	0.023
EA25P1D	Nemrut Dag (EA25)	0.024
EA25P1C	Nemrut Dag (EA25)	0.029
EA25R1	Nemrut Dag (EA25)	0.041
EA25P2C	Nemrut Dag (EA25)	0.044
EA25P3	Nemrut Dag (EA25)	0.045
EA25P2D	Nemrut Dag (EA25)	0.048
EA25P2A	Nemrut Dag (EA25)	0.050
EA25P2B	Nemrut Dag (EA25)	0.055

Elements: Ti, Zr, Ba

A-Rank:	Nemrut Dag (EA25)	7
B-Rank:	Nemrut Dag (EA22)	3

Specimen	*Location*	*E.D.*
EA25P1D	Nemrut Dag (EA25)	0.032
EA25P1A	Nemrut Dag (EA25)	0.034
EA25P1B	Nemrut Dag (EA25)	0.034
EA25P1C	Nemrut Dag (EA25)	0.044
EA25R1	Nemrut Dag (EA25)	0.044
EA25P3	Nemrut Dag (EA25)	0.047
EA22P8B	Nemrut Dag (EA22)	0.056
EA25P2C	Nemrut Dag (EA25)	0.056
EA22P6B	Nemrut Dag (EA22)	0.058
EA22P7A	Nemrut Dag (EA22)	0.058

Elements: Ti, Fe, Zr, Ba, Zn

A-Rank:	Nemrut Dag (EA22)	6
B-Rank:	Nemrut Dag (EA25)	4

Specimen	*Location*	*E.D.*
EA25P2C	Nemrut Dag (EA25)	0.057
EA25P1D	Nemrut Dag (EA25)	0.074
EA25P1A	Nemrut Dag (EA25)	0.075
EA22P7A	Nemrut Dag (EA22)	0.077
EA25P1B	Nemrut Dag (EA25)	0.078
EA22R1	Nemrut Dag (EA22)	0.081
EA22P3	Nemrut Dag (EA22)	0.084
EA22P1D	Nemrut Dag (EA22)	0.085
EA22P5B	Nemrut Dag (EA22)	0.087
EA22P1C	Nemrut Dag (EA22)	0.093

Elements: Ti, Al, Fe, Mn, Ca, Zr, Ba

A-Rank:	Nemrut Dag (EA25)	10
B-Rank:	-	-

Specimen	*Location*	*E.D.*
EA25P1A	Nemrut Dag (EA25)	0.038
EA25P1B	Nemrut Dag (EA25)	0.043
EA25P1C	Nemrut Dag (EA25)	0.049
EA25R1	Nemrut Dag (EA25)	0.050
EA25P3	Nemrut Dag (EA25)	0.052
EA25P1D	Nemrut Dag (EA25)	0.054
EA25P2C	Nemrut Dag (EA25)	0.063
EA25P2B	Nemrut Dag (EA25)	0.066
EA25P2A	Nemrut Dag (EA25)	0.068
EA25P2D	Nemrut Dag (EA25)	0.068

Table D.1 - Source Assignments of Artifacts based on Euclidean Distance to Centroids of Geological Specimens

Artifact: J2 q99-1 f42 k33

A-Rank: Nemrut Dag (EA24) 54
B-Rank: **Bingol A*** **13**

Elements: Fe, Ti, Ba

A-Rank: **Bingol A*** **10**
B-Rank: - -

Specimen	*Location*	*E.D.*
EA48P5	Bingol A	0.039
EA48P2C	Bingol A	0.047
EA48R2A	Bingol A	0.047
EA48P3	Bingol A	0.050
EA48P2B	Bingol A	0.051
EA48P4	Bingol A	0.051
EA48P1B	Bingol A	0.052
EA48R2B	Bingol A	0.052
EA48P1A	Bingol A	0.053
EA48P2A	Bingol A	0.053

Elements: Fe, Zr, Ba

A-Rank: Nemrut Dag (EA24) 10
B-Rank: - -

Specimen	*Location*	*E.D.*
EA24P1B	Nemrut Dag (EA24)	0.096
EA24P1C	Nemrut Dag (EA24)	0.102
EA24P2A	Nemrut Dag (EA24)	0.102
EA24P6A	Nemrut Dag (EA24)	0.102
EA24P1A	Nemrut Dag (EA24)	0.103
EA24P2B	Nemrut Dag (EA24)	0.105
EA24P6B	Nemrut Dag (EA24)	0.106
EA24P5A	Nemrut Dag (EA24)	0.108
EA24P8A	Nemrut Dag (EA24)	0.112
EA24R1	Nemrut Dag (EA24)	0.113

Elements: Ti, Fe, Zr, Ba

A-Rank: Nemrut Dag (EA24) 10
B-Rank: - -

Specimen	*Location*	*E.D.*
EA24P1B	Nemrut Dag (EA24)	0.097
EA24P1C	Nemrut Dag (EA24)	0.103
EA24P6A	Nemrut Dag (EA24)	0.103
EA24P2A	Nemrut Dag (EA24)	0.104
EA24P1A	Nemrut Dag (EA24)	0.105
EA24P2B	Nemrut Dag (EA24)	0.107
EA24P6B	Nemrut Dag (EA24)	0.107
EA24P5A	Nemrut Dag (EA24)	0.109
EA24P8A	Nemrut Dag (EA24)	0.114
EA24P3	Nemrut Dag (EA24)	0.116

Elements: Ti, Fe, Mn, Ca, Zr, Ba

A-Rank: Nemrut Dag (EA24) 9
B-Rank: Nemrut Dag (EA21) 1

Specimen	*Location*	*E.D.*
EA24P1A	Nemrut Dag (EA24)	0.120
EA24P1C	Nemrut Dag (EA24)	0.120
EA24P2A	Nemrut Dag (EA24)	0.128
EA24P8A	Nemrut Dag (EA24)	0.129
EA24P1B	Nemrut Dag (EA24)	0.132
EA24P6A	Nemrut Dag (EA24)	0.133
EA24P2B	Nemrut Dag (EA24)	0.135
EA24R1	Nemrut Dag (EA24)	0.135
EA21R1A	Nemrut Dag (EA21)	0.136
EA24P5A	Nemrut Dag (EA24)	0.137

Elements: Fe, Ti, Zr

A-Rank: Nemrut Dag (EA24) 10
B-Rank: - -

Specimen	*Location*	*E.D.*
EA24P1B	Nemrut Dag (EA24)	0.096
EA24P6A	Nemrut Dag (EA24)	0.102
EA24P1C	Nemrut Dag (EA24)	0.103
EA24P1A	Nemrut Dag (EA24)	0.104
EA24P2A	Nemrut Dag (EA24)	0.104
EA24P2B	Nemrut Dag (EA24)	0.106
EA24P6B	Nemrut Dag (EA24)	0.107
EA24P5A	Nemrut Dag (EA24)	0.108
EA24P7	Nemrut Dag (EA24)	0.114
EA24P8A	Nemrut Dag (EA24)	0.114

Elements: Ti, Zr, Ba

A-Rank: Nemrut Dag (EA24) 7
B-Rank: Nemrut Dag (EA21) 1

Specimen	*Location*	*E.D.*
EA24P1B	Nemrut Dag (EA24)	0.052
EA21R1A	Nemrut Dag (EA21)	0.062
EA24P1A	Nemrut Dag (EA24)	0.062
EA24P1C	Nemrut Dag (EA24)	0.062
EA24P2A	Nemrut Dag (EA24)	0.062
EA23P1B	Nemrut Dag (EA23)	0.066
EA24P6A	Nemrut Dag (EA24)	0.069
EA22P5A	Nemrut Dag (EA22)	0.070
EA24P2B	Nemrut Dag (EA24)	0.072
EA24P6B	Nemrut Dag (EA24)	0.073

Elements: Ti, Fe, Zr, Ba, Zn

A-Rank: Nemrut Dag (EA22) 5
B-Rank: **Bingol A*** **3**

Specimen	*Location*	*E.D.*
EA22P5B	Nemrut Dag (EA22)	0.206
EA22P7A	Nemrut Dag (EA22)	0.209
EA22R1	Nemrut Dag (EA22)	0.211
EA22P1D	Nemrut Dag (EA22)	0.224
EA24P2A	Nemrut Dag (EA24)	0.227
EA22P3	Nemrut Dag (EA22)	0.229
EA24P5A	Nemrut Dag (EA24)	0.235
EA48P2B	Bingol A	0.237
EA48P3	Bingol A	0.239
EA48P5	Bingol A	0.239

Elements: Ti, Al, Fe, Mn, Ca, Zr, Ba

A-Rank: Nemrut Dag (EA24) 8
B-Rank: Nemrut Dag (EA21) 2

Specimen	*Location*	*E.D.*
EA24P1A	Nemrut Dag (EA24)	0.145
EA24R1	Nemrut Dag (EA24)	0.147
EA24P1C	Nemrut Dag (EA24)	0.148
EA21R1A	Nemrut Dag (EA21)	0.149
EA24P2A	Nemrut Dag (EA24)	0.152
EA24P8A	Nemrut Dag (EA24)	0.154
EA21P2	Nemrut Dag (EA21)	0.155
EA24P6A	Nemrut Dag (EA24)	0.157
EA24P1B	Nemrut Dag (EA24)	0.158
EA24P5A	Nemrut Dag (EA24)	0.158

* "Bingol A" is the correct source based on the CNK/A vs. NK/A peralkalinity plot and scatterplots of critical elements identified by Poidevin (1998): Al, Fe, and Ba plus Ti.

Table D.1 - Source Assignments of Artifacts based on Euclidean Distance to Centroids of Geological Specimens

Artifact: J3 q146.1 f100 k13

A-Rank: **Nemrut Dag (EA25)** **52**
B-Rank: Nemrut Dag (EA22) 24

Elements: Fe, Ti, Ba

A-Rank:	Nemrut Dag (EA25)	10
B-Rank:	-	-

Specimen	*Location*	*E.D.*
EA25R2	Nemrut Dag (EA25)	0.042
EA25P2A	Nemrut Dag (EA25)	0.046
EA25P2C	Nemrut Dag (EA25)	0.046
EA25P2D	Nemrut Dag (EA25)	0.047
EA25P1C	Nemrut Dag (EA25)	0.049
EA25P2B	Nemrut Dag (EA25)	0.054
EA25P1A	Nemrut Dag (EA25)	0.056
EA25P1B	Nemrut Dag (EA25)	0.057
EA25P1D	Nemrut Dag (EA25)	0.060
EA25R1	Nemrut Dag (EA25)	0.064

Elements: Fe, Zr, Ba

A-Rank:	Nemrut Dag (EA22)	8
B-Rank:	Nemrut Dag (EA21)	2

Specimen	*Location*	*E.D.*
EA21P1	Nemrut Dag (EA21)	0.074
EA22P5A	Nemrut Dag (EA22)	0.077
EA22P7A	Nemrut Dag (EA22)	0.077
EA22P6A	Nemrut Dag (EA22)	0.084
EA22P4	Nemrut Dag (EA22)	0.085
EA22P6B	Nemrut Dag (EA22)	0.085
EA22P7B	Nemrut Dag (EA22)	0.085
EA22P5B	Nemrut Dag (EA22)	0.086
EA21R1B	Nemrut Dag (EA21)	0.087
EA22P3	Nemrut Dag (EA22)	0.087

Elements: Ti, Fe, Zr, Ba

A-Rank:	Nemrut Dag (EA25)	8
B-Rank:	Nemrut Dag (EA22)	1

Specimen	*Location*	*E.D.*
EA25P1A	Nemrut Dag (EA25)	0.088
EA25P1B	Nemrut Dag (EA25)	0.088
EA25P1C	Nemrut Dag (EA25)	0.088
EA25P1D	Nemrut Dag (EA25)	0.089
EA22P7A	Nemrut Dag (EA25)	0.095
EA25P2C	Nemrut Dag (EA25)	0.099
EA25P2D	Nemrut Dag (EA25)	0.103
EA22P6B	Nemrut Dag (EA22)	0.104
EA21P1	Nemrut Dag (EA21)	0.105
EA25P2A	Nemrut Dag (EA25)	0.105

Elements: Ti, Fe, Mn, Ca, Zr, Ba

A-Rank:	Nemrut Dag (EA25)	10
B-Rank:	-	-

Specimen	*Location*	*E.D.*
EA25P1C	Nemrut Dag (EA25)	0.088
EA25P1A	Nemrut Dag (EA25)	0.089
EA25P1B	Nemrut Dag (EA25)	0.092
EA25P1D	Nemrut Dag (EA25)	0.099
EA25P2C	Nemrut Dag (EA25)	0.103
EA25P2A	Nemrut Dag (EA25)	0.109
EA25P2D	Nemrut Dag (EA25)	0.109
EA25R1	Nemrut Dag (EA25)	0.111
EA25P2B	Nemrut Dag (EA25)	0.115
EA25R2	Nemrut Dag (EA25)	0.116

Elements: Fe, Ti, Zr

A-Rank:	Nemrut Dag (EA25)	6
B-Rank:	Nemrut Dag (EA22)	4

Specimen	*Location*	*E.D.*
EA25P1D	Nemrut Dag (EA25)	0.066
EA25P1A	Nemrut Dag (EA25)	0.067
EA25P1B	Nemrut Dag (EA25)	0.068
EA25P1C	Nemrut Dag (EA25)	0.073
EA22P7A	Nemrut Dag (EA22)	0.083
EA25R1	Nemrut Dag (EA25)	0.086
EA25P2C	Nemrut Dag (EA25)	0.088
EA22P8B	Nemrut Dag (EA22)	0.089
EA22P6B	Nemrut Dag (EA22)	0.090
EA22P5A	Nemrut Dag (EA22)	0.091

Elements: Ti, Zr, Ba

A-Rank:	Nemrut Dag (EA22)	5
B-Rank:	Nemrut Dag (EA25)	4

Specimen	*Location*	*E.D.*
EA22P7A	Nemrut Dag (EA22)	0.080
EA25P1A	Nemrut Dag (EA25)	0.088
EA25P1B	Nemrut Dag (EA25)	0.088
EA25P1C	Nemrut Dag (EA25)	0.088
EA22R1	Nemrut Dag (EA22)	0.089
EA25P1D	Nemrut Dag (EA25)	0.089
EA21P1	Nemrut Dag (EA21)	0.091
EA22P2	Nemrut Dag (EA22)	0.093
EA22P6B	Nemrut Dag (EA22)	0.093
EA22P7B	Nemrut Dag (EA22)	0.093

Elements: Ti, Fe, Zr, Ba, Zn

A-Rank:	Nemrut Dag (EA22)	6
B-Rank:	Nemrut Dag (EA25)	4

Specimen	*Location*	*E.D.*
EA22P7A	Nemrut Dag (EA22)	0.096
EA25P2C	Nemrut Dag (EA25)	0.100
EA22R1	Nemrut Dag (EA22)	0.106
EA25P1A	Nemrut Dag (EA25)	0.106
EA25P1D	Nemrut Dag (EA25)	0.107
EA25P1B	Nemrut Dag (EA25)	0.109
EA22P3	Nemrut Dag (EA22)	0.113
EA22P7B	Nemrut Dag (EA22)	0.113
EA22P5B	Nemrut Dag (EA22)	0.118
EA22P1C	Nemrut Dag (EA22)	0.119

Elements: Ti, Al, Fe, Mn, Ca, Zr, Ba

A-Rank:	Nemrut Dag (EA25)	10
B-Rank:	-	-

Specimen	*Location*	*E.D.*
EA25P1A	Nemrut Dag (EA25)	0.089
EA25P1C	Nemrut Dag (EA25)	0.089
EA25P1B	Nemrut Dag (EA25)	0.093
EA25P1D	Nemrut Dag (EA25)	0.101
EA25P2C	Nemrut Dag (EA25)	0.104
EA25P2A	Nemrut Dag (EA25)	0.110
EA25P2D	Nemrut Dag (EA25)	0.110
EA25R1	Nemrut Dag (EA25)	0.111
EA25P2B	Nemrut Dag (EA25)	0.116
EA25R2	Nemrut Dag (EA25)	0.116

Table D.1 - Source Assignments of Artifacts based on Euclidean Distance to Centroids of Geological Specimens

Artifact: J3 q150.3 f105 k22

A-Rank: **Nemrut Dag (EA22)** **38**
B-Rank: Nemrut Dag (EA25) 25

Elements: Fe, Ti, Ba

A-Rank:	Nemrut Dag (EA25)	10
B-Rank:	-	-

Specimen	*Location*	*E.D.*
EA25P1B	Nemrut Dag (EA25)	0.014
EA25R2	Nemrut Dag (EA25)	0.015
EA25P1A	Nemrut Dag (EA25)	0.016
EA25R1	Nemrut Dag (EA25)	0.016
EA25P1C	Nemrut Dag (EA25)	0.017
EA25P2A	Nemrut Dag (EA25)	0.018
EA25P3	Nemrut Dag (EA25)	0.018
EA25P2B	Nemrut Dag (EA25)	0.020
EA25P2C	Nemrut Dag (EA25)	0.021
EA25P1D	Nemrut Dag (EA25)	0.022

Elements: Fe, Zr, Ba

A-Rank:	Nemrut Dag (EA22)	7
B-Rank:	Nemrut Dag (EA21)	3

Specimen	*Location*	*E.D.*
EA22P5A	Nemrut Dag (EA22)	0.115
EA21R1A	Nemrut Dag (EA21)	0.119
EA21P1	Nemrut Dag (EA21)	0.120
EA21R1B	Nemrut Dag (EA21)	0.122
EA22P7A	Nemrut Dag (EA22)	0.122
EA22P6A	Nemrut Dag (EA22)	0.123
EA22P3	Nemrut Dag (EA22)	0.125
EA22P4	Nemrut Dag (EA22)	0.125
EA22P5B	Nemrut Dag (EA22)	0.125
EA22P8B	Nemrut Dag (EA22)	0.127

Elements: Ti, Fe, Zr, Ba

A-Rank:	Nemrut Dag (EA22)	7
B-Rank:	Nemrut Dag (EA21)	3

Specimen	*Location*	*E.D.*
EA22P5A	Nemrut Dag (EA22)	0.127
EA22P7A	Nemrut Dag (EA22)	0.127
EA21P1	Nemrut Dag (EA21)	0.132
EA21R1B	Nemrut Dag (EA21)	0.133
EA22P8B	Nemrut Dag (EA22)	0.134
EA22P3	Nemrut Dag (EA22)	0.135
EA22P6A	Nemrut Dag (EA22)	0.135
EA22P4	Nemrut Dag (EA22)	0.136
EA21R1A	Nemrut Dag (EA21)	0.137
EA22P6B	Nemrut Dag (EA22)	0.137

Elements: Ti, Fe, Mn, Ca, Zr, Ba

A-Rank:	Nemrut Dag (EA25)	6
B-Rank:	Nemrut Dag (EA22)	3

Specimen	*Location*	*E.D.*
EA25P1A	Nemrut Dag (EA25)	0.144
EA25P1B	Nemrut Dag (EA25)	0.145
EA25P1D	Nemrut Dag (EA25)	0.148
EA25P1C	Nemrut Dag (EA25)	0.150
EA22P7B	Nemrut Dag (EA22)	0.159
EA25R1	Nemrut Dag (EA25)	0.163
EA22P4	Nemrut Dag (EA22)	0.164
EA25P2C	Nemrut Dag (EA25)	0.166
EA21P1	Nemrut Dag (EA21)	0.167
EA22P6A	Nemrut Dag (EA22)	0.167

Elements: Fe, Ti, Zr

A-Rank:	Nemrut Dag (EA22)	7
B-Rank:	Nemrut Dag (EA21)	3

Specimen	*Location*	*E.D.*
EA22P5A	Nemrut Dag (EA22)	0.127
EA22P7A	Nemrut Dag (EA22)	0.127
EA21P1	Nemrut Dag (EA21)	0.132
EA21R1B	Nemrut Dag (EA21)	0.133
EA22P8B	Nemrut Dag (EA22)	0.134
EA22P3	Nemrut Dag (EA22)	0.135
EA22P6A	Nemrut Dag (EA22)	0.135
EA22P4	Nemrut Dag (EA22)	0.136
EA21R1A	Nemrut Dag (EA21)	0.137
EA22P6B	Nemrut Dag (EA22)	0.138

Elements: Ti, Zr, Ba

A-Rank:	Nemrut Dag (EA22)	6
B-Rank:	Nemrut Dag (EA21)	3

Specimen	*Location*	*E.D.*
EA22P7A	Nemrut Dag (EA22)	0.117
EA22P5A	Nemrut Dag (EA22)	0.120
EA21P1	Nemrut Dag (EA21)	0.122
EA21R1B	Nemrut Dag (EA21)	0.124
EA22P8B	Nemrut Dag (EA22)	0.126
EA21R1A	Nemrut Dag (EA21)	0.127
EA22P3	Nemrut Dag (EA22)	0.127
EA22P6A	Nemrut Dag (EA22)	0.127
EA24P1B	Nemrut Dag (EA24)	0.127
EA22R1	Nemrut Dag (EA22)	0.129

Elements: Ti, Fe, Zr, Ba, Zn

A-Rank:	Nemrut Dag (EA22)	9
B-Rank:	Nemrut Dag (EA25)	1

Specimen	*Location*	*E.D.*
EA22P7A	Nemrut Dag (EA22)	0.151
EA22P5B	Nemrut Dag (EA22)	0.161
EA22R1	Nemrut Dag (EA22)	0.166
EA22P3	Nemrut Dag (EA22)	0.177
EA22P1D	Nemrut Dag (EA22)	0.184
EA25P2C	Nemrut Dag (EA25)	0.185
EA22P1C	Nemrut Dag (EA22)	0.195
EA22P7B	Nemrut Dag (EA22)	0.196
EA22P6A	Nemrut Dag (EA22)	0.205
EA22P8B	Nemrut Dag (EA22)	0.206

Elements: Ti, Al, Fe, Mn, Ca, Zr, Ba

A-Rank:	Nemrut Dag (EA25)	8
B-Rank:	Nemrut Dag (EA22)	2

Specimen	*Location*	*E.D.*
EA25P1A	Nemrut Dag (EA25)	0.144
EA25P1B	Nemrut Dag (EA25)	0.145
EA25P1D	Nemrut Dag (EA25)	0.148
EA25P1C	Nemrut Dag (EA25)	0.150
EA22P7B	Nemrut Dag (EA22)	0.163
EA25R1	Nemrut Dag (EA25)	0.163
EA25P2C	Nemrut Dag (EA25)	0.166
EA22P4	Nemrut Dag (EA22)	0.168
EA25P3	Nemrut Dag (EA25)	0.168
EA25P2D	Nemrut Dag (EA25)	0.171

Table D.1 - Source Assignments of Artifacts based on Euclidean Distance to Centroids of Geological Specimens

Artifact: J3 q152.1 f101 k13

A-Rank: **Nemrut Dag (EA25)** **45**
B-Rank: Nemrut Dag (EA22) 27

Elements: Fe, Ti, Ba

A-Rank:	Nemrut Dag (EA25)	10
B-Rank:	-	-

Specimen	*Location*	*E.D.*
EA25P2C	Nemrut Dag (EA25)	0.013
EA25P1C	Nemrut Dag (EA25)	0.014
EA25P2B	Nemrut Dag (EA25)	0.015
EA25P2D	Nemrut Dag (EA25)	0.015
EA25P1B	Nemrut Dag (EA25)	0.016
EA25R2	Nemrut Dag (EA25)	0.017
EA25P1D	Nemrut Dag (EA25)	0.018
EA25P1A	Nemrut Dag (EA25)	0.019
EA25P2A	Nemrut Dag (EA25)	0.019
EA25R1	Nemrut Dag (EA25)	0.022

Elements: Fe, Zr, Ba

A-Rank:	Nemrut Dag (EA22)	7
B-Rank:	Nemrut Dag (EA21)	3

Specimen	*Location*	*E.D.*
EA22P5A	Nemrut Dag (EA22)	0.051
EA21P1	Nemrut Dag (EA21)	0.057
EA22P7A	Nemrut Dag (EA22)	0.057
EA21R1A	Nemrut Dag (EA21)	0.058
EA21R1B	Nemrut Dag (EA21)	0.059
EA22P4	Nemrut Dag (EA22)	0.059
EA22P6A	Nemrut Dag (EA22)	0.059
EA22P5B	Nemrut Dag (EA22)	0.060
EA22P3	Nemrut Dag (EA22)	0.061
EA22P8B	Nemrut Dag (EA22)	0.062

Elements: Ti, Fe, Zr, Ba

A-Rank:	Nemrut Dag (EA25)	4
B-Rank:	Nemrut Dag (EA22)	4

Specimen	*Location*	*E.D.*
EA22P7A	Nemrut Dag (EA22)	0.073
EA25P1D	Nemrut Dag (EA25)	0.076
EA25P1A	Nemrut Dag (EA25)	0.078
EA25P1B	Nemrut Dag (EA25)	0.078
EA22P5A	Nemrut Dag (EA22)	0.080
EA22P8B	Nemrut Dag (EA22)	0.080
EA22P6B	Nemrut Dag (EA22)	0.082
EA25P1C	Nemrut Dag (EA25)	0.083
EA21P1	Nemrut Dag (EA21)	0.085
EA21R1B	Nemrut Dag (EA21)	0.085

Elements: Ti, Fe, Mn, Ca, Zr, Ba

A-Rank:	Nemrut Dag (EA25)	10
B-Rank:	-	-

Specimen	*Location*	*E.D.*
EA25P1A	Nemrut Dag (EA25)	0.082
EA25P1C	Nemrut Dag (EA25)	0.083
EA25P1B	Nemrut Dag (EA25)	0.085
EA25P1D	Nemrut Dag (EA25)	0.093
EA22P7B	Nemrut Dag (EA22)	0.104
EA25P2C	Nemrut Dag (EA25)	0.104
EA25R1	Nemrut Dag (EA25)	0.104
EA25P3	Nemrut Dag (EA25)	0.108
EA25P2D	Nemrut Dag (EA25)	0.110
EA25P2A	Nemrut Dag (EA25)	0.111

Elements: Fe, Ti, Zr

A-Rank:	Nemrut Dag (EA22)	4
B-Rank:	Nemrut Dag (EA25)	4

Specimen	*Location*	*E.D.*
EA22P7A	Nemrut Dag (EA22)	0.073
EA25P1D	Nemrut Dag (EA25)	0.075
EA25P1A	Nemrut Dag (EA25)	0.078
EA25P1B	Nemrut Dag (EA25)	0.078
EA22P5A	Nemrut Dag (EA22)	0.080
EA22P8B	Nemrut Dag (EA22)	0.080
EA22P6B	Nemrut Dag (EA22)	0.082
EA25P1C	Nemrut Dag (EA25)	0.083
EA21R1B	Nemrut Dag (EA21)	0.084
EA21P1	Nemrut Dag (EA21)	0.085

Elements: Ti, Zr, Ba

A-Rank:	Nemrut Dag (EA22)	6
B-Rank:	Nemrut Dag (EA25)	3

Specimen	*Location*	*E.D.*
EA22P7A	Nemrut Dag (EA22)	0.063
EA22P8B	Nemrut Dag (EA22)	0.073
EA22R1	Nemrut Dag (EA22)	0.073
EA22P5A	Nemrut Dag (EA22)	0.074
EA22P6B	Nemrut Dag (EA22)	0.075
EA21P1	Nemrut Dag (EA21)	0.076
EA25P1D	Nemrut Dag (EA25)	0.076
EA21R1B	Nemrut Dag (EA21)	0.077
EA25P1A	Nemrut Dag (EA25)	0.077
EA25P1B	Nemrut Dag (EA25)	0.077

Elements: Ti, Fe, Zr, Ba, Zn

A-Rank:	Nemrut Dag (EA22)	6
B-Rank:	Nemrut Dag (EA25)	4

Specimen	*Location*	*E.D.*
EA25P1D	Nemrut Dag (EA25)	0.076
EA25P1A	Nemrut Dag (EA25)	0.079
EA25P1B	Nemrut Dag (EA25)	0.079
EA22P8B	Nemrut Dag (EA22)	0.080
EA22P6B	Nemrut Dag (EA22)	0.083
EA22P6A	Nemrut Dag (EA22)	0.087
EA22P7B	Nemrut Dag (EA22)	0.088
EA25P1C	Nemrut Dag (EA25)	0.092
EA22P3	Nemrut Dag (EA22)	0.094
EA22R2	Nemrut Dag (EA22)	0.095

Elements: Ti, Al, Fe, Mn, Ca, Zr, Ba

A-Rank:	Nemrut Dag (EA25)	10
B-Rank:	-	-

Specimen	*Location*	*E.D.*
EA25P1A	Nemrut Dag (EA25)	0.083
EA25P1C	Nemrut Dag (EA25)	0.085
EA25P1B	Nemrut Dag (EA25)	0.087
EA25P1D	Nemrut Dag (EA25)	0.095
EA25R1	Nemrut Dag (EA25)	0.104
EA25P2C	Nemrut Dag (EA25)	0.106
EA25P3	Nemrut Dag (EA25)	0.108
EA25P2D	Nemrut Dag (EA25)	0.112
EA25P2A	Nemrut Dag (EA25)	0.113
EA25P2B	Nemrut Dag (EA25)	0.114

Table D.1 - Source Assignments of Artifacts based on Euclidean Distance to Centroids of Geological Specimens

Artifact: Georgia-nS1, Anaseuli

A-Rank: **Chikiani** **51**
B-Rank: Golludag 9

Elements: Fe, Ti, Ba

A-Rank:	Chikiani	6
B-Rank:	Damlik	2

Specimen	*Location*	*E.D.*
GE11nS5	Chikiani	0.025
GE04iD1	Chikiani	0.027
GE10nS1	Chikiani	0.037
AR69rB1	Damlik	0.038
GE08rB1	Chikiani	0.038
CA21P2	Golludag	0.039
AR13jB1	Ankavan	0.041
GE12nS1	Chikiani	0.041
AR69rB2	Damlik	0.043
GE08rB2	Chikiani	0.045

Elements: Fe, Zr, Ba

A-Rank:	Chikiani	5
B-Rank:	Golludag	3

Specimen	*Location*	*E.D.*
CA21P2	Golludag	0.015
GE11nS5	Chikiani	0.016
CA21R1A	Golludag	0.027
GE04iD1	Chikiani	0.027
GE10nS1	Chikiani	0.033
CA21R2B	Golludag	0.035
GE08rB1	Chikiani	0.036
EA37P4	Kars-Digor	0.037
EA37R1	Kars-Digor	0.037
GE12nS1	Chikiani	0.038

Elements: Ti, Fe, Zr, Ba

A-Rank:	Chikiani	6
B-Rank:	Golludag	2

Specimen	*Location*	*E.D.*
GE11nS5	Chikiani	0.026
GE04iD1	Chikiani	0.027
GE10nS1	Chikiani	0.037
GE08rB1	Chikiani	0.038
CA21P2	Golludag	0.039
AR13jB1	Ankavan	0.041
GE12nS1	Chikiani	0.041
AR69rB1	Damlik	0.043
GE08rB2	Chikiani	0.045
CA21R1A	Golludag	0.047

Elements: Ti, Fe, Mn, Ca, Zr, Ba

A-Rank:	Chikiani	6
B-Rank:	Golludag	2

Specimen	*Location*	*E.D.*
GE11nS5	Chikiani	0.026
GE04iD1	Chikiani	0.039
GE08rB1	Chikiani	0.041
GE12nS1	Chikiani	0.041
GE10nS1	Chikiani	0.045
GE08rB2	Chikiani	0.048
AR69rB1	Damlik	0.056
AR13jB1	Ankavan	0.058
CA21R2B	Golludag	0.064
CA21R2C	Golludag	0.064

Elements: Fe, Ti, Zr

A-Rank:	Chikiani	9
B-Rank:	Hatis	1

Specimen	*Location*	*E.D.*
GE07kM1A	Chikiani	0.003
GE02iD1A	Chikiani	0.007
GE02iD1B	Chikiani	0.010
GE07kM1B	Chikiani	0.011
GE13nS1	Chikiani	0.011
GE04iD1	Chikiani	0.012
GE05iD1	Chikiani	0.012
GE11nS1	Chikiani	0.012
GE11nS4	Chikiani	0.015
AR08jB1	Hatis	0.016

Elements: Ti, Zr, Ba

A-Rank:	Chikiani	6
B-Rank:	Ankavan	2

Specimen	*Location*	*E.D.*
AR13jB1	Ankavan	0.008
GE08rB2	Chikiani	0.009
GE12nS1	Chikiani	0.018
AR14jB1	Ankavan	0.020
GE11nS5	Chikiani	0.023
GE04iD1	Chikiani	0.025
GE08rB1	Chikiani	0.030
AR69rB1	Damlik	0.033
GE10nS1	Chikiani	0.034
AR69rB3	Damlik	0.035

Elements: Ti, Fe, Zr, Ba, Zn

A-Rank:	Chikiani	7
B-Rank:	Golludag	1

Specimen	*Location*	*E.D.*
GE11nS5	Chikiani	0.041
GE10nS1	Chikiani	0.042
GE08rB2	Chikiani	0.048
GE08rB1	Chikiani	0.052
GE12nS1	Chikiani	0.058
CA21R2C	Golludag	0.064
AR43kM1	Pokr Arteni	0.079
GE07kM1C	Chikiani	0.079
GE11nS4	Chikiani	0.080
AR13jB1	Ankavan	0.087

Elements: Ti, Al, Fe, Mn, Ca, Zr, Ba

A-Rank:	Chikiani	6
B-Rank:	Golludag	3

Specimen	*Location*	*E.D.*
GE11nS5	Chikiani	0.049
GE04iD1	Chikiani	0.058
GE12nS1	Chikiani	0.058
GE08rB1	Chikiani	0.059
GE10nS1	Chikiani	0.059
GE08rB2	Chikiani	0.063
CA21R2C	Golludag	0.064
CA21R2B	Golludag	0.065
CA21R1A	Golludag	0.070
AR69rB1	Damlik	0.076

Table D.1 - Source Assignments of Artifacts based on Euclidean Distance to Centroids of Geological Specimens

Artifact: Georgia-nS2a, Chachuna

A-Rank: **Chikiani** **61**
B-Rank: Damlik 3

Elements: Fe, Ti, Ba

A-Rank:	Chikiani	7
B-Rank:	Damlik	1

Specimen	*Location*	*E.D.*
GE07kM1C	Chikiani	0.010
GE11nS4	Chikiani	0.010
GE07kM1B	Chikiani	0.019
AR60sK1	Damlik	0.021
GE07kM1A	Chikiani	0.025
GE02iD1A	Chikiani	0.027
GE11nS1	Chikiani	0.027
GE05iD1	Chikiani	0.031
AR43kM1	Pokr Arteni	0.034
AR29ipS1	Unknown	0.037

Elements: Fe, Zr, Ba

A-Rank:	Chikiani	7
B-Rank:	Gollu Dag	2

Specimen	*Location*	*E.D.*
GE11nS4	Chikiani	0.009
GE07kM1A	Chikiani	0.012
CA21P1	Gollu Dag	0.015
GE07kM1B	Chikiani	0.015
GE07kM1C	Chikiani	0.019
AR60sK1	Damlik	0.021
GE02iD1A	Chikiani	0.021
GE11nS1	Chikiani	0.025
GE05iD1	Chikiani	0.029
CA21R1B	Gollu Dag	0.030

Elements: Ti, Fe, Zr, Ba

A-Rank:	Chikiani	7
B-Rank:	Damlik	1

Specimen	*Location*	*E.D.*
GE11nS4	Chikiani	0.013
GE07kM1B	Chikiani	0.021
GE07kM1C	Chikiani	0.021
AR60sK1	Damlik	0.025
GE07kM1A	Chikiani	0.025
GE02iD1A	Chikiani	0.028
GE11nS1	Chikiani	0.028
GE05iD1	Chikiani	0.031
AR43kM1	Pokr Arteni	0.036
AR29ipS1	Unknown	0.037

Elements: Ti, Fe, Mn, Ca, Zr, Ba

A-Rank:	Chikiani	8
B-Rank:	Damlik	1

Specimen	*Location*	*E.D.*
GE11nS4	Chikiani	0.016
GE07kM1B	Chikiani	0.021
GE07kM1C	Chikiani	0.023
AR60sK1	Damlik	0.026
GE02iD1A	Chikiani	0.029
GE11nS1	Chikiani	0.030
GE07kM1A	Chikiani	0.031
GE05iD1	Chikiani	0.032
AR29ipS1	Unknown	0.039
GE02iD1C	Chikiani	0.040

Elements: Fe, Ti, Zr

A-Rank:	Chikiani	10
B-Rank:	-	-

Specimen	*Location*	*E.D.*
GE11nS6	Chikiani	0.001
GE02iD1C	Chikiani	0.002
GE01jB1	Chikiani	0.009
GE03iD1	Chikiani	0.009
GE05iD1	Chikiani	0.010
GE02iD1B	Chikiani	0.011
GE13nS1	Chikiani	0.011
GE13nS2	Chikiani	0.011
GE11nS4	Chikiani	0.012
GE11nS1	Chikiani	0.016

Elements: Ti, Zr, Ba

A-Rank:	Chikiani	5
B-Rank:	Ttvakar	2

Specimen	*Location*	*E.D.*
AR43kM1	Pokr Arteni	0.012
GE11nS4	Chikiani	0.012
AR70rB1	Ttvakar	0.018
AR29ipS1	Unknown	0.019
GE07kM1B	Chikiani	0.021
GE07kM1C	Chikiani	0.021
AR70rB2	Ttvakar	0.023
AR60sK1	Damlik	0.024
GE07kM1A	Chikiani	0.025
GE06iD1	Chikiani	0.026

Elements: Ti, Fe, Zr, Ba, Zn

A-Rank:	Chikiani	8
B-Rank:	Armenia, Unk	1

Specimen	*Location*	*E.D.*
GE07kM1B	Chikiani	0.022
GE02iD1A	Chikiani	0.033
GE05iD1	Chikiani	0.045
GE07kM1A	Chikiani	0.045
GE06iD1	Chikiani	0.051
AR29ipS1	Armenia, Unk	0.052
GE04iD1	Chikiani	0.057
GE07kM1C	Chikiani	0.063
AR43kM1	Pokr Arteni	0.069
GE11nS1	Chikiani	0.074

Elements: Ti, Al, Fe, Mn, Ca, Zr, Ba

A-Rank:	Chikiani	9
B-Rank:	Damlik	1

Specimen	*Location*	*E.D.*
GE11nS4	Chikiani	0.027
GE07kM1B	Chikiani	0.033
GE07kM1C	Chikiani	0.035
GE05iD1	Chikiani	0.038
GE11nS1	Chikiani	0.038
GE02iD1A	Chikiani	0.040
AR60sK1	Damlik	0.045
GE02iD1C	Chikiani	0.046
GE07kM1A	Chikiani	0.048
GE13nS1	Chikiani	0.049

Table D.1 - Source Assignments of Artifacts based on Euclidean Distance to Centroids of Geological Specimens

Artifact: Georgia-nS2b, Chachuna

A-Rank: **Chikiani** **58**
B-Rank: Hasan Dag 19

Elements: Fe, Ti, Ba

A-Rank:	Chikiani	7
B-Rank:	Hasan Dag	3

Specimen	*Location*	*E.D.*
GE11nS6	Chikiani	0.007
GE01jB1	Chikiani	0.014
GE03iD1	Chikiani	0.018
GE13nS2	Chikiani	0.023
GE11nS3	Chikiani	0.024
GE11nS2	Chikiani	0.025
CA29R1	Hasan Dag	0.036
GE02iD1B	Chikiani	0.037
CA29R2	Hasan Dag	0.039
CA29P3B	Hasan Dag	0.043

Elements: Fe, Zr, Ba

A-Rank:	Chikiani	7
B-Rank:	Hasan Dag	3

Specimen	*Location*	*E.D.*
GE11nS6	Chikiani	0.012
GE03iD1	Chikiani	0.020
GE01jB1	Chikiani	0.021
GE13nS2	Chikiani	0.022
GE11nS2	Chikiani	0.025
GE11nS3	Chikiani	0.026
CA29R2	Hasan Dag	0.034
CA29R1	Hasan Dag	0.035
GE02iD1B	Chikiani	0.037
CA29P2A	Hasan Dag	0.041

Elements: Ti, Fe, Zr, Ba

A-Rank:	Chikiani	8
B-Rank:	Hasan Dag	2

Specimen	*Location*	*E.D.*
GE11nS6	Chikiani	0.012
GE03iD1	Chikiani	0.020
GE01jB1	Chikiani	0.021
GE13nS2	Chikiani	0.023
GE11nS2	Chikiani	0.025
GE11nS3	Chikiani	0.026
GE02iD1B	Chikiani	0.039
CA29R1	Hasan Dag	0.043
CA29R2	Hasan Dag	0.044
GE13nS1	Chikiani	0.046

Elements: Ti, Fe, Mn, Ca, Zr, Ba

A-Rank:	Chikiani	7
B-Rank:	Hasan Dag	3

Specimen	*Location*	*E.D.*
GE11nS6	Chikiani	0.013
GE03iD1	Chikiani	0.021
GE13nS2	Chikiani	0.023
GE11nS2	Chikiani	0.027
GE11nS3	Chikiani	0.028
CA29R1	Hasan Dag	0.045
GE02iD1B	Chikiani	0.045
CA29R2	Hasan Dag	0.049
GE01jB1	Chikiani	0.049
CA29P4	Hasan Dag	0.051

Elements: Fe, Ti, Zr

A-Rank:	Chikiani	10
B-Rank:	-	-

Specimen	*Location*	*E.D.*
GE13nS2	Chikiani	0.009
GE11nS2	Chikiani	0.011
GE11nS6	Chikiani	0.012
GE02iD1C	Chikiani	0.014
GE11nS3	Chikiani	0.015
GE11nS4	Chikiani	0.015
GE01jB1	Chikiani	0.016
GE13nS1	Chikiani	0.016
GE11nS1	Chikiani	0.017
GE02iD1B	Chikiani	0.018

Elements: Ti, Zr, Ba

A-Rank:	Chikiani	7
B-Rank:	Hasan Dag	3

Specimen	*Location*	*E.D.*
GE11nS6	Chikiani	0.010
GE03iD1	Chikiani	0.011
GE01jB1	Chikiani	0.021
GE13nS2	Chikiani	0.022
GE11nS3	Chikiani	0.023
GE11nS2	Chikiani	0.024
CA28P4	Hasan Dag	0.032
CA29R1	Hasan Dag	0.034
CA29R2	Hasan Dag	0.036
GE02iD1B	Chikiani	0.038

Elements: Ti, Fe, Zr, Ba, Zn

A-Rank:	Chikiani	7
B-Rank:	Hasan Dag	3

Specimen	*Location*	*E.D.*
GE11nS6	Chikiani	0.026
GE11nS2	Chikiani	0.029
GE13nS2	Chikiani	0.043
CA29P5B	Hasan Dag	0.052
GE02iD1B	Chikiani	0.053
GE02iD1C	Chikiani	0.056
CA29P1A	Hasan Dag	0.063
GE11nS3	Chikiani	0.065
CA29R1	Hasan Dag	0.068
GE11nS1	Chikiani	0.069

Elements: Ti, Al, Fe, Mn, Ca, Zr, Ba

A-Rank:	Chikiani	5
B-Rank:	Hasan Dag	5

Specimen	*Location*	*E.D.*
GE11nS6	Chikiani	0.024
GE03iD1	Chikiani	0.032
GE11nS2	Chikiani	0.037
GE11nS3	Chikiani	0.037
GE13nS2	Chikiani	0.037
CA29R1	Hasan Dag	0.046
CA29R2	Hasan Dag	0.050
CA29P4	Hasan Dag	0.052
CA29P3B	Hasan Dag	0.053
CA28P2	Hasan Dag	0.054

Table D.1 - Source Assignments of Artifacts based on Euclidean Distance to Centroids of Geological Specimens

Artifact: Georgia, nS3, Dzudzuana

A-Rank: **Chikiani** **62**
B-Rank: Hasan Dag 6

Elements: Fe, Ti, Ba

A-Rank:	Chikiani	9
B-Rank:	Damlik	1

Specimen	*Location*	*E.D.*
GE11nS1	Chikiani	0.006
GE02iD1A	Chikiani	0.009
GE07kM1B	Chikiani	0.009
GE05iD1	Chikiani	0.010
AR60sK1	Damlik	0.011
GE07kM1A	Chikiani	0.014
GE07kM1C	Chikiani	0.016
GE02iD1C	Chikiani	0.022
GE11nS4	Chikiani	0.022
GE13nS1	Chikiani	0.024

Elements: Fe, Zr, Ba

A-Rank:	Chikiani	9
B-Rank:	Damlik	1

Specimen	*Location*	*E.D.*
GE11nS1	Chikiani	0.006
GE07kM1A	Chikiani	0.009
GE02iD1A	Chikiani	0.011
GE05iD1	Chikiani	0.012
GE07kM1B	Chikiani	0.016
AR60sK1	Damlik	0.020
GE02iD1C	Chikiani	0.021
GE11nS4	Chikiani	0.023
GE13nS1	Chikiani	0.024
GE07kM1C	Chikiani	0.028

Elements: Ti, Fe, Zr, Ba

A-Rank:	Chikiani	9
B-Rank:	Damlik	1

Specimen	*Location*	*E.D.*
GE11nS1	Chikiani	0.007
GE05iD1	Chikiani	0.012
GE02iD1A	Chikiani	0.014
GE07kM1A	Chikiani	0.015
GE07kM1B	Chikiani	0.017
AR60sK1	Damlik	0.021
GE02iD1C	Chikiani	0.022
GE11nS4	Chikiani	0.023
GE13nS1	Chikiani	0.024
GE07kM1C	Chikiani	0.028

Elements: Ti, Fe, Mn, Ca, Zr, Ba

A-Rank:	Chikiani	8
B-Rank:	Ttvakar	1

Specimen	*Location*	*E.D.*
GE07kM1A	Chikiani	0.018
GE11nS1	Chikiani	0.020
GE05iD1	Chikiani	0.023
GE02iD1A	Chikiani	0.025
GE02iD1C	Chikiani	0.029
GE07kM1B	Chikiani	0.034
GE07kM1C	Chikiani	0.034
GE13nS1	Chikiani	0.036
AR70rB1	Ttvakar	0.037
AR29ipS1	Unknown	0.039

Elements: Fe, Ti, Zr

A-Rank:	Chikiani	10
B-Rank:	-	-

Specimen	*Location*	*E.D.*
GE13nS1	Chikiani	0.001
GE11nS4	Chikiani	0.004
GE05iD1	Chikiani	0.005
GE11nS1	Chikiani	0.005
GE02iD1B	Chikiani	0.007
GE13nS2	Chikiani	0.008
GE02iD1C	Chikiani	0.010
GE11nS6	Chikiani	0.011
GE04iD1	Chikiani	0.013
GE07kM1A	Chikiani	0.013

Elements: Ti, Zr, Ba

A-Rank:	Chikiani	6
B-Rank:	Ttvakar	2

Specimen	*Location*	*E.D.*
GE11nS1	Chikiani	0.007
AR70rB1	Ttvakar	0.008
AR70rB2	Ttvakar	0.012
GE05iD1	Chikiani	0.012
GE02iD1A	Chikiani	0.014
GE07kM1A	Chikiani	0.015
GE07kM1B	Chikiani	0.017
AR60sK1	Damlik	0.019
AR29ipS1	Unknown	0.021
GE06iD1	Chikiani	0.021

Elements: Ti, Fe, Zr, Ba, Zn

A-Rank:	Hasan Dag	5
B-Rank:	Chikiani	2

Specimen	*Location*	*E.D.*
AR60sK1	Damlik	0.021
GE11nS4	Chikiani	0.027
AR70rB2	Ttvakar	0.046
CA29P1A	Hasan Dag	0.051
GE11nS3	Chikiani	0.051
CA29P1C	Hasan Dag	0.053
CA29P4	Hasan Dag	0.055
CA29P1B	Hasan Dag	0.060
AR70rB1	Ttvakar	0.065
CA30R1A	Hasan Dag	0.065

Elements: Ti, Al, Fe, Mn, Ca, Zr, Ba

A-Rank:	Chikiani	9
B-Rank:	Hasan Dag	1

Specimen	*Location*	*E.D.*
GE11nS1	Chikiani	0.039
GE05iD1	Chikiani	0.040
GE02iD1C	Chikiani	0.044
GE02iD1A	Chikiani	0.045
GE13nS1	Chikiani	0.047
GE07kM1A	Chikiani	0.050
GE07kM1B	Chikiani	0.050
GE07kM1C	Chikiani	0.050
CA29P1C	Hasan Dag	0.053
GE06iD1	Chikiani	0.053

Table D.1 - Source Assignments of Artifacts based on Euclidean Distance to Centroids of Geological Specimens

Artifact: Georgia-iD1, Tetritsqaro

A-Rank: **Chikiani** **40**
B-Rank: Golludag 14

Elements: Fe, Ti, Ba

A-Rank:	Chikiani	7
B-Rank:	Damlik	1

Specimen	*Location*	*E.D.*
GE11nS4	Chikiani	0.012
GE07kM1C	Chikiani	0.018
GE07kM1B	Chikiani	0.027
GE07kM1A	Chikiani	0.030
AR60sK1	Damlik	0.031
GE04iD1	Chikiani	0.032
AR43kM1	Pokr Arteni	0.034
AR29ipS1	Unknown	0.035
GE02iD1A	Chikiani	0.036
GE11nS1	Chikiani	0.039

Elements: Fe, Zr, Ba

A-Rank:	Golludag	5
B-Rank:	Chikiani	4

Specimen	*Location*	*E.D.*
CA21P1	Golludag	0.011
CA21R1B	Golludag	0.014
GE07kM1C	Chikiani	0.020
CA21R2A	Golludag	0.021
GE11nS4	Chikiani	0.022
CA21R2B	Golludag	0.023
CA21R2C	Golludag	0.024
GE07kM1B	Chikiani	0.026
GE07kM1A	Chikiani	0.029
AR60sK1	Damlik	0.030

Elements: Ti, Fe, Zr, Ba

A-Rank:	Chikiani	6
B-Rank:	Damlik	2

Specimen	*Location*	*E.D.*
GE07kM1C	Chikiani	0.020
GE11nS4	Chikiani	0.022
GE07kM1B	Chikiani	0.027
AR60sK1	Damlik	0.031
GE07kM1A	Chikiani	0.031
AR43kM1	Pokr Arteni	0.034
GE04iD1	Chikiani	0.034
AR29ipS1	Unknown	0.036
GE02iD1A	Chikiani	0.036
AR69rB1	Damlik	0.043

Elements: Ti, Fe, Mn, Ca, Zr, Ba

A-Rank:	Chikiani	6
B-Rank:	Damlik	2

Specimen	*Location*	*E.D.*
GE07kM1C	Chikiani	0.023
GE07kM1A	Chikiani	0.031
GE04iD1	Chikiani	0.034
GE07kM1B	Chikiani	0.034
GE11nS4	Chikiani	0.036
AR29ipS1	Unknown	0.037
GE02iD1A	Chikiani	0.038
AR43kM1	Pokr Arteni	0.039
AR60sK1	Damlik	0.042
AR69rB1	Damlik	0.045

Elements: Fe, Ti, Zr

A-Rank:	Chikiani	9
B-Rank:	Damlik	1

Specimen	*Location*	*E.D.*
GE07kM1B	Chikiani	0.005
GE07kM1C	Chikiani	0.008
GE02iD1B	Chikiani	0.009
GE02iD1A	Chikiani	0.010
GE05iD1	Chikiani	0.010
AR60sK1	Damlik	0.011
GE01jB1	Chikiani	0.012
GE02iD1C	Chikiani	0.013
GE04iD1	Chikiani	0.014
GE11nS6	Chikiani	0.014

Elements: Ti, Zr, Ba

A-Rank:	Chikiani	5
B-Rank:	Damlik	2

Specimen	*Location*	*E.D.*
AR43kM1	Pokr Arteni	0.012
AR29ipS1	Unknown	0.020
GE07kM1C	Chikiani	0.020
GE11nS4	Chikiani	0.022
GE07kM1B	Chikiani	0.027
AR60sK1	Damlik	0.029
GE06iD1	Chikiani	0.029
AR69rB3	Damlik	0.030
AR70rB2	Ttvakar	0.031
GE07kM1A	Chikiani	0.031

Elements: Ti, Fe, Zr, Ba, Zn

A-Rank:	Chikiani	8
B-Rank:	Pokr Arteni	1

Specimen	*Location*	*E.D.*
GE07kM1C	Chikiani	0.021
AR43kM1	Pokr Arteni	0.035
AR29ipS1	Unknown	0.039
GE11nS1	Chikiani	0.046
GE05iD1	Chikiani	0.049
GE02iD1C	Chikiani	0.057
GE07kM1B	Chikiani	0.063
GE02iD1B	Chikiani	0.068
GE11nS4	Chikiani	0.072
GE02iD1A	Chikiani	0.078

Elements: Ti, Al, Fe, Mn, Ca, Zr, Ba

A-Rank:	Chikiani	6
B-Rank:	Damlik	2

Specimen	*Location*	*E.D.*
GE07kM1C	Chikiani	0.024
GE07kM1A	Chikiani	0.031
GE04iD1	Chikiani	0.035
GE07kM1B	Chikiani	0.035
AR29ipS1	Unknown	0.037
GE02iD1A	Chikiani	0.038
GE11nS4	Chikiani	0.038
AR43kM1	Pokr Arteni	0.040
AR60sK1	Damlik	0.042
AR69rB1	Damlik	0.045

Table D.1 - Source Assignments of Artifacts based on Euclidean Distance to Centroids of Geological Specimens

Artifact: Georgia-iD2, Tetritsqaro

A-Rank: **Chikiani** **65**
B-Rank: Hasan Dag 12

Elements: Fe, Ti, Ba

A-Rank:	Chikiani	8
B-Rank:	Hasan Dag	2

Specimen	*Location*	*E.D.*
GE11nS3	Chikiani	0.004
GE13nS2	Chikiani	0.008
GE11nS2	Chikiani	0.010
GE02iD1B	Chikiani	0.015
GE13nS1	Chikiani	0.021
GE02iD1C	Chikiani	0.024
GE11nS6	Chikiani	0.024
CA29P3B	Hasan Dag	0.028
GE03iD1	Chikiani	0.028
CA29P4	Hasan Dag	0.029

Elements: Fe, Zr, Ba

A-Rank:	Chikiani	5
B-Rank:	Hasan Dag	5

Specimen	*Location*	*E.D.*
GE13nS2	Chikiani	0.009
GE02iD1B	Chikiani	0.013
GE11nS2	Chikiani	0.013
GE11nS3	Chikiani	0.015
CA29P1A	Hasan Dag	0.016
GE13nS1	Chikiani	0.019
CA29P2A	Hasan Dag	0.021
CA29P3A	Hasan Dag	0.021
CA29P4	Hasan Dag	0.021
CA29P1C	Hasan Dag	0.022

Elements: Ti, Fe, Zr, Ba

A-Rank:	Chikiani	9
B-Rank:	Hasan Dag	1

Specimen	*Location*	*E.D.*
GE13nS2	Chikiani	0.010
GE11nS2	Chikiani	0.015
GE11nS3	Chikiani	0.015
GE02iD1B	Chikiani	0.016
GE13nS1	Chikiani	0.021
GE02iD1C	Chikiani	0.024
GE11nS6	Chikiani	0.024
GE03iD1	Chikiani	0.029
CA29P4	Hasan Dag	0.033
GE05iD1	Chikiani	0.034

Elements: Ti, Fe, Mn, Ca, Zr, Ba

A-Rank:	Chikiani	9
B-Rank:	Hasan Dag	1

Specimen	*Location*	*E.D.*
GE13nS2	Chikiani	0.010
GE11nS2	Chikiani	0.016
GE11nS3	Chikiani	0.017
GE11nS6	Chikiani	0.024
GE02iD1B	Chikiani	0.026
GE02iD1C	Chikiani	0.026
GE13nS1	Chikiani	0.028
GE03iD1	Chikiani	0.029
CA29P4	Hasan Dag	0.033
GE05iD1	Chikiani	0.036

Elements: Fe, Ti, Zr

A-Rank:	Chikiani	10
B-Rank:	-	-

Specimen	*Location*	*E.D.*
GE02iD1C	Chikiani	0.007
GE11nS6	Chikiani	0.007
GE03iD1	Chikiani	0.008
GE05iD1	Chikiani	0.009
GE11nS4	Chikiani	0.009
GE13nS2	Chikiani	0.009
GE13nS1	Chikiani	0.010
GE02iD1B	Chikiani	0.012
GE11nS1	Chikiani	0.013
GE01jB1	Chikiani	0.014

Elements: Ti, Zr, Ba

A-Rank:	Chikiani	8
B-Rank:	Unknown	2

Specimen	*Location*	*E.D.*
GE13nS2	Chikiani	0.007
GE11nS2	Chikiani	0.014
GE02iD1B	Chikiani	0.015
GE11nS3	Chikiani	0.015
GE13nS1	Chikiani	0.021
GE02iD1C	Chikiani	0.024
GE11nS6	Chikiani	0.024
CA29P4	Unknown	0.029
GE03iD1	Chikiani	0.029
CA29P3A	Unknown	0.032

Elements: Ti, Fe, Zr, Ba, Zn

A-Rank:	Chikiani	10
B-Rank:	-	-

Specimen	*Location*	*E.D.*
GE03iD1	Chikiani	0.030
GE05iD1	Chikiani	0.039
GE13nS2	Chikiani	0.041
GE02iD1B	Chikiani	0.044
GE01jB1	Chikiani	0.051
GE02iD1A	Chikiani	0.056
GE02iD1C	Chikiani	0.056
GE07kM1B	Chikiani	0.057
GE11nS6	Chikiani	0.059
GE11nS2	Chikiani	0.066

Elements: Ti, Al, Fe, Mn, Ca, Zr, Ba

A-Rank:	Chikiani	6
B-Rank:	Hasan Dag	4

Specimen	*Location*	*E.D.*
CA29P4	Hasan Dag	0.038
GE11nS3	Chikiani	0.038
GE11nS2	Chikiani	0.039
GE11nS6	Chikiani	0.039
GE13nS2	Chikiani	0.039
CA29P1C	Hasan Dag	0.042
CA29P3B	Hasan Dag	0.042
CA29R1	Hasan Dag	0.044
GE03iD1	Chikiani	0.044
GE13nS1	Chikiani	0.044

Table D.1 - Source Assignments of Artifacts based on Euclidean Distance to Centroids of Geological Specimens

Artifact: Georgia-iD3, Tetritsqaro

A-Rank: **Chikiani** **60**
B-Rank: Hasan Dag 3

Elements: Fe, Ti, Ba

A-Rank:	Chikiani	9
B-Rank:	Damlik	1

Specimen	*Location*	*E.D.*
GE11nS1	Chikiani	0.008
GE02iD1A	Chikiani	0.010
GE07kM1B	Chikiani	0.012
GE05iD1	Chikiani	0.013
GE07kM1A	Chikiani	0.013
AR60sK1	Damlik	0.018
GE07kM1C	Chikiani	0.019
GE02iD1C	Chikiani	0.025
GE11nS4	Chikiani	0.025
GE13nS1	Chikiani	0.025

Elements: Fe, Zr, Ba

A-Rank:	Chikiani	8
B-Rank:	Damlik	1

Specimen	*Location*	*E.D.*
GE11nS1	Chikiani	0.008
GE05iD1	Chikiani	0.013
GE07kM1A	Chikiani	0.013
GE02iD1A	Chikiani	0.016
GE07kM1B	Chikiani	0.019
GE02iD1C	Chikiani	0.022
GE13nS1	Chikiani	0.024
GE11nS4	Chikiani	0.025
AR60sK1	Damlik	0.026
AR70rB1	Ttvakar	0.027

Elements: Ti, Fe, Zr, Ba

A-Rank:	Chikiani	8
B-Rank:	Damlik	1

Specimen	*Location*	*E.D.*
GE11nS1	Chikiani	0.009
GE05iD1	Chikiani	0.014
GE07kM1A	Chikiani	0.015
GE02iD1A	Chikiani	0.016
GE07kM1B	Chikiani	0.019
GE13nS1	Chikiani	0.025
AR60sK1	Damlik	0.026
GE02iD1C	Chikiani	0.026
GE11nS4	Chikiani	0.026
AR70rB1	Ttvakar	0.028

Elements: Ti, Fe, Mn, Ca, Zr, Ba

A-Rank:	Chikiani	5
B-Rank:	Ttvakar	2

Specimen	*Location*	*E.D.*
AR70rB1	Ttvakar	0.028
AR70rB2	Ttvakar	0.029
GE07kM1A	Chikiani	0.032
GE11nS1	Chikiani	0.038
CA29P1A	Hasan Dag	0.041
GE05iD1	Chikiani	0.041
AR43kM1	Pokr Arteni	0.042
GE02iD1A	Chikiani	0.042
GE06iD1	Chikiani	0.042
CA31P2	Hasan Dag	0.044

Elements: Fe, Ti, Zr

A-Rank:	Chikiani	10
B-Rank:	-	-

Specimen	*Location*	*E.D.*
GE11nS1	Chikiani	0.008
GE04iD1	Chikiani	0.009
GE11nS4	Chikiani	0.009
GE13nS1	Chikiani	0.010
GE05iD1	Chikiani	0.011
GE07kM1A	Chikiani	0.012
GE02iD1B	Chikiani	0.014
GE13nS2	Chikiani	0.015
GE02iD1A	Chikiani	0.016
GE07kM1B	Chikiani	0.017

Elements: Ti, Zr, Ba

A-Rank:	Chikiani	6
B-Rank:	Ttvakar	2

Specimen	*Location*	*E.D.*
GE11nS1	Chikiani	0.004
AR70rB2	Ttvakar	0.010
AR70rB1	Ttvakar	0.011
GE02iD1A	Chikiani	0.013
GE05iD1	Chikiani	0.013
GE07kM1A	Chikiani	0.013
GE07kM1B	Chikiani	0.018
AR60sK1	Damlik	0.020
AR29ipS1	Unknown	0.021
GE06iD1	Chikiani	0.021

Elements: Ti, Fe, Zr, Ba, Zn

A-Rank:	Chikiani	9
B-Rank:	Armenia, Unk	1

Specimen	*Location*	*E.D.*
GE02iD1A	Chikiani	0.019
GE07kM1B	Chikiani	0.019
GE07kM1A	Chikiani	0.032
GE06iD1	Chikiani	0.039
GE05iD1	Chikiani	0.042
AR29ipS1	Armenia, Unk	0.054
GE04iD1	Chikiani	0.069
GE02iD1B	Chikiani	0.071
GE03iD1	Chikiani	0.073
GE07kM1C	Chikiani	0.074

Elements: Ti, Al, Fe, Mn, Ca, Zr, Ba

A-Rank:	Chikiani	5
B-Rank:	Hasan Dag	3

Specimen	*Location*	*E.D.*
CA29P1A	Hasan Dag	0.041
GE11nS1	Chikiani	0.044
CA31P2	Hasan Dag	0.045
GE05iD1	Chikiani	0.046
GE06iD1	Chikiani	0.046
GE07kM1A	Chikiani	0.048
CA29P3A	Hasan Dag	0.049
AR43kM1	Pokr Arteni	0.050
AR70rB1	Ttvakar	0.050
GE02iD1A	Chikiani	0.050

Table D.1 - Source Assignments of Artifacts based on Euclidean Distance to Centroids of Geological Specimens

Artifact: Georgia-iD4, Tetritsqaro

A-Rank: **Chikiani** **45**
B-Rank: Golludag 7

Elements: Fe, Ti, Ba

A-Rank:	Chikiani	6
B-Rank:	Ttvakar	2

Specimen	*Location*	*E.D.*
AR43kM1	Pokr Arteni	0.015
AR29ipS1	Unknown	0.016
GE11nS4	Chikiani	0.020
GE07kM1C	Chikiani	0.024
AR70rB2	Ttvakar	0.027
AR70rB1	Ttvakar	0.028
GE06iD1	Chikiani	0.029
GE07kM1B	Chikiani	0.029
GE07kM1A	Chikiani	0.031
GE02iD1A	Chikiani	0.037

Elements: Fe, Zr, Ba

A-Rank:	Golludag	4
B-Rank:	Chikiani	2

Specimen	*Location*	*E.D.*
AR29ipS1	Unknown	0.018
GE11nS4	Chikiani	0.020
CA21P1	Golludag	0.021
AR43kM1	Pokr Arteni	0.023
CA21R2A	Golludag	0.026
AR70rB2	Ttvakar	0.027
CA21R2C	Golludag	0.027
AR70rB1	Ttvakar	0.030
CA21R1B	Golludag	0.030
GE07kM1A	Chikiani	0.031

Elements: Ti, Fe, Zr, Ba

A-Rank:	Chikiani	6
B-Rank:	Ttvakar	2

Specimen	*Location*	*E.D.*
AR29ipS1	Unknown	0.020
GE11nS4	Chikiani	0.021
AR43kM1	Pokr Arteni	0.024
AR70rB2	Ttvakar	0.028
AR70rB1	Ttvakar	0.030
GE07kM1A	Chikiani	0.033
GE07kM1B	Chikiani	0.034
GE06iD1	Chikiani	0.036
GE07kM1C	Chikiani	0.036
GE11nS1	Chikiani	0.039

Elements: Ti, Fe, Mn, Ca, Zr, Ba

A-Rank:	Chikiani	8
B-Rank:	Armenia, Unk	1

Specimen	*Location*	*E.D.*
GE11nS4	Chikiani	0.022
AR29ipS1	Armenia, Unk	0.036
GE07kM1B	Chikiani	0.037
GE07kM1C	Chikiani	0.043
AR60sK1	Damlik	0.045
GE11nS1	Chikiani	0.046
GE02iD1A	Chikiani	0.047
GE07kM1A	Chikiani	0.047
GE05iD1	Chikiani	0.050
GE04iD1	Chikiani	0.055

Elements: Fe, Ti, Zr

A-Rank:	Chikiani	5
B-Rank:	Ttvakar	2

Specimen	*Location*	*E.D.*
AR29ipS1	Unknown	0.017
AR70rB1	Ttvakar	0.017
AR70rB2	Ttvakar	0.018
GE04iD1	Chikiani	0.018
GE11nS1	Chikiani	0.020
GE11nS4	Chikiani	0.020
AR33ipS2C	Pokr Sevkar	0.022
EA03P1A	Sarikamis	0.022
GE03iD1	Chikiani	0.022
GE05iD1	Chikiani	0.022

Elements: Ti, Zr, Ba

A-Rank:	Chikiani	5
B-Rank:	Ttvakar	2

Specimen	*Location*	*E.D.*
GE11nS4	Chikiani	0.006
AR29ipS1	Unknown	0.017
AR43kM1	Pokr Arteni	0.021
AR70rB2	Ttvakar	0.025
GE07kM1A	Chikiani	0.026
AR70rB1	Ttvakar	0.027
GE07kM1B	Chikiani	0.028
GE07kM1C	Chikiani	0.030
AR60sK1	Damlik	0.032
GE06iD1	Chikiani	0.032

Elements: Ti, Fe, Zr, Ba, Zn

A-Rank:	Chikiani	7
B-Rank:	Armenia, Unk	1

Specimen	*Location*	*E.D.*
AR29ipS1	Armenia, Unk	0.020
AR43kM1	Pokr Arteni	0.035
GE07kM1C	Chikiani	0.044
GE05iD1	Chikiani	0.045
GE07kM1B	Chikiani	0.052
GE11nS1	Chikiani	0.052
GE02iD1C	Chikiani	0.062
GE02iD1A	Chikiani	0.065
GE06iD1	Chikiani	0.065
AR14jB1	Ankavan	0.067

Elements: Ti, Al, Fe, Mn, Ca, Zr, Ba

A-Rank:	Chikiani	6
B-Rank:	Golludag	3

Specimen	*Location*	*E.D.*
GE11nS4	Chikiani	0.066
CA21R2C	Golludag	0.068
GE07kM1B	Chikiani	0.075
CA21P1	Golludag	0.076
CA21R2B	Golludag	0.077
GE05iD1	Chikiani	0.079
GE07kM1C	Chikiani	0.079
GE11nS1	Chikiani	0.079
AR29ipS1	Unknown	0.080
GE06iD1	Chikiani	0.081